PROCEEDINGS

ESB 2026

35th Annual Conference

of the European Society for Biomaterials

7 - 11 September 2026 • Antwerp, Belgium

ESB 2026

7 - 11 September 2026
Antwerp, Belgium

35th Annual Conference of the
European Society for Biomaterials

Symposia

S1
3D printing photopolymerization at micro- and nanoscale design of devices and materials for bioapplications

S1 – K1
Two-photon 3D-printed modular microfluidic platform for controlled formulation of targeted nanogels

Colli C.[1], Matining V.[1], Jacchetti E.[1], Raimondi M.T.[1], Colosimo B.M.[2], Rosano L.[3], Moscatelli D.[1], Mauri E.[1]
[1]Dept.of Chemistry, Materials and Chemical Engineering, Politecnico di Milano, Milan; [2]Dept. of Mechanical Engineering, Politecnico di Milano, Milan; [3]Institute of Molecular Biology and Pathology, National Research Council, Rome, Italy

Introduction
The performance of targeted nanotherapies critically depends on the controlled synthesis and surface functionalization of the nanosystems. Among them, polymeric nanogels are relevant for different tumoral scenarios. Conventional batch fabrication offers limited control over particle size distribution and ligand decoration, leading to variability that can compromise therapeutic outcomes. Microfluidics can address these limitations, through the design via two-photon polymerization (2PP) 3D printing of platforms with high-resolution features, structural stability, and greater architectural flexibility compared to conventional soft-lithography. In this context, the 2PP-based fabrication of modular microfluidic units enabling a continuous workflow — from controlled nanoparticle synthesis to in-chip decoration with selected ligands, and direct recovery of fully engineered nanoscaffolds at the outlet — would represent a straightforward approach to produce customizable nanosystems.

Materials and Methods
Quantum X Shape 3D printer (Nanoscribe GmbH) was used for the 2PP fabrication of the microfluidic units (Fig.1a): (i) a micromixer ensuring efficient blending of reactive polymer solutions, (ii) a droplet generator producing uniform microdroplets in which nanoscaffold formation occurs under controlled conditions, and (iii) a microinjection “decorator” module enabling in-flow surface functionalization with ligands. Computational fluid dynamics (CFD) simulations were performed to support the design and optimization of flow behavior within the modules. The feasibility of the modular platform was validated through the synthesis and decoration of nanogels using hyaluronic acid and polyethylene glycol/polyamine as reactive polymers, and an inhibitory molecule targeting ovarian cancer cells as decorating agent. The resulting NGs were further evaluated as drug delivery systems by exploiting their swelling behavior for cisplatin encapsulation. Biological performance was assessed in vitro on OVCAR3 cells by Western blot and MTT assay. Comparisons with conventional batch synthesis were performed.

Results
The 2PP-fabricated microfluidic platform demonstrated robust performance over repeated synthesis cycles, maintaining structural and functional stability for at least one week of continuous operation. CFD simulations enabled optimization of mixing efficiency and droplet formation, in agreement with experimental observations. NGs produced on-chip exhibited a narrow size distribution (polydispersity index < 0.05) and over 50% higher ligand decoration efficiency compared to batch synthesis. In vitro studies showed enhanced inhibition of ovarian cancer cell proliferation and reduced metabolic activity for microfluidic-derived NGs relative to batch-produced counterparts, confirming improved therapeutic potential (Fig.1b).

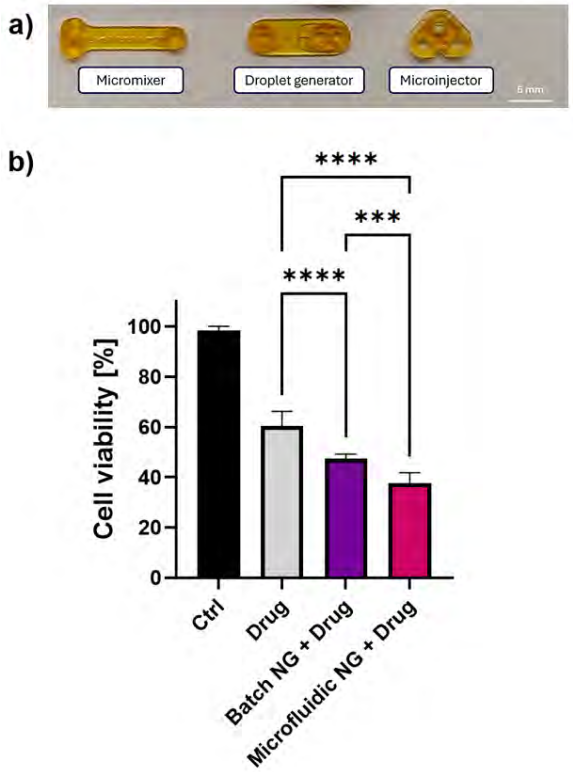

Figure 1. *a) 2PP-3D printed microfluidic units; b) MTT assay of drug-loaded decorated NGs, administered to OVCAR3 cells after 24 h.*

Conclusion

Two-photon polymerization enables the fabrication of highly precise and robust microfluidic systems with minimal geometrical constraints. The proposed modular platform provides a reproducible and versatile strategy for continuous NG production and tailored surface functionalization. This approach represents a powerful tool for the development of next-generation nanotherapeutics, allowing customizable design of nanocarriers in terms of composition and targeting ligands.

Acknowledgements

PRIN 2022 - European Union – Next Generation EU, Mission 4, Component 1, CUP B53C24007220006.
Part of the experimental activities were performed in a laboratory co-funded by Regione Lombardia DGR3637/2020 (lab BIO-3D PRINTING 4.0).

S1 – O1

Combining 2-photon-polymerization with microfluidic on-chip setups for complex multicompartment scaffolds as osteochondral tissue model

Reisbitzer A.[1], Rothe H.[1], Rost J.[1], Schirmer U.[1], Hildebrand G.[1], Boelke F.[2], Töpfer E.[2], Gärtner C.[2], Kruppke B[1,3]
[1]Dept. of Biomaterials, Institute for Bioprocessing and Analytical Measurement Techniques e.V., Heilbad Heiligenstadt; [2]Microfluidic ChipShop GmbH, Jena; [3]Institute for Organic and Macromolecular Chemistry, Friedrich Schiller University Jena, Jena, Germany

Introduction

Physiologically relevant 3D tissue and disease models require precise control over scaffold architecture, mechanics, cell nutrition and co-cultivation. In osteochondral tissues and bone marrow niches, spatially separated yet biochemically coupled microenvironments govern cell fate and disease progression. Conventional scaffold fabrication and cell culture set-ups lack the printing resolution and accessibility of scaffolds to generate complex, perfusable, multicompartment systems within closed microfluidic platforms.

Materials and Methods

We combine a tailored photoreactive copolymer (lactide-caprolactone-methacrylate) with a high-efficiency two-photon photoinitiator to enable direct laser writing inside sealed microfluidic chips. Using two-photon polymerization (2PP), triply periodic minimal surface (TPMS) architectures based on the Schwarz-P geometry were fabricated as bicontinuous scaffolds (5 × 5 mm footprint, and up to 3 mm height). The design separates a cellular and a vascular compartment. Furthermore, different scaffold structures can be written with 2PP directly on top of each other, as is necessary in osteochondral models, for example. The resolution of 2PP technique allows, to write micropores into the scaffold walls (~5 µm nominal perforation), allowing diffusive exchange while preventing uncontrolled cell migration.
Scaffolds were printed directly into multi-directional perfusion chips with independent medium circuits. Computational fluid dynamics simulations were used to prove the uniform supply to the cells and homogeneous flow conditions of the separate channel structures within the entire scaffold. Mechanical properties were tuned via polymer composition and geometry to generate osteogenic and chondrogenic microenvironments.

Results

In-chip 2PP enabled high-precision fabrication of bicontinuous, perfusable scaffolds without post-assembly steps, minimizing leakage and fluid short circuits. Distinct inner (cellular) and outer (vascular) flow paths were maintained under perfusion. For osteochondral models, phase-specific stiffness based on the scaffold design was achieved. The material/cell interaction remained unaffected, enabling efficient seeding and culture of cells in subcompartments of scaffolds in the chip system. Combining on-chip microfluidics and 2PP scaffolds was successfully applied not only to osteochondral designs but also to disease models of acute myeloid leukaemia and osteoarthritis to optimally adapt cell cultivation.

Conclusion

The integration of two-photon polymerized Schwarz-P multicompartment scaffolds inside microfluidic chips establishes a versatile platform for complex biphasic and niche-specific tissue and disease models. This approach unites materials engineering, high-resolution additive manufacturing and microfluidic systems, providing a scalable route toward physiologically relevant bone, osteochondral and hematopoietic in vitro models for drug testing and mechanistic studies.

Acknowledgements

This work was supported by TAB-funded projects “Arthrosis-on-a-Chip” (2023 VFE 0024), Bone-Infection-on-an-Chip” (2021 VF 0034), and “3D-Tumor-on-Chip analysis” (2024 VFE 0040).

S1 - O2

A 3D microstuctured scaffold reveals the mechanobiology of cancer multi-drug resistance

G. Buccioli[1], C. Cortesi[1], C. Martinelli[1], C. Conci[1], A. Nardini[2], R. Martínez Vázquez[2], M.T. Raimondi[1], E. Jacchetti[1]
[1] Dept. of Chemistry, Materials and Chemical Engineering "G. Natta", Politecnico di Milano, Milan, Italy;[2] Institute for Photonics and Nanotechnologies, CNR, Milan, Italy

Introduction

Multi-drug resistance (MDR) remains a major obstacle in cancer therapy and is often driven by ATP-driven drug efflux pumps [1]. Importantly, drug resistance is not governed by transporter abundance alone. Instead, MDR is conditioned by the mechanobiological state of the cell, where membrane organisation and mechanics are set by the coupling between cholesterol-rich domains and the cortical actin network. In parallel, MDR commonly occurs with a glycolytic metabolism and is functionally linked to cholesterol biosynthesis. Because conventional 2D cultures impose an artificial, highly spread cell morphology, they often fail to reproduce the membrane–cortex organisation and cell metabolism, required to recapitulate MDR. Here, we present a biocompatible 3D microscaffold, fabricated via two-photon polymerization in the SZ2080 resin, as a biomaterial platform that reproduces key tumour mechanical cues and MDR phenotypes, demonstrating how the biomaterial-defined microenvironment jointly modulates plasma-membrane mechanobiology, metabolic state, and drug efflux pump activity.

Materials and Methods

We used a custom-made 3D microstructured scaffold (the "Niche"), consisting of a lattice of cubic pores 15×15×15 μm^3 [2]. MCF7 and MDA-MB-231 breast cancer cell lines were cultured on 2D glass or within the 3D Niche. After 24 h, cells were treated with the traditional chemotherapeutic drug Doxorubicin at their specific IC50 (4.4 µM on glass; 103.5 µM in the Niche), with or without the cholesterol-biosynthesis inhibitor Lovastatin (1 µM). Viability assays were performed to quantify drug response. Cortical actin organisation was assessed by immunofluorescence imaging, and fluorescence lifetime imaging microscopy (FLIM) was used to characterisemetabolic shifts.

Results

Inhibition of cholesterol biosynthesis with Lovastatin had no effect on Doxorubicin cell response in 2D cultures, but significantly increased cancer chemosensitivity within the micro-architected 3D scaffold (Fig. 1e). This 3D-specific sensitisation was associated with a marked disruption of cortical actin organisation following cholesterol depletion (Fig. 1c-d), whereas only modest cytoskeletal changes were observed on flat substrates (Fig. 1a-b). Consistently, FLIM analysis revealed a metabolic shift emerging predominantly in 3D, with lifetime signatures (τ_{mean}) indicative of reduced glycolytic cell metabolism (Fig. 1f).

Conclusion

This work demonstrates that a micro-engineered biocompatible scaffold can faithfully recapitulate the mechanobiological and metabolic context underlying tumour drug resistance, a relationship that is largely obscured in conventional 2D cell culture. In conclusion, we highlight the potential of precision-engineered biomaterials as advanced *in vitro* platforms for tumour modelling and for the identification of new therapeutic targets in drug-resistant cancers.

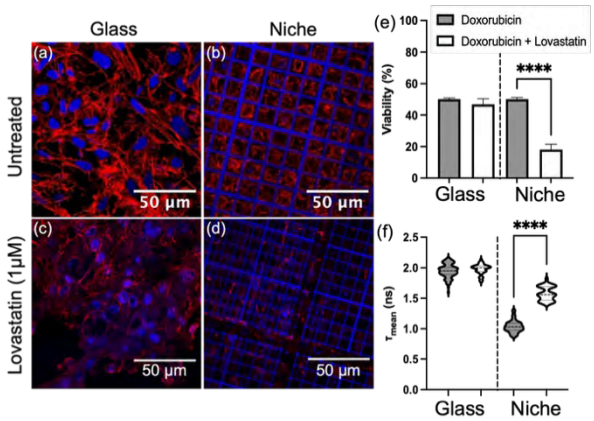

Figure 1: Immunofluorescence images of MDA-MB-231 cells cultured in (a) 2D and (b) the 3D Niche show distinct actin organization. After Lovastatin treatment, (c) flat-cultured cells show no major change in cortical actin, whereas (d) Niche-cultured cells display a disrupted cortical actin (blue, nuclei/Niche; red, F-actin). (e) Cell viability of MDA-MB-231 within the Niche in presence of Doxorubicin decreases significantly upon co-treatment with Lovastatin, indicating a marked chemosensitization when cholesterol synthesis is inhibited. (f) NAD(P)H FLIM mean lifetime (τ_{mean}) in MDA-MB-231 increases in the Niche upon Lovastatin treatment, consistent with a shift toward a less glycolytic metabolic signature.

Acknowledgements

MIUR (PRIN2022-VISION, cod. 2022FLXS8T); ERC (project BEACONSANDEGG, G.A. 101053122); European Union's Horizon 2020 research and innovation programme (project flIMAGING3D, G.A. 101073507)

References

[1]Buccioli et al, Sci Rep 14, 20298, 2024
[2]Martinelli et al, Mater Today Bio 35, 102328, 2025

S1 – O3

Thermoresponsive granular bioinks based on elastin-like recombinamers

Puertas-Bartolomé M.[1], Acosta S.[1], Blanco Escribano A.[1], Alonso M.[1], Rodríguez-Cabello J. C.[1]
[1]BIOFORGE (Group for Advanced Materials and Nanobiotechnology), University of Valladolid- CIBER BBN-LADIS, Valladolid, Spain

Introduction

3D bioprinting enables the precise and automated deposition of bioinks to fabricate complex tissue models, but a key challenge remains in identifying materials that balance mechanical strength, biocompatibility, and responsiveness to stimuli. Elastin-like recombinamers (ELRs), inspired by the extracellular matrix, offer a promising solution due to their resilience, elasticity, tunable bioactivity, and thermosensitivity, making them ideal candidates for bioink development.

Aim

This study presents a stimuli-responsive bioink composed of ELR-based microgels combined with a granular 3D printing approach. ELRs were engineered using a modular design that includes cell-binding motifs and temperature responsiveness, and they were processed as packed microgels to form a granular bioink. We aim to obtain a formulation capable of replicate the innate viscoelasticity of elastic tissues, while also offering superior porosity, improved nutrient transport, and enhanced cell viability compared to bulk hydrogels, maintaining excellent printability, combining material innovation with advanced printing techniques.

Materials and Methods

Microgels were fabricated via a batch emulsion method, using two functionalized ELRs mixed through a double-syringe system equipped with a static mixer. Crosslinking occurred in situ via click chemistry during emulsification. After purification, microgels were jammed to form the granular ink. Methacrylate groups were also incorporated to enable additional photocrosslinking between microgels post-printing. Printability was assessed using extrusion-based bioprinting, and structural properties, porosity, and hMSC viability were evaluated.

Results

The ELR-based microgels (~200 µm diameter) showed spherical morphology and excellent stability. After jamming, the ink exhibited shear-thinning behavior and rapid recovery under stress, ideal for extrusion printing. A temperature-induced phase transition caused ~80% volume shrinkage in the microgels, improving printing resolution and enabling a defined extrusion window. The dual-crosslinking approach—click chemistry during microgel formation and photocrosslinking post-printing—enhanced mechanical strength and shape fidelity of the constructs. The jamming process produced an interconnected porous network, which facilitated oxygen and nutrient diffusion, promoting high cell viability and proliferation of hMSCs. The constructs maintained structural stability over time and preserved the thermoresponsive behavior of the ELRs.

Conclusion

This granular ELR-based bioink demonstrates excellent printability, tunable mechanical properties, and biological performance. The integration of thermosensitivity and dual-crosslinking strategies results in a robust platform suitable for fabricating 3D scaffolds with high fidelity and cell-supportive environments, making it a promising candidate for tissue engineering and regenerative medicine applications.

Acknowledgements

This project has received funding from the European Union's Horizon Europe research and innovation programme under the Marie Skłodowska-Curie grant agreement No 101155569.

S1 – O4

Evaluation of scaffold-induced immune response in chicken embryo chorioallantoic membrane studies

Cortesi C.[1], Cherubin L.[1], Buccioli G.[1], Lodola G.[1], Conci C.[1], Martinelli C.[1], Colosimo B.M.[2], Moscatelli D.[1], Mauri E.[1], Raimondi M.T.[1], Jacchetti E.[1]
[1]Dept. of Chemistry, Materials and Chemical Engineering 'Giulio Natta', Politecnico di Milano; [2]Dept. of Mechanics, Politecnico di Milano, Milan, Italy

Introduction

The chicken embryo chorioallantoic membrane (CAM) provides a rapid, accessible, and cost-effective platform for biomaterials screening, enabling the evaluation of early responses to implants [1]. Understanding how scaffold architecture and material properties influence host response is essential for the development of implantable biomaterials and for the preliminary characterization of their *in vivo* effects. In this work, we investigated the host response to implantation of microscaffolds fabricated by two-photon polymerization (2PP), focusing on the effect of scaffold design and material properties on extracellular matrix (ECM) remodeling and immune cell recruitment within the CAM model.

Materials and Methods

Three-dimensional highly-porous microscaffolds were fabricated in IP-S photoresist (E=2.1GPa, v=0.3, ρ =1111kg/m^3) employing Quantum X Shape system (λ=780nm, PRR=80MHz, 25x objective, NA0.8) (Nanoscribe, GmbH). Fertilized eggs were cultured *ex ovo*, and microscaffolds were implanted directly onto CAM regions on embryonic incubation day (EID) 8. On EID14, CAM samples were harvested, fixed in 4% paraformaldehyde, and processed for immunofluorescence (Hoechst-33342, Phalloidin, KUL01 antibody, Anti-chicken collagen-I antibody). Tissue organization and ECM remodeling were investigated by combining confocal microscopy with two-photon excitation fluorescence (TPEF) (λ_{ex}=800nm), and label-free SHG imaging (λ_{ex}=910nm), using Nikon A1R+ (40× objective, NA1.15).

Results

Implanted acellular microscaffolds maintained structural integrity after implantation, indicating mechanical stability under physiological conditions. CAM imaging revealed multilayered tissue organization, as well as localized host responses to the implant, characterized by ECM remodeling and cell migration and infiltration within scaffold pores (Fig.1a). Collagen-I accumulation within the scaffold architecture was detected by immunostaining (Fig.1a), while SHG imaging revealed the formation of a fibrillar collagen capsule surrounding the implant. Capsule geometry followed microscaffolds architecture, suggesting that scaffold design may influence collagen deposition and fiber orientation. Immunostaining with KUL01 showed recruitment of macrophages and monocytes in stromal and peri-implant regions (Fig.1b), indicating an innate immune response to the implant.

Conclusion

CAM model provides a powerful platform for early evaluation of host responses to biomaterial implantation. These results highlight the importance of understanding how scaffold architecture and material properties influence host response, to guide the design of implantable biomaterials. The acellular model establishes a baseline host response that will support future studies using cellularized microscaffolds, to investigate the contribution of different cell types to the implant response.

Acknowledgements

ERC, project BEACONSANDEGG, G.A. 101053122; PRIN2022-VISION, cod. 2022FLXS8T; EU, MSC-DN, project flIMAGIN3D, G.A. 101073507.

References

[1]Conci C. et al., In vivo label-free tissue histology through a microstructured imaging window. *APL Bioengineering,* 2024; 8,016102.

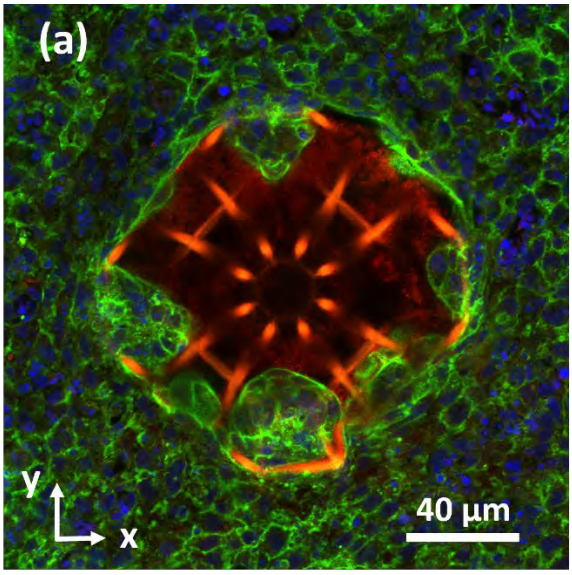

Nuclei, F-actin,
Collagen-I, Scaffold

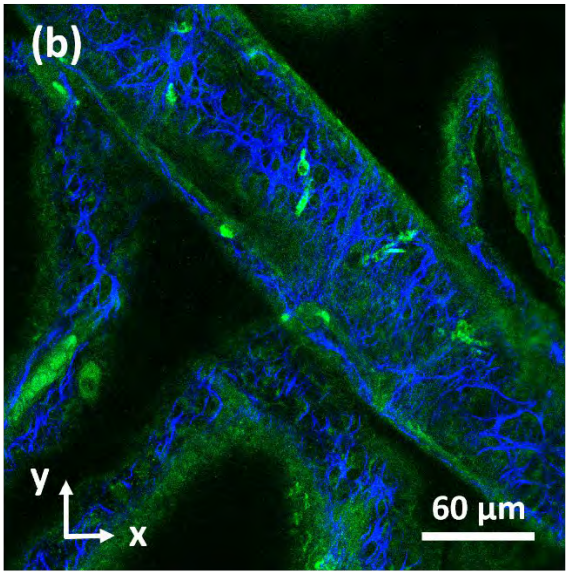

Collagen (SHG), Macrophages,
CAM autofluorescence

Figure 1a: Confocal image of the acellular microscaffold implanted on the CAM, showing host cell migration and infiltration within scaffold pores, together with the deposition of non-fibrillar collagen inside the architecture.
Figure 1b: SHG imaging of a vascularized CAM region, revealing collagen surrounding the vessel (SHG), as well as macrophage-like cells inside the vessel and in the surrounding region (KUL01 immunostaining).

S1 – O5

Scaling up microscale architectures for 2PP bioprinting applications

Santoni S.[1,2], Carpentier N.[1,2], Cooley I.[3], Vuillod B.[4], Dallaywater W.[5], Wildman R. D.[4], Rose F. R. A. J.[1,2]
[1]School of Pharmacy, University of Nottingham, Nottingham; [2]Nottingham Biodiscovery Institute, University of Nottingham, Nottingham; [3]Dept. of Chemical Engineering, Loughborough University, Loughborough; [4]Faculty of Engineering, University of Nottingham, Nottingham; [5]Faculty of Medicine & Health Sciences, University of Nottingham, Nottingham, UK

Introduction

Two photon polymerization (2PP) allows the generation of the smallest features via additive manufacturing up to the sub-micron range. However, its main drawbacks are the high printing time and the possibility of cell damage while bioprinting. This work aims at increasing the volume throughput of 2PP bioprinted samples via printing parameters optimisation and formulation tuning, to achieve a high resolution and functional 3D construct with uniform cell distribution along its depth, while allowing 3D cell spreading.

Materials and Methods

GelMA and GelNB were synthetized according to the literature and used in combination with a photoinitiator and a thiolated PEG crosslinker in case of GelNB. The inks were mixed with L929 fibroblasts and printed using an UpNano NanoOne printer. The processability window under varying printing parameters was assessed by fabricating a reference structure, followed by confocal imaging and image analysis. Printing time was modeled by measuring the fabrication of cubes of different sizes using a full-factorial DoE. The effect of printing parameters on cell viability was evaluated via live/dead™ assays on bioprinted cubes after 24 hours incubation. A surrogate model was developed using four printing parameters as descriptors to predict cell viability, with a randomised 80/20 train-test split. Selected printing conditions were further examined comparing bulk structures with lattice geometries of different pore sizes, with live/dead™ assays at day 1 and quantification of F-actin expression in larger samples at day 7.

Results

Using a formulation printed in the gel state, sedimentation of the cells was successfully avoided. Printing rates were reduced from below 1 µL/hr to >8 µL/hr while maintaining the resolution. The processability window of the investigated materials was correlated with the cell viability in the bioprinted structures. A comparative analysis across eight candidate models returned a good fit to the experimental data (R^2>0.8). A selected model was used to identify a sub-region of the processability domain of the tested materials where the viability was >70%. The use of different porosities improved cell spreading and actin-F expression within the bioprinted structures compared to bulk structures obtained with the same printing parameters.

Conclusion

Within this work, a methodology for the optimisation of volume throughput and cell viability while keeping microscale resolution was developed. These strategies can be transferred to the production of relevant tissue structures with viable cells throughout the hydrogel.

Acknowledgements

This work was funded by UKRI EPSRC programme grant EP/W017032/1

S1 – O6

Design of bio-based photocurable non-isocyanate polyurethanes for two-photon polymerization 3D printing of biocompatible microstructures

Carlucci S. L.[1], Caserio L.[1], Matining V.[1], Jacchetti E.[1], Raimondi M. T. [1], Moscatelli D.[1], Mauri E.[1]
[1]Dept. of Chemistry, Materials and Chemical Engineering "Giulio Natta", Politecnico di Milano, Milan, Italy

Introduction

Two-Photon Polymerization (2PP) is an advanced micro- and nanoscale additive manufacturing technique enabling the fabrication of highly resolved 3D architectures for biomedical applications. Its capability to precisely reproduce complex geometries makes it particularly suitable for mimicking cell niches and engineered microenvironments. In this context, the development of photo-curable materials that combine high printing resolution, tunable and cell-friendly physico-mechanical properties, and biocompatibility is of primary importance. Furthermore, sustainable resin synthesis, aligned with circular economy principles, remains a key challenge for current materials[1]. While polyurethanes are promising, conventional isocyanate-based routes are increasingly restricted under EU regulations (Regulation 2020/1149). Non-isocyanate polyurethanes (NIPUs), offering tunable properties and safer synthetic pathways, represent a sustainable alternative. This work focuses on the design, synthesis, and characterization of bio-based, photo-curable NIPU resins tailored for 2PP microfabrication and validated as new candidate materials for biomedical applications.

Materials and Methods

NIPUs were synthesized via a multi-step route, starting from aminolysis of ethylene carbonate using a bio-based diamine, yielding bis(hydroxyethyl) carbamate (BHEC), followed by melt polycondensation with a bio-derived diol. The resulting prepolymer was functionalized with vinyl groups through two alternative pathways to tune mechanical properties: methacrylic anhydride (NIPU-MA) and a glycol diacrylate derivative (NIPU-NPGDA)[2]. Materials were characterized by ^{1}H-NMR, FT-IR, GPC, DSC, and rheological/mechanical testing. Photoresins were formulated and processed via 2PP using a Nanoscribe Quantum X system. Microstructures (e.g., lattice and scaffold-like geometries) were fabricated with feature resolution down to ~10 µm. Degradation was assessed at pH 4, 7.4, and 10, over 7 days. Biocompatibility was evaluated according to ISO 10993-5, alongside preliminary cell adhesion and viability studies using breast cancer cells (Live/dead assay) (Fig.1).

Results

Both resins were successfully synthesized and confirmed by ^{1}H-NMR and FT-IR. GPC analysis showed comparable molecular weights (~4.7 kDa), consistent with oligomeric architectures suitable for photopolymerization. Polymers were characterized by low glass transition temperatures (< −30 °C), indicating flexible, fully amorphous structure. After photocrosslinking, NIPU-MA exhibited higher stiffness ($G' \approx 3 \times 10^5$ Pa) and elastic recovery, while NIPU-NPGDA showed lower viscosity and increased flexibility/softness ($G' \approx 6 \times 10^4$ Pa). Both resins enabled the fabrication of complex microstructures with high fidelity (Printability Index > 85%). Degradation studies confirmed stability under physiological conditions and tunable degradation under alkaline conditions. Biocompatibility tests demonstrated non relevant cytotoxic behavior of the resins, with cell viability around 80% at day 7 (Fig.2). Cell seeding experiments revealed effective adhesion and homogeneous cell distribution within the microstructures.

Conclusion

Bio-based, photo-curable NIPU resins were developed as sustainable alternatives for 2PP microfabrication. By tuning the functionalization strategy, materials with distinct mechanical and processing properties were obtained. Both systems demonstrated excellent printability, physiological stability, controlled degradability, and suitability for cell adhesion. These results position NIPU-based resins as promising candidates for bio-scaffolding and broader cell-based and cell-free biomedical applications.

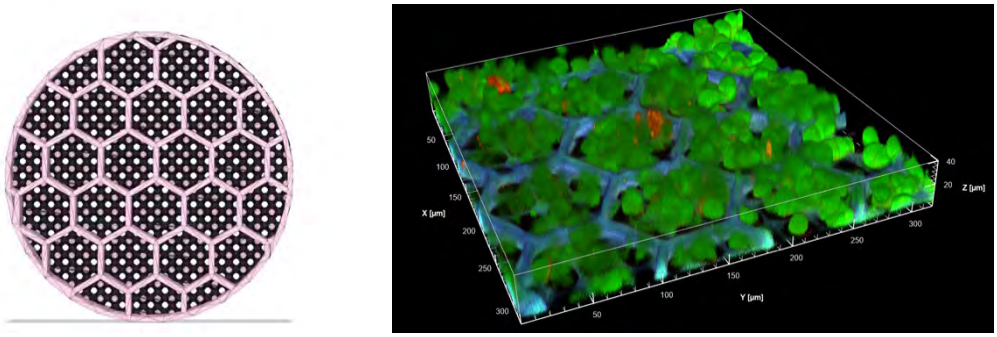

Figure 2. *On the left, an image of the STL model of the 2PP printed microstructures (D = 100 µm); on the right, a confocal microscopy image illustrates cell adhesion on the NIPU–NPGDA sample structure.*

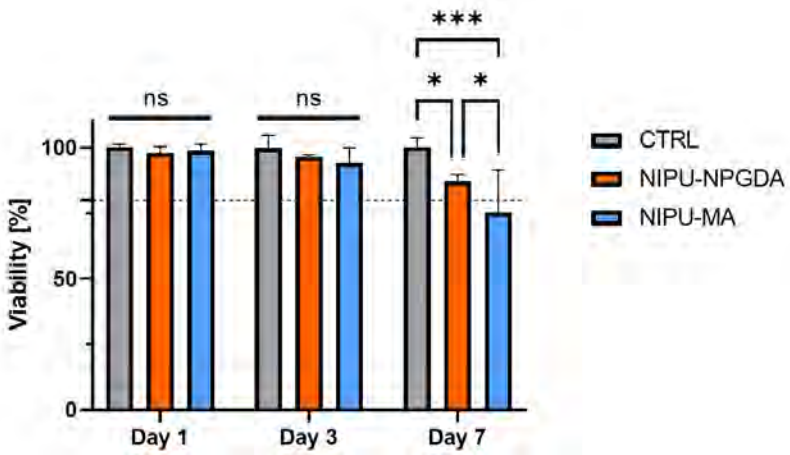

Figure 2. *MTT assay according to ISO-10993-5 was conducted: cell viability after administration of the conditioned medium collected from NIPU-NPGDA and NIPU-MA specimens incubated in culture medium for 1, 3, and 7 days. Results are expressed as normalized viability (%) relative to the control group (CTRL) and reported as mean ± SD from three independent experiments. Statistical analysis was performed using one-way ANOVA test (*p < 0.05, **p < 0.01, ***p < 0.001, ****p < 0.0001, ns = not significant).*

Acknowledgements

Part of the experimental activities were performed in a laboratory co-funded by Regione Lombardia DGR3637/2020 (lab BIO-3D PRINTING 4.0).

References

[1] Seán O'Halloran, Abhay Pandit, Andreas Heise, and Andrew Kellett. Two-Photon Polymerization: Fundamentals, Materials, and Chemical Modification Strategies. Advanced Science, March 2023, 10(7):2204072.

[2] Xinqi Zhang, Xinxin Zan, Jiangdi Yin, and Jiaxi Wang. Non-Isocyanate Urethane Acrylate Derived from Isophorone Diamine: Synthesis, Characterization and Its Application in 3D Printing. Molecules, June 2024, 29(11): 2639.

S1 – O7

Bioprinted silk fibroin-based auxetic metamaterials as platform for modeling cardiovascular diseases

Spessot E.[1], Agostinacchio F.[1], Tirella A.[1], Maniglio D.[1], Motta A.[1]
[1]BIOtech Research Centre, Dept. of Industrial Engineering, University of Trento, Trento, Italy

Introduction

Cardiovascular diseases (CVD) are the leading causes of health issues and mortality worldwide affecting roughly 1 in 12 individuals [1].
To develop 3D *in vitro* models for studying CVDs, biomaterials that closely recapitulate the complex biochemical environment and the dynamic mechanical properties of the cardiac tissue are needed. Natural polymer-based isotropic hydrogels often fail to adapt the mechanical requirements of beating cardiac tissue. Thus, natural polymers can be engineered into auxetic structures – i.e. architectures characterized by a negative Poisson's ratio – to expand in multiple direction under longitudinal strain and adapt the anisotropic mechanics of the beating heart.

Aim

Design of a biomaterial ink composed of a blend of a fibrous protein (silk fibroin, SF), and a polysaccharide (tyramine-modified alginate, Alg-Tyr). Light-based bioprinting was explored to manufacture 4D auxetic structures with controlled time-dependent viscoelastic properties resembling the progression from healthy to fibrotic cardiac tissue.

Materials and Methods

Silk Fibroin (SF) was extracted from *Bombyx Morii* cocoons and regenerated as in [2]. Tyramine-modified alginate (Alg-Tyr) was obtained via EDC/NHS chemistry as in [3]. Rheological properties of biomaterial inks were characterized, and the formulation was optimized. The printability was assessed using a Digital Light Processing (DLP) bioprinter varying the intensity and exposure to light and the infill density of the printed structures. The time-dependent viscoelastic properties and structural rearrangements of SF were monitored by using microindentation and Fourier-transformed infrared (FT-IR) spectroscopy, respectively.

Results

The synergistic combination of a structural protein (SF) with a polysaccharide (Alg-Tyr) successfully enhanced the biochemical cues and mechanical tunability of the resulting bioprinted hydrogels, creating an ideal microenvironment mimicking cardiac tissue both in physiological and diseased condition. Optimized SF-AlgTyr biomaterial inks demonstrated good printability via DLP and structural stability over 28 days. Mechanical evaluations depicted a highly concentration-dependent relationship on the final hydrogel properties. DLP bioprinting achieved spatial resolutions allowing the manufacturing of customizable auxetic design. This system demonstrated a progressive stiffening from few kPa to >100 kPa after 28 days. This effect was driven by the conformational rearrangement of SF, as confirmed via FT-IR spectra deconvolution of Amide I peak. Preliminary *in vitro* evaluations validated the cytocompatibility of the SF-AlgTyr hydrogels and ongoing studies will assess the impact of the 4D system and the auxetic design on contractile functionality of the material.

Conclusion

The combination of SF and Alg-Tyr to design biomaterial inks allowed the manufacturing of 4D bioprinted auxetic metamaterials that mimic the mechanical switch from a healthy to a fibrotic cardiac tissue, as a dynamically adapting *in vitro* platform.

Acknowledgements

This work received fundings from Piano Sviluppo e Coesione-Ministero della Salute, LIFE4HUB-T4-CN-05/0022998 (14/11/2022) and from Fondazione Caritro (grant 'Progettazione di sistemi 3D in vitro per la medicina personalizzata').

References

[1]Brown B., Williams H., Egbulonu S., et al. Augmented Flow-Induced Outward Remodelling Occurs with Ageing in Mice. *International Journal of Molecular Sciences*, 2025; 26(21); 10274.
[2]Rockwood, D., Preda, R., Yücel, T. et al. Materials fabrication from Bombyx mori silk fibroin. *Nature Protocols,* 2011; 6, 1612–1631.
[3]Perin F., Mota C., Mancini I., et al. Photo-enzymatic dityrosine crosslinking for bioprinting. P*olymer,* 2022; 252; 124941.

S2
4D printing and smart biomaterials for regenerative medicine

S2 - K1
4D Printing across scales: Design, mechanics, and shape morphing

Mohammad J. Mirzaali Mazandarani

Four-dimensional (4D) printing enables additively manufactured structures to change their shape or properties in response to external stimuli. Its successful implementation relies on the coordinated selection of responsive materials, geometrical design and manufacturing strategies, and the type of stimulus.
In this talk, I will present three examples illustrating how these elements can be combined across different length scales. First, I will discuss shape-memory polymer structures fabricated by fused deposition modeling, in which printing-induced anisotropy and defects are used to tune mean and Gaussian curvatures and create shape-changing concepts for drug delivery. Second, I will present the two-photon polymerization of temperature-responsive poly(N-isopropylacrylamide) hydrogels, enabling reversible shape morphing in three-dimensional microstructures at very small length scales. Finally, I will show how magnetic particles embedded in printed hydrogels can be remotely actuated to control the effective elastic modulus of the substrate.
These examples demonstrate that 4D printing is not governed by responsive materials alone. Instead, its functionality emerges from the interplay between material behavior, structural design, manufacturing, and external stimulation. This integrated approach provides opportunities for developing adaptive biomaterials, dynamic tissue-engineering platforms, and remotely controlled biomedical devices.

S2 – O1

From biodegradation to “smart” hydrogels: Graphene derivatives for biomedical applications

Martín C.[1,2], Alcaide J.[1,2], Vázquez E.[1,2]
[1]Instituto Regional de Investigación Científica Aplicada (IRICA); [2]Facultad de Ciencias y Tecnologías Químicas (UCLM), Ciudad Real, Spain

Introduction

Graphene-based hydrogels have emerged as advanced biomaterials due to their mechanical robustness, electrical conductivity and biocompatibility. The incorporation of graphene derivatives, including graphene oxide and few-layer graphene, into polymeric matrices enables the development of multifunctional three-dimensional (3D) scaffolds. These systems are particularly attractive for tissue engineering applications because of their ability to mimic the native extracellular matrix and promote cell adhesion and proliferation.

Aim

This work aims to investigate the role of graphene derivatives in polymeric hydrogels and to evaluate the enhancements they provide in biodegradability, biological response and multifunctional performance for advanced tissue engineering and therapeutic applications.

Materials and Methods

Graphene derivatives were integrated into polymeric hydrogel networks to obtain responsive and mechanically stable 3D scaffolds. Their physicochemical properties were evaluated, including rheological behavior relevant for injectability and biofabrication. Enzymatic degradation studies of graphene-based materials were performed to assess biodegradability, focusing on interactions with human peroxidases. Biological performance was investigated through in vitro cell culture models, and antibacterial activity was evaluated to determine suitability for wound healing environments. Responsiveness to near-infrared irradiation was analyzed to explore photothermal therapeutic potential.

Results

Graphene-enhanced hydrogels exhibited improved mechanical properties and biocompatibility compared to pristine polymeric systems. The presence of graphene derivatives promoted cell adhesion and proliferation in neural and skin-related models. Enzymatic assays demonstrated that graphene-based materials undergo biodegradation mediated by human peroxidases, supporting their potential long-term biocompatibility. Additionally, the composite hydrogels displayed antibacterial activity and photothermal responsiveness, broadening their applicability in infection-prone environments. Some hydrogels exhibited shear-thinning behavior and viscosity profiles compatible with 3D bioprinting, allowing extrusion-based manufacturing of customized scaffolds.

Conclusion

Graphene-containing hydrogels represent versatile platforms for regenerative and personalized medicine. By combining structural support, biodegradability, antibacterial properties and photothermal responsiveness, these 3D scaffolds bridge material science and biomedical innovation. Our findings demonstrate that the incorporation of graphene derivatives provides a synergistic enhancement of structural, biological and functional properties.

Acknowledgements

C.M. acknowledges support from the CONEX-Plus program, funded by “Universidad Carlos III de Madrid” and the European Union’s Horizon 2020 Research and Innovation Programme under the Marie Sklodowska-Curie Grant (grant agreement no. 801538) and EU Graphene Flagship project (no. 785219). The authors acknowledge financial support from MCIN/AEI/10.13039/501100011033, RYC2024-048/685-I (C.M.); JCCM SBPLY/24/180225/000155 (C.M.); and University of Castilla-La Mancha (2025-GRIN-38256). IRICA instrumental service is gratefully acknowledged.

S2 – O2

Optimizing NaOH treatment of 4D printed PCL networks: Trade-off between biological, mechanical, and shape-memory performance

Bonetti L.[1], Mira E.[1], Scalet G.[1]
[1]Dept. of Civil Engineering and Architecture, University of Pavia, Pavia, Italy

Introduction

Semi-crystalline polymer networks based on polycaprolactone (PCL) have been widely investigated for their shape-memory behavior and recently proposed for extrusion-based 4D printing. Despite its advantages (e.g., biocompatibility, biodegradability), PCL is limited by its hydrophobic nature which limits cell adhesion. Surface modification techniques can enhance these properties; however, achieving an optimal trade-off between improved biological performance and preserved material's functional properties requires careful investigation.

Aim

This study investigates the effects of NaOH-induced hydrolysis on the physico-mechanical, shape-memory, and biological properties of PCL-based specimens fabricated by extrusion-based 4D printing.

Materials and Methods

Specimens (30 x 5 x 0.4 mm) were 4D printed with a pneumatic bioprinter, using methacrylated PCL (M_n = 10 kDa) and achieving photo-crosslinking (λ = 365 nm) directly on the printbed in the presence of a suitable photo-initiator. Samples were then divided into four groups: untreated control (G0) and three groups treated with aqueous NaOH solutions at increasing concentrations (G4, G8, G10 = 5, 10, 20 M). All samples underwent hydrolytic treatment at 37 °C for 48 h and were characterized by weight change, contact angle, tensile, shape-memory, and in vitro biological tests.

Results

Increasing NaOH molarity increased specimen weight loss (22.2 vs. 0 % for G12 and G0) and hydrophilicity (θ_C = 21.3 vs. 72.1 ° for G12 and G0). Mechanically, all treated samples showed a ~25% reduction in Young's modulus, suggesting similar impacts across different molarities. One-way shape-memory tests showed comparable strain fixity and recovery ratios (R_f ~ 95 %, R_r ~ 96 %) for all specimens; interestingly, two-way shape-memory performance improved after treatment (AM = 13.5 vs. 18.9 %, RM = 84.2 vs. 91.7% for G0 and G12). No cytotoxic effects were detected when challenging material extracts with HS-5 cells. Moreover, higher NaOH molarity qualitatively enhanced cell adhesion on the specimen surfaces (Figure 1).

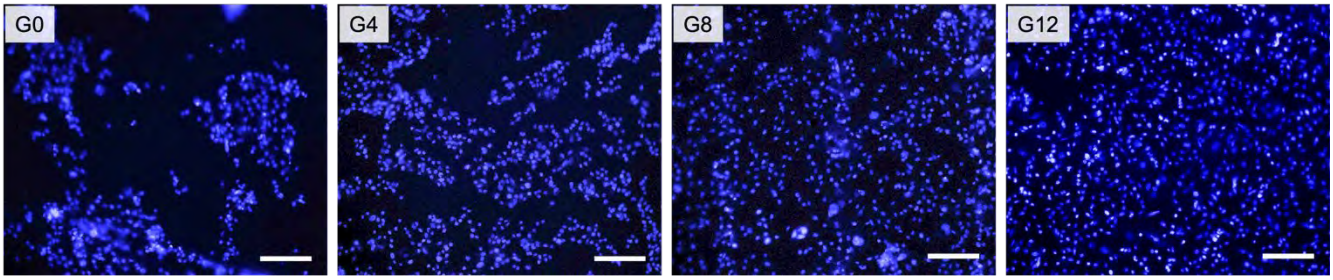

Figure 1 - Immunofluorescence micrographs (blue = nuclei) 24 h after HS-5 cell seeding, showing increased cell adhesion on PCL surfaces with increasing NaOH treatment molarity. Scalebar = 100 µm.

Conclusion

NaOH-induced hydrolysis effectively modulates the surface properties of PCL networks, enhancing their biological performance while preserving their mechanical and shape-memory behavior.

Acknowledgements

This work was funded by the European Union ERC CoDe4Bio Grant ID 101039467.

S2 – O3

NeoNectin-functionalized 3D-printed polymeric stents promote endothelialisation and reduce thrombogenicity

Cano-Morenilla M.[1], Pino M.[2], Díaz-Ricart M.[2], Wang X.[4], Baker D.[4], Pegueroles M.[1,3], Guillem-Marti J.[1,3]
[1]Biomaterials, Biomechanics and Tissue Engineering Group (BBT), Dept. of Materials Science and Engineering, Barcelona Research Center in Multiscale Science and Engineering (CCEM) and Institute for Research and Innovation in Health (IRIS), Universitat Politècnica de Catalunya-BarcelonaTech, Barcelona, Spain; [2]Hematopathology, Pathology Dept., Centre de Diagnòstic Biomèdic, Institut d'Investigacions Biomèdiques August Pi i Sunyer, Hospital Clínic, Universitat de Barcelona, Barcelona, Spain; [3]Centro de Investigación Biomédica en Red-Bioingeniería, Biomateriales y Nanomedicina (CIBER-BBN), Instituto de Salud Carlos III, Madrid, Spain; [4]Institute for Protein Design, University of Washington, Seattle, United States

Introduction

Congenital heart diseases remain the main cause of children decease worldwide. Pediatric aortic coarctation, an abnormal narrowing of the aorta, lacks of specific treatment devices. Bioresorbable stents are a promising solution as they can adapt to the growing aorta, although their surfaces do not promote endothelial cell adhesion. Functionalization with extracellular matrix (ECM) proteins or ECM-derived peptides improves adhesion but lacks specificity for endothelial cells and may increase thrombosis. To address these limitations, NeoNectin, a *de novo* computationally designed protein that specifically binds $\alpha_5\beta_1$ integrin[1], is proposed as a biofunctionalization strategy. Since $\alpha_5\beta_1$ integrin is involved in endothelial cell adhesion and migration but it is marginally expressed in platelets, NeoNectin could promote stent endothelialisation while preventing thrombus formation.

Aim

This study aims to functionalize bioresorbable polymeric 3D-printed cardiovascular stents with NeoNectin and evaluate their capabilities to promote endothelialisation and to reduce thrombogenicity.

Materials and Methods

PLCL copolymer with 85:15 (P85) PLLA:PCL ratio and a blend (B70) of P85 and 70:30 (P70) PLLA: PCL molar ratio, respectively, films and 3 mm diameter stents were fabricated by solvent-cast direct-ink writing (SC-DW)[2]. The ink consisted in the selected polymer-chloroform solution at 30.25% w/v. After thermal treatment (65ºC, 12h), surfaces were functionalized with NeoNectin via O_2 plasma activation and EDC/NHS coupling. Fibronectin- and non-functionalized samples served as controls. Functionalization was verified by XPS. Endothelial adhesion and proliferation (HUVEC, HAoEC) were assessed on 2D films, while antithrombogenicity was evaluated on 3D-printed stents by platelet adhesion after whole-blood perfusion.

Results

Different PLCL bioresorbable stents were successfully 3D-printed by SC-DW technique, and XPS confirmed surface functionalization by an increase of N atomic percentage in functionalized samples. After 24 h, HAoEC and HUVEC (*Figure 1a)*) exhibited increased spreading and attachment on PLCL surfaces, especially on NeoNectin immobilized. NeoNectin effect is comparable to Fibronectin for both cell lines after 14 days (*Figure 1b)*). Noteworthy, adhered platelets' percentage was significantly lower on NeoNectin functionalized P85 stents (*Figure 2a)*). For B70 samples, NeoNectin showed a similar trend, reducing platelet adhesion compared to bare PLCL surface, although the differences were not statistically significant (*Figure 2b)*).

Conclusion

NeoNectin functionalization is a promising strategy for PLCL cardiovascular stents. NeoNectin promotes endothelial cell adhesion and proliferation on PLCL surfaces with an efficiency comparable to Fibronectin, while significantly reducing the thrombogenic potential of these materials.

Acknowledgements

Project PID2024-161387OB-C22 funded by MICIU/AEI/10.13039/501100011033 and by FEDER, UE. María de Maeztu CEX 2023-001300-M/AEI/10.13039/501100011033, Administration of University and Research Grants (AGAUR) of the Generalitat de Catalunya (2023 FI Joan Oró-00794). The Ramon y Cajal grant

(RYC2022-0380006-I) funded by MCIN/AEI/10.13039/501100011033.

References

[1] Wang X, Guillem-Marti J, Kumar S, Lee DS, Cabrerizo-Aguado D, Werther R, Alamo KAE, Zhao YT, Nguyen A, Kopyeva I, Huang B, Li J, Hao Y, Li X, Brizuela-Velasco A, Murray A, Gerben S, Roy A, DeForest CA, Springer T, Ruohola-Baker H, Cooper JA, Campbell MG, Manero JM, Ginebra MP, Baker D. De Novo Design of Integrin α5β1 Modulating Proteins to Enhance Biomaterial Properties. *Adv Mater*. 2025; 37(34): e2500872.
[2] Chausse V, Schieber R, Raymond Y, Ségry B, Sabaté R, Kolandaivelu K, Ginebra MP, Pegueroles M.; Solvent-cast direct-writing as a fabrication strategy for radiopaque stents. *Additive Manufacturing*. 2021; 48.

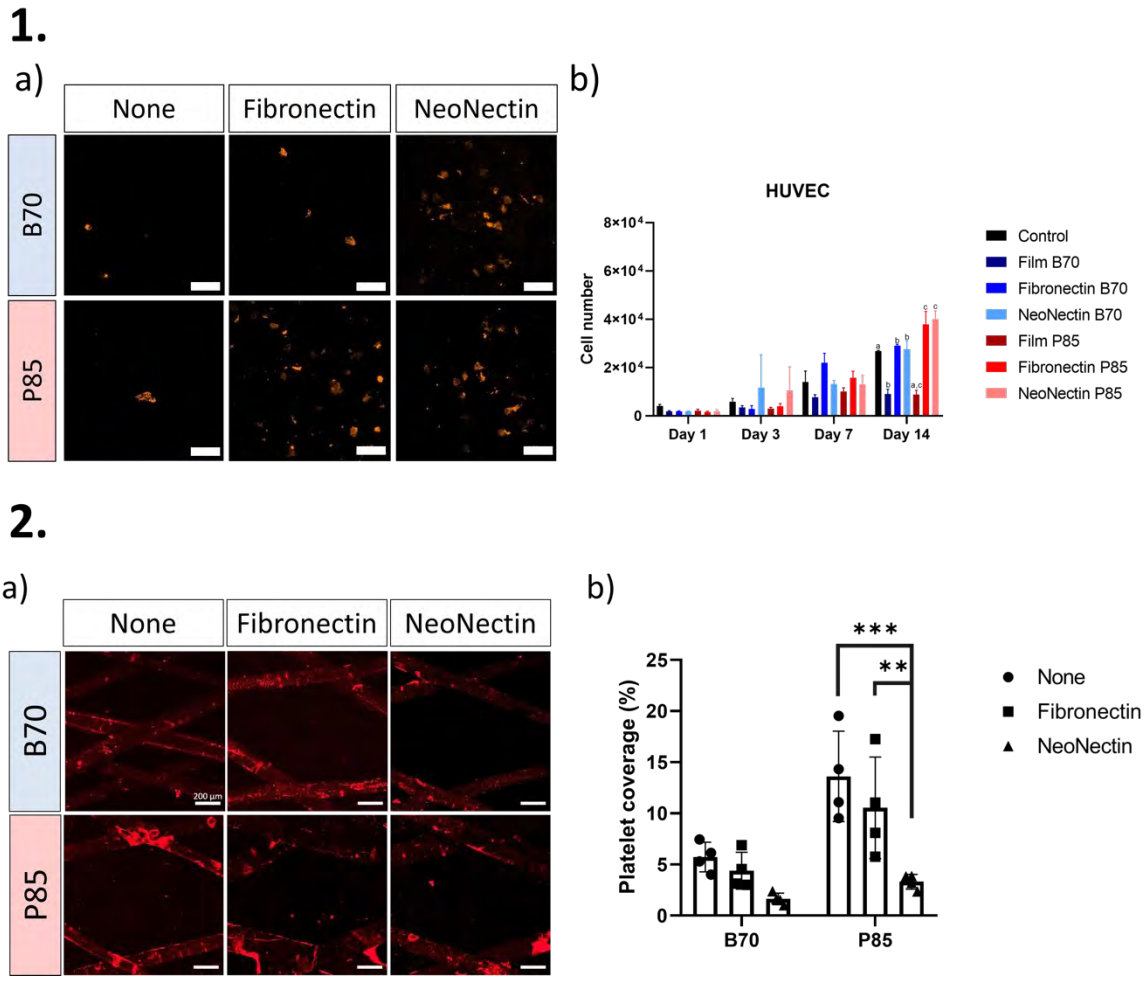

***Figure 1*: Results of non-functionalized (None) and functionalized (Fibronectin and NeoNectin) PLCL 2D films for: a) HAoEC 24h adhesion. Scale bar: 100 µm; b) HUVEC 14-day proliferation.**

***Figure 2*: Platelet adhesion on non-functionalized (None) and functionalized (Fibronectin and NeoNectin) PLCL cardiovascular stents: a) Immunofluorescence staining of CD36. Scale bar: 200 µm; b) Platelet coverage percentage.**

S2 – O4

Tailoring bone mimetic matrices: Nanocomposite injectable formulations and 3D printing for personalized therapies and tissue regeneration

Campodoni E.[1], Vicinelli G.[1], Panocchia A.[1], Mazzoleni A.[2], Martin I.[2], Muraro M.[2], Sandri M.[1]
[1]CNR-ISSMC Institute of Science, Technology and Sustainability for Ceramics, Faenza (RA), Italy; [2]Dept. of Biomedicine, University Hospital Basel, Basel, Switzerland

Introduction

Despite significant advances in recent decades in elucidating the pathological mechanisms of bone-associated diseases and developing targeted pharmacological therapies, finding effective therapeutic solutions remains extremely challenging for most of these diseases.

Bone organoids, miniaturized in vitro structures recapitulating natural tissue, offer advantages over animal and 2D cell models. However, existing vitro systems remain limited. Three-dimensional (3D)-printed tissues are expected to overcome the shortcomings of traditional tissue engineering by providing precise structural control and supporting cell-laden constructs. However, progress in bioprinting is hindered by the shortage of biomaterials that enable printing, ensure cell viability and deliver tissue-specific cues.

Materials and Methods

In this contest, our research focused on developing biomimetic, injectable nanocomposite hydrogels in which collagens from different sources are functionalized with biomimetic hybrid magnesium-doped-hydroxyapatite (bMgHA) particles. bMgHA hybrid particles are synthesized via a bioinspired mineralization process studied to obtain a nano-structured mineral phase that is highly bioactive and bioavailable. The composite formulations are optimized in terms of rheological properties and printability and processed using extrusion-based printing. The printed structures are then dried by freeze-casting and chemically stabilized via dehydrothermal treatment.

Results

bHA hybrid particles exhibit a crucial multiple functions: (i) enhancing the rheological behavior of the hydrogel to enable high-fidelity 3D printing; (ii) introducing osteoinductive properties through their nanostructured, bioactive composition; (iii) improving the mechanical behavior of constructs. The presence of the organic phase is essential for obtaining more hydrophilic particles that are ideal for use in stable, homogeneous composite injectable hydrogels. This formulation enables the creation of 3D matrices with a controlled macro-geometry that recapitulates the complexity of the bone niche microenvironment. Furthermore, freeze-drying enables the structure to be decorated with a dense network of micro-pores, which is essential for improving the internal surface area, fluid absorption, cell permeation and connection, and compatibility with perfusion bioreactors.

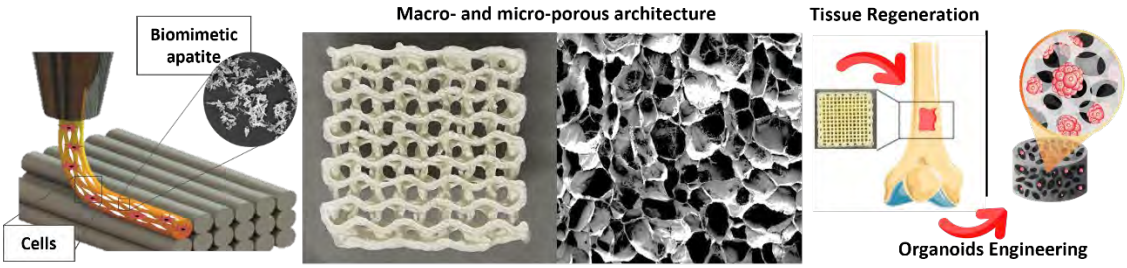

Conclusion

The 3D-printed scaffolds are validated, employing a dynamic in vitro setting where human bone marrow-derived mesenchymal stromal cells (hBM-MSCs) were cultured for 28 days. They maintained structural stability, supported homogeneous cell colonization, and promoted osteogenic differentiation, highlighted by ECM deposition and gene expression of osteogenic markers. Additionally, the printed constructs supported a second, more complex dynamic co-culture involving both osteoblast- and osteoclast-lineage cells. Without the addition of supraphysiological

stimulants, the scaffold sustained osteoclastogenesis via osteoblast-mediated signaling, demonstrating the matrix's capacity to support key elements of bone remodeling under physiological conditions

References

Campodoni E., Mazzoleni A., Montanari M., Vicinelli G., Possetti V., Inforzato A., Martin I., Muraro M.G., Sandri M. Injectable nanocomposite biomaterial for 3D printing of personalized matrices and their use in bioreactors for bioengineering advanced cell culture models. *ACS Applied Materials & Interfaces* (2025), 17, 68440-68456

S2 – O5

AddGraft: A biocompatible and versatile additive for light-based 3D patterning within crosslinked hydrogel networks.

Falandt M.[1], Bonhomme C.[1], Florczak S.[1], Vermonden T.[2], Bernal P.N.[1,3], Levato R.[1,3]
[1]Dept. of Clinical Sciences, Faculty of Veterinary Medicine, Utrecht University; [2]Division of Pharmaceutics, Faculty of Sciences, Utrecht University; [3]Dept. of Orthopedics, University Medical Center Utrecht, Utrecht, The Netherlands

Introduction

Replicating the time-dependent changes in the physicochemical microenvironment of native tissues remains a key challenge in biofabrication. While 3D bioprinting enables the creation of complex cell-laden architectures, the resulting constructs are mostly static. New strategies, like photo-grafting, can introduce spatiotemporal modifications in a contact-less manner, but often rely on specific chemistries, requiring complex synthetic steps and optimization for new materials.

Aim

In this study, we propose an off-the-shelf biocompatible additive, AddGraft, enabling post-gelation modification via thiol-ene click chemistry into any acrylated network. AddGraft's compatibility with volumetric bioprinting allows for tomographic light patterns-driven freedom of design for distributing grafted molecules across a wide range of biomaterials.

Materials and Methods

AddGraft was synthesized as a heterobifunctional polyethylene glycol (PEG) with an acrylate and a norbornene group. AddGraft was incorporated in different concentrations into gelatin methacryloyl (GelMA), alginate methacryloyl (AlgMA), and PEG diacrylate (PEGDA). The hydrogels were crosslinked with lithium phenyl(2,4,6-trimethylbenzoyl)phosphinate (LAP) as photoinitiator. Before photo-grafting, the constructs are infused with LAP and either thiolated crosslinkers, such as 8-arms-PEG_{10kDa}-SH, to induce matrix stiffening, or thiolated fluorescent probes, like SH-PEG_{5kDa}-Cy3, to assess 3D photo-grafting. A second volumetric printing step enables spatiotemporal stiffening or patterning of the hydrogels. Compression testing was performed to assess the stiffening, and the fluorescent patterning was evaluated through lightsheet microscopy. Finally, human mesenchymal stem cells (hMSCs) were encapsulated in the gels, and their viability, metabolic activity, and morphology were compared pre-and post-photografting.

Results

The incorporation of the additive into GelMA did not affect bulk stiffness, crosslinking kinetics, or physical properties, and maintained a high hMSCs viability (>95%). Up to a 3-time fold increase in the stiffness of AddGraft-containing GelMA hydrogels was observed upon grafting different thiol crosslinkers. Volumetric photografting enabled high-resolution patterning of fluorescent molecules (60.8±13.4 µm features), including grafting of multiple compounds. Grafting density is light-dose dependent, enabling the formation of gradients upon greyscale illumination. Comparable results were achieved when using AlgMA and PEGDA with incorporated AddGraft. Finally, encapsulated hMSCs exhibited high viability post-stiffening (>85%) and significant changes in morphology and circularity.

Conclusion

AddGraft provides a versatile and biocompatible strategy for on-demand spatiotemporal modifications of acrylated hydrogels. This control over the hydrogels' properties over time allows for studying specific cells' behavior. Its compatibility with light-based biofabrication techniques, such as volumetric printing, and widely used acrylate-based hydrogels, positions AddGraft as a powerful tool for 4D bioprinting strategies, with a strong potential in regenerative medicine and relevant *in vitro* modelling.

S2 – O6

Self-Rolling Vascular Scaffolds Fabricated via Combined Melt Electrowriting and Melt Electrospinning

Piontek A.[1], Gaspar Gonçalves Fernandes M. [2], Włodarczyk-Biegun M.K.[1,2]
[1]Biotechnology Center, The Silesian University of Technology, Gliwice, Poland; [2]Zernike Institute for Advanced Materials, University of Groningen, Groningen, The Netherlands

Introduction

Self-rolling is a promising strategy for producing tubular structures from planar sheets via externally applied, controlled stimuli. Melt electrowriting (MEW) and melt electrospinning (MES) are advanced additive manufacturing techniques that enable the creation of fine fibers from polymer melt under the influence of an electric field. While MEW allows precise and controlled fiber deposition, MES produces dense and randomly oriented fibrous structures. In this research, these two approaches were combined within a single fabrication process to create multimaterial self-rolling scaffolds for vascular tissue engineering.

Materials and Methods

Two types of poly(ethylene oxide terephthalate)/poly(butylene terephthalate) (PEOT-PBT) block copolymers with different swelling properties were used. First, two layers of parallel fibers made of a more hydrophobic material (PEOT-PBT300) were fabricated using the MEW technique (BioScaffolder 3.3, GeSiM). Subsequently, a more hydrophilic polymer (PEOT-PBT1000) was deposited on top using MES to produce dense structure. The ratio of the two materials in the structure was adjusted, and the fabrication parameters for each technique were optimized. Planar scaffold microstructure was characterized using optical microscopy and scanning electron microscopy (SEM). The self-rolling behavior was evaluated by placing the scaffolds in phosphate-buffered saline (PBS). The microstructure of the self-rolled scaffolds was examined by cryogenic SEM (cryoSEM). Mechanical properties of the tubular scaffolds were assessed through tensile testing. Endothelial cell studies were conducted to evaluate cell adhesion and distribution within the tubular scaffolds.

Results

Differences in swelling behavior between the two materials induced self-rolling of the constructs, resulting in tubular structures with a central lumen of 800 µm. The external and internal tube diameters could be tuned by adjusting the material ratio and scaffold dimensions before rolling. MEW fibers guided the rolling direction, while the MES layer provided a microenvironment favorable for endothelial cell attachment and monolayer formation, mimicking the structure of native blood vessels.

Conclusion

The conducted research demonstrates the successful integration of two materials and two fabrication techniques within a single process to produce self-rolling tubular scaffolds. Such structures show potential as functional and patient-specific grafts for vascular tissue engineering.

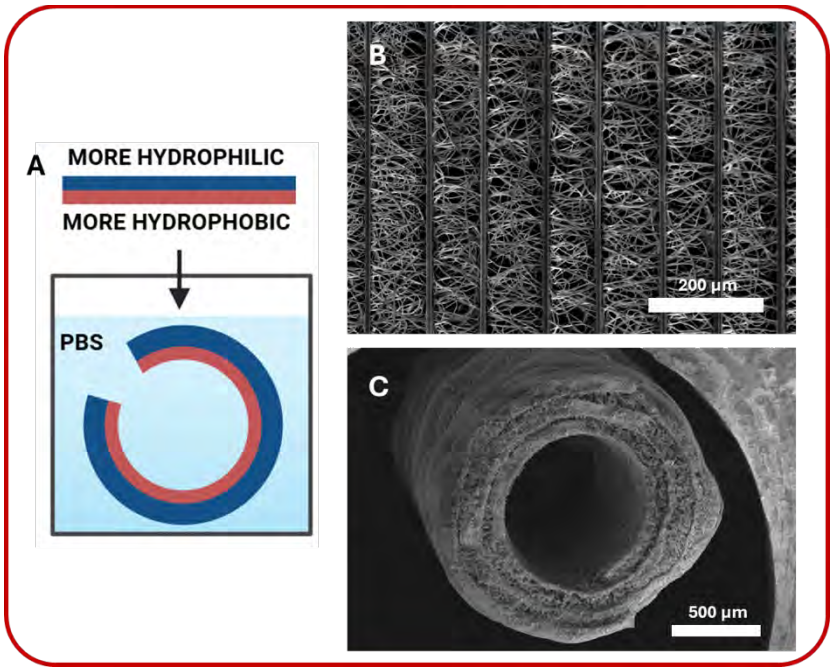

Figure 1. A. Mechanism of self-rolling of scaffolds in a wet environment. B. SEM image of scaffold's microstructure before rolling. C. Cryo-SEM image of self-rolled tubular scaffold.

S2 – PO7

Recombinant spider silk-enriched alginate scaffolds for long-term bovine mesenchymal stem cell expansion

Cohen S[1], Rottenberg Fromm M[1], Sklan E[2], Tavor Re'em T[1]
[1]Dept. of Pharmaceutical Engineering, Azrieli College of Engineering, Jerusalem, Israel; [2]Seevix Material Sciences Ltd., Hadassah Ein-Karem Jerusalem, Israel

Introduction

Harnessing the potential of bovine mesenchymal stem cells (bMSCs) for cultured meat production requires the design of new scaffolds that support cell growth and tissue formation. Alginate, a biocompatible polysaccharide, is commonly used for scaffolding due to its biocompatibility and ability to mimic the extracellular matrix. However, it has limited mechanical properties, such as strength and stability. Recombinant spider silk biopolymer (SVX, Seevix) is biocompatible, highly porous, and has previously been shown to enhance alginate bioinks for cell bioprinting, due to its strength and elasticity. This study aims to develop edible, alginate-based scaffolds for cultured meat by incorporating SVX particles to enhance mechanical properties and cell functionality.

Materials and Methods

SVX particles were produced using an E. coli expression system (Seevix). bMSCs were evaluated in a stepwise platform progression including spontaneously formed spheroids, bioprinted ring-shaped constructs, bulk edible alginate hydrogels, and macroporous freeze-dried edible scaffolds. Bioprinting was performed using the Allevi 2 bioprinter. Scaffold mechanical properties were evaluated using a tensiometer, while cell viability was assessed using a CellTiter-Glo assay. Large-scale edible scaffolds with an approximate diameter of 5 cm were fabricated, and cell distribution was assessed by spatial biopsies.

Results

SVX supplementation (0.02%) supported viable bMSC spheroid formation, improved long-term viability in bioprinted ring constructs (Figure 1 A), and enhanced the mechanical performance of both research-grade and food-grade alginate hydrogels. In 1.5 cm-diameter freeze-dried macroporous scaffolds, cultured for 29 days, SVX-alginate demonstrated improved long-term cell viability (Figure 1 B-C). The large-scale edible scaffold remained culture-compatible for more than 31 days and achieved an approximately 19-fold expansion, with an estimated final yield of approximately 3.16 × 10^7 viable cells per scaffold based on five spatial biopsies used to assess uniformity.

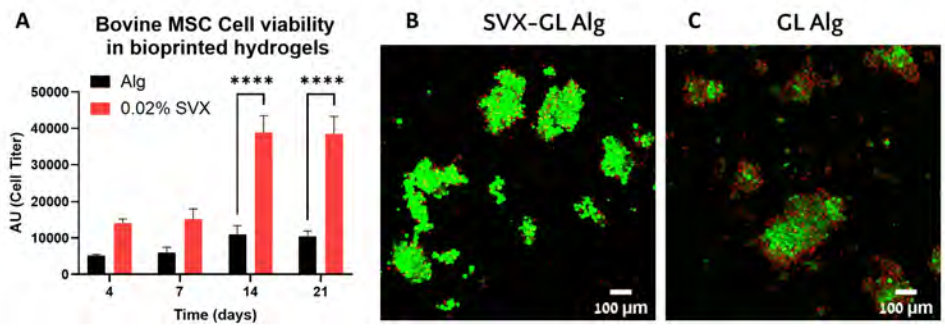

Figure 1: Enhanced bMSC cell viability in SVX-enriched alginate models in bioprinted models, assessed by CellTiter-Glo (A), and in SVX-enriched edible GL alginate macroporous scaffolds, by confocal live/dead imaging on day 29 (Calcein-AM – green; propidium iodide – red)

Conclusion

These findings identify SVX-alginate as an edible, mechanically reinforced scaffold strategy for prolonged bMSC culture across scales. By improving both handling robustness and long-term cell support, this platform addresses practical bottlenecks in scalable 3D cultivated-meat manufacturing and highlights recombinant spider-silk-like particles as promising functional additives for next-generation food biomaterials.

Acknowledgements

We thank Dr. Sharon Shelezinger, the Hebrew University of Jerusalem, for providing the bMSCs, and the Israeli Cultivated Meat Consortium, and the Azrieli College of Engineering, Jerusalem for their financial support.

S3
4D tissue engineering widening the control over cell's microenvironment

S3 - K1
Engineering mechanical heterogeneity in 3D cell environments with light

Castilho M.[1]
[1]Biomaterials Engineering and Biofabrication, Biomedical engineering Dept., Eindhoven University of Technology, Eindhoven, The Netherlands

Our tissues are multi-component, highly organized structures that perform specialized and coordinated functions to maintain the body's overall physiology. Tissues such as bone can naturally remodel and repair small defects, but when their function becomes irreversibly impaired, regenerative medicine seeks to restore it by delivering engineered cells, tissues, or organs. Stem cells play a central role in this context because of their immunomodulatory potential, broad differentiation capacity, and sensitivity to mechanical cues. Because stem cells are furthermore mechanosensitive, one approach of regenerative medicine is to carefully guide their behavior with controlled mechanical cues. In native tissues, mechanical signals are both spatially and temporally dynamic, yet it remains unclear to what extent this mechanical heterogeneity must be replicated in engineered environments to guide stem cell fate effectively. Controlling and analyzing such cues in three dimensions remains a significant challenge. Current biomaterial fabrication technologies—including 2D lithographic methods, multiphoton lithography, and conventional volumetric printing—offer great promise as they can introduce spatial patterns but cannot encode mechanical heterogeneity with true 3D freedom. Similarly, available characterization tools provide limited ability to map evolving mechanical properties at high spatial resolution.
This lecture explores how controlled mechanical heterogeneity can be implemented in 3D tissue models. Particularly it introduce a novel grayscale light-sheet volumetric bioprinting approach that enables fully 3D control of biomaterial mechanical heterogeneity, and demonstrate how non-destructive Brillouin microscopy can monitor the evolution of local mechanical properties over time. Together, these advances open new directions for precisely steering cell and organoid behavior and for studying mechanical cell–matrix interactions, providing powerful tools for mechanobiology and ultimately enabling functional tissue regeneration.

S3 – O1

Chemical 4D reconstruction of extracellular matrices using ion-pair-engineered click hydrogels

Tera M.[1*], Fukue R.[1], Shimada K.[1], Hosokawa K.[1]
[1]Graduate School of Technology, Tokyo University of Agriculture and Technology, Tokyo, Japan

Introduction

Engineering synthetic extracellular matrices (ECMs) that dynamically regulate cellular microenvironments remains a central challenge in biomaterials science. Although many hydrogel systems allow control of mechanical or biochemical properties during gel formation, post-gelation reconstruction of ECM architectures in space and time remains difficult. Here we report a modular click-hydrogel platform based on strain-promoted azide–alkyne cycloaddition (SPAAC) between azide-modified hyaluronic acid (HA–N_3) and ion-pair-engineered water-soluble dibenzo-cyclooctadiyne crosslinkers (WS-CODYs), enabling independent control of gel mechanics, biochemical ligand presentation, and post-gelation structural reconstruction (**Figure 1**).

Materials and Methods

Click hydrogels were prepared by mixing HA–N_3 (0.75 wt%) with WS-CODY crosslinkers in PBS under physiological conditions. The polarity of WS-CODY side chains was designed to regulate electrostatic interactions with the HA backbone, enabling predictable modulation of hydrogel network formation and mechanical stiffness. Cell encapsulation experiments were performed using multiple mammalian cell types including C2C12, HDF, HUVEC, PC-9, and HL-60 cells. Bioactive ligands were introduced via azide-modified RGD peptides incorporated through SPAAC during gel formation. Sequential gel–gel attachment and injectable gel-in-gel assembly were used to generate spatially heterogeneous hydrogel architectures.

Results

Ion-pair-engineered WS-CODY crosslinkers enabled ultrafast gelation and hydrogel formation at polymer concentrations below 1 wt%, producing injectable matrices with tunable stiffness. The click gels supported cytocompatible encapsulation of diverse cell types with >90% viability. Incorporation of RGD peptides restored integrin-mediated adhesion and induced differentiation of C2C12 myoblasts into multinucleated myotubes. Matrix stiffness further modulated cell morphology independently of ligand density, demonstrating orthogonal control of mechanical and biochemical cues. Sequential injection of HUVEC-containing click-gel precursor into fibroblast-conditioned click gel after 3 days of HDF culture resulted in rapid endothelial network expansion within 24 h (**Figure 1**). Residual azide groups within the network also enabled sequential covalent attachment of hydrogel modules, allowing post-gelation reconstruction of ECM architectures.

Conclusion

This ion-pair-engineered click-hydrogel platform enables chemical 4D reconstruction of extracellular matrices, allowing independent and dynamic control of mechanical, biochemical, and structural modalities. The approach provides a versatile strategy for constructing programmable biomaterials for tissue engineering, regenerative medicine, and advanced 3D cell culture models.

This research is supported by KAKENHI (23K17989 to M.T.), Terumo Foundation, and Fuji Seal Foundation.

References

[1]Tera M., Harati-Taji Z., Luedtke N.W. Intercalation-enhanced “Click” Crosslinking of DNA. *Angew. Chem. Int. Ed.,* 2018; 57; 15405-15409.

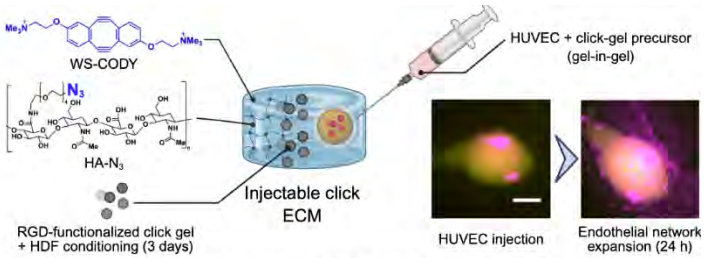

Figure 1. Injectable click ECM enables gel-in-gel vascular reconstruction.
WS-CODY crosslinkers react with azide-modified hyaluronic acid (HA–N_3) via SPAAC to form an injectable click hydrogel. HDF are cultured in RGD-functionalized click gels for 3 days to establish a fibroblast-conditioned matrix. HUVECs are then injected together with click-gel precursor to generate a gel-in-gel architecture, leading to rapid endothelial network expansion within 24 h. Scale bar = 1 mm

S3 – O2

Mechanistic modelling and experimental validation of a biocompatible and biodegradable 3D IPMC actuator

Murray R. T.[1], Burgess M. K.[1], Nair M.[1]
[1]Institute of Biomedical Engineering, Dept. of Engineering Science, University of Oxford, Oxford, UK

Introduction

Ionic polymer–metal composites (IPMCs) have been extensively investigated for applications in drug delivery, self-powered wearables, and soft robotics. However, clinical translation remains limited. Major barriers include non-biodegradable materials that can release toxic byproducts. Furthermore, fabrication methods are typically limited to thin-film geometries.

Aim

This work aims to develop a biodegradable and biocompatible 3D IPMC actuator, to validate its electromechanical performance under enzymatic degradation, and to validate a continuum-mechanics model of actuation to expand the biomedical applicability of IPMCs.

Materials and Methods

A continuum-mechanics model coupling ion transport (Poisson-Nernst-Planck), fluid flow (Darcy) and structural mechanics (poroelasticity) was developed to predict the actuation of porous IPMCs. For validation, biodegradable three-dimensional extracellular matrix (ECM)-based ionic polymer scaffolds were fabricated by producing a suspension of 1 w/w% collagen, 0.5 w/w% elastin and 1 w/w% taurine in 0.05 M acetic acid, frozen at -70°C and dried at 0°C, 0.53 mbar for 26 hr. Scaffolds with and without taurine were crosslinked with 200% genipin in sodium phosphate buffer for 24 hours, followed by sputter coating of thin gold electrodes to form an IPMC. Samples were subject to enzymatic degradation (10 U/ml, 7 days, 37 °C) and assessed for changes to microstructure (microCT) and deflection under an applied electric field at discrete time points.

Results

Taurine functionalisation to produce ECM-based 3D IPMCs (CETG) resulted in enhanced ion-driven actuation alongside increased enzymatic degradation rates. Progressive mass loss of CETG confirms biodegradability under physiological conditions, with uncrosslinked CE degrading most rapidly and genipin-crosslinked CEG retaining 73% of its mass at Day 7 (Fig. 1). The steady-state electromechanical responses observed experimentally were quantitatively reproduced by the coupled multiphysics model (Fig. 2).

Conclusion

This work demonstrates the feasibility of fabricating three-dimensional biodegradable and biocompatible IPMCs for active biomedical applications. Our multiphysics continuum-mechanics model was experimentally validated to capture degradation-coupled electromechanial behaviour accurately, providing a predictive framework to aid the design of 4D biomaterials devices.

Acknowledgements

This work was supported by the Engineering and Physical Sciences Research Council (EP/Y004434/1, EP/W524311/1).

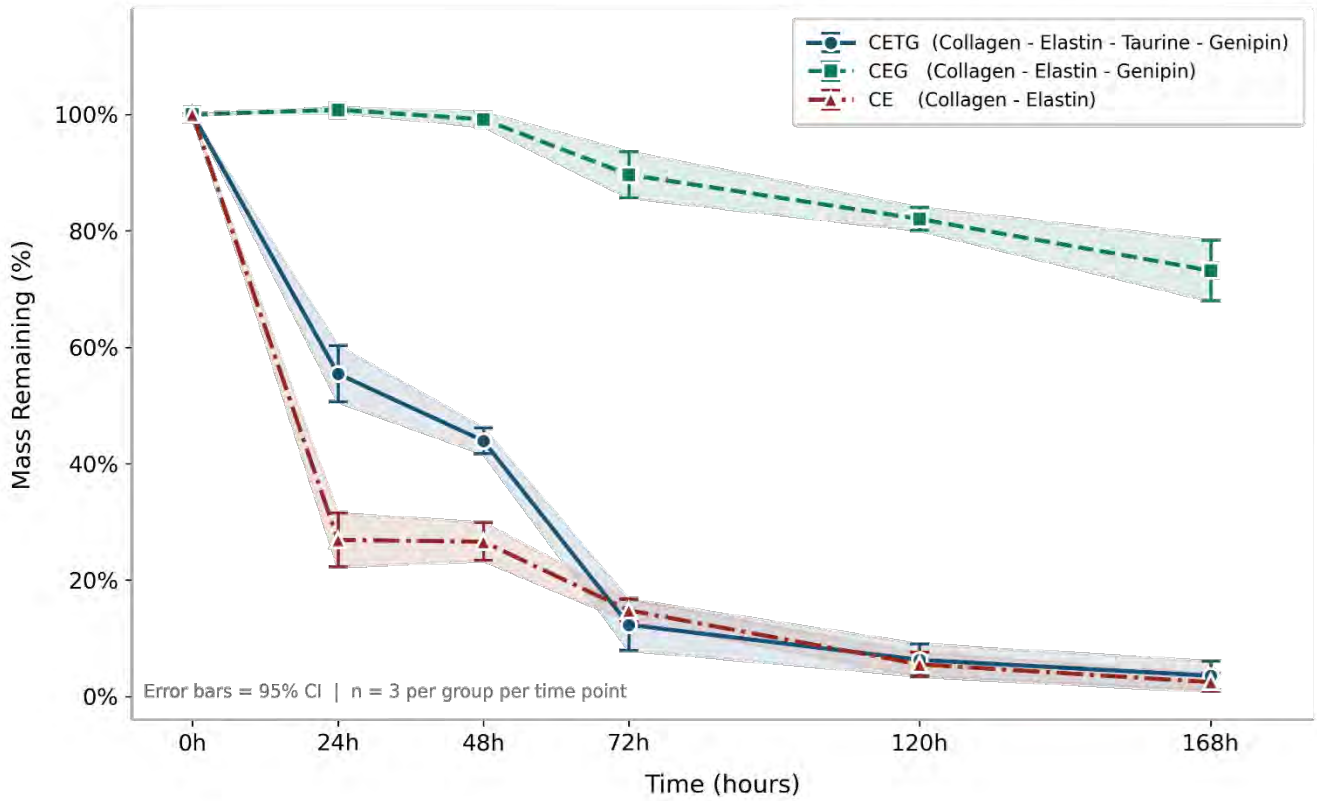

Figure 1 IPMC Enzymatic Degradation study with collagenase Type I 10U/ml at 37 °C for the 3 groups of samples.

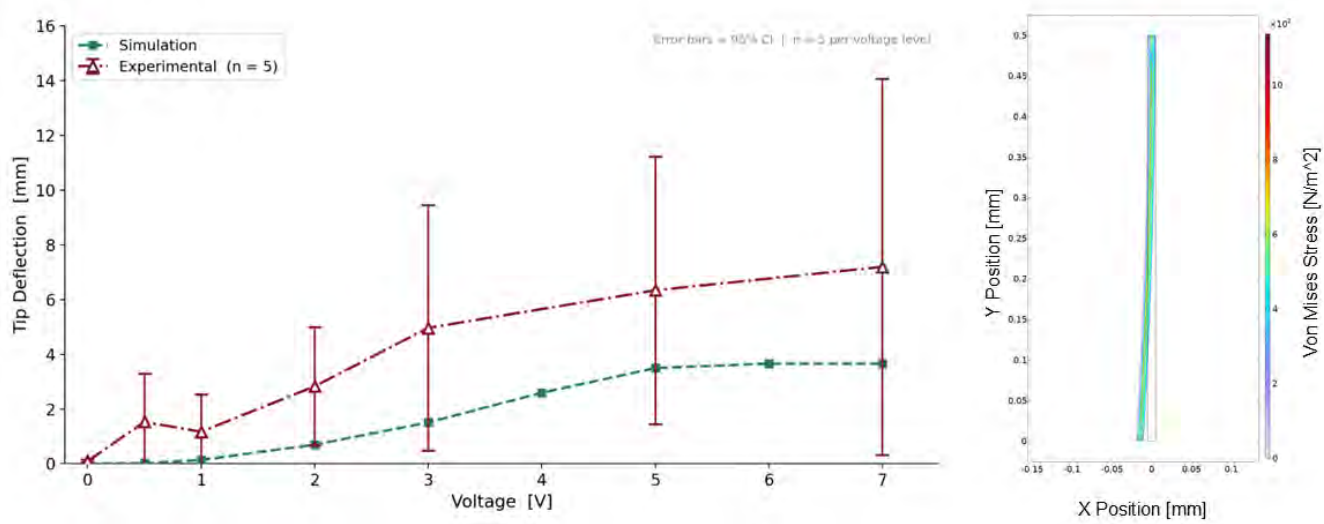

Figure 2. (Left) Steady-state IPMC tip deflections (0-7 V). (Right) von Mises stress distribution in an undegraded IPMC segment.

S3 – O3

Biocompatibility and precision in xolography-baed bioprinting: Validation of new additives across broad range of cell types

König N F[1], Brauer E[2], Garmshausen Y[1], Leonhard J[1], Madalo L[1], Lima L V[1], Roychoudhury A[1]
[1]xolo GmbH, Volmerstrasse 9B; [2]Institute of Chemistry, Humboldt-Universität zu Berlin, Berlin, Germany

Introduction

Xolography is a scalable volumetric 3D printing method enabling high-resolution fabrication of complex hydrogel structures. Its adaptation to opens new avenues for tissue engineering and regenerative medicine, although standard bioresins like GelMA face reactivity limitations.

Aim

This study aims to optimize bioresins for rapid, high-resolution Xolographic volumetric bioprinting of cell-laden constructs.

Materials and Methods

We present a novel dual-color photoinitiator and newly designed additives compatible with iodixanol-based GelMA formulations, enabling high-precision bioprinting at cell densities exceeding 20 million cells/mL. A theoretical model supports refractive index tuning to optimize light confinement and polymerization kinetics.

Results

Constructs larger than 1 cm^3 were printed in under three minutes using the Xube² system, achieving fine structural resolution and >95% cell viability.

Conclusion

These findings establish Xolography as a robust light-based 3D printing platform for fast, accurate, and cytocompatible volumetric bioprinting, across various cell types.

S3 – O4

Engineered mechanical heterogeneity through light-sheet grayscale volumetric bioprinting enables spatial and temporal control of cellular fate

Stoecker L.[1], Van Hattem T.C.[1], Oliva M.A.G[2], Albertazzi L[1], Salmeron-Sanchez M.[2], Castilho M.[1]
[1]Dept. of Biomedical Engineering, Eindhoven University of Technology, Eindhoven, The Netherlands; [2]Institute for Bioengineering of Catalonia, Barcelona, Spain;

Introduction

Traditional biomaterials support long-term cell survival but typically are unable to provide the dynamic mechanical cues, particularly (visco)elasticity, that guide cell fate and tissue development. However, current biomaterial manufacturing methods offer limited control over mechanical heterogeneity in 3D and lack tools to analyse these properties with high spatial resolution. To address this, we introduce grayscaled light sheet volumetric bioprinting [3] to achieve microscale, fully 3D spatial control of mechanical properties through grayscale-modulated light exposure.

Aim

Using this approach, we aimed to achieve spatially defined and spheroid-position-driven (visco)elastic patterning, hypothesizing that grayscale-modulated crosslinking could regulate human mesenchymal stem differentiation via local mechanical cues and that Brillouin microscopy could track the spatiotemporal evolution of these properties.

Materials and Methods

Grayscaled light-sheet volumetric printing was used to create cell-laden gelatin methacryloyl-based hydrogels with controlled heterogeneous (visco)elasticity in the Pa to lower kPa range. Brillouin microscopy tracked (visco)elastic evolution at day 3, 6, and 20. Fate commitment was assessed by immunofluorescence. Nanoindentation measurements were conducted as a reference for obtained Brillouin shifts. To enable cell-position-driven print design, an in-situ microscope was developed to map spheroid positions in 3D, which were used to generate customized encapsulation geometries and (visco)elastic-patterned microenvironments.

Results

Printed cellular environments with mechanical heterogeneity (Fig 1.) showed Brillouin shifts between 6.25±0.01 and 6.28±0.01 GHz, corresponding to elasticities of 0.2–2.0 kPa for softer and stiffer regions, respectively. Mechanical control was possible down to a length scale of 60 µm in cell-free and laden hydrogels. Differences in the 3D mechanical environment affected cellular behavior. Under dual osteogenic/adipogenic supplementation, stiff zones showed increased calcium accumulation, indicative of osteogenic commitment. Stiffness-patterned microenvironments, adaptively defined by spheroid position, modulated spheroid outgrowth within the soft environment.

Conclusion

The herein introduced combination of grayscale Xolography for spatially and cell-position-driven controlled elasticity and Brillouin microscopy for spatiotemporal analysis of cell-material interactions, together with integrated in-situ microscopy for spheroid-aware fabrication of stiffness-patterned microenvironments, offers a unique platform opening new avenues for adaptive mechanobiological studies in 3D.

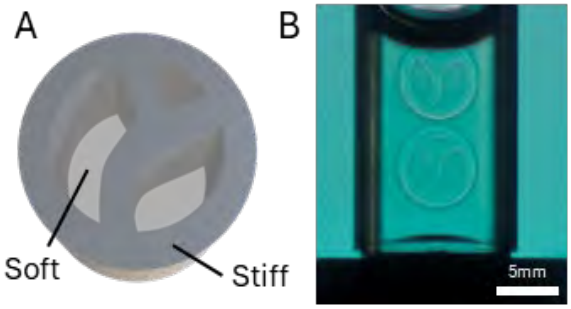

Figure 1. Grayscaled xolography print of a simplified trabecular structure. A) CAD model showing spatially defined stiff and soft regions. B) Schlieren image of the printed construct in a cuvette.

Acknowledgements
All authors acknowledge funding from the Institute for Complex Molecular Systems and the Dutch Ministry of Education, Culture, and Science, Gravitation program 024.003.013 (Materials Driven Re-generation).

References

[1] Saraswathibhatla A., Indana D., Chaudhuri O. Cell-extracellular matrix mechanotransduction in 3D. *Nature Reviews Molecular Cell Biology* 2023; 24; 495-516.

[2] Stoecker L., Cedillo-Servin G., König N.F., de Graaf F.V., García-Jiménez M., Hofmann S., Ito K., Wentzel A.S., Castilho M. Xolography for Biomedical Applications: Dual-Color Light-Sheet Printing of Hydrogels With Local Control Over Shape and Stiffness. *Advanced Materials* 2025; 37(10);

S3 – O5

A delayed dissolution, digital light processing bioprinting approach towards vascularized osteogenesis

Parmentier L.[1], Van Damme L.[1], Pien N.[1], Lim K. S.[2], Van Vlierberghe S.[1]
[1]Polymer Chemistry and Biomaterials group, Centre of Macromolecular Chemistry, Dept. of Organic and Macromolecular Chemistry, Ghent University, Ghent, Belgium; [2]Light-Activated Biomaterials Group, Charles Perkins Centre, School of Medical Sciences, University of Sydney, Sydney, Australia

Introduction

Vascularization remains a critical limitation in large-scale bone tissue engineering, restricting nutrient delivery, osteogenic maturation, and clinical translation of grafts. Achieving precise spatiotemporal control over vascular network formation is therefore essential. Digital light processing (DLP) bioprinting provides high spatial resolution, while delayed dissolution (DD) bioresins offer temporal control over channel formation. Combining these approaches has the potential to guide both angiogenesis and osteogenesis within engineered constructs.

Aim

This study aimed to optimize delayed dissolution bioresins for DLP bioprinting and subsequent embedding within a 5 w/v% GelNBNBSH hydrogel (norbornene-norbornene-modified gelatin crosslinked with thiolated gelatin) to maximize vascularized osteogenesis.[1,2]

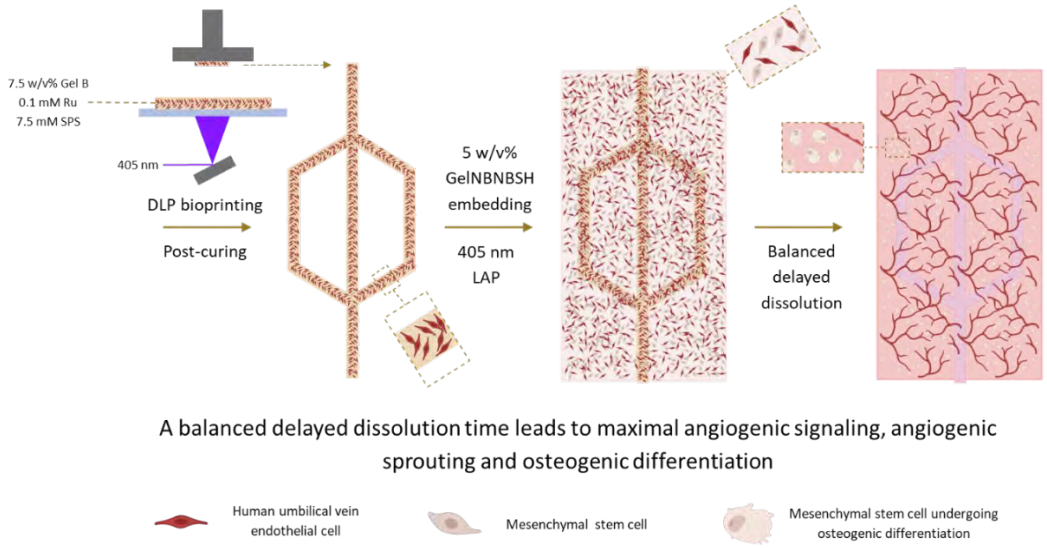

Materials and Methods

Constructs were bioprinted via DLP and embedded in 5 w/v% GelNBNBSH hydrogels using specific light wavelengths (315–525 nm) to achieve distinct delayed dissolution times (DD-2, DD-6, DD-11). HUVECs and MSCs (1.25:1.25 × 10^6 cells/mL) were co-cultured in the hydrogel. Angiogenesis and osteogenesis were assessed by signaling at day 7, network formation at day 14, ALP activity at days 7 and 14, and calcium deposition at day 21.

Results and Discussion

Modulation of bioresin composition and embedding conditions enabled tuning of delayed dissolution times, producing DD-2 (2 ± 1 days), DD-6 (6 ± 2 days), and DD-11 (11 ± 2 days). Constructs with an intermediate delayed dissolution time (DD-6, 5 w/v% GelNBNBSH, 0.18 mM LAP, 405 nm UV-A) exhibited the highest angiogenic signaling at 7 days and network formation by 14 days. Incorporation of a co-culture (HUVEC:MSC, 1.25:1.25 million cells/ml) further enhanced vascular network formation, eliminating the need for exogenous biochemical cues. Enhanced angiogenesis directly supported osteogenic maturation, as reflected by elevated ALP activity at 7 and 14 days and increased calcium deposition by 21 days.

The intermediate delayed dissolution provides an optimal balance between channel stability and timely cell infiltration, highlighting the critical role of temporal control in guiding vascularized osteogenesis. Co-culturing HUVECs and MSCs synergized with delayed dissolution, demonstrating that the combination of spatial and temporal cues can outperform biochemical supplementation alone. These results underscore the importance of integrating precise spatiotemporal control in engineered constructs to achieve maximal angiogenic and osteogenic outcomes.

Conclusion

This approach provides a framework for incorporating spatiotemporal control in complex tissue-engineered grafts.

References

[1]Duquesne J., Parmentier L., Vermeersch E., Lemaire F., Won Seo J., Dmitriev R.I., Van Vlierberghe S. Volumetric bioprinting of the osteoid niche. *Biofabrication* 2025; 17; 2; 025002.

[2]Parmentier L., D'Haese S., Carpentier N., Dmitriev R.I., Van Vlierberghe S. Bottom-up extrusion-based biofabrication of the osteoid niche. *Macromolecular Bioscience* 2024; 24; 4; 2300395.

S3 – O6

Ice-templated IL-2 loaded collagen matrices mimic regulatory T cells tissue microenvironment

Bouabdallah M.[1,2], Dorgham K.[2], Haddouche A.[2], Hassan J.[2], Cretet-Rodeschini C.[2], Miyara M.[2,3], Trichet L.[1], Fernandes F.M.[1]

[1]Laboratoire de Chimie de la Matière Condensée de Paris, Sorbonne Université; [2]Centre d'Immunologie et des Maladies Infectieuses, Inserm; [3]Hôpital Pitié Salpêtrière, AP-HP, Paris, France

Introduction

Controlling the immune environment following material transplantation remains a major challenge for successful biointegration. Regulatory T cells (Tregs), a subset of CD4+ T cells, have emerged as pivotal mediators of tissue repair, yet the mechanisms governing their pro-regenerative functions remain unclear. Tregs exhibit phenotypic heterogeneity and can be subdivided into fractions based on stability, proliferation, and suppressive activity. Tissue Tregs, a subset residing in non-lymphoid tissues, have been recently highlighted for their active role in tissue repair. Deciphering the interplay between Tregs and their surrounding tissue microenvironment is thus central to developing effective pro-regenerative tissue engineering strategies. Given the essential role of interleukin-2 (IL-2) in Tregs' survival and expansion, IL-2–loaded materials mimicking the extracellular matrix (ECM) provide a unique approach to elucidate regenerative processes.

Materials and Methods

Type I collagen scaffolds were fabricated by ice-templating followed by topotactic fibrillogenesis to mimic the ECM architecture and mechanical properties. Different IL-2 doses were encapsulated within the collagen constructs by impregnation. CD4+ T cells, total CD25+FOXP3+ Tregs and naive CD25+FOXP3+CD45RA+ Tregs (nTregs) were cultured with IL2-loaded collagen constructs or with equivalent IL2 dose in the culture medium. Cell phenotype was characterized by regular and spectral flow cytometry and cell-material interactions were observed by confocal microscopy coupled to second harmonic generation.

Results

Our collagen matrices supported CD4+ T cells migration, even in the absence of IL-2. Intermediate amount of IL2 supported highest colonization of the materials surface by CD4+ T cells and total Tregs (Figure 1). Moreover, $CD4^+$ T-cell viability was favored for infiltrated cells under stringent conditions, as well as Treg survival under standard culture, compared to counterparts in suspension. Additionally, cultured nTregs showed higher expression of FOXP3*,* hallmark of Treg phenotype, among expanded CD4+ cells infiltrating the collagen matrices (Figure 2). Cultured nTregs also presented increased CD69 and PD-1 expression when in suspension around IL2 releasing materials, and even greater expression when infiltrating the materials, compared with controls. These markers are respectively involved in Tregs stability and activation, and are also considered as markers of tissue retention overexpressed in tissue Treg.

Conclusion

IL-2–enriched collagen matrices represent a promising tool to investigate immune signaling in regenerative medicine and an innovative platform for enhanced immune cell culture. This work paves the way to the development of biomimetic scaffolds for organ replacement while deepening our fundamental knowledge on pro-regenerative immune cues following organ transplantation.

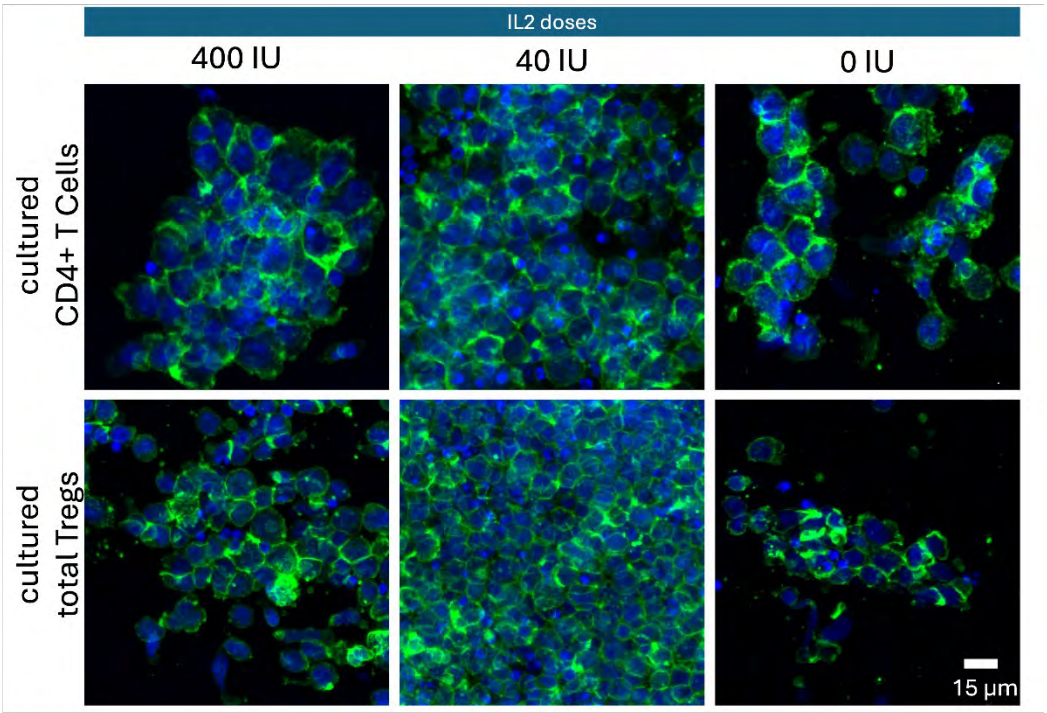

Figure 1. Confocal images of cultured T cells adhering on the collagen constructs after 6 days. (Actin= green, nuclei= blue, collagen= not shown)

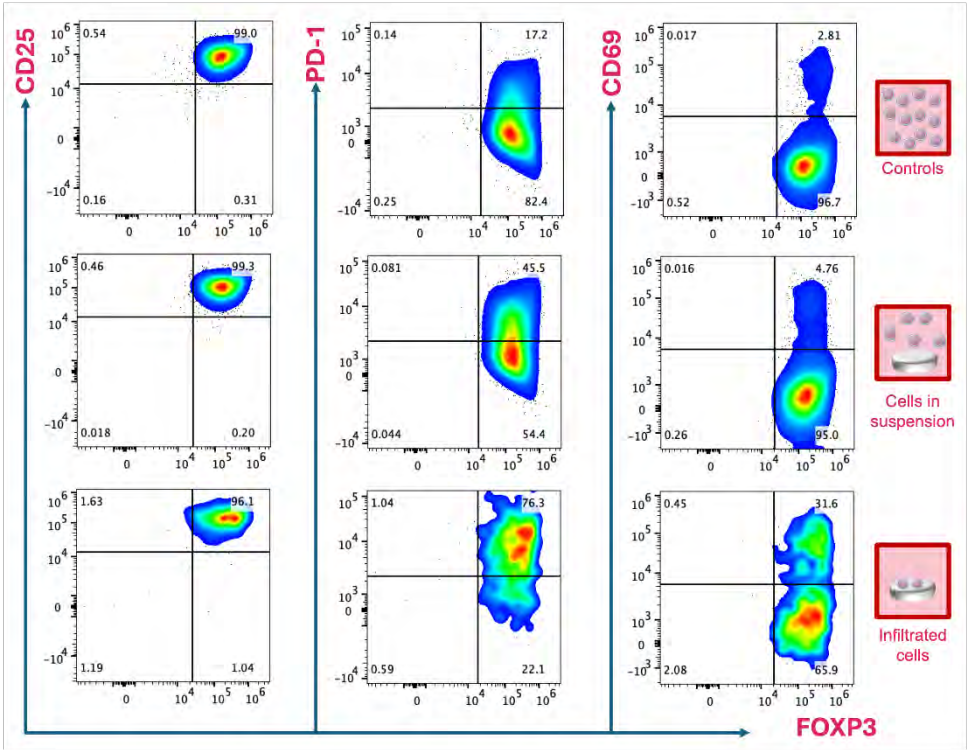

Figure 2. Co-expression of FOXP3 with CD25, PD-1 and CD69 within expanded nTregs after 6 days of culture. Materials were loaded with 40 IU of IL2 and controls correspond to equivalent IL2 dose supplemented in the medium.

S3 – O7

Design heterogeneous microenvironments via light-directed biochemical and mechanical patterning of ha hydrogels

Finne-Wistrand A.[1], Behroozi Kohlan T.[1], Kivijärvi T.[1]
[1]Dept. of Fibre and Polymer Technology, School of Engineering Sciences in Chemistry, Biotechnology and Health, KTH Royal Institute of Technology, Stockholm, Sweden

Introduction

The ability to control biochemical and mechanical cues within hydrogels with high spatial and temporal precision is central to designing microenvironments that mimic the complexity of native tissues. Light-responsive materials provide a powerful means to achieve this, enabling user-defined modification of chemical functionalities in three-dimensional networks. This research, which will be presented, focuses on developing hyaluronic acid (HA) hydrogels that can be photopatterned to locally regulate biochemical presentation and mechanical behaviour, thereby expanding the design space for advanced biomaterials and mechanobiological studies.

Aim

The overarching aim was to create light-responsive HA hydrogels in which (1) biochemical cues can be selectively introduced and released in predefined time and regions, and (2) mechanical properties can be adjusted locally through light-directed conversion of dynamic covalent crosslinks. Together, these strategies sought to develop versatile tools for constructing complex, heterogeneous microenvironments.

Materials and Methods

Coumarin-based photocages masking amine (Cou-DAB), hydrazine (Cou-Hyd), or hydroxylamine (Cou-Oxy) groups were synthesized via multi-step procedures and characterized by absorbance and fluorescence spectroscopy, hydrolytic stability testing, and uncaging kinetics using ^{1}H NMR. These photocages were grafted onto HA, which was subsequently crosslinked. Photophysical behavior of the polymer-conjugated photocages was assessed under one-photon (365 nm) and two-photon (760–800 nm) excitation. Mechanical photopatterning was implemented using HA modified with aldehyde groups, and HA modified with adipic acid dihydrazide (ADH) and Cou-Oxy (HA-ACOxy) to enable hydrazone-to-oxime conversion upon irradiation. Hydrogel properties were analyzed using swelling studies, FTIR, SEM, in situ photorheology, stress relaxation measurements, and confocal microscopy for region-specific patterning.

Results

The synthesized photocages exhibited distinct photochemical behavior, Cou-Oxy and Cou-Hyd uncaged rapidly, while Cou-DAB showed longer hydrolytic stability and photostability. After conjugation to HA, photocages retained photoactivity, allowing dose- and time-dependent liberation of reactive groups within hydrogels. Two-photon excitation enabled 3D patterning with resolutions of 10–100 µm.

In mechanical tuning studies, irradiation of HA-ACOxy-containing hydrogels released hydroxylamine, driving competitive oxime formation and replacing hydrazone bonds. This transition led to immediate increases in storage modulus and slower stress relaxation, with mechanical changes dependent on photocage loading and irradiation time. Region-specific irradiation produced localized photolysis and mechanical modification, confirmed by fluorescence tracking of irradiated versus non-irradiated regions.

Conclusion

This work demonstrates a robust strategy for photopatterning both biochemical and mechanical cues within HA hydrogels. By integrating photocaged reactive groups with dynamic covalent chemistry, these materials enable high-resolution spatial tuning of hydrogel microenvironments. The platform provides valuable tools for investigating cell-matrix interactions and designing next-generation biomaterials with programmable complexity.

Acknowledgements

The authors gratefully acknowledge financial support from the Swedish Research Council (2020-03427) and Sweden's Innovation Agency VINNOVA, through the AM4Life Competence Centre (contract number 2024-03847).

S4
Advancing biomaterials through biointerfacial reaction mechanisms

S4 - K1
Carbonated apatite as a platform for stem cell-based regenerative medicine

Ishikawa K.[1]
[1]Dept. of Biomaterials, Faculty of Dental Science, Kyushu University, Fukuoka, Japan

Carbonate apatite (CA) artificial bone
The inorganic component of bone is carbonate apatite (CA), not hydroxyapatite (HA), containing 9–12 mass% carbonate within the apatite structure. Although CA cannot be fabricated by sintering due to thermal decomposition, it can be produced via a dissolution–precipitation process using calcium carbonate as a precursor. CA artificial bone is currently used clinically in Japan, the United States, Malaysia, and Taiwan.
Unlike sintered HA, CA is resorbed by osteoclasts and replaced with new bone, and exhibits higher osteoconductivity than sintered HA, β-TCP, and bovine bone. CA honeycomb scaffolds form bone marrow–like tissue within their pores when placed on the rat cranium. At 12 weeks, histological features were comparable to femoral bone marrow. Hematopoietic stem cells were confirmed by $CD34^{+}$ staining and flow cytometry of $CD45^{-}CD34^{+}$ cells.

Restoration of hematopoietic stem cells (HSCs) function by carbonate apatite
Mice do not survive following bone marrow ablation. However, survival was achieved when CA honeycomb scaffolds, preconditioned on the calvarial bone of GFP-expressing rats, were subsequently implanted subcutaneously into bone marrow–ablated mice.
The intensity of GFP fluorescence in the mouse peripheral blood gradually increased after transplantation of the CA honeycomb scaffold. Essential immune cells for host defense, including monocytes, lymphocytes, T cells, B cells, and NK cells, were fully restored.
These findings indicate that CA honeycomb scaffolds are capable of forming hematopoietic stem cell niche units and that their transplantation restores hematopoietic and immune functions in immunocompromised mice to normal levels.

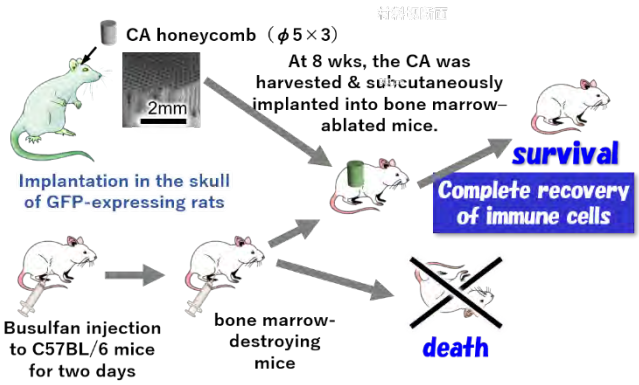

Regeneration of the osteochondral unit by carbonate apatite
Bone marrow contains not only hematopoietic stem cells but also mesenchymal stem cells (MSCs), which have the capacity to differentiate into chondrocytes. Therefore, porous CA was implanted into osteochondral defects in the femoral trochlea of rabbits to assess osteochondral unit regeneration.
At 4 weeks after implantation, new bone formed on the surface of the porous CA, and hyaline-like cartilage was observed. At 12 weeks after implantation, the porous CA was completely replaced with new bone.
These results suggest that porous CA has the capability to regenerate the osteochondral unit.

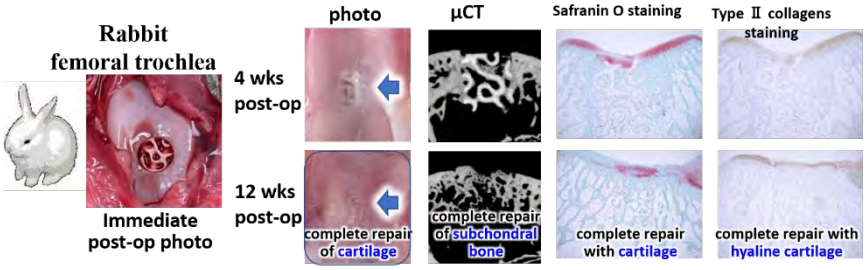

Conclusion

Carbonate apatite has strong potential as a platform material for stem cell–based regenerative medicine.

S4 – O1

Coupling-agent-free biofunctionalization of nitinol stent retrievers to enhance thrombus engagement in mechanical thrombectomy

Guyot D.[1,2,3], Kersani D.[1], Ho-Tin-Noe B.[2]
[1]Balt Extrusion, Research & Development – Biotechnology Division; [2]Inserm, U1144, Team 4; [3]CEA, Université Paris-Saclay, Paris, France

Introduction

Mechanical thrombectomy with stent retrievers is the standard treatment for ischemic stroke caused by large vessel occlusion. However, efficacy remains limited by insufficient device–thrombus interaction, leading to clot fragmentation, distal embolization, repeated retrieval attempts, and prolonged procedures associated with reduced first-pass recanalization and poorer outcomes[1]. Stroke thrombi exhibit substantial compositional variability, influencing device–thrombus interactions and retrieval performance. However, fibrin and neutrophil extracellular traps (NETs) are consistently present as major structural components[2]. Improving thrombus capture without altering device mechanics or endovascular practice remains a key challenge. Surface functionalization of stent retrievers is a promising strategy to enhance thrombus engagement while preserving established workflows.

Materials and Methods

A coupling-agent-free chemical activation strategy was developed to enable direct biomolecular grafting onto nitinol. Antibody immobilization was performed on full-scale nitinol discs and clinical stent retrievers. Functionalization was characterized using multi-scale, multi-technique quantitative and qualitative approaches combining fluorescence imaging, XPS, AFM and FTIR to assess grafting homogeneity and reproducibility across complex geometries. Mechanical robustness was evaluated under friction cycles, chemical exposure, and simulated thrombectomy conditions. Biological performance was assessed using in vitro thrombus models enriched in fibrin and NETs, and in a 3D neurovascular model mimicking realistic endovascular conditions.

Results

The strategy enabled reproducible and homogeneous antibody immobilization on flat nitinol substrates and complex geometries. Fluorescence analysis confirmed low inter-sample variability and strong retention of the grafted layer after mechanical stress, chemical exposure. Surface analyses (XPS, FTIR and AFM) confirmed protein immobilization, supporting a homogeneous organic layer. Functionalized surfaces showed increased thrombus binding compared with non-functionalized controls, with preferential interactions for fibrin- and NET-rich thrombi in vitro (Figure 1). The grafted layer remained mechanically stable in a 3D neurovascular model, supporting compatibility with clinical deployment and retrieval conditions (Figure 2).

Conclusion

This work demonstrates a robust coupling-agent-free surface engineering strategy for nitinol-based neurovascular devices that preserves mechanical integrity while enabling biologically active functionality. These results establish a robust framework for the future evaluation of biofunctionalized stent retrievers to enhance thrombus capture during mechanical thrombectomy.

Acknowledgements

This work was supported by Balt Extrusion and conducted within the RHU BOOSTER programme, in collaboration with Inserm and CEA.

References

[1]Koo A., et al. Impact of procedure time on first pass effect in mechanical thrombectomy for anterior circulation acute ischemic stroke. *Neurosurgery 2024;* 95(1) 128-136.
[2]Desilles J-P. et al. Composition and organization of acute ischemic stroke thrombus: implications for therapeutic strategies. *Front Neurol* 2022; 13:870331.

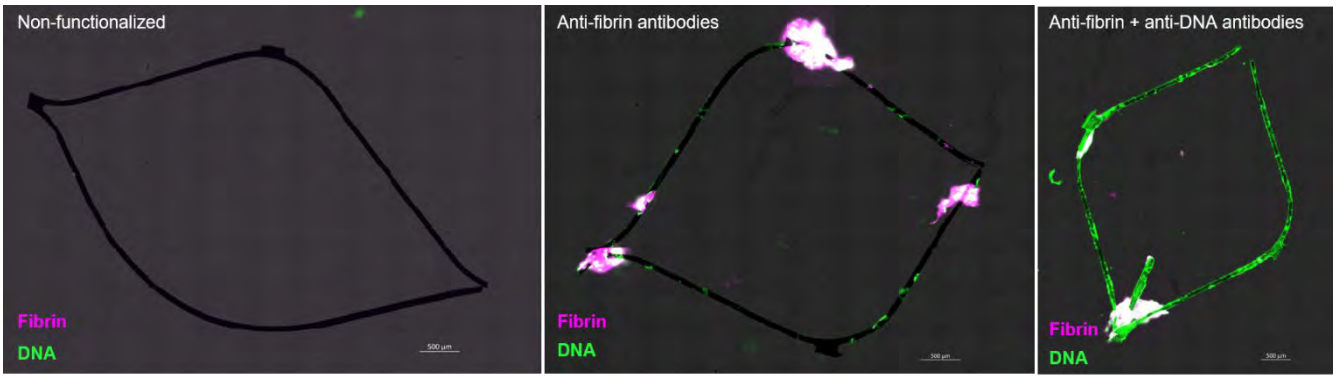

Figure 1: Interaction with fibrin-rich thrombi

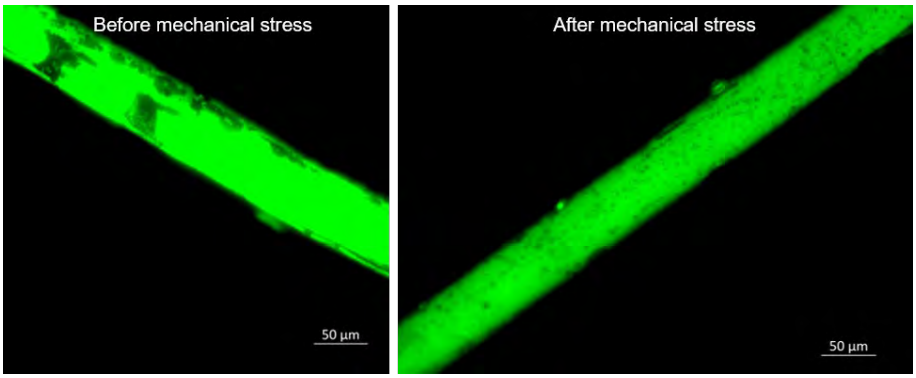

Figure 2: Coating is robust after mechanical stress.

S4 – O2

Effect of residual alumina particles after blasting on apatite formation and osteoblast activity on titanium surfaces

Ogura A.[1], Phuc T.M.L.[2], Gallab M.[3], Yamaguchi S.[3]
[1]Division of Functional Structure, Dept. of Morphological Biology, Fukuoka Dental College, Fukuoka, Japan; [2]Institute of Biology, Vietnam Academy of Science and Technology, Hanoi, Vietnam; [3]Dept. of Biomedical Sciences, College of Life and Health Sciences, Chubu University, Kasugai, Japan

Introduction

Various surface treatments of titanium (Ti) implants have been universally studied, seeking better osseointegration. Blasting/acid-etching is one of the popular surface modifications to enhance cell activity. We found a simple heat treatment following acid treatment provides a high apatite-formation capability, which may promote early bone bonding [1,2]. Although residual alumina from blasting media is often observed on Ti surfaces after treatment, it remains unclear how this residual alumina affects the apatite formation and cell activity of blast-treated Ti.

Aim

To investigate the effect of alumina residue on apatite formation and osteoblast activity after acid and heat treatment following blast treatment.

Materials and Methods

Pure Ti plates were blasted by alumina particles (425-600µm) at 500kPa and then subjected to an acid and heat treatment with the condition as previously reported [1,2]. The treated surfaces were soaked in simulated-body-fluid (SBF) for 3-28 days and their apatite formation was analyzed by SEM, XRD and EDX. Cell viability, alkaline phosphatase (ALP) activity, and mineralization ability (Alizarin Red; ARS) of MC3TC-E1 on the treated Ti and those formed with apatite by soaking in SBF were evaluated.

Results and Discussions

Ti samples after blasting exhibited surface roughness on the order of several-tens micrometer and a large amount of residual alumina particles (10-100µm). Most of the residual particles were found to be removed by the subsequent acid treatment while additional microscale texture was uniformly produced on the sample surfaces, which remained even after the heat treatment. When the acid-heat treated samples with or without blast treatment were soaked in SBF, apatite formation was observed on both surfaces within 3 days. However, apatite formation on the blast-acid-heat treated samples was delayed in regions where the large alumina particles had remained following the blasting treatment (Fig.1). This may be attributed to insufficient acid treatment caused by residual alumina particles. In the cell experiment, blast-treated samples exhibited lower ALP activity and ARS than untreated samples despite several-tens micrometer roughness that is preferential for cell activation. This is also probably due to the residual alumina particles. Subsequent acid treatment significantly increased ARS levels while restoring ALP activity compared to untreated samples. Both ARS and ALP were maintained after heat treatment and further increased when the surface was covered with apatite.

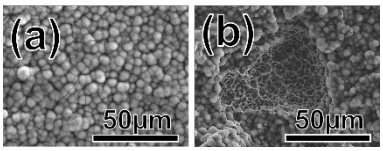

Fig.1 SEM images of the Ti surface (a)without or (b)with the blasting, followed by acid-heat treatment and soaking into SBF for 3 days.

Conclusion

Residual alumina after blasting gives negative effects on apatite formation and osteoblast differentiation. These effects can be improved by removing alumina residue by acid treatment and providing the capacity of apatite formation by heat treatment.

References

[1]T.Kawai, et al. Bone-bonding properties of Ti metal subjected to acid and heat treatments. *J Mater Sci Mater Med*. 2012;23:2981-2992.
[2]A.Ogura, et al. The effect of simple heat treatment on apatite formation on grit-blasted/acid-etched dental Ti implants already in clinical use. *J Biomed Mater Res.* 2021;1–11.

S4 – O3

Improving ion release properties of iodine-containing calcium-deficient calcium titanate for simultaneous osteogenesis and antibacterial activity

Yamaguchi S.[1]
[1]Dept. of Biomedical Sciences, College of Life and Health Sciences, Chubu University, Kasugai, Japan

Introduction

Titanium (Ti) implants, such as artificial hip joints and mandibular fixation plates, require both osteoconductivity and antibacterial activity to prevent loosening and infection. We previously demonstrated that both properties can be imparted to Ti without cytotoxicity by forming an iodine-containing calcium-deficient calcium titanate (I-CDCT) layer through NaOH–$CaCl_2$–heat–ICl_3 treatment[1]. The antibacterial activity depends on the amount of iodine ions released; however, the treated surface tends to exhibit burst release within the first day. Such an initial burst release should be suppressed to prevent infections over the medium to long term. This suppression could be achieved by densifying the characteristic three-dimensional network structure of I-CDCT.

Aim

To investigate the effects of coexisting ion species in the initial NaOH treatment on the nanoscale network structure. By controlling them, this study aims to elucidate a structure that exhibits controlled-release properties by regulating the initial ion release.

Materials and Methods

Ti plates were soaked in 5M NaOH solution with 9 types inorganic and organic additives including K, Cs, Ca, Ga, Tetramethylethylenediamine, and aceton at 60˚C for 3-24 h. The surfaces and cross sections of the treated samples were observed under SEM, EDX and Raman. Among the treated samples, those with a thickness of approximately 1 µm, comparable to the standard NaOH-treated sample, and possessing either dense or sparse network structures were selected and subjected to $CaCl_2$–Heat–ICl_3 treatment according to the previously reported method[1]. Iodine ion release from the sample into PBS was measured by ICP and their initial release ratio was evaluated using the cumulative release within the first 3 days as a reference.

Results and Discussions

The addition of Ca or K in the NaOH treatment resulted in dense or sparse network structure as shown in Fig.1. Other inorganic ions including Ga, Si Cs, Li and organic additives suppressed growth of titanate layer. The samples treated with 5M NaOH+0.3mM $Ca(OH)_2$ (noted as Na+Ca) and KOH for 3h were subjected to $CaCl_2$ treatment that completely replaced surface Na or K ions with 3.3% or 4.1%Ca that are similar to 3.7% Ca of NaOH-treated sample. Subsequent heat and ICl_3 treatment induced 0.7 and 2.0% iodine to Na+Ca and KOH samples, respectively, indicating different ion exchange capacity. In the Ion release tests, the Na+Ca sample reduced ion release ratio within 1 h by 12% compared with the NaOH-treated sample, whereas the KOH sample showed a 9% increase.

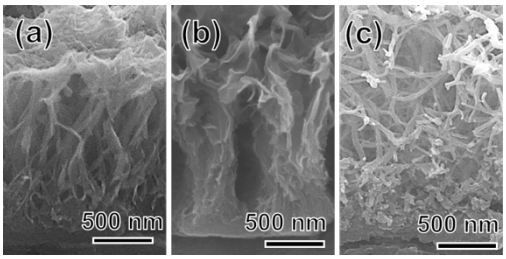

Cross sectional SEM images of (a) NaOH, (b) Na+Ca and (c) KOH samples.

Conclusion

The additives in the initial NaOH treatment affected a structure and ion exchange capacity of I-CDCT layer, which resulted in a significant influence on the release behavior of iodine ions. Na+Ca sample showed the densest structure that effectively suppressed ion release within the first hour.

References

[1]S Yamaguchi, et al. Iodine-Loaded Calcium Titanate for Bone Repair with Sustainable Antibacterial Activity Prepared by Solution and Heat Treatment *Nanomaterials*. 2021;11:2199.

S4 – O4

An extracellular matrix–based blood–brain barrier model for evaluating nanoplastic toxicity

Kobayashi M.[1], Zhao Y.[1], Washihira N.[1], Fujii S.[2], Tanabe T.[3], Kimura T.[4], Yamamoto M.[1]
[1]Dept. of Materials Processing, Graduate School of Engineering, Tohoku University, Sendai; [2]Dept. of Science, Faculty of Science, Yamagata University, Yamagata; [3]College of Engineering and Design, Shibaura Institute of Technology, Tokyo; [4]Dept. of Biomedical Engineering, Faculty of Life Sciences, Toyo University, Saitama, Japan

Introduction

In vitro blood–brain barrier (BBB) models are widely used to study substance transport across the BBB, which regulates exchange between the bloodstream and the central nervous system. Brain microvascular endothelial cells form tight junctions that restrict paracellular diffusion and control entry of compounds and nanoparticles. Conventional BBB models are typically constructed using collagen; however, they do not reproduce the extracellular environment of brain tissue. The extracellular matrix (ECM) regulates endothelial cell behavior and barrier formation. Decellularized extracellular matrix (dECM), derived from tissues after removal of cellular components, provides a biomimetic microenvironment that may better support BBB function. In this study, we developed a BBB model using brain-derived dECM combined with collagen and evaluated its response to oxidized low-density polyethylene (LDPE) nanoplastics (NPs).

Materials and Methods

Brain-derived dECM was prepared by high hydrostatic pressure decellularization and characterized by residual DNA and SDS–PAGE. A BBB model was constructed using ACBRI498 and hCMEC/D3 cells with hydrogel or thin-coating ECM pretreatments. Barrier integrity was evaluated by transendothelial electrical resistance (TEER), sodium fluorescein permeability, tight junction analysis, and P-glycoprotein (P-gp) activity. Oxidized LDPE nanoplastics were prepared using an advanced oxidation process. Particle size and morphology were analyzed by dynamic light scattering and scanning electron microscopy, and surface oxidation by X-ray photoelectron spectroscopy, Fourier-transform infrared spectroscopy, and zeta potential measurements. The BBB model was exposed to oxidized LDPE NPs.

Results

Hydrogel ECM pretreatment formed a thick matrix layer that hindered compact endothelial monolayer formation, whereas the thin-coating approach enabled stable barrier formation. dECM-coated membranes significantly improved cell adhesion and barrier function, as confirmed by lower sodium fluorescein permeability and a higher P-gp efflux ratio. In particular, brain-derived dECM combined with collagen produced a BBB model with higher TEER, lower permeability, and enhanced tight junction protein expression compared with conventional coatings.
Oxidized LDPE NPs (~460 nm, negatively charged) induced a transient decrease in TEER and increased permeability, which partially recovered over time. Morphological observations suggested membrane remodeling and particle aggregation near the cell surface.

Conclusion

Brain-derived dECM combined with collagen improved the structural and functional properties of the *in vitro* BBB model. The developed platform enabled evaluation of BBB responses to nanoplastics, demonstrating that oxidized LDPE NPs can transiently disrupt barrier integrity. These results suggest that the dECM-based BBB model is a useful tool for investigating the biological impact of nanoplastics on the BBB.

Acknowledgements

This work was supported by JST, CREST Grant Number JPMJCR21L6.

S4 – O5

Protein adsorption and macrophage responses for nanoparticles with different oxidation degrees

Yamamoto M.[1,2], Perez Arana S.[1], Washihira N.[1], Fujii S.[3], Tanabe T.[4], Kimura T.[5], Hirano A.[6], Kobayashi M.[1]
[1]Grad. Sch. Eng., Tohoku University, Sendai; [2]Grad. Sch. Biomed. Eng., Tohoku University, Sendai; [3]Fac. Sci., Yamagata University, Yamagata; [4]Fac. Design Eng., Shibaura Institute of Technology, Tokyo; [5]Fac. Life Sci., Toyo University, Saitama; [5]AIST, Tsukuba, Japan

Introduction

Protein adsorption has been widely demonstrated as a key factor governing the biointerface between cells and/or tissues and biomaterials. Surface properties, such as wettability, surface charges, chemical compositions, can influence protein adsorption behaviors, thereby modulating subsequent cellular interactions. The formation of a protein corona through protein adsorption on the surface of nanomaterials, such as carbon nanotubes, has been extensively investigated to understand their in vivo fate in blood circulation. More recently, nanoplastics (NPs), an emerging class of exogenous nanomaterials, have been detected in several organs in humans and are now recognized as a potential environmental threat to living organisms.

Aim

The objective of this study is to investigate the biointerface between macrophages and NPs with different oxidation degrees, focusing on how protein adsorption governs the formation of the protein corona and subsequently influences macrophage responses.

Materials and Methods

NPs with different oxidation degrees were fabricated from low density polyethylene (LDPE) and poly(ethylene terephthalate) (PET) by controlling ultraviolet (UV) irradiation. The resulting NPs were characterized in terms of size, surface charges, chemical composition via dynamic light scattering, electrophoretic light scattering, and X-ray photoelectron spectroscopy, respectively. Protein adsorption onto the surface of NPs were evaluated using bovine serum albumin (BSA). Macrophage responses for NPs were investigated using human THP-1 cells genetically edited with HiBiT-tag on the downstream of interleukin-1β gene (IL-1β) for a non-invasive and highly sensitive method[1].

Results

UV irradiation induced surface oxidation with the introduction of carbonyl groups on LDPE and PET nanoparticles. Protein adsorption was influenced by the degree of surface oxidation of the NPs, irrespective of polymer type. Exposure to NPs induced IL-1β secretion in M1-polarized macrophages, whereas pre-adsorption of BSA onto the NPs surface suppressed IL-1β secretion. Pyrolysis–gas chromatography–mass spectrometry (Py-GC/MS) revealed that the amount of NPs uptaken by macrophages decreased by increasing BSA concentration in the pre-adsoption process.

Conclusion

These results suggest that macrophages internalize NPs by recognizing proteins adsorbed onto the nanoparticle surface, and subsequently secrete IL-1β in a manner dependent on the amount of NPs internalized.

Acknowledgements

This work was supported by JST, CREST Grant Number JPMJCR21L6.

References

[1]Washihira N., Murakami M., Kimura T, Yamamoto M. et al. Application of a genetically engineered macrophage cell line for evaluating cellular effects of UV/US-treated poly(ethylene terephthalate) microplastics. *Colloids and Surfaces B: Biointerfaces* 2023; 234; 113735.

S4 – O6

Spontaneous macrophase separation strategy for fabricating bilayer hydrogels with seamless interfaces and programmable biointerfacial structures

Jie Z.[1]
[1]Dept. of Biomedical and Chemical Engineering, University of Texas at San Antonio, San Antonio, TX, USA

Introduction

Bilayer hydrogels and double-network (DN) hydrogels are two distinct classes of soft-wet materials: bilayer hydrogels feature anisotropic two-layer configurations for stimuli-responsive actuation, while DN hydrogels consist of two interpenetrating networks providing exceptional mechanical strength. A unified fabrication strategy bridging both types has been lacking. Conventional methods (layer-by-layer assembly, 3D/4D printing) require multiple steps and often produce weak interfaces prone to delamination.

Aim

We present a spontaneous macrophase separation strategy that leverages differential polymerization rates and sol-to-gel phase transitions for one-pot, one-step fabrication of bilayer hydrogels with seamless biointerfacial structures, controllable layer thicknesses, and programmable stimuli-responsive functions.

Materials and Methods

Three macrophase separation strategies were developed. (1) Heat-induced: polymer pairs (e.g., PDMAE/gelatin) where one undergoes sol-to-gel transition upon cooling while the other exhibits LCST-driven hydrophilic-to-hydrophobic separation. Reactants were mixed in one pot, heated to 60°C for phase separation, cooled, and UV-polymerized. (2) Polymerization rate-induced: vinyl monomers (e.g., NIPAM) and zwitterionic styryl monomers (e.g., VBPS) with distinct radical reactivities were combined; faster-polymerizing vinyl monomers formed the first network while slower styryl monomers phase-separated into a second layer. (3) Stimuli-responsive-induced: polymer pairs combining LCST with salt/pH-responsive transitions. Structures were characterized by SEM-EDS, FTIR-ATR, UV-vis, mechanical testing, and 90° peeling tests.

Results

The strategy produced bilayer hydrogels with separation efficiencies of 20–99%, seamless interfaces confirmed by SEM-EDS, and layer thicknesses from micrometers to millimeters. Interfacial toughness reached 257–467 J/m², exceeding most conventional bilayer hydrogels (50–200 J/m²). The polymerization rate-induced strategy was validated across acrylamide-styryl pairs (AAm/VBPS, NIPAM/VBPS, HEAA/VBPS; 48–90% efficiency) and acrylate-styryl pairs (SBMA/VBPS, HEMA/VBPS; 45–70%). Fluorescent bilayer hydrogels with spiropyran mechanophores exhibited reversible shape and color changes in response to pH and solvent stimuli. Micro-leaf actuators (~200 µm thickness) achieved ultrafast actuation within 2–5 s, 70–240 times faster than macroscopic counterparts. By controlling fabrication temperature relative to LCST, the same polymer pairs produced either bilayer or DN structures, bridging the fabrication gap between both hydrogel classes.

Conclusion

The macrophase separation strategy provides a versatile, one-pot platform for bilayer hydrogels with seamless biointerfacial structures, high interfacial toughness, and programmable stimuli-responsive functions. This approach overcomes limitations of conventional multistep methods and bridges the design gap between bilayer and DN hydrogels, offering new opportunities for biomaterials in soft robotics, tissue engineering, and biosensing.

Acknowledgements

This work was supported by NSF (DMR-2311985, 2603321) and ACS PRF (ND-65277).

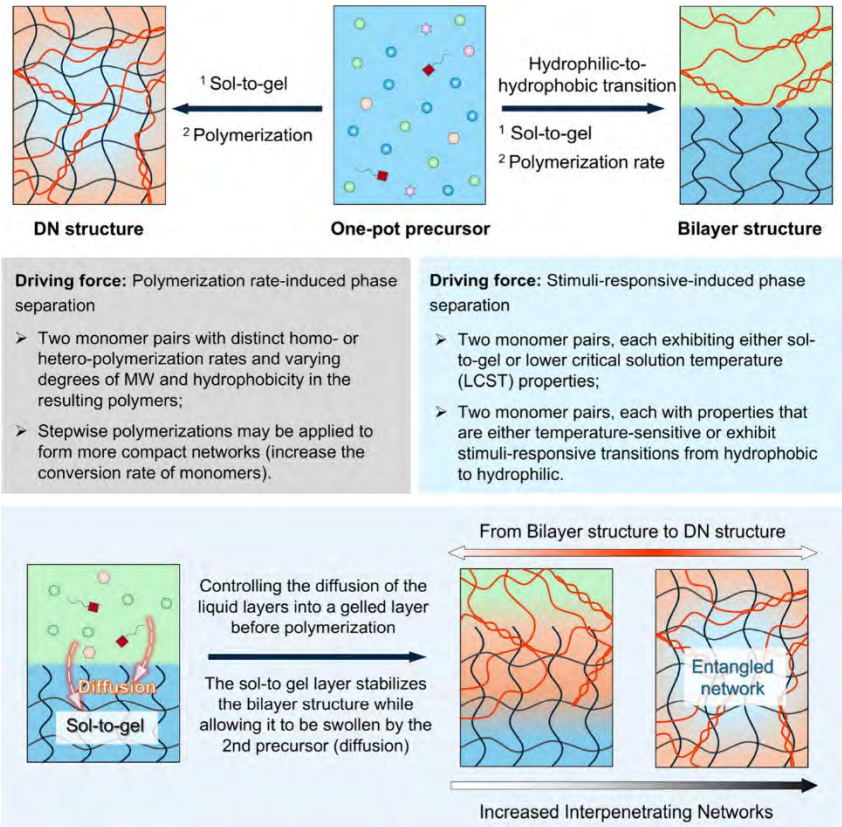

Figure 1. Macrophase separation strategy for bridging hydrogels from bilayer to DN structure.

References

[1]Zhang D., Tang Y., Zhang K., Xue Y., Zheng S.Y., Wu B., Zheng J. Multiscale bilayer hydrogels enabled by macrophase separation. *Matter* 2023; 6; 1484-1502.

[2]Zhang D., Tang Y., He X., Gross W., Yang J., Zheng J. Bilayer hydrogels by reactive-induced macrophase separation. *ACS Macro Lett.* 2023; 12; 598-604.

[3]Zhang D., Chen Q., Chen H., Tang Y., Zheng J. Spontaneous macrophase separation strategy for bridging hydrogels from bilayer to double-network structure. *Acc. Mater. Res.* 2024; 5; 1415-1427.

S4 – O7

Bypassing endocytosis for DNA delivery using amphiphilic phospholipid-mimetic polymers

Goda T.[1]
[1]Dept. Biomed. Eng., Toyo Univ., Asaka, Saitama, Japan

Introduction

The rapid emergence of therapeutic modalities such as nucleic acids, peptides, and antibodies has intensified the need for advanced intracellular drug delivery systems. Amphiphilic phospholipid-mimetic polymers, particularly poly(MPC_{30}-*r*-BMA_{70}) (PMB30W; MPC: 2-methacryloyloxyethyl phosphorylcholine; BMA: n-butyl methacrylate), have attracted attention due to their ability to penetrate cell membranes via energy-independent mechanisms without disrupting membrane integrity[1]. This process is hypothesized to involve the transient formation of inverse micelle-like structures, enabling direct cytoplasmic delivery[2]. While PMB30W has been successfully applied to hydrophobic drug delivery, its application to hydrophilic macromolecules remains challenging because they cannot spontaneously traverse lipid bilayers.

Aim

The objective of this study is to determine whether amphiphilic phospholipid-mimetic polymers can enable the non-endocytic intracellular delivery of hydrophilic model drugs, and to elucidate how the molecular weight and structural properties of DNA cargos influence their energy-independent membrane translocation, thereby identifying the key factors governing delivery efficiency.

Materials and Methods

PMB30W was synthesized via RAFT polymerization using azide-functionalized initiators. The ω-terminal group was converted to a thiol and labeled with Rhodamine B via thiol–Michael addition. Cy5-labeled single- and double-stranded DNA (ssDNA and dsDNA) bearing strain-promoted alkyne groups were conjugated to the α-terminal azide via click chemistry. Polymer structure and properties were characterized by ^{1}H NMR, GPC, FT-IR, dynamic light scattering, and surface tension measurements. Membrane permeability was evaluated using HepG2 cells at 4°C to suppress endocytosis, and intracellular localization was analyzed by confocal microscopy. Cytotoxicity and cell proliferation were assessed to evaluate biological effects.

Results

Azide-functionalized PMB30W with controlled molecular weights (Mn = 7.54–18.6 kDa) was successfully synthesized via RAFT polymerization. Subsequent fluorescent labeling and DNA conjugation did not disrupt the amphiphilic nature of the polymer, as confirmed by DLS and surface tension measurements, which indicated the formation of stable nanoscale aggregates (~10 nm).

Cellular uptake studies under energy-independent conditions demonstrated that membrane translocation behavior is highly dependent on cargo structure. Specifically, increasing the chain length of single-stranded DNA led to a marked reduction in permeability, whereas double-stranded DNA retained high permeability even at larger sizes. These results indicate that molecular rigidity and effective hydrodynamic size, rather than molecular weight alone, play dominant roles in the translocation process.

These observations support a transport mechanism based on inverse micelle formation within the lipid bilayer, where compatibility of the cargo with the transient hydrophobic environment is critical. Safety evaluations confirmed negligible membrane damage and low cytotoxicity.

Conclusion

This study demonstrates that the membrane permeability of PMB30W–DNA conjugates is governed by cargo structural properties. Amphiphilic phospholipid-mimetic polymers enable energy-independent intracellular delivery of DNA without membrane disruption. These findings provide important insights for the rational design of next-generation drug delivery nanocarriers.

Acknowledgements

This work was supported in part by Mr. K. Yokoo at Toyo University, Toyo University Top Priority Research Program (Grant No. 2024T1) and Research Facility Center, Asaka, Toyo University.

References

[1]Goda T., Goto Y., Ishihara K. Cell-penetrating macromolecules: Direct penetration of amphipathic phospholipid polymers across plasma membrane of living cells, *Biomaterials*, 2010; 31; 2380-2387.

[2]Goda T., Imaizumi Y., Hatano T. Matsumoto A. Ishihara K. Miyahara Y. Translocation mechanisms of cell-penetrating polymers identified by induced proton dynamics, *Langmuir*, 2019; 35; 8167-8173.

S5
AI-Integrated approaches for Next-Generation tissue regeneration

S5 – K1

Marchal J.A.
University of Granada - Spain

S5 – O1

Morphology-aware machine learning framework for predicting nanoparticle transfection efficiency across cell types

Kamaliasl S.[1], Dunne N.[2], McCarthy HO.[1]
[1]School of Pharmacy, Queen's University Belfast, Belfast, United Kingdom
[2] School of Mechanical and Manufacturing Engineering, Dublin City University, Dublin, Ireland

Introduction

Efficient intracellular delivery remains a major challenge in RNA therapeutics and biomaterial-based gene delivery systems. Nanoparticle-mediated delivery performance is influenced by multiple interacting parameters, including physicochemical properties, formulation conditions, and biological characteristics of target cells.[1] Current optimisation strategies rely on empirical screening approaches, which are time-consuming and often poorly transferable between cell types. Recent advances in artificial intelligence (AI) enable analysis of complex, high-dimensional datasets; however, most predictive models focus primarily on nanoparticle properties while neglecting cellular morphological characteristics that influence uptake and intracellular processing.[2,3] In this study, we developed a morphology-aware machine learning framework integrating biomaterial design parameters with quantitative cell morphology descriptors to predict nanoparticle-mediated transfection efficiency.

Materials and Methods

Experimental datasets were generated using cell-penetrating peptide nanoparticles across multiple cell lines. Biomaterial features included peptide physicochemical descriptors, nanoparticle formulation parameters such as N:P ratio, and nanoparticle size characteristics. In parallel, quantitative cell morphology features were extracted from microscopy images using image analysis pipelines. These features were integrated into a unified dataset representing both biomaterial and cellular parameters. Machine learning models, including Random Forest and gradient boosting, were trained to predict transfection efficiency and cell viability. Model performance was evaluated using cross-validation and independent testing datasets.

Results

The morphology-aware modelling framework was evaluated across multiple cell lines representing distinct cellular morphologies and biological contexts. Models trained using nanoparticle parameters alone achieved moderate predictive performance. Incorporating morphology descriptors improved predictive accuracy by approximately 10% compared with biomaterial-only models, and this improvement was consistent across cell lines. Feature importance analysis identified cell area, circularity, and aspect ratio among the most informative predictors alongside N:P ratio and peptide charge. These findings indicate that cell morphology influences nanoparticle-cell interactions and uptake dynamics. Representative transfection outcomes are shown in Figure 1A, with improved agreement between predicted and experimentally observed transfection efficiencies across conditions (Figure 1B).

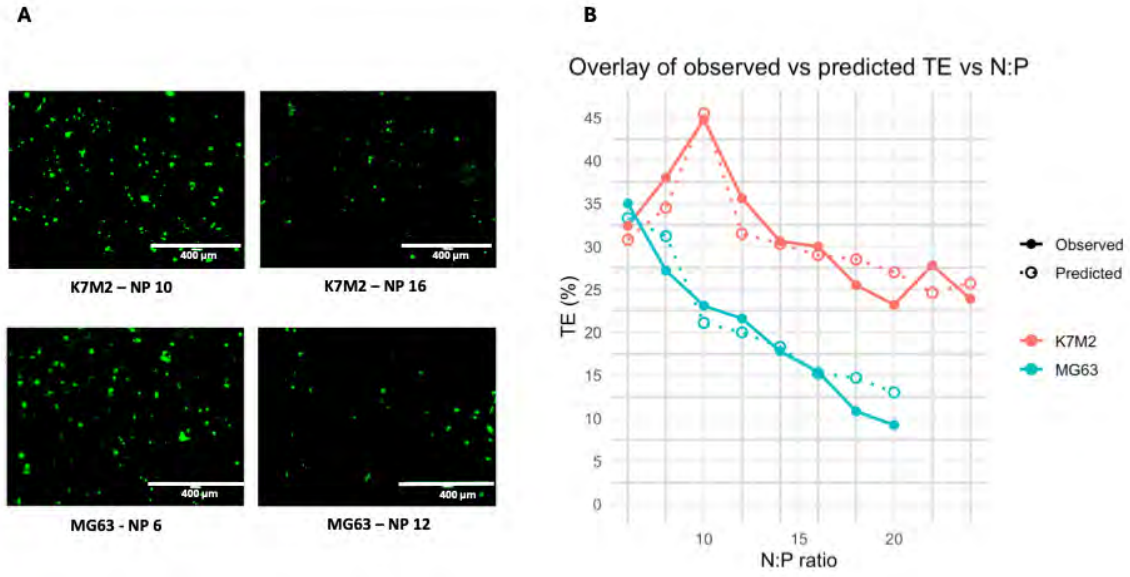

Figure 1. Transfection efficiency and model prediction across N:P ratios. (A) Green fluorescent Protein (GFP) fluorescence images of K7M2 and MG63 cells at indicated N:P ratios (scale bar = 400 µm). (B) Observed and predicted transfection efficiency (%) showing ~10% agreement.

Conclusion

Incorporating cell morphology descriptors into machine learning models enhances prediction of nanoparticle-mediated transfection efficiency, yielding an approximate 10% improvement across multiple cell lines. These findings highlight cellular geometry as a critical determinant of biomaterial delivery performance. The proposed framework reduces reliance on empirical screening and provides a scalable, data-driven strategy for rational design of nanoparticle delivery systems, with broader applicability to RNA therapeutics and gene delivery platforms.

Acknowledgement

This research was funded by the Department for the Economy (DfE), Northern Ireland.

References

[1]Johansson J.M., Du Rietz H., Hedlund H., et al. Cellular and biophysical barriers to lipid nanoparticle mediated delivery of RNA to the cytosol. Nature Communications 2025; 16; 1–12.
[2]A Gong D., Ben-Akiva E., Singh A., et al. Machine learning guided structure function predictions enable in silico nanoparticle screening for polymeric gene delivery. Acta Biomaterialia 2022; 147; 1–12.
[3] Luo G., Jiang X., Hu C., et al. Artificial intelligence-powered nanomedicine. Chemical Society Reviews 2026; 55; 1–15.

S5 – O2

Digital twin and machine learning pipeline for the microfluidic generation of mineralized gellan-alginate microgels for osteochondral tissue engineering

Marecik S.[1], Stępień J.[2], Hallo F.[3], Marcjan Ł.[3], Pietryga K.[4], Pamuła E.[1]
[1]Dept. of Biomaterials and Composites, Faculty of Materials Science and Ceramics, AGH University of Krakow, Krakow; [2]Faculty of Medicine, Jagiellonian University Medical College, Kraków; [3]Dept. of Applied Computer Science and Modeling, Faculty of Metals Engineering and Industrial Computer Science, AGH University of Krakow, Krakow; 4Silesian Park of Medical Technology Kardio-Med Silesia, Zabrze, Poland

Introduction

Microfluidic systems enable precise microgel fabrication for biomedical applications, including osteochondral tissue engineering. However, empirical optimization is highly time-consuming and leads to excessive reagent consumption. This study aimed to develop a digital twin combined with a machine learning (ML) pipeline for polymer microgel generation. This synergistic computational approach allows for rapid parameter screening and process optimization.

Materials and Methods

The aqueous phase comprised 2% (w/v) gellan gum (Gelzan, Sigma-Aldrich) and 0.5% (w/v) sodium alginate (Sigma-Aldrich). Two formulations were evaluated: a non-mineralizing variant processed at 60°C and a mineralizing variant processed at 75°C, supplemented with 0.1M Na_2HPO_4 (Avantor Performance Materials). Crosslinking and concurrent mineralization were induced in a 1M $CaCl_2$ bath (Avantor Performance Materials). The continuous phase was light mineral oil (Sigma-Aldrich) with 2% (v/v) Span 80 (Sigma-Aldrich). Droplets were generated in a custom temperature-controlled microfluidic chip, 3D-printed (Asiga MAX X27) from KeyGuide resin (KeyPrint). The shear-thinning behavior of the aqueous phase, measured via an oscillatory rheometer (MCR 302, Anton Paar), was incorporated into a Volume of Fluid (VOF) multiphase model in Ansys Fluent software. The simulation maintained a courant number below 0.25 with residuals converging to 10^{-5}. Additionally, a two-stage ML pipeline was developed to complement the analysis of experimental data. In the first stage, the flow regime was classified as stable or unstable based on phase flow rates using classifiers including Decision Tree, Support Vector Machine, and Logistic Regression. In the second stage microgel diameter was predicted for samples classified as stable using regressors including Ridge, Support Vector Regression, and Decision Tree. Different combinations of classification and regression models were investigated using nested cross-validation with hyperparameter optimization, enabling a systematic evaluation of the two-stage pipeline. Flow rates ranged from 1 to 8 µl/min for the dispersed phase and 1 to 160 µl/min for the continuous phase.

Results

Experimentally, the platform enabled the stable generation of droplets with diameters between 250 and 350 µm, alongside successful brushite precipitation. VOF simulations predicted microgel diameters with a relative error of less than 5% (Figure 1). The ML pipeline demonstrated excellent performance. The flow regime classification achieved a balanced accuracy of 98.75%, an F1-score of 0.9867 for the stable regime, and a confusion matrix consisting of 36 true positives, 16 true negatives, zero false positives, and one false negative. For stable regimes, the optimal regression model accurately predicted droplet diameters, yielding a mean absolute error of 6.57 µm and an R^2 of 0.9076.

Conclusion

Integrating a VOF-based digital twin with a robust ML pipeline provides a highly accurate framework for predicting non-Newtonian multiphase flows. This synergy paves the way for AI-driven systems autonomously optimizing microgel production for specific clinical applications like osteochondral regeneration, drastically reducing reagent waste and accelerating laboratory workflows.

Acknowledgements

We acknowledge the National Science Center, Poland for the financial support provided by Preludium project (ID 2025/57/N/ST8/03399).

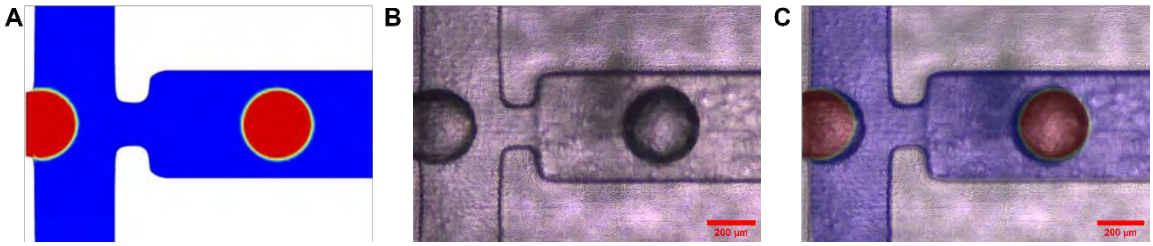

Figure 1. Multiphase VOF simulation (A), experimental droplet formation (B), overlay comparison between the simulation predictions and experimental results (C), for a formulation containing 2% (w/v) gellan gum and 0.5% (w/v) sodium alginate. Flow rates: 1 µl/min for the aqueous phase and 10 µl/min for the oil phase.

S5 – O3

Optical tomography enables density based adaptive and context-aware volumetric printing

Größbacher G.[1,2], Levato R.[1,2]
[1]Dept. of Orthopaedics, University Medical Center Utrecht; [2]Dept. of Clinical Sciences, Utrecht University, Utrecht, The Netherlands

Introduction

Tomographic volumetric printing enables the rapid fabrication of three-dimensional structures within photosensitive resin. Our group previously introduced GRACE[1], a multi-wavelength light-sheet system that registers fluorescently stained objects within the printing vial, enabling parametric printing tailored to vial contents. However, the requirement for fluorescent staining limits compatibility with many biologically relevant samples.

Aim

To address this, we developed a label-free object registration strategy for volumetric printing combining optical tomography with machine learning classification, broadening compatibility with biologically relevant samples and enabling autonomous, object-specific fabrication with a simple, low-cost camera setup.

Materials and Methods

The fluorescence detection system of GRACE was replaced with diffuse backlit LED illumination. Six wavelengths (selected between 650 and 1040 nm) were screened for optimal transmission, contrast-to-noise ratio, and optical density reconstruction quality. Biological constructs, including blood vessel and cystic fibrosis organoids and pancreatic islets were scanned and reconstructed without fluorescent staining. Both supervised and unsupervised machine learning approaches were applied to demonstrate automated classification from optical density reconstructions. A CUDA-based fast Radon library was developed to implement next-generation optimizers (L-BFGS, FISTA), which were benchmarked against the previously used OSMO algorithm and the inverse rendering framework DrTVAM[2].

Results

White light produced up to 6.9x higher noise than 1040 nm illumination, nevertheless, precise construct registration was achieved across all tested wavelengths. 1040 nm also offered substantially higher transmission, enabling volumetric optical density reconstruction of all sample types. Label-free reconstruction was successfully demonstrated across multiple construct types, and optical density-based machine learning classification allowed automated discrimination of biological objects within complex microenvironments. Shadow correction using L-BFGS completed in under three minutes for a 10×6.4 mm cylindrical sample, yielding improved contrast at biologically relevant speeds compared to the OSMO/GRACE pipeline.

Conclusion

This work presents a novel, fluorescent label-free strategy for object registration in volumetric printing. By replacing fluorescence detection with NIR backlit tomography and filtered back projection, the system achieves µm-scale registration accuracy without labelling, broadening compatibility with a wide range of biologically relevant samples. The addition of machine learning-driven classification based on intrinsic optical density profiles further enhances the precision and autonomy of object-specific fabrication. This approach represents a significant advance toward fully automated, biology-aware volumetric bioprinting.

References

[1] Florczak, Sammy, et al. Adaptive and Context-Aware Volumetric Printing. *Nature* 2025; 645; 108-114.
[2] Nicolet, Baptiste, Felix Wechsler Inverse Rendering for Tomographic Volumetric Additive Manufacturing. *ACM* 2024; 228; 1-17.

S5 – O4Preserving myoblast viability in extrusion bioprinting: An FEM-driven machine learning surrogate for extrusion parameter optimization

Tavangari Z.[1], Maghami A.[2], Papangelo A.[2], Ciofani G.[3], Genchi G.G.[1,3]
[1]Dept. of Bioscience, Biotechnology and Environment, University of Bari "Aldo Moro", Bari; [2]Dept. of Mechanics, Mathematics and Management, Polytechnic University of Bari, Bari; [3]Smart Bio-Interfaces, *Istituto Italiano di Tecnologia*, Pontedera (Pisa), Italy

Introduction

Extrusion-based bioprinting exposes cells to shear and extensional stresses often compromising viability and forcing a trade-off between print fidelity and process-induced damage. For skeletal muscle constructs, which demand both high cell viability and alignment, this extrusion parameter window is particularly narrow. Here, we develop an integrated finite element-Gaussian process (FEM–GP) framework, grounded in a validated mechanobiological damage law for L8 myoblasts, to predict flow rate and total cell damage due to pressure and needle diameter, and identify a viable bioprinting window.

Materials and Methods

We implemented an FEM model (DOLFINx 0.10)[1] of the full Nordson EDF stepped needle geometry (barrel diameter Ø: 4.2 mm, with middle Ø: 2.0 mm and tip Ø: 100–330 µm), solving the incompressible power-law Stokes' equations with Neumann traction pressure boundary conditions and a viscosity-continuation Newton solver. FEM outputs were used to train a GP surrogate with Matérn kernel v=2.5 on 29 parameter combinations, by using leave-one-out cross-validation (LOO-CV: Q error < 9%, Dt error < 0.1 %) to map the bioprinting parameter space across 4 needles and 8 applied pressures. Cell damage was quantified based on a published mechanobiological model[2], decomposing total damage Dt into shear (Dst) and extensional (Det) contributions.

Results

Wall shear stress agreed with previous experimental data within 3%, and volumetric flow rate within 28% across the 50–400 kPa pressure range, capturing the nonlinear shear-thinning response (Fig. 1a,b). Dt was nearly pressure-independent at fixed needle diameter, driven primarily by geometry: Dt decreased from 85% (Ø: 100 µm) to 71% (Ø: 330 µm), without any pressure adjustment (Fig. 1c). Shear damage dominated in all conditions (Dst ≈ 70–86%), with extensional stress contributing 3–13% at higher pressures where entrance effects become significant (Fig. 1d). Across the full surrogate-predicted parameter space, a viable bioprinting window (Dt <80%, Q ≥1 µL/s) emerged only for needle diameter ≥200 µm (Fig. 2).

Conclusion

Coupling of an FEM description of the stepped extrusion needle with a GP surrogate enables rapid exploration of the extrusion parameter space without time-consuming FEM simulations. Our framework suggests needle diameter, rather than pressure, is the dominant determinant of predicted cell damage. The resulting FEM–GP framework offers groundwork for bioprinting condition screening, in the future, adaptable to other cell–bioink systems and operating parameters.

Acknowledgements

Agenzia Spaziale Italiana grant 2024-59-HH.0 (CUP: F93C24000580001).

References

[1]*Baratta I.A. et al. "DOLFINx: The next generation FEniCS problem solving environment." Zenodo 2025;10447665;1–28.*
[2]*Ning L. et al. "Characterization of Cell Damage and Proliferative Ability during and after Bioprinting."* ACS Biomater. Sci. Eng. 2018; 4(11); 3906–3918.

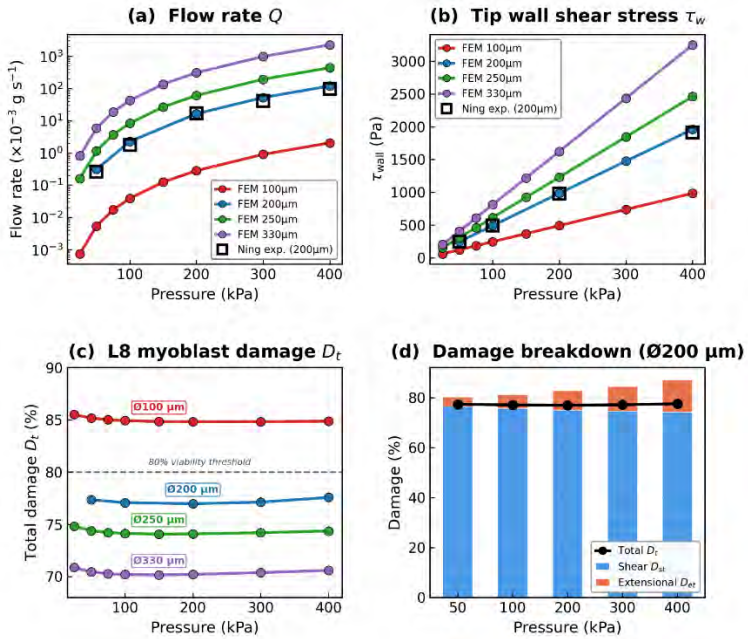

Figure 1. FEM-predicted: flowrate Q (a), wall shear stress τ_w (b), cell damage D_t (c) and damage breakdown with Dst and Det contributions to Dt (d).

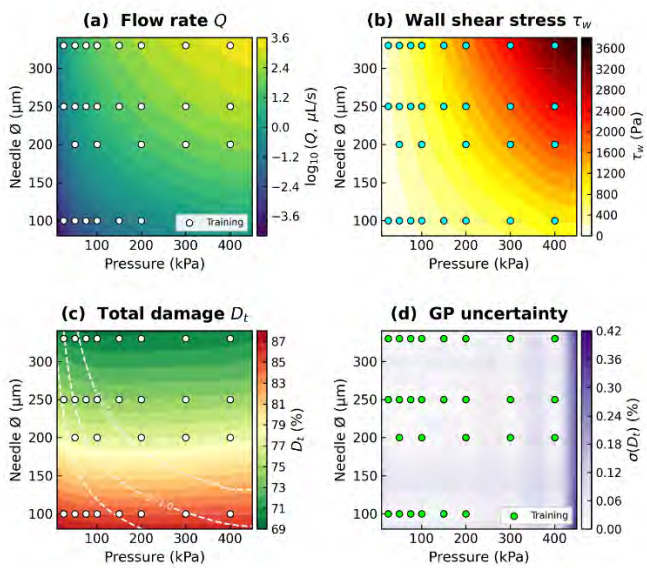

Figure 2. Gaussian Process surrogate predictions over the full bioprinting parameter space: Flow rate (a), Wall shear stress (b), Total cell damage Dt with iso-flow-rate contours (c), and GP predictive uncertainty (d).

S5 – O5

AI-driven analysis of pore geometry–dependent mineralization in silk fibroin scaffolds using synchrotron imaging

Dei Rossi G.[1], Buccino F.[1,2], Longo E.[3], Tromba G.[3], Vergani L.M.[1,2]
[1]Dept. of Mechanical Engineering (DMEC), Politecnico di Milano, Milan; [2]IRCCS Galeazzi-Sant'Ambrogio, Milan; [3]Elettra-Sincrotrone Trieste ScpA, Basovizza, Trieste, Italy

Introduction

Silk fibroin scaffolds provide tunable porous architectures for bone tissue engineering; however, establishing predictive structure-function relationships remains challenging. Although pore size is widely regarded as a key determinant of osteogenesis, mineralized matrix formation arises from complex three-dimensional geometric interactions. Artificial Intelligence (AI) enables automated volumetric analysis, pore recognition, and predictive modelling of scaffold heterogeneity to identify quantitative osteogenic outcomes[1].

Aim

To develop an AI-assisted multi-scale framework combining high-resolution imaging with automated pore identification, morphometric extraction, and statistical modelling to identify pore configurations and connectivity patterns governing osteogenic mineral deposition in silk fibroin scaffolds.

Materials and Methods

Silk fibroin scaffolds were seeded with human bone marrow-derived mesenchymal stem cells and cultured for four weeks under osteogenic conditions with human platelet lysate. Constructs were analysed by synchrotron X-ray phase-contrast microtomography for non-destructive high-resolution 3D visualization of mineralized tissue (Fig. 1).

A convolutional neural network enabled automated segmentation of scaffold and mineral phases and pore identification, extracting morphometric descriptors (equivalent radius, internal surface area, sphericity, principal axis alignment) and graph-based connectivity metrics. Given non-Gaussian distributions ($p < 0.05$), non-parametric statistics (Kruskal-Wallis), nonlinear regression, ANOVA, k-means clustering, and cross-validated machine learning evaluated geometric contributions to mineral density.

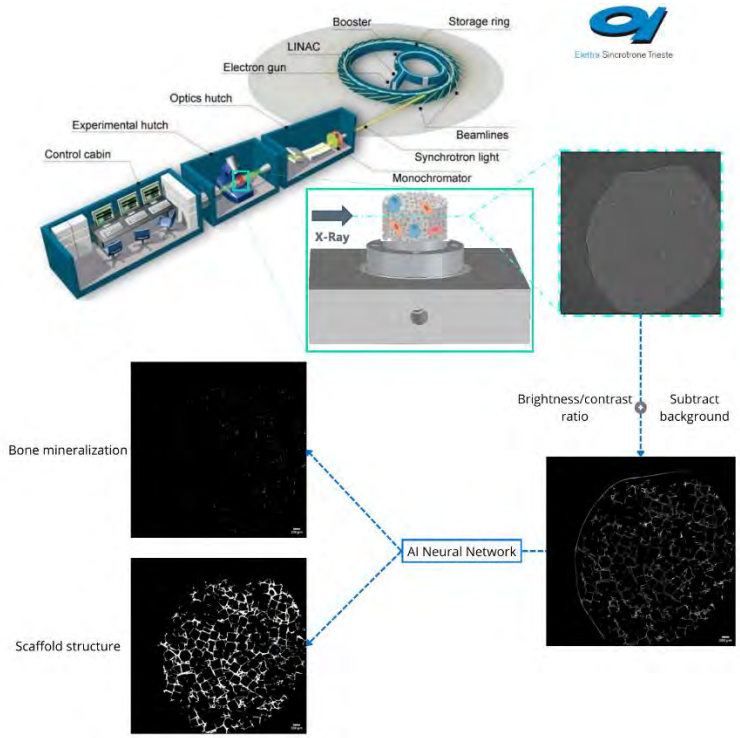

Fig. 1: Schematic workflow of the study. Silk fibroin scaffolds are scanned by synchrotron X-ray phase-contrast microtomography to obtain high-resolution 3D datasets. After image preprocessing, a convolutional neural network enables automated segmentation of mineralized bone and scaffold structure. This approach allows quantitative analysis of pore morphology and evaluation of pore-bone interactions.

Results

Most porosity parameters showed non-normal distributions ($p < 0.05$).

Mineral deposition preferentially localized within pores exhibiting equivalent radii of 110-120 µm, high internal surface area, and intermediate sphericity (0.65 – 0.75). Significant nonlinear associations were observed between mineral density and radius, surface area, and sphericity ($p<0.0001$), whereas pore alignment showed no independent predictive value.

Graph-based connectivity analysis demonstrated that highly interconnected pores exhibited enhanced mineral accumulation, indicating that interconnectivity amplifies osteogenesis beyond individual geometric descriptors. Multivariate machine learning identified a synergistic morphometric-connectivity pore class associated with higher mineral density (ANOVA, $p<0.0001$), indicating that optimal osteogenesis depends on coordinated three-dimensional architecture rather than pore size alone.

Conclusions

Integration of synchrotron imaging with AI-driven segmentation, graph modelling, distribution-based statistical validation, and predictive analysis identifies quantitative three-dimensional design rules linking pore geometry and interconnectivity to mineralized matrix formation. This framework supports rational optimization of silk fibroin scaffold architectures for bone tissue engineering.

Acknowledgements

The authors acknowledge: Prof. Sandra Hofmann (TU/e), Euro-BioImaging ERIC Elettra-Sincrotrone Trieste S.C.p.A., Alta Scuola Politecnica, MSCA GAP 101120290 and ARCHIMEDES – CUP D53D23003940006.

References

[1]F. Mukasheva, L. Adilova, A. Dyussenbinov, B. Yernaimanova, M. Abilev, D. Akilbekova. Optimizing scaffold pore size for tissue engineering: insights across various tissue types. *Front. Bioeng. Biotechnol.* 2024; 12.

S5 – O6

Morphology-driven cell sorting based on AI inference enriches dental pulp stromal cells for regenerative tissue engineering

Yuan D.[1], Van Wijngaarden M.[2], Zhao Z.[3], Huang M.[4], Sturms J.[4], Van Meerbeek B.[1], Van den Bosch T.P.P.[4], Van der Spek P.J.[2], EzEldeen M.[1,5], Pedano De Piero M.S.[1]

[1]Dept. of Oral Health Sciences, BIOMAT & UZ Leuven, Dentistry, KU Leuven, Leuven, Belgium; [2]Dept. of Pathology and Clinical Bioinformatics, Erasmus MC, University Medical Center Rotterdam, Rotterdam, The Netherlands; [3]Dept. of Oral Health Sciences, Orthodontics, Dentistry, KU Leuven, Leuven, Belgium; [4]Dept. of Pathology, Erasmus MC, University Medical Center Rotterdam, Rotterdam, The Netherlands; [5]Dept. of Oral Health Sciences, Paediatric Dentistry and Special Dental Care, UZ Leuven, Leuven, Belgium

Introduction

Tissue engineering and regenerative medicine mostly relies on the surface-marker based enrichment, such as fluorescence-activated cell sorting (FACS) and magnetic-activated cell sorting (MACS). Their applications are limited by the specificity and stability of the surface markers. To address these limitations, a live-cell imaging, AI inference, and smart sorting platform [REM-I (Deepcell)] was used to characterize the heterogeneity of human dental pulp stromal cells (hDPSCs) and support real-time cell sorting based on cell morphology.

Aim

To establish a high-resolution morphological database of hDPSCs and correlate cell morphological features with transcriptional signatures, thereby providing a basis for morphology-driven cell sorting.

Materials and Methods

hDPSCs from 10 healthy donors (<18y) were imaged using the 'Deepcell' platform followed by deep-learning feature extraction and single-cell clustering. Sixty-four AI-derived and 51 morphometric features were used to construct a 2D UMAP to reveal distinct cell morphotypes. Afterwards, morphotypes were classified, sorted out and subjected to scRNA-seq to match the morphological features with transcriptome signatures. hDPSCs from another 4 independent donors were subsequently sorted using the same morphological classification scheme and induced toward odontogenic differentiation for 21 days, with functional assays used to validate the correspondence between the morphology-driven cell sorting and transcriptomic profiling.

Results

A high-resolution morphological database of hDPSCs was established, enabling visualization of intracellular contents. This database showed no overlap with the immune cells, indicating that hDPSCs exhibit distinct morphological clustering patterns and confirming the specificity of the generated databases. After removing debris and doublets, eight morphotypes with pronounced differences in cell size, contour, texture, and intracellular structural complexity were identified. Among them, six morphotypes, each representing 7.9%–13.63% of the cell population, were sorted for in vitro culture and exhibited distinct proliferative capacities.

Conclusion

Deepcell reveals the intrinsic heterogeneity of monolayer cultured hDPSCs independent of marker labeling, functional annotation, and transcriptomic profiling. This morphology-driven cell sorting approach provides a new strategy to enrich cell sources for stem cell research and regenerative applications.

S7
Antimicrobial biomaterials and biocoatings

S7 – K1
Targeting oral biofilms: Biomaterial-based approaches for modern dental therapies

Deb S.
Kings College Londen - UK

S7 – K2

Antimicrobial materials for biomedical applications: From personal protective equipment to implantable devices

Serrano-Aroca Á.[1]
[1]Biomaterials and Bioengineering Lab, Dept. of Biotechnology, Catholic University of Valencia, Spain

Abstract

This keynote will explore how the COVID-19 pandemic, the continued emergence of viral threats, and the accelerating global crisis of antimicrobial resistance have exposed critical gaps in infection prevention across materials used in biomedical applications, spanning from everyday protective tools to advanced implantable devices. Conventional materials used in many biomedical applications often lack intrinsic antimicrobial properties and therefore are unable to actively inactivate viruses, bacteria, and fungi, including multidrug-resistant strains. The lecture will present recent advances in biofunctional antimicrobial technologies designed to rapidly inactivate a broad spectrum of pathogens while maintaining safety, usability, and translational potential. Real-world examples will include next-generation protective tools, such as enhanced face masks, face shields, and antimicrobial lipsticks, showing rapid antiviral, antibacterial, and antifungal performance, with a clear pathway toward scalable and sustainable industrial implementation. Beyond personal protection, the keynote will also highlight how distinct antimicrobial design strategies are being developed for biomedical applications, where infection remains a major cause of implantable device failure. In particular, the talk will showcase the development of antimicrobial hernia repair meshes and tissue engineering scaffolds engineered to simultaneously prevent microbial colonization and support tissue regeneration. This dual functionality aims to reduce complications, improve healing, and increase the long-term success of implantable devices. To accelerate progress in this field, the lecture will also introduce antimicrobial biomaterial characterization methods developed by the research group to enable faster and more reliable screening and benchmarking of antiviral, antibacterial, and antifungal performance. By facilitating standardized and comparative evaluation across different material families, these approaches can shorten development cycles and help identify promising candidates more efficiently, supporting the discovery of next-generation antimicrobial biomaterials. The keynote will highlight how the integration of antimicrobial performance, biosafety, and manufacturability is driving the development of a new generation of protective and implantable technologies for safer and more effective biomedical solutions.

Acknowledgements

The authors gratefully acknowledge the Fundación Universidad Católica de Valencia San Vicente Mártir for the grant 2025-231-001UCV, and the Spanish Ministry of Science and Innovation for the grant PID2024-157498OB-I00

S7 – O1

Borosilicate-based bouncy bioglass with antimicrobial properties

Lam T.S.T.[1], Claireaux H.[1], Babut C.[2], Tsigkou O.[2], Ramasamy A.[3], Jones J.R.[1]
[1]Dept. of Materials, Imperial College London, London; [2]Dept. of Materials, School of Natural Sciences, Faculty of Science and Engineering, The University of Manchester, Manchester; [3]Dept. of Bioengineering, Imperial College London, London, UK

Introduction

Organic-inorganic hybrids are materials comprising bioactive glass and polymer co-networks at the molecular scale. The aim of sol-gel hybrids is to obtain synergy of the properties of the individual networks – stiffness and bioactivity of the inorganic and toughness of the polymers, while maintaining controlled biodegradation. Tallia et al developed "Bouncy Bioglass", which showed unprecedented combination of mechanical properties and controlled degradation.[1] Li et al. showed Bouncy Bioglass scaffolds with a channel size of 250 µm were able to induce chondrogenic differentiation of hBMSCs. The cells preferentially produced collagen Type II as opposed to collagen Type I, indicating differentiation into hyaline cartilage.[2] Scaffolds with antimicrobial properties are desired to prevent post-surgical infection.

Aim

The aim was to incorporate borate into the inorganic network of Bouncy Bioglass scaffolds, and to test their antibacterial properties and angiogenic ability.

Materials and Methods

Synthesis was based on introducing borate sol-gel precursors into the synthesis of "Bouncy Bioglass", a silica/poly(tetrahydrofuran)/poly(caprolactone-diCOOH) hybrid (SiO_2/PTHF/PCL-diCOOH), modifying the protocol from Tallia et al.[1] The resulting sol was transferred into syringes. Using direct ink writing, scaffolds with a 250 µm pore size were fabricated, aged for 4 days, and dried for 3 days. 5 mm diameter scaffold discs were extracted using a surgical punch.

Time-kill analyses were performed by culturing 10^5 CFU ml^{-1} *E. coli* and MRSA in Mueller-Hinton broth (MHB) with the scaffolds at 37 °C with shaking at 180 rpm. At 24 h and 48 h, aliquots were taken, serially diluted in PBS, then plated on MHB agar for CFU enumeration. Cytotoxicity of the scaffolds was tested on hMSCs using media conditioned with the scaffolds. The potential for blood vessel ingrowth evaluated in vitro by culturing HUVECs and MSCs on the Borate Bouncy Bioglass scaffolds over 21 days, with and without a supporting gel. Confocal microscopy was used to observe vessel formation.

Results

We have successfully incorporated borate into Bouncy Bioglass scaffolds without phase separation. A scaffold and SEM micrograph are shown in Figure 1a and 1b respectively. Interconnected channels of mean size 215±41 µm were obtained.

Borate Bouncy Bioglass exhibited more effective antibacterial properties compared to borate-free Bouncy Bioglass scaffolds (Figure 2). Bouncy Bioglass scaffolds had effects similar to no treatment control, while 50 mg mL^{-1} Borate Bouncy Bioglass scaffolds inhibited the growth of *E. coli*. 100 mg mL^{-1} of the same scaffold led to elimination of the bacteria. For MRSA, Bouncy Bioglass scaffolds at concentrations ≥ 50 mg mL^{-1} were able to kill the bacteria. Borate Bouncy Bioglass was able to demonstrate this killing effect at a lower concentration of 25 mg mL^{-1}.

Conclusion

Borosilicate/PTHF/PCL-diCOOH hybrids can be 3D printed and show antimicrobial activity above a concentration of 50 mg mL^{-1}.

References

[1]Tallia F., Russo L., Li S., et al. Bouncing and 3D printable hybrids with self-healing properties. *Mater. Horiz.* 2018; 5; 849-860.

[2]Li S., Tallia F., Mohammed A.A., et al. Scaffold channel size influences stem cell differentiation pathway in 3-D printed silica hybrid scaffolds for cartilage regeneration. *Biomater. Sci.* 2020; 8; 4458-4466.

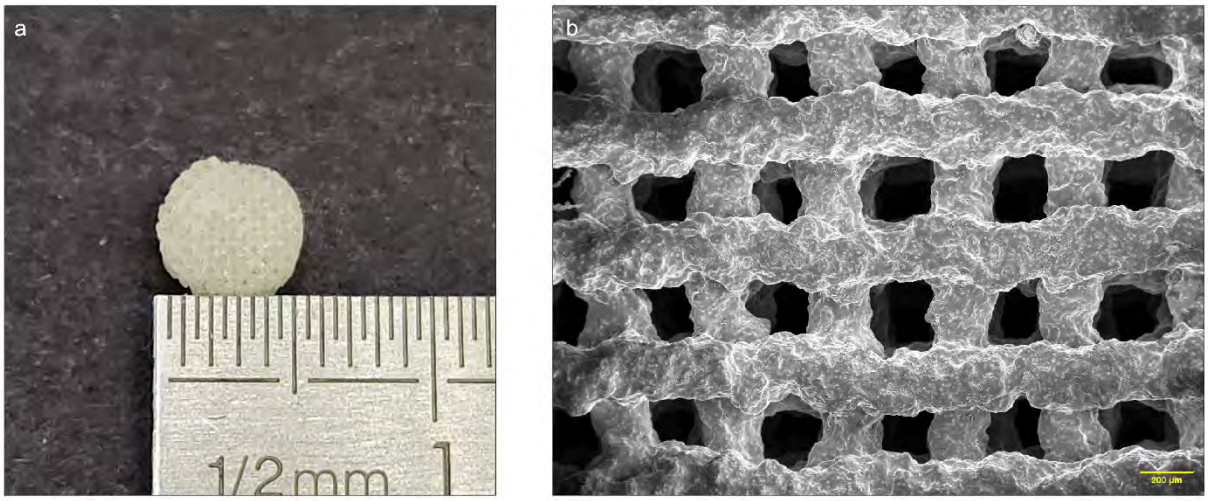

Figure 1 – (a) Printed Borate Bouncy Bioglass scaffold. (b) Scanning electron microscopy image of the scaffold top surface. Pore sizes measured using Image J.

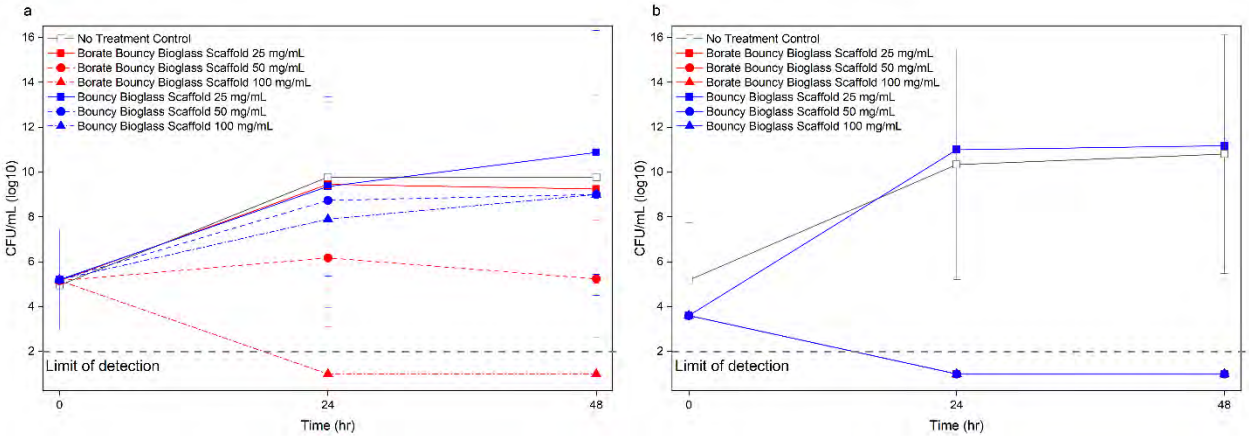

Figure 2 – Time-kill analyses of (a) *E. coli* (b) MRSA cultured with varying amounts of Borate Bouncy Bioglass and borate-free Bouncy Bioglass. Error bars represent standard deviation.

S7 – O2

Degradable PLGA coatings incorporating organometallic complexes for controlled antibacterial activity on implants

Gamage D.L.[1], Fan M.S.J.[2], Soukup C.R.M.[2], Duffin R.N.[2], Meagher L.[1], Andrews P.C.[2]
[1]Dept. of Materials Science and Engineering, Monash University; [2]School of Chemistry, Monash University, Clayton, Australia

Introduction

Implant-associated infections (IAIs) contribute significantly to implant failure due to biofilm formation that resists host defenses and antibiotics.[1] Conventional antimicrobial coatings often exhibit limited stability, poor adhesion, and uncontrolled release.[2] Novel coatings offering sustained antibacterial activity while preserving cytocompatibility are therefore critically needed.

Materials and Methods

In this study, degradable antimicrobial coatings were developed by incorporating organometallic bismuth (Bi) and indium (In) complexes into poly(lactide-*co*-glycolide) (PLGA) matrices and depositing them onto substrates via spray coating. Coating formulations were optimised by systematically varying solvents and deposition parameters. Ethyl acetate enabled stable suspensions and consistent film formation. Optimal coatings were obtained using 1% (w/v) polymer concentration, a 0.1 $mLmin^{-1}$ flow rate, and post-annealing at 80°C for 24 h, producing uniform and morphologically stable coatings. Cytocompatibility was evaluated using L929 mouse fibroblasts following ISO 10993-5 guidelines. Antibacterial activity was assessed according to ISO 22196:2011 against *Escherichia coli* (ATCC 8739) and two multidrug-resistant *Klebsiella pneumoniae* strains (ATCC BAA-2814 and RH201207). Elemental release from the coatings was quantified using inductively coupled plasma mass spectrometry (ICP-MS).

Results

Coatings containing 5 wt% Bi and 5 wt% In complexes maintained L929 fibroblast viability above the ISO 10993-5 cytotoxicity threshold of 80% across all tested dilutions. All coatings exhibited significant antibacterial activity against the tested strains. Indium-based coatings produced greater bacterial reductions than the bismuth-based, likely reflecting their higher solubility and increased release from the polymer matrix. As shown in Figure 1, both Bi- and In-complex-containing coatings produced strong antibacterial activity across all tested strains, achieving log reductions above 2 and, in some formulations, approaching 4 and beyond, equivalent to ≥99.9% bacterial inhibition. ICP-MS analysis revealed higher cumulative release of indium (6.74%) compared with bismuth (2.27%), consistent with the observed antibacterial performance.

Conclusion

These findings demonstrate that Bi- and In-complex-loaded PLGA coatings provide strong, sustained antibacterial activity across multiple bacterial strains (including drug-resistant strains), while maintaining cytocompatibility, highlighting their potential as infection-resistant surfaces for metallic implants.

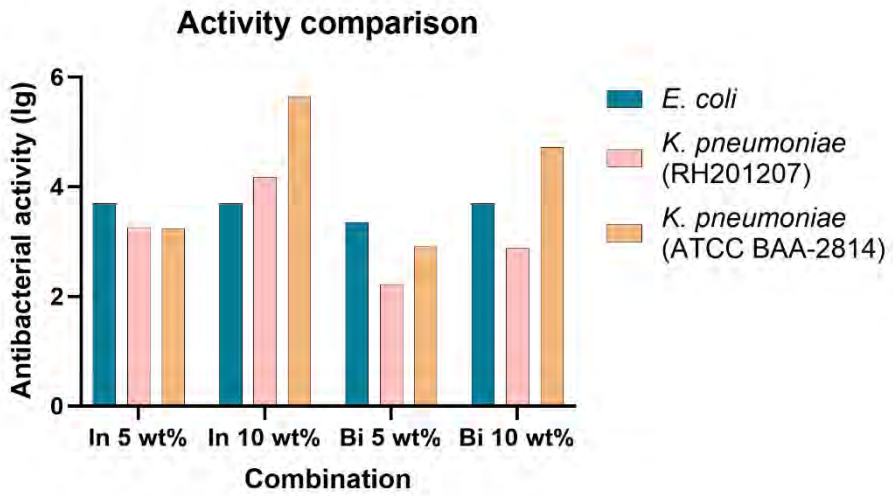

Figure 1: Antibacterial efficacy of Bi and In coatings at varying concentrations against tested bacterial strains.

Acknowledgements
The authors thank the Australian Research Council (DP220103632) and Monash University for financial support, and Prof. Anton Peleg (Monash Centre to Impact AMR) for providing multidrug-resistant bacterial samples.

References
[1] Naghavi M., Vollset S.E., Ikuta K.S., et al. Global burden of bacterial antimicrobial resistance 1990–2021: a systematic analysis with forecasts to 2050. The Lancet 2024; 404: 1199–1226.
[2] Alt V. Antimicrobial coated implants in trauma and orthopaedics–A clinical review and risk-benefit analysis. Injury 2017; 48: 599–607.

S7 – O3

Lights on, resistance off? Investigating bacterial resistance to light-activated graphene

Lazaro B.[1,2], Brites A.[1], Gomes R.[1], Henriques A.P.[1,2], Gonçalves I.C.[1,2]
[1]i3S- Institute for Research and Innovation in Health; [2]GOTECH Antimicrobial, Porto, Portugal.

Introduction

Antimicrobial resistance, the ability of microorganism to withstand antimicrobial drugs, poses a critical global health threat. Light-activated graphene shows promise as an antimicrobial, but its potential to induce bacterial resistance remains unclear. Only one study has explored resistance in irradiated graphene composites, but not graphene on its own.

Aim

This work aims to investigate the potential for bacterial resistance to light-activated graphene oxide (GO) in Staphylococcus epidermidis.

Materials and Methods

GO films were produced by vacuum filtration and characterized before and after irradiation regarding degree of surface morphology (SEM), oxidation degree (XPS), and wettability (contact angle measurements). To assess the potential for bacterial resistance, a sublethal irradiation time (defined as 1 to 2 $\log_{10}$ reduction in viable counts) was determined. A bacterial suspension of *S. epidermidis* ($6{,}65 \times 10^5$ CFU/mL) was subjected to exposures of GO films irradiated with NIR light laser (850 nm, at 130 mA) during different times (2h, 3h and 4h). Bacteria were then exposed to sublethal irradiation time across 15 cycles and colony-forming units were quantified at each irradiation cycle to monitor phenotypic changes. To detect potential genotypic changes, DNA was extracted from bacteria collected at cycles 1 and 15 and analysed by whole-genome sequencing. Control groups assessed the influence of GO films alone and of NIR light alone.

Results

GO films' surface morphology, chemistry and wettability are kept upon NIR irradiation, showing graphene sheets fusion with a wrinkled-like morphology and similar oxidation degree (31%). 3-hour irradiation of GO films with NIR light was defined as the sublethal dose, leading to a reduction of 2 log CFU/mL. Following 15 cycles of repeated exposure and regrowth, the antimicrobial effect was maintained, suggesting no evidence of resistance development. Although small colony variants emerged in the NIR-activated GO condition, their frequency remained stable over time and was not associated with increased survival. This suggests a reversible physiological adaptation rather than a fixed resistance mechanism. Whole-genome sequencing at cycle 15 revealed no resistance-associated exonic mutations in bacteria exposed to NIR-activated GO, whereas a single exonic mutation in an IS110 family transposase was detected exclusively in the GO-alone condition.

Conclusion

These findings provide evidence that NIR-activated GO, under sublethal stress, does not promote resistance in *S. epidermidis* and supports its potential as antibiotic-free and resistance-sparing antimicrobial therapy.

Acknowledgements

Authors acknowledge the financial support from Wellcome Trust Foundation [WT223940/Z/21/Z]

S8
Beyond biocompatibility advanced biomaterials for therapy and repair the DAEDALUS and HYDROHEAL projects

S8 - K1
Bioinspired biomineralized biomaterials with antimicrobial properties for hard tissue regeneration

Aparicio C.[1,2]
[1]Bioinspired Oral Biomaterials and Interfaces (BOBI), Dept. of Materials Science and Engineering, Barcelona East School of Engineering (EEBE), Universitat Politècnica de Catalunya–BarcelonaTech (UPC); [2]Catalan Institution for Research and Advanced Studies (ICREA), Barcelona, Spain

Advanced biomaterials are transforming healthcare by moving from passive biocompatibility to systems that sense, respond and adapt to their environment. This keynote will explore how injectable, printable and 4D biomaterials, capable of changing their 3D structure under thermal, mechanical, electrical or light stimuli, are opening new avenues for minimally invasive regeneration, local drug delivery and smart implants. The keynote lecture will discuss strategies to engineer materials with tailored mechanical behaviour (viscoelasticity, shape-memory, self-healing), controlled degradation and on-demand release, and how these properties can be exploited to modulate cell fate, tissue regeneration and immune responses. Particular attention will be given to antibacterial, anti-infective and inmunomodulatory biomaterials that address the growing challenge of antimicrobial resistance without relying solely on conventional antibiotics. The lecture will also highlight the role of digital tools (modelling, simulation, AI-assisted design and advanced characterization) in accelerating the development and scaling of these systems, and how sustainability considerations, including bio-degradable and bio-absorbable designs, are being integrated in line with emerging regulatory and circular-economy frameworks. Overall, the keynote will provide a perspective on current achievements, bottlenecks and future directions for translating advanced biomaterials into safer, more effective and more sustainable healthcare solutions.

Acknowledgements
This research is part of the EU-funded HYDROHEAL project (101178398, HORIZON Innovation Actions programme).

S8 – O1

Tuning the synthesis of methacrylated alginate hydrogels for enhanced bone regeneration

Reinal I.[1], Traldi C.[2,3,4], Tonda-Turo C.[2,3,4], Gómez-Tejedor J.A.[1,5], Gallego-Ferrer G.[1,5], Gentile P.[1,5]
[1]Center for Biomaterials and Tissue Engineering (CBIT); [2]Dept. of Mechanical and Aerospace Engineering, Politecnico di Torino, Turin, Italy; [3]POLITO BIOMedLAB, Politecnico di Torino, Turin, Italy; [4]Interuniversity Center for the Promotion of the 3Rs Principles in Teaching and Research, Italy; [5]Biomedical Research Networking Centre on Bioengineering, Biomaterials and Nanomedicine (CIBER-BBN), Carlos III Health Institute, Valencia, Spain

Introduction

The prevalence of bone-related disorders has increased in recent decades due to the rising incidence of conditions such as osteoporosis, trauma, infections, and cancer. These pathologies frequently result in fractures that significantly impair quality of life and may be difficult to treat when bone regenerative capacity is compromised. Current clinical strategies rely on autografts, allografts, and commercially available bone substitutes, including ceramic scaffolds, collagen-based matrices, and polymer–ceramic composites. However, many of these materials present important limitations, such as limited osteoinductive capacity, insufficient vascularization, slow or incomplete integration with host tissue, and restricted control over degradation and mechanical properties. In this context, injectable hydrogels have emerged as promising biomaterials due to their minimally invasive administration, ability to adapt to irregular defect geometries, and capacity to provide a supportive microenvironment for tissue regeneration. Among them, alginate-based hydrogels are particularly attractive for bone tissue engineering because of their biocompatibility, tunable physicochemical properties, and ease of chemical modification.

Aim

Develop photocrosslinkable hydrogels based on methacrylated alginate (AlgMA) with tunable physicochemical and mechanical properties suitable for injectable applications in bone regeneration and fracture repair.

Materials and Methods

Alginate was chemically modified through methacrylation to obtain photocurable polymers capable of forming hydrogels under light exposure. A Box–Behnken experimental design was employed to optimize synthesis parameters and control the degree of methacrylation. The resulting AlgMA formulations were chemically characterized using Fourier-transform infrared spectroscopy (FTIR), proton nuclear magnetic resonance (^{1}H-NMR), and size exclusion chromatography (SEC) to confirm successful functionalization and evaluate polymer properties. In addition, rheological analyses were performed to investigate gelation kinetics and viscoelastic behavior, allowing the identification of formulations compatible with injectable delivery and *in situ* crosslinking.

Results

Spectroscopic characterization confirmed the successful incorporation of methacrylate groups into the alginate backbone. The experimental design enabled the identification of synthesis conditions that provided controlled levels of functionalization while maintaining suitable polymer characteristics. Rheological testing demonstrated that the resulting hydrogels exhibited tunable gelation times and mechanical properties, supporting their potential use as injectable materials capable of forming stable networks after photocrosslinking.

Conclusion

The optimized AlgMA hydrogels display physicochemical and rheological properties compatible with injectable biomaterials intended for bone tissue regeneration. These findings represent an important step toward the development of adaptable hydrogel-based scaffolds designed to overcome some of the limitations associated with current bone fracture treatments.

Funding

This work is carried out with the support of EU-funded HYDROHEAL project (101178398, HORIZON Innovation Actions programme).

S8 – O2

Stimuli-responsive composite hydrogels for the treatment of vertebral and alveolar fractures

Traldi C[1,2], Reinal I.[3], Peletto M.[1,2], Madureira D.[4], Coelho C.[4], Gentile P.[3,5], Tonda-Turo C.[1,2],
[1]Dept. of Mechanical and Aerospace Engineering, Politecnico di Torino, Turin, Italy; [2]POLITO BIOMedLAB, Politecnico di Torino, Turin, Italy; [3]Center for Biomaterials and Tissue Engineering (CBIT), Valencia, Spain; [4]FLUIDINOVA S.A., Portugal. [5]Biomedical Research Networking Centre on Bioengineering, Biomaterials and Nanomedicine (CIBER-BBN), Carlos III Health Institute, Valencia, Spain

Introduction

The treatment of bone atrophy and complex fractures remains a significant clinical challenge. Indeed, osteoporosis, infections or trauma may lead to severe bone defects, requiring external interventions to be restored and allow effective healing. Current therapeutic approaches relying on synthetic cements and bone grafts are limited by surgical invasiveness, risk of infections, immune rejection, which can compromise the clinical outcomes. To address these drawbacks, injectable hydrogels have emerged as promising alternatives to develop novel biomaterial-based solutions for bone repair.

Aim

In this study, we propose the design of multi-functional hydrogels, composed of naturally derived polymers and substituted nano-hydroxyapatite, aiming at supporting bone regeneration after vertebral and alveolar fractures.

Materials and Methods

Chitosan and alginate were selected to develop injectable hydrogel formulations, by exploiting both physical and chemical crosslinking strategies. Thermosensitive chitosan-based hydrogels were obtained through the incorporation of β-glycerophosphate, enabling sol-gel transition under physiological conditions. Methacrylated chitosan and alginate were synthetized to obtain photosensitive polymers and achieve fast crosslinking after visible light exposure. The hydrogels were characterized in terms of rheological behaviour, injectability, mechanical properties and biological activity.

Results

According to the results, chitosan/β-glycerophosphate hydrogels showed thermo-induced gelation within 5 minutes and stable gel-like behaviour in physiological conditions. On the other hand, methacrylated polymers were demonstrated to form a chemically crosslinked network in response to blue light irradiation for 2 minutes. In addition, the here developed hydrogel formulations presented shear-thinning behaviour, enabling injectability and tuneable mechanical properties according to polymer and nano-hydroxyapatite concentrations. Lastly, the biocompatibility of hydrogels was also assessed.

Conclusion

The here proposed hydrogels meet essential requirements for *in vivo* applications, representing innovative solutions to develop minimally invasive methods in bone regeneration. Future studies will be aimed at exploring the use of these systems as functional platforms for the local administration of therapeutic compounds.

Acknowledgements

This work is carried out with the support of EU-funded HYDROHEAL project (101178398, HORIZON Innovation Actions programme).

S8 – O3

Bio-orthogonally cross-linked alginate-based hydrogel for bone tissue engineering

Marrone A.M.[1,2], Salthouse D.[2], Tonda-Turo C.[1], Mattu C.[1], Gentile P.G.[3,4], Ferreira-Duarte A.[2]
[1]Dept. of Mechanical and Aerospace Engineering, Politecnico di Torino, Turin, Italy; [2]School of Engineering, Newcastle University, Newcastle Upon Tyne, NE1 7RU, UK; [3]Center for Biomaterials and Tissue Engineering (CBIT), Valencia, Spain; [4]Biomedical Research Networking Centre on Bioengineering, Biomaterials and Nanomedicine (CIBER-BBN), Carlos III Health Institute, Valencia, Spain

Introduction

Bone fractures are common traumatic injuries whose incidence is increasing due to osteoporosis and population ageing. Current treatments based on bone grafts and synthetic biomaterials remain limited by surgical invasiveness and poor tissue integration. Injectable alginate hydrogels are emerging as promising alternatives for bone repair due to their ability to form hydrogels *in situ* under mild physiological conditions. In this context, strain-promoted azide–alkyne cycloaddition (SPAAC) offers a cell-compatible strategy to engineer hydrogels with improved structural stability and tunable mechanical properties.
Here, we developed a SPAAC-crosslinked injectable alginate hydrogel system and investigated how the degree of substitution (DS) influences hydrogel network properties.

Materials and Methods

Alginate was functionalised with alkyne groups via carbodiimide-mediated coupling chemistry and reacted with an azide-based crosslinker to obtain SPAAC-crosslinked injectable hydrogels. The DS of alginate carboxyl groups was tuned to control crosslinking density and hydrogel mechanical properties. Principal component analysis (PCA) was used to identify the main reaction parameters influencing DS activation and to guide the optimisation of the functionalisation process. DS was assessed by ^{1}H NMR, while hydrogels were characterised in terms of mechanical, viscoelastic and injectability properties**.**

Results

PCA indicated that DS was mainly influenced by reaction conditions, particularly reagent concentration and coupling parameters. Chemical characterisation confirmed the successful functionalisation of alginate, enabling the orthogonal SPAAC crosslinking reaction. Rheological and mechanical analyses showed that hydrogel properties varied with DS, highlighting its influence on the structure, viscoelastic behavior, mechanical performance, and injectability of the hydrogel network.

Conclusions

The proposed SPAAC-crosslinked alginate hydrogels represent a promising injectable and cytocompatible platform for bone tissue engineering. The possibility to tune the degree of substitution enables control over the crosslinking density and the resulting mechanical properties. These systems may provide innovative solutions for minimally invasive bone regeneration strategies.

Acknowledgements

This work is carried out with the support of EU-funded HYDROHEAL project (101178398, HORIZON Innovation Actions programme).

S8 – O4

Lipid-composite microspheres (LCM) by CryoXpand® technology: Biocompatible carriers for statins delivery in bone tissue regeneration

Esposito P.[1], Danan H.[1], Cota Carrera P.[1,2], Reinal I.[3], Gentile P. [3,4]
[1] SITEC pharmabio SL, Barcelona; [2] Dept. of Bioengineering, IQS Instituto Quimico de Sarría, Barcelona; [3]Center for Biomaterials and Tissue Engineering (CBIT), Valencia; [4] Biomedical Research Networking Centre on Bioengineering, Biomaterials and Nanomedicine (CIBER-BBN), Carlos III Health Institute, Valencia, Spain

Introduction

The rising incidence in bone fractures and bone-damaging pathologies in aging patients necessitates the development of novel and effective treatments for bone tissue regeneration. In this context, localized delivery of osteogenic statins(1) using biocompatible and biodegradable drug carriers is a promising strategy for introducing better, patient-friendly therapies. Lipid-composite microspheres (LCM) are designed with specific functional and structural properties to enable the delivery of drugs with diverse physico-chemical and biological properties. Lipids can act as biodegradable structuring materials to modulate statins release and locally maintain drug concentrations within the osteogenic window for extended periods. Furthermore, lipids within bone marrow serve as a valuable nutrition source for osteoblasts during the energy-intensive process of bone matrix generation(2).

Aim

To develop biodegradable, lipid-composite microspheres using CO_2-cryospraying technology for the localized and controlled delivery of statins in bone regeneration therapies.

Materials and Methods

Statins-excipients combinations were selected on the basis of Hansen solubility parameters and subsequently confirmed experimentally. Simvastatin-LCM and rosuvastatin calcium-LCM were prepared by combining structuring lipid materials (stearic acid or glyceryl-monostearate) with different functional lipids or polymeric materials. Solid microspheres were produced from liquid, composite blends using CryoXpand®, a cryogenic spraying technology based on liquid-CO_2 expansion and phase transition(3). Microspheres morphology was evaluated by optical microscopy, SEM, and Z-potential by DLS. Drug content and in-vitro drug release profiles in PBS pH 7.4, were determined by UV-VIS spectroscopy. Characterization of statins in microspheres bulk (by DSC and XRD) and on surface (by XPS-ESCA) is ongoing.

Results

LCM-statins were produced by CryoXpand®, as easy-to-handle, flowable powders. Drug content in LCM was 10% for liposoluble simvastatin (encapsulation efficiency >95%), and 5% for water-soluble rosuvastatin calcium (encapsulation efficiency >85%). The resulting microparticles were spherical, with diameters below 100µm (Figure 1). Drug release studies on simvastatin microspheres in PBS showed a “burst” release of 10% at 6 hours, and 30% to 40% after 5 days. Optical microscopy images suggest a diffusion, self-emulsification mechanism (Figure 2). In contrast, rosuvastatin exhibited rapid release (hours), suggesting a preferential drug distribution on particle surface and highlighting the need for formulation optimization. Z-potential values were negative for all microparticles studied, from -11.8 to -62.5 mV for simvastatin-LCM, and -19.2 to -33.9 mV for rosuvastatin-LCM, with differences attributed to excipients combinations.

Conclusions

LCM for localized, controlled delivery of osteogenic statins can be produced by CryoXpand® technology. Particles size and high drug loading facilitate local injectability and offer dosing flexibility. High Z-potential also makes LCM a promising scaffold for surface modification through electrostatic layering of polyelectrolytes.

Acknowledgements

Work funded by EU. HYDROHEAL project (101178398, HORIZON Innovation Actions Program)

References

[1]Granat M., Eifler-Zydel J., Kolmas J. Statins-Their Role in Bone Tissue Metabolism and Local Applications with Different Carriers. *Int.J. Mol. Sci.,* 2024,25, 2378,1-21.
[2]Nandy A, Helderman R., Thapa S., Jayapalan S., Richards A, Narayani N., Czech M., Rosen C., Rendina-Ruedy E. Lipolysis supports bone formation by providing osteoblasts with endogenous fatty acid substrates to maintain bioenergetic status. *Bone Research,* 2023,11: 62, 1-19
[3]Danan H., Esposito P., Caramés J. Process and apparatus for the manufacture of solid microparticles. *PCT/EP2022/084162, EP4440732B1*

Figures

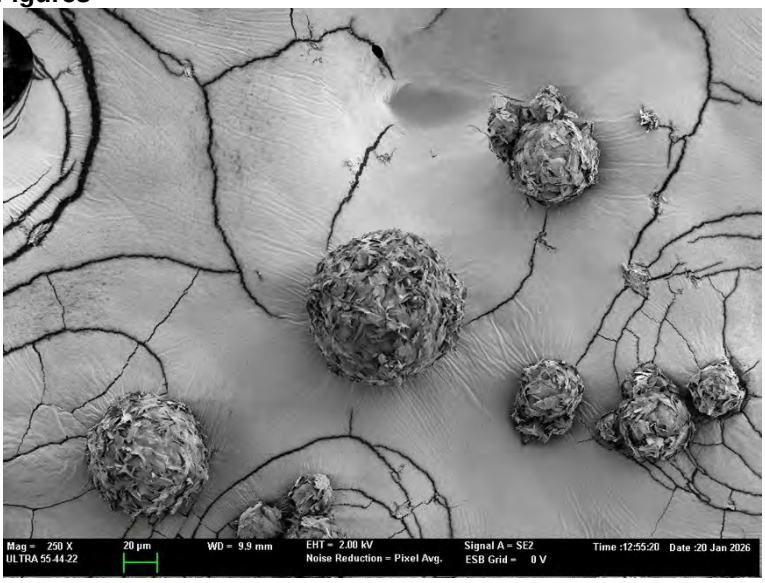

Fig.1. SEM image of simvastatin-Lipid Composite Microparticles

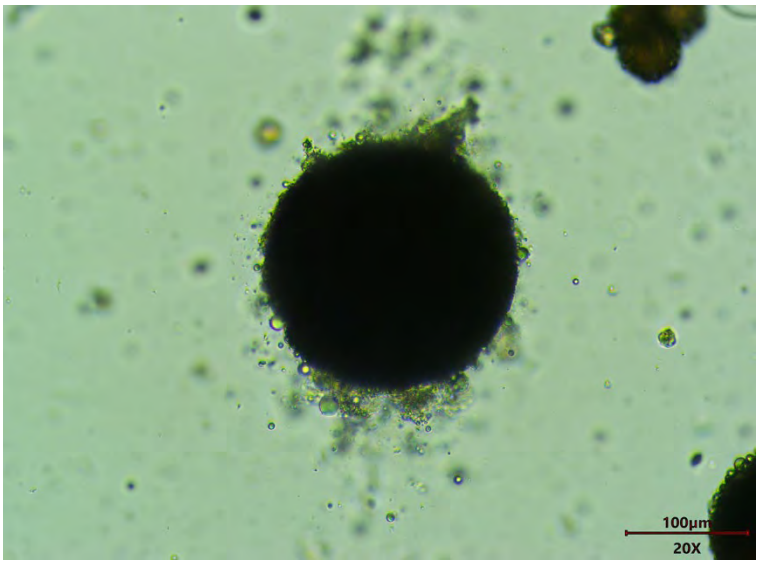

Fig. 2. Optical microscopy (200x) showing formation of diffusional layer and release of oily droplets from simvastatin-LCM (at 30 min in PBS)

S8 – O5

Hemidesmosome-promoting and antimicrobial peptide nanocoatings for transepithelial titanium implants: Evaluation in a post-infection co-culture model

Moreno D.[1], Roquette M.[1], Mallor I.[1], Aparicio C.[1,2]
[1]Bioinspired Oral Biomaterials and Interfaces (BOBI), Dept. of Materials Science and Engineering, Barcelona East School of Engineering (EEBE), Universitat Politècnica de Catalunya–BarcelonaTech (UPC); [2]Catalan Institution for Research and Advanced Studies (ICREA), Barcelona, Spain

Introduction

Transepithelial limb prostheses offer amputees improved comfort and mobility compared with socket-based systems, but their long-term success is limited by inadequate soft tissue sealing and recurrent infections at the skin–implant interface [Ref1: https://doi.org/10.1002/adhm.201770105Digital Object Identifier (DOI)]. Poor epithelial attachment facilitates bacterial colonization, leading to chronic inflammation and eventual failure. Inspired by natural transcutaneous interfaces such as teeth and claws, this work targets to formulate biomimetic multifunctional nanocoatings on Ti6Al4V that upregulate keratinocyte hemidesmosome formation for epithelial sealing [ref2: https://doi.org/10.1016/j.bioactmat.2022.03.019]and suppress methicillin-resistant *Staphylococcus aureus* (MRSA) to avoid microbial infection, comparing two peptide immobilization strategies, and challenging such coatings in a eucaryote-procaryote cell co-culture that modeled early post-implantation infection.

Materials and Methods

Ti6Al4V substrates were functionalized with dual-peptide nanocoatings by covalent co-immobilization of a hemidesmosome-promoting peptide derived from Netrin-1 (Net1) and an antimicrobial peptide derived from salivary secretory proteins (DJK-2). Two immobilization routes were evaluated: (i) silanization with CPTES and (ii) copper-free click-chemistry. Surface wettability and chemistry were characterized by water contact angle and X-ray photoelectron spectroscopy. Biofunctional performance was assessed in three in vitro models: (i) HaCaT keratinocyte monocultures (1 and 3 days) to evaluate adhesion and hemidesmosome-associated marker (α6β4 integrin) via immunofluorescence; (ii) MRSA monocultures (overnight) to quantify biofilm formation, viability (LIVE/DEAD), and metabolic activity (Resazurin); and (iii) a keratinocyte–MRSA co-culture that simulates early infection after implantation. Unmodified Ti6Al4V and single-peptide coatings were used as controls. Statistical analysis was performed using ANOVA with Tukey's post-hoc test ($p<0.05$).

Results

Both silanization and click-chemistry produced multifunctional coatings with increased hydrophilicity and higher C/Ti and N/Ti ratios, confirming effective peptide immobilization. In keratinocyte monocultures, dual-peptide surfaces from both chemistries enhanced cell attachment and hemidesmosome expression after 1 and 3 days compared with unmodified control. A marked reduction in viable MRSA and biofilm formation was assessed on DJK-2 coatings, irrespective of the peptides immobilization route. The co-culture model confirmed the multifunctionality of the dual-peptide coatings in a simulated infection post-implantation condition. Although no major differences were detected between silanization and click-chemistry at the level of main biological outcomes, the click-based coatings yielded more robust responses, attributed to the higher specificity and efficiency provided by this coating method.

Conclusion

The proposed biomimetic nanocoatings provided a multifunctional interface that promoted robust epithelial sealing while limiting MRSA colonization on Ti6Al4V surfaces. By directly comparing silanization and click-chemistry and validating performance in a keratinocyte–bacteria co-culture model, this work supports the translational potential of dual-peptide functionalization strategies to improve long-term stability of dental and transepithelial implants for amputees.

Acknowledgements

Financial support was provided by the MCIN/AEI/10.13039/501100011033 and FSE+ under award PREVENTITIS-PID2022-137496OB-I00 as well as by the Assistant Secretary of Defense for Health Affairs through the Peer Reviewed Orthopaedic Research Program (PRORP) under Applied Research Award No W81XWH-20-1-0563 (CA). The U.S. Army Medical Research Acquisition Activity, 839 Chandler Street, Fort Detrick MD 21702-5014 is the awarding and administering acquisition office. Opinions, interpretations, conclusions, and recommendations are those of the authors and are not necessarily endorsed by the Department of Defense.

References

[1]Abdallah M.-N., Badran Z., Ciobanu O., Hamdan N., Tamimi F. Osseointegrated implants: strategies for optimizing the soft tissue seal around osseointegrated implants. *Advanced Healthcare Materials* 2017; 6: 1700105

[2]Fischer N.G., Aparicio C. Junctional epithelium and hemidesmosomes: tape and rivets for solving the "percutaneous device dilemma" in dental and other permanent implants. *Bioactive Materials* 2022; 18: 178-198.

S8 – O6

Design of an interoperable digital repository of structured and contextualized hydrogel experimentation

Sánchez-García D.[1], Ferri P.[1], Durà-Hernández M.[1], Reinal-Ferre I.[2], Alba-Pérez A.[2], Gallego-Ferrer G.[2,3], Gentile P.[2,3], García-Gómez J.M.[1,3]

[1]Biomedical Data Science Lab, Universitat Politècnica de València; [2]Centro de Biomateriales e Ingeniería Tisular, Universitat Politècnica de València; [3]Biomedical Research Networking Centre on Bioengineering, Biomaterials and Nanomedicine (CIBER-BBN), Carlos III Health Institute, Valencia, Spain

Introduction

Research in hydrogels generates massive experimental data, frequently recorded in analog or unstructured formats. This lack of systematic digitalization leads to critical information loss and hinders trial reproducibility. Currently, no specific repository exists to centralize knowledge for future hybrid in-silico & wet-lab experimentation. Performing cross-sectional analyses between experimental batches remains extremely costly. This is mainly because the contextual information (medatada) such as instrumentation and environmental variables are not usually structurally stored alongside the experimental results, preventing of including them as confounding factors in potential statistical or machine learning models. Consequently, there is an operational need to transform manual workflows of data storage into a digital ecosystem that ensures every experiment is recorded, traceable, and searchable.

Materials and Methods

In this study we introduced a digital repository for structuring and storing data from hydrogel syntheses and characterizations. The platform operates through two complementary streams. First, researchers may directly upload wet-lab experiments through a visual standard interface, including experimental results along with a structured description of the experimental environment. Second, the system integrates Artificial Intelligence (AI) and Natural Language Processing (NLP) modules to extract data from legacy publications, converting unstructured text into usable records. To maintain integrity, the software implements a mandatory "Curated" or "Non-Curated" flag, distinguishing between human verified entries and automated extractions awaiting review. Furthermore, a REST API guarantees interoperability with other laboratory management systems or external analysis tools.

Results

The implementation establishes a centralized digital infrastructure that consolidates all experimental activity. Key outcomes include a fully indexed hydrogel repository designed to support computational simulation models and advanced workflows. By automating data ingestion from both new trials and existing literature, the platform optimizes operational costs and drastically reduces time spent on manual searching and comparison. The REST API architecture ensures the system is scalable and compatible with modern laboratory technological ecosystems.

Conclusion

This study provides the essential foundation of a digital repository for hybrid hydrogel research. By centralizing data and enabling interoperability, the platform eliminates knowledge fragmentation and reduces costs associated with manual data management. This solution facilitates the integration of physical laboratory workflows with in-silico experimentations, accelerating biomaterial discovery aligned to the Common European Data strategy.

Acknowledgements

This research is part of the HYDROHEAL project, funded by the European Union.

S8 – O7

Star-shaped PEG-PLA copolymer/ Gelatin hydrogels for tunable layered materials in colorectal tissue regeneration

Montassier J.[1], Pinese C. [1,2], Vandeputte H.[3], Vozzi G.[4], Van Vlierberghe S.[3], Nottelet B.[1,2]
[1]Polymers for Health and Biomaterials, IBMM, ENSCM, University of Montpellier, CNRS, Montpellier, France; [2]Dept. of Pharmacy, Nîmes University Hospital, Nîmes, France; [3]Polymer Chemistry and Biomaterials Group, Centre of Macromolecular Chemistry, Ghent University, Gent, Belgium; [4]Research Centre "E. Piaggio" and Dept. of Information Engineering, University of Pisa, Pisa, Italy

Introduction

Surgical treatment of colorectal diseases often involves mucosal and submucosal resection, leading to tissue dysfunction. Regenerative approaches require biomimetic constructs reproducing their layered organization. In that frame, the combination of degradable synthetic polymers, providing structural support, with natural polymers, providing improved biocompatibility or even bioactivity, is of advantage to generate layers with tunable mechanical properties. In this contribution, we explore the combination of PEG-PLA star-shaped copolymers with gelatine. The impact of the polymers ratios and of the chemistry used to yield chemically crosslinked hydrogel networks, methacrylate chain-growth versus thiol-ene step-growth, is explored and discussed with respect to tissue engineering application. An overview of both strategies is presented in Figure 1.

Materials and Methods

Multifunctional PEG-PLA star-shaped copolymers were synthesized bearing methacrylate (MA), thiol (SH), or norbornene (NB) groups, enabling chain-growth or step-growth crosslinking. These copolymers were combined with complementary functional-gelatins at varying gelatin-to-polymer ratios to prepare three families of hydrogels: GelMA/PEG-PLA-MA, GelSH/PEG-PLA-NB, and GelNB/PEG-PLA-SH. (Photo)rheological studies were carried out to assess network formation and quantified storage (G′) and loss (G″) moduli as a function of formulation and composition.

Results and Discussion

Preliminary photorheological measurements on GelMA/PEG-PLA-MA show that increasing the PEG-PLA fraction enhances gel-like behavior, with higher G′ and G″ values indicating a more robust network. These trends support the ability of this formulation to form mechanically reinforced hydrogels suitable for further optimization toward layered colorectal tissue constructs. Ongoing work extends this approach to GELSH/PEG-PLA-NB and GELNB/PEG-PLA-SH systems to compare chain-growth and step-growth networks and identify the most promising candidates for mucosa-submucosa regeneration.

Conclusions

The modular combination of methacrylated, thiolated, and norbornene-functionalized star copolymers with complementary gelatin matrices establishes a versatile platform for engineering biomimetic hydrogel architectures. This strategy enables precise control over network chemistry and mechanics, offering a pathway toward layer-specific constructs that replicate the organization of colorectal tissues. Such tunable systems hold significant potential to advance 3D bioprinting and regenerative approaches aimed at restoring complex mucosal structures.

Acknowledgments

This project is funded by the European Union (DAEDALUS G.A.101178568).

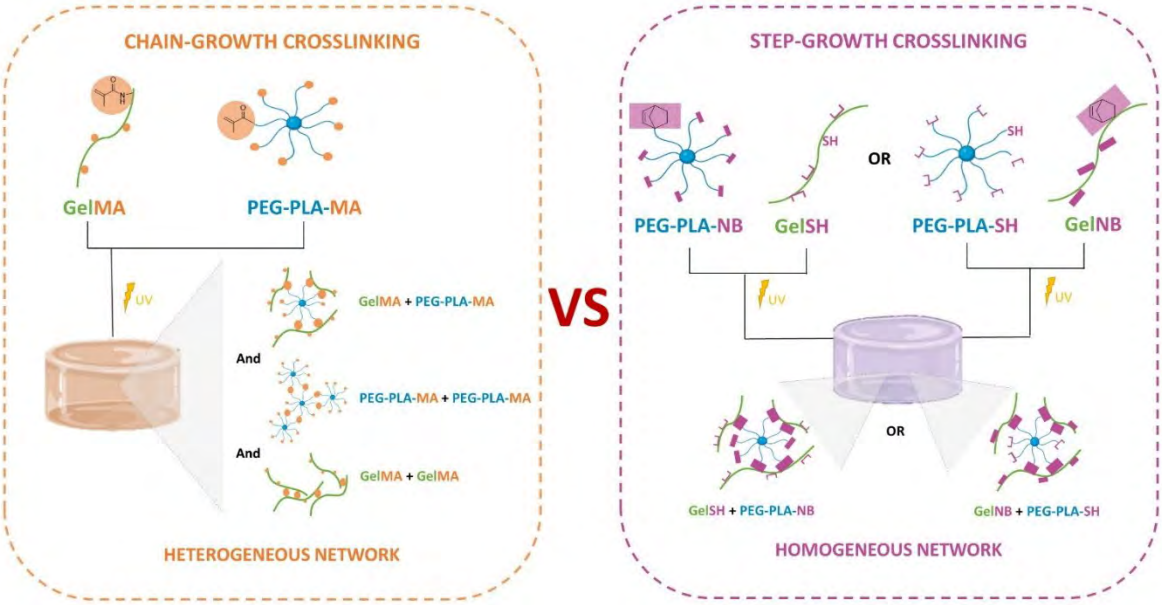

Figure 1: Summary of core concepts

S9
Beyond methacrylates advanced chemistries for dynamic, bioactive hydrogels

S9 - K1
Interactive and anisometric colloidal building blocks for regenerative medicine and tissue engineering

De Laporte L.[1]
[1]DWI – Leibniz Institute for Interactive Materials; [2]Institute of Technical and Macromolecular Chemistry, Macromolecular Materials for Medicine, RWTH; [3]Institute of Applied Medical Engineering, University Hospital Aachen, Advanced Materials for Biomedicine, University Hospital RWTH Aachen, Germany

Introduction
We apply polymeric molecular and micron-scale building blocks to assemble into soft 3D biomaterials with anisotropic and dynamic properties. We focus on injectable materials that can be pipetted using automated systems, bioprinted or delivered *in vivo* in a low invasive manner.

Materials and Methods
Spherical and rod-shaped microgels and fibers are produced by microfluidics, in-mold polymerization, and fiber spinning. To arrange the building blocks in a spatially controlled manner, self-assembly mechanisms and alignment by magnetic fields are employed.

Results
Reactive and/or bioactive spherical and rod-shaped microgels interlink and form macroporous constructs facilitating 3D cell growth and cell-cell interactions or cells are able to use microgels as bricks to build their own house.[1] Chemically defined poly(ethylene glycol)-based microgels, produced via parallelized step-emulsification microfluidics, self-organize with induced pluripotent stem cells (iPSCs) into 3D constructs by robust cell-material interactions.[2] The iPSCs expand and retain their pluripotency, after which they can be differentiated into the three germ layers, providing a suitable platform for organoid differentiation, which was exemplary demonstrated for cardiac organoids. This new organoid production technology enables iPSC expansion and differentiation in the same construct in a reproducible and scalable manner, compatible with high-throughput automation. On the other hand, magneto-responsive rod-shaped microgels form the core of the patented Anisogel technology, which offers a low-invasive therapy to regenerate sensitive tissues with an oriented architecture.[3] It can be injected and structured *in situ* to guide cells in a linear manner. Finally, a thermoresponsive hydrogel system, encapsulated with plasmonic gold-nanorods, actuates by oscillating light and elucidates how rapid hydrogel beating affects cell migration, focal adhesions, extracellular matrix production, and nuclear translocation of mechanosensitive proteins, depending on the amplitude and frequency of actuation.[4] The time spent in the *in vitro* gym seems to affect myoblast differentiation and fibrosis, while actuation seems to induce mesenchymal stem cell differentiation into bone cells.

Conclusion
Injectable colloidal building blocks with a variety of structural, mechanical, and biochemical properties are produced and rendered responsive to external triggers. When combined with cells, they are able to support 3D cell expansion, interaction, differentiation, alignment and mechanical actuation, supporting tissue formation.

1. Bulut S*, Günther D*, Bund M, Haats C, Bissing T, Bastard C, Wessling M, De Laporte L[§], Pich A[§]. Cellular architects at work: cells building their own microgel houses. Advanced Healthcare Materials 2023, 13: e2302957.
2. Klasen L, Mork M, Nasehi R, Krishnamurthy VT, Zeevaert K, Babendreyer A, Di Russo J, Wagner W, De Laporte L. Microgels enable iPSCs to assemble, expand, and differentiate into organoids – from sizable to high throughput. BioRxiv DOI: 10.1101/2025.10.20.683388.
3. Babu S, Chen I, Vedaraman S, Gerardo-Nava J, Licht C, Kittel Y, Haraszti T, Russo JD, De Laporte L. How do the local physical, biochemical, and mechanical properties of a synthetic Anisogel affect oriented nerve growth? Advanced Functional Materials 2022, 32: 2202468.
4. Castro Nava A*, Doolaar IC*, Labude N, Malyaran H, Babu S, Chandorkar Y, Di Russo J, Neuss S[§], De Laporte L[§]. Actuation of soft thermoresponsive hydrogels mechanically stimulates osteogenesis in human mesenchymal stem cells without biochemical factors. ACS Appl. Mater. Interfaces 2024, 16: 30.

S9 – O1

Engineering dynamic covalent hydrogels: Impact of polymer architecture and multivalency on functional properties

Joshi S.[1], Baker M.B.[1]
[1]Dept. of Instructive Biomaterial Engineering, MERLN, Maastricht University, Maastricht, The Netherlands

Dynamic covalent chemistry (DCvC) provides a versatile strategy for constructing adaptive polymer networks with tunable stability and responsiveness. In particular, dynamic hydrogels have attracted increasing attention for applications in soft biomaterials, biofabrication, and 3D printing because their mechanical and dynamic properties can be controlled through molecular design.

In this work, we investigate how polymer architecture influences hydrogel properties by systematically varying crosslinking motifs, linker length, and multivalency. Hydrazine functionalities are introduced onto a polymer backbone through chemical modification using different dihydrazide linkers. These functionalized polymers then crosslinked with aldehyde-based crosslinkers of varying valency (2-, 4-, and 8-arm) and different spacer lengths to form dynamic hydrazone-linked hydrogels.

By comparing ladder-like and network-like architectures, we aim to understand how crosslinker structure and multivalency influence macroscopic material properties. Rheological characterizations are used to evaluate hydrogel stiffness, viscoelastic behavior, and stress relaxation dynamics. Understanding these structure–property relationships is essential for designing materials with predictable mechanical and adaptive behavior.

Overall, this study demonstrates how DCvC can be used as a modular chemical platform to engineer hydrogels with tunable architecture and mechanical properties, providing valuable design principles for future applications in soft biomaterials, biofabrication, and biomedical engineering.

S9 – O2

Sacrificially templated multiscale porous 3D bone models using photo-crosslinkable star-shaped polymers for cell-driven vascularisation

Sert E.[1], Aldemir Dikici B.[1]
[1]Dept. of Bioengineering, Izmir Institute of Technology, Izmir, Turkey

Introduction

Syringe-based 3D printing is widely used for scaffold fabrication; however, low-viscosity emulsions tend to spread during extrusion, resulting in poor structural fidelity[1]. To address this, a reverse engineering strategy integrating emulsion templating based on functionalised PCL with sacrificial PVA templates fabricated *via* FDM is employed, enabling the generation of high-fidelity macrochannels while preserving emulsion-derived microporosity. This approach enables the fabrication of multiscale porous scaffolds for bone regeneration by supporting infiltration and vascular ingrowth[2], and the aim of this study is establishing a reproducible hierarchically porous platform to investigate osteogenic and angiogenic responses using hMSCs and HUVECs cross-talk.

Materials and Methods

Four- and six-arm PCL pre-polymers (4PCLMA and 6PCLMA) were synthesised, methacrylated, and characterised by ^{1}H-NMR, MALDI-TOF, gel fraction, contact angle, and compression testing. Emulsion-templated discs (polyHIPEs) were fabricated and investigated for mechanical properties, swelling, accelerated degradation, protein adsorption, and cytocompatibility (Saos-2, hMSCs and HUVECs). Multiscale scaffolds were produced using FDM-printed PVA templates filled with emulsions, photopolymerised, and template-dissolved. Printing accuracy, morphology, and initial hMSCs responses were evaluated. Ongoing studies include hMSCs-HUVECs co-culture on scaffolds with osteogenic and angiogenic assessment *via* ex ovo CAM and *ex vivo* chick femur organotypic culture.

Results

^{1}H-NMR confirmed methacrylation (~100%), while MALDI-TOF indicated similar molecular weights for pre-polymers. Gel fractions exceeded 90% and contact angles remained below 90°. Mechanical testing revealed a stiffer network for 6PCLMA. PolyHIPEs showed markedly improved mechanical performance in the 6PCLMA, reaching up to ~20-fold higher values, with reduced swelling and slower degradation due to the higher degree of branching. Both polyHIPEs exhibited pronounced protein adsorption and supported the robust viability of Saos-2, hMSCs and HUVECs, while higher metabolic activity and enhanced cell infiltration were observed on the 6PCLMA polyHIPE. SEM confirmed preserved macrochannels, continuous microporosity and high-fidelity in reverse-engineered scaffolds. hMSCs attached and spread effectively on multiscale porous 6PCLMA scaffolds.

Conclusion

Overall, this study introduces a multiscale fabrication strategy that combines reverse engineering with emulsion templating to produce architecturally defined and biologically active scaffolds, extending beyond the microporosity typically observed in polyHIPE structures. These constructs provide controlled platforms for studying cell-driven osteogenic-angiogenic interactions and represent promising platforms for vascularised bone modelling and next-generation bone tissue engineering.

Acknowledgements

We acknowledge funding from the Scientific and Technological Research Council of Turkey (TUBITAK, 2209-A, 1919B012206638), thank Özgü Özkendir and Ece Özmen for contributions to polymer synthesis and characterisation, and acknowledge the TUBITAK 2224-A Programme (2026/2 call, application pending).

References

[1]Sears N.A. et al. Emulsion inks for 3D printing of high porosity materials. Macromolecular Rapid Communications 2016; 37; 1369-1374.
[2]Du S. et al. Bioactive polymer composite scaffolds fabricated from 3D printed negative molds enable bone formation and vascularization. Acta Biomaterialia 2024; 186; 260–274.

S9 – O3

Development of tissue-like microenvironments using dynamic cell-crosslinked hyaluronic acid based hydrogels

Konecna M.[1], McGrath M.[1], Browne S.[1,2,3]
[1]Tissue Engineering Research Group (TERG), Dept. of Anatomy and Regenerative Medicine, Royal College of Surgeons in Ireland (RCSI), Dublin; [2]CÚRAM, Centre for Research in Medical Devices, University of Galway, Galway; [3]Trinity Centre for Biomedical Engineering (TCBE), Trinity College Dublin, Dublin, Ireland.

Introduction

Conventional cell-rich hydrogels fail to adequately mimic native tissue, they lack dynamic mechanical properties like stress-relaxation, as high cell densities interfere with crosslinking. Cell cross-linked hydrogels overcome these limitations and offer a route to develop tissue-like microenvironments with stress-relaxing properties, which have been shown to be critical for cell proliferation and differentiation. Hyaluronic acid (HyA)-based hydrogels offer a tunable system which can be functionalised to enable assembly using cells as active cross-linkers. This approach provides a cell rich hydrogel platform that closely mimics native tissue dynamics. This study uses azide-modified cells as active crosslinkers to develop hydrogels with native tissue-like dynamic properties that support cell function.

Materials and Methods

HyA was modified with dibenzocyclooctyne (DBCO)-amine producing HyA-DBCO, with degree of modification verified by H^1 NMR. Fluorescent microscopy confirmed modification of cell surface glycans of human dermal fibroblasts (HDF) with Ac_4ManNAz introducing azide groups. Cell cross-linked hydrogels were formed by copper-free click chemistry reaction between HyA-DBCO and azide-modified HDF cells. Cell survival was assessed by alamar blue, Live/Dead staining and image analysis focusing on cell elongation visible through F-actin and nuclei staining. Biophysical characterization included stress-relaxation and compression testing was also performed.

Results

Modification of HyA with DBCO groups (12.5%) was confirmed by H^1 NMR, expression of azide groups on cell surface of HDFs was confirmed by microscopy. Maximum azide modification was demonstrated at 150 μM (Figure 1A, 1B) with no impact observed on cell number (Figure 1C). Addition of azide modified HDFs to HyA-DBCO supported stable hydrogel formation. Cell survival was demonstrated post-hydrogel formation (Figure 2A), while extensive cell spreading and elongation of HDFs inside cell cross-linked hydrogels was seen compared to rounded HDFs in poly(ethylene glycol) (PEG)-bisazide cross-linked hydrogels (Figure 2B). Furthermore, cell-crosslinked hydrogels demonstrated stress-relaxing properties (Figure 2C), with a half relaxation time ($\tau_{1/2}$) of 80 seconds comparable to PEG cross-linked hydrogels which did not demonstrate any significant relaxation over time.

Conclusion

Azide functionalised HDF combined with HyA-DBCO enables the formation of a stable hydrogel system. Despite the lack of additional adhesion ligands, azide modified cells rapidly spread in cell-crosslinked hydrogels. Cell-crosslinked hydrogels exhibit stress-relaxation properties that closely mimic viscoelastic behaviour of soft tissues including skin. Cell-crosslinked hydrogels offer a platform technology with great potential to study cell behaviour and for the development of *in vitro* tissue models that more faithfully recapitulate native tissue dynamics.

Acknowledgements

This project is funded by the Health Research Board (ILP-POR-2024-023)

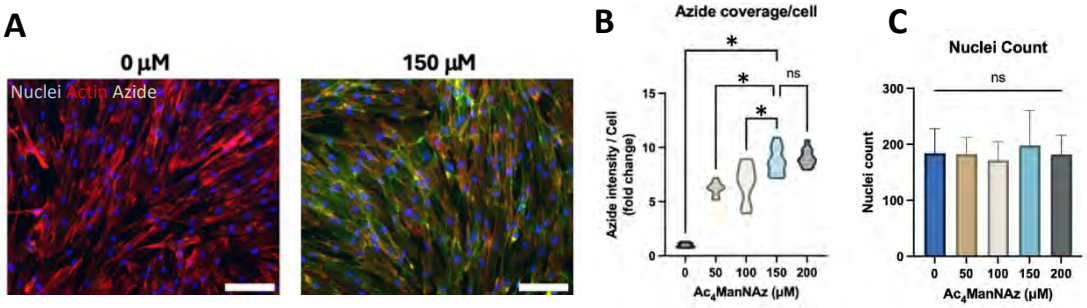

Figure 1: Human dermal fibroblast (HDF) modified with increasing concentrations of Ac_4ManNAz (azides) A) HDF cells modified with 150 µM Ac_4ManNAz and control sample. Scale bar = 150 µm. **B)** Azide coverage per cell showing 150 µM of Ac_4ManNAz results in greatest azide modification **C)** Nuclei count shows no differences across azide concentrations when compared to control. * indicates $p<0.05$.

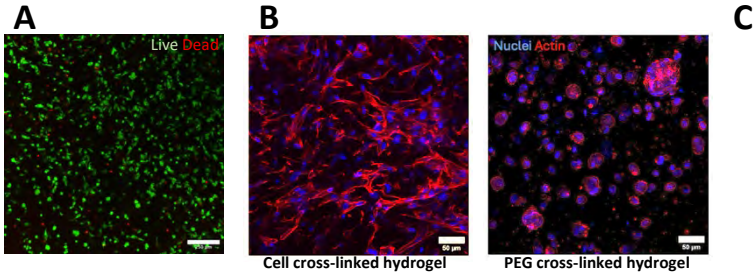

Figure 2: Cell-crosslinked gels support cell spreading and demonstrate stress relaxation comparable with soft tissue A) Live/Dead staining of cell-crosslinked hydrogels after 24 hours. Scale bar = 250 µm **B)** Fluorescent images of cells encapsulated in HyA-DBCO cell cross-linked hydrogels and PEG-bisazide cross-linked hydrogels. Scale bar = 50 µm Blue = nuclei, Red = F-actin. **C)** Stress-relaxation of PEG-bisazide and cell-crosslinked hydrogels showing a clear difference in the viscoelastic behaviour.

S9 – O4

Combining light-based chemistries with supramolecular biomaterials for tissue engineering applications

Sampon T.[1], Pierrard A.[1], Helsen A.[1], Baker M.[1]
[1]Dept. of Instructive Biomaterials Engineering (IBE), MERLN Institute for Technology-Inspired Regenerative Medicine (Maastricht University), Maastricht, The Netherlands

Introduction

The development of synthetic extracellular matrices (ECMs) for tissue engineering requires materials that combine structural hierarchy, mechanical resilience, and dynamic responsiveness. Supramolecular polymers based on benzene-1,3,5-tricarboxamide (BTA) offer an attractive platform due to their ability to self-assemble into one-dimensional fibrils that mimic ECM nanostructure. However, the relatively weak mechanical properties of supramolecular hydrogels limit their use in load-bearing applications. In this study, we combine BTA-based supramolecular polymers with light-based chemistries to reinforce the hierarchical network while enabling stereolithography-based 3D printing and spatiotemporal biofunctionalization.

Materials and Methods

Novel BTA-based supramolecular polymers were synthesized based on previously reported methods[1] and functionalized with methacrylate and norbornene groups, enabling chain-growth and step-growth photopolymerization, respectively. Polymer blends with varying ratios of these functionalities were prepared and characterized using rheology to study their mechanical properties. Supramolecular self-assembly was visualized using cryogenic transmission electron microscopy (cryo-TEM). In addition, the printability and cytocompatibility of the biomaterial were evaluated, alongside strategies for biofunctionalization of this fully synthetic platform.

Results

The polymers were successfully synthesized and characterized using ^{1}H NMR spectroscopy. Rheological analysis of the different polymer blends revealed clear structure-property relationships, demonstrating tunable stiffness, photocuring kinetics, and stress relaxation behavior. Cryo-TEM imaging confirmed the formation of fibrillar supramolecular assemblies at the nanoscale. Ongoing studies investigating printability and cytocompatibility indicate that these light-responsive supramolecular polymers demonstrate potential for mechanically tunable, hierarchical biomaterials suitable for tissue engineering applications.

Funding

This work is supported by the European Union through a European Research Council (ERC) Consolidator Grant under the Horizon Europe programme (Grant agreement ID: 101088285).

References

[1]Hafeez S., Wen Ooi H. Baker M. Desymmetrization via Activated Esters Enables Rapid Synthesis of Multifunctional Benzene-1,3,5 tricarboxamides and Creation of Supramolecular Hydrogelators. *Journal of the American Chemical Society* 2022; 144-9.

S9 – O5

Dynamic hydrogels enable volumetric bioprinting of functional iPSC-derived heart constructs for in vitro cardiac modelling

Bernal P.N.[1,2,3], Janssen J.[3,4], Größbacher G.[1,3], Chirico N.[3,4], Falandt M.[1,3], Cervera i Barea A.[3,4], Brice C.[1,3], Florczak S.[1,3], Mesfin J.[5], Dokter I.[3,4], Snijders Blok C.J.B.[3,4], Christman K.[5], Sluijter J.[3,4], Malda J.[1,2,3], van Mil A.[3,4], Levato R.[1,2,3]

[1]Dept. of Clinical Sciences, Utrecht University, Utrecht, The Netherlands; [2]Dept. of Orthopaedics, University Medical Center Utrecht, Utrecht, The Netherlands; [3]Regenerative Medicine Centre Utrecht, University Medical Centre Utrecht and Utrecht University, Utrecht, The Netherlands; [4]Experimental Cardiology Laboratory, University Medical Center Utrecht, Utrecht, Netherlands; [5]Dept. of Bioengineering, University of California, California, United States

Introduction

Cardiovascular disease is the leading cause of mortality worldwide, yet existing *in vitro* cardiac models struggle to reproduce the structural and functional complexity of human heart tissue. Conventional testing platforms, including 2D cultures and engineered heart tissues, often fail to capture physiologically relevant cell-cell interactions and anatomical organization. To address these limitations, we developed an anatomically-relevant *in vitro* cardiac model using high-speed, contactless volumetric bioprinting (VBP)[1]. This approach enables the rapid fabrication of complex, cell-laden cardiac structures within tens of seconds, overcoming scalability and geometric limitations of conventional bioprinting methods. To induce coordinated contractility, the bioprinted heart platform incorporates HybriGel, a novel dynamic hydrogel that provides enhanced viscoelasticity and structural stability while promoting cell-cell interactions and cardiomyocyte network formation.

Materials and Methods

Bi-chamber heart models were fabricated via VBP using a co-culture of human induced pluripotent stem cell-derived cardiomyocytes (iPSC-CMs) and cardiac fibroblasts (10:1 ratio, $10x10^6$cells/mL) embedded in HybriGel. HybriGel enables covalent bonding via methacryloyl groups under light exposure, and supramolecular assembly through cyclodextrin-adamantane host-guest interactions, creating a dynamic matrix conducive to cellular organization. Cell viability, network formation, and structural organization were assessed using LIVE/DEAD assays and immunofluorescence imaging. Functional characterization included beating rate analysis and calcium handling imaging. To evaluate disease modelling capabilities, myocardial infarction was simulated via cryoinjury at the apex of the heart constructs, followed by histological, functional, and RNA sequencing analysis.

Results

Heart models (~165mm³, printing time=21s) showed high shape fidelity to the original STL file (**Fig1A**). VBP enabled the generation of complex geometries, including asymmetric chambered structures and a four-chamber heart replica (Fig1B). iPSC-CMs cultured in HybriGel maintained >75% viability and exhibited enhanced network formation compared with fully covalent GelMA controls over two weeks of culture (Fig1C,D). The printed hearts displayed coordinated contractions and directional calcium waves within one week of culture. Immunofluorescence imaging confirmed alignment of cardiomyocyte networks along chamber walls and septal regions. Cryoinjury induced localized disruption of calcium signaling and signal asynchrony throughout the entire heart wall. RNA sequencing of injured vs. control samples revealed upregulation of genes associated with fibrotic remodeling and ECM deposition, mirroring clinical patterns observed post-myocardial infarction.

Conclusion

The bioprinted heart model introduced here demonstrates that VBP combined with dynamic biomaterials enables the rapid fabrication of anatomically relevant cardiac tissues that support functional cardiomyocyte organization and injury responses. This scalable platform offers a promising tool for disease modelling, drug screening, and the development of personalized cardiac therapies.

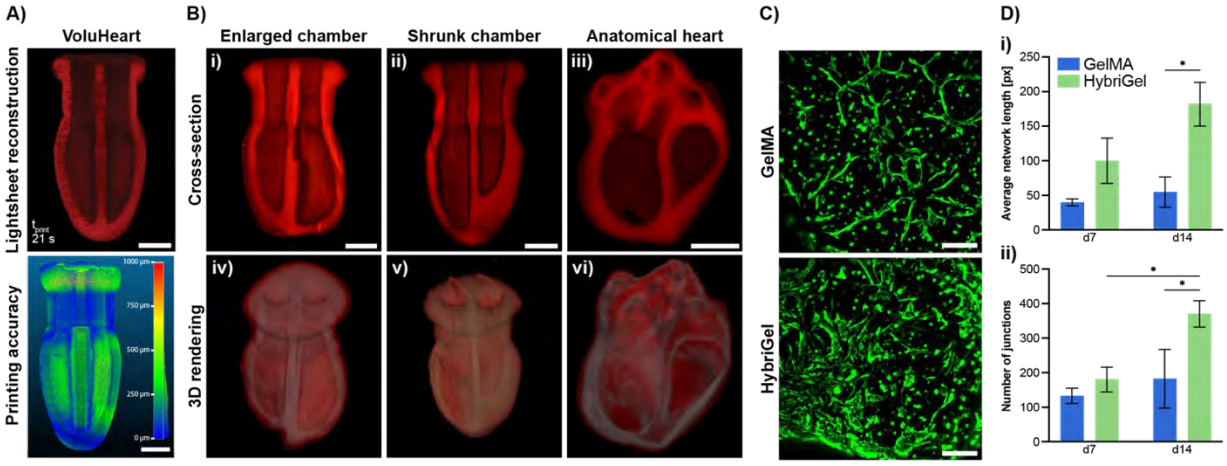

A) Lightsheet reconstruction of the bi-chamber VoluHeart and cloud-to-cloud distance difference map showing the size variation of the volumetric heart compared to the original STL file (scale bar = 2 mm). Bi-iii) Cross-sectional views and iv-vi) full 3D renderings of complex heart models depicting: i,iv) an enlarged chamber, ii,v) a shrunk chamber and iii,vi) an anatomical heart model (without valve structures) obtained through lightsheet microscopy (scale bars = 2 mm). C) Fluorescent images of volumetrically printed iPSC-derived cardiomyocytes stained with cardiac troponin T after 14 days of culture in gelMA hydrogels and the dynamic HybriGel resin (scale bars = 200µm), and D) quantification of the resulting cellular networks formed over this culture period, showing i) average network length and ii) the number of intercellular junctions.

References

[1] P. N. Bernal, *et al.*, *Advanced Materials* **2019**, *31*, DOI 10.1002/adma.201904209.
[2] J. W. Buikema, *et al.*, *Cell Stem Cell* **2020**, *27*, DOI 10.1016/j.stem.2020.06.001.
[3] M. Falandt, *et al.*, **2025**, DOI 10.1101/2025.01.06.631505.

S9 – O6

Development of boronate ester-based biomaterial inks for 3D bioprinting: Correlating rheology and printing

Tewari H.[1], Babilotte J.[1], Saint-Pé G.[1], Terriac L.[1], Loll F.[1], Garnier C.[2], Boutet M. A.[1], Blanchard F.[1], Delplace V.[1,]
[1]Université de Nantes, CHU Nantes, INSERM, Regenerative Medicine and Skeleton (RMeS) UMR 1229; [2]INRAE, UR1268 Biopolymères Interactions Assemblages, Nantes, France

Introduction

3D bioprinting is a promising technology for fabricating tissue-like constructs in tissue engineering and regenerative medicine. As the field of extrusion bioprinting advances, the development of suitable bioinks becomes equally essential. These cell-laden biomaterials must exhibit smooth extrusion while maintaining good resolution and structural stability. However, bioink printability remains poorly understood, particularly regarding rheological properties.

Aim

Through this project, we aimed to investigate the relationship between rheology and printing in dynamic hydrogels using boronate ester (BE) networks.[1] We have recently demonstrated that BE hydrogels are extrudable, yet limited in printing resolution, particularly in cell media.[2] This study identifies key rheological parameters impacting their performance as biomaterial inks for extrusion bioprinting.

Materials and methods

Using hyaluronic acid (HA; 1% [w/v]) as a base polymer and a common culture medium (α-MEM medium), we established a library of BE hydrogels combining *ortho*-aminomethylphenylboronic acid (*o*-AM-PBA) and glucamine-modified HA precursors across different MWs (10 to 200 kDa). Rheological properties, including storage and loss moduli, viscosity, yield stress, thixotropy, stress relaxation, and shear-thinning index, were systematically evaluated. Printability was assessed using extrusion printing by varying nozzle and needle diameters, as well as printing pressure and speed. Printing performance was characterised by assessing filament diameter, stacking ability, and printability index. Rheological parameters were then correlated with printing outcomes. We next investigated the stability of selected BE hydrogel formulations by monitoring mass and dimensions using various crosslinking strategies, such as methacrylation and click chemistry (i.e., Inverse Electron-demand Diels-Alder).

results and discussion

We first assessed the effect of needle versus conical nozzles on the printing of standard BE hydrogel formulations and demonstrated that needles produced more uniform filaments with shape fidelity, allowing printing down to 500 µm using a 30G needle (up to 5 layers). As shown by lower extrusion pressures and smaller filament diameters, combining high- and low-MW HA precursors (e.g. 200 kDa with 10 kDa) improved printability in comparison to using only high or low MW combinations. We identified that complete thixotropy (full recovery of G') is essential for homogeneous printing, while storage modulus influences the printing pressure and needle selection, with a range of viscosity indicating smooth extrusion. These insights played an important role in achieving improved printing resolution than ever before with our BE hydrogels (approx. 400-500 µm). The particular combination of *o*-AM-PBA-modified HA (100 kDa) and Glucamine-modified HA (10 kDa) showed a suitable set of rheological properties (i.e., thixotropy, G' of 50 Pa, and viscosity of 7 Pa.s), enabling the fabrication of 5-layer grids with a filament resolution of 500 µm. However, this formulation showed limited stability (approx. 10 hours) in culture medium after printing. To improve stability, methacrylation was used for photo-crosslinking post-printing, resulting in stability (i.e., minimal change in mass) at physiological conditions up to 28 days. As a light-free alternative, a second-step click crosslinking using IEDDA was explored, providing stable constructs and potentially enabling post-printing modifications. Ongoing work is focused on evaluating the cytocompatibility of the complete system to enable its broader applications in 3D bioprinting.

Conclusion

Overall, this work establishes how key rheological parameters, specifically thixotropy, storage modulus, and viscosity, influence the printability of BE-based dynamic bioinks. The identified rheological window and optimised BE formulation provide a practical framework for achieving high-resolution and stable 3D printing in cell medium. While methacrylation and click chemistry approaches improved structural stability and enabled more complex architecture, further expansion of the range of physical properties and evaluation of cytocompatibility with different cell types will support their translation to 3D and 4D bioprinting applications.

References:

1. Terriac, et al., Chem. Mater. 36, 6674–6695 (2024)
2. Tournier, et al., Advanced Science 10, 2300055 (2023)

S9 – O7

Thiol-ene PEG-tuned ha-norbornene hydrogels enhance brain organoid diffusion and maturation

Vilche A.[1,3], Katimi V.[5,6], Mañez J.[1], Rodriguez S.[1], Xuriguera E.[2], Ortega J.A.[5,6], Alvarez Z.[1,7], Castaño O.[3,4,7,8]

[1]Biomaterials for Neural Regeneration Group, Institute for Bioengineering of Catalonia (IBEC), The Barcelona Institute of Science and Technology (BIST); [2]Materials Science and Physical Chemistry, University of Barcelona, Barcelona; [3]Electronics and biomedical engineering, University of Barcelona, Barcelona, Spain. [4]Biomaterials for Regenerative Therapies, Institute for Bioengineering of Catalonia (IBEC), The Barcelona Institute of Science and Technology (BIST), Barcelona; [5]Pathology and Experimental Therapeutics, Institute of Neurosciences, University of Barcelona, L'Hospitalet de Llobregat, Barcelona; [6]Institut d'Investigacio Biomèdica de Bellvitge (IDIBELL), L'Hospitalet del Llobregat, Barcelona; [7]CIBER en Bioingeniería, Biomateriales y Nanomedicina, CIBER-BBN, Madrid; [8]Institute of Nanoscience and Nanotechnology (IN2UB), University of Barcelona (UB), Barcelona, Spain

Introduction

Matrigel variability limits brain organoid reproducibility and standardization[1]. The complex organization of the central nervous system (CNS) is difficult to reproduce in vitro, limiting the development of physiologically relevant neural models[2]. Conventional HA-methacrylate hydrogels couple mechanics and mesh size, forming dense networks that restrict molecular and cellular diffusion. To address this limitation, we introduce PEG-tuned HA-norbornene hydrogels formed by thiol-ene photochemistry, providing defined porous CNS-like matrices that support brain organoid growth and maturation[3, 4]

Materials and Methods

HA was functionalized with norbornene groups and combined with PEG-dithiol crosslinkers of 2000-5000 Da to modulate hydrogel porosity. Networks were formed by photopolymerization with controlled light intensity. Hydrogel architecture, mechanics, and transport properties were characterized using SEM, swelling assays, rheology, and diffusion studies. Bioinks were then combined with pre-formed human brain organoids to evaluate integration, viability, and maturation during long-term culture. HA-methacrylate hydrogels were used as controls.

Results

FTIR and NMR confirmed HA-norbornene and HA-methacrylate functionalization. Hydrogels showed storage moduli between 0.1 and 2.4 kPa, within the reported range of CNS tissue[2]. SEM revealed tunable microarchitectures, while diffusion coefficients for a 70 kDa dextran were 8-fold higher in HA-norbornene than HA-methacrylate controls. When combined with human brain organoids, the bioinks supported robust neural cell integration, sustained viability, and progressive maturation while maintaining structural integrity.

Conclusion

PEG-tuned HA-norbornene hydrogels formed by thiol-ene photochemistry create defined networks with CNS-like mechanics and larger mesh size than HA-methacrylate controls, which allows faster diffusion of biomolecules. These matrices support long-term brain organoid culture and reduce Matrigel-driven variability, offering a controlled platform for more reproducible neural disease and drug testing models.

Acknowledgements

We acknowledge the financial support from the European Union's Horizon Europe research & innovation program (EIC-2021-PATHFINDER-OPEN-01-01-101047099 4DBR) and Grants, PID2021-124839OA-I00, PID2020-114407RA-100 and PID2024-159777OB-I00 funded by the Ministry of Science and Innovation of Spain (MCINAEI/10.13039/501100011033). Grant R01AG086270, funded by the National Institute on Aging of the National Institutes of Health (NIH); Grant P199, supported by the IRP Research Foundation. Funded by the European Union (ERC, 101230979 - SpineCraft) under the European Union's Horizon Europe research and innovation program. We acknowledge support from the Ramón y Cajal Program RYC2020-028732-I. Institutional support was provided by IBEC, which acknowledge the Centro de Excelencia Severo Ochoa (Grant CEX2023-001282-S, funded by MICIU/AEI/10.13039/501100011033).

References

[1]Kim, D., Youn, J., Kim, J., From organoid culture to manufacturing: technologies for reproducible and scalable organoid production. *Npj Biomadical innovations* 2026, 3; 12.

[2]Axpe, E., Orive, G., Franze, K., Towards brain-tissue-like biomaterials. *Nature communications* 2020, 11; 10-13.

[3]Nisbet, D., Crompton, K., Horne, M., Neural Tissue Engineering of the CNS Using Hydrogels. *Journal of Biomedical Materials Research - Part B Applied Biomaterials* 2008, 87, 251-263.

[4]Madhusudanan P., Raju G., Shankarappa S. Hydrogel systems and their role in neural tissue engineering. *J. R. Soc. Interface* 2020, 17.

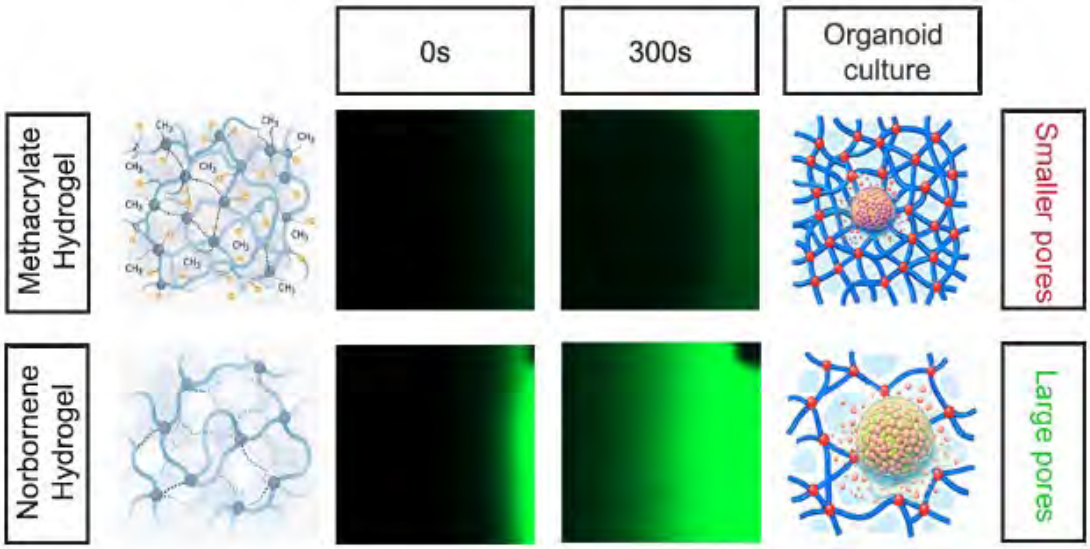

Figure: Comparison of Methacrylate and Norbornene hydrogel networks.

S10
Bio-fabrication and bioactive biomaterials for regulating the host-graft interactions advances and challenges in the field

S10 - K1
Exploiting keratin versatility to produce novel templates for biomedical applications

Ng K.W.[1,2,3]
[1]School of Materials Science and Engineering, Nanyang Technological University; [2] Nanyang Environment and Water Research Institute; [3] Skin Research Institute of Singapore, Singapore

Introduction
A variety of waste biomass sources are being explored as raw materials to produce sustainable biomaterial platforms. Keratinous wastes such as hair, feather and wool are recent examples. In particular, keratins derived from human hair are one of the few human-derived materials that are readily accessible in abundance, and could circumvent pathogenic, immunological, cultural and religious concerns associated with animal-derived materials. These keratins are easily processed into a variety of physical formats that are capable of inducing positive cell and tissue responses to support repair and regeneration. This presentation showcases our recent efforts in developing two novel keratin-based templates for practical applications.

Materials and Methods
In the first development, we adopted the technique of Interfacial Polyelectrolyte Complexation (IPC) to produce keratin-based fibers.[1] Oppositely charged keratins were allowed to interact physically. A solid phase formed at the interface was unidirectionally drawn to produce a continuous fiber. Physical and mechanical properties were characterized and the suitability of this fiber as a suture was tested *in vivo* using an incisional wound model in mice. In the second development, thiolate interaction with cations was used to produce a gradient hydrogel.[2] Specifically, we used silver as the crosslinker to effect silver-thiolate complexation with keratins. By exploiting simple diffusion of silver ions through a keratin solution, we produced a gradient hydrogel in a single-step process. This hydrogel was tested *in vivo* using an excisional wound model in mice.

Results
The keratin-based IPC fibers were of consistent morphology, stable, flexible and strong enough to be knotted. These fibers functioned well as sutures to support closing of full-thickness cutaneous wounds in mice. The fibers evoked minimal host tissue response over 3 weeks, comparable to commercial sutures made from synthetic polymers, with onset of biodegradation after 1 week. Separately, the keratin-based gradient hydrogels presented variations of large to small pore size microarchitecture across high to low silver ion concentration diffusion gradient. These gels released silver ions as an antimicrobial agent as they degraded. When used as a dressing on full-thickness excisional wounds, the hydrogels induced more collagen production in the wound bed compared to controls.

Conclusion
Using established and simple fabrication techniques, it is possible to produce functional keratin-based biomaterials in the forms of fibers and gradient hydrogels for potential use as sutures and tissue regeneration templates, respectively. This work demonstrated the potential of using human hair keratins to produce practical and sustainable biomaterial platforms.

References
[1]Foo L.L.E., Logeshwari M.N., Czarny B., Ng K.W. Development of Keratin-based Fibers Fabricated by Interfacial Polyelectrolyte Complexation for Suture Applications. *Biomaterials* 2024; 314; 122878.
[2]Yee M.Z.L., Lim Y.W., Logeshwari M.N., Czarny B., Ng K.W. One-Step Tunable Human Hair Keratin Gradient Hydrogel with Antibacterial Activity for Tissue Engineering. *SMALL* 2025; 21(52); e09775.

S10 - O1

Light-addressable liquid crystal elastomer metamaterial scaffolds for dynamic skeletal muscle regeneration

Banerjee H.[1], Kim D.[1], Kar-Narayan S.[1]
[1]Dept. of Materials Systems Engineering, Max Planck Institute for Dynamics of Complex Technical Systems (MPI-DCTS), Magdeburg, Germany

Introduction

Skeletal muscle regeneration and functional organization are strongly governed by dynamic mechanical cues that regulate myoblast alignment, fusion, and maturation. However, most biomaterial scaffolds used in tissue engineering provide static mechanical environments and therefore fail to reproduce the spatiotemporally varying mechanical signals present in native extracellular matrices. Developing biomaterials capable of delivering programmable mechanical stimulation within engineered tissues therefore remains a key challenge in regenerative medicine. Liquid crystal elastomers (LCEs) are anisotropic soft materials in which molecular orientation is coupled to macroscopic deformation, enabling reversible and controllable actuation. Here we investigate photocurable LCE metamaterial scaffolds fabricated via architected additive manufacturing as light-addressable biomaterial matrices capable of generating localized mechanical stimulation within engineered skeletal muscle microenvironments (Figure 1).

Materials and Methods

Photocurable LCE resins were processed using extrusion-based printing and melt electrowriting to fabricate architected metamaterial scaffolds with controlled filament orientation and hierarchical porosity. Shear-induced alignment during printing programmed the nematic director orientation within the LCE network, producing anisotropic mechanical properties following photopolymerization. The resulting porous architectures were designed to support cell infiltration, nutrient transport, and mechanical compliance comparable to skeletal muscle extracellular matrices.

To achieve optical addressability, the LCE networks incorporated photothermal components capable of converting visible or near-infrared illumination into localized thermal stimuli that induce controlled LCE deformation. Spatially focused light stimulation generated programmable actuation in selected scaffold regions. C2C12 murine myoblasts were cultured on the printed scaffolds to evaluate cell–material interactions. Cellular responses were analyzed using fluorescence microscopy, immunostaining of myogenic markers, and quantitative assessment of cellular alignment and morphology.

Results

Initial experiments demonstrate that the printed LCE architectures undergo reversible deformation under external light stimulation, enabling localized modulation of strain fields within the scaffold. Optical actuation produced spatially confined deformation of printed filaments, indicating that light-addressable mechanical stimulation can be achieved within the architected matrix. Preliminary in vitro studies with C2C12 myoblasts show sustained cell attachment and viability during early culture. Quantitative fluorescence imaging indicates preferential cellular alignment along printed filament directions. Compared with non-actuated controls, dynamically actuated scaffolds exhibit increased cellular elongation and directional organization. The interconnected porous architecture further supports nutrient transport and multicellular organization within the scaffold.

Conclusion

Photocurable LCE metamaterials provide a promising strategy for engineering dynamic biomaterial scaffolds capable of delivering localized mechanical stimulation. By integrating architected additive manufacturing with light-addressable actuation, this platform enables spatially programmable mechanical environments for studying mechanobiology and guiding skeletal muscle tissue formation.

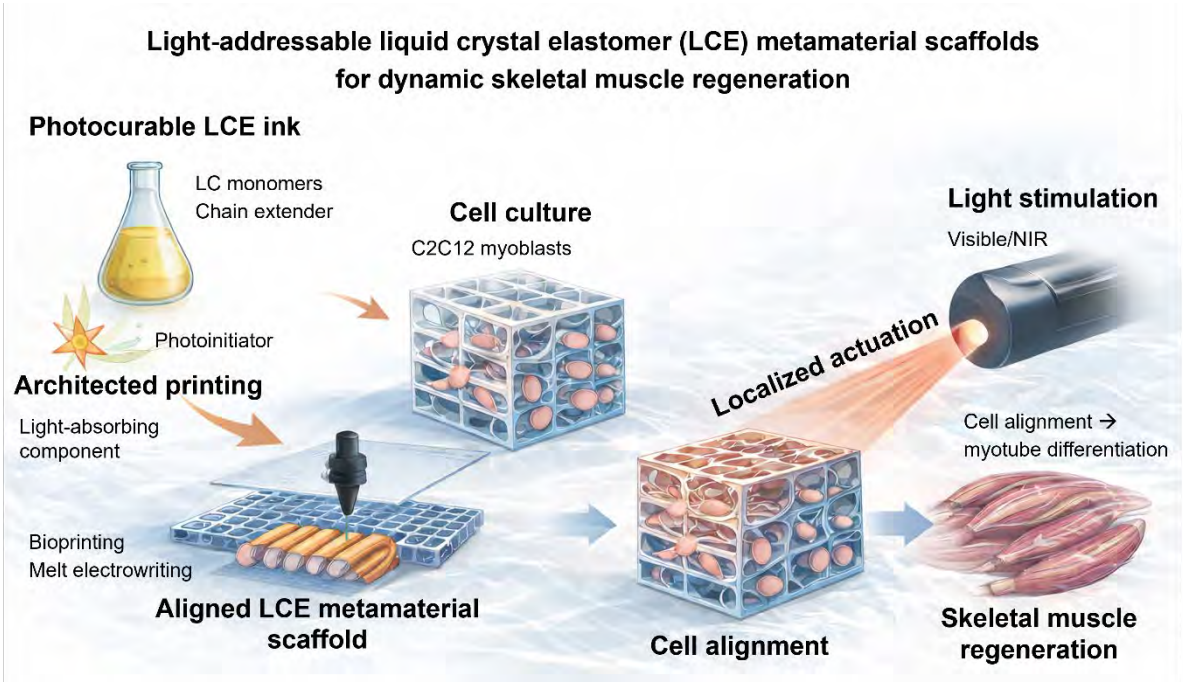

Figure 1: Light-addressable liquid crystal elastomer metamaterial scaffolds for dynamic skeletal muscle regeneration.

S10 – O2

Bioactive implant surface coatings using biomolecules derived from probiotic microflora

Lohar R.[1,2], Nikutta K.[1,2], Stiesch M.[1,2], Rahim I.R.[1,2]
[1]Dept. of Dental Prosthetics and Biomedical Materials, Hannover Medical School; [2]Lower Saxony Centre for Biomedical Engineering, Implant Research and Development (NIFE), Hannover, Germany

Introduction

Probiotic microflora-derived biomolecules are involved in adhesion, biofilm formation, and host interactions. Their diverse structures underlie varied biological properties and are increasingly studied for biomedical use due to their biocompatibility and immunomodulatory potential. Since implant surface properties influence microbial colonization and host responses, such biomolecules that inhibit pathogen adhesion and biofilm formation while remaining compatible with mammalian cells are promising candidates for implant coatings that reduce infection risk and support host integration.

Materials and Methods

Biomolecules were isolated from anaerobic cultures of probiotic bacteria and coated on cell culture plates and titanium discs. Biofilm assays were performed with *Porphyromonas gingivalis* and a dysbiotic oral multispecies consortium comprising *Streptococcus oralis*, *Veillonella parvula*, *Actinomyces naeslundii*, and *Fusobacterium nucleatum*. Bacterial growth was assessed by OD_{600} measurements, CFU counts, and live/dead imaging. Biocompatibility was evaluated by culturing human cell lines on biomolecule-coated surfaces, followed by live/dead imaging before studying complex tissue models.

Results

Coated plates reduced OD_{600} values and CFUs of *P. gingivalis* compared with controls. Live-dead imaging confirmed reduced bacterial attachment and biofilm formation, with only sparse planktonic cells on coated surfaces, while controls showed dense biofilms. The coating also reduced the proportion of viable cells in dysbiotic multispecies biofilms, along with lower OD_{600} values and CFU counts, indicating inhibited growth. Biomolecule coating on titanium discs prevented a 72-h *P. gingivalis* biofilm formation and reduced bacterial growth in the surrounding medium, indicating antibacterial and antibiofilm activities. MG63 cells adhered and maintained normal morphology on coated surfaces, while THP-1-derived macrophages showed spindle-like morphologies consistent with polarization toward an M2-like anti-inflammatory phenotype.

Conclusion

Probiotic-derived biomolecule coatings significantly inhibit pathogenic oral biofilm formation while maintaining compatibility with mammalian cells and promoting anti-inflammatory macrophage responses. These combined antibacterial, antibiofilm, and immunomodulatory effects highlight the potential of probiotic biomolecules as multifunctional coatings for biomedical implants, particularly where prevention of infection and improved host integration are critical.

S10 – O3

Biofilm prevention and quorum-sensing interference via surface-bound peptoid

Najmi Z.[1], Gamna F.[2], Cochis A.[1], Penteado Battesini Carretero G.[3], Mojsoska B.[3], Malesevic M.[4], Rimondini L.[1], Spriano S.[2]
[1]Università del Piemonte Orientale UPO, Dept. of Health Sciences, Center for Translational Research on Autoimmune and Allergic Diseases–CAAD, Novara, Italy; [2]Politecnico di Torino, Turin, Italy; [3]Dept. of Science and Environment, Roskilde University, Roskilde, Denmark; [4]Institute of Molecular Genetics and Genetic Engineering, University of Belgrade, Belgrade, Serbia

Introduction

The emergence of antibiotic resistance has ushered in a post-antibiotic era, highlighting the urgent need for alternative, cytocompatible antimicrobial strategies. Among these, antimicrobial peptides (AMPs) are promising to overcome antibacterial resistance, being at the same time cytocompatible, but they are limited by fast enzymatic degradation. Peptoids are synthetic and bio-mimetic biomolecules that overcome the limitations of AMPs with resistance to proteolytic degradation. This study examined the inhibitory effect of biofilm formation on the titanium implants loaded with peptoid, GN2-Npm9, via interference with the quorum-sensing (QS) system.

Materials and Methods

Ti6Al4V samples were chemically pre-treated (CT) to favour osteointegration and functionalization with GN2-Npm9, synthesized via solid-phase chemistry and purified by reverse-phase HPLC. Physicochemical properties of the functionalized CT samples and the release characteristics of peptoid from the samples were evaluated. The peptoid's antibacterial efficacy was validated using multi-species oral microbiota isolated from the plaque of patients affected by periodontitis. This approach allowed us to test the efficacy of the functionalization in a model much closer to the clinical scenario and to understand the specific effect of the peptoid on the different populations by proteomics. Finally, a deep evaluation of the interference of GN2-Npm9 with QS systems was performed using a culture of *Pseudomonas aeruginosa*.

Results

Zeta potential titration curves indicated an electrostatic attraction between the peptoid and the CT substrate on the functionalized samples. XPS analysis and fluorescence microscopy confirmed the presence of the peptoid on CT_GN2-Npm9 and evidenced a uniform distribution. The functionalized samples were subjected to biological assays against oral plaque collected from patients affected by periodontitis, showing a biofilm reduction of 60% in comparison to CT and a specific effect towards pathogens, as evidenced by proteomics studies (Figure 1). To investigate the mechanism of biofilm prevention, a culture of *P. aeruginosa* was performed by conditioning the culture medium with the supernatant from the plaque test, demonstrating that the biofilm of *P. aeruginosa* was significantly reduced due to a peptoid's indirect effect, due to down-regulation of the expression of genes involved in the quorum-sensing network and the elastase gene (lasB).

Conclusion

These findings demonstrate how a rationally designed synthetic peptoid can be integrated onto a clinically relevant titanium surface, not only to reduce microbial colonization but also to modulate bacterial communication pathways. Furthermore, the application of complementary surface analyses, combined with proteomic and gene expression studies, provided a detailed mechanistic understanding of the material–biofilm interface.

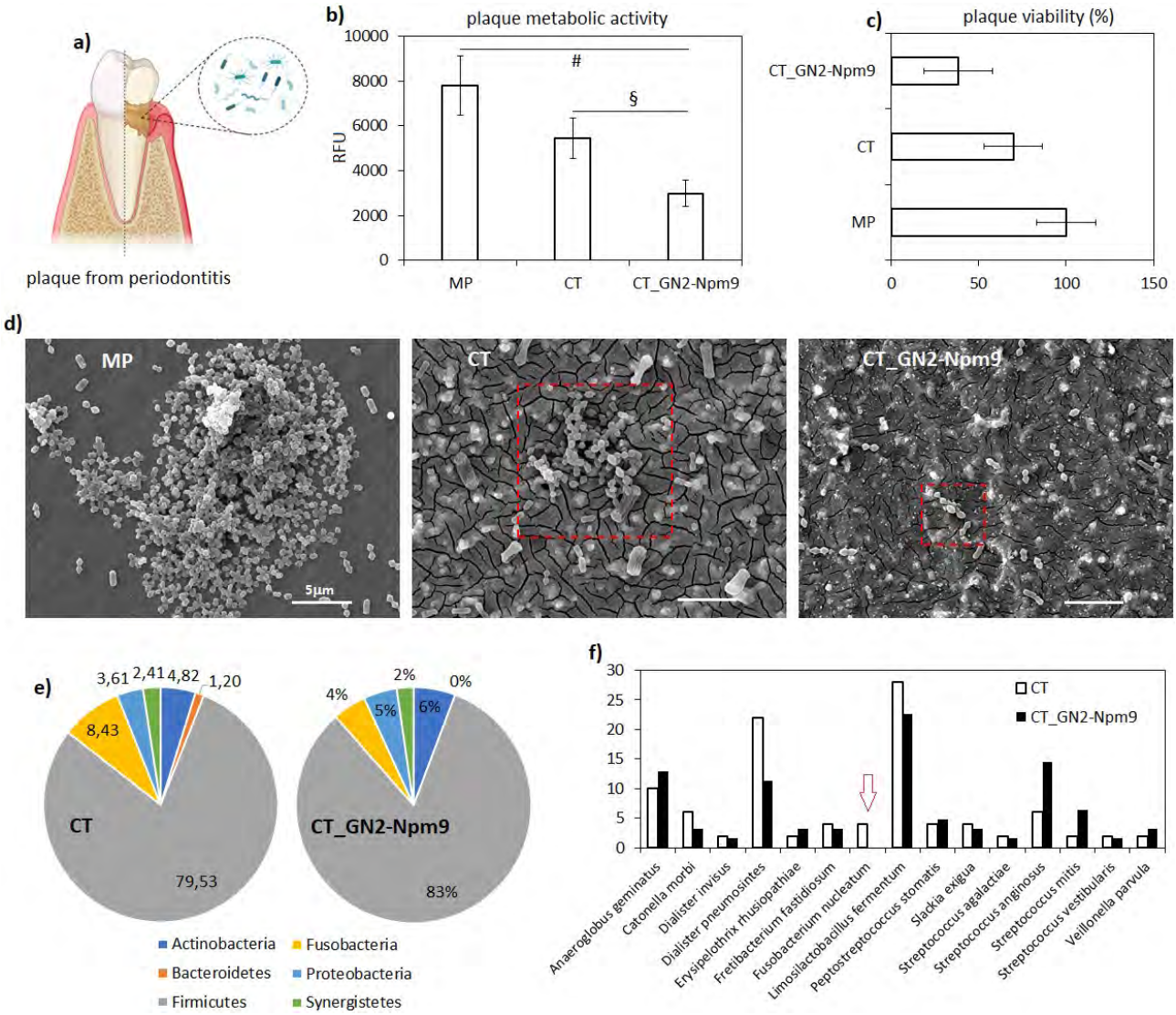

Figure 1. Peptoid's antibacterial activity using oral plaque from periodontitis. (a) Schematic design of plaque in periodontitis, (b) The metabolic activity of plaque bacteria ($p<0.05$, indicated by # and §, respectively), (c) Viability of plaque, (d) SEM images, biofilm-like aggregates are shown in the red box. Scale bar = 5 µm, (e) Proteomics analysis at the level of bacterial phyla, (f) Proteomics analysis at the level of bacterial species.

S10 – O4

Competitive protein adsorption on nanocellulose substrates: Real-time insights into Vroman-type behavior by QCM-D

Borges-Vilches J.[1], Valle-Delgado J.J.[1], Österberg M.[1]
[1]Dept. of Bioproducts and Biosystems, Espoo, Finland

Introduction

Nanocellulose networks have been extensively surveyed as biocompatible interfaces for biomedical applications, including wound dressings and tissue engineering scaffolds, owing to their intrinsic biocompatibility, high water retention capacity, and tunable physicochemical properties [1]. The biological performance of nanocellulose has been commonly associated with their tunable surface chemistry, swelling and mechanical behaviors, which can be tailored to modulate cell-material interactions within their networks [2]. However, despite these advantages, the interactions between nanocellulose surfaces and complex biological fluids remain insufficiently understood. In particular, when materials are exposed to blood or serum, the rapid adsorption of proteins leads to the formation of a dynamic protein layer that largely defines the biological identity of the interface. The competitive adsorption and exchange of proteins over time, commonly referred to as the Vroman effect, has been widely studied on rigid and non-porous surfaces, yet it has been far less investigated on soft, porous, bio-based polymers such as nanocellulose. In this work, Quartz Crystal Microbalance with Dissipation (QCM-D) monitoring was employed to examine, in real time, the adsorption behavior of different plasma proteins on nanocellulose films with varied surface functionality.

Aim

This work aims to address plasma protein adsorption not as an isolated biochemical event but as a surface-structure-dependent phenomenon intrinsically related to the nanocellulose surface properties, thus providing insights into the dynamic biointerfacial processes governing the performance of nanocellulose-based biomaterials in physiologically relevant environments.

Materials and Methods

Model thin films made from TEMPO-oxidized cellulose nanofibers (TCNF) of varied surface properties were prepared by spin-coating onto gold-coated QCM sensors. QCM-D measurements were performed under flow conditions at physiological temperature using both individual and mixture of plasma proteins, e.g., albumin, fibrinogen, and globulin that mimic plasma protein conditions. Real-time frequency and dissipation changes were monitored over time, and the adsorbed protein masses were estimated using the Sauerbrey equation. This approach enabled correlation of TCNF surface properties with adsorption kinetics, interfacial viscoelasticity due to protein conformational changes, and protein displacement phenomena.

Results

Initial exposure of individual plasma proteins to the various TCNF films resulted in significant differences in the adsorption kinetics, mainly due to surface charge-dependent interactions. Sequential protein adsorption experiments (e.g., albumin followed by globulin) indicated time-dependent changes in adsorption behavior that may reflect competitive interactions between proteins with different affinities for the surface. The magnitude of displacement and final viscoelastic properties depended strongly on the TCNF surface characteristics, highlighting the role of surface functionality in modulating competitive protein adsorption dynamics and subsequent biomaterial performance.

Conclusions

These findings demonstrate that QCM-D provides real-time, mechanistic insight into competitive protein adsorption on nanocellulose substrates. By bridging material design parameters with competitive adsorption mechanisms, this work provides valuable guidelines for the rational design and optimization of nanocellulose-based biomaterials with controlled biointerfacial properties.

References

[1] A. Subhedar, S. Bhadauria, S. Ahankari, H. Kargarzadeh, Nanocellulose in biomedical and biosensing applications: A review, International Journal of Biological Macromolecules 166 (2021) 587–600. https://doi.org/10.1016/j.ijbiomac.2020.10.217.
[2] R. Curvello, V.S. Raghuwanshi, G. Garnier, Engineering nanocellulose hydrogels for biomedical applications, Advances in Colloid and Interface Science 267 (2019) 47–61. https://doi.org/10.1016/j.cis.2019.03.002.

S10 – O5

Magnetically responsive antimicrobial nanosystems: An ally against biofilms

Campos F.[1,2,3], Pires A.[3], Rocha M.[3], Gomes A[4]., Gomes P.[4], Martins M. C. L.[1,2,5], Pereira A.[3], Monteiro C.[1,5]
[1]i3S – Institute for Research and Innovation in Health, University of Porto; [2]ICBAS - School of Medicine and Biomedical Sciences, University of Porto; [3]Institute of Physics for Advanced Materials, Nanotechnology and Photonics, University of Porto; [4]LAQV/REQUIMTE - Dept. of Chemistry and Biochemistry, Faculty of Sciences, University of Porto; [5]INEB, National Institute of Biomedical Engineering, University of Porto, Porto, Portugal

Introduction

Over 60% of chronically infected wounds harbor biofilms, bacterial communities that hinder antibiotic penetration and promote resistance. Biofilms are commonly associated with Gram-negative bacteria, with *Pseudomonas aeruginosa* being one of the main biofilm producers. Antimicrobial peptides (AMPs) are promising candidates to manage biofilm-associated infections.

Aim

Therefore, this work explores the development of magnetic-responsive nanoparticles to be pulled as “nano-knives” across biofilm layers.

Materials and Methods

Manganese ferrite ($MnFe_2O_4$) nanoparticles were synthetized by salt dissolution and aqueous coprecipitation, stabilized by capping with oleic acid, and encapsulated into poly(D,L-lactide-co-glycolide) with polyethylene glycol (PLGA-PEG) by nanoprecipitation to form mNPs. Finally, the AMP MSI78/Pexiganan® was covalently linked through a thiol-maleimide Michael addition (MSI78-mNPs).
Size and surface charge of mNPs were characterized by Dynamic/Eletrophoretic Light Scattering, while magnetic properties were evaluated by Superconducting Quantum Interference Device (SQUID). Grafted MSI78 was quantified by amino acid analysis (AAA) and mNP chemical composition was characterized by Raman spectroscopy and Fourier-Transform Infrared Spectroscopy (FTIR). Finally, mNPs were observed by Transmission Electron Microscopy (TEM) to decipher their morphology. MSI78-mNPs were first tested against *P. aeruginosa* in Muller-Hinton Broth (MHB) for 24h at 150 rpm, and secondly evaluated in Phosphate Buffered Saline (PBS) against a 24h-established biofilm for 3h under the application of an external magnetic field.

Results

MSI78-mNPs and bare mNPs showed a hydrodynamic diameter of 525±19 and 417±73 nm, and a zeta potential of +5 and -9 mV, respectively. According to SQUID, MSI78-mNPs and bare mNPs exhibited a saturation magnetization of 20 and 28 emu/g, respectively. Raman spectra confirmed the presence of $MnFe_2O_4$ nanoparticles in mNPs without structural modification, whereas FTIR displayed the peaks assigned to the PLGA-PEG groups and AMP amides. Finally, TEM revealed that mNPs were round-shaped enclosing the $MnFe_2O_4$ nanoparticles (Figure 1). After 24h-direct contact with bacteria, MSI78-mNPs were bactericidal at an AMP concentration of 40-80 µg/mL (AAA quantification). Furthermore, MSI78-mNPs led to a reduction of bacteria on biofilm surfaces.

Conclusion

In conclusion, mNPs were successfully produced by nanoprecipitation, with the inorganic part maintaining its chemical composition and crystallographic structure. The presence of MSI78 was detected by different techniques and the formulation demonstrated antimicrobial and antibiofilm activity against *P. aeruginosa.*

Acknowledgements

FCT (2023.02018.BD); COMPETE2030-FEDER-00737800; Mobilise (European Union’s Horizon 2020 - 951723)

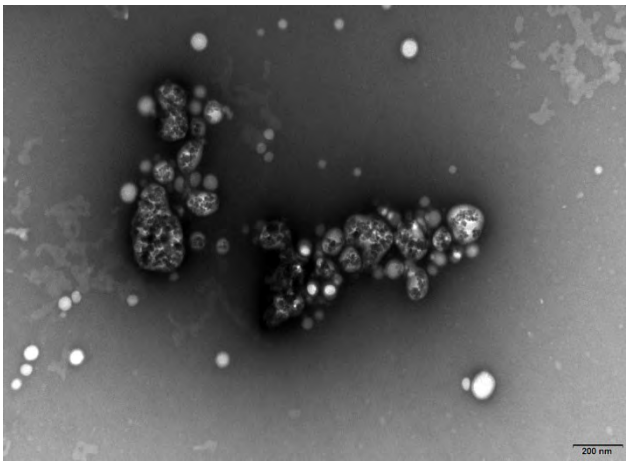

Figure 1 – TEM micrograph of MSI78-mNPs

S10 – O6

Evaluation of microbial degradation of phytic acid and its effect on caco-2 intestinal cells

Muganli Z.[1], Yazici M.A.[1], Ozturk L.[1], Mustafaoglu N.[1, 2, 3]
[1]Faculty of Engineering and Natural Sciences, Sabanci University, Tuzla 34596; [2]Nanotechnology Research and Application Center (SUNUM), Sabanci University, Tuzla 34596; [3]Center of Excellence for Functional Surfaces and Interfaces for Nano Diagnostics (EFSUN), Sabanci University, Tuzla 34956, Istanbul, Turkey

Introduction

Nutrient deficiency remains a global health concern, often caused by insufficient uptake or absorption of essential micronutrients including macrominerals (such as Ca and Mg) and microminerals (such as Fe and Zn), as well as vitamins.[1] The intestinal barrier plays a critical role in regulating nutrient absorption, and its dysfunction can lead to disorders associated with deficiencies, including impaired immunity and metabolic diseases.[1] Phytic acid, a common component of plant-based foods, is a key dietary factor that reduces mineral availability by chelating essential ions.[2,3] Although it exhibits antioxidant and anticancer properties, its antinutritional effects limit mineral absorption. Humans and other monogastric organisms have negligible endogenous phytase activity; therefore, external phytase is required to hydrolyze phytic acid and improve mineral availability.[4]

Aim

This study aims to evaluate the effect of phytic acid on Zn uptake in intestine epithelial (Caco-2) cells in the presence of microbial phytase.

Materials and Methods

Microbial degradation of the phytic acid was quantified by the phosphomolybdate blue assay. For this purpose, the bacteria were treated with 2mM phytic acid for 24 hours and the supernatant was tested for the inorganic orthophosphate formation which is the sign for the phytic acid hydrolysis. Cell viability of different concentrations of phytic acid, $ZnSO_4$, and bacterial eluents were assessed by the MTT assay on intestinal epithelial (Caco-2) cells for 24 hours. Zinc uptake assay was conducted on Caco-2 cells for two hours period as control, only 100 µM $ZnSO_4$ and 100 µM/2mM phytic acid and Zn concentration was measured using the inductively coupled plasma optical emission spectrometry (ICP-OES).

Results

Microbial treatment significantly increased the degradation of the phytic acid compared to the control groups and demonstrated the production of extracellular phytase in the tested bacteria (**Figure 1D**). Cell viability analysis showed that phytic acid concentrations above 3 mM were cytotoxic (**Figure 1B**), whereas $ZnSO_4$ (0-200 µM) and bacterial eluents (0-20%) did not exhibit significant toxicity. ICP-OES results demonstrated that phytic acid reduced Zn uptake in Caco-2 cells (**Figure 1C**).

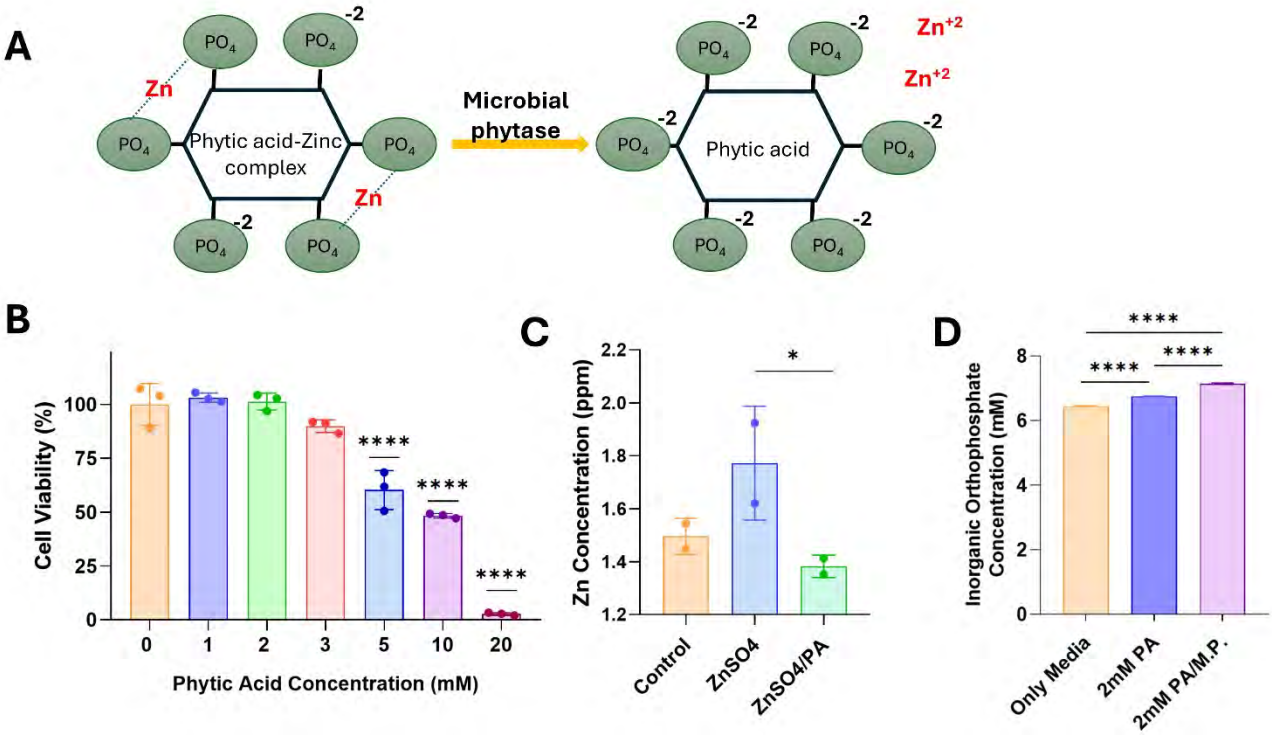

Figure 1. A) Degradation of the phytate complex (phytic acid-zinc chelate) degradation by microbial phytase**. B)** Cell viability of Caco-2 cells after treatment with different concentrations of phytic acid. Bar graph shows the percentage viability of Caco-2 cells exposed to increasing concentrations of phytic acid (0–20 mM). **C)** Zn uptake in Caco-2 cells treated with $ZnSO_4$ and phytic acid (PA), compared to untreated controls, quantified by ICP-OES (n=2, **p**<0.5). **D)** Phytic acid degradation by the microbial phytase (M.P.) evaluated by the phosphomolybdate blue assay, compared to control groups. Data are presented as mean ±SD (n=3). Statistical significance was determined using one-way ANOVA followed by Dunnet's multiple comparisons test (**p**<0.0001 compared to control)

Conclusion

These findings indicate that microbial phytase can effectively degrade phytic acid through extracellular phytase activity and reduce its antinutritional effects. The decrease in the Zn uptake observed in the presence of phytic acid, indicates the inhibitory effect of phytic acid on mineral absorption. Consequently, the degradation of phytic acid enhances Zn uptake in intestinal epithelial cells, emphasizing microbial phytase as a promising strategy to improve mineral bioavailability and support nutrient absorption.

Acknowledgment

This project was supported by JTC2022 - Cerebrovascular: BiotaBB project (TUBITAK Project No: 123N410).

References

1. A. K. Kiani, K. Dhuli, K. Donato, B. Aquilanti, V. Velluti, G. Matera, A. Iaconelli, S. T. Connelly, F. Bellinato, P. Gisondi and M. Bertelli, *Journal of preventive medicine and hygiene*, 2022, **63**, E93-e101.
2. H. W. Lopez, F. Leenhardt, C. Coudray and C. Remesy, *International Journal of Food Science and Technology*, 2002, **37**, 727-739.
3. S. M. G. Pires, R. S. Reis, S. M. Cardoso, R. Pezzani, E. Paredes-Osses, A. Seilkhan, A. Ydyrys, M. Martorell, E. Sönmez Gürer, W. N. Setzer, A. F. Abdull Razis, B. Modu, D. Calina and J. Sharifi-Rad, *Frontiers in chemistry*, 2023, **11**, 1174109.
4. S. Rizwanuddin, V. Kumar, B. Naik, P. Singh, S. Mishra, S. Rustagi and V. Kumar, *Journal of Agriculture and Food Research*, 2023, **12**, 100559.

S11 Bioactive coatings and electrophoretic deposition from design to biomedical applications

S11 – K1

Electrophoretic Deposition as versatile technique for developing advanced antibacterial and bioactive coatings

Boccaccini AR[1], Hadzhieva Z[1]
[1]Institute of Biomaterials, University of Erlangen-Nuremberg, 91058 Erlangen, Germany

Introduction

Insufficient osseointegration and bacterial infections are two major challenges limiting the performance of orthopedic and dental metallic implants. Electrophoretic deposition (EPD) is a versatile room temperature coating method that offers the possibility to functionalize the surface of metallic implants by creating composite or multi-material coatings composed of bioactive materials, biopolymers and bioactive molecules[1]. Such coatings are promising candidates to induce bone tissue integration and to prevent infections around orthopaedic and dental implants.

Aim. The current work aimed to develop coatings based on natural polymers (e.g. chitosan, zein) and silicate bioactive glass (BG) particles doped with biologically active ions on titanium or Ti alloy substrates by EPD.

Materials and Methods

For the preparation of the suspensions usually the biopolymer (zein, chitosan) is dissolved in a mixture of ethanol and water, sometimes with addition of glycerol. The coatings are produced by using direct current (DC)-EPD on Ti or Ti alloy substrates with applied voltages (usually 10 V) and deposition time of 3-5 min. Different types of BG particles, both melt-derived and sol-gel derived, can be considered as second phase in the biopolymer matrix, for example of composition: 70 mol.% SiO_2, 25 mol.% CaO and 5 mol.% P_2O_5. Such bioactive particles induce bioactivity and bone bonding capability. Additionally, BGs doped with biologically active ions (e.g. F, Cu, Sr) are considered. The morphological, mechanical and chemical properties of the coatings are evaluated. Furthermore, bioactivity of the coatings is assessed by immersion in simulated body fluid (SBF) and by cell biology tests.

Results

The results confirmed the successful incorporation of the glass particles in the zein or chitosan coating matrix. A typical cross-sectional image of the zein based coatings is shown in Fig. 1, exhibiting a coating thickness of around 50 µm. The coating bioactivity was confirmed by hydroxyapatite formation after 3 days of immersion in SBF. In addition, ion doping is key to enhance the antibacterial properties.

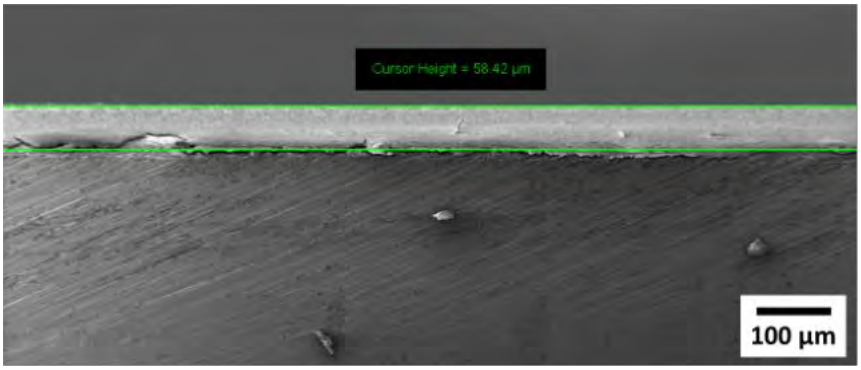

Figure 1: SEM cross-sectional image of a typical zein-BG coating obtained by EPD.

Conclusion

EPD is a versatile coating technology for biomedical applications. Incorporating silicate BG particles in biopolymer coatings imparts bioactive properties while doping with metallic ions leads to enhanced antibacterial performance. The results highlight the strong potential of EPD to produce multifunctional coatings for use in orthopedic and dental applications.

Acknowledgements
The authors thank the German Research Foundation (DFG) (project BO 1191/25–1) for funding.

References

[1] Z. Hadzhieva et al., *Current Opinion in Biomedical Engineering*, 2022; 21; 100367.

S11 – O1

Electrophoretic deposition of epidermal-inspired collagen films for wound healing

Citak M.K.[1], Truman G.[1], Cameron R.E.[1], Best S.M.[1]
[1]Department of Materials Science and Metallurgy, University of Cambridge, Cambridge, United Kingdom

Introduction

Collagen, the primary structural protein in skin, is widely used in wound care. However, conventional casting methods offer limited control over collagen film thickness and density, parameters that directly influence mechanical stability, degradation behaviour and barrier function. Improved structural control is required to develop epidermal-inspired materials that provide barrier properties comparable to healthy skin, which exhibits a water vapour transmission rate (WVTR) of approximately 204 g m^{-2} day^{-1}. This study investigates electrophoretic deposition (EPD) as a processing route to fabricate collagen films with tuneable thickness and density and compares their degradation and water barrier properties with conventionally cast films.

Materials and Methods

Insoluble type I collagen suspensions were deposited onto conductive substrates using direct current EPD at 15 V and 30 V for deposition times between 1 and 120 minutes. Deposition kinetics were analysed by fitting deposited film mass data to the Sarkar and Nicholson model[1]. Film thickness was measured by micrometry and density was calculated from mass and volume measurements. Deposition yield was determined as the ratio of dry film mass to total collagen mass in deposition suspension. Cast collagen films were prepared as controls, using the same suspensions. Degradation behaviour was assessed by incubating films in deionised water at 37 °C for 21 days, a timescale relevant to the haemostasis, inflammation and proliferation phases of skin wound healing. Water permeability was evaluated using a Systech Illinois 7101 Water Vapour Permeation Analyser at 35 °C and 50% relative humidity to assess the barrier performance of the cast and EPD films.

Results

EPD showed rapid deposition kinetics followed by a plateau as the remaining suspension concentration decreased during deposition. This behaviour is consistent with the theoretical model[1] (Figure 1a). Increasing deposition time and applied voltage increased deposition yield (Figure 1b), thickness and density (Figure 1c–d), demonstrating controllable structural properties via processing parameters. EPD films displayed substantially higher densities than cast controls. The densest films (30 V, 60 min) were selected for degradation analysis. Over 21 days, EPD films showed significantly reduced mass loss compared with cast films at early time points, with statistically significant differences observed except at day 18 (Figure 2a). The barrier properties of the films were assessed to determine the differences between films of differing thicknesses and fabrication methods. Permeability increased linearly with film thickness across cast and EPD samples (Figure 2b), indicating that the WVTR of the films was uniform in the tested range of film thicknesses with a value of 357 g m^{-2} day^{-1}.

Conclusion

EPD enables the fabrication of density-enhanced epidermal-inspired collagen films with tuneable structural and functional properties. Increased film thickness and density achieved via EPD did not compromise water vapour transport. EPD of insoluble type I collagen can thus provide a controllable strategy to achieve degradation and barrier properties relevant for wound healing requirements.

Acknowledgements

The authors acknowledge support from the Gates Cambridge Scholarship.

References

[1]P. Sarkar., P. S. Nicholson. Electrophoretic Deposition (EPD): Mechanisms, Kinetics, and Application to Ceramics. *Journal of the American Ceramic Society*; 1996; 8; 1987–2002.

S11 – O2

Electrophoretic Deposition as a One-Pot Strategy to Fabricate Multifunctional Chitosan Patches Embedding Alginate Microspheres for Drug and Cell Delivery

Fiorati A. Pavarini M. Altomare L
Department of Chemistry, Materials and Chemical Engineering "G. Natta", Politecnico di Milano

Introduction

Chitosan electrodeposition is a well-established technique for producing polymeric scaffolds for tissue engineering and drug delivery. This approach offers several advantages, including process simplicity, precise control over coating properties, and mild deposition conditions that may allow incorporation of biological components while preserving their functionality [1]. However, electrodeposition of living cells remains highly challenging because cell viability is often compromised during the process. To date, successful examples of eukaryotic cell electrodeposition have not been reported in the literature.

Aim

This study aims to develop a versatile platform based on Electrophoretic Deposition (EPD) of chitosan (CS) combined with alginate microspheres (MS) to enable both drug and cell loading and release.

Materials and Methods

To preserve cell viability during EPD, an acid-free chitosan solution was prepared. Chitosan (2% w/v) was initially dissolved in an aqueous acetic acid solution (0.07% v/v) and neutralized to pH > 7. The resulting hydrogel was collected and washed until the rinse water conductivity dropped below 30 µS/cm. The gel was then dissolved using CO_2 gas and diluted to a final concentration of 1% w/v [2]. Alginate microspheres were produced by extrusion dripping with coaxial laminar flow into a $CaCl_2$ solution (100–900 mM) to control the crosslinking degree and obtain microspheres smaller than 1 mm. Two formulations were prepared using low-viscosity (LV) and medium-viscosity (MV) alginate. L929 cells and curcumin (model drug) were encapsulated within the microspheres, which were subsequently dispersed in the acid-free chitosan solution. EPD was performed at 30–50 V for 3 minutes for drug-loaded films and 1–3 minutes for cell-loaded patches. Cell viability and proliferation were evaluated using Live/Dead staining and Alamar Blue assays.

Results

Curcumin-loaded microspheres exhibited controlled release kinetics in both PBS and acetate buffer (AB) (Figure 1a). During electrodeposition, the microspheres were successfully incorporated into chitosan films, and curcumin diffusion from the microspheres to the surrounding chitosan matrix was evidenced by a visible color shift (Figure 1b). The resulting patches remained structurally stable and did not fully degrade. L929 cells encapsulated in both LV and MV alginate microspheres survived the EPD process and proliferated within the patches. Alamar Blue assays confirmed cell metabolic activity for up to 10 days of culture (Figure 1c), and viable cells were clearly visible through Live/Dead staining after 10 days (Figure 1d).

Figure 1 – (a) Curcumin-loaded MS release in AB. (b) Curcumin diffusion in the CS patch in different media. (c) Metabolic activity trend of L929 cells electrodeposited with different EPD times. (d) Live/Dead assay on EPD L929 cells in alginate MS after 10 days of incubation.

These findings demonstrate that the acid-free chitosan dissolution strategy, combined with microsphere encapsulation, provides a non-cytotoxic environment suitable for electrodeposition. The microspheres effectively protected cells during the EPD process. Nevertheless, cell viability decreased with increasing electrodeposition time.

Conclusion

This study demonstrates the feasibility of producing multifunctional chitosan-alginate patches via EPD capable of incorporating both drugs and living cells. By tuning alginate viscosity and crosslinking degree, the release profile can be modulated, making this platform promising for future applications in drug delivery and tissue regeneration

References

[1] Avcu, et a , Prog Mater Sci, 2019, 103, 69–108, doi: 10.1016/J.PMATSCI.2019.01.001.
[2] Casalini et al., Carbohydrate Polymers 2024, 331, 121842. doi: 10.1016/j.carbpol.2024.121842

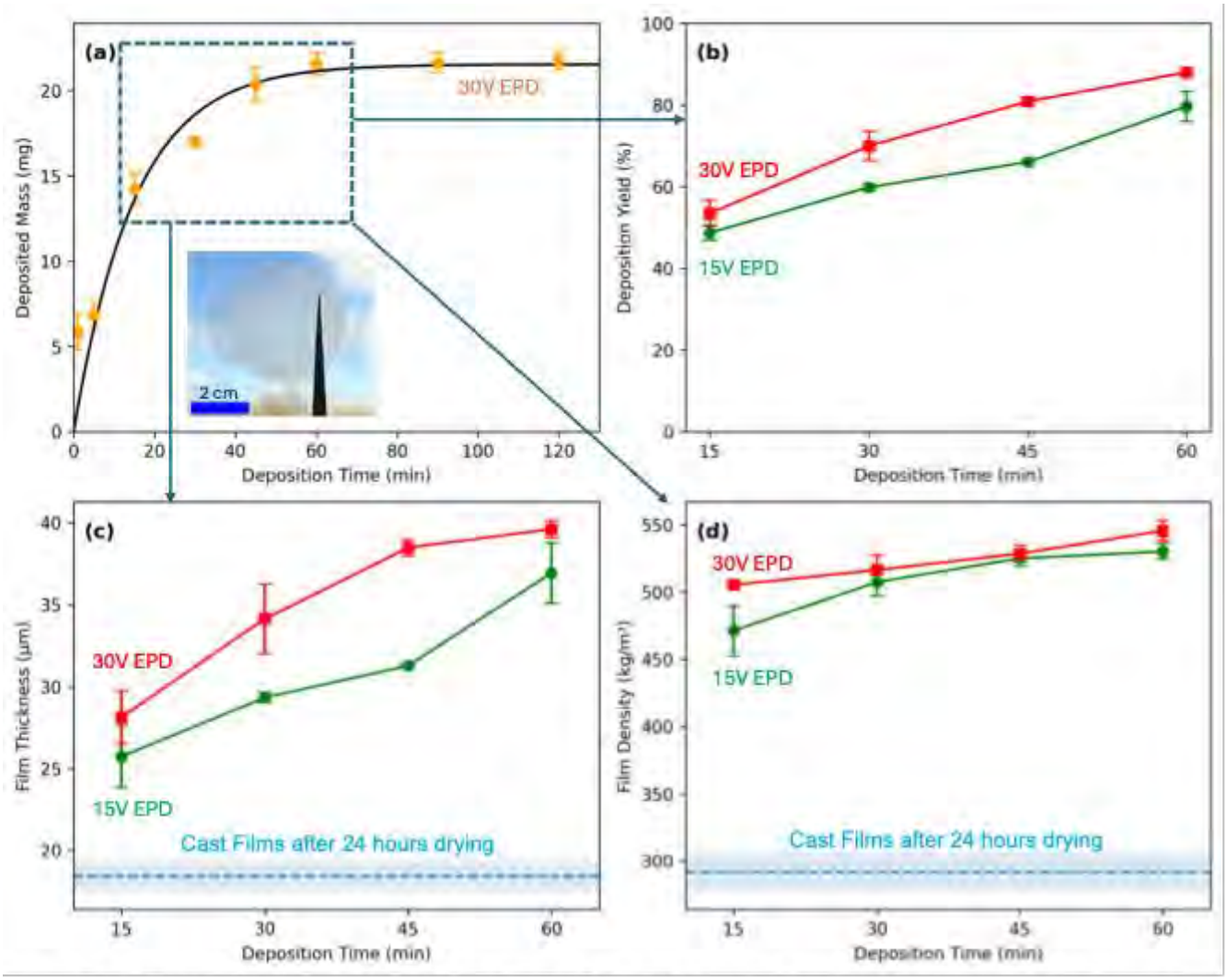

Figure 1. (a) Deposition kinetics of collagen films showing the mass deposited over time. Experimental points (orange) are fitted using the Sarkar & Nicholson model[1] (black line). Inset shows a free-standing collagen film, fabricated via EPD (scale bar: 2 cm) , (b) Deposition yields at 15 V (green) and 30 V (red) for 15–60 min, (c) Film thickness as a function of deposition time for 15 V (green) and 30 V (red) EPD films. The dashed blue line and light blue band indicate the mean and standard deviation of cast films, (d) Film density as a function of deposition time for 15 V (green) and 30 V (red) EPD films, with cast film reference shown as a dashed line and blue band.

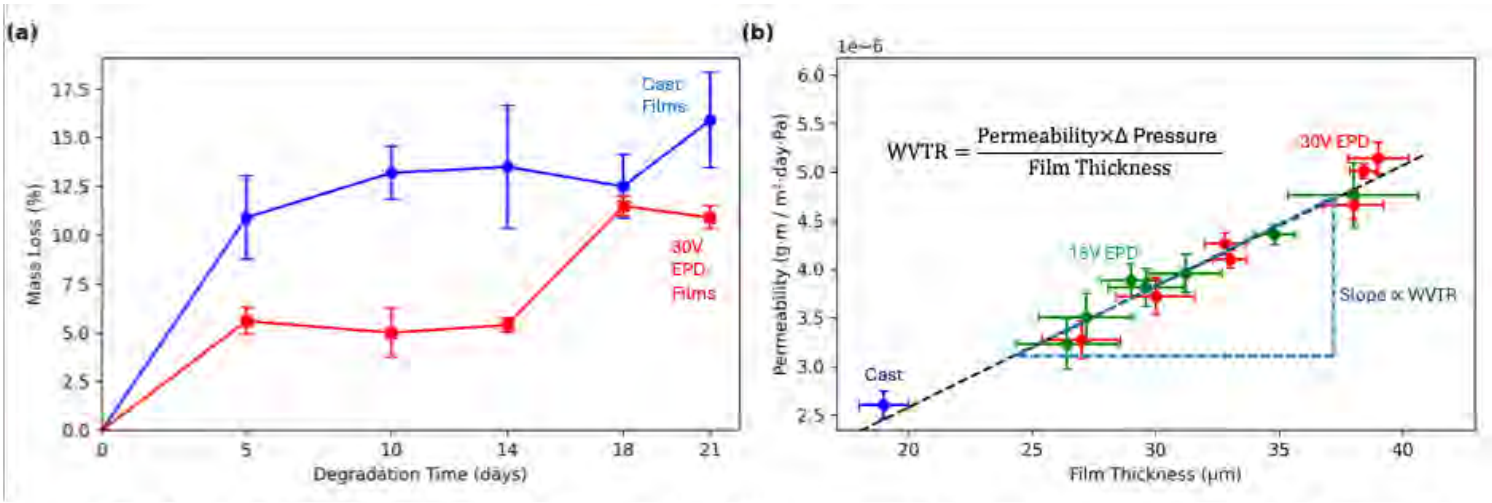

Figure 2. (a) Mass loss (%) of cast and EPD films over 21 days. EPD films demonstrated a more controlled degradation profile compared with cast films, with statistically significant differences at all time points except day 18 ($p < 0.05$). (b) Master curve of water vapour permeability as a function of film thickness, showing a positive linear correlation (dashed line indicates linear fit). WVTR is defined as the permeability multiplied by the applied water vapour partial pressure gradient (Δ Pressure) and divided by film thickness. The linear relationship indicates consistent transport behaviour across thicknesses and fabrication methods, corresponding to a uniform WVTR of 357 g m^{-2} day^{-1}.

S11 – O4
Sono-Electrodeposited CaP–Sr Coatings on Carbon Cloth for Bone Repair

Nenni K[123], Calcagno V[2], Ben Allah L[3], Gallet O[1], Alfonsi S[3], Hindié M[1]*

* Presenting author

1 ERRMECe EA1391, CY Cergy Paris Université, Cergy, France
2 Institut des Matériaux (I-MAT), CY Cergy Paris Université, Cergy, France
3 Laboratoire de Physicochimie des Polymères et des Interfaces (LPPI), CY Cergy Paris Université, Cergy, France

Introduction

Critical-size bone defects remain challenging due to insufficient regeneration capacity beyond a certain threshold. Conventional calcium phosphate (CaP) ceramics are bioactive but brittle, limiting their use in irregular or load-bearing defects. Flexible supports like activated carbon cloth (ACC) provide high tensile strength, radiolucency for artifact-free imaging[1], and a large accessible surface area suitable for functional coatings. Incorporating strontium into CaP enhances osteogenic activity and early matrix mineralization[2], motivating the development of a conformable CaP–Sr coating strategy for textile-based implants. We aimed to develop a sono-electrodeposition route for depositing homogeneous, adherent CaP coatings doped with strontium (Sr) on ACC. Two electrochemical deposition modes—cyclic voltammetry (CV) and chronoamperometry (CA)—were implemented under continuous sonication, and their resulting coatings were compared. We then assessed how post-deposition heat treatment further modified their morphology, crystallinity, stoichiometry, stability in a physiological-like medium, and pre-osteoblast response.

Materials and Methods

ACC (Zorflex® FM50K) was cut, solvent-cleaned using a high-pressure SpeedExtractor (120 °C, 100 bar, 28 min) and dried under vacuum. CaP–Sr coatings were produced by sono-electrodeposition in a three-electrode setup (ACC working electrode confined between two Pt grids, SCE reference, Pt counter-electrode) immersed in a $Ca^{2+}/Sr^{2+}/H_2PO_4^-$ electrolyte (5 mM (Ca^{2+}+Sr^{2+}), 3 mM $H_2PO_4^-$, Ca/P = 1.67, 5 % Sr substitution, pH 4.8). Continuous sonication (35 kHz) was applied during deposition. Two electrochemical strategies were compared: (1) cyclic voltammetry (CV) with optimized parameters (20 mV/s, 30 cycles, −1.6 V to +1.1 V, 70 °C bath), enabling a 2 h deposition; (2) chronoamperometry (CA) at −0.63 V/SCE for 6 h. Heat treatments (400 °C or 600 °C, 4 h, N_2) were applied to improve crystallinity and remove non-apatitic species. Coatings were analysed by SEM/EDX, FTIR-ATR and BET surface area measurements. Stability was assessed by 7-day immersion in HEPES buffer (10 mM, pH 7.4, 37 °C). STRO-1$^+$A pre-osteoblasts were seeded on sterilized samples (dry heat, 180 °C/2 h) and evaluated at days 1, 3 and 7 using Live/Dead staining and confocal microscopy.

Results

CA produced thicker, more uniform apatitic layers relative to CV, which showed higher surface roughness and needle-like crystal clusters. Heat-treated CA coatings exhibited the highest crystalline order and resistance to dissolution. After HEPES immersion, CA samples maintained a stable (Ca+Sr)/P ratio and coherent microstructure, whereas CV coatings showed greater pitting and compositional drift. Biologically, CaP–Sr coatings promoted high cell viability (>99%) and enhanced spreading, with CA outperforming CV in promoting extended filopodia and cytoskeletal organization. Cell morphology and early osteogenic behavior were consistent with the pro-osteogenic effect of Sr incorporation.

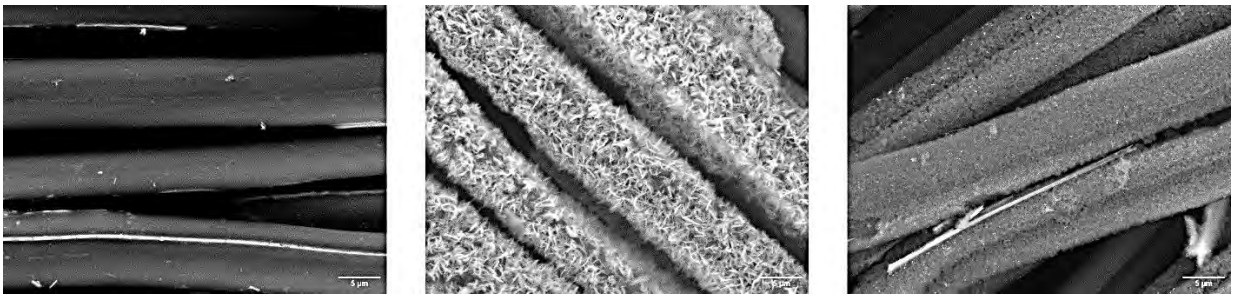

Figure 1 – SEM micrographs of ACC, CV-derived CaP–Sr, and CA-derived CaP–Sr. Scale bars: 5 µm.

Conclusion

Sono-electrodeposition enables reproducible CaP–Sr coatings on flexible ACC substrates. CA, particularly when combined with heat treatment, provides superior homogeneity, stability, and biological performance. These results position ACC-based CaP–Sr coatings as promising candidates for next-generation, conformable implants designed for irregular or critical-size bone defects.

Acknowledgements This work was supported by the CY Initiative – EMERGENCE program, which funded the E-BIOMIMOS project.

References

1. Yeung C.M. et al. Carbon Fiber Implants in Orthopaedic Oncology. J Clin Med. 2022.

2. Olivier F. et al. Strontium incorporation into Ca-deficient HA. Mater Sci Eng C. 2020.

ESB
2026

S11 – O5

A combination of plasma polymerization and plasma etching to control the antibacterial properties of biomaterial in dental care

Federico Apolloni, UGent

S12
Bioadhesives – Strengthening the bond

S12 – K1
From formulation to preclinical translation: A bioinspired calcium phosphate adhesive for fragility fracture repair

Redmond J.[1], Agarwal S.[1], Jaiswal S.[1], Tzagiollari A.[2], Insley G.[3], Levingstone T.[1], Dunne N.[1]
[1]School of Mechanical and Manufacturing Engineering, Dublin City University, Dublin; [2]Biodesign Europe, Dublin City University, Dublin; [3]Biomimetic Innovations Ltd, affiliate of PBC Biomed, Limerick, Clare, Ireland; [3]PBC Biomed, Accelerating Medical Innovation, Limerick, Clare, Ireland

Introduction
Fragility and osteoporotic fractures remain difficult to stabilise with conventional metallic fixation, particularly in comminuted and poor-quality bone[1]. A phosphoserine-modified calcium phosphate cement (PM-CPC), OsStic®, was developed as an injectable, bioresorbable bone adhesive capable of bonding wet cortical and cancellous surfaces while engaging bone repair pathways. This keynote will present the development of OsStic® from formulation and scale-up through *in vitro* and *in vivo* evaluation and will examine how a cell-instructive adhesive reframes the role of fragile bone fixation.

Materials and Methods
A DoE approach was used to optimise α-tricalcium phosphate (α-TCP)/phosphoserine/liquid ratios to achieve targeted rheology, setting behaviour, compressive strength and bone-to-bone bond strength within clinically acceptable windows, and robustness to ten-fold increases in powder volume was assessed[2]. The optimised PM-CPC was then examined by *in vitro* and *in vivo* studies. Pre-osteoblast MC3T3-E1 and human mesenchymal stem cells were used to assess cytocompatibility, proliferation, biomineralisation and expression of osteogenic markers relative to α-TCP and HydroSet™ controls. RAW 264.7 macrophages were used to characterise osteoclastogenesis, sealing zone formation and biomarker release (CAII, TRAP and MMP-9) on OsStic® versus control cements. Translational performance was evaluated in mini-pig dental implant stabilisation and ovine long-bone defect models, focusing on early mechanical fixation, interfacial strength and new bone formation at and within the adhesive.

Results
DoE analysis identified the optimal PM-CPC (Fig.1A) that satisfied target ranges for setting (60-200 s), compressive strength (≥10 MPa) and adhesive strength (≥2.5 MPa), with comparable performance at 1 g, 5 g and 10 g scales[2]. ISO 10993-5-compliant extraction tests showed no cytotoxicity (Fig.1B), while direct-contact assays demonstrated superior attachment quality and proliferation kinetics (Fig.1C) on OsStic® versus α-TCP and HydroSet™, corroborated by SEM, LIVE/DEAD™ and actin–nuclei staining. Osteoblast cultures on OsStic® exhibited extensive biomineralisation (Fig.1D) and increased expression of ALP (Fig.1E), osteopontin, osteocalcin and BMP-2, and osteoclast assays revealed multinucleated cells (Fig.1F) with well-defined sealing zones (Fig.1G) and elevated CAII release (Fig.1H) on the PM-CPC surface compared with controls. In dental and long-bone models, OsStic® provided immediate mechanical stabilisation, sustained gains in torque and pull-out strength and substantial new bone volume within and around OsStic®, consistent with progressive replacement rather than long-term material persistence.

Conclusion
OsStic® has emerged not only as a wet-field adhesive that meets mechanical handling specifications, but as a transient, cell-instructive interface that integrates into the osteoblast–osteoclast feedback loop. The keynote will use OsStic® to explore how design constraints from surgery, preclinical evidence and device-level considerations can be combined to redefine fixation in fragile bone as a time-limited support that hands control back to physiological bone turnover.

References
[1.]Tzagiollari A, McCarthy HO, Levingstone TJ, Dunne NJ. Bioengineering. 2022 Jun 10;9(6):250.
[2.]Tzagiollari A, Redmond J, McCarthy HO, Levingstone TJ, Dunne NJ. Acta Biomaterialia. 2024 Jan 15;174:447-62.

Acknowledgments

This research was funded through the Disruptive Technologies and Innovation Fund (DT20200177) by the Dept. of Business, Enterprise and Innovation, Ireland.

Word count – 400/400

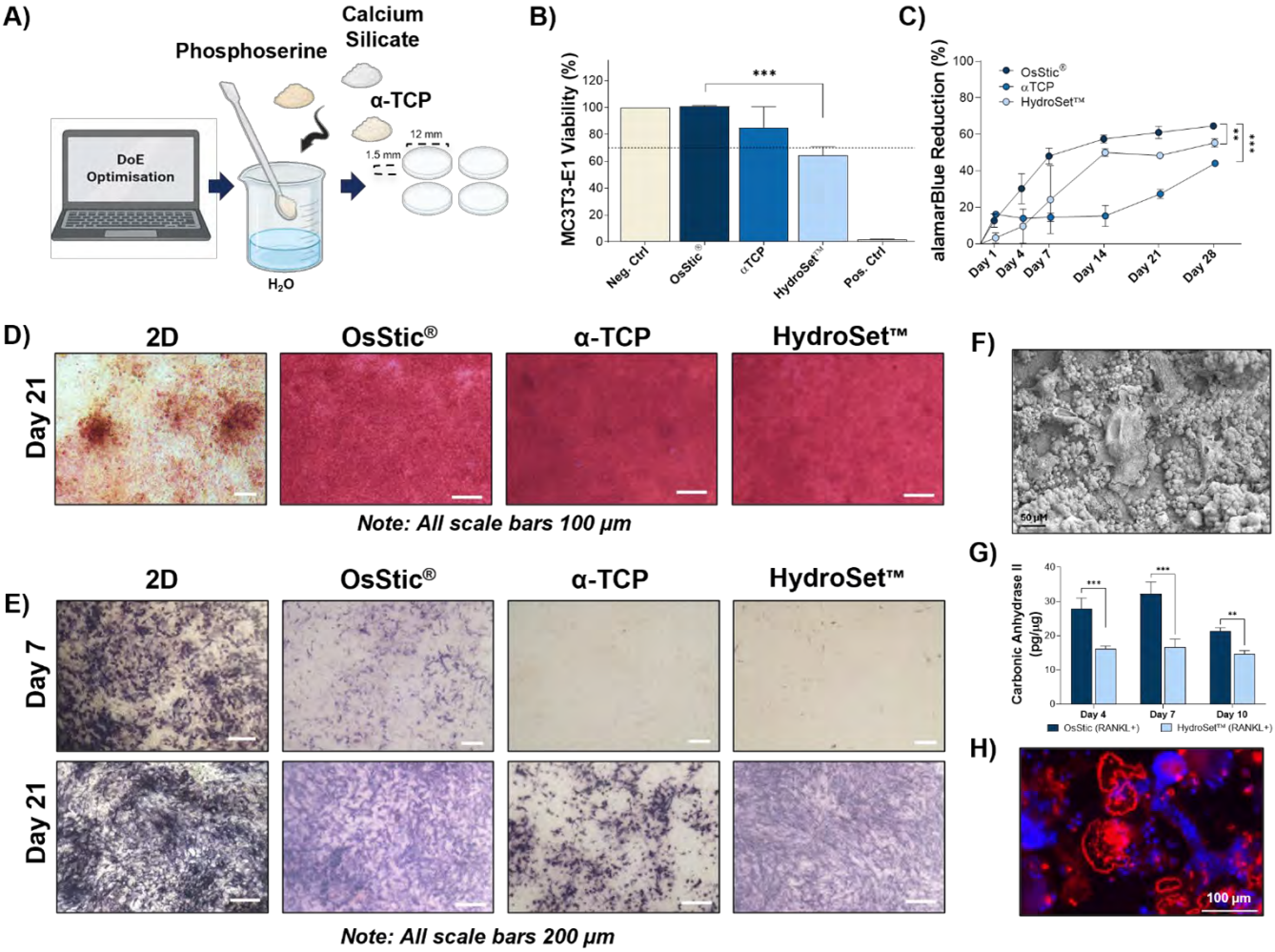

Figure 1. A) OsStic® optimisation via DoE was completed, producing a final material that satisfied the clinical requirements for setting, handling and mechanical properties. B) Pre-osteoblast cell viability (indirect culture) confirmed no material-related cytotoxicity. C) Pre-osteoblast proliferation (direct culture) demonstrated superior kinetics on the PM-CPC. D) Alizarin Red staining confirmed significant biomineralisation by mature osteoblast cells. E) ALP staining demonstrated earlier induction of ALP activity on the PM-CPC compared to both controls. F) SEM micrograph of mature osteoclasts on OsStic® surface. G) CAII ELISA demonstrated significantly higher release levels of this key functional marker on the PM-CPC at all timepoints. H) F-actin and DAPI staining showing a large mature osteoclast with significant sealing zone activity.

S12 – O1

Multicomponent reaction-derived self-healing bioadhesive for treatment of chronic wounds

Afshari R.,[1] Annabi N. [1]
[1]Dept. of Chemical and Biomolecular Engineering, University of California, Los Angeles, Los Angeles, California 90095, US

Introduction

Chronic wounds caused by trauma, burns, surgery, and diabetes remain difficult to treat, as most current dressings provide only passive coverage and lack integrated antibacterial, anti-inflammatory, and regenerative functions, while requiring complex multi-step syntheses that limit their tunability and translational potential. To address this challenge, we developed UgiGel, a gelatin-based self-healing bioadhesive synthesized using a one-pot Ugi four-component reaction (Ugi-4CR). This combinatorial chemistry enables rapid generation of pseudopeptide-functionalized networks with programmable physicochemical and biological properties, offering a versatile platform for engineering multifunctional adhesives. Our preliminary work describes the synthesis and physicochemical characterization of UgiGel,[1] using dynamic boronate-ester crosslinking that causes self-healing, antioxidant and antibacterial activity, and favorable mechanical properties.

Fig. 1. **Schematic overview of UgiGel synthesis and its multifunctional performance for wound closure and repair.**

Aim

Our ongoing work focuses on the translational evaluation of UgiGel for chronic wound repair. Specifically, we are engineering formulations with thermoresponsive painless detachability, and assessing their therapeutic performance in advanced wound-healing models (**Fig. 1**).

Materials and Methods

UgiGel bioadhesives were fabricated via a one-pot multicomponent reaction strategy followed by *in situ* crosslinking under physiological conditions.[1] Mechanical properties were evaluated using rheology, lap-shear, and burst-pressure testing on porcine skin. *In vitro* bioactivity was assessed using fibroblast cells to evaluate cytocompatibility, along with antibacterial and antioxidant assays. To better recapitulate tissue responses, a 3D injured skin model was established and treated with UgiGel patches following laser-induced injury. In parallel, linear incisional and splinted excisional wound models were used to evaluate wound closure, regeneration, angiogenesis, and immune responses compared with sutures and a commercial hydrogel dressing.

Results

UgiGel exhibited significantly higher wet-tissue adhesion strength (~140 kPa) and burst pressure (~14 kPa) compared with methacrylated gelatin (GelMA) and commercial sealants (Evicel® and Coseal®) (**Fig. 2A-B**). UgiGel demonstrated excellent cytocompatibility, supporting high fibroblast viability and proliferation (**Fig. 2C**). In addition, UgiGel displayed antibacterial activity against both strains (**Fig. 2D**). A 3D injured skin construct was established to evaluate the

Fig. 2. **Mechanical performance and translational evaluation of UgiGel.** (**A-B**) Adhesion strength and burst pressure compared with GelMA and commercial sealants. (**C**) Fibroblast viability and proliferation, demonstrating cytocompatibility. (**D**) Antibacterial activity against *P. aeruginosa*. (**E**) 3D injured skin construct used to evaluate tissue responses to UgiGel treatment. (**F**) Representative images from a murine wound model showing minimal inflammation following UgiGel application after 7 days.

interaction of UgiGel with damaged tissue (**Fig. 2E**). *In vivo* murine wound-healing studies have been initiated to assess the translational potential of UgiGel (**Fig. 2F**).

Conclusion

UgiGel demonstrates how combinatorial chemistry can enable the rapid synthesis of multifunctional biomaterials through a simple and sustainable strategy. The resulting self-healing bioadhesive combines strong wet-tissue adhesion with antibacterial, antioxidant, and thermoresponsive, skin-friendly detachability. Evaluation in wound-healing models will establish UgiGel as a versatile platform for next-generation wound dressings.

References

[1] Afshari R., Roy A., Jain S., Lum K., Huang J., Denton S., Annabi N. One-pot synthesis of antibacterial and antioxidant self-healing bioadhesives using Ugi four-component reactions. *J Biomed Mater Res B: Appl Biomater* 2025; 113; e35584.

S12 – O2

Volumetric additive manufacturing of cell-loaded hydrogel adhesives for hard-to-soft tissue interfaces

Nottegar A.[1], Karami P.[1], Pioletti D.P.[1]
[1]Laboratory of Biomechanical Orthopedics, EPFL, Lausanne, Switzerland;

Introduction

Hard-to-soft tissue interfaces, such as cartilage-to-bone and tendon-to-bone junctions, exhibit complex gradients in composition, structure, and mechanical properties that are critical for effective load transfer and long-term function. Hydrogel adhesives are promising tools for promoting healing at these interfaces, as they can conform to irregular defect sites, provide immediate fixation in wet physiological environments, and support integration between dissimilar tissues while maintaining a cell-supportive microenvironment. However, replicating these interfaces remains challenging, as current fabrication approaches often lack spatial precision, require prolonged processing times, and fail to achieve robust and durable adhesion to native tissues. This study aims to develop a rapid and versatile strategy based on volumetric additive manufacturing (VAM) to fabricate hydrogel adhesives capable of mimicking and integrating hard-to-soft tissue interfaces.

Materials and Methods

Photoresponsive hydrogel precursor solutions incorporating adhesive polymers were engineered to enable VAM while maintaining cytocompatibility and tunable mechanical properties. Poly(acrylic acid) functionalized with NHS esters (PAA_{NHS}) was used as the adhesive polymer. Thiol–ene photoclick chemistry was employed to achieve crosslinking during the VAM process. Lithium phenyl(2,4,6-trimethylbenzoyl)phosphinate (LAP) was used as a photoinitiator at a concentration of 0.05% (w/v) to induce photocrosslinking. VAM was performed using a Tomolite Performance v2.0 printer in combination with Apparite software (Readily 3D, Lausanne, Switzerland). Mechanical properties, including stiffness and interfacial adhesion energy to biological substrates, were characterized using a ZwickRoell uniaxial testing system. In vitro assays using bovine chondrocytes were conducted to assess cytocompatibility and cell encapsulation capacity.

Results

Three-dimensional constructs mimicking native soft-to-hard tissue interfaces were fabricated within seconds, eliminating the need for layer-by-layer deposition while enabling spatial control over composition and mechanical gradients and preserving high cell viability (Fig. 1A). Multi-material overprinting facilitated the formation of graded constructs that closely mimic native interfaces (Fig. 1B). Mechanical testing demonstrated tunable stiffness gradients across the constructs. The incorporation of PAA_{NHS} enabled strong covalent bonding to amine-rich biological tissues, resulting in interfacial adhesion energies exceeding 100 J/m^2 under physiological conditions (Fig. 1C–F). In vitro studies confirmed high cytocompatibility and successful cell encapsulation, indicating that the fabrication process preserves cell viability and supports biological function.

Conclusion

This study demonstrates that VAM is a powerful platform for the rapid fabrication of cell-loaded hydrogel adhesives for hard-to-soft tissue interfaces. The ability to generate spatially graded, tissue-adhesive, and cytocompatible constructs offers a promising approach for improving interfacial tissue repair and advancing regenerative medicine strategies.

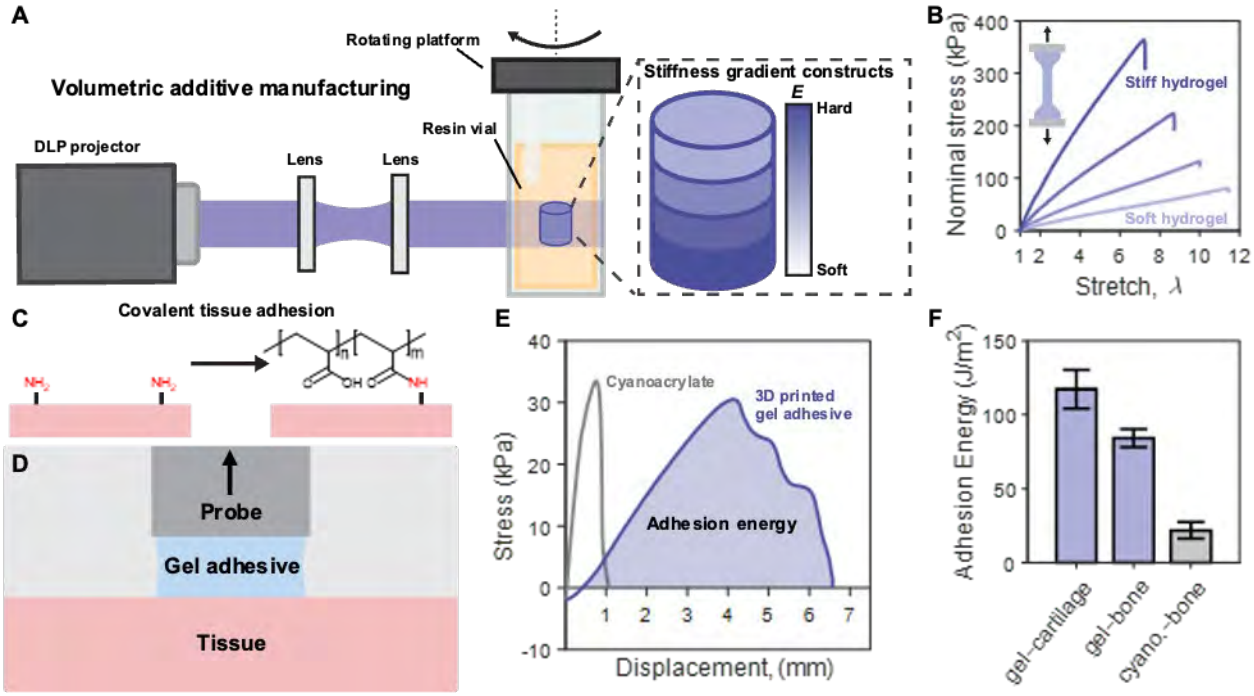

Figure. 1. Design principles of 3D printed hydrogel adhesives for hard-to-soft tissue interfaces. (**A**) Volumetric additive manufacturing of. (**B**) Stress-stretch curves showing the different stiffness of hydrogel resins. (**C**) Schematic showing the covalent tissue adhesion mechanism via NHS esters reacting with amines present on the tissue surface. (**D**) Schematic showing the set-up for the testing of the interfacial adhesion energy of printed hydrogels. (**E**) Stress-displacement curves of adhesion between 3D printed gel adhesives to cartilage and cyanoacrylate to bone. (**F**) Adhesion energy of 3D printed hydrogels and cyanoacrylate (cyano.) to various biological substrates.

S12 – O3

The role of a phosphoserine-modified calcium phosphate adhesive in augmenting osteoclast response and bone remodelling

Redmond J.[1], Agarwal S.[1], Jaiswal S.[1], Tzagiollari A.[2], Insley G.[3], Levingstone T.[1], Dunne N[1]
[1]School of Mechanical and Manufacturing Engineering, Dublin City University, Dublin; [2]Biomimetic Innovations Ltd, affiliate of PBC Biomed, Limerick, Clare; [3]PBC Biomed, Accelerating Medical Innovation, Limerick, Clare, Ireland

Introduction

A phosphoserine-modified calcium phosphate adhesive, 'OsStic®', has been developed to address unmet clinical needs in fracture stabilisation and bone repair. Previous studies showed that the bioadhesive demonstrated excellent adhesive and cohesive properties in wet-field environments and met clinical requirements for setting time, mechanical properties, degradation and injectability. Additionally, OsStic® has demonstrated biocompatibility, supporting the culture and functioning of stem cells, osteoblasts and osteoclasts. Herein, we present findings of enhanced osteoclast activity and the underlying biological mechanisms of the adhesive.

Materials and Methods

OsStic® samples were prepared to a previously optimised composition containing phosphoserine, alpha-tricalcium phosphate (α-TCP) and calcium silicate. For controls, an α-TCP-only material and the commercially available HydroSet™ were used as comparators. RAW 264.7 (murine) cells were used for all *in vitro* studies, with osteoclast differentiation induced through RANKL supplementation.

Results

RAW 264.7 cells attached readily to all materials. Proliferation kinetics were similar regardless of material, with an early peak in cell numbers followed by a plateau and eventual decline. TRAP staining was observed on all materials, although OsStic® provided a more suitable surface for fusion and cell enlargement. The comparator materials were primarily populated by a dense TRAP-positive layer of mononuclear cells. F-actin staining demonstrated superior multinucleated osteoclast formation on OsStic®, with enhanced sealing zone activity (Fig.1(a)). Enhanced osteoclast activity on the OsStic® surface was further confirmed via ELISA of various biomarkers (Fig.1(b-d)), notably Carbonic Anhydrase II (CAII), where significantly higher levels of CAII were recorded at all timepoints (Fig.1(d)).

Conclusion

Work within our lab suggests the addition of phosphoserine to the calcium phosphate cement (CPC) promotes enhanced osteoclast attachment, formation and resorption capabilities. These *in vitro* findings corroborate with *in vivo* data, whereby OsStic® demonstrates substantial levels of bone remodelling and does not behave as a bioinert CPC that persists at the implant site long-term. We believe the sustained ion release (calcium and phosphate) by OsStic® is crucial in promoting the bone remodelling observed *in vivo*, allowing for the material to effectively 'hijack' the body's natural bone turnover due to its intrinsic biomimetic properties. Through its bioactivity and physiochemical properties, the OsStic® material enhances the macrophage/osteoclast response post material implantation, which drives the concurrent recruitment of required cell populations to induce osteogenesis and ultimately replaces the OsStic® with new bone.

Acknowledgments

This research was funded through the Disruptive Technologies and Innovation Fund (DTIF) by the Dept. of Business, Enterprise and Innovation, Ireland. Award number DT20200177.

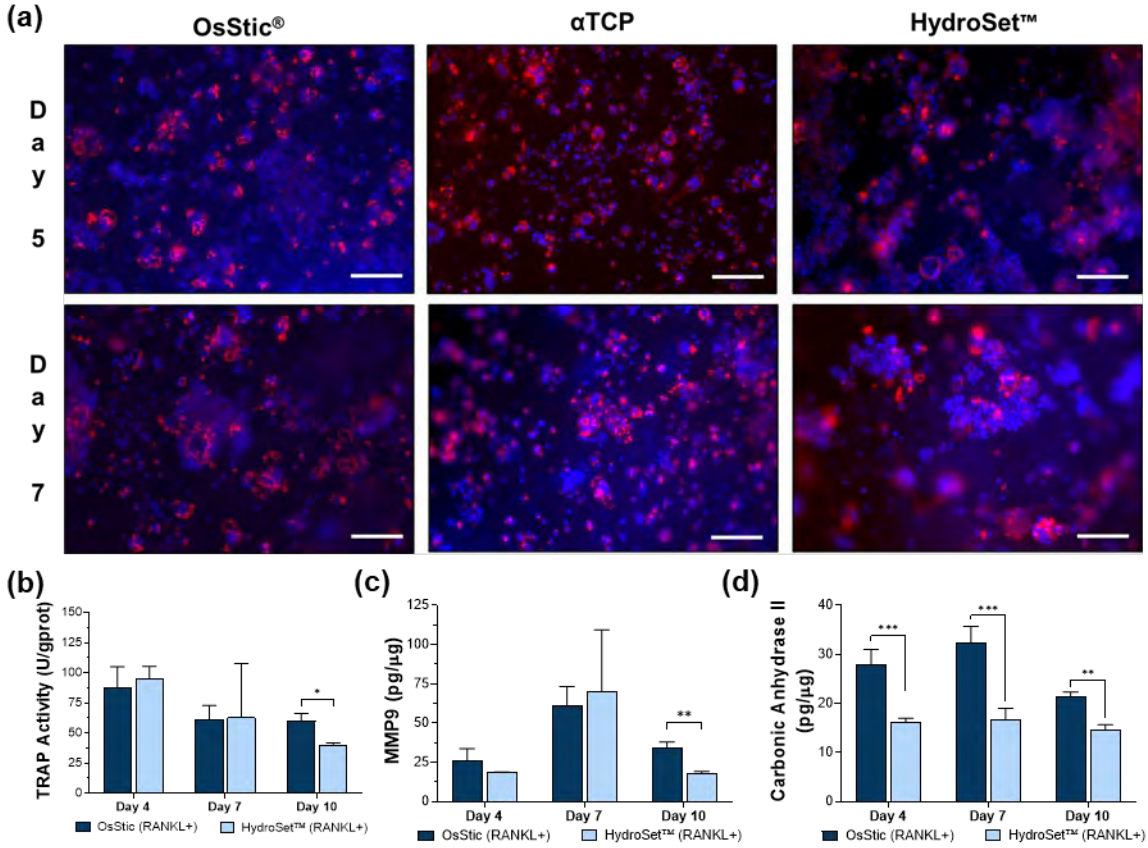

Figure 1 (a) F-actin and DAPI staining at Days 5 and 7 showing enhanced sealing zone activity on the OsStic® material, scale bars 100 µm. (b) ELISA quantifications of osteoclast formation and function-related markers TRAP, MMP9 and CAII.

S12 – O4

Lubricating nanoparticles with sheltered cationic charges maintain cartilage adhesion and lubrication

Austin W.[1,2], Mertens S.[3] Lee D.[1,2], Adibnia V.[1,2,3]
[1]School of Biomedical Engineering, Dalhousie University; [2]Dept. of Biomaterials and Applied Oral Sciences, Dalhousie University; [3]Dept. of Chemistry, Dalhousie University, Halifax, Canada

Introduction

Osteoarthritis (OA), a degenerative joint disease, is the leading cause of adult disability. Cartilage degradation and OA development arise from increased surface roughness and mechanical wear of the articular surfaces.[1] There is no cure for OA nor an effective intervention to delay its progression. Phytoglycogen nanoparticles (PhG-NP) are biosourced superlubricants with exceptional performance in boundary regime through hydration lubrication.[2] However, due to their size, they have low residence time in the joint. Approaches to improve PhG-NP retention in the joint through electrostatic adhesion have proven successful, but sacrifice the PhG-NPs lubricating capabilities.[3] **Aim.** In this study, we will use zwitterionic charge shielding to maintain electrostatic adhesion between PhG-NPs and cartilage surfaces while restoring the PhG-NP's superlubrication properties.

Materials and Methods

PhG-NPs are highly branched polysaccharide polymers sourced from sweet corn. The particle surface is chemically modified with varying concentrations of ethylenediamine (EDA) using Schiff-base reaction, imbuing a tunable cationic charge. The cationic PhG-NPs are then surface-modified with phosphatidylcholine (PC), a lubricating zwitterionic molecule found on articular cartilage surfaces, providing tunable degrees of charge shielding. Characterization of these novel particles includes zeta potential, dynamic light scattering (DLS), nuclear magnetic resonance (NMR), and TNBS assay. *In vitro* analysis of lubrication and adhesion include cartilage-on-cartilage tribology, surface force apparatus (SFA), and isothermal calorimetry (ITC).

Results

Following EDA-modification, PhG-NPs showed no significant change in hydrodynamic diameter while surface amine concentration and zeta potential increased with higher amounts of EDA addition. PC addition to cationic PhG-NPs did not alter particle size or charge while surface amine concentration decreased. NMR analysis of the particles verified both modifications. ITC analysis of particle adhesion to cartilage components (hyaluronic acid and chondroitin sulphate) showed increased thermal adhesion energy with increasing EDA modification. Cartilage tribology indicated that PC addition to cationic PhG-NPs improved their lubrication capabilities. Statistical analysis included one-way Analysis of Variance and Tukey's post-hoc using R v4.2.2.

Conclusion

To summarize, surface modification of cationic PhG-NPs with zwitterionic PC functional groups maintains particle adhesion to articular cartilage surfaces *in vitro* while shielding the cationic charge, maintaining ultralow friction coefficients.

References

[1]Temple-Wong M.M., et al. Biomechanical, structural, and biochemical indices of degenerative and osteoarthritic deterioration of human articular cartilage of the femoral condyle. *Osteoarthr. Cartil.* 2009; 17; 1469-1476.
[2]Adibnia V., et al. Phytoglycogen nanoparticles: nature-derived superlubricants. *ACS Nano* 2021; 15; 8953-8964
[3]Ma Y., et al. Phytoglycogen nanolubricants with extended retention time in joints. *Adv. Funct. Mater.* 2025; 35; 2413525.

S12 – O5

A mucoadhesive hydrogel stent approach for managing esophageal mucosal ulcers

Zarur M.[1], Yuts Y.[2], Leroux J.C.[2], Concheiro A.[1], Alvarez-Lorenzo C.[1]
[1]Dept. de Farmacología, Farmacia y Tecnología Farmacéutica, I+D Farma (GI-1645), Facultad de Farmacia, Materials Institute iMATUS and Health Research Institute of Santiago de Compostela (IDIS), Universidade de Santiago de Compostela, Spain; [2]Institute of Pharmaceutical Sciences, Dept. of Chemistry and Applied Biosciences, ETH Zurich, Switzerland

Introduction

Esophageal ulcers arise from multiple causes including reflux disease, inflammation, chemical injury, and malignancy, often leading to severe mucosal damage and complications. Endoscopic stenting is commonly used to maintain esophageal patency and manage advanced lesions when conventional treatment fails[1]. However, current self-expanding metal and plastic stents, which only provide passive mechanical support, are associated with complications such as migration, pain, and tissue overgrowth. Hydrogel-based materials offer a promising alternative due to their soft, tissue-like properties, swelling-driven expansion, and potential for improved mucoadhesion and therapeutic delivery[2].

Aim

To develop 3D-printed drug-loadable stent hydrogels via DLP using aqueous photopolymers to produce stents capable of providing combined mechanical support and localized therapy for enhanced treatment of esophageal mucosal lesions.

Materials and Methods

Poly(ethylene glycol) diacrylate (PEGDA), sodium carboxymethyl cellulose (CMC), methacrylic anhydride (MA), lithium phenyl-2,4,6-trimethylbenzoylphosphinate (LAP) and tartrazine were used. This study involves the methacrylation of CMC using MA, followed by dialysis for purification and freeze-drying. Aqueous photocurable inks containing 25% w/w PEGDA, methacrylated CMC (M-CMC), LAP as photoinitiator, and tartrazine as photoabsorber were formulated and optimized for printability. A lattice stent with defined geometry was designed using computer-aided design software and fabricated using a custom top-down DLP 3D printer. Printed stents were washed, UV post-cured and dried overnight in a desiccator at room temperature prior to characterization.

Results

PEGDA-based inks enabled the successful DLP printing of hydrogel stents with well-defined lattices and high geometric fidelity (Figure 1). A PEGDA blend (700/575, 60:40) provided a balance between crosslink density, flexibility and swelling capacity required for structural stability. Incorporation of M-CMC narrowed the printing window, with 0.5% w/w identified as the optimal concentration for maintaining the lattice resolution. The addition of tartrazine effectively controlled curing depth, preventing overcuring and preserving fine structural features. Dimensional analysis confirmed reproducible fabrication with minimal deviation from the CAD design and consistent lattice architecture.

Conclusion

Optimized water-based DLP formulations allowed high-resolution fabrication of expandable PEGDA/M-CMC hydrogel stents with well-defined lattice architectures and improved biocompatibility under environmentally friendly conditions, addressing a significant clinical challenge in esophageal ulcer management.

References

[1]Sharma P, Kozarek R. Role of Esophageal Stents in Benign and Malignant Diseases. *Am J Gastroenterol* 2010;105:258–73.
[2]Choi JR, Yong KW, Choi JY, Cowie AC. Recent Advances in Photo-Crosslinkable Hydrogels for Biomedical Applications. *BioTechniques* 2019;66:40–53.

Acknowlegments
The work was supported by Spain Ministerio de Ciencia, Innovación y Universidades MICIU/AEI/ 10.13039/501100011033 [PID2023-150422OB-I00], ERDF A way of making Europe, co-funded by the European Union, and Xunta de Galicia [ED431C 2024/09].

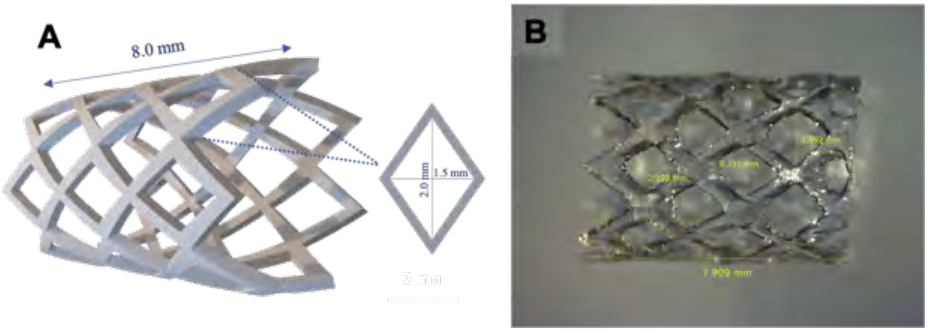

Figure 1**.** (A) CAD design of the stent geometry. (B) DLP-printed hydrogel stent showing defined diamond unit-cell architecture.

S12 – O6

Bioinspired pullulan-based adhesive coacervate films for targeted buccal delivery of peptides

Sacramento M.M.A.[1,2], Ezazi N.Z.[2,4], Pantazoglou E.[2], Lund P.M.[2], van de Weert M.[3], Zhang Z.[2], Vitorino R.[5], Bahuon F.[6], Berthelsen R.[6], Buckley S.T.[6], Untracht G.R.[2], Andersen P.E.[2], Brayden D.J.[7], Silva A.S.[1], Rodrigues J.M.M.[1], Nielsen L.H.[2], Mano J.F.[1]

[1]CICECO – Aveiro Institute of Materials, University of Aveiro, Aveiro, Portugal; [2]Dept. of Health Technology, Technical University of Denmark, Lyngby, Denmark; [3]Dept. of Pharmacy, University of Copenhagen, Copenhagen, Denmark; [4]KTH Royal Institute of Technology, Stockholm, Sweden; [5]iBiMED, University of Aveiro, Aveiro, Portugal; [6]Novo Nordisk A/S, Måløv, Denmark; [7]University College Dublin, Dublin, Ireland

Introduction

Peptide therapeutics are typically administered by injection due to poor oral bioavailability. Buccal delivery offers a non-invasive alternative, enabling systemic absorption through the vascularized oral mucosa while avoiding gastrointestinal degradation. However, buccal delivery of peptides remains challenging due to limited mucosal permeability and short residence time. In previous work, we developed mussel-inspired tannic acid–pullulan methacrylate (TA|PUL-MA) adhesive coacervates with strong wet adhesion.[1] Here, we extend this bioinspired platform to engineer mucoadhesive dual-layer films for buccal delivery of a glucagon-like peptide-1 receptor agonist (GLP-1-RA).

Aim

To engineer a mussel-inspired adhesive dual-layer buccal film for GLP-1-RA delivery and evaluate how polymer methacrylation degree (MD) influences adhesion, release, and transbuccal permeation.

Materials and Methods

Adhesive coacervates were formed by mixing TA with PUL-MA (1.5% and 3% MD). The dense coacervate phase was incorporated into a mucoadhesive layer containing the permeation enhancer sodium glycodeoxycholate (GDC) and the GLP-1-RA. Dual-layer buccal films were fabricated using scalable slot-die coating, consisting of an active mucoadhesive layer and a cellulose-based backing layer. Films were characterized in terms of rheology, morphology, mechanical properties, mucoadhesion, drug release, and peptide structural integrity. Film swelling and structural evolution were monitored on tissue using optical coherence tomography (OCT) under simulated oral conditions. Buccal permeation and retention were evaluated using *ex vivo* porcine buccal tissue models.

Results

Coacervate morphology and material properties were strongly influenced by the PUL-MA MD. Increasing MD enhanced film mechanical properties and mucoadhesive performance. The 3% methacrylation formulation exhibited the highest work of adhesion (~102.6 ± 14.2 J/m²), approximately five times higher than conventional buccal films. Dual-layer films enabled controlled release of GLP-1-RA and GDC while preserving the peptide secondary structure. *Ex vivo* permeation studies suggest that the enhanced mucoadhesion of the 3% methacrylation formulation improved tissue residence and facilitated peptide transport across buccal mucosa, achieving permeation values up to ~5.4% (Figure 1).

Conclusion

This study demonstrates a coacervate-based platform integrating mussel-inspired adhesion chemistry with scalable film manufacturing to enable buccal peptide delivery, highlighting their potential as a non-invasive and novel strategy for peptide administration.

Acknowledgements

This work was supported by the European Union's Horizon Europe research and innovation program, 101091765 ─ BUCCAL-PEP ─ HORIZON-CL4–2022-RESILIENCE-01. M.M.A.S acknowledge the Portuguese Foundation for Science and Technology for funding her individual PhD grant (DOI 10.54499/2020.07156.BD).

References

[1]Sacramento M., et al. Natural Polymer-Polyphenol Bioadhesive Coacervate with Stable Wet Adhesion, Antibacterial Activity, and On-Demand Detachment. *Advanced Healthcare Materials* 2024; 13; 2304587.***igure* 1.** Dual-layer buccal films for peptide delivery. A) Schematic illustration and photographs of the adhesive coacervate production stages resultant from the mixture of TA and PUL-MA, the precursor material of the mucoadhesive layer (ML). B) Mucoadhesive dual-layer film design, comprising a cellulose-based backing layer (BL) and the coacervate ML for the release of GLP-1-RA and the GDC. C) Schematic of the dual layer-film production process, comprising i) the coacervate precursor solution, ii) GDC and GLP-1-RA introduction into the coacervate precursor, iii) cast of the mucoadhesive coacervate precursor solution through slot-die coater, iv) solvent evaporation for ML fabrication, and v) cast and solvent evaporation of the BL solution for production of the dual-layer films. D) SEM image of the 3% MD dual-layer film cross-sectional view. Scale bar: 250 µm. E) Work of adhesion as indicator of mucoadhesive strength. F) Ex vivo permeation assays of GDC and GLP-1-RA: i) schematics of the ex vivo permeation set up with isolated porcine buccal tissue, ii) cumulative permeation of GDC and GLP-1-RA from the 3% MD dual-layer film across buccal tissue, in PBS at 37 °C, and iii) H&E staining images and the corresponding Coherent anti-Stokes Raman scattering (CARS) microscopy images of the epithelial buccal tissue layers following the permeability assays. CARS imaging (2850 cm^{-1}) showed increased CH_2 signal in GDC-exposed tissues from the positive control (GDC) solution, while dual-layer film–treated samples preserved tissue morphology. White arrows indicate the cell membrane; black arrows indicate the nuclei.

S12 – O7

Electroactive poly (L-lactic) acid thin films as platforms for modulation of PC12 cells

Fernandes M. [1], Ivanov M.[1], Vilarinho P.M.[1]
[1]Dept. of Materials and Ceramic Engineering, UA, Aveiro, Portugal

Introduction

The nervous system depends on precise electrical signals for intercellular communication, and disruptions from trauma or disease can impair function. Studies in neural tissue engineering show that electrical cues enhance neurite growth, cell adhesion, and differentiation. Because conventional stimulation is invasive, electroactive biomaterials have emerged as a promising alternative. Among these, piezoelectric polymers such as poly (L-lactic acid) (PLLA) are particularly attractive due to their ability to transduce mechanical stimuli into electrical signals. PLLA additionally offers biocompatibility, biodegradability, and U.S. Food and Drug Administration approval for certain medical applications. Here, to modulate membrane and action potentials in PC12 cells, semicrystalline PLLA thin films have been developed as electrically active platforms with periodic surface potentials.

Materials and Methods

A 2.5 wt% PLLA solution was prepared and deposited on top of stainless steel 316L substrates by spin coating. The resulting films were crystallized under different atmospheres (air, oxygen, nitrogen, and vacuum) using a Rapid Thermal Annealing furnace.

Results

Morphological analyses showed that crystallization atmosphere strongly affects PLLA spherulite formation, with nitrogen producing smaller, more uniform spherulites with clear Maltese-cross patterns and periodicity comparable to PC12 cell size, while vacuum suppressed crystallization, resulting in amorphous films. SEM analysis revealed atmosphere-dependent spherulite boundary features, with nitrogen films showing hierarchical growth between larger and smaller spherulites, oxygen films rigid boundaries, and air films less-defined interfaces. XRD and FTIR confirmed α-phase crystallinity in air, oxygen, and nitrogen, and amorphous structure under vacuum**.** AFM and KPFM results revealed that these crystalline surfaces generate local electrical polarization patterns in air and nitrogen, with nitrogen films exhibiting the strongest signals. All crystalline films were moderately hydrophilic, favoring cell adhesion to the spherulitic surfaces. In addition, they proved to be non-cytotoxic, supporting L929 viability, and immunocompatible, showing no NF-κB activation in THP-1 cells.

Conclusion

PLLA thin films with tailored periodic crystalline properties can generate localized electrical cues intrinsically, highlighting their potential as platforms for neural tissue engineering. Among the tested conditions, nitrogen-crystallized films showed the most favorable properties for effective neuron–film interaction.

Acknowledgements

This work was developed within the scope of the project CICECO – Aveiro Institute of Materials, UID/50011/2025 & LA/P/0006/2020 (DOI 10.54499/LA/P/0006/2020), financed by national funds through the FCT/MCTES (PIDDAC).

S13
Bioengineered platforms for studying environmental toxicity

S13 - K1
Biomaterial-engineered *in vitro* platforms to investigate the impact of environmental pollutants on cardiovascular tissues

Boffito M.[1], Vozzi F.[2], Sartori S.[1], Ciardelli G.[1]
[1]Dept. of Mechanical and Aerospace Engineering, Politecnico di Torino, Turin; [2]Institute of Clinical Physiology, National Research Council (IFC-CNR), Pisa, Italy

Introduction
Environmental pollutants, including hazardous chemicals as well as micro- and nanoplastics, represent an emerging class of contaminants whose interactions with human tissues are still poorly understood. Their potential impact on cardiovascular tissues poses growing concerns for human health. In this context, advanced *in vitro* models are gaining increasing relevance as predictive and ethically sustainable alternatives to conventional two-dimensional cell cultures and animal experimentation. Biomaterials play a key enabling role in this transition, as their tuneable chemical, mechanical and structural properties allow the creation of sophisticated three-dimensional microenvironments that better reproduce native tissue architecture and function. This contribution highlights recent advances in biomaterial-based *in vitro* systems designed to emulate relevant features of the cardiac tissue at different stages of ageing and exposed to environmental toxicants.

Materials and Methods
Advanced biomaterial platforms were developed through the bottom-up design of block-poly(ester urethane)s and the ad-hoc bulk functionalization of natural polymers. These materials can be processed into complex three-dimensional architectures capable of reproducing key aspects of the native extracellular matrix and tissue microstructure at different stages of ageing. Combined with advanced biofabrication approaches, these biomaterials support the development of *in vitro* bioengineered cardiac tissue models. Such systems enable the establishment of physiologically relevant culture conditions and controlled exposure scenarios for pollutant studies.

Results
Biomaterial-engineered platforms demonstrated the ability to enhance the maturation and functionality of human induced pluripotent stem cell-derived cardiomyocytes at both the cellular and molecular levels. Furthermore, our findings showed that, through the precise modulation of model physico-chemical and mechanical properties, distinct stages of myocardial aging can be effectively recapitulated. Indeed, myocardial aging was associated with increased levels of specific biomarkers related to cardiac damage, mitochondrial dysfunction, protein degradation, lipid impairment leading to membrane disorganization, as well as alterations in muscle contraction processes and inflammatory pathways. Overall, the developed models provide an advanced platform for investigating cellular responses to environmental pollutants under physiologically relevant conditions.

Conclusion
By integrating advanced biomaterials with physiologically relevant *in vitro* systems, the developed 3D bioengineered cardiac tissue models represent powerful platforms for investigating pollutant–tissue interactions with enhanced predictive capability, while accounting for the influence of ageing on tissue responses. Their further development and validation may facilitate the implementation of next-generation alternative methods for toxicity testing, supporting more human-relevant environmental risk assessment and reducing reliance on animal models.

Acknowledgements
This work was supported by the European Union’s Horizon 2020 research and innovation program (grant #101037090 and #814495). The content of this manuscript reflects only the author’s view, and the Commission is not responsible for any use that may be made of the information it contains.

S13 – O1

LbL nanocoating to improve biomimicry of aged cardiac tissue 3D models for cardiotoxicity screening

Cassa M.A.[1,2], Licciardello M.[2], Tonda-Turo C.[1,2], Gentile P.[3], Ciardelli G.[1,2] and Carmagnola I.[1,2]
[1]Dept of Aerospace and Mechanical Engineering (DIMEAS), Politecnico di Torino, Torino, Italy; [2]Polito BIOmed Lab, Politecnico di Torino, Torino, Italy; [3]Centre for Biomaterials and Tissue Engineering, Universitat Politècnica de València, València, Spain

Introduction

Current standards for chemicals and pharmaceuticals toxicity testing rely greatly on animal and 2D *in vitro* human models, facing both ethical issues and discrepancies from actual human *in vivo* scenarios. H2020 project ALTERNATIVE focused on the development of a high-throughput cardiotoxicity screening platform based on 3D bioengineered control and aged human cardiac *in vitro* constructs cultured on melt-extruded polymeric scaffolds based on polycaprolactone (PCL).

Aim

Development of a nanostructured biomimetic Layer-by-Layer (LbL) coating composed of cardiac extracellular matrix (cECM) proteins abundant in hypertrophic, aged cardiac tissue to be applied on polymeric substrates for cardiac tissue engineering (TE).

Materials and Methods

The LbL coating (COLL1/FIB) was composed of 6 bilayers, the selected polycations were collagen type I (COLL1) in the first 3 bilayers and a mix of fibronectin (FIB) and COLL1 in the last 3 bilayers. The polycations were alternated with negatively charged hyaluronic acid (HA). PCL was used as a model substrate to study the coating deposition and its stability behaviour in terms of physico-chemical (WCA, ATR-FTIR, XPS, QCM-D) and morphological (SEM, profilometry) properties. Then the coating was applied onto porous LbL-coated PCL scaffolds and preliminary biological characterizations were carried out with murine cardiac myoblasts (H9C2 cell line) via Live/Dead and phalloidin staining.

Results

The QCM-D deposition study estimated a final coating thickness of 30 nm. The coating greatly improved the hydrophobicity of pristine PCL and resulted stable in physiological conditions up to 48h (Figure 1a). Surface topography showed web-like patterns and aggregates ascribable to the LbL deposition (Figure 1b), with a final roughness around 85 nm. Viability of H9C2 onto LbL-coated substrates was 95% after only 3 days of culture. Cells greatly colonized the 3D scaffolds and showed a well-spread morphology (Figure 2).

Conclusion

A nanocoating resembling the composition of aged cECM with suitable physico-chemical properties for TE applications was successfully developed. Ongoing work is evaluating the potential coating ability to support H9C2 differentiation into cardiomyocytes. The developed LbL coating represents an easy, versatile and tunable strategy to reproduce different pathological and physiological ECM compositions on substrates intended for TE, avoiding the use of organic solvents and producing minimum toxic chemical waste for a more sustainable process.

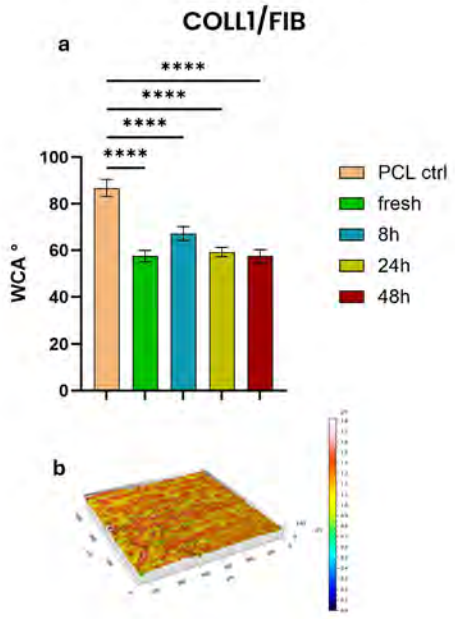

Acknowledgements

This work was supported by the European Union's Horizon 2020 research and innovation program (grant n. 101037090). The content of this manuscript reflects only the author's view, and the Commission is not responsible for any use that may be made of the information it contains.

///

S13 – O2

3D Bioprinted Fibro-Lung Model as tool to predict the mineral fiber-induced fibrosis

De Biagi L.A.[1], Petrachi T.[1], Veronesi E.[1], Fantini R.[2], Colombo F.[2], Gualtieri A.F.[2]
[1]TPM-Tecnopolo Mario Veronesi, Mirandola; [2]Dept. of Chemical and Geological Sciences, University of Modena and Reggio Emilia, Modena, Italy

Introduction

Mineral fibres can pose significant health risks, as shown by asbestos exposure. They trigger occupational diseases like pneumoconiosis, characterized by excessive extracellular matrix deposition. As toxicity varies across mineral species, reliable screening tools are essential. We present a patented 3D Fibro-Lung Model (FLM) to investigate biological responses to fibres in a physiologically relevant 3D system, providing an alternative to 2D cultures.

Materials and Methods

FLM consists of bioprinted Normal Human Lung Fibroblasts (NHLFs) encapsulated in a type-I collagen-based bioink (3D Bioplotter, EnvisionTEC). After 72h maturation, scaffolds were exposed (50 µg/mL) to: Crocidolite (CRO, mineral positive control) and Wollastonite (NYAD, mineral negative control). TGFβ1 (10 ng/mL) served as a biological positive control, while non-treated (N.T.) scaffolds were used as a negative baseline control. Assessments at 1, 3, 7, and 14 days included cell viability, fibronectin expression (immunofluorescence), collagen deposition (Masson's Trichrome), and mechanical analysis via nanoindentation. Data are expressed as mean±SD.

Results

FLM successfully discriminated between stimuli through distinct mechanisms. At day 1, TGFβ1 promoted a significant initial collagen deposition ($p < 0.001$ vs NYAD), while CRO significantly upregulated fibronectin expression over N.T. baseline ($p < 0.01$). By day 14, Masson's Trichrome quantification demonstrated a massive accumulation of collagen in positive controls, with CRO (60712.96±18504.50µm^2) and TGFβ1 (74431.34±10917.94µm^2) showing a 2-fold increase compared to negative controls, NYAD (25525.54±7777.73µm^2) and N.T. (31205.80±10503.1µm^2) ($p < 0.0001$). These findings were corroborated by nanoindentation data, which highlighted a significant stiffening of the scaffolds: at day 14, the Young's Modulus for CRO (6.99±0.76kPa) and TGFβ1 (16.46±1.16kPa) was significantly higher than the baseline measured for N.T. (3.58±0.45kPa) and NYAD (3.71±0.80kPa) ($p < 0.0001$), confirming the model's ability to replicate the mechanical hallmarks of lung fibrosis.

Conclusion

FLM is a robust tool for studying lung fibrosis induced by mineral stimuli. Our findings demonstrate that the model discriminates between hazardous fibers and inert minerals, replicating the complex biological and mechanical changes of fibrotic tissue. This validates the 3D bioprinted platform as a reliable tool for the safety assessment of mineral materials.

Acknowledgements

Supported by the Project 101113855 – LIFE22-ENV-IT-LIFE ReWo co-funded by the European Union, and Project POR FESR 2014–2020 (CUBIBOX).

S13 – O3

High-throughput neuro-nanotoxicity studies of manufactured nanomaterials with complex microfluidic BBB models

Lefevre, M.C.[1], Feregotto, G.[1,2], Ceccarelli, M.C.[1,2], Gigante, G.[1,2], Bernardeschi, M.[1], Ciofani, G.[1]
[1]Smart Bio-Interfaces, Istituto Italiano di Tecnologia, Viale Rinaldo Piaggio 34; [2]The BioRobotics Institute, Scuola Superiore Sant'Anna, Viale Rinaldo Piaggio 34, Pontedera, Italy

Introduction

Nanoparticles (NPs) are increasingly used in industry and medicine, raising concerns about human exposure and accumulation in sensitive organs such as the brain. Some NPs can cross or disrupt the blood-brain barrier (BBB), potentially triggering inflammation and neurotoxicity. Reliable in vitro BBB models are therefore needed to assess neuro-nanotoxicity. Here, we developed a sensorized high-throughput microfluidic BBB-on-chip platform that recreates the 3D BBB microenvironment under flow and enables real-time barrier monitoring to evaluate the effects of benchmark and manufactured nanomaterials.

Materials and Methods

The platform was fabricated in polydimethylsiloxane by soft lithography and bonded to a glass substrate integrating thin-film platinum microelectrodes. Immortalized human astrocytes (IM-HA) embedded in Geltrex represented the brain parenchyma, while immortalized human brain microvascular endothelial cells (IM-HBMEC) formed the vascular barrier along an array of 10 µm-spaced pillars. Vascular channels were perfused with culture medium at 20 µL/min for 24 h. Barrier integrity was assessed in real time by electrochemical impedance spectroscopy (EIS) using *in situ* electrodes on both sides of the BBB. The system was then scaled into a multi-BBB-on-chip format comprising 10 groups of 8 interconnected units. Benchmarked SiO2, silver, and graphene NPs, together with graphene-based manufactured nanomaterials from different companies, were tested at concentrations ranging from 50 to 0.005 µg/mL. Proteomic analyses were additionally performed to investigate molecular changes associated with nanomaterial exposure.

Results

The platform was first optimized on a single organ-on-chip model to evaluate the effect of the fluid flow on BBB integrity and permeability. After 2 days of maturation, the IM-HBMEC formed a vessel-like structure along the pillars in the perfusion channels. The system was connected to a microfluidic pump and perfused for 24 hours, during which the BBB integrity was monitored via EIS (Figure 1.a). Impedance remained stable for the first 6 hours and then slightly decreased at intermediate to high frequencies (>100 Hz), with values significantly higher than those observed in a disrupted BBB (Figure 1.b). This model was scaled in parallel to a multi-BBB-on-chip model consisting of 10 groups of 8 connected single-BBB models, which can be independently monitored, enabling higher-throughput nanotoxicity studies (Figure 1.c). While benchmark SiO2, silver, and graphene NPs did not measurably affect barrier integrity under the tested conditions, the platform discriminated among manufactured graphene-based nanomaterials according to their detrimental effects on the BBB (Figure 1.d).

Conclusion

This sensorized multi-BBB-on-chip platform combines physiological relevance, real-time EIS monitoring, and high-throughput capacity for neuro-nanotoxicity assessment. The model maintained a stable and functional barrier under flow and distinguished subtle differences in BBB toxicity among manufactured graphene-based nanomaterials. Combined with proteomic profiling, it represents a promising tool for screening neurotoxic risks associated with engineered nanomaterials and for supporting safer-by-design nanotechnology.

Acknowledgements

This research has received funding from the European Health and Digital Executive Agency (iCare, 101092971).

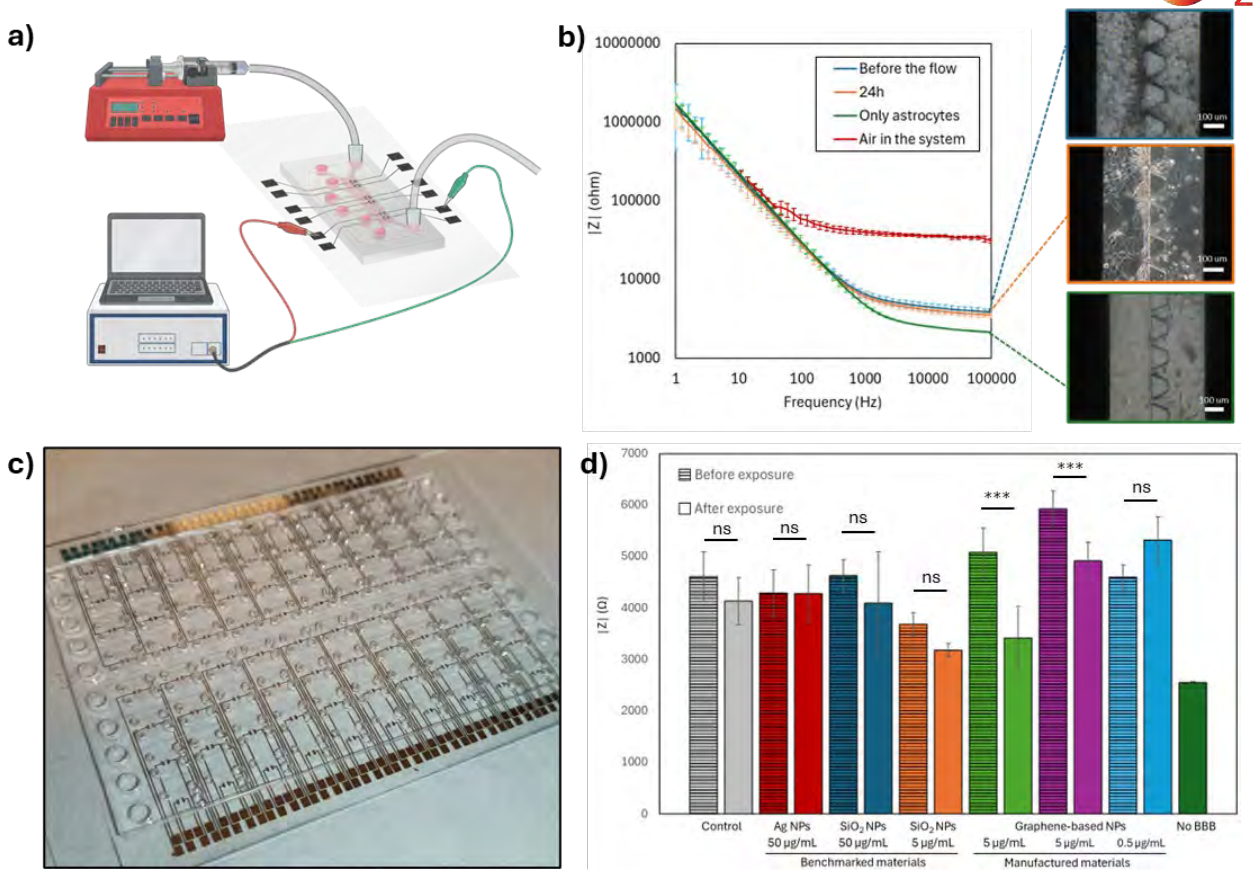

Figure 1: Development and application of the sensorized multi-BBB-on-chip platform for neuro-nanotoxicity studies. (a) Schematic of real-time electrochemical impedance spectroscopy (EIS) monitoring of BBB integrity during 24 h perfusion in the single BBB-on-chip model. (b) Impedance profile of the BBB under fluidic conditions compared with a disrupted barrier, showing maintenance of barrier integrity over time. (c) Image of the high-throughput multi-BBB-on-chip platform composed of 10 groups of 8 interconnected single BBB models, independently monitored by integrated thin-film microelectrodes. (d) Evaluation of the effects of benchmark and manufactured nanomaterials on BBB integrity by impedance measurement at 10 kHz, showing the ability of the platform to discriminate the detrimental impact of different graphene-based manufactured nanomaterials. Data are presented as mean ± SD (∗∗∗, $p < 0.0005$).

S13 – O4

A porous alveoli-like 3D lung model for investigating microplastic interactions with lung tissue

Chiudaroli L.[1], Capotorto E.[1], Pionato S.[2], Acosta S.[2], Rodriguez Cabello J.C.[2], Farè S.[1,3]
[1]Dept. of Chemistry, Materials and Chemical Engineering G. Natta, University of Politecnico di Milano, Milano; [2]GIR Bioforge, Universidad de Valladolid, CIBER-BBN, Valladolid, Spain; [3]National Interuniversity Consortium of Materials Science and Technology (INSTM), Florence, Italy

Introduction

Institutional and public attention on the environmental pollution has increased significantly in recent years. In particular, microplastics represent an emerging concern for human health. These particles can enter the body through ingestion, dermal exposure, and inhalation, accumulating in various organs. However, their biological effects and potential contribution to pulmonary diseases remain poorly understood.

Aim

To address this knowledge gap, we propose the development of a porous alveoli-like 3D *in vitro* lung model based on a blend of GelMA and elastin-like recombinamers (ELR-MA) and sodium alginate sacrificial microbeads (MBs) to generate a platform intended to investigate interactions between microplastics and lung tissue.

Materials and Methods

MBs (2% w/v sodium alginate, Alg) were fabricated using an optimized setup based on a coaxial needle connected to an air flow system [1]; 100 mM calcium chloride was used for the crosslinking. The morphology of the MBs was characterized by optical microscope. L929 cells were encapsulated into the Alg MBs. GelMA was synthetized and its methacrylation degree was verified through H-NMR analysis and TNBSA assay. The Alg MBs were embedded in 10% w/v GelMA. To avoid cell damage induced by UV exposure, visible light photocrosslinking was performed using riboflavin and sodium persulfate. The composite scaffold was immersed in 50 mM trisodium citrate to dissolve the Alg MBs to allow cell release within the pores generated in the GelMA matrix. To verify the complete dissolution of Alg, aminoethyl Rhodamine B (Rh-B) was synthesized and Alg was functionalized via amidic bond [2]. Cell metabolic activity after the release from the Alg MBs was assessed via AlamarBlue assay over 14 days. Cells viability and organization was investigated through Live/Dead assay.
Alongside, ELR-MA was synthesised and methacrylation were verified through H-NMR. Preliminary compression and rheological mechanical tests on GelMA, ELR-MA and blend were performed.

Results

H-NMR and TNBSA assay confirmed a 60% degree of methacrylation for GelMA. Morphological study of the Alg MBs highlighted diameters in the range 100-400 µm, consistent with the physiological alveolar structure (Figure 1). Functionalization with Rh-B allowed to verify, through optical and fluorescence analysis, the complete dissolution of Alg within the GelMA matrix. AlamarBlue demonstrated good cellular metabolism, while Live/Dead assay confirmed high cells viability. Fluorescence analysis showed cells distribution along the inner walls of the pores formed after Alg dissolution (Figure 2).
The TNBSA test revealed a 2.3 ratio between the functional groups concentration of ELR-MA and GelMA. Considering this result, along with the physiological balance of lung components (approximately 60% collagen and 40% elastin), the optimal hydrogel formulation was set at 77.5% GelMA and 22.5% ELR-MA.

Conclusion

This work demonstrates the feasibility of developing a porous 3D lung model that mimics lung parenchyma tissue architecture. The results show good structural properties and cell viability, highlighting the potential of this platform as a relevant *in vitro* model to study interactions between microplastics and lung tissue.

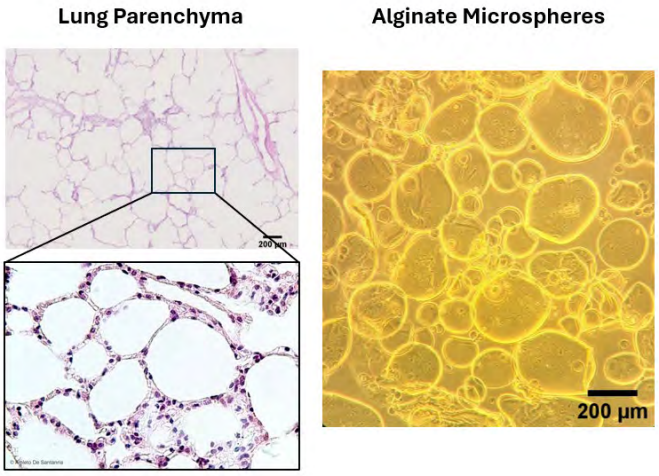

Figure 1: comparison between lung parenchyma and Alginate microspheres

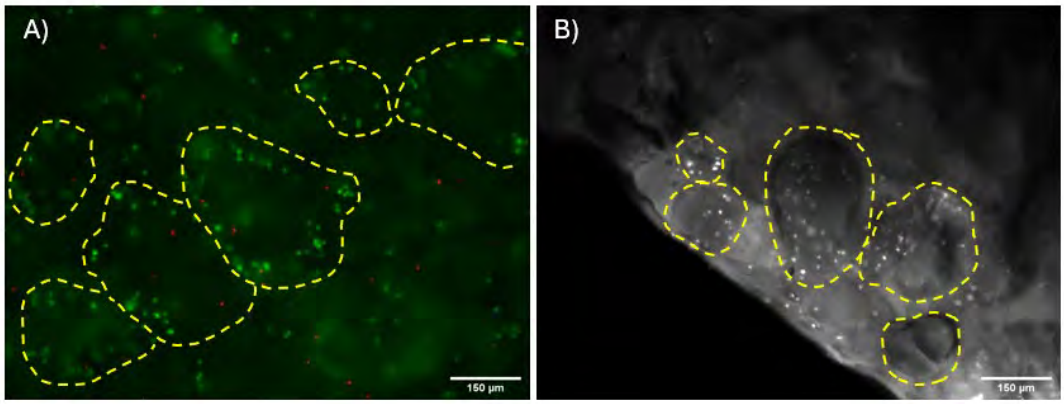

Figure 2: A) Live/Dead staining; B) optical image of a slice of sample; in both the images the perimeters of the alveolar-like structure are highlighted in yellow.

Acknowledgements

This work was funded by the National Plan for NRRP Complementary Investments in the call for the funding of research initiatives for technologies and innovative trajectories in the health and care sectors (Directorial Decree n. 931 of 06-06-2022) - project n. PNC0000003 - AdvaNced Technologies for Human-centrEd Medicine (ANTHEM).

References

[1] N. Contessi Negrini, M Bonnetier, G Giatsidis, D P Orgill, S Farè, B Marelli, “Tissue-mimicking gelatin scaffolds by alginate sacrificial templates for adipose tissue engineering”, Acta Biomaterialia, 2019, 87, 61–75

[2] R. Bernasconi, E. Mauri, A. Rossetti, S Rimondo, R Suriano, M Levi, A Sacchetti, S Panè, L Magagnin, F Rossi, “3D integration of pH-cleavable drug-hydrogel conjugates on magnetically driven smart microtransporters”, Materials and Design, 2021, 197

S13 – O5

3D engineered human cardiac tissues as platforms for cardiotoxicity assessment

Pochettino E.[1,2], Alliaud A.[1], Gisone I.[3], Fernandez-Arroyo S.[4], Boffito M.[1], Sartori S.[1], Cecchettini A.[5], Ceccherini E.[3], Vozzi F.[3], Ciardelli G.[1]

[1]Dept. of Mechanical and Aerospace Engineering, Politecnico di Torino, Turin, Italy; [2]Dept. of medical and surgical sciences, Università di Torino, Turin, Italy; [3]Institute of Clinical Physiology IFC-CNR, Pisa, Italy; [4]Centre for Omic Sciences, Joint Unit Eurecat-Universitat Rovira i Virgili, Reus, Spain; [5]Dept. of Clinical and Experimental Medicine, University of Pisa, Pisa, Italy

Introduction

Humans are constantly exposed to a wide range of environmental and pharmaceutical compounds, some of which may exert cardiotoxic effects. However, cardiotoxicity remains insufficiently investigated, particularly in relation to age-related differences in cardiac tissue response. Structural and functional changes occurring during myocardial aging can significantly influence cellular susceptibility to toxic agents. Therefore, reliable *in vitro* models capable of reproducing different stages of myocardial maturation are essential for more accurate evaluation of drug and chemical toxicity.

Aim

The aim of this work was to develop bioengineered 3D cardiac models that mimic different stages of myocardial aging as platforms for cardiotoxicity assessment.

Materials and Methods

The models consisted of fibronectin-functionalized scaffolds fabricated via melt-extrusion additive manufacturing using a custom-made poly(caprolactone)(PCL)-based polyurethane (PUR). These scaffolds were combined with photocurable gelatin methacryloyl (GelMA) hydrogels at 5% and 10% w/v concentration to reproduce the mechanical properties of young and mature myocardium, respectively. GelMA served as a carrier for a co-culture of human-induced pluripotent stem cell-derived cardiomyocytes and human coronary artery endothelial cells in an 80:20 ratio. The cellularized GelMA precursor was pipetted into the PUR scaffolds and subsequently photo-crosslinked (365 nm, 10 mW/cm², 30 s) to obtain the final biphasic constructs. Multi-omics approaches consisted of transcriptomics (RNA-seq by Illumina platform), untargeted proteomics (by nLC-Orbitrap-MS), and targeted metabolomics and lipidomics (by LC-QqQ-MS).

Results

PUR synthesis was confirmed by infrared spectroscopy and size exclusion chromatography, while differential calorimetry and thermogravimetric analyses provided information on its thermal transitions and stability. Scaffolds with anisotropic architecture (filament diameter of *ca.* 0.41 mm) were produced and surface-functionalized with fibronectin to enhance biomimicry of cardiac extracellular matrix. Photo-rheological characterization of GelMA hydrogels revealed Young's modulus values of approximately 10 kPa and 55 kPa for 5% and 10% formulations, reproducing the mechanical properties of young and mature myocardium, respectively. Scanning electron microscopy of the assembled constructs revealed strong PUR–GelMA integration and an interconnected porous network that supports nutrient and oxygen diffusion. The cell-based models were cultured for up to 11 days, during which cell viability and oxidative stress were monitored. Multi-omics analyses (transcriptomics, proteomics, and metabolomics) revealed that myocardial aging was associated with mitochondrial dysfunction, loss of calcium homeostasis, enhanced protein degradation, impaired cell-cell adhesion, and alterations in amino acid and lipid metabolism, ultimately affecting contractile function and cellular maturation.

Conclusion

The developed 3D cardiac models successfully reproduced key features of young and mature myocardial tissue *in vitro*. These platforms represent promising tools for investigating age-related cardiac physiology and for improving the predictive assessment of chemical-induced cardiotoxicity.

Acknowledgements

This work was supported by the European Union's H2020 research and innovation program (ALTERNATIVE project, grant#101037090). The content of this abstract reflects only the author's view, and the Commission is not responsible for any use that may be made of the information it contains.

S13 – O6

Sacrificial scaffolds as a reproducible and scalable platform for perfusable microvascularized 3D tissue models

Kuntschke P.[1], de Silva L.[1], Theis K.[1], Di Gravina G.M.[1], Raduechel A.[1], Groll J.[1], Ryma M.[1]
[1]Dept. of Functional Materials in Medicine and Dentistry, University Hospital Wuerzburg, Wuerzburg, Germany

Introduction

The lack of reproducible vascularization remains a major bottleneck in the development of physiologically relevant in vitro tissue models. While advanced biofabrication techniques can generate microvascular structures, many approaches lack scalability, reproducibility, and compatibility with industrial manufacturing. Here, we present a bioreactor-based platform enabling the generation of perfusable and endothelialized microvascular networks within hydrogel matrices using sacrificial polymer scaffolds. By combining Murray's law–guided vascular design with scalable fabrication strategies, this work aims to establish a reproducible and user-friendly platform for vascularized 3D tissue models.

Materials and Methods

Sacrificial vascular templates were designed using bifurcating and interconnected network architectures based on Murray's law (Fig. 1) to achieve physiologically relevant flow distributions. Scaffolds were fabricated from poly(2-oxazoline) using high-resolution vacuum casting and injection molding to enable scalable production of complex microvascular geometries. The sacrificial templates were integrated into custom-designed bioreactor chambers produced via additive manufacturing. Following embedding in hydrogel matrices (fibrin and gelatin methacryloyl), the sacrificial templates were dissolved to generate perfusable microchannel networks. Geometric fidelity of mother and daughter vessel diameters was quantified before and after template dissolution to evaluate structural accuracy and hydrogel swelling effects. Endothelial cells were seeded into the channels under dynamic perfusion to generate endothelialized lumens. Immunofluorescence staining was used to assess endothelialization and vessel maturation. Compatibility with embedded cells and spheroid cultures was evaluated to demonstrate platform versatility.

Results

The sacrificial scaffolds enabled reproducible fabrication of interconnected microvascular channels within hydrogel matrices. Quantitative analysis demonstrated high structural fidelity of the templated networks and predictable diameter changes following hydrogel formation. The generated channels supported immediate perfusion and endothelial cell seeding, resulting in continuous endothelialized lumens characterized by CD31 and collagen IV expression (Fig. 2A, B, D). Angiogenic sprouting from the perfused vessels into the surrounding hydrogel matrix was observed, indicating active endothelial remodeling (Fig. 2C). The platform further supported co-culture with embedded cells and spheroid-based tissue models, demonstrating the ability to establish barrier-free interactions between vascular networks and surrounding tissue constructs.

Conclusion

This work presents a scalable sacrificial scaffold strategy enabling reproducible fabrication of perfusable and endothelialized microvascular networks within a modular bioreactor platform. By integrating flow-optimized vascular design, scalable manufacturing, and biological functionality, the developed system provides a versatile platform for vascularized 3D tissue models. Such ready-to-use vascularized culture systems offer a promising route toward standardized in vitro models for tissue engineering, disease modeling, and high-throughput drug testing.

Acknowledgements

The authors thank the Horizon EIC Transition project Vasc-on-Demand (project number 101156395) for financial support.

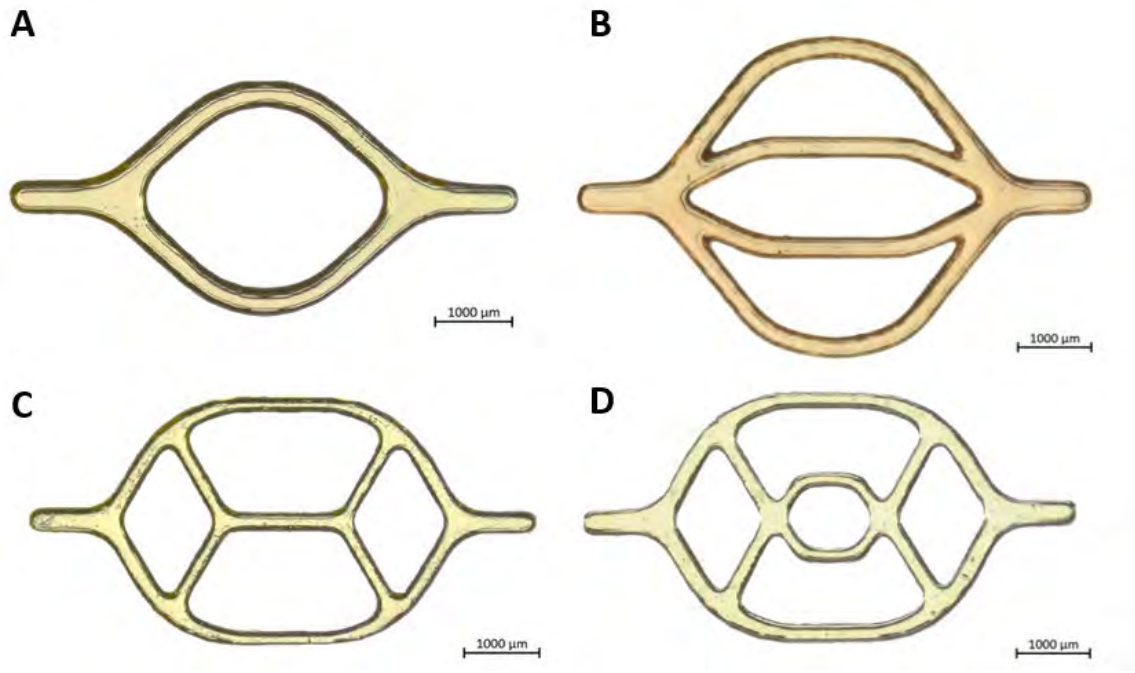

Figure 1. Sacrificial scaffold designs fabricated from poly(2-oxazoline).
(A) Simple bifurcating scaffold design. (B) Four-branch scaffold. (C) Interconnected scaffold geometry. (D) Circular interconnected scaffold. Scale bars: 1000 µm.

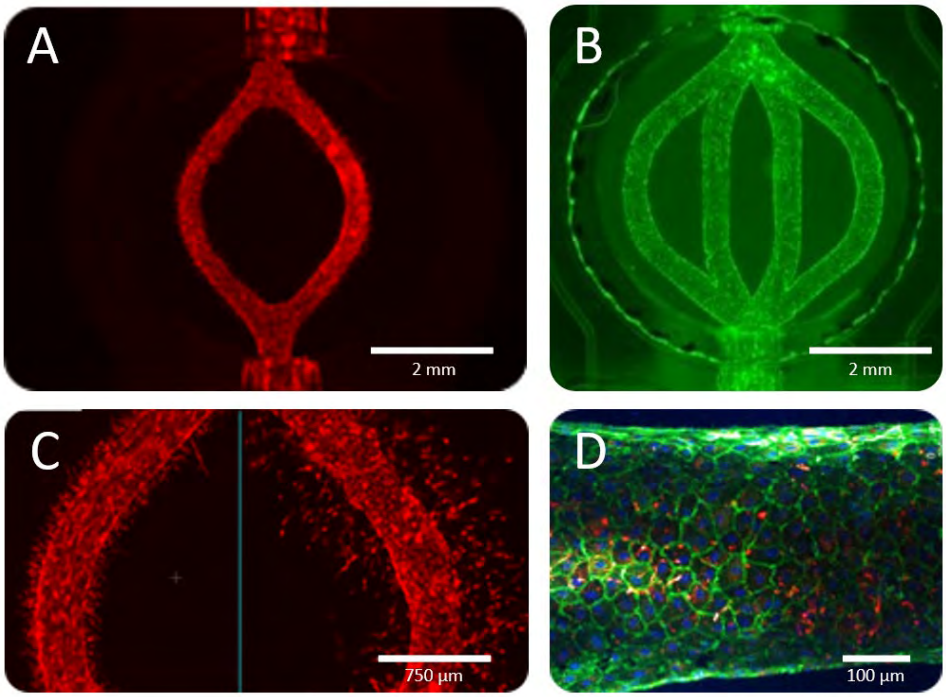

Figure 2. Sacrificial scaffold–templated microvascular networks in hydrogels.
(A) Bifurcating channel architecture with endothelial cells (red). (B) Perfused four-branch channel network seeded with GFP-HUVECs. (C) Angiogenic sprouting from the endothelialized vessel into the surrounding hydrogel matrix. (D) Confocal image of an endothelialized lumen showing CD31 (green) and collagen IV (red). Scale bars: 2 mm (A,B), 750 µm (C), 100 µm (D).

S13 – O7

Electrospun fiber-based scaffolds for *in vitro* cardiac tissue modeling

Ruocco G.[1,2,3], Nicoletti L.[1,2,3], Paoletti C.[1,2,3], Zoso A.[1,2,3], Carmagnola I.[1,2,3], Chiono V[1,2,3]
[1]Dept. of Mechanical and Aerospace Engineering, Politecnico di Torino; [2]PolitoBIOMed Lab, Politecnico di Torino; [3]Interuniversity Center for the Promotion of 3Rs Principles in Teaching and Research, Politecnico di Torino, Turin, Italy

Introduction

The development of predictive *in vitro* models is essential for advancing the study of environmental toxicity and reducing reliance on animal testing. Cardiac tissue is particularly vulnerable to toxic insults, yet conventional 2D cultures fail to reproduce the complex microenvironment and cell-cell interactions of the human myocardium. In this context, biomimetic scaffolds represent a promising strategy to engineer physiologically relevant platforms for toxicity assessment.

Aim

This study aims to develop and validate an electrospun fiber-based *in vitro* cardiac tissue model and to assess its suitability for investigating cytotoxicity and cellular responses.

Materials and Methods

Electrospun poly(ε-caprolactone) (PCL) fibrous scaffolds were fabricated and functionalized with extracellular matrix proteins to promote cell adhesion and activation. Human cardiac fibroblasts (HCFs) and human induced pluripotent stem cell-derived cardiomyocytes (hiPSC-CMs) were cultured on these substrates to establish *in vitro* cardiac tissue models. A custom-designed multiwell platform enabled reproducible scaffold handling and compatibility with standard assays (Figure 1). Biological validation included immunofluorescence, gene expression analysis, and functional assays. To evaluate the platform for toxicity studies, cells were exposed to RNA-loaded nanoparticle-based delivery systems, and cytocompatibility, cytotoxicity, and cellular uptake were assessed.

Results

The electrospun scaffolds supported fibroblast activation and extracellular matrix deposition, enabling the development of a physiologically relevant fibrotic cardiac model. Co-culture systems demonstrated spatial organization and intercellular communication between HCFs and hiPSC-CMs. The platform showed high reproducibility and compatibility with high-content imaging. Exposure to nanoparticle-based delivery systems revealed cell-type-specific responses, with functionalized nanoparticles showing enhanced uptake in fibroblasts and improved cytocompatibility compared to non-functionalized systems (Figure 2). These results highlight the ability of the platform to detect differential cytotoxic effects and uptake mechanisms in a multicellular cardiac environment.

Conclusion

This study presents a scalable and biomimetic in vitro cardiac platform based on electrospun fibrous scaffolds, suitable for investigating tissue-level responses to environmental and nanomaterial-related toxicity. In particular, the system enables the evaluation of cytotoxicity and targeting efficiency of nanoparticle-based delivery systems in a human-relevant cardiac model, supporting its application as a bioengineered platform for advanced toxicological screening and preclinical safety assessment.

Acknowledgements

This study has received funding from European Union - Next Generation EU, Mission 4 - Component 2 through MERIT project (CN00000041_1; CUP E63C22000940007) and NANOMIRC project (CN00000041; CUP C93C22002780006).

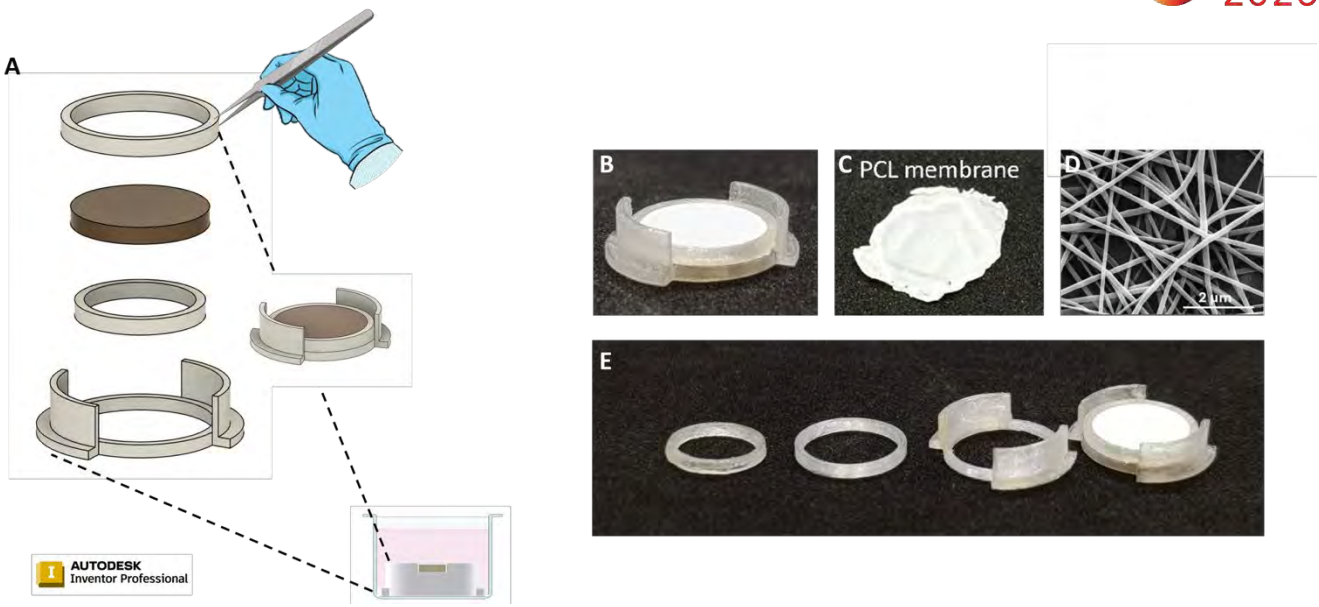

Figure 1. Design and fabrication of the holder and poly(ε-caprolactone) (PCL) nanofibrous scaffold.
(A) Schematic representation of the assembly process of the culture platform components, including insertion of the membrane into the supporting ring structure. (B) Photograph of the assembled membrane holder. (C) Representative image of PCL scaffold used as cell culture substrate. (D) Scanning electron microscopy (SEM) image of the electrospun PCL scaffold showing a fibrous architecture; scale bar: 2 µm. (E) Disassembled components of the culture platform, including supporting rings and membrane holder, prior to assembly.

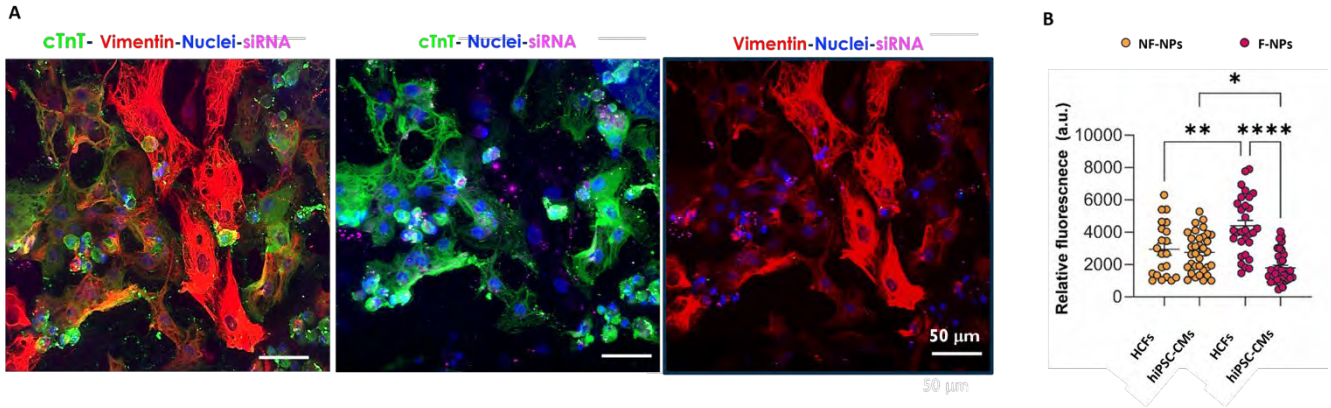

Figure 2. Nanoparticle uptake in the ReF co-culture model assessed by immunofluorescence.
(A) Representative immunofluorescence images of the co-culture model showing uptake of Cy5-labeled siRNA-loaded nanoparticles. Cardiomyocytes were identified by cardiac troponin T (cTnT, green), fibroblasts by vimentin (red), nuclei by DAPI (blue), and internalized siRNA is shown in magenta (Cy5). Merged and single-channel images highlight preferential nanoparticle accumulation in fibroblasts compared with cardiomyocytes. Scale bars: 50 µm. (B) Quantification of Cy5 fluorescence intensity is shown on the right and expressed as relative fluorescence (a.u.) in HCFs and hiPSC-CMs. Data are presented as individual data points with mean ± SD. Statistical significance is indicated as *$p < 0.05$, **$p < 0.01$, ****$p < 0.0001$.

S14
Biofabrication of complex tissues and models using functional biomaterials

S14 – K1
3D printing and biofabrication of engineered tissues in vitro

Kim BS[1]

[1]School of Biomedical Convergence Engineering, Pusan National University, Republic of Korea

Introduction

Three-dimensional (3D) printing and biofabrication technologies provide powerful strategies for engineering complex, cell-laden tissues with controlled architecture, material properties, and biological function. These approaches are particularly useful for constructing physiologically relevant in vitro models that bridge conventional two-dimensional cell culture and native tissue environments. However, the successful fabrication of engineered tissues requires the coordinated design of printing processes, bioink properties, and biological cues to support structural fidelity, cell viability, and tissue-specific function.

Materials and Methods

Our laboratory has developed and integrated multiple biofabrication platforms, including planar-based printing, rotational-based printing, customized coaxial nozzles, embedded printing, cellular spheroid-based assembly, and perfusion-friendly printing. Bioink formulation and process parameters were considered together to regulate printability, shape stability, perfusability, and cellular responses. These engineering strategies were applied to generate skin, tumor, and vascular tissue models, with emphasis on epithelial organization, morphogenesis, shear stress-mediated vascular responses, mechanical loading, and matrix stiffness-dependent tumor microenvironments.

Results

The developed biofabrication approaches enabled the construction of diverse in vitro tissue platforms, including healthy and wounded skin models, blood-vessel-on-a-chip systems, vascularized 3D tissues, and vascularized metastatic tumor models. Skin models were designed to reproduce layered tissue organization and pathological wound environments. Perfusable vascular channels and vessel-on-a-chip platforms allowed the investigation of flow and shear stress-related biological responses. Tumor-associated models incorporated vascular and matrix components to better represent tumor-vessel interactions and microenvironment-dependent therapeutic responses. The overall concept and representative applications are summarized in Fig. 1.

Conclusion

By combining advanced printing technologies with biomaterial and microenvironmental design, 3D biofabrication can generate more relevant in vitro models of skin, tumor, and vascular tissues. These platforms provide useful tools for studying tissue morphogenesis, disease progression, and treatment response, and may contribute to the broader development of functional bioartificial organs.

Acknowledgements

This work was supported by the National Research Foundation of Korea (NRF) grant funded by the Korean government (RS-2025-14383075)

Keywords: 3D printing, bioprinting, biofabrication, engineered tissue, vascularized tissue, tumor microenvironment

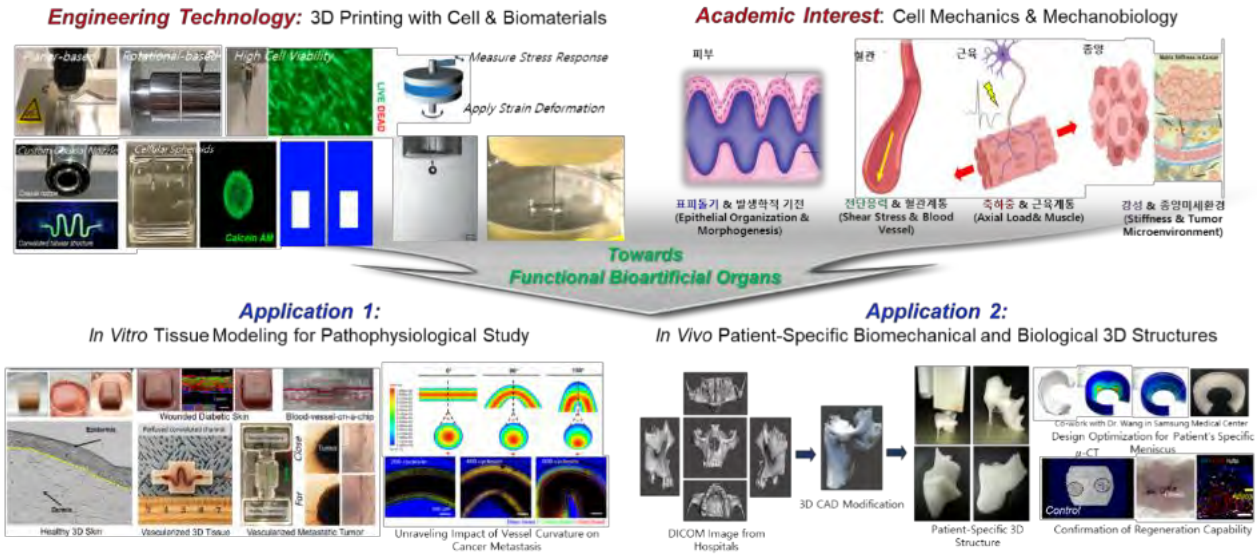

Fig. 1. Overview of engineering technologies, academic interests, and applications of 3D printing and biofabrication for engineered tissues in vitro.

S14 – K2
Novel Bioinks for 3D printing and Biofabrication of 3D tissue models

Vozzi, Giovanni

S14 – O1

Engineering a 3D model of bone metastasis with citrate-functionalized hydroxyapatite nanocrystals and microfluidics to investigate the role of citrate in prostate cancer progression

Pasquarelli A.[1], Cavassi E.[1], Bucchi L.[1], Boanini E.[3], Di Pompo G.[2], Lipreri M.V.[2], Perut F.[2], Bouidida Y.[4], Sonveaux P.[4,5], Rubini K.[3], Montesissa M.[2], Santonocito R.[2], Baldini N.[1,2], Avnet S.[1]

[1]Dept. of Biomedical and Neuromotor Sciences, University of Bologna, Bologna, Italy; [2]Biomedical Science, Technologies, and Nanobiotechnology Lab, IRCCS Istituto Ortopedico Rizzoli, Bologna, Italy; [3]Dept. of Chemistry 'Giacomo Ciamician', University of Bologna, Bologna, Italy; [4]Pole of Pharmacology and Therapeutics, Institut de Recherche Expérimentale et Clinique (IREC), Université catholique de Louvain (UCLouvain), Brussels, Belgium; [5]WEL Research Institute Research Institute, Walloon Excellence in Life Sciences and Biotechnology (WELBIO) Dept., Wavre, Belgium

Introduction

Prostate cancer (PCa) is one of the most common malignancies in men and is characterised by an energy metabolism centred on citrate consumption. PCa also frequently metastasises to bone, a tissue rich in citrate embedded within the mineralised matrix. The relationship between metastatic PCa and bone-derived citrate is currently unknown, partly owing to the lack of suitable 3D models of the bone microenvironment.

Aim

This study aimed to investigate the role of citrate metabolism in PCa metabolic reprogramming during bone metastatic progression, through the development of a 3D microfluidic bone model that recapitulates key chemical, physical, and biological features of the bone microenvironment.

Materials and Methods

To mimic the bone microenvironment, synthetic hydroxyapatite nanocrystals (HA-Nc) functionalised with citrate at different concentrations were produced. These nanoparticles were incorporated into a Matrigel®/Type I collagen mixture to obtain an osteomimetic matrix, which was used with PCa cells in either a 3D microfluidic chip or a custom 2.5D device to reproduce bone architecture, and gradients relevant to PCa progression. PC3 and LNCaP cells were used as models of aggressive and non-aggressive PCa, respectively. Cell viability, migration, clonogenicity, citrate transporter expression, and metabolic pathways were assessed by live/dead staining, transwell assay, Seahorse and Resipher analyses, live-cell confocal microscopy, flow cytometry, RT-qPCR, and capillary western blotting.

Results

In our system, HA-Nc released citrate at concentrations comparable to those found in bone. The released citrate promoted PCa osteotropism and clonogenicity within the bone-like matrix. Expression of the plasma membrane citrate transporter (pmCTP), which mediates citrate uptake, was higher in the more aggressive PC3 cells and was further upregulated by extracellular citrate. Citrate induced a shift in mitochondrial dynamics, increasing mitochondrial mass without a corresponding increase in OXPHOS. Lipid metabolism was unaffected. By contrast, glycolysis was reduced, alongside increased pyruvate and lactate secretion, suggesting a metabolic signature characterised by citrate uptake, mitochondrial biogenesis, and lactate fermentation. In addition, HA-Nc-derived citrate counteracted the drop in extracellular pH caused by the highly glycolytic activity of PCa cells. This buffering effect also increased the survival of PCa cells in an acidic microenvironment.

Conclusion

Our 3D microfluidic model of bone metastasis, combined with citrate-funcionalised HA-Nc, enables investigation of the role of citrate in PCa progression within bone, and may support the identification of novel therapeutic avenues for this common cancer. More broadly, this platform represents a valuable tool to study cancer–bone interactions in other tumour types metastasising to bone.

Acknowledgements
The work was supported by Italian Association for Cancer Research (AIRC IG 2021—ID 25749).

S14 – O2

Engineering bruch's membrane-mimicking substrates for ARPE-19 barrier maturation: A comparative study of electrospun PLGA and gelatin membranes

Di Stasi M[1,2*], Esposito A[2*], Fortunato G.M[2,3*], De Maria C[2,3], Nieri P[1,2], Vozzi G[2,3]
[1]Dept. of Pharmacy, University of Pisa, Pisa, Italy; [2]Research Center "E. Piaggio", University of Pisa, Pisa, Italy; [3]Dept. of Information Engineering, University of Pisa, Pisa, Italy; **These authors contributed equally to this work.*

Introduction

Recreating a functional analogue of Bruch's membrane that can sustain a stable retinal pigment epithelium (RPE) monolayer is a key challenge in the design of physiologically relevant outer retinal models and, ultimately, in the development of cell-based therapeutic strategies. ARPE-19, a well-characterized human RPE cell line, is widely used for *in vitro* barrier studies given its ability to form polarized monolayers with defined tight-junction organization and paracellular selectivity[1]

Aim

This study examined whether electrospun poly(lactic-co-glycolic acid) (PLGA) and gelatin membranes could function as Bruch's membrane-mimicking substrates for ARPE-19 cellularization, comparing both against Transwell® permeable supports as planar controls.

Materials and Methods

ARPE-19 cells were seeded onto electrospun PLGA, electrospun gelatin, or Transwell® supports and cultured for 28 days. Cytocompatibility was assessed by MTT (3-(4,5-dimethylthiazol-2-yl)-2,5-diphenyltetrazolium bromide) and LDH (lactate-dehydrogenase) assays. Barrier maturation was evaluated by transepithelial electrical resistance (TER) and FITC-dextran paracellular permeability,[2] and tight-junction organization by ZO-1 immunofluorescence. Days 21 and 28 were selected as assessment time points based on TER kinetics: day 21 captured barrier stabilization, day 28 confirmed its persistence. Data were analyzed by one-way ANOVA with Tukey's post hoc test.

Results

Both electrospun membranes supported monolayer formation more effectively than the planar control, with MTT and LDH data confirming cytocompatibility across all substrates. The clearest differences emerged at the functional level. TER increased progressively and plateaued by day 21 on electrospun substrates, with PLGA sustaining the highest values throughout. FITC-dextran flux followed the inverse pattern, lowest on PLGA and highest on Transwell®, indicating tighter paracellular restriction. ZO-1 staining was continuous in all groups, but sharper, more intense, and consistently circumferential on PLGA, reflecting greater tight-junction maturity (**Figure 1**).

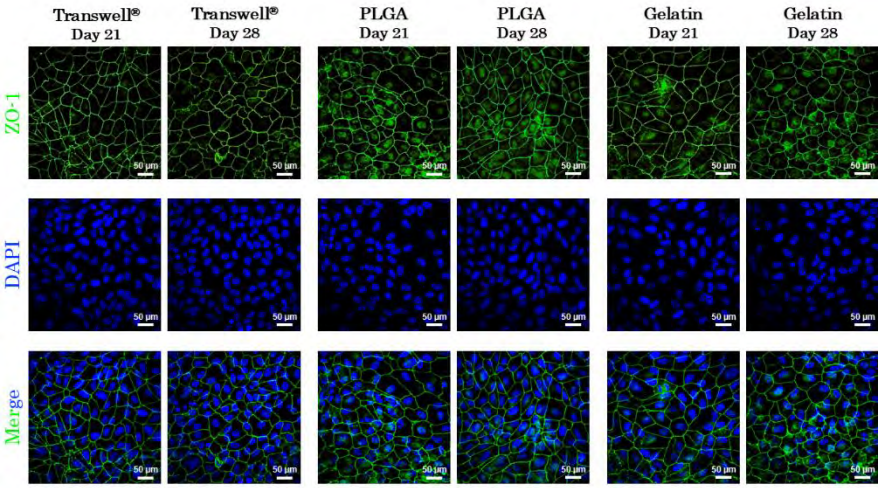

Figure 1. Confocal immunofluorescence images of ZO-1 expression in ARPE-19 cells cultured on Transwell® supports, electrospun PLGA membranes, and electrospun gelatin membranes at days 21 and 28.

Conclusion

Among all substrates tested, electrospun PLGA provided the most favorable environment for ARPE-19 barrier maturation, combining cytocompatibility, superior transepithelial resistance, and well-organized tight junctions. These findings support its use as a scaffold for biomimetic outer retinal modeling and as a reliable *in vitro* tool for evaluating drug permeability across the retinal barrier.

References

[1]Dunn K.C., Aotaki-Keen A.E., Putkey F.R., Hjelmeland L.M. ARPE-19, a human retinal pigment epithelial cell line with differentiated properties. Experimental Eye Research 1996; 62; 155-169.

[2]Zhang F., Liu L., Zhang H., Liu Z.-L. Effect of Platelet-Activating Factor on Barrier Function of ARPE-19 Cells. Drug Design, Development and Therapy 2020; 14; 4205-4214.

S14 – O3

Development and in vitro evaluation of 3D-printed biodegradable hydroxyapatite bioscaffolds

L.Baghdasaryana, L.Mkhitaryana, M.A. Rodríguezb, S. Hovhannisyanc V. Rstakyana
aA.B. Nalbandyan Institute of Chemical Physics, NAS RA, P. Armenia; b Instituto de Cerámica y Vidrio, Spain
c Research Institute of Biology, Yerevan State University, Yerevan, Armenia

Introduction

Hydroxyapatite (HA) is widely used in bone tissue engineering due to its chemical similarity to the mineral component of natural bone and its excellent biocompatibility. Additive manufacturing (AM) technologies enable the fabrication of patient-specific bioscaffolds with precisely controlled internal structure and porosity. However, achieving an optimal balance between mechanical stability and controlled biodegradation remains a major challenge in the development of HA-based scaffolds.

Aim

The aim of this study was to fabricate 3D-printed HA-based ceramic bioscaffolds using vat photopolymerization (VPP) and to evaluate their structural, mechanical, and biological performance through in vitro investigations (Fig. 1).

A ceramic slurry containing 50 vol% HA powder dispersed in a biocompatible photopolymer was formulated and optimized for VPP processing. A suitable dispersant was incorporated to control slurry rheology and ensure homogeneous particle dispersion and stable suspension behavior. After optimization of the slurry formulation and printing parameters, green bodies were fabricated in a layer-by-layer manner. The printed structures were subsequently subjected to thermal debinding followed by sintering at 1250 °C to obtain consolidated ceramic scaffolds.

The sintered bioscaffolds were characterized in terms of microstructure and mechanical properties, while biocompatibility was evaluated using cell viability and adhesion assays. Cytotoxicity was assessed using an MTT assay, and biodegradability was investigated through immersion tests in Tris–HCl buffer (pH 7.4) and simulated body fluid (SBF). The mechanical behavior of the scaffolds was evaluated by compressive strength testing to assess their suitability for bone applications. The fabricated scaffolds exhibited a stable ceramic microstructure with interconnected porosity favorable for tissue ingrowth and demonstrated sufficient mechanical strength for potential use in non-load-bearing bone defects. In vitro results confirmed good cell attachment and proliferation, indicating favorable bioconductive properties and the potential of vat photopolymerization for the fabrication of bioactive HA scaffolds for bone regeneration.

Figure 1. Schematic Workflow of Hydroxyapatite Scaffold Fabrication and Evaluation by DLP Printing.

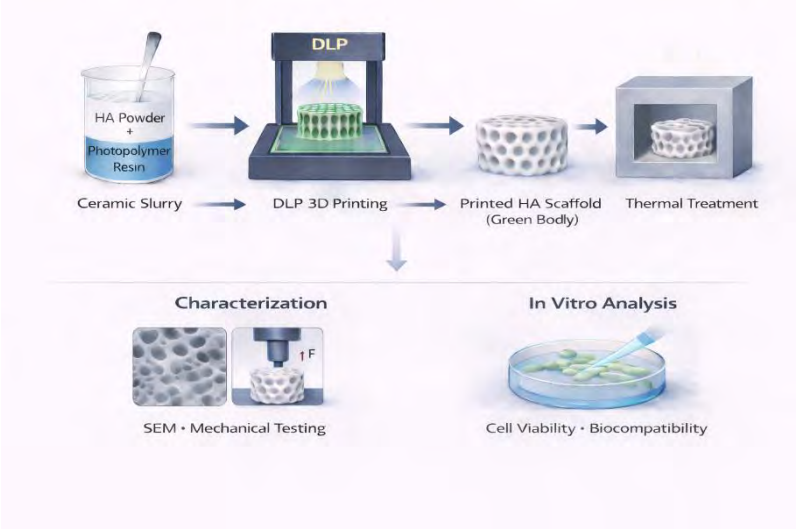

S14 – O4

From avascular constructs to living tissues: Engineering vascularized bioprinted skin

A.P.B[1,2], C.T[3], M.D[2], A.S[4], A.R[1], J.W[1]

[1]Blond McIndoe Laboratories, School of Medical Sciences, University of Manchester; Manchester, UK; [2]Henry Royce Institute, University of Manchester, Manchester, UK; [3]Image Regenerative Clinic, Italy; [4]Division of Developmental Biology and Medicine; School of Medical Sciences, University of Manchester, Manchester, UK

Introduction

Chronic wounds, including diabetic foot ulcers, represent a growing and largely unmet healthcare challenge. In the UK alone, an estimated 2.2–3.8 million people are affected annually, placing a substantial burden on healthcare systems and, in severe cases, leading to mortality. Despite significant advances in tissue-engineered skin models, most current constructs lack integrated vascular networks, which are essential for maintaining tissue homeostasis and accurately recapitulating the wound healing process. Consequently, key mechanisms underlying impaired healing in chronic wounds remain poorly understood. 3D bioprinting has emerged as a powerful strategy to overcome these limitations, enabling the fabrication of complex, vascularised tissue constructs and offering new opportunities to study wound healing in a more physiologically relevant context.

Aim

The aim of this work is to address a key limitation in tissue engineering: the lack of vascularized constructs. This was achieved by combining photocrosslinkable biomaterials to provide structural support with fibrin to enhance bioactivity and promote vascular network formation within the hydrogel.

Materials and Methods

Gelatine methacryloyl (GelMA), hyaluronic acid methacryloyl (HaMA), and human fibrinogen were used to fabricate a three-layered, vascularised bioprinted skin equivalent. Human dermal fibroblasts and keratinocytes were incorporated to recapitulate the dermal and epidermal compartments, respectively, while human umbilical vein endothelial cells (HUVECs) were included to promote vascular network formation within the construct. An adipose-derived component was integrated to mimic the hypodermal layer. The functionality of the engineered skin was assessed by PCR, and key markers of keratinocyte differentiation and barrier formation, including KRT14, involucrin, and ZO-1, were evaluated by immunofluorescence. Endothelial network formation was further characterised using CD31 staining.

Results

Bioprinted constructs showed high viability and structural integrity, with well-defined epidermal stratification (KRT14 basal, KRT10 suprabasal). HUVECs formed extensive CD31-positive vascular-like networks, confirming robust endothelial self-organisation and vascularization within the matrix

Conclusion

The GelMA/HaMA/fibrin bioink demonstrated strong potential for generating structurally and functionally relevant skin models. Importantly, bioprinting enables the precise spatial organisation of vascular components, representing a significant advancement in skin tissue engineering and a promising strategy for the fabrication of more complex, vascularised tissues.

Acknowledgements

The author would like to thank the EPSRC-funded Centre for Doctoral Training in Advanced Biomedical Materials, grant reference EP/S022201/1, and the Henry Royce Institute, grant reference EP/R00661X/1, EP/S019367/1, EP/P025021/1, and EP/P025498/1 for funding this work.

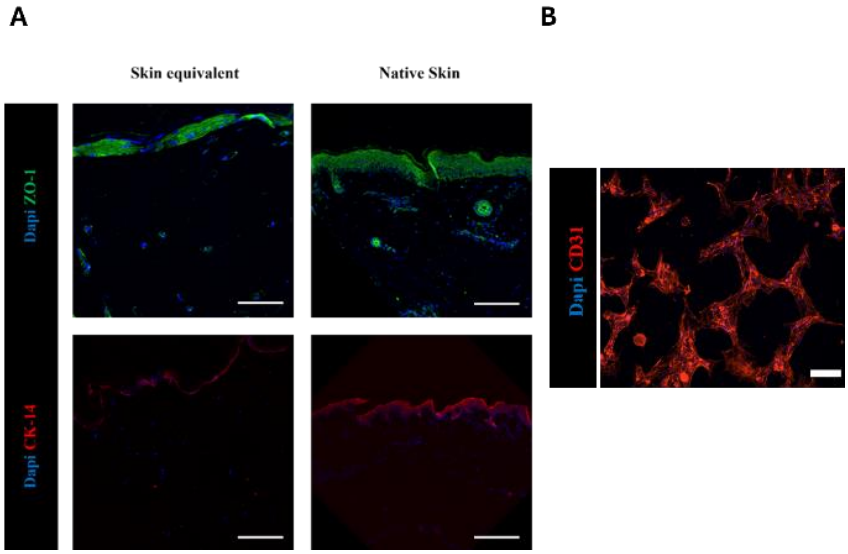

Fig. 1: A) Comparison between skin model and native skin. B) Vascular formation within the construct marked by CD31 staining. Scale bar 100 µm.

S14 – O5

Collagen substrates allow independent control over physical properties and biological functionality for in-vitro culture of renal primary cells

Thursfield E.D.[1], Bilican B.[2], Woollard K.J.[3], Cameron R.E.[1], Best S.M.[1]
[1]Dept. of Materials Science and Metallurgy, University of Cambridge, Cambridge, UK; [2]Applied Stem Cell Sciences, Discovery Sciences, AstraZeneca, Gothenburg, Sweden; [3]Bioscience Renal - Early CVRM – BioPharmaceuticals R&D, AstraZeneca, Cambridge, UK

Introduction

Human renal proximal tubule epithelial cells (RPTECs) are the most abundant cell type in the kidney and are commonly used to model kidney injury in-vitro. These are primarily cultured as 2D monolayers on plastic or as spheroids in 3D suspension culture, both representing non-physiological conditions. This work considers the suitability of air-dried collagen films and freeze-dried collagen scaffolds to provide optimised RPTEC culture systems, with the cellular response upon varying physical properties and biological functionality being investigated.

Materials and Methods

Collagen (insoluble, bovine dermal, type I) films and scaffolds were crosslinked using varying concentrations of 1-ethyl-3-(3-dimethylaminopropyl) carbodiimide hydrochloride (EDC) and N-hydroxy-succinimide (NHS), ranging between 0%-100% of the standard condition (a 5:2:1 EDC:NHS:Collagen molar ratio), giving control over the physical properties of the substrates. Collagen substrates were further functionalised via biomolecular decoration with laminins, collagen IV, fibronectin and elastin to provide tailored biofunctionality. Lactate dehydrogenase (LDH) activity assays and PrestoBlue activity assays were used to investigate cellular attachment, proliferation and health. Confocal fluorescence microscopy and 2-photon microscopy were used to investigate cellular morphology and proliferation. Kim-1 ELISAs were used to measure cellular health.

Results

Collagen scaffolds supported prolonged RPTEC culture, with viability being maintained over 40 days. The cellular response of RPTECs on 2D collagen films and 3D scaffolds was found to be invariant upon crosslinking condition – with adhesion, proliferation, morphology and health being consistent across all conditions, as shown in Figure 1. RPTEC adhesion was confirmed to be non-integrin mediated via inhibition of the β1 integrin binding site, possibly explaining the consistency across crosslinking conditions. In contrast, functionalisation via decoration with varying biomolecule density was shown to significantly affect the cellular adhesion and morphology, as shown in Figure 2. Optimal coating densities were found for laminin peptides, collagens I & IV and fibronectin, all improving RPTEC spreading.

Conclusion

Collagen substrates provide 2D and 3D cell culture systems with highly controllable mechanical properties, which can be varied independently of the cellular response of RPTECs. Furthermore, optimised culture conditions were found by controlling the functionality of the substrates through biomolecular coating.

Acknowledgements

This work has been undertaken as part of an AstraZeneca-funded, non-clinical studentship at the University of Cambridge. This work was supported by the Henry Royce Institute for advanced materials through the Equipment Access Scheme enabling access to the Cambridge 3D Bioelectronics Facility, through Cambridge Royce facilities grant EP/P024947/1 and Sir Henry Royce Institute recurrent grant EP/R00661X/1.

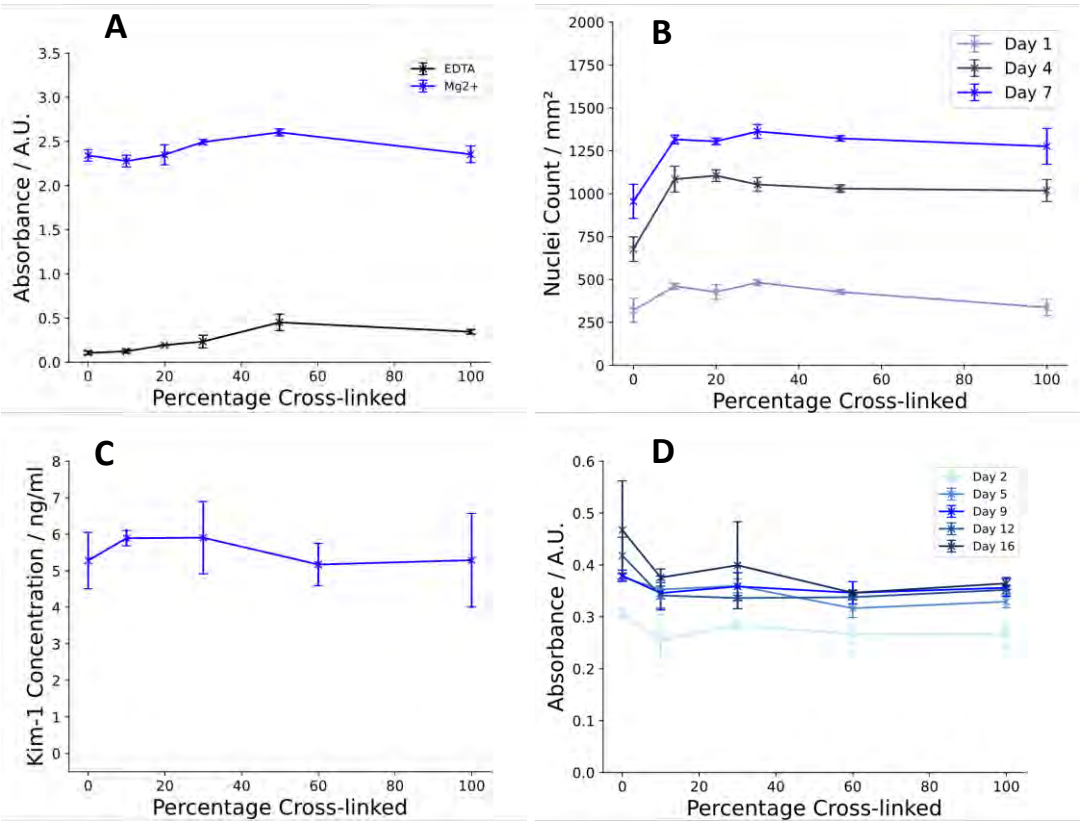

Figure 1. Collection of data showing consistent cellular response of RPTECs to collagen films and scaffolds with varying crosslinking density.

A) RPTEC attachment to collagen films shown via LDH activity assay. B) RPTEC proliferation on collagen films shown via nuclear counts from fluorescence microscopy. C) RPTEC health on collagen scaffolds shown via KIM-1 ELISA. D) RPTEC viability on collagen scaffolds over 16 days, shown via PrestoBlue activity assay.

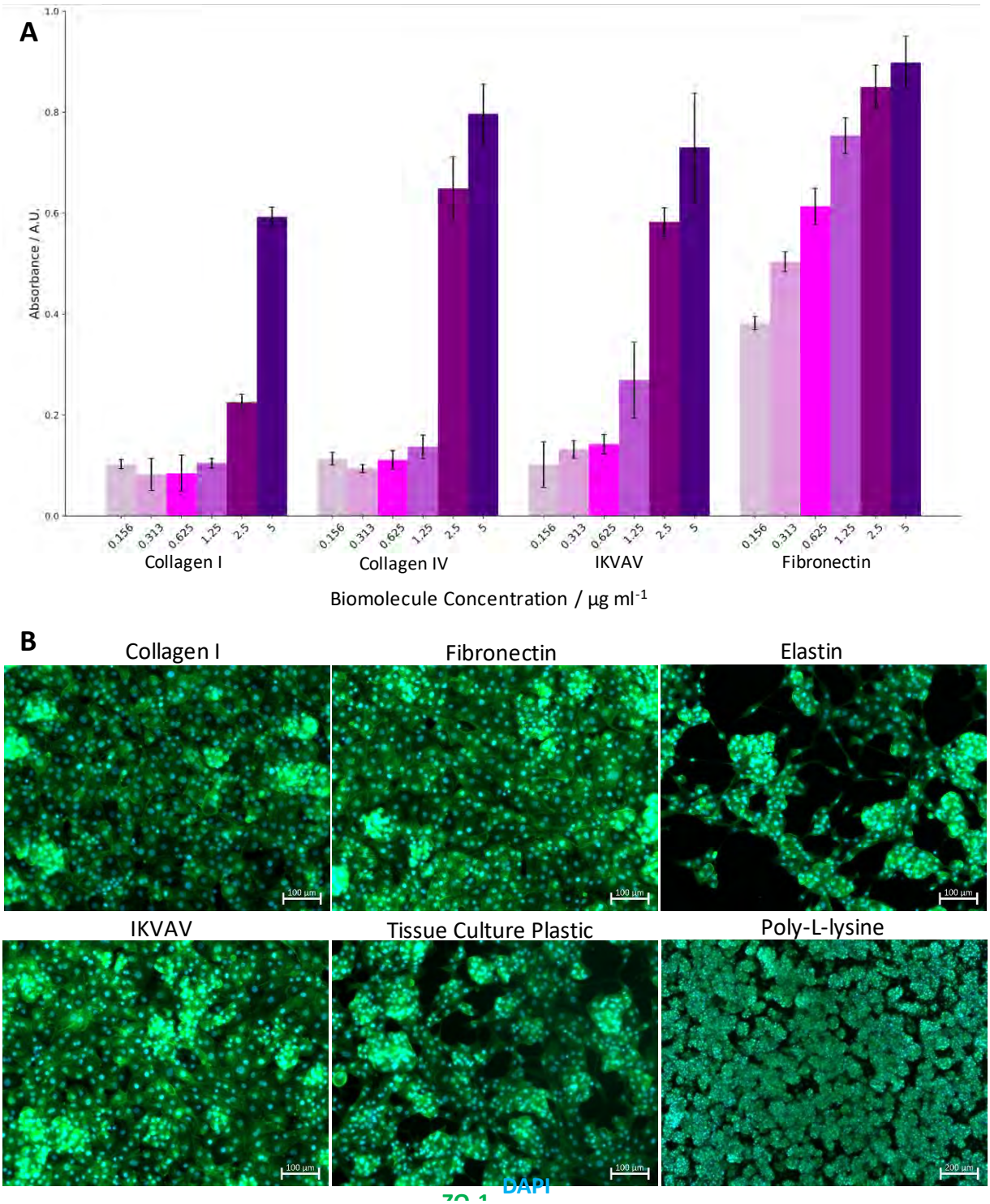

Figure 2. Collection of data showing varied response of RPTECs to surfaces functionalised via biomolecular coating.

A) Bar chart showing RPTEC attachment to surfaces with varying biomolecular coating densities shown via LDH activity assay; B) Fluorescence microscopy images showing varied RPTEC morphology on functionalised surfaces.

S15
Biofabrication using photoactivated materials

S15 - K1
Advances in tomographic volumetric additive manufacturing for organ-on-chips

Rizzo R.[1], Wechsler F.[1], Sgarminato V. [1,2], Zhang Q. [1], Moser C.[1]
[1]Laboratory of Applied Photonics Devices, École Polytechnique Fédéral Lausanne (EPFL), Lausanne, Switzerland ; [2]Dipt. di Ingegneria Meccanica e Aerospaziale (DIMEAS), Politecnico dit Torino, Turin, Italy

Introduction
Human organ-on-chip (OoC) platforms are emerging tools for drug discovery and safety testing that replicate essential aspects of organ physiology and reduce reliance on animal models. Most OoCs rely on soft-lithography microfluidics, which are scalable but limited to rigid materials and simplified 2.5D geometries that constrain physiological relevance (Figure 1A). Although 3D bioprinting has improved structural complexity, current approaches are slow and require multiple post-processing and assembly steps (Figure 1A). Tomographic volumetric additive manufacturing (TVAM) enables rapid fabrication of complex 3D structures but still depends on manual construct transfer and chip assembly.

Aim
Develop strategies to directly 3D print high-complexity, high-cell-density perfusable models within preassembled, leak-proof TVAM compatible chips featuring integrated fluidics (TVAM-in-a-chip, Figure 1B).[1]

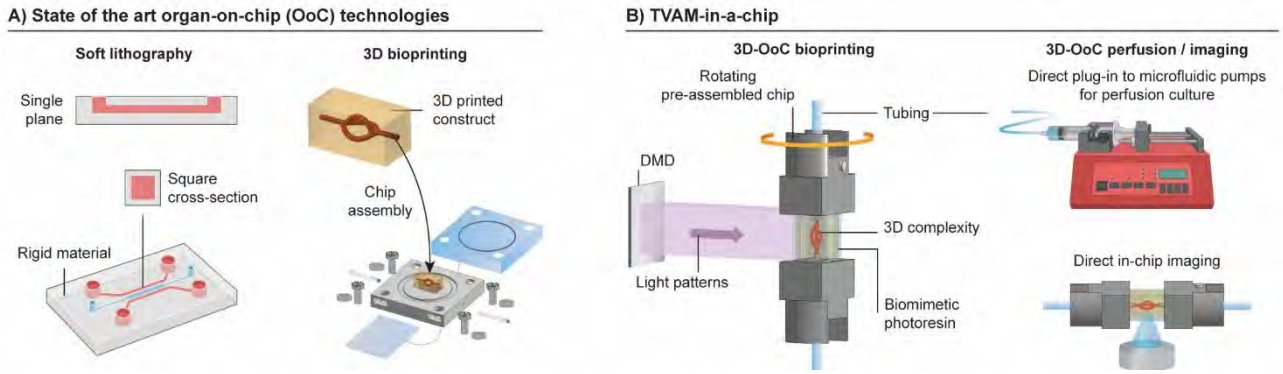

Figure 1. Schematic of state-of-the-art OoC technologies (A) and proposed TVAM-in-a-chip strategy (B).

Materials and Methods
Biocompatible photosensitive resins are used for TVAM-in-a-chip printing in custom flat quartz-based containers sealed with SLA-printed caps featuring microfluidic connectors. Pattern optimization in square geometry (chip), overprinting scenarios (presence of light occluding inlets / outlets) and highly scattering media (cell-laden resin) is performed with open-source optical framework Dr.TVAM.[2] Following printing, chips are seeded with endothelial and/or epithelial cells and cultured under flow. Tissue maturation is monitored via confocal microscopy directly in the chip.

Results
TVAM-in-a-chip enables rapid fabrication of single- and multichannel 3D OoCs within universal, imaging-compatible chips. The platform supports diverse natural and synthetic photoresins spanning different chemistries, viscosities, and stiffnesses. Moreover, it allows for printing with highly scattering bioresins featuring high cell densities (≥10-15 million cells mL^{-1}) and multicellular printing. This approach also enables the generation of high-resolution channels (≤250 µm), complex 3D architectures, and successful epithelialization and endothelialization under perfusion culture. Overall, this approach provides a versatile route toward biomimetic 3D scaffold-guided tissue morphogenesis.

Conclusion

This study introduces a versatile biomanufacturing approach with far-reaching potential, termed TVAM-in-a-chip, that overcomes some key limitations of current OoC platforms, paving the way for more complex biomimetic 3D OoC platforms.

References

[1]Rizzo R., Sgarminato V., Wechsler F., Moser C. Tomographic Printing in a Chip: A Versatile Platform for Biomimetic 3D Organ-on-Chip. *bioRxiv* 2026. https://doi.org/10.64898/2026.02.26.708161.

[2]Nicolet B., Wechsler F., Madrid-Wolff J., Moser C., Jakob W. Inverse Rendering for Tomographic Volumetric Additive Manufacturing. ACM *Trans Graph* 2024; 43 (6). https://doi.org/10.1145/3687924.

S15 – O1

Peptide-encapsulated 3D bioprintable hydrogels for bone tissue engineering: In-vitro evaluations

Durukan E.[1], Turan M.F.[2], Karaca M.A.[3], Ozatay Gok O.[4]
[1]Dept. of Biomedical Engineering, Institute of Natural and Applied Sciences, Acibadem Mehmet Ali Aydinlar University; [2]Dept. of Biomaterials, Institute of Natural and Applied Sciences, Acibadem Mehmet Ali Aydinlar University; [3]Dept. of Medical Biotechnology, Institute of Health Sciences, Acibadem Mehmet Ali Aydinlar University, Istanbul; [4]Dept. of Biomedical Engineering, Faculty of Engineering and Natural Sciences, Acibadem Mehmet Ali Aydinlar University, Istanbul, Türkiye

Introduction

Hydrogels are promising materials in bone tissue engineering due to their extracellular matrix (ECM)-like architecture and cell-friendly properties. This study aims to develop novel peptide-encapsulated natural and synthetic polymer blends to fabricate biocompatible and biomimetic peptide encapsulated scaffolds using 3D bioprinting, specifically targeting bone tissue regeneration.

Materials and Methods

Natural polymers were modified with methacrylic anhydride to enable UV-light crosslinking. To enhance mechanical strength, these methacrylated polymers were blended with a synthetic biodegradable polymer, Poly(ethylene glycol) di-methacrylate (PEGdiMA). An osteoblast cell-adhesive KRSR peptide, synthesized via solid-phase peptide synthesis (SPPS), was incorporated into the polymer blend.

The hybrid hydrogels were characterized using FT-IR Spectroscopy, Scanning Electron Microscopy (SEM), swelling capacity tests, and rheological analysis. In vitro cytotoxicity was evaluated using L929 mouse fibroblasts via CCK-8 assay. Osteoblast response was assessed using the hFOB 1.19 human fetal osteoblast cell line through time-dependent live/dead assay to evaluate cell adhesion and Alizarin Red S staining was performed to determine mineralization rate.

Results

FT-IR and rheological analysis confirmed successful methacrylization. The hybrid hydrogels exhibited a high and stable mechanical strength, with a storage modulus (G') of approximately 48.9 MPa and a loss modulus (G'') of 2.2 MPa. These rates confirmed the formation of a robust, highly elastic, and frequency-independent gel network. SEM imaging revealed a highly porous and interconnected architecture favorable for cell infiltration. The CCK-8 assay demonstrated over 70% cell viability, indicating the non-toxic nature of the hybrid system.

Most importantly, the incorporation of the KRSR peptide significantly promoted osteoblast adhesion in a time-dependent manner and effectively enhanced the mineralization rate as confirmed by Alizarin Red S staining compared to peptide-free controls.

Conclusion

This study introduces a novel hybrid hydrogel system combining methacrylated natural/synthetic polymers with the KRSR peptide. The results highlight that UV-crosslinkable biomaterial inks provide structural integrity and bioactivity. The system shows great promise as a next-generation biomaterial inks for 3D bioprinting applications in bone tissue engineering.

S15 – O2

Macroporous mineralizing photoresins for bone tissue engineering

Hui I. B.[1], Puiggalí-Jou A.[1], Amstad E.[2], Fernández-Rico C.[3], Zenobi-Wong M.[1]
[1]Dept. Health Sciences & Technology, ETH; [2]Dept. Material Science, EPFL, Lausanne; [3]Dept. Materials, ETH, Zürich, Switzerland

Introduction

Large bone defects arising from trauma or pathological conditions remain a major clinical challenge. Treatment often involves autologous bone grafting, despite limitations such as donor site morbidity and restricted graft availability. Bone tissue engineering has therefore emerged as a promising strategy for promoting bone regeneration. However, biomaterials that simultaneously reproduce the architecture, composition, and mechanical properties of native bone are still lacking. To address this gap, we engineered macroporous mineralizing photoresins that mimic the properties of native tissue.

Materials and Methods

To obtain a structure mimicking trabecular bone, the target morphology and pore size were optimized by analyzing different resin compositions containing norbornene-functionalized polyethylene glycol (PEG-NB) and dextran. Upon light irradiation, polymerization-induced phase separation (PIPS) gels were formed. Porosity assessment of PIPS gels was carried out using confocal microscopy and quantitative image analysis, while photorheology was used to establish the link between polymerization rate and pore size. The alkaline phosphatase (ALP) enzyme was then added to the resin to enable mineralization of the scaffolds and mimic bone's composition. Mineralization was confirmed by micro-computed tomography (µCT), mechanical testing, and scanning electron microscopy.

Results

The engineered PIPS hydrogels replicated the interconnected architecture of trabecular bone, demonstrating broad pore size tunability ranging from 10 to 400 µm. This tunability was achieved by modulating the hydrogel composition and light intensity to balance the polymerization rate against the competitive phase-separation coarsening rate. Furthermore, the incorporation of ALP enabled scaffold mineralization, yielding calcium phosphate-enriched composite materials. µCT imaging confirmed that the mineral phase develops within the gel matrix, yielding a trabecular bone-like structure in porous gels (Figure 1). Mechanically, these mineralized scaffolds exhibited a compressive strength of 1.5 MPa.

Conclusion

We developed a tunable macroporous photoresin that accurately mimics the complex architecture, composition, and mechanical strength of native trabecular bone. This biomaterial offers dual clinical utility: it can serve as an injectable resin that is photopolymerized *in situ* to fill irregular bone defects, or it can be used to pre-fabricate customized scaffolds prior to implantation. Ultimately, this photoresin provides a promising alternative for the treatment and regeneration of bone defects.

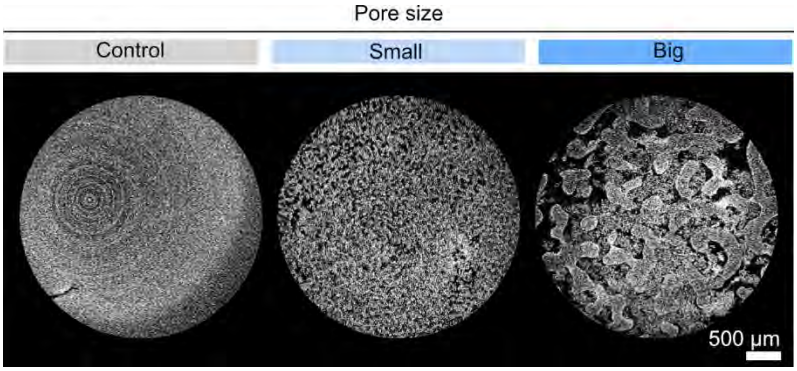

Figure 1: µCT images of mineralized PIPS hydrogels comparing a control with two distinct pore sizes.

S15 – O3

Methacrylated Pluronic (PluMA) hydrogels for high-resolution 3D printing and biofabrication

Babilotte J.[1], Pech de Laclause M.[1,2], Biscaccianti V[1], Charbonnier B.[1], Paré A.[2], Delplace V.[1]
[1]Nantes Université, INSERM, Regenerative Medicine and Skeleton, RMeS, UMR France; [2]Dept. of Maxillofacial and Plastic Surgery, University Hospital of Tours, France

Introduction

Achieving high-resolution hydrogel biofabrication while maintaining structural stability remains a major challenge. Photocrosslinkable methacrylated polymers are widely used in biofabrication because light-triggered crosslinking enables rapid stabilization of hydrogel networks. However, these materials (e.g., gelatin or hyaluronic acid derivatives) often require blending or additional strategies to achieve sufficient printability and shape fidelity, particularly for high-resolution extrusion. In contrast, Pluronic F127 is a thermoresponsive polymer widely used in 3D printing due to its excellent printability, but displays limited stability in aqueous environments as a physically assembled micellar hydrogel. Here, we develop methacrylated Pluronic (PluMA), combining printability with photocrosslinking-enabled structural stability to improve shape fidelity and resolution compared to conventional methacrylated hydrogels.

Aim

This study aims to develop and characterize PluMA hydrogels for high-resolution hydrogel 3D biofabrication.

Materials and Methods

PluMA was synthesized by methacrylation of Pluronic using methacrylic anhydride. The optimized polymer was purified by dialysis, freeze-dried, and characterized by ^{1}H NMR to confirm successful methacrylation. Printability was evaluated at 37°C using 20–25% (w/v) PluMA by varying deposition pressure and speed with a 30G nozzle, while filament diameter was measured. Rheological properties relevant to printing, including shear-thinning behavior and dynamic recovery, were characterized. Hydrogels were photocrosslinked using LAP photoinitiator (0.1-0.2 wt%) under 405 nm irradiation for 15-60 s. The influence of polymer concentration and light exposure time on hydrogel mechanical properties was evaluated by compression testing. Cytocompatibility was evaluated using L929 fibroblasts cultured on PluMA scaffolds, and cell viability was monitored over time.

Results

We first investigated the printability of PluMA hydrogels. With 20% PluMA, filament diameters ranged from 365 ± 42 µm to 765 ± 4 µm depending on printing parameters. Increasing concentration to 25% significantly improved resolution, enabling filaments as small as 147.0 ± 8.5 µm, with diameter precisely controlled by printing parameters. The ability to stack filaments and generate multi-layered structures and complex geometries was also investigated. Rheological analysis revealed pronounced shear-thinning behavior together with immediate viscosity recovery after shear removal. In three-interval thixotropy test (3-ITT), the storage modulus recovered to ~100% of its initial value, demonstrating efficient structural recovery after shear. Together, these rheological properties support extrusion, stable filament deposition, and shape retention after printing, a key limitation of many conventional methacrylated hydrogels. Following photocrosslinking, compression tests showed that Young's modulus increased with both PluMA concentration and light exposure time. For instance, modulus increased from 4.40 ± 1.05 kPa (20% PluMA, 30 s crosslinking) to 26.98 ± 0.70 kPa (25% PluMA, 30 s) and reached 36.65 ± 16.09 kPa (25% PluMA, 60 s). All hydrogels exhibited elastic recovery after compression, indicating structural resilience. Finally, cells cultured on PluMA scaffolds showed 50–60% viability after 24h, indicating mild cytotoxicity, followed by recovery in proliferation after 7 days.

Conclusion

PluMA hydrogels provide a promising platform for high-resolution hydrogel-based biofabrication strategies. Future work will explore hybrid constructs combining PluMA scaffolds with biocompatible, cell-laden hydrogels to improve biological performance. These results open new opportunities to investigate how scaffold architecture and mechanical cues influence stem cell behavior and tissue-specific differentiation.

Acknowledgements

This work was supported by the French National Research Agency (ANR) through the DYNAM-OA project (ANR-22-CE19-0020) and by the Fondation des *Gueules Cassées* (Convention No. 72–2025).

S15 – O4

Physiologically inspired three-dimensional architecture enhances proximal tubule epithelial organization in vitro

Sinnona F.[1,2], Sgarminato V.[1,2], De Nisco G.[1], Meiburger K.M.[1], Hitomi H.[3], Ciardelli G.[1,2], Tonda-Turo C.[1,2]
[1]Dept. of Mechanical and Aerospace Engineering, Politecnico di Torino, Torino, Italy; [2]Bioinside Lab, Politecnico di Torino, Torino, Italy; [3]Dept. of iPS Stem Cell Regenerative Medicine, Kansai Medical University, Osaka, Japan

Introduction

The nephron, the functional unit of the kidney, consists of specialized segments, among which the proximal tubule exhibits a highly convoluted three-dimensional (3D) organization essential for its transport function. *In vivo*, proximal tubule epithelial cells are confined within curved and continuous architectures that promote polarization and epithelial integrity. However, most biomaterial-based *in vitro* models simplify this organization into straight or low-complexity tubular systems, overlooking the intrinsic convoluted geometry of the native tubule. Evaluating how increasing geometric complexity alone influences epithelial organization is therefore essential.

Materials and Methods

A hydrogel platform based on Gelatin Methacryloyl (GelMA) and GelMA-Thiolate Hyaluronic Acid (HASH) formulations was optimized by screening different polymer concentrations and compositions to identify conditions that ensure homogeneous cell attachment and long-term mechanical stability. Using the selected formulation, three geometries of increasing architectural complexity were engineered while maintaining constant biochemical and mechanical properties: planar constructs, straight tubular structures, and physiologically inspired convoluted tubules reproducing continuous curvature. Distinct fabrication strategies were employed to generate each configuration while preserving identical crosslinking conditions. For tubular designs, a dedicated supporting platform (Fig.1) was developed to host the constructs and facilitate handling. The platform enables cell seeding and medium perfusion through the lumen under static culture conditions. In addition, inlet and outlet ports allow connection to external tubing, enabling future implementation of dynamic perfusion systems.
Human proximal tubule epithelial cells (RPTEC-TERT1) were seeded under identical culture conditions. Epithelial organization was evaluated through analysis of cytoskeletal structure, cell alignment, junctional continuity, and polarization. Maintenance of proximal tubular phenotype was assessed to confirm segment-specific identity.

Results

A formulation providing structural integrity and cell adhesion across all fabrication approaches was identified. While all geometries supported cell viability, epithelial organization differed as a function of architectural configuration. Planar constructs showed heterogeneous orientation and distribution. Straight tubular geometries promoted partial circumferential alignment and improved epithelial cohesion. Convoluted architectures induced more uniform cytoskeletal organization, enhanced junction continuity, and more consistent polarization patterns. Quantitative analysis revealed increased structural coherence and reduced variability in epithelial organization within the physiologically inspired geometry.

Conclusion

By integrating hydrogel formulation optimization with controlled geometric design, this study demonstrates that physiologically inspired convoluted architecture significantly enhances proximal tubule epithelial organization compared to planar or simple tubular configurations. These findings identify 3D architectural complexity as an independent and critical design parameter in biomaterial-based kidney models, supporting the incorporation of geometric biomimicry in renal tissue engineering strategies.

Acknowledgements

The PhD scholarship of Federico Sinnona runs under the joint agreement between Kansai Medical University and Politecnico di Torino

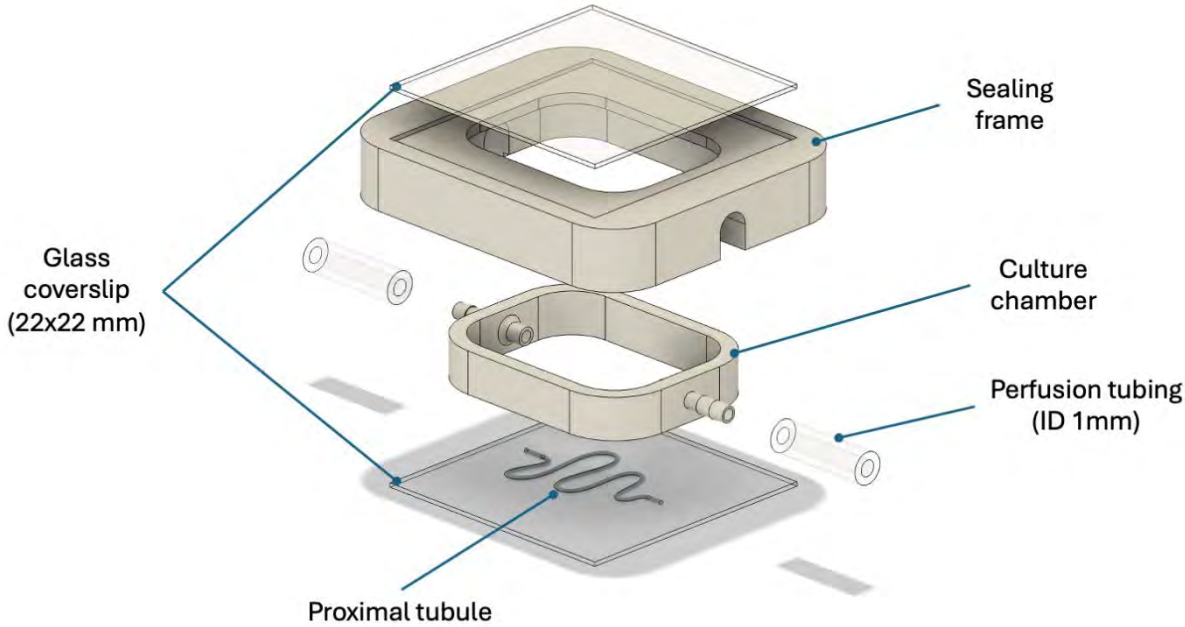

Figure 1: Exploded view of the modular platform for culture and perfusion of engineered proximal tubule constructs.

S15 – O5

Ultrafast volumetric bioprinting enables precise morphological control of perfusable stem cell-derived microphysiological endocrine pancreatic units

Brice C.[1], Català P.[1], Ribezzi D.[1], Größbacher G.[1], Riemers F.[1], van Rijen M.[1], Stillitano F.[1], Caiazzo M.[2], Westendorp B.[1], Levato R.[1]

[1]Regenerative Medicine Centre Utrecht, University Medical Centre Utrecht and Utrecht University,; [2]Dept. of Pharmaceutics, Utrecht University, Utrecht, The Netherlands

Introduction

Functional islets from induced pluripotent stem cells (iPSCs) hold great promise as a renewable cell source for pancreatic tissue engineering. Despite advances in differentiation protocols, iPSC-derived islets often remain immature and lack the complex microenvironmental cues necessary for full functionality. This limits the development of robust *in vitro* platforms, impeding deeper insights into islet biology and function.

Aim

To develop and evaluate an engineered pancreatic construct that integrates iPSC-derived islets within a gelatine methacryloyl (GelMA) matrix using light-based volumetric bioprinting, in order to create advanced endocrine units that better replicate the pancreatic microenvironment.

Materials and Methods

iPSC-derived pancreatic islets were generated using an established protocol (*Fig1A*).[1] Upon differentiation, islets were suspended in varying concentrations of GelMA (4-7% (w/v)) and bioprinted using shear stress-free, light-based VBP. Constructs were analysed by immunofluorescence (IF) imaging, single-cell transcriptomics, and glucose-stimulated insulin secretion (GSIS) assays under static and dynamic conditions. Dynamic GSIS assays were further performed in the presence of a known anti-diabetes drug, a GLP-1 analogue, to assess the potentiation of insulin secretion, as well as following streptozotocin treatment to evaluate β-cell susceptibility within the engineered constructs.

Results

VBP enabled rapid fabrication of centimetre-scale constructs (6% (w/v) GelMA, t<30 s), preserving iPSC-islet viability and metabolic activity for at least 21 days. Notably, islets bioprinted and matured within the 6% (w/v) GelMA matrix exhibited an increased insulin secretory capacity compared to non-printed controls (*Fig1B*). These constructs contained mature, single-hormone producing β-, α-, and δ-cells, confirmed by IF staining and single-cell transcriptomics. Mathematically-defined gyroidal structures (strut size:750μm, infill:40%) containing a homogenous distribution of iPSC-islets were successfully perfused for up to 21 days and further functionally validated using dynamic GSIS assays (*Fig1C,D*). The perfusable constructs supported anti-diabetic drug screening as shown by their significant increase in insulin secretion in response to the administration of a GLP-1 analogue (*Fig1E,F*). Additionally, the streptozotocin-treated constructs showed no insulin release capacity, with the selective β-cell toxicity being confirmed through immunofluorescence analysis.

Conclusion

This study established VBP as a rapid and versatile strategy for fabricating perfusable pancreatic constructs containing iPSC-derived pancreatic islets within GelMA. The engineered architectures support high cell viability, preserve the endocrine phenotype, and enabled dynamic functional assessment of insulin secretion in response to physiological and pharmacological stimuli. Together, this platform provides a scalable, more physiological relevant system for studying islet biology, disease modelling, and high-throughput drug screening, while advancing the development of engineered pancreatic tissues.

References

[1]Balboa D., *et al*. Functional, metabolic and transcriptional maturation of human pancreatic islets derived from stem cells. *Nature Biotechnology* 2022; 40; 1042-1055.

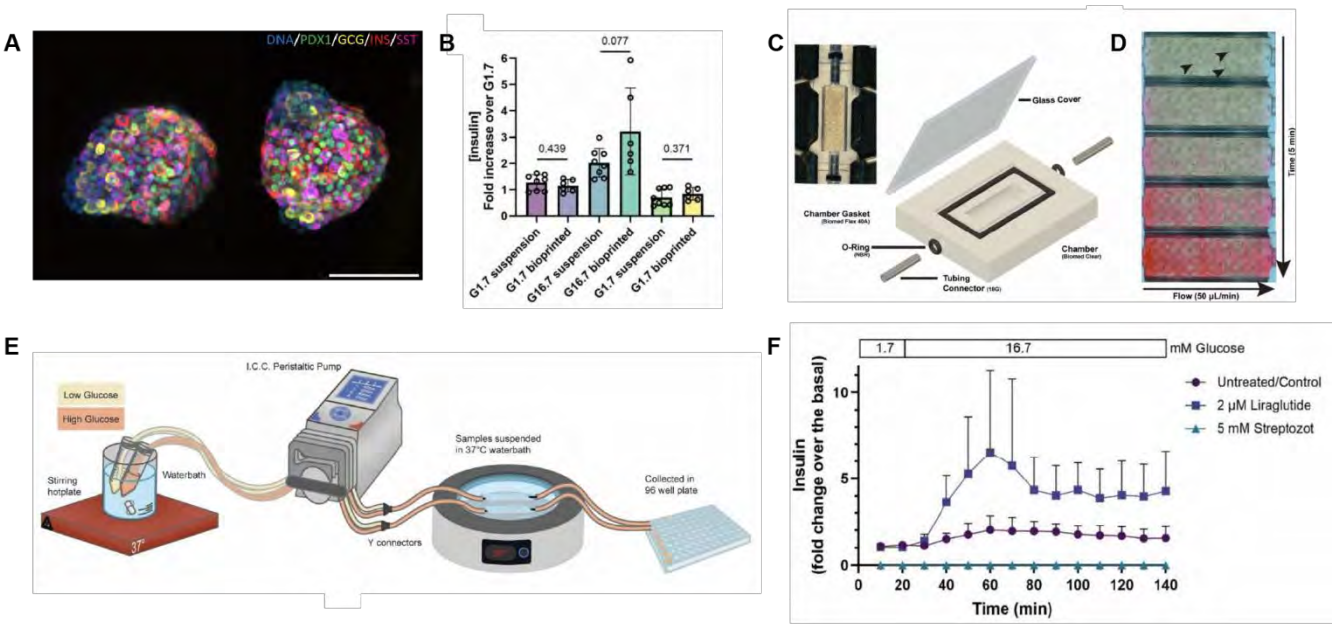

Figure 1. A. Immunofluorescence imaging of iPSC-derived pancreatic islets, revealing protein expression of PDX1 (green), glucagon (GCG, yellow), insulin (INS, red), and somatostatin (SST, magenta). Scale bar represents 200 µm. B. Glucose-stimulated insulin secretion (GSIS) results between samples matured in suspension versus those matured in 6% (w/v) GelMA. G1.7: 1.7 mM glucose solution, G16.7: 16.7 mM glucose solution. C. A volumetrically bioprinted gyroidal construct containing a homogenous distribution of iPSC-derived islets, within a perfusion chamber. D. Efficient perfusion of the constructs at 50 µL/min. E. Schematic representation of the experimental setup used to perform dynamic GSIS assays on bioprinted endocrine pancreatic units. F. The platform enables pharmacological testing, demonstrated by enhanced insulin secretion following treatment with the glucose-sensitising agent liraglutide (N=6), compared to untreated controls (N=8). In contrast, treatment with the β-cell cytotoxic agent streptozotocin (N=2) abolished insulin secretion, confirming its deleterious effect on the bioprinted constructs.

S15 – O6

An immunocompetent bioprinted dextran-based skin model for studying chronic wound inflammation

Downs-Ford, R. L.[1], Warde, D.[3], Cartmell, S. H.[2], Domingos, M.[1]

[1]Dept. of Mechanical and Aerospace Engineering, The University of Manchester, Manchester; [2]Dept. of Materials, The University of Manchester, Manchester; [3]Solventum, Loughborough, UK

Introduction

Chronic wounds are a major healthcare challenge, with 40–60% failing to heal within three months. They are characterised by persistent inflammation, impaired cellular activity and excessive extracellular matrix degradation. Existing in vitro wound models often fail to reproduce the complex cellular interactions and inflammatory signalling that drive chronic wound pathology, particularly the role of immune cells. In addition, commonly used biomaterials such as collagen present challenges related to variability, cost and limited printability. There is therefore a need for reproducible and physiologically relevant in vitro models that better replicate the chronic wound microenvironment.

Aim

The aim of this study was to develop an immunocompetent, bioprinted dextran-based full-thickness skin model capable of reproducing key inflammatory and cellular characteristics of chronic wounds.

Materials and Methods

Photocrosslinkable dextran-based hydrogels were developed as a bioink for extrusion-based 3D bioprinting. Dextran was functionalised with glycidyl methacrylate (DexGMA) to produce a shear-thinning hydrogel suitable for printing and rapid photocrosslinking. Bilayered skin constructs were fabricated with human dermal fibroblasts in the dermal layer and keratinocytes forming an epidermal layer cultured at an air–liquid interface. After tissue maturation, reproducible wounds were introduced and chronic inflammatory conditions were induced.

Macrophages were incorporated to investigate immune responses through M1/M2 polarisation and migration towards wound sites. Cytokine secretion was quantified by ELISA for IL-6, IL-8, IL-1α, TNF-α and TGF-β. Matrix remodelling was assessed by MMP-2 and MMP-9 quantification, while quantitative PCR was used to evaluate fibroblast and keratinocyte activity.

Results

Dextran based hydrogels demonstrated favourable rheological properties and rapid photocrosslinking, enabling reliable extrusion-based printing of bilayered constructs. The resulting skin models supported high cell viability, structural stability during extended culture and keratinocyte stratification under air-liquid interface conditions.

Controlled wounding enabled reproducible monitoring of healing behaviour. Under chronic inflammatory stimulation, wound closure was delayed compared with healthy controls. Macrophage integration further altered the wound microenvironment, with increased secretion of pro-inflammatory cytokines including IL-6, IL-8 and TNF-α. Chronic stimulation also altered MMP-2 and MMP-9 levels, suggesting changes in the extracellular matrix remodelling. Gene expression analysis revealed altered fibroblast and keratinocyte activity consistent with impaired healing responses.

Conclusion

This study demonstrates the development of an immunocompetent, bioprinted dextran-based skin model that reproduces key features of chronic wound pathology, including sustained inflammatory signalling, altered cellular behaviour and dysregulated matrix remodelling. The platform provides a reproducible in vitro system for investigating chronic wound biology and evaluating emerging therapies.

Acknowledgements

The authors would like to thank the EPSRC funded Centre for Doctoral Training in Advanced Biomedical Materials grant reference EP/S022201/1 for funding this work.

We also acknowledge the Henry Royce Institute for Advanced Materials (grant no. EP/R00661X/1, EP/S019367/1, EP/ P025021/1, and EP/P025498/1) for support and equipment use.

S15 – O7

Light-activated mechanostimulation of hiPSC-derived cardiomyocyte microtissues using a 4D printed hybrid scaffold

Valenzuela-Segura L.[1,2], Anaut I.[3], Urigoitia-Asua A.[1,2], Larequi E.[3], Mazo M.M.[3,4,5], Henriksen-Lacey M.[1,6], Jimenez de Aberasturi D.[1,7]

[1]CIC biomaGUNE, BRTA, Donostia-San Sebastián; [2]Dept. of Applied Chemistry, University of the Basque Country, Donostia-San Sebastián; [3]Bioengineering Program, Technological Innovation Division, Cima Universidad de Navarra, 31008 Pamplona; [4]Instituto de Investigación Sanitaria de Navarra (IdiSNA), 31008 Pamplona; [5]Hematology and Cell Therapy, Cancer Center Clínica Universidad de Navarra (CCUN), Pamplona; [6]CIBER-BBN, 20014 Donostia-San Sebastián; [7]Ikerbasque, Basque Foundation for Science, 48009 Bilbao, Spain

Introduction

Limited maturation is a significant hindrance for the application of human induced pluripotent stem cell-derived cardiomyocytes (hiPSC-CMs). Be it as a regenerative therapeutic, or as the basis of in vitro cardiac models to study the pathology of human cardiovascular diseases (CVDs), fetal-like gene expression, structure and function precludes application, limiting their ability to accurately represent native tissue. Mechanical stimulation is reported to induce a significant enhancement of maturity but often relies on invasive methods involving the use of potentially toxic metals, or complex devices. Here, we present an optically responsive hybrid ink, compatible with 3D printing, which can be used as a scaffold to support the generation of 3D engineered cardiac tissues by embedding hiPSC-CMs in fibrin (Figure 1); by applying irradiation with NIR light sources, cyclic contraction and expansion of the material can be achieved leading to controlled hiPSC-CM mechanostimulation (Figure 2). By employing biocompatible light sources and materials, and defining cyclic irradiation parameters, hiPSC-CM microtissue maturation can be achieved.

Materials and Methods

Scaffolds, fabricated using a previously published hybrid ink [1], were printed using Liquid Crystal Display (LCD) printing, sterilised and seeded with 2 million hiPSC-CMs embedded in a fibrin-thrombin gel. Cardiomyocyte differentiation and microtissue fabrication was performed following previously reported protocols.[2] Cytotoxicity of the hybrid scaffold material was evaluated using Live/Dead staining and Alamar Blue assay. Mechanical stimulation treatment consisted of 1h/day pulsed NIR laser irradiation, for 5 days. Viability and CM maturation were evaluated by counting beating rate, Alamar Blue, RT-qPCR, RNA-seq and immunofluorescence (IF) staining.

Results

We successfully fabricated an LCD-printed biocompatible scaffold featuring diamond-shaped micropores that showed highly reproducible expansion and contraction in response to NIR irradiation. Laser irradiation conditions (power density, irradiation time, spot size) were optimized to achieve a temperature change optimal for the contractile capability of the hybrid ink (33-38 ºC) under physiological conditions. We observed that irradiation treatment led to a higher hiPSC-CM maturation, as measured by RT-qPCR of cardiac genes and bulk RNA-seq, and IF staining. Importantly, no negative effects in any of the measured variables were observed.

Conclusion

We have successfully developed an LCD-printable and biocompatible scaffold capable of stimulating mechanotransduction pathways in hiPSC-CM microtissues enhancing their maturation profile at electrophysiological levels.

Acknowledgements

Ministerio de Ciencia e Innovación de España (#PID2022-143248OB-I00 and PID2022-142562OB-I00) and Ikerbasque Foundation.

References

[1]Urioitia-Asua A. et al., *Adv. Optical Mater.* (2025), 13, e01142.
[2]Iglesias-Garcia O. et al., *Adv. Funct. Mater.* (2025): 35, 2420106.

Figures

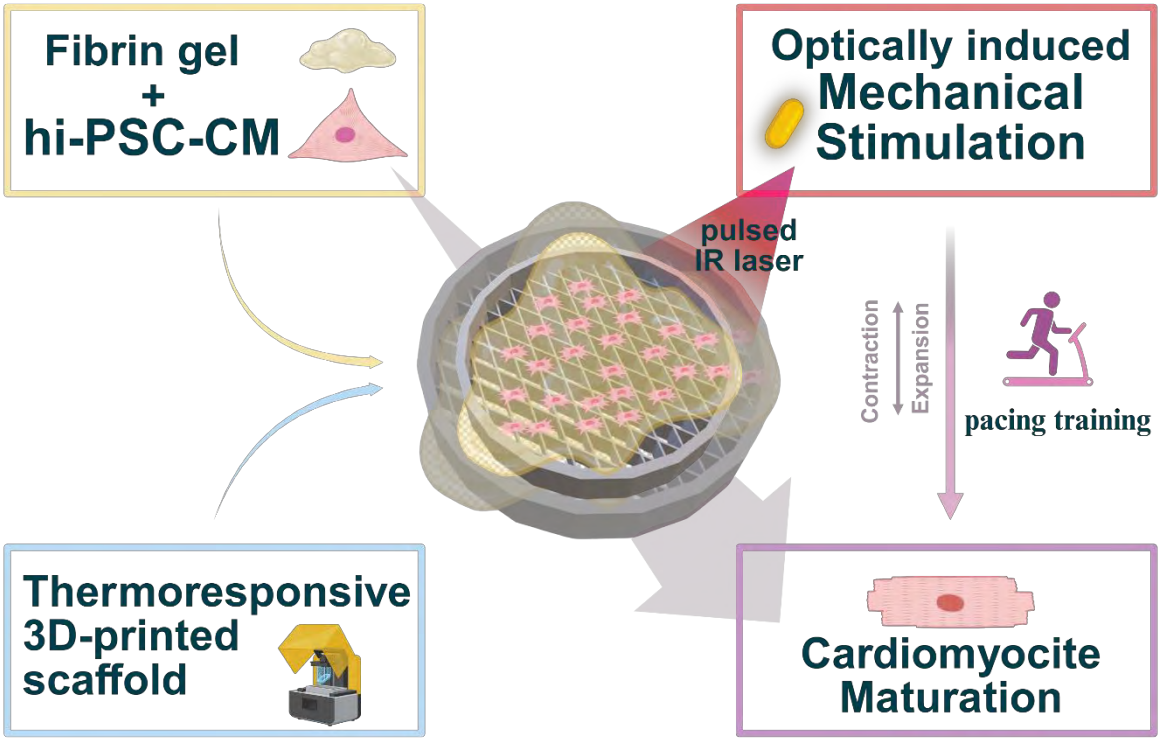

Figure 1. Visual abstract of the composition, functioning and aim of the optically responsive platform applied to the mechanostimulation of the hiPSC-CM microtissues.

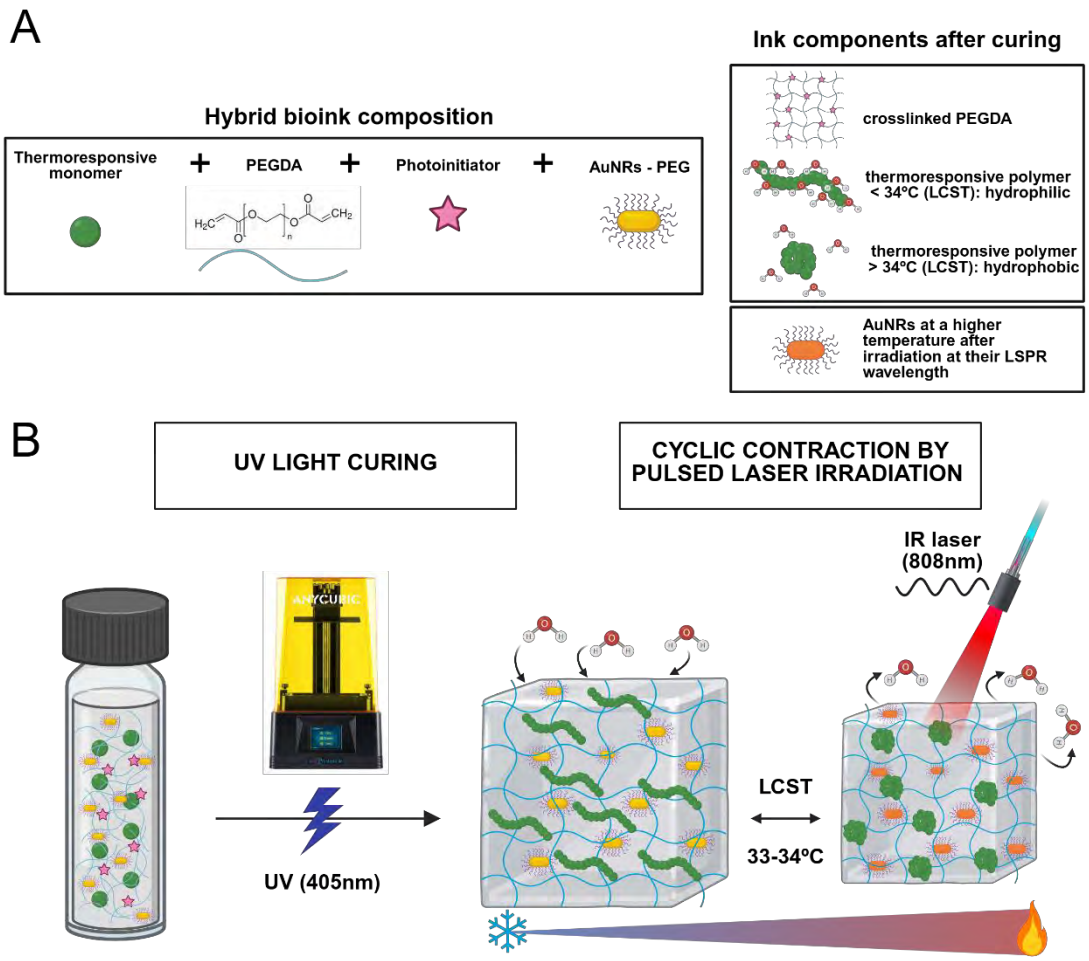

Figure 2. Scheme of the composition and functioning of the 3D-printable hybrid bioink. **A.** Formulation and depiction of its components before and after UV curing. **B.** Illustration of the process of the hydrogel ink crosslinking and the functioning of the pulsed irradiation as a cyclic contraction and expansion mechanical force.

S16
Biological macromolecules for the biofabrication of tissue-like microenvironments

S16 – K1
Human-derived proteins for the biofabrication of tissue-like structures

Mano J.F.
University of Aveiro, Aveiro, Portugal

S16 – O1

Controlling self-assembly in protein-based materials via sequence engineering and post-processing approaches

Lopez Barreiro D.
Manufacturing Futures Lab, Dept. of Chemical Engineering, University College London, UK

Introduction

The biofabrication of recombinant structural proteins with a range of mechanical or structural features usually relies on the generation of protein libraries displaying variations in terms of amino acid composition, block structure, molecular weight, or physical/chemical crosslinking sites. This approach, while highly successful in generating a wealth of knowledge regarding the links between design features and material properties, has some inherent limitations related to its low throughput. This slows down the pace of the development of *de novo* recombinant structural proteins. Here, we combine traditional sequence engineering approaches with postprocessing methods to tune the viscoelastic properties of thermoresponsive hydrogels made of silk-elastin-like polypeptides (SELPs). Specifically, we focus on three aspects:

- Type, number and location of structural building block throughout the protein sequence (e.g., silk-like GAGAGS, elastin-like VPGXG and IPAVG).
- Influence of non-structural peptide building blocks (specifically, antimicrobial peptides, hydroxyapatite biomineralising peptides and graphene-binding peptides) on the self-assembly of thermoresponsiveness of SELP hydrogels.
- Effect of postprocessing methods – formic acid treatment, ethanol annealing or shear – that alter the topology of SELP networks prior to gelation, from highly disordered to highly ordered.

Materials and Methods

We use SELPs formed by structural and functional building blocks inspired by natural proteins, such as silk or elastin. Our *de novo* proteins are recombinantly expressed in *E. coli*, purified via inverse temperature cycling, and subjected to multiscale characterisation using techniques such as NMR, rheology, AFM, SEM and fluorescence recovery after photobleaching. These array of techniques allow us to understand their multiscale self-assembly and their ability to form thermoresponsive (ir)reversible hydrogels.

Conclusion

Our results highlight the deleterious effect of charged amino acids for the overall viscoelastic properties of SELP hydrogels, especially when solvent treatments such as ethanol annealing are applied. We also identify optimal positions for functional building blocks within the SELP sequences that enhance the self-assembly propensity of SELPs. Finally, we also identify the number of silk-like block clusters (rather than the overall number of silk-like blocks) as a key element on the irreversible gelation of SELP hydrogels.

Acknowledgements

The author acknowledges financial support from UK Research and Innovation (UKRI) via the Engineering and Physical Sciences Research Council (EPSRC) New Investigator Award (UKRI128).

S16 – O2

Physioink: Platform for physiological bioinks to reproduce human extracellular matrix structure and composition

Hettrich, K.[1], Protz R.[1], Hettrich, C.[2], Uhlig, K.[2], Flechner, M.[2], Hautmann, A.[3], Salazar, C.S.S.[3], Friedmann, A.[3], Schmelzer, C.[3], Probst, J.[4], Weigel, T.[4]
[1]Fraunhofer Institute of Applied Polymer Research IAP Potsdam; [2]Branch of Bioanalytics and Bioprocesses, Fraunhofer Institute for Cell Therapy and Immunology IZI-BB, Leipzig; [3]Fraunhofer Institute for Microstructure of Materials and Systems IMWS, Halle (Saale); [4]Translational Center Regenerative Therapies TLC-RT, Fraunhofer Institute for Silicate Research ISC, Würzburg, Germany

Introduction

Bioinks/Hydrogels are in development for more than two decades. However, the reproduction of the real ECM structure, composition and material density is still an unsolved issue. For better standardization and printability, biological materials are denaturated and/or chemical modified resulting in superior printing properties and cell compatibility due to remaining biological groups. But as the microscopic structure is completely lost, advanced cell functions and tissue maturating are handicaped. On the other side, the application of natural ECM like collagen 1 (Col1) is limited due to uncontrolled gelation, need for pH shift, limited applicable concentrations and high viscosities.

In our approach, we just physically formulate the ECM molecules to polyelectrolyte complexes which can overcome all drawbacks and maintains all biological and structural properties. Similar to sulfated glycans in most tissues we designed cellulose sulfates (CS) to bind to solubilized ECM like Col1. By adjusting the molecular structure of CS, the triggerable binding and gelation properties can be customized to the individual ECM without any modifications on the biological proteins.

Materials and Methods

Various types/sources of cellulose were used to synthesise CS. By varying reaction parameters, such as composition of reagents, reaction temperature and time, degrees of substitution between 0.4 and 2.0 were achieved. The CS were characterized in terms of their solubility and viscosity in water, sulphur content, rheological behaviour and molar mass distribution. Attractive molecular interactions between CS and ECM (Col1, Elastin, Collagen 4) were performed by SPR and measurements of optical density/scattering, screening CS structure, pH, temperature, concentration and proportions. Gelation and further characterization of resulting Col1 inks/gels occurred optically, by rheology, nanoindentation and SEM. Thereby, applicable collagen concentrations were evaluated and tested in biological interaction concerning their detailed composition. Finally, the printing properties of the ink were evaluated and first applications in tissue models tested.

Results

Binding properties between ECM molecule and CS improved with increasing degree of sulfation and decreasing chain length. For Col1, the formulation resulted in lower viscosities, improved physiological structure and strong shift in gelation start for low concentrations of 10 or 20mg/ml (compared to pure collagen) and enabled to further increase the applicable collagen concentration to >50mg/ml. Bioprinting experiments showed improving printing properties with higher concentrations (viscosities) and also strongly reduced tissue contraction in applied tissue models.

Conclusion

By formulating defined ECM molecules as a polyelectrolyte complex with anionic cellulose sulfate, the applicability was highly improved and generated a basic instrument to be applied on all ECM types.

S16 – O3

Pre-vascularized skin constructs as a basis for vascular wall engineering

Bacakova L.[1], Tomsu J.[1], Wu Y.-C.[1], Doubkova M.[1], Broz A.[1], Svobodova L.[1], Lukas D.[2]
[1]Laboratory of Biomaterials and Tissue Engineering, Institute of Physiology of the Czech Academy of Sciences, Prague; [2]Faculty of Science, Humanities and Education, Technical University of Liberec, Liberec, Czech Republic

Introduction

Pre-vascularization of *in vitro*-engineered tissues is a key strategy to prevent necrosis after *in vivo* implantation and to develop *in vitro* tissue models that are more relevant for various experimental studies.

Aim

Our initial goal was to develop a pre-vascularized bilayer dermal-epidermal skin equivalent. At a certain stage in the construction process, it was transformed into a structure resembling the *tunica intima* and *media* of a blood vessel wall.

Materials and Methods

An electrospun nanofibrous membrane made from a synthetic degradable polymer, such as polylactide or polycaprolactone, was modified with a fine fibrin mesh and seeded with either normal human dermal fibroblasts (NHDFs) or human subcutaneous adipose tissue-derived stem cells (ADSCs), isolated from lipoaspirates obtained via liposuction. After reaching subconfluence, the ADSCs were overlaid with a collagen-based hydrogel loaded with human umbilical vein endothelial cells (HUVECs).

Results

Both NHDFs and ADSCs gradually migrated into the hydrogel, supporting pre-capillary formation by acting as pericytes. However, the pre-capillary network was more developed with ADSCs. When the construct was seeded with human keratinocytes, pre-capillaries stopped growing beneath its surface. The keratinocytes then matured phenotypically and stratified at an air-liquid interface, resulting in a dermal-epidermal skin equivalent. However, when keratinocytes were not seeded on top of the construct and pre-capillaries reached its surface, they created openings, and the HUVECs formed a confluent layer on top (Figure 1). The ADSCs in the hydrogel could differentiate into vascular smooth muscle cells (VSMCs). As a result, the construct transformed into a structure resembling the *tunica intima* and *media* of a blood vessel wall. Still, a conflict remains between pre-vascularization, endothelial cell layer formation, and VSMC differentiation that needs to be resolved. A similar conflict was also observed between pre-vascularization and osteogenic differentiation of ADSCs, although it was milder.

Conclusion

Tissue-engineered constructs can be pre-vascularized by co-culturing endothelial and mesenchymal stromal cells. These cells naturally form tubular, capillary-like structures within a hydrogel-based three-dimensional (3D) environment. This approach can be used to develop soft tissue equivalents, such as skin and vascular walls. With proper reinforcement, it can also be used to produce hard-tissue equivalents, such as bone.

Acknowledgements

Supported by the P JAC Project „EXREGMED“ (No. CZ.02.01.01/00/22_008/0004562) of the Ministry of Education, Youth and Sports of the Czech Republic, co-funded by the European Union, and by the *Praemium Academiae* grant (No. AP2202) of the Czech Academy of Sciences.

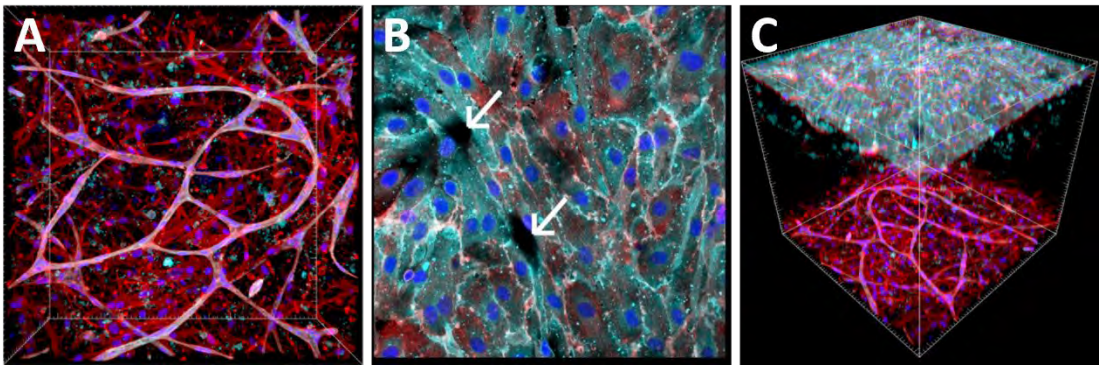

Figure 1. A. ADSCs and HUVECs spontaneously form pre-capillaries in a collagen hydrogel. **B**. Pre-capillaries end on the hydrogel surface, and HUVECs form a confluent layer. **C**. Side view of a pre-vascularized structure that resembles the *tunica intima* and *media* of the vascular wall.

S16 – O4

Light-based 3D cell bioprinting: Implications of bioink for an artificial skin prototype

Resina L.[1,2], Peréz-Madrigal M.M.[1,2], Alemán C.[1,2,3]
[1]IMEM-BRT Group, Departament d'Enginyeria Química, EEBE, Universitat Politècnica de Catalunya - BarcelonaTech (UPC); [2]Barcelona Research Center in Multiscale Science and Engineering (CCEM), Universitat Politècnica de Catalunya - BarcelonaTech (UPC); [3]Institute For Bioengineering of Catalonia (IBEC), The Barcelona Institute of Science and Technology, Barcelona, Spain

Introduction

Despite its resilience, skin is highly vulnerable to traumatic injuries, which are often complicated by infection, and delayed repair. Effective wound healing depends largely on fibroblast activity, as these cells produce extracellular matrix proteins that drive tissue remodelling. Although 3D bioprinting has emerged as a powerful strategy for engineering biomimetic skin substitutes and advanced wound dressings, the development of bioinks that simultaneously provide structural integrity, cytocompatibility, and bioactivity remains challenging.

Aim

To understand how human fibroblasts behave within gelatin methacryloyl and tannic acid (GelMA+TA) scaffolds and how these systems could be optimized as prototypes of artificial skin. The present work aimed to design and 3D bioprint human skin cells within a scaffold based on GelMA+TA to serve as a prototype for future applications as a next-generation wound dressing and artificial skin prototype.

Materials and Methods

GelMA–based hydrogels incorporating TA were developed via digital light processing (DLP) bioprinting to fabricate 3D scaffolds as prototypes of artificial skin and wound dressings. The bioprinted scaffolds were characterized by SEM, micro-CT and FTIR, and their mechanical and antibacterial properties were assessed, as well as TA release for 25 days. Human fibroblasts and monkey epithelial cells were also bioprinted within the scaffolds, cell viability, adhesion and proliferation were studied by MTT and confocal microscopy over time.

Results

The incorporation of TA significantly enhanced hydrogel stability, mechanical stiffness, and antibacterial activity (against *E. coli* and *S. aureus*), while maintaining high water content and print fidelity. Structural characterization revealed that TA promoted the formation of a more compact and homogeneous porous network, consistent with the observed increase in Young's modulus and delayed degradation under physiological conditions. Importantly, 3D bioprinting and encapsulation studies demonstrated cell type–dependent biological responses. Human skin fibroblasts exhibited robust long-term viability and proliferation within pure GelMA scaffolds, while TA-containing hydrogels promoted early cell–material interactions but limited long-term fibroblast proliferation. In contrast, epithelial cells showed improved viability and morphology under encapsulation conditions in GelMA+TA scaffolds.

Conclusion

These results highlight the critical interplay between macromolecular composition, 3D microenvironment, and cell response, demonstrating the potential of GelMA+TA bioinks as tunable platforms for bioactive wound dressings and artificial skin scaffolds.

Acknowledgements

This publication is part of the I+D+i projects PID2021-125257OB-I00, PID2021-125767OB-I00, PDC2025-165847-I00, and the Maria de Maeztu Units of Excellence Programme CEX2023-001300-M, both funded by MCIN/AEI/10.13039/501100011033. C.A. was also supported through the prize "ICREA Academia" for excellence in research funded by the Generalitat de Catalunya.

S16 – O5

Dual-functional GelMANB hydrogels crosslinked with thiolated elastin with tunable mechanics for volumetric bioprinting

Willemarck R.[1,2], Bogaert B.[1], Dehaene I.[2], Van Vlierberghe S.[1], Pien N.[1]
[1]Polymer Chemistry and Biomaterials Group, Centre of Macromolecular Chemistry (CMaC), Ghent University; [2]Dept. of Obstetrics and Gynaecology, Ghent University Hospital, Ghent, Belgium

Introduction

Photocrosslinkable gelatin derivatives have emerged as excellent biomaterials for light-based bioprinting methods. Among these, gelatin-methacryloyl (GelMA) and gelatin-norbornene (GelNB) are well established due to their favorable mechanical properties, processability, and biocompatibility[1]. Building on these advantages, a new dual-functional derivative, gelatin-methacryloyl-norbornene (GelMANB), combining both chain-growth and step-growth polymerization, has been developed.

Aim

This work assesses the influence of different, frequently used thiolated crosslinkers, such as dithiothreitol (DTT), polyethylene glycol dithiol (PEG2SH), thiolated gelatin (GelSH), and compares them with a newly designed thiolated elastin crosslinker (ElnSH).

Materials and Methods

GelMANB was synthesized and characterized by proton nuclear magnetic resonance spectroscopy (^{1}H-NMR) to quantify the degrees of substitution (DS) of methacryloyl and norbornene groups. Both GelSH and ElnSH were synthesized, and the DS was quantified using an o-phthaldialdehyde assay. GelMANB resins with different crosslinkers were prepared at 5, 7.5, and 10 w/v% and underwent physico-chemical characterization including photorheology, tensile testing, frequency sweep analysis, gel fraction, and mass swelling assessment. Processability was further investigated through volumetric additive manufacturing (VAM). Scaffolds were printed to evaluate mechanical behavior. Bioinks containing lung fibroblasts (MRC5, 1.5 million/mL) were prepared, and VAM printed to assess post-printing viability and proliferation using live/dead staining and MTS assays.

Results

^{1}H-NMR confirmed successful functionalization of gelatin, resulting in a DS of 66% for methacryloyl and 25% for norbornene. Thiolated polymers GelSH and ElnSH were synthesised with DS values of 69% and 34%, respectively. Photorheology of 7.5 w/v% resin formulations showed that GelMANB/GelSH produced the highest storage moduli (10.6 ± 0.9 kPa), whereas GelMANB/DTT and GelMANB/ElnSH displayed the lowest (3.9 ± 0.2 kPa and 0.9 ± 0.08 kPa). Notably, the storage modulus of 10 w/v% GelMANB/ElnSH matched that of 7.5 w/v% GelMANB/DTT (Fig.1A). Tensile testing showed that the Young's modulus of 10 w/v% GelMANB/ElnSH (18.5 ± 1.1 kPa) was reduced relative to GelMANB-hydrogels without additional crosslinker (28.35 ± 2.1 kPa), indicating increased elasticity despite higher crosslink density (Fig.1B). An optimal printing dose was assessed to be 125 mJ/cm² for 10w/v% GelMANB/ElnSH using VAM (Fig. 1C).

Conclusion

Eln-SH shows promising potential as a new water-soluble, cell-interacting, and non-toxic thiol crosslinker suitable for volumetric printing. Future work should evaluate their relevance in soft- or elastic-tissue cell models.

Acknowledgements

The authors acknowledge the Research Foundation Flanders (FWO) for a Hercules grant (grant number I003922N)

References

[1]Pien N, Bogaert B, et al. Additive Manufacturing 2025; 109; 104850, DOI: 10.1016/j.addma.2025.104850.

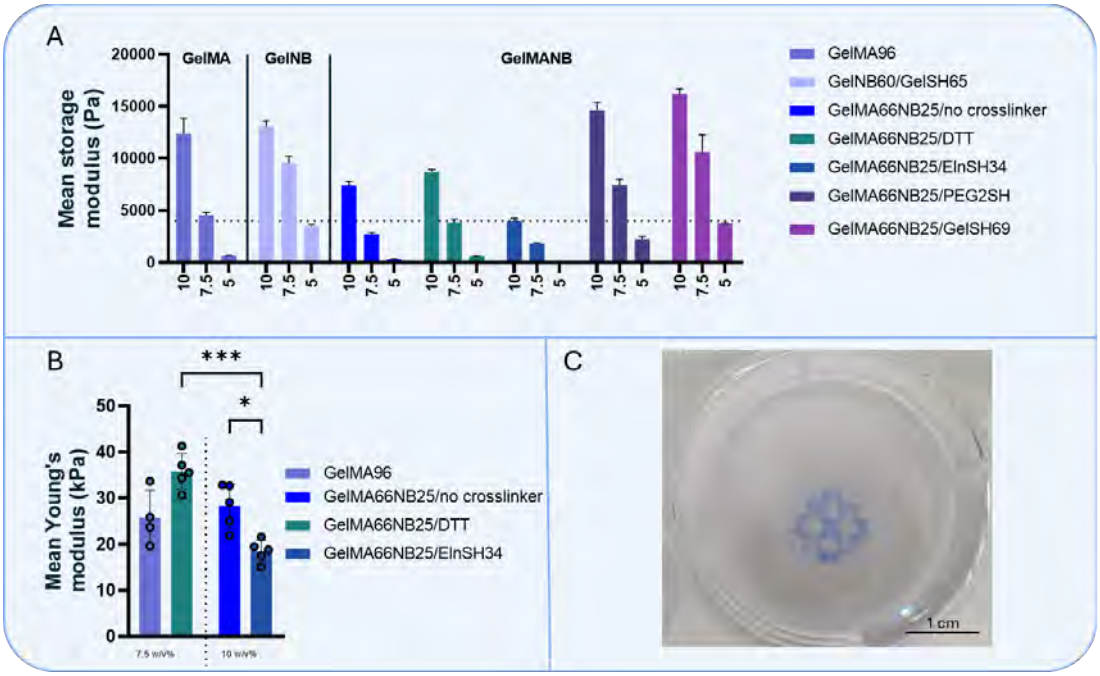

Figure 1: (**A**) mean storage modulus of the gelatin-based resins, measured using photorheology, (**B**) mean Young's modulus using tensile testing (* = p-value ≤ 0.0332; *** = p-value ≤ 0.002), (**C**) 125 mJ/cm² 10w/v% GelMA66NB25/ElnSH34 print in 6-well plate

S16 – O6

Shaping biomaterials: Optimization of a novel fibrillar collagen ink for 3D bioprinting

Gallo N.[1,2], Natali M.L.[2], Kodra C.[2], Sannino A.[3], Salvatore L.[2]

[1]Dept. Engineering for Innovation, University of Salento, Lecce; [2]Typeone Biomaterials Srl, Calimera; [3]Dept. Experimental Medicine, University of Salento, Lecce, Italy

Introduction

Three-dimensional bioprinting has emerged as a powerful strategy for fabricating biomimetic constructs for regenerative medicine. Among available biomaterials, type I collagen is particularly attractive due to its intrinsic advantages. However, the development of collagen-based bioinks remains challenging, as native fibrillar collagen often exhibits poor printability, limited mechanical stability, and are not soluble in physiological conditions. Recently, an innovative collagen ink has been developed in order to overcome collagen bioink limits. Indeed, it has been designed to be composed of fibrillar collagen, be stable at neutral pH, be self-standing, and ready-to-use, making it directly applicable as a bioink for extrusion bioprinting. Despite these advancements, further optimization is required to enhance its rheological and structural performances.

Aim. This study aims to optimize an innovative fibrillar collagen ink, with a specific focus on elucidating the effect of collagen concentration and cryo-crosslinking on its rheological properties, printability, and structural stability.

Materials and Methods Fibrillar collagen inks were subjected to cryo-crosslinking and resuspended at several concentrations. First of all, morphological and physico-chemical characterization was performed, Then, rheological analyses were conducted. Printability was assessed through extrusion-based printing tests, filament formation, and shape fidelity evaluation.

Results

Collagen concentration played a key role in modulating the rheological profile of the bioink, with higher concentrations leading to increased viscosity and improved viscoelastic behavior, enhancing filament formation and print fidelity. Cryo-crosslinking further reinforced the fibrillar network, promoting structural stability and resistance to deformation after extrusion. The combined effect of optimized concentration and cryo-treatment resulted in a bioink exhibiting pronounced shear-thinning behavior, rapid recovery, and improved shape retention. No pre-processing related modifcation of collagen fibrillar structure were observed.

Conclusion

The synergistic modulation of collagen concentration and cryo-crosslinking significantly improves the performance of this ready-to-use fibrillar collagen bioink. This optimized system represents a promising platform for the fabrication of biomimetic constructs in regenerative medicine, with potential applications in tissue engineering and in vitro models.

S17
Biomaterial-Engineered microphysiological systems for disease modeling and regeneration

S17 – K1
Engineering biomaterial platforms to study the tumour-stromal crosstalk in the context of pancreatic cancer

Velliou, E.[1]
[1]Centre for 3D Models of Health and Disease, Division of Surgery and Interventional Science, University College London, London, UK

Introduction
Pancreatic ductal adenocarcinoma (PDAC) is a very aggressive cancer characterised by poor prognosis and very low rates of survival, i.e., 5-year survival is below 10%. Further to lack of early detection tools, these disappointing statistics are also due to the highly complex tumour tissue microenvironment (TME) of PDAC, which drives treatment resistance. More specifically, the TME of PDAC is characterised by high levels of fibrosis/desmoplasia. Desmoplasia is the result of the deposition of very high amounts of Extracellular Matrix (ECM) proteins by the stellate cells, which get activated when the tissue is diseased (like in cancer). Desmoplasia is a hallmark of the disease, promoting its' aggressiveness, treatment resistance and metastatic cascade.
Therefore, when studying the disease evolution and treatment response, it is of paramount importance to reproduce robustly the complexity of the fibrotic PDAC TME.

Materials and Methods
To that end, using biomaterials we have generated spatially complex, zonal dynamic models of the PDAC TME which can capture in a tuneable way key features of the tumour tissue such (i) cellular complexity (ii) fibrosis/desmoplasia and stroma reprogramming (iii) interstitial tissue fluid flow. Furthermore, we have performed treatment in our models. More specifically we have performed, (chemotherapy X-ray radiotherapy, chemoradiotherapy and novel proton radiotherapy followed b mapping how different TME features affect the biological response and/or potential resistance to treatments.

Results
We see changes in aggressiveness of the cancer as well as changes in the fibrotic levels induced by activated stellate cells depending on the matrix proteins introduced in the models as well as depending on interstitial flow rates. In return, such changes affect the cellular response to the applied treatments.

Conclusion
The therapy responses we observe generally correspond to patient data, confirming the suitability of our novel biomaterial-based models for high throughput screening of therapies for PDAC as well as for personalised treatment design. Herein, key advances of our animal-free high throughput platform will be presented and discussed.

S17 – O1

Volumetrically printed porous hydrogels as tissue-mimetic platforms for ultrasound-enhanced drug delivery

Stanny J.[1,2], Noirot I. [1,3], Li M.[1], Clavier L.[1], Marcotulli M.[2], Nair M.[2], Carugo D.[2], Stride E.[2], Shavandi A.[1]

[1]Université libre de Bruxelles (ULB), 3BIO-BioMatter, Avenue F.D. Roosevelt, 50 - CP 165/61, 1050 Brussels, Belgium; [2]Institute of Biomedical Engineering, University of Oxford, Windmill Road, Oxford, OX3 7LD, UK; [3]École Supérieure de Biologie Biochimie Biotechnologies (ESTBB), Université Catholique de Lyon (UCLy), Lyon, France

Introduction

Ultrasound (US) and cavitation-mediated drug delivery hold substantial promise for improving the therapeutic index of drugs including chemotherapeutics. However, optimization of acoustic parameters remains challenging because microbubble dynamics are highly sensitive to the mechanical and transport properties of the surrounding tissue microenvironment. Conventional mechanically homogeneous gel phantoms, fail to reproduce physiologically relevant transport limitations (~100–200 µm) and often undergo brittle fracture under cavitation, limiting their predictive value.

Materials and Methods

Volumetric bioprinting was used to fabricate porous GelMA–PEGDA hydrogel constructs with digitally tunable pore and channel architectures. Porosity and perfusable vascular-like channels (1 mm diameter) were introduced as programmable design parameters, enabling control over pore size, orientation, and connectivity. Transport properties were evaluated under static and perfusion conditions using model solutes of varying size and charge, including fluorescent dextrans of defined molecular weight (***Fig.***). Mechanical properties were assessed by rheological measurements. Ultrasound-mediated cavitation experiments were performed under perfusion at acoustic pressures 1 to 5 MPa to evaluate structural stability and acoustic compatibility and resulting acoustic signals were processed in MATLAB.

Results

Engineered porosity enhanced both passive diffusion and perfusion-driven convection. Interconnected pore networks reduced the storage modulus from ~2000 Pa in bulk hydrogels to ~900–1000 Pa and increased effective solute penetration by more than twofold under flow (***Fig.***). In contrast, closed-pore architectures softened the matrix but did not significantly improve permeability. Transport remained strongly dependent on molecular properties: small cationic molecules diffused rapidly (~1.8 mm in 30 min), whereas larger or highly anionic species exhibited restricted penetration due to steric and electrostatic interactions. Comparisons with near-neutral fluorescent dextrans enabled separation of size- and charge-mediated transport effects.

Under ultrasound exposure, porous constructs effectively transmitted acoustic energy and sustained stable cavitation at therapeutic pressures up to 3 MPa without structural failure, whereas bulk hydrogels exhibited crack-like damage. Structural damage in porous systems was observed only above 5 MPa (***Fig.***).

Conclusion

Volumetrically printed porous hydrogels provide a mechanically stable and transport-relevant platform integrating passive diffusion, convection, and ultrasound-driven delivery. By quantitatively linking architecture, mechanics, transport, and cavitation response, this system establishes a predictive framework for optimizing ultrasound-assisted drug delivery.

Acknowledgements

This study was supported by an Aspirant fellowship from the Fonds National de la Recherche Scientifique de Belgique (FNRS) (grant number 46599), 2022 awarded to Julia Stanny. Additional support to J.S. was provided by the SofinaBoël Fellowship, and the Fondation Philippe Wiener – Maurice Anspach.

Figure

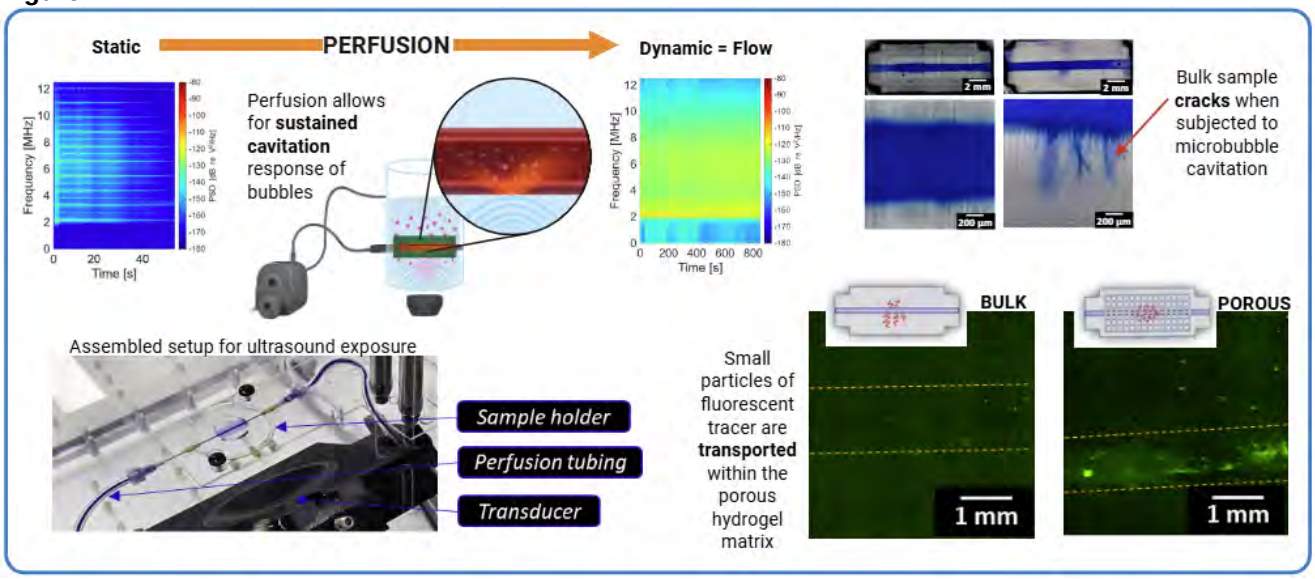

FIGURE: Ultrasound and perfusion-enhanced transport in porous hydrogels. Dynamic flow sustains microbubble cavitation compared to static conditions, promoting tracer particle transport through interconnected pores. The experimental setup (transducer, sample holder, and perfusion tubing) enables controlled ultrasound exposure, while bulk samples exhibit cracking under cavitation, highlighting the role of matrix structure in transport behavior.

S17 – O2

Chemically modified decellularized extracellular matrix combined with a microfluidic chip to model the early stages of pancreatic tumorigenesis

Neukelmance A.[1,2], Martin L.[2], Hoang A.[1], Caullet P.[2], Sacchi M.[1], Bertacchi N.[2], Clément F.[2], Texier I.[1]
[1]Univ. Grenoble Alpes, CEA, LETI-DTIS; [2]Univ. Grenoble Alpes, CEA, Inserm, IRIG, UA13 BGE, Biomics, France

Introduction

Pancreatic ductal adenocarcinoma (PDAC) is one the most aggressive cancers, which poor outcome is largely due to late diagnosis and the limited performance of current biomarkers. Recreating the pancreatic microenvironment to develop relevant models and identify early disease biomarkers is therefore an urgent need. Most in vitro models of PDAC rely on collagen or Matrigel® to mimic the tissue microenvironment while decellularized extracellular matrix (dECM) provides a more physiologically relevant environment by preserving all native biochemical cues and growth factors. However, dECM exhibits limited mechanical properties. To overcome this limitation, dynamic covalent bonds can be incorporated to enhance its mechanical stability while allowing matrix remodelling in response to cell-generated stresses.

Aim. This project aims to recreate the pancreatic microenvironment within a microfluidic chip using a dynamic dECM hydrogel in order to identify new early biomarkers for PDAC diagnosis.

Materials and Methods

dECM was prepared from adipose tissues of consenting donors, chemically modified to introduce functions amenable to dynamic crosslinking, and characterized. A PDMS microfluidic chip comprising a perfusable lumen embedded in a chamber filled with the dECM was designed and manufactured.

Results

The extracellular matrix was decellularized to remove all cellular components while preserving its native biochemical composition (1 to 5% dry weight recovery compared to initial tissue) (Fig. 1A). The obtained dECM was functionalized with functional groups to enable dynamic crosslinking (Fig. 1B). The PDAC model chip was designed to exhibit perfusable lumen structures to mimic exocrine ducts and endocrine islets within the dECM hydrogel (Fig. 1C). The developed microfluidic chip presents a chamber containing the hydrogel with a hollow tubular structure that allows stable perfusion for at least 21 days (Fig. 1D). The dynamic bonds introduced in the dECM are expected to enhance matrix stability while allowing cell-mediated remodelling. Furthermore, the dECM will be functionalized in the future with metabolic or environmental factors, such as glucose or pollutants, to investigate their effects on the initial stages of pancreatic tumorigenesis.

Conclusion

In summary, our experimental approach integrates chemical functionalization, co-culture of exocrine and endocrine cells, and microfluidics, to investigate early pancreatic tumorigenesis and identify new PDAC biomarkers.

Acknowledgements

We acknowledge the financial support of the “Material and Processes” CEA-PTC program. LETI-DTIS is supported by the French National Research Agency (ANR, CBH-EUR-GS (ANR-17-EURE-003) and ANR-15-IDEX-02 programs). Biomics is supported by ANR (JCJC ADOC (ANR-24-CE19-3753-01)) and Association Espoir Isère Cancer.

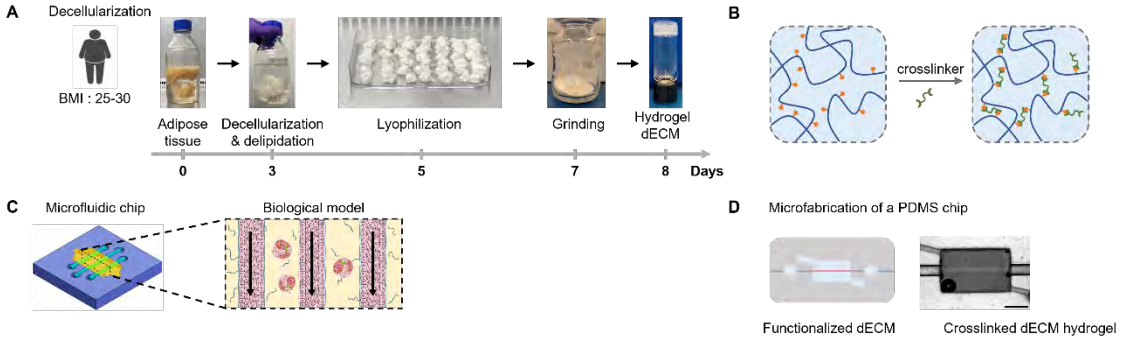

Figure 1. *A) Decellularization process for the formation of a dECM hydrogel.* ***B)*** *Chemical modification of dECM for dynamic crosslinking.* ***C)****Model of the pancreatic microenvironment integrating exocrine ducts and endocrine islets in a dECM hydrogel in a microfluidic chip.* ***D)*** *PDMS microfluidic chip containing a perfusable lumen embedded in a chamber filled with hydrogel. Scale bar: 1200µm.*

S17 – O3

Dormancy-inducing 3D engineered matrices to model breast cancer dormancy across scales: The role of adhesion and stiffness in ER+ luminal breast cancer cell lines and patient-derived models

Heras U.[1,2], Pardo-Sánchez J.M.[1], Berasain J.[1,3], Iturriaga L.[1], Aguirresarobe R.[4], Calafel I.[4], del Carcer G.[5], Arizaga E.[1,6], Riestra A.[7,8], Mitxelena-Iribarren O.[1], Cipitria A.[1,9]

[1]Group of Bioengineering in Regeneration and Cancer, Biogipuzkoa Health Research Institute, Donostia/San Sebastian; [2]Dept. of Cell Biology and Histology, Faculty of Medicine and Nursing, University of the Basque Country UPV/EHU, Leioa; [3]Dept. of Advanced Polymers and Materials: Physics, Chemistry and Technology, Faculty of Chemistry, University of the Basque Country UPV/EHU, San Sebastian; [4]POLYMAT and Dept. of Polymers and Advanced Materials: Physics, Chemistry and Technology, Faculty of Chemistry, University of the Basque Country UPV/EHU, Donostia/San Sebastian; [5]Cell Cycle and Cancer Biomarkers Group, Dept. of Cancer Biology, Instituto de Investigaciones Biomédicas Sols-Morreale (IIBM, CSIC-UAM), Madrid; [6]Dept. of Radiology, Donostia University Hospital, Donostia/San Sebastian; [7]Dept. of Pharmacy, Fundación Onkologikoa Fundazioa, Donostia/San Sebastian; [8]Dept. of Medicine, University of Deusto, Bilbao; [9]IKERBASQUE, Basque Foundation for Science, Bilbao, Spain

Introduction

Cancer dormancy is a collective phenomenon of single cells, tumor masses and active micrometastases, evolving across spatiotemporal scales (1). 3D bioengineered models demonstrate that extracellular matrix (ECM) confinement induces breast cancer (BC) dormancy through high density and/or low adhesion (2).**Aim**

Recapitulate BC dormancy using stiffness-matched inert alginate versus adhesive and degradable GelMA hydrogels to dissect dormancy and provide drug screening platforms.

Materials and Methods

MCF7-FUCCI2 cells were encapsulated in i) norbornene-modified alginate and ii) adhesive and degradable GelMA. Stiffness was evaluated by rheology. Single cells and tumor masses were stained with F-actin, 3D-imaged with confocal microscopy and segmented using deep learning to quantify volume and sphericity. We correlated these with a macromolecular crowding biosensor and immunofluorescence for p27 (dormancy), H3K4me3 (chromatin accessibility), and SOX9 and NR2F1 (transcription factors). We validated a dormancy signature by RT-qPCR (day 5) and dormancy scape by 7 days in 2D culture post-retrieval. Retrieved cells were implanted into chicken chorioallantoic membrane (CAM) models for tumor formation. ER+ patient-derived cells were tested with tamoxifen for drug resisntance.

Results

We obtained soft (1 kPa) and stiff (10 kPa) matrices for alginate and GelMA. Soft alginate significantly maintained single cells, whereas soft GelMA promoted tumor mass formation. Morphogenesis analysis demonstrated that single cells reduced in volume and tumor masses expanded in GelMA over time (Fig. 1). We observed significantly higher nuclear p27 expression in alginate groups compared to GelMA, demonstrating that low adhesion and low degradability promote dormancy. Thus, soft alginate promoted stem-like dormancy characterized by H3k4me3^{low}/SOX9^{high} expression together with protective and anti-apoptotic genes (SOX9, DEC2 and FHL2). Stiff alginate significantly increased macromolecular crowding, active chromatin sites (H3k4me3^{high}) and NR2F1 nuclear localization in single cells, with upregulated pro-apoptotic genes (p53, p21 and p57) (Fig. 2). Cells retrieved from soft alginate reawakened in 2D culture post-retrieval, but failed to form tumors in CAM models, whereas cells retrieved from stiff alginate had limited survival. Drug testing with patient-derived cells showed higher IC50 values (21.34 µM) for dormant cells in soft alginate compared to proliferative cells in soft GelMA (11.06 µM).

Conclusion

Adhesion and degradability modulate single cells (alginate) vs. tumor mass (GelMA) formation. In alginate, soft gels support stem-like dormancy through protective phenotypes, allowing partial reawakening under favorable conditions, whereas stiff gels promote macromolecular crowding, active chromatin sites and pro-apoptotic phenotypes. These platforms are clinically relevant to evaluate therapy resistance.

Acknowledgements

We acknowledge financial support from IKERBASQUE Basque Foundation for Science, the Spanish Ministry of Science and Innovation (PID2021-123013OB-I00 funded by MCIN/AEI/10.13039/501100011033/FEDER, UE);

Fundación Científica Asociación Española Contra el Cáncer, (grant numbers LABAE223466CIPI and POSTD234723MITX); the Basque Government Dept. of Education (PRE_2024_2_0005 and PRE_2025_2_0097) and the European Research Council Consolidator Grant (DORMATRIX, 101123883).

References

1. Heras, U., Pardo-Sánchez, J.M., Fallert. L., Jiménez de Aberasturi, D., Mitxelena-Iribarren. O., Cipitria, A. Cancer Dormancy as a Collective Phenomenon Across Scales in Length and Time: Biological Observations and Advanced 3D Bioengineered Models. Annual Review of Cancer Biology 2025; 381.
2. Bakhshandeh, S., Heras, U., Taïeb, H. M., Varadarajan, A. R., Lissek, S. M., Hücker, S. M., Lu, X., Garske, D. S., Young, S. A. E., Abaurrea, A., Caffarel, M. M., Riestra, A., Bragado, P., Contzen, J., Gossen, M., Kirsch, S., Warfsmann, J., Honarnejad, K., Klein, C. A., Cipitria, A. Dormancy-inducing 3D engineered matrix uncovers mechanosensitive and drug-protective FHL2-p21 signaling axis. Science Advances 2024; 10, 45, eadr3997.

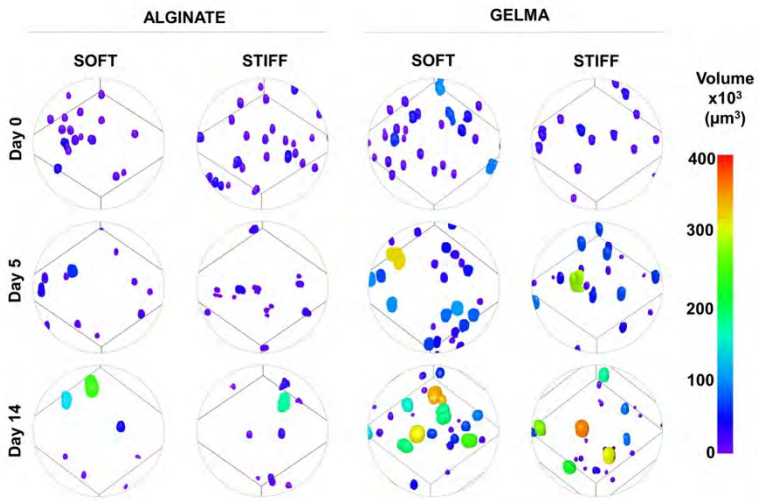

Figure 1

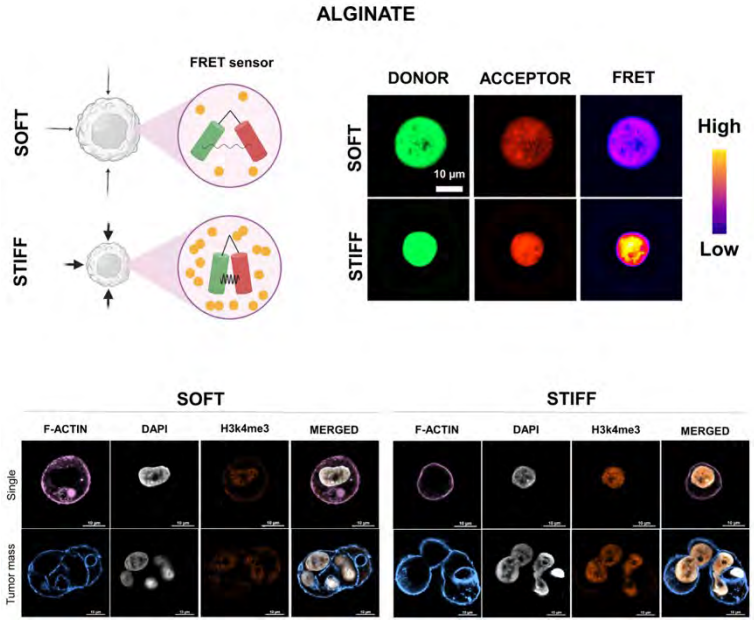

Figure 2

S17 – O4

An alternative supercritical CO_2 decellularization approach for breast tissue-derived cancer models

Gato-Diaz U.[1], López-Iglesias C.[1,2], Concheiro A.[1,2], García-González .CA.[1,2], Alvarez-Lorenzo C.[1,2], Blanco-Fernandez B.[1,2]
[1]I+D Farma Group (GI-1645), Dept. of Pharmacology, Pharmacy and Pharmaceutical Technology, Faculty of Pharmacy and Institute of Materials (iMATUS), University of Santiago de Compostela, Santiago de Compostela; [2]Health Research Institute of Santiago de Compostela (IDIS), Complexo Hospitalario Universitario de Santiago de Compostela, Santiago de Compostela, Spain

Introduction

Breast cancer extracellular matrix (ECM) plays a critical role in tumor progression and clinical outcomes. Therefore, its biochemical and structural complexity must be considered when designing breast cancer models that aim to replicate tumor behavior. In this context, tissue-derived matrices (TDMs) can recreate the full complexity of the ECM. Breast tissues (BT) and tumors are typically decellularized with detergent-based protocols, although these approaches frequently remove important ECM biomolecules.

In this study, we explored an alternative decellularization method for BT based on supercritical CO_2 and developed hydrogels using the resulting biomaterial. Breast cancer models were generated by supplementing this matrix with different ECM components. The resulting biomaterial provides a versatile platform for engineering clinically translatable breast cancer models, as it can be tuned to better reproduce tumor ECM characteristics. Moreover, this approach offers a more sustainable and scalable strategy, since it does not rely on patient-derived tumor samples, enabling the generation of ECM-based scaffolds compatible with high-throughput drug screening.

Materials and Methods

Porcine breast tissue underwent four distinct supercritical CO_2-based decellularization protocols, and the resulting TDMs were characterized through dsDNA, glycosaminoglycans, and collagen quantification, together with histological and proteomic profiling. The most suitable matrix was used to engineer breast cancer models together with gelatin-methacrylamide, fibronectin, and collagen. The proliferation and cell morphology of MDA-MB-231 cells encapsulated in the hydrogels were assessed. Furthermore, invasiveness assays, along with genetic and proteomic analyses, were performed to evaluate whether the models induced the tumorigenic phenotype typically observed *in vivo*.

Results

The decellularization process yielded a biomaterial with low dsDNA content and high concentrations of glycosaminoglycans and collagen. Proteomic analysis revealed the presence of many tumor ECM proteins in the TDM. All designed prototypes promoted cellular proliferation (Figure 1A) and the invasiveness of cancer cells (Figure 1B). Moreover, cells upregulated the expression of genes and proteins related to ECM remodeling and invasion, highlighting the potential of these models to replicate the malignancy markers of breast tumors.

Conclusion

Overall, these findings demonstrate that supercritical CO_2-decellularized BT provides a promising and tunable platform for the development of biomimetic breast cancer models. This approach represents a scalable and reproducible strategy to generate physiologically relevant *in vitro* models for studying tumor-ECM interactions and for future drug screening applications.

Acknowledgements

This research was funded by MICIU/AEI/10.13039/501100011033 and ESF+ (RYC2022-037421-I) and PID2023-147892OA-I00 funded by MICIU/AEI/10.13039/501100011033 and ERDF/EU and Xunta de Galicia (ED431F 2024/19).

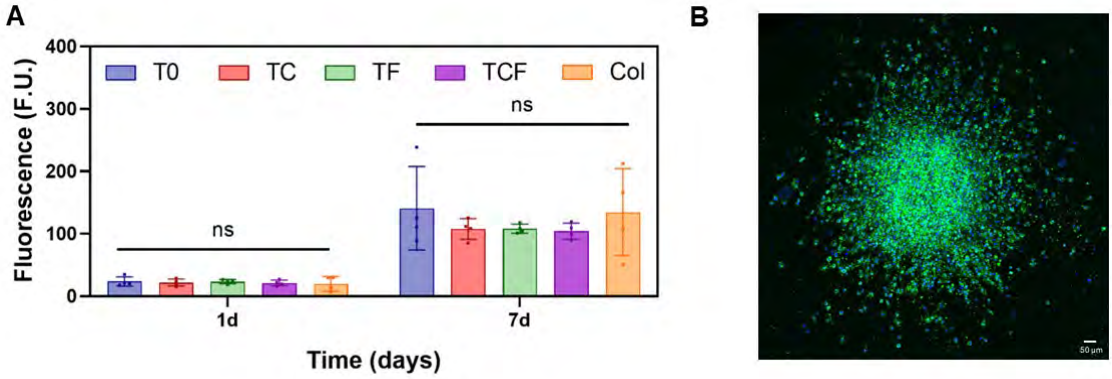

Figure 1. Proliferation (A) and invasive potential (B) of MDA-MB-231 cells in the designed models.

S18
Biomaterials & bioprinting powering the next generation of Organs-on-Chip (in collaboration with the international MPS Society) MPSS)

S18 - K1
From biomaterials to living systems: Biofabrication strategies enabling advanced microphysiological systems

Moroni L.[1]
[1]Complex Tissue Regeneration Dept., MERLN Institute for Technology-Inspired Regenerative Medicine, Maastricht University, Universiteitssingel 40, 6229 ER Maastricht, The Netherlands

The development of predictive human microphysiological systems requires biomaterials that do more than support cells. They have to actively instruct cellular behavior in space and time. A major limitation of current *in vitro* models is the limited control over cell–material interactions, which restricts the ability to reproduce tissue organization, maturation, and physiological function. Traditional approaches, including soluble factor delivery, surface functionalization, or bulk material tuning, have improved cell performance but remain limited in their capacity to recreate the dynamic and hierarchical microenvironments found in human tissues.

Here, we highlight how biofabrication technologies enable the design of instructive biomaterial systems with enhanced regulation of biological, physicochemical, and mechanical functions across multiple length scales. By integrating material engineering with automated fabrication platforms, we generate biological constructs in which spatial organization, mechanical heterogeneity, and biochemical signaling are programmed during manufacturing. Through selected examples, we show how these approaches allow controlled modulation of stem cell fate, tissue patterning, and multicellular interactions, leading to more physiologically relevant human 3D *in vitro* models. Such biofabricated systems bridge key gaps between conventional organ-on-chip platforms and native tissue complexity by enabling vascularized, compartmentalized, and dynamically responsive microenvironments.

Collectively, emerging convergent technologies combining biomaterials science, bioprinting, and micro-physiological systems provide a powerful framework for engineering functional human tissue models. Future advances will focus on tighter integration between biofabrication and microfluidic platforms to achieve real-time control over tissue development and function. These innovations position biomaterials and bioprinting as central drivers for the next generation of organs-on-chip, accelerating drug discovery, disease modeling, and ultimately the translation of human-relevant testing platforms into biomedical research and clinical innovation.

S18 – O1

Engineering a modular, perfusable bone-on-chip system by leveraging granular hydrogel design

Sanaei F.[1], Zhao Y.[1,2], Rühl L.L.[1], Borsen L.[1], Van den Beucken J.J.J.[1], Leeuwenburgh S.C.G.[1], Diba M.[1]
[1]Dept. of Dentistry-Regenerative Biomaterials, Research Institute for Medical Innovation, Radboud University Medical Center, Nijmegen, The Netherlands; [2]School of Bioengineering, Dalian University of Technology, Dalian, China

Introduction

Bone (re)generation is a dynamic process in which mesenchymal stromal cells (MSCs) initially form an interconnected cellular network in a supporting matrix. This network is a key factor for MSC differentiation into osteocytes, the terminally differentiated bone cells embedded in the mineralized matrix. Together with mechanical cues driven by fluid flow, the cellular network orchestrates key aspects of bone development. However, current in vitro platforms are unable to support both network formation and fluid flow within a three-dimensional (3D) matrix, which limits their physiological relevance and translational potential.

Aim: We present a modular, perfusable bone-on-chip (BoC) through the design of a 3D extracellular matrix (ECM)-mimicking granular system. This matrix is composed of polyethylene glycol (PEG) microgels, facilitating flow-mediated mineralized bone-like tissue formation.

Materials and Methods

A polydimethylsiloxane (PDMS)-based BoC fluidic chip was fabricated to accommodate the ECM-mimicking matrix. Microgels were synthesized using thiol–ene click chemistry and droplet microfluidics, mixed with MSCs and jammed *in situ* within the central channel of the chip (Figure 1a). Cell behavior and osteogenic progression were assessed by DNA quantification, alkaline phosphatase (ALP) activity, immunofluorescent imaging, and gene expression of key osteogenic markers.

Results

The matrix modularity allowed for tuning physicochemical properties such as functionalising microgels with RGD peptide and adjusting the stiffness. The PDMS chip successfully accommodated the *in situ* jamming of engineered PEG-based microgels, forming a confined and microporous matrix stable over the culture period. As shown in Figure 1, the matrix architecture supported homogeneous cell distribution shortly after cell-microgel injection and promoted formation of an interconnected 3D cellular network within the interstitial pores (Fig. 1b). This organization was associated with abundant extracellular matrix deposition, including collagen I (Fig. 1c–e). Biological analyses demonstrated progressive osteogenic differentiation, with increased ALP activity relative to baseline and upregulation of Runt-related transcription factor 2 (RUNX2). Importantly, immunofluorescent staining confirmed dentin matrix protein 1 (DMP1) expression together with extracellular matrix mineralization, indicating progression toward an early osteocyte-like phenotype (Fig. 1c–e).

Conclusions

The developed BoC supports stable MSC network formation in a 3D granular matrix, representing a critical step toward the fabrication of mature bone-like tissue. The observed transition of osteoblasts toward early osteocyte phenotypes underscores the platform's capacity to recapitulate key stages of bone formation *in vitro*.

Future studies will integrate active perfusion, employ molecular and functional analyses to quantitatively assess the fidelity of the engineered tissue model, with comparisons to woven bone serving as a biological benchmark.

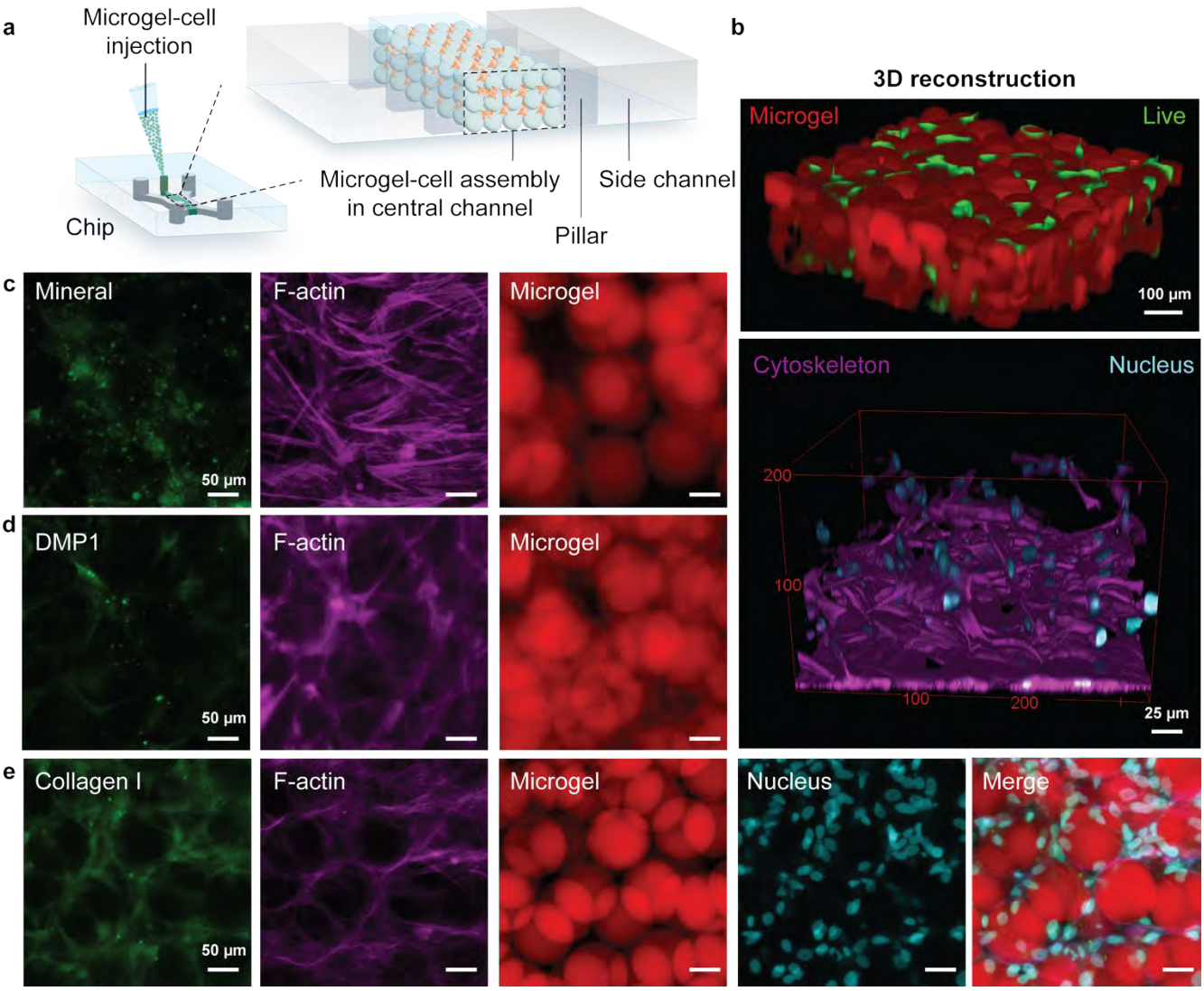

Figure 1. Overview of bone-on-chip immunofluorescent evaluation (a) Schematic illustration of the bone-on-chip platform, showing injection of microgel-cell mixture into the central channel of the chip and formation of a microgel–cell assembly within the central channel, confined by pillar structures and flanked by side channels. (b) Upper Panel: Representative 3D reconstruction of the engineered construct, showing the 3D distribution and confinement of live cells (green) within the interstitial pores of microgels (red) at 4 hours after injection. Lower Panel: Representative 3D reconstruction of the fixated cells (magenta) and nuclei (cyan), demonstrating the cellular network formed by differentiated osteoblasts. (c–e) Representative fluorescence Z-projection images showing key features of osteogenic tissue formation within the chip, including mineral deposition, DMP1 expression, and collagen I deposition (green), together with F-actin staining of the cytoskeleton (magenta), microgels (red), cell nuclei (cyan), and the corresponding merged view with microgels.

S18 – O2

A multicompartment vascularized melanoma-on-a-chip: Recapitulating the tumour microenvironment and metastatic potential

Mattioda C.[1], Ciardelli G.[1] ,Mattu C.[1]
[1]Dept. of Mechanical and Aerospace Engineering (DIMEAS), Politecnico di Torino, Turin, Italy

Introduction

Malignant melanoma remains a major clinical challenge due to its aggressive metastatic potential and the presence of a protective tumour microenvironment (TME), frequently promoting treatment resistance. Conventional *in vitro* models often fail to reproduce the complex architecture of the tumour niche, limiting their predictive value.
This work aims at the development of a multicompartment model to recapitulate key structural and functional features of melanoma and at integrating the model within a microfluidic platform, potentially enabling its connection with additional tissue models to investigate metastasis development and spreading.

Materials and Methods

The primary melanoma model was obtained in trans-well inserts, using a biomimetic hydrogel composed of bovine collagen type I and methacrylated hyaluronic acid (Col-HAMA), that mimic the physiological mechanical properties and composition of the human derma. Human dermal fibroblasts were embedded within the hydrogel, while the epidermal layer was obtained by seeding human keratinocytes on the surface. Melanoma spheroids were incorporated at the dermal–epidermal interface. The system was cultured at the air–liquid interface to reproduce physiological conditions. To recreate the vascular compartment, human umbilical vein endothelial cells were seeded in the basal chamber of the insert. The integration of the construct within a microfluidic platform enabled perfusion, which favored endothelial maturation and vessel sprouting.

Results

The hydrogel supported fibroblast viability and proliferation for up to 21 days and promoted extracellular matrix remodelling through the deposition of native ECM proteins (fig. 1). Melanoma spheroids showed progressive growth and invasion into the surrounding matrix. Interestingly, in co-culture with fibroblasts, spheroids appeared less invasive, suggesting a modulatory role of stromal cell. Compared to conventional 2D cultures, an enhanced secretion of melanoma-associated cytokines (IL-6, IL-8) was observed. Dynamic perfusion within the microfluidic platform promoted the formation of a thick and continuous endothelial layer, which was not observed under static conditions. Moreover, confocal microscopy confirmed the development of self-assembled capillary-like networks within the matrix (fig. 2).

Conclusion

This study reports the development of a multicompartment vascularized melanoma-on-a-chip model that recapitulates key aspects of the native TME. By integrating biomimetic materials, relevant cell populations, and dynamic culture, this system allows the study of tumour behaviour under physiological conditions. This model represents a promising tool to investigate melanoma progression, invasion and metastasis development in a more realistic setting.

Acknowledgements

Part of this project was founded by “D34H—Digital Driven Diagnostics, prognostics and therapeutics for sustainable Health care” (PNC0000001), Spoke 4 funded by MUR, the European Union – Next Generation EU, Mission 4 – Component 2 – through 3DPathoSkin project (PE_00000019 – HEAL ITALIA; CUP E93C22001860006), and PON "Ricerca e Innovazione" 2014-2020 Azione IV.R "dottorato su tematiche green".

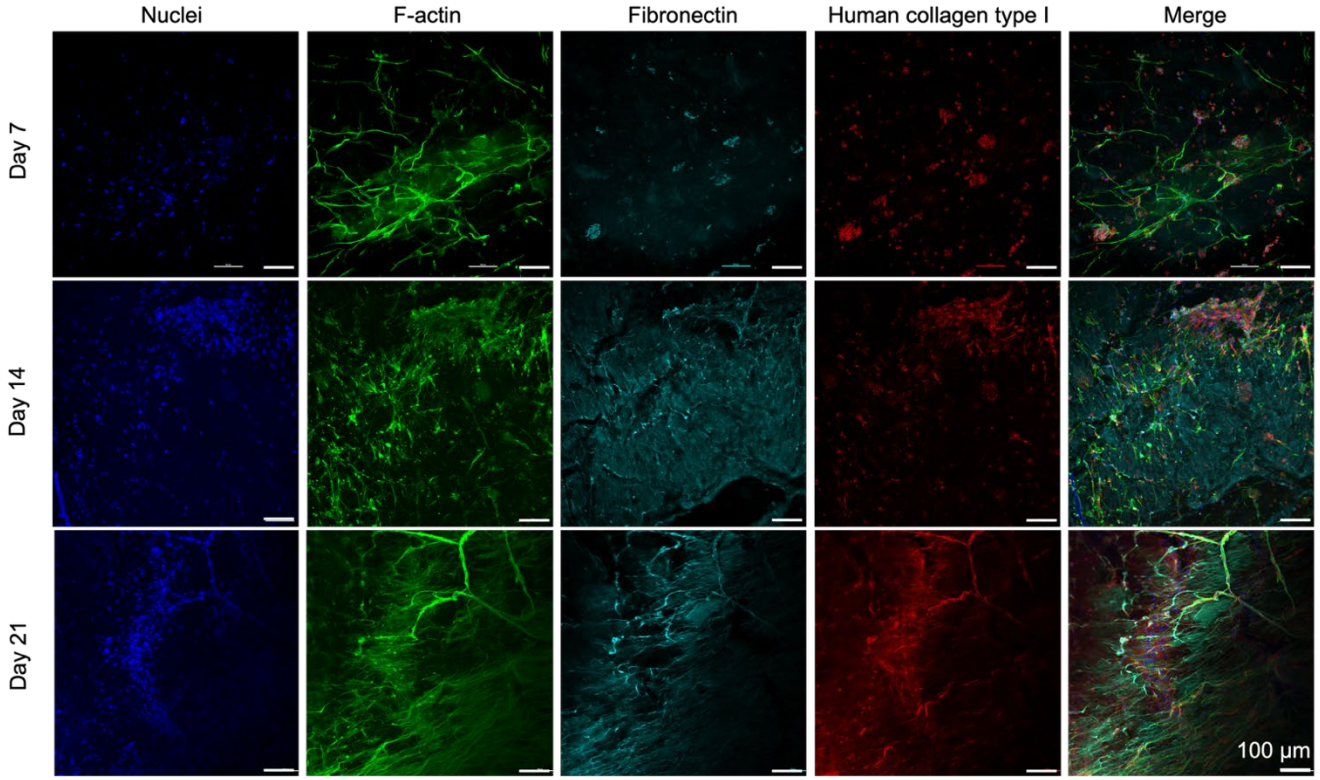

Figure 2: Immunofluorescence analysis of the progressive deposition of native extracellular matrix proteins (human collagen type I and fibronectin) within the fibroblasts seeded matrix.

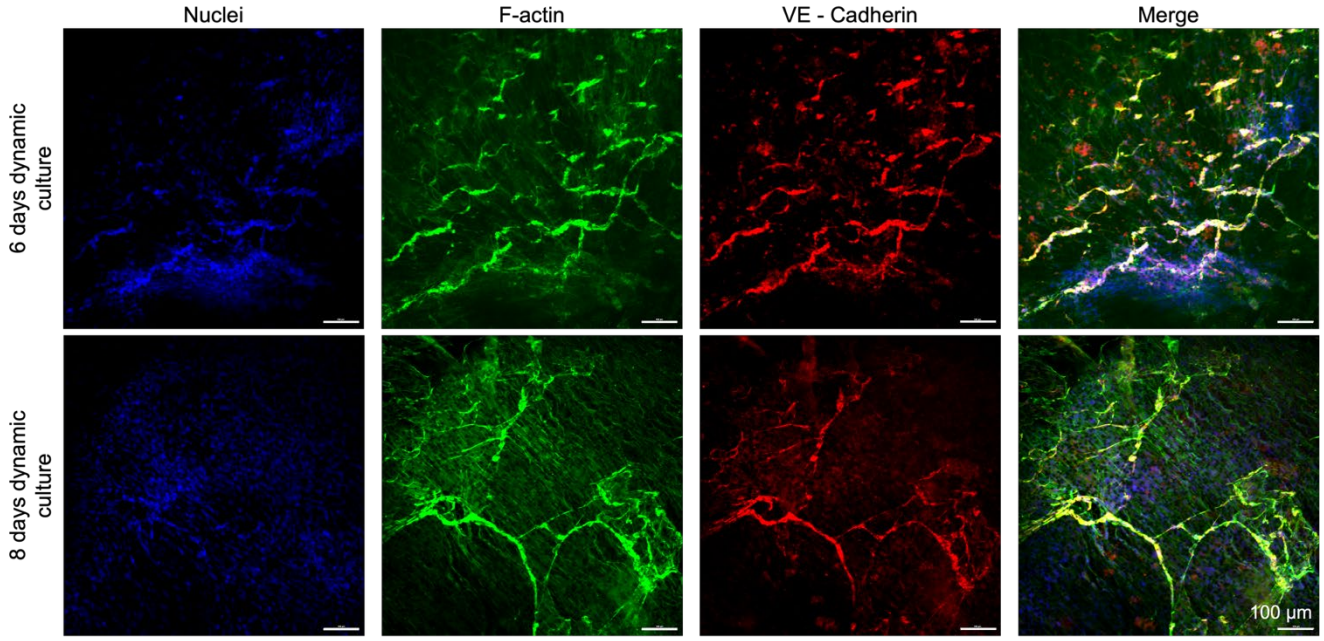

Figure 3: Immunofluorescence images of self-assembled capillary-like structures within the Col-HAMA hydrogel following 6 and 8 days of endothelial cells dynamic culture.

S18 – O3

Alveoleye – An alveoli-on-a-chip model to recapitulate lung microarchitecture

F Farina F.[1,2], Licciardello M.[1,2], Moroni L.[3], Ciardelli G.[1,2,4], Tonda-Turo C.[1,2]
[1]Dept. of Mechanical and Aerospace Engineering, Politecnico di Torino, Italy; [2]Bioinside Lab, Politecnico di Torino, Italy; [3]Dept. of Complex Tissue Engineering, MERLN Institute for Technology-Inspired Regenerative Medicine, Maastricht University, Maastricht, the Netherlands; [4]Biomedical Engineering Center, Kansai Medical Univ., Osaka, Japan

Introduction

Alveolar tissue exhibits a highly complex multiscale morphology, consisting of a thin epithelial layer arranged in a three-dimensional architecture and surrounded by a branched capillary network. Most current lung-on-chip platforms rely on flat membranes that inadequately reproduce native alveolar geometry, limiting structural biomimicry and physiological relevance.

Aim

The aim of this work was to develop a biomimetic alveoli-on-a-chip integrating a patterned scaffold and a cell-laden hydrogel to better recapitulate alveolar packing within a controlled microfluidic environment.

Materials and Methods

A Voronoi-based scaffold reproducing the spatial organization of alveolar sacs was fabricated via digital light processing (DLP) using a flexible biocompatible resin. The scaffold was designed to generate physiologically relevant pore dimensions within a defined circular area for epithelial cell seeding.
The scaffold was positioned onto a fibrin hydrogel intended for co-encapsulation of human umbilical vein endothelial cells (HUVECs) and lung fibroblasts (MRC-5). The hydrogel was laterally confined within a DLP-fabricated bottomless microfluidic chip (Figure 1, center-right) featuring micropillars to ensure mechanical retention. Adjacent microchannels enabled medium perfusion. The device was sealed to a glass substrate to allow optical monitoring during culture, and a removable lid enabled controlled air exposure.

Results

The Voronoi design yielded a reproducible alveolus-like architecture with controlled pore size and high printing fidelity (Figure 1, left). Integration between scaffold, hydrogel, and microfluidic chip was successfully achieved, with stable positioning of the hydrogel ensured by the micropillar array.
Perfusion tests confirmed the proper functionality of the microfluidic channels and demonstrated hydraulic sealing of the gel compartment without leakage or gel displacement under flow conditions. The overall device showed structural integrity and compatibility with optical inspection.
Biological validation of the vascularized compartment is currently ongoing.

Conclusion

The proposed alveoli-on-a-chip combines additive manufacturing and hydrogel-based tissue engineering strategies to recreate key structural features of the alveolar niche within a perfusable microfluidic platform. This system represents a promising foundation for future studies on lung physiology and pollutant-induced pulmonary fibrosis in a controlled in vitro setting.

Acknowledgements

S This work was carried out within the BREATH project (Bioprinted alveolaR lung-on-chip devicE to assess The role of inHaled pollutants towards pulmonary fibrosis onset), funded by the European Union – Next Generation EU within the PRIN 2022 – PNRR program (D.D. 104 - 02/02/2022, Italian Ministry of University and Research).

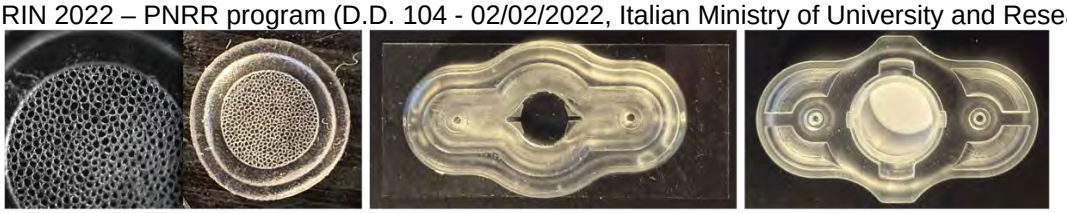

Figure 4 Voronoi-based alveolar scaffolds (left), Base of the microfluidic chip (center) and lid of the microfluidic chip (right)

S18 – O4

Microfluidic Neurovascular Microenvironments for High-Throughput Benchmarking of Emerging Nanotherapies

Bezze A.[1], Muccio S.[1], Mattioda C.[1], Ciardelli G.[1,2], Mattu C.[1]
[1]Dept. of Mechanical and Aerospace Engineering, Politecnico di Torino, Turin, Italy; [2]Biomedical Engineering Center, Kansai Medical University, Osaka, Japan

Introduction

The blood-brain barrier (BBB) is a vital interface regulating the central nervous system (CNS) homeostasis and molecule trafficking. The complex BBB alterations associated with neurological disorders and brain malignancies severely impair treatment efficacy. However, these interactions are poorly recapitulated by conventional 2D cell cultures or 3D *in vitro* models. More sophisticated BBB models have been proposed but are often non-scalable, limiting their utility in high-throughput screening. In this work, human-relevant BBB-on-a-chip models were developed using high-throughput microfluidic platforms of increasing complexity to assess barrier behavior in physiological and pathological conditions. These systems were applied to investigate nanoparticle (NP) or microglia extravasation, potentially allowing the validation of nanomedicines and/or cell-based drug delivery systems.

Materials and Methods

Human Brain Endothelial Cells, alone or co-cultured with pericytes, were seeded in commercial microfluidic platforms to form functional vessels separated by a collagen hydrogel mimicking the brain extracellular matrix (ECM). Pathological states were induced by exposing mature vessels to neuroinflammatory stimuli (Interferon-γ) or via co-culture with glioblastoma (GBM) cells. To more accurately recapitulate the brain tumor microenvironment, vessel sprouting was induced through angiogenic factors after incorporating GBM spheroids within the ECM gel. Barrier integrity was verified by immunostaining for junctional markers (ZO-1, VE-Cadherin, CD-31) and quantified via permeability assays using FITC-Dextran in healthy and pathological vessels. Additionally, the transendothelial penetration of NPs and microglia cells was assessed across the different BBB models.

Results

The high-throughput microfluidic systems produced physiologically relevant homogeneous vessels (Fig. 1A) with stable barrier properties (Fig. 1B) and robust junctional organization (Fig. 1C). Pathological alterations were successfully modelled after stimulation, accurately reproducing the increased permeability (Fig. 2A), enhanced NP extravasation, and facilitated immune cell recruitment observed *in vivo*. Critically, the implementation of a complex, branched vascular bed supported the vascularization of GBM spheroids (Fig. 2B), providing a superior replication of transport patterns in GBM. Furthermore, this model demonstrated that microglia-based carriers significantly enhanced nanomedicine accumulation across the ECM-like gel and the microvasculature (Fig. 2C), providing a more effective targeting than free NPs.

Conclusion

Microphysiological systems were successfully engineered to replicate the complex architecture and characteristics of the brain microvasculature in physio/pathological conditions. While simplified BBB-on-chips remain effective for preliminary screenings, tridimensional microenvironment models are essential to capture the interactions guiding disease progression and therapeutic accumulation. These scalable platforms provide a robust benchmarking tool, facilitating reliable preclinical validation for a wide range of brain disorders.

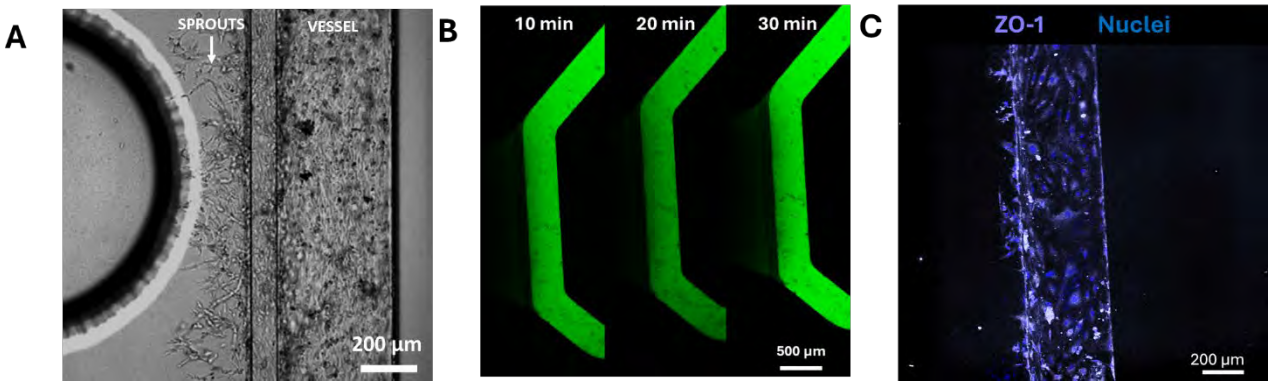

Figure 1. A) Endothelial vessels forming branched sprouts inside the microfluidic chip. B) Fluorescent dextran (green) retention by the vessel over time. C) Immunofluorescence staining showing the homogeneous expression of tight junction proteins.

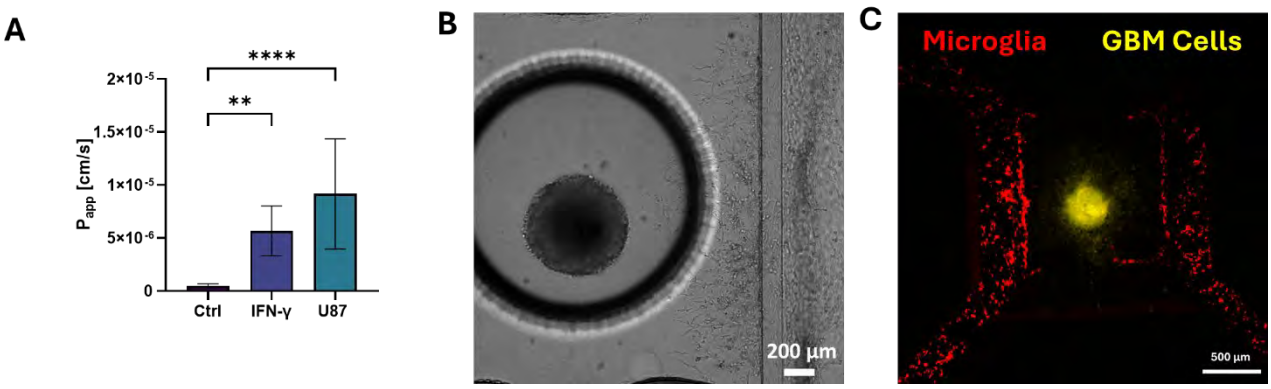

Figure 2. A) Apparent permeability (P_{app}) of vessels after pathological stimulation. B) Vascularization of GBM spheroids in the microfluidic chip. C) Microglia extravasation across brain vessels towards GBM spheroids.

S18 – O5

A versatile 3D printed platform for the assembly and perfusion of breast tumor cell clusters

Sayer S.[1,2,3], Lunzer M.[1,3], Ovsianikov A.[2,3]
[1]Dept.A, Institution A, City, Country; [2]Research Group 3D Printing and Biofabrication, Institute of Materials Science and Technology, TU Wien, Vienna, Austria; [3]Austrian Cluster for Tissue Regeneration

Introduction

Animal models have been the gold standard for testing chemotherapeutic drugs, but less than 5 percent of drugs passed clinical trials between 2000 and 2015 [1]. Furthermore, regulatory agencies are mandating to reduce animal testing [2]. We propose a tumor-on-a-chip model facilitated by multiphoton lithography (MPL), a high-resolution 3D printing technology that enables the fabrication of structures inside of microfluidic chips [3]. Gelatin-based hydrogel structures facilitating the automatic clustering of cells in a predefined spatial pattern were fabricated.

Materials and Methods

The microfluidic chip was printed using the SLA 3D printer Form 3 (Formlabs GmbH) using the resin Clear v4.1 (Formlabs GmbH). The chips were coated with polydopamine (Sigma-Aldrich). To create the cell distribution structure, a gelatin-based hydrogel (HYDROBIO INX U200, BIO INX) was structured using the commercial MPL system NanoOne (UpNano GmbH). MDA-MB-231 triple-negative breast cancer (TNBC) cells (CeMM) were used in the model to study the effects of carboplatin (Sigma-Aldrich). Human umbilical vein endothelial cells (HUVECs, PELOBiotech GmbH) were used for the endothelialization of the microchannels.

Results

3D structure enabling the clustering of cells in predefined micropatterns was designed. These structures were printed using an MPL-compatible gelatin-based hydrogel inside custom-made well plates and microfluidic chips. Cells were added in suspension, leading to the formation of clusters which were then fully embedded by a UV-sensitive gelatin layer. Figure 1 gives an overview of the printed cell clustering structures inside the well-plate. Live/ dead staining shows a high cell viability after embedding and showcases the distribution of cell clusters within the hydrogel. Live/dead staining shows high cell viability after embedding and showcases the distribution of cell clusters within the hydrogel. MDA-MB-231 cells were embedded within the hydrogel structures surrounded by perfusable microchannels. Carboplatin was added to the microchannels and differences between 2D cultures and the 3D model were observed.

Conclusion

This work demonstrates the fabrication of a gelatin-based hydrogel structure that facilitates the automatic clustering of cells according to predefined patterns. The structures were printed in a microfluidic chip and microchannels with diameters down to 50 µm were successfully perfused.

References

[1]Wong C. H., Siah K. W., and Lo A. W. Biostatistics. 2019
[2]Adashi E. Y., O'Mahony D. P., and Cohen I. G. The American Journal of Medicine. 2023
[3]Dobos A. et al. Biofabrication. 2020

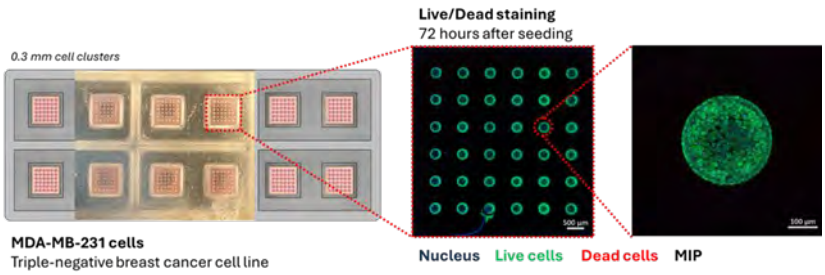

Figure 5: Overview of the 3D printed well plate with MDA-MB-231 cell clusters embedded in gelatin. Each cluster has a diameter of 0.3 mm, a height of 0.2 mm and contains 3 500 cells.

S19
Biomaterials and the immune system

S19 - K1
Hidden architectures in plant biomaterials: Gluten peptide assemblies and their immunological footprint

Dodero V.I.
Faculty of Chemistry, Bielefeld University, Bielefeld, Germany

Plant proteins are increasingly being explored as sources for developing biomaterials for skin regeneration and wound healing. Among them, wheat gluten proteins (WG)—a mixture of gliadin and glutenin—are particularly attractive due to their soft, stretchable "loop-and-train" network and relatively low cost. Electrospun WG nanofibers have recently been applied in drug delivery, biological scaffolding, and active food packaging (1). WG is highly resistant to enzymatic proteolysis; the resulting products, known as proteolytically resistant wheat gluten peptides (PRGPs), form nanostructures that activate innate immune responses, but the mechanisms remain unclear.
We investigated the self-assembly behavior of WG and their PRGPs (2) and how they influence the activation of Toll-like receptors (TLRs)—membrane-bound receptors that recognize structurally conserved molecular patterns and play a crucial role in immune surveillance.
Here, I will present our recent work on the self-assembly capabilities of PRGPs and their effects on TLRs, in specialized and non-specialized cells. Our findings highlight the need to evaluate innate responses to plant biomaterials and demonstrate the relevance of molecular structure, shape, and size in modulating TLR signaling.

Acknowledgements
This work is supported by Deutsche Forschungsgemeinschaft (DFG) - Projektnummer 430578458

References
[1]K. Marszalik, M. Polak, J. Knapczyk-Korczak, K. Berniak, M. N. G. Ibrahim, Q. Su, X. Li, B. Ding, U. Stachewicz. Skin Regeneration and Wound Healing by Plant Protein-Based Electrospun Fiber Scaffolds and Patches for Tissue Engineering Applications. *Macromol. Rapid Commun.*2025, 46, 2500196.
[2]M. G. Herrera, L. Ciccone, L. H. Moleiro, N. Tonali, V. I. Dodero. Endogenous Aβ and Exogenous Wheat Gluten Nanostructures: Understanding Peptide Self-Assembly in Disease. *ACS Nano* 2025, 19, 34, 30688–30719

S19 – O1

Laser surface texturing of bulk metallic glass promotes protein adsorption and tissue-regenerative macrophage phenotypes

Green T.D.[1], Bigot S.[2], Brousseau E.[2], Bhaduri D.[2], Nishio W.[1]
[1]Cardiff University School of Dentistry, Cardiff; [2]School of Engineering, Cardiff University, Cardiff, UK

Introduction

Revision surgery of orthopaedic implants due to aseptic loosening affects 20,000 patients yearly across the EU, costing public healthcare services €600 million annually. Bulk metallic glasses (BMGs) offer a promising solution, exhibiting advantageous physical properties (high wear and corrosion resistance, high elasticity) compared to traditional implant alloys. BMG laser surface texturing (LST) promotes osseointegration, although immunomodulation of LST remains to be elucidated. This research investigates whether LST can modulate the host response to orthopaedic implants, with the goal of enhancing long-term integration.

Material and Methods

AMLOY-ZR02, a BMG with nominal composition: $Zr_{65}Cu_{16}Ni_{12}Al_4Ti_3$, underwent groove-micropatterning via nanosecond LST. Adsorption of immunomodulatory proteins (complement C3b, immunoglobulin G (IgG), fibronectin) from human serum were quantified using BCA assay and ELISAs. A CCK-8 assay assessed AMLOY-ZR02 biocompatibility to THP-1 macrophages. Subsequently, mean cell area and aspect ratio of macrophages were quantified using ImageJ, and ELISAs assessed THP-1 secretion of anti-inflammatory cytokines, IL-10 and TGF-β1.

Results

Augmentations in laser fluence significantly influenced total protein adsorption to BMGs following 24-hour incubation in human serum ($P<0.001$). LST did not affect fibronectin or C3b adsorption, however IgG adsorption significantly increased with fluence at all incubation periods (10 mins, 2 hours, 24 hours) ($P<0.05$); these protein adsorption differences reflect fluence-dependent changes in surface topography and wettability. Although initial macrophage attachment was reduced relative to tissue culture polystyrene ($P<0.05$), all groups maintained consistent cellular proliferation across 72-hours, indicating no LST elicited cytotoxicity. No difference in cell area was observed between surfaces, although macrophage aspect ratio increased following micropatterning ($P<0.01$), consistent with cellular alignment with grooves. No difference in IL-10 was measured between sample supernatants, however macrophage TGF-β1 secretion increased significantly upon micropatterned surfaces ($P<0.001$).

Conclusion

Laser fluence augmentations during LST promoted immunoregulatory protein adsorption and macrophage elongation via modifications in surface wettability and topography. An increased secretion of M2-phenotypic cytokines was associated with topography-mediated macrophage elongation, consistent with the literature, and highlighting the potential of LST to promote peri-implant tissue remodelling. Further phenotypic characterisation will be conducted via secretome analysis. Future work will establish the molecular pathways involved in topography-mediated polarisation via RNA sequencing.

Acknowledgements

This work was supported by the Engineering and Physical Sciences Research Council (EPSRC) Doctoral Training Partnership.

S19 – O2

Bioprinted hyaluronic acid/gelatin hydrogel 3d model for studying extracellular histone effects in sepsis-related renal injury

Amaro-Prellezo E.[1,2], Yau D.[1], Calpe-Fortea R.[3,4], Nacher-Sendra E.[3,4], Arias-Muñoz V.[1], Tolosa L.[2,5], García-Gimenez J.L.[3,4,6], G. Gallego-Ferrer[1,2]

[1]Centre for Biomaterials and Tissue Engineering (CBIT), Universitat Politècnica de València; [2]Biomedical Research Networking Centre on Bioengineering, Biomaterials and Nanomedicine (CIBER-BBN); [3]Epigenomics and Translational Epigenetics Research Group, Health Research Institute INCLIVA; [4]Faculty of Medicine and Dentistry, Dept. of Physiology, University of Valencia; [5]Experimental Hepatology Unit, Health Research Institute La Fe (IISLAFE), Valencia, 46026; [6]Biomedical Research Networking Centre on Rare Diseases (CIBER-ER), Valencia, Spain

Introduction

Sepsis frequently causes acute kidney injury (AKI), significantly increasing mortality. Extracellular histones released during tissue damage are key mediators of cytotoxicity in septic AKI. Conventional 2D models fail to replicate the complexity of the renal microenvironment. To address this, we developed a bioprinted 3D hyaluronic acid (HA) (80%)/gelatin (GEL) (20%) hydrogel model to study histone-induced cellular damage in HEK293 cells.

Aim

This study aimed to develop a bioprinted 3D HA/GEL hydrogel model to investigate the effects of extracellular histones on HEK293 cells in sepsis-associated kidney injury.

Material and Methods

HA-Tyr/GEL-Tyr conjugates were enzymatically crosslinked to generate 3D hydrogels encapsulating HEK293 cells. Rheological analysis of different HA/GEL ratios, with and without histones, was performed and compared to native kidney tissue. Equilibrium water content (EWC) and gelation time were also measured. Based on rheology, the HA/GEL (80/20) gels were selected as bioink for cellular models. Cell viability was monitored over time, with or without histones. Expression of apoptosis and oxidative stress-related genes was quantified by RT-qPCR to evaluate histone-induced cellular responses.

Results

The HA/GEL (80/20) formulation exhibited mechanical properties closely matching native kidney tissue. Upon exposure to extracellular histones, the hydrogel stiffness further shifted while remaining within the physiological renal range. EWC and gelation time were also evaluated in the presence and absence of histones. HEK293 viability decreased over culture time, with histones inducing a dose-dependent reduction. Histone exposure also modulated the expression of genes related to apoptosis and oxidative stress.

Conclusion

The HA/GEL (80/20) hydrogel provides a biomimetic 3D platform that can be successfully bioprinted to generate stable 3D cellular constructs with kidney-like mechanical properties. It effectively models histone-induced cytotoxicity, representing a promising *in vitro* tool to study sepsis-associated kidney injury.

S19 – O3

M2 macrophage-derived exosome-functionalized fibrous scaffolds regulate the foreign body response and the coupling of angio/osteoclasto/osteogenesis

Jin S.[1]

[1]Dept. of Orthopedics, Southwest Hospital, Army Medical University, Chongqing 400038, China

Introduction

The foreign body response (FBR) is a complex immunological process. Designing scaffolds that can regulate the innate immune response and promote vascularized bone regeneration holds promise for bone tissue engineering.

Aim

Providing insights into under- standing nanofibrous scaffold-mediated FBR and vascularized bone regeneration and a strategy to achieve biological repair of bone defects.

Materials and Methods

Combining physical and biological cues into the scaffold, M2 macrophage–derived exosome-functionalized electrospun nanofibrous scaffold (PP-Exo) was fabricated. The cellular uptake of exosomes by target cells and its effects on cell functions such as tube formation by endothelial cells, osteogenic differentiation of BMSCs, and macrophage polarization *in vitro*. The FBR mediated by exosome-functionalized scaffolds was studied by subcutaneous implantation in mice. This study investigated whether M2 macrophage–derived exosomes functionalized nanofibrous scaffold could mediate vascularized bone regeneration via rat cranial bone critical-sized defects model.

Results

M2 macrophage–derived exosomes were successfully immobilized on the electrospun nanofibrous scaffold by surface modification with cationic PEI. *In vitro* cell experiments showed that exosomes could promote tube formation of HUVECs, osteogenic differentiation of BMSCs, and anti-inflammatory macrophage polarization of RAW264.7. Animal experiments demonstrated that the exosome-functionalized fibrous scaffolds efficiently dampened the inflammatory response via the activation of M2 macrophages to enable sustained anti-dysfunctional angiogenesis and anti-fibrotic development. Micro-CT analysis demonstrated that the exosome-functionalized PP-Exo scaffolds were comparable with the commercial Bio-Gide in terms of bone augmentation and trabecular microarchitecture, almost closing the bone defects after 10 weeks of repair. Histological staining results indicated that the PP-Exo scaffold showed a significantly higher frequency of the type H bone vessel subtype, coupling angiogenesis, and osteogenesis.

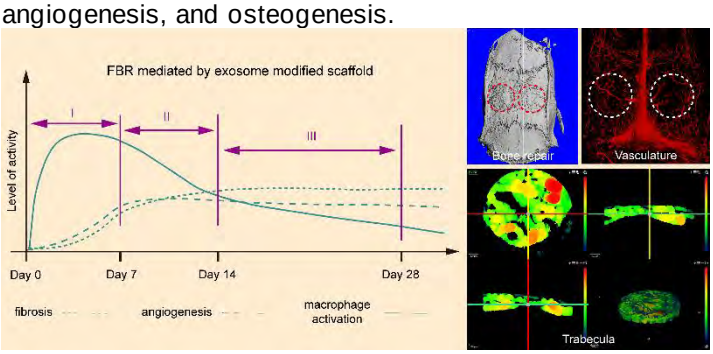

Figure 1. The foreign body reaction and vascularized bone regeneration mediated by the PP-Exo scaffold.

Conclusion

M2 macrophage–derived exosomes could activate anti-inflammatory M2 macrophages to direct the development of a regenerative immune niche during the FBR. The PP-Exo scaffold could regulate the coupling of neoangiogenesis, osteogenesis, and osteoclastogenesis by stimulating the formation of type H vessels, ultimately mediating vascularized bone regeneration. We believe that these findings will contribute to the design and new paradigm of scaffolds in orthopedics and maxillofacial surgery.

Acknowledgements

This work was supported by the National Natural Science Foundation of China (32401132, 82172394).

S19 – O4

Dual action fibrin hydrogels enhance macrophage polarisation and angiogenesis to support regenerative healing

Sousa A.B.[1,2,3], Barrias C.C.[1,2,3], Barbosa J.N.[1,2,3]
[1]i3S - Instituto de Investigação e Inovação em Saúde, Universidade do Porto; [2]INEB - Instituto de Engenharia Biomédica; [3]ICBAS - Instituto de Ciências Biomédicas Abel Salazar, Universidade do Porto, Portugal

Introduction

The global incidence of chronic wounds is rising, creating a substantial clinical and socioeconomic burden. Conventional treatments, namely topical agents to prevent infection and anti-inflammatory drugs to control inflammation, often fail to restore tissue structure or function. To address these limitations, we propose a fibrin-based hydrogel containing zein nanoparticles loaded with maresin-1 (MaR-1), a specialized pro-resolving mediator that actively promotes the resolution of inflammation, to suppress excessive inflammation and promote regeneration. By guiding macrophage polarization toward an M2-like phenotype and enhancing angiogenesis, the developed hydrogel aims to coordinate immune and vascular responses essential for sustained wound healing.

Aim

By integrating maresin-1-loaded zein nanoparticles into a fibrin hydrogel, we expect to deliver maresin-1 in a sustained manner and create an immunomodulatory and pro-angiogenic biomaterial to enhance tissue repair.

Materials and Methods

A fibrinogen solution (2 mg/mL) was mixed with (i) maresin-1 (Fib+MaR-1), (ii) maresin-1-loaded zein nanoparticles (Fib+MaR-1 NPs), or (iii) maresin-1 combined with maresin-1-loaded zein nanoparticles (Fib+MaR-1 NPs+MaR-1). Thrombin (2 U/mL) was then added to initiate polymerisation for 30 min at 37 °C. Human macrophages isolated from buffy coats were cultured on the resulting hydrogels to evaluate their M2-polarising capacity. A scratch assay was performed to determine the ability of the hydrogels to promote wound closure in vitro. To assess their angiogenic potential, a chorioallantoic membrane (CAM) assay was also conducted.

Results

A degradation assay confirmed that the hydrogels remained structurally intact for eight days. The release assay demonstrated a sustained seven-day delivery of maresin-1 from fibrin hydrogels. All formulations showed high biocompatibility, with no macrophage cytotoxicity. Both the Fib+MaR-1 NPs and the Fib+MaR-1 NPs+MaR-1 hydrogels effectively promoted M2 macrophage polarisation, confirming their immunomodulatory capacity. Regarding the scratch assay, a faster wound closure was observed when MaR-1 was present in the hydrogel. Furthermore, in the CAM assay, the results showed a tendency toward increased formation of new blood vessels in the Fib+MaR-1 NPs and Fib+MaR-1 NPs +MaR-1 hydrogels compared with empty fibrin hydrogels.

Conclusion

Fibrin hydrogels incorporating maresin-1-loaded zein nanoparticles were biocompatible, promoted M2 macrophage polarisation, and increased angiogenic potential. Together, these findings highlight their promising potential as multifunctional biomaterials to guide macrophage-mediated tissue repair and angiogenesis, thereby enhancing regenerative outcomes.

Acknowledgements

This work was supported by Fundo Europeu de Desenvolvimento Regional (FEDER) and national funds, operation no. 16784, operation code COMPETE2030-FEDER-00796700, under the Call for Applications no. MPr-2023-12. (DOI: https://doi.org/10.54499/2023.18474.ICDT).

S19 – O5

The architecture of exclusion: Collagen fibril alignment as a mechanical regulator of immune dysfunction

Teo J.[1,2]

[1]Division of Engineering, York University Abu Dhabi, Abu Dhabi, UAE; [2]Dept. of Mechanical and Biomedical Engineering, New York University, Brooklyn, NY USA

Introduction

The desmoplastic reaction in solid tumors is characterized by the transition of the extracellular matrix (ECM) from a disorganized meshwork to a highly linearized, aligned collagen architecture. While alignment is a known driver of cancer cell invasion, its role in modulating the immune contexture remains a critical frontier.

Materials and Methods

We investigated how collagen fibril alignment serves as a mechanical regulator of immune cell dysfunction using 3D collagen-based scaffolds with tunable fibril alignment gradients[1]. We integrated these biomimetic models with human dendritic cells, macrophages, and T-lymphocytes, utilizing multiparametric flow cytometry, metabolic profiling, and live-cell imaging to quantify mechanobiological shifts induced by ECM anisotropy.

Results

Our data demonstrate that collagen fibril alignment dictates immune dysfunction through three primary mechanisms:

Dendritic Cells (DCs): As the "intelligence officers" of immunity, DCs are mechanically silenced across maturation states. In immature DCs (iDCs), alignment enhances pro-inflammatory chemokine secretion without impacting antigen uptake; however, a downregulation in mitochondrial ATP production forces a metabolic shift toward glycolysis. This shift fails to maintain sufficient ATP, restricting iDC migratory characteristics. Conversely, while mature DCs (mDCs) maintain an unaltered phenotype, the aligned microarchitecture significantly dampens their interactions with T-cells, suppressing T-cell activation and proliferation[2].

Macrophages: Acting as "traffic controllers," macrophages are driven toward a pro-tumor, M2-like phenotype by matrix stiffness. RNA-sequencing revealed enhanced, integrin-mediated PI3K signaling in response to matrix tension, potentially supporting an IL-4 autocrine positive feedback loop. Ultimately, fibril alignment and matrix crosslinking work in tandem to suppress pro-inflammatory activity, sequestering macrophages into a suppressive state[3].

T-lymphocytes (T-cells): As the "workhorse" of adaptive immunity, T-cell efficacy is compromised via structural and molecular reprogramming. In aligned collagen, activated T-cells exhibit increased protrusions and reduced actin content, leading to a marked reduction in migratory capacity. Furthermore, matrix stiffness and alignment suppress T-cell activation and proliferation. Crucially, this suppression is reversible through the inhibition of YAP signaling, which improves T-cell activation within aligned matrices[4].

Conclusion

Our findings establish that the physical microarchitecture of the stroma is a primary determinant of the immune-excluded phenotype. By identifying the YAP, PI3K, and OXPHOS axes as key mechanosensitive nodes, we propose that future immunotherapies must prioritize matrix-normalizing strategies to bypass these barriers and restore immune infiltration and function.

Acknowledgements

New York University Abu Dhabi (NYUAD) Faculty Research Fund (AD266)

References

1. Sapudom J., Karaman S., Quartey B.C., Mohamed W.K.E., Mahtani N., Garcia-Sabaté, A., Teo, J. Collagen Fibril Orientation Instructs Fibroblast Differentiation Via Cell Contractility. *Advanced Science* 2023; 19, 2301353.
2. Quartey B.C., Sapudom J., Tipay P.S., Hunashal Y., Alshehhi S., Arnoux M., Cardoso T., Quilez J. Piano F., Teo J.C.M. Hydrogel-Based Tumor Tissue Microarchitecture Reshapes Dendritic Cell Metabolic Profile and Functions. *Advanced Healthcare Materials* 2025; 13.
3. Sapudom J., Tipay P.S., Teo J.C.M. Mechano-mediated M2 macrophage polarization and immune suppression in stiffened tumor microenvironment. bioRxiv 2024; 07.29.605566
4. Sapudom J., Alatoom A., Tipay P.S., Teo J.C.M. Matrix Stiffening from Fibril Density and Alignment Modulates YAP-mediated T-cell Immune Suppression. *Biomaterials* 2025; 315:122900

S19 – O6

Chirality-programmed self-assembling peptides fine-tune macrophage inflammation revealed by targeted secretomics

Wychowaniec J.K.[1], Bektas E.I.[1], Patt-Lafitte G.[2], Sapudom J.[3], Šrejber M.[4], Otyepka M.[4], Teo J.[3], Eglin D.[2], D'Este M.[1]
[1]AO Research Institute Davos, Davos, Switzerland; [2]Mines Saint-Étienne, Univ Jean Monnet, INSERM, U1059 Sainbiose, Saint-Étienne, France; [3]Laboratory for Immuno Bioengineering Research and Applications, Division of Engineering, New York University Abu Dhabi, Abu Dhabi, UAE; [4]Regional Centre of Advanced Technologies and Materials, Czech Advanced Technology and Research Institute (CATRIN), Palacký University Olomouc, Olomouc, Czech Republic

Introduction

Numerous chronic inflammatory conditions involve prolonged immune imbalance, with macrophages (MΦs) and their crosstalk with stromal cells playing a central role in dictating healing. Biomaterial-based strategies can guide MΦ responses toward regeneration, particularly in severe injuries.

Aim

Inspired by nature's homochirality, we evaluated an extended family of tyrosine-modified β-sheet-forming self-assembling peptides (SAPs) to influence MΦ behaviour and promote resolution of chronic inflammation toward a pro-healing state.

Materials and Methods

By varying hydrophobic/hydrophilic residues and tyrosine placement, as well as choosing the overall chirality state (L- versus D-), we were able to tune the physicochemical properties and interactions of SAPs with MΦs. These SAPs were comprehensively characterized using physicochemical and molecular dynamics analyses, and their effects on MΦ polarization were evaluated in THP-1 and donor-derived PBMC-derived cells through molecular and cellular assays, including a targeted Olink® Target 96 Inflammation panel.

Results

Among L-variants, we identified two negatively charged key modulators, EF8, which induced an anti-inflammatory M2 response (CD105, CD163, CD206 upregulation, IL-10 secretion), and YEF8, which favoured an M1-like phenotype (increased HLA-DR expression and TNF-α secretion), whilst EF8Y not inducing strong responses. Olink analysis showed: (i) YEF8 > EF8 for selected chemokines and remodelling markers (e.g., MCP-3/4, MMP-1, uPA), indicating a moderately higher inflammatory tone; (ii) YEF8 > M_0 MΦs with strong increases in CCL23, CCL20, CXCL5/6, MMP-1; and (iii) EF8 20 mM hydrogel ≫ EF8 in medium, with large elevations in IL-6, VEGFA, MMP-1, CXCL1/CXCL6, consistent with robust innate activation. Notably, EF8, YEF8, and EF8Y did not elevate IFN/STAT1-linked chemokines (CXCL10/11) nor IL-18, suggesting a comparatively restrained secretome lacking strong TLR/IFN or inflammasome signatures. Homochiral D-variants of $EF8_D$ and $YEF8_D$ confirmed immunomodulatory induction of polarization, albeit with lower response as compared to L-variants.

Conclusion

SAP chemistry and chirality enable graded immunomodulation of MΦs. Across the secretome, EF8 hydrogel and BSA control produced the most pro-inflammatory profiles, whereas soluble EF8 remained immuno-quiet and YEF8 showed selective chemokine upshifts without IFN/ECM surges. These data position EF8 as a promising pro-resolving cue and YEF8 as a tuneable activator, offering a spatiotemporal toolkit to steer musculoskeletal inflammation toward regeneration and informing rational design of peptide-based immunotherapies.

Acknowledgements

This work was supported by the AO Foundation, EU H2020-MSCA-IF-2019 (no.893099-ImmunoBioInks), European Research Council (ERC, no. 101219936-DeCodeGels), LEADING HOUSE MENA Research Partnership (RPG-2022-38) and Consolidation (COG-2023-35) grants, and COST Action SNOOPY (CA23111).

S19 – O7

Co-assembled fluorescent self-assembling peptide probes enable visualization of macrophage uptake and polarization

Venegas Bustos D.[1] Wychowaniec J.K.,[2]
[1] Bioforge Lab, LaDIS, CIBER-BBN, Edificio LUCIA, Universidad de Valladolid, Valladolid, Spain; [2] AO Research Institute Davos, Davos, Switzerland

Introduction

Macrophages (MΦs) constitute basic innate immune cells responsible for directing regenerative capacity in disrupted tissues. Understanding how self-assembling peptides (SAPs) are internalized and trafficked within MΦs is essential for designing next-generation immuno-active biomaterials. Yet, conventional fluorophore–peptide conjugation often disrupts peptide assembly or alters biological behaviour.

Aim. To overcome this, our aim was to develop a modular strategy in which a fluorescent dye–peptide conjugate co-assembles with native immunomodulatory SAPs: anti-inflammatory **EF8** and pro-inflammatory **YEF8**, preserving structural integrity while enabling high-resolution visualization of cellular interactions.

Materials and Methods

We investigated the co-assembly behaviour, optical properties, and uptake dynamics of FCA-tagged peptides mixed with parent β-sheet-forming SAPs and assessed their suitability as minimally perturbative probes for live imaging of macrophage engagement. FCA-labelled **EF8** and **YEF8** SAP analogues were co-assembled with unmodified peptides at three molar ratios (1, 5 and 10 mol%). Structural integrity of the mixed assemblies was analysed using oscillatory rheology and Fourier transform infrared spectroscopy. Fluorescence properties and quenching behaviour were evaluated across environmental conditions, confirming preservation of dye emissivity within co-assembled fibrils. Uptake studies were performed in PBMC-derived MΦs using confocal microscopy to track internalization kinetics and intracellular distribution.

Results

FCA conjugation at the terminal lysine yielded a stable, assembly-competent probe that reliably co-assembled with EF8 and YEF8 SAPs without altering their β-sheet secondary structure. Mixed fibrils displayed homogeneous fluorescence and retained their native morphology. Co-assembled FCA-containing hydrogels retained fluorescent across all molar ratios (Fig. 1) and allowed quantitative assessment of uptake efficiency, enabling discrimination between SAPs that engage macrophages primarily via surface interaction versus those demonstrating stronger intracellular accumulation.

Conclusion

FCA-labelled co-assembling peptides provide a powerful, non-perturbative fluorescent platform for real-time visualization of immunomodulatory SAPs–MΦs interactions. This strategy preserves native self-assembly behaviour while enabling precise tracking of interactions with immune cells. Such probes open new opportunities to map how peptide chemistry and chirality govern immune engagement, ultimately facilitating rational design of immuno-active peptide biomaterials.

Acknowledgements

This work was supported by the AO Foundation, EU H2020-MSCA-IF-2019 (no.893099-ImmunoBioInks), European Research Council (ERC, no. 101219936-DeCodeGels), LEADING HOUSE MENA Research Partnership (RPG-2022-38) and Consolidation (COG-2023-35) grants, and COST Actions SNOOPY (CA23111) and TENET (CA22170).

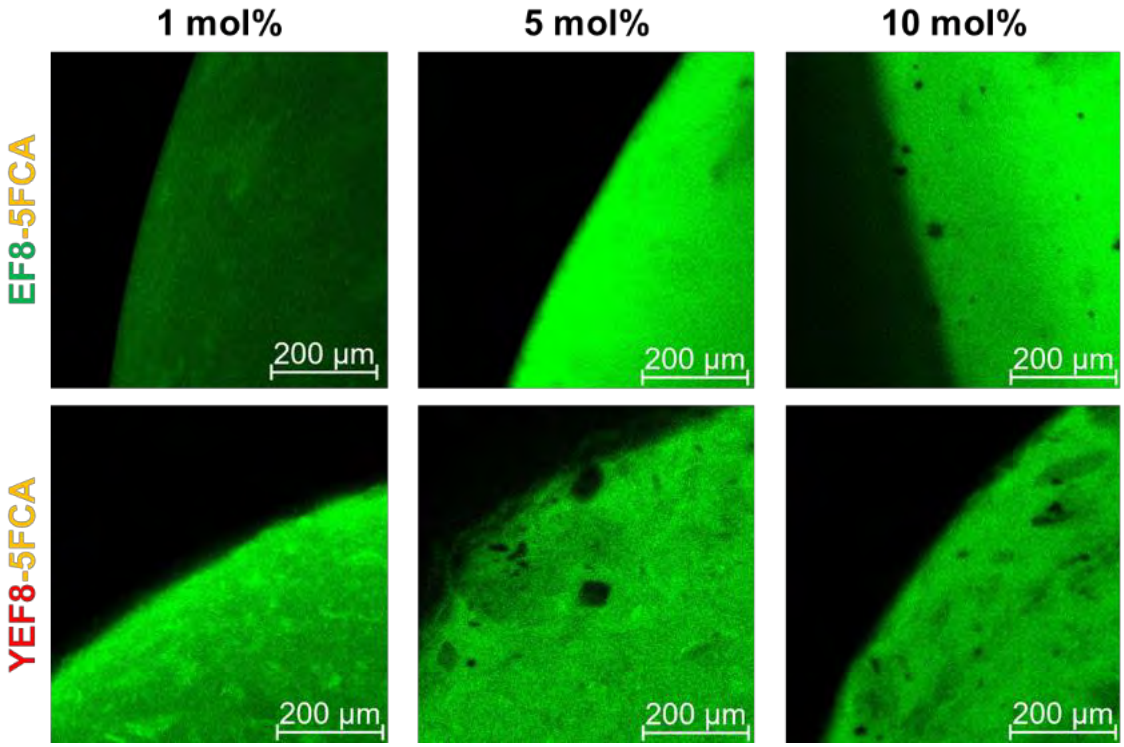

Figure 1. Confocal microscopy of co-assembled **EF8** and **YEF8** fluorescent probes at three molar ratios (1, 5 and 10 mol%).

S20
Biomaterials designed from particulate building blocks

S20 – K1
From particles to immune niches: Engineering regeneration

Segura T.
[1]Duke University; [2]Dept. of Biomedical Engineering, Durham, USA

Particulate biomaterials offer a powerful framework for engineering biological function by assembling discrete building blocks into complex microenvironments. In this talk, I will present how particle-based design enables control over both tissue regeneration and immune modulation.
We developed microporous annealed particle (MAP) scaffolds that assemble into injectable, tissue-integrating networks. By incorporating immunogenic cues, these materials form localized immune niches that recruit and activate antigen-specific B cells directly within injured tissue, reprogramming inflammation and promoting regenerative healing.
In parallel, we developed computational tools to quantify how particle packing governs pore architecture, revealing how particle properties define void space, connectivity, and accessibility.
Together, these studies illustrate how particulate building blocks can be used to program immune responses and guide endogenous regeneration through control of material architecture.

Acknowledgements
I like to thank my lab for their hard work and creative science. I also like to thank the USA National Institutes of Health for funding. Part of the work presented in this keynote presentation is a collaboration with Joel Collier and lead by a co-mentored student Pablo Cordero.

S20 – O1

Design of a photocrosslinkable organic-inorganic colloidal hydrogel

Donderwinkel I.[1], Leeuwenburgh S.C.G.[1], Diba M.[1]
[1]Dept. of Dentistry, Regenerative Biomaterials, Radboudumc, Nijmegen, The Netherlands

Introduction

Hydrogels have been effectively reinforced with inorganic nanoparticles, rendering them promising materials for "bottom-up" scaffold fabrication. Here, we functionalised silica nanoparticles (SiO_2 NPs) with silane-polyethylene glycol-acrylate (silane-PEG-Ac) and mixed them with gelatin NPs to create biocompatible photo-reactive extrudable hydrogels with enhanced shape fidelity, addressing extrusion-based limitations.

Aim

Preparation of a photo-crosslinkable hybrid colloidal hydrogel as a tough extrudable biomaterial.

Materials and Methods

SiO_2 NPs were synthesized by the Stöber method[1] and functionalised with silane-PEG_{1k}-Ac or silane-PEG_{10k}-Ac at targeted densities of 0.1 or 1.0 PEG/nm^2. As a control, PEG-free SiO_2-Ac NPs were synthesized by reaction with hydrolyzed 3-(trimethoxysilyl)propyl methacrylate (MPS). Gelatin nanoparticles were synthesized by ethanol-induced desolvation followed by EDAC/NHS crosslinking and purification using crossflow filtration. NPs were analyzed by 1) Dynamic Light Scattering and Scanning Electron Microscopy (wet and dry size, respectively); 2) Laser Doppler Electrophoresis (surface charge), 3) and Fourier Transform Infrared spectroscopy (chemical structure). Hydrogels were prepared at a particle volume fraction (φ) of 0.1 in Phosphate Buffered Saline (PBS) using 10mM lithium phenyl-2,4,6-trimethylbenzoylphosphinate (LAP) as photo-initiator followed by irradiation (405 nm, 10 mW/cm^2). Viscoelastic properties were analysed by oscillatory rheology.

Results

SiO_2 NPs were reproducibly synthesized with a hydrodynamic radius (r_H) of 115±16 nm, a polydispersity (Đ) of 0.15, a zeta-potential of ζ=-36±2 mV and dry size of 73±8 nm. Functionalised SiO_2 NPs showed low polydispersity (~0.2) and characteristic infrared absorption peaks corresponding to acrylate (1703 cm^{-1}) and PEG-acrylate groups (1703, 2850, 2918 cm^{-1}). Gelatin nanoparticles showed a r_H of 613±26 nm (Đ=0.15) and ζ=+17±0.1 mV. Silane-PEG-Ac-functionalised SiO_2 (SiO_2-PEG-AC) NPs remained stable upon addition of PBS, whereas SiO_2 and SiO_2-Ac NPs dispersed. Upon irradiation, SiO_2-PEG-Ac hydrogels (φ=0.1) showed an increase in storage modulus in presence of LAP from 3 to 7.5 kPa (0.1 silane-PEG_{1k}-Ac/nm^2), 1.5 to 12 kPa (1.0 silane-PEG_{1k}-Ac/nm^2), 3 to 13 kPa (0.1 silane-PEG_{10k}-Ac/nm^2), and 5.5 to 20 kPa (1.0 silane-PEG_{10k}-Ac/nm^2).

Conclusion

SiO_2-PEG-Ac NPs formed more elastic hydrogels than SiO_2 and SiO_2-Ac controls with tunable mechanical properties depending on PEG molecular weight and functionalization density. These findings indicate that photoreactive SiO_2 NPs are promising building blocks for mechanically reinforced hybrid colloidal hydrogels. Future work will focus on combining gelatin NPs with SiO_2-PEG-Ac NPs to form extrudable hydrogels.

Acknowledgements

ID acknowledges funding by the European Union (101107724).

References

1. Stöber, W., Fink, A., Bohn, E. Controlled growth of monodisperse silica spheres in the micron size range. *Journal of Colloid and Interface Science* 1968; 26(1); 62-69

S20 – O2

Glycopeptide-based hydrogels as storage depots that promote vascularisation

Araújo A.R.[1,2], Castro V.I.B.[1,2] , Rodrigues D.B.[1,2], Reis R.L.[1,2], Pirraco R.P.[1,2], Pires R.A.[1,2]
[1]3B's Research Group, I3Bs, Research Institute on Biomaterials, Biodegradables and Biomimetics, University of Minho, Headquarters of the European Institute of Excellence on Tissue Engineering and Regenerative Medicine; [2]ICVS/3B's PT Government Associated Laboratory, Braga/Guimarães, Portugal

Introduction

Glycosaminoglycans (GAGs) are one of the most abundant class of biomolecules that constitute the extracellular matrix (ECM) of living tissues. They have a series of bioactivities, as for example: participation in cell-cell communication; mediation of ligand-receptor recognition (i.e., act as co-receptors); enable long term storage of proteins maintaining them in their bioactive conformation (i.e., act as storage depots); among others.[1] Importantly, the vascularization of constructs plays a critical step in tissue engineering, as it provides oxygen and metabolites to the cellular components and removes metabolic products from the extracellular space.
Herein, we designed a glycopeptide (i.e., Fmoc-FF-Glucosamine-6-sulfate) that self-assembles into nanofibers and gels under physiological conditions, mimicking the sulphated GAGs/proteoglycans present in the ECM.[2] We hypothesise that these hydrogels can act as storage depots and promote vascularisation.

Materials and Methods

Glycopeptides were synthesised via chemical conjugation of the peptide amphiphile Fmoc-FF with the respective monosaccharide moiety, i.e., glucosamine-6-sulfate (GlcN6S), using EDC/NHS coupling chemistry. The generated amphiphile is able to self-assemble into nanofibers and forms hydrogels when in contact with solutions at physiological ionic strength (e.g., cell culture media). Self-assembly into nanofibers can be promoted by different strategies, including: a heating–cooling cycle (solubilisation at high temperature, e.g., 90 °C, followed by assembly at physiological temperature, i.e., 37 °C); the induction of a pH switch (solubilisation at high pH followed by assembly at neutral pH); and through a solvent switch approach (solubilisation in DMSO followed by dilution into water). Growth factors (GFs), such as VEGF, can be encapsulated in these systems by their loading into the soluble precursor solution prior to the self-assembly and/or gelation, that only occurs upon exposure to cell culture media.

Results

The biocompatibility of the generated supramolecular hydrogels was confirmed using human dermal microvascular endothelial cell (hDMECs) cultures by live/dead staining and AlamarBlue® assays. These hydrogels were then loaded with angiogenic factors, e.g., vascular endothelial growth factor (VEGF) at concentrations of 10 and 20 ng/mL, to promote vascularisation (Fig.1A).[3] The encapsulation of VEGF in the supramolecular hydrogels, induced microvascularization during 4 days using a combination of hDMECs and adipose-derived stromal/stem cells (hASCs), as demonstrated through the formation of capillary-like structures, validated by immunofluorescence imaging (lectin-FITC) on day 4 of cell culture (Fig.1B)

Conclusions

Our results show that the proposed glycopeptide-based supramolecular hydrogel can capture angiogenic factors, such as VEGF, maintain them in their bioactive conformation (as observed for sulphated GAGs in living tissues) and promote the pre-vascularisation of supports for tissue engineering and regenerative medicine applications.

Acknowledgements

Supported by FCT (Portugal), the European Commission, CCDR Norte, and La Caixa Foundation through UID/PRR/50026/2025 (DOI:10.54499/UID/PRR/50026/2025), Norte-01-0145-FEDER-022190, ERA4Health partnership (CARDINNOV/0001/2023-AmnioSMART) and LaCaixa-OCEANIC (HR24-00056).

References

1. Gandhi, N. S. & Mancera, R. L. The structure of glycosaminoglycans and their interactions with proteins. Chem. Biol. Drug Des. (2008). 72, 455–482.
2. Castro, V. I. B. et al. Glycopeptide-Based Supramolecular Hydrogels Induce Differentiation of Adipose Stem Cells into Neural Lineages. ACS Appl. Mater. Interfaces (2023) 15, 29998–30007.
3. Song, J., Shao, L., Yu, H., Meng, C. & Li, G. Self-Assembly of Sulfate-Containing Peptides Sequesters VEGF for Inhibiting Cancer Cell Invasion. Biomacromolecules (2024) 25, 3087–3097.

S20 – O3

Surface-functionalized hybrid silica–hydrogel biomaterials for stimuli-responsive pH sensing at cellular scale

Iuele H., Onesto V., Siciliano A. C., Forciniti S., del Mercato L.L.
Nanotechnology Institute of National Research Council (Cnr-NANOTEC), Lecce, Italy

Introduction

Extracellular pH regulation plays a fundamental role in cellular metabolism, tissue homeostasis, and disease progression. In pathological conditions such as cancer, metabolic alterations induce extracellular acidification, strongly influencing cell behavior and cell–material interactions.[1] However, reliable and spatially resolved monitoring of extracellular pH within biomaterial-based systems remains challenging. There is a growing need for nanostructured biomaterials that integrate surface functionalization with smart, stimuli-responsive sensing capabilities.

Aim

The aim of this study was to develop a modular, customizable, surface-functionalized biomaterial platform capable of stable, high-resolution, and stimuli-responsive extracellular pH sensing in live-cell environments.

Materials and Methods

A modular biomaterial system based on biocompatible silica microparticles was developed through surface functionalization with polymerizable linkers, enabling the controlled growth of hydrogel shells with tunable chemical and mechanical properties.[2] The hydrogel layers were engineered to allow covalent immobilization of ratiometric pH-responsive fluorophores, ensuring optical stability and long-term functionality. Sensor performance was evaluated by bulk fluorimetric analysis and single-particle confocal imaging. Optimized sensor formulations were embedded into electrospun polycaprolactone nanofibrous scaffolds to generate extracellular matrix–mimicking, pH-responsive biomaterials suitable for live-cell studies.[3]

Results

The modular hybrid silica–hydrogel biomaterials (Fig. 1a) exhibited robust, reversible, and stable ratiometric pH responses across the physio-pathological range (Fig. 1b-c). Surface modification via hydrogel shells preserved fluorophore sensitivity while preventing dye leaching (Fig. 1d). When integrated into nanofibrous scaffolds, the sensors enabled real-time, spatially resolved mapping of extracellular pH in live-cell cultures (Fig. 1e-n). Distinct extracellular acidification profiles were detected between healthy (Fig. 1e-f-i) and malignant cells (Fig. 1j-k-n), and dynamic pH shifts were observed following metabolic perturbation (Fig. 1g-h-1, Fig. 1l-m-n), confirming the stimuli-responsive behavior of the system.

Conclusion

A nanostructured and nanocomposite biomaterial platform combining surface-functionalized silica particles with smart hydrogel networks for extracellular pH sensing is presented. The modularity, biocompatibility, and responsiveness of the system make it suitable for investigating cell–material interactions and microenvironmental dynamics in advanced biomaterial-based models.

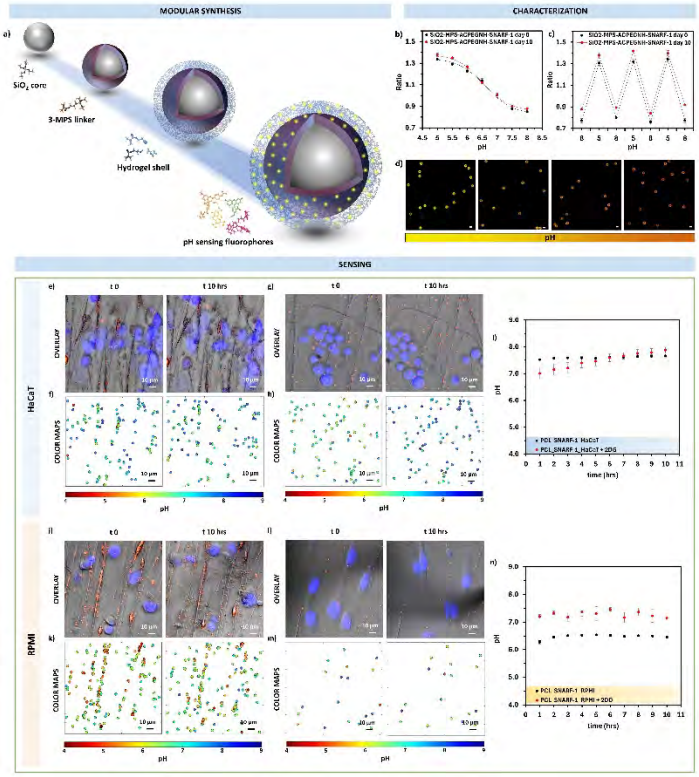

Figure 1. (a) Schematic representation of the synthetic route employed for producing hybrid silica-hydrogel pH-sensing particles: formation of SiO2 core particles; surface silanization with MPS; polymerization of hydrogel shells from; covalent conjugation of pH sensing fluorophores. Stability and Signal Reversibility of Functionalized pH Microsensors. Spectrofluorimetric characterization of hybrid silica-hydrogel pH sensors in L15 medium adjusted across physiological pH values (5.0-8.0): (b) calibration curves for SiO2-MPS-ACPEGNH-SNARF-1, (c) reversibility and aging tests based on the three pH switching cycles (pH 5.0 to 8.0). (λEX SNARF-1= 555 ± 16 nm, λEM SNARF-1= 540 nm ± 8 and 700 ± 8 nm); ratios calculated as λEM MAX1 SNARF-1 (590 nm)/λEM MAX2 SNARF-1 (640 nm).Values expressed as mean (±SE). (d) Representative confocal laser scanning microscopy (CLSM) images of SiO_2–MPS–ACPEGNH–SNARF-1 of hybrid silica–hydrogel pH sensors at pH 5.0 - 6.0 - 7.0 and 8.0 showing green/red emission channels. Green channel (false color, λEX= 543 nm, λEM1 = 556-603 nm)/Red channel (λEX= 543 nm, λEM2 = 603-700 nm). Real-time monitoring of extracellular pH dynamics using SNARF-1-loaded electrospun nanofibers of HaCaT and RPMI cells with or without 2-DG stimulation. Representative CLSM micrographs and pH scatter plots at t 0 and t 10 hours of 2-DG unstimulated (e-f) or stimulated (h-g) HaCaT cells cultured on SNARF-1-based fibers and corresponding pH quantification over time and space during a 10h time lapse monitoring (i). 2-DG unstimulated (j-k) or stimulated (l-m) RPMI-7951 cells on SNARF-1-based fibers and corresponding measurements quantification at t 0 and t 10 hours (n). (field of view in 141.42 × 141.42 µm; step size 2.50 µm, z-projection of 16 sections, 1 data point every hour) (False color channel overlay: green channel (false color, λEX SNARF-1 = 543 nm, λEM1 SNARF-1 = 556-603 nm)/red channel (λEX SNARF-1 = 543 nm, λEM2 SNARF-1 = 603-700 nm), blue = nuclear stain (λEX Hoechst = 405 nm, λEM Hoechst = 440-500 nm)). Scale bars = 10 µm. Values expressed as mean (±SE).

References

1. E. Boedtkjer. "The acidic tumor microenvironment as a driver of cancer." *Annual review of physiology.*
2. H. Iuele, et al. “Modular hybrid silica–hydrogel sensors enable high-resolution extracellular pH sensing in tumor and healthy cell models.” *Chemical Engineering Journal.*
3. V. Onesto, et al. "Probing Single-Cell Fermentation Fluxes and Exchange Networks via pH-Sensing Hybrid Nanofibers." *ACS nano.*

S20 – O4

Zinc-doped mesoporous bioactive glass nanoparticles for treating intracellular infections

Andrée L.[1], Adigun A.E.[1], Langel A.[2], Joziasse L.S.[1], Harhangi H.R.[3], van Niftrik L.[3], Deng D.[2], Yang F.[1]
[1]Dept of Dentistry, Regenerative Biomaterials, Radboud University Medical Center, Nijmegen; [2]Dept. of Preventive Dentistry, Academic Center for Dentistry Amsterdam (ACTA), University of Amsterdam and Vrije Universiteit Amsterdam; [3]Dept. of Microbiology, Radboud Institute for Biological and Environmental Sciences, Radboud University, Nijmegen, The Netherlands

Introduction

Antibiotic resistance has become a major health concerns worldwide. An often-overlooked factor in antibiotic resistance is the presence of intracellular bacteria, which are shielded from both the host immune system and many antibiotics due to limited cellular penetration. Staphylococcus aureus (S. aureus) is a key intracellular pathogen and the leading cause of recurrent bone infections, with recurrence rates of 20-30%.[1] Nanoparticles offer a strategy to overcome this barrier by enabling intracellular drug delivery. Mesoporous bioactive glass nanoparticles (MBGNs), silica-based particles doped with calcium ions, exhibit high cargo loading capacity and efficient cellular internalization, favoring intracellular drug delivery.[2] Here, we developed zinc-doped MBGNs (Zn-MBGNs) to enhance antibacterial activity and evaluated their cytocompatibility and bacteriostatic efficacy.

Materials and Methods

Zinc-doped MBGNs were synthesized via the surfactant-assisted sol–gel method and thoroughly characterized with respect to particle morphology, size and mesoporosity. Cellular internalization in murine pre-osteoblastic MC-3T3 cells was assessed by confocal microscopy. Cytocompatibility was evaluated after 1 and 3 days of exposure (31.25–250 µg/mL) via metabolic activity and DNA quantification. Antibacterial activity against S. aureus was determined by monitoring bacterial growth over 24 hours using optical density measurements.

Results

Spherical MBGNs (~85 nm) with radial mesopores were obtained independent of zinc content. Efficient cellular internalization was observed, with particles localizing in endolysosomal compartments. After 3 days, Zn-MBGNs maintained cell viability comparable to controls at concentrations ≤125 µg/mL. Notably, MBGNs with a high zinc dopant content (10 mol% Zn relative to Ca) reduced S. aureus growth up to ~50% at these concentrations and completely inhibited growth at 250 µg/mL, comparable to antibiotic treatment. In contrast, undoped MBGNs reduced cell viability but showed no significant antibacterial effect.

Conclusion

Zn-MBGNs were successfully synthesized and demonstrated strong bacteriostatic activity while maintaining cytocompatibility. At 10 mol% zinc doping, they effectively inhibited S. aureus growth, highlighting their potential for intracellular antibacterial therapy. Future work will assess their efficacy in co-culture models of intracellular bacteria and in combination with additional antibacterial agents.

Acknowledgements

The authors thank the Radboud Electron Microscopy and Radboudumc Technology Center for Microscopy, and Dutch Research Council funding (NWO, project 20339).

References

1. K. D. Alder et al., Intracellular Staphylococcus aureus in bone and joint infections: A mechanism of disease recurrence, inflammation, and bone and cartilage destruction. *Bone*; 2020; 141; 8756-3282.
2. S. Van Rijt, et al., Calcium Phosphate and Silicate-Based Nanoparticles: History and Emerging Trends. *Tissue Eng. - Part A*; 2022; 28(11-12); 461-477.

S20 – O5

Supramolecular glycohelices: Control of handedness and cytotoxicity

Castro V.I.B.[1,2], Ge J.[1,2,3], Chen J.[3] Reis, R.L.[1,2], Pashkuleva I.[1,2], Pires R.A.[1,2]
[1]3B's Research Group, I3Bs, Research Institute on Biomaterials, Biodegradables and Biomimetics, University of Minho, Headquarters of the European Institute of Excellence on Tissue Engineering and Regenerative Medicine, Barco, Guimarães, Portugal; [2]ICVS/3B's–PT Government Associate Laboratory, Braga/Guimarães, Portugal; [3]Dept. of Chemical Engineering, School of Environmental and Chemical Engineering, Shanghai University, China

Introduction

Supramolecular helices are used by biological systems in different processes such as biorecognition, coding and transferring information, replication.[1] Their handedness is determined by the chirality of the building blocks and the assembly conditions but the exact mechanisms are not clear.[1,2] Herein, we used two enantiomeric glucosamine amphiphiles, namely Fmoc-D-GlcN and Fmoc-L-GlcN, and studied their assembly in aqueous environment.

Materials and Methods

Fmoc-D-GlcN and Fmoc-L-GlcN were synthesised in one-step reaction from the respective glucosamine enantiomers and N-fluorenyl methoxycarbonyl chloride (Fmoc-Cl). The structure and purity were confirmed by NMR, MS, and HPLC. Supramolecular assembly was induced by a heating-cooling cycle: the amphiphiles were suspended in water, heated at 80°C until complete dissolution and then cooled to room temperature at different rates. The process was followed in real time by CD, and the assemblies were characterized by AFM and SEM. The cytotoxicity was assessed using L929 cell line.

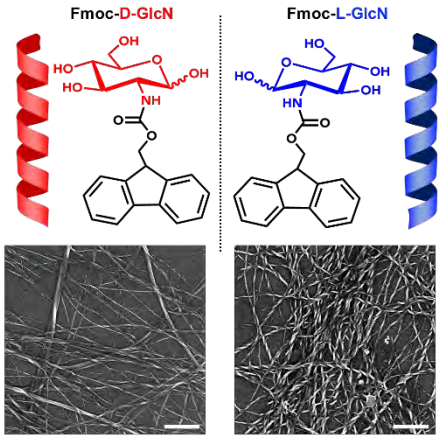

Figure 1. Chemical structure of the synthesized Fmoc-D-GlcN and Fmoc-L-GlcN. Representative SEM images of the helical fibres obtained from 12mM solution of the respective enantiomer (Scale bar 500nm)

Results

At the studied concentration range (6 -16 mM), both isomers formed nanofibrous hydrogels upon cooling but the helicity of the fibres was different: Fmoc-D-GlcN formed right-handed (P-) helices, while Fmoc-L-GlcN generated left-handed (M-) helices. Real time follow up of the assembly at slow cooling rate suggested distinct stability and cooperative assembly pathways for the enantiomers. Rheology measurements showed higher stiffness for the gels assembled from the D-enantiomer than for the L-isomer. Cytotoxicity of the gels assembled from Fmoc-D-GlcN was significantly higher than the ones generated by Fmoc-L-GlcN.

Conclusion

Our data provide mechanistic insides about transferring chiral information by carbohydrates in water. The distinct mechanical properties and toxicity of the gels assembled from the two enantiomers show that the use of unnatural L-carbohydrates can be further explored in the development of biocompatible materials that retain characteristic properties of carbohydrates but are not recognized by the cell surface receptors.

Acknowledgements

We acknowledge the financial support from the Portuguese FCT (2023.17561.ICDT, DOI:10.54499/2023.17561.ICDT), European Commission, CCDR Norte and La Caixa Foundation: LaCaixa-Oceanic (HR24-00056), UID/PRR/50026/2025 and Norte-01-0145-FEDER-022190.

References

1. Castro VIB, Reis RL, Pires RAP, Pashkuleva I, Chem Soc Rev 2025 54:8325
2. Castro VIB et al, J Mat Chem 2024, 12, 6996

S20 – O6

Bioactive glass scaffolds loaded with Superparamagnetic Iron Oxide Nanoparticles (SPIONs): A multifunctional approach for bone regeneration and hyperthermia in bone cancer treatment

Giacobbi S.[1], Gobbo V. A.[1], Koivisto J.T.[1], Miola M.[2], Verné E.[2], Massera J.[1]
[1]Faculty of Medicine and Health Technology, Tampere University, Finland; [2]Dept. of Applied Science and Technology, Institute of Materials, Physics and Engineering, Biomaterials Laboratory, Politecnico di Torino, Turin, Italy

Introduction

Conventional bone cancer treatments are often associated with critical size bone defects and cancer cells remnants, after tumor resection[1]. Magnetic hyperthermia in combination with bioactive glass, may allow bone tissue regeneration while preventing cancer cells proliferation via hyperthermia, without being invasive[2]. Bioactive glass (BAG) 1393B20 is promising for bone regeneration, due to overcoming the crystallization tendencies of traditional silicate glasses, while promoting angiogenesis/osteogenesis and mineralization/collagen formation *in vitro* and *in vivo*[3].

Aim

This study aims at processing a multifunctional 3D printed magnetic scaffold, made of BAG 1393B20 and Superparamagnetic Iron Oxide Nanoparticles (SPIONs), able to repair critical bone defects while eradicating residual cancer cells.

Materials and Methods

SPIONs were synthesized via co-precipitation method and incorporated into an ink composed of 1393B20 BAG powder/Pluronic F-127. The BAG/SPIONs ratios were 100:0 wt%, 95:5 wt% wet, 95:5 wt% dry, 90:10 wt% dry ("wet" or "dry": SPIONs in liquid solution or dry powder). The impact of SPIONs addition on the ink rheology and on the scaffolds mechanical, bioactive and magnetic properties were assessed. The heating capacity, as a function of SPIONs loading was also evaluated. Magnetic scaffold cytocompatibility was studied with human adipose stem cells.

Results

Porous cylindrical scaffolds (h = 1 mm, ϕ = 5 mm) were successfully fabricated for all compositions. The mechanical properties of 100:0 wt% and 95:5 wt% dry fell within the range of trabecular bone, whereas 95:5 wt% wet and 90:10 wt% dry showed lower results. Scaffolds exhibited superparamagnetic properties and an increase of up to 10 °C was recorded after 10 min under an alternating magnetic field. All the compositions proved to be bioactive (precipitation of hydroxyapatite layer in SBF). Human adipose stem cells, cultured on the scaffolds, exhibited a spread morphology. Presence of SPIONs had no significant effects on cell viability and proliferation.

Conclusion

The lower mechanical properties of 95:5 wt% wet and 90:10 wt% dry were mostly due to SPIONs aggregates within the glass matrix that acted as impurities. Nonetheless, scaffolds enabled increasing the temperature of the medium within a range suitable for hyperthermia treatment. The presence of SPIONs didn't interfere with both the bioactivity of the scaffolds and cell viability and proliferation, indicating promising cytocompatibility. This study represents an innovative step towards offering new, multifunctional treatments able to repair bone, while preventing cancer cells proliferation, migration and post-surgery recurrence.

Acknowledgements

This research received funding from the RCF (MAXHEAL project #361159).

References

1. American Cancer Society. Surgery for Bone Cancer. *Bone Cancer* 2021.
2. Yazdanpanah A. et al. Threatening sarcoma with combinational therapies: Magnetic hyperthermia using nanoparticles. *Nano Select 2023*; 4; 353-367.
3. Szczodra A. et al. Boron substitution in silicate bioactive glass scaffolds to enhance bone differentiation and regeneration. *Acta Biomaterialia* 2024; 186; 489-506.

S20 – O7

DLP fabrication of amorphous borate bioactive glass composite scaffolds incorporating mesoporous bioactive glass nanoparticles

Chen S.[1], Kurtuldu F. [1], Nohut S.[2], Schwentenwein M.[2], Galusek D.[1,3], Michálek M.[1]
[1]FunGlass, A. Dubček University of Trenčín, Trenčín; [2]Lithoz GmbH, Vienna, 1060, Austria; [3]Joint Glass Centre of the IIC SAS, Trenčín, Slovakia

Introduction

In our previous work, 1393B3 borate bioactive glass (BG) scaffolds for bone regeneration were successfully fabricated via DLP-based additive manufacturing, achieving high densification while preserving the amorphous state. The feasibility of composite system printing was also demonstrated by incorporating silicate-based BG nanoparticles into the borate BG raw materials. Subsequent characterization of the scaffolds showed that their high densification resulted in favorable mechanical properties, while the amorphous state of the 1393B3 preserved their high bioactivity. In the present study, we systematically investigated the incorporation of different amounts of silicate-based mesoporous bioactive glass nanoparticles (MBGNs) into a 1393B3 matrix to enable composite system printing. MBGNs can incorporate specific therapeutic ions and provide mesoporous structures within the scaffolds, enabling efficient drug loading. They can be internalized by cells through endocytosis, facilitating more effective intracellular delivery of therapeutic ions or loaded drugs and enhancing their biological functions. In addition, incorporating MBGNs at varying concentrations alters the scaffold surface, thereby promoting cell adhesion and spreading.

Materials and Methods

1393B3 was prepared by a conventional melt–quenching method and subsequently ball-milled and sieved to obtain powders with particle sizes below 20 µm. MBGNs were synthesized via an alkali-catalyzed sol–gel process. The powders containing different amounts of MBGNs (0–32 vol%) relative to 1393B3 were mixed with a binder supplied by Lithoz GmbH using a centrifugal mixer to prepare printable slurries. Gyroid scaffolds with different dimensions were fabricated using a Lithography-based Ceramic Manufacturing system from Lithoz. The printed structures included 6 × 6 × 6 mm cubes for compressive strength testing, 3 × 5 × 25 mm bars for bending tests, and 4 × 4 × 4 mm cubes for further material characterization, including SEM–EDX, confocal microscope, XRD, bioactivity testing, and cytocompatibility evaluation.

Results

SEM and confocal microscopy revealed that the incorporation of MBGNs induced a hierarchical surface morphology on the scaffolds, consisting of micrometer-scale features and nanoscale structures originating from the MBGNs. SEM images of scaffold cross-sections showed that the 1393B3 matrix was nearly fully densified, while XRD confirmed that all samples remained amorphous. EDX mapping analysis further demonstrated that MBGNs were uniformly distributed within the 1393B3 matrix. Mechanical testing showed that the flexural strength decreased with increasing MBGN content.

Conclusion

1393B3 scaffolds with MBGN contents of up to 32 vol.% were successfully fabricated. All scaffolds remained amorphous, while the 1393B3 matrix exhibited good densification. The incorporation of MBGNs generated hierarchical micro/nano scale surface features and allowed homogeneous distribution within the borate glass matrix, at the expense of a gradual reduction in flexural strength with increasing MBGN content.

Acknowledgements

This work has received funding from the European Union’s Horizon Europe research and innovation programme under grant agreement No 101120555. Views and opinions expressed are however those of the author(s) only and do not necessarily reflect those of the European Union or European Research Executive Agency (REA). Neither the European Union nor the granting authority can be held responsible for them. Financial support for this work through the grants APVV-22-0036 and VEGA 1/0057/23 is gratefully acknowledged.

S21
Biomaterials for women's health bridging gaps in regenerative medicine and disease modeling

S21 - K1
Engineering adipo-mimetic niches and microphysiological systems to model high grade serous ovarian cancer

Gonzalez Molina J.[1], Bosch-Fortea M.[1], di Cio S.[1], Dibble M.[1], Joy J.[2], Balkwill F.[2], Gautrot J.E.[1]
[1]School of Engineering and Materials Science, Queen Mary, University of London; [2]Barts Cancer Institute, Queen Mary University of London, UK

Introduction
Adipose tissues, such as the omentum, sub-cutaneous fat or the bone marrow, constitute unique microenvironments playing key roles in stem cell biology and the development of cancer. Mesenchymal stem cells (MSCs) and haematopoietic stem cells (HSCs) reside in these microenvironments with unique microstructure and mechanics, in which 90% of the volume of the tissue is constituted of adipocytes nested in a network of ECM proteins and other tissue resident cells. During metastasis, adipose tissues not only regulate cancer cell invasion, but also remodel significantly. We propose that recreating the biochemical (matrix composition, adhesive motifs) and physical (microstructure, mechanics) of adipose tissues will enable enhanced control of stem cell phenotypes and the study of cancer progression, with application in the study of woman biology and regenerative medicine.

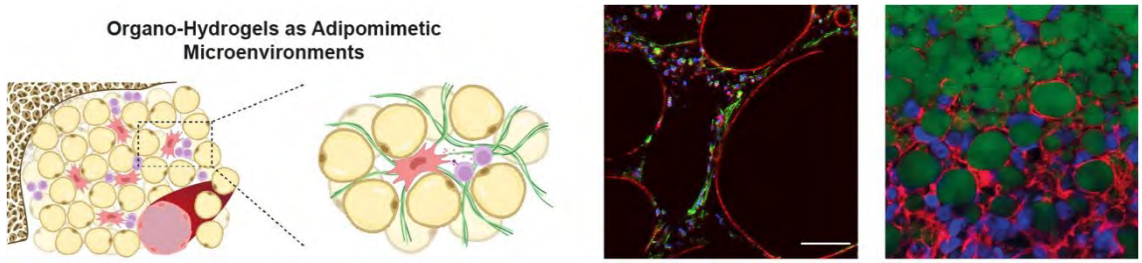

Fig.1 Engineering of adipo-mimetic biomaterials for the design of stem cell niches and the study of ovarian cancer cell development.

Results
To develop adipo-mimetic microenvironments, we explore the engineering of cell-instructive organo-hydrogels, hydrogel-like materials in which adipocyte-mimicking microdroplets are crosslinked together. This enables the control of microstructure (microporosity), mechanics (nanoscale mechanics, toughness and local mechanical anisotropy) and biochemistry (cell adhesion motifs, degradation) of resulting biomaterials. We show that this environment is particularly well-suited for the culture of MSCs and HSCs in vitro and recreates key properties regulating the progression of ovarian cancer. We find that cancer cell migration is regulated by the biophysical properties of adipose tissues and that this controls tumour progression, matrix remodelling and malignancy. Beyond fundamental studies, we demonstrate how the development of advanced biomimetic in vitro models can help identify novel therapeutics for the treatment of ovarian cancer, such as CAR T-cells.

Acknowledgements
Funding for this work from the European Research Council (ProLiCell, 772462 and ProBioFac, 966740) is gratefully acknowledged.

References
[1]Bosch-Fortea, M.; Marciano, D.; Gautrot, J.E. *Biomaterials* 2026, 325, 123612.
[2]Gonzalez-Molina, J.; Nabili, P.; Marciano, D.; Abdelnabi, A.; Gultekin, O.; Rasul, M. F.; Zhang, Y.; Nadal, C.; Chrysanthou, A.; Alkasalias, T.; Salehi, S.; Balkwill, F.; Lehti. K.; Gautrot, J.E. *Nature Communications* 2025, 16, 8541.
[3]Mojares, E. ; Chrysanthou, A.; Gautrot, J.E. *Adv. Mater.*, 2024, *36*, 2406333.
[4]Joy, J.D; Malacrida, B.; Laforets, F.; Kotantaki, P.; Maniati, E.; Manchanda, R.; Annibaldi, R.; Hopkins, S.; Garrobo-Calleja, I.; Gautrot, J.; Balkwill, F.R. *Cancer Res.* 2024, 84 (15), 2432-2449.

S21 - K2

Evaluation of microgravity-dependent alterations on ovarian follicles in an organ-on-a-chip system

Emanet M.[1], Gigante G.[1], Lefevre M.C.[1], Carmignani A.[1], Ciofani G.[1]
[1]Smart Bio-interfaces Group, Italian Institute of Technology, Pontedera (PI), Italy

Introduction

Gravity is a key physical force shaping living systems, from cytoskeletal organization and intracellular transport to cell proliferation, differentiation, polarity, and communication[1]. Because ovarian follicles rely on tightly coordinated local and endocrine signals, ovarian function is especially vulnerable to physical stressors such as altered gravity[2]. To assess potential reproductive risks during spaceflight, we investigated the effects of simulated microgravity (S-µG), generated by a random positioning machine, on KGN granulosa spheroids and H295R theca-like cultures, developing 3D human ovarian follicle models. Follicular activity was supported with follicle-stimulating hormone (FSH) and luteinizing hormone (LH). We then examined how S-µG affected paracrine signaling, cellular stress responses, and cell death compared with earth-gravity controls.

Materials and Methods

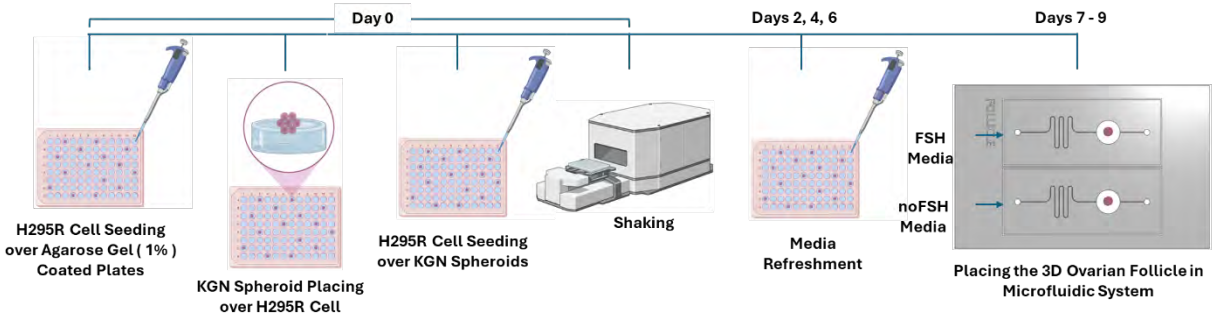

Figure 1. Schematic illustration of the 3D ovarian follicle model development procedure

Results

The 3D ovarian follicle model was structurally characterized by confocal microscopy following staining of nucleic acids with Hoechst and F-actin with phalloidin-FITC (Figure 2A-C). The distinct nuclear morphology of KGN and H295R cells enabled rough spatial discrimination within the construct, with KGN cells organized into a central spheroid surrounded by an outer layer of H295R cells. This arrangement was further confirmed by histological evaluation of sectioned samples stained with hematoxylin and eosin, which supported the confocal observations (Figure 2D). Functional analyses showed that FSH or LH modulated steroidogenic enzyme expression under both earth gravity and S-µG (Figure 2E and F). In KGN cells, FSH treatment significantly increased CYP19A1 expression regardless of gravitational status. In contrast, CYP17A1 expression in H295R cells was significantly reduced under S-µG, although LH treatment partially restored its levels. S-µG also induced a significant ROS production in both cell types (Figures 2G and H), and KGN cells exhibited altered necrosis and late apoptosis under S-µG without FSH treatment (Figures 2I and J).

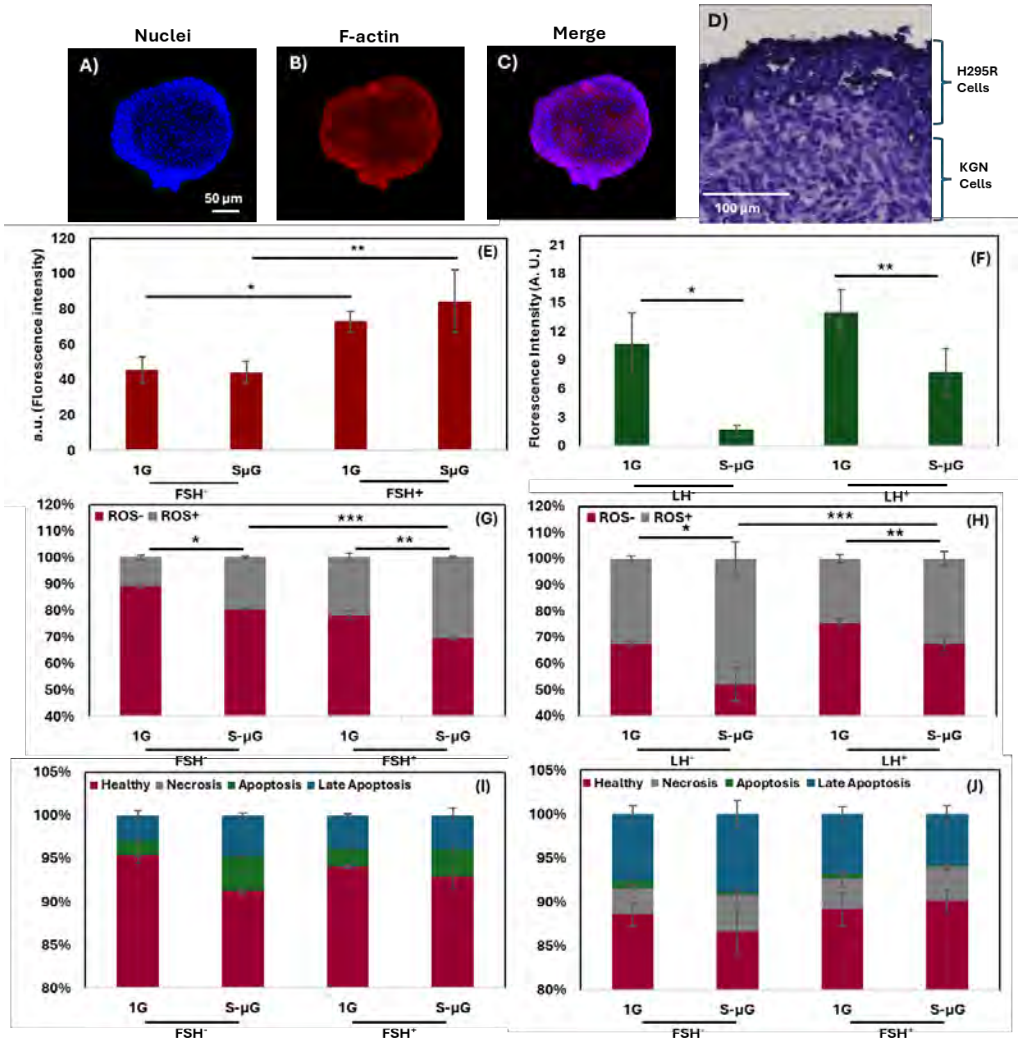

Figure 2. Representative confocal microscopy images of the nuclei (A), f-actin (B), and their merging (C); histological images (D) of the 3D ovarian follicle model. Quantitative analysis of CYP19A1 and CYP17A1 confocal microscopy images (E and F), ROS (G and H), and apoptosis and necrosis (I and J) performed on KGN and H295R cells, respectively.

Conclusion

The 3D ovarian follicle model successfully recapitulated follicular architecture, with KGN spheroids centrally enclosed by H295R cells, as confirmed by confocal and histological analyses. Functionally, gonadotropin signaling partly preserved steroidogenic competence under S-µG: FSH sustained CYP19A1 expression, whereas CYP17A1 declined despite partial LH rescue. S-µG also increased oxidative stress and selectively promoted KGN apoptotic/necrotic vulnerability in this model.

Acknowledgements

This research has received funding from the European Space Agency (4000145476).

References

[1] H Winkler, L. Human Physiological Limitations to Long-Term Spaceflight and Living in Space, Aerospace Medicine and Human Performance (2023) 94;444.

[2] Liu, M. Ultrastructure of isolated mouse ovarian follicles cultured in vitro, Reproductive Biology and Endocrinology (2011) 9;1.

S21 - O1

Engineering a 3D human peritoneal endometriosis model using self-assembling peptide hydrogel composites

Silva R.[1], Fischer D.[2], Marshall K.[2], Gough J.[3], Miller A.[4], Saiani A.[4], Herrick S.[1]
[1]Division of Cell Matrix Biology and Regenerative Medicine, University of Manchester; [2]Division of Pharmacy and Optometry, University of Manchester; [3]Dept. of Materials & Henry Royce Institute, University of Manchester, UK; [4]Manchester Institute of Biotechnology, University of Manchester, UK

Introduction

Endometriosis is characterised by the establishment of endometrial-like tissue outside the uterus, most commonly on the peritoneal surface. Progress in understanding early lesion formation is limited by the lack of reproducible human-relevant *in vitro* models. We propose that defined synthetic biomaterial scaffolds will provide an improved microenvironment to investigate early lesion formation compared with conventional animal-derived matrices. The aim of this study was to engineer a defined 3D human peritoneal endometriosis model using self-assembling peptide hydrogel composites and relevant primary human patient- derived cell populations.

Materials and Methods

Primary human fibroblasts were embedded within self-assembling peptide hydrogels and mesothelial cells were seeded on the gel surface to generate a peritoneal construct. Peptide formulations with differing stiffness, charge and pH as well as combination of other matrix components were comparatively assessed for handling, construct stability, cell distribution and viability for peritoneal model development. In parallel, patient-derived endometrial epithelial organoids were established and combined with stromal cells to generate an endometrial-like tissue component. Cell distribution, morphology and associated marker expression was analysed to assess model relevance and reproducibility.

Results

Comparative screening identified peptide hydrogel-collagen I composites as the most suitable scaffold for peritoneal construct development, providing improved mechanical stability and handling relative to single-component peptide hydrogel matrices. The composite system also supported favourable uniform fibroblast distribution and sustained cell viability. Mesothelial cells formed a surface monolayer on the construct, while demonstrating expected marker expression consistent with a peritoneal-like tissue architecture. Patient-derived endometrial epithelial organoids co-cultured with stromal cells displayed gland-like morphology and endometrial lineage-associated features. Together, these components provide the basis for an integrated 3D human model of early peritoneal endometriosis lesion development.

Conclusion

Self-assembling synthetic composites support the development of a reproducible 3D human peritoneal endometriosis model incorporating relevant stromal, mesothelial and endometrial components. This defined biomaterial-based *in vitro* model platform offers a promising approach for analysing mechanisms in endometriosis development in a controlled and human-relevant microenvironment.

Acknowledgements

The authors would like to thank the EPSRC-funded Centre for Doctoral Training in Advanced Biomedical Materials (grant reference EP/S022201/1) for funding this work, and the patients who provided informed consent and the clinical colleagues at the Northern Care Alliance Endometriosis Centre at Royal Oldham Hospital for their support. Tissue collection was conducted under ethical approval.

S21 - O2

Evaluation of *in vivo* inflammation reaction induced by ascorbic acid 2-phosphate-releasing poly(L-lactide-co-ε-caprolactone) materials for pelvic organ prolapse applications

Ala-Mononen K.[1,2], Harju P.[1,2], Lindén J.[3], Miettinen S.[1,2], Sartoneva R.[1,2,4]
[1]Adult Stem Cell Group, Faculty of Medicine and Health Technology, Tampere University; [2]Tays Research Services, Wellbeing Services County of Pirkanmaa, Tampere University Hospital; [3]Dept. of Veterinary Biosciences and Finnish Centre for Laboratory Animal Pathology, Faculty of Veterinary Sciences, University of Helsinki; [4]Dept. of Obstetrics and Gynaecology, Wellbeing Services County of South Ostrobothnia, Seinäjoki, Finland

Introduction

Pelvic organ prolapse (POP) is a common gynecological condition among elderly women. It is caused by weakening of the pelvic floor connective tissues, which leads to descent of pelvic floor organs into or through the vagina. First-line surgical approach for POP is to suture the patient's own tissues to reinforce the supporting structures in the pelvic floor. Non-degradable vaginal polypropylene (PP) meshes have been used for recurrent prolapses. However, they have been associated with various complications, including mesh erosion, infections, and pain. Therefore, biodegradable materials allowing tissue regeneration and causing shorter-term inflammatory reactions could be attractive alternatives for POP applications. The inflammatory reaction and its duration have a significant impact on biomaterial integration and tissue remodeling. Ascorbic acid 2-phosphate (A2P) is a more stable derivative of ascorbic acid that has been demonstrated to enhance extracellular matrix synthesis and modulate immune responses. Therefore, A2P-releasing biodegradable poly(L-lactide-co-ε-caprolactone) (PLCL) could be a promising candidate for POP treatment.

Materials and Methods

Commercial PP mesh, PLCL and A2P-releasing PLCL (4 and 8 wt-%) membranes were implanted on the abdominal fascia of female rats. Rats without a material implantation and having a sham operation were used as controls. The systemic inflammation reaction was assessed by analysing blood smears and 14 different inflammatory markers from serum 3 days, 1 week, and 1 month after implantation with ProcartaPlex assay. Local inflammation reactions such as swelling, leukocyte infiltration, and macrophage reaction on the material surface were analysed from hematoxylin and eosin (HE) stainings 1 week and 1 month after implantation. Local inflammation reactions were analysed based on ISO 10993-6:2016 Annex E.

Results

Our results demonstrated that all PLCL-based materials caused transient acute inflammation reactions that resolved within one month, and no prolonged inflammatory reactions were detected on the systemic or local level. A2P-releasing PLCL materials caused similar systemic and local inflammation reactions compared to pure PLCL. In contrast, PP meshes induced a prolonged local inflammation response, marked by continuous lymphocyte and polymorphonuclear leukocyte infiltration and stronger surface reaction.

Conclusion

Our findings demonstrate that A2P does not affect the *in vivo* inflammatory response induced by biodegradable PLCL materials. Further, PLCL-based materials cause shorter-term inflammatory responses compared to commercial PP mesh. Therefore, A2P-releasing PLCL could be a promising biodegradable option for POP applications.

Acknowledgements

This study was funded by the Academy of Finland, the State funding for university-level health research, and Nationwide and Häme Regional Fund of the Finnish Cultural Foundation.

S21 - O3
3D-Printable Biomaterials with Integrated Diagnostic Functionality

Kolouchova K.[1], Groborz O.[2], Herynek V.[3], Humajova J.[3], Matous P.[3], Van Damme L.[1,4], Quaak A.[1], Van Durme B.[1], Ritter N.[1], Van Vlierberghe S.[1]
[1]Polymer Chemistry and Biomaterials group, Centre of Macromolecular Chemistry, Dept. of Organic and Macromolecular Chemistry, Ghent University, Belgium; [2]Institute of Biophysics and Informatics, Charles University, First Faculty of Medicine, Prague, Czech Republic; [3]Center for Advanced Preclinical Imaging, First Faculty of Medicine, Charles University, Prague, Czech Republic; [4]Tissue BV, Technologiepark-Zwijnaarde 48, Belgium

Introduction
To ensure optimal clinical outcomes, accurate determination of the biodegradation and dissolution rates, as well as the in vivo fate of administered synthetic systems and biomaterials, is essential. However, monitoring the biodegradation of biomaterials in vivo using non-invasive imaging techniques remains highly challenging and largely unexplored for the majority of existing systems, which significantly hampers their clinical translation. For example, currently available data on the biodegradation of hydrogel-based implants used in regenerative medicine are limited and rely predominantly on ex vivo analyses following in vivo animal studies. This destructive approach not only substantially increases animal sacrifice but is also inherently incompatible with clinical application in humans.

Materials and Methods
In this research, we introduce diagnostic modalities enabling non-invasive, real-time monitoring of biomaterial fate in vivo. The first approach employs fluorine magnetic resonance imaging (^{19}F MRI), a highly attractive non-invasive imaging technique that can be used alongside conventional ^{1}H MRI. Due to the negligible fluorine background in biological tissues, ^{19}F MRI provides high-contrast images and has gained increasing attention over recent decades. For this purpose, thermoresponsive poly[N-(2,2-difluoroethyl)acrylamide] polymers were developed, offering excellent ^{19}F MRI detectability owing to their favorable relaxation properties, while their thermoresponsive behavior enables broad applicability in biomedical settings. As a second strategy, a diagnostic modality compatible with conventional micro-computed tomography (µCT) imaging was introduced. Although µCT presents certain limitations, including patient exposure to ionizing radiation, it remains one of the most widely applied imaging techniques in clinical practice. For this purpose, the hydrophilic radiopaque monomer 5-acrylamido-2,4,6-triiodoisophthalic acid (AATIPA) was developed and successfully incorporated into polymeric systems.

Results
Both diagnostic modalities were implemented into a broad range of advanced polymeric platforms and crosslinked biomaterials, spanning smart nanoparticle-based theranostic systems, injectable and implantable hydrogels for drug delivery, tissue engineering, and cell therapy, as well as 3D-printable polyester-based scaffolds. Their in vivo fate was systematically evaluated, demonstrating excellent biocompatibility and the absence of long-term bioaccumulation.

Conclusion
Altogether, this work establishes a versatile and clinically translatable toolbox for real-time, non-invasive monitoring of biomaterial degradation and biodistribution, paving the way toward safer, smarter, and more predictable next-generation medical implants.

Acknowledgements
K.K. gratefully acknowledges the financial support provided by Research Foundation—Flanders (FWO, Fonds Wetenschappelijk Onderzoek—Vlaanderen, project no. 1229422N and 1247425N). This work benefited from access to the Center of Advanced Preclinical Imaging (CAPI), part of the Euro-BioImaging research infrastructure. Financial support was provided by the European Union's Horizon Europe research and innovation programme under grant agreement number 101058620 canSERV.

References

[1]Kolouchova, K., Herynek, V., Groborz, O., Karela, J., Van Damme, L., Kucka, J., Šafanda, A., Bui, Q. H., Sefc, L., & Van Vlierberghe, S. ^{19}F MRI *In Vivo* Monitoring of Gelatin-Based Hydrogels: 3D Scaffolds with Tunable Biodegradation toward Regenerative Medicine. *Chemistry of Materials*, 2024, 36, 4417–4425.

[2]Kolouchova, K., Humajova, J., Matous, P., Ritter, N., Van Damme, L., Hovorakova, M., Pavlikova, Z., Dalecka, L., Steklikova, K., Zeman, J., Kucka, J., Hruby, M., Groborz, O., Sefc, L., & Van Vlierberghe, S. Non-destructive *in vivo* tracking of gelatin hydrogels for advancing tissue engineering. Communications Materials, 2025, 6, 112.

[3]Kolouchova, K., Thijssen, Q., Groborz, O., Van Damme, L., Humajova, J., Matous, P., Quaak, A., Dusa, M., Kucka, J., Sefc, L., Hruby, M., & Van Vlierberghe, S. Next-Gen Poly(ε-Caprolactone) Scaffolds: Non-Destructive In Vivo Monitoring and Accelerated Biodegradation. Advanced Healthcare Materials, 2025, 14, 2402256.

S21 - O4

Towards replacing animal models: Z 3D *in vitro* bone model for breast cancer bone metastasis research

Eroglu F.[1,2], Harrison H.[3], Clarke R.[3], Tsigkou O.[1,2]

[1]Dept. of Materials, School of Natural Science, Faculty of Science and Engineering, The University of Manchester; [2]The Henry Royce Institute, Royce Hub Building, The University of Manchester; [3]Breast Biology Research Group, Division of Cancer Sciences, School of Medical Sciences, Faculty of Biology, Medicine and Health, The University of Manchester, UK

Introduction

Breast cancer frequently metastasises to bone, yet current research relies heavily on animal models, which raise ethical concerns and often fail to mimic human physiology. There is a pressing need for 3D in vitro models that can reduce animal use in line with the 3Rs principles[1]. In this study, we develop a 3D in vitro bone model by seeding bone marrow-derived mesenchymal stem cells (BM-MSCs) onto 3D-printed hydroxyapatite-poly (lactic-co-glycolic acid) (HA-PLGA) scaffolds under osteogenic conditions, incorporating collagen type I as a cell-carrier matrix to mimic the native bone extracellular matrix[2]. The aim is to establish a functional bone model and investigate its interaction with breast cancer cells towards an in vitro bone metastasis platform.

Materials and Methods

Scaffolds were fabricated via 3D printing. BM-MSCs were seeded onto them either in osteogenic medium alone (HA-PLGA) or embedded within collagen type I hydrogel in osteogenic medium (HA-PLGA collagen). Osteogenic differentiation was assessed through ALP quantification, Alizarin Red staining, and µCT imaging. Gene expression of osteogenic markers was analysed by qPCR, and immunofluorescence confirmed expression of bone-specific proteins.

Results

ALP activity and Alizarin Red quantification were significantly higher in the HA-PLGA collagen group at day 28, indicating enhanced mineralisation. µCT analysis confirmed greater calcium deposition in the collagen group at days 14, 21, and 28. qPCR revealed significantly upregulated OPG and ALP expression at day 14, and OSX and COL1A1 at days 4 and 7 in the collagen group, suggesting both early and sustained osteogenic progression. OCN, RUNX2, and BMP2 showed no significant differences between groups. Immunofluorescence confirmed positive expression of OPN, OCN, and COL1A1, validating the osteogenic capacity of the model. Preliminary data on the interaction between breast cancer spheroids and the bone model will also be presented.

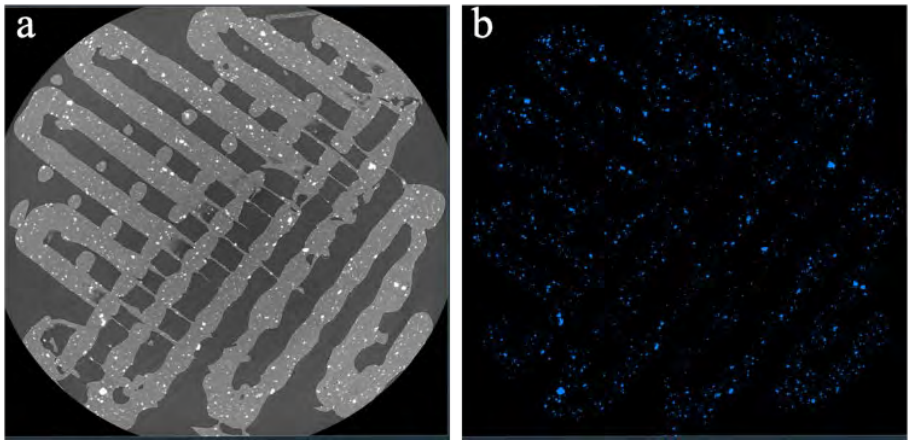

Fig *1*. µCT analysis of scaffolds. (a) Top-down view of the 3D printed scaffold architecture, where bright spots indicate the presence of hydroxyapatite particles within the polymer matrix. (b) HA particles (blue) segmented from the scaffold for mineral content quantification.

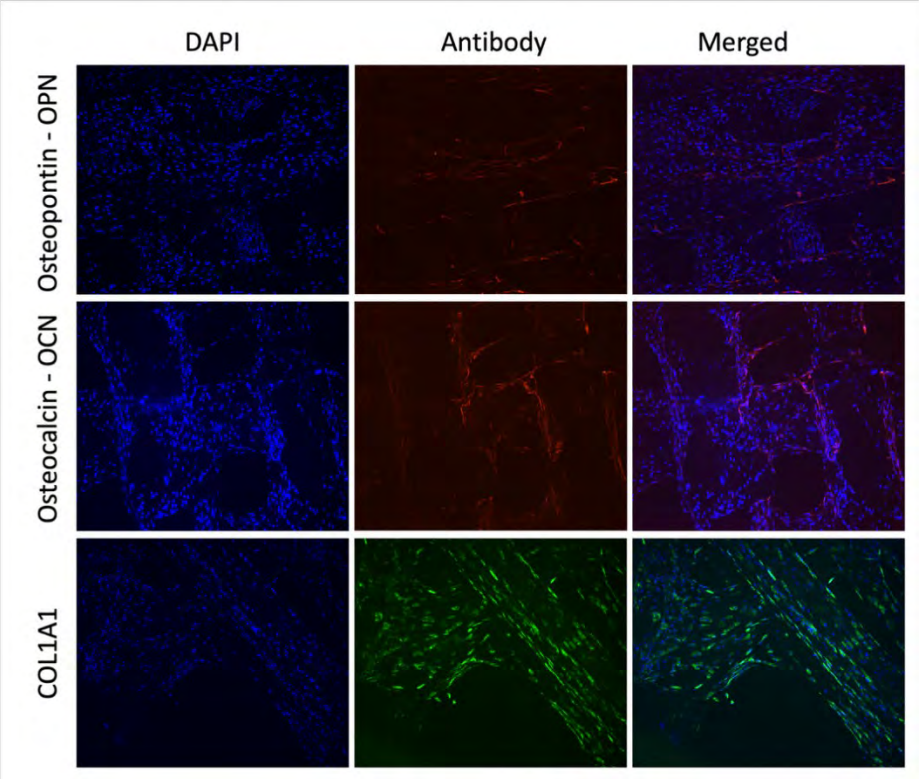

Figure 2. Immunofluorescence staining of HA-PLGA collagen scaffolds after 28 days of culture in osteogenic medium, showing the staining for osteopontin (OPN), osteocalcin (OCN), and collagen type I (COL1A1). DAPI nuclear staining (blue), antibody-specific staining (red for OPN and OCN; green for COL1A1), and merged images, confirming positive expression of key osteogenic proteins within the engineered bone model.

Conclusion

HA-PLGA scaffolds support osteogenic differentiation of BM-MSCs, with collagen type I further enhancing this by providing a more biomimetic environment. The collagen-enhanced model exhibited superior mineralisation and earlier expression of osteogenic markers, supporting its suitability as a functional 3D bone model. This platform offers a promising in vitro alternative aligned with the 3Rs principles for studying breast cancer metastasis to bone. Future work will integrate breast cancer cells and fluidic systems to recapitulate the metastatic niche.

References

[1]K. S.Higgins, A. J.Yu, and C. T.Gomillion. 3D *In Vitro* Models of Breast Cancer: Current Challenges and Future Prospects Toward Recapitulating the Microenvironment and Mimicking Key Processes. Advanced Biology (2025); 9; no. 11: e00846.

[2]Z. Ebrahimi, S. Irani, A. Ardeshirylajimi, E. Seyedjafari. Enhanced osteogenic differentiation of stem cells by 3D printed PCL scaffolds coated with collagen and hydroxyapatite. Scientific Reports (2022); 12(1); 12359.

S21 - O5

Matrix stiffness modulates estrogen receptor signalling and endocrine therapy response in patient-derived breast cancer models

Koikalethu A.T.[1], Adams M.N.[1], Morenc M.[1], Reinhardt J.[1], Thompson, E.W.[1], Bock N.[1]
[1]School of Biomedical Sciences, Faculty of Health, Queensland University of Technology (QUT) and Translation Research Institute (TRI), Brisbane; [2]Centre for Biomedical Technologies, QUT, Brisbane; [3]Max Planck Queensland Centre, Brisbane; [4]Centre for Genomics and Personalised Health, QUT, Brisbane, Australia

Introduction

Breast cancer progression is governed by dynamic interactions between biochemical signalling and the mechanical properties of the tumour microenvironment (TME). In hormone responsive disease, estrogen receptor (ER) signalling forms the basis of endocrine therapy, the primary treatment for ER-positive (ER+) tumours. However, progressive stiffening caused by extracellular matrix remodelling can influence cellular behaviour and therapeutic response. Despite growing recognition of mechanotransduction in cancer biology, most in vitro models assess hormonal signalling without physiologically relevant mechanical context. This limitation is particularly pronounced in patient-derived systems where matrix properties are rarely controlled. Here, we investigate how matrix stiffness influences ER signalling and endocrine therapy response using a tuneable three-dimensional (3D) culture platform.

Materials and Methods

A photopolymerizable gelatin methacryloyl (GelMA) hydrogel system was employed to generate 3D matrices spanning physiologically relevant stiffness ranges. ER+ breast cancer cell lines and patient-derived breast tumour spheroids were encapsulated under defined estrogen supplementation conditions. Cell viability, metabolic activity and proliferation were quantified across stiffness conditions. Nuclear morphology and cytoskeletal organisation were assessed. ER expression and estrogen responsive transcription were measured using immunofluorescence and gene expression analysis. Mechanotransduction pathways were interrogated through analysis of cytoskeletal and signalling regulators, including CK8/18ROCK1/2 and YAP.

Results

Matrix stiffness emerged as a key regulator of endocrine responsiveness. Cell line spheroids exhibited stiffness-dependent metabolic ad transcriptional adaptations, including altered expression of CK8/19, ROCK1/2 and YAP. These changes were accompanied by stiffness dependent shifts in proliferation, nuclear morphology and estrogen-responsive gene expression. In contrast, patient-derived spheroids displayed pronounced heterogeneity and responses that were largely inverse to those observed in cell lines, with distinct ER expression patterns and sensitivity to combined mechanical and hormonal cues. Notably, increased matrix stiffness attenuated the efficacy of ER blockade in selected patient samples sustaining metabolic activity despite endocrine therapy.

Conclusion

This study demonstrates that tumour mechanics are a critical determinant of endocrine therapy response in breast cancer. Integrating tuneable biomaterials with patient-derived models provide a physiologically relevant platform to interrogate biochemical and biophysical interactions governing endocrine signalling and highlight the importance of mechanical context in predictive cancer drug testing.

Acknowledgements

Funding from Max Planck Queensland Centre for Materials Science of Extracellular Matrices, Advance Queensland, Tour De cure, TRI and Australian Research Council is acknowledged.

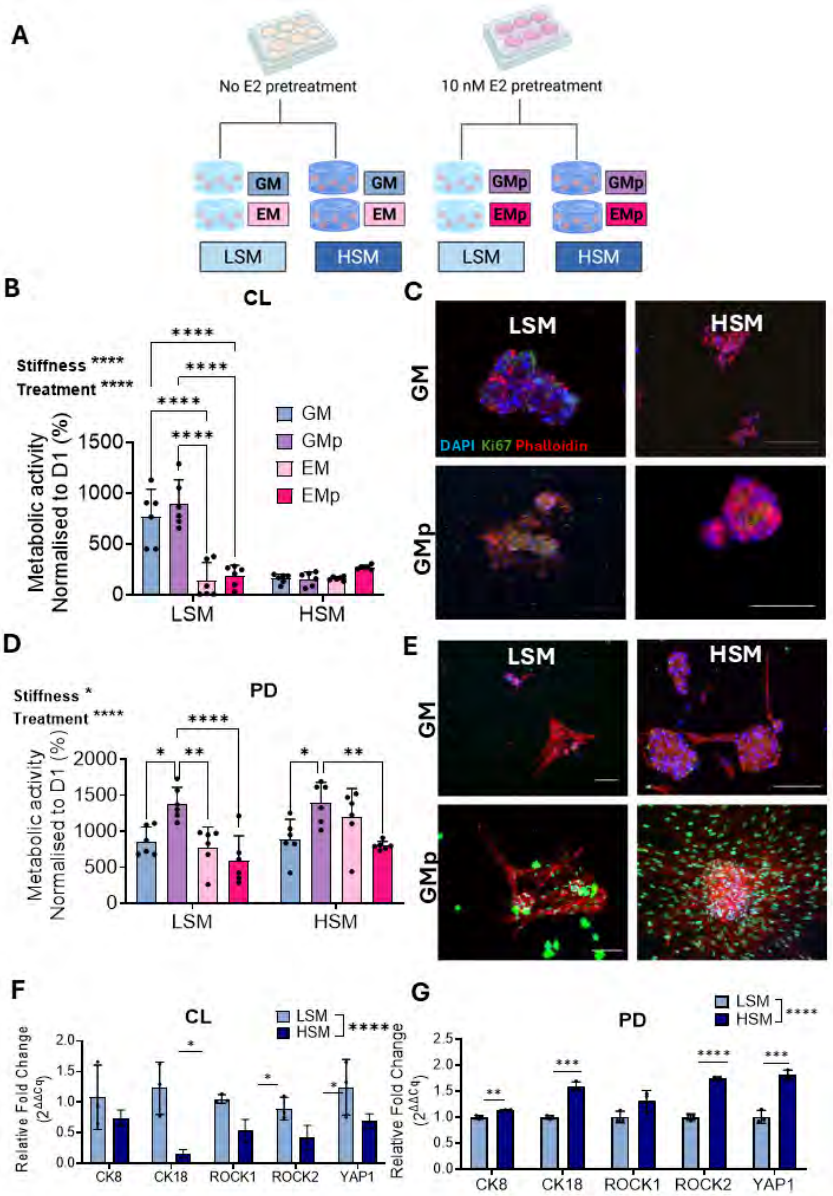

Figure 3:Influence of stiffness, pretreatment and continual exposure to estrogen in 3D cell line and patient-derived spheroids (A) Schematic outlining of the experimental design for eight treatment groups, combining hydrogel stiffness, (Low stiffness matrix (LSM) or High Stiffness Matrix (HSM), estrogen pretreatment status (pretreated (p) or unpretreated), and continual supplementation (continued: EM or withdrawn: GM). Created with Biorender.com. (B) Metabolic Activity for CL spheroids of all treatment groups at Day 7 normalized to Day 1 (Mean + SD, n = 6; two-way ANOVA) (C) Representative immunofluorescence images of CL spheroids stained for the proliferation marker Ki67 (green) and actin filaments (red). Scale bar = 100 µm. (D) Metabolic Activity for PD spheroids of all treatment groups at Day 7 normalized to Day 1 (Mean + SD, n = 6; two-way ANOVA) (E) Representative immunofluorescence images of PD spheroids stained for the proliferation marker Ki67 (green) and actin filaments (red). Scale bar = 100 µm (F) Gene expression analysis (qPCR) showing the relative fold change of CK8, CK18, ROCK1, ROCK2, and YAP1 in CL spheroids cultured in LSM versus HSM (Mean ± SD, two-way ANOVA) (G) Gene expression analysis (qPCR) showing the relative fold change of CK8, CK18, ROCK1, ROCK2, and YAP1 in PD02 spheroids cultured in LSM versus HSM (Mean ± SD, two-way ANOVA) For all tests, statistical significance was indicated by *p < 0.05 *p < 0.01, ***p < 0.001, ****p < 0.0001. PD spheroids stained for the proliferation marker Ki67 (green) and actin filaments (red). Scale bar = 100 µm. For all tests, statistical significance was indicated by *p<0.05 *p < 0.01, ***p < 0.001, ****p < 0.0001.

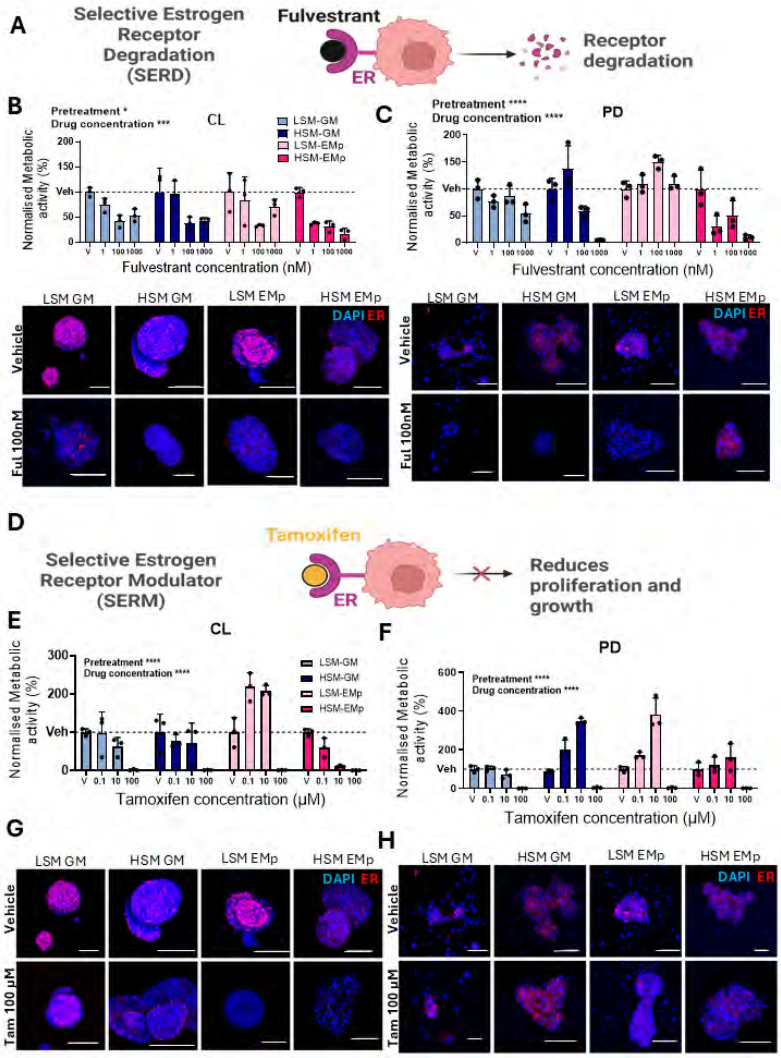

Figure 4: Influence of Endocrine Therapy on CL and PD spheroids (A) Schematic showing mechanism of action of SERD (Fulvestrant). Created with Biorender.com. (B) Metabolic activity of CL spheroids in LSM and HSM, with or without estrogen, following 4 days of treatment with varying concentrations of fulvestrant (Mean + SD, n = 6; two-way ANOVA). Representative immunofluorescence images of CL spheroids stained for ER (Red) following vehicle or 100 nM fulvestrant treatment. Scale bar = 100 µm. (C) Metabolic activity of PD spheroids in LSM and HSM, with or without estrogen, following 4 days of treatment with varying concentrations of fulvestrant (Mean + SD, n = 6; two-way ANOVA). Representative immunofluorescence images of PD spheroids stained for ER (Red) following vehicle or 100 nM fulvestrant treatment. Scale bar = 100 µm. (D) Schematic showing mechanism of action of SERM (Tamoxifen). Created with Biorender.com. (E) Metabolic activity of CL spheroids in LSM and HSM, with or without estrogen, following 4 days of treatment with varying concentrations of fulvestrant (Mean + SD, n = 6; two-way ANOVA). Representative immunofluorescence images of CL spheroids stained for ER (Red) following vehicle or 100 nM tamoxifen treatment. Scale bar = 100 µm. (F) Metabolic activity of PD spheroids in LSM and HSM, with or without estrogen, following 4 days of treatment with varying concentrations of tamoxifen (Mean + SD, n = 6; two-way ANOVA). Representative immunofluorescence images of PD spheroids stained for ER (Red) following vehicle or 100 µM tamoxifen treatment. Scale bar = 100 µm. For all tests, statistical significance was indicated by *p<0.05 *p < 0.01, ***p < 0.001, ****p < 0.0001.

S21 - O6

Biodegradable PLLA platform for curcumin delivery in breast cancer: Evaluation in 2D and 3D models

Schiera V.[1], Rigogliuso S.[2], Poma P.[2], Brucato V.[1], Carfì Pavia F.[1]
[1]Dept. of Engineering, University of Palermo; [2]Dept. of Biological, Chemical and Pharmaceutical Sciences and Technologies (STEBICEF), University of Palermo, Italy

Introduction

Breast cancer remains one of the leading causes of cancer-related mortality worldwide, highlighting the need for innovative therapeutic strategies able to overcome the limitations of conventional treatments, including multidrug resistance[1]. Curcumin (Cur), a natural polyphenolic compound derived from *Curcuma longa*, has shown promising anticancer activity but its clinical use is limited by low bioavailability and rapid metabolism. Polymeric drug delivery systems represent a promising strategy to enhance the stability and controlled release of such bioactive molecules[2].

Aim

This study aimed to develop a biodegradable Poly(L-Lactic Acid) (PLLA) platform for sustained curcumin delivery to enhance its therapeutic potential against breast cancer.

Materials and Methods

The polymeric system was fabricated by thermally induced phase separation (TIPS) from a ternary solution of PLLA, ultrapure water, and 1,4-dioxane. Cylindrical samples (diameter 4mm, thickness 2mm) were then loaded with Cur (purity ≥94%, curcuminoid content ≥80%) via solvent casting using an ethanol solution (0.15 wt% of Cur). The resulting samples were characterized by Raman spectroscopy, scanning electron microscopy, and calorimetric analysis. *In vitro* curcumin release was monitored by UV–Vis spectroscopy. The anticancer activity of the system was evaluated using human breast cancer MCF-7 cells, including both doxorubicin-sensitive and resistant lines. Therapeutic performance was assessed in both 2D monolayer cultures and 3D tumour-like *in vitro* model.

Results

The polymeric platform exhibited a well-defined interconnected porous architecture, which remained morphologically stable after the curcumin loading. Raman spectroscopy confirmed the homogeneous distribution of Cur within the polymer matrix and suggested interactions with PLLA. These interactions enabled a sustained and controlled release profile over time, as confirmed by UV-Vis release studies.
Biological assays demonstrated that the produced platform can induce cell death in both 2D and 3D models. Notably, the 3D model provided a more physiologically relevant environment, allowing a more comprehensive evaluation of the therapeutic response of cancer cells.

Conclusion

The developed polymeric platform enables the sustained delivery of Cur. Evaluating it in 3D breast cancer models provided a more physiologically relevant assessment of the therapeutic response, highlighting its potential for localised breast cancer therapy.

References

1 Harbeck N., Penault-Llorca F., Cortes J., Gnant M., Houssami N., Poortmans P., Ruddy K., Tsang J., Cardoso F. Breast cancer. Nature Reviews Disease Primers 2019; 5; 66.
2 Liu Y., Shi Y., Zhang M., Han F., Liao W., Duan X. Natural polyphenols for drug delivery and tissue engineering construction: A review. International Journal of Biological Macromolecules 2022; 199; 1–17.

S22
Biomaterials for wound healing opportunities and challenges to solve clinical needs

S22 – K1

Racan F.
Charité - Universitätsmedizin Berlin – Germany

S22 – O1

New plant-based nanovesicles based on alkyl polyglucosides surfactants and β-sitosterol as topical drug delivery systems

Alcaina-Hernando M.[1,2], Ferraboschi I.[3], Huck-Iriart C.[4], Bianchera A.[5], Pedersen J.S.[6], Ferrer-Tasies L.[1], Pescina S.[5], Sissa C.[3], Ventosa N.[2,7], Córdoba A.[1]
[1]Nanomol Technologies S.L., Bellaterra, Spain; [2]Institut de Ciència de Materials de Barcelona (ICMAB-CSIC), Bellaterra, Spain; [3]Dept. of Chemistry, Life Sciences and Environmental Sustainability, University of Parma, Italy; [4]ALBA Synchrotron Light Source, Cerdanyola del Vallès, Spain; [5]Dept. of Chemistry, Life Sciences and Environmental Sustainability, University of Parma, Italy; [6]Dept. of Chemistry and Interdisciplinary Nanoscience Center (iNANO) Aarhus University, Denmark; [7]Centro de Investigación Biomédica en Red de Bioingeniería, Biomateriales y Nanomedicina, Instituto de Salud Carlos III, Bellaterra, Spain

Introduction

Most of the delivery systems (DSs) used in healthcare are not suitable for vegan consumers or patients, so there is the need of new DSs. We present a new platform of nanovesicles (NVs) formed by self-assembly of β-Sitosterol (Sit) and alkyl polyglucosides, biodegradable and biocompatible components from vegetal origin. They can integrate and deliver topically a large variety of hydrophobic and hydrophilic payloads, presenting here new results on their functionality after encapsulation.

Materials and Methods

NVs were formulated combining Sit and alkyl polyglucosides using DELOS technology, a sustainable production method based on compressed fluids[1,2]. Physicochemical characterization was carried out, size, PdI, surface charge (DLS-ELS), morphology (CryoTEM and SAXS), and stability. Skin compatibility was evaluated using *in vitro* reconstructed epidermis models. The loading of different payloads such as hydrophilic proteins (growth factors) or hydrophobic molecules (α-tocopherol (TCP) or 7-dehycrhocolesterol (7-DHC)) and their functionality after encapsulation was assed by different techniques. Finally, skin penetration in porcine ear explants was determined with multiphoton microscopy.

Results

For the first time, small unilamellar NVs have been produced combining Sit with different types of alkyl polyglucoside surfactants as membrane components[3,4]. The combination of Sit with Lauryl Glucoside (LGL), a neutral charged surfactant, and Lauryl Glucose Carboxylate (LGC), a negatively charged surfactant, at different molar ratios allowed the tunning of a nanovesicular platform with different physicochemical properties (from size of 220 to 150 nm and surface charge from -40 mV to -70 mV). The loading capacity of these new NVs has been tested with growth factors and small hydrophobic molecules like TCP and 7-DHC and in all cases it has been seen that they maintained their functionality after encapsulation through specific functional assays for each payload. At physicochemical level they presented similar properties compared to blank NVs. *In vitro* assays with reconstructed human epidermis showed that the novel delivery platform is compatible with the skin and non-irritant. Finally, *ex vivo* skin retention studies showed that the NVs seem to penetrate down to epidermis without reaching the dermis.

Conclusion

A new drug delivery platform has been developed, using plant-derived ingredients that self-assemble in stable small unilamellar NVs. This novel delivery platform is completely biocompatible with the skin and can help to the retention of loaded actives in the epidermis, important characteristics for topical delivery applications in pharma and cosmetics. Thus, covering an unmet need for vegan patients and consumers.

Acknowledgements

This work was supported by grants of Industrial Doctorates Plan of Ministerio de Ciencia e Innovaci´on (DIN2019–010396) and Industrial Doctorates Plan of Agaur-Generalitat de Catalunya (2020 DI 14). The research leading to these results has also received funding from the European Union's Horizon 2020 research and innovation programme under the Marie Skłodowska-Curie grant agreement No 712949 (TECNIOspring PLUS) and from the Agency for Business Competitiveness of the Government of Catalonia. This project has received funding from the European Union's Horizon 2020 research and innovation programme under the Marie Sklodowska–Curie grant agreement number 101007804 (Multifunctional nanocarriers for nonlinear microscopy: new tools for biology and

medicine (Micro4Nano)). This project has received funding from the European Union´s Horizon 2020 research and innovation programme under grant agreement no. 101004728 via the TamaTA-INNOV call for access to the BL11-NCD-SWEET beamline from the ALBA synchrotron. The work has also been supported by the Spanish Ministry of Science and Innovation through grants "MOL4BIO" (PID2019–105622RB-I00), "ARMONIA" (PID2022–137332OB-I00) and the FUNFUTURE-FIP-2020 Severo Ochoa project, and by the Generalitat de Catalunya through grant 2021 SGR 00438.

References

[1]I. Cabrera, et al., Multifunctional nanovesicle-bioactive conjugates prepared by a one-step scalable method using CO2-expanded solvents, *Nano Lett* 2013, 13, 3766–3774,

[2]J. Merlo-Mas, et al., Application of Quality by Design to the robust preparation of a liposomal GLA formulation by DELOS-susp method, *The Journal of Supercritical Fluids* 2021, 173, 105204.

[3]Patent Application Number: WO2024028283. A. Córdoba. (2023)

[4]M. Alcaina-Hernando, et al., A new plant-based drug delivery platform based on alkyl polyglucosides and β-sitosterol nanovesicles for topical delivery, *Applied Materials Today* 2024, 41, 102467.

S22 - O2

Multifunctional Quatsome-based nanomedicines: A versatile platform for protected biomolecule delivery and advanced wound care

Guasch E.[1,2,] Ferrer-Tasies L.[1,2,3], Cabrera-Puig I.[1,2], González-Mira E.[1,2], Ballell-Hosa L.[1,2,3], Castellar-Álvarez C.3, Córdoba A.3, Merlo-Mas J.[3], Moreno-Calvo E.[1,2], Tomsen-Melero J.[1,2], Köber M.[1,2], Ratera I.[1,2], Sala S.[3]; Veciana J.[1,2,3], Ventosa N.[1,2,3]

[1]ICMAB-CSIC, Cerdanyola del Vallès; [2]CIBER-BBN, Madrid; [3]Nanomol Technologies SL, Cerdanyola del Vallès, Spain

Introduction

Chronic wound healing is often hindered by impaired tissue regeneration due to a hostile proteolytic environment. Conventional therapies frequently fail to provide sustained bioactivity of growth factors at the wound site, necessitating multifunctional approaches that can ensure effective delivery and protection of therapeutic agents.

Aim

In this study, we present a nanomedicine candidate designed to enhance regenerative therapies by exploiting the active role of the nanocarrier. The strategy utilizes nanovesicles composed of cholesterol and surfactants (quatsomes, QS) for the delivery of Recombinant Human Epidermal Growth Factor (rhEGF). While initial research has focused on understanding the platform's intrinsic properties and its therapeutic efficacy, current efforts involve its clinical translation through the development of patient-friendly formats, such as hydrogels and sprays, to expand therapeutic options.

Materials and Methods

This nanomedicine candidate was synthesized using the green DELOS-susp methodology [1,2], a one-step and easily scalable process that enables stable electrostatic conjugation of rhEGF. Cytotoxicity and safety of the rhEGF-loaded Quatsomes were validated using in vitro dermal irritancy tests (Episkin). Protection against protease degradation and cellular proliferation were assessed in vitro and ex vivo. Therapeutic efficacy was validated in diabetic mouse models and a clinical pilot study with Diabetic Foot Ulcer (DFU) patients [3]. Advanced application forms, including hydrogels and sprayable dispersions, were developed by incorporating the nanovesicles into biocompatible polymeric matrices.

Results

The QS scaffold demonstrated excellent biocompatibility and reduced cytotoxicity compared to free surfactants, while providing additional functional benefits that complement the growth factor's action. Crucially, the platform shielded rhEGF from enzymatic degradation, maintaining its bioactivity in proteolytic environments. Nanostructuration of rhEGF on the Quatsome surface further promoted dimerization-dependent signaling, enhancing regenerative potential compared to the free protein. Clinically, full re-epithelialization or significant wound reduction was observed in DFU patients after 12 weeks [3]. The successful incorporation of the nanovesicles into hydrogels and sprayable systems was achieved, maintaining the structural integrity and stability of the platform.

Conclusions

This nanomedicine candidate ensures the enhanced stability and bioactivity of protected rhEGF, offering a clear advantage over free biomolecules for tissue regeneration. The robust scale-up potential of the DELOS-susp process, combined with the transition to patient-ready formats like gels and sprays, highlights the platform's readiness for clinical translation. Furthermore, the versatile nature of the QS scaffold opens new therapeutic possibilities, acting as a modular and synergistic system for the protected delivery of other biomolecules.

References

[1]Köber M, Illa-Tuset S, Ferrer-Tasies L, et al. Stable nanovesicles formed by intrinsically planar bilayers. J. Colloid Interface Sci.. 2023;631:202-211

[2]Córdoba A. Method for obtaining nano-disperse systems. Patent WO2026032777 2026; Feb 12; 1-58

[3]Ferrer-Tasies L., Santana H., Cano-Sarabia M., et al. Recombinant human epidermal growth factor/quatsome nanoconjugates: a robust topical delivery system for complex wound healing. Adv. Therap. 2021; 4; 2000260.

S22 – O3

A bioactive three-layered ECM-based hydrogel for enhanced wound healing and skin regeneration

Pleguezuelos-Beltrán P.[1,2,3], Chocarro-Wrona C.[1,2,3], López de Andrés J.[1,2,3], Antich C.[1,3,4], de Vicente J.[5], Gálvez-Martín P.[6], López-Ruiz E.[2,3,7], Marchal J.A.[1,2,3]

[1]BioFab i3D - Biofabrication and 3D (bio)printing laboratory, Dept. of Human Anatomy and Embryology, University of Granada, Spain; [2]Biopathology and Regenerative Medicine Institute (IBIMER), Center for Biomedical Research (CIBM), University of Granada, Spain; [3]Instituto de Investigación Biosanitaria ibs.GRANADA, University Hospitals of Granada, University of Granada, Spain; [4]National Center for Advancing Translational Sciences, National Institute of Health, Rockville, USA; [5]F2N2Lab, Magnetic Soft Matter Group, Dept. of Applied Physics, University of Granada, Spain; [6]Bioibérica S.A.U., Barcelona, Spain; [7]Dept. of Health Sciences, University of Jaén, Spain

Introduction

Skin tissue engineering (TE) aims to develop substitutes for damaged skin, yet conventional approaches often lack the complexity required to replicate the structure and function of native skin. To address these limitations, 3D biofabrication strategies are being explored to enhance biomimicry in engineered skin models. However, most substitutes focus on recreating dermal and epidermal layers while neglecting the hypodermis, which plays a key role in epidermal differentiation and provides mechanical and thermoregulatory support. In this study, we developed biomimetic hydrogels to biofabricate a three-layered (BT) skin substitute based on the main extracellular matrix (ECM) components of the epidermal, dermal, and hypodermal layers, aiming to better replicate native skin structure and function.

Materials and Methods

Hydrogels for dermal and hypodermal layers were based on agarose and type I collagen supplemented with ECM components (dermatan sulfate, hyaluronic acid, and elastin) and loaded with human dermal fibroblasts (hDFs) or human mesenchymal stromal cells (hMSCs), respectively. The epidermal hydrogel was formulated using type I collagen supplemented with keratin and sphingolipids and seeded with human epidermal keratinocytes (hEKs). After evaluating the physicochemical, mechanical, and biological properties of the formulations, a three-layered BT Skin substitute was biofabricated and characterized in vitro, and its wound healing potential was assessed in a full-thickness murine skin wound model.

Results

Physicochemical analyses showed that each hydrogel formulation presented suitable viscosity, gelation time, and pH. The BT Skin exhibited favorable swelling and degradation kinetics and mechanical properties within the range of human skin. Both individual hydrogels and the complete BT Skin model showed high cell viability and stable metabolic activity over three weeks while maintaining the integrity of the three-layered structure. Both cell-free and cell-loaded BT Skin demonstrated strong wound healing capacity in vivo, promoting faster wound closure than autografting, restoring skin barrier integrity and homeostasis parameters, and supporting effective dermal and epidermal regeneration.

Conclusion

This bioactive and biomimetic three-layered BT Skin incorporates cells and biomolecules characteristic of epidermal, dermal, and hypodermal layers to better replicate the native skin ECM. The construct supports wound healing and skin regeneration by restoring skin homeostasis and barrier function, showing strong potential for applications in skin TE and wound healing therapies, including burn and chronic wound treatment. Additionally, BT Skin may serve as a versatile in vitro platform for skin biology studies, drug testing, and disease modeling.

S22 – O4

Beyond traditional wound dressings: Glucose-responsive poly(ether urethane)-based patches patient-personalized through AI- and XR-technologies

Laurano R.[1], Secco J.[2], Ulrich L.[3]

[1]Dept. of Mechanical and Aerospace Engineering, Politecnico di Torino, Turin, Italy; [2]Dept. of Electronics and Telecommunications, Politecnico di Torino, Turin, Italy; [3]Dept. of Management and Production Engineering, Politecnico di Torino, Turin, Italy

Introduction

Diabetic foot ulcers (DFUs) represent a growing and costly public health burden worldwide, with significant implications for patient quality of life and healthcare sustainability. The major challenge in DFU management lies in the lack of patient-personalization characterizing currently available commercial wound dressings. In this regard, the advancement in multi-stimuli-responsive biomaterial design, AI-guided analyzes and XR-based customization tools can bring high potential in the development of personalized treatments.

Aim

To engineer a glucose-responsive drug-loaded biomaterial ink for the 3D extrusion of personalized patches to smartly treat DFUs.

Materials and Methods

An amphiphilic poly(ether urethane) bearing secondary amines was synthesized according to a two-step procedure and functionalized with 3-carboxyphenylboronic acid through water-based carbodiimide chemistry. Size Exclusion Chromatography (SEC), infrared (IR) and Nuclear Magnetic Resonance (NMR) spectroscopies and a colorimetric assay were used to chemically characterize the polymer (G-DHP407). Swelling tests were conducted on G-DHP407 hydrogels in wound-simulated conditions. The potentialities as smart drug carrier were investigated by encapsulating hydrophobic and hydrophilic model drugs and controlling their release in response to glucose levels (range: 0.5-4mg/mL). G-DHP407 hydrogel processing in complex 3D patches was assessed by extruding different structures. The cytocompatibility was tested according to the ISO10993:5.

Results

SEC, IR and NMR first confirmed the synthesis of a high molecular weight poly(ether urethane) (Mn 20kDa) bearing 1E19 -NH/$g_{polymer}$. Then, carbodiimide-mediated functionalization revealed a feed-dependent glucose-responsive molecule grafting, giving 1E18 units/$g_{polymer}$ in the optimal -COOH:-NH molar ratio. G-DHP407 hydrogels showed: (i) high stability in contact with fluids (i.e., ca. 20% dry weight loss at 7 days); (ii) capability to encapsulate both hydrophobic (Ibuprofen) and hydrophilic (ibuprofen sodium salt) drugs (at concentration indicated by AI-analyses) within the micellar network and, (iii) release the payload in response to glucose levels for up to 5 days without burst release. Moreover, G-DHP407 processability in 3D patches characterized by patient-specific morphologies as designed through XR-technologies was assessed by extruding structures of different shapes. Lastly, G-DHP407 formulations were found to be cytocompatible (i.e., cell metabolic activity > 98%) when tested on a 2D monolayer of murine fibroblasts.

Conclusion

By enabling both therapeutic and morphological personalization, the engineered patch seeks to overcome the main limitations of commercial products and drastically increase the healing outcomes in the management of DFUs.

Acknowledgements

This work was financed by PERSEUS project (Patient-specific engineering of smart responsive wound dressings for enhanced diabetic foot ulcer management through AI- and XR-technologies) with the support of Politecnico di Torino, Fondazione Compagnia San Paolo and Fondazione CRT.

S22 - O5

Cannabidiol-loaded PLGA nanoparticles prepared by microfluidics for burn wound treatment

Echevarria-Torres P.L.[1,2,3], Palao-Suay R.[1,2], Benito-Martínez S.[2,4,5], Pascual G.[2,4,5], García-Fernández L.[1,2], Rojo L.[1,2], Rancan F.[6], Aguilar M.R[1,2]

[1]Instituto de Ciencia y Tecnología de Polímeros (ICTP), CSIC, Madrid, España; [2]CIBER de Bioingeniería, Biomateriales y Nanomedicina, Instituto de Salud Carlos III, (CIBER-BBN, ISCIII), Madrid, España; [3]Dept. de Bioquímica y Biología Molecular, Facultad de Ciencias Químicas, Universidad Complutense de Madrid, Madrid, España; [4]Dept. de Medicina y Especialidades Médicas, Facultad de Medicina y Ciencias de la Salud, Universidad de Alcalá, Alcalá de Henares, España; [5]Instituto Ramón y Cajal de Investigación Sanitaria (IRYCIS), Madrid, España; [6]Dept. Dermatology, Venereology and Allergology, Clinical Research Center for Hair and Skin Science, Charité - Universitätsmedizin Berlin, Germany.

Introduction

Burn wound healing is influenced by cytokine signalling, oxidative stress, and microbial infection[1]. Cannabidiol (CBD) shows antioxidant, anti-inflammatory and antimicrobial effects, but its therapeutic potential is limited by low solubility and poor bioavailability[2]. Here CBD-loaded poly(lactic-co-glycolic acid) (PLGA) nanoparticles (CBD-NPs) were obtained by microfluidics and characterized physicochemically and biologically in the burn wound healing context.

Materials and Methods

PLGA (5 mg/mL) and CBD (1.5, 3 and 5% w/w) were mixed with water (1:3, v:v, 4 mL/min) in a staggered herringbone micromixer using a microfluidic mixer (Elveflow, France). CBD-NPs were dialyzed (72 h) and stored at 4 °C. Size and polydispersity (DLS), zeta potential (Doppler electrophoresis), morphology (SEM) and stability over 56 days were assessed. Loading capacity and release were quantified spectrophotometrically. Antioxidant (DPPH assay), cytocompatibility (AlamarBlue assay in RAW 264.7, HEK and HDF) and antibacterial activity against *Staphylococcus aureus* (inhibition test, MIC and MBC) were tested. Burn healing was evaluated in *ex vivo* human skin with standardized burns treated with vehicles, free CBD, CBD-NPs or Bepangel. Explants were cultured to 12 days with medium collection at days 0, 1, 4, 6, 8 and 12. Cytotoxicity (LDH assay) and cytokines (IL-1α, IL-1β, IL-6 and IL-8, ELISA) were analyzed at all time points, whereas histology (H&E) and re-vascularization (CD31 immunostaining) were evaluated at days 6 and 12.

Results

CBD-NPs shows ~130 nm, monodisperse distribution, negative charge and spherical morphology, stable for 56 days. CBD-NPs5 showed the highest encapsulation (82.2 ± 4.3%) and loading capacity (4.11 ± 0.21%), with release peaking at 6 h. It shows antioxidant effect (EC50 0.026 mg/mL) with bacterial inhibition growth at 0.625 mg/mL maintained over 72 hours, MIC 0.313 mg/mL and bacteriostatic effects against *S. aureus*. Cytocompatibility was observed in cells and skin. CBD-NPs induce partial closure of the wound at day 12 (Figure 1) and accelerate CD31 expression at day 6 with reduction at day 12 (Figure 2). A decreasing trend for IL-8 at day 1, IL-1β from day 1 to 6, and IL-6 and IL-1α from day 1 to 12 was observed.

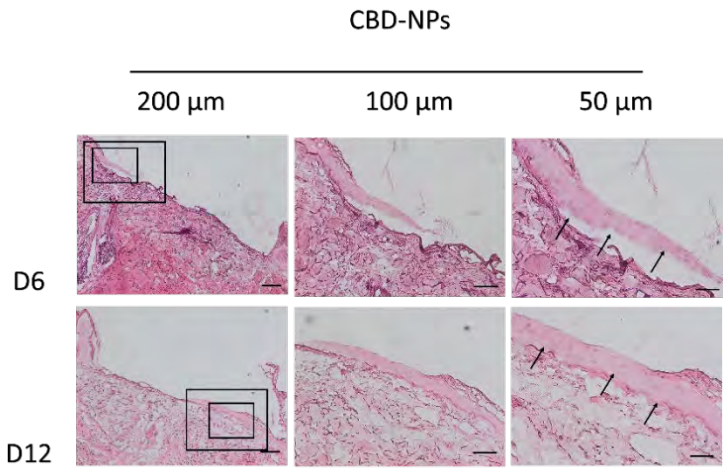

Figure 1. H&E micrographs taken in the wound centre.

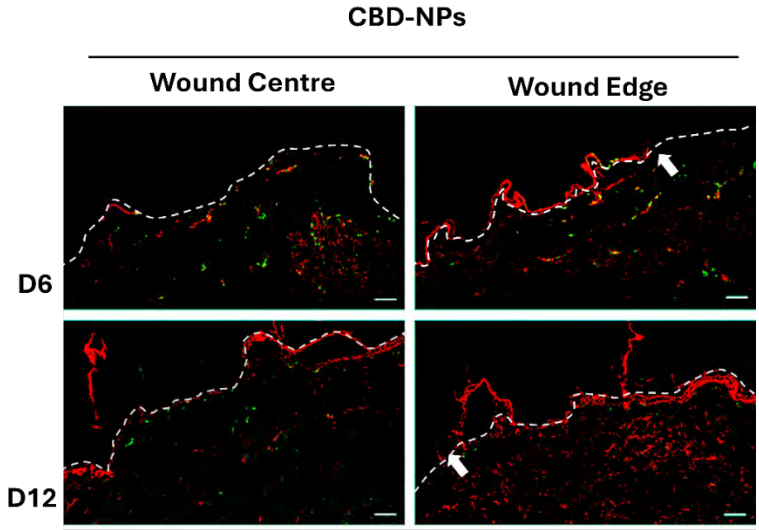

Figure 2. CD31 (green) immunostaining and PI nuclei staining (red) in the wound centre and edge. Dotted lines show the surface of the wound/skin. Arrows show the transition from skin wound. Scale bar 200 µm.

Conclusion

CBD-NPs synthesized via microfluidics demonstrated physicochemical stability and enhance burn wound healing through combined antibacterial, antioxidant, anti-inflammatory and pro-regenerative actions.

Acknowledgements

CAM (S2022/BMD-7406), MICINN (PID2020-114086RB-I00 and PRE2021-096868), MICIU PID2023-149301OB-I00

References

[1]Al-Mehdar AA, et al. 2026, 10.2147/JEP.S575002.
[2]Grifoni L, et al. 2022, 10.3390/MOLECULES27186070.

S22 – O6

SCOBY nanocellulose dressings enriched with L-carnosine for chronic wound care

Baran A.[1], Reczyńska-Kolman K.[1], Pamuła E.[1]
[1]Dept. of Biomaterials and Composites, Faculty of Materials Science and Ceramics, AGH University of Krakow, Poland

Introduction

Nanocellulose can be produced in the fermentation of black tea and sucrose by symbiotic culture of bacteria and yeast (SCOBY) [1]. This simple and cost-effective process provides nanocellulose with high liquid retention capacity that could be used as wound dressing [1]. L-carnosine is a low-cost dipeptide that has been reported to promote wound closure and reduce inflammation [2].

Aim

We aimed at producing and characterising dressing from SCOBY nanocellulose enriched with L-carnosine for chronic wounds.

Materials and Methods

The SCOBY pellicle was purified with 1.5M NaOH, bleached with 1.5% H_2O_2, washed in MilliQ water and freeze-dried. The resulting SCOBY nanocellulose was enriched with different amounts of L-carnosine. The swelling of the dressing was tested in FBS as an exudate-simulating liquid. Dressings were analysed by FTIR spectroscopy and SEM. The L-carnosine release profile was determined using a BCA protein assay. Cytocompatibility and cell proliferation studies were performed using the AlamarBlue assay and live-dead staining. A wound closure model in HaCaT keratinocytes and L929 fibroblasts was used to assess the effect of the dressing on cell proliferation. A direct observation of cell morphology was analysed by optical tomography (Nanolive).

Results

The results show that SCOBY nanocellulose is a transparent hydrogel and, after freeze-drying, forms a highly porous scaffold consisting of thin nanofibers (86 ± 19 nm in diameter). It can absorb a large amount of model exudate (FBS); at least 60 times its own weight. Release studies show that at an 8 h time point around 70% of L-carnosine is released followed by a sustainable delivery until 24 h. *In vitro* studies show satisfactory cytocompatibility of nanocellulose in contact with fibroblasts and keratinocytes as judged from metabolic activity, fluorescence staining, and label-free timelapse images of cells. The released L-carnosine promoted wound closure in the scratch assay in HaCaT and L929 cells.

Conclusion

SCOBY nanocellulose dressing is cytocompatible and effectively releases L-carnosine while absorbing wound exudate. It was found to enhance wound closure *in vitro;* thus, it has potential of being a more economical alternative to other active dressings due to low-cost components.

Acknowledgements

This study was supported by the Programme ‘Excellence Initiative – Research University” for AGH and by the National Science Centre, Poland (2025/57/B/ST5/01898).

References

[1]Sharma C. Biotransformation of fermented black tea into bacterial nanocellulose via symbiotic interplay of microorganisms. *International Journal of Biological Macromolecules*, 2019, 132, 166–177.

[2]Ansurudeen I. Carnosine enhances diabetic wound healing in the db/db mouse model of type 2 diabetes. *Amino Acids* 2012, 43, 127–134.

S22 - O7

Multifunctional 3D-printable biomaterials for enhanced wound repair

Nunes J.S.[1], Force Repair consortium[1]
[1]smart and multifunctional 3D printable pro-Regenerative biological matrix modulating mechanot Ransduction as advanced therapy to treat skIn chronic wounds (FORCE REPAIR), Horizon Europe grant n. 101092243.

Introduction

Chronic wounds are skin injuries that fail to heal properly due to persistent inflammation, bacterial colonization and exudate production. Current therapies present several limitations: most do not effectively combine tissue regeneration with infection and inflammation control; suitable animal models representing human chronic wounds are scarce; and personalized treatments tailored to patient and wound specific characteristics remain limited. As a result, existing approaches often do not address the multifactorial nature of chronic wound healing. In this way, this work aims to overcome these challenges by developing a smart, multifunctional and cost-effective 3D printed personalized wound dressing for the treatment of chronic wound (CW). The dressing is designed to control bacterial infection and inflammation, reduce skin tension, and promote tissue regeneration to accelerate healing.

Materials and Methods

Initial work focused on functionalizing the hyaluronic acid (HA) and selecting a sterile, printable hyaluronic-silver hydrogel as the base material. Three different inks were then developed: an antibiotic and an anti-inflammatory inks, each containing nanocapsules with therapeutics agents, and a proregenerative ink loaded with elastin-like peptide (ELP), Wharton Gel Complex (WGC) and innervation peptides to promote tissue regeneration. The effect of incorporating nanocapsules and active agents on hydrogel stability, rheology, and printability were evaluated. In vitro studies assessed cytotoxicity, antibacterial performance and neuronal growth support using relevant cell models. Bioadhesion tests with porcine dermal tissue examined tissue interaction. Finally, an acute wound model in piglets was used to evaluate the in vivo biocompatibility and therapeutic efficacy.

Results

All inks exhibited rheological properties suitable for injection and 3D printing, forming solids constructs easy to handle, without any post-processing crosslinking. All formulations significant bioadhesive properties. Stability studies revealed strong medium absorption, beneficial for exudate management, and enzyme-responsive degradation in the presence of hyaluronidase, reflecting chronic wounds conditions. In vitro, materials were non-cytotoxic and preserved fibroblast viability and morphology. The antibacterial ink successfully eradicated the polymicrobial biofilm comprised by *S. aureus* and *P. aeruginosa*. The proregenerative formulation enhanced neurite extension compared to HA alone. Finally, in vivo studies in acute wounds using the proregenerative ink showed a clear improvement in healing when compared to the control (normal dressing), with wounds already half-closed after just 5 days.

Conclusion

The biomaterials produced in this work exhibited key features required for multifunctional wound dressings and demonstrated strong in vitro and in vivo performance, offering a promising personalized and cost-effective solution for improved wound recovery.

Acknowledgements

This study was funded by the European Union, Horizon-CL4-2022-RESILIENCE-01 (Force Repair, 101092243).

S23
Biomaterials science lectureship symposium

S23 - K1
Engineering biomaterials for glucose-responsive diabetes therapy

Webber, M.J.
Chemical & Biomolecular Engineering, University of Notre Dame, IN USA

Introduction
Despite major advances in insulin formulations and diabetes technologies, achieving autonomous regulation of blood glucose remains a central challenge in diabetes therapy. Current approaches often fail to replicate physiological feedback control, contributing to risks of both hyperglycemia and hypoglycemia. Biomaterials that directly sense glucose and dynamically regulate therapeutic release offer a promising strategy to restore metabolic responsiveness. Here, we describe the development of glucose-responsive biomaterials that integrate dynamic-covalent chemistry, supramolecular self-assembly, and glucose-directed phase behavior to enable autonomous delivery of insulin or glucagon in response to changing glycemic conditions.

Aim
Engineer glucose-responsive biomaterials that autonomously regulate the delivery of insulin and glucagon, enabling long-lasting and physiologically adaptive diabetes therapy.

Materials and Methods
A range of glucose-responsive biomaterial platforms were engineered using phenylboronic acid (PBA) and high-affinity diboronate (DiPBA) glucose-binding motifs. Dynamic-covalent hydrogels were prepared through reversible boronate ester crosslinking, while insulin delivery systems were constructed through DiPBA-mediated complexation of insulin with diol-functionalized dendrimer carriers to form injectable nanocomplex depots. In parallel, glucose-responsive supramolecular assemblies and liquid–liquid phase-separated (LLPS) materials were designed to regulate glucagon release through glucose-dependent modulation of material stability. Material properties, glucose responsiveness, therapeutic release kinetics, and in vivo efficacy were evaluated using biochemical characterization and diabetic animal models.

Results
Glucose-responsive materials exhibited tunable assembly, phase behavior, and therapeutic release profiles across multiple delivery formats, including injectable depots (***Fig 1***). Dynamic-covalent hydrogels demonstrated reversible network remodeling and glucose-triggered modulation of cargo release. DiPBA-based insulin nanocomplexes formed stable depots under physiological conditions but underwent glucose-dependent dissolution through competitive glucose binding, resulting in accelerated insulin release during hyperglycemia. In streptozotocin-induced diabetic mice, a single administration restored normoglycemia and maintained glucose control for up to five days while preserving responsiveness to repeated glucose challenges. In diabetic swine, glucose-responsive insulin delivery maintained glycemic control for at least one week. Complementary LLPS and self-assembling glucagon systems exhibited glucose-dependent transitions that enabled hormone release under low-glucose conditions, providing a strategy for hypoglycemia prevention.

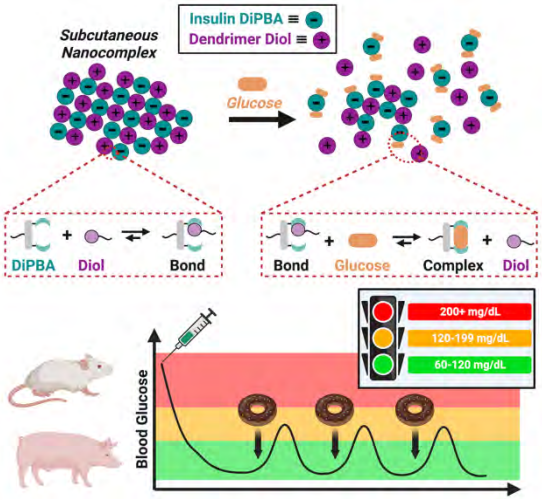

Fig 1: *Glucose-responsive complexes for long-term blood glucose control, demonstrated in mice and pigs.*

Conclusion
These studies demonstrate how molecular engineering principles can be leveraged to create biomaterials that dynamically interact with physiological glucose levels and autonomously regulate therapeutic delivery. By integrating dynamic-covalent chemistry, supramolecular assembly, and glucose-directed phase behavior, these

platforms provide long-lasting and metabolically responsive control over insulin and glucagon release. Such biomaterials represent a promising foundation for next-generation diabetes therapies capable of mimicking key aspects of endogenous glucose regulation.

S23 – O1

Assessing the humidity effects on fracture behavior in polycrystalline alumina: A microcantilever study and phase-field modeling of slow crack growth

Birocco M.[1], Erlacher A.[1], Minnert C.[1], Blugan G.[1], Gao C.[3], Michler J.[2], Schwiedrzik J.[1]
[1]Laboratory for High-Performance Ceramics, Empa, Swiss Federal Laboratories for Materials Science and Technology, Dübendorf, Switzerland; [2]Laboratory for Mechanics of Materials and Nanostructures, Empa, Swiss Federal Laboratories for Materials Science and Technology, Thun, Switzerland; [3]Dept. of Mechanical and Industrial Engineering, NTNU - Norwegian University of Science and Technology, Trondheim, Norway

Introduction

Due to its excellent chemical stability and biocompatibility, alumina is widely adopted for biomedical components, particularly in orthopedic and dental systems. Nevertheless, alumina is inherently brittle, and its fracture behaviour is influenced by environmental conditions. In particular, the presence of moisture promotes slow crack growth (SCG), progressively lowering the effective fracture resistance and potentially compromising the long-term reliability of components operating in physiological conditions.

Materials and Methods

The present work explores how slow crack growth (SCG) affects the fracture behavior of polycrystalline alumina at the microscale under a wide range of controlled humidity environments. Microcantilevers were prepared via laser ablation and plasma-focused ion beam milling and subsequently tested using a displacement-controlled nanoindenter in a controlled-humidity environment. To interpret the experimental observations, phase-field modeling was employed, incorporating SCG effects through a humidity-dependent degradation of the fracture properties derived from the observed Kp–RH trend.

Results

Examining the dependence of fracture resistance (Kp) on environmental humidity highlighted two distinct regimes following a sigmoidal trend. At low relative humidity (RH), the measured stress intensity factor at fracture Kp=2.53 MPa√m indicated negligible SCG activity. With increasing RH, SCG was clearly activated, with Kp decreasing to 1.92 MPa√m. The developed numerical model was able to accurately replicate the experimentally observed fracture behavior, reaching a Concordance Correlation Coefficient of 0.93. This outcome provides a first contribution toward the numerical modeling of SCG phenomena in brittle materials.

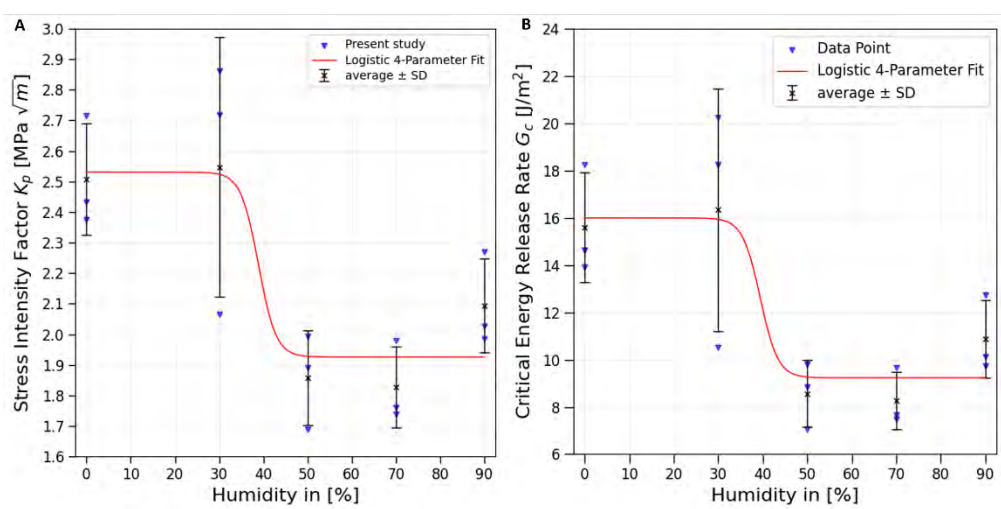

Conclusion

These results provide deeper insight into fracture behavior in bioceramics and introduce, for the first time, a numerical model aimed at describing SCG phenomena in brittle materials. They also support future model calibration and improved FEM-based predictive capabilities, ultimately contributing to the optimized design of components intended to operate in hydrated environments, such as dental implants and crowns.

Acknowledgements

This project has received funding from the European Union Horizon Europe research and innovation programme under the Marie Skłodowska-Curie (MSCA) grant agreement No 101120290 (GAP).

S23 – O2

Porous microcrystalline diamond bio-interfaces for ultrasensitive early detection of CEA and CYFRA 21-1 biomarkers

Joshi S.[1], Ramachandra Rao M.S.[2], Sudhakar S.[3], Arunachalam N.[1]
[1]Dept. of Mechanical Engineering, Indian Institute of Technology Madras; [2]Dept. of Physics, Nano Functional Materials Technology Centre and Materials Science Research Centre, Indian Institute of Technology Madras; [3]Dept. of Applied Mechanics and Biomedical Engineering, Indian Institute of Technology Madras, Chennai, India

Introduction

Early diagnosis of lung cancer relies on the reliable detection of protein biomarkers at extremely low concentrations in complex biological media. Sensitive detection of lung cancer biomarkers such as carcinoembryonic antigen (CEA) and cytokeratin-19 fragment (CYFRA 21-1) at sub-pg/mL levels remains challenging with existing electrochemical platforms[1]. Most two-dimensional electrodes, including metallic nanostructures and carbon-based materials, suffer from restricted bioreceptor loading, limited analyte transport, and surface fouling, leading to limits of detection that exceed clinically relevant thresholds. Boron-doped diamond (BDD)[2] is well known for its wide potential window, low interfacial capacitance, chemical robustness, and resistance to biofouling, making it attractive for bioelectronic sensing. However, conventional planar or porous BDD architectures still provide insufficient three-dimensional interface for achieving the sensitivity required for early-stage diagnosis[3].

Materials and Methods

In this work, we develop a three-dimensional BDD nanopillar interface by combining femtosecond laser patterning with microwave plasma chemical vapor deposition (MPCVD). Periodic micro-wells are first inscribed onto silicon substrates using femtosecond laser pulses (800 nm, 120 fs, 1 kHz), which serve as controlled nucleation sites for diamond growth. Subsequent MPCVD under CH_4/H_2 plasma (750°C, 2% CH_4) results in selective formation of boron-doped diamond nanopillars within these laser-defined regions. A post-growth acid treatment (HNO_3/HF, 3:1, 80°C, 24 h) eliminates graphitic and amorphous carbon, revealing clean nanopillars anchored within porous silicon cavities as shown in Figure 1. This architecture increases the effective surface area by approximately 50-100 times compared to flat BDD films.

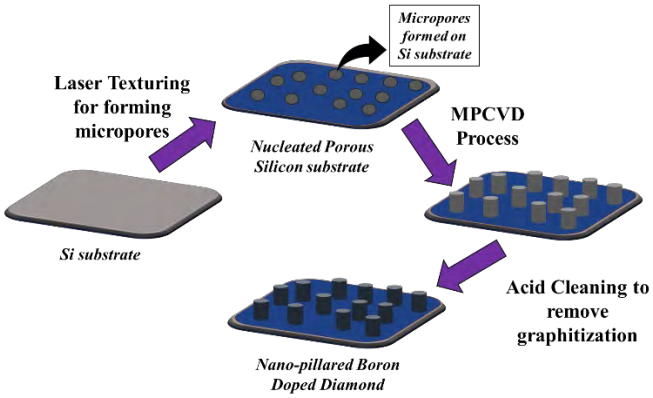

Figure 1: Schematic Diagram for fabricating Boron doped Nanopillars for Biosensing interfaces

Results

SEM revealed uniform nanopillar arrays with dramatic ~50-100× surface area enhancement over flat BDD, ideal for high-density bioreceptor loading. Raman spectroscopy confirmed pristine sp^3 diamond bonding with characteristic boron-doping Fano profile (~1300 cm^{-1} peak shift) and complete absence of graphitic D/G bands, ensuring superior electrochemical stability. FTIR displayed sharp N-H/O-H amination signatures alongside robust antibody conjugation peaks, validating stable bio-functionalization. Preliminary electrochemical transduction via steady-state current shifts from antigen-antibody binding demonstrated exceptional sensitivity across the clinically-critical 100 ng/mL–1 pg/mL CEA/CYFRA 21-1 range (full sub-pg/mL validation in progress).

Conclusion

The characterization validated 3D BDD nanopillar bio-interface which overcomes the 2D electrode limitations, delivering antifouling stability and 50-100x enhanced sensitivity for scalable point-of-care detection of lung cancer biomarkers CEA/CYFRA 21-1.

Acknowledgements

The authors thank the Ministry of India for the Prime Minister Research Fellowship for conducting this work.

References

1. Thomas, D. S.; Fourkala, E. O.; Apostolidou, S.; Gunu, R.; Ryan, A.; Jacobs, I.; Menon, U.; Alderton, W.; Gentry-Maharaj, A.; Timms, J. F. Evaluation of Serum CEA, CYFRA21-1 and CA125 for the Early Detection of Colorectal Cancer Using Longitudinal Preclinical Samples. *Br. J. Cancer 2015*, *113* (2), 268–274.
2. Zhou, Y.; Zhi, J. The Application of Boron-Doped Diamond Electrodes in Amperometric Biosensors. *Talanta*. Elsevier, *2009*, pp 1189–1196. 3. Li, X.; Li, H.; Li, M.; Li, C.; Sun, D.; Lei, Y.; Yang, B. Preparation of a Porous Boron-Doped Diamond/Ta Electrode for the Electrocatalytic Degradation of Organic Pollutants. *Carbon N. Y. 2018*, *129*, 543–551.

S23 – O3

Poly(alkylene terephthalate)s as a platform material for melt electrowriting

Van Daele L.[1], Braig J.[2], Brancart J.[3], Van Vlierberghe S.[1], Jungst T.[2], Dubruel P.[1]
[1]Polymer Chemistry and Biomaterials Group (PBM), Centre of Macromolecular Chemistry (CMaC), Dept. of Organic and Macromolecular Chemistry, Ghent University, Belgium; [2]Dept. of Functional Materials in Medicine and Dentistry, Institute of Biofabrication and Functional Materials, University of Würzburg and KeyLab Polymers for Medicine of the Bavarian Polymer Institute (BPI), Germany; [3]Physical Chemistry and Polymer Science (FYSC), Vrije Universiteit Brussel, Belgium

Introduction

Melt electrowriting (MEW) is a state-of-the-art additive manufacturing technique, often used in tissue engineering, that enables the high-resolution production of constructs composed of accurately positioned and stacked microscale fibres. One of the major limitations of MEW is the small pool of available processable polymers. This limits the variety of chemical, thermal, mechanical and other properties that are required for different applications.

Aim

We aim to introduce poly(alkylene terephthalate)s (PATs) and their tuneable thermo-mechanical properties to the MEW toolbox, thereby expanding the application potential of both.

Materials and Methods

PATs with an alkyl chain length varying from 5 to 12 were synthesized via a catalyst-free single-step solution polycondensation reaction. These polymers were processed using MEW and the resulting scaffolds were visualized and characterized thermally and mechanically.

Results

The polymers were successfully synthesized and consecutively processed using MEW. Interestingly, besides varying the applied voltage difference, all other parameters could be kept the same for processing all PATs. Nonetheless, a difference in printing behaviour (i.e. fiber stacking) depending on the alkyl chain length was observed. The PATs demonstrated a broad range of thermal and mechanical properties, with a T_g in the range of -2.8 to 16.3°C, a T_m between 94.3 and 149.9°C and Young's moduli of the MEW scaffolds between 76 and 533 MPa. As a proof-of-concept, one specific PAT was selected to fine-tune the processing parameters and push the boundaries of MEW fabrication by up- and downscaling and by generating highly complex scaffold architectures (i.e. rectangular, hexagonal, sinusoidal and shifted sinusoidal) that are on par with the gold-standard reference PCL. These scaffolds were then characterized mechanically, revealing excellent shape memory behaviour (cfr. Figure), outperforming previously reported MEW polymers in terms of activation temperature and applied strains, while maintaining a high shape fixity (typically around 90%) and recovery (between 84 and 100 %) .

Conclusion

With shape memory activation near body temperature, excellent biocompatibility, processability, and thermo-mechanical tunability, the PAT material platform offers broad potential for MEW applications in biomedical engineering and soft robotics.

Acknowledgements

We acknowledge the Fund for Cardiac Surgery, the Research Foundation Flanders (FWO), the German research Foundation (DFG) and the European Union's Horizon 2020 research and innovation programme for their financial support.

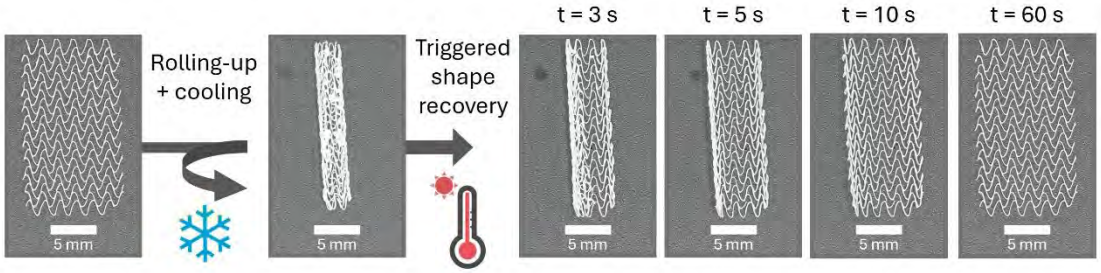

S23 – O4

Development and characterization of albumin-based materials

Akbarpour Z.[1], Hirtzel J.[1], Jmal H.[2], Beurton J.[1], Lavalle P.[1], Frisch B.[1], Reisch A.[1]
[1]Biomaterials and Bioengineering, Inserm UMR_S 1121, CNRS EMR 7003, Université de Strasbourg; [2] Laboratoire ICube (UMR 7357), équipe MMB, Dépt. de Mécanique, Université de Strasbourg, France

Introduction

Protein-based materials are increasingly valued for their ecological benefits and versatility, with applications spanning food packaging to tissue engineering [1]. A critical challenge is to develop mechanically resistant materials using gentle methods that preserve protein functionality. Our laboratory has developed a salt-assisted compaction method based on the simple drying of bovine serum albumin (BSA) solutions in the presence of salts such as NaBr at 37°C. This process produces water-insoluble materials with excellent mechanical properties, biodegradability, and biocompatibility, without the need for chemical crosslinkers or harsh conditions [1,2].

Aim

Here, we aim to better understand the formation of these materials and to control their properties. We investigate the role of protein surface chemistry in determining material properties.

Materials and Methods

Surface amine or carboxylate groups of BSA were modified with groups of different charge and hydrophobicity, using anhydride and carbodiimide chemistries to target accessible amine and carboxylate groups on the protein surface, respectively. Modified proteins were characterized by mass spectrometry, primary amine quantification, and electrophoresis. These proteins were then used to assemble materials through salt-assisted compaction at 37°C. Dynamic mechanical analysis and tensile testing were used to evaluate the resulting mechanical properties.

Results

We studied the influence of variations in the number and nature of charged groups, as well as in BSA hydrophobicity, on material assembly and properties. Material assembly remained possible for proteins bearing up to at least 10 modified amine or carboxylate groups. Modification of carboxylate groups led to a decrease in water content and an increase in rigidity, whereas modification of amine groups resulted in more swollen materials with lower rigidity.

Conclusion

This work shows that protein surface functionalization is an effective strategy to tailor material properties. By controlling surface charge and hydrophobicity, it becomes possible to design handleable, biocompatible, and sustainable protein-based materials obtained under mild conditions.

Acknowledgements

Zahra Akbarpour acknowledges a PhD fellowship from the Doctoral School ED 182 (Physique-Chimie, Université de Strasbourg). This study was also supported by the Carnot MICA SoyMAT project and the Fondation Jean-Marie Lehn project. The authors gratefully acknowledge the Plate-forme Protéomique Strasbourg Grand Est (LSMBO, UMR 7178, IPHC) for mass spectrometry analyses.

References

1. S. M. Choi, P. Chaudhry, S. M. Zo, S. S. Han, in Cutting-Edge Enabling Technologies for Regenerative Medicine (Eds.: H. J. Chun, C. H. Park, I. K. Kwon, G. Khang), *Springer Singapore, 2018*, pp. 161-210.
2. E. Aloui, J. Beurton, C. Medembblik, L. Hugoni, I. Clarot, A. Boudier, Y. Arntz, M. De Giorgi, J. Combet, G. Fleith, E. Mathieu, N. Kharouf, L. Kocgozlu, B. Heinrich, D. Favier, M. Brender, F. Boulmedais, P. Schaaf, B. Frisch, P. Lavalle, *Adv Healthcare Materials 2025*, 14, 2403385.

S23 – O5

Development of composite acrylic bone cements: Effect of hema/mma ratio on the formulation

Dartus J.[1, 2,3], Desoutter P.[3,1], Maton M.[1], Vienne A.[1], Negrach A.[1], Hennart B.[4], Chai F.[1], Carpentier O.[3], Putman S.[2], Monchau F.[3], Blanchemain N.[1]

[1]Université de Lille, INSERM, CHU Lille, U1365 Advanced Drug Delivery Systems; [2]CHU Lille, Université de Lille, Dept. universitaire de chirurgie orthopédique et traumatologique, hôpital Roger-Salengro; [3]Université d'Artois, IMT Nord Europe, Junia, Univ. Lille, ULR 4515, Laboratoire de Génie Civil et géo-Environ nement (LGCgE), Béthune; [4]CHU Lille, Université de Lille , ULR 4490, Laboratoire de Toxicologie, France

Introduction

Bone infections are a major complication in orthopaedic surgery. Conventional PMMA-based bone cements, widely used for local antibiotic delivery, have a high modulus that can cause stress shielding and limit bone integration. In addition, antibiotic-loaded PMMA cements have limited release, leaving much of the drug trapped and poorly bioavailable. To overcome these limitations, we have developed a HEMA/MMA cement incorporating calcium filler to confer bioactivity and polysaccharides to modulate the release of gentamicin. This study aims to evaluate the influence of the HEMA/MMA ratio on swelling, drug release and mechanical properties in order to optimise the balance between structural performance and local therapeutic delivery.

Experimental Methods

HEMA/MMA cement formulations were prepared using different HEMA/MMA mass ratios (90/10, 70/30 and 50/50), keeping calcium phosphate and polysaccharide loads constant. Gentamicin was incorporated as antibiotic. Swelling behaviour was studied in PBS (37°C, 80 rpm) as a function of HEMA content, while gentamicin release was monitored by Clone Enzyme Donor Immunoassay for 64 days in PBS (37°C, 80 rpm) and the antibacterial activity of release media was tested against *Staphylococcus aureus* and *Escherichia coli.* The mechanical properties were investigated using compression tests carried out on a machine fitted with a 10 kN load cell. The tests were conducted at a crosshead travel speed of 20 mm/min in order to assess the effect of the HEMA/MMA ratio on compressive strength and Young's modulus.

Results and discussion

An increase in the proportion of HEMA leads to a rise in the swelling ratio, varying from 13% to 20% depending on the HEMA content, thereby promoting the release of gentamicin. The release kinetics study shows that, depending on the HEMA/MMA ratio, up to 66% of the initial gentamicin load can be released after 64 days, compared with approximately 32% for a commercial cement (Palacos®). Throughout this period, the release media contain gentamicin concentrations higher than the MICs for *Staphylococcus aureus* and *Escherichia coli*. Furthermore, an increase in the HEMA content is accompanied by a decrease in compressive strength and Young's modulus, with values approaching those of cancellous bone.

Conclusion

The HEMA/MMA ratio is a key parameter that influences swelling, drug release kinetics and the mechanical properties of bone cement. In the formulations developed, the local bioavailability of gentamicin is significantly improved compared with commercial cements, whilst maintaining effective and sustained antibacterial activity against pathogens commonly implicated in bone infections, which represents a promising strategy for clinical applications.

S24
Biomimetic horizons: Engineering advanced ES constructs

S24 - K1
Electrospun medical devices: Ten years of experience on the market

Cirstea M.[1]
[1]The Electrospinning Company Limited, Harwell Science and Innovation Campus, Oxfordshire, UK

Introduction
Over the past fifteen years, electrospinning has evolved from an academic technique into a reliable manufacturing platform for implantable medical devices. A key driver is its ability to create biomimetic architectures replicating human extracellular matrices. As a Contract Development and Manufacturing Organization (CDMO), we have supported the commercialization of multiple electrospun constructs, successfully navigating the transition from early-stage research to approved medical devices. This involvement across diverse therapeutic areas provides a broad perspective on the technical, manufacturing, and regulatory factors determining successful clinical translation.

Materials and Methods
While specific device details remain proprietary, representative mechanistic findings are illustrated through comparable systems. In ophthalmology, an electrospun keratoprosthesis skirt anchors an intraocular lens to the sclera. Controlling fibre diameter, thickness, and bulk density achieved a consistent pore size distribution, analysed via synchrotron X-ray tomography and fluorescence confocal microscopy. In cardiovascular repair, a patch for aortic dissection was designed to replicate the human aorta, targeting a physiological modulus of 0.5–3 MPa. Modulating inter-fibre bonding to allow fibre sliding tuned mechanical compliance. A third case involved an electrospun corneal epithelial patch for limbal epithelial cell (LEC) transplants, which progressed to a first-in-human trial in India. This highlighted early regulatory engagement during process development.

Results
Proxy data illustrate the relationships between process parameters, fibre morphology, and performance. Ophthalmic scaffolds achieved consistent porosity, enabling predictable tissue integration (Figure 1). For cardiovascular patches, optimising fibre connections successfully reduced initial stiffness from ~10 MPa to the physiological ~2 MPa (Figure 2). In the LEC application, meeting strict Indian regulatory limits for residual solvents necessitated altered drying protocols. This produced a more brittle scaffold, demonstrating how stringent regulatory requirements can inadvertently alter carefully engineered biomimetic properties. This unexpected handling characteristic required surgeon retraining and delayed the trial, yet ultimately yielded successful safety outcomes, emphasizing the critical role of process–property mapping.

Conclusion
These examples illustrate the complexities of bringing biomimetic electrospun devices to the clinic. For researchers and developers, successful translation relies not only on precise process control and quantitative material characterisation but equally on understanding how early-stage design choices impact downstream regulatory compliance, clinical usability, and surgical handling. Future efforts should focus on predictive modelling and standardised mechanical–biological correlations to accelerate the reliable commercialization of constructs pushing the biomimetic horizons of regenerative medicine.

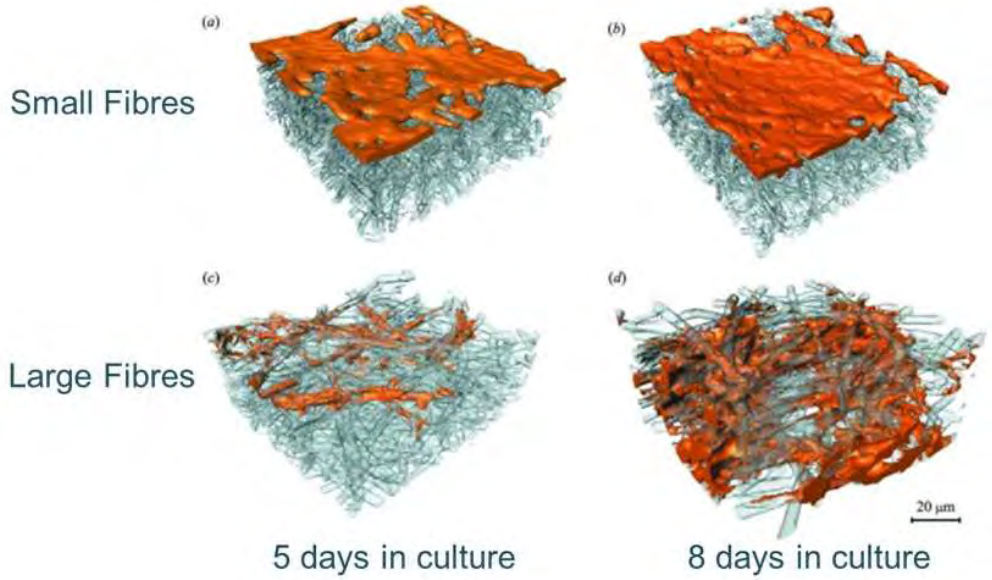

Figure 1: Synchrotron X-ray tomography showing different fibre diameters and stained cells.

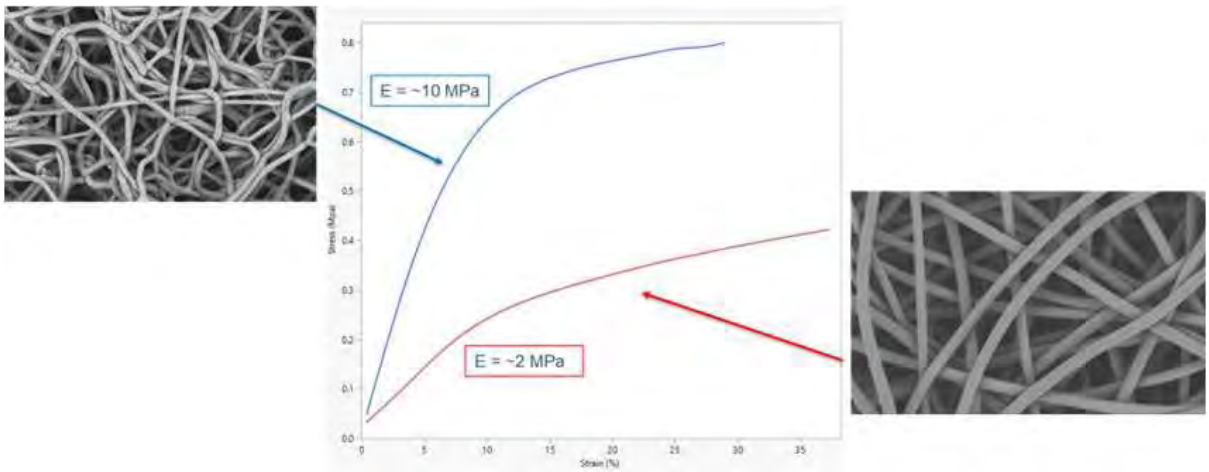

Figure 2: Tensile testing data for scaffolds with varying inter-fibre bonding.

ESB 2026

S24 – O1

Polydopamine-functionalized electrospun PCL/PLA/PEG scaffolds for sustained biomolecule delivery in advanced wound dressing systems

Martinez-Ramirez F.[1,2]; Zawadzka A.[1,2]; Schmieder P.[3]; Beshchasna N.[3]; Klimczak A.[1]; Kraśkiewicz H.[1,2]
[1]Laboratory of Biology of Stem and Neoplastic Cells, Institute of Immunology and Experimental Therapy PAS, Wrocław, Poland; [2]Group of Biological Activity Studies of Medical Biomaterials, Institute of Immunology and Experimental Therapy PAS, Wrocław, Poland; [3]Biofunctional Materials and Point-of-Care Diagnostics, Fraunhofer Institute for Ceramic Technologies and Systems IKTS, Dresden, Germany

Introduction

Electrospun scaffolds are studied for wound dressing applications due to their high surface area and tunable structural properties. Mesenchymal stem/stromal cell (MSC) secretome provides a cell-free source of regenerative paracrine factors with potential to support wound repair. However, rapid burst release of regenerative molecules and paracrine factors loaded onto scaffolds remains a limitation for therapeutic delivery. Surface functionalization strategies for improving biomolecule binding and release kinetics are essential for developing advanced wound-care materials.

Aim

This study aimed to develop a biointerface-engineered electrospun scaffold enabling sustained biomolecule delivery using enhanced MSC spheroid-derived secretome.

Materials and Methods

Electrospun poly(ε-caprolactone)/polylactic acid/polyethylene glycol (PCL/PLA/PEG) monoaxial fibers were produced using a custom electrospinning setup under optimized *in-house* parameters. The resulting scaffolds were characterized by scanning electron microscopy (SEM) and transmission electron microscopy (TEM) to confirm fiber morphology and structure. Scaffolds were surface-functionalized using a polydopamine (PDA) coating to create a bioactive interface for protein binding, optimized to ensure uniform deposition. To enhance regenerative proteins and paracrine factors secretion, MSC spheroid-derived secretome was generated in a controlled bioreactor system and used as protein cargo. Protein loading and release kinetics were evaluated under physiologically relevant conditions. *In vitro* biocompatibility of PDA-coated scaffolds was assessed using ATP quantification via Luciferase across three cell lines and live/dead staining with fluorescence microscopy. The resulting wound dressing system was designed as a biomaterial platform for delivery of MSC secretome and future incorporation of bacteriophages toward clinically relevant wound-care biomaterials.

Results

Electrospun membranes (10×21cm) were successfully fabricated, with SEM and TEM confirming formation of fibers. PDA functionalization produced a stable bioactive interface for protein immobilization. Non-functionalized scaffolds exhibited burst release within 24h, whereas PDA-coated scaffolds demonstrated controlled and sustained protein release profiles for up to five days with statistically distinct kinetics ($p<0.05$; $f_2<50$). Biocompatibility assays confirmed that PCL/PLA/PEG scaffolds supported high cell viability, with no adverse effects observed after PDA functionalization. The triple-component scaffold design improved mechanical properties compared to previously developed systems, with an additional enhancement following PDA coating. Additionally, MSC spheroid-derived secretome produced in a bioreactor exhibited 24% higher protein yield and broader paracrine factor diversity, supporting enhanced regenerative potential for biomaterial-based therapeutic delivery.

Conclusion

Polydopamine-functionalized PCL/PLA/PEG scaffolds enable controlled biomolecule release while maintaining biocompatibility and enhanced mechanical performance. Combined with MSC spheroid-derived secretome, this platform offers a multifunctional and clinically relevant strategy for advanced wound dressing development and regenerative biomaterial applications.

ESB 2026

S24 – O2

Electrospinning a mechanocompatible external support for the Ross procedure

Vervenne T.[1,2], Hendrickx A.[3], Schols M.[3], Rega F.[3], Famaey N.[1], Mignon A.[2]
[1]Soft Tissue Biomechanics, Dept. of Mechanical Engineering, KU Leuven; [2]Smart Polymeric Biomaterials, Dept. of Materials Engineering, Campus Group T, KU Leuven; [3]Cardiac Surgery, Dept. of Cardiovascular Sciences, KU Leuven, Belgium

Introduction

The Ross procedure is the only aortic valve replacement technique that restores long-term survival while preserving quality of life. In this procedure, the patient's own pulmonary valve is implanted in the aortic position, forming a pulmonary autograft. However, its long-term durability is limited by progressive autograft dilatation under systemic pressures. Although existing textile reinforcements can reduce dilatation, they are often excessively stiff and fail to replicate the biomechanical behavior of native arterial tissue.

Aim

In this study, we use electrospinning to develop a mechanocompatible external support designed to stabilize autograft diameter while preserving arterial compliance.

Materials and Methods

Biodegradable tubular scaffolds were fabricated by electrospinning blends of poly(ε-caprolactone) and elastin. As a preclinical proof-of-concept, supported and unsupported pulmonary arteries were transplanted into the abdominal aorta of rats to mimic the mechano-biological conditions of the Ross procedure. Contrast-enhanced micro-computed tomography (µCT) was used to assess diameter changes of the autografts both postoperatively and after 8 weeks. Upon sacrifice, Verhoeff's van Gieson (VVG) staining was performed to histologically evaluate biological adaptations.

Results

Figure 1 shows the successful surgical implantation of both supported and unsupported autografts in rats. In addition, Figure 1 presents histological analysis of explanted tissue after eight weeks, demonstrating benign biological integration of the electrospun tubular support. Figure 2 highlights the evolution of vessel diameter assessed by µCT. Supported autografts maintained their wall diameter over eight weeks, whereas unsupported autografts exhibited pronounced dilatation. Quantitative µCT analysis revealed diameters of 1.40 ± 0.10 mm for the native aorta, 3.57 ± 0.41 mm for unsupported autografts, and 2.65 ± 0.07 mm for supported autografts (Fig. 2).

Conclusion

Overall, our electrospun polymer–elastin blends represent a promising strategy to prevent dilatation while preserving autograft remodeling. This approach provides a translational pathway for further material optimization and electrospinning process development, with the potential to improve surgical outcomes of polymer-based external supports in cardiovascular applications.

Acknowledgements

This work was supported by a doctoral fellowship from the Research Foundation Flanders (FWO) to Thibault Vervenne (SB1SE2125N). The animal studies were funded by the KU Leuven Fund for Cardiac Surgery (ref. 489715 and 489742).

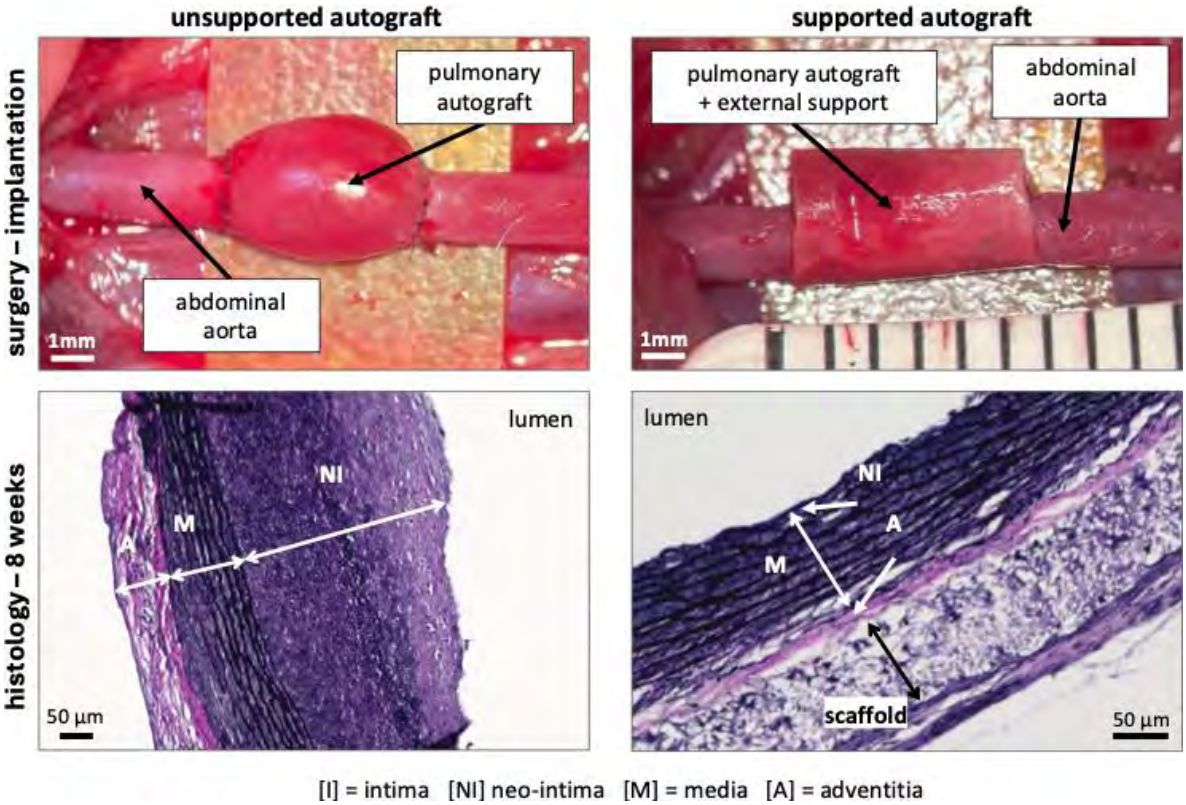

Figure 1: Surgical implantation of supported and unsupported pulmonary autografts in the rat abdominal aorta. Representative histological images of explanted tissue at 8 weeks with Verhoeff's van Gieson (VVG) staining.

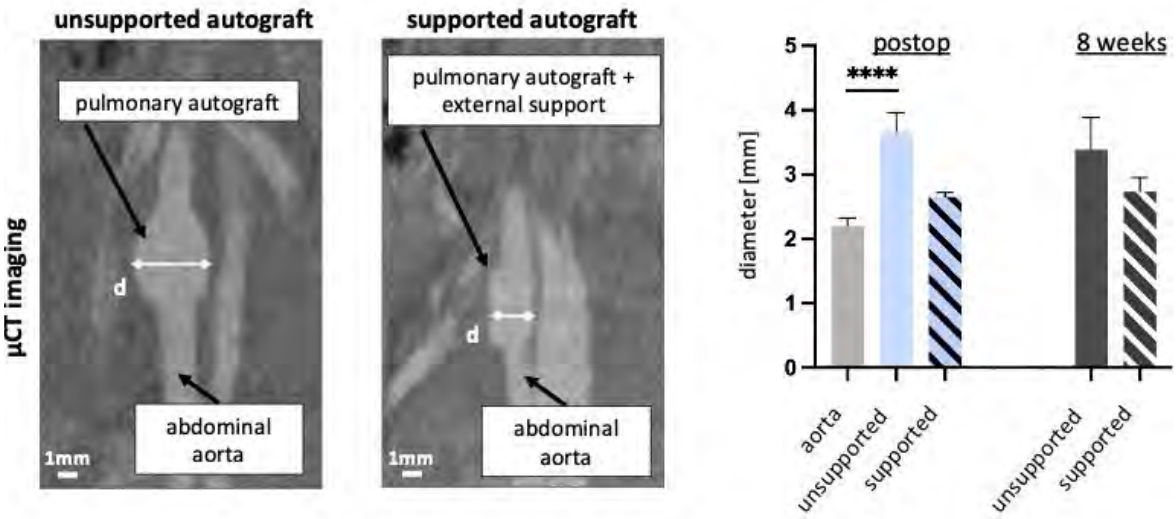

Figure 2: Contrast-enhanced µCT imaging of supported and unsupported autografts postoperatively and at 8 weeks. Quantification of vessel diameter for native aorta, supported autografts, and unsupported autografts.

ESB 2026

S24 – O3

Programmable skeletal muscle organization using MEW-patterned thin films

Vannozzi L.,[1] Ricci A.,[1] Boccoli L.,[1] Trucco D.,[1] Ricotti L.[1]
[1]The BioRobotics Institute, Scuola Superiore Sant'Anna, Pisa, Italy

Introduction

Skeletal muscle function strongly depends on the spatial organization of myofibres, which form specific architectures such as parallel, fusiform or pennate arrangements. Reproducing these physiologically relevant structures *in vitro* remains challenging, as most culture systems promote only uniform cell alignment. Melt electrowriting (MEW) enables the precise deposition of microscale polymer fibres that can act as topographical guidance cues for cell organization. However, when used alone, MEW typically generates open fibre scaffolds that lack a continuous supporting surface, which limits the ability to recreate physiologically relevant skeletal muscle architectures on compliant substrates.[1]

Aim

This study aims to combine the MEW with thin-film technology to provide a continuous and flexible substrate that supports and directs myotube organization according to predefined fibre architectures. MEW-patterned thin films therefore represent a promising platform to guide myotube alignment and recreate biomimetic skeletal muscle architectures, with potential applications in skeletal muscle tissue engineering and in vitro muscle models.

Materials and Methods

Thin films were fabricated from polycaprolactone (PCL, 40 mg/mL in chloroform) by spin coating, and the resulting films were then placed onto the RegenHU platform, where melt electrowriting (MEW) was used to deposit fibre patterns made of PCL at different spacing (200, 500 and 1000 µm) directly onto the thin film surface, at a temperature of 80 °C (**Figure 1**). Muscle cell viability and organization were evaluated using C2C12 myoblasts. Prior to cell seeding, the substrates were plasma-treated and subsequently functionalized with fibronectin (5 µg/mL) to enhance cell adhesion. After seeding, cells were cultured in growth medium for 3 days, followed by 7 days in differentiation medium. Cells were stained for myosin heavy chain, and myotube formation was quantified.

Results

Thin PCL films produced from a 40 mg/mL solution exhibited a thickness of 1.67 ± 0.26 µm, whereas films prepared from an 80 mg/mL solution showed a thickness of 5.59 ± 2.27 µm. MEW filaments were printed directly onto the PCL thin films, with an average filament diameter of approximately 11 µm, demonstrating high stability due to thermal bonding between the deposited fibres and the substrate during printing. Three parallel patterns were initially tested to evaluate cellular behaviour by varying the inter-fibre spacing and the number of deposited filament layers (1 and 4) (**Figure 2**). In all cases, cells robustly aligned along the printed fibres, demonstrating that MEW patterns effectively guide myotube organization even at large inter-fibre spacings (1000 µm). Increasing the pattern height (4 layers) had a more pronounced effect at larger spacings, where myotubes tended to form and organize around the printed filaments.

Conclusion

This work demonstrates that MEW-patterned thin films provide a simple and robust platform to control myotube orientation on compliant substrates. C2C12 cells align along the printed fibres even at large inter-fibre spacings, highlighting the effectiveness of MEW-derived topographical cues. This approach opens the possibility to engineer programmable skeletal muscle architectures beyond simple parallel alignment.

Acknowledgements

This work received financial and technical support from INAIL, project MioPRO2, grant n.PR23-CR-P1.

References

[1]Ranat K. et al. Advancements in musculoskeletal tissue engineering: the role of melt electrowriting in 3D-printed scaffold fabrication. *Journal of Functional Biomaterials 2025,* 16, 163.

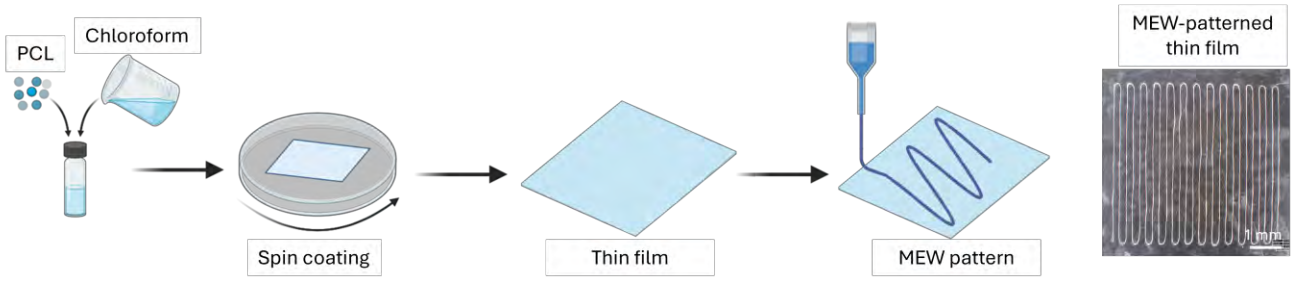

Figure 1: Fabrication of MEW-patterned PCL thin films. PCL dissolved in chloroform was spin-coated to produce thin films, which were then patterned by melt electrowriting (MEW) to deposit fibre architectures directly onto the film surface.

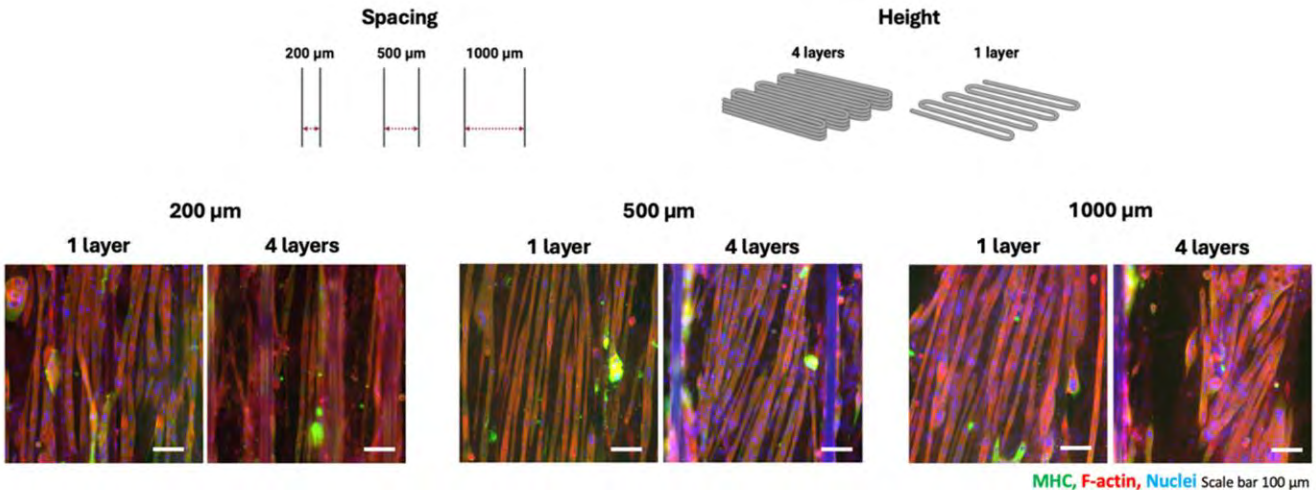

Figure 2: Effect of MEW pattern spacing and height on C2C12 organization. Patterns with spacings of 200, 500, and 1000 µm and heights of 1 or 4 layers were tested. Cells aligned along the fibre direction in all conditions, with increased organization around the filaments at larger spacings and higher pattern height. MHC (green), F-actin (red), nuclei (blue). Scale bar: 100 µm.

ESB 2026

S24 – O4

Manufacturing of bioartificial eardrum replacements for middle ear surgery

Sestini M.[1,2], Fricker A.[1], Ramachandran R. [2], Milazzo M.[2], Forli F. [1,3], Danti S.[2], Berrettini S.[1,3]
[1]U.O. Otorinolaringoiatria, Audiologia e Foniatria, Azienda Ospedaliero-Universitaria Pisana, Pisa; [2]Dept. of Civil and Industrial Engineering, University of Pisa; [3]Dept. of Surgical, Medical, Molecular Pathology and Emergency Medicine, University of Pisa, Italy

Introduction

Conductive hearing loss may arise from infections, trauma or congenital defects affecting the outer and middle ear (ME). Reconstructive surgery typically involves removal of damaged tissues and their replacement with passive ME prostheses; however, prosthesis extrusion remains a significant complication of synthetic biomaterials. Tympanic membrane (TM) perforation represents a widespread damage, yet replicating TM hierarchical fibrous architecture responsible for its acoustic performance remains challenging. In this work, bioartificial ultrafine fiber meshes containing polysaccharides and protein, in addition to synthetic components, were developed to manufacture scaffolds mimicking TM extracellular matrix (ECM).

Materials and Methods

A polymeric blend of poly(ethylene oxide terephthalate)/poly(butylene terephthalate) (PEOT/PBT), chitosan (CS) and collagen peptides (CP) was investigated. Different solvent systems including hexafluoroisopropanol (HFIP), acetic acid (AA), water and trifluoroacetic acid (TFA) were explored to overcome solubility limitations of (PEOT/PBT)/CS/CP blends and find a miscibility area. Electrospinning was performed by varying applied voltage, flow rate and tip-to-collector distance to identify stable processing conditions. TM-mimetic fibre collectors were designed in SolidWorks. The structure consisted of intersecting radial and circumferential elements arranged in two separated layers to enable potential electrical independence. The collectors were fabricated via masked Stereolithography Apparatus (MSLA) 3D printing.

Results

We obtained (PEOT/PBT)/CS/CP continuous fibers with minimal bead formation in the blends with 50:5:45 (w/w/w) composition using HFIP/AA (90% in water) at 10:3 (w/w) ratio. Optimized electrospinning conditions were: 15 kV applied voltage, 0.5 ml/h flow rate and 15 cm tip-to-collector distance. Scanning Electron Microscopy (SEM) analysis revealed a narrow fibre diameter distribution in the range of 90–115 nm, consistent with ECM collagen type II fibers in TM (Figure 1A). Complex biomimetic collector with superimposed radial and circumferencial pattern was designed and fabricated (Figure 1B).

Conclusion

This study demonstrates the feasibility of electrospinning (PEOT/PBT)/CS/CP blends into fibre scaffolds with size in the nano-domain, which resembled the polysaccharide and protein elements and fibrous structure of the TM. The results highlighted the importance of optimizing solvent composition and electrospinning parameters. In parallel, the design and fabrication of modular collectors provided a promising strategy to guide fibre alignment and reproduce the characteristic radial–circumferential architecture of the native TM.

Acknowledgements

European Union - Next Generation EU – PNRR, Mission 6 Component 2 Investment 2.1 “Enhancement and strengthening of biomedical research in the NHS”, project “Biomanufacturing of advanced tissues and devices for middle ear surgery (acronym: MAGIC-EAR)”, POC-2023-12377924, CUP master D53C24000870001.

S24 – O5

Beyond poly(ε-caprolactone): Poly(ester amide) scaffolds fabricated by electrospinning and melt electrowriting for flexor tendon repair

Brebels J.[1],Saraiva S.[2], Agten H.[1], Smet M.[3], Fonseca A. C.[2], Bloemen V.[1] and Mignon A.[1]
[1]Dept. of Materials Engineering, Surface, and Interface Engineered Materials (SIEM), KU Leuven, Belgium; [2]CEMMPRE, ARISE, Dept. of Chemical Engineering, University of Coimbra, Portugal; [3]Dept. of Chemistry, Laboratory of Organic Material Synthesis, KU Leuven, Belgium

Introduction

Scaffolds engineered by electrospinning (ES) and melt electrowriting (MEW) offer promising strategies to mimic the hierarchical structure of native tendon tissue. However, most reported approaches rely on poly(ε-caprolactone) (PCL), despite its slow biodegradation and accompanied inflammatory response due to acidic degradation products. In this study, α-amino acid–based poly(ester amide)s (AAA-PEAs) are investigated as alternative biomaterials for flexor tendon repair.

Materials and Methods

AAA-PEAs derived from L-phenylalanine were synthesized and characterized in terms of their physicochemical properties. The polymer was processed by ES and MEW to fabricate homogeneous fibrous sheets and highly aligned multilayered structures. Characterization included water contact angle measurements (WCA), *in vitro* degradation, and mechanical testing. Cytocompatibility and cell proliferation were evaluated using indirect Live/Dead and AlamarBlue assays. Finally, a proof-of-concept double-layered tubular scaffold was fabricated by consecutively combining MEW and ES, employing a novel MEW design with a reduced winding angle compared to existing tubular architectures.

Results

L-phenylalanine-based PEA (Phe-PEA$_{44.5k}$) synthesis was confirmed by chromatographic analysis and ^{1}H-NMR. WCA measurements indicated reduced hydrophobicity (115.91 ± 2.9°) compared to PCL (134.6 ± 3.9°), suggesting improved cell-material interactions. Phe-PEA$_{44.5k}$ was successfully processed by ES, yielding excellent fiber quality outcomes with a fiber diameter of 1.54 ± 0.40 µm. Most interestingly, Phe-PEA$_{44.5k}$ showed great promise for MEW processing up to 15 layers. *In vitro* degradation in PBS revealed a sufficiently slow degradation (>80% remaining after 8 weeks), while being significantly faster compared to PCL. Tensile testing of the fibrous materials revealed its highly elastic behaviour with a strain to failure value above 400%, combined with an ultimate tensile strength over 30 MPa. Biocompatibility experiments concluded a cell viability above 95% and a cell proliferation between 450 - 550% after 5 days of incubation. The double-layered tubular scaffold exhibited a highly aligned MEW inner layer and an ES outer layer that partially infiltrated inward (Figure 1). Ongoing work focuses on direct *in vitro* studies using tenocytes and *ex vivo* mechanical testing on cadaveric human flexor tendons

Conclusion

In this study, ES and MEW processing of Phe-PEA$_{44.5k}$ resulted in excellent outcomes, adding a novel polymer to the materials library of MEW. Phe-PEA$_{44.5k}$ showed accelerated biodegradation and improved mechanical properties when compared to PCL. Biocompatibility testing confirms its potential as biomaterial for flexor tendon repair. The fabrication of a biomimetic double-layered tubular scaffold highlights the potential of AAA-PEAs for flexor tendon repair and opens the way for further biological and mechanical validation.

Acknowledgements

This work was supported by the Research Foundation – Flanders (FWO), grant: 1SH1D24N, fellow: J.B.

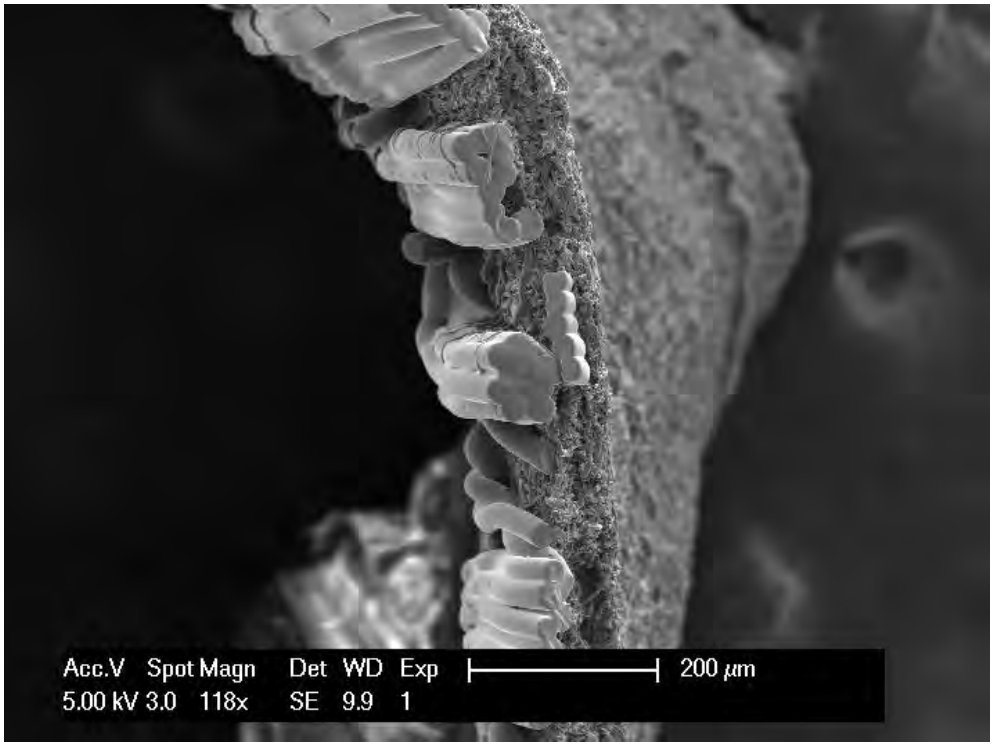

Figure 1. Double-layered tubular scaffold combining ES and MEW from Phe-PEA$_{44.5k}$

S24 – O6

Graphene oxide-decorated electrospun architectures for macrophage gene delivery

Ghitman J.[1,2], Gradisteanu G.[1], Vasile E.[3], Iliescu C.[2], Hovu H.[1,2]
[1]Advanced Polymer Materials Group, National University of Science and Technology Politehnica Bucharest; [2]eBio-hub Center of Excellence in Bioengineering, National University of Science and Technology Politehnica Bucharest; [3]Dept. of Oxide Materials Science and Engineering, National University of Science and Technology Politehnica Bucharest, Romania

Introduction

Non-viral gene therapy enables modulation of gene expression in specific cells through the delivery of exogenous genetic material. Developing efficient delivery systems targeting macrophages remains challenging due to their limited specificity and strong phagocytic activity. Electrospun fibrous architectures offer a promising platform for integrating gene carriers and enabling controlled spatial and temporal release of gene vectors, potentially overcoming limitations of systemic administration.

Aim

In this work we report a biodegradable hybrid gelatin-alginate electrospun architecture decorated with carboxylated graphene oxide (HAG/G) as versatile substrate for local and controlled delivery of PEI/pDNA nanoparticles (Np) to macrophages an alternative to systemic gene delivery carriers.

Materials and Methods

PEI/pDNA nanoparticles were formed by electrostatic interactions at different N/P ratios and characterized by DLS and TEM. The nanoparticles were immobilized on electrospun gelatin–alginate/graphene oxide (HAG/G) scaffolds, with loading controlled by the content of GO-COOH and evaluated by surface zeta potential (SZP). GFP-encoding plasmid DNA was used to assess cytocompatibility, transfection efficiency, and immunomodulatory activity in macrophages cultured *in vitro*.

Results

The dispersion of GO-COOH sheets shifts the surface zeta potential of HAG/G to high negative value (SZP = -16.8 ± 2.21 mV) and increases the encapsulation efficiency of PEI/pDNA Np on the hybrid HAG/G electrospun architectures to ~ 69 % (HAG/G-Np). Besides the fibrous structure of hybrid electrospun architectures, SEM micrographs highlighted very well the presence of PEI/pDNA Np that were distributed onto the surface of scaffolds or integrated between the fibersThe in vitro biological investigations show a good metabolic activity of macrophages seeded onto the HAG/G-Np (MTT assay), while the gene expression experiments show a 30% increase in transient transfection efficiency of macrophages cultured in the presence of HAG/G-Np as compared to those incubated with free PEI/pDNA Np.

Conclusion

These results demonstrate that the HAG/G electrospun architecture represents a promising platform for the local and controlled delivery of gene vectors, enhancing macrophage transfection efficiency while maintaining good cytocompatibility.

Acknowledgements

This work was supported by the European Union's Horizon Europe framework program 2021–2027, under the Coordination and Support Actions, HORIZON-WIDERA-2022-TALENTS-01 (grant agreement—101087007—eBio-hub). Funded by the European Union. Views and opinions expressed are those of the authors only and do not necessarily reflect those of the European Union or European Research Executive Agency (REA).

S25
Bioresorbable metallic implants alloy design, biological performance and clinical translation

S25 - K1
Architecting the next generation of bioresorbable metallic implants: From alloy design to predictive biomaterials engineering

Shabadi R.
Univ. Lille, CNRS, INRAE, Centrale Lille, UMR 8207 - UMET - Unité Matériaux et Transformations, France

Permanent metallic implants have transformed modern orthopaedic and cardiovascular medicine, yet their long-term presence in the body can lead to complications including stress shielding, chronic inflammation, implant failure and revision surgeries. Bioresorbable metallic implants have therefore emerged as a promising paradigm for regenerative medicine, offering temporary mechanical support while gradually degrading and being replaced by natural tissue. Among the various candidate materials, magnesium-based alloys and related degradable metallic systems have attracted considerable attention due to their favourable mechanical properties, biocompatibility and physiological degradation pathways.

Over the past decade, significant advances have been achieved in alloy development, microstructural engineering and surface modification strategies aimed at controlling degradation behaviour and improving biological performance. Alloying strategies involving elements such as Zn, Ca and selected rare-earth elements have enabled improvements in strength, corrosion resistance and cytocompatibility. At the same time, advanced thermomechanical processing techniques—including severe plastic deformation, grain refinement approaches and microstructural tailoring—have demonstrated the ability to tune both mechanical properties and degradation kinetics. Surface functionalisation strategies further enable modulation of early corrosion behaviour, interfacial biological interactions and tissue integration.

Despite these advances, major scientific and translational challenges remain. The degradation behaviour of bioresorbable metals is governed by complex interactions between alloy chemistry, microstructure, processing history, surface condition and the physiological environment. This multi-parameter dependency often results in variability in corrosion kinetics and biological responses, complicating reliable prediction of in vivo performance. Furthermore, the path toward clinical translation requires improved reproducibility, robust preclinical validation and a deeper understanding of the relationships between materials design, degradation mechanisms and tissue response.

In this keynote lecture, recent progress in the design and engineering of next-generation bioresorbable metallic implants will be discussed from a materials science perspective. Particular emphasis will be placed on the concept of alloy architecture, where composition, microstructure and processing routes are deliberately engineered to achieve controlled degradation while maintaining adequate mechanical integrity during the healing process. Emerging approaches that integrate microstructural design with surface engineering strategies to tailor degradation pathways and biological interactions will be highlighted.

Looking forward, the field is increasingly moving toward a predictive biomaterials engineering paradigm, in which experimental materials development is complemented by advanced modelling and data-driven approaches. The integration of digital materials engineering concepts—including microstructure–property modelling, physics-informed computational approaches and data-assisted materials optimisation—offers new opportunities to accelerate the discovery and design of degradable metallic systems with predictable in vivo performance. Such approaches can shorten development cycles and enable more rational design of implant materials tailored to specific clinical indications.

By bridging alloy design, processing science, biological performance and emerging predictive frameworks, bioresorbable metallic implants are poised to play a central role in the development of next-generation regenerative biomaterials. The lecture will conclude with perspectives on future research directions and translational challenges, highlighting how integrated materials engineering approaches can help realise the full clinical potential of degradable metallic implants.

S25 - K2
Biological response to biodegradable alloys

Willumeit-Römer R.
Helmholtz-Centre Hereon, Institute for Metallic Biomaterials, Geesthacht, Germany

Introduction

Biodegradable metals become more and more important in clinical application. However, we still have not reached a full understanding of all processes during the degradation of such implants and regeneration of the surrounding tissue. Beside the standard interaction of cell attachment, matrix formation and finally tissue regeneration which is observed similar as to non-degradable metallic implants we also have to deal with the effects of the degradation process. We might have to consider changes in pH, gas evolution, ion concentrations or solubility of degradation products. While in many cases the material part is studied in much detail, this talk will give an overview of current knowledge of the biological response to degradable metal implants.

Materials and Methods

The talk will introduce the effect of Mg degradation on different cell types: musculoskeletal cells, stem cells, microglia and astrocytes as well as antibacterial activity against *S. aureus*. *In vivo* data is based on mice, rat and rabbit models. Materials (Mg and alloys containing eg. Gd, Ag, Zn or Li) were produced, machined to discs (cell culture) or pins resp. screws for the animal experiments and characterised by Helmholtz Center Hereon. Animal experiments were conducted at the Hereon Outstation at MOIN CC, Kiel. Ex vivo studies were performed at the Hereon Outstation at DESY, Hamburg.

Results

Magnesium promotes bone formation[1] and shows immune modulatory capacity[2, 3]. Antibacterial and anti-cancer activity was shown *in vivo*[4].

Conclusion

Magnesium is in many respects an atypical implant metal: it degrades and has a strong interplay on biological process in cells and the tissue. This offer the potential for tailored and complete tissue regeneration if we understand the complexity of interactions.

References

[1] Y. Sun, H. Helmholz, O. Will, T. Damm, B. Wiese, M. Luczak, E. Peschke, B. Luthringer-Feyerabend, T. Ebel, J.-B. Hövener, C.-C. Glüer, R. Willumeit-Römer: Dynamic in vivo monitoring of fracture healing process in response to magnesium implant with multimodal imaging: Pilot longitudinal study in a rat external fixation model. *Biomater. Sci. 2022,* 10,1532-1543.

[2] H. Ben Amara, D.C. Martinez, F.A. Shah, A. Johansson Loo, L. Emanuelsson, B. Norlindh, R. Willumeit-Römer, T. Plocinski, W. Swieszkowski, A. Palmquist, O. Omar, P. Thomsen: Magnesium implant degradation provides immunomodulatory and proangiogenic effects and attenuates peri-implant fibrosis in soft tissues. *Bioactive Materials 2023* 26, 353–369..

[3] Q. Wang, L. Xu, H. Helmholz, R. Willumeit-Römer, B.J.C. Luthringer-Feyerabend: Effects of degradable magnesium on the paracrine signaling between human umbilical cord perivascular cells and peripheral blood mononuclear cells. *Biomater. Sci. 2020* 8, 5969–5983.

[4] N. Anisimova, M. Kiselevskiy, N. Martynenko, R. Willumeit-Römer, E. Kornyushenkov, M. Rodionov, S. Dobatkin, Y. Estrin: Anti-tumour activity of Mg-6%Ag and Mg-10%Gd alloys in mice with inoculated melanoma. *Materials Science & Engineering C 2021* 130, 112464..

S25 – O1

Magnesium alloy development for additive manufacturing of biodegradableo implants: The effect of powder size and morphology on the sinterability

Azadi A.[1], Hyeonsok K.[1], O'Cearbhaill D.E.[1], Celikin M.[1,2]
[1]School of Mechanical and Materials Engineering, University College Dublin; [2]UCD Conway Institute, Dublin, Ireland

Introduction

The use of biodegradable magnesium (Mg) alloys for bone fixation devices have potential to improve patients' quality of life by avoiding the necessary secondary operations conducted regularly for the removal of implants fabricated from conventional non-resorbable alloys. Having excellent biocompatibility and biodegradability along with a low modulus of elasticity (decreased bone-shielding) leads to clinical uses as bone-fixation screws (Magnezix®, Syntellix) and coronary stents (Magmaris®, Biotronik). Next generation Mg implants necessitate patient-specific designs, which can be realised most effectively via Additive Manufacturing (AM). AM processes based on Powder Bed Fusion have not been widely adopted for Mg-alloys due to safety concerns raising from the intrinsic properties of Mg, such as high affinity to oxygen, low boiling temperature and high vapor pressure. Fused Deposition Modelling (FDM) is a cost-efficient 3D-printing technique commonly used to produce polymer-based components. Employing FDM that operates at low temperatures (<200˚C) can offer key technological advancement in the customisation of patient-specific Mg alloys with maximum design flexibility. The key limiting factor is the low sinterability of Mg and its alloys. This study focuses on the development of novel Magnesium-Strontium-Calcium (Mg-Sr-Ca) based alloys with superior sinterability for extrusion AM. The role of liquid-phase sintering (LPS) process on the densification was analysed.

Materials and Methods

Thermodynamic calculations (Thermo-Calc) and Differential Scanning Calorimetry (DSC) are used to predict and evaluate the liquid phase fraction in order to optimise sinterability and porosity levels. Materials characterisation was conducted to validate the thermodynamic modelling results using optical and scanning electron microscopy (SEM/EDS) as well as X-ray Diffraction (XRD). Final porosity levels were determined using X-ray Computed Tomography (CT). Developed alloys were 3D-printed via extrusion AM, and the mechanical performance was evaluated in comparison to cast alloys via compression testing.

Results

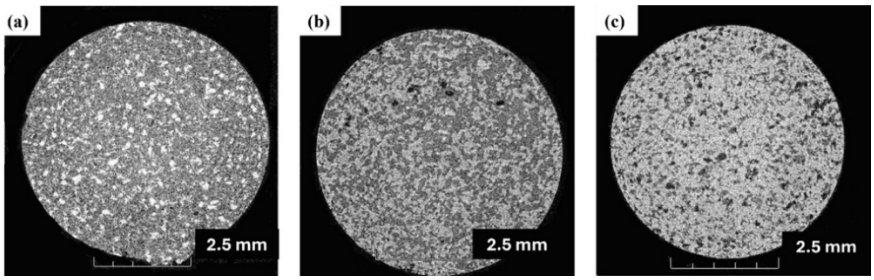

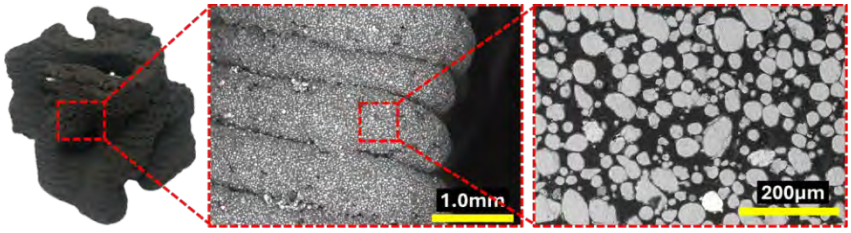

Acknowledgements

This publication has emanated from research conducted with the financial support of Research Ireland under Grant No. 20/FFP-P/8868.

S25 – O2

Influence of macrophage on the electrochemical corrosion of Mg-based Implants

Sahu M.R.[1,2], Yamamoto A.[2]
[1]Japan Society for the Promotion of Science (JSPS) International Research fellow; [2]Research Center for Macromolecules and Biomaterials, National Institute for Materials Science (NIMS), Tsukuba, Japan

Introduction

A major critical challenge faced in Mg-based implants during clinical trails is its uncontrolled degradation in the patients' bodies; its degradation rate varies differently in each patient and also as per the implantation sites. Besides this, the degradation rate also depends on the host's inflammatory response accompanied by pH reduction in the tissue fluid, which is largely governed by the activity of immune cells, particularly macrophages[1]. Therefore, in the present work, we develop *in vitro* corrosion model incorporating macrophages to understand the effect of inflammation on corrosion of Mg-based materials *in vivo*. We investigate the effect of macrophage activation level on Mg-based material by electrochemical impedance spectroscopy (EIS) and potentiodynamic polarization (PDP) test.

Materials and Methods

The *in vitro* model was prepared by the addition of human lymphoma-derived U937 monocytes into the cell culture medium (RPMI + 10 % FBS) with different conditions. The cells were differentiated (activated) with supplementary addition of 1 µM PMA for 24 h, and further treated with the addition of 1 µg/mL LPS for hyperactivation. The corrosion behaviour was evaluated by performing the electrochemical tests of 24 h at 37 ℃ under an atmosphere of 5 % CO_2 in humidified air using WE43 alloy. After 24 h of macrophage culture with the WE43 specimen, the H_2O_2 in the supernatant was quantified by a calorimetric assay.

Results and Discussion

The test results of both EIS and PDP test showed an increase in corrosion rate in presence of macrophages with a trend of RPMI + 10 % FBS < steady state U937 < activated U937 < hyperactivated U937. The corrosion rate also increased with progress of time for activated and hyperactivated conditions which is conformed from the decreased impedance with time. The H_2O_2 test showed highest reactive oxygen species (ROS) for hyperactivated U937 indicating its highest corrosion rate. The cellular metabolic reaction could alter the microenvironment at the alloy/medium interface, including pH reduction and secretion of biomolecules, thus accelerating the alloy corrosion. The highest corrosion rate with hyperactivated macrophages demonstrates that the secretion of ROS involved in acceleration of the alloy corrosion probably due to the destruction of oxide and/or insoluble salt layer on the specimen surface by ROS.

Conclusion

This work demonstrates that macrophage activation significantly influences Mg alloy corrosion; hyperactivated macrophages accelerated the corrosion rate with ROS secretion.

References

[1]M. P. Kwesiga, A. A. Gillette, F. Razaviamri, et al., Biodegradable magnesium materials regulate ROS-RNS balance in pro-inflammatory macrophage environment, Bioactive materials 2023; 23; 261-273.

S25 – O3

Comparison of bone healing using β-titanium alloy and Ti-6Al-4V plates with matched axial stiffness

Nakai M.[1], Miyazaki D.[2], Tanaka K.[2], Yamamoto E.[3], Ueki K.[2], Sakata S.[2]
[1]Laboratory for Biomaterials and Bioengineering, Institute of Science Tokyo, Tokyo; [2]Dept. of Mechanical Engineering, Kindai University, Higashiosaka; [3]Dept. of Biomedical Engineering, Kindai University, Wakayama, Japan

Introduction

Stress shielding caused by high-modulus metal bone plates reduces mechanical stimulation of bone, impairing remodeling and increasing the risk of bone atrophy and refracture. β-type titanium alloy Ti-29Nb-13Ta-4.6Zr (TNTZ; E ≈ 60 GPa), developed by our research group, has approximately half the elastic modulus of Ti-6Al-4V (Ti64; E ≈ 110 GPa) while maintaining excellent biocompatibility, making it a promising candidate for next-generation orthopedic implants. Previous studies comparing low- and high-modulus plates used identical plate geometries, thereby confounding the effects of elastic modulus and structural stiffness. Through geometric design, however, axial stiffness can be equalized between materials of different moduli. Such geometric adjustment inevitably produces substantial differences in bending stiffness because bending stiffness scales with the cube of plate thickness. This study aimed to evaluate the effects of plate elastic modulus and structural stiffness on bone healing using an experimental design that partially decouples these two mechanical factors.

Materials and Methods

Three plate conditions were prepared: (1) TNTZ with a thickness of 0.5 mm (TNTZ-0.5 mm); (2) Ti64 with a thickness of 0.27 mm (Ti64-0.27 mm)—axial stiffness–matched to condition (1) but with approximately 3.5-fold higher bending stiffness; and (3) TNTZ with a thickness of 1.5 mm (TNTZ-1.5 mm)—identical modulus to condition (1) but with approximately 27-fold higher bending stiffness. Plates (25.0 × 5.0 mm) were fixed with stainless steel screws across a 5.0-mm hemi-cylindrical femoral defect in skeletally mature female rabbits (mean body weight: 3.0 ± 0.5 kg; n = 5 per group). At 3 weeks, femora were retrieved and callus area was quantified from micro-CT images using ImageJ. At 6 weeks, Goldner trichrome staining was performed for conditions (1) and (3) to evaluate mineralized tissue distribution. Group differences at 3 weeks were analyzed statistically.

Results

At 3 weeks, callus area was significantly greater in TNTZ-0.5 mm than in both Ti64-0.27 mm and TNTZ-1.5 mm. At 6 weeks, the mineralized area was markedly larger in TNTZ-0.5 mm than in TNTZ-1.5 mm, indicating more advanced bone healing in the low-modulus, low-stiffness group.

Conclusion

TNTZ-0.5 mm showed significantly greater bone healing than Ti64-0.27 mm despite equivalent axial stiffness, demonstrating that equalizing axial stiffness through geometric design is insufficient to produce equivalent bone healing outcomes. This difference is likely attributable to additional mechanical factors—particularly the 3.5-fold difference in bending stiffness. Comparison between TNTZ-0.5 mm and TNTZ-1.5 mm further demonstrates that higher plate stiffness suppresses bone healing even when the elastic modulus is identical, consistent with stress shielding. Taken together, these findings indicate that material selection, rather than geometric design alone, is a critical determinant of bone healing outcomes in fracture fixation.

S25 – O4

Bioactive PLGA-plasma electrolytic oxidation coatings on β- titanium alloys for an increased antibacterial activity

N.M.E.[1], L.G.[2], K.L.[3], D.A.[1], D.P.[3], P.C.[1], T.F.[1], B.K.[3], A.M.[2], R.P.[1]
[1]Dept. of Chemistry and Materials Science, University of Turin; [2]Instituto de Nanosciencia y Materials de Aragón, Zaragoza, Spain [3]Dept. of Industrial Engineering, University of Padova, Italy

Introduction

β-Titanium alloys are promising candidates as the next-generation orthopedic implants, due to their excellent biocompatibility and a Young's modulus closer to that of the human bone. Implant failure due to antibiotic-resistant bacterial infections, caused by common bacterial pathogens colonizing the implant's surface, i.e. Methicillin-resistant *Staphylococcus aureus* (MRSA), remains a major concern and urges for the development of antibacterial implant surfaces that do not exhibit cytotoxicity against eucaryotic cells. Micron-sized porosity is known to promote cell adhesion and growth, but it could favour bacterial adhesion and proliferation leading to biofilm formation. One promising way to avoid bacterial adhesion on such type of surfaces is to further functionalise them with antifouling or antimicrobial compounds. This study aims to fabricate bioactive coatings on β-Titanium substrates, consisting of a permanent titanium oxide (TiO_2) micron-sized-porous layer and a biodegradable antimicrobial-loaded poly(lactic-co-glycolic acid) (PLGA) microparticle-based layer, that would inhibit bacterial adhesion and biofilm formation, without compromising cytocompatibility.

Materials and Methods

Two β-Titanium alloys, Ti45Nb and Ti-24Nb-4Zr-8Sn (Ti2448) underwent Plasma Electrolytic Oxidation (PEO) in an electrolyte containing hydroxyapatite and Gallium to create the permanent TiO_2 layer, and electrospraying to deposit the biodegradable antimicrobial-loaded PLGA microparticle-based coating. Surface composition and morphology were characterized by Scanning Electron Microscopy (SEM), Energy-Dispersive Spectroscopy (EDS) and X-ray Photoelectron Spectroscopy (XPS). Wettability was evaluated by contact angle measurements (CA). Gallium leaching was quantified by Inductively Coupled Plasma-Mass Spectrometry (ICP-MS) after incubating the samples in a physiological solution for 7 days at 37°C. Cytotoxicity was assessed using mouse Mesenchymal Stem Cells (mMSCs) and fibroblasts. Haemolysis assays (HA) were performed to evaluate their haemocompatibility.

Results

SEM images revealed the typical micron-sized porous PEO morphology and the PLGA microparticles attachment to the surface (Fig.1). EDS and XPS confirmed the incorporation of HaP and Ga on the PEO coating. CA measurements showed the PEO coatings to be hydrophilic, with values around 20°. SEM analysis after 7 days of incubation revealed not fully hydrolysed microparticles, which support a sustained release of the encapsulated antimicrobial. ICP-MS analysis showed Ga leaching, with the highest amount released within 24 hours, and a slower release over the 7-day-incubation. HA indicated haemocompatibility and preliminary cell viability assays showed that mMSCs are adhering and proliferating on the PEO coatings (Fig.2).

Conclusion

The PEO coatings exhibit promising cytocompatibility, although further *in-vitro* assays are required. The slow hydrolysis of the PLGA microparticles suggests possible controlled antimicrobial release. Future work will evaluate the antimicrobial loading and release profiles of the antimicrobial-loaded microparticles. MRSA will be used to assess the coatings' bactericidal effect.

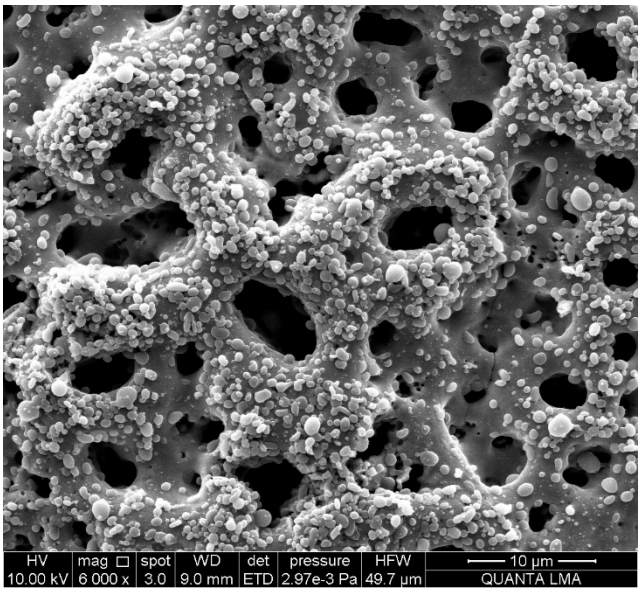

Figure 1: SEM image of Ti2448 after PEO treatment and electrospinning of PLGA microparticles for 1 hour.

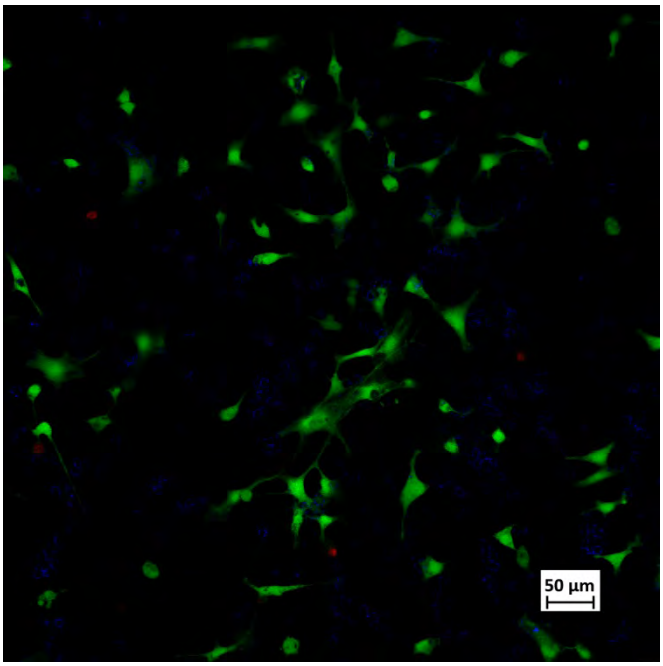

Figure 2: Confocal image of PEO treated Ti2448 with live-dead staining of mMSCs.

S26
Closing the loop green biomaterials and technologies for tissue engineering and regenerative medicine

S26 – K1

Carmagnola I.
Politecnico di Torino, Torino, Italy

S26 – O1

Tailored resveratrol-loaded patches for chronic wound treatment

Mazzanti C.[1], Laurano R.[1,2], Boffito M[1,2]., Cassino C[3]., Bronco S.[1], Ciardelli G.[1,2]
[1]Institute for Chemical-physical Processes, National Research Council (CNR-IPCF), Pisa; [2]Dept. of Mechanical and Aerospace Engineering, Politecnico di Torino, Turin; [3]Dept. of Science and Technological Innovation and Magnetic Resonance Platform (PRISMA-UPO), Università del Piemonte Orientale, Alessandria, Italy

Introduction

During the years, a variety of clinical approaches have been explored to support skin regeneration in hard-to-heal wounds, However, due to persistent challenges in effective wound care management, chronic wound treatment remains a significant unmet clinical need.

Aim

A green, patient-specific wound dressing was engineered to release Resveratrol (Res), a naturally occurring therapeutic agent with antioxidant properties.

Materials and Methods

The hydrogel matrix consisted of Hyaluronic Acid (HA) and Alginate (Alg) and was dual crosslinked for enhanced structural integrity. HA was functionalized with Tyramine (Tyr) using a green, carbodiimide-mediated grafting reaction, enabling Horseradish Peroxidase (HRP) catalyzed enzymatic crosslinking. Optimal enzymatic crosslinking parameters, including HRP and H_2O_2 concentrations, were identified by the tube inverting test, while ionic crosslinking parameters in terms of ions concentration (Ca^{2+} and Mg^{2+}) and immersion time (15,30,60 min) were established via frequency sweep tests. The self-healing properties were investigated using a creep and recovery test. Using an Incredible+ bioprinter, different geometries were printed. The hydrogel's capability to absorb exudate was analyzed through swelling tests over five days. Res was complexed with β-cyclodextrins (Res/βCDs) to overcome its poor water solubility, stability, and bioavailability. The synthesis was optimized for temperature and reaction time (24,48,72h), with the amount of encapsulated Res quantified through UV-Vis spectroscopy. Res/βCDs were characterized by infrared (IR) and Proton Nuclear Magnetic Resonance (^{1}H-NMR) spectroscopies, respectively. The antioxidant property of Res/βCDs was analyzed using the 2,2-diphenyl-1-picrylhydrazyl (DPPH) assay. Lastly, Res/βCDs were incorporated into the hydrogel, with release kinetics assessed up to 72h and cytocompatibility evaluated using the CellTiter-Blue assay.

Results

Functionalization was confirmed by IR (amide bands at 1540, 1640, 1725 cm^{-1}) and ^{1}H-NMR spectroscopy, showing phenolic peaks (6.6 – 7.3 ppm). Optimization of HRP, H_2O_2, and $CaCl_2$/$MgCl_2$ concentrations enabled the formation of a printable, shape-stable (up to 5 days), and self-healing hydrogel (recovery of 80%). Complex synthesis success was confirmed by IR, ^{1}H-NMR, and UV-Vis spectroscopy with an approximate yield of 75%. βCDs preserved Res antioxidant activity, as confirmed by the DPPH assay (80% activity). UV-Vis spectroscopy revealed sustained Res release over 72 hours. All formulations demonstrated cytocompatibility tested in accordance with ISO 10993:5 regulation, giving cell viability < 95%.

Conclusion

This customized hydrogel exhibited significant potential as drug delivery system and advanced bioink for fabricating antioxidant, biocompatible, patient-specific wound dressings.

Acknowledgements

This work was supported by the ATTITUDE project titled "vAlorization of wasTe products for the fabrication of sustainable paTient-personalIzed paTches targeting different phases of the woUnD hEaling cascade", which was financed by Fondazione Pisa (Italy) Call 2022 "Scientific and Technological Research" in macroarea of Biomedicine

S26 – O2

Lignin nanoparticles: Green tools to support tissue regeneration

Pezzuto M.F.[1], Crivello G.[2], Thakur S. [3], Villani S. [4], Alifano P.[5], Demitri C.[5], Ciardelli G.[1], Mattu C.[1]
[1]Dept. of Mechanical and Aerospace Engineering, Politecnico di Torino; [2]Dept. of Agricultural and Food Sciences, University of Bologna, Cesena; [3]Dept of Applied Science and Technology, Politecnico di Torino; [4]Dept. of Engineering for Innovation, University of Salento, Lecce; [5] Dept. of Experimental Medicine, University of Salento, Lecce, Italy

Introduction

Lignin is one of the most abundant natural polymers and a major by-product of the paper and biorefinery industries. Despite its widespread availability, it remains largely underexploited and is often treated as waste. Therefore, converting lignin into circular bio-based materials represents an attractive strategy for developing sustainable biomaterials for regenerative medicine [1]. Recently, lignin-based nanomaterials have emerged as promising green platforms for wound-related biomedical applications [2]. Thanks to its polyphenolic structure, lignin exhibits intrinsic antioxidant properties that could modulate the pathological microenvironment of chronic wounds, characterized by persistent inflammation, oxidative stress, and bacterial infection.

Aim

This study aims at developing nanoparticles derived from biomass-derived lignin and at evaluating their potential as sustainable antimicrobial platforms in chronic wound applications. Strategies to enhance antibacterial activity of lignin-based nanoparticles were explored by tuning the surface charge of lignin nanoparticles using *Staphylococcus aureus* as the model bacteria. Functionalization with positively charged ligands could increase electrostatic attraction to negatively charged bacteria, and promote membrane disruption, thereby amplifying the photothermal antibacterial effect.

Materials and Methods

Lignin was first enzymatically functionalized with polyphenolic compounds through a laccase-mediated reaction carried out in aqueous conditions, thus increasing the phenolic content of the material while avoiding strong oxidants and toxic organic solvents [3]. The modified lignin was then used to prepare lignin-based nanoparticles incorporating cobalt-phthalocyanine complexes as functional antimicrobial components. The nanoparticles were characterized in terms of morphology, size distribution, and surface charge. Antioxidant activity was evaluated through radical scavenging assays, while cytocompatibility was assessed on fibroblasts and keratinocytes. The biocompatibility was also evaluated on zebrafish larvae. Antibacterial activity against Staphylococcus aureus was investigated through colony-forming unit assays. Surface charge tuning strategies were explored to modulate the ζ-potential and improve interactions with bacteria.

Results

The obtained lignin nanoparticles showed a nanoscale size distribution and good colloidal stability. Their polyphenolic composition provided antioxidant activity together with cytocompatibility on fibroblasts and keratinocytes. Zebrafish larvae exposed to the nanoparticles showed high survival rates and no evident signs of mutations/alterations. Surface charge tuning shifted the nanoparticle ζ-potential toward positive values, enhancing electrostatic interactions with bacterial membranes and resulting in enhanced antibacterial activity against *S. aureus*.

Conclusion

The results show that lignin, a widely available biomass-derived polymer, can be valorized into multifunctional nanomaterials through sustainable synthetic strategies. By combining lignin functionalization, incorporation of antimicrobial components, and surface charge tuning, lignin-based nanoparticles represent promising green platforms for modulating the pathological microenvironment of chronic wounds.

Acknowledgements

This study was funded by the European Union - Next Generation EU, Mission 4 - Component 2 through 3DPathoSkin project (PE_00000019 - HEAL ITALIA; CUP E93C22001860006).

References

[1]Figueiredo P., Lintinen K., Hirvonen J.T., Kostiainen M.A., Santos H.A. Properties and chemical modifications of lignin: Towards lignin-based nanomaterials for biomedical applications,. *Progress in Materials Science 2018,* 93; 233-269.
[2]Crivello G., Pezzuto M.F., Armanetti P., Cassino C., Ceresa C., Fracchia L., Catarinicchia C., Villani S., Alifano P., Demitri C., Menichetti L., Tzanov T., Ciardelli G., Mattu C. Lignin nanoparticles containing cobalt-cyanine complexes: Potential multifunctional platforms for photoacoustic imaging and photothermal treatment of bacterial biofilms in chronic wounds. *Macromolecular Bioscience 2026,* 26, e00532-e00532.
[3]Morena A.G., Tzanov T. Enzymatic functionalization of lignin with polyphenols for biomedical applications. *Industrial & Engineering Chemistry Research 2020,* 59, 10787-10796.

S26 – O3

Sustainable drug-releasing bacterial cellulose patch for antioxidant and antibacterial wound healing

Tivano F.[1], Marcello E.[1], Amadi E.[2], Hinchliffe J.[2], Ceresa C.[3], Zoso A.[1], Fracchia L.[3], Carmagnola I.[1], Roy I.[2], Chiono V.[1]

[1]Dept. of Mechanical and Aerospace Engineering, Politecnico di Torino, Italy; [2]Dept. of Materials Science & Engineering, University of Sheffield, UK; [3]Dept. of Pharmaceutical Sciences, Università del Piemonte Orientale "A. Avogadro", Novara, Italy

Introduction

Wound care often requires repeated dressing changes, causing patient discomfort and generating significant medical waste, highlighting the need for sustainable dressing solutions based on renewable materials. Bacterial cellulose (BC) has recently gained attention as an eco-friendly alternative to plant-derived cellulose, and its clinical use already demonstrates clear advantages in wound management. However, native BC lacks intrinsic bioactive properties, essential for advanced wound care aimed at reducing inflammation and accelerating healing.

Aim

In this study, we developed a multifunctional sustainable BC patch by embedding antioxidant and anti-inflammatory curcumin-loaded zein nanoparticles (CurZNPs) and the antibacterial biosurfactant rhamnolipid R89.

Materials and Methods

BC pellicles were produced using *Gluconacetobacter xylinus* and scale-up production was explored. CurZNPs (2.5–10 µg/mL) were prepared by nanoprecipitation and characterized. Their *in vitro* biocompatibility was assessed on HaCaT keratinocytes after 24 h. CurZNPs loading into BC was optimized, and curcumin content and release kinetics from BC pellicles were evaluated. Antioxidant and anti-inflammatory activity of CurZNPs/BC systems were investigated using HaCaT and RAW 264.7 cells. Subsequently, loading of the biosurfactant rhamnolipid R89 was optimized. Finally, CurZNPs and R89 were simultaneously incorporated into BC pellicles, and the resulting R89/CurZNPs/BC system was evaluated for antibacterial and antibiofilm activity against *Staphylococcus aureus*.

Results

BC pellicles were successfully produced using *Gluconacetobacter xylinus*, with a dry yield of 1.07 g/L. CurZNPs exhibited high encapsulation efficiency (85%), sustained curcumin release, and strong antioxidant and anti-inflammatory activity. *In vitro* biocompatibility was confirmed on human keratinocytes after 24 h. CurZNPs incorporation into BC was optimized, achieving high curcumin loading within BC pellicles (86%) and enabling sustained release. *In vitro* studies with keratinocytes under oxidative stress and inflamed macrophages suggested that CurZNPs/BC pellicles exert a therapeutic effect by reducing oxidative damage and inflammatory signaling. R89 loading and release from BC pellicles were also investigated, and the optimal concentration (0.5 mg/mL) was selected based on biocompatibility results. The final R89/CurZNPs/BC system maintained high cell viability and demonstrated antibacterial and antibiofilm activity against *Staphylococcus aureus* (Figure 1).

Conclusion

Overall, this study successfully developed a sustainable BC wound dressing capable of delivering antioxidant and anti-inflammatory CurZNPs and antibacterial R89. The multifunctional system enables controlled drug release while combining therapeutic efficacy with environmentally sustainable material design.

Acknowledgements

FT acknowledges support from Research and Innovation NOP 2014-2020 for Doctoral Research programmes (Action IV.5) and INJECTHEAL Project, funded by the European Union, through the Horizon Europe research and innovation programme under the Grant Agreement no. 101177924. Views and opinions expressed are however those of the author(s) only and do not necessarily reflect those of the European Union or European Health and Digital Executive Agency (HADEA). Neither the European Union nor the granting authority can be held responsible for them.

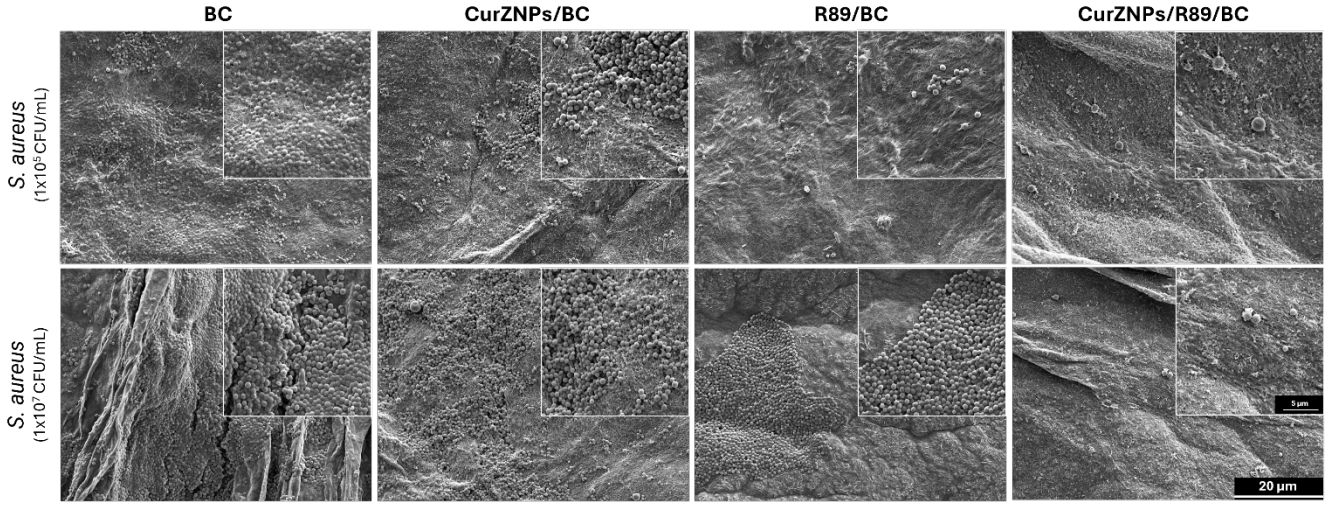

Figure 1. Scanning electron microscope (SEM) images of BC, CurZNPs/BC, R89/BC and CurZNPs/R89/BC against S. aureus.

S26 – O4

Bio-based injectable self-healing hydrogel from modified pectin and gelatin for chronic wound treatment

Cutietta G.[1], Tivano F.[1], Zoso A.[1], Khan S. [2], Pochettino E.[1], Boffito M.[1], Carmagnola I.[1], Chiono V.[1]
[1]Dept. of Mechanical and Aerospace Engineering, Politecnico di Torino, Italy; [2]Tissue Click Ltd, The Knoll Business Centre, Old Shoreham Rd, Hove, UK

Introduction

Chronic wounds affect 1–2% of the global population, impair quality of life, and represent a major healthcare burden. They are characterized by persistent inflammation, infection, and impaired extracellular matrix remodeling, delaying healing and limiting the efficacy of conventional dressings. Injectable hydrogels based on natural polymers can conform to irregular wound geometries and enable localized therapeutic delivery. Here, we developed a green, self-healing injectable hydrogel composed of oxidized pectin (OPec) and carbohydrazide-modified gelatin (G-CDH), designed for rapid in situ crosslinking via dynamic Schiff base chemistry and controlled release in chronic wound environments.

Materials and Methods

OPec was synthesized by periodate oxidation of citrus pectin (2.5 and 5 mol.% oxidation), while G-CDH was prepared via carbodiimide-mediated coupling. Two hydrogel compositions were selected: OPec_2.5/G-CDH (70:30% w/w) and OPec_5/G-CDH (50:50% w/w). Network structure and release properties were investigated using fluorescein-dextran (4 and 70 kDa), along with water absorption and weight loss properties in phosphate buffered saline (PBS). Injectability through G27–G30 needles was analyzed in 3D-printed wound phantoms. Litmus was loaded for real-time pH monitoring, then validated in PBS at pH 5, 7, and 9. Hyperbranched poly(ε-lysine) dendrons (0.1–1% w/w) were loaded into hydrogels to analyze their effect on rheological properties and cytocompatibility using Human Umbilical Vein Endothelial Cells (HUVECs) and Human Dermal Fibroblasts (HDFs).

Results

OPec_2.5/G-CDH (70:30% w/w) and OPec_5/G-CDH (50:50% w/w) hydrogels exhibited rapid gelation with a crosslinking degree of ~70 mol%. Rheological analysis confirmed shear-thinning behavior and rapid structural recovery. Dendron loading did not alter the storage modulus G' (~28 Pa and ~20 Pa for the 50:50 and 70:30 formulations, respectively), while it accelerated the crosslinking kinetics. Injection tests confirmed homogeneous filling of wound phantom channels (Figure 1). Water absorption and weight loss studies showed faster degradation/dissolution of the 70:30 hydrogel within 14 days, whereas the 50:50 hydrogel remained stable over the same period. Fluorescein dextran diffusion tests showed size-dependent permeability, while litmus-loaded hydrogels enabled real-time pH monitoring through color changes at pH 5, 7, and 9 (Figure 2). Cytocompatibility assays confirmed high cell viability.

Conclusion

The OPec/G-CDH hydrogel demonstrated adequate physicochemical and biological properties for use as a multifunctional platform for use in therapeutic delivery in minimally invasive chronic wound treatment.

Acknowledgements

Support was provided by INJECTHEAL, funded by the European Union, through the Horizon Europe research and innovation programme under Grant Agreement no. 101177924. The views and opinions expressed are, however, those of the author(s) only and do not necessarily reflect those of the European Union or European Health and Digital Executive Agency (HADEA). Neither the European Union nor the granting authority can be held responsible for them. GC is supported by the joint PhD program in Bioengineering and Medical-Surgical Sciences at Politecnico di Torino and University of Turin.

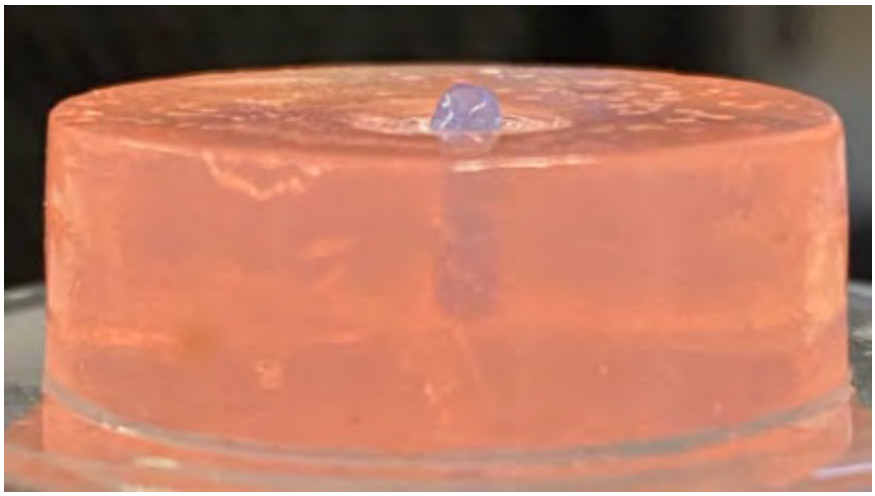

Figure 1 Representative image of OPec/G-CDH hydrogel injected into a single-channel wound phantom model. The hydrogel exhibited shear-thinning behavior during injection and underwent *in situ* gelation within the confined cavity, supporting its suitability for minimally invasive treatment of tunneling chronic wounds.

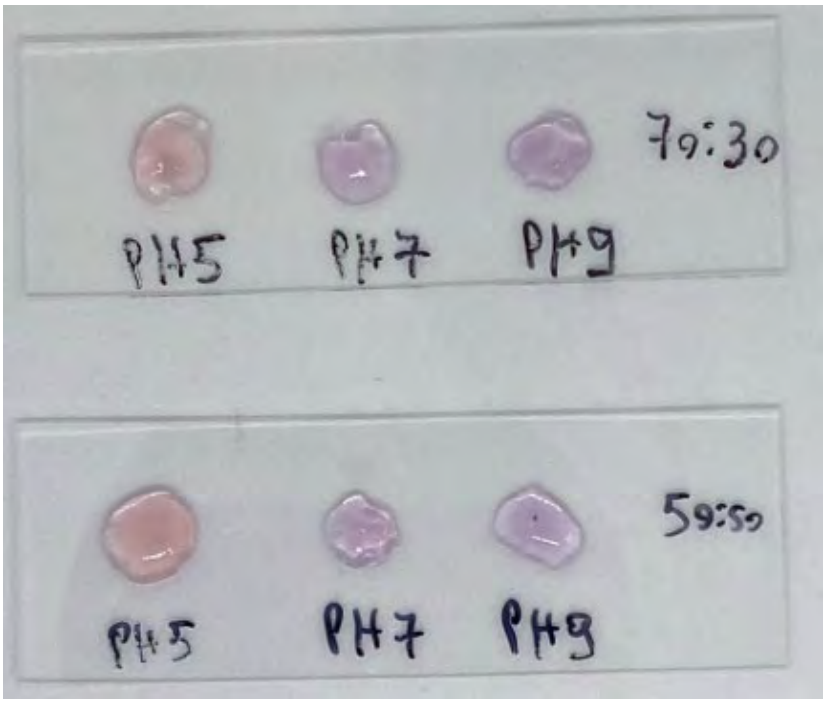

Figure 2 - Photographs of OPec/G-CDH hydrogels loaded with litmus after incubation in PBS at pH 5, 7, and 9. Upper row: OPec_2.5/G-CDH 70:30; lower row: OPec_5/G-CDH 50:50. Both hydrogels showed color transitions from pink at pH 5 to light purple at pH 7 and deeper purple at pH 9. The RGB color composition was extracted and quantified using the Color Recognizer application on a mobile phone.

S26 – O5

Bio-based antibacterial gelatin-alkali lignin membranes as multifunctional interfaces for soft tissue engineering

Sousa L.M.[1,2,3], Maia F.R.[1,2], Pina S.C.A.[1,2], Consonni S.R.[2], Reis. R.L.[1,2], Silva-Correia J.[1,2], Oliveira J.M.[1,2]
[1]3B's Research Group, I3Bs, Research Institute on Biomaterials, Biodegradables and Biomimetics, University of Minho, Guimarães, Portugal; [2]ICVS/3B's, PT Government Associate Laboratory, Guimarães/Braga, Portugal; [3]Dept. of Structural and Functional Biology, Institute of Biology (IB), State University of Campinas (Unicamp), Brazil

Introduction

Membrane-based biomaterials are widely used in tissue engineering applications such as guided tissue regeneration, wound healing and soft tissue repair, where they act as temporary interfaces that provide mechanical support and regulate cell-tissue interactions[1]. However, infection and poor integration remain major challenges. Gelatin and lignin are sustainable biopolymers with growing relevance for biomaterials development. While gelatin provides excellent biocompatibility and bioactivity, lignin – an abundant by-product of the pulp and paper industry – remains largely underutilized despite its intrinsic antioxidant and antibacterial properties[2].

Aim

Herein, we developed hybrid membranes composed of gelatin (Gel) and alkali lignin (AL) and evaluated their physicochemical and biological properties (Fig.1), exploring their potential as multifunctional biointerfaces for soft tissue engineering applications, including for pelvic organ prolapse (POP) repair.

Materials and Methods

Hydrogel membranes were prepared using Gel and AL, designated as GelxALy, where x and y represent the polymer concentrations (% w/v). Gel10AL5 membranes were produced by mixing the two polymers under controlled heating and stirring, followed by casting and crosslinking with 0.01% w/v genipin overnight under agitation and at RT. Physicochemical characterization included rheology, tensile testing, contact angle, surface energy determination and atomic force microscopy (AFM). Hemocompatibility and inflammatory response were assessed through haemolysis and cytokine quantification (IL-6, IL-10, IL-1β). For biological evaluation, L929 fibroblasts were cultured on the membranes for 1, 3 and 7 days to assess viability, metabolic activity, proliferation and cell morphology. The angiogenic response was assessed using the chick chorioallantoic membrane (CAM) assay. Antibacterial activity was evaluated against *Escherichia coli* using CFU quantification and Live/Dead assays.

Results

The incorporation of AL enhanced the viscoelastic properties of the membranes, supporting frequencies up to ~40 Hz compared to ~20 Hz for Gel-only membranes. Tensile testing demonstrated adequate mechanical properties for soft tissue support. Surface characterization revealed moderate hydrophilicity (contact angle 49.2° with water), surface energy of 65 mN/m and homogeneous nanoscale topography. The membranes exhibited excellent hemocompatibility and no detectable inflammatory response, as evidenced by stable levels of cytokines. *In vitro* assays confirmed high cytocompatibility, with fibroblasts displaying normal morphology, adhesion and proliferation throughout the culture period. Gel10AL5 membranes did not induce adverse reactions in the CAM and prevented endothelial cell infiltration, supporting their biocompatibility and barrier function. Importantly, AL incorporation conferred intrinsic antibacterial activity, significantly reducing *E. coli* proliferation as compared to Gel-only membranes.

Conclusion

This study demonstrates that bio-based GelAL membranes combine mechanical stability, cytocompatibility and intrinsic antibacterial properties, making them promising candidates for multifunctional soft tissue engineering interfaces. Their performance highlights the potential of lignin-derived biomaterials for regenerative medicine applications, including POP repair and other membrane-guided tissue regeneration strategies.

Acknowledgements

The authors thank the UID/50026:3B's-Biomaterials, Biodegradables and Biomimetics Research Group, University of Minho. This work was supported by IVDisCHIP (Project nº 15772, COMPETE2030-FEDER-

00687900), co-funded by ERDF/COMPETE 2030 (Portugal 2030) and FCT, and by the EngVIPO project (HORIZON-MSCA-2023-SE-01-101183041) through EU-EC. LMS acknowledges São Paulo Research Foundation (FAPESP 2024/17913-3), and JSC acknowledges FCT Tenure Program (nº1467/2024).

References

[1]Dziki J.L., Badylak S.F. Biomaterials for soft tissue reconstruction. Nature Reviews Materials *2018,* 3, 160-170.
[2]Sugiarto S., Leow W.R. How far is lignin from being a biomedical material? Materials Today Bio *2022,* 13, 100193.

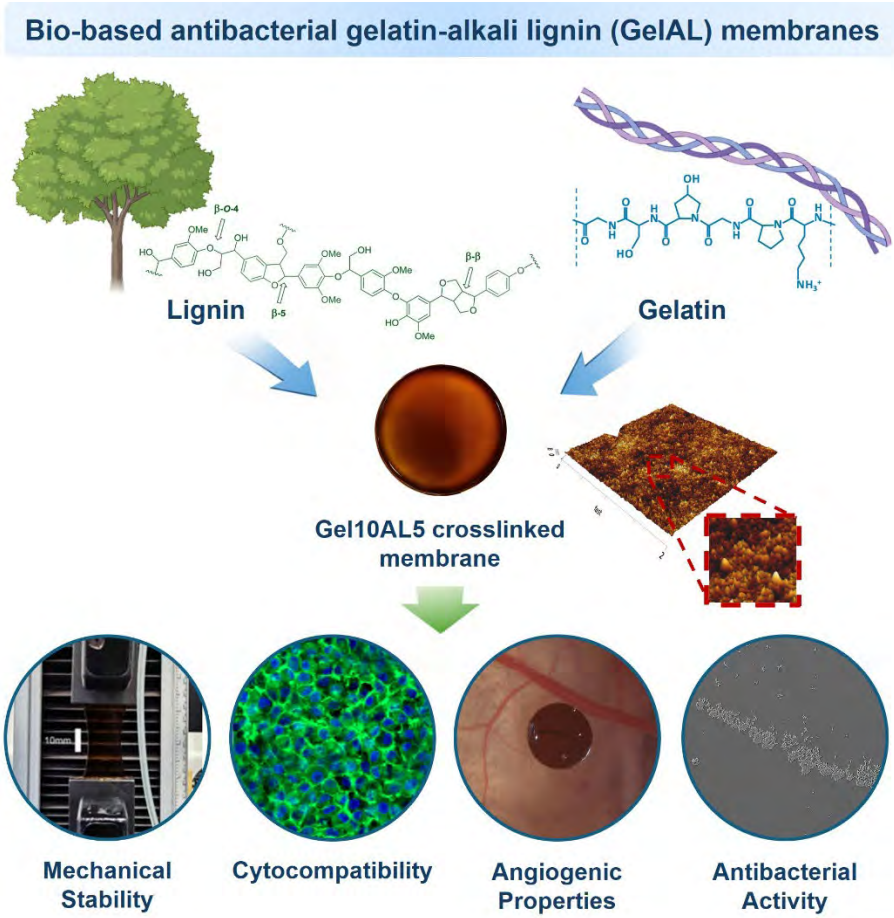

Fig. 1

S26 – O6

Recombinant spider silk films for vascular tissue engineering

Melo S.F.[1], Schmuck B.[2], Stadlmayr S.[1], Gross B.[2], Lu L.[2], Rising A.[1,2]
[1]Dept. of Medicine, Huddinge (MedH), Karolinska Institutet (KI), Stockholm; [2]Dept. of Animal Biosciences (HBIO), Swedish University of Agricultural Sciences (SLU), Uppsala, Sweden

Introduction

Silk-derived materials have been explored for cardiovascular applications, including vascular graft research. Spider silk is particularly attractive due to its mechanical strength, biocompatibility, and tuneable biodegradation. However, native spider silk is difficult to harvest in large quantities, making recombinant production a promising alternative. The Rising group developed a scalable process for biomimetic recombinant spider silk production, enabling high-yield generation of the silk proteins (spidroins). Unpublished results show that concentrated spidroin solutions can be processed into flexible thin films, which are now being tested for degradation, mechanical properties, and hemo/biocompatibility *in vitro*. Our main goal is to assess the potential of these films for blood-contacting medical applications.

Materials and Methods

By genetic engineering, we introduced different cytophilic amino acid motifs into the miniature spidroin $(A_3I)_3$-A_{14}. Proteins were produced using *E. coli* bioreactor fermentations and purified with a semi-automated protocol.[1] Concentrated solutions of $(A_3I)_3$-A_{14} and modified versions thereof were processed into films, optionally containing artificial spider silk fibers, also made from $(A_3I)_3$-A_{14}. Optimal film production parameters (temperature, relative humidity, incubation time, immersion bath) were identified to produce flexible and transparent films. Films' degradability was measured in solutions containing different enzymes over 63 days at 37°C, under static and dynamic conditions. Films' Young modulus (E) and stress at break (σ) were determined using an Instron tensile tester equipped with a BioBath, enabling mechanical testing in physiological-like conditions (37°C, 0.9% NaCl). Hemo/biocompatibility was assessed using human blood and primary human umbilical vein endothelial cells (HUVEC), and statistically compared to medical grade Gore-Tex.

Results

Degradation studies showed progressive slow decrease in spidroin films mass in all tested protease solutions, in contrast to control (1x PBS), where no degradation was observed. Mechanical tests revealed tensile properties compatible with vascular applications, with E ranging from 5 to 17 MPa, and σ from 1 to 4 MPa. The highest values were obtained for fiber-incorporating films. Hemolysis assays indicated that none of the spidroin-based films induced hemolytic effects, with hemolysis levels remaining below 1% under all tested conditions. Cytocompatibility was confirmed after direct seeding of HUVECs onto the films. Cells remained metabolically active throughout 21 days of culture on all film types and exhibited a normal cobblestone-like morphology when observed by fluorescence microscopy.

Conclusion

Artificial spider silk-based films represent a hemo/biocompatible tissue engineering platform that benefits from the intrinsic excellent properties of silk and the modifications allowed by recombinant protein production.

References

1. Arndt, T. *et al.*, *Advanced Functional Materials 2022*, 32, 2200986

S26 – O7

Geometric optimisation of 3D-printed auxetic meshes enabling lung-mimetic biaxial straining of collagen scaffolds

Chen J.[1], Cameron R.E.[1], Best S.M.[1]
[1]Dept. of Materials Science and Metallurgy, University of Cambridge, UK

Introduction

Ice-templated collagen scaffolds provide structural and biochemical mimicry of lung parenchyma but are typically evaluated under static conditions. Physiological lung alveoli experience cyclic biaxial strains of 5 to 12 percent during normal breathing, with a negative Poisson's ratio close to -1.[1] These strains regulate extracellular matrix remodelling and cellular behaviour.

Existing biaxial stretching systems rely on elastic membranes or rigid clamping, which generate non-uniform strain fields or damage fragile three-dimensional scaffolds. Re-entrant auxetic meshes offer a promising strategy for converting uniaxial tension into synchronous biaxial expansion.

Aim

This study aims firstly to optimise auxetic mesh geometry to maximise auxeticity and suppress in-plane instability caused by out-of-plane folding, thereby achieving physiologically relevant biaxial strain for scaffold stretching. Secondly, we aim to quantify scaffold structural deformation under strain using both the optimised auxetic mesh and an equivalent non-auxetic honeycomb mesh.

Materials and Methods

Re-entrant and honeycomb polypropylene meshes were fabricated by programmable G-code 3D-printing with systematic variation of re-entrant angle, strut width and strut thickness. Quasi-static uniaxial tensile testing was performed using a Tinius Olsen 1st testing machine to obtain force-strain responses. Poisson's ratio and critical strain were quantified at both the full mesh and central unit cell levels using digital image analysis. Optimised auxetic and honeycomb meshes were subsequently integrated with ice-templated collagen scaffolds and straining effects were assessed macroscopically and by two-photon microscopy to quantify pore deformation and anisotropy.

Results

Mesh geometry strongly governed auxetic performance (Figure 1). Increasing re-entrant angle produced more negative Poisson's ratios but reduced the critical strain before folding, while greater mesh thickness allowed higher strain capacity. Narrower struts prompted strut rotation, resulting in stronger auxetic expansion and lower deformation force. An optimised configuration (40° angle, 0.78 mm strut width, 0.82 mm thickness) achieved a Poisson's ratio of -0.84 and sustained in-plane auxetic behaviour up to 9% longitudinal strain, matching the physiological strain range of lung alveoli.

When integrated with collagen scaffolds, the auxetic mesh produced uniform biaxial scaffold expansion with nearly equal orthogonal strains. Two-photon microscopy revealed isotropic pore enlargement with minimal change in structural anisotropy across the strain range. In contrast, scaffolds strained using the equivalent honeycomb mesh exhibited pore elongation along the loading direction with increasing structural anisotropy (Figure 2).

Conclusion

Auxetic mesh designs can be optimised for mechanical stability and response through control of re-entrant angle, strut width and mesh thickness, demonstrating effective biaxial strain transfer to lung mimetic collagen scaffolds. The platform provides a mechanically compatible foundation for future dynamic bioreactor development and mechanobiological investigation of engineered lung constructs.

References

[1]Nossa R., Costa J., Cacopardo L., Ahluwalia A.. Breathing in vitro: Designs and applications of engineered lung models. *Journal of Tissue Engineering. 2021* Jan, 12:204173142110086.

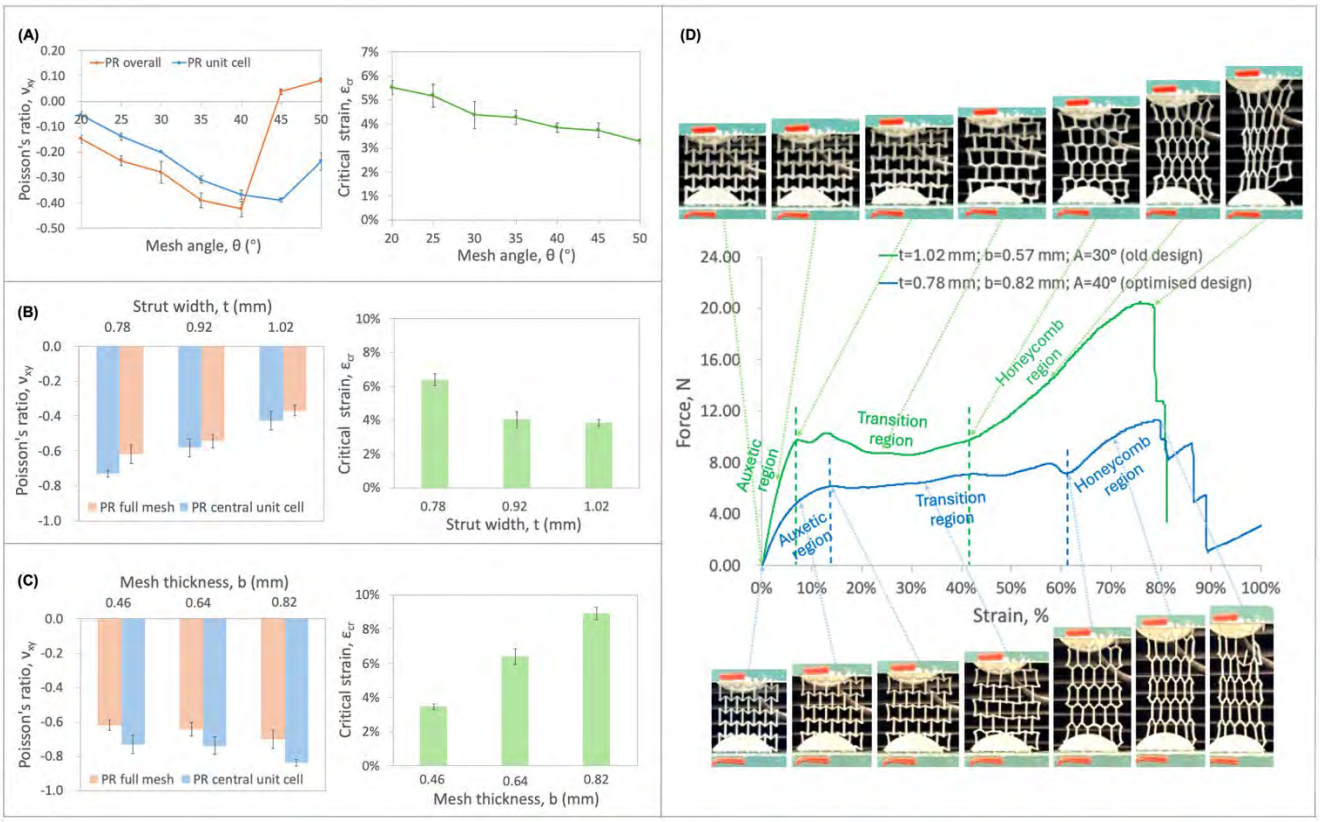

Figure 1. Influence of mesh geometry on mechanical performance and auxetic deformation behaviour. (A) Variation of Poisson's ratio (left) and critical longitudinal strain (right) with re-entrant angle, measured at both the central-unit-cell and full-mesh levels. Increasing angle produces more negative Poisson's ratios but reduces the attainable strain range. (B) Influence of strut width on Poisson's ratio (left) and critical strain (right) at a fixed re-entrant angle of 40° and a comparable mesh thickness of approximately 0.6 mm. A strut width of 0.78mm yields the most negative Poisson's ratio while sustaining the largest strain range. (C) Influence of mesh thickness on Poisson's ratio (left) and critical strain (right) at a constant strut width of 0.78 mm. A mesh thickness of 0.82 mm (five printed layers) improves structural stiffness and achieves the highest strain capacity. (D) Force-strain response of the previous and optimised mesh designs. The deformation behaviour is divided into three regimes: in-plane expansion of the auxetic structure, which is elastic and recoverable; a transitional region associated with the out-of-plane strut rotation; and a honeycomb region where the polypropylene material undergoes direct stretching. The optimised mesh (blue curve) requires lower force to initiate deformation while sustaining a wider auxetic strain range.

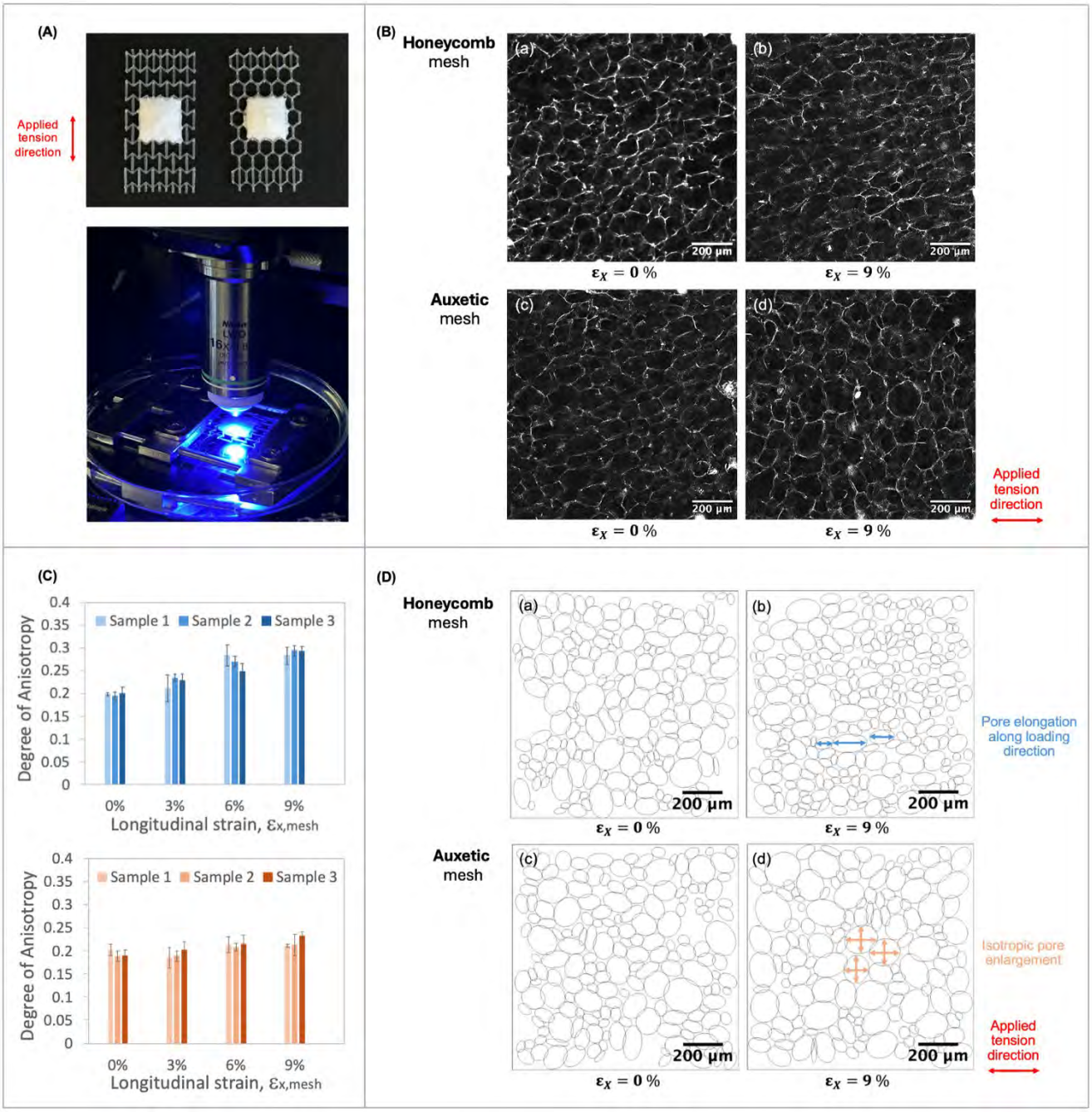

Figure 2. Biaxial strain transfer from auxetic meshes to collagen scaffolds. **(A)** Freeze-dried collagen scaffolds integrated with honeycomb and re-entrant auxetic meshes (top), and the experimental setup for two-photon imaging of mesh-embedded scaffolds during tensile loading (bottom). **(B)** Representative two-photon microscopy images of scaffold microstructure at longitudinal strains of 0% and 9% for scaffolds embedded with (a, b) honeycomb meshes and (c, d) re-entrant auxetic meshes. **(C)** Evolution of scaffold pore anisotropy with applied strain (0%, 3%, 6% and 9%) for honeycomb (top) and auxetic (bottom) mesh systems. Auxetic mesh-embedded scaffolds maintain near constant anisotropy during deformation. **(D)** Pore morphology visualised using watershed segmentation and elliptical fitting for honeycomb (a, b) and auxetic (c, d) mesh-embedded scaffolds at longitudinal strains of 0% and 9%. Auxetic meshes induce isotropic pore enlargement within the scaffold structure.

S27
Converging towards Mechano-Transduction in bone cartilage interface

S27 – K1
Biofabrication and Bioprinting Strategies for Cartilage, Bone and Osteochondral Tissue Engineering

Kelly D.J.
Trinity College Dublin – Ireland

Our musculoskeletal system has a limited capacity for repair. This has led to increased interest in the development of tissue engineering and biofabrication strategies for the regeneration of musculoskeletal tissues. This talk will demonstrate how different musculoskeletal tissues, specifically cartilage, bone and osteochondral defects, can be engineered or repaired using emerging biofabrication and 3D bioprinting strategies. The talk will first describe how different emerging bioprinting platforms can be used to spatially combine cells, supporting biomaterials and biochemical and/or biophysical cues to engineer different musculoskeletal tissues with user defined extracellular matrix architectures. We will then demonstrate how such bioprinting platforms can be used to provide spatially defined boundary conditions to cells to engineer zonally defined articular cartilage whose collagen architecture varies biomimetically through the depth of the tissue. Finally, this talk will demonstrate how osteoconductive biomaterials can be integrated into such biofabrication platforms in order to engineer osteochondral grafts,and will assess their capacity to support synovial joint regeneration in preclinical large animal models.

Acknowledgement
This work was funded by the European Research Council (ERC, 4D-BOUNDARIES #101019344).

S27 – O1

Clarifying the contributions of time and strain dependent mechanical dynamics toward the determination of cell fate in human-derived scaffolds

Ladeira B.M., Custódio C.A., Mano J.F.
Dept. of Chemistry, CICECO, University of Aveiro, Portugal

Introduction and Objectives

Cell fate is informed by myriad biomechanical cues received from the surrounding extracellular matrix (ECM). Although the individual influence of such signals on cell behavior has been increasingly clarified, cell response to these cues is context-sensitive and potential interactions between different mechanical signals remain unexplored. The aim of this work is to generate mechanically controllable scaffolds from human ECM, derived from decellularized placenta (dPC), to assess how separate mechanical cues cooperatively determine stem cell behavior in human tissue-like environments.

Materials and Methods

Photopolymerizable moieties were introduced in dPC either by covalent functionalization with methacryloyl groups, or through host-guest interactions with acryloyl β-cyclodextrin. By combining the two systems in different proportions, hydrogels with differing viscoelastic and strain-stiffening behavior could be generated, as assessed by rheological characterization. Mesenchymal stromal cells isolated from human umbilical cord were then encapsulated in the combined placenta (cPC) scaffolds to assess the cooperative influence of such mechanical cues on cell morphology, metabolism, mechanotransduction (YAP signalling) and osteogenic differentiation. Further experiments were conducted in osteogenic induction medium to assess how biochemical stimuli may interfere with cell perception of biomechanical cues.

Results

Matrix viscoelasticity and strain-stiffening behavior could be tuned independently from hydrogel stiffness as shown in Figure 1, unveiling potential trade-offs between time-dependent mechanical behavior and non-linear elasticity on cell behavior. Increasing matrix viscoelasticity promoted the activation of mechanotransduction pathways, resulting in enhanced cell spreading. Osteogenic differentiation was promoted in highly viscoelastic matrices only in the presence of osteogenic induction factors and was otherwise inhibited by increased viscoelasticity. By contrast, hydrogels exhibiting pronounced stiffening could trigger osteogenic differentiation without additional stimulation.

Conclusion

Mechanically controllable hydrogels could be generated from human placenta, clarifying the roles of matrix viscoelasticity and strain-stiffening behavior on cell behavior, and how they modulate cell response to additional cues cells may receive from their surrounding environment.

Acknowledgements

ERC – REBORN (ERC-2017-ADG-883370); EU's Horizon Europe – SUPRALIFE (101079482); FCT – individual contract 2020.01647.CEECIND, doctoral grant 2022.10626.BD. CICECO - Aveiro Institute of Materials (DOI 10.54499/UID/50011/2025 & 10.54499/LA/P/0006/2020), through FCT/MCTES (PIDDAC).

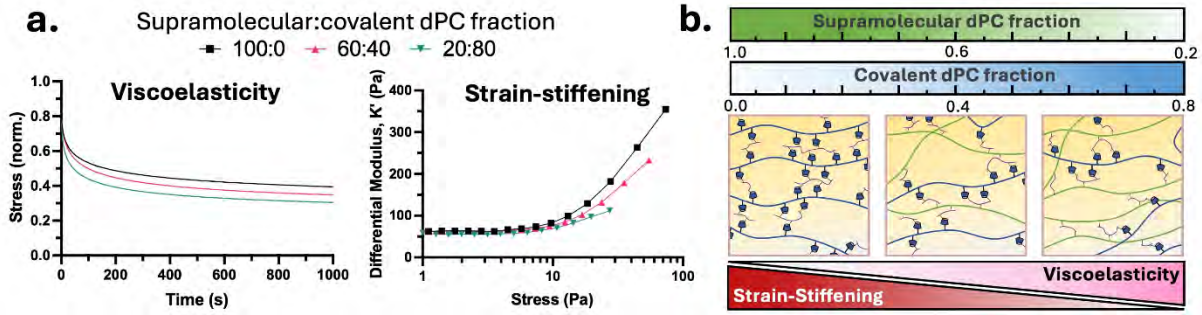

Figure 1. Mechanical tunability of cPC hydrogels. (a) Stress relaxation (left) and strain-stiffening behavior (right) can be adjusted independently from stiffness at rest. (b) Schematic representation of trade-off between matrix viscoelasticity and stiffening in cPC hydrogels.

S27 – O2

Toward rational design: How hydrogel characteristics drive the biomechanical response and matrix deposition of encapsulated chondrocytes

van de Looij S.M.[1], Peters J.R.[2], Ito K.[2], Callens S.J.P.[2], van Ravensteijn B.G.P.[1], Vermonden T.[1]
[1]Division of Pharmaceutics, Utrecht University, The Netherlands; [2]Orthopaedic Biomechanics (OPB), Dept. of Biomedical Engineering, Eindhoven University of Technology, The Netherlands

Introduction

Hydrogels are frequently used in tissue engineering because their material characteristics can be tuned to mimic natural extracellular matrices (ECM). As highly mechanosensitive cells, chondrocytes are known to sense and respond to variations in stiffness, viscoelasticity and matrix architecture of their local environment. Depending on the specific cues, they may enhance chondrogenesis and ECM production, or undergo dedifferentiation and hypertrophy. In this research, we developed a library of fifteen hyaluronic acid-based hydrogels varying in polymer concentration, crosslinking chemistry and crosslinking density (Fig. 1A). By leveraging bovine articular chondrocyte (bAC) mechanosensitivity after encapsulation, we aim to correlate early mechanobiological response and late stage ECM deposition to the hydrogel properties (Fig. 1B).

Materials and Methods

Sodium hyaluronate (103 kDa) was modified to obtain methacrylated hyaluronic acid (HAMA). HAMA co-functionalized with methylfuran or β-cyclodextrin was used to prepare three classes of hydrogels: (i) static networks formed via methacrylate crosslinking only, (ii) semi-dynamic-covalent networks incorporating methacrylates and Diels-Alder crosslinks (between methylfuran and 4-arm PEG-maleimide), and (iii) semi-dynamic networks combining methacrylates and host/guest interactions (between β-cyclodextrin and 4-arm PEG-adamantane). Young's modulus and creep deformation were measured to assess stiffness and viscoelasticity. bACs were encapsulated at 5 x 10^6 cells/mL. Cell viability (live/dead staining) and early mechanobiological response (qPCR, YAP/Taz nuclear localization) were evaluated in the first seven days of culture. ECM deposition was assessed after 28 days using qPCR, histology and immunohistochemistry.

Results

Photocrosslinking of methacrylate groups resulted in comparable baseline stiffness contributions across all hydrogel types. In static and semi-dynamic hydrogels, stiffness was primarily governed by methacrylate crosslinks (Fig. 2AC). In contrast, semi-dynamic-covalent hydrogels exhibited a significant additional stiffness contribution from Diels-Alder crosslinks (Fig 2B). As expected, hydrogels crosslinked with methacrylates as well as host/guest interactions displayed a higher viscoelasticity than fully static and semi-dynamic-covalent gels at the same polymer concentration. The type of crosslinking influenced the viability of bACs in the first days after hydrogel encapsulation.

Conclusion

We established a hyaluronic acid-based hydrogel library with controlled variations in polymer concentration, crosslink chemistry and crosslink density. Hydrogels displayed distinct differences in stiffness, viscoelasticity and swelling behaviour, enabling a systematic investigation of how material properties regulate chondrocyte mechanobiology and long-term matrix formation. Ongoing work focuses on elucidating activated mechanotransduction pathways in encapsulated cells, as well as assessing extracellular matrix deposition over extended culture periods.

Acknowledgement

We thank the Dutch Research council (NWO) for funding: LS-NeoCarE (NWA.1389.20.192) and VICI (18673).

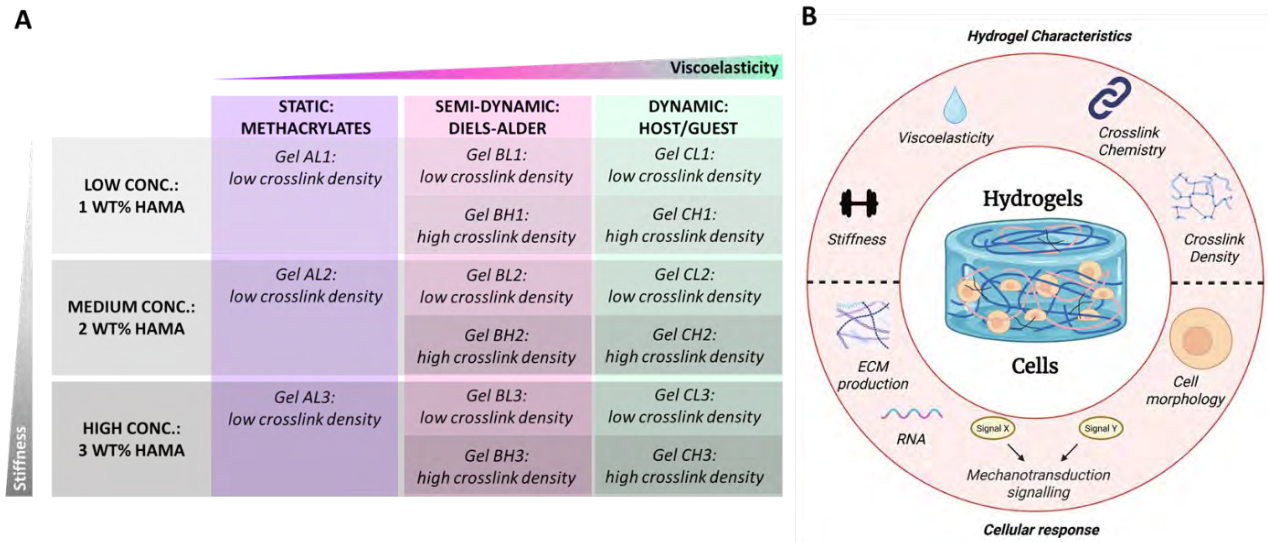

Figure 1: *Overview of research work. (A) Visual representation of the hydrogel library used in this work, including hydrogels with varying crosslink chemistry (horizontal), polymer concentration (vertical) and crosslink density. (B) Schematic overview of research aims and investigated parameters. Which hydrogel characteristics induce a certain cellular response?*

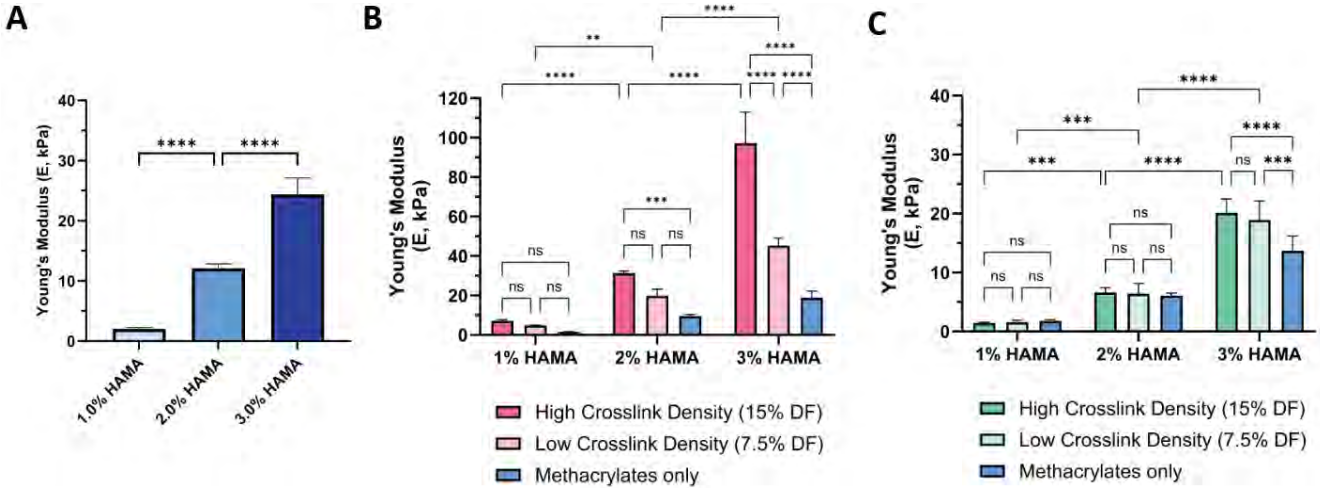

Figure 2: *Stiffness profile as measured with Young's modulus of hydrogels made with (A) HAMA and 4-arm PEG-OH, (B) HAMA-methylfuran and 4-arm PEG-maleimide and (C) HAMA-cyclodextrin and 4-arm PEG-adamantane. Panels B and C show the contributions of methacrylate crosslinking within the hydrogels in blue. Bars represent average Young's modulus ± st.dev for n = 4 replicates. Statistical significance is denoted with * ($p < 0.05$), ** ($p < 0.01$), *** ($p < 0.001$) or **** ($p < 0.0001$).*

S27 – O3

DLP bioprinted functionally graded SFMA–κ-carrageenan–TCP scaffolds with selective barrier properties for guided bone regeneration

Pahurkar N.[1], Latiyan S.[2], Chatterjee K.[3]
[1]Dept. of Materials Engineering, Indian Institute of Science; [2]Dept. of Materials Engineering, Indian Institute of Science; [3]Dept. of Bioengineering, Indian Institute of Science, Bengaluru, India

Introduction

Guided bone regeneration (GBR) is widely used in periodontal and cranio-maxillofacial reconstruction to facilitate selective bone formation while preventing rapid soft tissue invasion into defect sites. However, conventional GBR membranes largely function as passive barriers and lack the structural integration and bioactivity. Furthermore, most existing biomaterials fail to replicate the hierarchical organisation present at the native soft tissue–bone interface. To address these limitations, this study shows a DLP bioprinted functionally graded scaffold composed of silk fibroin methacrylate (SFMA), κ-carrageenan, and tricalcium phosphate (TCP) designed to integrate selective barrier functionality with osteoconductive support for bone regeneration.

Materials and Methods

A photocrosslinkable composite bioink was reinforced with bioactive TCP particles and fabricated using digital light processing (DLP) bioprinting. The scaffold was engineered as a functionally graded construct, comprising a dense upper layer designed to inhibit fibroblast infiltration and a porous lower layer facilitating osteogenic cell migration and extracellular matrix deposition. SFMA provided mechanical stability and photocrosslinking capability, while κ-carrageenan contributed hydrophilicity and matrix-forming properties. TCP served as an osteoconductive ceramic. Mechanical properties, degradation behaviour, morphological and swelling characteristics were evaluated. In vitro studies were conducted to assess MC3T3-E1 cell viability, proliferation, and NIHT3T (fibroblast cell line) migration to evaluate barrier functionality. Furthermore, biomineralisation assays were performed to confirm osteogenesis.

Results

The DLP bioprinted 15%SFMA–2%κ-carrageenan–3%TCP scaffolds demonstrated excellent printing fidelity and well-defined gradient architecture. Incorporation of TCP showed enhanced compressive strength to approximately ~125kPa, providing sufficient mechanical stability. The dense barrier region significantly restricted fibroblast infiltration, reducing soft tissue migration by approximately 60–65% compared to non-gradient scaffolds. In contrast, the porous osteogenic region supports high cell viability (>90%) and promotes osteogenic differentiation, with alkaline phosphatase activity increased approximately 1.5 fold relative to non-TCP scaffolds. ARS assay demonstrated enhanced calcium deposition within the TCP-enriched scaffolds after 14–21 days, indicating progressive extracellular matrix mineralisation.

Conclusion

By combining a dense barrier layer that limits soft tissue infiltration with a porous osteogenic region that promotes bone formation, the scaffold mimics the hierarchical interface required for effective guided bone regeneration.

S27 – O4

Engineering poly(glycerol adipate)-based elastomeric biomaterials for tissue regeneration

Gazińska M.A.[1], Krokos A.[1], Rudnicka K.[2], Płociński P.[2], Szwed-Georgiou A.[2], Biernat M.[3], Żywicka B.[4], Vukomanovic M.[5], Rodziewicz-Motowidło S.[6]

[1]Dept. of Polymer Engineering and Technology, Wrocław University of Science and Technology, Poland; [2]Dept. of Immunology and Infectious Biology, University of Lodz, Poland; [3]Łukasiewicz Research Network - Institute of Ceramics and Building Materials, Kraków, Poland; [4]Pre-clinical Research Centre, Wrocław Medical University, Poland; [5]Advanced Materials Dept., Jožef Stefan Institute, Ljubljana, Slovenia; [6]Dept. of Biomedical Chemistry, University of Gdańsk, Poland

Introduction

Poly(glycerol adipate) (PGA) is primarily used as a drug delivery carrier. Despite its similarity to poly(glycerol sebacate), widely applied in tissue engineering, *in vivo* studies on cross-linked PGA remain limited. Here, we demonstrate that elastomeric PGA exhibits strong potential for tissue engineering. The presence of hydroxyl groups in each repeating unit enables effective biofunctionalization and cross-linking, allowing precise control over mechanical properties, degradation behavior, and release kinetics.

Aim

To demonstrate the applicability of polymer-ceramic biocomposites based on poly(glycerol adipate), incorporating ceramic particles and pro-regenerative and antibacterial peptides, as implantable materials for the regeneration of small bone defects, and to indicate the suitability of PGA-based materials for soft tissue regeneration.

Materials and Methods

Tri-component elastomer composites were fabricated as bulk materials. The pro-regenerative peptide was incorporated into the matrix for sustained release, while the antimicrobial peptide was applied to the surface for rapid antibacterial action. Viscoelastic properties were assessed by Dynamic Mechanical Analysis, and peptide release kinetics, along with *in vitro* and *in vivo* biological performance, were evaluated. The selected biocomposite was further tested *in vivo* as a hip trochanter implant in a rabbit model.

Results

The storage modulus (1 Hz, 37°C) can be tuned over six orders of magnitude depending on the cross-linking method, ranging from a few Pa (prepolymer) to several kPa (thermally crosslinked elastomer) and up to a few MPa (chemically crosslinked elastomer)[1,2]. Incorporation of ceramic particles increases stiffness and broadens the rubbery plateau[3]. PGA-based materials exhibit high cytocompatibility, supporting cell adhesion, spreading, and proliferation, and promote osteogenic cell recruitment *in vitro*. *In vivo*, the composite show pronounced early osteostimulatory effects (up to 30 days), with spongy bone formation and abundant trabeculae observed around the implants.

Conclusion

The rubbery plateau modulus of PGA-based elastomers at physiological temperature closely matches that of osteoid and soft tissues. Combined with favorable *in vitro* outcomes, this highlights their potential for cartilage and osteochondral regeneration.

Acknowledgements

The research was supported by projects “Multifunctional composite material with antimicrobial and pro-regenerative properties for bone tissue reconstruction”, (TECHMATSTRATEG 2/406384/7/NCBR/2019) and “REvolutionising bone and cartilaGE reconstruction through Novel cell-instructive biomaterial and peptide-Enhanced Stem cell Immobilization Strategy” (M-ERA.NET3/2024/98/REGENESIS/2025), financed by the National Centre for Research and Development.

References

[1]Gazińska M.A., Ortyl E., Krokos A., Grzymajło M., Kobielarz M., Dąbrowski P., Kressler J. Relationship between the poly(glycerol adipate) prepolymers chain microstructure and linear viscoelastic properties of the elastomers. *Reactive and Functional Polymers*, *2024*, 199, 105891.

[2]Gazinska M.A., Krokos A., Tunable structure and linear viscoelastic properties of poly(glycerol adipate urethane) based elastomeric composites for tissue regeneration. *Journal of the Mechanical Behavior of Biomedical Materials*, *2024*, 153, 106493.

[3]Gazińska M.A., Rudnicka K., Sawicka J., Włodarczyk M., Krokos A., Grzmajło M., Ciołek L., Krupa A., Ortyl E., Biernat M., Rodziewicz-Motowidło S. Bioactive elastomeric composites based on poly(glycerol adipate urethane), bioactive glass, and anoplin-derived peptide for improved antimicrobial properties. *Materials & Design*, *2025*, 260, 15251.

S27 – O5

Decoupling Bone and Cartilage: Biphasic biofabrication of the osteochondral unit using wild-type and RUNX2 KO human MSCs

Puiggalí-Jou A.[1], Ponta S.[1], Chen S.[1], Stoddart M.J.[2], Zenobi-Wong M.[1]
[1]Dept. Health Sciences & Technology, ETH, Zürich; [2]AO Research Institute Davos, Switzerland

Introduction

The osteochondral (OC) unit is a hierarchical tissue composed of hyaline cartilage, calcified cartilage, and subchondral bone, enabling load-bearing and joint stability. Despite its functional integration, the mechanisms that maintain distinct oxygenation, vascularization, and mechanical properties across layers remain poorly understood, complicating *in vitro* replication. Existing approaches rely on multi-material systems or complex microfluidics. Here, we propose a simplified strategy that uses a single biomaterial and uniform culture conditions, while generating zonal specificity via genetically engineered mesenchymal stem cells (MSCs). MSCs are widely used due to their accessibility and differentiation potential; however, their tendency to undergo endochondral ossification (EO), driven by RUNX2, limits stable cartilage formation. Taking advantage of this, we developed biphasic OC constructs combining RUNX2-knockout (KO) MSCs for cartilage formation and wild-type (WT) MSCs for bone formation, aiming to recapitulate native tissue organization.

Materials and Methods

Primary human MSCs were genetically modified using CRISPR/Cas9 to generate RUNX2-KO cells. Single-layer and biphasic constructs were fabricated using Filamented Light (FLight) 3D bioprinting, enabling rapid generation of anisotropic architectures. A bioresin composed of hyaluronic acid and decellularized extracellular matrix was used. KO MSCs were first evaluated in single-layer constructs under chondrogenic and hypertrophic conditions. Subsequently, bilayer OC grafts were fabricated by spatially patterning KO MSCs in the cartilage region and WT MSCs in the bone region (Figure 1a). Constructs were assessed using histology, micro-computed tomography (µCT), mechanical testing, and scanning electron microscopy (SEM).

Results

KO MSCs showed enhanced chondrogenesis compared to WT MSCs, with increased glycosaminoglycan deposition and mechanical properties (1204 ± 296 kPa) comparable to native cartilage. Importantly, KO constructs resisted hypertrophic differentiation, maintaining GAG content and exhibiting low expression of hypertrophic markers (Collagen X, ALP, Osteocalcin). Calcification was minimal (0.29 ± 0.26 mm^3) compared to WT controls (2.70 ± 1.73 mm^3). In biphasic constructs, a well-defined interface was achieved, with a calcified WT region and a stable KO-derived cartilage layer. This spatial organization was confirmed by histology (Figure 1b), µCT, mechanical analysis, and SEM-EDX.

Conclusion

RUNX2 KO enables stable hyaline cartilage formation by preventing hypertrophy and mineralization. Combining KO and WT MSCs in a single-material construct creates a distinct osteochondral interface, offering a promising strategy for OC repair.

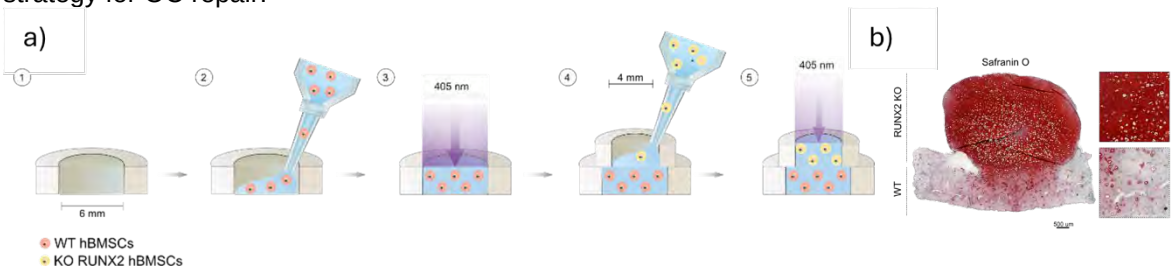

Figure 1. a) Illustration of the osteochondral (OC) unit biofabrication process. b) Safranin O of the construct cultured for 4 weeks in chondrogenic media, followed by 4 weeks in hypertrophic media.

S27 – O6

Decoupling mechanical and biochemical cues in 3D cell culture using biomimetic adaptable materials

Thibieroz N.[1], Machillot P.[1], Dutheil R.[2], Neri C.[1], Marchadier L.[1], Bradshaw A.[1], Picart C.[1], Migliorini E.[1]
[1]Univ. Grenoble-Alpes, INSERM U1292 Biosanté, France

Introduction

The limited predictive power of current in vitro models remains a major bottleneck in drug development, with up to 90% of candidate molecules failing during preclinical and clinical phases. This is largely due to the widespread use of 2D culture systems, which fail to recapitulate the mechanical and biochemical complexity of native tissues. While 3D models have emerged as promising alternatives, many rely on poorly defined matrices, which lack tunability and reproducibility. There is therefore a critical need for biomimetic platforms enabling precise and independent control of extracellular matrix (ECM) parameters.

Materials and Methods

We developed biomimetic adaptable materials (BAM), consisting of a 3D scaffold with different architectures combined with a functionalized coating allowing independent tuning of mechanical and biochemical properties (Figure 1). Stiffness can be modulated within a physiologically relevant range (5–120 kPa), while the biochemical composition can be adjusted through controlled incorporation of glycosaminoglycans, adhesion ligands and morphogens. A proprietary and patented process enables scalable fabrication and functionalization of these materials, compatible with high-content imaging and analysis workflows. Human neuroblastoma cells were cultured in BAM and compared to 2D conditions.

Results

BAM exhibits robust and reproducible architecture across batches, with stable chemical composition over several weeks under storage conditions.
In this context, BAM enables the growth and organization of neuroblastoma cells over a month. Upon treatment with retinoic acid, a differentiation-inducing agent used as treatment for aggressive neuroblastomas, cells cultured in BAM display a reduced sensitivity compared to standard 2D conditions with a stiffness-dependent effect. This differential response highlights the impact of the 3D microenvironment and ECM properties on therapeutic response.

Conclusion

BAM provides a versatile and tunable platform to decouple and control mechanical and biochemical cues in 3D cell culture. By enabling precise modulation of ECM properties and compatibility with high-content analysis, this approach addresses key limitations of existing *in vitro* systems. These results support the potential of BAM as a platform technology for more predictive preclinical models in drug screening and disease modeling.

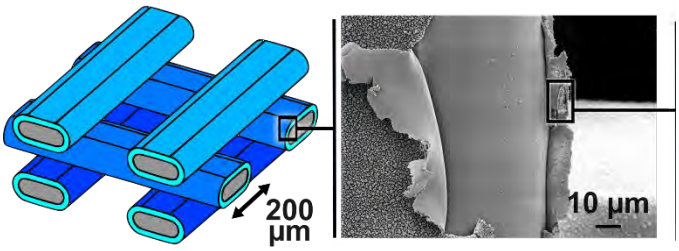

Figure 1: Left: schematic representation of BAM with the 3D printed scaffold with variable pore size and with a coating that permit the tuning of its mechanical and the chemical properties. **Right:** SEM image of an intentional scratch to the surface of the BAM which shows the scaffold backbone and the homogenous coating

Acknowledgements

EM acknowledge the Région Auvergne-Rhone alpes for the Ambition Internationale 2024 funding, the FRM prematuration grant and BFT lab from BPI France. This work is also supported by the French National Research Agency in the framework of the "Inves7ssements d'avenir" program (ANR-15-IDEX-02).

S27 – O7

Mechanotransduction activated by stimuli-responsive biomaterials: Multidoped hydroxyapatite in piezoelectric polymeric matrix

Vukomanović M.[1], Gazvoda L.[1], Zabčić, M[1], Agjelovikj, V.[1], Spreitzer M.[1], Szwed-Georgiou, A.[2] Rudnicka K[2], Mantovani D.,[3] Gazinska, M.[4]
[1]Jožef Stefan Institute, Advanced Materials Dept., Ljubljana, Slovenia; [2]University of Lodz, Faculty of Biology and Environmental Protection, Poland; [3]Laboratory for Biomaterials and Bioengineering, Laval University, Canada; [4]Wrocław University of Science and Technology, Dept. of Polymer Engineering and Technology, Poland

Introduction

In bioinspired materials, hierarchical architectures and chemically active cues facilitate the conversion of mechanical stimuli, such as body motion, into electrochemical signals that are subsequently translated into biological responses. Replicating this strategy in synthetic electroactive polymers combined with bioactive bone-like minerals opens promising new avenues for mechanotransduction-based bone and cartilage repair.

Materials and Methods

Hydroxyapatite was co-doped with multiple bioactive ions to obtain a multi-doped mineral phase (mHAp). The resulting material was incorporated as a filler into a poly-L-lactide (PLLA) matrix and further processed into layered piezoelectric constructs comprising electrospun fibers and uniaxially drawn films. Alongside chemical, structural, mechanical, surface, and morphological characterization, electromechanical activation was evaluated through measurements of mechanically induced surface charge and voltage generation. Cells cultured on these constructs and their components were subsequently analyzed for stimulus-mediated proliferation, differentiation, and actin filament expression.

Results

The hierarchical polymer architecture, consisting of electroactive piezoelectric layers with embedded ion-containing mHAp as chemically active cues, acted as an active functional system that governed mechanically induced electromechanical coupling. Plasma-assisted bonding of the piezoelectric layers enhanced interfacial adhesion, provided additional shear, thereby promoting coupling under cyclic mechanical loading. This effect resulted from both filler-enhanced piezoelectricity and strain generated at the interfaces between adjacent layers. The resulting electromechanical response was effectively translated to biological systems. The piezoelectric fibrous surface supported cell adhesion and enabled efficient transfer of mechanically generated electrical cues to adherent cells, particularly affecting directional migration and cytoskeletal organization, with increased actin expression as a marker of mechanosensing. Beyond electrical effects, the bioactive ion-containing mHAp also enhanced cell proliferation and osteogenic differentiation, further promoting osteogenesis.

Conclusion

The hierarchical structures presented here combine soft, mechanically active organic piezoelectric layers, mimicking fibrous extracellular matrix architecture, with a bioactive ion-releasing mineral phase, mimicking the chemistry of bone mineral. Together, they define a new class of chemically programmed interfaces and stimulus-responsive biomaterials capable of electromechanical transduction and efficient delivery of generated stimuli to cells adhered to their surface. This bioinspired materials design holds strong potential for the development of bioactive bioelectronics in regenerative medicine, particularly for bone and cartilage repair.

Acknowledgement

Work was funded by projects REGENESIS (M-era.net 2024, PR-13605), BoneFill (ARIS- and CNC- funded Weave collaboration), and ARIS funded fundamental research programme P2-0091.

S28
Current advancements in oral, dental and craniofacial tissue regeneration

S28 – K1

Bottino M.
University of Michigan School of Dentistry - USA

S28 – K2

Human epithelial tooth organoids reveal direct causal links between common pharmacological agents and ameloblast dysfunctions

Hasevoets S.[1], Hermans F.[1], Meyns J.[2], Vankelecom H.[3], Declercq H.[4], Wolfs E.[1], Lambrichts I.[1], Bronckaers A.[1]
[1]Biomedical Research Institute (BIOMED), Hasselt University, Diepenbeek; [2]Dept. of Oral and Maxillofacial Surgery, General Hospital St-Jan, Genk; [3]Dept. of Development and Regeneration, KU Leuven; [4]Dept. of Development and Regeneration, KU Leuven campus KULAK, Kortrijk, Belgium

Introduction

Dental enamel formation is a tightly regulated developmental process that is vulnerable to disruption during early life, leading to permanent enamel defects such as 'molar incisor hypomineralization'. While previous studies have associated environmental factors and medical treatments to enamel problems, we still lack direct causal evidence. Recently our team developed Epithelial tooth organoids (ETOs), which are long-term expandable 3D models derived from human dental follicle tissue isolated from unerupted wisdom teeth. These organoids accurately recapitulate the stemness phenotype of the epithelial cell rests of Malassez and possess the intrinsic capacity to differentiate into functional ameloblast-like cells1.

Materials and Methods

ETO were subjected to different concentrations of amoxicillin, bisphenol A, vinblastine, and vincristine. The effect of this exposure on ameloblast differentiation and maturation was investigated using mRNA analysis and Western Blot.

Results

Amoxicillin, vinblastine, and vincristine significantly impeded ameloblast differentiation, as evidenced by reduced expression of the mature enamel matrix proteins AMTN and ODAM. Transcriptomic analysis (bulk RNASeq) following amoxicillin treatment revealed targeted suppression of metabolic and secretory pathway programs, including oxidative phosphorylation, glycolysis, and unfolded protein response. Importantly, ETO also recapitulated the established mechanistic effects of the tested chemotherapeutic agents, such as α-tubulin depolymerization as demonstrated by Western Blot.

Conclusion

In conclusion, these results establish ETO as a robust, high-fidelity platform for investigating the molecular etiology of enamel defects. By revealing how drugs directly interfere with ameloblast differentiation, this work underscores the potential of human tooth organoid systems as study tool for environmental and pharmacological risks to dental health.

Acknowledgements

This work was supported by a grant of the 'Bijzonder Onderzoeksfonds Universiteit Hasselt' (grant BOF22KP12), and by the Fund for Scientific Research (FWO) - Flanders (grant G083626N).

References

Hemeryck L., Hermans F., Chappell J., Kobayashi H., Lambrechts D., Lambrichts I., Bronckaers A., Vankelecom H. Organoids from human tooth showing epithelial stemness phenotype and differentiation potential. *Cell Mol Life Sci 2022*, 79(3), 153.

S28 – O1

From spheroids to macro tissues: Vasculogenic potential of DPSC spheroids for dental pulp tissue engineering

Şenel Demirtaş B.[1], Bronckaers A.[2], Declercq H.[1]
[1]Development and Regeneration, KU Leuven Campus KULAK, Kortrijk; [2]Group of Morphology, Biomedical Research Institute, Hasselt University, Diepenbeek, Belgium

Introduction

Dental pulp is a highly vascularized tissue, responsible for supplying nutrients and oxygen critical for maintaining tooth vitality and function[1]. Despite its critical function, pulpal diseases remains a common oral pathology [2]. Current clinical strategies are lacking in restoring the biological vitality of the pulp, underscoring the need for tissue engineering approaches. Successful regeneration of the pulp depends mainly on the harmony between endothelial cells (ECs) and dental pulp stem cells (DPSCs) within a conducive microenvironment[3]. To address this, we developed a strategy to obtain prevascular microtissue with tissue-specific ECs and DPSCs, enhancing angiogenic potential to support vascular integration and pulp regeneration.

Materials and Methods

Microtissues were generated as bioprintable spheroids to support EC differentiation. Spheroids were formed in chips containing 2865 pores with 200 µm diameter. Differentiation was induced by supplementing EGM2-MV culture medium with Vascular Endothelial Growth Factor (VEGF165) on day 1[3]. EC differentiation was evaluated by confocal imaging of VE-cadherin, von Willebrand factor (vWF),VEGFR1 and VEGFR2 alongside by flow cytometric evaluation of CD31 expression, after enzymatic and mechanical dissociation. In parallel, mesenchymal cell characteristics were assessed by flow cytometry using an MSC panel (CD73, CD90, CD105, CD34, and CD45) (Figure 1). Sprouting assay was performed on Matrigel with VE-cadherin staining to assess angiogenic potential. To investigate tissue-level properties, spheroids were encapsulated in fibrin gel disks and analyzed for spheroid fusion and macro-scale tissue organization. Endothelial–pericyte crosstalk was assessed in both micro and macro scale tissue constructs by alpha-smooth muscle actin (α-SMA) expression.

Results

Differentiation within the spheroids showed strong VE-Cadherin and vWF expression, mainly at the outer layer. Angiogenic potential was further supported by VEGFR1 and VEGFR2 expression and by sprouting assays, which revealed increase in vascular sprouts over time, sprouts also expressing VE-cadherin. Flow cytometry confirmed CD31 positivity, indicating endothelial differentiation significantly higher than in traditional 2D cultures. Simultaneously, expression of the MSC marker panel decreased, consistent with a phenotypic transition. In addition, α-SMA positivity suggested the presence of pericyte-like support cell features. Together, these findings support the vasculogenic potential of DPSC spheroids, characterized by early sprouting behavior and progressive endothelial marker expression during spheroid formation.

Conclusion

This method establishes a robust platform for endothelial and pericyte-like differentiation beyond conventional 2D culture approaches. We believe these microtissues provides a closer mimic of the native dental pulp microenvironment, enhancing physiological relevance. Ongoing optimizations and validation are critical to fully characterize the spheroids and refine the bioprinting strategies for macro-tissue constructs, paving the way for advanced dental pulp regeneration therapies.

Acknowledgements

Acknowledgement: The research is funded by Fonds Wetenschappelijk Onderzoek-Vlaanderen (FWO, G083623N)

References

1. Rombouts, C., Giraud, T., Jeanneau, C. & About, I. Pulp Vascularization during Tooth Development, Regeneration, and Therapy. *Journal of Dental Research vol. 96 2017.*
2. Jakovljevic, A. et al. Prevalence of Apical Periodontitis and Conventional Nonsurgical Root Canal Treatment in General Adult Population: An Updated Systematic Review and Meta-analysis of Cross-sectional Studies Published between 2012 and 2020. *Journal of Endodontics vol. 46 2020.*
3. Bento, L. W. et al. Endothelial differentiation of SHED requires MEK1/ERK signaling. *J Dent Res 92, 2013*

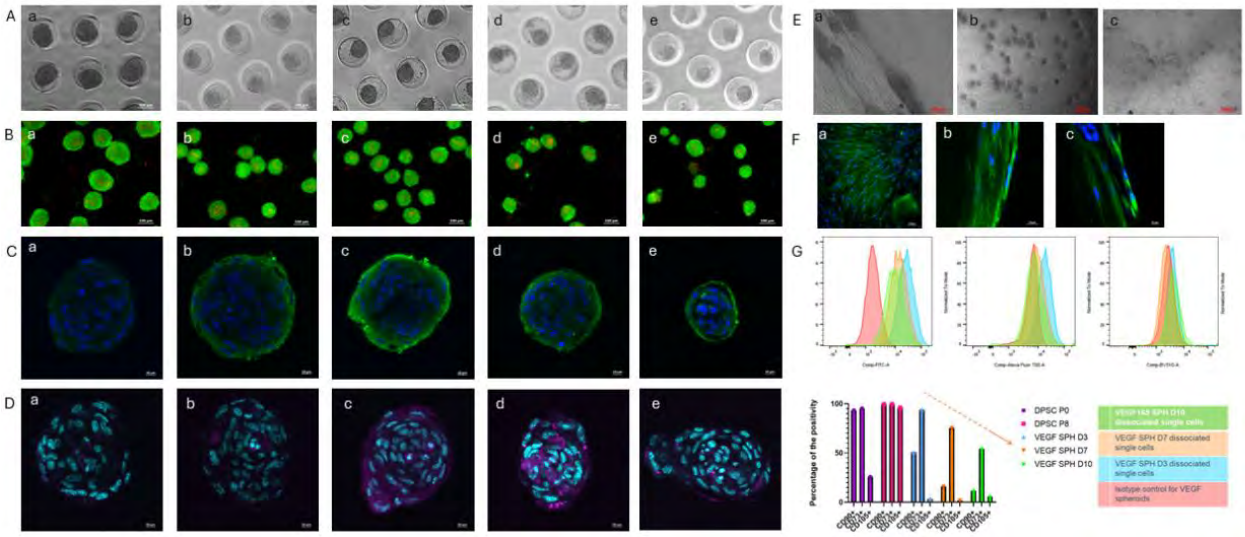

Figure 1. My own data showing: Formation and characterization of DPSC Spheroids supplemented with VEGF165 (1M/2865 spheroids). (A) Brightfield images showing spheroid formation at days 3 (a), 7 (b), 10 (c), 20 (d), and 30 (e) following seeding. (B) Live/dead analysis illustrating spheroid viability at days 3 (a), 7 (b), 10 (c), 20 (d), and 30 (e) (C) Confocal images of immunofluorescence staining for markers VE-cadherin (green) and DAPI (blue) days 3 (a), 7 (b), 10 (c), 20 (d), and 30 (e) (D) Confocal images of immunofluorescence staining for markers VWF (violet) and DAPI (turquoise) at days 3 (a), 7 (b), 10 (c), 20 (d), and 30 (e) (E) Spheroids encapsulated in fibrin gel showing (a) fusion and formation of elongated vascular cord-like structures at day 3; (b) day 10 spheroids cultured in fibrin gel for 3 days; and (c) day 10 spheroids cultured in fibrin gel for 10 days. (F) Confocal imaging of VE-cadherin (green) and DAPI (blue) in day 10 spheroids cultured in fibrin gel, demonstrating cord-like vascular structures. (G) Flow cytometric analysis of mesenchymal stem cell (MSC) markers (CD73, CD90, CD105, CD34, CD45), showing downregulation consistent with endothelial lineage commitment.

S28 – O2

Bioengineered HA-internalizing osteoblasts and osteonectin synergistically boost bone regeneration

Yang W., Li X.[1]
[1]State Key Laboratory of Oral Diseases, West China Hospital of Stomatology, Sichuan University, China

Introduction

Traditional bone scaffolds face limitations in early osteogenesis due to slow calcium/phosphate (Ca/P) ion release from hydroxyapatite (HA) nanocrystals and insufficient biological stimulation. To address this, we proposed a strategy utilizing HA-internalized osteoblasts (OHA) with osteonectin (ON) to enhance early bone regeneration. OHA accelerates Ca/P ion release via lysosomal degradation of internalized HA nanocrystals, activating the PI3K/Akt pathway to promote osteogenic differentiation. ON promotes Ca/P deposition and collagen binding, to jointly enhance early bone regeneration and improve osteogenic quality.

Materials and Methods

Terbium-doped HA (HA-Tb) nanocrystals were synthesized hydrothermally for fluorescence tracing. Polycaprolactone/HA (PHA) scaffolds were fabricated via 3D printing. Rat osteoblasts were pre-incubated with 100 µg/mL HA-Tb to generate OHA. Scaffold groups included PHA (control), PHA+ON, and PHA+ON+OHA. *In vitro* assays assessed osteogenic gene expression (COL1, BMPR, OCN, and OPN), mineralization (Alizarin Red S staining), ion release kinetics (ICP-MS), and lysosomal inhibition validation (BafA1 treatment). *In vivo* evaluations included r rat subcutaneous ectopic implantation (1–4 months) and rabbit femoral critical-sized defects (6 months), analyzed via micro-CT, histology (H&E, Masson), and immunohistochemistry (RUNX2, OCN).

Results

PHA+ON+OHA scaffolds demonstrated superior osteogenic potential *in vitro*, with upregulated osteogenic genes and enhanced mineralization. ICP-MS confirmed rapid Ca/P release from OHA via lysosomal degradation, which was abolished by BafA1. *In vivo*, subcutaneous implantation revealed that PHA+ON+OHA scaffolds induced ectopic bone formation, with increased collagen maturation and angiogenesis. In the rabbit femoral defect model, PHA+ON+OHA scaffolds exhibited significantly higher bone volume (BV/TV), bone mineral density (BMD), and trabecular integrity at 6 months compared to controls. Immunostaining showed sustained RUNX2 and OCN expression, indicating enhanced osteogenic differentiation and matrix mineralization.

Conclusion

The OHA+ON synergistic strategy addresses the limitations of traditional scaffolds by enabling rapid Ca/P release via lysosomal degradation and promoting matrix maturation via ON. This dual-pathway approach enhances early osteogenesis and long-term bone quality, offering a promising solution for complex bone defect repair, including ischemic and load-bearing environments.

Acknowledgements

This work was supported by the National Natural Science Foundation of China (Grant No. 32071335).

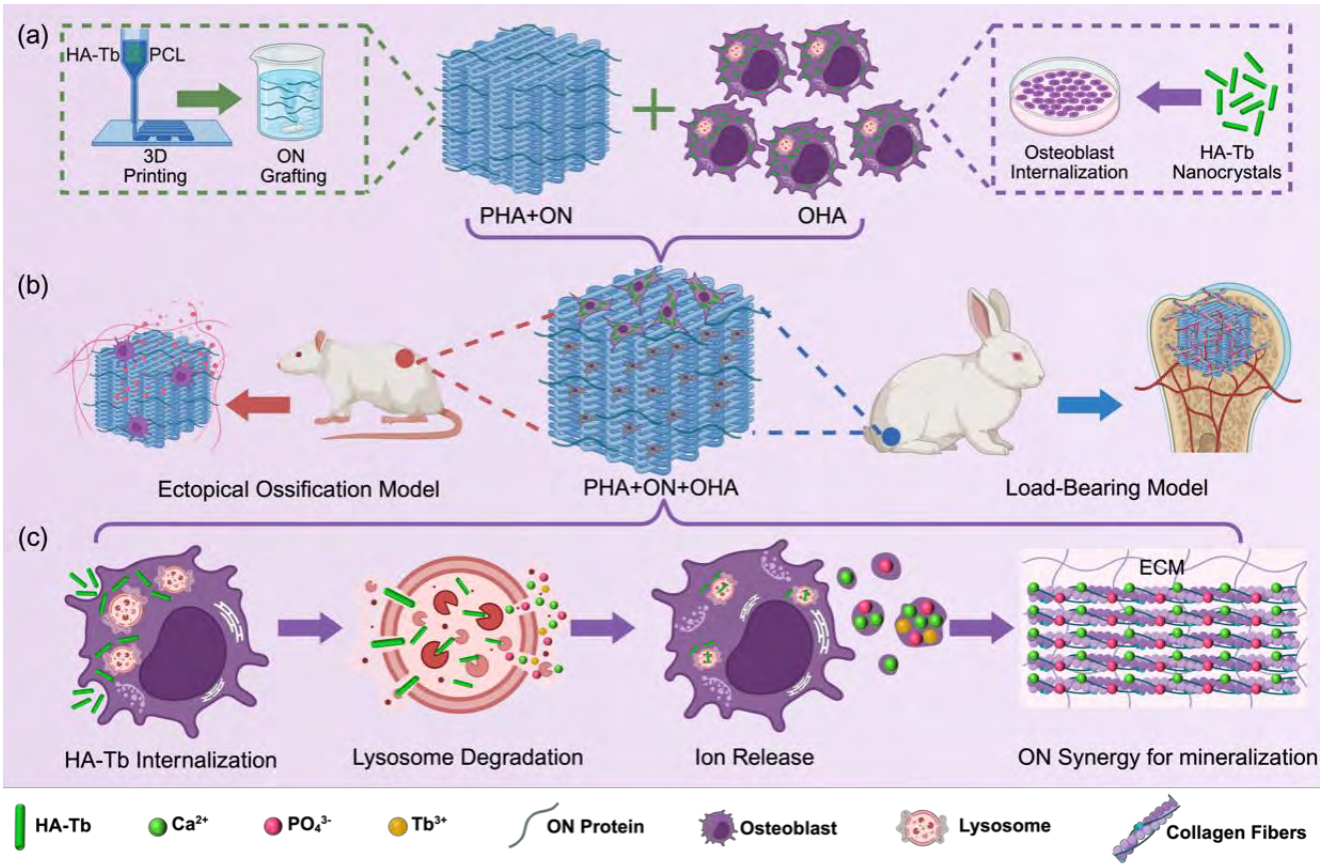
(a)
HA-Tb
PCL
3D Printing
ON Grafting
PHA+ON
OHA
Osteoblast Internalization
HA-Tb Nanocrystals
(b)
Ectopical Ossification Model
PHA+ON+OHA
Load-Bearing Model
(c)
ECM
HA-Tb Internalization
Lysosome Degradation
Ion Release
ON Synergy for mineralization
HA-Tb
Ca2+
PO43-
Tb3+
ON Protein
Osteoblast
Lysosome
Collagen Fibers

S28 – O3

Design and processing of UV-curable calcium phosphate Inks for direct ink writing of tooth root scaffolds

Alexandridis A.[1], Koos E.[2], Vleugels J.[1], Jacobs R.[3], EzEldeen M.[3,4], Braem A.[1]
[1]KU Leuven Dept. of Materials Engineering; [2]KU Leuven Dept. of Chemical Engineering; [3]KU Leuven Dept. of Imaging and Pathology; [4]KU Leuven Dept. of Oral Health Sciences, Belgium

Introduction

Traumatic dental injuries (TDIs) affect approximately 20% of children and adolescents and often lead to permanent tooth loss, creating significant functional and aesthetic challenges. Current treatment strategies such as tooth auto-transplantation or orthodontic alignment are limited by donor tooth availability and compatibility, while conventional titanium implants are unsuitable due to ongoing dentoalveolar development. Regenerative dental therapies represent a promising alternative, and additive manufacturing can play a key role by enabling the fabrication of patient-specific bioceramic scaffolds that accurately reproduce the geometry of the tooth root. Calcium phosphates (CaPs), including β-tricalcium phosphate (β-TCP) and hydroxyapatite (HAp), are widely used in mineralized tissue engineering due to their compositional similarity to dentin and bone. However, successful fabrication of CaP scaffolds via UV-assisted direct ink writing (UV-DIW) requires optimization of the entire processing route, from ink formulation and rheology to printing parameters and post-processing, to achieve high shape fidelity and adequate mechanical performance.

Materials and Methods

UV-curable ceramic inks composed of β-TCP, HAp, or biphasic calcium phosphate (BCP) powders combined with acrylate-based reactive monomers, a non-reactive diluent, dispersant, and photoinitiator were formulated for UV-DIW processing. Rheological characterization was performed to evaluate flow behavior and structural response in order to assess printability. The influence of solid loading and dispersant concentration on suspension stability was investigated through rheological measurements and zeta potential analysis. Printing parameters, including extrusion pressure, printing velocity, layer height, and line spacing, were optimized using a design-of-experiments (DoE) approach. UV-DIW entails a curing step after each layer deposition; therefore, curing depth was evaluated to ensure sufficient interlaminar adhesion while avoiding overcuring. Following printing, scaffolds were sintered using composition-specific thermal cycles to optimize densification and minimize phase transformation and grain growth. Dimensional accuracy and internal defects were evaluated using micro-focus computed tomography (micro-CT), and mechanical performance was assessed through uniaxial compression testing.

Results

All formulations exhibited pronounced shear-thinning behavior, enabling stable extrusion and filament shape retention during printing. Combined rheological and zeta potential analyses identified the optimal dispersant concentration and solid loading for each composition, demonstrating that dispersant oversaturation increased both flow and yield stress, resulting in unstable extrusion and restricted material flow through the nozzle. DoE-based optimization revealed a narrow processing window in which extrusion pressure and printing speed must be carefully balanced to maintain consistent filament diameter and dimensional fidelity. Sintering evaluation showed densification levels above 98% for all compositions without formation of the α-TCP phase. For BCP compositions, however, further densification appeared limited by the different sintering behavior of the constituent phases. Micro-CT analysis indicated that raster orientation and stacking sequence significantly influenced defect formation, with unidirectional architectures exhibiting the highest number of internal defects. Compression testing revealed distinct mechanical responses among β-TCP, HAp, and BCP scaffolds, reflecting differences in microstructure, densification, and printing conditions.

Conclusion

This study establishes a systematic framework linking ink formulation, rheological behavior, and process parameters to the fabrication of high-fidelity CaP scaffolds using UV-DIW. The findings demonstrate that controlled ink design and process optimization enable reliable fabrication of β-TCP, HAp, and BCP scaffolds with tailored mechanical properties, providing a foundation for patient-specific bioceramic dental root scaffolds for regenerative therapies in growing patients.

Acknowledgements

KU Leuven Internal founding IDN/23/008#57610364
DREIMS Project

S28 – O4

In situ photocrosslinked thiol-ene/dithiolane nanocomposite hydrogels based on modified-hyaluronic acid and dendritic polymer for bone regeneration

Lo Re A.[1], Biscari G.[1], Tesfaye A.[2], Pitarresi G.[1], Palumbo F.S.[1], Malkoch M.[2], Fiorica C.[1]
[1]STEBICEF, University of Palermo, Italy; [2]Coating Technology, KTH Royal Institute of Technology, Stockholm, Sweden

Introduction

Bone tissue engineering is widely used in orthopedics, dentistry, and maxillofacial surgery. The increasing incidence of bone diseases, such as osteoporosis, is expected to raise graft demand. In situ-forming biopolymer hydrogels provide promising regenerative support, particularly as fillers for irregular bone defects, due to their site adaptability and controlled degradability, which enable scaffold replacement and regulate cell behavior. Hydroxyapatite (nHAp) incorporation improves osteoconductivity, mechanical properties, and similarity to native bone. Among in situ crosslinking strategies, thiol-based photo-click chemistry is attractive for its rapid and controllable gelation. Upon irradiation, thiyl radicals react with vinyl groups via thiol-ene chemistry (TEC) or recombine to form disulfide bonds, for example from lipoic acid (LA) functionalities, enabling efficient formation of injectable, tunable hydrogels for bone repair.

Materials and Methods

An amine derivative of hyaluronic acid (HA) was functionalized with LA via EDC/NHS coupling. LA incorporation enabled light-triggered formation of dual-crosslinked networks via disulfide exchange and TEC coupling with the DLD's allyl. Injectable nHAp-loaded hydrogels were developed and photocrosslinked under 405 nm irradiation using the HA derivative and an allyl-terminated dendritic-linear-dendritic (DLD) polymer, without photoinitiator (Fig.A,B). Network morphology was examined by SEM. Swelling and stability were monitored for up to one month under physiological-mimicking conditions, including susceptibility to reducing environments. Rheological behavior was investigated before and after irradiation. Radical-scavenging activity was quantified using the ABTS assay, and intracellular ROS levels were measured in FD-MSC cells using the DCFH-DA probe. Cytotoxicity was tested in FD-MSCs.

Results

Photo-rheology confirmed rapid gelation, which was not affected by nHAp incorporation, while amplitude and frequency sweep demonstrated the formation of mechanically stable viscoelastic networks suitable for in situ bone defect filling. The hydrogels exhibited high stability under physiological conditions and responsiveness to reducing environments. Notably, nHAp incorporation increased the swelling ratio and contributed to maintaining hydrogel stability. In particular, the presence of nHAp mitigated hydrogel degradation under reducing conditions, indicating a protective effect against reductive environments. The systems also displayed radical-scavenging activity. Cell viability assays demonstrated good cytocompatibility along with enhanced cell proliferation (Fig. B). Lastly, SEM analysis revealed homogeneous and interconnected porous architecture (Fig.C).

Conclusion

This dual-crosslinked hydrogel forms networks under light without photoinitiators, with tunable crosslinking, environmental responsiveness, and radical-scavenging activity conferred by LA. Its injectability, cytocompatibility, ECM-mimetic design, HA-driven acceleration of cell proliferation, and the osteoinductive potential of nHAp make it a promising minimally invasive scaffold for repairing complex or critically sized bone defects.

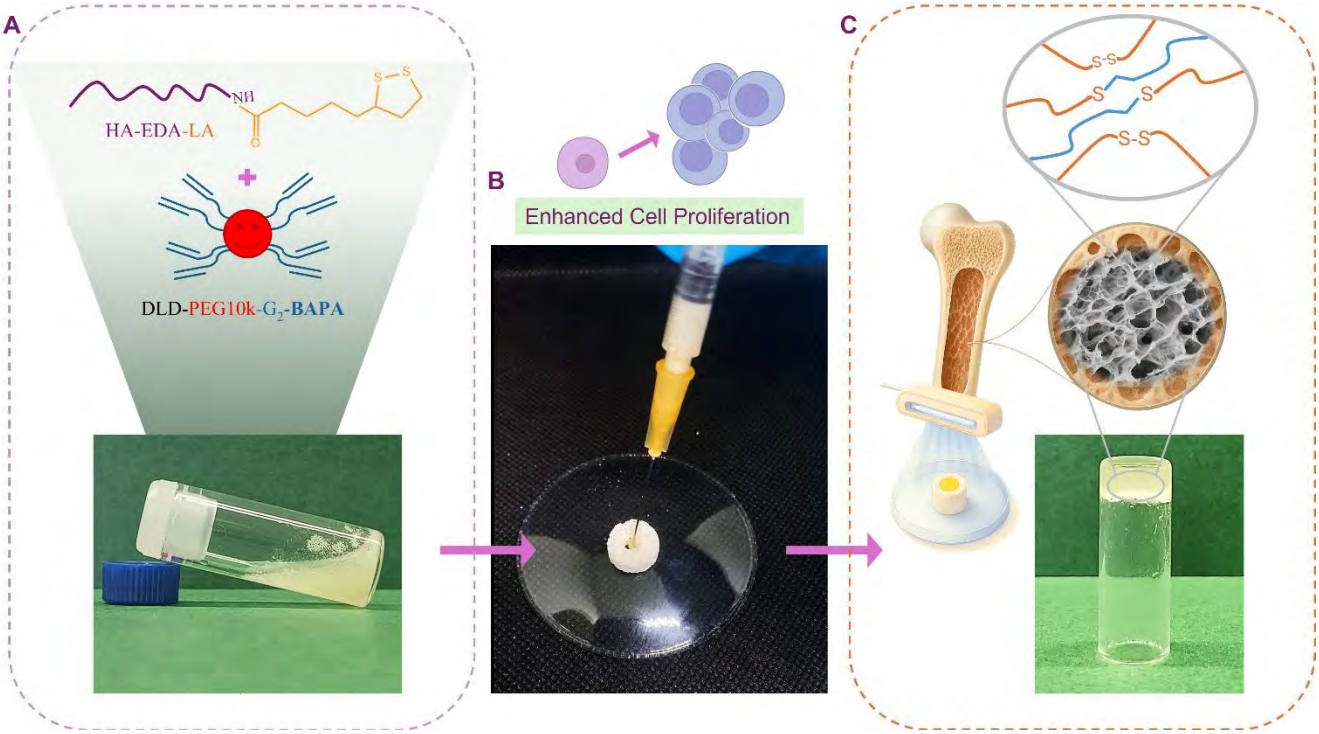
A
HA-EDA-LA
NH
S
S
DLD-PEG10k-G2-BAPA
B
Enhanced Cell Proliferation
C
S-S
S
S
S-S

S29
Current concepts in orthopaedic device-related infection

S29 – K1
Biomaterials for multidrug-resistant implant infection: bacteriophages and beyond

Moriarty F.
A.O. Research Institute – Switserland

S29 – K2
Animal models for testing efficacy of antimicrobial biomaterials

Animal models for testing efficacy of antimicrobial biomaterials

Siverino C.[1], Moriarty T.F.[1,2], D'Este M.[1], Metsemakers W.J.[3]
[1]AO Research Institute Davos, Davos Platz, Switzerland; [2]Center for Musculoskeletal Infections, Department of Orthopaedic and Trauma Surgery, University Hospital Basel, Basel, Switzerland; [3]Department of Trauma Surgery, University Hospitals Leuven, Leuven, Belgium

Introduction
Orthopaedic device-related infections (ODRI) remain a major clinical challenge, often leading to implant failure, prolonged treatment, and increased healthcare costs. The development of antimicrobial biomaterials has emerged as a promising strategy to prevent and manage these infections. However, reliable preclinical evaluation is essential before clinical translation, and animal models play a critical role in assessing efficacy and safety.

Aim. To provide an overview of current animal models used to evaluate antimicrobial biomaterials in ODRI and to highlight key considerations for their translational relevance.

Materials and Methods
A structured overview of preclinical in vivo models was performed, focusing on commonly used species, implant systems, and infection protocols. Models were analyzed according to their ability to replicate clinical conditions, including bacterial inoculation strategies, biofilm formation, host immune response, and surgical procedures.

Results
Animal models are essential for evaluating antimicrobial biomaterials, as in vitro systems cannot replicate complex host-pathogen interactions, immune responses, and pharmacokinetics. A spectrum of models exists, ranging from rodent models for mechanistic and high-throughput studies to large animal models that approximate human anatomy and surgical conditions.
Model selection is highly dependent on the research question, with increasing complexity required for translational validation. Clinically relevant models incorporate resistant pathogens, realistic implants, and soft tissue involvement. However, challenges remain in standardization, model sensitivity, and reproducibility.
Preclinical studies demonstrate that antimicrobial biomaterials, particularly local delivery systems, can reduce bacterial burden and biofilm formation. Importantly, in vivo models reveal critical factors such as spatial antibiotic distribution and the differences between prophylactic and therapeutic efficacy, which cannot be captured in vitro.

Conclusion
Animal models are indispensable for assessing the efficacy of antimicrobial biomaterials in ODRIs. Careful selection and design of models are essential to ensure clinical relevance. Future efforts should focus on standardization and the development of complex, clinically representative models to improve translational success.

S29 – K3
Strategies for the prevention of implant-associated infection

Wildemann B.
Experimental Trauma Surgery, Jena University Hospital, Friedrich-Schiller-University, Jena, Germany

Implant-associated infections remain a major challenge in modern medicine, often leading to impaired healing, implant failure, and the need for revision surgery. Conventional approaches to infection prevention, including systemic antibiotic therapy, are increasingly limited by antimicrobial resistance and the inability to effectively target bacteria at the implant–tissue interface. Engineering infection-preventing implants therefore represents a promising strategy to prevent bacterial adhesion, biofilm formation, and subsequent infection.

This presentation will explore emerging strategies for modifying implant surfaces and materials to enhance their antimicrobial properties while maintaining biocompatibility and functional performance.

S29 – K4

Soft biomaterials for antibiotic delivery: A design journey guided by surgical practice

Nylund P.[1], Siverino C.[1], Röschli B.[1], Richards R.G.[1], Montali A.[2], Moriarty T.F.[1], D'Este M.[3]
[1]AO Research Institute Davos; [2] AO Innovation Translation Center, Davos, Switzerland

Introduction

Fracture-related infections (FRI) represent a major complication in orthopedic trauma surgery, often resulting in prolonged treatment periods and substantial socioeconomic burden. Systemic antibiotic therapy can be ineffective in this context due to impaired vascularization and tissue damage at the infection site, limiting the ability to achieve therapeutic drug concentrations. Local antibiotic delivery using biomaterials such as bone cements can overcome some of these limitations by providing local drug release; however, these materials typically require surgical removal, introducing additional patient morbidity, costs, and infection risk.
To address these challenges, we developed a bioresorbable, injectable, emulsion-based GEl for Delivery of Antibiotics (GEDAI) tailored for the treatment of FRI.

Aim

To present a translation-driven development pathway for a soft, bioresorbable biomaterial enabling localized delivery of gentamicin, vancomycin, and tobramycin, from formulation and comprehensive in vitro characterization, to assessment of antimicrobial performance.

Materials and Methods

A questionnaire was administered to orthopaedic surgeons from a referral center of musculoskeletal infections to gain feedback on preferred formulations and design input of biomaterials for antibiotic delivery.
A parametric study to determine a formulation matching the design criteria was followed by physico-chemical characterization including rheological behavior, droplet size, zeta potential, antibiotic release kinetics and antimicrobial activity. Adhesion energy on gloves and metals was measured, as well as ATR FT-IR to characterize the surface chemistry determining the adhesion properties.

Results

Tack test indicated good adhesion to metal and leather, and poor adhesion to surgical gloves, likely due to preferential deposition of hydrophobic components on surgical gloves as indicated by FT-IR analysis. This feature was included in the design based on input from the surgeons. Macroscopic stability was confirmed by zeta potential measurements, as well as submicron droplet size in the dispersed oil phase. Rheological profile (Figure 1) confirmed shear thinning, injectability and elastic recovery, preserved in presence of gentamicin and tobramycin (G and T in Figure 1, respectively). Gentamicin and vancomycin were released in 24-48 h in vitro, preserving planktonic and biofilm bacteria-killing activity. Importantly, GEDAI can be sterilized with methods widely used in industry and recognized by regulatory authorities.

Conclusion

The innovative potential of the antibiotic-loaded GEDAI lies in fulfilling surgeon-driven design goals for its physicochemical properties, thereby addressing the unmet clinical needs in infection management for orthopedic trauma. Its composition reflects these design goals and offers several unique translational advantages over existing solutions.

Acknowledgements

The AO Foundation and the AO Innovation Translation Center for financial support.

Figure 1

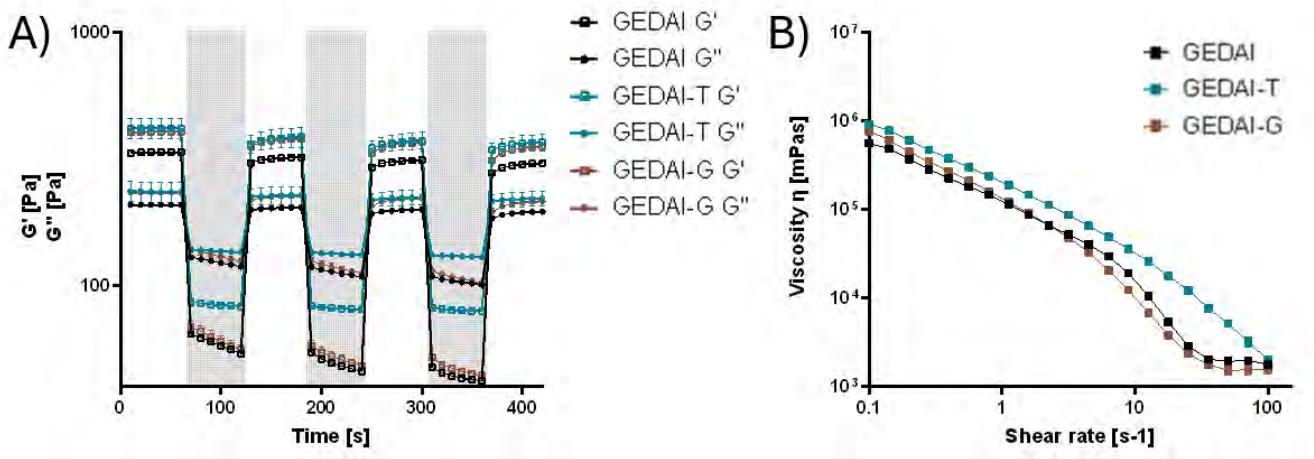
A)
1000
100
G' [Pa]
G'' [Pa]
0
100
200
300
400
Time [s]
GEDAI G'
GEDAI G''
GEDAI-T G'
GEDAI-T G''
GEDAI-G G'
GEDAI-G G''
B)
10^7
10^6
10^5
10^4
10^3
Viscosity η [mPas]
0.1
1
10
100
Shear rate [s-1]
GEDAI
GEDAI-T
GEDAI-G

S29 – O1

Development of propolis-loaded alginate dry hydrogels with antibacterial properties for osteomyelitis treatment

Gomes R.[1,2], Monteiro F.J.[1,2,3,4], Martins M.C.L.[1,2,4,5], Barros J.[1,2]
[1]Bioengineered Surfaces, I3S, Instituto de Investigação e Inovação em Saúde, Universidade do Porto; [2]INEB, Instituto de Engenharia Biomédica, Universidade do Porto; [3]FEUP, Faculdade de Engenharia da Universidade do Porto; [4]PCCC, Porto Comprehensive Cancer Center Raquel Seruca; [5]ICBAS, Instituto Superior de Ciências Biomédicas Abel Salazar, Universidade do Porto, Portugal

Introduction

Osteomyelitis is a severe bone infection with a significant impact on healthcare systems and patients' quality of life, resulting in high morbidity and mortality rates. This infection is primarily caused by *Staphylococcus aureus* and is associated with biofilm formation, antibiotic resistance, and impaired bone regeneration. Current treatments rely on prolonged systemic antibiotic therapy and surgical intervention, leading to poor outcomes and the formation of large bone defects.

Aim

This work aimed to develop a biomaterial that is easy to transport, store, and handle, enabling direct implantation into bone defects to provide temporary structural support and localised, high-dose delivery of antibacterial agents. Considering these requirements, propolis (Ps)-loaded alginate (Alg) dry hydrogels were developed as natural and multifunctional scaffolds. Nano-hydroxyapatite (NanoHAp) and hyaluronic acid (HA) were incorporated to enhance the structural and regenerative properties of the material.

Materials and Methods

Alg-based hydrogels (2% w/v) incorporating Ps, NanoHAp (30% w/w), and HA (1.5% w/w) were fabricated by casting, freeze-drying, calcium crosslinking, and a second lyophilisation. Structural and morphological characterisation was performed by scanning electron microscopy (SEM), histology, confocal microscopy, and micro-computed tomography. Physicochemical properties were assessed by Fourier transform infrared spectroscopy (FTIR), swelling ratio, water content, and pH stability. Ps release was quantified by UV–Vis spectroscopy. Biological evaluation included cytocompatibility (L929 cells, ISO 10993-5), HET-CAM irritation assay, and antibiofilm activity against *S. aureus*.

Results

The two-step lyophilisation strategy yielded homogeneous and stable scaffolds with improved storage capacity and reproducibility. Upon hydration, they recover their hydrogel form, exhibiting typical hydrogel behaviour.
All components were successfully incorporated into the Alg network, as confirmed by FTIR and confocal microscopy. Distinct internal structures and pore morphologies were observed by SEM. HA-containing formulations exhibited increased swelling, water content, and porosity, along with enhanced Ps release, resulting in improved antibiofilm activity (Fig. 1). This behaviour is attributed to the hydrophilicity of HA and electrostatic repulsion effects.
In contrast, NanoHAp incorporation reduced swelling and Ps release, leading to denser structures with lower porosity (Fig. 2) and higher mechanical strength, due to increased matrix density and packing efficiency.
Ps-loaded scaffolds demonstrated significant antibacterial activity against *S. aureus* biofilms in a concentration-dependent manner.

Conclusion

All formulations were cytocompatible and non-irritant. Ps-loaded Alg dry hydrogels represent a promising material for osteomyelitis treatment, offering a potential strategy for simultaneous infection control and bone regeneration. HA-containing scaffolds are suitable for rapid antibacterial action, while NanoHAp-based systems provide improved mechanical support and sustained release.

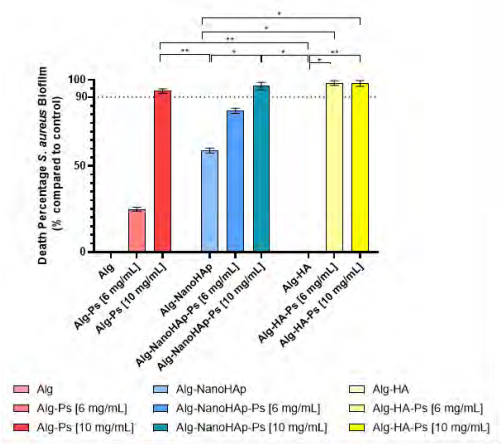

Figure 1 - Antibacterial activity against *Staphylococcus aureus* biofilm. Percentage of biofilm-associated *S. aureus* cell death relative to the control after 24 h treatment with the different hydrogel formulations (n=3).

Hydrogels	Connectivity	Total Porosity (%)	Open Porosity (%)	Closed Porosity (%)	Pore diameter (µm)	Wall Thickness (µm)
Alg	11288	59.77121	59.74236	0.07166	80.99	42.95
Alg-Ps	1392	28.88349	28.4749	0.57126	44.81	54.51
Alg-NanoHAp	8716	40.22484	40.01737	0.34588	52.25	55.61
Alg-NanoHAp-Ps	3777	46.15037	45.9221	0.42212	65.79	51.8
Alg-HA	9015	56.63586	56.57195	0.14716	88.84	55.31
Alg-HA-Ps	9310	40.3323	40.16308	0.28281	48.72	47.31

Figure 2 - Quantitative morphometric analysis obtained by micro-CT. Morphometric parameters obtained from micro-CT analysis, including connectivity density, total porosity, open and closed porosity (%), mean pore diameter, and wall thickness (µm) for each scaffold formulation.

S29 – O2

Localised corrosion and mechanical degradation in clinically used bone rasps

Ibrahim M.[1], Böregård I.-L.[2,3], Oxblom A.[2,4], Kalzén H.[2], Frostell C.[5], Björling G.[2,6,7], Aune R.E.[1]
[1]Dept. of Materials Science and Engineering, Norwegian University of Science and Technology, Trondheim, Norway; [2]Dept. of Anaesthesia, Operation, and Intensive Care, Södertälje Hospital, Region Stockholm, Södertälje, Sweden; [3]Dept. of Clinical Neuroscience, Karolinska Institute (KI), Stockholm, Sweden; [4]Dept. of Clinical Science, Intervention and Technology, KI, Stockholm, Sweden; [5]Dept. of Clinical Sciences Danderyd Hospital, KI, Stockholm, Sweden; [6]School of Health and Welfare, Jönköping University, Jönköping, Sweden; [7]Kaolrinska institutet, Dept. of Neurobiology, Care Sciences, and Society, Stockholm, Sweden

Introduction

Bone rasps are surgical instruments used to shape bones during orthopaedic procedures, where controlled material removal and surface precision are essential. During repeated clinical use, they are exposed to mechanical loading, sterilization cycles, and biological fluids, placing strict demands on mechanical integrity and cleanliness [1]. However, clear criteria for their removal from service remain poorly defined [2].

Most bone rasps are manufactured by CNC machining, producing surface geometries that directly influence wear, fluid interaction, and debris retention. These features can promote damage accumulation, corrosion, and retention of biological material, meaning surface integrity depends not only on material composition but also on manufacturing-induced geometry.

Aim

The aim of the present study was to identify degradation mechanisms in clinically used bone rasps and to assess how machining-induced surface features govern the localisation of corrosion and material accumulation, to support more informed decisions on instrument reuse and replacement.

Materials and Methods

Clinically used surgical bone rasps were analysed and compared with an unused control of identical design. Surface morphology and damage were characterised using stereomicroscopy and scanning electron microscopy. Elemental composition was analysed using X-ray fluorescence spectroscopy to identify the composition of the rasp.

Results

The used rasps exhibited pronounced mechanical degradation, including deformation and abrasive wear along cutting edges. Localised corrosion was confined to the central regions of individual grooves following CNC machining paths (Fig. 1), indicating non-random localisation governed by surface geometry. No comparable corrosion features were observed on the unused control. Material consistent with biological residues was present within groove crevices, confirming retention of organic matter after clinical use and standard cleaning and sterilisation.

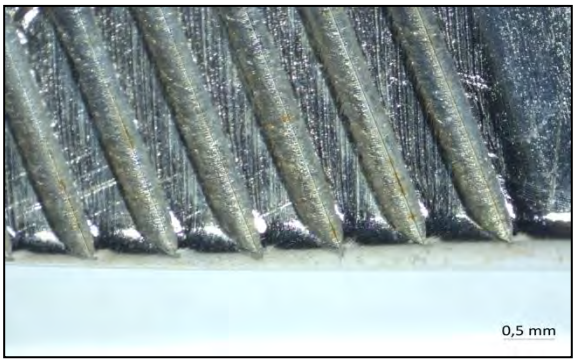

Fig.1: Stereomicroscopy image of a used bone rasp showing machining grooves with localised surface degradation concentrated in the groove centres.

Conclusion

Localised corrosion in surgical bone rasps is governed by machining-induced groove geometry, which creates confined regions that promote corrosion initiation and retention of debris and biological material. The interaction of mechanical damage, corrosion, and retained residues defines a coupled degradation mechanism driven by surface design and clinical exposure.
Degradation is not uniformly distributed and may remain undetected during routine inspection, highlighting the need for geometry-aware criteria to determine when instruments should be removed from service.

References

1. De Melo Costa, D., et al., *Evaluation of Stainless Steel Surgical Instruments Subjected to Multiple Use/Processing. Infection, Disease & Health, 2018*. 23(1): p. 3–9.
2. Lopes, L., et al., *Complex Design of Surgical Instruments as Barrier for Cleaning Effectiveness, Favouring Biofilm Formation. Journal of Hospital Infection, 2019*. 103(1): p. e53–e60.

S29 – O3

Development of Mg-Y-Zn based alloys for orthopaedic staple applications

Wiese B.[1], Helmholz H.[1], Sun Y. [1], Garcés G.[2], Wieland D.C.F.[1], Bohlen J.[3], Willumeit-Römer R.[1], Tolnai D.[1]
[1]Institute of Metallic Biomaterials, Helmholtz-Zentrum Hereon, Geesthacht, Germany; [2]Dept. of Physical Metallurgy, National Center for Metallurgical Research, CENIM-CSIC. Madrid, Spain; [3]Institute of Material and Process Design, Helmholtz-Zentrum Hereon, Geesthacht, Germany

Introduction

The Young's modulus of Mg alloys closely matches that of cortical bone, enabling favourable load transfer and minimizing stress shielding. Furthermore, their controlled degradation under physiological conditions eliminates the necessity for removal surgery, thereby improving patient comfort and reducing both surgical risks and healthcare costs. Alloying magnesium with yttrium and zinc enhances its mechanical performance as appropriate processing conditions promote the formation of LPSO structures, significantly increasing strength without compromising ductility. In combination with their demonstrated biocompatibility, Mg-Y-Zn alloys are promising candidates for next-generation biodegradable implant materials.

Materials and Methods

The material was produced by permanent-mould indirect chill casting. Four alloy compositions were prepared: a base alloy of Mg1.8Y0.6Zn, and three modified variants containing an additional 1.6 wt.% Gd, 1 wt.% Ag, and 0.4 wt.% Ca, respectively. The resulting ingots were homogenized at 400 °C for 24h and subsequently water-quenched. Indirect extrusion was carried out at 400 °C using an extrusion ratio of 1:25 and a ram speed of 1 $mm \cdot s^{-1}$. Microstructural characterization was performed by means of scanning- and transmission electron microscopy. Mechanical properties were evaluated at room temperature under constant initial strain rate of 10^{-3} s^{-1}. Degradation behaviour was assessed in SBF, and biocompatibility was investigated via cell viability tests using SCP-1 mesenchymal stem cells. In vivo tests with follow-ups of 8 weeks were involved to investigate the safety profiles.

Results

The microstructure of the alloys consists of Mg grains and the 18R-type LPSO structure formed during solidification. During homogenization it partially transforms into 14H-type structure that also precipitates from the Mg-matrix. The addition of Gd and Ag promotes the formation of 14H, while Ca stabilises the 18R structure. The mechanical tests show that the base alloy exhibits the highest yield strength 157±2 MPa, while the alloying additions increase both UTS and ductility. The degradation rates in SBF range between 0.11±0.3 mm/y (Mg-1.8Y-0.6Zn1-Ag) and 0.17±0.5 mm/y (Mg-1.8Y-0.6Zn-1Gd). In vitro assays confirm biocompatibility with viable cells observed on all sample surfaces. The preliminary in vivo evaluation in rat femur, demonstrated no adverse local reaction in response to Mg1.8Y0.6Zn1Ag.

Conclusion

Mg-Y-Zn–based alloys containing low concentrations of alloying elements exhibit adequate mechanical strength, low degradation rates, and favourable in vitro and in vivo biocompatibility. The incorporation of additional elements can further extend their functionality, e.g. antibacterial properties through Ag additions or enhancing sintering behaviour with Ca. Collectively, these characteristics render such alloys suitable for use as biodegradable implants in orthopaedic and trauma surgery.

S29 – O4

Marine waste shells as new biomaterials for orthopaedic application: Eco-friendly conversion route to obtain green hydroxyapatite and nanostructured coatings

Montesissa M.[1], Graziani G.[2], Fischetti T.[1], Perut F.[1], Boi M.[1], Sassoni E.[3] and Baldini N.[1,4]
[1]Biomedical Science and Technologies and NanoBiotechnologies Lab, IRCCS Istituto Ortopedico Rizzoli, Bologna; [2]San Raffaele Rome University; [3]Dept. of Civil, Chemical, Environmental and Materials Engineering, University of Bologna; [4]Dept. of Biomedical and Neuromotor Sciences, University of Bologna, Italy

Introduction

Synthetic bone substitutes are used in orthopaedics to promote osseointegration by mimicking the composition and structure of natural bone. Developing new biomaterials for nanostructured coatings remains challenging. Marine waste rich in calcium carbonate ($CaCO_3$) offers a promising sustainable source for producing green bone substitutes, particularly through its conversion into hydroxyapatite (HA), allowing the reduction of waste material in the food supply chain. However, conventional synthetic methods require high temperatures and toxic reagents, leading to significant energy consumption and environmental impact.

Aim

New mild-wet conversion of $CaCO_3$ from marine waste is proposed to obtain green HA. Subsequently, the use of green HA for coating fabrication is also explored.

Materials and Methods

Three $CaCO_3$ marine sources were used in coarse and powder form: cuttlefish bones, mussel and clam shells. A mild-wet treatment was performed for 48h at room temperature using an aqueous solution with different concentrations of diammonium phosphate (DAP, 0.1M and 1M) and the addition of ethanol (EtOH), isopropanol (IPA) and/or calcium chloride ($CaCl_2$). The converted materials were characterized by scanning electron microscopy (SEM-EDS) and FTIR spectroscopy. The preliminary biological response to the converted HA was tested on L929 fibroblasts using Alamar Blue assay. Coatings were fabricated using green HA by Ionized Jet Deposition (IJD) and characterized by SEM-EDS and FTIR.

Results

Cuttlefish bone and clams are composed of $CaCO_3$ in aragonite form and mussels in calcite form, with trace elements such as Na^+, Sr^{2+} and Mg^{2+}. FTIR showed that the conversion efficiency was higher for the powders than for the coarse form, and higher when using 1M DAP compared to 0.1M DAP. Moreover, the use of organic solvents improved HA formation. The best treatment conditions were different for each precursor, being 1M DAP for cuttlefish bone, 1M DAP + IPA + $CaCl_2$ for mussel and 1M DAP + IPA for clamshell. The converted powders had a spherical shape with undefined edges and Ca/P similar to biogenic HA (around 1.5). The converted powders were not cytotoxic on L929 cells using the correct amount and increased cell proliferation, underlined their potential use for coating fabrication. Nanostructured coatings of green HA were obtained by Ionized Jet Deposition, and SEM showed their morphology as globular aggregates uniformly covering the substrate surface. The coatings chemical composition was similar to the starting sputtering targets as confirmed by FTIR and EDS analyses, and they closely resembled human bone HA in terms of Ca/P, ion doping, and crystallinity. In addition, no cytotoxic effect on L929 cells was observed for the coatings.

Conclusion

$CaCO_3$ obtained from marine sources was converted successfully to green HA using a new mild-wet synthesis. The HA obtained was used for the development of new biomaterials such as nanocoatings for orthopaedic field.

S30
Designing functional biomaterials through Nano/Micro-Building blocks for targeted cancer therapy and regenerative application

S30 - K1
Theragenerative microaerogels with hydrogen and heat releasing properties for osteosarcoma management

Demidov Y.[1,2], Nayin A. [1,2], Thuir D. [1,2], Shafiei V. [1,2], Maleki H.H.[1,2]*
[1]Institute of Inorganic and Materials Chemistry, Dept. of Chemistry, University of Cologne; [2]Center of Molecular Medicine Cologne, CMMC Research Center, Germany

Introduction
Osteosarcoma (OS) is a highly malignant primary bone tumor that predominantly affects children and adolescents, with an annual incidence of approximately 15,000–20,000 cases worldwide. Current treatment approaches often fail to eliminate complete tumor cells after surgical removal together with the presence of irregular bone defects.

Aim
As a novel tumor therapeutic strategy, in this work, we aim to treat OS through combinatorial localized hydrogen-thermal therapy due to its selective tumor ablation with enhanced cytoprotection of surrounding tissues, offering more effective alternative to conventional high-temperature photothermal or chemotherapy. To this aim, we designed advanced hydrogen (H_2) and heat releasing micro-/aerogels by incorporating Ammonia Borane ($NH_3 \cdot BH_3$, AB, H_2 prodrug) loaded mesoporous black bioactive glass nanoparticles ($75SiO_{2-X}$ $25CaO$ $5P_2O_5$) (AB@MBBG) within a bisphosphonate (BP)-grafted silk fibroin methacrylate (SFMA-BP) self-assembled matrix for treating bone tumors and associated bone fractures.

Materials and Methods
Silk fibroin solution was extracted from *Bombyx mori* silkworm cocoon, methacrylated, and functionalized with BP via EDC/NHS chemistry to obtain SFMA-BP. Mesoporous Black Bioactive Glass (MBBG) nanoparticles were synthesized using a modified Stöber process, with subsequent calcination at 650 °C and magnesio-thermal reduction process, leading to photoresponsive black ceramic nanoparticles. In the next step, they were loaded with AB[3] to form AB@MBBG. SFMA-BP microgels incorporated with AB@MBBG nanoparticles were fabricated using flow-focusing microfluidics. The resulting microgels were then subjected to supercritical drying to obtain SFMA-BP@MBBG-AB microaerogels.

Figure 1. Enhanced elimination of MG-63 cells in proposed micro(aero)gels by synergistic action of PTT and H_2

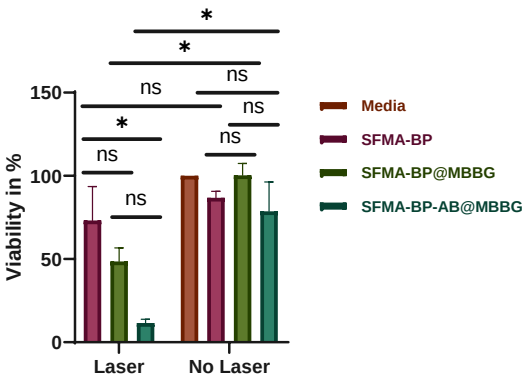

Results
The developed microaerogels exhibited a uniform size of approximately 200–300 µm and demonstrated pronounced

photothermal activity under near-infrared (808 nm) laser irradiation, attributed to the presence of MBBG-AB. In addition, they enabled hydrogen release under acidic conditions, contributing to the modulation of reactive oxygen species (ROS) in an in vitro bone tumor model. The microaerogels provided dual functionality, enabling effective eradication of MG63 cancer cells (Fig. 1), while simultaneously supporting osteoblast attachment and proliferation. This behavior is attributed to the biocompatible and osteoconductive three-dimensional porous aerogel matrix.

Conclusion

In this work, we successfully developed multifunctional theragenerative SFMA-BP@MBBG-AB microaerogels, for the first time. The developed microaerogels, due to their osteoblast-supportive microenvironment, NIR-activated photothermal effect and sustained and pH responsive hydrogen release, demonstrates strong potential as a minimally invasive theragenerative system for dual osteosarcoma treatment and subsequent bone healing.

S30 – O3

Selenium and magnesium functionalised collagen based scaffolds for dual bone regeneration and anti-cancer therapy

Pakenham E.[1], Ferreira A.[1], Johnston R.D.[1], Kaur K.[1,2], Lee T.C.[1], Curtin C. [1,3,4], Murphy C.M.[1,3,4]
[1]Dept. of Anatomy and Regenerative Medicine, Royal College of Surgeons in Ireland (RCSI); [2]School of Pharmacy and Biomolecular Sciences, RCSI; [3]Trinity Centre for Biomedical Engineering, Trinity College Dublin; [4]Advanced Material and Bioengineering Research (AMBER) Centre, Trinity College Dublin, Ireland

Introduction

Bone cancer related defects are difficult to treat due to disrupted bone formation and resorption inhibiting regeneration, while posing a risk of recurrence from residual cancer cells within the defect site. Incorporation of bioactive ions into biomaterials has gained attention for bone regeneration and cancer therapy. Magnesium (Mg) is capable of modulating resorption and formation to promote bone repair. Selenium (Se), has shown positive results as a cancer therapeutic exhibiting pro-oxidant and apoptotic effects against cancer cell lines. Nano-hydroxyapatite nanoparticles(nHA) are excellent candidates for ion delivery as their crystal structure can accommodate ionic substitution. This project will utilise nHA for the dual delivery of Mg and Se to inhibit bone resorption, enhance bone formation and obliterate cancer cells. Specific aims include developing and characterising a combined Se and Mg functionalised nHA to enhance the therapeutic effects of these ions followed by incorporation into a collagen-based scaffold to develop a multifunctional bone regenerative and anti-cancerous scaffold for the treatment of bone cancer defects.

Materials and Methods

Collagen-based scaffolds loaded with Se, Mg and Se/Mg functionalised nHA nanoparticles (1-10mM) were fabricated. FTIR was conducted to confirm successful loading of the ion functionalised nHA alongside assessing if incorporation affected scaffold architecture. RAW264.7 (pre-osteoclasts), mesenchymal stem cells (MSC) and prostate cancer cells (LNCaP) were cultured on the scaffolds to assess biocompatibility alongside the anti-cancer potential of the scaffolds using quantitative assays such as Alamar Blue™ and Pico Green™.

Results

FTIR displayed changes in peak intensity in -OH and PO_3^4 groups of nHA (500-1200cm^{-1}) confirming successful loading within the scaffold while having no effect on scaffold architecture (Figure 1A). Se/Mg-nHA displayed a concentration dependent effect on MSC proliferation while having no effect on pre-osteoclasts and enhancing LNCaP activity (Figure 1B-D). Se-nHA scaffolds (10mM) significantly reduced prostate cancer cell proliferation showing potential as a pro-regenerative and anti-cancerous scaffold (Figure 1D-E).

Conclusion

Based on these results, individually, Se/Mg-nHA enhanced MSC proliferation while Se-nHA exhibited anti-cancer activity at 10mM, showing potential for synthesising a pro-regenerative and anti-cancerous scaffold. However, when delivered together in a single particle, no significant changes were observed showing that delivery of Se and Mg separately, compared to being within a single nHA particle displays enhanced therapeutic potential. Future work involves assessing the osteogenic and osteoclastogenic differentiation capabilities of the ion-loaded scaffolds alongside in-depth analysis of the anti-cancer potential of the scaffolds.

Acknowledgements

Anatomical Society and Research Ireland Government of Ireland Postgraduate Fellowship GOIPG/2025/6128

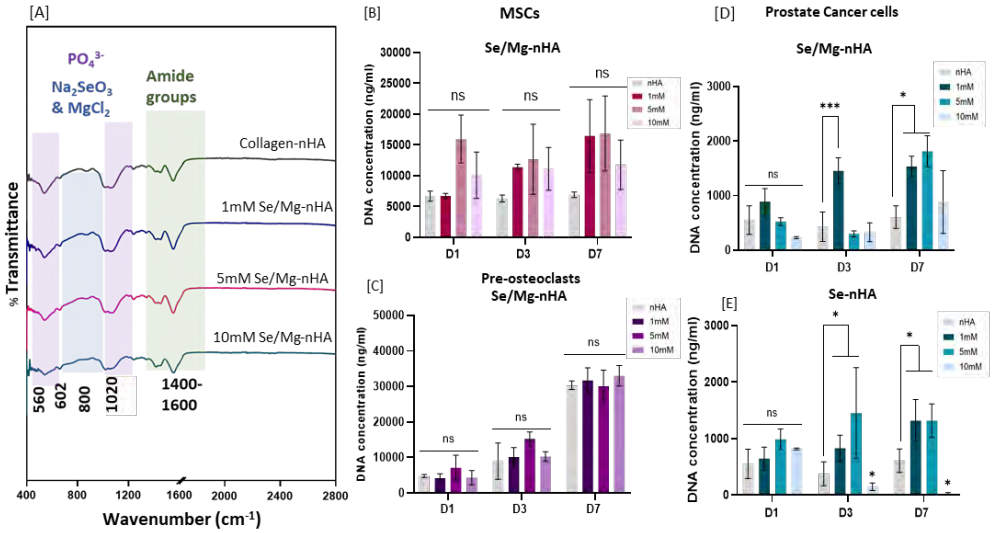

Figure 1. FTIR [A] of the ion loaded collagen-based scaffolds. Biocompatibility of MSCs [B], pre-osteoclasts [C] and LNCaP [D+E] cells cultured on scaffolds to assess the anti-cancer and pro-regenerative properties. *$p < 0.05$ compared to nHA control.

S30 – O4

Biomimetic dual-stimuli nanocarriers for targeted cancer therapy

Pancaro A.[1,2,3], Persy M.[1,2], Ajmeera S.[1,2], Oris A.[1,2,3], Geukens H-L.[1,2,3], Verstraelen S.[3], Nelissen I.[3], Ethirajan A.[1,2]

[1]Hasselt University, Institute for Materials Research (IUMAT), Nanobiophysics and Soft Matter Interfaces (NSI) group; [2]imec, IUMAT, Diepenbeek; [3]Flemish Institute for Technological Research (VITO), Environmental Intelligence Unit, Mol, Belgium

Introduction

Stimuli-responsive nanocarriers (NCs) have emerged as promising systems for controlled drug delivery in cancer therapy by exploiting specific conditions of the tumour microenvironment, such as elevated glutathione (GSH) levels and increased enzymatic activity. Poly(ε-caprolactone) diol (PCLD), a biodegradable polyester with hydrolysable ester bonds, represents an attractive building block for such systems due to its biocompatibility, non-toxicity, and tunable chemical functionality. In this work, we synthesized dual-stimuli-responsive NCs using PCLD and bis (4-hydroxyphenyl) disulfide (HPD) via the inverse miniemulsion technique, enabling enzymatic and GSH-triggered responsiveness, respectively. In addition, biomimetic strategies such as coating NCs with cancer cell membranes have attracted considerable interest for enhancing tumour targeting through homotypic recognition. Therefore, the NCs were functionalized with cancer cell membrane coatings to generate biomimetic NCs for targeted drug delivery.

Materials and Methods

Dual-stimuli-responsive polymeric NCs were synthesized via the inverse miniemulsion technique using an interfacial crosslinking reaction, enabling the formation of polymeric shells with dual responsiveness toward GSH and enzymatic activity. Sulforhodamine B (SRB) was encapsulated as a hydrophilic fluorescent model payload to evaluate encapsulation efficiency and cellular uptake. The physicochemical properties of the NCs were characterized using dynamic light scattering (DLS), transmission electron microscopy (TEM), and differential centrifugal sedimentation (DCS). Plasma membranes isolated from A549 cells were subsequently used to coat the NCs to generate biomimetic NCs. Cell viability (MTS assay) and cellular uptake (confocal microscopy and flow cytometry) of both coated and uncoated NCs were evaluated in A549 human lung adenocarcinoma cell line.

Results

The synthesized NCs exhibited uniform sizes below 200 nm, low polydispersity, good colloidal stability, high encapsulation efficiency, and stimulus-responsive release. *In vitro* assays demonstrated absence of cytotoxicity of both coated and uncoated NCs. While uncoated NCs showed no detectable cellular uptake, following coating with A549-derived plasma membranes clear changes in size, zeta potential, and morphology were observed, confirming successful membrane coating. Importantly, the biomimetic NCs showed no uptake in BEAS-2B bronchial cells but exhibited selective cellular uptake in A549 cells, highlighting the crucial role of the membrane coating in enabling effective cell-NC interactions.

Conclusion

This study demonstrates the successful synthesis and characterization of dual-stimuli-responsive NCs and their functionalization with cancer cell membrane coatings. The resulting biomimetic NCs exhibited favorable physicochemical properties, excellent biocompatibility, and selective cellular uptake. These findings highlight the potential of membrane-coated, dual-responsive NCs as a promising platform for targeted anticancer drug delivery.

Acknowledgements

AP is a post-doctoral fellow of Research Foundation Flanders (FWO project 12AR624N) and is additionally supported by VITO and Hasselt University (IUMAT).

S30 – O5

Development of navigator polymers for recruiting tumor-associated macrophages and promoting cancer cell phagocytosis

Funatomi R.[1], Kopinski-Grünwald O.[2], Homma K. [1], Ovsianikov A.[2], Matsusaki M.[1]
[1]Division of Applied Chemistry, Graduate School of Engineering, The University of Osaka, Japan; [2]Research Group 3D Printing & Biofabrication, Institute of Materials Science and Technology, TU Wien, Vienna, Austria

Introduction

Cancer recurrence after surgery remains a major challenge. Tumor-associated macrophages (TAMs), which constitute 30–50% of the tumor microenvironment, possess inherent phagocytic activity but are often suppressed by cancer cells via “don’t eat me” signals such as CD47. To overcome this, we designed biocompatible “navigator polymers” that actively recruit TAMs and enhance their interaction with cancer cells. These polymers incorporate phosphatidylserine (PS), one of the most potent “eat me” signals1 , and L-phenylalanine (Phe), which targets Ltype amino acid transporter 1 (LAT1) overexpressed on cancer cells2 . The navigator polymers enable selective co-localization of cancer cells and TAMs, and subsequently activate phagocytosis (Fig.1a).

Materials and Methods

Dextran (Mw ≈ 5 kDa) was chemically modified with succinic acid to introduce carboxyl groups, followed by conjugation with PS and Phe to obtain Dex5k-PS, Dex5k-Phe, and dual-functional Dex5k-Phe/PS (Fig.1b). The grafting degrees were determined by ^{1}H NMR analysis. Adsorption of the polymers were evaluated using THP-1-derived macrophages and MCF-7 breast cancer cells. Co-culture experiments were conducted to assess macrophage–cancer cell interactions. Quantitative fluorescence imaging was used to evaluate polymer adsorption and co-localization. Additionally, 3D spheroid models were employed to better mimic the tumor microenvironment and assess phagocytosis behavior.

Results

Dex5k-Phe and Dex5k-PS were successfully synthesized. Dex5k-PS exhibited higher adsorption onto macrophages compared to monocytes (Fig. 1c). Consistently, Dex5k-Phe showed higher adsorption to MCF-7 breast cancer cells compared to human mammary epithelial cells (HMECs) (Fig. 1d), indicating cancer cellselective affinity. The dual-functional Dex5k-Phe/PS was obtained with grafting degrees of 14% (Phe) and 11% (PS), and demonstrated enhanced co-localization of macrophages and cancer cells under co-culture conditions. Furthermore, in 3D spheroid models, macrophage adhesion onto cancer spheroids was observed in the presence of the polymers.

Conclusion

Dex5k-Phe and Dex5k-PS were successfully synthesized and shown to selectively interact with cancer cells and macrophages, respectively. Based on these results, we developed dual-functional navigator polymers designed to target both cell types. By promoting their co-localization, these polymers are expected to enhance macrophagemediated phagocytosis in the tumor microenvironment. This approach provides a potential platform for cancer immunotherapy and highlights the importance of material design in regulating cell–cell interactions.

References

1. Li B., Yuan Z., Jain P., Hung H. Jiang S., De novo design of functional zwitterionic biomimetic material for immunomodulation. *Science Advances, 2020,* Vol. 6, Issue 22.
2. Itani R., Mitsuyasu R., Dong-hee K., Homma K. Matsusaki M., Development of L-phenylalanine-grafted poly (vinyl alcohol) scaffold for selective capturing of cancer cells. *Talanta Open, 2024*, Vol. 9

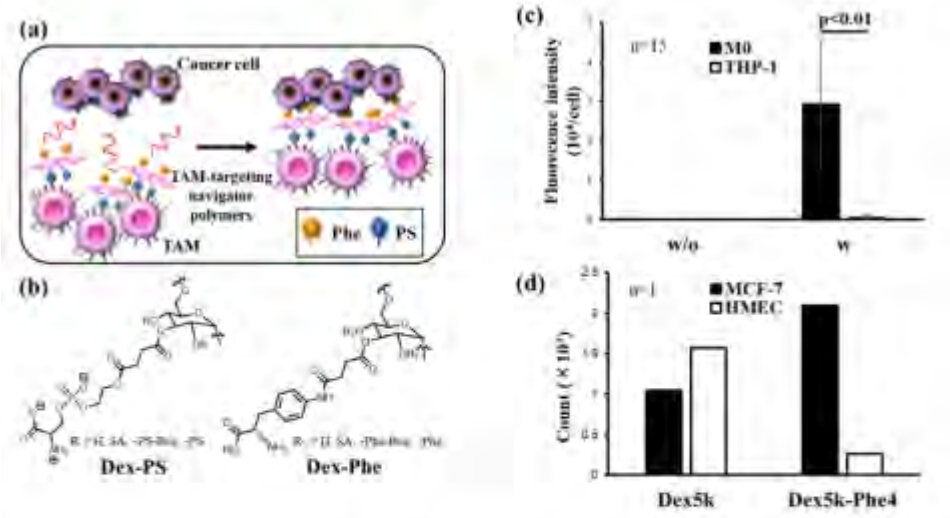

a) Schematic illustration of the concept of this study b) Chemical structures of phosphatidylserine (PS)– and phenylalanine (Phe)–grafted dextran polymers (Dex5k-PS and Dex5k-Phe). c) Quantification of Dex5k-PS2 adsorbed on THP-1 and macrophages after incubation with or without the polymer. d) Quantification of MCF-7 and HMEC cells adhered to each polymer surface by cell counting. The numbers (e.g., PS2, Phe4) indicate the grafting degree of each functional group determined by ^{1}H NMR.

S30 – O6

Unique properties of blue blood. Structural analysis of hemocyanin proteins with antibacterial and anticancer activity

Szpotkowski K., Skowronski L.
Division of Surface Science, Faculty of Chemical Technology and Engineering, Bydgoszcz University of Science and Technology, Kaliskiego 7, 85-796 Bydgoszcz, Poland

Introduction

Hemocyanins are proteins responsible for transporting oxygen in the hemolymph of mollusks. Latest research shows that they play a part in the cell-mediated immunity of theses animals. In the hemocyanin structures studied thus far, the basic quaternary structure is a cylindrical decamer with a diameter of about 3.5 nm. The active site usually contains two copper ions which form a complex with six histidines. In this kind of spatial structure, the oxygen O_2 molecule is reversibly bound between two copper atoms. The knowledge about hemocyanins in mussels is quite limited. Knowledge about hemocyanins is very fragmentary; however, even their incomplete characterization allows us to recognize their significant application potential

Aim

The aim of the conducted research is to determine the structure of hemocyanins from the great pond snail *Lymnaea stagnalis* and the swan mussel *Anodonta anatina*. The second objective is to confirm their antibacterial and anticancer properties.

Materials and Methods

The structural analysis of the isolated hemocyanins was carried out based on small-angle X-ray scattering data, circular dichroism, and infrared spectroscopy. Their anticancer properties were studied in cell cultures using cervical cancer, ovarian cancer, and pancreatic cancer cell lines. To evaluate antibacterial activity, a range of pathogens associated with difficult-to-heal wounds was used.

Results

Based on SAXS data, it was found that at physiological pH the analyzed hemocyanins form decamers, whereas increasing the pH to around 10 causes these proteins to occur in monomeric form. Analysis of the secondary structure showed that these proteins are composed mainly of α-helices (average content of about 70%). Such a high α-helix content is responsible for the high thermal stability of hemocyanins. These proteins are stable within the temperature range of 0–80 °C.

It was demonstrated that the analyzed hemocyanins induce the death of cancer cells in cervical, ovarian, and pancreatic cancer cell lines. Antibacterial activity of hemocyanins was also demonstrated against the bacteria *Staphylococcus aureus*, *Pseudomonas aeruginosa*, *Acinetobacter baumannii*, and *Klebsiella pneumoniae*.

Conclusion

- the analyzed hemocyanins form decamers under physiological conditions,
- interaction with phospholipids switches the hemocyanins into phenoloxidase mode,
- antibacterial and anticancer properties have been confirmed.

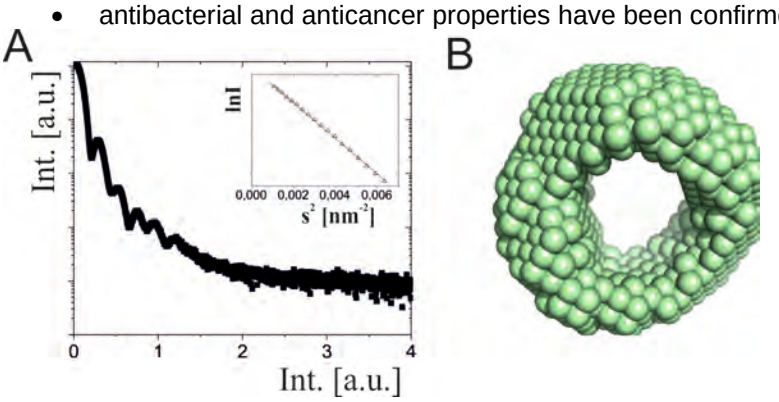

Fig. SAXS results for hemocyanin from the great pond snail. (A) SAXS curve for the protein at a concentration of 2 mg/mL and pH 7.5, and the Guinier plot (insert) and corresponding *ab initio* structure (B).

S31
Dynamic and stimuli-responsive nanocomposite engineering materials adaptability to instruct cellular responses

S31 - K1
Remotely activated nanomodulators of microglia for glioblastoma immunotherapy

Ciofani G.
Smart Bio-Interfaces, Italian Institute of Technology, Pontedera, Italy

Introduction
Microglia, the resident immune cells of the central nervous system, play a dual role in glioblastoma (GBM): while capable of antitumor activity, they are often co-opted by the tumor microenvironment into an immunosuppressive M2-like state that promotes disease progression. To reprogram these cells toward a therapeutically beneficial, pro-inflammatory phenotype, we developed a set of nanoplatforms designed for precise, remotely controlled immunomodulation.

Materials and Methods & Results
Our approach integrates piezoelectric [1] or magnetic [2] nanotransducers capable of converting external physical stimuli—ultrasound or alternating magnetic fields—into localized electrical or thermal cues at the cellular interface. When exposed to these stimuli, the nanoparticles induced M1-like microglial polarization characterized by upregulation of CD40 and CD86, increased secretion of IL-6, IL-8, and TNF-α, and enhanced intracellular calcium signaling. The activated microglia, in turn, released factors that impair the proliferation and viability of both immortalized and patient-derived glioblastoma cells, promoting immunogenic cell death.

Conclusion
Collectively, these findings highlight the potential of remotely activatable or intrinsically responsive nanoparticles as next-generation tools for non-pharmacological immunotherapy, offering a tunable and minimally invasive strategy to harness microglia in the fight against glioblastoma.

References
1 Montorsi M., Pucci C., De Pasquale D., Marino A., Ceccarelli M.C., Mazzuferi M., Bartolucci M., Petretto A., Prato M., Debellis D., De Simoni G., Pugliese G., Labardi M., Ciofani G. Ultrasound-activated piezoelectric nanoparticles trigger microglia activity against glioblastoma cells. Advanced Healthcare Materials, 2024, 13, 2304331.
2 Ceccarelli M.C., Paravizzini G., Marino A., Gigante G., Carmignani A., Catalano F., Prato M., Pugliese G., Fiaschi P., Battaglini M., Ciofani G. Thermo-magnetic induction of pro-inflammatory microglia: A lipid-based nanovector strategy for glioblastoma immunotherapy. ACS Applied Materials and Interfaces, 2025, 17, 63253-63271.

S31 - K2

Microenvironment-responsive mesoporous silica nanoparticles for osteosarcoma therapy and bone repair

van Rijt S.
Instructive Biomaterials Engineering, MERLN Institute for Technology-Inspired Regenerative Medicine, Maastricht University, Maastricht, The Netherlands

Introduction

Effective treatment of osteosarcoma remains challenging because therapeutic strategies must simultaneously eradicate tumour cells while preserving or restoring the surrounding bone tissue. Biomaterial-based nanotherapeutics offer promising opportunities to address this challenge by enabling targeted drug delivery combined with regenerative support. In particular, mesoporous silica nanoparticles (MSNs) provide a versatile platform for cancer therapy due to their high surface area, tunable porosity, and flexible surface chemistry, which allow efficient incorporation of therapeutic ions and drugs as well as responsive release mechanisms.
Our research focuses on engineering bioactive MSNs for osteosarcoma treatment using tumor-microenvironment-responsive strategies. Selenium-based therapeutics are particularly attractive due to their ability to induce oxidative stress and selectively inhibit cancer cell activity. However, systemic delivery can lead to toxicity in healthy tissues. Nanoparticle-based delivery systems therefore offer opportunities to improve therapeutic selectivity while enabling localized treatment strategies that can be combined with bone-regenerative biomaterials.

Materials and Methods

Selenium-incorporated MSNs were developed and further functionalized to incorporate chemotherapeutic agents. Stimuli-responsive systems were developed to enable pH- and redox-triggered drug release under osteosarcoma microenvironment conditions. In addition, hybrid nano-microparticle systems were created by immobilizing functional nanoparticles on calcium phosphate granules using pH-responsive linkers. The therapeutic performance of these systems was evaluated using osteosarcoma cell models and osteosarcoma-on-a-chip platforms.

Results

Selenium-incorporated MSNs demonstrated strong anticancer activity against osteosarcoma cells by inducing oxidative stress while maintaining improved selectivity compared with conventional treatments. Incorporation of doxorubicin within these systems enabled combination therapy approaches that further enhanced tumour cell inhibition. Stimuli-responsive nanoparticle designs allowed drug release to be triggered under acidic and redox conditions characteristic of the tumour microenvironment, thereby improving targeting of cancer cells.
To further integrate therapeutic and regenerative strategies, nanoparticle-based drug delivery systems were combined with bone-mimetic scaffolds. This nano-microparticle strategy allows localized cancer therapy while maintaining the osteoconductive properties of calcium phosphate materials used for bone repair. Ongoing work explores osteosarcoma-on-a-chip models that enable evaluation of these biomaterials in microenvironments and facilitate the study of tumour–bone interactions during treatment.

Conclusion

Nanomaterials provide promising opportunities for osteosarcoma therapy by combining targeted drug delivery with biomaterial-mediated tissue regeneration. By integrating therapeutic nanoparticles with bone-regenerative biomaterials, these strategies aim to develop next-generation treatments that eradicate tumour cells while supporting bone repair.

Acknowledgements

This work was supported by the Dutch Research Council (NWO) through the Gravitation Program “Materials Driven Regeneration” (024.003.013) and by the European Research Council (ERC) through the Consolidator Grant Nano4Bone.

S31 – O1

Magnetic field-induced drug delivery: An insight on the role of magnetoelectric nanoparticles size, shape and surface functionalization

Tommasini A.[1,2], Bonato M.[1], Gallucci S.[1], Fiocchi S.[1], Chiaramello E.[1], Cortese B.[3,4,5], Parazzini M.[1], Ravazzani P.[1], Suarato G.[1]

[1]Cnr-Istituto di Elettronica e di Ingegneria dell'Informazione e delle Telecomunicazioni, Milano, Italy; [2]Politecnico di Milano, Milano, Italy; [3]Interventional Coronary Center, University Hospitals Harrington Heart & Vascular Institute, Cleveland, Ohio, USA; [4]Fondazione Ricerca e Innovazione Cardiovascolare, Milan, Italy; [5]DCB Academy, Milan, Italy

Introduction

Magnetoelectric nanoparticles (MENPs) have gained considerable attention in nanomedicine due to their unique ability to wirelessly convert magnetic energy into localized electrical signals. Their working principle arises from the interface coupling of a magnetostrictive material with a piezoelectric one. MENPs electrical outputs are tunable by varying geometry, size, and magnetic stimulation[1],[2] and versatility can be enhanced via functionalization ensuring bioavailability, cell targeting and on-demand therapeutics delivery. Their clinical potential can be explored in interventional cardiology, where timely and localized administration of anti-proliferative agents is crucial for effective therapeutic outcomes. MENPs effectiveness for drugs release is herein computationally evaluated. Transitioning from a static to an alternating magnetic field (H_{field}) induces oscillations in the MENPs surface electric potential, which translates in a "shaking effect" able to modulate the ionic charge density (Q_{ionic}) of a MENP-drug bond, thus facilitating drug dissociation. The analysis focuses on optimizing the electrical outputs by examining the impact of MENPs shape, size, and PEGylation.

Materials and Methods

As previously validated by our group[2], MENPs magnetoelectric activation was modeled in COMSOL Multiphysics®5.6. A parametric sweep study was conducted under a static H_{field} of 300mT varying the nanoparticles size and morphology, maintaining a constant core/shell ratio. The analysis also incorporated 1–2nm PEG-layer to evaluate its effects on the generated electric field. In a second step, the MENPs dynamic response under alternating H_{field} (6.5mT, 100Hz) was analyzed to trigger drug release. Using the previous setup of the parametric sweep, a prediction of the cargo molecule release efficiency was derived.

Results

Figure1 (left) confirms the magnetization of the core and the consequent generation of an electric field, induced by the dipole behavior resulting from the mechanical deformation transmission at the core-shell interface. Configurations with thinner PEG-layers show higher electric field values (Figure1, right).

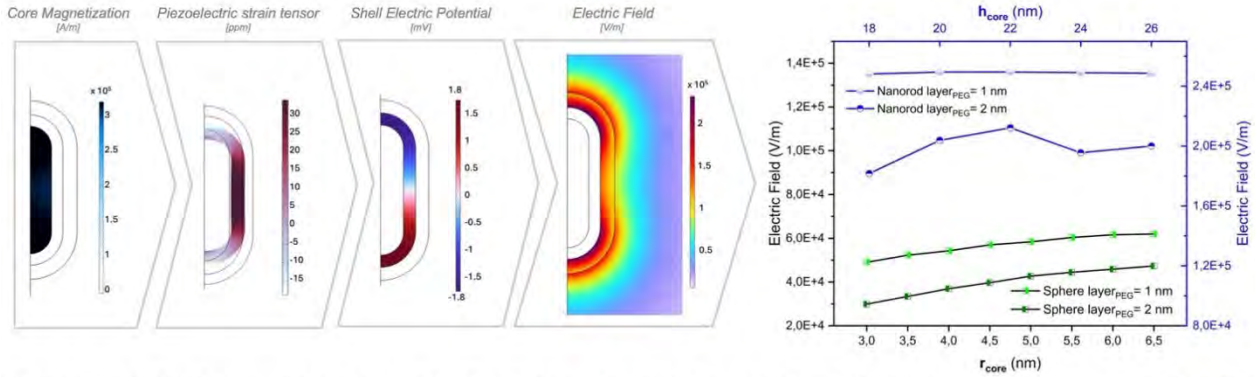

Figure 1. *Left*: Baseline behavior under a 300 mT static H_{field}. *Right*: Profiles of the E_{field} 99th percentile registered in the blood vessel wall with respect to the characteristic lengths of the nanoparticles (nanosphere core radius = r_{core} and nanorod core height = h_{core}) and the PEG coating thicknesses

Under alternating H_{field} conditions, a hypothetical drug-MENP ionic bond would experience a displacement of its charges from their equilibrium positions, whose values can be correlated with more intense electric potential differences at the MENP surface (Figure2, left), and with the nanoparticles geometrical features (Figure2, right).

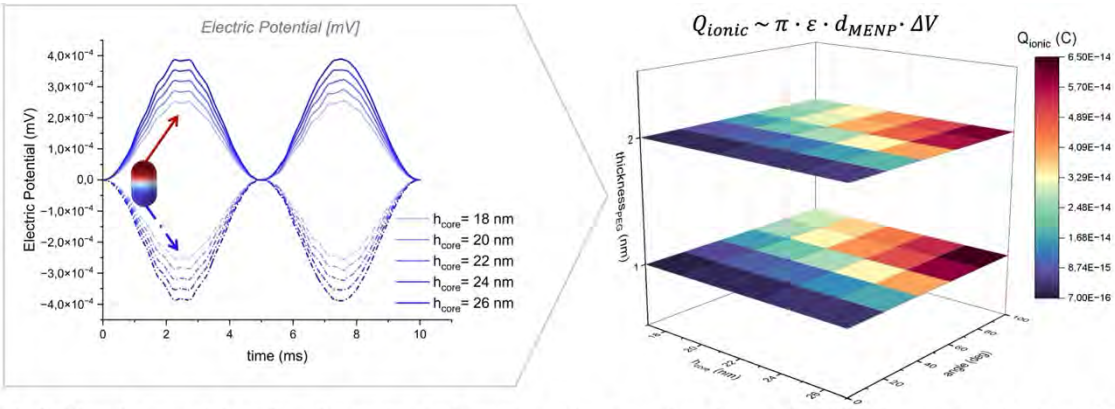

Figure 2. *Left*: Electric potential profile of negative and positive poles over time for rod-like MENPs coated with 1 nm PEG. *Right*: charge displacement in the hypothetical drug-MENP ionic bond values proportional to the dielectric constant (**ε**), the distance between the two poles (d_{MENP}), and the potential difference generated on the surface of the nanoparticle (ΔV). The 3D color map shows the variation of Q_{ionic} (expressed in Coulombs) as a function of three key parameters: PEG coating thickness, core size, and the surface sampling angle

Discussion and conclusion

This study demonstrates MENPs' efficiency in releasing a therapeutic cargo under an external magnetic stimulus is governed by the particle morphology and its magnetostrictive core size. Nanorods outperform spheres (data not shown) through optimized core-shell stress transmission and homogeneous strain, significantly enhancing electrical polarization. PEG functionalization introduces a slight damping effect; however, 1nm coatings do not compromise the overall response. Under alternating H_{field}, oscillations of the surface electric potential reverberate onto the Q_{ionic} profile, facilitating drug-bond dissociation. Larger cores and elongated geometries maximize this release mechanism. Varying parameters such as morphology, size and functionalization leads to a nano-system capable of generating on-demand a localized electrical output that finely modulates the drug delivery phenomenon.

References

1. Tommasini A., Suarato G., Fiocchi S., Chiaramello E., Marrella A., Lenzuni M., Parazzini M., Cortese B., Ravazzani P. Exploring magnetoelectric nanoparticles for advanced nano-electroporation and drug delivery in interventional cardiology. *Nanoscale Advances* 2025; 7; 5978-5992
2. Marrella A., Suarato G., Fiocchi S., Chiaramello E., Bonato M., Parazzini M., Ravazzani P. Magnetoelectric nanoparticles shape modulates their electrical output. *Frontiers in Bioengineering and Biotechnology* 2023; 11; 1219777

S31 – O2

Mechanically active hydrogel platform for targeted glioblastoma therapy: TrapKill

Clarke T.[2,3,4], Fernandez Real J.M.[2,3,4], Fahy Y.[1,3,4], Nadig K.[2,3,4], Biggs M.[2,3,4], Shamieva S.[5], Van Vlierberghe S.[5], Vallejo-Giraldo C.[1,2,3,4]

[1]Regenerative Medicine Institute (REMEDI), Advanced Therapies, School of Medicine, College of Medicine, Nursing and Health Sciences, University of Galway, Galway, Ireland; [2]Biomedical Engineering, School of Engineering, College of Science and Engineering, University of Galway, Galway, Ireland; [3]Institute for Health Discovery and Innovation, Bioscience Building, University of Galway, Galway, Ireland; [4]CÚRAM - Research Ireland Center for Research in Medical Devices, Galway, Ireland; [5]Polymer Chemistry and Biomaterials Group, Center of Macromolecular Chemistry, Department of Organic and Macromolecular Chemistry, Ghent University, Ghent, Belgium

Introduction

Glioblastoma remains the most common and aggressive primary malignant brain tumour with a median patient survival of 14-18 months[1]. Therapeutic resistance and tumour recurrence remain major challenges, highlighting the urgent need for innovative treatment strategies. This study investigates a hydrogel-based biomaterial platform that harnesses principles of mechanobiology to mechanically perturb cellular integrity through engineered microscale geometries designed to impair the DNA repair capacity of glioblastoma cells.

Materials and Methods

Gel Fabrication: GelMA-NB hydrogels[2] of different concentrations were fabricated to provide defined mechanical properties. Mechanical characterisation was performed, with bulk properties and nanoscale stiffness assessed via rheology and nanoindentation, respectively. Chemical characterisation of the polymer network was conducted using High-Resolution Magic Angle Spinning Nuclear Magnetic Resonance (HRMAS NMR) to assess network composition and crosslinking behaviour.

Geometrical Functionalisation: Microscale geometries were manufactured using two-photon polymerisation (2PP) to generate spatially confined architectures. Structural fidelity of the geometries was evaluated under varying fabrication conditions, assessing deviation of the pattern from the original design.

Cellular Response: Human glioblastoma cells were introduced to the platform to investigate the impact on varying levels of geometric confinement using markers associated with cytoskeletal changes (pFAK, F-Actin) and DNA damage (γH2AX, 53BP1).

Results

Mechanical testing demonstrated reproducible tuning of hydrogels stiffness across different gel types and concentrations (*Fig. 1A*), while the 2PP post-microfabrication process produced defined geometries with dimensions as small as 1 µm (*Fig. 1B*). Cell confinement within the engineered architectures induced pronounced cellular elongation, with nuclei adopting a filamentous morphology (*Fig. 1C*). Immunostaining for γH2AX, a marker of the DNA damage response, revealed increased signalling, suggesting impaired DNA repair under conditions of mechanical confinement within the hydrogel platform.

Conclusion

The TrapKill platform demonstrates that mechanically engineered hydrogel platforms can disrupt nuclear repair processes through cellular confinement, highlighting a promising mechanobiological strategy for glioblastoma therapy.

Funding

Funded by the European Union (ERC, TrapKill, 101163850). Views and opinions expressed are however those of the author(s) only and do not necessarily reflect those of the European Union or the European Research Council. Neither the European Union nor the granting authority can be held responsible for them. This work is also supported by the CMNHS Scholarship, University of Galway.

References

[1] Królikowska K., Błaszczak K., Ławicki S., Zajkowska M., Gudowska-Sawczuk M. Glioblastoma—A Contemporary Overview of Epidemiology, Classification, Pathogenesis, Diagnosis, and Treatment: A Review Article. International Journal of Molecular Sciences 2025; 26; 12162.

[2] Maes L., Szabó A., Van Haevermaete J., Geurs I., Dewettinck K., Vandenbroucke R.E., Van Vlierberghe S., Laukens D. Digital light processing of photo-crosslinkable gelatin to create biomimetic 3D constructs serving small intestinal tissue regeneration. Biomaterials Advances 2025; 171; 214232

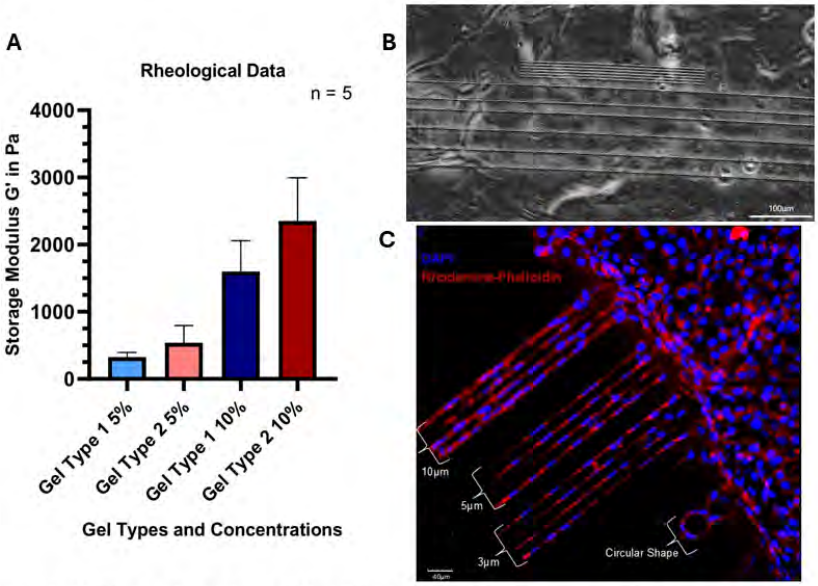

Figure 1. Optimised hydrogel platform offers tuneable stiffness, high fidelity geometries with the capacity to modulate cell response

(A) Rheological assessment of GelMA-NB bulk properties; (B) 1 µm-diameter micro-geometries produced under different fabrication conditions, Scale bar = 100µm; (C) Glioblastoma cells confined to engineered architectures, F-Actin (Red, Rhodamine-Phalloidin) and Nuclei (Blue, DAPI), Scale bar = 40 µm

S31 – O3

Biodegradable piezoelectric poly-L-lactic acid nanoparticles for wireless electrical stimulation in tissue engineering

Pucci C.,[1] Orlando F.,[1] Cavallini B.,[1] Vannozzi L.,[1] Trucco D.,[1] Redondo J.,[1] Boccoli L.,[1] Gruppioni E.,[2] Ricotti L.[1]
[1]The BioRobotics Institute, Scuola Superiore Sant'Anna, Pisa; [2]Centro Protesi INAIL, Bologna, Italy

Introduction

Ultrasound-activated piezoelectric nanomaterials enable non-invasive localized electrical stimulation that modulate cell behavior and promote tissue regeneration. However, most inorganic piezoelectric materials lack biodegradability, limiting clinical translation. Developing biodegradable and biocompatible piezoelectric nanomaterials is therefore crucial for safe ultrasound-mediated wireless stimulation in regenerative medicine.
This study aims to develop biodegradable piezoelectric poly-L-lactic acid nanoparticles (PLLA NPs) by optimizing crystallinity, evaluating biodegradability, cytocompatibility, and cellular internalization in muscle cell models for ultrasound-mediated wireless stimulation in regenerative medicine and tissue engineering.

Materials and Methods

PLLA NPs were synthesized by single emulsion, followed by thermal annealing. NPs were characterized by dynamic light scattering (DLS), scanning electron microscopy (SEM), differential scanning calorimetry, piezoresponse force microscopy. Biodegradability was evaluated over 30 days in buffers and relevant enzymes (lipase, cathepsin L). Cytocompatibility was tested on C2C12 myoblasts. Internalization was investigated in 2D cultures and 3D cell-laden hydrogels using confocal microscopy.

Results

The optimized formulation yielded monodisperse PLLA NPs with diameter of 252±11 nm and zeta potential of -39.4±0.6 mV (Figure 1.A,B). As-prepared NPs exhibited low crystallinity (36±5%). However, thermal annealing increased the crystalline fraction to 68±14% without altering size or charge. This enabled the emergence of piezoelectricity; while as-prepared NPs showed no response, annealed NPs exhibited a piezoelectric coefficient of 40±17 pm/V. To the best of our knowledge, this is the first report demonstrating piezoelectric behavior in PLLA NPs.
Biodegradability studies showed that PLLA NPs degraded only in presence of lipase and cathepsin L, capable of cleaving PLLA chains; the degradation started from an aggregation phase followed by breakdown of PLLA (>20 days). Cytotoxicity assays on C2C12 cells treated with NPs up to 1 mg/mL showed no significant effects on viability and metabolic activity.
Since internalization is a key factor for piezoelectric stimulation-mediated regeneration we investigated the ability of PLLA NPs to be taken up by cells. Studies revealed rapid, dose- and time-dependent uptake in 2D cultures (Figure 1.C). In 3D cell-laden hydrogels, NPs maintained high biocompatibility, did not impair myogenic differentiation, and remained internalized throughout the process.

Conclusion

This work demonstrates the development of biodegradable piezoelectric PLLA NPs with controlled size and crystallinity. Combined with enzymatic degradability, cytocompatibility, and efficient cellular internalization in 2D and 3D muscle models, these results highlight PLLA NPs as a promising, clinically relevant platform for ultrasound-mediated intracellular stimulation and electrically induced cell differentiation in tissue engineering.

Acknowledgements

This work received financial and technical support from INAIL, project MioPRO2, grant n.PR23-CR-P1

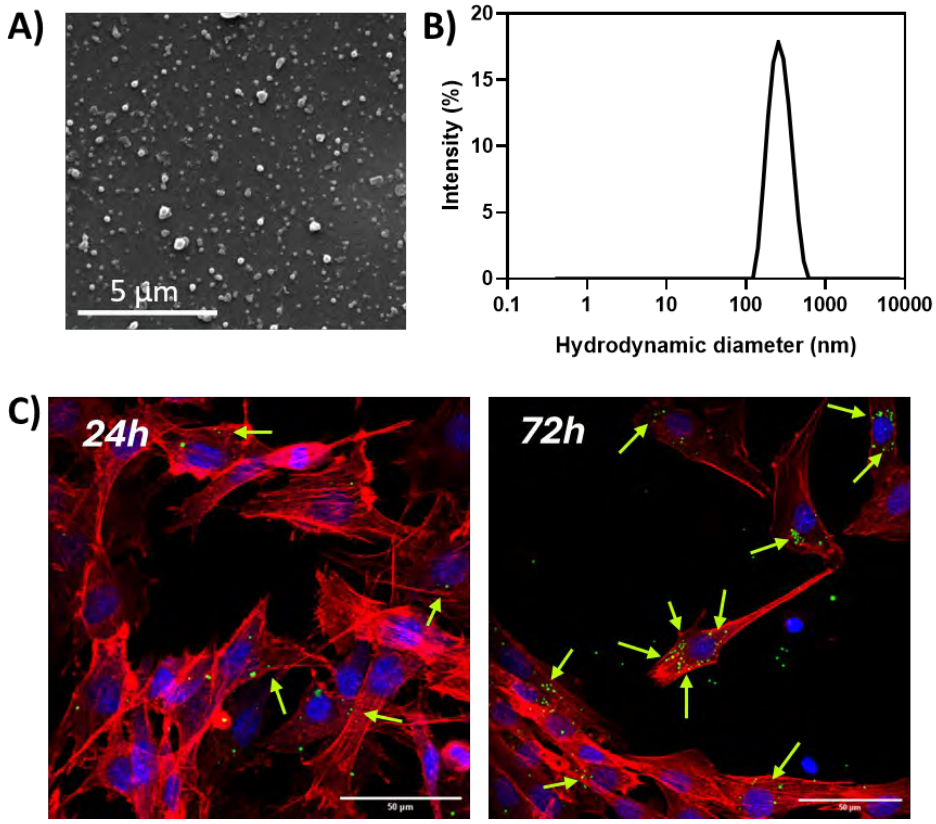

Figure 1. A) SEM image of PLLA NPs B) Hydrodynamic diameter (nm) distribution of PLLA NPs in water (250 µg/mL) C) Confocal images of C2C12 cells treated with PLLA NPs (250 µg/mL) for 24 and 72h (red: f-actin; blue: nuclei; green: PLLA NPs)

S31 – O4

4D piezoceramic-integrated scaffolds with bioelectric cues for skeletal muscle regeneration

Ravaglia N.[1,2], Rossi A.[1], Vignolo M.[3], Galizia P.[1], Pacheco D.[4,5], Arienti F.[1,6], Baldisserri C.[1], Guzzo C.M.[7], Montesi M.[1], Mancinelli R.[2], Labardi M.[8], Patrício T.M.F.[4], Glaum J.[8], Cunha C.[9], Mercadelli E.[1], Luciano G.[3], Panseri S.[1]

[1]Institute of Science, Technology and Sustainability for Ceramics (ISSMC), National Research Council of Italy, Faenza, Italy; [2]Dept. of Neuroscience, Imaging and Clinical Science, University of Studies "G. D'Annunzio", Chieti, Italy; [3]Institute of Chemical Sciences and Technologies "Giulio Natta" (SCITEC), National Research Council of Italy, Genova, Italy; [4]Centre for Rapid and Sustainable Product Development (CDRSP), Polytechnic Institute of Leiria, Marinha Grande, Portugal; [5]Coimbra Chemistry Centre-Institute of Molecular Sciences (CQC-IMS), Department of Chemistry, University of Coimbra, Coimbra, Portugal; [6]Dept. of Pharmacy and Biotechnology, University of Bologna, Bologna, Italy; [7]Dept. of Materials Science and Engineering, Faculty of Natural Sciences, Norwegian University of Science and Technology, Trondheim, Trøndelag, Norway; [8]Institute for Chemical-Physical Processes, National Research Council of Italy (CNR-IPCF), Pisa, Italy; [9]i3S - Instituto de Investigação e Inovação em Saúde, Universidade do Porto, Porto, Portugal

Introduction

Volumetric muscle loss (VML) poses a significant challenge due to the limited regenerative capacity of skeletal muscle. In this context, emerging four-dimensional (4D) regenerative strategies, which couple biomimetic scaffolds with external dynamic stimuli, have gained increasing attention for their potential to enhance repair outcomes. In this study, we developed a sustainable piezoelectric scaffold composed of egg white proteins (EWP) and piezoelectric barium titanate (BTO) particles designed to generate localized electrical stimulation under ultrasound (US) activation.

Materials and Methods

Piezoelectric scaffolds were fabricated through a rapid and versatile microwave-assisted method using EWP integrated with BTO particles at different ratios. The optimized EWP:BTO 1:1 composition demonstrated the most favourable combination of porosity, degradation, and mechanical compliance, closely mimicking native muscle tissue properties. To activate the piezoelectric phase, scaffolds were subjected to corona poling, which induced permanent polarisation of the BTO. *In vitro* biological performance was evaluated using C2C12 myoblasts to assess adhesion, proliferation, infiltration, and myogenic differentiation. 1-minute daily US application (900 mW/cm²) generated electromechanical cues, and gene expression analyses investigated mechanosensitive and electroactive responses. To assess immunomodulatory effects, monocyte-derived macrophages from healthy donor peripheral blood were cultured with scaffolds under direct and indirect conditions. Macrophage polarization was evaluated by qPCR of regeneration-associated genes and flow cytometry quantification of pro-regenerative markers. A pilot *in vivo* study assessed biocompatibility, structural integrity, local and systemic toxicity over a 28-day implantation period, and regenerative capacity in an orthopaedic muscle site using a VLM defect model.

Results

The EWP:BTO 1:1 scaffolds exhibited a highly porous architecture, suitable mechanical compliance, and controlled degradation kinetics, closely resembling the physical characteristics of native skeletal muscle tissue. *In vitro* experiments demonstrated that C2C12 myoblasts adhered efficiently to the scaffolds and showed enhanced proliferation, infiltration, and differentiation. The combination of scaffold polarisation and US stimulation produced a synergistic effect, upregulating early mechanosensitive and electroactive genes associated with myogenic signaling. *In vitro* immunological assays indicated that the scaffolds promote a pro-regenerative macrophage phenotype. *In vivo* study confirmed good biocompatibility, with the scaffolds maintaining structural integrity over 28 days and showing no signs of local inflammation or systemic toxicity, and enhanced tissue regeneration.

Conclusion

Overall, the EWP:BTO piezoelectric scaffold represents a sustainable, biocompatible platform capable of converting externally applied mechanical energy into localized electrical stimulation. The promising *in vitro* and *in vivo* results highlight its potential as a non-invasive strategy to enhance skeletal muscle regeneration and support functional repair in VML.

S31 – O5

Integrating conductive bioinks and laser-based processing for hybrid bioelectronics

Almeida H.[1], Pinheiro T.[1], Ureña C.[1], Igreja R.[1], Martins R.[1], Fortunato E.[1]
[1]CENIMAT|i3N, Dept. of Materials Science, School of Science and Technology, NOVA University Lisbon and CEMOP/UNINOVA, Caparica, Portugal

Introduction

The demand for scalable and flexible platforms in bioelectronics has driven the development of functional materials that merge robust electrical performance with biocompatibility. This study presents two complementary strategies to create hybrid bioelectronic interfaces integrating additive manufacturing with advanced laser processing techniques.

Materials and Methods

A. First, GelMA-based bioinks were enhanced with MXenes[1] and carbon nanotubes (CNTs) nanomaterials to achieve high electrical conductivity and mechanical stability. These bioinks were thoroughly characterized for their conductivity, rheological behavior, and printability and were employed in 3D bioprinting to fabricate complex architectures.
B. Secondly, we generated laser-induced graphene (LIG)[2] on lignin-polysaccharide membranes using CO_2 and UV lasers. Lignin's natural biocompatibility and the unique benefits of dual laser processing enabled scalable graphitization via CO_2 lasers and high-resolution patterning with UV lasers. Characterization confirmed the formation of high-quality conductive graphene. These LIG platforms exhibited tunable electrical properties and controlled morphology, making them ideal for integration into printed bioelectronics.

Results

A. Electrical stimulation tests demonstrated practical signal propagation and structural integrity, showcasing the potential of these bioinks for versatile bioelectronic applications, including wearable sensors and flexible circuits.
B. Characterization confirmed the formation of high-quality conductive graphene. These LIG platforms exhibited tunable electrical properties and controlled morphology, making them ideal for integration into printed bioelectronics.

Conclusion

By combining these approaches, we introduce a framework for hybrid bioelectronics that integrates conductive bioinks with precision graphene interfaces. This synergy enables the fabrication of multifunctional and flexible devices, paving the way for innovations in bioelectronic systems and hybrid interfaces.

Acknowledgements

This work was supported by FEDER via COMPETE 2020 and FCT projects LA/P/0037/2020, UIDP/50025/2020, UIDB/50025/2020, and LIGHEART 2022.08597.PTDC; Horizon 2020 Programme (Grant 101008701, EMERGE); and PRR projects Pacto Bioeconomia Azul (C644915664-00000026) and Fossil to Forrest (C644920945-00000036).

References

[1]Matias, M. L. et al. 3D printed MXene architectures for a plethora of smart applications. Mater Today Adv 23, 100512 (2024).
[2]Pinheiro, T. et al. Direct Laser Writing: From Materials Synthesis and Conversion to Electronic Device Processing. Adv Materials 36, (2024).

S32
Dynamic supramolecular biomaterials for regenerative medicine

S32 - K1
Supramolecular design of dynamic biomaterials to instruct cell functions

Borges J.
CICECO – Aveiro Institute of Materials, Department of Chemistry, University of Aveiro, Aveiro, Portugal

Introduction
Nature offers a rich toolbox of building blocks that inspire the creation of artificial biofunctional systems aiming to recreate living systems. One of the most prominent biological systems that has been gathering immense attention among the biomaterials community is the native extracellular matrix (ECM) – a dynamic supramolecular landscape formed through the highly orchestrated non-covalent self-assembly and reciprocal molecular recognition of mainly proteins and glycosaminoglycans. Despite the progress, synthetic biomaterial architectures developed to date do not fully emulate ECM's complex composition, dynamics and mechanical profile, thus limiting their potential as advanced therapies in regenerative medicine strategies.

In this keynote lecture, emphasis will be given to the synergistic interplay between naturally sourced biopolymers and synthetic self-assembling building blocks towards supramolecularly engineering cell-instructive biomaterials to better emulate the complex composition, nanostructural elegance and dynamic mechanical profile of the native ECM. We will discuss bottom-up nano/microtechnologies, including molecular self-assembly, 3D (bio)printing, and layer-by-layer assembly technology to assemble size- and shape-tunable, dynamic self-assembling biomaterials for directing cell functions. Their potential to act as advanced platforms for the encapsulation and on-demand controlled release of living cells will be discussed.

Acknowledgements
This work was funded by the European Union's Horizon Europe research and innovation programme under the Grant Agreement No. 101079482 ("SUPRALIFE"), and by FEDER - Fundo Europeu de Desenvolvimento Regional funds through the COMPETE 2030 in the framework of the project COMPETE2030-FEDER-00874400 ("SUPRANEURO") and national funds though Fundação para a Ciência e a Tecnologia (FCT), I.P., in the framework of the project 2024.16793.PEX ("SUPRANEURO"). J. Borges acknowledges FCT for the individual Assistant Researcher contract (2020.00758.CEECIND/CP1589/CT0007, DOI 10.54499/2020.00758.CEECIND/CP1589/CT0007). This work was developed within the scope of the project CICECO-Aveiro Institute of Materials, UID/50011/2025 (DOI 10.54499/UID/50011/2025) & LA/P/0006/2020 (DOI 10.54499/LA/P/0006/2020) & UID/PRR/50011/2025 (DOI 10.54499/UID/PRR/50011/2025), financed by national funds through the FCT/MEC (PIDDAC).

S32 - K2

Engineering supramolecular hydrogels as dynamic biomaterials for drug delivery and biofabrication

Ciardelli G.[1,2,3]
[1]DIMEAS Politecnico di Torino, Turin, Italy; [2]IPCF-CNR, Pisa, Italy, [3]Biomedical Engineering Center, Kansai Medical University, Osaka, 5731010, Japan

Introduction

Hydrogels are soft, hydrophilic three-dimensional networks of cross-linked macromolecules widely investigated for biomedical applications. Among them, physically cross-linked hydrogels are particularly attractive for drug delivery and cell encapsulation, as their mild gelation conditions preserve the stability of bioactive molecules and cell viability. However, designing stable systems based on weak physical interactions remains challenging, as phase separation and poor network integrity can compromise their performance. Supramolecular approaches offer a promising strategy to overcome these limitations by exploiting specific and reversible interactions, such as hydrogen bonding, host–guest recognition and hydrophobic interactions, to achieve tunable and dynamic hydrogel systems.

Materials and Methods

Supramolecular hydrogels were developed through the design of poly(ethylene glycol)-based poly(urethane)s engineered to interact with α-cyclodextrins via host–guest complexation. This bottom-up molecular design enables the formation of physically cross-linked networks with controlled architecture and properties. The resulting systems exhibit injectability and dynamic behavior, supported by their shear-thinning and self-healing characteristics. Their processability was further explored in combination with advanced biofabrication techniques, including extrusion-based and embedded three-dimensional bioprinting.

Results

The developed supramolecular hydrogels demonstrated suitable mechanical and rheological properties for biomedical use, including rapid recovery after shear and stable network formation. Their versatility was validated across multiple applications, including drug delivery systems for hydrophobic compounds (e.g., curcumin), biomaterial inks for three-dimensional bioprinting and support baths for embedded bioprinting processes. These results highlight the potential of supramolecular design to generate multifunctional platforms combining injectability, biocompatibility and structural adaptability.

Conclusion

Supramolecular hydrogels represent a versatile and powerful class of biomaterials for advanced therapeutics and biofabrication. By leveraging reversible molecular interactions, these systems enable the design of dynamic and functional platforms with enhanced performance. This keynote lecture provides an overview of current strategies and applications, setting the stage for further developments in dynamic supramolecular systems for regenerative medicine and drug delivery.

Acknowledgements

This work was carried out within BREATH project (CUP E53D23016840001) – funded by European Union – Next Generation EU within the PNRR, Mission 4, Component 2, Investment 1.1, PRIN PNRR 2022 program (D.D. 1409 14/09/2022 MUR).The content of this abstract reflects only the author’s view, and the Commission is not responsible for any use that may be made of the information it contains.

S32 – O1

Dynamic Nucleic Acid Bioengineered 3D Scaffolds for Cell Culture Applications

Thakur N[1,2], Jin M[1], Milkin P[3], Dam van C[1,2], Passier R[1,2], Meer van der A[1,2], Ionov L[3], and Paez J[1,2]
[1]Department of Bioengineering Technologies, [2]Cardiovascular Health Technology Centre, TechMed Centre, University of Twente, Drienerlolaan 5, 7522 NB, Enschede, The Netherlands, [3]Faculty of Engineering Science, University of Bayreuth, Universitätsstr. 30, 95440 Bayreuth, Germany.

Introduction

In tissue engineering and cell biology research, cell culturing entails exposing cells to a non-natural environment and there has yet to exist a material which could recapitulate the complexity of natural tissues and diverse cell-matrix interactions present in vivo. One line of action involves developing artificial 3D scaffolds to mimic key features of the native microenvironment of the cells. Bioinspired hydrogel matrices have demonstrated a broad range of applications, from facilitating cell encapsulation in advanced 3D culture and tissue models to supporting cell-based therapeutics and tissue engineering, but lack key properties such as dynamic mechanical features and conductivity.

Aim

Herein, we develop bio-inspired injectable hydrogel scaffolds with tunable properties and intrinsic conductivity for 3D cell culture applications. Our approach is to synthesize injectable, self-assembled nucleic acid inspired guanosine-quadruplex (GQ) hydrogels.

Materials and Methods

The GQ hydrogels were formulated as matrices using guanosine nucleotide with biopolymers and metal ions, under mild aqueous conditions. Mechanical properties of the hydrogels were characterized via rheology, morphological characterization was performed via SEM, AFM and confocal reflectance microscopy, and ion conductivity was measured via electrochemical impedance spectroscopy (EIS). Different cell types (*hMSCs, fibroblasts, hIPSC-CM*) were cultured on and within the hydrogels to test their cytotoxicity as well as ability to support cell culture.

Results

The physically crosslinked, bearing dynamic interactions, supramolecular GQ hydrogels showed rapid gelation under physiological conditions, tunable mechanics within values resemblant of soft tissues, fibrillar microstructure. The unique conductive and hierarchical 3D fibrous network, along with its excellent cytocompatibility, supported cell culture applications (Fig 1). The dynamic, GQ supramolecular hydrogels are injectable, 3D printable, self-recoverable and thermo-responsive, all desirable features for their application towards artificial tissue models. Importantly, GQ hydrogels are >10-times more conductive than other typical hydrogels used for cell culture (fibrin, collagen, Matrigel).

Conclusion

We demonstrate hydrogels successfully formulated as matrices for culture of various cells, showing fast gelation, fibrillar microstructure, dynamic and tunable mechanics, and ionic conductivity. These smart biomaterials are promising for cell culture and engineering tissue models.

Acknowledgements

NT and JP thank financial support from the EU (HORIZON-MSCA-PF, project no. 101067198 (RHYTHM)) and from Dutch Council Research, NWO-XS (OCENW.XS25.1.297).

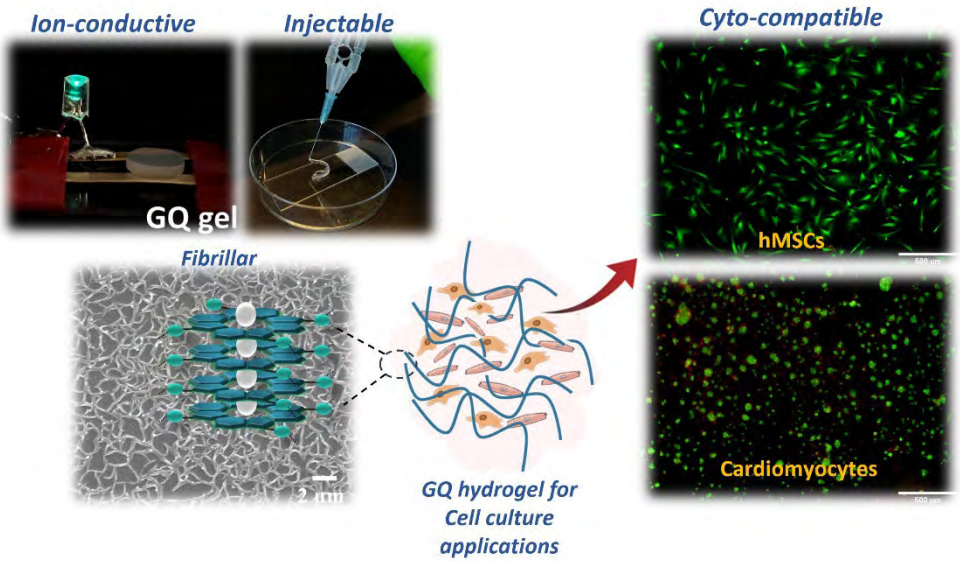

Fig 1. Injectable, conductive, fibrillar and cytocompatible GQ hydrogels for 3D cell culture applications.

S32 – O2

Multifunctional β-cyclodextrin polymer platform for drug delivery and supramolecular hydrogels in cartilage repair

Kalantarifard S.[1], Elmeligy, M.A.[1], Rasoulian, F.[2], Dinparvar, S.[3], Vojtová, L.[3], Lacik I.[1], Heydari A.[1,3]
[1]Dept. For Biomaterials Research, Polymer Institute of the Slovak Academy of Sciences, Bratislava, Slovakia; [2]Center for Regenerative Medicine, University of Continuing Education Krems, Austria; [3]Central European Institute of Technology, Brno University of Technology, Czech Republic

Introduction

Cartilage repair remains challenging due to limited self-regeneration and poor retention of therapeutics in the joint environment [1]. This study aims to develop a multifunctional β-cyclodextrin polymer (β-CDP)-based platform for combined drug delivery and supramolecular hydrogel formation to enhance chondrocyte performance and extracellular matrix (ECM) formation [2].

Materials and Methods

β-CDP was synthesized via crosslinking of β-cyclodextrin with epichlorohydrin and further functionalized with cyanoguanidine (CDP–CyG) to improve drug interaction and cellular uptake. Resveratrol was selected as a model therapeutic and encapsulated into CDP–CyG to evaluate drug loading, release behavior, and cellular internalization. Chondrocyte viability and ECM formation were assessed following treatment [3, 4].

For hydrogel formation, a supramolecular network was prepared via host–guest interactions between β-CDP and adamantane-functionalized alginate (Alg–Ad). The resulting hydrogels were characterized in terms of viscoelastic properties to determine their suitability for cartilage tissue engineering applications.

Results

CDP–CyG demonstrated efficient encapsulation of resveratrol and sustained release behavior, supporting its potential as a drug delivery carrier. Enhanced cellular uptake of the carrier system was observed in chondrocytes, leading to improved cell viability compared to control conditions. Furthermore, treated cells showed increased ECM deposition, indicating a positive effect on chondrocyte function.

The supramolecular hydrogels formed via β-CDP/Alg–Ad interactions exhibited tunable viscoelastic properties, with shear-thinning and self-healing behavior suitable for injectable or bioprintable systems. The dynamic host–guest interactions contributed to structural stability while maintaining a cell-friendly microenvironment.

Conclusion

The developed β-CDP-based system provides a versatile platform integrating drug delivery and injectable hydrogel formation. The combination of CDP–CyG-mediated resveratrol delivery and supramolecular hydrogel design enhances chondrocyte viability and ECM production, highlighting its potential for cartilage repair applications.

Acknowledgements

This work was supported by VEGA 2/0154/26, APVV-22-0568, APVV-22-0565, and FLAG-ERA grant GRAPH-OCD, by the Slovak Academy of Sciences under the grant number FLAG ERA III/2023/808/GRAPH-OCD.

References

1. L. Moroni, J.A. Burdick, C. Highley, S.J. Lee, Y. Morimoto, S. Takeuchi, J.J. Yoo, Biofabrication strategies for 3D in vitro models and regenerative medicine, Nature Reviews Materials 2018; 3(5) 21–37.
2. Q. Ling, H. Li, J. Zhao, W. Guo, H. Yu, Z. Li, Y. Hu, S. Wei, Y. Fu, Y. Zhang, K. Zhang, L. Bian, Mechanically heterogeneous hydrogel with cell-programmed network restructuring promotes tissue regeneration by mechano-epigenetic modulation, Nature Communications 2026; 17(1) 2184.
3. M. A. Elmeligy, F. Rasoulian, S. Kalantarifard, J. Filo, S. Dinparvar, A. M. Omer, L. Vojtová, S. Nehrer, I. Lacík, A. Heydari, Cyclodextrin-epichlorohydrin-cyanoguanidine polymer for resveratrol delivery to enhance human chondrocyte function in cartilage repair, 2025.
4. E. Kashani, S. Maghsoudi, H. Rezania, M. Yarazavi, M. Hajiabbas, G. Benkovics, E. Bilensoy, I. Lacik, A. Heydari, Cyclodextrin polymers containing ionizable and ionic groups: A comprehensive review from classifications and synthesis methods to applications, Materials Today Chemistry 2024; 39 102186.

S32 – O3

Supramolecular glycopeptide-based nanoparticles for the controlled delivery of perinatal stem cells' secretome for cardiac repair

Perioli A.[1,2], Gomes A.[1,2], Castro V.I.B.[1,2], Araujo A.R.[1,2], Arnaldi P.[3], Bollini S.[4,5], Silini A.[6], Spanò A.[7], Parolini O.[7,8], Reis R.L.[1,2], Pires R.A.[1,2]
[1]3B's Research Group, I3Bs – Research Institute on Biomaterials, Biodegradables and Biomimetics, University of Minho, Headquarters of the European Institute of Excellence on Tissue Engineering and Regenerative Medicine, Guimarães, Portugal; [2]ICVS/3B's–PT Government Associate Laboratory, Braga/Guimarães, Portugal; [3]IRCCS Azienda Ospedaliera Metropolitana (IRCSS AOM), Italy; [4]Dept. of Experimental Medicine (DIMES), University of Genova, Genova, Italy; [5]IRCCS Ospedale Policlinico San Martino, Genova, Italy; [6] Centro di Ricerca E. Menni, Fondazione Poliambulanza, Brescia, Italy; [7]Dipt. di Scienze della Vita e Sanità Pubblica, Università Cattolica del Sacro Cuore, Rome, Italy; [8] Fondazione IRCCS Casa Sollievo della Sofferenza, Foggia, Italy

Introduction
Cardiovascular diseases, particularly myocardial infarction, remain the leading cause of mortality worldwide. While current therapies rely on managing symptoms and restore blood flow, they cannot repair the necrotic myocardial tissue which has limited regenerative capacity.[1] Tissue engineering and regenerative medicine offer promising alternatives using cell-based and cell-free therapies; however, their clinical efficacy is often hindered by the low retention of cells/therapeutic molecules at the injury site.[2]

Materials and Methods
We prepared nanoparticles exploiting a water-in-oil-in-water (W/O/W) emulsion technique using the glycopeptide Fmoc-diphenylalanine-glucosamine-6-sulfate (Fmoc-FF-GlcN6S) which is designed to mimic the biofunctionality of glycoproteins found in the cardiac extracellular matrix, that can capture and preserve growth factors in their bioactive conformation.[3]

Results
The prepared nanoparticles exhibited an average diameter of 150 nm, a polydispersity index (PDI) < 0.2 and a surface charge of -20 mV, ensuring long-term stability and preventing aggregation. Stability assays in water, PBS at a pH 7.4 and PBS at a pH 6.8 confirmed their structural integrity in both physiological and inflammatory environments for several weeks. Afterwards, we used BSA as a model loading protein and we achieved a high encapsulation efficiency (~80%) across protein concentrations between 50–1000 µg/ml, followed by a controlled release profile for 1 week. In vitro studies using H9C2 cells demonstrated high cytocompatibility of the nanoparticles (2–1000 µg/ml), as well as successful cytoplasmic internalization. Further tests using perinatal stem cells' secretome as loading cargo confirmed the stability of the delivery system (during weeks at a pH between 6.5-7.5) with similar encapsulation efficiency and release profile as the one obtained with the model protein (i.e., BSA). Finally, to enhance therapeutic precision, a cardiac homing peptide (CHP, CSTSMLKAC) was conjugated to Fmoc-FF via a PEG spacer. The CHP tagged amphiphile was blended with Fmoc-FF-GlcN6S during the preparation of the nanoparticles. We found that this blended formulation facilitated their internalization in stressed cardiomyocytes.

Conclusion
The proposed glycopeptide-based delivery system represents a versatile and tunable strategy for targeted cardiac repair.

Acknowledgements
We acknowledge the financial support from the European Union (under Grant Agreement 101168752-SECRET DN), the Portuguese FCT and the ERA4Health partnership (CARDINNOV/0001/2023-AmnioSMART). We also acknowledge financial support from Portuguese FCT and CCDR Norte under grant agreements PINFRA/22190/2016 and Norte-01-0145-FEDER-022190.

References
[1]Vasu et al (2021). Biomaterials-based approaches for cardiac regeneration. *Korean circulation journal*, *51*(12), 943-960; [2]Gil-Cabrerizo et al (2023). Cardiac tissue engineering for myocardial infarction treatment. *European Journal of Pharmaceutical Sciences*, *185*, 106439; [3] Castro

et al (2023). Glycopeptide-based supramolecular hydrogels induce differentiation of adipose stem cells into neural lineages. *ACS Applied Materials & Interfaces*, *15*(25), 29998-30007.

S32 – O4

Engineered supramolecular hydrogels with tunable self-healing for embedded bioprinting applications

Grillo Coppola P.[1,2], Boffito M.[1], Pappalardo R.[1,3], Cassino C.[4], Ciardelli G.[1]
[1]Dept. of Mechanical and Aerospace Engineering, Politecnico di Torino, Turin; [2]Dept. of Surgical Sciences, Università degli Studi di Torino, Turin; [3]Inst. Chemical-Physical Processes (IPCF), National Center of Researches (CNR), Pisa; [4]Dept. of Sciences and Technlogical Innovation, Università del Piemonte Orientale, Alessandria, Italy

Introduction

Supramolecular hydrogels are emerging as attractive support materials for embedded 3D Bioprinting due to shear-thinning and self-healing behaviour. However, current support baths often show limited tunability, poor stability under culture conditions, or require harsh removal procedures that may compromise printed constructs. In this study, we developed a supramolecular hydrogel based on custom poly(ether urethane)s (PEUs) and α-cyclodextrins (CDs), as support baths for embedded bioprinting.

Materials and Methods

Two high molecular weight PEUs were synthesized from different macrodiols: poly(ethylene glycol) (3350 Da) and Poloxamer® 407 (12600 Da), yielding SHE and SHP, respectively[1,2]. By combining SHE and SHP at different weight ratios (total PEU 4% w/v) with CDs (9% w/v), we obtained physically crosslinked hydrogels driven by polypseudorotaxanes formation. The hydrogel with optimal composition was enriched with microbial transglutaminase (mTG) (5-10% w/v) to enable in situ enzymatic crosslinking of porcine gelatin bioinks (3-5% w/v) during printing.

Results

All formulations exhibited reproducible gelation (10-24 h), and stability up to 4 days, with more pronounced stability observed for hydrogels with higher SHP content. Rheological analyses confirmed gel-like behavior, with storage modulus G' consistently exceeding loss modulus G'' during frequency sweep tests, while self-healing strain tests revealed a G' recovery between 50% and 95% depending on the SHE/SHP ratio. Cytotoxicity tests on human fibroblasts confirmed high biocompatibility (80-100% cell viability). Among the tested compositions, the 30:70 SHE/SHP provided the best balance between mechanical recovery (87%), stability and cell viability (95%), and was selected as the optimal support bath. When enriched with mTG, the system enabled in situ enzymatic crosslinking of gelatin bioinks during printing, ensuring enhanced shape fidelity and structural retention of complex geometries (Fig. 1). Diffusion studies performed with fluorescein isothiocyanate–dextran, as model molecules for nutrients transport, confirmed the network permeability. Importantly, printed structures could be gently retrieved through washing with CD solution, enabling bath removal under mild, cell-compatible conditions.

Figure 1: Gelatin construct printed within support bath that maintains its structure after the bath removal.

Conclusion

This tunable supramolecular platform represents a versatile and cytocompatible alternative to conventional support baths, offering controlled network recovery, culture stability, nutrient permeability, and facile removal. These features make the system particularly promising for embedded bioprinting of complex, functional tissue constructs for regenerative medicine.

Acknowledgements

This work was performed within the BREATH project - funded by EU - Next Generation EU within the PRIN 2022-PNRR program (D.D. 104 02/02/2022 MUR). This abstract reflects only the authors' views and opinions, and the Ministry cannot be considered responsible for them.

References

[1]Boffito M. et al. Novel Polyurethane-based Thermosensitive Hydrogels as Drug Release and Tissue Engineering Platforms: Design and in Vitro Characterization. *Polymer International* 2016;65; 756-769.

[2]Pappalardo R., Boffito M. Schiff-base crosslinked hydrogels based on properly synthesized poly(ether urethane)s as potential drug delivery vehicles in the biomedical field: design and characterization;. *ACS Omega* 2024; 9(46); 45774-45788.

S32 – O5

Optimizing viscosity and dynamicity of alginate-based fibers to enhance bovine muscle generation for cultivated meat

Spaans S.[1], van Haaften T.[1], Beckers L.[1], Schaeken L.[1], Pötgens A.[1], Wieland E.[1], Post M.[1], Doğan A.[1]
[1]Mosa Meat B.V. Maastricht, The Netherlands

Introduction

Our aim is to create bioartificial muscle (BAMs) from cells obtained from a small biopsy from cows and use this as a high-quality ingredient to produce cultivated meat. For the generation of BAMs, bovine satellite cells (BSCs) are isolated, proliferated and finally differentiated within a three-dimensional (3D) biomaterial following previously established protocols1. It remains a challenge to fully mature muscle in the lab and, at the same time, also consider the scale, price and safety of the product. Various natural and synthetic biomaterials, such as Matrigel® or fibrin, have been used to form scaffolds for in vitro muscle tissue-engineered constructs; however, they have not reached the quality and price parity we aim to achieve and are not compatible for cultivated meat purposes. Alginate polymers have been extensively studied by us and were found to be a promising candidate for the generation of BAMs. To generate mature BAMs, we optimized the physical and mechanical properties of the alginate hydrogel matrix. This was achieved by modifying the alginate with cell-adhesive ligands based on well-known RGD peptides and mixing different alginates with varying mannuronic (M) and guluronic (G) acid compositions.

Materials and Methods

Sodium alginates with different viscosities and M and G content were used in this study and were formulated as high viscosity & low M HV-LM, high viscosity & high M HV-HM, low viscosity & low M LV-LM and low viscosity & high M LV-HM. RGD-modified alginate was synthesized as previously described[1]. BSCs fluorescent cell lines expressing either eGFP or mCherry were generated via lentiviral transduction. Briefly, BSCs were encapsulated at high densities in different alginate formulations and cultured in differentiation media for 12-14 days. Media was replenished every 7 days. 3D myogenic fusion percentage was determined by the overlapping area of two different fluorescently labeled BSCs (eGFP and mCherry) and dividing it over the area of the sum of both signals.

Results

BSCs were successfully encapsulated in different alginate formulations and 3D myogenic fusion was determined. For high viscosity alginates, a significant increase in 3D fusion was observed using high M containing alginates at total alginate concentration of 0.2 and 0.4 wt% (Figure 1A). For low viscosity alginates, a significant increase in 3D fusion was observed using high M containing alginates at total alginate concentration of 0.5 and 1.5 wt% (Figure 1B).

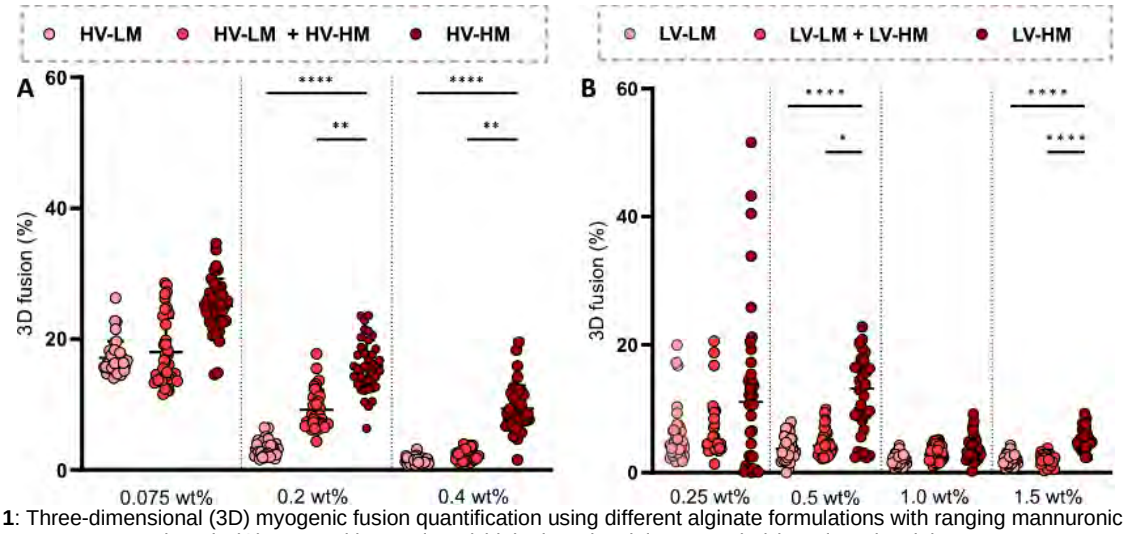

Figure 1: Three-dimensional (3D) myogenic fusion quantification using different alginate formulations with ranging mannuronic (M) and guluronic (G) compositions using A) high viscosity alginates and B) low viscosity alginates.

Conclusion

We have achieved an increased control over 3D myogenic fusion by tuning the physical and mechanical properties of RGD-modified alginate, which paves the way for a high-quality muscle ingredient for cultivated meat production.

References

[1]Melzener L., Schaeken L., Fros M., Messmer T., Raina D., Kiessling A, van Haaften T., Spaans S., Doğan A., Post M.J., Flack J.E. Optimisation of cell fate determination for cultivated muscle differentiation. *Communications Biology 2024*; 7; 1493.

S33
Emerging biomaterials and fabrication technologies for soft tissue regeneration

S33 - K1
Antimicrobial biodegradable mesh implants produced by melt electrowriting for pelvic organ prolapse repair

Silva E.[1], Martins J.[1], Mascarenhas T.[2], Fernandes A.A.[1]
[1]LAETA/INEGI, FEUP; [2]Dept. de Ginecologia, Centro Hospital de São João, Porto, Portugal

Introduction
Pelvic organ prolapse (POP) is a common condition that significantly impacts women's quality of life. Synthetic transvaginal meshes previously used for POP treatment were withdrawn from the United States market in 2019 due to complications such as infection, mesh erosion, and recurrent prolapse. Consequently, the development of biodegradable meshes has emerged as a promising alternative. In addition, 3D printing technologies enable the fabrication of meshes with controlled architecture and improved biological performance.
The use of antimicrobial coatings may reduce the risk of mesh-related infections, which, although relatively uncommon, can lead to severe complications and may require implant removal.

Aim
The aim of this study was to evaluate the antimicrobial effectiveness of antibiotic-coated polycaprolactone (PCL) mesh implants produced by melt electrowriting (MEW) in preventing bacterial biofilm formation associated with mesh infections.

Materials and Methods
PCL meshes were fabricated using MEW with Facilan™ PCL 100, a biodegradable polymer with a low melting point and rapid solidification suitable for this technique. The printed meshes were coated with antibiotics commonly used to treat genitourinary tract infections: azithromycin (0.15% and 0.20%), gentamicin sulfate (1% and 2%), and ciprofloxacin (0.9%).
The antimicrobial performance of the meshes was evaluated against bacterial strains commonly associated with mesh infections: *Escherichia coli* ATCC 25922, methicillin-susceptible *Staphylococcus aureus* (MSSA) ATCC 29213, and methicillin-resistant *Staphylococcus aureus* (MRSA) ATCC 43300.
Fourier transform infrared spectroscopy (FTIR) was used to analyse antibiotic incorporation in the meshes. Antibacterial activity and biofilm formation were assessed using inhibition zone assays, scanning electron microscopy (SEM), and biofilm quantification methods including XTT metabolic activity and crystal violet staining.

Results
FTIR analysis confirmed the presence of characteristic PCL peaks in all samples. A slight decrease in peak intensity was observed in antibiotic-coated meshes, suggesting the presence of additional compounds.
SEM images showed a clear reduction in bacterial colonization and biofilm formation in antibiotic-loaded meshes compared with the control (Figure 1 and 2). Ciprofloxacin-coated meshes demonstrated the highest antibacterial activity and the strongest reduction in biofilm formation for all tested bacterial strains. Gentamicin also showed notable antibiofilm activity, particularly against *E. coli* and MSSA. Azithromycin presented antibacterial activity but exhibited lower effectiveness in inhibiting biofilm formation.

Conclusion
Antibiotic-coated PCL meshes demonstrated significant antibacterial activity and reduced biofilm formation in bacterial strains associated with mesh infections. Among the tested antibiotics, ciprofloxacin showed the highest antimicrobial effectiveness. These findings support the potential use of antibiotic-loaded biodegradable meshes as a strategy to reduce infection risk in pelvic organ prolapse repair.

Acknowledgements
The authors acknowledge the Foundation for Science and Technology (FCT) for financial support to LAETA through project UID/50022/2025.

S33 – O1

Experimental and computational optimization of melt-electrowritten polycaprolactone scaffolds for hydrogel encapsulation in pelvic organ prolapse repair

Silva A.T.[1,2], Fernandes A.[1,2], Silva M.E.[1,2]
[1]LAETA, INEGI; [2]Faculty of Engineering, University of Porto, Porto, Portugal

Introduction

Pelvic Organ Prolapse (POP) affects millions of women worldwide and results from the weakening of pelvic floor supportive tissues. This condition can lead to pain, urinary dysfunction, and a significant reduction in quality of life. Current surgical treatments present several limitations, including recurrence, biocompatibility issues, and inflammatory responses associated with implanted materials. To address these limitations, we propose a minimally invasive device based on a bioactive hybrid hydrogel designed to promote muscle regeneration. To ensure mechanical stability and controlled degradation, the hydrogel is encapsulated within a polycaprolactone (PCL) membrane fabricated using Melt Electrowriting (MEW), a technique that enables the production of highly controlled micro-architectured scaffolds.

Aim

This study aims to optimize the geometric architecture of MEW-printed PCL scaffolds through an integrated computational and experimental framework.

Materials and Methods

The optimization framework combines computational modeling and experimental characterization. Different scaffold geometries were designed in SolidWorks and imported into Abaqus for compression simulations. These simulations evaluate the mechanical performance of both the isolated PCL membrane and the hydrogel-encapsulated PCL membrane.
Experimentally, PCL scaffolds are fabricated via MEW, using FullControl software (Python) for precise G-code generation. To assess the durability and functional lifespan of the device, degradation studies are being conducted. Additionally, uniaxial compression tests are performed on both dry PCL scaffolds and hydrogel-encapsulated membranes to evaluate compressive stiffness, structural integrity, and the influence of the hydrogel on the overall mechanical response.

Results

Preliminary numerical simulations indicate that scaffold geometry significantly influences the compressive response of the system. By correlating *in silico* finite element analysis with experimental data, we aim to identify the optimal geometric configuration that maintains stability throughout the degradation process. These results will define the architecture that provides the best balance between mechanical support, porosity for molecular diffusion, and structural persistence over time.

Conclusion

This strategy enables the rational design of mechanically stable and bioactive hybrid systems for regenerative medicine applications. The optimized scaffold architecture is expected to support hydrogel functionality while maintaining mechanical integrity during degradation, representing a promising minimally invasive approach for POP treatment.

Acknowledgements

The authors acknowledge the Foundation for Science and Technology (FCT) for financial support to LAETA through project UID/50022/2025. This research was also supported by the FCT PhD grant 2025.05959.BDANA.

S33 – O2
Taming biodegradation in peptide-crosslinked hydrogels

Kelchtermans K.[1], Marien N.[1], Adriaensens P.[1,2], Graulus G.-J.[1]
[1]UHasselt, Institute for Materials Research (IUMAT), Biomolecule Design Group, Diepenbeek; [2]UHasselt, Institute for Materials Research (IUMAT), Analytical and Circular Chemistry, NMR group, Diepenbeek, Belgium

Introduction

Over the past decades, cell-interactive hydrogels have made significant contributions to the progress in tissue engineering. Today, the ideal hydrogel is considered a dynamic environment that meets the needs of developing tissue. Regarding the scaffold's biodegradability, it is favorable to design hydrogels that remain stable during the initial phases of tissue development but fully degrade once the material has served its purpose. Therefore, in this project, a hydrogel is envisioned that is crosslinked with protease-sensitive peptide crosslinkers. These crosslinkers will be reversibly protected with a nitrobenzyl-based photocage. The introduction of suitable protecting groups is expected to prevent the protease from recognizing its substrate, thereby slowing down or even preventing degradation. When degradation is desired, the protecting group can be removed by UV exposure, returning the protease substrate to its native state (Figure 1).

Materials and Methods

Photocage synthesis: Fmoc-Glu-OtBu was converted to Fmoc-Glu(MNB)-OtBu using DMAP, DCC, and 1-(2-nitrophenyl)ethan-1-ol. To use the protected amino acid during the solid-phase peptide synthesis (SPPS) protocol, the tert-butyl group was removed with TFA.
Peptide synthesis: Peptides were synthesized via a standard Fmoc SPPS protocol, with DIC and Oxyma used as coupling reagents. Analysis of the samples was done via MALDI-TOF MS.
PEG modification: 4-arm PEG-OH was converted to 4-arm PEG-COOH using glutaric anhydride in the presence of DMAP and triethylamine. To enable crosslinking, the carboxylic acids were activated with DCC and NHS to form NHS-esters.
Peptide cleavage protocol: The degradability of the caged and uncaged peptides was assessed by incubating them with endoproteinase Glu-C and analyzing the resulting degradation products by MALDI-TOF MS.

Results

The protease-sensitive crosslinker (KGE//NLYFQSGK) was successfully synthesized, as confirmed by MALDI-TOF MS analyses. This peptide serves as a reference for the degradation rate in the presence of endoproteinase Glu-C. Peptides modified with a commercially available benzyl cage on the glutamic acid residue have been synthesized, and preliminary results indicate slowed enzymatic degradation of the peptide. These results are now being validated using the above-described nitrobenzyl-based photocage, which has already been successfully introduced on the peptide crosslinker. Furthermore, the conversion of the alcohol functionality on 4-arm PEG-OH to carboxylic acids and NHS esters was confirmed by NMR spectroscopy, setting the stage for in-gel validation.

Conclusion

Photocaged protease-sensitive peptides have been successfully synthesized in this project and are currently being explored to control the onset of biodegradation in model hydrogels.

Acknowledgements

This research is supported by Research Foundation Flanders (FWO) under project 11P4M24N.

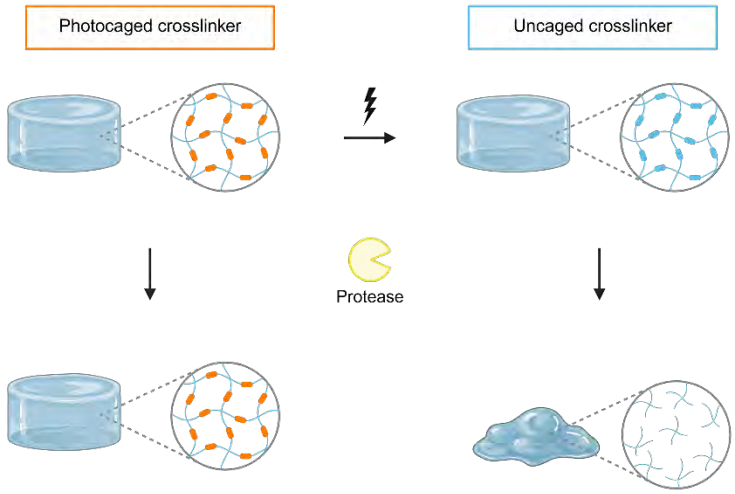

Figure 1: The protease cannot recognize its substrate while the photocage is present, leading to a stable hydrogel without enzymatic degradation. Degradation occurs only when UV light removes the photocage, thereby returning the protease substrate to its native state.

S33 – O3

Medical lace embroidery: Designing structural and mechanical heterogeneity in biotextiles

Haymon T.[1,2,3], Elschner C.[3], Tonndorf R.[3], Uhlig K.[3], Zybell L.[3], Scheibner H.[3], Mayer J.[2]
[1]Dept. of Health Sciences and Technology, ETH Zürich, Zürich, Switzerland; [2]Surgical Fusion Technologies GmbH, Schlieren, Switzerland; [3]Division Polymer Materials Engineering, Leibniz Institute for Polymer Research Dresden, Dresden, Germany

Introduction

Biotextiles encompass products from dressings to implanted meshes and are typically manufactured by weaving, knitting, braiding or non-wovens, which tend to produce spatially uniform structures. Lace embroidery, a familiar decorative technique, can be repurposed to produce free-standing, three-dimensional textiles on soluble backing. This technique, adapted to create self-supporting structures from biocompatible thread materials, is referred to as “medical lace embroidery.” It enables local control over porosity, anisotropy, and stiffness, so implants can be tailored to match the mechanical and structural properties of soft tissue.
The aim of the study was to record structure-property relationships in lace-embroidered biotextiles by investigating how embroidery patterns, machine settings, and individual pattern elements influence porosity and mechanical behavior.

Materials and Methods

Using SolidWorks and Ink/Stitch, mesh patterns featuring running and zigzag stitches, graded stitch density and distinct load-bearing strands were created (Figure 1a) and produced on Tajima embroidery machines using polypropylene monofilament and polyester multifilament threads (Figure 1b). Uniaxial tensile tests were performed to characterize mechanical behavior. Full-field deformation was measured by digital image correlation (DIC) processed with the VEDDAC software to compute displacement and strain maps (Figure 1c), while pore characteristics were quantified from digital-microscopy images using Python-based image analysis.

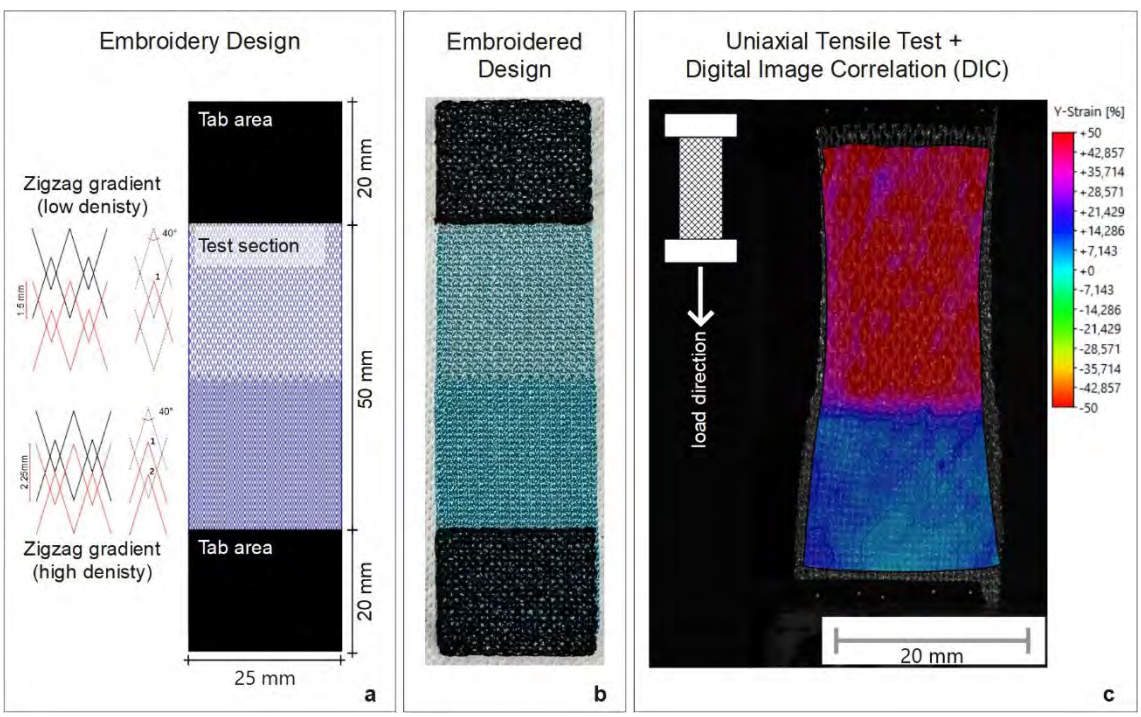

Figure 2. (a) The specimen design includes tab areas and a test section with low-density (top) and high-density (bottom) embroidery regions; (b) Embroidered specimen on substrate before testing; (c) Normal strain distribution (Y-strain, ± 50%) obtained by DIC showing that the low-density embroidery region deforms significantly more than the high-density region. The low-density region here exhibits a strain of 46 % while the high-density region shows only 6% strain. This demonstrates the reinforcing effect of increased stitch density.

Results

Using machine embroidery, biotextiles can be engineered with local mechanical heterogeneity and a tendon-like stress–strain response: an initial toe region, a defined linear region, and progressive failure instead of sudden rupture. Stitch topology dominates stiffness and anisotropy. Running stitches oriented with the loading direction produce a stiffer response, while zigzag stitches serve as an integrated thread reservoir that increases extensibility. Separate loading strands can be implemented to selectively take up load, while graded stitch density directs deformation to flexible regions. Production choices, such as thread tension and layering, influence the final shape and strand movement, which are important considerations for any implant-relevant design.

Conclusion

To produce biotextiles with customized spatial architecture and mechanics — designs that go beyond standard solutions for implantable textiles — machine lace embroidery can be used as a versatile fabrication method. Further research could focus on optimizing the pattern and process parameters to achieve the desired durability, biological compatibility, and ease of surgical handling.

S33 – O4

Engineered oxygen-delivery particles for advanced colorectal tissue engineering

Marta E.[1], Fiorilli S.L.[1], Van Vlierberghe S.[2], Groll J.[3], Vozzi G.[4], Vitale-Brovarone C.[1]
[1]Dept. of Applied Science and Technology, Politecnico di Torino, Turin, Italy; [2]Dept. of Organic and Macromolecular Chemistry, Ghent University, Ghent, Belgium; [3]Dept. for Functional Materials in Medicine and Dentistry, University of Würzburg, Würzburg, Germany; [4]Dept. of Information Engineering and Research Center 'E. Piaggio', Università di Pisa, Pisa, Italy

Introduction

The treatment of colorectal diseases frequently requires surgical removal of mucosal and submucosal layers, resulting in impaired tissue function. Addressing this unmet need requires regenerative strategies capable of restoring structure and physiological activity. Oxygen-releasing carriers offer a promising strategy to enhance tissue repair by improving oxygen availability. Here, we propose two particulate systems engineered for sustained oxygen delivery and integration into a 3D-printable, cell-laden, gelatin-based matrix for colorectal tissue engineering. The first system consists of PLGA microparticles encapsulating calcium peroxide (CaO_2) crystals, whose reaction with water generates oxygen[1]. The second consists of core-shell microparticles in which a polyvinylpyrrolidone (PVP) core complexing H_2O_2 is encapsulated within a gelatin shell, enabling *in situ* oxygen generation via endogenous catalase[2].

Materials and Methods

CaO_2 crystals were synthesized via aqueous precipitation, dispersed in a PLGA solution and sonicated to ensure uniform distribution before double-emulsion processing[1]. Core-shell particles containing PVP/H_2O_2 complexes were fabricated by co-axial electrospraying[2]. Both formulations were characterized morphologically and structurally using SEM, FESEM, EDS, FTIR, and XRD; degradation kinetics were also evaluated. Calcium incorporation was assessed via Alizarin Red staining, and H_2O_2 release quantified colorimetrically. Long-term oxygen release was evaluated at 37°C for up to 14 days. After embedding both formulations into a gelatin-based matrix, rheological characterization will confirm composite printability are on going.

Results

CaO_2 crystals exhibited the expected morphology and were effectively encapsulated within spherical PLGA microparticles (10-30µm), with homogeneous internal crystals distribution (*Figure 1*). Oxygen-releasing measurements demonstrate a sustained release profile, reaching dissolved oxygen levels of approximately 6mg/L. Optimized electrospraying parameters enabled the formation of core-shell particles with spherical morphology and size between 300nm and 3µm, as confirmed by structural analyses *(Figure 1)*.

Conclusion

These two engineered particulate systems provide complementary strategies for controlled oxygen delivery in regenerative medicine. When incorporated into a 3D-printable, cell-laden, gelatin-based matrix, they will support the development of advanced constructs for colorectal mucosa and submucosa regeneration, assisted by oxygen-release levels suitable for sustaining cell proliferation.

Acknowledgements

Funded by the European Union (DAEDALUS G.A.101178568).

References

[1]Mohseni-Vadeghani E., Karimi-Soflou R., Khorshidi S., Karkhaneh A. Fabrication of oxygen and calcium releasing microcarriers with different internal structures for bone tissue engineering: Solid filled versus hollow microparticles. *Colloids and Surfaces B: Biointerfaces* 2021;197.
[2]Guan Y., Niu H., Dang Y., Gao N., Guan J. Photoluminescent oxygen-release microspheres to image the oxygen release process in vivo. *Acta Biomaterialia* 2020; 115;333-342.

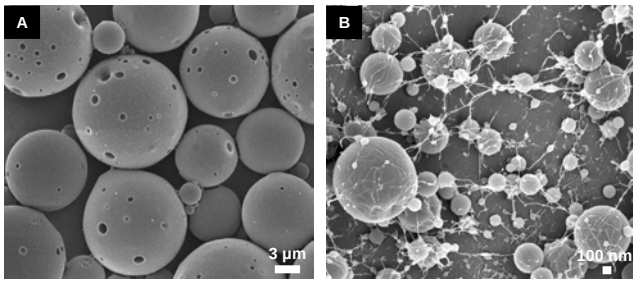

Figure 1. SEM images of A: PLGA microparticles incorporating CaO_2 crystals (scale bar 3 µm) and B: core-shell electrosprayed particles (scale bar 100 nm).

S33 – O5

Enhancing polyvinyl alcohol hydrogel stiffness via thermal and mechanical treatments for soft tissues repair

Confalonieri M.[1,2], Bettella L.[1], Pagot G.[2], Nifosì M.[1,2],Barbon S.[3], Stocco E.[3], Porzionato A.[3], Di Noto V.[2], Pavan P.G.[1,2], Todros S.[2]

[1]Fondazione Istituto di Ricerca Pediatrica Città della Speranza; [2]Dept. of Industrial Engineering, University of Padova; [3]Human Anatomy Section, Dept. of Neuroscience, University of Padova, Italy

Introduction

Polyvinyl Alcohol (PVA) hydrogels are promising biomaterials due to biocompatibility, hydrophilicity, high water content, and tunable mechanical properties. Their structural features make them suitable as synthetic grafts for soft tissues repair, such as cartilage, ligaments, and tendons. However, their mechanical performance remains a critical limitation. Thus, we evaluated two strategies to enhance PVA hydrogels stiffness (Figure 1): thermal treatment, enhancing hydrogen bonding and crystallinity, and mechanical treatment, to align polymer chains, improving directional mechanical and tribological properties.

Materials and Methods

PVA hydrogels 20% (w/v) were cast and physically crosslinked through four FT cycles (16 h at −20 °C; 8 h at 4 °C). Thermal treatment groups included: (i) *dried*, with samples dried for 16 h at 60 °C, and (ii) *annealed*, where the drying step was followed by annealing at 120 °C for 1 h. Finally, all samples were rehydrated for 48 h. Mechanical treatment employed a custom 3D-printed rig to deform samples stepwise up to 50%, 100%, or 200% strain. Characterization included measuring weight and volume variations, uniaxial tensile and compression tests, scanning electron microscopy (SEM) and thermogravimetric analysis (TGA).

Results

Thermal treatment of hydrogels enhanced both tensile and compressive stiffness (Figure 2A, B), with annealed samples approaching the range of native articular cartilage stiffness (200-5400 kPa). TGA revealed higher degradation temperatures and reduced water content (~50%) (Figure 2C), reflecting increased polymer concentration and crystallinity. In parallel, mechanical treatment induced an anisotropy within the material, resulting in increased stiffness along the direction of applied elongation; for instance, at 50% strain, stiffness along elongation direction was approximately 10% higher than in the transversal direction.

Conclusion

Overall, the applied thermal and mechanical treatments effectively enhanced the stiffness and structural organization of PVA hydrogels, highlighting their potential as optimized biomaterials to develop synthetic grafts and for future *in vivo* applications in soft connective tissue repair, especially as substitutive artificial cartilage in high-stress joints.

Acknowledgements

This activity was supported by BIRD 2024 Research Program of the University of Padova, Italy, grant number 2024DII1SIDPROGETTI-00281.

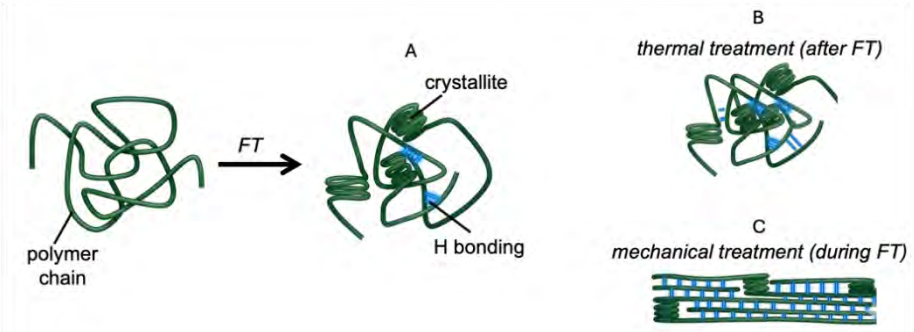

Figure 1: Schematic representation of PVA hydrogel chain conformation due to crosslinking via freeze-thawing (FT) (A), thermal (B) and mechanical (C) treatments.

Figure 2: Tensile (A) and compressive (B) behavior of thermally treated PVA. TGA profile (C): weight percentage vs temperature.

S33 – O7

Recombinant elastin-like polymer-based basement membrane for tissue-engineered skin regeneration

Escribano R.[1], Puertas M.[1], González I.[1], Santos M.[1], Rodríguez-Cabello J. C.[1]Alonso M.[1]
[1]BIOFORGE, LaDIS, CIBER-BBN, University of Valladolid, Valladolid, Spain

Introduction

Skin injuries caused by burns, chronic diabetic ulcers, or surgical procedures remain a major clinical challenge due to their impact on physiological function and the limitations of current treatments. The development of advanced skin substitutes capable of promoting tissue regeneration and protecting the wound environment is therefore essential [1]. This study aims to develop a basement membrane based on Elastin-Like Recombinamers (ELRs), bioinspired polymers derived from natural elastin, designed to mimic the native basement membrane and support skin regeneration [2].

Materials and Methods

Elastin-Like Recombinamers (ELRs) containing cell-adhesion (RGD) and enzymatically degradable (GTAR) sequences were used. The ELRs were functionalized with azide and cyclooctyne groups via NHS-ester chemistry to enable crosslinking. A laminin-derived peptide (PPFLMLLKGSTR), known to promote keratinocyte adhesion and migration, was synthesized by solid-phase peptide synthesis (SPPS) and incorporated into the system [3]. A biomimetic membrane was formed *in situ* by mixing the two ELRs components, RGD and GTAR.
ELRs were characterized by nuclear magnetic resonance (NMR) and, mass spectrometry, while thermal behavior was evaluated by differential scanning calorimetry (DSC). Membrane properties such as surface topography, wettability, porosity, mechanical strength, and enzymatic degradation were analysed. Biological performance was assessed *in vitro* using human fibroblasts (HFF-1) and keratinocytes (HaCaT) through viability, adhesion, and migration assays.

Results

The RGD ELRs functionalized with azide groups (15 groups per chain) and the GTAR ELRs functionalized with cyclooctyne groups (10 groups per chain) were successfully modified, enabling efficient in situ crosslinking via click chemistry. A laminin-derived peptide, synthesized with high purity by solid-phase peptide synthesis (SPPS), was covalently grafted onto the degradable ELR backbone (2 peptides per chain), providing the system with enhanced bioactivity. The resulting components formed a homogeneous membrane (~20 µm thick) under physiological conditions (Figure 1).
Rheological characterization revealed a complex modulus (G*) of ~3 kPa, consistent with soft tissue mechanics and suitable for handling and application. The membranes exhibited an exceptionally high-water content (98% equilibrium uptake at 37 °C) and showed controlled enzymatic degradation in the presence of urokinase-type plasminogen activator (580 U/mL), highlighting their dynamic and biomimetic nature.
In vitro assays demonstrated excellent biocompatibility and significantly enhanced cell–material interactions (Figure 2). Notably, laminin functionalization selectively boosted keratinocyte adhesion and migration, surpassing both fibroblasts and non-functionalized controls. This underscores its key role in promoting epithelial regeneration, which is a key process in tissue repair.

Conclusion

In summary, these findings highlight the potential of laminin-functionalized ELR membranes as a powerful strategy to selectively enhance keratinocyte-driven regeneration, paving the way for improved skin repair approaches.

Acknowledgements

The authors are grateful for funding from the Spanish Government (grants PID2021-122444OB-100 and PID2022-137484OB-I00 funded by MCIN/AEI/ 10.13039/501100011033 and by ERDF, EU, and grant PRE2022-104042 funded by MCIN/AEI/ 10.13039/501100011033 and by ESF+, EU), from the Department of Education, Junta de Castilla y León (grant VA188P23 and CLU-2023-1-05 cofunded by ERDF, EU), and from Centro en Red de Medicina Regenerativa y Terapia Celular de Castilla y León.

References

[1] Stashk T. S. Update on wound dressings: Indications and best use. *Clin. Tech. Equine Pract,* 2024., *3*, 148-163
[2] Flora, T. Use of proteolytic sequences with different cleavage kinetics as a way to generate hydrogels with preprogrammed cell-infiltration patterns imparted over their given 3D spatial structure. *Biofabrication*, 2019, 035008.
[3]Juanes D., Escribano R. Innovative elastin-like recombinamer hydrogels with laminin-derived peptides for enhanced wound healing. Cell Biomaterials., 2026, 100349

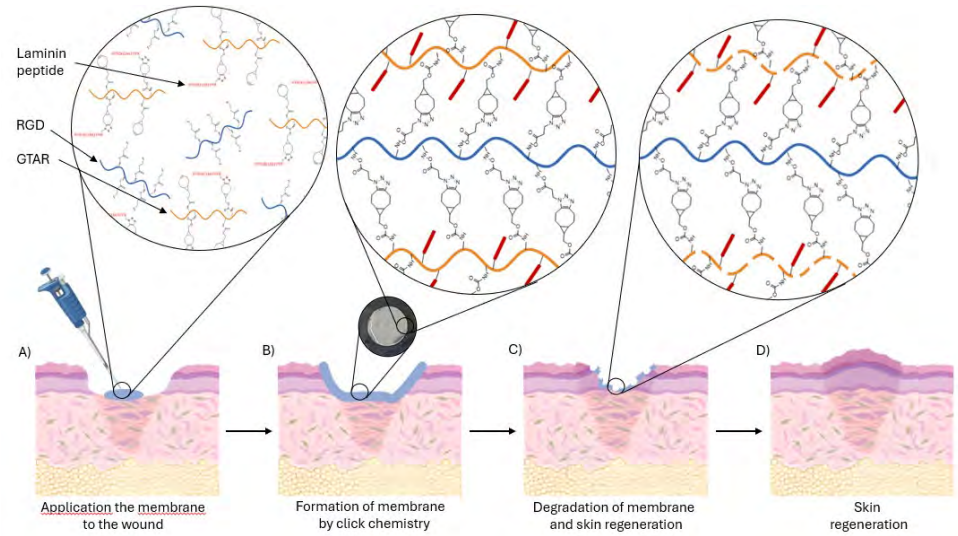

Figure 3. Schematic representation of the wound healing process with laminin membranes; (A) application of the membrane; (B) membrane formation; (C) membrane degradation; (D) and skin regeneration.

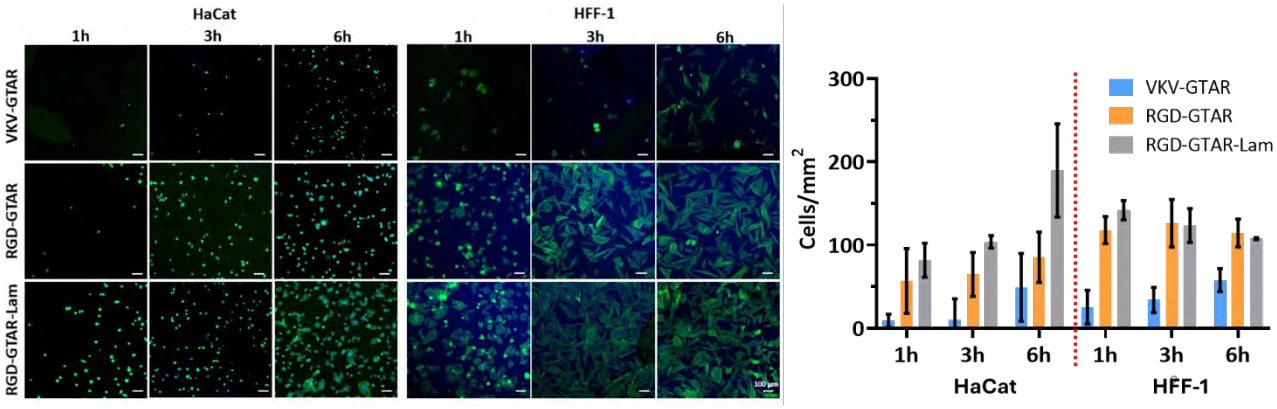

Figure 4. Cell adhesion assay. Representative images showing cell adhesion at different time points (1, 3, and 6 h) of HaCat and HFF-1 cells stained with Hoechst and phalloidin. Graphs depict the quantitative analysis of nuclei within a 1.18 mm² area.

S34
Engineering living materials for emerging health needs

S34 – K1
Engineering bioactive hydrogel-based living materials for infection control and bone regeneration

Ambrosio L.
IPCP – CNR – Italy
A. Mariano,[1] F. Zuppardi,[1] A. Soriente,[1] A. Bigham,[1] G. Gomez d'Ayala,[2] M.G. Raucci,[1] L. Ambrosio[1*]
Institute of Polymers, Composites and Biomaterials (IPCB) − CNR, Naples[1]/Pozzuoli[2], Italy.

Introduction
Biomaterials designed for bone repair and regeneration should not only provide structural support but also actively modulate the local microenvironment. Hydrogels are particularly attractive platforms, as their hydrated, extracellular matrix–like structure supports cell infiltration, nutrient diffusion, and dynamic interactions with surrounding tissues. Moreover, their physicochemical properties can be finely tuned to regulate cellular behavior. By incorporating bioactive components, hydrogels can promote osteogenic and angiogenic commitment while attenuating excessive inflammatory responses, thereby fostering a regenerative microenvironment conducive to effective bone healing. These bioactivated hydrogels will be loaded with natural (phages) or synthetic carriers (liposomes), containing modified genetic sequences, capable of transfecting biofilm-embedded bacteria to induce the production of osteoinductive proteins. As a result, the biofilm itself can be transformed into a biofactory, offering also a strategy to overcome antibiotic resistance.

Materials and Methods
Hydrogels were formulated using 23wt% Pluronic F127 and 1wt% alginate. Hydroxyapatite (5–10wt%) was incorporated via an in-situ sol–gel process, while bioactive glasses (2.5–5wt%) were synthesized through evaporation-induced self-assembly and introduced by physical blending. The resulting nanocomposite hydrogels were characterized by SEM, TEM, and Raman spectroscopy. Biocompatibility was evaluated through live/dead and Alamar Blue assays using human mesenchymal stem cells (hMSCs), human umbilical vein endothelial cells (HUVECs), and RAW 264.7 macrophages. Osteogenic differentiation was evaluated by monitoring the time-dependent expression of collagen I and osteocalcin, as well as cytoskeletal reorganization via immunofluorescence analysis. Angiogenic capacity was assessed in HUVECs through cell migration and capillary-like tube formation assays. Anti-inflammatory activity was examined by measuring nitrite and measuring reactive oxygen species (ROS) production and total superoxide dismutase (T-SOD) activity. M1/M2 macrophages polarization was studied via immunofluorescence analysis. Angiogenic potential was investigated using scratch wound and tube formation assays.

Results
The physical-chemical and rheology characterization demonstrated the stability and injectability of the biohydrogels. Biocompatibility of the hydrogels was first confirmed hMSCs, HUVECs, and RAW 264.7 macrophages, demonstrating that the developed nanocomposite hydrogels provide a safe and supportive cellular environment. Higher levels of bioactive signals promoted a more pronounced osteogenic response, as evidenced by the upregulation of collagen I and osteocalcin expression and enhanced cytoskeletal organization during hMSCs differentiation. Similarly, angiogenic activity in HUVECs, assessed through migration and capillary-like tube formation assays, improved with increasing bioactive content. In parallel, the immunomodulatory effects observed in RAW 264.7 macrophages were more evident at higher concentrations of both HA and BGs, with greater regulation of ROS and nitrite production, modulation of T-SOD activity, and a shift toward a pro-regenerative M2 phenotype.

Conclusion
The developed nanocomposite hydrogels provide a physical and biologically supportive environment while actively influencing key regenerative pathways. The incorporation of bioactive fillers confers the ability to regulate osteogenic differentiation, promote vascular-related responses, and modulate inflammatory signaling. This integrated functional profile positions these hydrogels as strategically engineered systems capable of orchestrating

multiple aspects of the bone healing cascade, supporting their advancement as instructive platforms for bone tissue regeneration.

Acknowledgements
HORIZON-EIC-2022-PATHFINDEROPEN-01 (GA 101098972): Bacteria Biofilm as bio-factory for tissue regeneration – BIOACTION. CUP: B63C23000240006.

S34 – K2
Bacteria-based materials in cell engineering

Salmeron-Sanchez M.
Institute for Bioengineering of Catalonia, IBEC, Barcelona, Spain & Centre for the Cellular Microenvironment, University of Glasgow, Glasgow, UK

Introduction
Engineered living materials combine synthetic materials with bacteria to add new properties to materials systems. We use genetically modified bacteria to engineer a new class of living biomaterials able to confer dynamic presentation of proteins and growth factors to mammalian cells. We focus on *L.lactis* as a non-pathogenic strain with low production of extracellular matrix. We have engineered *L.lactis* to produce fibronectin as a membrane protein and also secrete controlled concentrations of growth factors, seeking to control adhesion and differentiation of mesenchymal stem cells.

Materials and Methods
We have genetically engineered *L.lactis* to respond dynamically to controlled concentrations of nisin in the medium. This leads to increased expression of fibronectin as a membrane protein and BMP-2 (a potent osteogenic growth factor) either as a membrane protein or secreted to the medium. We use a range of synthetic materials to co-culture the genetically engineered bacteria and mesenchymal stem cells.

Results
We demonstrate the ability of these strains to colonise different synthetic materials, and also to be part of 3D hydrogels. We show that the expression of fibronectin and BMP-2 is controlled by the concentration of nisin in the medium. Co-culture of genetically engineered *L.lactis* with mesenchymal stem cells enables adhesion to the fibronectin-expressing bacteria and osteogenic differentiation of mesenchymal stem cells in co-culture with BMP-2 secreting bacteria.

Conclusion
Genetically modified bacteria can be included in synthetic materials to control the adhesion and differentiation of mesenchymal stem cells.

S34 – O1

Lysozyme amyloid nanofibril-reinforced carrageenan–CMC bioinks for high-fidelity 3D bioprinting of living wound healing patches

Teixeira M.C.[1], Carvalho J.P.F.[1], Lameirinhas N.S.[1], Luís J.[2], Oliveira H.[3], Oliveira J.M.[2], Silvestre A.J.D.[1], Vilela C.[1], Freire C.S.R.[1]
[1]CICECO – Aveiro Institute of Materials, Department of Chemistry, University of Aveiro, Aveiro, Portugal; [2]CICECO – Aveiro Institute of Materials, EMaRT Group, University of Aveiro, Oliveira de Azeméis, Portugal; [3]Department of Biology & CESAM, University of Aveiro, Aveiro, Portugal

Introduction

Severe skin injuries remain a major clinical challenge due to infection risk, delayed healing and impaired tissue regeneration. Recent advances in extrusion-based 3D bioprinting allow the fabrication of personalized, cell-laden constructs that mimic the architecture of native tissues. Natural polymer hydrogels are promising bioink matrices due to their biocompatibility and ability to support cellular activity; however, many still lack optimal printability and mechanical stability for high-fidelity bioprinting. Here, lysozyme amyloid nanofibrils (LNFs) are explored as multifunctional nano-reinforcing agents to simultaneously enhance bioink printability, mechanical performance and biological functionality.

Aim

This study aimed to develop a multifunctional polysaccharide-based hydrogel bioink reinforced with LNFs for high-fidelity extrusion 3D bioprinting of keratinocyte-laden living wound healing patches (Figure 1).

Materials and Methods

Hydrogel bioinks were prepared from a carrageenan–carboxymethyl cellulose (Crg–CMC) matrix reinforced with LNFs (5, 10 and 15 wt.% relative to the polymer content). Rheological behavior, printability, mechanical properties, porosity, degradation and cytocompatibility were evaluated. The optimal formulation was loaded with human keratinocytes (HaCaT, 3×10^6 cells mL^{-1}) and dexpanthenol (Dex, 5 wt.%) as a therapeutic agent. Cell-laden constructs were fabricated using extrusion-based 3D bioprinting and cultured for up to 21 days. Cell viability was assessed using LIVE/DEAD assays and fluorescence microscopy.

Results

The incorporation of LNFs significantly improved the rheological performance of the Crg–CMC bioinks, reducing gelation temperature to ~31 °C and enabling extrusion printing under physiological conditions. LNFs enhanced printing fidelity, yielding constructs with high shape accuracy and printability values close to 0.9. The resulting hydrogels exhibited suitable porosity and mechanical strength (~360–500 kPa), within the physiological range of native skin tissue. The optimized Crg–CMC–LNFs (10%) bioink supported long-term keratinocyte survival, with cell viability exceeding 91% after 21 days. The presence of Dex did not compromise cell viability while providing additional therapeutic potential.

Conclusion

The developed Crg–CMC–LNFs nanocomposite bioink exhibited excellent rheological, mechanical and biological performance for extrusion-based 3D bioprinting. LNFs significantly enhanced printability and structural stability while maintaining high keratinocyte viability. These findings demonstrated the potential of LNF-reinforced polysaccharide bioinks as a promising platform for the fabrication of living wound healing patches and next-generation skin tissue engineering constructs.

Acknowledgements

This work was developed within the scope of the projects CICECO – Aveiro Institute of Materials, UID/50011/2025 (DOI 10.54499/UID/50011/2025) & LA/P/0006/2020 (DOI 10.54499/LA/P/0006/2020), and CESAM (UID/50006 & LA/P/0094/2020 (doi.org/10.54499/LA/P/0094/2020)), financed by national funds through the FCT/MCTES (PIDDAC), and financially supported by the project I&D "NANOBIOINKS- Engineering bio-based nanofibers for the development of high-performance nanostructured bioinks for 3-D bioprinting, CENTRO-01-0145-FEDER-031289" funded by the Operational Program of the Center Region, in its FEDER/FNR component, and by national funds (OE), through FCT/MCTES

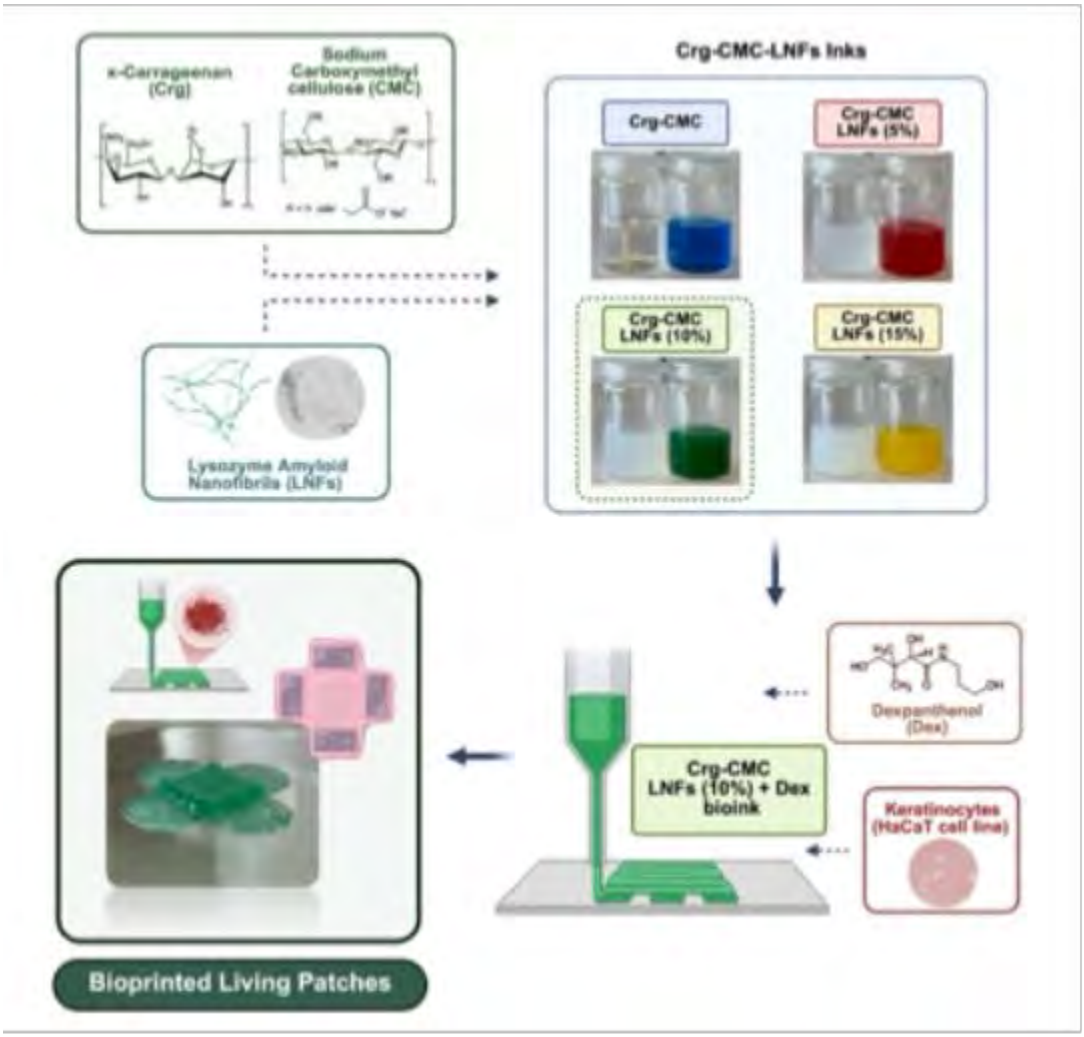

Figure 1 - Schematic representation of the preparation of the Crg-CMC-LNFs inks and the bioprinting living patches using the Crg-CMC-LNFs bioink loaded with Dex and keratinocytes.

S34 – O2

Photosynthetic biomaterials based on microalgae for oxygen generation and metabolic activity analysis

Podstawczyk D.[1], Sajbura N.[1], Nizioł M.[1], Gozdowska M.[1], Szyszka M.[1], Dawiec-Liśniewska A.[2], Bastrzyk A.[1], Jurga A.[3], Miller U.[3], Brandić Lipińska M.[4]

[1]BioSS lab, Dept. of Process Engineering and Technology of Polymer and Carbon Materials, Faculty of Chemistry, Wroclaw University of Science and Technology, Norwida 4/6, 50-373 Wroclaw, Poland; [2]Dept. of Advanced Materials Technologies, Faculty of Chemistry, Wroclaw University of Science and Technology, Smoluchowskiego 25, 50-372 Wroclaw, Poland; [3]Dept. of Environmental Biology and Air Protection, Faculty of Environmental Engineering, Wroclaw University of Science and Technology, Wybrzeże Stanislawa Wyspianskiego 27, 50-370 Wroclaw, Poland; [4]Integrative Design | Extremes, Dept. of Experimental Architecture, Innsbruck University, Technikerstraße 21, 6020 Innsbruck, Austria

Introduction

Microalgae-based biomaterials are increasingly explored as platforms for developing functional living systems with integrated biological activity. Embedding photosynthetic cells within hydrogel matrices enables the combination of material properties with biological functionality, such as oxygen generation and metabolite production. However, maintaining cell viability and activity within structured biomaterials remains a key challenge.

Aim

The aim of this study was to develop and characterize microalgae-laden hydrogel biomaterials capable of oxygen generation and metabolite production.

Materials and Methods

Microalgae (*Chlamydomonas reinhardtii*) were immobilized within hydrogel matrices based on alginate and GelMA. Bioinks were formulated to ensure printability and cell compatibility and processed using extrusion-based and coaxial 3D bioprinting. Coaxial printing enabled the fabrication of perfusable core-shell structures with defined architecture and spatial organization of materials and cells.

Cell viability was assessed using fluorescence-based assays, and photosynthetic activity was monitored under controlled light conditions. Oxygen production was measured in aqueous media, while metabolic activity was evaluated through quantitative analysis of selected compounds, including proteins, lipids, carbohydrates, and flavonoids, using spectrophotometric methods.

Results

The developed constructs (**Fig. 1**) supported cell viability and maintained photosynthetic activity over several days of cultivation. Oxygen production was detected in the range of ~6-8 mg/L, depending on experimental conditions such as cell density and illumination intensity. Metabolite analysis confirmed the presence of key primary and secondary compounds, including proteins, lipids, carbohydrates, and flavonoids, indicating retained metabolic activity of immobilized microalgae. The fabricated structures exhibited good shape fidelity and structural integrity after printing and crosslinking. Coaxial bioprinting enabled the formation of perfusable constructs with controlled architecture, supporting the development of more complex biomaterial systems.

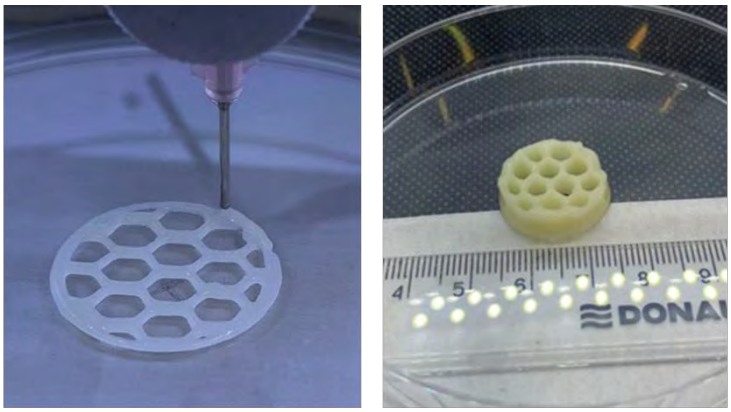

Fig. 1. 3D bioprinting proces of microalgae-laden constructs (left) and printouts (right)

Conclusion

Microalgae-laden hydrogel biomaterials provide a platform for integrating biological activity within structured materials. The presented approach enables oxygen generation and metabolite production within 3D constructs while maintaining cell functionality. These results support further development of photosynthetic biomaterials for potential applications in bioactive systems and oxygen-generating materials.

Acknowledgements
This research was funded by the National Science Centre, Poland, under grant no. 2023/49/B/ST8/03834.

S34 – O3

Species-dependent biofunctionalization of Ti6Al4V surfaces using microalgae-derived biomolecules

Hart M[1], Gutierrez Púa L.[3], Saez A[2], Paredes Mendez V.[3]
[1]Department of Mechanical Engineering, Universidad del Norte, Puerto Colombia, Barranquilla, 081008, Colombia, [2]School of Applied Sciences and Engineering, Universidad de EAFIT, Medellín, Colombia, [3]Biomedical Engineering Department, Universidad Simón Bolívar, Barranquilla 080002, Colombia

Introduction

Surface biofunctionalization is a key strategy to enhance the biological performance of titanium-based biomaterials used in orthopedic and dental implants. Recently, natural biomolecules have gained attention as sustainable alternatives for developing bioactive coatings. Microalgae represent a particularly attractive source of proteins, polysaccharides, lipids, and bioactive compounds with potential biomedical functionality. However, the influence of microalgal species on the physicochemical characteristics of biofunctionalized metallic surfaces remains largely unexplored. To date, the biofunctionalization of metallic biomaterials using microalgae-derived biomolecules has been scarcely reported.

Aim. The aim of this study is to compare the biofunctionalization of Ti6Al4V surfaces using biomolecules derived from two microalgae species, Spirulina platensis and Scenedesmus, in order to identify species-dependent differences in the resulting surface chemistry and morphology.

Materials and Methods

Ti6Al4V substrates were activated using piranha solution to increase surface reactivity and subsequently functionalized with (3-aminopropyl)triethoxysilane (APTES). Biomolecules derived from Spirulina platensis and Scenedesmus were immobilized onto the surface as biomass and protein extracts at concentrations of 1–5 g/L and immersion times of 3 h and 14 h. The resulting surfaces were characterized by Fourier-transform infrared spectroscopy (FTIR), X-ray photoelectron spectroscopy (XPS), scanning electron microscopy (SEM), and energy-dispersive X-ray spectroscopy (EDS) to evaluate chemical composition and surface morphology (Figure 1).

Results

Surface characterization confirmed the successful immobilization of microalgae-derived biomolecules on Ti6Al4V. FTIR and XPS analyses revealed the incorporation of carbon-, oxygen-, and nitrogen-containing functional groups associated with proteins and polysaccharides. SEM observations revealed pronounced species-dependent differences in coating morphology. Coatings derived from *Spirulina platensis* produced heterogeneous aggregated structures consistent with the filamentous nature of this cyanobacterium, while *Scenedesmus*-derived coatings generated more homogeneous granular deposits. EDS analysis further confirmed the incorporation of bioorganic elements (C, O and N) associated with microalgal biomolecules The elemental composition and surface morphology were strongly influenced by both microalgal species and biomolecule type, indicating distinct biofunctionalization mechanisms for each system.

Conclusion

Both microalgae successfully generated biomolecular coatings on Ti6Al4V surfaces, confirming that microalgae-derived biomolecules can act as effective biofunctionalization agents for metallic biomaterials. The comparative analysis revealed a clear species-dependent biofunctionalization behavior, with *Spirulina platensis* producing heterogeneous aggregated structures and *Scenedesmus* generating more homogeneous granular coatings. These differences demonstrate that microalgal species selection significantly influences the resulting surface chemistry and morphology. Overall, this study highlights the potential of microalgae-derived biomolecules as sustainable platforms for tailoring bioactive coatings on titanium-based implants.

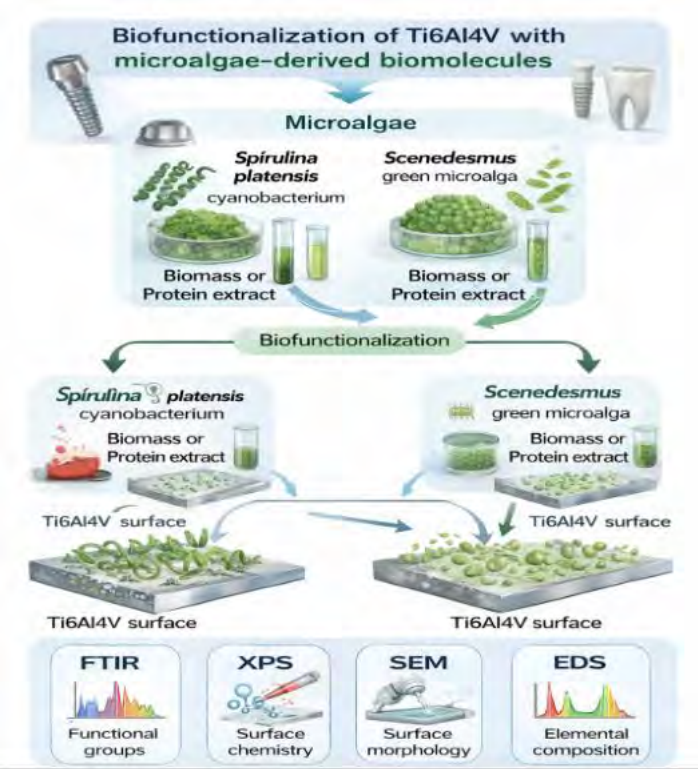

Figure 1. Schematic representation of Ti6Al4V surface biofunctionalization using microalgae-derived biomolecules.

S34 – O4

Dynamic perfusion enhances vascular network formation in human platelet lysate–derived hydrogels

Militão L.[1], Rufino A[2], Mano J.[1], Custódio C.[1,2]
[1]Dept. of Chemistry, CICECO – Aveiro Institute of Materials, University of Aveiro, Aveiro; [2]Metatissue, PCI - Creative Science Park Aveiro Region, Ílhavo, Portugal

Introduction

Vascularization remains a major challenge in tissue engineering, particularly when developing three-dimensional (3D) models free of animal-derived components. Human platelet lysate–derived hydrogels (hPLMA) provide a xeno-free, bioactive platform for supporting cell growth. Co-culture systems combining endothelial and stromal cells have shown potential to promote vascular organization in vitro, and integrating these systems into dynamic platforms, such as organ-on-a-chip (OOC), allows recreation of physiologically relevant microenvironments. This combination of human-derived biomaterials and microfluidic culture enables more accurate modeling of vascularization in 3D human tissues.

Aim

This study aimed to investigate the potential of hPLMA hydrogels as a xeno-free matrix for vascular network formation, comparing ASC–HUVEC co-cultures under static and dynamic conditions in a barrier-free OOC platform.

Materials and Methods

Adipose-derived stem cells (ASCs) and human umbilical vein endothelial cells (HUVECs) were encapsulated in 11% (w/v) hPLMA solution (Metatissue®) at a 1:1 ratio (total density 10×10^6 cells/mL) and subsequently photopolymerized. Hydrogels were maintained either under static culture conditions or in a barrier-free OOC for dynamic culture. Cell viability, morphology, and endothelial organization were assessed over time, including analysis of Live/Dead staining and immunostaining, with quantitative analysis of vascular networks.

Results

ASC–HUVEC co-cultures encapsulated in hPLMA hydrogels maintained high viability and supported endothelial organization in 3D culture. Under static conditions, cells progressively formed CD31-positive endothelial networks, with the emergence of interconnected structures over time. In contrast, dynamic culture within the organ-on-a-chip platform resulted in significantly larger vascular networks (Figure 1), characterized by increased network area and a higher number of branching junctions compared to static cultures (Figure 2). These results demonstrate that microfluidic perfusion enhances endothelial organization and vascular network complexity within the hPLMA matrix.

Conclusion

hPLMA hydrogels provide a fully human, xeno-free platform that supports endothelial network formation from stromal–endothelial co-cultures in 3D systems. Dynamic culture in an organ-on-a-chip platform enhances endothelial network formation compared to static conditions, highlighting the potential of combining human-derived biomaterials with microfluidic culture systems to develop physiologically relevant vascularized models for tissue engineering applications.

Acknowledgements

This work was supported by the European Research Council (ERC) under the European Union's Horizon 2020 research and innovation programme (ERC Advanced Grant 2019, Grant Agreement No. 883370 – REBORN project) and by the European Union's Horizon 2020 research and innovation programme under Grant Agreement No. 101080445 (MIti2 project).

Figures

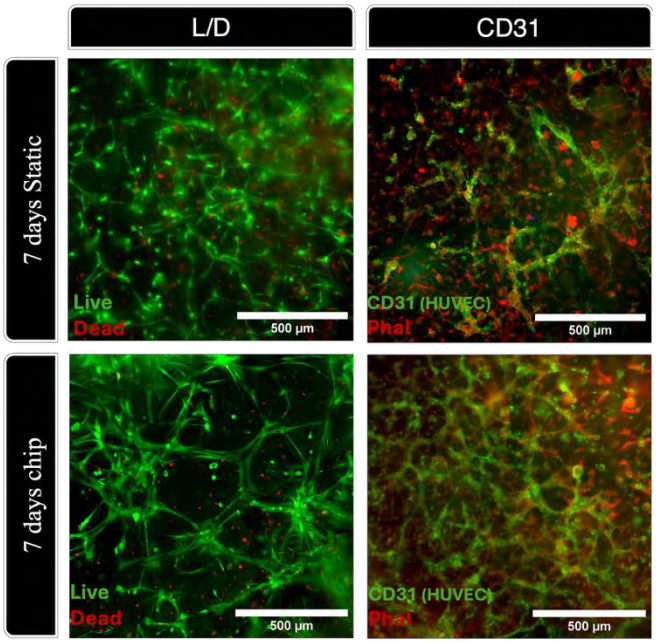

Figure 1. Live/Dead staining and immunostaining (CD31 and phalloidin) of ASC–HUVEC co-cultures encapsulated in 11% (w/v) hPLMA hydrogels after 7 days of culture under static and dynamic conditions.

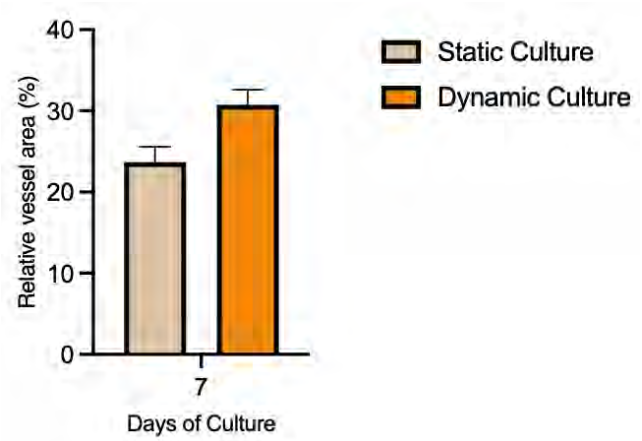

Figure 2. Quantification of relative vessel area in ASC–HUVEC co-cultures encapsulated in 11% (w/v) hPLMA hydrogels after 7 days of culture under static and dynamic conditions.

S35
Ethical by design designing biomaterials for replacement, reduction and refinement

S35 - K1
Engineering tuneable, animal-free, biomaterial scaffolds for 3D cell culture

Walsh-Korb Z.[1,2,3]
[1]School of Mechanical and Materials Engineering and Centre for Biomedical Engineering, University College Dublin, Ireland; [2]Conway Institute for Biomedical Sciences, University College Dublin, Ireland; [3]Dept. of Biomedical Engineering, University of Basel, Switzerland

Introduction
Interest in new approach methodologies (NAMs), like organoids and organ-on-chip models, in biomedical science to reduce animal model usage in line with the 3Rs, is growing. Yet, biomaterials used for cell and tissue culture are often animal-derived, e.g., basement membrane matrices are obtained from Engelbreth-Holm-Swarm mouse sarcomas. Increasing interest in NAMs, to reduce animal models, paradoxically runs the risk of increasing animal sacrifice for culture matrix production. Moreover, basement membrane struggles to replicate the complex mechanical cues of the native extracellular matrix, resulting in less physiologically relevant tissue models.

Aim.
By exploiting the unique molecular scale properties of mechano/chemo-responsive protein complexes as cross-links in macroscale hydrogels, we aim to develop a new class of mechanically dynamic hydrogels that could remodel, and be remodelled by, growing organoids, in a dynamic feedback loop. Producing proteins recombinantly and using biomass-derived polymers as scaffolds, means we can define hydrogel composition, enhance reproducibility and remove animal-derived components from the matrix, improving NAMs alignment with the 3Rs.

Results
Comparing nanoscale behaviours of protein complexes to macroscale properties of protein-functionalised hydrogels, highlights how properties and responsivity translate across length scales and dimensions. This is a valuable tool matrix refinement across tissue types. The hydrogels' micromechanical and structural properties are characterised using rheology, AFM-nanoindentation and microrheology and scanning electron microscopy (SEM) to gain insight into how protein-ligand interactions control viscoelastic properties locally and in bulk. We introduced organoids (from different sources (mouse vs human) and tissues) to study how environmentally responsive matrices interact with, or influence complex biological structures. Examining the morphology, structure and biological function of various organoid models using IF staining, proteomics and computed nanotomography, we have refined these animal-free hydrogels towards specific tissue properties, enhancing their physiological relevance.

Conclusion
Investigating the organoid-matrix feedback provides insight into the role of micromechanical cues in cell growth and differentiation. We are employing this knowledge to rationally refine and design responsive culture matrices with defined biochemical, viscoelastic and structural properties tuned to induce specific cellular outcomes in multi-cellular structures. In this way we hope to enhance the physiological accuracy of organoid models for biomedical science, while improving the 3Rs alignment of NAMs, and develop new insights into mechanical drivers of health and disease.

Acknowledgements
This project has been funded by a Horizon 2020 MSCA International Fellowship (CatchGel, 842043), a Swiss National Science Foundation Spark Grant (221019), University College Dublin and a UCD STEM Challenge Grant.

S35 – O1

From food to animal-free *in vitro* testing: Engineering photocrosslinkable gastric-dECM materials

Perin F.[1], Troncoso-Afonso L.[2], Muñoz A.M.M.[1], García-Astrain C.[1,2,3]
[1]POLYMAT, Applied Chemistry Dept., Faculty of Chemistry, University of the Basque Country UPV/EHU, Donostia−San Sebastián; [2]CIC biomaGUNE, Basque Research and Technology Alliance (BRTA), Donostia-San Sebastián; [3]IKERBASQUE - Basque Foundation for Science, Bilbao, Spain

Introduction

Regulatory bodies worldwide are reducing animal testing due to ethical concerns and poor translation of results to humans. Thus, increased research efforts have been placed in building more relevant in vitro models, particularly using three-dimensional cultures, like spheroids, organoids or biofabricated constructs. Advanced culturing techniques rely heavily on the use of solubilized basement membrane matrices, such as Matrigel® or Geltrex™, extracted and purified from Engelbreth-Holm-Swarm tumors grown in lab animals. These materials are costly, show batch variability, differ from native tissue composition, and paradoxically depend on the use of laboratory animals. As an alternative, the use of decellularized extra cellular matrix (dECM) is raising to overcome ethical issues while obtaining tissue-specific materials with superior biomimicry. Chemical modification of the dECM is recently emerging to fine tune the crosslinking and rheology of the obtained hydrogels, expanding the biofabrication possibilities to techniques such as light-based photocrosslinking.

Aim. The aim of this research is to obtain photocrosslinkable gastric-dECM for in vitro modelling of the stomach mucosa, by sourcing porcine stomachs from the food industry, as schematized in Figure 1.

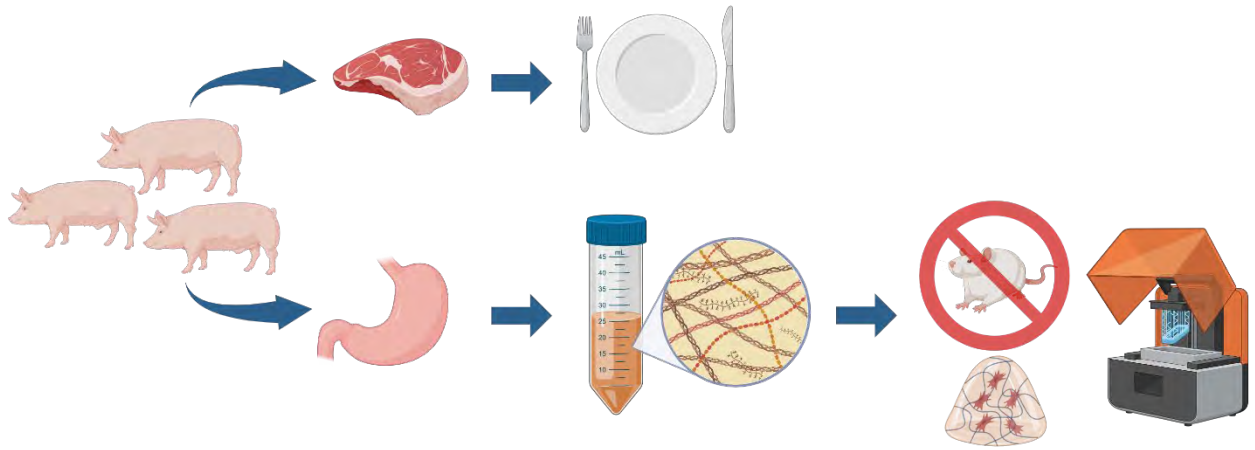

Figure 1 Scheme of the presented research to turn porcine stomachs from food industry into photo-crosslinkable dECM as alternative to solubilized basement membrane.

Materials and Methods

Porcine stomachs from three donors were obtained from a local butcher, decellularized to obtain dECM, characterized, and pooled to minimize batch-to-batch variability.The obtained matrix was reacted by acylation with anhydrides to produce photocrosslinkable derivatives: dECM-methacryloyl (dECM-MA), dECM-norbornene (dECM-NB), and dECM-pentanoate (dECM-PA). ^{1}H-NMR was used to identify the degree of functionalization of the reacted dECM. Proteomics was carried out to characterize the protein composition of the obtained materials, compared to the one of native tissues. The viscoelastic properties and crosslinking kinetics of the photo-dECM materials were investigated via photorheology. Moreover, the obtained materials were used as inks for SLA printing. Printing parameters were optimized with cell-free experiments, following a design of experiments approach (DOE). Finally, the photo-dECM hydrogels were subjected to preliminary biological testing with gastric cell lines (metabolic activity measurements and immunofluorescence staining).

Results
Porcine stomachs were sucessfully turned into photocrosslinkable-dECM derivatives, with tunable viscoelastic properties. Photo-dECM showed superior proteomic composition compared to commerical basement membrane matrix. Moreover, photo-dECM could be used to prepare inks for SLA printing and showed promising results in preliminary biological testing.

Conclusion
Photo-dECM derivatives showed promising preliminary results to produce relevant in vitro stomach models. In future experiments, further biological testing will be carried out to test the materials for culturing organoids and to bioprint stomach mucosa models.

Acknowledgements
Financial support was provided by the Spanish MICIU PID2024-162567OA-I00 and a 2025 Leonardo Grant for Scientific Research and Cultural Creation from the BBVA Foundation. We acknowledge support from the María de Maeztu Excellence Unit CEX2023-001303-M funded by MCIN/AEI/10.13039/501100011033.

S35 – O2

Multicellular bone tumour microenvironment platforms for high-content imaging analysis and drug screening

Krolinski A.[1,2,3], Morenc M.[2,3,4], Friedrich O.[1], Hutmacher D.W.[2,3,4], Bock N.[2,3,4]
[1]School of Biomedical Sciences, Faculty of Health, Queensland University of Technology (QUT) and Translation Research Institute (TRI), Brisbane, Australia, [2]Centre for Biomedical Technologies, QUT, Brisbane, Australia, [3]Friedrich-Alexander University of Erlangen–Nuremberg, Germany, [4]Max Planck Queensland Centre, Brisbane, Australia

Introduction

Tumour microenvironment (TME) components strongly influence cancer progression and therapeutic response, yet many preclinical drug-screening models fail to incorporate physiologically relevant extracellular matrix (ECM) interactions and spatially organised multicellular niches. Conventional high-throughput 2D systems lack cell–cell and cell–matrix interactions, while complex 3D models often remain incompatible with scalable screening workflows. To address these limitations, we developed a spatially organised, bioprinted multicellular tumour microenvironment platform compatible with high-content imaging and drug-screening applications. The system aims to model aspects of the bone metastatic niche by integrating cancer cells with osteoblast and adipocyte microenvironmental components.

Materials and Methods

Multicellular 3D constructs were generated in 96-well plates using drop-on-demand bioprinting (Rastrum™, Inventia Life Sciences) with biofunctionalised polyethylene glycol (PEG) hydrogels containing RGD, GFOGER and DYIGSR motifs. Constructs were organised into spatially defined compartments containing human breast (MCF-7) or prostate (LNCaP) cancer cells together with stromal microenvironment cells, including MC3T3-E1 osteoblasts and 3T3-L1 adipocytes using the 'Triple Matrix Model' (figure 1). Matrix stiffness was optimised within the physiological range (~0.7–3.0 kPa) to support cell viability, differentiation and tumour spheroid formation. Cell viability, metabolic activity and differentiation were monitored for up to 21 days using fluorescence-based live/dead assays and metabolic readouts. High-content imaging was performed using an Operetta CLS system, and image analysis was conducted through automated segmentation pipelines combining Ilastik pixel classification and Cellpose-SAM deep-learning algorithms.

Results

Bioprinted constructs demonstrated high post-printing cell viability (>85%) and sustained metabolic activity during long-term culture. Osteoblast and adipocyte monocultures remained viable for 21 days and maintained differentiation potential across the tested stiffness range, enabling selection of a lower-stiffness matrix (~1.1 kPa) that improved printing fidelity without compromising cell function. Cancer cells cultured in softer hydrogels (~0.7 kPa) self-assembled into multicellular spheroids and exhibited increasing metabolic activity over time. High-content imaging enabled longitudinal quantification of spheroid morphology and viability. Drug responses were assessed using multiplexed live-cell imaging assays including mitochondrial activity and membrane-impermeant SYTOX-based cell death staining, enabling real-time monitoring of treatment-induced cytotoxicity. Automated segmentation and image analysis generated quantitative single-cell and spheroid-level readouts suitable for high-content drug screening.

Conclusion

This study establishes a spatially organised, bioprinted multicellular TME platform that supports stromal differentiation, cancer spheroid formation and automated high-content imaging analysis. By integrating relevant bone-associated microenvironment cells within a scalable bioprinted architecture, the platform provides a physiomimetic system for investigating tumour–stroma interactions and developing imaging-based drug-screening strategies.

Acknowledgements

Funding from Max Planck Queensland Centre for Materials Science of Extracellular Matrices, Advance Queensland, Tour De cure, TRI and Australian Research Council is acknowledged.

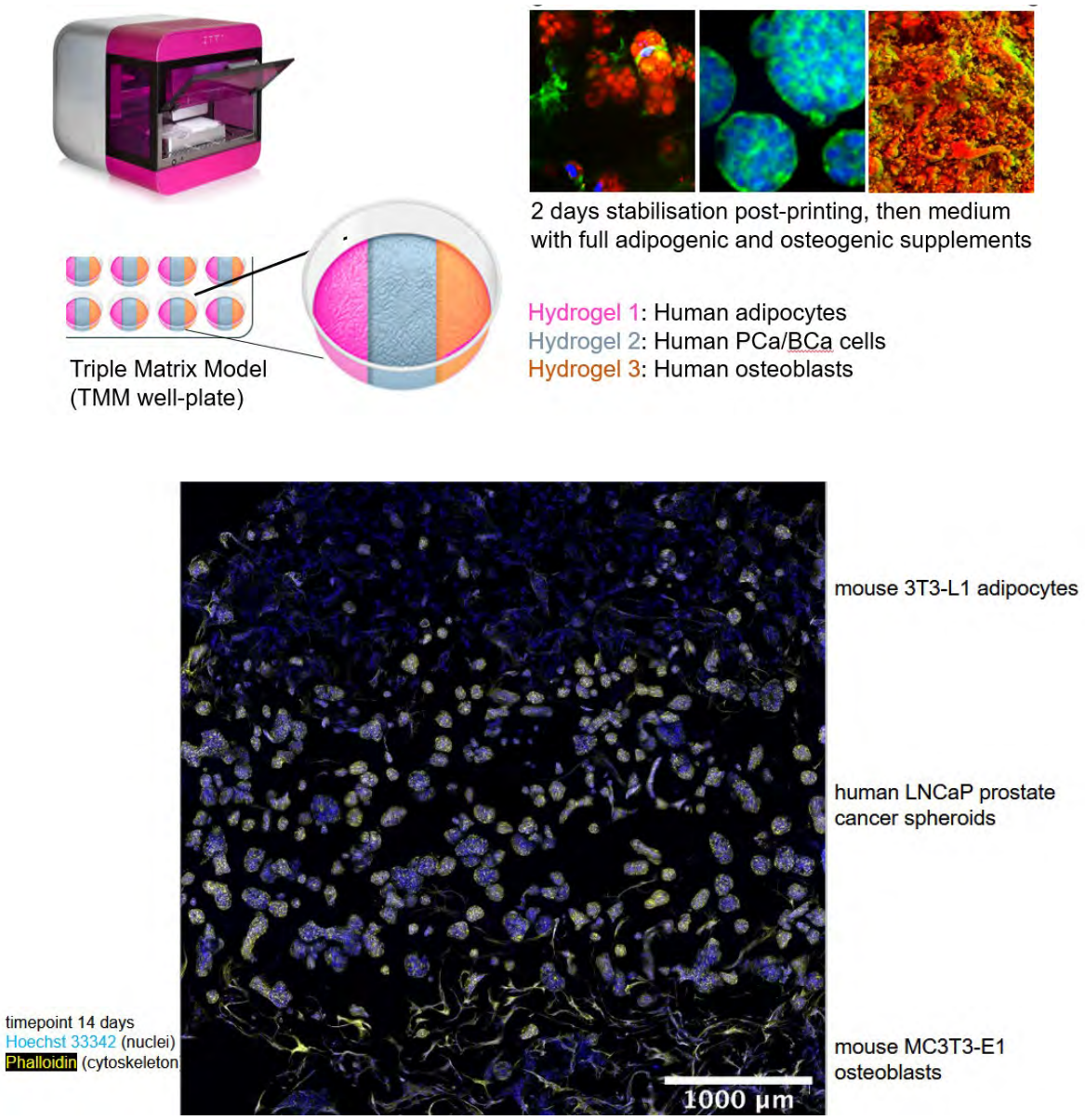

Figure 1. Concept of the human bone tumour microenvironment model using the 'Triple Matrix Model' (TMM), Rastrum Bioprinter and proof of concept of bioprinted TMM with human/mouse cell lines stained for nuclei and cytoskeleton.

S35 – O3

Investigating the effects of electrical stimulation on the motility and morphology of glioblastoma cells in vitro for improved engineered glioblastoma in vitro cell models

Duc D.[1], Lawson M.[1], Thompson D.[1]
[1]School of Pharmacy and Pharmaceutical Sciences, Cardiff University, Cardiff, UK

Aims and Objectives

Gliomas are high-prevalence primary brain tumours(42.8%)[1]. Glioblastomas (GBM) are the most prevalent and malignant subtype with a low survival(2 years)[1,2]. The discovery of novel treatments necessitates accurate and reproducible in vitro models due to challenges of reproducing the complexity of GBM. This study investigates the influence of electrical stimulation(ES) on GBM cell motility and morphology as potential technique to create improved GBM models in vitro.

Methods

The motility of U87-MG glioblastoma cells under electrical stimulation(ES) was assessed in vitro using a migration assay. Cells were stimulated using a biphasic rectangular waveform at 1V for 10milliseconds, 20Hz for 1 hour (Day 0) using C-Pace EM 100 (Ion Optix, Westwood, MA, United States). High-resolution brightfield microscopy was employed to investigate cell migration (wound closure) and cell morphology (orientation of cell extensions) at 24h and 48h after ES. Expression of cytoskeletal proteins under ES were evaluated using (1)live cell fluorescence imaging of actin and tubulin(CellLight™BacMam2.0), and (2)immunocytochemistry staining of F-actin, β3-tubulin, vimentin and nestin. Trypan blue assay (TBA) was further used to assess cytotoxicity after ES.

Results

Analysis of U87-MG cells revealed positive cell migration under ES with a wound closure of 74.2% from Day0 to Day2(one-way ANOVA; Tukey multiple comparisons,$p<0.001$). No statistical difference in wound closure was obtained in comparison with no electrical stimulation(one-way ANOVA,$p>0.05$). However, image analysis of orientation of the glioblastoma cell extensions revealed a preferential orientation towards the positive electrode, indicating an effect of ES on cell morphology. Assessment of cytoskeletal proteins expression via fluorescence microscopy further showed topographical cytoskeletal protein expression (e.g. actin and tubulin) under ES. No significant cell cytotoxicity was detected under ES (TBA).

Conclusion

This work showed that ES can influence glioblastoma cells morphology in vitro by potentially affecting cytoskeletal protein expression[2]. This supports further exploration of ES as viable tool for engineering reproducible glioma models in vitro.

Acknowledgement

We thank the Wellcome Trust (315564/Z/24/Z) for financial support and Dr Ewan Fowler for the ES equipment.

References

1. Eur J Med Res(2023);doi.org/10.1186/s40001-023-01011-y
2. Oncotarget(2016)doi:10.18632/oncotarget.11372.

S35 – O4

Pulsed electromagnetic fields (PEMF) reduce inflammation and immune cell recruitment in an in vitro osteoarthritis model

Ferla F.[1], Scalia A.C.[1], Cochis A.[1], Rimondini L.[1]
[1]Dept. of Health Sciences, Center for Translational Research on Autoimmune and Allergic, Disease - CAAD, Università Del Piemonte Orientale (UPO), 28100 Novara, Italy

Introduction

Osteoarthritis (OA) is a chronic degenerative joint disease characterized by cartilage breakdown, synovial inflammation, and progressive loss of function. Pro-inflammatory cytokines such as IL-1β and TNF-α drive the catabolic phenotype of resident cells, promoting matrix degradation and immune cells recruitment. Pulsed electromagnetic fields (PEMF) have emerged as a promising non-invasive approach to modulate inflammation; however, its mechanisms remain unclear.[1,2]

This study aimed to establish an *in vitro* OA-like inflammatory model using human bone marrow-derived mesenchymal stem cells (hBMSCs) and to investigate whether PEMF can modulate inflammatory signaling and functionally regulate immune cell recruitment.

Materials and Methods

hBMSCs (clone Y201) were exposed to a pro-inflammatory environment induced by IL-1β (10 ng/ml), TNFα (20 ng/ml), or their combination. After 24 hours, cells were stimulated with PEMF (1.5 mT, 75 Hz) for 2, 4, or 8 hours using devices provided by IGEA Clinical Biophysics. The inflammatory response was assessed by qRT-PCR analyzing the expression of pro- and anti-inflammatory cytokine.

To evaluate immune cell recruitment, peripheral blood mononuclear cells (PBMCs) were used in a transwell migration assay. PBMCs were seeded in the upper chamber (pore size 0.8 µm), while inflamed hBMSCs were cultured in the lower chamber. Migrated PBMCs were stained with May-Grünwald-Giemsa method.

To assess the potential protective role of PEMF on chondrocyte-like cells, hBMSCs were differentiated toward the chondrogenic lineage for 21 days, exposed to inflammatory cytokines, and stimulated with PEMF for three consecutive days (1 hour/day).

Results

Inflammatory stimulation upregulated pro-inflammatory cytokines (IL-1β, TNFα) and mediators (COX2, CXCL8). PEMF stimulation reduced their expression while increasing the anti-inflammatory cytokine IL-10. Among the tested conditions, the combination of cytokines showed the strongest effect and was selected as the optimal experimental condition.(Fig.1A) Transwell assays demonstrated that cytokine-stimulated hBMSCs significantly increased PBMCs migration, whereas PEMF treatment reduced immune cell recruitment, consistent with reduced expression of chemotactic mediators CXCL8 (Fig.1B). During chondrogenic differentiation under inflammatory conditions, PEMF reduced pro-inflammatory markers while increasing anti-inflammatory mediators (IL-10, TSG6), indicating that its immunomodulatory effects are maintained also in chondrocyte-like cells. (Fig.2)

Conclusion

PEMF stimulation effectively modulates inflammation in hBMSCs exposed to OA-like conditions, reducing pro-inflammatory mediators and immune cells recruitment, while increasing anti-inflammatory signaling. Importantly, these effects are preserved during chondrogenic differentiation, suggesting a potential protective role of PEMF in cartilage-like cells under inflammatory stress. These findings support PEMF as a promising non-invasive strategy to control inflammation in osteoarthritic environments and to potentially improve cartilage repair outcomes.

References

[1]Charlier E, et al. Chondrocyte dedifferentiation and osteoarthritis (OA). Biochem Pharmacol. 2019 Jul.
[2]Ross CL, et al. The Use of Pulsed Electromagnetic Field to Modulate Inflammation and Improve Tissue Regeneration: A Review. Bioelectricity. 2019 Dec 1.

Figure 1:Gene expression of pro-inflammatory genes IL-1β and TNF-α, under inflammatory conditions, with or without PEMF stimulation. All results were normalized with respect to control. Data are expressed as mean ± SD.

Figure 1:Gene expression of pro-inflammatory genes IL-1β and TNF-α, under inflammatory conditions, with or without PEMF stimulation. All results were normalized with respect to control. Data are expressed as mean ± SD.

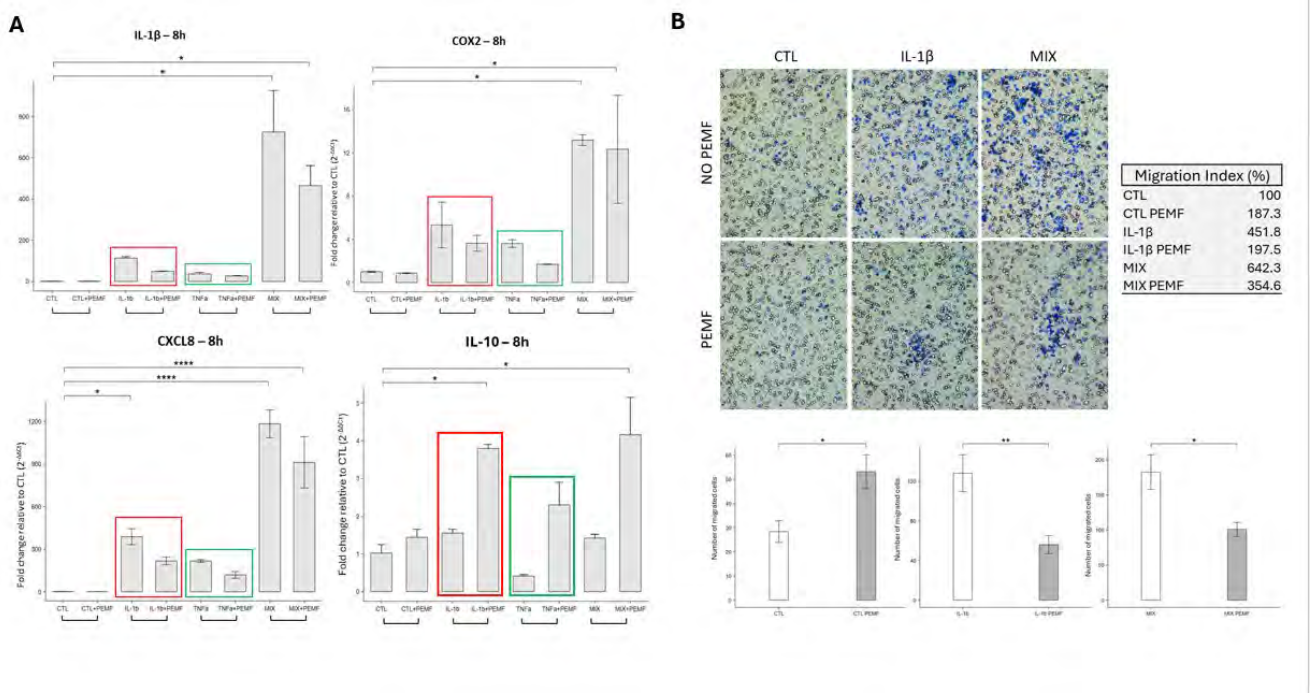

Figure 1

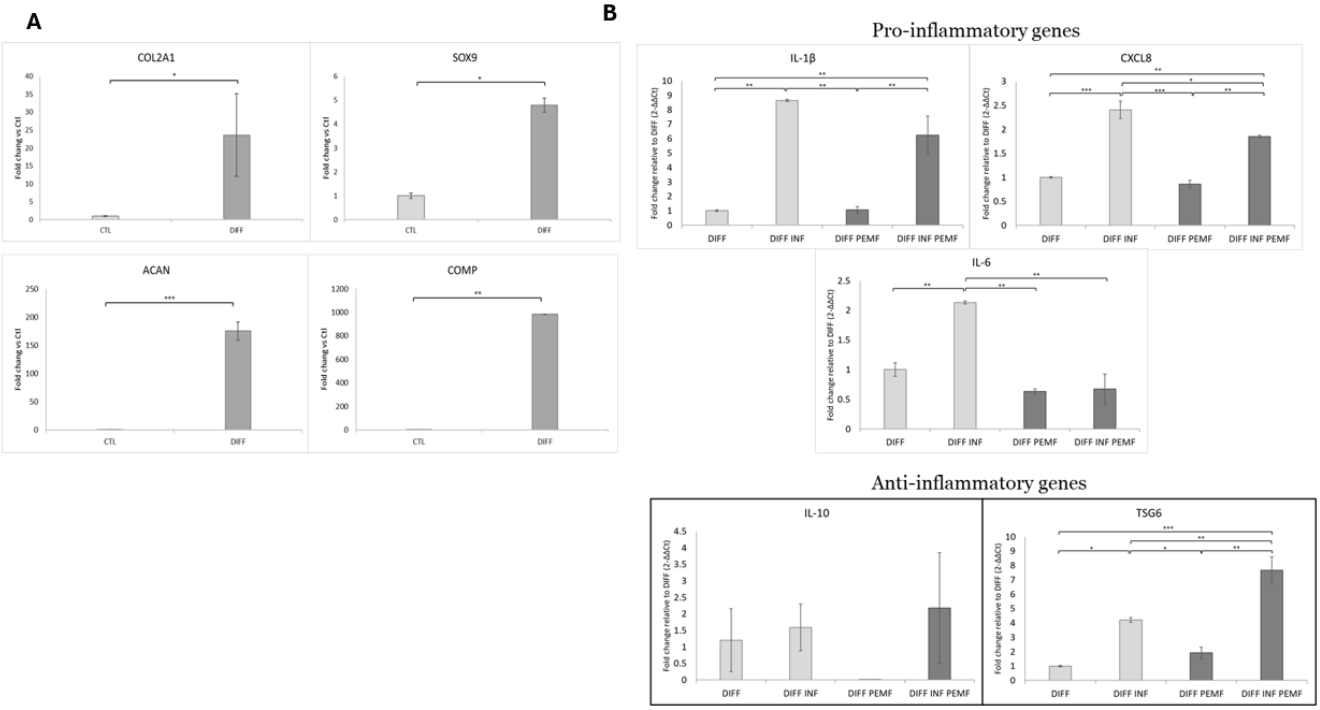

Figure 2

S35 – O5

Evolving strategies in organ-on-a-chip technologies enabled by human-derived biomaterials integration

Monteiro Cátia F.[1], Deus Inês A.[1], Martins Elisa A.G.[1], Ferreira Rita S.[1], Pereira Eva F.[1], Custódio Catarina A.[1], Mano João F.[1]
[1]Chemistry Dept., CICECO – Aveiro Institute of Materials, University of Aveiro, Aveiro, Portugal

Introduction

Organ-on-chip (OoC) technologies have evolved from rigid microfluidic devices toward increasingly biomimetic systems in which materials, architecture, and perfusion recreate key physiological aspects. Biomaterials have transitioned from passive structural fillers to active design elements that dictate fluid, cell, and microenvironmental signaling. Here, we present complementary strategies illustrating how human-derived biomaterials can be integrated into OoC platforms, expanding the design space of perfusable *in vitro* tissues.

Materials and Methods

Human platelet lysate (hPLMA) hydrogels were integrated into predefined PDMS microchannels to microengineer tumor-on-a-chip model. Low- and high-metastatic tumor spheroid were co-cultured with MSCs and a doxorubicin testing was performed. Beyond this configuration, we combined OoC with 3D bioprinting to engineer perfusable channels within photocrosslinkable human ECM proteins. Two strategies were explored: (i) sacrificial printing of Pluronic in a granular hydrogel bath, followed by ink removal and endothelialization, and (ii) printing of a macromolecular crowder solution into hPLMA-rich bath to induce interfacial protein precipitation for lumen creation. In parallel, in-gel perfusion was achieved exploring human amniotic membrane cryogels with highly interconnected macroporous networks. Both randomly and aligned pores were created into cryogels, where endothelial and stem cells were cultured under osteogenic differentiation conditions.

Results

Aligned with the most common strategy, hPLMA hydrogels were successfully incorporated into conventional PDMS OoC devices without changing classical fabrication workflows. This configuration enabled a dynamic tumor-stem cell crosstalk, supporting the study of the invasiveness capacity of tumor spheroids exhibiting distinct metastatic ability, while capturing the early metastatic invasion and drug response. (Fig.1A)
The combination of 3D bioprinting with OoC demonstrated that sacrificial Pluronic F-127 printing into a human ECM-based granular hydrogel bath produced stable channels that could be endothelialized. (Fig.1Bi) In a more innovative strategy, macromolecular crowding-based printing in an hPLMA-rich bath generated perfusable lumens while simultaneously creating a basement-membrane-like interface via interfacial protein precipitation that allowed cells to adhere. (Fig.1Bii)
Shifting to macroporous biomaterials, amniotic membrane cryogels enabled fluid transport mimicking interstitial flow. Here, randomly porous architectures supported diffusion-dominated transport, whereas aligned pores promoted directional flow. When integrated into a perfused device, these cryogels supported the osteogenic differentiation of co-cultured endothelial and stem cells. (Fig.1C)

Conclusion

Collectively, these strategies illustrate how biomaterials can progressively assume structural, functional, and fluidic roles within OoC systems, enabling new levels of physiological relevance, design freedom, and translational potential.

Acknowledgements

This work was supported by CICECO, UID/50011/2025&LA/P/0006/2020, FCT/MCTES (PIDDAC); the ERC-AdG No.883370 (REBORN); and the HORIZON-RIA grant ORTHO-ALLO-UNION (no.101137464).

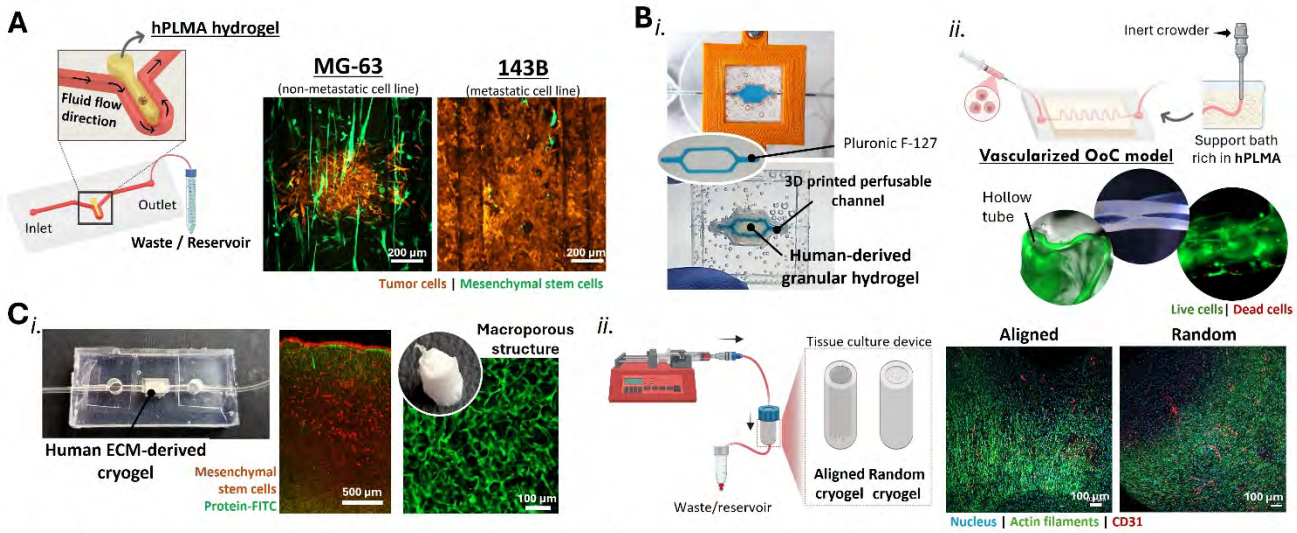

Figure 1. Integrating human-derived biomaterials into organ-on-a-chip platforms. (A) Tumor-on-a-chip model incorporating hPLMA hydrogel to demonstrate the different metastatic ability of tumor cells. **(B)** Printing perfusable channels into **(i)** a human protein-derived granular hydrogel using a sacrificial ink or **(ii)** a support bath rich in hPLMA using an inert macromolecular crowder. **(C)** In-chip human ECM-derived cryogels with **(i)** random and **(ii)** aligned macroporous, allowing fluid perfusion and cell infiltration for osteogenic differentiation purposes.

S35 – O6

Integrating microfluidics and layer-by-layer assembly for the development of scalable RNAi nanocarriers targeting PTSD

Mares-Bou S.[1], Michavila-Gil R.[1], Agramunt-Solaz L.[1], Guinart-Estelles D.[1], Rodenas-Rochina J.[1], Gallego-Ferrer G.[1,2], Giron-Hernandez J.[1,2], Gentile P.[1,2]
[1]Center for Biomaterials and Tissue Engineering, Universitat Politecnica de Valencia (CBIT-UPV); [2]Biomedical Research Networking Centre on Bioengineering, Biomaterials and Nanomedicine (CIBER-BBN), Carlos III Health Institute, Valencia, Spain

Introduction

The development of nanocarrier platforms capable of efficiently delivering RNA interference (RNAi) molecules represents a promising strategy for precision therapeutics in neuropsychiatric disorders such as post-traumatic stress disorder (PTSD), a debilitating condition characterized by dysregulated neuronal signaling and neuroinflammation, for which conventional often show limited efficacy or tolerability[1,2].

Aim

The aim of this work was to develop and characterize a scalable nanocarrier platform for efficient delivery of therapeutic RNAi molecules targeting PTSD. Specifically, a polyplex core composed of chitosan and PLGA encapsulating RNAi was designed and coated via layer-by-layer (LbL) assembly to obtain RNAi@LbL-polyplex nanocarriers with tunable physicochemical properties and controlled RNAi release.

Materials and Methods

The nanocarrier design was adapted to RNAi payload and number of LbL layers to achieve tunable release kinetics. The therapeutic RNAi molecules included (1) siRNA-PPP6C, targeting the regulation of the neuronal potassium channel Kv3.2[1], and (2) miRNA-511, involved in the transcriptional regulation of FKBP5 and inflammatory signaling pathways relevant to PTSD[2]. Polyplex core production was optimized using COMSOL Multiphysics® to model microfluidic mixing and nanoparticle formation, comparing a commercial microchip and an improved in-house design. Experimental validation enabled reproducible control of size, surface charge, and yield, allowing scalable and automated synthesis. Surface properties were tuned by LbL assembly using alternating pectin/chitosan bilayers, while tangential flow filtration (TFF) was integrated during deposition to remove excess polyelectrolytes and improve scalability[3].

Results

Physico-chemical characterization by DLS confirmed controlled nanoscale size distribution (200-400 nm) and tunable ζ-potential (core/pectin-layer/chitosan-layer: 25.2±1.8 / -38.6±0.4 / 47.8±1.2 mV), while fluorescence-based assays demonstrated high encapsulation efficiencies of RNAi (85-98 %). Analysis under TEM revealed uniform morphology and well-defined multilayer coatings (**Fig.1**). Release studies in PBS (37 °C) showed sustained release of RNAi dependent on number of layers. Finally, *in vitro* evaluation in SH-SY5Y neuroblastoma cell line differentiated into neurons (retinoic acid and BDNF protocol, qPCR verification) demonstrated excellent cytocompatibility of RNAi@LbL-polyplex systems. In addition, dexamethasone at different doses was used as 2D *in vitro* pharmacological stressors to reproduce PTSD molecular alterations, and therapeutic activity of RNAi@LbL-polyplex was analyzed by qPCR.

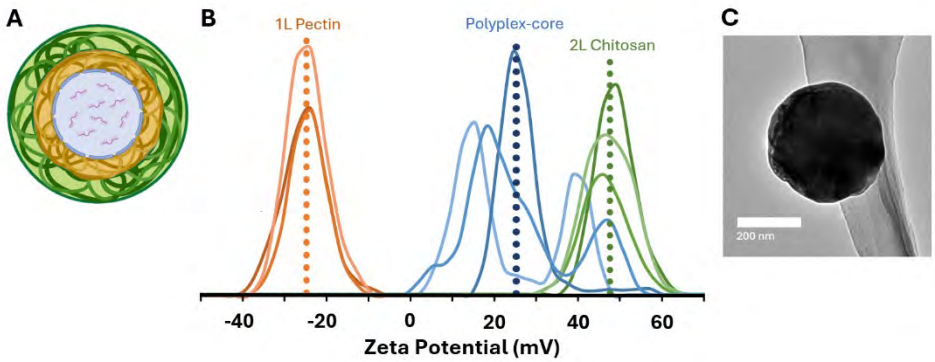

Fig.1. Schematic illustration of RNAi@LbL-polyplex (**A**); ζ-potential of core, 1st layer (pectin), and 2nd layer (chitosan) (**B**); and its TEM image (**C**).

Conclusion

RNAi@LbL-polyplex enables scalable production of multilayer nanocarriers with tunable physicochemical properties and controlled RNAi release, while integration of microfluidic synthesis with TFF improves manufacturing reproducibility and scalability, highlighting its potential as a platform for RNAi-based therapeutic approaches targeting PTSD.

Acknowledgements

Mares-Bou S. and Gentile P. acknowledge support from ATRAE program (ATR2023-145518).

References

[1]Xiao H., Xi K., Wang K., Zhou Y., Dong B., Xie J., et al. Restoring the function of thalamocortical circuit through correcting thalamic Kv3.2 channelopathy normalizes fear extinction impairments in a PTSD mouse model. *Advanced Science* 2024; 11; 2305939.
[2]Zheng D., Sabbagh J.J., Blair L.J., Darling A.L., Wen X., Dickey C.A. MicroRNA-511 binds to FKBP5 mRNA, which encodes a chaperone protein, and regulates neuronal differentiation. *Journal of Biological Chemistry* 2016; 291; 17897–17906.
[3]Correa S., Choi K.Y., Dreaden E.C., Renggli K., Shi A., Gu L., et al. Highly scalable, closed-loop synthesis of drug-loaded, layer-by-layer nanoparticles. *Advanced Functional Materials* 2016; 26; 991–1003.

S35 – O7
PDAC-on-hand – A microfluidic device for drug screening

Bortolameazzi M.[1], Peletto M.[1], Rubicondo M.[1], Mattu C.[1], Ciardelli G.[1], Sgarminato V.[1], Tonda-Turo C.[1]
[1]BioInside Lab, Dept. of Mechanical and Aerospace Engineering, Politecnico of Turin, Italy

Introduction

Pancreatic ductal adenocarcinoma (PDAC) is one of the most aggressive malignancies, largely due to late diagnosis and the limited effectiveness of current therapies. A key factor in PDAC progression and drug resistance is the dense desmoplastic tumor microenvironment, where stromal cells and extracellular matrix (ECM) components limit drug penetration. Biomimetic microfluidic platforms represent a promising strategy to reproduce tumor-stroma interactions under physiologically relevant conditions.

Materials and Methods

Two complementary *in vitro* models were developed to reproduce PDAC tumor-stroma interactions. A modified transwell system was established by replacing the commercial membrane with an electrospun polycaprolactone/gelatin (PCL/Gel) nanofibrous membrane acting as a biomimetic substrate for tumor cells. Pancreatic cancer cells were seeded on the basal side of the membrane, while fibroblasts were embedded in a type I collagen hydrogel in the apical compartment, reproducing the stromal barrier. This model was used to investigate drug delivery across the stromal barrier using both free drugs and hybrid lipid-polymeric nanoparticles (hNPs), administered in the apical compartment and diffusing toward the tumor cells.
In parallel, a PDMS-based PDAC-on-chip device was designed in Fusion 360 and fabricated by replica molding. The platform consists of three compartments: a lateral channel for medium perfusion, a central fibroblast-laden collagen channel mimicking the stroma, and a tumor chamber where PDAC cells are cultured on the electrospun membrane positioned by a holder (Figure 1).

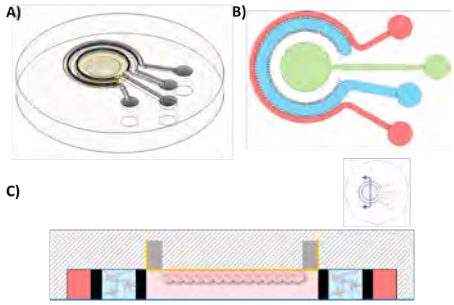

Figure 2: PDAC-on-chip design generated in Fusion 360. A) **Three compartments arrangement of the device.** B) **Top view of the PDAC-on-chip layout highlighting the medium channel (red), stromal channel (blue), and central chamber for PDAC cell culture (green).** C) **Cross-sectional view of the PDAC-on-chip.**

Results

The modified transwell model confirmed the barrier effect of the fibroblast-laden collagen hydrogel, which reduced molecular diffusion compared with the 2D configuration. Treatment with hNPs showed that nanoparticles were able to cross the stromal compartment and reach PDAC cells cultured on the basal side of the membrane. Flow cytometry analysis revealed significantly higher hNP internalization in PDAC cells than in fibroblasts, indicating preferential accumulation in the tumor compartment.
In parallel, optimization of the fabrication process enabled the production of the first PDAC-on-chip prototypes integrating the electrospun nanofibrous membrane and the collagen-based stromal hydrogel. The microfluidic architecture allows controlled molecular exchange between compartments and direct visualization of tumor–stroma interactions (Figure 2).

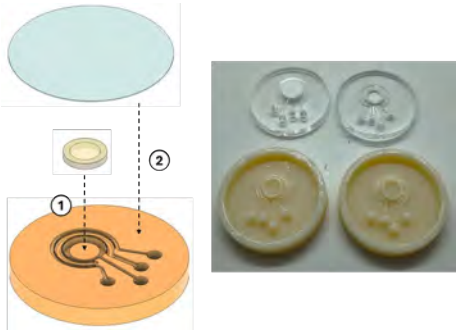

Figure 3: assembly scheme: (1) insertion of the electrospun PCL/Gel membrane holder into its housing; (2) device sealing by plasma bonding. Representative photos of the molds and of the first assembled PDAC-on-chip prototypes are shown on the right.

Conclusion

The proposed PDAC-on-chip integrates biomimetic materials and microfluidics to reproduce key features of the pancreatic tumor microenvironment, providing a platform to study tumor–stroma interactions and nanoparticle-based therapies.

Acknowledgements

This project was partially supported by Fondazione Compagnia di San Paolo - Trapezio Call for Proposals (Target 1), project ERATOSTHENES.

S36
Extracellular vesicles and biomaterials new horizons for targeted therapies

S36 – K1
Engineered extracellular vesicles: Advancing next-generation theranostics tools in regenerative medicine

Jesus C.[1,2], Mimoso S.[1,2,3], Barão M.[1,2], Deus C.[1,2,3], Blanco-Elices C.[1,2,3], Carvalho D.[1,2,3], Serra-Caetano J.[4], Banerjee A.[1,2], Jones J,[2], Ferreira L.[1,2,4], Fernandes H.[1,2,3,5]
[1]CIBB – Center for Innovative Biomedicine and Biotechnology, Rua Larga, University of Coimbra, 3004-504 Coimbra; [2]CNC – Center of Neuroscience and Cell Biology, Rua Larga, University of Coimbra, 3004-504 Coimbra; [3]MIA – Portugal – Multidisciplinary Institute of Ageing, University of Coimbra, 3004-504 Coimbra; [4]Faculty of Medicine, University of Coimbra, 3030-789 Coimbra; [5]IIIUC – Institute of Interdisciplinary Research, University of Coimbra, 3030-789 Coimbra, Portugal

Introduction
Extracellular vesicles (EVs) are key mediators of intercellular communication, encapsulating and delivering bioactive cargos to recipient cells. EVs can also be used as a fingerprint of the cell´s proteome, metabolome and transcriptome making them an appealing source for biomarker discovery. Given their intrinsic biocompatibility and ability to cross biological membranes, EVs have been used as a highly efficient drug delivery system in several pathological contexts. In their native form, however, EV therapeutic efficacy is often limited.

Aim
Explore bioengineering tools to enhance EV bioactivity and/or targeting potential.

Materials and Methods
EVs isolated from multiple sources were isolated and characterized according to ISEV guidelines. High-content screening was used to identify miRNAs with biological activity in multiple contexts, particularly metabolic and ischemic-related diseases. The most promising miRNAs identified in the assays were loaded into EVs using various strategies (e.g., electroporation, detergent-based methods, cholesterol conjugation and commercial reagents). Cell-based assays were used to study the internalization mechanism(s) and bioactivity of miRNA-engineered EVs. In vivo assays were used to study the biodistribution of miRNA- or scramble-engineered EVs and their functional impact was analysed in in vivo disease models.

Results
We have shown that miRNA-engineered EVs can improve wound healing in diabetic mice, ameliorate motor deficits in a Parkinson disease mouse model and rescue glucolipotoxicity-induced cell beta cell death in the context of diabetes/obesity. Furthermore, we utilized EV-miRNA signatures from human samples for risk stratification in the context of diabetes, with preliminary results showing that exosomal miRNA signatures hold potential to identify patients at risk of developing diabetes and/or assess the efficacy of antidiabetic therapies.

Conclusion
These results establish the use of engineered EVs as a powerful and versatile platform for disease management from diagnosis to therapy.

Acknowledgements
This work was co-funded by the European Union's Horizon 2020 research and innovation program under Grant Agreement No. 857524, European Regional Development Fund (FEDER) through the Innovation and Digital Transition Thematic Program PORTUGAL COMPETE2030-FEDER-00670600, operation No. 15628 & 15621, "targeted anti-senescence formulations (2022.07615.PTDC) and "Engineering extracellular vesicles to permeabilize the blood-brain barrier (2023.15026.PEX), European Regional Development Fund (ERDF) through the Centro 2023 Regional Operational Programme under project CENTRO2030-FEDER-02360400 and EU Recovery and Resilience Facility and Portuguese national funds via FCT – Fundação para a Ciência e a Tecnologia, under projects, LA/P/0058/2020, UID/PRR/4539/2025 and UID/04539/2025.

S36 – O1

Extracellular vesicle-based senotherapeutics for targeting vascular aging

Guímaro C.[1], Sá Ferreira R.[1], Barão M.[1], Padrão J.[1], Castro R.[1], Panek J.[2], Fielder E.[2], Huete Acevedo J.[3], Viktor Korolchuk[2], Borras C.[3], R. Pitrez P.[1,4], Ferreira L.[1,4]
[1]Center for Neuroscience and Cell Biology, Univeristy of Coimbra, Portugal; [2]Biosciences Institute, Newcastle University, UK; [3]Faculty of Medicine. University of Valencia, Spain; [4]Faculty of Medicine, University of Coimbra, Portugal

Introduction

Vascular aging is driven by the accumulation of senescent endothelial cells (ECs), which exhibit irreversible cell-cycle arrest and a pro-inflammatory secretory phenotype (SASP) [1]. These cells act as the underlying foundation for systemic physiological decline and fuels progression of cardiovascular diseases (CVDs) [2], a critical challenge to global health. Current senotherapeutics often lack cell-type specificity, leading to off-target risks.

Aim. We propose biomimetic extracellular vesicles (EVs) designed to selectively modulate senescent ECs to improve vascular dysfunction [3].

Materials and Methods

Senescence was induced in human coronary artery endothelial cells (HCAECs) and mouse aortic endothelial cells (MAECs) via γ-irradiation. High-throughput screening of a bioactive library identified candidates that selectively modulate senescent ECs without affecting healthy cell viability. Top candidates were encapsulated into biomimetic EVs for delivery. Formulations were characterised for size, concentration, polydispersity and morphology using nanoparticle tracking analysis (NTA), dynamic light scattering (DLS) and cryo-EM. Mechanistic insights were performed via RNA-Seq, PCR and immunocytochemistry. *In vivo* efficacy was evaluated in aged C57BL/6 mice through systemic administration, with subsequent functional tests.

Results

In HCAECs and MAECs, EVs reversed senescent markers, evidenced by a robust decrease in p21, p16, and SA-β-gal (40%) and a 3-fold increase in Ki-67 proliferation. SASP profiling revealed a rescue of factors normally downregulated in senescence (PDGF-AA, RANTES, IL-15) and a downregulation of pro-inflammatory factors (G-CSF, GM-CSF, IL-1α, IL-8). Mitochondrial health was restored through the rescue of mitophagy events, reduced MitoSox levels (50%) and aged mitochondrial network morphology. A specific pathway was identified by RNA-Seq as the main target of our treatment. Immunofluorescence (25%) and PCR (50%) confirmed that the significant upregulation of a protein in senescence was reversed during treatment. Systemic administration in aged mice stabilised body weight and improved frailty and pre-frailty scores *in vivo*. Furthermore, we have also confirmed that our treatment reduced pro-inflammatory lipid mediators produced by the targeted pathway, both *in vitro* (40%) and *in vivo* (30%).

Conclusion

These findings demonstrate that EVs delivering a bioactive therapeutic can effectively target and modulate senescent ECs. This novel senotherapeutic suppressed a specific pathway in ECs and rescued mitochondrial mitophagy. This approach offers a targeted, biomimetic strategy that avoids off-target risks of current senotherapeutics, creating new avenues for treating CVDs.

Acknowledgements

Supported by FCT (2022.07615.PTDC, TREATABLE), EC (952266, RESETageing), and co-funded by EU Recovery & Resilience Facility and Portuguese national funds via FCT under projects LA/P/0058/2020, UID/PRR/04539/2025, and UID/04539/2025 [DOI: 10.54499/LA/P/0058/2020].

References

1. J., G., *Aging and aging-related diseases: from molecular mechanisms to interventions and treatments.* Signal Transduction and Targeted Therapy, 2022.
2. C., L.-O., *Hallmarks of aging: An expanding universe.* Cell, 2023.
3. P., P., *Vulnerability of progeroid smooth muscle cells to biomechanical forces is mediated by MMP13.* Nature Communications, 2020.

S36 – O2

Room-temperature radiolabeling of small extracellular vesicles with $^{89}Zr^{4+}$ for monitoring transient blood-brain barrier opening

Banerjee A.[1,3], Hrynchak I.[2,4,5], Jesus C.[1,3], Sereno J[2,4], Marques T.M.[6], Girao H.[6], Ferreira M.J.[2,6,7], Abrunhosa A. [2,4,5], Ferreira L.[1,3]

[1]Faculty of Medicine, University of Coimbra, 3004-504 Coimbra; [2]ICNAS – Institute for Nuclear Sciences Applied to Health; University of Coimbra, Coimbra-3000-548; [3]CNC-Center for Neurosciences and Cell Biology, University of Coimbra, 3004-517 Coimbra; [4]Coimbra Institute for Biomedical Imaging and Translational Research (CIBIT), University of Coimbra, Coimbra-3000-548; [5]Institute for Nuclear Sciences Applied to Health (ICNAS Pharma), Polo das Ciências da Saúde, University of Coimbra, 3000-548 Coimbra; [6]Center for Innovative Biomedicine and Biotechnology, University of Coimbra, 3004–504 Coimbra; [7]Cardiology Dept., Centro Hospitalar e Universitário de Coimbra, Praceta Prof. Mota Pinto, 3000-075, Coimbra, Portugal

Introduction

Drug delivery to the brain is challenging due to the restrict permeability of the blood brain barrier(BBB). Recent studies indicate that BBB permeability increases over time during physiological aging likely due to factors (including extracellular vesicles (EVs)) that exist in the bloodstream. Therefore, inspiration can be taken from aging to develop new strategies for the transient opening of the BBB for drug delivery to the brain. This growing interest in sEV-based interventions underscores the importance of developing reliable methods for long-term in vivo tracking, where positron emission tomography (PET) plays a key role. Zirconium-89 ($^{89}Zr^{4+}$) is particularly advantageous for PET due to its long physical half-life of 78.4 hours, low positron emission energy (395.5 keV), and cost-effective production. Conventionally, deferoxamine (DFO) is used as the chelator for $^{89}Zr^{4+}$, forming complexes rapidly at room temperature. However, several preclinical studies have reported instability, with $^{89}Zr^{4+}$dissociating from the DFO complex within an hour of administration. An alternative chelator, DOTA, yields more stable complexes but requires high temperatures (90 °C), making it less suitable for sEV labeling.

Results

Our objective was to develop a chelator for $^{89}Zr^{4+}$ that could form a stable complex at room temperature and be used in PET imaging. Our chelator successfully complexed $^{89}Zr^{4+}$within one hour at room temperature. Radiolabeling of sEVs was achieved through a two-step strategy: conjugating the chelator (L1) to the vesicles, followed by $^{89}Zr^{4+}$ incorporation. The resulting EV-L1-$^{89}Zr^{4+}$ construct demonstrated a radiochemical yield of approximately 60% and retained ~80% stability in plasma for up to seven days. Importantly, the labeling process preserved the structural integrity, surface protein profile, and RNA content of the vesicles. Finally, we successfully imaged EVs in mice after injecting EV-chelator-^{89}Zr intravenously and measured the bio-distribution of it in different organs including the different parts of the brain for a prolonged time.

Conclusion

This work introduces a robust and stable strategy for radiolabeling sEVs with $^{89}Zr^{4+}$, offering a powerful platform for non-invasive imaging. The approach holds promise for enhancing diagnostic capabilities and advancing regenerative medicine applications in crossing the BBB.

Acknowledgements

Project ‘LABEL’ (POCI-01-0247-FEDER-049268) under the Portugal 2020 program, FCT project reference TargetingHeart 2022.02803.PTDC and 2023.15026.PEX, Pizo4spine- grant agreement No 101098597 (European Union’s Horizon Europe research and innovation programme), Reborn- 101091852 (European Union or the European Health and Digital Executive Agency (HADEA)) Authors have no conflicts of interest to declare.

References

1. M. Tkach and C. Thery, *Cell*, 2016, **164**, 1226-1232.
2. J. P. Holland, V. Divilov, N. H. Bander, P. M. Smith-Jones, S. M. Larson and J. S. Lewis, *Journal of Nuclear* Medicine, 2010, 51, 1293-1300.
3. D. N. Pandya, N. Bhatt, H. Yuan, C. S. Day, B. M. Ehrmann, M. Wright, U. Bierbach and T. J. Wadas, Chemical science, 2017, 8, 2309-2314.
4. J. P. Holland, Y. Sheh and J. S. Lewis, Nuclear medicine and biology, 2009, 36, 729-739.

S36 – O3

TEM and AI-Based morphological profiling of extracellular vesicles and mitovesicles for ALS Diagnosis

Cansever Mutlu E.[1], Odabasi Bagci J.[2], Kaya O.[3], Aydin Turkoglu S.[4], Yildirim M.[5], Yazici O.C.[5], Hombrebueno J.R.[6], Ben-Nissan B.[7], Stamboulis A.[1]

[1]Biomaterials Research Group, School of Metallurgy and Materials, University of Birmingham, UK; [2]Programme of Neurosciences, Abant Izzet Baysal University, Bolu, Turkiye; [3]Dept.Biology, Abant Izzet Baysal University, Bolu, Turkiye; [4]Dept.Clinical Neurosciences, Faculty of Medicine, Abant Izzet Baysal University, Bolu, Turkiye; [5]Dept.Chemistry, Abant Izzet Baysal University, Bolu, Turkiye; [6]Institute of Inflammation and Ageing, University of Birmingham, Birmingham, UK; [6]Institute of Inflammation and Ageing, University of Birmingham, Birmingham, UK; [7]School of Life Sciences, University of Technology Sydney, P.O. Box 123, Broadway, NSW, 2007, Australia

Introduction

Extracellular vesicles (EVs) and mitovesicles carry critical biomarkers in neurodegenerative disorders such as amyotrophic lateral sclerosis (ALS). Conventional characterization methods fail to capture their structural heterogeneity and dynamic behaviour. In addition, there is not any disease specific TEM or Cryo-TEM marker in the biomaterial literature[1]. An appropriate biomarker design could be promising for early diagnosis of ALS and possibly prognosis. In this study, TEM imaging combined with AI-driven image analysis offers a novel approach to identify disease-specific morphological signatures and provide new perspective about biomaterials design[2].

Aim

The aim of this study is to develop novel TEM-based biomarkers by synthesizing peptide and non-peptide motifs that target cell-free mitovesicles in amyotrophic lateral sclerosis (ALS) for diagnostic applications.

Materials and Methods

EVs were isolated from cerebrospinal fluid (CSF) samples of ALS patients and polyneuropathy control subjects. A new oxadiazole-based non-peptide motif was synthesized, and molecular docking studies were performed to evaluate its interactions with mitochondrial proteins such as TIMM23[3]. Nanoparticle tracking analysis (NTA) was conducted, followed by incubation of exosomes with the oxadiazole derivative. Transmission electron microscopy (TEM) imaging was performed to visualize vesicular subtypes, followed by AI-based analysis of membrane thickness and geodesic diameter. Clustering algorithms categorized mitovesicles into distinct groups based on cristae integrity and membrane fragility. Comparative profiling was conducted to identify ALS-specific cell-free double-membrane patterns as study framework.

Results

TEM revealed significant heterogeneity among double membrane exosomes in ALS patients, including disrupted inner membranes and expanded subtypes absent in control samples. AI-assisted clustering was capable to identify three major groups with varying degrees of inner membrane heterogeneity just like cristae. These structural variations could be correlated with mitochondrial stress and vesicle remodelling, suggesting their potential as diagnostic markers. Additionally, motion profiling indicates that EVs function as subgroups dependent of size, opening new avenues for biomaterials integration considering motion profiling as a significant classification parameter that should be considered in the next MISEV classification guideline.

Conclusion

New peptide and non-peptide motifs combined with TEM and computational analysis provide a promising approach for extracellular vesicle characterization and enable the identification of disease-associated morphological signatures. These findings may contribute to the development of diagnostic strategies for rare diseases and support future biomaterial-based platforms for vesicle analysis. Future studies will aim to expand the sample size and integrate vesicle omics with dynamic motion profiling to provide a deeper understanding of vesicle heterogeneity in neurodegenerative diseases.

Acknowledgements

This work was supported by collaborative efforts between the Biomaterials Group at the University of Birmingham, College of Engineering and Physical Sciences and Abant Izzet Baysal University, School of Medicine and School of Pure and Applied Sciences. Abant Izet Baysal University supported this work with 2023-TRD-6.12.56-0006 AIBU-BAP founding.

References

1. Cansever Mutlu, E.; Kaya, M.; Küçük, I.; Ben-Nissan, B.; Stamboulis, A., Exosome structures supported by machine learning can be used as a promising diagnostic tool. *Materials* **2022,** *15* (22), 7967.
2. Mutlu, E. C.; Gkoutos, G. V.; Ben-Nissan, B.; Stamboulis, A., Applications and Future Trends of Extracellular Vesicles in Biomaterials Science and Engineering. In *Extracellular Vesicles-Applications and Therapeutic Potential*, IntechOpen: 2023.
3. Ahmed, H. I.; Yazıcı, O. C.; Abdullah, F. O.; Yildirim, M.; Ameen, B. A. H., Synthesis, in vitro and in silico anticancer evaluations of novel styryl 1, 3, 4-oxadiazole-sulfonamide hybrids for colorectal cancer. *Bioorganic & Medicinal Chemistry* **2025**, 118409.

S36 – O4

Engineered bone marrow stem cell-derived extracellular vesicles for bone repair and regeneration

Bochti E.A., Tsimbouri P.[1], Dalby M.J.[1], Berry C.C.[1]
[1]Centre for the Cellular Microenvironment (CeMi), University of Glasgow, Glasgow, Scotland, UK

Introduction

Bone is the second most transplanted tissue worldwide, with over 4 million procedures performed annually (1,2). Current treatments rely on autologous grafts, which are limited by donor site morbidity and availability, or bone graft substitutes that lack osteoinductive and osteoconductive capacity (3). Bone marrow-derived stromal cells (BMSCs) are widely used in bone tissue engineering due to their osteogenic potential, with emerging evidence suggesting their therapeutic effects are mediated in part through extracellular vesicles (EVs) (3,4). This study aims to develop a novel EV-based microenvironment by encapsulating osteogenically primed BMSC-derived EVs within hydrogel beads for localized, cell-free bone regeneration.

Materials and Methods

BMSCs were osteogenically primed for 28 days using (i) chemical induction (osteogenic media) or (ii) mechanical induction, via nanoscale vibrational stimulation named “nanokicking”. BMSC osteogenic differentiation was confirmed at gene, protein, and histological levels. BMSC-derived EVs were isolated during the early osteogenesis (days 7 and 14) and characterised by shape (TEM) size & concentration (NTA, TRPS, DLS, microBCA), and bioactive cargo (cytokines and metabolites). Their regenerative and angiogenic potential was assessed using wound healing and angiogenesis assays while their osteogenic-inducing potential was confirmed by incubating osteogenic-primed EVs with naive BMSCs. Gelatine-alginate hydrogel beads were generated using microfluidics and their biocompatibility was confirmed following BMSC encapsulation.

Results

Both chemical and mechanical stimulation successfully induced osteogenesis in BMSCs. Isolated EVs displayed characteristic size (60–250 nm), morphology, and surface markers (TSG101, ALIX, CD63, CD81, FLOT1). Osteogenically primed EVs exhibited enriched cargo associated with osteogenesis (osteopontin), angiogenesis (angiopoietin-1/2, VCAM-1), and regeneration (FGF-7, FGF-19, EMMPRIN) compared to negative control EVs. Functionally, these EVs enhanced wound healing in primary osteoblasts and promoted osteogenic differentiation in naïve BMSCs. Osteogenic EVs were successfully encapsulated within the biocompatible gelatin–alginate hydrogels while their osteogenic efficacy is currently under investigation.

Conclusion

Osteogenically primed EVs promote osteogenesis and exhibit pro-angiogenic and regenerative properties, supporting their potential for cell-free bone repair strategies. Notably, differences in cytokine and metabolite profiles were observed between mechanically and chemically primed EVs, with chemically induced EVs showing greater enrichment. Ongoing work will evaluate the osteogenic efficacy of EV-loaded hydrogel beads in naïve BMSCs.

Acknowledgements

I would like to express my gratitude to Medical Research Scotland (MRS) for funding my research project (Project Reference: PHD-50388-2021), my former EPO Sphere Bio, MVLS College at the University of Glasgow and a special thank my supervisors and colleagues from the CeMi group.

References

1. NHS Golden Jubilee (2024, January 25). “NHS Golden Jubilee Research Paper Exploring 3D bio-printing for bone regeneration gains international recognition”. Accessed: Jan. 25, 2024. [Online]. Available: https://www.nhsgoldenjubilee.co.uk/news/press-releases/press-releases-2024/nhs-golden-jubilee-research-paper-exploring-3d-bio-printing-bone-regeneration-gains-international-recognition#:~:text=Bone%20is%20the%20second%20most,annually%20to%20treat%20bone%20defects
2. Zhou X *et al*. Pharmaceutics 14-5: 1012, 2022
3. Iaquinta M R *et al.* Front. Cell Dev. Biol 7, 2019
4. Liu F *et al.* Front. Bioeng. Biotechnol. 11, 2023

S36 – O5

Engineering the next generation of biologically active vascular grafts

Clarke J.[1], Boumpouli M.[2], Salmeron-Sanchez, Paterson N.[2], Berry C.[1]
[1]Centre for the Cellular Microenvironment (CeMi), University of Glasgow; [2]Terumo Aortic, Glasgow, UK

Introduction

Cardiovascular diseases (CVDs) are the leading cause of death globally.[1] The use of synthetic Polyethylene Terephthalate (PET) vascular grafts has shown great promise in treating CVDs however, they are still at risk of developing acute thrombosis and intimal hyperplasia over time.[2,3] Mesenchymal stromal cell (MSC) derived extracellular vesicles (EVs) will be investigated as a biologically active graft coating to promote endothelialisation and limit blood clot formation.

Materials and Methods

MSCs were primed in normal and hypoxic culture to generate MSC-EVs with enhanced angiogenic factors.[4] The EVs were characterised by size, concentration and membrane markers. Then EV cargo was assessed for angiogenic and wound healing effects using human umbilical vein endothelial cells (HUVECs) for tube formation and migration assays, as well as analysing cytokine and metabolite cargo. PET graft samples were prepared with a proprietary coating to facilitate EV binding via integrins. HUVECs were then cultured on uncoated and bioactive coated surfaces to assess angiogenic properties and morphology changes over time. Human whole blood interaction was recorded at pre, 30min and 2hr timepoints under flow conditions, to observe surface activation of the coagulation cascade.

Results

Normal and hypoxic MSC-EVs had a similar size and concentration, with hypoxic EVs exhibiting more angiogenic factors and promoting wound healing. MSC-EVs successfully adhered to the graft material, with its woven topography manipulating EV distribution across the surface. HUVECs contact guided along the graft fibres, with the bioactive coating encouraging cell growth and junction formation across the fibres. Platelet activation was reduced by the bioactive coating in comparison to the uncoated PET graft under flow conditions.

Conclusion

Overall, the bioactive coating shows promise to reduce thrombosis alongside the hypoxic EVs promoting endothelialisation, therefore resulting in better graft integration within the injured blood vessel. Future work will involve assessing the endothelial monolayer on the bioactive coating under static and flow conditions.

Acknowledgements

I would like to thank my funders from EPSRC/UKRI for the LifETIME centre for doctoral training (CDT) and industry sponsor Terumo Aortic.

References

1. World Health Organization, “Cardiovascular diseases (CVDs).” Accessed: Nov. 28, 2022. https://www.who.int/news-room/fact-sheets/detail/cardiovascular-diseases-(cvds)
2. T. Pennel and P. Zilla, Tissue-Engineered Vascular Grafts, 3–34, 2020.
3. K. Yoshizawa et al. J Neurointerventional Surgery, 2022.
4. C. Almeria et al., Front Bioeng Biotechnol, vol.7, Oct.2019

S36 – O6

Engineered plant-derived extracellular vesicles tagged with magnetic nanoparticles as novel antitumoral agents

Conte M.[1], Selzer S.[1], Ambrosone A.[2], Moros M.[1]
[1]Instituto de Nanociencia y Materiales de Aragón, INMA (CSIC-Universidad de Zaragoza), Zaragoza, Spain;
[2]Dept. of Pharmacy, University of Salerno Fisciano, Italy

Introduction

Extracellular vesicles (EVs) are emerging as highly promising biological nanocarriers for drug delivery and cancer therapy due to their intrinsic biocompatibility, ability to transport bioactive molecules, and capacity to cross biological barriers. Despite the extensive investigation of mammalian-derived EVs, their clinical translation remains limited by safety concerns, poor scalability, and high production costs.

Plant-derived EVs represent a promising alternative, as they are non-immunogenic, non-toxic, and suitable for large-scale production. Moreover, increasing evidence supports their involvement in cross-kingdom communication and their intrinsic antitumoral activity. However, current isolation methods based on whole plants or fruits often result in heterogeneous EV preparations and limited reproducibility, highlighting the need for standardized production and purification strategies optimized for nanomedicine applications.

Aim

Plant cell cultures (PCCs) provide a controlled system for the production of plant-derived extracellular vesicles (EVs), enabling standardized yields and high-purity preparations. The present work aims to establish a scalable nanomedicine platform by integrating these EVs with magnetic nanoparticles (MNPs). EVs are selectively isolated from conditioned media using antibody-functionalized MNPs, resulting in hybrid nanocomplexes (MNP@EVs) designed to combine targeted capture with potential applications in drug delivery and hyperthermia-based strategies, offering a multifunctional therapeutic approach.

Materials and Methods

MNPs were synthesized via a one-step thermal decomposition method [1] and transferred to water using a PMAO coating. Their morphology, size, and composition were characterized by TEM and ICP-OES, while magnetic properties and colloidal stability were evaluated by SQUID magnetometry, DLS, and zeta potential. MNPs were then functionalized with antibodies ensuring a proper surface orientation. *Arabidopsis thaliana* PCC were generated by inducing callus from explants on media supplemented with 2,4-D and kinetin.

Results

To evaluate their suitability for the proposed applications, the synthesized MNPs were characterized for morphology, composition, magnetic behavior, colloidal stability, and functionalization efficiency. The nanoparticles exhibited a uniform cubic morphology with a size of ~25 nm and displayed superparamagnetic behavior with good colloidal stability in water, a slightly negative surface charge, and minimal aggregation. Antibody conjugation was successfully optimized, yielding ~80% functionalized particles, and preliminary experiments confirmed their efficient target-capturing ability, supporting their potential application for selective immunocapturing.

Conclusion

These preliminary results demonstrate the potential of the proposed platform for the selective capture of plant-EVs and pave the way for the development of novel EV-based nanoplatforms, with potential applications in drug delivery and magnetic hyperthermia.

Acknowledgements

This work is supported by the European Union through the Marie Skłodowska-Curie Postdoctoral Fellowship (Grant Agreement No. 101210929)

References

[1]Del Sol-Fernández S., De Simone M., Fernández-Afonso Y., Garcia-Gonzalez D., Martínez-Vicente P., van Zanten T.S., Fratila R.M., Moros M. MagPiezo: A magnetogenetic platform for remote activation of endogenous Piezo1 channels in endothelial cells. Advanced Functional Materials 2026; e29076.

S36 – O7

Unravelling the potential of *star*-shaped PolyLactic acid functionalized with β-cyclodextrin for doxorubicin delivery in osteosarcoma cells

Scala A.[1], Piperno A.[1], Coulembier O.[2], Nocito G.[3], Mazzaglia A.[3], Montesi M.[4]
[1]Dept of Chemical, Biological, Pharmaceutical and Environmental Sciences (CHIBIOFARAM), University of Messina, Italy; [2]Center of Innovation and Research in Materials and Polymers (CIRMAP), Laboratory of Polymeric and Composite Materials, University of Mons, Belgium; [3]CNR-ISMN, National Council of Research, Institute for the Study of Nanostructured Materials, URT of Messina *c/o* DeptCHIBIOFARAM, University of Messina, Italy; [4]CNR-ISSMC, Institute of Science, Technology and Sustainability for Ceramics, Faenza, Italy

Introduction

Star-shaped polymers are emerging biomaterials of considerable interest for biomedical applications, particularly as injectable drug delivery systems. Their unique architecture, consisting of multiple linear polymeric arms radiating from a central *core*, provides physicochemical properties that cannot be achieved with conventional linear polymers. [1] Moreover, amphiphilic copolymers, characterized by both hydrophilic and hydrophobic segments of tunable length, represent versatile drug delivery platforms due to the ability to self-assemble into micelles, vesicles, and other nanostructures.

Aim

Within our ongoing efforts to develop polymer-based nanotherapeutics, [2-4] we recently synthesized a novel three-armed *star* PolyLactic Acid functionalized with β-cyclodextrin (*star* PLA-CD) and we exploited its ability to encapsulate the antitumoral drug Doxorubicin (Dox) serving as long-lasting delivery nanosystem for osteosarcoma treatment.

Materials and Methods

The novel *star* PLA-CD was obtained through a multistep synthetic strategy combining ring-opening polymerization (ROP) of L-lactide initiated by glycerol, Steglich esterification, and copper-catalyzed azide-alkyne 1,3-dipolar Huisgen cycloaddition (CuAAC). Stable micellar nanoassemblies encapsulating Dox were obtained by nanoformulation in water (*star* PLA-CD@Dox). Physicochemical properties (*i.e,* particle size, zeta potential), drug loading, encapsulation efficiency, drug release profile were assessed. The biological profile was investigated on a panel of osteosarcoma cells (U2, MG63, Saos-2, MNNG-HOS-GFP, 143B) and on healthy cells (bone marrow derived mesenchymal stem cells, BM-MSCs). Cellular uptake and MTT assays at 72 h were performed; IC50 and Selectivity Index (SI) were calculated. Preliminary *in vivo* studies on healthy mice were also performed.

Results

Covalent and supramolecular approaches were employed for the design of *star* PLA-CD@Dox nanostructures. Leveraging controlled polymerization strategies and coupling chemistry, a high degree of structural precision was achieved. During nanoformulation, Dox was loaded with a very high encapsulation efficiency exploiting both the polymeric micellar core and the CD cavity forming nanoassemblies of about 100 nm. The positive zeta potential value of drug-loaded *star* PLA-CD@Dox (ζ + 19 mV) respect to the negative "empty" system (ζ - 25 mV) might suggest that Dox likely fit into the CD cavity by the quinone side exposing the protonated sugar moiety at the nanoassembly surface. A sustained and prolonged drug release from star PLA-CD@Dox was promoted by acidic pH that stimulated nanoparticles disassembly together with DOX protonation. *In vitro* biological studies on U2, MG63, Saos-2, MNNG-HOS-GFP, and 143B osteosarcoma cells pointed out the ability of our *star* PLA-CD@Dox to effectively inhibit tumoral cells proliferation, without toxicity on BM-MSCs. Preliminary *in vivo* studies on healthy mice excluded toxicity in major organs (heart, lungs, liver, kidneys, spleen), confirming the biocompatibility of the nanosystem.

Conclusion

Overall, these findings highlighted the great potential of amphiphilic *star* PLA-CD as a promising nanoplatform for anticancer therapy preserving Dox activity and acting as a pH-responsive slow-release *"drug reservoir"* that ensured prolonged biological activity over the time.

References

[1] Kubisa P., Lapienis G., Biela T. *Polym. Adv. Technol.* 2021; 10; 3857-3866.
[2] Torcasio S. M., Oliva R., […], Scala A. *Biomat Adv* 2022; 140; 213043.
[3] Oliva R., Ginestra G., […] Scala A. *Int. J. Pharm.* 2023; 642; 123067.
[4] Oliva R., Torcasio S. M. […], Scala A. *Int. J. Pharm.* 2024; 657; 124183.

S37
From bioactive materials to 3D-printed solutions: Advancing spinal fusion and back pain therapies

S37 - K1
Pathology- and patient-adapted spinal materials and implants

Persson C.[1]
[1]Div. Biomedical Engineering, Dept. Materials Science and Engineering, Uppsala University, Sweden

Introduction
Spinal pathologies such as osteoporotic vertebral compression fractures and degenerative disc disease require treatments that account for pathology-specific biomechanics. Conventional bone cements used in vertebroplasty exhibit high stiffness, which has been linked to increased adjacent-level fracture risk due to modulus mismatch with osteoporotic bone. Similarly, standard fusion cages often lack optimized load distribution, motivating computational design approaches to improve their mechanical and clinical performance. In addition, bioactive and biodegradable materials may further improve the treatment possibilities and patient outcomes.

Aim
To develop pathology-adapted spinal treatments, and where appropriate, patient-specific such.

Materials and Methods
Low-modulus cements have been developed by the addition of small amounts of softener that significantly reduces elastic modulus while maintaining adequate handling properties and biocompatibility. These cements have been thoroughly characterized, from key laboratory properties to preclinical tests and a randomized clinical trial in four countries.

Topology-optimized intervertebral fusion cages have been designed by employing optimization frameworks, mechanical validation, additive manufacturing, and incorporation of osteoinductive bioceramics. These design strategies were verified through numerical simulations and experimental mechanical testing to evaluate load-sharing and structural integrity. Early investigations into completely degradable composite materials have also been done.

Results
Low-modulus cements demonstrated substantial stiffness reductions compared with commercial controls, while retaining sufficient compressive strength for vertebral augmentation. Studies further indicate beneficial alterations in discoplasty biomechanics and reduced endplate stress. Recent insights from the largest ever randomized clinical trial performed on this type of material shows a statistically confirmed reduced fracture risk.

Topology-optimized fusion cages showed improved mechanical efficiency, increased graft-packing volume, and reliable structural performance. Designs supported incorporation of bioactive materials while maintaining cage integrity, with strong correlation between computational predictions and mechanical testing outcomes.

Conclusion
Together, low-modulus bone cements and topology-optimized fusion cages represent promising pathways toward personalized spinal care, for vertebral bodies as well as intervertebral discs. The work provides foundational contributions enabling pathology- and patient-specific mechanical compatibility, reduced complication risks, and potentially improved long-term outcomes in spinal interventions.

S37 – O1

Xenogeneic spinal cord ECM bioink for 3D printing application to restore sensorimotor function through axonal reconnection in rat complete spinal cord transection

Chaudhari L.R.[1], Kawale A.A.[1], Sonkawade O.R.[1], Patil J.[2], Desai S.S.[3], Joshi M.G.[1,4]
[1]Dept. of Stem Cells and Regenerative Medicine, CIR, D Y Patil Education Society (Deemed to be University), Kolhapur, MS; [2]Dept. of Radiology, D Y Patil Medical College Hospital and research center, Kolhapur, MS; [3]Dept. of Obstetrics and Gynecology, D Y Patil Medical College, Kolhapur, 416003, MS; [4]Stem Plus Biotech Pvt. Ltd., SMK Commercial Complex, C/S No. 1317/2, Near Shivaji Maharaj Putla, Bus Stand Road, Gaon Bhag, Sangli, MS – 416416

Background

Spinal cord injury (SCI) remains a major clinical challenge due to poor intrinsic regeneration, formation of inhibitory scar tissue, and lack of effective treatment options that restore the functionality of the damaged spinal cord. To address these concerns, study developed a bioinspired 3D printed spinal cord extracellular matrix conduit to reestablish a favorable microenvironment for regeneration.

Methods

Fabrication of biomimetic 3D-printed conduit using PVA-gelatin bioink functionalized with xenogeneic spinal cord extracellular matrix (xSC-ECM) and fibronectin. These scaffolds were fabricated to model the viscoelastic and topographical properties of native spinal cord. A series of physicochemical, viscoelastic, mechanical, biochemical, histological, in vitro, and in vivo characterizations were performed to assess scaffold composition, functionality, and in vivo regenerative efficacy.

Results

The xSC-ECM-loaded scaffold demonstrated favorable viscoelastic properties (thixotropy ~4,511 Pa/s), controlled biodegradation rate, and pore sizes (500–1200 µm) and porosity % (67.72%) supportive of axonal infiltration. In vitro characterization confirmed excellent cytocompatibility (~100% viability) and hemocompatibility (<5%), and chorioallantoic membrane assays demonstrated robust angiogenic potential. Rats receiving xSC-ECM conduits showed significant functional recovery, with Basso–Beattie–Bresnahan locomotor scores (13.3 ± 0.5, $p < 0.001$**), compared to injury controls. MRI, retrograde tract tracing, and gene expression profiling revealed complete lesion bridging and reinnervation. Mechanistically, xSC-ECM conduits promoted neuroprotection through GFAP+ astrocytic border attenuation (1.3 ± 0.1 folds), enhanced angiogenesis (5.5 ± 0.1 folds in VEGF), and tissue remodeling (2.6 ± 0.1 folds in TGF-β).

Conclusion

This study demonstrates that xSC-ECM-functionalized bioprinted conduits promote neuroprotection, angiogenesis, and sensorimotor recovery following complete SCI while establishing a translatable and clinically promising ECM-based biofabricated conduit for spinal cord repair.

S37 – O2

Comparative analysis of simulated degeneration strategies for the development of intervertebral disc biomaterials

Todescato F.[1,2], Pasini M.[3], Palanca M.[3], Cristofolini L.[3], Fernandes P.R.[1,2], Öhman-Mägi C.[2], Castro A.P.G.[1,4], Persson C.[2]

[1]IDMEC, Instituto Superior Técnico, Lisbon, Portugal; [2]Dept. of Materials Science and Engineering Sciences, Uppsala University, Uppsala, Sweden; [3]Dept. of Industrial Engineering, Alma Mater Studiorum - University of Bologna, Bologna, Italy; [4]ESTSetúbal, Instituto Politécnico de Setúbal, Setúbal, Portugal

Introduction

Percutaneous Cement Discoplasty (PCD) is a minimally invasive technique for treating Intervertebral Disc Degeneration (IVDD). Although spinal fusion remains the gold standard, PCD shows promising outcomes in patients with advanced IVDD presenting a vacuum phenomenon (VP). However, its clinical potential, including the development of new materials for this treatment method, require further investigation, supported by reliable standardized models. In preliminary studies, IVDs from animals provide greater standardisation, enabling more reliable comparisons across different degeneration methods for modelling IVDD. Among these methods, papain digestion and surgical nucleotomy are well-established degeneration strategies in ovine and porcine models. Collagenase-II digestion is another technique, mainly used in human IVDD. Papain digests collagen and proteoglycans in the nucleus pulposus, whereas collagenase II selectively degrades type I and II collagen.

Aim

The aim of this study is to compare three artificial degeneration methods to identify the most reliable strategy to model VP in ex-vivo porcine IVD. In this abstract, only the results from enzymatic methods are presented.

Materials and Methods

Porcine functional spinal units (FSU) were harvested from 5-month-old Yorkshire/Hampshire pigs. Lower thoracic and lumbar FSUs were used to evaluate two strategies based on enzymatic digestion, papain and collagenase II. The enzyme solution was injected into the disc through a 19 G needle. After injection, FSUs were incubated at 60°C for 16 h for papain digestion, or at 37°C for 2 h when treated with collagenase II. The extent of degeneration was evaluated by quantifying axial stiffness via pure compression and by analyzing void formation using micro-computed tomography (micro-CT).

Results

Papain digestion successfully created a void in the porcine IVD, replicating the VP (Figure 1). Collagenase-II also produced signs of VP, but the effect was not clear from CT images. Compression tests were conducted for both enzymatic strategies and showed a more pronounced reduction in compressive stiffness after papain digestion, with a mean decrease of −18.8% ± 15.0% (n = 5). Collagenase-II digestion resulted in a smaller reduction in stiffness (−9.7% ± 6.8% (n = 4)) after the first cycle of injection, indicating a milder biomechanical alteration compared to papain treatment (Figure 2).

Conclusion

Papain digestion showed promising results in replicating the characteristic NP void, and resulted in notable shifts in mechanical properties. The collagenase II approach requires further optimization before it can be reliably used in animal models and may ultimately provide a protocol for inducing graded IVDD, to enable the development of new biomaterials for this indication.

Acknowledgements

This work was supported by Fundação para a Ciência e a Tecnologia (FCT), Portugal, through LAETA (project UID/50022/2025), PhD Grant 2024.00399.BD, and COST Action EuroCurvoBioNet CA22153, supported by COST (European Cooperation in Science and Technology).

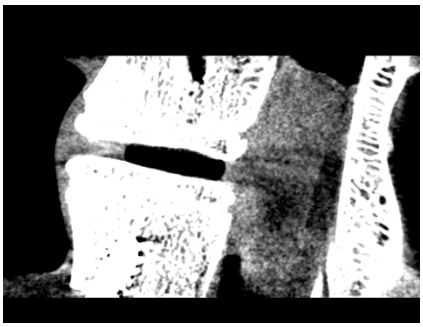

Figure 1: Papain-induced vacuum in a porcine IVD.

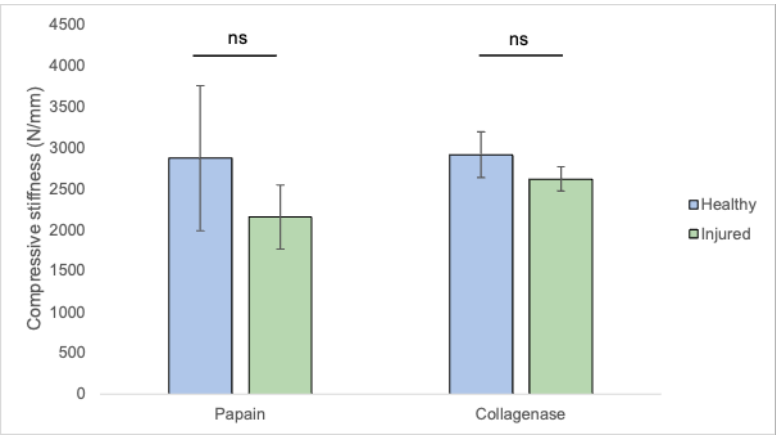

Figure 2: Compressive stiffness of Healthy and Injured samples, as induced from papain and collagenase digestion.

S37 – O3

Bioactive and load-bearing calcium phosphates for developing biomimetic spine fusion implants

Massel B.F.[1], Truckenmüller R.[1], Habibović P.[1], Tahmasebi Birgani Z.N.[1]
[1]Dept. of Complex Tissue Regeneration, MERLN Institute of Technology-Inspired Regenerative Medicine, Maastricht, the Netherlands

Introduction

Intervertebral disc degeneration is a major contributor to chronic back pain, responsible for 30–40% of cases and ranking among the top causes of disability globally. When conservative therapies fail, spinal fusion using cages made of titanium or polyetheretherketone remains the standard treatment. However, these bioinert and non-degradable materials often show poor osseointegration, limited osteoinductivity, and mechanical mismatches with surrounding bone, which may lead to delayed fusion, implant failure, and degeneration of adjacent vertebrae.

Aim

This study aims to develop bioactive and mechanically competent calcium phosphate (CaP) porous scaffolds that could serve as biomimetic spinal fusion implants. We hypothesize that combining hydroxyapatite (HA) nanowires with β-tricalcium phosphate (β-TCP) nanofibers can yield fibrous, bioactive CaP scaffolds with enhanced elasticity and strength suitable for spinal fusion.

Materials and Methods

Ceramic slurries combining in-house synthesized β-TCP nanofibers and HA nanowires were prepared to fabricate porous CaP scaffolds. The total solid content (4–20 wt%) was adjusted to tailor scaffold strength while preserving partial elasticity for load-bearing applications. β-TCP nanofibers were obtained by sintering hydrothermally synthesized precursors (Ca/P = 1.5), and HA nanowires were produced via hydrothermal treatment at 200 °C for 4 h. The two components were mixed at varying ratios for 2 h, cast into molds, and frozen at −80 °C overnight. Porous scaffolds were then formed by freeze-drying. Scaffold morphology and phase composition were analyzed using scanning and transmission electron microscopy, and X-ray diffraction. Mechanical properties were assessed via uniaxial and cyclic compression tests. Planned in vitro studies will examine human mesenchymal stem cell compatibility and osteogenic differentiation.

Results

Preliminary morphological and chemical analyses confirmed the successful synthesis of HA nanowires and β-TCP nanofibers and their integration into fibrous CaP scaffolds. Mechanical testing showed that increasing the slurry solid content led to a corresponding increase in scaffold stiffness. Mechanical testing revealed that increasing solid content enhanced stiffness while preserving partial elasticity. Fibrous architecture appears to mitigate the intrinsic brittleness typically associated with ceramic biomaterials, suggesting improved mechanical adaptability for load-bearing applications.

Conclusion

The developed HA–β-TCP fibrous scaffolds demonstrate tunable mechanical properties and improved elasticity compared with conventional brittle CaP ceramics. These findings highlight HA–β-TCP fibrous scaffolds as promising candidates for developing next-generation bioactive spinal fusion implants.

S37 – O4

ROS-responsive hydrogen-releasing scaffolds for sustained miRNA sponge delivery in spinal cord injury

Pan W.C.[1], Hwang E.[2], Liu Z.H.[3], Hu S.H.[1]
[1]Dept. Biomedical Engineering and Environmental Sciences, National Tsing Hua University, Hsinchu; [2]Dept. Biological Science and Technology, National Yang Ming Chiao Tung University, Hsinchu; [3] Dept. Neurosurgery, Chang Gung Memorial Hospital, Taoyuan, Taiwan

Introduction

Spinal cord injury (SCI) remains a devastating condition with limited therapeutic options. Excessive accumulation of reactive oxygen species (ROS) at the lesion site drives neuroinflammation and neuronal loss, creating a hostile microenvironment that impedes neural repair[1]. Gene therapy offers a promising strategy to modulate regenerative pathways; notably, delivery of miR6236 sponges can activate signaling that promotes axonal regrowth[2]. However, effective therapy requires localized gene delivery while overcoming oxidative stress. Here, we develop a ROS-responsive transfectant microgel scaffold (RTMS) integrating ammonia borane–mediated hydrogen release with sustained gene delivery. Upon hydrolysis, ammonia borane generates therapeutic hydrogen that scavenges ROS and restores a permissive niche for neural transfection, while enabling prolonged release of miRNA sponge plasmids. This platform mitigates inflammation, enhances transfection efficiency, and promotes functional recovery after SCI.

Materials and Methods

RTMS microgels were fabricated by loading ammonia borane onto PEI-modified GelMA microgels, followed by electrostatic incorporation of miR6236-targeting sponge (mts) plasmids. DNA binding and hydrogen release were characterized by gel electrophoresis and gas chromatography. In vitro, primary NSCs were treated with RTMS to evaluate transfection and differentiation. In vivo, rat spinal cords were analyzed by immunofluorescence and TEM to assess immune modulation, neural regeneration and myelination, while electrophysiology and behavioral tests evaluated functional recovery.

Results

The highly biocompatible RTMS exhibited potent ROS scavenging via hydrogen release, alleviating oxidative stress and facilitating efficient delivery of miRNA sponge plasmids into neurons (Figure 1). This modulation neutralized the neurogenic inhibitor miR6236[3], establishing a permissive microenvironment for neurogenesis and neurite outgrowth. Under oxidative conditions, RTMS also induced the highest levels of neural growth–related factors among all treatments. In SCI rat models, RTMS achieved effective transfection at the lesion site and significantly reduced acute neuroinflammation and glial scarring. Partial reconstruction of neurofilaments and remyelination was observed during a 6-week recovery period. Functional assessments further demonstrated that RTMS-treated rats exhibited the greatest improvements in motor coordination and electrophysiological responses, leading to accelerated behavioral recovery compared with control groups (Figure 2).

Conclusion

We demonstrate that a hydrogen–gene dual-functional microgel establishes a self-regulated therapeutic niche through complementary mechanisms. ROS-triggered H_2 release rapidly scavenges cytotoxic radicals and suppresses neuroinflammation, limiting secondary damage. Meanwhile, sustained delivery of miR6236 sponges reactivates intrinsic regenerative pathways by modulating genes involved in axonal growth and neuronal differentiation. This synergistic strategy couples redox regulation with genetic modulation, providing an adaptive biomaterial platform for neuroprotection and regeneration after spinal cord injury.

Acknowledgements

This work was financially supported by the Ministry of Science and Technology of the Republic of China, Taiwan under contracts MOST 111-2314-B-007-003-MY3, MOST 111-2636-E-007-021 and MOST-110-2634-F-007-025, MOST 111-2320-B-A49-015-MY3, National Tsing Hua University (111Q2715E1 and 111F7MELE1) in Taiwan.

References

[1]Ahuja, C.S., Wilson, J.R., Nori, S., Kotter, M., Druschel, C., Curt, A., Fehlings, M.G. Traumatic spinal cord injury. *Nature Reviews Disease Primers* 2017; 3, 1-21.

[2]Pan, W.C., Lin, Y.H., Iao, H.M., Chang, Y.H., Chen, Y.H., Liu, H.C., Tran, N.T., Lee, I.C., Lien, H.W., Hwang, E., Chu, L.A., Hu, S. H. In situ magnetoelectric generation of miRNA sponges and wireless electric stimulus by conductive granular scaffolds for nerve regeneration. *Advanced Materials* 2025; 37, 2500650.

[3]Chen, Y. J., Huang, Y. A., Ho, C. T., Yang, J. M., Chao, J. I., Li, M. C., Hwang, E. A nanodiamond-based surface topography downregulates the microRNA miR6236 to enhance neuronal development and regeneration. *ACS Applied Bio Materials* 2020; 4, 890-902.

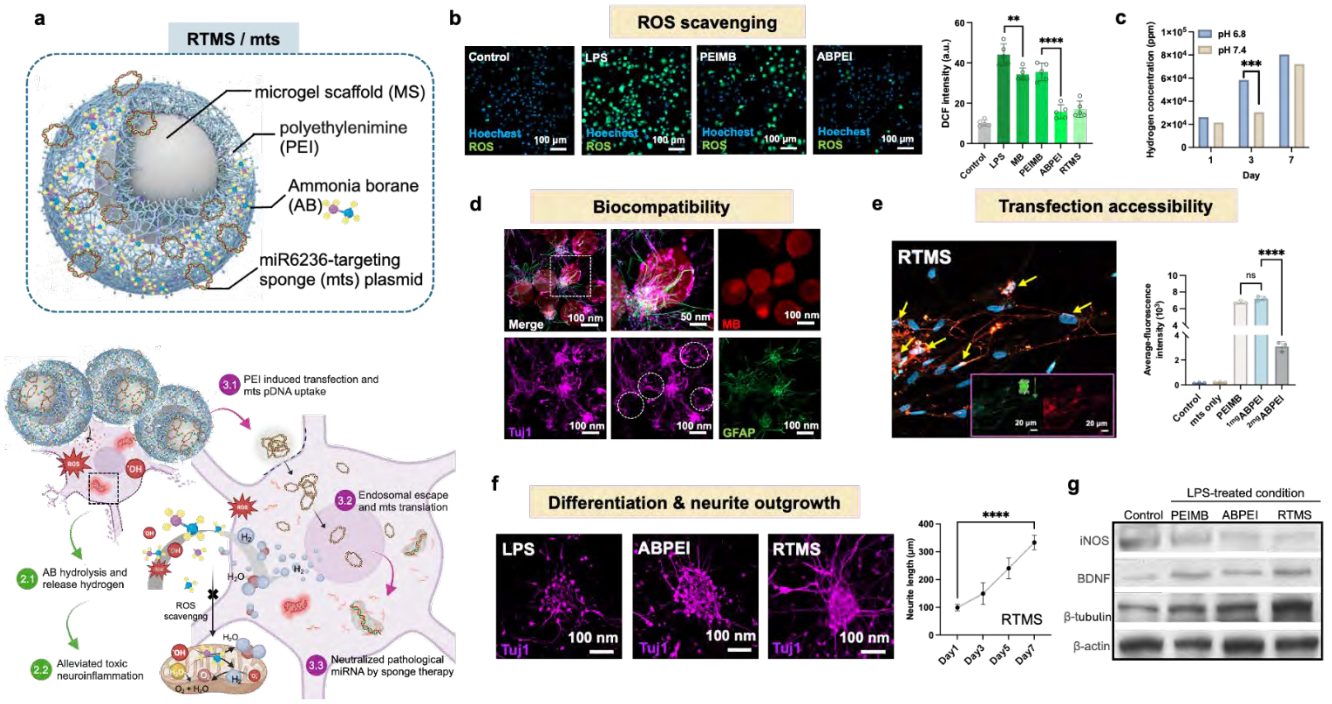

Figure 1. The novel RTMS therapy for SCI. (a) Schematic illustration of the RTMS formulation and workflow for ROS scavenging and gene delivery into neurons. (b) Confocal images showing that RTMS has superior ROS depletion ability. (c) Hydrogen release profile under different pH conditions. (d) Biocompatibility of RTMS when cultured with neural stem cells. (e) Neuronal transfection resulting in miR6236 depletion. (f) Confocal images demonstrating neural differentiation and neurite outgrowth across different groups. (g) Western blot assay showing that RTMS therapy induces the highest expression of neural growth–related factors with efficient immunomodulation.

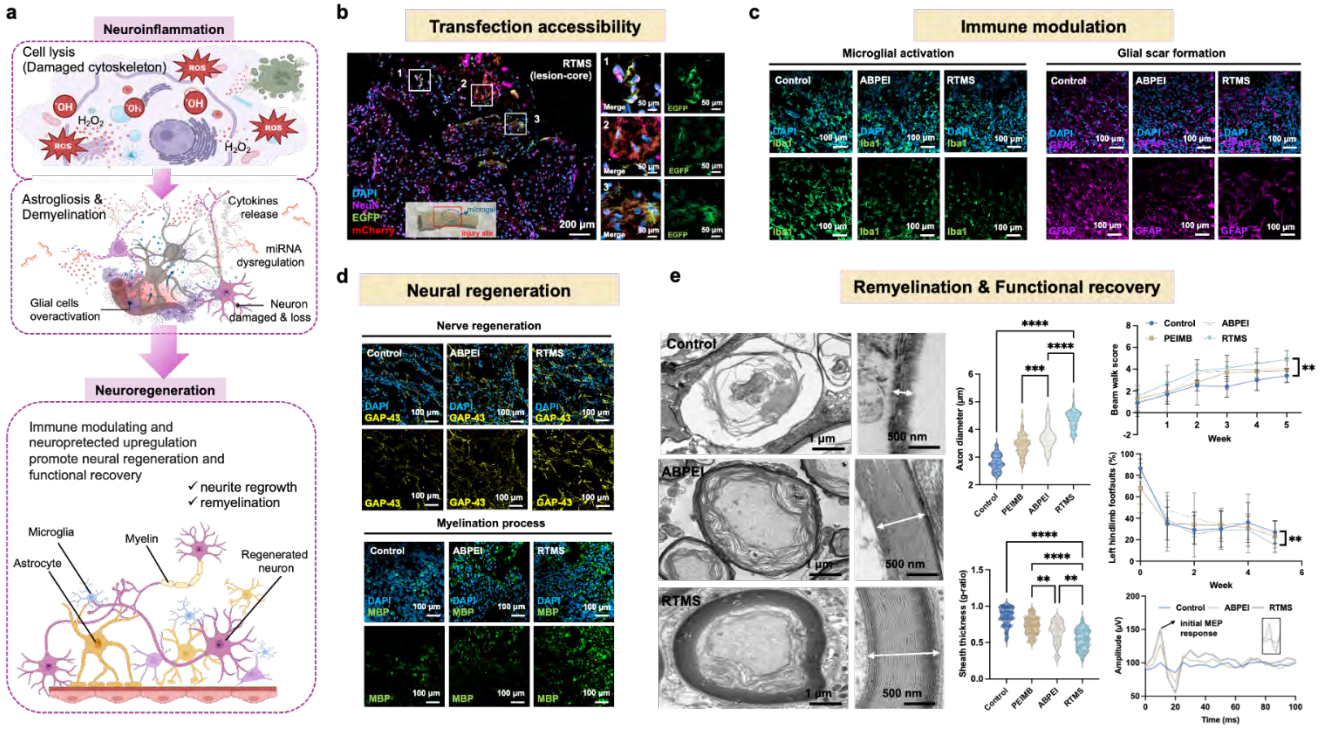

Figure 2. In vivo therapeutic efficacy of RTMS. (a) Schematic illustration showing how RTMS alleviates neuroinflammation and promotes tissue regeneration. (b) In vivo transfection at the lesion-core area. (c–d) Confocal images showing that RTMS not only reduces microglial activation and glial scarring, but also partially restores neurofilament and myelin. (e) TEM images demonstrating remyelination. Behavioral tests and electrophysiological recordings were used to evaluate functional recovery.

S37 – O5

Electrically conductive nanocomposite silk fibroin hydrogel for spinal cord injuries repair

Benazzato S.[1,2], Borah R.[3], Casalini S.[1,2], Monaghan M.[3], Menna E.[1,2]
[1]Dept. of Chemical Sciences, University of Padova, Padova, Italy; [2]Consorzio Interuniversitario Nazionale per la Scienza e Tecnologia dei Materiali (INSTM), Firenze, Italy; [3]Dept. of Mechanical, Manufacturing and Biomedical Engineering, Trinity College Dublin, Dublin, Ireland

Introduction

This work aims to design an injectable silk fibroin hydrogel incorporating functionalized multi-walled carbon nanotubes (MWCNT) and PEDOT: PSS to promote neural development for spinal cord injuries (SCI) repair. SCI recovery is limited by poor endogenous repair and a hostile inflammatory environment. To address this issue, electrically conductive scaffolds for cell transplantation represent a promising strategy. The hydrogel serves as a structural support and delivery platform for cells, exploiting its conductivity to restore neural communication and stimulate tissue regeneration. This approach offers a promising strategy to overcome biological barriers and enhance functional recovery.

Materials and Methods

Two MWCNT derivatives, functionalized with glucose (MWCNT-Gluc) and sulfonate (MWCNT-S) functional groups respectively, were obtained through a diazotization reaction and characterized through thermogravimetric analysis (TGA), dynamic light scattering (DLS), Z potential, Raman spectroscopy, and infrared (IR) spectroscopy. Six optimized silk-based composite hydrogel formulations were subsequently developed and characterized through SEM spectroscopy, rheological tests, swelling behavior in PBS, *in vitro* biodegradability, mechanical compression tests and electrochemical profiling. Finally, the biocompatibility of the scaffolds was assessed via live/dead assays with Calcein AM using the C3H10 cell line, while the materials ability to promote neural differentiation was evaluated through β tubulin and DAPI staining using the PC12 cell line.

Results

All tested formulations exhibited rheological and mechanical properties compatible with their intended use as injectable hydrogels. SEM microscopy and swelling assays allowed the characterization of the porosity across the different compositions. The scaffolds demonstrated excellent biocompatibility toward C3H10 fibroblasts, supporting both 2D surface adhesion and 3D encapsulation. Furthermore, preliminary investigations into the axonal outgrowth of encapsulated PC12 cells yielded promising results; specifically, formulations incorporating MWCNT-Gluc showed enhanced neurite development, highlighting their potential for promoting neural regeneration.

Conclusion

These findings demonstrate that silk-based nanocomposite hydrogels represent a promising platform for spinal cord injury treatment. The synergistic integration of silk fibroin, PEDOT:PSS, and functionalized MWCNT provides the necessary mechanical, electrical, and biological cues to support neural regeneration. Future investigations will focus on characterizing the scaffold's immunomodulatory properties and evaluating the impact of applying an electrical stimulation on the axonal formation. Overall, this study sets the suitability of these injectable scaffolds as tools for cell delivery and functional tissue repair.

Acknowledgements

European Molecular Biology Organization (EMBO) Scientific Exchange Grants

S37 – O6

Placenta-derived ECM as a bioinstructive biomaterial for spinal cord tissue engineering

Barceló X.[1], Ortega J.A.[4,5], Álvarez Z.[1,2,3]
[1]Biomaterials for Neural Regeneration Group, Institute for Bioengineering of Catalonia (IBEC), The Barcelona Institute of Science and Technology (BIST), Barcelona, Spain; [2]CIBER en Bioingeniería, Biomateriales y Nanomedicina, CIBER-BBN, Madrid, Spain; [3]Simpson Querrey Institute for BioNanotechnology, Northwestern University, Chicago, Illinois, USA; [4]Institut d'Investigació Biomèdica de Bellvitge (IDIBELL), L'Hospitalet del Llobregat, Spain; [5]Department of Pathology and Experimental Therapeutics, Institute of Neurosciences, University of Barcelona, L'Hospitalet de Llobregat, Spain

Introduction

Understanding the pathophysiology of spinal cord injury (SCI) and related neurological disorders requires advanced human-relevant *in vitro* models that faithfully recapitulate the complexity of the spinal cord (SC). Current models often fail to mimic the native tissue architecture, which limits their predictive potential for therapeutic development. Therefore, the development of biomaterials capable of mimicking the native SC microenvironment is essential. Decellularized extracellular matrix (ECM)-derived biomaterials are promising candidates due to their ability to retain tissue-specific proteins and signaling molecules. Human placenta represents an abundant and ethically accessible source of ECM enriched in structural and regulatory proteins that overlap with those present in neural tissues.

Aim

Here, we investigated placenta-derived ECM as a bioinstructive biomaterial for SC tissue engineering and evaluated its integration within bioprinted human spinal cord exoskeletons designed to recapitulate the anatomical organization of grey and white matter.

Materials and Methods

Placenta-derived ECM was obtained through decellularization of human placental tissue and processed to generate ECM-based biomaterials suitable for biofabrication. Proteomic characterization was performed to assess the similarity between placental ECM and human fetal and adult SC ECM, focusing on the presence of key structural proteins. The resulting ECM was formulated into bioinks optimized for inkjet bioprinting to ensure appropriate viscosity, and preservation of cell viability.

Results

Proteomic analysis of placenta-derived ECM revealed a substantial overlap of structural proteins with native fetal and adult SC ECM, supporting its potential as a bioinstructive biomaterial for neural tissue engineering. The ECM-based bioinks exhibited suitable rheological properties for inkjet bioprinting and maintained high neural cell viability following deposition. When integrated within the GelMA exoskeleton scaffold, the ECM bioink enabled spatially defined patterning of neural cell populations corresponding to anatomically relevant compartments. Printed constructs maintained structural integrity and demonstrated robust cell survival over time. Preliminary observations suggested early cellular self-organization within the ECM microenvironment.

Conclusion

This work demonstrates the potential of human placenta-derived ECM as a bioinstructive biomaterial for SC tissue engineering. By combining human-derived ECM with advanced bioprinting strategies, this platform provides a promising approach for developing biomimetic *in vitro* models of the human SC.

Acknowledgements

Supported by grants PID2024-162574OB-I000 (10.13039/501100011033, ERDF/EU), R01AG086270 (NIA, NIH), and P199 (IRP Research Foundation); fellowships/programs JDC2023-051798-I (Juan de la Cierva, MICIU/AEI/10.13039/501100011033, ESF+), RYC2020-028732-I (Ramón y Cajal), and EU funding (ERC, 101230979 – SpineCraft, Horizon Europe).

S37 – O7

Mechanical microenvironment dictates astrocyte fate in human cortical organoids

Garhwal A.[2,4], Fahy Y.[1,3,4], Nadig K.[2,3,4], Qian X.[2], Pandit A.[4], Vallejo-Giraldo C.[1,2,3,4]
[1]Regenerative Medicine Institute (REMEDI), Advanced Therapies, School of Medicine, College of Medicine, Nursing and Health Sciences, University of Galway; [2]Biomedical Engineering, School of Engineering, College of Science and Engineering, University of Galway; [3]Institute for Health Discovery and Innovation, Bioscience Building, University of Galway; [4]CÚRAM - Research Ireland Center for Research in Medical Devices, Galway, Ireland

Introduction

Mechanical cues within the cellular microenvironment are key regulators of cell fate and tissue development. In the central nervous system, mechanical properties such as stiffness, cytoskeleton tension and cell-matrix interaction influence cellular differentiation through mechanotransduction pathways.[1] Astrocytes are highly responsive to mechanical cues and play a central role in neural tissue remodelling and injury responses, including astrogliosis in traumatic brain injury (TBI). While the mechanical regulation of glial differentiation has been widely studied in 2D environments, it remains poorly understood in complex 3D models such as human brain organoids. In particular, the influence of spatiotemporal mechanobiological cues – including geometric constraints, shear stress and hydrostatic pressure on growth and development remains unclear. This study investigates how these mechanical cues regulate growth and astrocyte maturation with the broader goal of establishing a stable model for TBI analysis.

Materials and Methods

Cortical organoids were generated from induced pluripotent stem cells (iPSCs) using an adapted protocol from [2]. Organoids were cultured under varying spatial constraints and hydrodynamic shear stress induced by orbital shaking, and their growth was quantified through surface area and volume measurements over time. Nanoindentation was performed to determine local Young's modulus, which informed finite element analysis (FEA) in COMSOL Multiphysics to model stress distribution and fluid–structure interactions. Astrocyte differentiation was evaluated using astrocyte-specific markers through combinatorial analysis of flow cytometry, immunostaining, and proteomics.

Results

Organoids cultured under varying spatial and hydrodynamic conditions exhibited distinct growth dynamics, as reflected in surface area and volumetric expansion (Fig. a–c). Nanoindentation revealed condition-dependent differences in local Young's modulus, indicating that extrinsic mechanical cues influence intrinsic organoid mechanics. Computational modeling suggested that these conditions generated discrete shear stress and pressure gradients, which correlated with the observed differences in growth and astrocyte differentiation (Fig. d–e).

Conclusion

This study demonstrates that spatial and hydrodynamic differences in organoids culture can be used to experimentally demonstrate the influence of mechanical factors on tissue growth and astrocyte differentiation. This 3D platform provides a robust system for investigating mechanotransduction in organoids and builds towards a model for studying TBI.

Funding

The lifETIME CDT was supported by Science Foundation Ireland 18/EPSRC-CDT/3583 and the Engineering and Physical Sciences Research Council EP/S02347X/1. This work emanated from research supported in part by a grant from Science Foundation Ireland (SFI) and the European Regional Development Fund (ERDF) under grant number 13/RC/2073_P2.

References

1) Engler A. J., Sen S., Sweeney H. L. & Discher D. E. Matrix Elasticity Directs Stem Cell Lineage Specification. *Cell* 2006; 126, 677–689
2) Eigenhuis KN., Somsen HB., van der Kroeg M., et al. A simplified protocol for the generation of cortical brain organoids. *Front. Cell. Neurosci.* 2023; 17:1114420

Figure

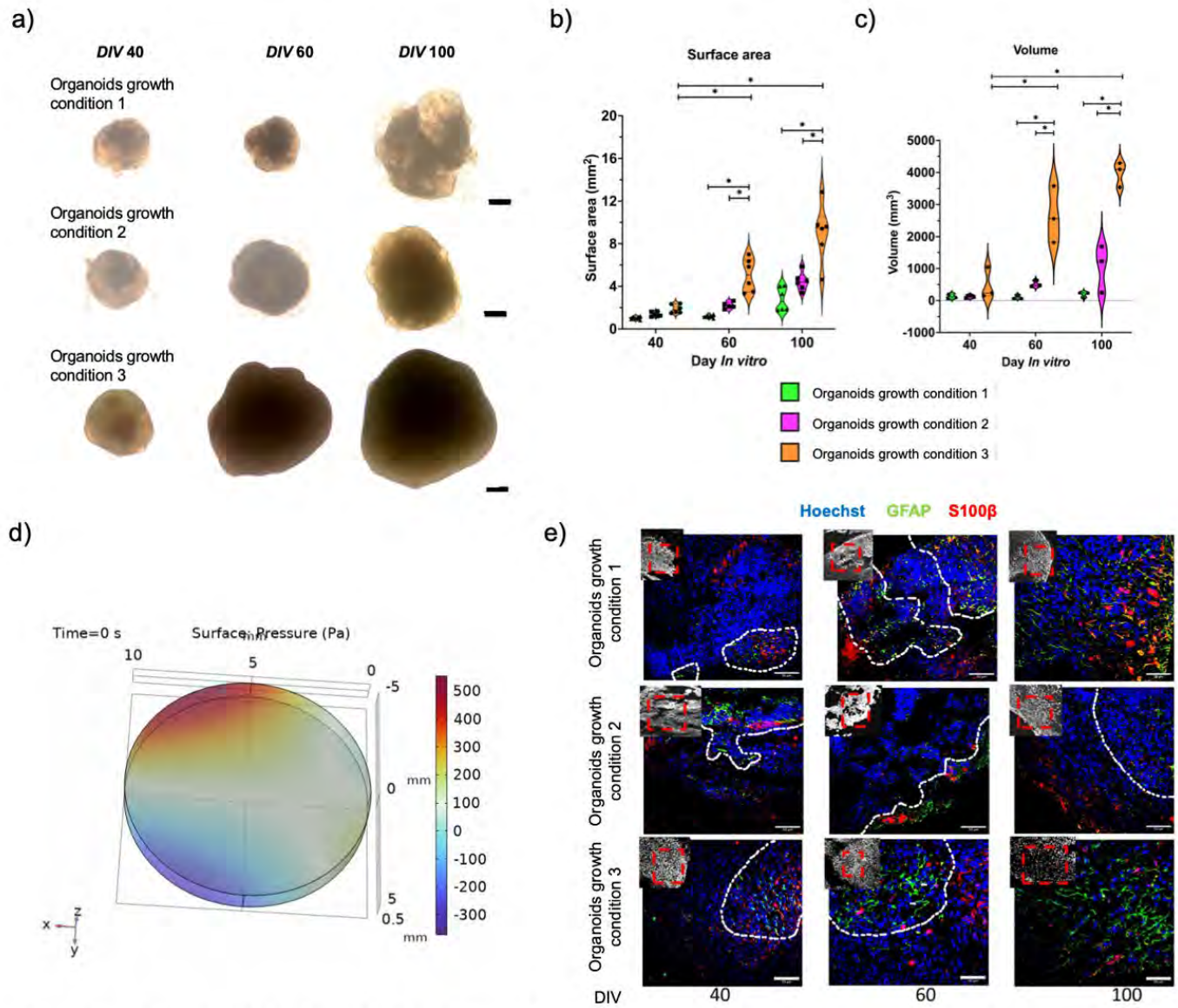

Astrocyte Growth is Modulated by Spatial and Hydrodynamic Cues
(a) Representative brightfield images of organoids cultured under different growth conditions. Scale bar = 500 µm. Quantification of organoid surface area (b) and volume (c) under the different conditions. Data represent n ≥ 3. Two-way ANOVA with Bonferroni's post-hoc correction was used. *p < 0.05, **p < 0.01, ***p < 0.001. Representative pressure profile for a spatially constrained culture condition, generated using finite element simulations in COMSOL Multiphysics, (d). Astrocyte marker staining (GFAP and S100β) under different culture conditions, showing astrocyte differentiation. Scale bar = 50 µm. The dotted line indicates the region containing GFAP-positive cells, which expands over time (e).

S38
Form muscle to tendon – advanced biomaterials for vitro models and therapeutic development

S38 – K1
TENET: Strengthening tendon regeneration research through cooperation

Gomez-Florit M.
IDISBA - Health Research Institute of the Balearic Islands, Palma, Spain

S38 – K2

Development and evaluation of precision biomaterials and biomanufacturing for treatment of volumetric muscle loss injuries

Christ G.J.
Depts. of Biomedical Engineering & Orthopaedic Surgery, University of Virginia, Charlottesville, USA

Introduction

Volumetric muscle loss (VML) resulting from battlefield trauma, vehicular accidents, tumor resection, or congenital deficits represents a major unmet medical need with no satisfactory treatment options. Current therapeutic development largely ignores the fact that VML exists along a continuum of injury magnitudes and complexities, potentially requiring a spectrum of regenerative solutions rather than a one-size-fits-all approach. Moreover, despite the prevalence of craniofacial VML, preclinical research remains overwhelmingly focused on extremity muscles, neglecting muscle-specific features that may be critical for therapeutic efficacy.

Materials and Methods

We address this knowledge gap through systematic evaluation of multiple biomaterial form factors across anatomically diverse VML models, including extremity (tibialis anterior, gastrocnemius, rotator cuff), trunk (latissimus dorsi), and craniofacial (masseter) muscles. Our technology platform encompasses: (1) sheet-based decellularized ECM as a cell delivery vehicle for tissue engineered muscle repair (TEMR), (2) injectable and implantable form factors of MuscleMatrix™, a tunable hyaluronic acid-based hydrogel and cryogel, and (3) KeraStat powder, a keratin-based hydrogel.

Results

Rigorous multiscale functional assessments enable direct comparison of regenerative efficacy across diverse injury sites and severities. This comparative approach enables therapeutic discovery efforts that are more focused on injury-specific, impairment-based therapeutics, essentially precision medicine for neuromuscular trauma.

Conclusion

Our findings highlight the need for incorporating muscle-specific design principles into VML repair strategies to further enable the translational potential of biomanufacturing strategies that integrate material science with regenerative pharmacology. This approach should enable creation of a roadmap for developing customized treatment strategies that move beyond current limitations toward more complete functional recovery.

Acknowledgements

NIH Award DE026914 and DoD awards W81XWH-22-2-0013 & W81XWH-20-1-0839.

S38 - K3

Decoding mechanosignaling in bioengineered tendon models for regenerative strategies

Domingues R.M.A.
Domingues Research Group, INL – International Iberian Nanotechnology Laboratory, Braga, Portugal

Introduction

Tendons are highly mechanosensitive tissues with complex physiology and limited regenerative capacity, making tendinopathy a major clinical challenge. Their heterogeneous cellular composition interacts within a dynamic extracellular matrix (ECM) whose architecture and biochemical cues are context-dependent. Mechanical forces are transduced through specialized membrane mechanoreceptors, yet the molecular mechanisms driving tendon homeostasis and disease remain poorly understood. A critical bottleneck is the limited availability of representative human *in vitro* models capable of dissecting these mechanotransduction pathways, particularly those mediated by force sensitive cell receptors.

Results

To address these challenges, we have developed advanced bioengineering strategies to create 3D human-based microphysiological systems. This talk will highlight two complementary tendon-on-chip platforms: (i) conventional microfluidic devices and (ii) automated 3D writing within support matrices. Both approaches aim to replicate the anisotropic architecture and cellular organization of the intrinsic tendon core while enabling bidirectional crosstalk with extrinsic compartments, including nervous, vascular and immune components. Leveraging these humanized platforms, we explore how the established cellular communication affects tendon cells fate under deferent healthy and diseases microenvironments. Furthermore, we introduce a novel technology to design tailor-made nanoswitches for wireless, submolecular control of PIEZO channels in tendon-relevant cells. We show how this molecularly designed nanoactuators opens new avenues for probing cell mechanosignaling. Furthermore, we discuss how mechanical actuation with submolecular precision may help to unveil previously unrecognized PIEZO-mediated force transduction mechanism, which can potentially be explored for developing regenerative interventions.

Conclusion

By integrating these platforms, we aim to provide powerful tools to unravel tendon biology and pathology and to accelerate the discovery of targeted therapeutic strategies. Ultimately, these findings will contribute to develop nanomaterials-enabled, mechanobiology-driven regenerative medicine approaches for tendinopathy.

Acknowledgements

EU Horizon Europe ERC (Grants No. 772817 and 101171765), FCT project 10.54499/2022.05526.PTDC, and TENET COST Action CA22170.

S38 – O1

Fibrin-gelatin hybrid hydrogels as a platform for biomimetic mechanically active *in vitro* tendon modelling

Meeremans M.[1,2], Oleinik E.O.[3,4], Gross F.[3], Lebedeva A.N.[3], Pien N.[1,2], Monforte Vila X.[4], Peelman L.[5], Teuschl-Woller A.H.[4], Thurner P.J.[3], Van Vlierberghe S.[2], De Schauwer C.[1]
[1]VetSCRU, Dep. of Translational Physiology, Infectiology and Public Health, Faculty of Veterinary Medicine, Ghent University, Belgium; [2]PBM, Centre of Macromolecular Chemistry, Faculty of Sciences, Ghent University, Belgium; [3]ILSB, TU Wien, Vienna, Austria; [4]Dep. Life Science Engineering, University of Applied Sciences Technikum Wien, Vienna, Austria; [5]Laboratory of Animal Genetics, Dep. of Veterinary and Biosciences, Faculty of Veterinary Medicine, Ghent University, Belgium

Introduction

Tendon injuries remain a major clinical challenge in both human and veterinary medicine due to limited intrinsic regeneration and high reinjury rates. Progress in tendon mechanobiology and regenerative therapy development is constrained by the lack of biomimetic *in vitro* models that integrate extracellular matrix composition, viscoelastic mechanics, and cellular responses under physiological loading.

Materials and Methods

In this study, we developed a mechanically active three-dimensional tendon model based on circular hydrogel ring constructs composed of fibrin, norbornene-functionalized gelatin (gelNB, crosslinked using 1,4-dithiothreitol), and their hybrid. To our knowledge, the combination of fibrin with gelNB into a covalently crosslinked hybrid network has not previously been reported. Physicochemical evaluation included swelling and stability assays, SEM imaging, tensile testing, and AFM micro-indentation. Subsequently, primary equine tenocytes were encapsulated and cultured for 21 days under cyclic stimulation (10 % 6h/day 0.5 Hz) or non-stimulated conditions (controls). Cell number, viability, elongation, and alignment were assessed, alongside mRNA and protein expression, and mechanical properties of cell-encapsulated rings.

Results

Hybrid hydrogels integrated the fibrous architecture and energy dissipation of fibrin with the tunable covalent network of gelNB, enabling modulation of viscoelastic properties. While fibrin exhibited the highest bulk tensile modulus (6.7±0.3kPa), hybrids demonstrated enhanced microscale stiffness (6.1±4.1kPa), tendon-like hysteresis (34.6±9.3%), and intermediate long-term stress relaxation (15.3±0.7%). Under cyclic loading, hybrid constructs promoted superior tenocyte elongation, alignment, collagen I/III deposition, and strain-stiffening behaviour resembling native tendon.

Conclusion

Collectively, fibrin-gelNB hybrids provide a bioactive and mechanically instructive platform capturing the interplay between matrix composition, viscoelasticity, and tenocyte function. This system represents a physiologically relevant *in vitro* tendon model with translational potential for mechanobiology studies and regenerative therapy screening, and highlights the promise of fibrin-gelNB hybrids for advanced tissue engineering applications.

Acknowledgements

FWO funding (1S02822/24N, V418424N and 12E4523N), TENET COST Action (CA22170, STSM grant) and Austrian Science Foundation (MatureTissue DK, DOI: 10.55776/DFH28).

Graphical Abstract

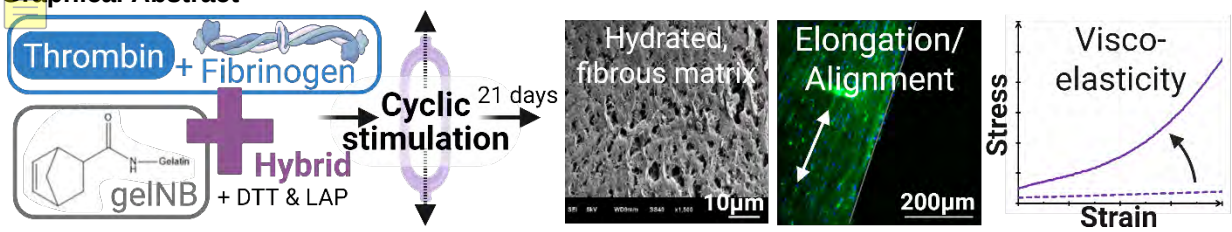

S38 – O2

Toward non-invasive muscle stimulation mediated by NIR-activated polydopamine nanoparticles

Gigante G.[1,2], Carmignani A.[1], Lefevre M.C.[1], Ciofani G.[1]
[1]Istituto Italiano di Tecnologia, Smart Bio-Interfaces; [2]Scuola Superiore Sant'Anna, BioRobotics Institute, Pontedera, Italy

Introduction

Remote stimulation of muscle tissue has long been of interest to the research community, both for traditional biomedical research and, more recently, in the development of biohybrid actuators. Advancements in nanotechnology have introduced photoresponsive nanoparticles as a non-invasive alternative to traditional stimulation techniques. In particular, polydopamine nanoparticles (PDNPs) combine efficient near-infrared (NIR) photothermal conversion with high biocompatibility and antioxidant properties, and have been shown to trigger the contraction of single C2C12 myotubes in 2D cultures upon NIR irradiation[1]. Here, we aim to extend this approach to engineered 3D muscle microtissues and evaluate potential systemic effects in multi-organ platforms, as a next step toward in vivo–relevant applications.

Materials and Methods

Microfluidic devices were fabricated using multilayer photolithography and PDMS-replica moulding. PDNPs were synthesized from dopamine hydrochloride, as previously described[1], and characterized with scanning electron microscopy (SEM) and dynamic light scattering (DLS). In vitro experiments were conducted on C2C12 murine myoblasts cultured in conventional 2D conditions and within microfluidic devices to generate 3D muscle constructs in a collagen/Matrigel matrix. Myoblasts were differentiated into myotubes using low-serum medium, both on dishes and on-chip. The interaction between myotubes and PDNPs was investigated in terms of cytocompatibility, nanoparticle internalization, and potential effects on muscle differentiation. Myotube formation and PDNPs internalization were evaluated by confocal microscopy.

Results

PDNPs exhibit a spheroidal morphology with a narrow size distribution and a strongly electronegative zeta potential (Figure 1a-c). Their uptake by C2C12 cells was evaluated both during myoblast differentiation and in previously differentiated myotubes. Confocal images revealed comparable internalization in both conditions (Figure 1d), suggesting that tissue maturation does not hinder nanoparticle uptake. Microfluidic devices were designed to obtain a self-standing muscle microtissue between two deformable attachment sites (Figure 2a,b), enabling non-invasive monitoring of muscle contraction and quantitative assessment of PDNP-mediated photothermal stimulation. Within this platform, C2C12 cells progressively compacted into a fiber-like microtissue, showing typical characteristics of mature muscle tissue, such as cytoskeletal alignment and multinucleated myotubes (Figure 2c,d).

Conclusion

These findings demonstrate that PDNPs can be efficiently internalized by differentiated C2C12 cells, which are able to organize into mature 3D muscle microtissues on-chip. This establishes a robust platform for investigating PDNP-assisted NIR photothermal stimulation in engineered muscle tissues and for studying remote actuation strategies. Ongoing studies focus on demonstrating NIR-induced contraction of PDNP-loaded muscle microtissues on-chip and on evaluating nanoparticle biodistribution and systemic effects in a liver–muscle multi-organ microphysiological system.

References

[1]Carmignani A., Yamazaki T., Battaglini M., Vu C.Q., Marino A., … & Ciofani G. Cellular activity modulation mediated by near-infrared irradiated polydopamine nanoparticles: in vitro and ex vivo investigation. ACS Nano; 2025; 19(17); 16267-16286.

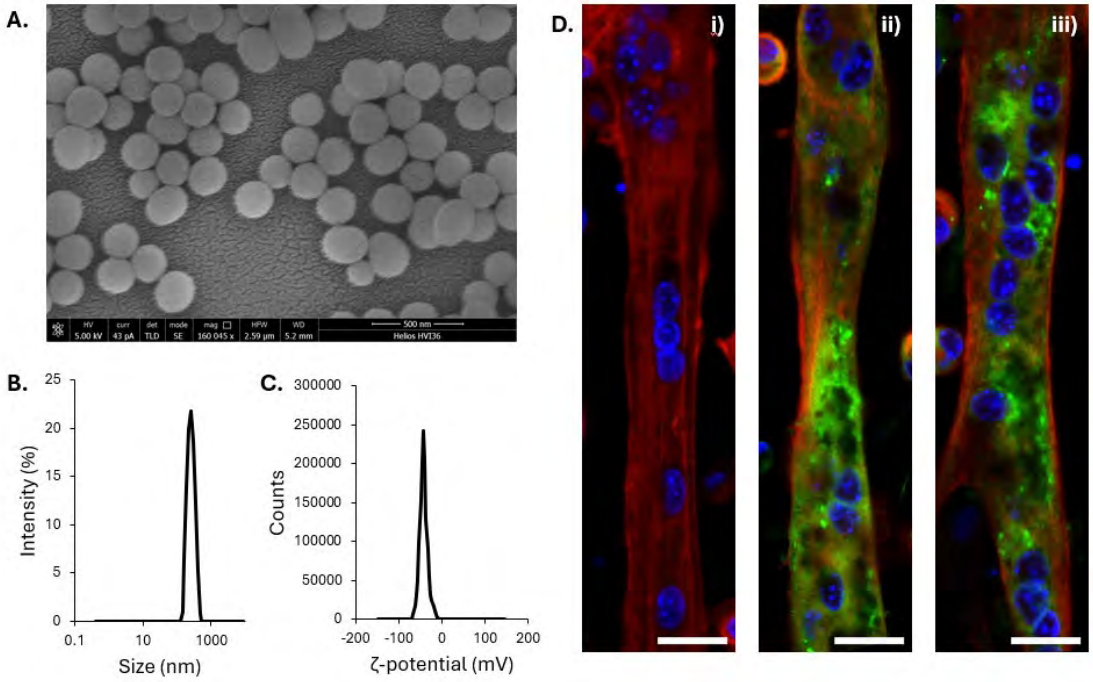

Figure 1. PDNPs characterization and cellular uptake. (A) Representative SEM image. (B) Hydrodynamic diameter and (C) ζ-potential analysis. (D) Nanoparticle internalization (ii) during myoblast differentiation and (iii) on differentiated myotube compared to (i) non-treated control (nuclei in blue, F-actin in red, PDNPs in green). Scale bars 20µm.

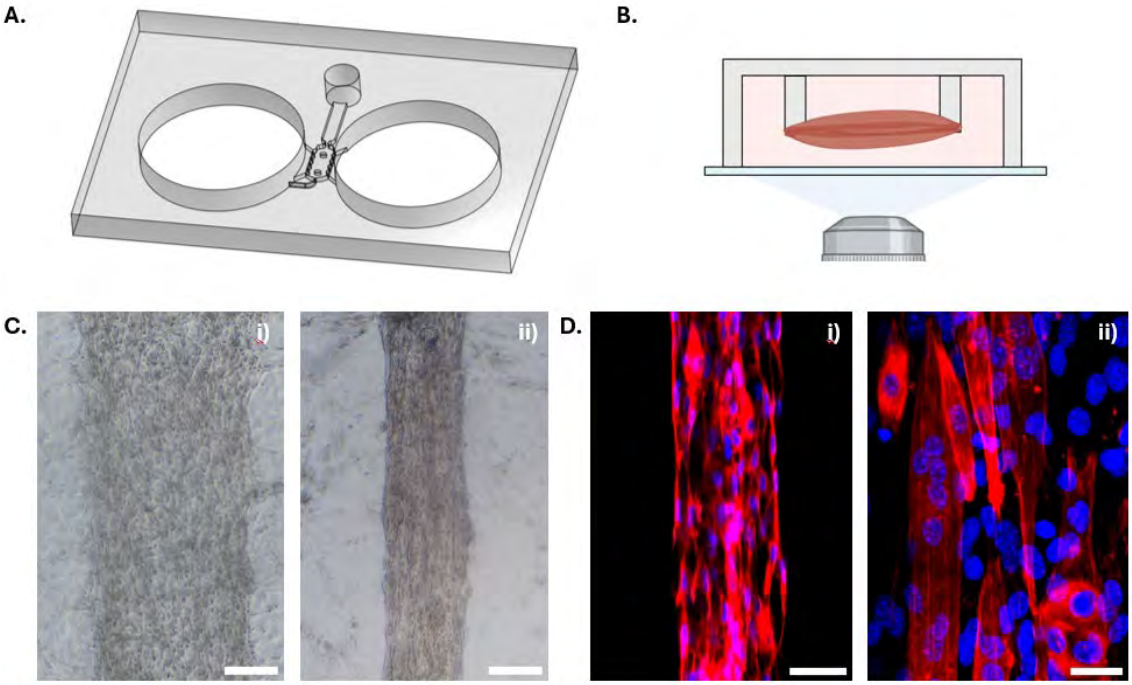

Figure 2. Muscle-on-chip design and characterization. (A) Device design and (B) schematic illustration of muscle microtissue placement on the anchors. (C) Microtissue compaction from (i) day 1 to (ii) day 9 of differentiation in the device. Scale bars 200µm. (D) Muscle microtissue maturation (nuclei in blue, F-actin in red). Scale bars (i) 50µm, (ii) 30µm.

Adipose-derived stromal cells as a model for evaluating peptide-functionalized chitosan biomaterials for musculoskeletal tissue regeneration

Pikuła M.[1], Tymińska A.[1], Skoniecka A.[1], Zawrzykraj M.[2], Karska N.[3], Banach-Kopeć A.[4], Mania S.[4], Kondej K.[5], Tylingo R.[4], Rodziewicz-Motowidło S.[2]
[1]Laboratory of Tissue Engineering and Regenerative Medicine, Division of Embryology, Medical University of Gdańsk (MUG); [2]Division of Clinical Anatomy, MUG; [3]Dept. of Biomedical Chemistry, University of Gdańsk (UG); [4]Dept. of Chemistry, Technology and Biotechnology of Food Gdańsk, University of Technology (UT); [5] Dept. of Plastic Surgery, MUG, Poland

Introduction

The development of instructive biomaterials capable of directing stem cell behavior represents a central challenge in musculoskeletal tissue engineering[1]. Adipose-derived mesenchymal stromal cells (AD-MSCs) constitute an abundant and clinically relevant cell source that can be readily isolated from adipose tissue obtained during routine surgical procedures. Due to their high proliferative capacity and multipotent differentiation potential, AD-MSCs provide a valuable translational model for studying cell- biomaterial interactions[2]. Chitosan, a naturally derived polysaccharide, has emerged as a versatile scaffold material due to its biocompatibility, biodegradability, and chemical versatility[3-4]. In this study we propose a biomaterial design strategy based on peptide-functionalized chitosan scaffolds aimed at instructing AD-MSCs responses toward musculoskeletal tissue regeneration.

Materials and Methods

Human AD-MSCs were isolated from subcutaneous adipose tissue using enzymatic digestion (collagenase) and expanded *in vitro*. Cell phenotype was confirmed by flow cytometry analysis of surface markers (CD73, CD90, CD105 positive; CD34, CD45 negative) and by *in vitro* differentiation. Bioactive peptides derived from copine (CPNE) proteins were synthesized using solid- phase peptide synthesis and incorporated into chitosan-based biomaterial constructs. Cell viability and cytotoxicity were analyzed using XTT metabolic activity and lactate dehydrogenase (LDH) release assays. Lineage-specific differentiation (adipocytes, osteocytes, chondrocytes) was assessed using biochemical and histological analyses of collagen synthesis, glycosaminoglycan (GAG) production and calcium deposition.

Results

Chitosan scaffolds supported proliferation and survival of AD-MSCs confirming their high cytocompatibility. Functionalization of chitosan with copine-derived peptides enhanced cellular responses, including increased migration and extracellular matrix production and promoted lineage-specific differentiation. Elevated markers of chondrogenesis and osteogenesis were observed in peptide-functionalized biomaterials compared with non-functionalized controls. Importantly, the constructs showed no detectable cytotoxic or immunogenic effects.

Conclusion

The results demonstrate that peptide-functionalized chitosan scaffolds can act as instructive biomaterials capable of directing mesenchymal stromal cell behavior. This approach highlights the potential of combining biofunctionalized biomaterials with clinically relevant stem cell models for the development of advanced regenerative strategies targeting musculoskeletal tissues, including cartilage and bones.

Acknowledgements

This work was supported by the National Center for Research and Development, Poland (Grant TECHMATSTRATEG2/ 410747/11/2019, acronym BIONANOVA)

References

1. Deptuła M, Zawrzykraj M, Sawicka J, Banach-Kopeć A, Tylingo R, Pikuła M. Application of 3D- printed hydrogels in wound healing and regenerative medicine. Biomed Pharmacother. 2023 Nov;167:115416. doi: 10.1016/j.biopha.2023.115416.
2. Czerwiec K, Zawrzykraj M, Deptuła M, Skoniecka A, Tymińska A, Zieliński J, Kosiński A, Pikuła M. Adipose-Derived Mesenchymal Stromal Cells in Basic Research and Clinical Applications. Int J Mol Sci. 2023 Feb 15;24(4):3888. doi: 10.3390/ijms24043888.
3. Tymińska A, Karska N, Skoniecka A, Zawrzykraj M, Banach-Kopeć A, Mania S, Zieliński J, Kondej K, Gurzawska-Comis K, Skowron PM, Tylingo R, Rodziewicz-Motowidło S, Pikuła M. A novel chitosan-peptide system for cartilage tissue engineering with adipose-derived stromal cells. Biomed Pharmacother. 2024 Dec;181:117683. doi: 10.1016/j.biopha.2024.117683.
4. Banach-Kopeć A, Mania S, Tylingo R, Wawrzynowicz A, Pawłowska M, Czerwiec K, Deptuła M, Pikuła M. Thermosensitive composite based on agarose and chitosan saturated with carbon dioxide. Preliminary study of requirements for production of new CSAG bioink. Carbohydr Polym. 2024 Jul 15;336:122120. doi: 10.1016/j.carbpol.2024.122120.

S38 – O4

Synthesis of a highly soluble, biodegradable and conducting copolymer for biomedical engineering applications

Alves D.M.[1], Torresi S.I.C.[1], Catalani L.H.[1]
[1]Institute of Chemistry, University of São Paulo, São Paulo, Brazil

Introduction

3D printing of biomaterials remains constrained due to the limited diversity of resins, particularly for high-resolution technologies. This gap becomes even more pronounced in the context of smart biomaterials, which hold the promise of enabling a wide range of therapeutic applications[1,2].

Conductivity is a valuable property in tissue engineering, as most cellular structures rely on electrical signals for communication. Conducting polymers (CPs) are particularly promising due to their unique combination of conductivity and versatility in their material properties. Within this class, poly(3,4-ethylenedioxythiophene) (PEDOT) is particularly suitable for biomedical applications, offering superior redox stability in biological environments with low potential excursions[2].

Nevertheless, CPs are challenging to process due to their low solubility. Common strategies to improve processability include blending or copolymerization. The latter approach yields a more homogenous surface and can enhance biocompatibility and biodegradability by incorporating a biodegradable polyester block[3].

3D printing techniques impose additional material requirements. For instance, Digital Light Processing (DLP) requires materials that form a gel upon light exposure. To meet this criterion, the material must contain functional groups that can undergo photocrosslinking. A viable approach is to introduce acryloyl groups into the copolymer structure to enable such behavior[1].
Here, we aimed to integrate these properties into a single copolymer to overcome limitations in resin diversity, thereby enabling the fabrication of smart scaffolds via advanced 3D printing for tissue engineering applications.

Materials and Methods

The macromonomer (EDOT-PCl) was synthesized through ring-opening polymerization of caprolactone and further polymerized through radical polymerization, yielding PEDOT-g-PCl. Following, the material was functionalized with acryloyl groups (PEDOT-g-PCl-AC) (Fig. 1). Curing of the resins was performed in a UV chamber (405nm). Rheological and crosslinking properties of the materials were characterized by photorheology. Cyclic voltammetries of coated electrodes were performed in a ferro-/ferricyanide solution.

Results

The copolymers and their acryloyl derivatives had their structure elucidated by ^{1}H NMR, MALDI-TOF, and GPC. Cyclic voltammetry (Fig. 2) confirmed the electroactive properties of PEDOT-g-PCl, PEDOT-g-PCl-AC and the crosslinked film, revealing that the material retained its ability to allow electron transfer even after curing. Storage and loss modulus of the resins before and after UV exposure revealed that the resins had a gelation time of 12 seconds.

Conclusion

Synthesis of a functionalized, conductive, and highly soluble PEDOT derivative was successfully achieved, alongside the development of potential resins for 3D biomedical applications. Furthermore, this material shows potential across a wide range of applications involving conducting polymers.

Acknowledgements

The authors acknowledge funding by FAPESP (#2018/13492-2), CAPES and CNPq.

References

[1]Yu, C.; et al.; Photopolymerizable Biomaterials and Light-Based 3D Printing Strategies for Biomedical Applications. *Chem. Rev.*; 2020, 120, 10695–10743.
[2]Balint, R.; Cassidy, N. J.; Cartmell, S. H.; Conductive polymers: towards a smart biomaterial for tissue engineering. *Acta Biomater.*; 2014, 10, 2341-2353.
[3]Guimard, N. K.; Gomez, N.; Schmidt, C. E.; Conducting polymers in biomedical engineering. *Prog. Polym. Sci.*; 2007, 32, 876-921

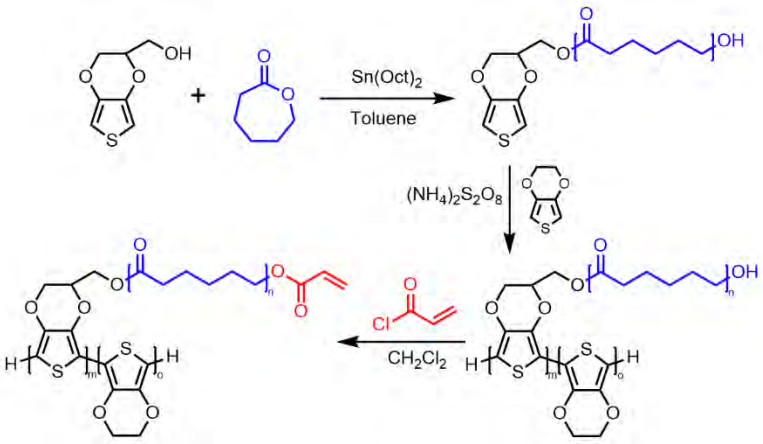

Fig. 1: Schematic representation of ring opening polymerization of the macromonomer, followed by copolymerization and further acryloyl chloride modification.

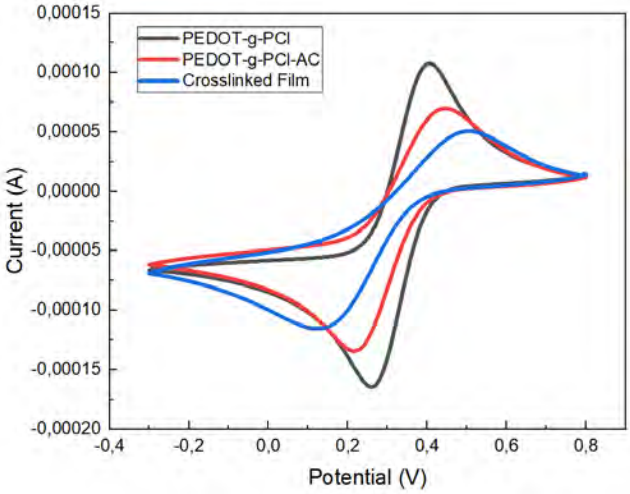

Fig. 2: Cyclic voltammograms obtained for the conducting copolymer, conducting copolymer acrylate and crosslinked film in 0,1 M KCl solution. The ferro-/ferricyanide redox couple was used as a probe.

S38 – O5

Linking multi-omics, spatial imaging, and contractile function to benchmark engineered skeletal muscle maturation

Celikkin N.[1,2], Volpi M.[3], Maulliari F.[1], Promovych Y.[1], Vandenbosch M.[2], Heeren M.A.R.[2], Costantini M.[1]
[1]Institute of Physical Chemistry, Polish Academy of Sciences, Warsaw, Poland; [2]M4i, Maastricht University, Maastricht, The Netherlands; [3]Materials Science and Engineering, Warsaw University of Technology, Warsaw, Poland

Introduction

Engineered skeletal muscle is commonly evaluated using morphological and endpoint molecular markers, yet these measures alone do not adequately capture functional maturity. Because contractile performance emerges from coordinated changes in tissue architecture, molecular composition, and spatial organization, there is a need for benchmarking strategies that link these layers to force generation. Multi-omics and multi-model imaging now offer an opportunity to identify the structural and molecular programs associated with improved function in engineered muscle tissues.

Materials and Methods

A *multimodal omics workflow* was established to characterize engineered skeletal muscle across maturation stage, architecture, and training condition. For integrated lipidomics and proteomics, lipids and proteins were isolated from the same fresh-frozen constructs using a single-step extraction protocol. Lipids were extracted with methyl tert-butyl ether, re-extracted from the aqueous phase, dried, reconstituted in ACN:IPA, and analyzed by LC-MS/MS using a Vanquish UHPLC system coupled to an Orbitrap Exploris 480. Proteins from the aqueous fraction were extracted in 5 M urea, separated by SDS-PAGE, fractionated, and subjected to in-gel tryptic digestion following reduction, alkylation, destaining, washing, and peptide extraction. Peptides were analyzed by nanoUHPLC-Q Exactive HF in DIA mode, and raw data were processed in DIA-NN v1.8.1 against the SwissProt Mus musculus database. In parallel, *a multi-model imaging workflow* combining spinning-disk microscopy, targeted two-photon imaging, optional second-harmonic generation, and confocal microscopy was designed to quantify 3D alignment, bundle continuity, laminin organization, nuclear anisotropy, and sarcomeric periodicity.

Results

The integrated lipidomic and proteomic profiling revealed a coordinated maturation of the engineered skeletal muscle constructs marked by coupled metabolic and membrane remodeling. During maturation, enrichment of bioenergetic, calcium-signaling, trafficking, redox, and lipid-remodeling proteins were observed together with selective depletion of triacylglycerol, diacylglycerol, phosphatidylethanolamine, cardiolipin, ceramide, and glycosphingolipid species. This consistent shift from storage to matrix-dominant remodeling strongly indicated the mitochondrial specialization and active phospholipid reorganization.
Relative increases in lysophosphatidylcholine, cholesteryl ester, and selected ether-phosphatidylcholine species further supported activation of membrane remodeling pathways linked to lysophospholipid turnover, glycerolipid mobilization, and mitochondrial phospholipid homeostasis. Collectively, these data identified candidate protein-lipid interaction axes that distinguish maturation of engineered muscle states and suggest that functional maturation is accompanied by a metabolic handover toward a more bioenergetically organized tissue phenotype. These molecular signatures have also been coincided with imaging-based hallmarks of structural maturation, including enhanced 3D alignment, improved bundle continuity, more continuous laminin organization, greater nuclear anisotropy, and more pronounced sarcomeric periodicity in mature constructs.

Conclusion

These preliminary results demonstrate the potential of combining multi-omics, hierarchical imaging, and contractile force measurements to resolve maturation-associated states in engineered skeletal muscle. The integrated approach suggests that progression toward a mature phenotype is accompanied by coordinated metabolic, membrane, and structural remodeling and provides a framework for identifying candidate protein-lipid interaction linked to functional performance. Collectively, this work aims to establish a more predictive and mechanistically informative benchmark for engineered skeletal muscle maturation and performance.

Acknowledgements

The results are based on research funded by the National Science Centre, Poland, under the SONATINA 2023/48/C/ST5/00230 project. We acknowledge the Laboratory of Imaging Tissue Structure and Function, at the Nencki Institute, the Leader of the Polish Euro-BioImaging Node “Advanced Light Microscopy NodePoland” supported by the Minister of Education and Science based on contract No 2022/WK/05, for their assistance.

S39
Functional and biodegradable nanomaterials innovations and nanotoxicological insights from alternative models

S39 – K1
Next-generation tools for nanotoxicology: New approach methodologies to assess nanomaterial safety

Alfaro-Moreno E.
International Iberian Nanotechnology Laboratory

The rapid expansion of engineered nanomaterials (ENMs) across industrial, medical, and consumer applications highlights the urgent need for reliable and human-relevant approaches for their safety assessment. Traditional toxicity testing frameworks, relying on animal models and traditional 2D in vitro models, often fall short in capturing the complex interactions of nanomaterials with relevant biological systems and in the case of animal models, ethical concerns are reducing their use. New Approach Methodologies (NAMs) provide an integrative, mechanistically informed path forward for nanotoxicology.

Here we explore how NAMs—encompassing advanced in vitro, in vivo, and in silico systems—are transforming our understanding of nanomaterial toxicity/safety. Advanced multi-cellular (2.5 and 3D models) and organoid systems further enhance physiological relevance by capturing complex intercellular interactions. Organ-on-chip platforms, including lung- and skin-on-chip models, allow simulation of realistic tissue microenvironments and dynamic exposures, bridging the gap between cellular assays and whole-organism biology. In parallel, alternative in vivo models such as Caenorhabditis elegans, planarians, and Galleria mellonella provide efficient, ethically acceptable ways to study organismal responses and conserved toxicity pathways. These experimental approaches can be enriched using in silico models, including computational toxicology, structure–activity relationships, and physiologically based kinetic modeling, offering predictive power. Together, these NAMs form a synergistic toolbox capable of generating mechanistic data, helping hazard assessment, and supporting regulatory decision-making for nanomaterials.

Acknowledgement
This work is funded by the European Commission under the HORIZON-CL4-2022-DIGITAL-EMERGING-01 (N.101092971)

S39 – K2
Engineered materials based on natural eutectic solvents to embed functional entities

Beloqui Elizazu A.
POLYMAT, Spain

S39 – O1

Fucoidan-functionalized multilayer nanoparticles for targeting activated endothelial cells

Mansoori-Kermani A.[1,2,3], Battaglini M.[2], Inchaurraga-Llamas A.[4], Guevara-Pantoja P.E.[4], Benito-Lopez F.[4], Basabe-Desmonts L.[4,5], Ciofani G.[2], Larrañaga A.[1]
[1]Dept. Mining-Metallurgy Engineering and Materials Science, Polymat, University of the Basque Country, Bilbao, Spain; [2]Smart Bio-Interfaces Group, Istituto Italiano di Tecnologia, Pontedera; [3]The Biorobotics Institute, Scuola Superiore Sant´Anna, Pontedera, Italy; [4]Analytical Microsystems & Materials for Lab-on-Chip Group, University of the Basque Country, Vitoria-Gasteiz; [5]Basque Foundation of Science, IKERBASQUE, Bilbao, Spain

Introduction

In this study, we fabricated multilayered polymer nanoparticles and functionalized their surface with fucoidan (FUC), aiming to enhance their interaction with P-selectin—an adhesion molecule upregulated in activated endothelial cells of the blood–brain barrier.[1] The main aim of this work is to examine in detail the behavior and interactions of FUC-functionalized nanoparticles under biologically relevant conditions, employing complex biological fluids (e.g., human serum), microfluidic platforms, and in vitro cellular models.

Materials and Methods

Multilayered nanoparticles were fabricated using the layer-by-layer assembly strategy, employing FUC as the outermost layer. The resulting nanoparticles were characterized in terms of surface ζ-potential, morphology, and colloidal stability in biological fluids. The dynamic interaction of the nanoparticles with P-selectin was assessed in real time using a custom microfluidic micropatterned platform, with bovine serum albumin (BSA) serving as a non-specific binding control. Cytocompatibility, neuro-inflammatory responses, and cellular uptake were evaluated in nervous system–relevant cell models, including murine microglia and brain endothelial cells, both in resting and activated conditions.

Results

The prepared formulations yielded stable multilayered nanoparticles displaying a strongly negative surface ζ-potential (< -20 mV). FUC functionalization improved colloidal stability in both phosphate-buffered saline and biological fluids, maintaining a narrower size distribution throughout the incubation period (Figure 1). Under dynamic flow conditions, FUC-coated nanoparticles exhibited reduced nonspecific interaction with BSA while markedly enhancing their binding to P-selectin (Figure 2A-C). None of the formulations showed cytotoxicity at concentrations up to 100 µg/mL, nor did they induce up-regulation of pro-inflammatory markers in murine microglia (tumor necrosis factor-α, TNF-α; interleukin-1β, IL-1β; interleukin-6, IL-6), supporting the biosafety of the developed nanoparticles. Additionally, uptake of FUC-functionalized nanoparticles by activated endothelial cells was significantly enhanced—showing more than a two-fold increase compared with non-activated cells (Figure 2D).

Conclusion

These findings demonstrate that surface functionalization of nanoparticles with FUC effectively promoted their specific interaction with P-selectin and their uptake by activated endothelial cells. We are currently evaluating the ability of these FUC-functionalized nanoparticles to traverse the BBB using advanced microfluidic models incorporating human iPSC-derived endothelial cells and primary astrocytes.

Acknowledgement

We acknowledge the financial support of TheraTools (Ref. 101073404. HORIZON-MSCA-2021-DN-01).

Reference

[1]Tylawsky D.E., Kiguchi H., Vaynshteyn J., Gerwin J., Shah J., Islam T., Boyer J.A., Boué D.R., Snuderl M., Greenblatt M.B., Shamay Y., Raju G.P., Heller D.A. P-selectin-targeted nanocarriers induce active crossing of the blood-brain barrier via caveolin-1-dependent transcytosis. *Nature Materials* 2023; 22(3); 391-399.

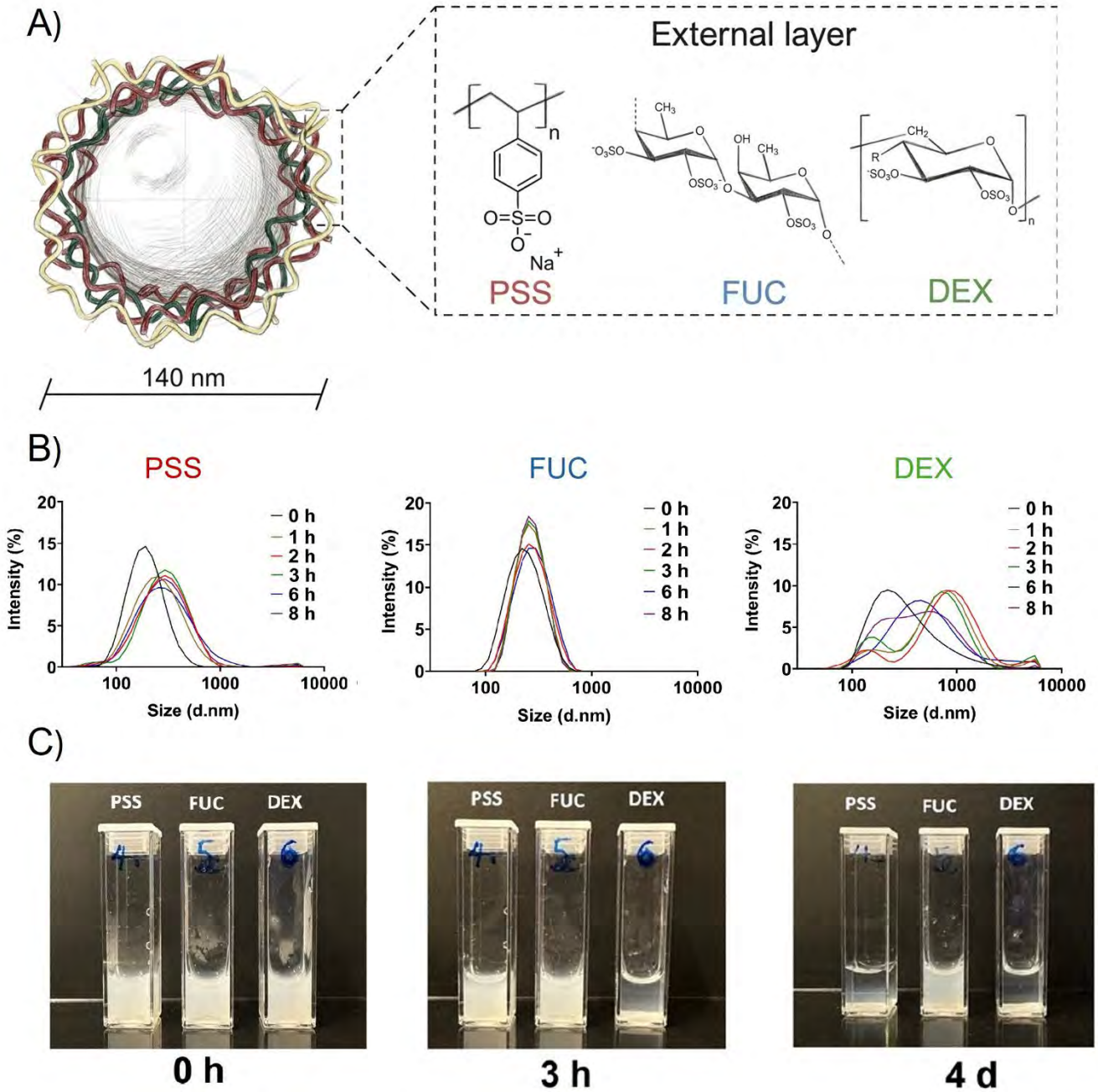
A)
External layer
PSS
FUC
DEX
140 nm
B)
PSS
FUC
DEX
Intensity (%)
Size (d.nm)
0 h
1 h
2 h
3 h
6 h
8 h
C)
PSS
FUC
DEX
0 h
3 h
4 d

Figure 1.

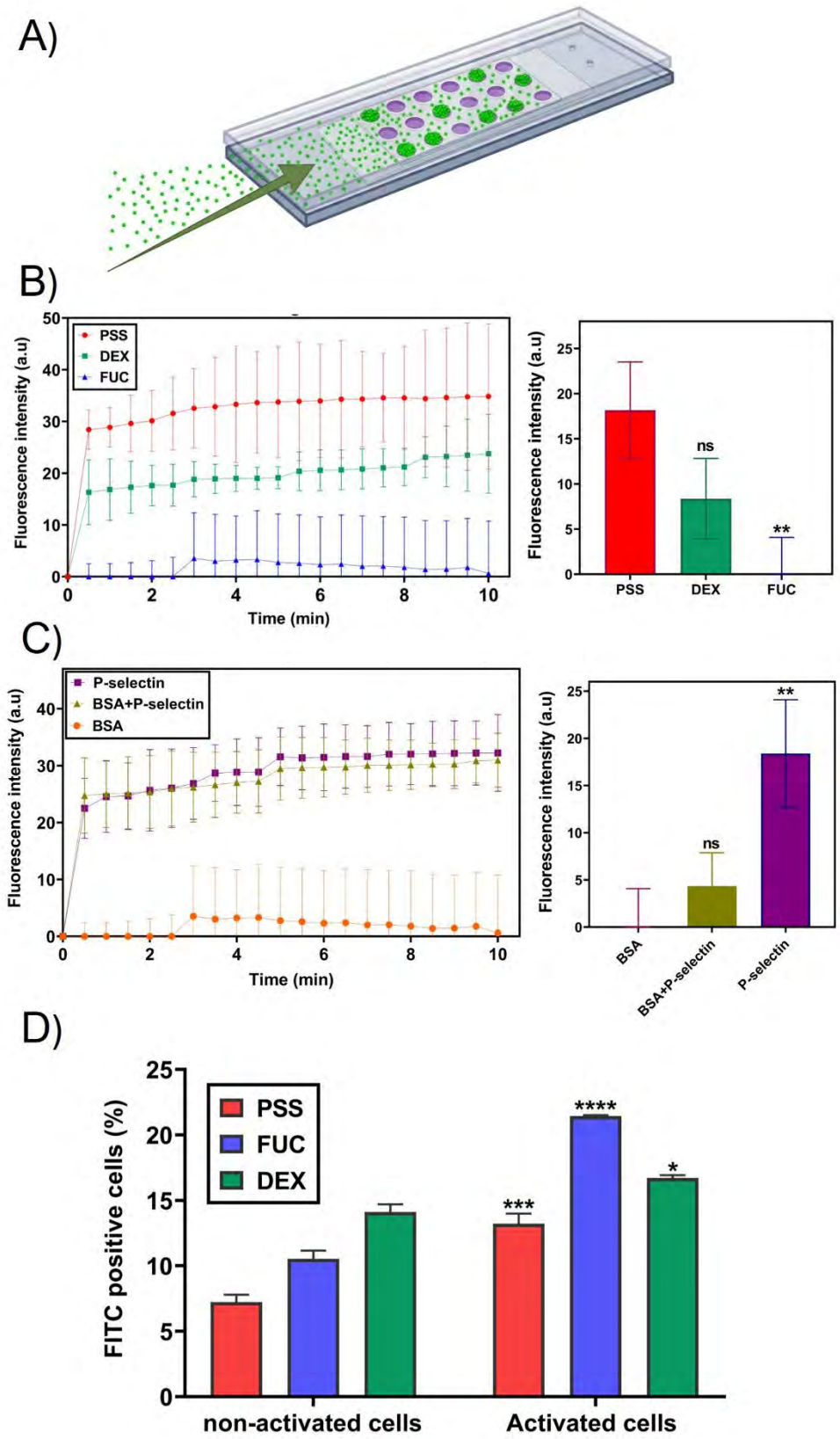
A)
B)
PSS
DEX
FUC
Fluorescence intensity (a.u)
Time (min)
ns
**
C)
P-selectin
BSA+P-selectin
BSA
D)
FITC positive cells (%)
non-activated cells
Activated cells
***
****
*

Figure 2.

S39 – O2

Cell membrane-coated polydopamine nanoparticles for photothermal therapy against glioblastoma

Carmignani A.[1], De Campo M.[1,2], Lefevre M.C.[1], Emanet M.[1], Battaglini M.[1], Marino A.[1], Beola L.[1], Ciofani G.[1]
[1]Center for Materials Interfaces, Istituto Italiano di Tecnologia, Pontedera; [2]Dept. of Mechanical and Aerospace Engineering, Politecnico di Torino, Torino, Italy

Introduction

Glioblastoma remains one of the most aggressive and treatment-resistant brain tumors, highlighting the need for more effective and selective therapeutic strategies. Photothermal therapy (PTT) mediated by near-infrared (NIR)-responsive nanomaterials is emerging as a promising approach for local tumor ablation. In this work, we developed polydopamine nanoparticles (PDNPs) coated with cell membranes (CM-PDNPs) derived from patient-derived glioblastoma cells (GBM-P1), to exploit homotypic targeting to improve nanoparticle internalization and enhance PTT efficacy. The study investigated the biocompatibility, cellular uptake, and therapeutic performance of these biomimetic nanoparticles in 2D and 3D models.

Materials and Methods

Patient-derived glioblastoma cells obtained from surgical resection were used to perform experiments and prepare CM-PDNPs (GBM-P1 and GBM-P2). Nanoparticles' biocompatibility was assessed in 2D cultures in the absence of laser irradiation. The effect of membrane coating on nanoparticle internalization was then evaluated in 2D under both static conditions and dynamic conditions, as well as in GBM spheroids. For photothermal treatment, cells or spheroids incubated with CM-PDNPs were exposed to NIR laser irradiation for 10 min/day over 3 consecutive days. Therapeutic efficacy was assessed by monitoring tumor cell proliferation arrest and cell death. Moreover, a more advanced *in vivo*-like validation is currently being investigated by grafting patient-derived glioblastoma spheroids onto the chorioallantoic membrane (CAM) of quail embryos (*Coturnix japonica*), followed by intravenous nanoparticle administration and localized NIR irradiation.

Results

Polydopamine nanoparticles showed excellent biocompatibility, indicating that the nanoplatform itself did not induce relevant cytotoxic effects under non-irradiated conditions. Membrane functionalization improved nanoparticle internalization, consistent with a homotypic targeting effect. This enhancement was observed not only in conventional 2D static cultures but also under dynamic microfluidic conditions (Figure 1a) and in 3D spheroid models, supporting the robustness of the targeting strategy in increasingly complex experimental settings. The membrane functionalization also proved to be patient-specific (Figure 1b). Upon NIR irradiation, the combination of CM-PDNPs and NIR laser treatment induced a marked anti-tumor effect in both 2D and 3D models, resulting in strong inhibition of tumor cell proliferation and pronounced cell death (Figure 2).

Conclusion

This study demonstrates that cell CM-PDNPs represent a promising biomimetic platform for glioblastoma photothermal therapy. The nanoparticles are biocompatible, display enhanced uptake in patient-derived tumor models, and effectively induce tumor growth arrest and cell death upon NIR stimulation. Ongoing studies in the quail embryo CAM model will provide further insight into the translational potential of this approach in a more complex and clinically relevant setting.

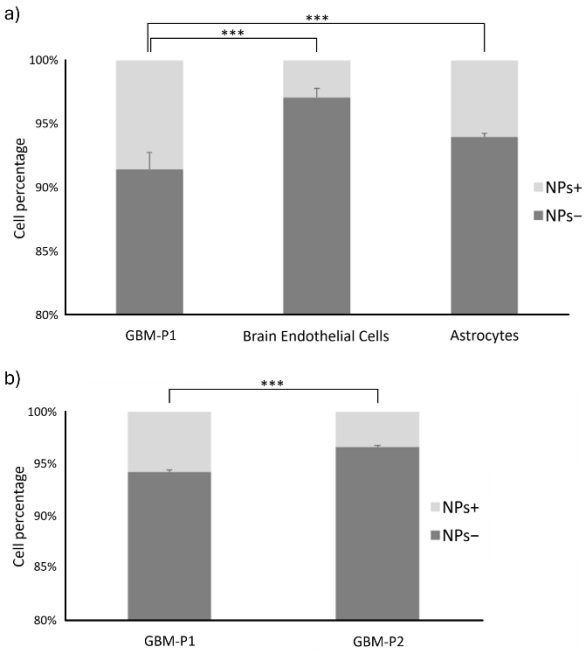

Figure 2. Nanoparticle internalization in 2D dynamic conditions. a) CM-PDNPs uptake evaluated in GBM patient-derived cells, brain endothelial cells, and astrocytes. NP-positive cells (NPs+) are shown in light gray, and NP-negative cells (NPs-) in dark gray. b) CM-PDNPs uptake comparison between different GBM patient-derived cell populations. NPs+ are shown in light gray while NPs- are shown in dark gray (*** = $p < 0.001$).

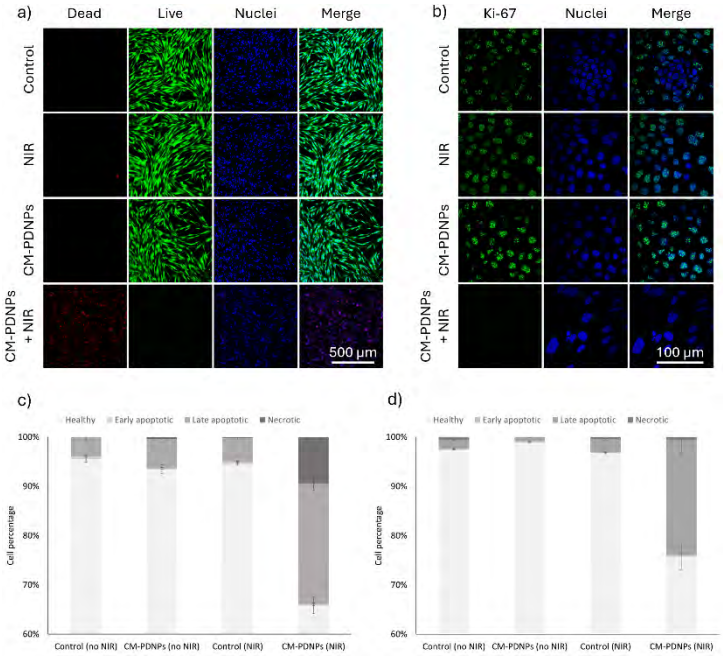

Figure 1. Analysis of photothermal treatment on GBM patient-derived cells. a) Representative confocal microscopy images of LIVE/DEAD assay (dead cells in red, live cells in green, nuclei in blue). b) Representative confocal microscopy images of Ki-67 proliferative marker expression (Ki-67 in green, nuclei in blue). c) and d) apoptosis/necrosis levels performed respectively on 2D and 3D cultures.

S39 – O3

Evaluating cytotoxicity of fibrous and hydrogel biomaterials to inform scaffold design for conjunctival repair

Hollett J.A.[1], Williams R.L.[1], Liptrott N.J.[2], Bosworth L.A.[1]
[1]Dept. of Eye and Vision Science, University of Liverpool; [2]Immunocompatibility Group, Department of Pharmacology and Therapeutics, University of Liverpool, Liverpool, UK

Introduction

The conjunctiva is a mucosal membrane which covers the sclera and inside of the eyelids and contributes to the maintenance of the ocular surface. When a substantial amount of conjunctiva has been injured, traditional surgical interventions (primary closure, conjunctival autografts) are not always suitable due to insufficient healthy tissue remaining, and the alternative, amniotic membrane, carries a risk of graft rejection and transmission of infectious disease. Thus, a need remains for an optimal tissue replacement that facilitates regeneration of the conjunctiva.

Aim

To evaluate novel substrates - electrospun (ELSP) fibres, melt-electrowritten (MEW) fibres and hydrogels - for cytotoxicity and subsequent suitability as a potential therapeutic replacement for native conjunctival tissue in the form of a fibre/gel composite scaffold (Fig.1).

Materials and Methods

ELSP fibres were fabricated from 10%w/v poly(ε-caprolactone) (PCL) in 1,1,1,3,3,3-hexafluoroisopropanol, and spinning parameters: 21cm needle-collector distance, 5mL/hour flow rate, voltage of +20kV (needle) and -4kV (collector), fibres collected on a rotating mandrel (200rpm). MEW fibres were fabricated from PCL with a needle-collector distance of 3.5mm and +5kV applied voltage. Hydrogel samples were prepared as per manufacturer protocols for PhotoGel (50 and 95) and PhotoAlginate, and poly-epsilon-lysine (PeK) hydrogels were prepared via either diacid crosslinking (PeK-DA) or methacrylation and subsequent UV-crosslinking (PeKMA).
Materials were disinfected in 70% ethanol for 1 hour, then rinsed in sterile PBS for 5 minutes x 3.
Using an immortalised human conjunctival epithelial cell line (IM-HConEpiC; 5×10^4 cells/mL), WST-1 and lactate dehydrogenase (LDH) assays were performed. Assays included a cell free control, a negative control with known outcome (lysis buffer) and an untreated control (cells seeded into well without material). Assays were performed either direct (cells seeded onto materials in the well for 24h) or indirect (cells treated with media which had been incubated with material for 72 hours prior to treatment).

Results

Both direct and indirect cytotoxicity assays demonstrated comparable metabolic activity and LDH release to untreated controls across all materials, indicating no overt cytotoxic effects from either direct scaffold contact or potential leachates in the initial screening at the chosen time-points (Fig.2).

Conclusion

All materials demonstrated cytocompatibility comparable to untreated controls. This preliminary screening suggests that both fibrous and hydrogel systems may represent promising components for future scaffold design aimed to support conjunctiva repair. Further evaluation of biocompatibility and sensitisation in accordance with ISO-10993 standards will be required before translational applications can be considered.

Funding

This PhD work was funded by the University of Liverpool.

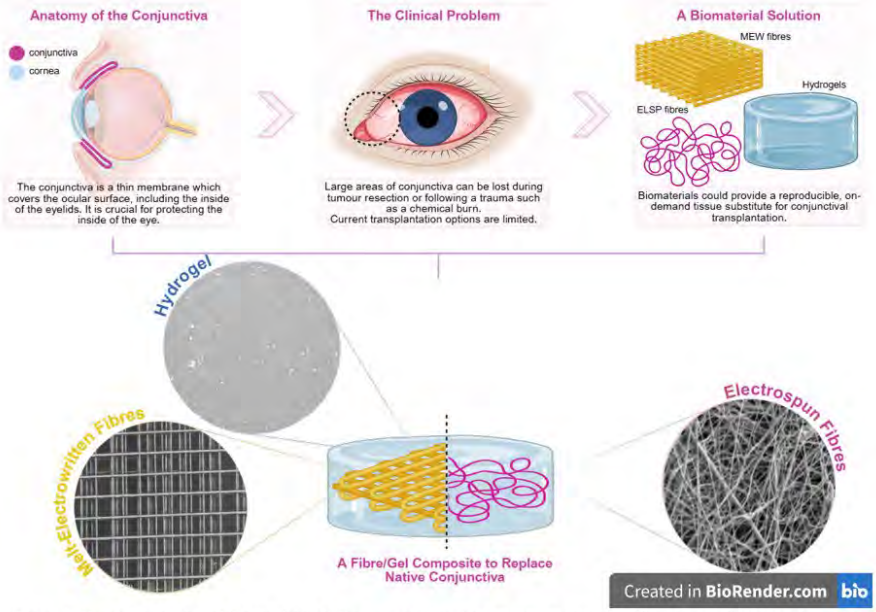

Figure 1. Graphic overview of the anatomy of the conjunctiva, the key clinical issue and the proposed composition of a biomaterial composite tissue replacement for conjunctival transplantation, composed of either a hydrogel reinforced with electrospun fibres, or a hydrogel reinforced with melt-electrowritten fibres. Scanning electron microscopy images of a hydrogel, electrospun fibres and melt-electrowritten fibres are included to show topographical differences between the materials. (Created in BioRender.com)

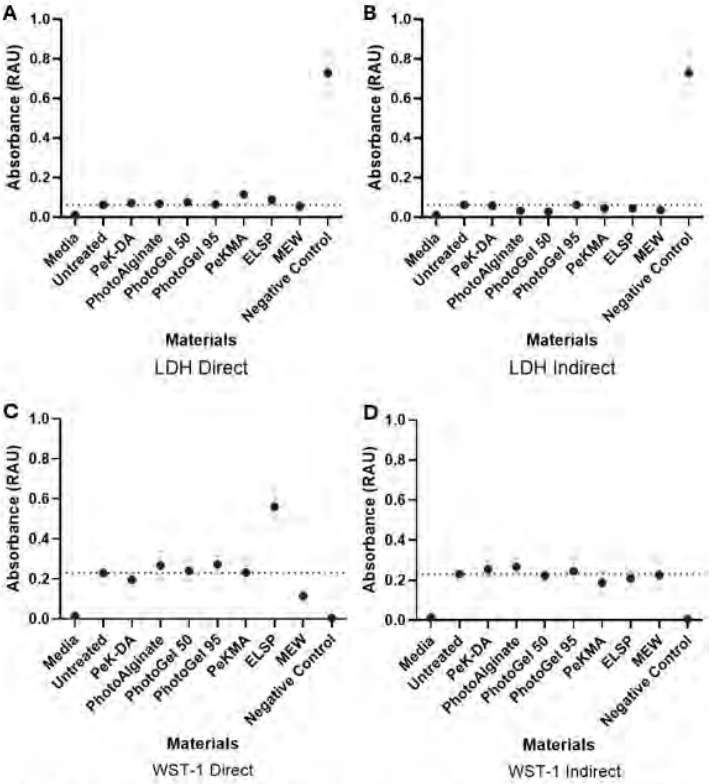

Figure 2. Cytotoxicity assays on all material groups shown as Relative Absorbance Units. Experimental controls: Media (media without cells), Untreated (cells seeded into a well with no treatment added), Negative Control (lysis buffer). Line = Average of untreated control, n=3. Kruskal-Wallis showed no statistical significance between RAU of materials compared to the untreated control.

S39 – O4

Development of tacrine and gallic acid conjugated nanotherapeutics for Alzheimer's disease

İğdeli G.[1], Temel B.A.[2]
[1]Dept. of Biotechnology, Institute of Health Sciences, Bezmialem Vakif University; [2]Dept. of Pharmaceutical Chemistry, Faculty of Pharmacy, Bezmialem Vakif University, Istanbul, Türkiye

Introduction

Alzheimer's disease (AD) is a progressive neurodegenerative disorder characterized by memory loss and cognitive decline, accounting for approximately 60–80% of dementia cases worldwide. Although no curative treatment currently exists, available therapies can alleviate symptoms and partially slow disease progression. Acetylcholinesterase inhibitors (AChEIs) represent the first approved pharmacological agents for AD treatment. Among these compounds, tacrine exhibits strong AChE inhibitory activity and a simple molecular structure, making it an attractive scaffold for the development of multitarget-directed agents. In addition, gallic acid, a naturally occurring polyphenolic compound, shows strong antioxidant and neuroprotective effects by reducing reactive oxygen species (ROS) formation and preventing apoptosis. This study aims to develop a nanotherapeutic strategy for AD treatment through the synthesis of polymer–drug conjugates incorporating tacrine and gallic acid.

Materials and Methods

Three amphiphilic copolymers incorporating tacrine and gallic acid at different positions within the polymer architecture were synthesized *via* reversible addition–fragmentation chain transfer (RAFT) polymerization to develop multifunctional nanotherapeutic systems for AD (Figure 1). The resulting polymers were characterized using chromatographic and spectroscopic techniques, to confirm their molecular structure and composition. Subsequently, the amphiphilic copolymers were allowed to self-assemble in aqueous media to form polymeric micelles, whose size distribution and morphology were determined using dynamic light scattering (DLS) and transmission electron microscopy (TEM). Furthermore, the antioxidant and anticholinesterase activities of the micellar systems were evaluated to investigate their potential multifunctional therapeutic effect. Finally, the cytotoxicity and cell viability of the developed nanostructures were assessed and compared using the human neuroblastoma cell line (SH-SY5Y).

Results

The synthesized amphiphilic copolymers successfully self-assembled into nanosized polymeric micelles in aqueous media, as confirmed by DLS and TEM analyses. Comparative evaluation of the micellar systems showed that micelles containing both tacrine and gallic acid exhibited antioxidant and anticholinesterase activities comparable to those of micelles containing only tacrine or gallic acid. Cell viability studies on the SH-SY5Y cell line showed that the developed micellar systems exhibited acceptable cellular compatibility.

Conclusion

The developed polymer–drug conjugate systems represent promising nanotherapeutic platforms for Alzheimer's disease, where the amphiphilic architecture enables micelle formation that may enhance drug stability and delivery efficiency. These findings highlight the potential of tacrine and gallic acid conjugated polymeric nanostructures as multifunctional nanotherapeutic systems combining cholinesterase inhibition and antioxidant activity for neurodegenerative diseases.

Acknowledgement

This work was financially supported by the Scientific and Technological Research Council of Türkiye (Project No: 124Z487).

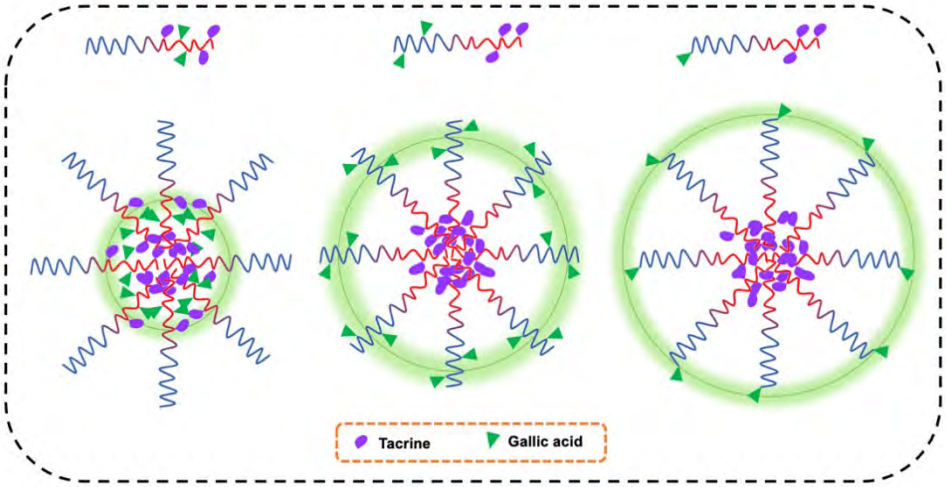

Figure 1. Schematic representation of tacrine and gallic acid conjugated nanotherapeutics.

S40
Hydrogel fibre composites for enhanced functionality in engineered tissues

S40 – K1

Freire C.
CICECO/Department of Chemistry- University of Aveiro - Portugal

S40 – O1

Melt electrowritten fiber reinforcement of OHA–GEL hydrogels enables tunable neural microenvironments

Unalan I. [1], Jain R.[2], Boccaccini A.R.[3]
[1]Dept. of Materials Science and Engineering Institute of Biomaterials, Friedrich-Alexander-University, Erlangen-Nuremberg, Germany

Introduction

The mechanical properties of the central nervous system (CNS) play an important role in regulating cellular behavior. Hydrogels that reproduce brain-like mechanics are increasingly used to investigate processes such as brain development, disease, and regeneration. However, very soft hydrogels with brain-like stiffness often show limited mechanical stability during long-term culture.

Materials and Methods

To address this challenge, oxidized hyaluronic acid–gelatin (OHA–GEL) hydrogels with brain-relevant stiffness were reinforced with anisotropic melt electrowritten (MEW) poly(ε-caprolactone) (PCL) microfiber scaffolds to improve structural stability while maintaining soft mechanical properties. Melt electrowriting (MEW) is a high-precision additive manufacturing technique that enables the fabrication of well-defined microfiber architectures with controlled fiber orientation and pore geometry. In this work, MEW structures with different architectures and pore sizes were designed to introduce controlled anisotropy within the composite matrices. Highly porous MEW scaffolds were integrated with OHA–GEL hydrogels at different concentrations (2.5, 7.5, and 10 wt%). The chemical composition of the hydrogels was analyzed by Fourier transform infrared spectroscopy (FTIR). Representative digital and scanning electron microscopy (SEM) images illustrate the formation of hydrogel–MEW composite constructs and the structural support provided by the MEW microfiber architecture to the soft hydrogel matrix (Figure 1). SEM observations further confirmed stable integration between the hydrogel phase and the MEW microfiber network.

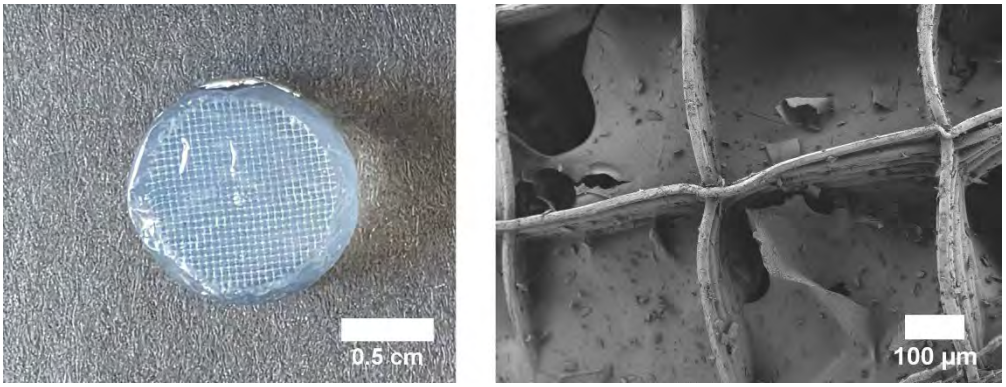

Figure 1. Representative digital and SEM images of OHA–GEL hydrogels integrated with PCL MEW scaffolds, demonstrating the formation of hydrogel–MEW composite constructs and the structural support provided by the MEW microfiber architecture.

Results/conclusion

Additionally, mechanical testing showed that the MEW architectures enhanced the structural stability of the soft hydrogels and enabled tuning of the mechanical response through fiber orientation and hydrogel composition. Preliminary in vitro studies with neural cells demonstrated that the hybrid OHA–GEL–MEW matrices provide a supportive three-dimensional microenvironment for cell viability and matrix interactions. Confocal microscopy and scanning electron microscopy were used to visualize cell distribution, morphology, and interactions with the microfiber-reinforced hydrogel architecture. The results indicated that neural cells remained viable within the composite matrices and established interactions with the surrounding structural framework.

These results demonstrate that anisotropic MEW scaffolds provide a promising strategy to stabilize brain-mimicking hydrogels and develop tunable platforms for mechanobiological studies of neural

microenvironments.Keywords: Melt electrowriting; brain-mimicking hydrogels; neural tissue engineering; hydrogel–fiber composites; mechanobiology; anisotropic scaffolds

Acknowledgements
We acknowledge the financial support of the Deutsche Forschungsgemeinschaft (DFG, German Research Foundation) under project number 460333672 – CRC 1540 “Exploring Brain Mechanics” (Subproject X03). We also thank Dr. Renato Frischknecht and Ms. Ezgi Erterek for their support with the neural cell studies.

References
1. K. Franze, P.A. Janmey, J. Guck, Mechanics in neuronal development and repair, Annu. Rev. Biomed. Eng. 2013.
2. M. Lorke, S. Kuth, R. Frischknecht, A.R. Boccaccini, Development of oxidized hyaluronic acid based hydrogels for neuronal tissue engineering: Effects of matrix stiffness on primary neurons, Acta Biomater. 2025.
3. P.D. Dalton, Melt electrowriting with additive manufacturing principles, Curr. Opin. Biomed. Eng. 2017.

S40 – O2

From nanofibrils to scaffolds: Bacterial cellulose as a structural reinforcement for hydrogels

Malandain N.[1, 2], Fraile H.[2], Farré R.[3], Otero J.[2], Roig S.[4], Iglesias-Mejuto A.[5], García-González C.[6], Roig A.[7], Laromaine A.[8]

[1]Institut de Ciència de Materials de Barcelona (ICMAB-CSIC), Campus Universitat Autònoma de Barcelona; [2]Unit of Biophysics and Bioengineering, School of Medicine and Health Sciences, Universitat de Barcelona; [3]AerogelsLab, I+D Farma Group (GI-1645), Dept. of Pharmacology, Pharmacy and Pharmaceutical Technology, Faculty of Pharmacy, iMATUS and Health Research Institute of Santiago de Compostela (IDIS), Universidade de Santiago de Compostela, Spain

Introduction

Natural biomaterial-based hydrogels are increasingly used for 3D cell culture because they mimic physiological environments, but many lack the mechanical strength required for tissue-like scaffolds or biofabrication. To address this, various reinforcement strategies—such as adding nanoparticles, nanofibers, or hybrid polymers—are being explored. Bacterial cellulose (BC) fibers represent a promising natural reinforcing material due to their high purity, strong nanofibrillar network, excellent mechanical properties, and ease of functionalization. Produced by bacteria such as *Komagataeibacter xylinus*, BC lacks plant-derived impurities and blends well with other polymers, making it highly suitable for strengthening hydrogels, developing printable biomaterial inks, and supporting structurally demanding biomedical applications.

In our work, BC fibers biosynthesized from *K. xylinus* pellicles were combined with various biopolymers, including type I collagen. Confocal and scanning electron microscopy confirmed a homogeneous distribution of both polymers throughout the composite matrix. Mechanical tests demonstrated that BC incorporation increased the stiffness of the hydrogels by over 40% while preserving their viscoelastic profile. Human bone marrow–derived mesenchymal stromal cells embedded within reinforced matrices showed high viability, proliferation, and adhesion over 7 days, validating the system's biocompatibility. Additionally, BC fibers were produced with alternative compositions, such as iron oxide, polypyrrole, or gold nanoparticles, broadening their functionality. These fibers can form interpenetrating networks, blend efficiently with natural polymers, be printed without additional crosslinking, and support cell encapsulation during fabrication.

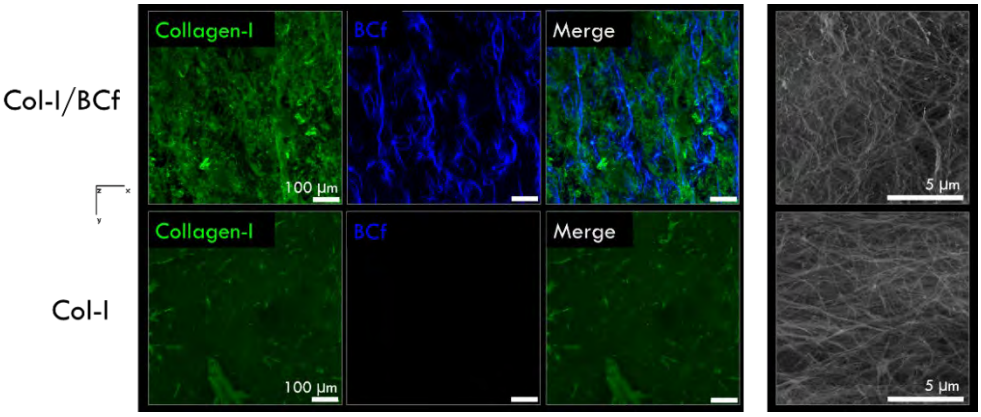

Overall, collagen hydrogels reinforced with BC fibers represent a versatile and robust platform with potential for 3D *in vitro* organ modeling, tissue engineering, mechanobiology, and next-generation biofabrication technologies.

Acknowledgements

This work was supported by the Spanish Ministry of Science and Innovation through PID2021-122645OB-I00 and PID2019-108958RB-I00 projects, the “Severo Ochoa” Programme for the Center of Excellence in R&D (CEX2019-000917), and the Generalitat de Catalunya (2021SGR00446 grant). N.M. acknowledges the Ph.D. scholarship (PRE2019-089754) in the framework of the Biotechnology Ph.D. program of the UAB. A.I.-M. acknowledges to Xunta de Galicia for her postdoctoral fellowship (ED481B-2025/032).

References

[1]Roig-Sanchez, S.; Kam, D.; Malandain, N.; Sachyani-Keneth, E.; Shoseyov, O; Magdassi, S.; Laromaine, A.; Roig, A. . *Carbohydrate Polymers* 2022, 294, 119778.
[2]Malandain, N.; Sanz-Fraile, H.; Farré, R.; Otero, J.; Roig, A.; Laromaine, . *ACS Applied Bio Materials* 2023, 6, 9, 3638–3647.
[3]Iglesias-Mejuto, A.; Malandain, N.; Ferreira-Gonçalves, T.; Ardao, I.; Pinto Reis, C.; Laromaine, A.; Roig, A.;García-González, C. A. . *Cellulose*2024. 31, 515-534.

S40 – O3

Electrically conductive and magnetic microfluidic-spun fiber-laden hydrogels for muscle tissue engineering

Luís S.[1], Kehoe T.[1], Neuhäusler A.[1], Schätzlein E.[1], Roshanbinfar K.[1], Blaeser A.[1,2]
[1]Institute for BioMedical Printing Technology, Technical University of Darmstadt; [2]Centre for Synthetic Biology, Technical University of Darmstadt, Germany

Introduction

Large muscle defects represent a major clinical challenge, as effective regenerative solutions remain unavailable. Myofibrils are muscle cells that are fused and form aligned structures. Fiber-laden hydrogels represent a promising strategy to induce cell alignment by providing physical cues from the fibers within hydrogels.

Aim

Investigate microfluidic-spun aligned collagen fibers functionalized with magnetic nanoparticles (mNPs, Streptavidin MagneSphere® Paramagnetic Particles) or conductive polymers (PEDOT:PSS) to enable remote stimulation or enhanced cellular connectivity, promoting improved orientation of C2C12 myoblasts in fiber-reinforced collagen hydrogels.

Materials and Methods

Aligned collagen mNPs or PEDOT:PSS-functionalized fibers were produced using a custom microfluidic-spinning system to generate continuous, uniaxially oriented fiber mats. Fiber composition was characterized (ATR-FTIR,SEM), and fibers were collected in cell crowns to preserve alignment. Aligned fibers were also embedded in collagen hydrogels to create fiber-laden constructs mimicking native muscle anisotropy. C2C12 myoblasts were seeded onto these constructs and cultured under differentiation conditions. Cell viability was assessed by CTB-Blue assay, while morphology and alignment were evaluated by immunofluorescence, with nuclear orientation relative to the fiber axis quantified in ImageJ.

Results

C2C12 myoblasts showed comparable cytocompatibility across all microfluidic-spun fibers (<90%). After 28 days, C2C12 cells cultured on aligned pure (Ø≈13.34 µm), mNP-functionalized (Ø≈10.82 µm), and PEDOT:PSS-functionalized (Ø≈8.02 µm) collagen fibers showed pronounced elongation and alignment along the fiber axis (nuclear angles clustered ≈0°), whereas control cells seeded on well plates exhibited regionally random orientation. Differences in fiber diameter resulted from adjustments in collagen concentration required to obtain spinnable solutions. ATR-FTIR confirmed collagen fiber functionalization; mNP-containing fibers retained magnetic properties, and impedance measurements confirmed the conductivity of PEDOT:PSS-functionalized fibers. Fiber-reinforced collagen hydrogels further demonstrated that embedded aligned fibers promote greater cellular alignment and elongation compared to unpatterned controls. Magnetic collagen microfibers enabled remote stimulation of C2C12 cells using a magnetic field, resulting in enhanced alignment, while collagen–PEDOT:PSS microfibers promoted improved cellular alignment and connectivity.

Conclusion

Our data showed that microfluidic-spun collagen fibers provide a versatile platform to effectively guide cellular alignment and represent a promising platform for engineering anisotropic tissues, supporting the development of aligned skeletal muscle patches for regenerative therapies.

Acknowledgement

Funded by the European Union (trainLSE-101126497).

Reference

[1] Neuhäusler A., Bioact Mater., *et al* 2025,

S40 – O4

A 3D co-cultured hydrogel-fibre cardiac perfusion model

Steedman O.F. [1], Tung T. [2], Krishnamoorthi K.V.[3], Melo P.[4], Ferreira A.M.[5], Dalgarno K. [6]
[1]School of Engineering, Newcastle University, Claremont Road, NE1 7RU Newcastle Upon Tyne

Introduction

There is a pressing need for human cardiac tissue models to provide insights into the development of cardiac diseases, the potential value of new cardiac therapies, and the toxicity of new drugs for a wide range of conditions.

Aim

This study aims to develop a human in vitro ventricular cardiac chamber, which supports pulsatile perfusion flow through a cylindrical tissue engineered chamber, to create a new model of cardiac function for early-stage evaluations of novel therapies.

Materials and Methods

The first stage of the process is electrospinning of polycaprolactone to create a 5 mm diameter cylindrical fibre scaffold. The reactive jet impingement (ReJI) bioprinting process [1] is then used to print a human cardiac fibroblast/cardiomyocyte onto the cylinder, using a purpose designed rotational stage to allow printing over the cylinder surface area. Co-cultures have been developed using human cardiac fibroblasts (HCF), and two different sources of cardiomyocytes: the AC16 cell line and iPSC derived cardiomyocytes. The co-cultures are encapsulated within a collagen-alginate-fibrin hydrogel bio-ink [2], so that after printing a cylindrical cell-hydrogel-fibre composite has been created. The cylindrical structure is then positioned in-line within a unique purpose-built perfusion test rig, with initial static culture for a period of up to a week followed by perfusion culture for a period of up to two weeks, at pressures of up to 2 kPa and flowrates of up to 30 mL/min.

Results

PCR, immunocytochemistry and immunohistochemical analysis show that the fibroblast/cardiomyocyte co-cultures maintain phenotype and deposit extracellular matrix, creating tissue-like structures and demonstrating that a biomimetic perfusable ventricular heart chamber model can be developed and cultured over extended time periods.

Conclusion

These findings demonstrate the successful in vitro model of a biomimetic, perfusable human ventricular chamber model capable of sustaining functional cardiac co-cultures for extended evaluation of emerging cardiac therapies.

Acknowledgement

This project has received funding from the European Union's Horizon Europe research and innovation program under grant agreement No. 101091852.

References

[1] Kotlarz, M., Ferreira, A.M., Gentile, P. *et al.* Droplet-based bioprinting enables the fabrication of cell–hydrogel–microfibre composite tissue precursors. *Bio-des. Manuf.* **5**, 512–528 (2022).
[2]Bowes, A., Collins, A., Oakley, F., Gentile, P., Ferreira, A. M., & Dalgarno, K. (2024). Bioprinted High-Cell-Density Laminar Scaffolds Stimulate Extracellular Matrix Production in Osteochondral Co-Cultures. *International Journal of Molecular Sciences 2024*, *25*(20).

S40 – O5

Designing conductive hydrogel-based bioinks with polysaccharides and metal-protein nanohybrids for the 3D bioprinting of cardiac tissue platforms

Carvalho J.P.F.[1], Teixeira M.C.[1], Luís J.L.[2], Tavares B.L.[1], Oliveira H.[3], Oliveira J.M.[2], Silvestre A.J.D.[1], Vilela C.[1], Freire C.S.R.[1]

[1]CICECO, Aveiro Institute of Materials, Dept. of Chemistry, University of Aveiro; [2]CICECO, Aveiro Institute of Materials, EMaRT Group - Emerging: Materials, Research, Technology, School of Design, Management and Production Technologies Northern Aveiro, Oliveira de Azeméis; [3]CESAM, Centre for Environmental and Marine Studies, Dept. of Biology University of Aveiro, Portugal

Introduction

3D bioprinting relies on the layer-by-layer deposition of cell-laden biomaterials ("bioinks") to originate 3D living structures for biomedical applications. Biopolymer-based hydrogels present great potential for cell survival and proliferation due to their high-water content, facile crosslinking using mild conditions, resemblance to the native extracellular microenvironment, and cytocompatibility. These key factors have made biopolymeric hydrogel-based bioinks the most frequent option for 3D bioprinting applications. However, some human tissues have specific functionalities (*e.g.,* electrical conductivity) that are not naturally shown by common biobased hydrogels.

Materials and Methods

This work explores the design and thorough characterization of an electrically conductive hydrogel-based bioink by combining gellan gum (1.5 wt.%), carboxymethyl cellulose (1 wt.%), and a nanostructured hybrid of lysozyme nanofibrils and gold nanoparticles (LNFs:AuNPs), for the 3D bioprinting of cardiac cells (H9c2).

Results

The developed ink formulations reveal suitable rheological properties, showing a proper shear-thinning behavior and notorious *G'* recovery rate (above 85%), good printability, and improved conductivity (~3.0 mS cm^{-1}) imparted by the presence of LNF:AuNPs. Furthermore, the resulting crosslinked hydrogels mimic the stiffness of cardiac tissue (<100 kPa) and present a porous microstructure (>70%). The inclusion of LNF:AuNPs also significantly reduces their degradation rate (from above 30% to 13.8 ± 2.4%) and enhances the antioxidant activity (from 22.0 ± 0.8% to 75.1 ± 0.3%).

Conclusion

The complex 3D structures bioprinted with the formulations developed herein are able to sustain high H9c2 cell viability (90%) for up to 7 days, confirming the biocompatibility of the formulations and their potential for the development of living structures that may be used as conductive cardiac tissue platforms for biomedical applications.

Acknowledgements

This work was developed within the scope of the projects CICECO – Aveiro Institute of Materials, UID/50011/2025 (DOI 10.54499/UID/50011/2025) & LA/P/0006/2020 (DOI 10.54499/LA/P/0006/2020), and CESAM (UID/50006 & LA/P/0094/2020 (doi.org/10.54499/LA/P/0094/2020)), financed by national funds through the FCT/MCTES (PIDDAC), and financially supported by the project I&D "NANOBIOINKS- Engineering bio-based nanofibers for the development of high-performance nanostructured bioinks for 3-D bioprinting, CENTRO-01-0145-FEDER-031289" funded by the Operational Program of the Center Region, in its FEDER/FNR component, and by national funds (OE), through FCT/MCTES. FCT is acknowledged for the doctoral grants to J.P.F.C (2020.09018.BD, DOI 10.54499/2020.09018.BD) and the research contracts under Scientific Employment Stimulus to C.S.R.F. (DOI 10.54499/CEECIND/00464/2017/CP1459/CT0033), C.V. (DOI 10.54499/2021.01571.CEECIND/CP1659/CT0024) and H.O. (DOI 10.54499/CEECIND/04050/2017/CP1459/CT0023).

S40 – O6

Cellulose-supported 3D printing: Unlocking complex, anisotropic hydrogel structures for biomimetic aorta models

Pint D. [1], Steindorfer T. [2], Lackner F. [3], Mohan T. [4], Gruber-Woelfler H. [5], Kargl R. [6], Stana Kleinschek K.[7]
[1]Institute of Chemistry and Technology of Biobased Systems (IBioSys), Graz University of Technology; [2]Institute of Process and Particle Engineering (IPPE), Graz University of Technology, Austria

Introduction

Extrusion based 3D printing of hydrogels enables biomedical and soft material applications. Unsupported hydrogel filaments can deform or collapse during printing. This limits overhangs, internal channels, and tall structures. We report a cellulose based sacrificial support that stabilizes Nanofibrillated Cellulose/Sodium Alginate (NFC/ALG) hydrogel prints in open air direct ink writing (DIW) and improves shape fidelity and stability. The method uses mild ionic crosslinking and is designed for accessible and reproducible workflows. A schematic overview of the workflow is depicted in Figure 1.

Materials and Methods

The structural ink combined nanofibrillated cellulose (NFC) with sodium alginate (ALG). NFC provided shear thinning and shape retention properties. ALG enabled Ca2+ crosslinking to maintain geometry after deposition. The sacrificial support ink contained NFC 2.5 wt%, Hydroxyethylcellulose (HEC) 15 wt%, and CaCl2 2 wt%. HEC was gradually incorporated into NFC with dissolved CaCl2, then hydrated for 24 to 48 h at 4 °C before cartridge and printer loading. Direct ink writing used tapered nozzles in the 580 to 840 µm range. A layer height set to 50% of nozzle diameter and pressures of 140 to 160 kPa for the structural NFC/ALG ink and 175 to 235 kPa for the support NFC/HEC/CaCl2 ink yielded continuous strands and strong interlayer bonding. Immediately after printing, constructs were immersed in 30 mM CaCl2 solution for 24 h. Support dissolution proceeded under gentle shaking at 60 rpm over about 3 days to preserve shape fidelity during crosslinking and enable clean release of fine structures.

Results

Unsupported NFC/ALG tubes collapsed during printing, while tubes printed with surrounding support walls remained stable at 50 mm height even when tilted to 45 degrees. Printed tubes were watertight when the layer height was reduced to 50% of the nozzle diameter. Reducing layer height from 840 µm to 420 µm improved surface quality from rough and porous to smooth and sealed, yielding watertight tubular prints suitable for perfusion. The method reproduced complex geometries, including a human aorta, which retained fine features after crosslinking and complete support removal (Figure 2).

Conclusion

A cellulose based sacrificial support ink stabilizes NFC/ALG hydrogel prints in open air DIW. The approach enables high aspect ratio and complex geometries with improved surface quality and watertightness. Support dissolution in 30 mM CaCl2 over about 3 days maintains integrity during crosslinking and allows full release. The method is inexpensive and uses mild ionic chemistry. It is reproducible and suitable for future cell laden adaptations.

Acknowledgements

This research project (grant number: 911658) was funded by COMET – Competence Centers for Excellent Technologies – through BMIMI, BMWET, and the co-financing federal provinces (Styria through SFG, Upper Austria, Vorarlberg) and carried out with the participation of scientific and company partners. The COMET program is managed by FFG.

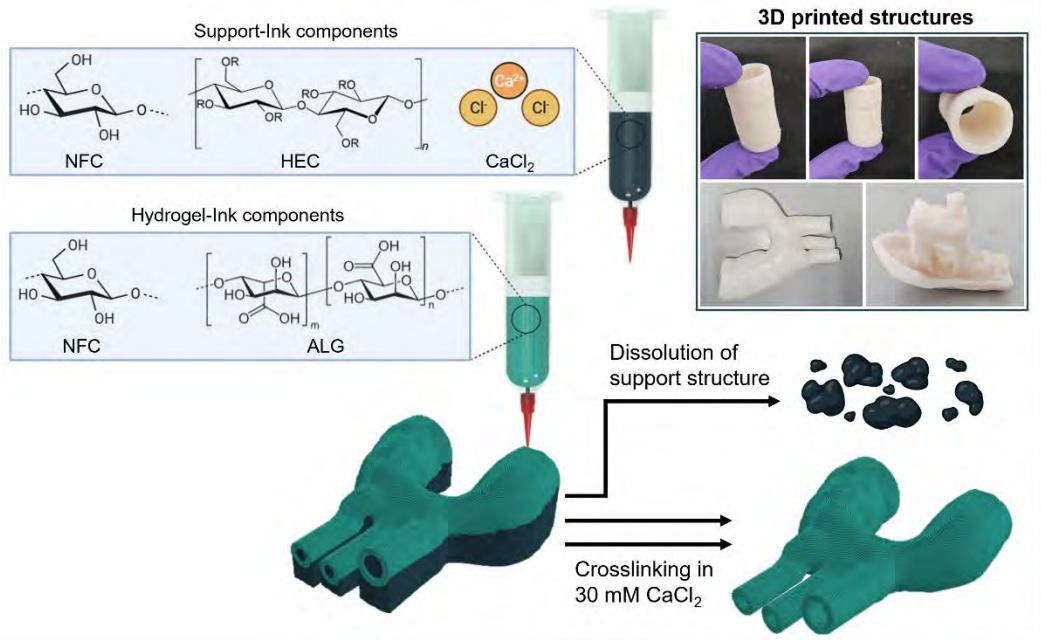

Figure 1: Schematic overview of the complete fabrication workflow.

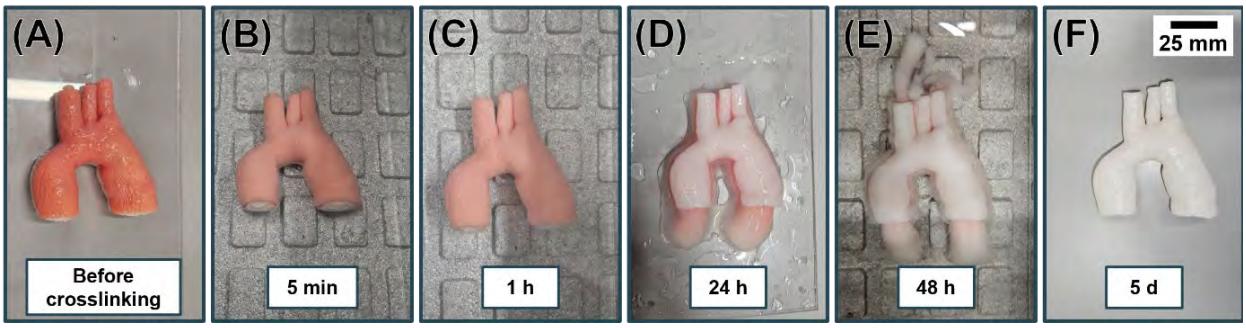

Figure 2: Time-lapse sequence of a printed hydrogel aorta during crosslinking and support removal in 30 mM $CaCl_2$ solution.

S40 – O7

Development and characterization of fiber-reinforced hydrogel scaffolds for osteochondral repair

Niendorf C.[1], Barkow P.[1], Waletzko-Hellwig J.[2], Freiin Grote V.[2], Polley C.[2], Kissel H.[3], Boccaccini A. R.[3], Bader R.[2,4] and Seitz H.[1,4]
[1]Faculty of Mechanical Engineering and Marine Technology, Chair of microfluidics, University of Rostock, Rostock; [2]Rostock University Medical Center, University of Rostock, Rostock; [3]Institute of Biomaterials, Friedrich-Alexander-University Erlangen-Nuremberg, Erlangen; [4]Department Life, Light & Matter, University of Rostock, Rostock, Germany

Introduction

Cartilage and osteochondral defects remain a major clinical challenge in regenerative medicine. Despite advances in current treatments such as microfracture or matrix-assisted autologous chondrocyte implantation, the resulting repair tissue can consist of fibrocartilage rather than native hyaline cartilage. It therefore fails to meet the mechanical and tribological demands of load-bearing joints. Hydrogels represent promising candidates for cartilage repair because they provide a supportive matrix for chondrocytes and mesenchymal stem cells. However, tailoring hydrogel systems to withstand the mechanical environment of articular cartilage while maintaining cell-permissive conditions remains difficult. Here, we present an approach that integrates melt electrowritten (MEW) fiber scaffolds with hydrogels to create fiber-reinforced constructs for osteochondral tissue engineering.

Materials and Methods

In the present study, we combined an extracellular-mimicking matrix made of alginate-dialdehyde-gelatin formulations with highly oriented MEW meshes fabricated from polycaprolactone that functions as a bone phase. Two scaffold architectures with rectangular and triangular pore geometries were investigated. The hydrogels were subsequently stabilized using a dual-crosslinking strategy involving Ca^{2+} ions and microbial transglutaminase. The resulting reinforced hydrogels underwent comprehensive mechanical characterisation, including compressive testing, dynamic-mechanical analysis, and relaxation assays, and were compared with non-reinforced hydrogels.

Results

Preliminary results suggest that MEW reinforcement significantly improves the mechanical performance of the hydrogel constructs, indicating greater potential for load-bearing cartilage applications.

Conclusion

In summary, our findings highlight the capability of combining MEW-fabricated scaffolds with tailored hydrogel systems to engineer functional substitute materials for osteochondral defects.

Acknowledgement

Research funding: This study is funded by the Deutsche Forschungsgemeinschaft (DFG, German Research Foundation) – SFB 1270/3,4-299150580.

S41

Innovative strategies to integrate gasotransmitters and signalling molecules into biomaterials for therapeutic action

S41 - K1

Hydration-controlled nitric oxide delivery from S-nitrosothiol-integrated biomaterials

de Oliveira M.G.
Institute of Chemistry, University of Campinas, UNICAMP, SP, Brazil

Introduction

Localized delivery of nitric oxide (NO) from biomaterials has potential benefits in several clinical settings. In wound care, NO can support healing, improve local blood flow, and reduce bacterial burden. In cardiovascular devices such as intracoronary stents, NO may help limit restenosis and promote endothelialization after angioplasty. These therapeutic effects have motivated the development of polymer systems capable of releasing NO. Because NO is a short-lived gas, such systems typically incorporate NO-donor molecules or attach NO-releasing groups to polymer chains. Both approaches require mechanisms that control when and how much NO is released. We developed NO-releasing biomaterials with 3D printable controlled architectures, designed to remain stable in the dry state and release NO at tunable rates upon hydration.

Materials and Methods

S-nitrosoglutathione (GSNO) and *S*-nitroso-*N*-acetylpenicillamine (SNAP) were synthesized by *S*-nitrosation of their thiolated precursors. These compounds were incorporated into several polymer matrices, including Pluronic F127 (F127), F127/poly(acrylic acid) (PAAc), gelatin/hyaluronic acid, and polysilsesquioxane/F127/PEG systems. Incorporation was achieved by absorbing donor solutions into crosslinked polymer networks followed by lyophilization. The F127/PAAc hybrid hydrogel was prepared by thermal polymerization of acrylic acid in a micellar F127 solution. F127 was methacrylated using methacrylic anhydride in a microwave-assisted reaction. Methacrylated poly(dodecanediol citrate)s were synthesized by esterification of citric acid with 1,12-dodecanediol and mercaptosuccinic acid, followed by methacrylation with glycidyl methacrylate. Hydrogel and polyester constructs were fabricated using photo-induced 3D printing. Nitric oxide release was monitored in real time by chemiluminescence.

Results/Conclusion

The resulting hydrogels and crosslinked polyesters functioned as matrices for localized NO delivery from GSNO, SNAP, or *S*-nitrosothiol groups incorporated into the polymer structure. These materials remained stable during storage under dry conditions, addressing the known instability of *S*-nitrosothiols in aqueous environments. Upon hydration, NO release occurred through donor decomposition or hydrolysis processes. This mechanism allows NO delivery to be initiated by exposure to physiological fluids, such as wound exudate or blood contact with vascular devices. The materials also allow adjustment of release rates through polymer composition and structure. Overall, these hydration-responsive systems provide a platform for controlled NO delivery with potential applications in wound treatment and vascular implants.

Acknowledgements

This work was supported by the São Paulo Research Foundation, FAPESP, grant 2022/14645-2.

References

[1]de Almeida H.V. et al. Integrating 3D printing of biomaterials with nitric oxide release. *Biomater. Sci.*, 2025, 13, 1-17.
[2]de Almeida H.V. et al. Nitric oxide-releasing PHEMA/polysilsesquioxane photocrosslinked hybrids. *RSC Adv.*, 2025, 15, 45048–45060.

S41 – O1

Design and optimization of nitric oxide (NO) releasing hybrid supramolecular hydrogels for cardiovascular applications

Deepa D[1,2], Paez J.I[1,2]

[1]Dept. of Bioengineering Technologies, [2]Cardiovascular Health Technology Centre, TechMed Centre, University of Twente, Enschede, Netherlands

Introduction

Cardiovascular diseases are accountable for >17 million deaths annually. Despite advances like bypass graft surgery and percutaneous coronary intervention, their potential to repair damaged heart tissue is still limited. Therapeutically administered nitric oxide (NO) has appeared as a plausible strategy because of its antiproliferative and antiinflammatory properties. Hydrogels have proved significant potential as platforms for local delivery due to tunable viscoelastic properties, controlled release of bioactive molecules and drugs, including NO. However, traditional hydrogels often show rapid degradation and uncontrolled NO release. Herein, we propose the development of NO-releasing supramolecular hybrid hydrogels to overcome the uncontrolled NO release of conventional hydrogels for sustained cardiovascular therapy.

Aim

Development and characterization of hybrid supramolecular hydrogels loaded with NO donors, and evaluation of the effect of NO donor loading on hydrogel viscoelastic properties, cytotoxicity and cellular response. Ultimately, we aim to estimate the potential of NO release of these hydrogels and their therapeutic prospects to support repair of cardiac tissue.

Materials & Methods

Hybrid supramolecular hydrogels were fabricated using different concentrations of nucleotide, biopolymers, fibrin, and (diverse types of) NO donors including small molecules and nanoparticles; and characterized them by rheology. Cytotoxicity of hydrogels was assessed using live-dead assay with immortalized human mesenchymal stem cells (SCP-1, ihmsc). NO release was quantified by Griess assay.

Results

Optimized hydrogels were fabricated with controlled gelation rate and improved homogeneity, by tuning the concentration and ratio of components. Small-molecule NO donors were successfully loaded in the hydrogels, and showed to enhance the curing rate and mechanical strength of the materials. Cell viability studies showed that hydrogels with 1 mM, 0.1 mM, and 0.01 mM GSNO maintained moderate viability in-gel and high viability out-gel (**Figure.1**). These findings highlight concentration dependent balance between localized effects and overall cytocompatibility. Ongoing studies compare small molecule NO donors vs NO releasing nanoparticles, to assess the optimal approach for controlled release and therapeutic activity.

Conclusion

Supramolecular hybrid hydrogels loaded with NO donors are an innovative platform for local NO delivery in cardiovascular applications. Enhanced viscoelastic properties along with high cytocompatibility, at optimized NO donor concentrations, highlight their potential in treatment of cardiovascular diseases. Ongoing work explores controlled NO release kinetics to further improve the therapeutic potential in cardiac repair.

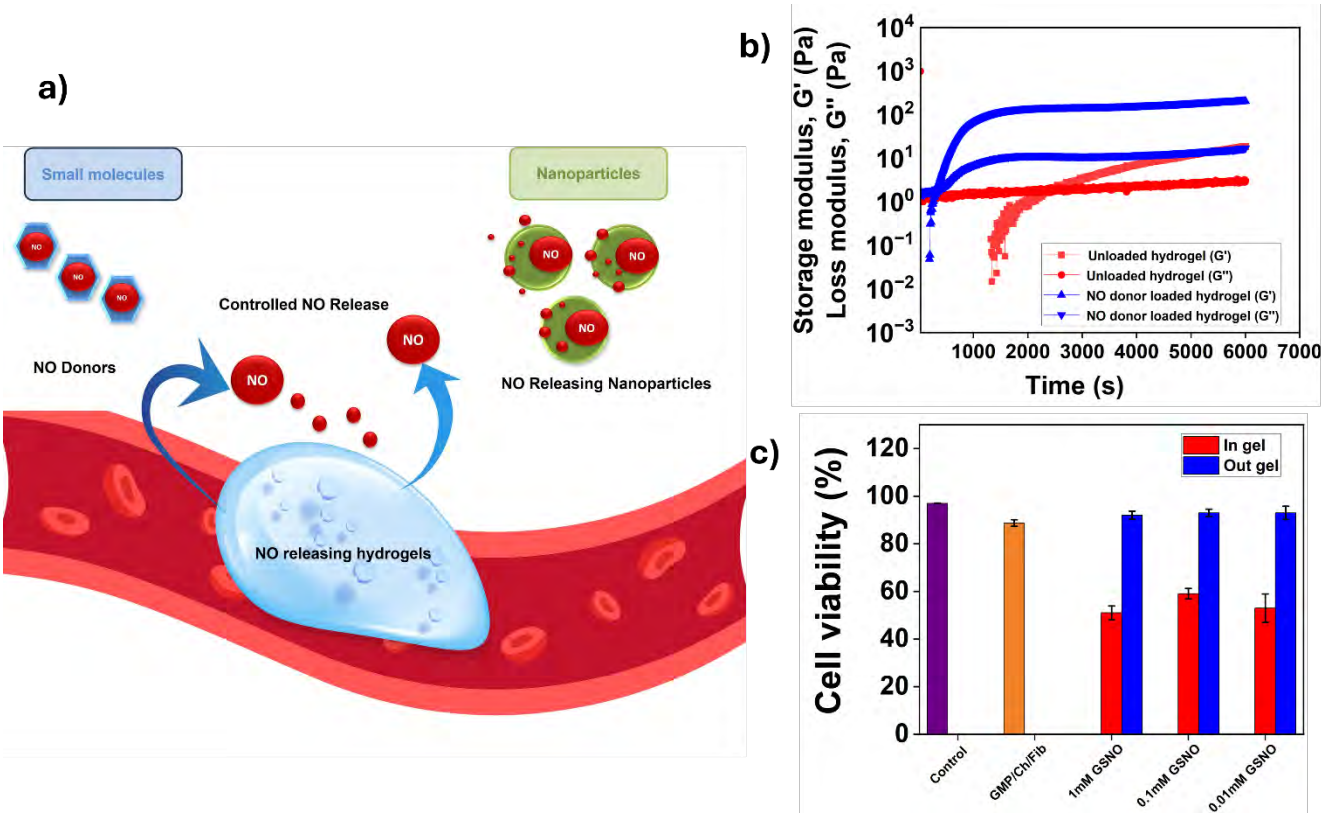

Figure 1. a) Schematic representation of nitric oxide (NO) delivery strategies in hydrogels. b) Time sweep rheological curve of hydrogels. c) Live-dead assay of hydrogels. n = 3, mean ± SD.

S41 – O2

Nitric oxide release from S-nitrosoglutathione preserves vasodilation and reduces infarct size after myocardial ischemia-reperfusion

Guizoni, D.M.[1,2], Pinto Junior, E.A.[1], Gomes, E.I.[2], Davel, A.P.[3], Sposito, A.C.[2], de Oliveira, M.G.[1]
[1]Institute of Chemistry, University of Campinas - UNICAMP, SP; [2]Laboratory of Vascular Biology and Atherosclerosis (Aterolab), School of Medical Sciences, University of Campinas - UNICAMP, SP; [3]Institute of Biology, University of Campinas - UNICAMP, SP, Brazil

Introduction

Ischemia-reperfusion (I/R) injury significantly contributes to increase myocardial damage following acute myocardial infarction, highlighting the urgent need for effective cardioprotective therapies. S-nitrosoglutathione (GSNO), an endogenous S-nitrosothiol that functions as a physiological nitric oxide (NO) donor, exhibits vasodilatory, cytoprotective, and redox modulating properties. However, the therapeutic potential in myocardial I/R injury remains insufficiently explored. This study assessed the potential of GSNO to reduce I/R induced cardiac injury by improving coronary vasodilation and perfusion in an isolated rat heart model.

Materials and Methods

S-nitrosoglutathione (GSNO) was synthesized by S-nitrosation of glutathione and purified by acetone precipitation and lyophilization. Stability and nitric oxide (NO) release in Krebs-Henseleit solution was analyzed by UV-Vis spectroscopy and chemiluminescence. In vitro cytotoxicity was evaluated in H9c2 cardiomyoblasts and HUVEC endothelial cells treated with GSNO for four hours using the CCK-8 assay. Cardiovascular effects were assessed in isolated rat hearts using the Langendorff I/R model with GSNO (200-500 µM). Hemodynamic parameters, coronary flow, infarct size by Evans Blue/TTC staining, and vascular reactivity in aortic and coronary arteries were analyzed.

Results

GSNO synthesis was confirmed by UV-Vis spectroscopy, showing characteristic absorption bands at 336 and 545 nm. In Krebs-Henseleit solution, GSNO exhibited an initial NO burst followed by sustained release, with steady fluxes of 3.45 and 8.20 nmol mL^{-1} min^{-1} for 200 and 500 µM, respectively. In the Langendorff I/R model, GSNO increased coronary flow and reduced coronary resistance compared with controls. Treatment with 200 µM GSNO significantly decreased infarct size (~40%) versus controls (~65%), whereas 500 µM showed no cardioprotection (Fig. 1). GSNO also reduced cell viability dose-dependently, with cardiomyoblasts more sensitive than endothelial cells, and induced strong vasorelaxation in coronary arteries.

Conclusion

GSNO exhibited potent vasodilatory and cardioprotective effects in the isolated rat heart I/R model. Treatment with 200 µM GSNO improved coronary perfusion and significantly reduced myocardial infarct size, while higher concentrations did not confer additional protection, indicating a dose-dependent therapeutic window. GSNO also induced strong vasorelaxation in coronary arteries and showed cell type dependent cytotoxicity in vitro. These findings highlight the potential of GSNO as a nitric oxide donor for cardiovascular applications and support its further development as a therapeutic strategy or as a component of NO releasing biomaterials for myocardial protection.

Acknowledgements

This work was supported by the São Paulo Research Foundation, FAPESP, grants 2022/14645-2 (to M.G.O.), 2025/00254-0 (to D.M.G), 2024/08075-4 (to E.A.P.J.) and, 2023/17022-9 and 2018/26080-4 (to A.P.D.).

.

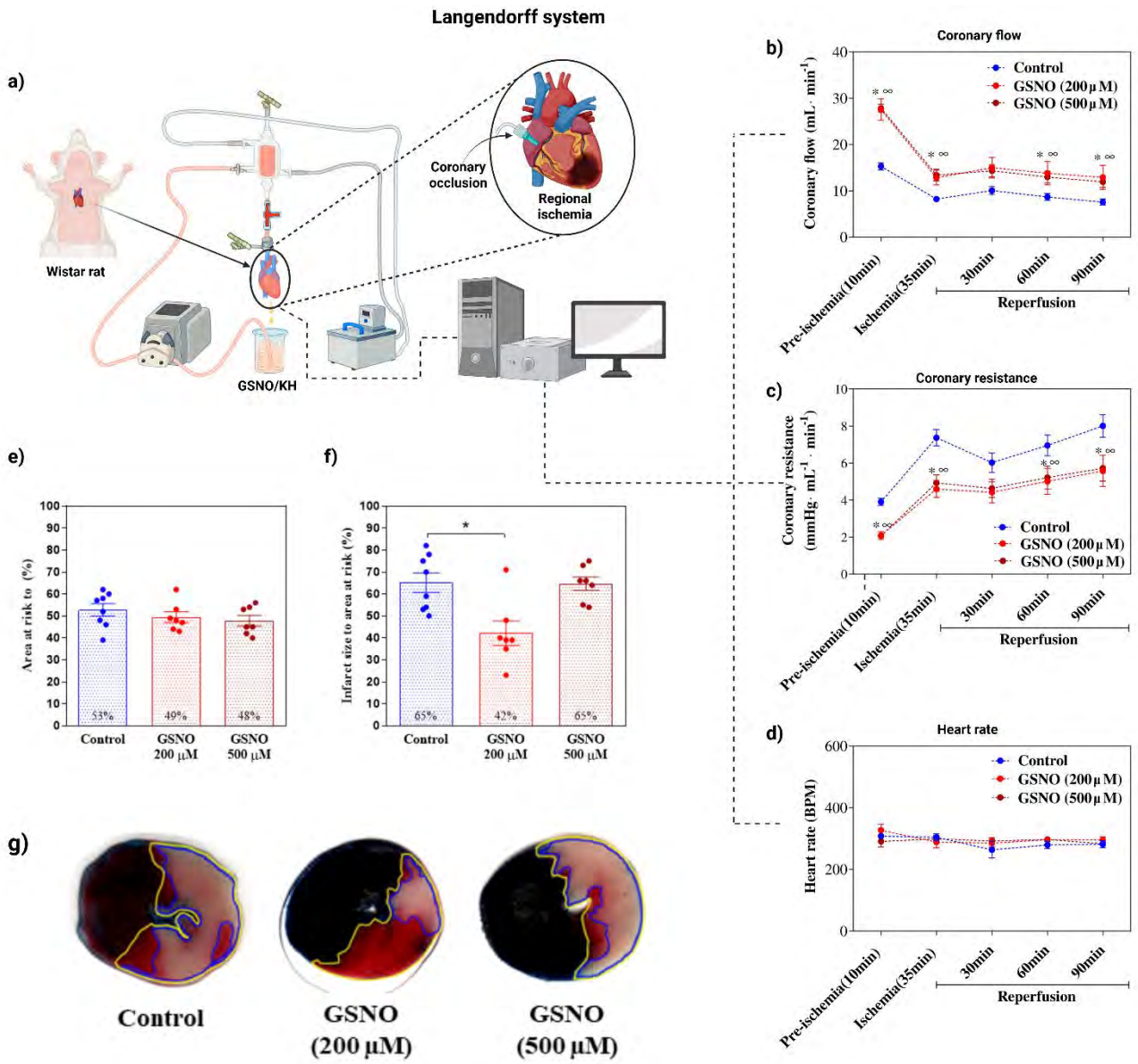

Figure 1. (a) Schematic of the Langendorff perfusion system. (b–d) Coronary flow, coronary resistance, and heart rate in isolated hearts from control and GSNO-treated groups (200 or 500 μM). (e–f) Quantification of area at risk and infarct size after ischemia–reperfusion. Data are mean ± SEM (n = 7–8), statistical analysis by ANOVA

S41 – O3

Nitric oxide-releasing methacrylated pluronic hydrogels for antileishmanial therapy

Rosa L.B.[1,2], Pinto Junior E.A.[1], Bomediano M.P.[1], Miguel D.C.[2], Oliveira, M.G.[1]
[1]Dept. of Physical Chemistry, Institute of Chemistry, University of Campinas (UNICAMP); [2]Dept. of Parasitology, Institute of Biology, University of Campinas (UNICAMP), Brazil

Introduction

Leishmaniasis is a neglected tropical disease with limited therapeutic options and treatments often associated with significant toxicity. Nitric oxide (NO) plays an important role in macrophage-mediated killing of *Leishmania* parasites, supporting the development of NO-releasing biomaterials for localized therapy. Methacrylated Pluronic (F127-DM) forms photocrosslinked hydrogels that can act as thermosensitive and biocompatible matrices for NO delivery. Hydrogels loaded with *S*-nitrosoglutathione (GSNO) (F127-DM/GSNO) may provide localized microbicidal activity whitouth systemic effect. This study evaluated the antileishmanial activity and selectivity of F127-DM/GSNO against *Leishmania amazonensis* and *Leishmania braziliensis*, and assessed cytotoxicity toward bone marrow–derived macrophages.

Materials and Methods

GSNO was synthesized by *S*-nitrosation of glutathione, followed by purification through acetone precipitation and lyophilization. The terminal hydroxyl groups of Pluronic F127 were methacrylated using methacrylic anhydride under microwave-assisted conditions, producing F127-DM with approximately 95% methacrylation. Antileishmanial activity of free GSNO and F127-DM/GSNO was evaluated against promastigotes of *L. amazonensis* and *L. braziliensis*. Parasites were cultured in Medium 199 (pH 7.4, 26 °C), while bone marrow-derived macrophages (BMDM) were maintained in RPMI (pH 7.4, 37 °C, 5% CO_2). Cells were exposed to free GSNO or F127-DM/GSNO for 24 or 48 h. Cell viability was measured using the MTT assay. Cytotoxicity toward BMDM was used to calculate the selectivity index (SI).

Results

Free GSNO showed dose-dependent antileishmanial activity against *L. amazonensis* and *L. braziliensis*, with IC_{50} values ranging from 87.5 to 250.4 µM after 24–48 h. Cytotoxicity toward macrophages remained low ($CC_{50} \approx 3.2$–4.0 mM), resulting in favorable selectivity indices. F127-DM/GSNO also reduced parasite viability and produced complete inhibition at 10 mM, particularly against *L. braziliensis*, while maintaining high macrophage viability (>89%). Infection assays confirmed a reduction in intracellular amastigotes. NO measurements indicated an initial burst followed by sustained release over 60 min, which was associated with enhanced antiparasitic activity and minimal toxicity to host cells.

Conclusion

Methacrylated Pluronic hydrogels containing GSNO provide a platform for localized NOe delivery in leishmaniasis treatment. The system showed antileishmanial activity while maintaining low toxicity toward macrophages, resulting in high selectivity. Sustained NO release from the F127-DM/GSNO may contribute to improved therapeutic effects while limiting systemic exposure. These findings support further investigation of this platform as a topical or injectable approach for treating cutaneous leishmaniasis.

Acknowledgements

This work was supported by the São Paulo Research Foundation, FAPESP, grants 2022/14645-2 (to M.G.O.), 25/26666-2 (to L. B. R),)2023/17022-9 (to E.A.P.J.) and 22/13352-1 (to M. P. B).

a)

	L. amazonensis	*L. braziliensis*	BMDM	*L. amazonensis*	*L. braziliensis*
	Free GSNO IC50 (µM)		CC50 (µM)	S. I.	
24h	134.5	87.52	3203	23.81	36.59
48h	250.4	145.4	3967	15.84	27.28

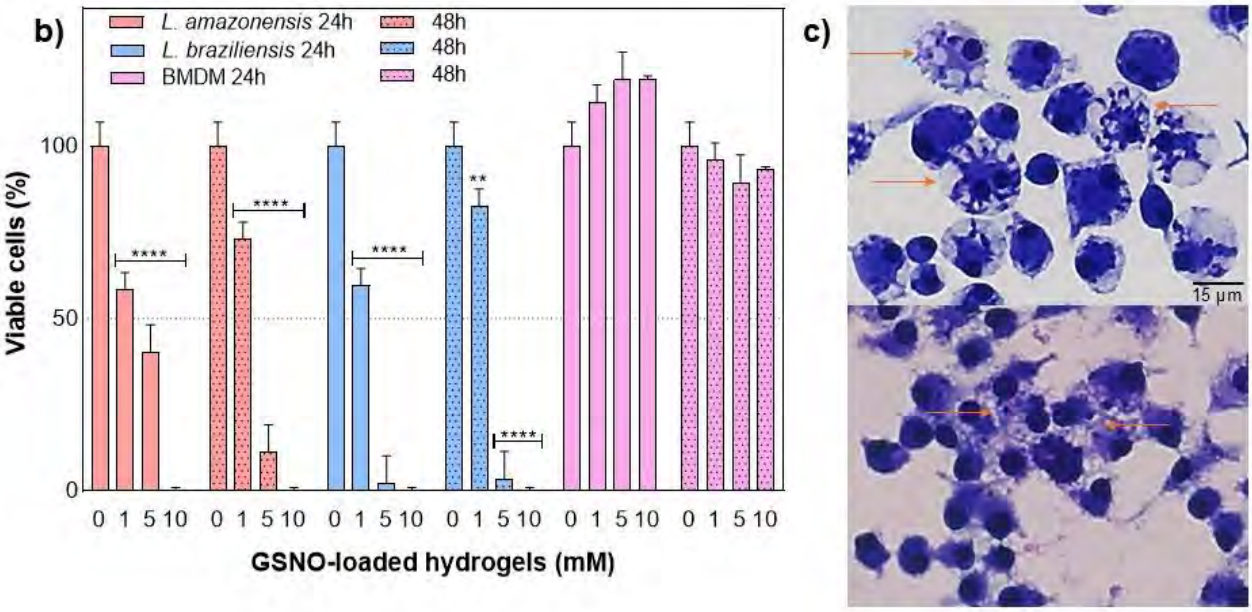

Figure 1: Antileishmanial activity and cytotoxicity of GSNO and GSNO-loaded hydrogels, a) IC_{50} values of free GSNO against L. amazonensis and L. braziliensis after 24 h and 48 h, along with CC_{50} values for BMDM and the corresponding selectivity index, b) Viability of L. amazonensis, L. braziliensis, and BMDM treated with GSNO-loaded hydrogels (0-10 mM) for 24 and 48 h (mean ± SD; **$p < 0.01$, ****$p < 0.0001$) and c) Representative microscopy images of infected macrophages showing intracellular amastigotes before and after treatment. Scale bar: 15 µm.

S41 – O4

Gasotransmitter-modulating MOF nanoparticles for immunometabolic reprogramming in triple-negative breast cancer

Abdo A.[1], Boran A.[2], González-Gómez R. [2], Revill H.[1], Farràs P.[1,2], Pandit A.[1]
[1]CÚRAM, Research Ireland Centre for Medical Devices, University of Galway; [2]School of Biological and Chemical Sciences, Ryan Institute, University of Galway, Ireland

Introduction

The tumour microenvironment (TME) of Triple-Negative Breast Cancer (TNBC) is characterized by metabolic competition and immunosuppressive signalling that impair antitumour immune responses.[1] Arginine (Arg) metabolism plays a central role in regulating nitric oxide (NO) production and T-cell metabolic fitness,[2] while carbon monoxide (CO) acts as a signalling gasotransmitter capable of modulating inflammatory and redox pathways.[3] Biomaterial-based delivery systems capable of locally regulating gasotransmitter signalling offer a promising strategy to reprogram tumour–immune interactions. Our aim was to engineer platforms for controlled delivery of arginine and CO to modulate immunometabolism and tumour behaviour in TNBC models.

Materials and Methods

Arg-loaded metal–organic framework nanoparticles (MOF-NPs) were synthesized using titanium- and zirconium-based frameworks and characterized by X-ray diffraction, electron microscopy, and loading efficiency analysis. Arg release was evaluated under physiological conditions. Immunometabolic effects were assessed in activated human T cells using Seahorse extracellular flux analysis to measure mitochondrial respiration following arginine exposure. Tumour responses were examined in inducible nitric oxide synthase (iNOS)-transduced MDA-MB-231 cells by assessing viability and migration in response to different unloaded and loaded MOF NPs. In parallel, CO-releasing systems based on CORM-2 were evaluated for their effects on inflammatory and redox signalling pathways associated with tumour progression and TNBC cell migration.

Results

Arginine-loaded MOFs showed efficient encapsulation and sustained release under physiological conditions (Fig. 1A–E). Released arginine significantly enhanced mitochondrial respiration in activated T cells, increasing basal and maximal oxygen consumption rates compared with untreated controls, indicating improved immunometabolic fitness (Fig. 1F). In TNBC models, arginine-releasing MOFs elevated intracellular NO levels (Fig. 1G,H) and modulated tumour cell migration (Fig. 2E,F), suggesting effects on tumour microenvironment signalling. CORM-2 loading into MOF nanoparticles was confirmed by SEM/EDX (Fig. 2A,B), and intracellular CO generation was verified (Fig. 2C,D). These CO-releasing nanoparticles further modulated redox and inflammatory signalling associated with tumour progression and immune suppression, while also inhibiting TNBC cell migration (Fig. 2E,F). Together, these results show that controlled gasotransmitter delivery can influence both immune cell metabolism and tumour cell behaviour.

Conclusion

This study demonstrates the potential of gasotransmitter-modulating biomaterials to regulate immunometabolism and tumour signalling in TNBC. Arginine-releasing MOFs enhance T-cell metabolic activity, while CO-releasing systems provide additional immunomodulatory signals. The integration of these biomaterial platforms represents a promising strategy to reprogram the TME and improve immunotherapeutic responses in TNBC.

Acknowledgements

Supported by Research Ireland (13/RC/2073_P2), the Irish Research Council (GOIPD/2023/1640; GOIPG/2025/8895), and the MedDevDoc Programme funded through Marie Skłodowska-Curie Actions (101126640).

References

[1]Bronte V, Zanovello P. Regulation of immune responses by L-arginine metabolism. *Nat. Rev. Immunol*; 2005; 5; 641-54.
[2]Geiger R, Rieckmann J.C, Wolf T, Basso C, Feng Y, Fuhrer T, Kogadeeva M, Picotti P, Meissner F, Mann M, Zamboni N, Sallusto F, Lanzavecchia A. L-arginine modulates T cell metabolism and enhances survival and anti-tumor activity. *Cell;* 2016; 167; 829-42.
[3]Loboda A, Jozkowicz A, Dulak J. HO-1/CO system in tumor growth, angiogenesis and metabolism - Targeting HO-1 as an anti-tumor therapy. Vascul. Pharmacol; 2015; 74; 11–22.

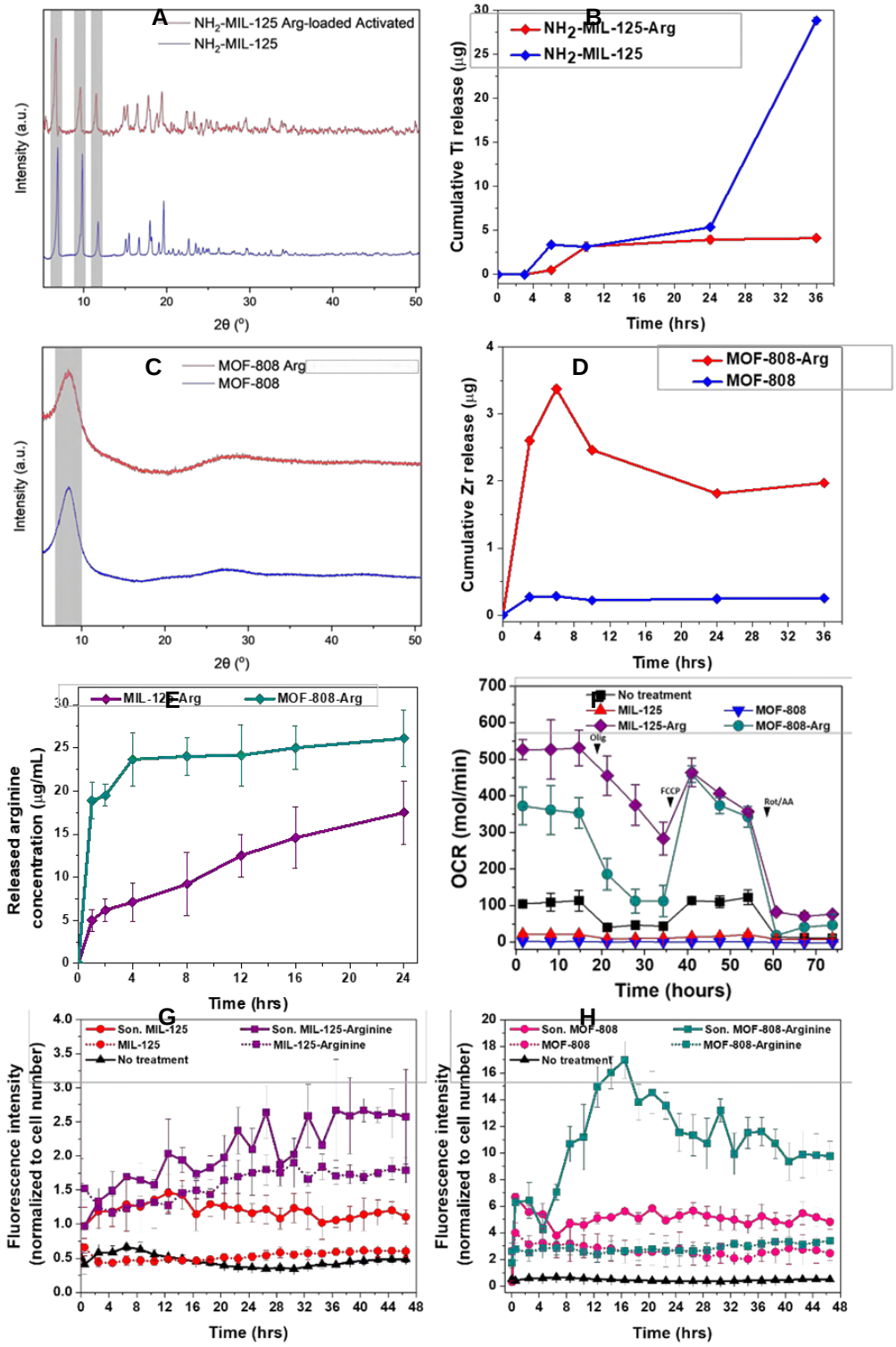

Figure 1. (A,B) PXRD patterns and cumulative Ti release from arginine (Arg)-free and Arg-loaded NH_2-MIL-125 nanoparticles (NPs), in PBS. **(C,D)** PXRD patterns and cumulative Ti release from Arg-free and Arg-loaded MOF-808 NPs in PBS. **(E)** In vitro Arg release from both MOF nanoparticles in PBS at 37 °C quantified by the ninhydrin assay. **(F)** Real-time oxygen consumption rate (OCR) of T cells treated with unloaded or Arg-loaded MOF NPs (50 µg/mL). **(G,H)** Time-dependent intracellular NO production in cells treated with sonicated or unsonicated NH_2-MIL-125 (G) and MOF-808 (H) NPs, either unloaded or Arg-loaded. Data are mean ± SD (n = 3 for OCR; n = 6 for migration).

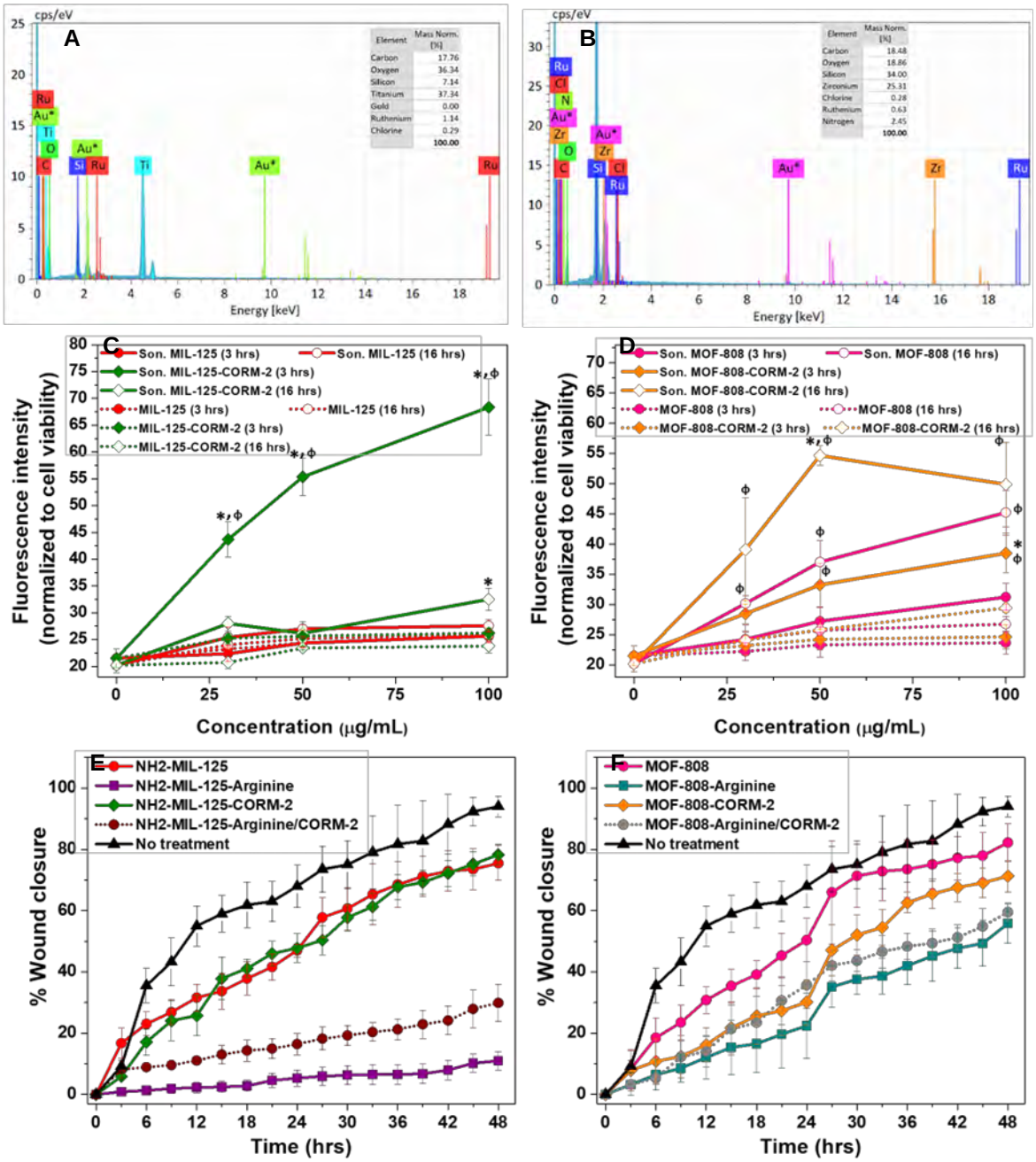

Figure 2 (A,B) EDX spectra of CORM-2–loaded NH_2-MIL-125 and MOF-808 nanoparticles (NPs). (C,D) Time-dependent intracellular CO generation following treatment with CORM-2–loaded NH_2-MIL-125 (C) and MOF-808 (D) NPs. (E,F) Wound closure over time in cells treated with unloaded, Arg-loaded, CORM-2–loaded, or Arg/CORM-2 co-loaded NH_2-MIL-125(Ti) and MOF-808(Zr) NPs. Data are presented as mean ± SD (n = 6).

S41 – O5

Insights into S-nitrosothiol decomposition: S-Nitroso-N-Acetylcysteine as a model for the design of next-generation NO• releasing wound-care materials

Boterberg V.[1], Minsart M.[1], Dubruel P.[1]
[1]Polymer Chemistry & Biomaterials Research Group, Dept. Organic and Macromolecular Chemistry, Ghent University, Belgium

Introduction

Nitric oxide (NO•) plays a key role in wound healing. Low, sustained levels promote tissue regeneration, whereas higher concentrations provide antimicrobial effects. However, its clinical use remains limited. This limitation stems from its instability, the difficulty of controlled delivery and the lack of a well-defined therapeutic window. S-nitrosothiols (RS-NOs) are promising NO• donors. However, their decomposition and NO• release depend strongly on environmental factors.

Aim

This work investigates the non-enzymatic RS-NO decomposition in absence of light and the resulting NO• release under physiologically relevant conditions. It focuses on low, sustained NO• levels for tissue regeneration.

Materials and Methods

S-nitroso-N-acetylcysteine (SNAC) was synthesized and served as primary model compound. All experiments were performed under light-excluded conditions. The study varied pH, buffer type and concentration, initial RS-NO concentration, temperature, chelators and media composition. The tested media included PBS, citrate buffer, HEPES, TRIS, MES, DMEM, simulated wound fluid (SWF) and microbial broth (MHB). SNAC decomposition was monitored using UV–Vis spectroscopy while NO• release was determined through electrochemical detection. In addition, rapid colorimetric assays (BCS, ABTS) enabled prediction of environmental effects on NO• release.

Results

SNAC decomposition and NO• release depended strongly on the environment. The surface area-to-volume ratio, a previously unreported factor, markedly affected decomposition rates. At ≤5 mM SNAC in citrate buffer or PBS, the system produced sustained low-dose NO• (<5 µM) for more than one week at room temperature. In contrast, MES, HEPES and TRIS did not support sustained release, whereas complex media such as DMEM, SWF and MHB did (max. 3 days tested). Higher pH (in range 3–7) slowed RS-NO decomposition, whereas unbuffered conditions caused rapid decomposition. Buffer strength (20–95 mM) had no significant effect. Chelator addition was not required in PBS and complex media, which already suppressed metal-catalyzed decomposition. Rapid assays successfully predicted environmental effects on NO• release.

Conclusion

NO• release from SNAC depends on a complex interplay of environmental factors. Buffer composition and media play key roles. The results identify conditions that enable sustained, low-dose NO• release, which supports tissue regeneration. We also show the need for standardized experimental conditions and introduce predictive assays that link *in vitro* results to physiological conditions. These findings provide a solid basis for designing controlled NO•-releasing systems, including smart wound dressings that combine sustained delivery with on-demand antimicrobial action (see figure). Light-triggered burst release for antimicrobial use was studied separately.

S41 – O6

Structure–property–function relationships of hydrogen- and nitrogen-modified titanium–amorphous carbon coatings for blood-contacting applications

Major R.[1], Zając Z.[1], Więcek-Chmielarz J.[1], Szawiraacz K.[1], Przemysław K.[2], Surmiak M.[3,4], Spuller M.[5], Kopernik M.[6], Major L. [1], Kot M.[5], Lackner Juergen M.[5]

[1]Institute of Metallurgy and Materials Science, Polish Academy of Sciences, Krakow, Poland; [2]Institute of Heart Prosthesis, Foundation of Cardiac Surgery Development, Zabrze, Poland; [3]2nd Dept. of Internal Medicine, Faculty of Medicine, Jagiellonian University Medical College, Krakow, Poland; [4]Center for the Development of Therapies for Civilization and Age-Related Diseases, Jagiellonian University Medical College, Krakow, Poland; [5]Joanneum Research Forschungsgesellschaft mbH, Materials, Institute for Sensors, Photonics and Manufacturing Technologies, Niklasdorf, Austria; [6] AGH University of Krakow, Poland

Introduction

Titanium-based amorphous carbon coatings modified with hydrogen and nitrogen are promising surface engineering solutions for blood-contacting biomedical devices [1,2]. In particular, the development of miniaturized ventricular assist devices (VADs) for paediatric patients requires materials that combine excellent mechanical durability with high hemocompatibility [3]. The project addresses the urgent clinical need for minimally invasive heart support systems for children aged 6–9 years by developing an extremely miniaturized VAD implantable via vascular access. However, current designs are prone to device-induced thrombus formation caused by unfavorable blood flow patterns, high shear stresses, and inadequate surface properties [4]. Therefore, advanced coating materials capable of reducing blood–material interactions while maintaining mechanical reliability are essential. This study investigates titanium–amorphous carbon coatings doped with hydrogen and nitrogen to establish structure–property–function relationships relevant for blood-contacting applications and to evaluate their potential for use in next-generation paediatric VAD technologies.

Materials and Methods

Titanium-based amorphous carbon coatings modified with hydrogen or nitrogen were deposited and systematically characterized in terms of surface, mechanical, structural, and biological properties. Surface roughness, wettability, and surface free energy were analyzed to evaluate potential blood–material interactions. Mechanical performance was assessed using tribological and scratch tests to determine friction behavior, wear resistance, and adhesion. Residual stress states were measured by X-ray diffraction, while transmission electron microscopy was used to analyze structural changes within wear tracks.

To simulate physiological flow conditions relevant to VAD operation, a three-dimensional finite volume model of a radial-flow cell detachment assay was developed to reproduce hydrodynamic loading on coated surfaces. The model predictions were validated against analytical solutions. Biological evaluation included lactate dehydrogenase (LDH) cytotoxicity testing. Cell detachment assays under flow conditions was used to assess blood-cell adhesion behavior. These investigations were performed in the context of developing advanced coating solutions suitable for highly miniaturized VAD components (Fig. 1) requiring excellent hemocompatibility and mechanical stability.

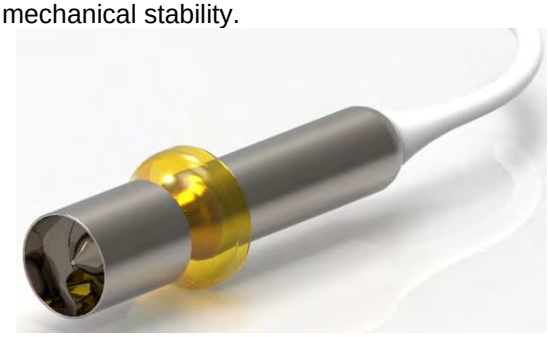

Fig. 1. Original concept elaborated by FRK of miniatural heart pump

Results

All investigated coatings exhibited relatively high surface free energy dominated by dispersive components. Nitrogen incorporation increased surface polarity and wettability. Tribological testing revealed that friction, wear resistance, and adhesion strongly depended on coating composition. Hydrogen- or nitrogen-doped titanium–amorphous carbon coatings demonstrated good mechanical stability and adhesion, whereas coatings containing both nitrogen and hydrogen showed premature failure due to reduced load-bearing capacity. X-ray diffraction measurements indicated very high compressive residual stresses in nitrogen-rich coatings, while hydrogen

incorporation significantly reduced stress, improving durability and adhesion. Transmission electron microscopy revealed friction-induced graphitization within wear tracks, which contributed to friction reduction but accelerated wear in mechanically weaker coatings.
Biological testing demonstrated good biocompatibility for all coatings. Hydrogen-doped coatings exhibited the lowest LDH release, The lowest critical shear stress for blood cell detachment, and reduced cell adhesion under hydrodynamic flow conditions (Table 1).

Tab.1. Critical stress values and its standard deviations

Sample	Critical Stress [Pa]
Ti+a:C-N	12.04±5.87
Ti+a:C-H-N (var. 1)	11.43±3.28
Ti+a:C-H-N (var. 2)	12.10±1.97
Ti+a:C-H	7.79±1.33

Conclusion

The results demonstrate that hydrogenated titanium–amorphous carbon coatings provide the most balanced combination of surface characteristics, mechanical reliability, and biological performance. These properties make them promising candidates for advanced surface engineering of blood-contacting components in miniaturized paediatric ventricular assist devices such as the KIDmicroBLOODpump. The integration of optimized coating materials with innovative VAD design and manufacturing technologies may contribute to reducing thrombogenic risks and improving the safety of minimally invasive heart support systems for children.

Acknowledgements

This work was supported by the Polish National Center for Research and Development project no. M-ERA.NET3/2023/98/KIDmicroBLOODpump/2024

References

1. Robertson J. Diamond-like amorphous carbon. *Materials Science and Engineering R 2002*; 37; 129–281.
2. Bewilogua K., Hofmann D. History of diamond-like carbon films. From first experiments to worldwide applications. *Surface and Coatings Technology 2014;* 242; 214–225.
3. Kirklin J.K., Naftel D.C., Pagani F.D. et al. Sixth INTERMACS annual report: a 10,000-patient database. *Journal of Heart and Lung Transplantation 2014*; 33; 555–564.
4. Bluestein D., Chandran K.B., Manning K.B. Towards non-thrombogenic performance of blood recirculating devices. *Annals of Biomedical Engineering 2010*; 38; 1236–1256.

S41 – O7

Influence of plasma electrolytic oxidation coatings on the corrosion resistance and biocompatibility of biodegradable Mg and Zn-based materials

Domínguez G.[1], Calero L.[1], Molina-Aldareguia J.M.[1,2], Sket F.[1], Llorca J.[1,2], Echeverry-Rendón M.[1]
[1]IMDEA Materials Institute, Getafe, Madrid; [2]Dept. of Material Science, Polytechnic University of Madrid/Universidad Politécnica de Madrid, Spain

Biodegradable metals have emerged as promising candidates for next-generation biomedical implants, particularly for temporary devices intended to support tissue regeneration and then gradually disappear once healing is complete. Among these materials, magnesium (Mg)- and zinc (Zn)-based alloys have attracted significant attention due to their favorable biological roles, suitable mechanical properties, and inherent degradability[1]. Magnesium alloys exhibit excellent mechanical compatibility with bone and good biocompatibility; however, their rapid corrosion in physiological environments may lead to premature mechanical failure and excessive hydrogen evolution. Zinc, on the other hand, degrades at a more moderate rate and presents good biocompatibility, but its limited mechanical strength and the release of Zn ions can negatively affect biological performance. Surface modification strategies are therefore essential to tailor the degradation behavior and biological response of these biodegradable metals. Plasma electrolytic oxidation (PEO) is a surface engineering technique capable of producing porous, ceramic-like oxide layers that improve corrosion resistance while potentially enhancing cell–material interactions. In this study, the influence of plasma electrolytic oxidation coatings on the corrosion resistance and biocompatibility of biodegradable Mg- and Zn-based materials was investigated. The work focused on optimizing key PEO parameters to achieve stable, homogeneous coatings and on evaluating their impact on degradation behavior and cellular response.

For Mg-Zn-Ca alloys, PEO treatments were performed using electrolytes containing either silicate or phosphate species, while varying voltage, current density, processing time, and electrolyte composition[2]. The resulting coatings exhibited uniform porous morphologies with thicknesses of approximately 5–6 µm. Corrosion behavior was evaluated by hydrogen evolution measurements, mass-loss analysis, degradation rate calculations, pH monitoring, and potentiodynamic polarization. The PEO-coated Mg-based samples showed improved corrosion resistance compared with the uncoated material, with lower corrosion current densities and reduced degradation rates. Among the evaluated treatments, phosphate-based PEO coatings provided superior corrosion protection while maintaining a similar surface morphology.

In parallel, phosphate-based PEO coatings were applied to pure Zn substrates to evaluate their effects on corrosion behavior and biological performance[3]. The influence of electrical parameters, including applied voltage and pulsed current modes, was investigated to control coating growth and surface characteristics. Higher voltages generally resulted in thicker coatings, whereas pulsed current conditions produced thinner layers due to reduced duty cycles and modified plasma discharge behavior. Surface characterization revealed that PEO treatment increased surface hardness and reduced contact angles, suggesting improved surface wettability that may favor cell adhesion.

Biological evaluation using osteoblastic cells indicated enhanced cytocompatibility for PEO-treated surfaces, likely due to controlled ion release and favorable surface topography. Overall, the results demonstrate that plasma electrolytic oxidation is an effective surface modification strategy for regulating degradation behavior and improving the biological response of biodegradable Mg- and Zn-based materials. These findings highlight the potential of PEO-coated biodegradable metals for future applications in temporary orthopedic devices and tissue regeneration.

References

1. López, G. D., Williams, P. L., England, E., Wang, J., Boehlert, C., LLorca, J., & Rendón, M. E. (2025). Mg-Zn-ca alloys for biodegradable medical implants. Part I: Effects of zinc and calcium on mechanical and corrosion behavior and cytocompatibility. Surface and Coatings Technology, 132519.
2. López, G. D., Williams, P. L., England, E., Wang, J., Boehlert, C., LLorca, J., & Echeverry-Rendón, M. (2025). Mg-Zn-Ca alloys for biodegradable medical implants. Part II: Surface modification using plasma electrolytic oxidation to improve corrosion resistance and biocompatibility. *Surface and Coatings Technology*, 518, 132860.
3. López, G. D., Williams, P. L., LLorca, J., & Echeverry-Rendón, M. Optimization of phosphate-based plasma electrolytic oxidation coatings on commercially pure zinc. *Surfaces and Interfaces 2025*, 107243.

S42
Macromolecular assemblies composed of peptides or proteins

S42 – K1
Protecting tissue surfaces using soft matter

Grover L.
Univeristy of Birmingham – UK

S42 – O1

Biofunctionalization of biomaterial surfaces using diazirine-based linkers from proof of concept to future applications

Rad N.[1], Marta Klak[1,2], Sylwester Domański[1]
[1]Polbionica S.A., Zielona Góra, Poland1, [2]Fundacja Badań i Rozwoju Nauki, Warsaw, Poland

Diazirines are essential reagents in photoaffinity labeling and attract significant interest in the functionalization of biological macromolecules. Their popularity stems from their ability to generate highly reactive carbene species upon exposure to UV/Vis light or elevated temperatures. The generated carbene can insert into nearby bonds or interact with adjacent groups, enabling targeted covalent attachment at specific sites where the diazirine moiety is localized. While this high reactivity offers advantages for photoaffinity labeling, it also poses challenges for achieving precise and controlled functionalization of biopolymers

Many natural polymers contain hydroxyl groups, and functionalization of these groups can expand the range of applications for such polymers. Traditional chemical cross-linking methods often produce significant quantities of byproducts, which can be undesirable. To address this issue, we aimed to develop a diazirine-based linker capable of selective insertion into hydroxyl bonds. We investigated the reactivity of 3-trifluoromethyl-3-aryldiazirine derivatives toward hydroxyl groups as potential linker molecules. These diazirines are characterized by a combination of high stability and photoaffinity. Additionally, the reactivity of this diazirine class can be modulated by the nature of substituents in the para position, enabling tailored reactivity profiles.

We identified conditions that minimize the formation of byproducts and conducted kinetic studies of the OH-insertion process to elucidate the underlying mechanism of the reaction.

S42 – O2

Soft scaffolds, smart delivery: Peptide hydrogels for sustained release of biologicals

Vu H.[1], Peeters E.[2], Hofkens K.[2], Vandemeulebroecke K.[3], T'Sas S.[2], Martin C.[4], Ballet S.[4], Hoogenboom R.[1], Goossens S.[2], Lammens T.[3], Van Trimpont M.[2], Madder A.[1]

[1]Dept. of Organic and Macromolecular Chemistry, Ghent University; [2]Dept. of Diagnostic Sciences, Ghent University; [3]Dept. of Pediatric Hematology-Oncology and Stem Cell Transplantation, Ghent University Hospital; [4]Dept. of Chemistry, Vrije Universiteit Brussel, Belgium

Introduction

Thixotropic peptide hydrogels are promising biomaterials for tissue engineering and controlled drug delivery due to their biocompatibility, biodegradability, and injectability. Our hydrogels are formulated from short, all-natural hexapeptides that self-assemble into networks via non-covalent interactions. The amphiphilic peptide sequences used here are the shortest known ionic self-complementary hydrogelators composed entirely of unmodified natural amino acids, making them attractive for scalable production. Previous studies have demonstrated their ability to release a variety of cargos, including small molecules, peptides, and proteins. In this work, we expand their application to biologicals by developing a sustained-release formulation of Erwinase, an FDA-approved asparaginase enzyme used as a second-line treatment for acute lymphoblastic leukemia (ALL).

Materials and Methods

This study investigates the loading capacity of different peptide hydrogel formulations and the factors influencing protein release. Insights from these analyses were used to design a sustained-release Erwinase formulation. Both *in vitro* and *in vivo* (pharmacokinetic) studies were conducted, measuring cumulative release and enzyme activity over time. The use of these hydrogels could enable sustained release from high-loading formulations and overcome the short in vivo half-life of Erwinase, thereby maintaining prolonged therapeutic plasma levels.

Results

Protein release profiles varied depending on cargo properties and hydrogel stability. Release was primarily governed by network erosion and electrostatic interactions between the peptide matrix and encapsulated proteins. High-loading Erwinase hydrogels with good injectability were successfully developed. *In vitro* studies showed sustained enzyme release over three days, with full retention of enzymatic activity. Pharmacokinetic studies demonstrated prolonged serum L-asparaginase activity compared to subcutaneously injected PBS control (Figure 1). While no significant extension in activity was observed relative to intramuscular injection, hydrogel encapsulation reduced the initial burst release, which may help decrease toxicity and side effects.

Conclusion

By tuning electrostatic interactions and formulation parameters, peptide hydrogels can allow high protein loading while maintaining injectability and controlled release. This study presents the first injectable peptide hydrogel formulation for sustained delivery of L-asparaginase. While circulation time remains comparable to existing treatments, the reduced initial burst highlights potential safety benefits. Given their high loading capacity, preserved enzyme activity, and simple "mix-and-go" preparation, these hydrogels offer a versatile platform for developing improved enzyme therapies and cancer treatments.

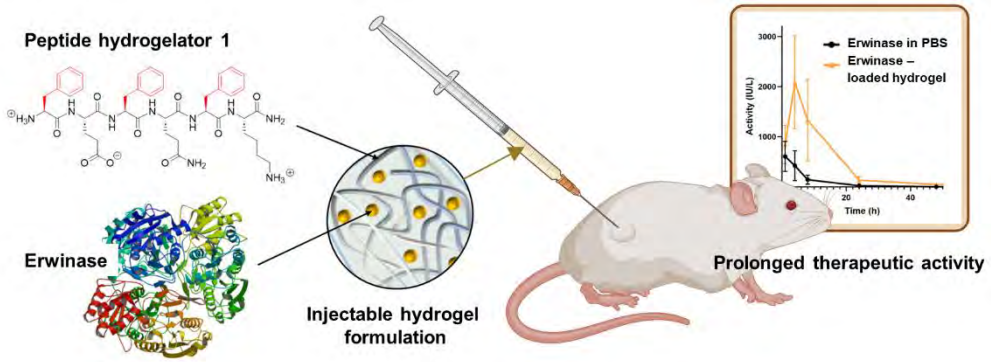

Figure 1. Peptide-based hydrogel formulations for sustained delivery of Erwinase

S42 – O3

Self-assembled peptide hydrogels with bioactive motifs for 3D lung cancer modeling

Sırma Tarım B.[1], Tamburacı S.[2], Top, A.[3]
[1]Dept. of Chemical Engineering, Izmir Institute of Technology, Türkiye

Introduction

Self-assembled peptide hydrogels can offer a promising platform for the development of three-dimensional (3D) in vitro cancer models to recapitulate the structural and biochemical complexity of the tumor microenvironment. Two-dimensional (2D) cultures fail to mimic the spatial arrangement, cell–matrix interactions, and mechanical properties of actual tumors, leading to poor predictive accuracy in drug screening and cancer biology research.[1] Self-assembled peptide hydrogels, which form under physiological conditions with ECM-like structures, can be used to encapsulate cancer cells and allow them to grow in a 3D microenvironment. Specific bioactive sequences can be incorporated into the hydrogel network to enhance bioactivity.[2] Thus, these 3D platforms can mediate to observe cancer progression and anticancer drug response in a more physiologically relevant manner.

Aim

The objective of this study is to incorporate cell attachment motifs and enzyme-degradable sequences into the peptide hydrogelators and evaluate their physicochemical and biological properties for 3D lung cancer model applications.

Materials and Methods

Peptide synthesis was carried out using the Fmoc-based solid-phase peptide synthesis method. Peptide purity was evaluated using MALDI-TOF-MS and RP-HPLC. The secondary structures of the peptides were confirmed by ATR-FTIR and CD spectroscopy. TEM and oscillatory rheometer measurements were used to determine morphological and viscoelastic properties of the hydrogels, respectively. A549 adenocarcinoma lung cancer cells and MRC-5 lung fibroblast cells were encapsulated into these hydrogels. Viability, proliferation and spreading of the encapsulated cells were investigated using Alamar Blue assay, live/dead staining, and DAPI/phalloidin staining, respectively. Anticancer drug response of the cells in 3D matrices was assessed.

Results

The molar mass and purity of the peptides were confirmed. ATR-FTIR and CD spectroscopy results supported the formation of β-sheet conformations. The peptides were shown to form self-supporting hydrogels in cell culture medium. TEM images revealed a nanofibrillar morphology of the peptide hydrogels. Frequency sweep measurements indicated that the storage moduli of the hydrogels were comparable to those of other peptide-based hydrogels. The hydrogels supported the viability, proliferation, cluster formation, and migration of encapsulated A549 cells. The cells cultured within the 3D matrices exhibited resistance to anticancer drugs after 7 days.

Conclusion

The bioactive peptide hydrogels containing cell attachment and enzyme-degradable sequences offer a promising platform for 3D cancer models.

Acknowledgements

This project was financially supported by The Scientific and Technological Research Council of Turkey (TÜBİTAK) (grant number: 122M821).

References

[1]Rauner, G., Gupta, P. B., & Kuperwasser, C. From 2D to 3D and beyond: the evolution and impact of in vitro tumor models in cancer research. *Nature Methods 2025*, *22*(9), 1776-1787.
[2] Marin, D., & Marchesan, S. Self-assembled peptide nanostructures for ECM biomimicry. *Nanomaterials 2022*, *12*(13), 2147.

S42 – O4

Designing peptide hydrogels as a localised delivery vehicle for adjuvant glioblastoma synergistic chemotherapy

Nasser N.[1,2], Tapeinos C.[1], Saiani A.[1,2]
[1]Division of Pharmacy & Optometry University of Manchester; [2]Manchester Institute of Biotechnology, University of Manchester, UK

Introduction

Glioblastoma (GB) is an aggressive brain cancer where current clinical modalities remain inadequate in preventing recurrence. Conventional drug administration has consistently shown limited efficacy, systemic toxicity(*1*), and poor cerebral penetration due to the blood-brain barrier (BBB)(*2*), leading to stagnant survival outcomes. Fully synthetic, biocompatible and non-inflammatory self-assembled peptide hydrogels (SAPHs)(*3*) offer a promising solution for intracerebral drug delivery(*4*), after tumour resection to localise chemotherapy, overcoming conventional administration challenges and reducing recurrence.

Aim

We investigate the use of injectable SAPHs as a localised cancer drug delivery vehicle following Glioblastoma resection to prevent recurrence and improve patient outcomes.

Materials and Methods

Three SAPHs of varying pH and charge were formulated with *Temozolomide* (TMZ) and *Thymoquinone* (TQ), where encapsulation and drug stability were characterised by UV-Vis spectroscopy. Release profiles were determined over 4 days by High Performance Liquid Chromatography (HPLC), and therapeutic co-delivery was modelled via Transwell® assay against U251 MG cells. Drug synergism was quantified using the Chou-Talalay method, and the biocompatibility of the lead formulation was assessed with non-cancerous glial cells.

Results

Three peptide designs - $(FEFK)_2$, $K(FEFK)_2K$ and $EE(FKFE)_2E$ - showed different gelation pH and charge profiles when forming self-supporting hydrogels. $(FEFK)_2$ demonstrated the most favourable sustained release, with low pH identified as a critical parameter for preventing both drugs' degradation. By optimising the drug loading ratio, the co-loaded hydrogel induced near-total U251 MG cell death (Combination Index, CI < 1). $(FEFK)_2$ showed no effect on the metabolic activity of non-cancerous glial cells.

Conclusion

$(FEFK)_2$ was the most promising formulation for co-delivering TMZ and TQ. The next phase of the investigation will be assessing formulation efficacy in relevant physiological models, including tumour spheroids and patient-derived tissues, to validate clinical relevance.

References

[1]J. L. Villano et al., Cancer Chemother Pharmacol 2012. 69, 107–113.
[2]S. Ostermann et al., Clinical Cancer Research 2004. 10, 3728–3736.
[3]A. Markey et al., Journal of Peptide Science 2017. 23, 148–154.
[4]F. Bolan et al., Transl. Stroke Res 2024. 15, 986–1004.

S42 – O5

Electrostatically tunable peptide hydrogels for embedded bioprinting and nanoparticle delivery

Taheri S.[1], Kilian K.A.[1]
[1]School of Chemistry, Australian Centre for NanoMedicine, UNSW Sydney, Australia

Introduction

Supramolecular peptide hydrogels are promising biomaterials for therapeutic delivery and biofabrication due to their injectability, dynamic mechanics, and extracellular matrix–like nanostructure. However, many systems exhibit slow gelation and limited mechanical stability, restricting their use in printing and translational applications. Here, we engineer charge-tunable tryptophan zipper (Trpzip) peptide hydrogels that rapidly assemble into supramolecular networks with tunable yield-stress mechanics. Beyond supporting cell growth and phenotype maintenance, these materials are promising as matrices for 3D bioprinting and carriers for nucleic acid-loaded lipid nanoparticles (NA-LNPs).

Materials and Methods

Oppositely charged Trpzip (T^+ and T^-) were mixed at defined ratios to form supramolecular hydrogels at 37 °C. Gelation and β-sheet assembly were evaluated by inversion tests and Thioflavin-T fluorescence, while surface charge and viscoelastic properties were characterized using zeta potential analysis and rheology. Bioactivity was assessed by encapsulating human adipose-derived stem cells (ADSCs) and measuring morphology (days 2 and 7) and metabolic activity using Alamar Blue assays. ADSC inks were bioprinted into droplet and line constructs within an oppositely charged Trpzip hydrogel support bath using a LulzBot 3D bioprinter and compared with gelatin microparticle baths. For delivery studies, nucleic acid–loaded lipid nanoparticles were entrapped in hydrogels and release-mediated transfection evaluated by fluorescence microscopy and flow cytometry.

Results

Mixing oppositely charged peptides accelerated gelation and increased β-sheet assembly, producing mechanically robust hydrogels. Increasing T^- content enhanced supramolecular crosslinking, raising the yield point ~4-fold in 0.75% T^+/0.25% T^- hydrogels compared with controls while maintaining pronounced shear-thinning and rapid thixotropic recovery (~75% modulus recovery after repeated shear cycles). Zeta potential decreased with increasing T^- content, correlating with enhanced gelation and supporting electrostatic attraction as a key driver of network stabilization and β-sheet assembly; ionic conditions in DMEM further influenced this behavior. These properties enable reversible network fluidization during extrusion while preserving structural stability after deposition. ADSCs encapsulated within hydrogels showed high viability and proliferation over 7 days (Figure 1a), while confocal morphometrics revealed formulation-dependent modulation of cell spreading, indicating electrostatic tuning of cell–matrix interactions (Figure 1b–d). During embedded printing, the yield-stress network enabled stable deposition and rapid self-healing. Unlike gelatin microparticle baths used in FRESH that liquefy near physiological temperatures, the peptide hydrogels remain stable at 37 °C, enabling printing under physiological conditions. The hydrogels also served as reservoirs for LNPs and ADSC-derived extracellular vesicles, enabling controlled release under varied conditions.

Conclusion

Charge-tunable Trpzip peptide hydrogels provide a modular supramolecular platform combining rapid assembly, yield-stress mechanics, strong shear recovery, and cytocompatibility. These materials function as stable support baths for embedded bioprinting and enable spatiotemporal release of nucleic acid–loaded LNPs in situ, highlighting their potential for regenerative medicine, gene therapy, and advanced biofabrication.

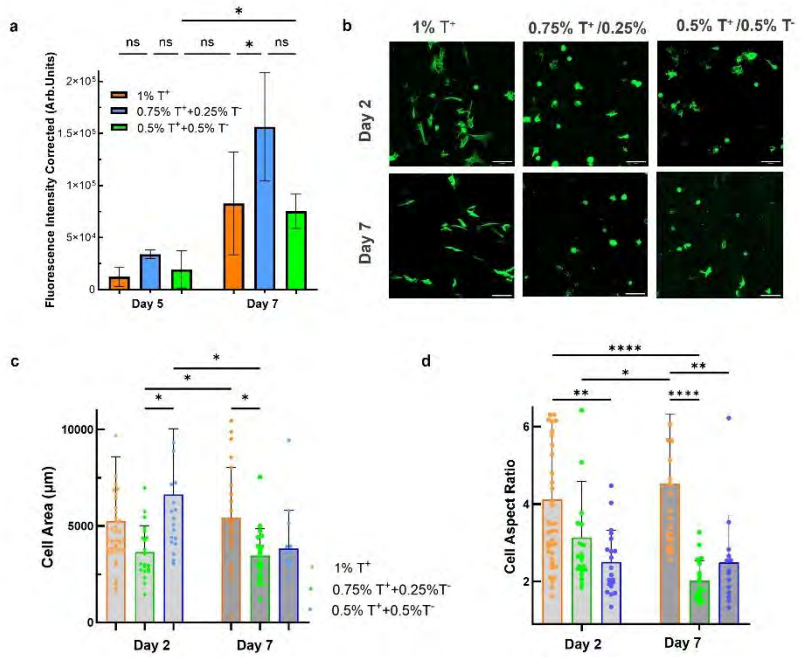

Figure 1. ADSC viability, proliferation, and morphology in charge-tunable Trpzip hydrogels. (a) ADSC metabolic activity in T^+/T^- hydrogels measured by Alamar Blue at days 5 and 7 (mean ± SD, n = 3). (b) Representative confocal images of ADSCs cultured in hydrogels at days 2 and 7 (F-actin staining, green; scale bar: 100 µm). Quantitative analysis of (c) cell spread area and (d) aspect ratio for ADSCs cultured in different hydrogel formulations. Statistical significance determined by one-way ANOVA.

S42 – O6

A barnacle-inspired mineralization peptide for dentin occlusion and bone repair

Song J.[1], Hu B.[1]
[1]National University of Defense Technology, Changsha, China

Abstract

Barnacles exhibit strong underwater bonding performance, relying on its multi component cements to permanently and firmly adhere to the surface of almost all underwater facilities, providing an excellent template for the development of biomimetic adhesives. For instance, the cement protein cp20k exhibits dual functionality: interfacial adhesion and the promotion of biomineralization. Based on this protein, our team designed a barnacle cement-derived peptide (CCP) that occludes dentinal tubules by combining adhesive properties with phosphate-triggered mineralization. Featuring a disulfide-stabilized structure, CCP selectively binds phosphate ions, rapidly nucleates amorphous calcium phosphate, and facilitates its conversion to hydroxyapatite. This process achieves deep tubule occlusion and restores the native mechanical strength of dentin in vitro. In contrast to conventional calcium-targeting peptides, CCP operates through a phosphate-sequestration mechanism, which results in exceptional retention of the mineral layer under oral abrasion in vivo. This offers a novel biomimetic strategy for durable dentin repair. Furthermore, cp20k-derived peptides have demonstrated unique self-assembly capabilities and the ability to promote osteoblast proliferation and differentiation, indicating broad application potential in areas such as bone repair.

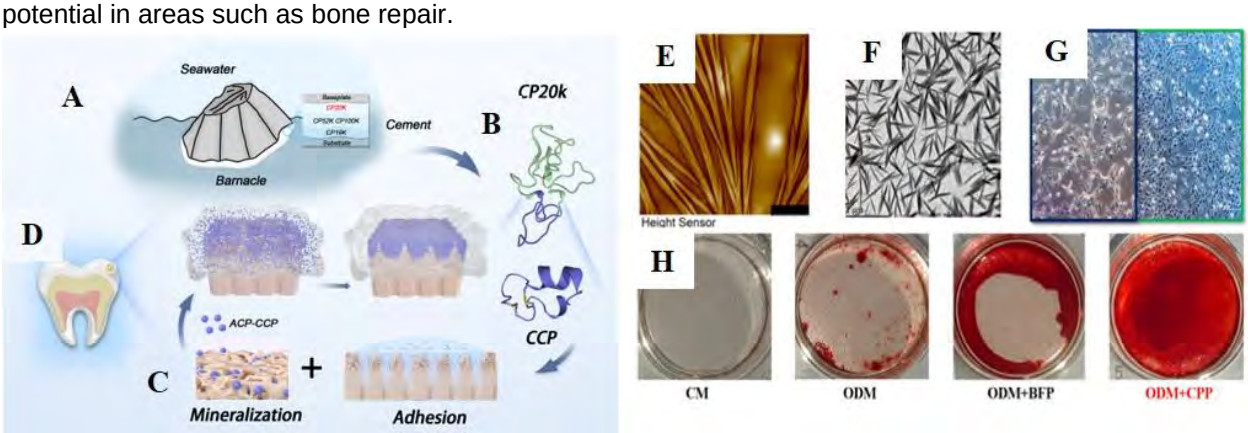

Figure 1. Application of CCP in the remineralization of demineralized dentin. **A)** In the multi-layer structure, cp20k is located at the top and primarily responsible for adhesion between the foreign substrate and the cement matrix. **B)** A segment of amino acid sequence CCP within cp20k. **C)** CCP can adhere to organic matrices on demineralized dentin surfaces and promote calcium phosphate mineralization. **D)** CCP induces a remineralization layer formation both inside and on the surface of demineralized dentinal tubules. **E/F)** AFM and TEM images of CCP self-assembly. **G)** CCP promotes the proliferation of BMSCs. H) Alizarin Red staining shows mineral deposition on the cell surface.

S42 – O7

Phlorotannin-inspired coatings for enhanced cytocompatibility and anti-inflammatory protection

Brosio, T.[1], Angelino, S.[2], Scalia, A. C.[1], Najmi, Z. [1], Alfieri, M. L.[2], Napolitano, A.[2], Cochis, A.[1], Rimondini, L.[1]
[1]Dept. of Health Sciences, University of Piemonte Orientale, Novara; [2]Dept. of Chemical Sciences, University of Naples Federico II, Italy.

Introduction

Acute and chronic wounds represent a significant clinical and economic burden. Acute wounds arise from sudden skin injuries and typically heal through the coordinated progression of the four phases of wound repair, leading to complete tissue regeneration. However, pathological conditions such as diabetes may prolong the inflammatory phase, promoting the transition to a chronic, non-healing state characterized by elevated levels of pro-inflammatory cytokines, neutrophils, and matrix metalloproteinases (MMPs). In this context, the development of wound dressings that support tissue regeneration while modulating inflammation is of great interest. Phlorotannins, found in brown algae, exhibit potent antioxidant and anti-inflammatory properties, yet the complexities of extraction and purification limit their large-scale application. Synthetic mimics of phlorotannins can be developed *via* a bottom-up approach involving phloroglucinol (FG) oxidative polymerization. This strategy is designed to overcome the drawbacks of natural compounds, yielding materials that should maintain similar structural features while providing enhanced functional properties.

Aim

The study has focused on the preparation of FG-based coatings to mimic these natural properties on glass substrates and gauzes.

Materials and Methods

Substrates were functionalized *via* the oxidative polymerization of phloroglucinol (10 mM) in the presence of hexamethylenediamine (HMDA) in carbonate buffer (pH 9.0) for 24 hours. Cytocompatibility was evaluated using human mesenchymal stem cells (hMSCs). The protective and anti-inflammatory effects were assessed after exposure to H_2O_2 and pro-inflammatory cytokines by monitoring intracellular ROS production and inflammatory gene expression. Finally, coating cytocompatibility and regenerative potential were investigated using a reconstructed human epidermis 3D model (EpiDerm).

Results

FG-based adhesive coatings have been successfully prepared through the oxidative polymerization of FG in the presence of HMDA. Biological assays revealed excellent cytocompatibility in monolayer. Under oxidative stress (H_2O_2), coated samples significantly maintained cellular metabolic activity relative to stressed controls. Furthermore, RT-PCR analysis confirmed a significant down-regulation of pro-inflammatory markers (TNFα, IL-1β, COX2) in cytokine-stressed cells. When in contact with the material, the 3D skin model showed remarkable cytocompatibility and showed no signs of irritation or tissue damage compared to Sodium Dodecyl Sulfate (SDS)-treated controls.

Conclusion

FG-HMDA coatings effectively mimic the bioactivity of natural phlorotannins, providing a cytocompatible and non-irritating surface. Their ability to mitigate oxidative stress and inflammation in both 2D and 3D models highlights their potential for functionalizing biomaterials in wound management and tissue engineering.

S43
Metabiomaterials and functional biomaterials: Bridging structure, mechnics and biology

S43 - K1
Leveraging additive manufacturing for orthopaedic metabiomaterials

Cox S.C.
Centre for Custom Medical Devices, University of Birmingham, UK

Introduction
Layer-by-layer processing of material via additive manufacturing (AM) technologies has opened new geometrical design possibilities for medical devices. Specifically for orthopaedics, metal AM processes such as powder bed fusion have been employed to create skeletal implants with intricate porous structures that can support tissue fixation. These lattice-based devices may also be customised to a patient's anatomy, offering surgeons new possibilities for reconstruction following complex operations such as revisions or limb salvage.
This talk will review the current use of porous structures for commercial skeletal implants and unpick the outstanding challenges in producing them via powder bed fusion (PBF). Beyond this the possibility to add further functionality to such devices, forming metabiomaterials will be discussed. Including exploration of novel biomedical alloys produced in-situ via PBF with regenerative biological functions, such as pro-osteogenic and antimicrobial to tackle outstanding clinical challenges.

Aim
Exploring the potential of metabiomaterials to solve outstanding clinical challenges within skeletal implants

Materials and Methods
Micro-computed tomography has been employed to explore on-market skeletal devices, specifically acetabular cups from a range of different manufacturers. This data provides a perspective on the quality of PBF implants from which process knowledge has been employed to refine reproducibility and accurate of such intricare structures. Beyond this, blended elemental powders were also processed by laser-based PBF to form a range of novel biomedical alloys in-situ. A range of characterisation and in-vitro tests were then employed to understand the performance of these new metabiomaterial structures.

Results and Conclusion
PBF is a widely employed technique to produce skeletal implants with intricare lattice structures (100-200um), which enhances fixation with surrounding tissue. Bringing together these advanced manufacturing process with new metal biomaterials presents the opportunity to functionalise such devices for specific biological processes. We demonstrate this with Cu-containing titanium alloy compositions and demonstrate that process parameters may play a significant role in tuning biological outcomes, such as bacterial adhesion. The opportunity to create pro-osteogenic metabiomaterials via AM is also presents through incorporation of elements such as Sn in titanium matrices.

Acknowledgements
The whole Centre for Custom Medical Devices team at the University of Birmingham are acknowledge for research delivery.

S43 - K2
Auxetic Metamaterials for Skeletal Muscle Regeneration

Kalogeropoulou M.,[1] Kaur P.,[2] Boffito M.,[2] Fucile P.,[1] Ciardelli G.,[2] Moroni L.[1]

[1]Department of Complex Tissue Regeneration, MERLN Institute for Technology - Inspired Regenerative Medicine, Maastricht University, Maastricht, The Netherlands;
[2]Department of Mechanical and Aerospace Engineering, Politecnico di Torino, Turin, Italy;

Introduction

Skeletal muscle tissue engineering faces a major challenge in replicating the structural and mechanical heterogeneity of native muscle. Current treatments for critical-size muscle defects, such as muscle flaps and allogenic transplants, are limited by donor site morbidity and immune complications. Although tissue engineering strategies are advancing, most fail to mimic the complex deformation behavior of skeletal muscle under physiological loading. Auxetic metamaterials, characterized by a negative Poisson's ratio, offer unique mechanical advantages, including enhanced energy absorption and deformation capacity, making them promising candidates for muscle regeneration.

Aim

This study aims to investigate the role of Poisson's ratio in regulating skeletal muscle differentiation and maturation under dynamic mechanical loading.

Materials and Methods

Nine auxetic unit cell geometries were analytically designed and optimized to achieve varying degrees of auxeticity while maintaining suitable pore sizes for cell seeding. These designs were fabricated as 2.5D lattices using melt extrusion printing with a PCL-PLLA copolymer. Mechanical properties were characterized through COMSOL simulations, tensile testing, and computer vision analysis of lateral expansion videos. Three geometries, namely tetrachiral, Lozenge, and arrowhead grids, were selected based on distinct auxetic responses and low elastic moduli. A typical 0-90 scaffold was also included as a positive Poisson's ratio control. Scaffolds were seeded with C2C12 myoblasts embedded in fibrin and subjected to cyclic tensile strain (0–3%) for 3 hours daily over 10 days. Cellular responses were assessed using immunostaining and qPCR analysis. The experimental pipeline is illustrated in **Figure 1.**

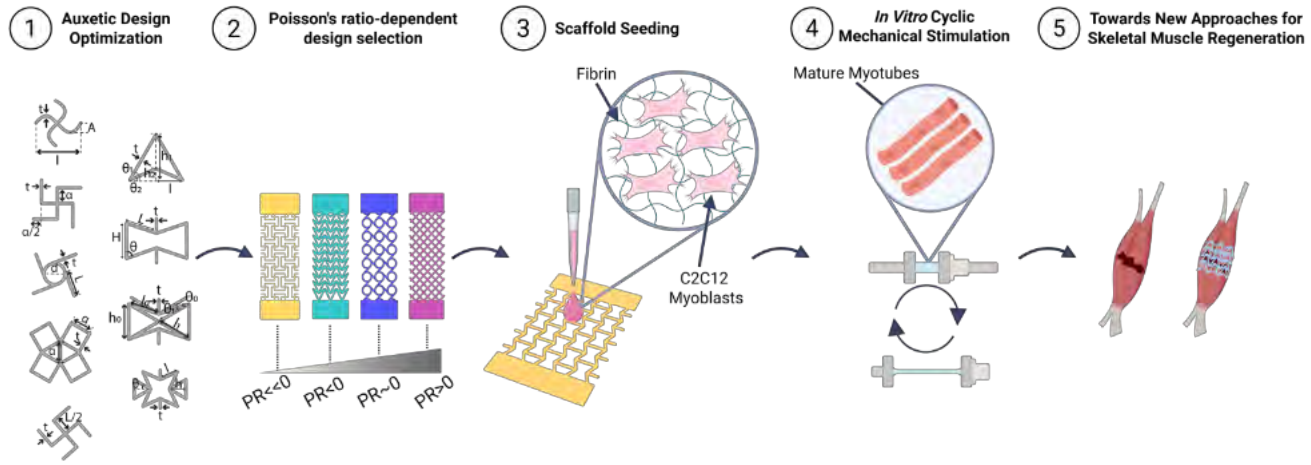

Figure 1. Experimental pipeline illustration of the present study.

Results

Results demonstrated a Poisson's ratio-dependent response in myotube fusion, alignment, and maturation. The expression of fusion, maturation and myofiber-type commitment genes (MYH1, MYH2, MYOG, MYOD1) followed a clear downward trend with decreasing Poisson's ratio during cyclic stimulation. Interestingly in static controls, the opposite trend was observed, hinting at the effect of the scaffold geometry on the passive tension established by the fibrin network. Additionally, mechanosensing-specific genes (YAP1, WWTR1) were affected by the degree of scaffold auxeticity. Finally, the Poisson's ratio was found to have an effect on myotube alignment, maturation index and hypertrophy. Hence, by isolating auxetic behavior from stiffness effects, the findings show that negative Poisson's ratio deformation is directly sensed by developing muscle cells and influences their maturation.

Conclusion

This work provides the first, to date, direct evidence that negative Poisson's ratio is an independent mechanical cue influencing skeletal muscle development. Auxetic metamaterials were found to not only enhance myogenic outcomes but also offer a tunable platform to better replicate the dynamic mechanical environment of native tissue. These findings highlight the significant potential of auxetic scaffolds in advancing functional skeletal muscle regeneration and addressing current limitations in the treatment of large volumetric muscle loss.

S43 – O1

Stochastic voronoi-based data-driven generation of trabecular bone surrogates with morphologically representative microarchitecture

Piacentini M.[1], Skallerud B.[2], Gao C.[1]
[1]Dept. of Mechanical and Industrial Engineering, Norwegian University of Science and Technology; [2]Dept. of Structural Engineering, Norwegian University of Science and Technology, Trondheim, Norway

Introduction

Trabecular bone is a porous cellular solid whose mechanical behavior is governed by the geometry and connectivity of individual trabeculae. Generating three-dimensional (3D) synthetic structures that faithfully reproduce trabecular morphology remains challenging, yet is essential for scaffold design, biomaterials research, and in silico testing. Voronoi tessellation offers a flexible framework for generating geometries resembling trabecular topologies. However, the mapping between generation parameters—such as seeding distributions, anisotropic growth rules, and post-processing operations—and resulting morphological descriptors is complex and underinvestigated. Data-driven strategies can bridge this gap by enabling systematic, target-driven generation of bone-mimicking microstructures.

Aim

This study develops a computational framework for generating 3D stochastic Voronoi-based structures whose morphological descriptors are statistically consistent with those of trabecular bone microarchitectures reconstructed from micro-CT imaging.

Materials and Methods

Trabecular bone samples reconstructed from micro-CT imaging are morphologically characterized using descriptors including bone volume fraction, connectivity density, degree of anisotropy, ellipsoid factor distribution, trabecular spacing and trabecular thickness. These define the morphological targets for generation. A stochastic Voronoi-based generation pipeline is developed, combining tunable seeding distributions and anisotropic growth parameters with graph-level post-processing operations including strut and plate nucleation, thickening, and pruning to modulate the cellular geometry. Machine learning surrogates are trained to predict morphological descriptor distributions as a function of generation parameters and to drive the post-processing operations on the Voronoi graph towards target morphologies. Generated structures are discretized and quantitatively verified against imaging-derived targets.

Results

Preliminary results show that Voronoi-based structures with controlled seeding, anisotropic growth, and targeted post-processing can reproduce plate-like and rod-like trabecular geometries. The machine learning surrogate effectively maps generation parameters to morphological outcomes, enabling guided parameter identification without exhaustive sampling. Quantitative comparison against micro-CT-derived targets identifies which morphological descriptors are most sensitive to specific generation choices, informing the design of the generation pipeline. A graph-evolution perspective in which post-processing operations are formulated as sequential decisions on the Voronoi graph emerges as a promising strategy for automated morphological optimization.

Conclusion

This work presents a data-driven framework for generating 3D Voronoi-based trabecular bone surrogates with morphologically representative microarchitecture. By coupling parametric tessellation with machine learning-assisted design, the approach offers a tractable pathway to produce synthetic microstructures that match key morphological descriptors of real trabecular bone. Potential applications include scaffold design for tissue engineering, biomaterials development, and large-scale in silico parametric studies.

Acknowledgements

The authors acknowledge the support from MSCA DN GAP project (No. 101120290).

S43 – O2

A molecular-weight-tuned fibrin–alginate IPN for modelling stiffness-linked cardiac ageing and fibrosis in 3D

Ribeiro J. S.[1], Sampon T.[1], Joglekar M. M.[1], Mota C.[1], Baker M. B.[1], Moroni L.[1]
[1]MERLN Institute for Technology-Inspired Regenerative Medicine, Maastricht University, The Netherlands

Introduction

Cardiac ageing is associated with progressive biomechanical and multicellular changes. Although matrix mechanics are increasingly recognized as important regulators of cardiac cell behaviour, many models vary stiffness together with matrix composition, ligand presentation, or architecture, making it difficult to isolate mechanical effects. Moreover, it remains unclear whether matrix stiffening is primarily a consequence of cardiac ageing and remodelling or whether it also acts as a driver of these phenotypic changes. In this study we aimed to establish a controllable biomaterial platform for probing these effects. We did so by engineering fibrin–alginate interpenetrating network (IPN) hydrogels in which mechanical properties are tuned through alginate molecular-weight blending rather than changes in protein content.

Materials and Methods

High- and low-molecular-weight alginates were combined at defined ratios while maintaining constant fibrin concentration, generating a five-condition formulation series. Alginate molecular-weight distributions were verified by GPC, and gel viscoelastic behaviour was assessed by oscillatory time sweep, frequency sweep, and stress-relaxation rheology. Additionally, the effect of CaCl2 crosslinking time on gel viscoelasticity and swelling behaviour was assessed to refine the accessible mechanical window and formulation stability. As an initial biological validation, hiPSC-cardiomyocytes were encapsulated in the softest and stiffest endpoint formulations and cultured for 7 days. Viability, metabolic activity, and spontaneous beating behaviour were assessed over time. Furthermore, selected soft, intermediate, and stiff formulations were further evaluated with iPSC-derived endothelial cells (hiPSC-ECs), cardiac fibroblasts (hiPSC-CFs), and their co-cultures.

Results

The IPN generated reproducible, ratio-dependent changes in viscoelastic behaviour, demonstrating that polymer molecular-weight distribution can be used to define mechanically distinct cardiac microenvironments, maintaining fibrin dose. Across the series, the platform spanned a stiffness ladder from the 0.2kPa to 16kPa range, and longer CaCl2 crosslinking further increased gel stiffness while modulating swelling behaviour. Both endpoint formulations supported hiPSC-cardiomyocyte viability and metabolic activity through day 7, while softer LMW-rich gels promoted more robust spontaneous beating (around 55bpm) than stiffer counterparts. In selected formulations, hiPSC-ECs, hiPSC-CFs, and their co-cultures were also supported in 3D culture and assessed for endothelial identity and fibroblast activation-associated features by CD31, vimentin, and αSMA immunofluorescence, extending the platform toward multicellular cardiac remodelling studies.

Conclusion

A molecular-weight-programmed fibrin–alginate IPN provides a practical route to generate mechanically distinct cardiac microenvironments while preserving constant fibrin content. By combining molecular-weight blending with controllable ionic crosslinking, the platform supports systematic interrogation of stiffness-dependent responses across cardiac cells, and is well suited for studying cardiac remodelling, ageing, and fibrosis.

Acknowledgements

This work was supported by the Dutch Research Council (NWO) through the Perspectief programme within the FAB4FUTURE project (P22.005).

S43 – O3

Bioprinting of phenotypically defined fibrocartilage microtissues into melt electrowritten scaffolds to engineer regionally defined meniscal grafts

Kronemberger, G.S.[1,2,3], Spagnuolo, F.D.[1,2,3], Roncada, T.[1,2,3], Chattahy, K.[1,2,3], Karam, A.S.[1,2,3], Gibney, R.[1,2,3], Wirth, M.[1,2,3] and Kelly, D.J.[1,2,3,4]

[1]Trinity Centre for Biomedical Engineering, Trinity Biomedical Sciences Institute, Trinity College Dublin; [2]Dept. of Mechanical, Manufacturing and Biomedical Engineering, School of Engineering, Trinity College Dublin; [3]Dept.of Anatomy and Regenerative Medicine, Royal College of Surgeons in Ireland, Dublin; [4]Advanced Materials and Bioengineering Research Centre (AMBER), Royal College of Surgeons in Ireland and Trinity College Dublin, Ireland

Introduction

Meniscal lesions are common in sports injuries and significantly increase osteoarthritis risk. Approximately 1.5 million meniscal repairs are performed annually in the US and Europe, representing one of the most common orthopedic procedures [1]. In tissue engineering, cellular aggregates, microtissues, and organoids are increasingly used as building blocks for scaled-up grafts [2]. These microtissues can be combined with 3D-printed scaffolds to guide fusion, remodeling, and enhance biomechanical properties, making them promising for meniscus regeneration [3]. This study aimed to deposit fibrocartilaginous microtissues generated from inner and outer meniscus progenitor cells (iMPCs and oMPCs) into melt-electrowritten (MEW) scaffolds to biofabricate zonally defined meniscus grafts.

Materials and Methods

Caprine meniscus tissues were obtained from Professor Pieter Brama (University College Dublin). iMPC- and oMPC-derived microtissues were fabricated using a high-throughput agarose hydrogel system, as previously described [4], and subjected to 48 hours of chondrogenic induction. Microtissues were either cast onto MEW scaffolds or encapsulated in 1% gelatin hydrogel bioink at 30,000 or 60,000/mL for bioprinting into polycaprolactone scaffolds with 15 µm fibers. Constructs were cultured in chondrogenic media for up to six weeks and analyzed histologically, biochemically, mechanically, and by gene expression.

Results

Scaffold pore architecture influenced microtissue fusion and tissue remodeling. PCL scaffolds with isotropic (0.8 × 0.8 mm) or anisotropic (0.4 × 1.6 mm) pores supported microtissue seeding, with successful fusion observed after 24 hours. SEM revealed dense ECM with aligned fibers in anisotropic scaffolds, indicating directional organization. Histology showed strong sGAG staining in isotropic scaffolds seeded with iMPCs, while anisotropic scaffolds exhibited greater collagen deposition with both iMPCs and oMPCs. No calcium deposition was observed, confirming stable fibrocartilaginous formation. Gene expression supported these trends, with elevated type I collagen in anisotropic scaffolds seeded with oMPCs, and increased aggrecan in isotropic scaffolds seeded with iMPCs. Tensile testing showed higher Young's modulus in anisotropic constructs, while compressive properties were similar. In a caprine meniscus explant model, oMPC-seeded scaffolds integrated robustly with native tissue. Bioprinting of oMPC microtissues into anisotropic scaffolds yielded uniform tissue with abundant sGAG and collagen deposition, and type I collagen distribution closely resembling native outer meniscus **(Fig. 1)**.

Conclusion

Integrating fibrocartilage microtissues with MEW scaffolds enables engineering of zonally defined meniscus grafts that replicate native structure and composition. This strategy shows strong potential for preclinical translation, improving meniscal repair outcomes, reducing osteoarthritis risk, and enhancing patient quality of life.

Acknowledgements

This work was funded by the European Research Council (ERC, 4D-BOUNDARIES #101019344) and the Research Ireland Postdoctoral Fellowship (GOIPD/2024/18).

References

[1]Makris, E. A., *et al 2011.* Biomaterials. 32(30):7411-7431.
[2]Achilli TM. *et al 2012.* Expert Opin Biol Ther. 2012.

[3]Kronemberger. *et al 2020.* World J Stem Cells. 12(2):110-122,
[4]Nulty. *et al 2021*. Front Bioeng Biotechnol. 9:661989, 2021.

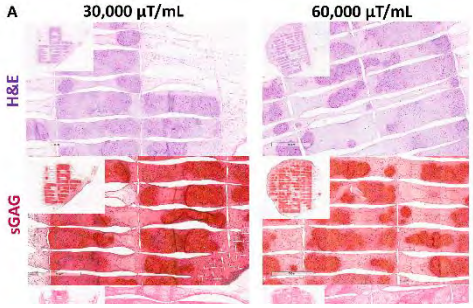

Figure 1: Engineered outer region meniscal grafts using MPC microtissues as biological building blocks bioprinted into MEW scaffolds. (**A**) Representative staining of oMPC microtissues bioprinted at densities of 30,000 and 60,000 microtissues/mL. Hematoxylin and Eosin (H&E), Safranin-O (sGAG), Picrosirius Red (Collagen), and immunohistochemical staining for type I collagen. (**B**) Biochemical analysis of total DNA, sGAG, and collagen content in oMPC microtissues bioprinted at densities of 30,000 and 60,000 microtissues/mL. Scale bar: 700 µm.

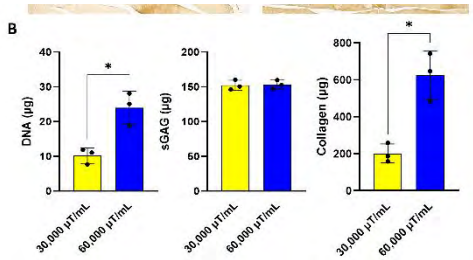

S43 – O4

Programming motion and shape-morphing in bioprinted heart tissues via dynamic magnetic fields

Chakraborty J.[1,2], Kelly D.[1,2], Czechowska I.[3], Daly A.C.[1,2]
[1]CÚRAM, SFI Research Centre for Medical Devices, University of Galway, Ireland; [2]Biomedical Engineering, University of Galway, Ireland [3]Faculty of Chemistry, Jagiellonian University, Krakow, Poland

Aim

Cardiac looping, an essential process during heart morphogenesis, involves a sequence of shape-changes to form a functional heart.[1] Conventional bioprinting produces static structures but bypasses the dynamic, self-organising morphogenetic processes essential for tissue maturation during embryonic development.
Herein, we leveraged induced pluripotent stem cell (iPSC) derived cardiomyocytes combined with externally applied, precisely controlled magnetic fields to replicate the shape-changes that occur during cardiac looping.
Our objectives are: a. To establish a bioprinting platform capable of directing 4D shape-morphing in bioprinted tissues using magnetic fieldsb. Replicate cardiac looping utilizing this platform and study the human iPSC-cardiomyocyte response to shape morphing

Materials and Methods

A custom-made bioprinter with a magnetic probe having X, Y, Z control was built in-house. 5 mg/ml of Fe_3O_4 magnetic nanoparticles (MNPs) were mixed with collagen (3mg/ml) and hyaluronic acid (4wt%) to form the acellular bioink. Multimeric bioink with/without MNPs was used to print different geometries in an agarose support bath (0.5%). Controlled magnetic actuation was applied to replicate the shape changes during cardiac looping. A live-dead assay was used to determine the viability of cell-laden constructs.

Results

We have developed a custom bioprinting platform featuring an integrated magnetic probe, which enables precise X, Y, and Z positioning, thereby facilitating the printing of MNP-based bioinks and their subsequent actuation. The bioinks exhibited shear-thinning properties, facilitating the bioprinter to produce diverse and precise geometries. We printed tubes with magnetic poles and actuated them to induce buckling. Furthermore, a whole ventricle was printed with the magnetic ink in between, mimicking the myocardium. We stimulated cardiac contractions by positioning the probe at the centre of the ventricle, which produced a bending and buckling pattern akin to the initial phases of cardiac looping. This illustrated the system's capability to convert magnetic inputs into consistent morphogenetic deformations.

Conclusion

The controlled magnetic actuation replicated the shape changes during cardiac looping. Current endeavours concentrate on the actuation of constructs encapsulated with iPSC-cardiomyocytes within multimeric bioinks, which is expected to significantly improve the functionality of iPSC-cardiomyocytes.

References

[1]J. Manner. *et al 2024.* Journal of Cardiovascular Development and Disease, 11(8), 252,

Figure 1:(A) A custom-made bioprinting platform with integrated magnetic probe having X, Y, Z control capable

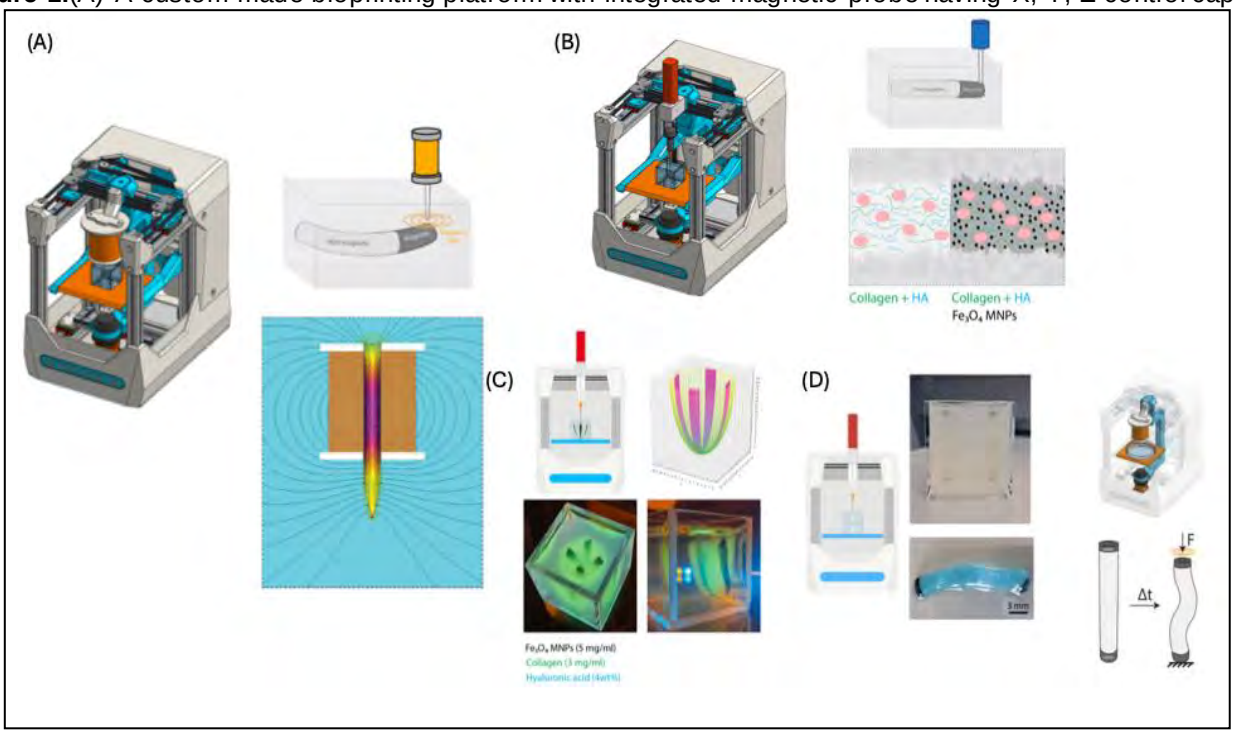

of inducing magnetic actuation, (B) Multimeric bioprinting with/without magnetic nanoparticles, (C), (D) Acellular bioprinting of whole ventricle and tube using multimeric inks, actuated by the magnetic probe.

Figure 2. Complex geometry printing using multi-material and actuation

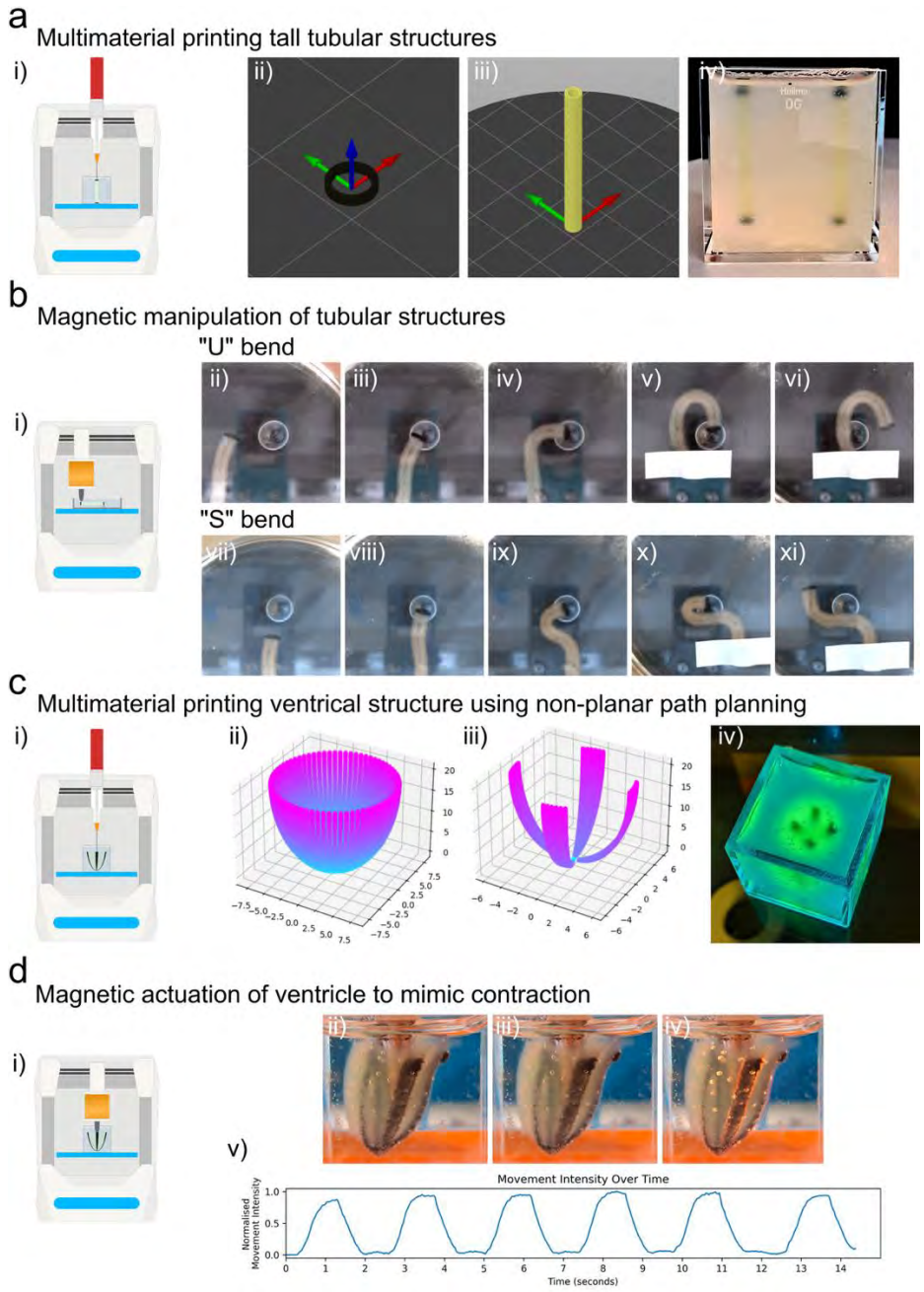

S43 – O5

Engineering collagen microarchitecture to modulate stromal differentiation and function in 3D lymphoid tissue models

ElGindi M.[1], Karaman S.[1], Teo J.[1,2]
[1]Division of Engineering, York University Abu Dhabi, UAE; [2]Dept. of Mechanical and Biomedical Engineering, New York University, Brooklyn, NY USA

Introduction

Three-dimensional (3D) lymphoid tissue models are increasingly used to study immune responses in controlled in vitro environments. However, most existing systems focus primarily on cellular composition while overlooking the role of extracellular matrix (ECM) microarchitecture in regulating stromal cell behavior. In native lymph nodes, fibroblastic reticular cells (FRCs) form highly organized networks that are strongly influenced by biophysical and structural cues from the surrounding matrix. This study aims to investigate how fibrillar collagen microarchitecture influences stem cell differentiation into FRC-like phenotypes and the resulting organization and function of engineered lymphoid tissue models.

Materials and Methods

Collagen-based hydrogels with tunable microarchitectural properties will be engineered by varying collagen concentration and inducing different degrees of fiber alignment. Stem cells will be embedded within these matrices and cultured under conditions promoting differentiation toward FRC-like phenotypes as previously published. Following stromal network formation, co-cultures with peripheral blood mononuclear cells (PBMCs) and antigen-primed dendritic cells will be established to assess functional immune interactions. Matrix architecture will be characterized using imaging approaches, while cellular differentiation and immune activity will be evaluated through flow cytometry, cytokine profiling, and antibody production assays.

Results

Previous work demonstrated the successful differentiation of stem cell-derived FRC-like cells and the formation of functional lymphoid-like environments in 3D collagen systems, including immune activation and antibody production. Conversely, current work investigates whether tuning collagen concentration and fiber alignment can promote a more robust FRC network formation and immune response. In addition, differences between different stem cells (mesenchymal and adipose derived) are also being explored in this context.

Conclusion

This work identifies collagen microarchitecture as a potential key regulator of stromal organization in engineered lymphoid tissues. By addressing the current limitations observed in 3D systems, this biomaterials-driven approach aims to enable the formation of functional lymphoid structures in vitro. Such platforms may support the development of more physiologically relevant models for studying immune responses and designing immunoengineered systems.

Acknowledgements

New York University Abu Dhabi (NYUAD) Faculty Research Fund (AD266)

S44
Microfluidic platforms for tissue modelling and micro nano-particle engineering

S44 – K1

Sochol R.
University of Maryland, College Park - USA

S44 – O1

Sterol-grafted chitosan nanoparticles as bactericidal nano-decoys for *Helicobacter pylori* eradication

Pinho A.S.[1, 2], Costa B.[1], Silva D.[1], Leiro V.[1], Müllertz A.[3,4], Martins M.C.L.[1,2,5,] Parreira P.[1]
[1]i3S, Instituto de Investigação e Inovação em Saúde, Universidade do Porto; [2]ICBAS, Instituto de Ciências Biomédicas Abel Salazar, Universidade do Porto; [3]Dept. of Pharmacy, University of Copenhagen, Denmark; [4] Bioneer: FARMA, Danish Drug Development Center, Dept. of Pharmacy, Faculty of Health and Medical Sciences, University of Copenhagen, Denmark; [5]INEB, Instituto de Engenharia Biomédica, Universidade do Porto, Portugal

Introduction

Helicobacter pylori chronically infects 50% of the worldwide population (~4 billion), accounting for 90% of all gastric cancer cases, one of the leading causes of cancer-related mortality worldwide. The effectiveness of standard treatment is increasingly compromised, highlighting the urgent need for alternative strategies. To persist within the host, *H. pylori* extracts cholesterol from gastric cells and incorporates it into its membrane. It also disrupts the lipid rafts, crucial elements of the immune response, escaping the host immune system, enhancing chronic infection and inflammation (1). Given its pivotal role in *H. pylori* pathogenesis and gastric infection, cholesterol and its analogues are an appealing target for the development of precision therapies, as demonstrated by us using 2D and 3D gold model surfaces(2).

Aim

Translate the proof-of-concept strategy into a biocompatible system by engineering ergosterol-functionalized chitosan nanoparticles for a targeted therapy against H. pylori.

Materials and Methods

Erg-PEG$_{75}$-SH (Erg) was produced in house using ergosterol (≥75%, Merck) through PEGylation and thiolation reactions (Fig.1). Then, commercial squid pen chitosan (degree of acetylation = 2%; molecular weight=355 ± 22 kDa; France Chitine) functionalized with norbornene groups was used to obtain chitosan nanoparticles (cNP) (3). These cNP were then grafted with Erg (Erg-cNP) via thiol–norbornene “photoclick” chemistry in a microfluidic system (Fig.2A) (3). Erg-cNPs were produced using two initial concentrations (2 and 4 mg/mL), and characterized by Nanoparticle Tracking Analysis (NTA), Attenuated Total Reflectance Fourier-Transform Infrared Spectroscopy (ATR-FTIR), and Transmission Electron Microscopy (TEM). The NPs' *in vitro* antimicrobial performance against *H. pylori* J99 strain (ATCC® 700824, highly pathogenic) was assessed by colony-forming units (CFU) counting after 24 hours. Cytotoxicity was evaluated using cell lines derived from human gastric carcinoma (AGS and MKN74) (3).

Results

Erg was obtained with a yield of 50%, allowing its conjugation with Norchit. The obtained Erg-cNP were round-shaped (TEM) with ~120 nm, while the cNP size was ~150 nm. Erg-PEG-SH grafting onto cNP was further confirmed by ATR-FTIR. Erg4-cNP were bactericidal at 10^{10} nanoparticles/mL, while Erg 2-cNP and cNP reduced bacteria by 2 and 1 logs, respectively. Furthermore, all nanoparticles were cytocompatible (metabolic activity above 70%, ISO 10993-5:2009).

Conclusion

Erg-cNP were successfully produced and effectively killed H. pylori, while also being cytocompatible on gastric cell lines. being promising for the development of targeted treatment for gastric infection.

Acknowledgements

Authors would like to acknowledge the project HELIPY, with Operation No. 15757 - COMPETE2030-FEDER-00686400 supported by PITD, Portugal 2030, and the European Union.

References

[1]Morey P., Pfannkuch L., Pang E., Boccellato F., Sigal M., Imai-Matsushima A., et al. *Helicobacter pylori* depletes cholesterol in gastric glands to prevent interferon gamma signaling and escape the host immune response. *Gastroenterology 2018*; 154(5): 1391–1405.
[2]Pinho A.S., Costa B., Silva D., Leiro V., Klitgaard M., Müllertz A., Martins M.C.L., Parreira P. Cholesterol-Functionalized Nanoparticles for Targeted *Helicobacter pylori* Eradication. *Advanced Healthcare Materials 2025*; article: e202404065.
[3]Fonseca D.R., Alves P.M., Neto E., Custódio B., Guimarães S., Moura D., Annis F., Martins M., Gomes A., Teixeira C., Gomes P., Pereira R.F., Freitas P., Parreira P., Martins M.C.L. One-Pot Microfluidics to Engineer Chitosan Nanoparticles Conjugated with Antimicrobial Peptides Using “Photoclick” Chemistry: Validation Using the Gastric Bacterium *Helicobacter pylori*. *ACS Applied Materials & Interfaces 2024*; 16(12): 14533-14547.

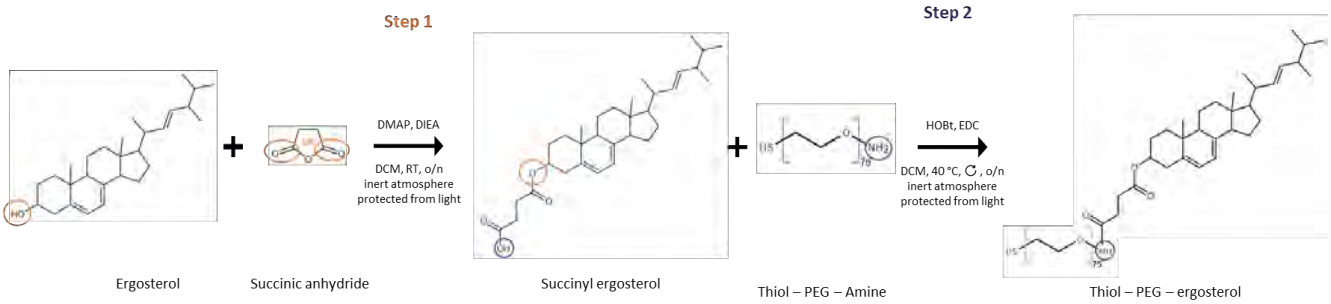

Fig. 1 - Schematic representation of the protocol for the synthesis of PEGylated and thiolated Ergosterol in two steps. DMAP – 4-dimethylaminopyridine; DIEA – N,N-diisopropylethylamine; DCM – anhydrous dichloromethane; DMF – anhydrous N,N-dimethylformamide; HOBt – hydroxybenzotriazole; EDC – 1-[3-(dimethylamino)propyl]-3-ethylcarbodiimide methiodide. (Molecules designed with IBM RXN for Chemistry).

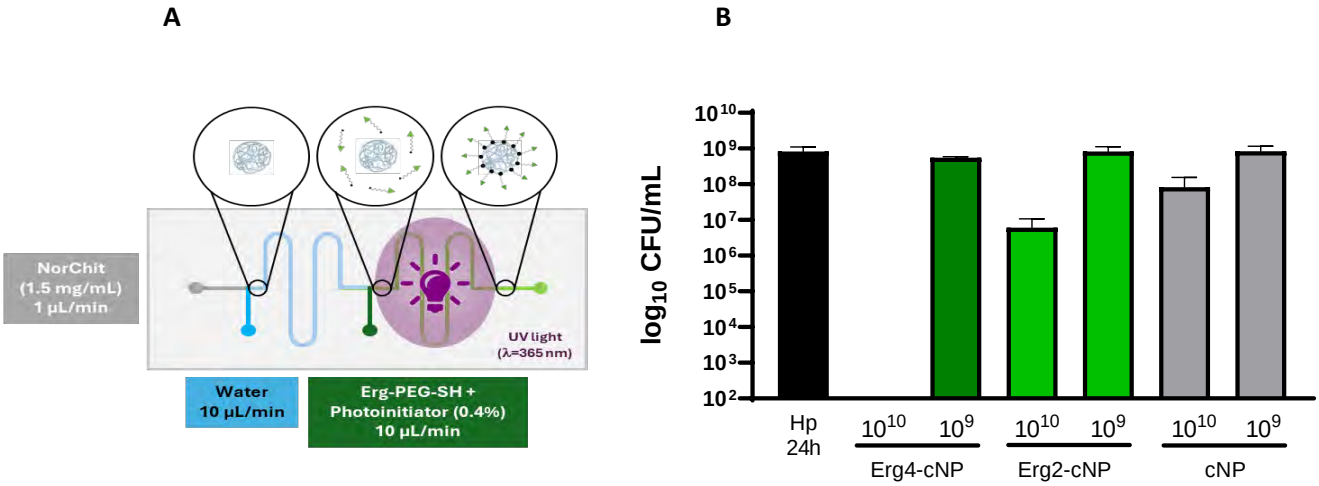

Fig. 2 – (A) Schematic representation of the microfluidic chip used for Erg-cNP production. (B) *H. pylori* J99 growth after incubation with Erg4-cNP, Erg2-cNP, and cNP over 24 h. Assays were performed in Brucella Broth+10%FBS. Values are mean ± SD, n=2.

S44 – O2

Real-time oxygen monitoring in 3D printed Organ-on-Chip using optical microsensors

Bisconti F.[1,2], Iuele H.[1,2], De Giorgi A.[1,2,3], Onesto V.[1,2], Corbezzolo N.[1,2,4], Scalera F.[1,2], Gigli G.[1,2,5], Stolfi F.[6,7], Chiocchetti A.[6,7], del Mercato L. L.[1,2], Gervaso F.[1,2,††], Polini A.[1,2]

[1]Institute of Nanotechnology, National Research Council (CNR-NANOTEC), Lecce; [2]Tecnomed Puglia, Technopole for Precision Medicine (Biotech Lecce Hub), Lecce; [3]Dept. di Matematica e Fisica E. de Giorgi, Università del Salento, Lecce; [4]Dept. di Ingegneria dell'Innovazione, Università del Salento, Lecce; [5]Dept. di Medicina Sperimentale, Università del Salento, Lecce; [6]Dept. di Scienze della Salute, Interdisciplinary Research Center of Autoimmune Diseases-IRCAD, Università del Piemonte Orientale, Novara; [7]Center for Translational Research on Autoimmune and Allergic Diseases, University of Piemonte Orientale, Novara, Italy

Introduction

Organ-on-Chip (OoC) technology is revolutionizing in vitro modeling, offering advanced platforms for studying physiology, toxicology, drug screening, and precision medicine.

In this context, oxygen availability plays a critical role in cellular metabolism and function, yet real-time and spatial monitoring within OoC systems remains a significant challenge, especially when cells are encapsulated in hydrogels, spheroids, or organoids, rather than cultured in traditional in 2D monolayers.

Aim

This study aimed to integrate optical ratiometric oxygen sensors within a 3D-printed microfluidic OoC platform to enable real-time monitoring of oxygen concentration in a physiologically relevant 3D cellular microenvironment.

Materials and Methods

A microfluidic OoC device was fabricated using Digital Light Processing (DLP) 3D printing. Patient-derived fibroblast-like synoviocytes (FLS) were encapsulated in a Gelatin Methacryloyl (GelMA) hydrogel together with silica-based ratiometric optical oxygen microsensors. The sensors consisted of silica microparticles functionalized with two fluorophores: one oxygen-sensitive probe and one oxygen-insensitive reference probe, enabling ratiometric measurements. The microsensors were uniformly dispersed throughout the 3D cellular construct to allow spatially resolved oxygen monitoring within the hydrogel matrix. Oxygen-dependent fluorescence signals were acquired and analyzed using confocal microscopy under dynamic perfusion conditions. Experimental measurements were compared with predictions obtained from computational fluid dynamics (CFD) simulations.

Results

Live/Dead assays demonstrated high cell viability (>80%) throughout the culture period, confirming the good biocompatibility of the platform. Moreover, DAPI–phalloidin staining showed that hFLS elongated within the GelMA matrix, adopting their characteristic spindle-like morphology.The integrated sensing platform enabled stable monitoring of oxygen concentration within the 3D construct for up to four days under dynamic culture conditions, providing spatial and temporal information on oxygen availability. The experimentally measured oxygen levels showed strong agreement with predictions from computational fluid dynamics (CFD) simulations, supporting the reliability of the sensing approach. The integration of ratiometric optical sensors within the 3D-printed microfluidic system allowed high-resolution oxygen mapping, improving the characterization of the cellular microenvironment.

Conclusion

The combination of DLP-based 3D printing and ratiometric optical sensing represents a powerful strategy to enhance the physiological relevance and analytical capabilities of OoC systems. By enabling real-time metabolic monitoring, this platform may support improved disease modeling and drug testing, contributing to bridging the gap between conventional in vitro models and in vivo conditions.

Acknowledgements

The authors acknowledge funding from the the European Union's Horizon 2020 research and innovation programme under grant agreement No. 953121 (FLAMIN-GO), the European Research Council (ERC) under the European Union's Horizon 2020 research and innovation program ERC Starting Grant “INTERCELLMED” (No. 759959), ERC Proof Of Concept “HySENSE” (No. 101212914), the “Tecnopolo per la medicina di precision” (TecnoMed Puglia) - Regione Puglia: DGR n.2117 of 21/11/2018, CUP: B84I18000540002).This research was also supported by European Union - NextGenerationEU” financing the PNRR Mission 4, Component 2 “From Research to Business” – Investment 1.4 “Strengthening research infrastructures and creation of national R&D champions on some Key Enabling Technologies”, Project Code CN00000033, Spoke 8, titled “National Biodiversity Future Center” (NBFC).

S44 – O3

Engineering a perfusable bicompartmental hydrogel for artery-perivascular tissue modelling

Perelli E.[1], Wu T.[1], Gall E.[1], Huang X.[1], Simon-Yarza T.[1], Chaubet F.[1]
[1]Laboratory for Vascular Translational Science, INSERM U1148, Université Sorbonne Paris Nord, Villetaneuse, France

Introduction

Arteries are involved in numerous diseases requiring new tools to understand their underlying mechanisms. The impact of pathological tissues surrounding the arteries on vascular homeostasis is often neglected. In particular, to our knowledge no 3D in vitro models have been developed to study these bidirectional interactions between arteries and perivascular tissues.

Aim. We propose a biomaterial-based model to study the interplay between an artery and its surrounding tissue. For that, we have developed a perfusable bicompartmental hydrogel made of a tubular scaffold, integrated inside a porous hydrogel that mimics a soft tissue.

Materials and Methods

The artery scaffold was composed of polyvinyl alcohol (PVA) to recapitulate the mechanical properties of arteries, and alginate and polyethylene glycol as porous agents. Physical crosslinking of PVA by a freeze-thawing-drying process led to a semi-interpenetrating network. To mimic the surrounding tissue, a double-network porous polysaccharide hydrogel made of pullulan, dextran, and alginate (PuDAlg) was obtained through chemical and ionic crosslinking followed by freeze-drying. A channel was formed within the PuDAlg hydrogel by needle templating to accommodate the artery scaffold. A fluidic chamber was engineered to perfuse the system.

Results

The artery scaffold presented a 900µm lumen diameter and a homogeneous inner porosity of 30.4% across its wall thickness (400µm). Pore size remained in the 0-10µm range, permitting macromolecule transport while preventing cell infiltration. Dynamic permeability studies confirmed the diffusion of 70kDa dextran with an apparent permeability of $3.98.10^{-7}$ cm/s. On the other hand, the PuDAlg hydrogel presented an interconnected porosity compatible with cell infiltration (pore size > 20µm). Its effective Young's modulus reached 36.5kPa falling within the range of soft tissues. Both materials were assembled to form a single construct and integrated within an engineered fluidic chamber made of a polydimethylsiloxane spacer clamped between two glass slides and connected to a peristaltic pump for intraluminal perfusion of fluids (Figure 1). This device enabled perfusion at arterial-like pulsative flow rates (1-5 mL/min). Cytocompatibility and 3D cell adhesion of vascular cells were validated for both materials, the artery scaffold and the soft matrix.

Conclusion

We developed a hydrogel-based system consisting of a small artery and a perivascular tissue that permits bidirectional communication between the lumen and the external environment. Ongoing studies focus on the cellularization of the system which will constitute a novel platform for the dynamic study of environmental and biochemical signals involved in vascular homeostasis.

Acknowledgements

Doctoral school ED146 Galilée funds E.P.'s scholarship.

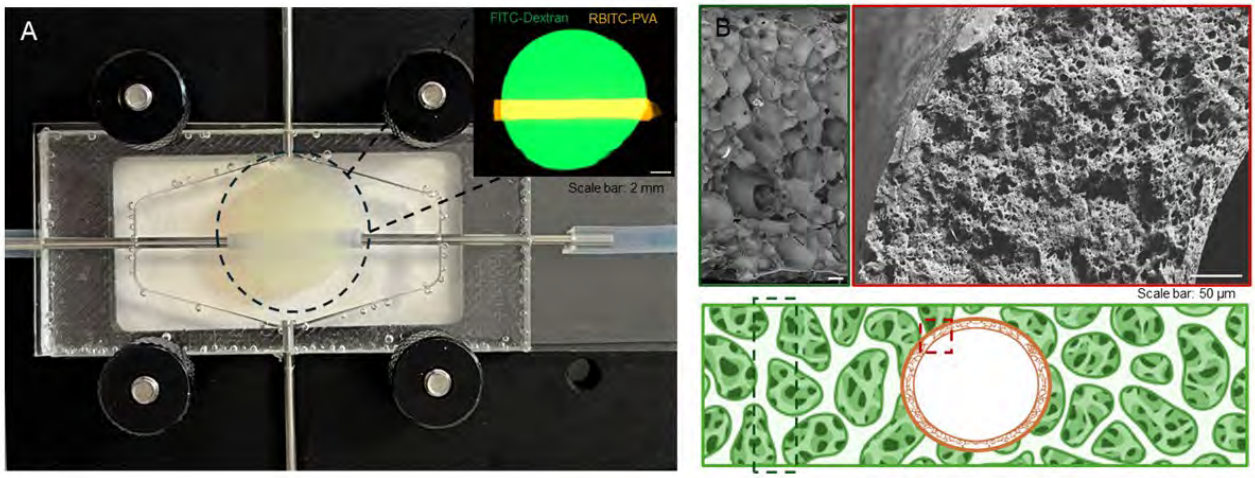

Figure 1: Representative images of the bicompartmental hydrogel within the engineered fluidic device (A) and its structure observed by scanning electron microscopy (B).

S45
Mimicking EMC for 3D bioprinted tissue models from bioinstructive inks to AI driven processes

S45 – K1

Russo L.
CNR IFC - Italy

S45 – O1

Human astrocyte to neuron reprogramming in hydrogels: Probing the influence of fibrin and stiffness

Distler T.[1,2], Konrad Daga K.[1], Bürkle M.[1], Simon T.[1], Vásquez-Sepúlveda S.[3,4], Franze K.[3,4,5], Götz M.[1,2,6], Masserdotti G.[1,2]

[1]Chair of Physiological Genomics, Biomedical Center (BMC), Faculty of Medicine, LMU Munich, Planegg-Martinsried, Germany; [2]Institute of Stem Cell Research, Helmholtz Center Munich, Neuherberg, Germany; [3]Max-Planck-Zentrum für Physik und Medizin, Erlangen, Germany; [4]Institute of Medical Physics and Microtissue Engineering, Friedrich-Alexander-Universität Erlangen-Nürnberg, Erlangen, Germany; [5]Dept. of Physiology, Development and Neuroscience, University of Cambridge, Cambridge, UK; [6]Excellence Cluster of Systems Neurology (SYNERGY), Munich, Germany

Introduction

Astrocytes are the most abundant glial cell type in the adult human brain. Following traumatic brain injury, they become reactive and can acquire stem cell–like properties. However, the influence of the surrounding extracellular matrix (ECM) environment – which is enriched in fibrin upon haemorrhagic injury – on astrocyte behaviour and on the re-acquisition of plasticity which may prime astrocytes for direct reprogramming into functional neurons, remains poorly understood.

Materials and Methods

To mimic the injury environment, we generated fibrin-based hydrogels with different properties, such as increased porosity and stiffness, and investigated how such changes affect astrocyte morphology, reactive state and transcriptome, and direct neuronal reprogramming. In particular, we generated fibrin hydrogels and compared them to interpenetrating-network hydrogels of fibrin and peptide-modified sodium alginate, called FAR. First, we analysed the hydrogel-microstructure and stiffness by multiphoton live-imaging and atomic force microscopy (AFM). We then evaluated the impact of different matrix density and hydrogel stiffness on human induced-pluripotent stem cell (iPSC)-derived astrocytes (hAstro) at different timepoints by analysing cell morphology, proliferation, and cell death. To investigate the molecular differences caused by the different environments, we performed bulkRNA-sequencing of astrocytes in 3D-Fibrin and 3D-FAR. Finally, we studied the potential to convert hAstro into induced neurons (iNeurons) in 3D hydrogels by using retroviral-mediated upregulation of Neurogenin2 via direct neuronal reprogramming.

Results

hAstro show profound differences in ramification, transcriptome, and conversion potential into neuronal cells depending on the 3D gel environment: While astrocytes are ramified and stationary in FAR, cells can migrate and proliferate to a higher extent in pure fibrin hydrogels. Strikingly, the transcriptomic profile revealed a more pronounced inflammatory signature in 3D-FAR ($CHI3L1^+$,$C3^+$), and a more proliferative cell-state in 3D-fibrin ($MKI67^+$,$HMGB2^+$). When transduced with Ngn2 coding viruses, human astrocytes fail to reprogram into neuronal cells in stiff FAR hydrogels but successfully reprogram in 3D-fibrin. Remarkably, reducing the stiffness and density of FAR partially rescues the direct reprogramming into iNeurons, indicating a decisive role of the 3D microenvironment and its physico-chemical properties on astrocyte state and conversion potential.

Conclusion

Here we show that tuning hydrogel mechanical properties and microstructure has a major impact on astrocyte behaviour, suggesting a major contribution of the environment to glial cell state. Importantly, these results have implications on how changes of the ECM microenvironment – such as stiffness increase in grade IV glioblastoma, or haemorrhage and accompanied fibrin accumulation – might affect astrocyte state and therefore functionality upon injury.

S45 – O2

Engineering a pectin hydrogel bioink for endothelial cell growth in soft neural like matrices

Leal, F.[1], Pêgo, A.P.[1,3,4], Granja P.L.[1]
[1]Instituto de Investigação e Inovação em Saúde, Universidade do Porto; [2]Faculdade de Engenharia, Universidade do Porto; [3]Instituto de Engenharia Biomédica, Universidade do Porto; [4]Instituto de Ciências Biomédicas Abel Salazar, Universidade do Porto, Portugal

Introduction

3D bioprinting offers new opportunities to create neurovascular tissues, but developing bioinks that meet the narrow biofabrication window remains challenging. In this context, pectin, a plant-derived polysaccharide with tunable gelation and extracellular matrix (ECM)-like properties, emerges as a promising candidate owing to its biocompatibility and biodegradability. However, its association with human umbilical vein endothelial cells (HUVECs), which are critical for angiogenesis, remains underexplored.

Aim

The aim of this study is to develop a norbornene-functionalized pectin hydrogel-based bioink modified with cell-adhesive and matrix metalloproteinase (MMP)-sensitive peptides to mimic the grey matter of the central nervous system, a region characterized by increased vascularity.

Materials and Methods

Pectin was purified and modified with tetrabutylammonium salt to facilitate dissolution in organic solvents. Afterwards, it was functionalised with carbic anhydride at a 1-fold molar excess to obtain norbornene-modified pectin (NorPec). Hydrogel fabrication employed a dual-crosslinking strategy: an initial ionic gelation step to achieve the viscosity required for 3D printing, followed by photocrosslinking to enhance structural fidelity and enable precise modulation of mechanical properties. During the photocrosslinking stage, cell-adhesive and MMP-sensitive peptides were conjugated to the pectin backbone. The norbornene functionalisation degree was estimated by ^{1}H NMR, while rheological and mechanical properties were characterized by varying calcium chloride ($CaCl_2$) and PVGLIG peptide concentrations. HUVECs were encapsulated in hydrogels and cultured for 7 days. *In vitro* cytocompatibility was further analysed using metabolic activity (resazurin), cell viability (live/dead staining), and cell morphology (DAPI/Phalloidin staining) assays.

Results

The degree of norbornene modification of NorPec was determined to be 24.7%. NorPec was successfully crosslinked using different concentrations of $CaCl_2$ and photocrosslinker. All hydrogel formulations demonstrated good printability, displaying adequate shear-thinning behaviour and a yield stress below 10 kPa. The elastic modulus ranged from 100 to 400 Pa, consistent with the inherently soft mechanical properties of neural tissues. Encapsulated HUVECs maintained viability above 70% and continued to proliferate within the hydrogels over a 7-day culture period.

Conclusion

A dual crosslinked hydrogel-based bioink was developed with a tunable rheological profile and good printability. Following hydrogel encapsulation, HUVECs demonstrated high viability and sustained proliferation for 7 days. Future studies will extend the culture duration to determine whether these cells can initiate capillary-like network formation.

Acknowledgements

The authors acknowledge Fundação para a Ciência e Tecnologia (FCT) for the PhD grant (2023.04235.BD), and the project IBEROS+ (0072_IBEROS_MAIS_1_E, Interreg-POCTEP 2021-2027) for funding. APP thanks the support of Air Force Office of Scientific Research (USA), under the award FA9550-23-1-0599.

S45 – O4

Enabling three-dimensional electrical stimulation of neural stem cells in decellularized extracellular matrix scaffolds using graphene-based electrodes

Martins P.A.[1,2,3], Barroca N.[1], Vieira S.I.[4], de Sousa B.M.[4], Gil G.[2,3], Cicuéndez M.[5], Casarrubios L.[6], Feito M.J.[6], Díez-Orejas R.[7], Pórtoles M.T.[6,8], Figueiredo B[9]., Silva R.[9], Garcia-Lizarribar A.[10], Fonseca P.[2,3], Alves L.N.[2,3], Marques P.A.A.P.[1]

[1]Dept. of Mechanical Engineering, Centre for Mechanical Technology Automation (TEMA), University of Aveiro, Portugal; [2]Dept. of Electronics, Telecomunications and Informatics, University of Aveiro, Portugal; [3]Instituto de Telecomunicações, Aveiro, Portugal; [4]Dept. of Medical Sciences, Institute of Biomedicine (iBiMED), University of Aveiro, Portugal; [5]Dept. de Química en Ciencias Farmacéuticas, Facultad de Farmacia, Universidad Complutense de Madrid (UCM), Instituto de Investigacion Sanitaria del Hospital Clínico San Carlos (IdISSC), 28040 Madrid, Spain; [6]Dept. de Bioquímica y Biología Molecular, Facultad de Ciencias Químicas, Universidad Complutense de Madrid (UCM), Instituto de Investigacíon Sanitaria del Hospital Clínico San Carlos (IdISSC), Madrid, Spain; [7]Dept. de Microbiologia y Parasitologia, Facultad de Farmacia, Universidad Complutense de Madrid (UCM), Instituto de Investigacion Sanitaria del Hospital Clínico San Carlos (IdISSC), Madrid, Spain; [8]CIBER de Bioingeniería, Biomateriales y Nanomedicina, Madrid, Spain; [9]Graphenest SA, Sever do Vouga, Portugal; [10]TECNALIA Basque Research and Technology Alliance (BRTA), San Sebastian, Spain

Introduction

Electrical stimulation (ES) has emerged as a promising strategy to modulate neural cell behaviour and enhance tissue regeneration. However, most *in vitro* electrostimulation systems rely on planar configurations or invasive electrodes, which fail to reproduce the three-dimensional (3D) microenvironment of neural tissues.

Aim

This work aims to develop a non-invasive platform based on screen-printed graphene electrodes capable of enabling controlled 3D electrical stimulation of neural stem cells (NSCs) cultured within biomimetic scaffolds composed of adipose-derived decellularized extracellular matrix (adECM) with or without reduced graphene oxide (rGO).

Materials and Methods

A conductive graphene-based ink composed of graphene, ethyl-cellulose and terpineol was formulated (Figure 1a) and screen-printed to fabricate electrodes (Figure 1b) integrated into a modified culture well plate (Figure 1c). The electrodes were electrically characterized and evaluated for cytocompatibility and macrophage response. Neural stem cells (NE-4C) were seeded onto adECM and adECM/rGO scaffolds and subjected to daily electrical stimulation (10 Hz, 200 µA, 1 h/day). Cell proliferation and neuronal differentiation were analysed through DNA quantification, immunocytochemistry (Tuj1, GFAP), neurite length measurements and immunoblotting of MAP2.

Results

The graphene electrodes showed stable electrical behaviour and good cytocompatibility, without increasing pro-inflammatory IL-6 secretion in macrophages. The developed platform, featuring these electrodes, enabled controlled 3D electrical stimulation while maintaining physiologically relevant impedance (<800 Ω). Electrical stimulation significantly enhanced NSC proliferation in adECM scaffolds and promoted neuronal differentiation (Figure 1d), evidenced by increased Tuj1 staining (Figure 1e) and MAP2 expression. In addition, ES stimulated neuritogenesis and increased neurite length, improving connectivity between neural cell clusters (Figure 1f). While rGO-containing scaffolds intrinsically promoted neuronal differentiation, electrical stimulation further enhanced neurite extension and network formation.

Conclusion

This work presents a simple and scalable graphene-based platform for non-invasive 3D electrical stimulation of cells within biomaterial scaffolds. The system enhances neuronal differentiation and neurite development of NSCs in biomimetic extracellular matrix scaffolds. These findings demonstrate the potential of combining graphene-based electrodes with 3D tissue engineering constructs to better mimic physiological environments and advance in vitro models for neural regeneration studies.

Acknowledgements
The authors gratefully acknowledge the support provided by national funds from FCT – Fundação para a Ciência e a Tecnologia, I.P., under the projects UID 00481/2025, Centre for Mechanical Technology and Automation (TEMA) and FEDER - Fundo Europeu de Desenvolvimento Regional funds through the COMPETE 2030 in the framework of the project COMPETE2030-FEDER-00744900 (3DNeuroStim project). Also the European Union's Horizon 2020 research and innovation programme support under grant agreement No 829060 (NeuroStimSpinal project).

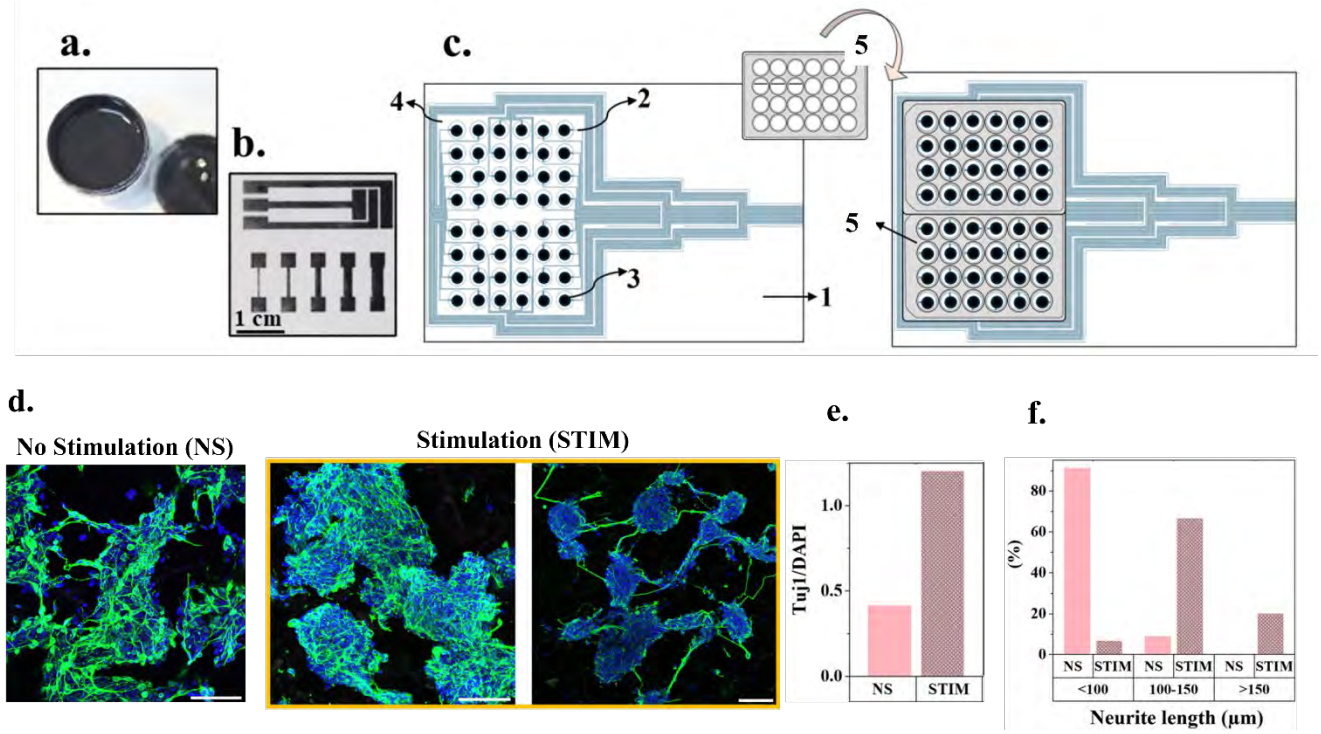

Figure 1: a) Photograph of final graphene-based ink; (b) examples of several screen-printed designs including interdigitated electrodes; c) schematic top view of the bottom electrodes and assembly with the bottomless well plate (1: polymeric sheet used as substrate for the screen printed electrodes; 2: silver tracks layer; 3: screen-printed electrodes layer that will be in direct contact with the scaffolds and the cell medium placed in each well; 4: screen-printed dielectric layer and 5: bottomless wells); d) Differentiation of NSCs on adECM scaffolds 10 days after RA-induced differentiation: confocal imaging of neuronal (Tuj1, green), astrocyte (GFAP, red) markers and cell nuclei (DAPI, blue) with (STIM) and without (NS) electrical stimulation; e) semi-quantitative analysis of NSCs differentiation by Tuj1/DAPI area and f) length of neurites branching out of cell clusters.

S45 – O4

Investigating the immune landscape of the gut-joint axis using a novel 3D bio-printed in vitro model of human synovium and its extracellular matrix

A. Heslington[1], C. Hilkens[2], A. Ferreira-Duarte[1], P. Melo[1]
[1]School of Engineering, Newcastle University; [2]Faculty of Medical Sciences, Newcastle University, UK

Introduction

The synovium, fundamental to healthy joint function, is often affected by systemic inflammatory disease including spondyloarthropathies (SpAs). 35% of inflammatory bowel disease (IBD) patients exhibit extra-intestinal manifestations, including those observed in SpAs[1]. Current two-dimensional (2D) lab models don't fully represent human physiological tissue environments or cellular interactions, including cell-extracellular matrix (ECM) interfaces. However, three-dimensional (3D) technologies, like bioprinting, offer improved physiological relevance for modelling immune-mediated inflammatory diseases (IMIDs), including SpAs[2].

Aim

This study aimed to i) develop a novel collagen-methacrylated-hyaluronic acid (MeHA) ECM-analogue bioink, ii) bioprint a physiologically-relevant *in vitro* synovial structure, iii) validate the healthy 3D model, and iv) assess responses to IBD-relevant stimuli, including bacterial metabolite and secretome exposure.

Materials and Methods

The novel collagen-MeHA-4-arm poly(ethylene) glycol (PEG) bioink (CHA-M), uses dual-stage crosslinking to achieve optimal printability (chemical) and physiological stiffness (light-based). Its physiochemical properties and printability, using extrusion-based bioprinting (EBB) have been characterised and optimised. Bioink components have been endotoxin-tested, with their immunomodulatory potential assessed via TNFa release. Both acellular and cellular CHA-M (using synovium-relevant cell types: monocytes (THP-1s), fibroblast-like synoviocytes (FLS) and macrophages (mTHP-1s)) have been printed. Bacterial secretome samples have been generated using the Aelius Biotech™ Colon Kit and introduced to 2D cultures. Immunomodulation studies with 3D co-cultures are currently ongoing.

Results

CHA-M demonstrated efficient nutrient uptake and shear-thinning behaviour, exhibiting similar storage modulus (G') to physiological synovium, with optimal photo-crosslinking at 365nm (40% intensity, 15 seconds). Dimensionality EBB analyses revealed comparable strand width and resolution to GelMA controls (Figure.1). Viability and morphology assays confirmed high cytocompatibility of CHA-M with THP-1s and FLS, in both mono-culture and co-culture, and when 3D printed, both cell types demonstrated sustained viability 24hrs post-printing (Figure.2). mTHP-1s have been successfully differentiated (M0, M1, M2) and co-cultured with tissue-relevant FLS (3D co-culture systems ongoing). Bacterial secretome samples (Aelius Biotech™ collaboration) demonstrated a mucus-dependent protective effect on THP-1 viability 24hrs post-treatment.

Conclusion

CHA-M exhibits favourable physiochemical and cytocompatible properties, in both mono-culture and co-culture, in 2D and 3D systems, and has been successfully EBB-printed. CHA-M encompasses both collagen and hyaluronic acid, key components of human synovium, and its stiffness is comparable to human synovium, thus validating CHA-M's physiological and biological relevance as a synovial ECM-analogue compared to existing *in vitro* models[3]. This 3D bioprinted system is a promising platform for modelling and exploring gut-joint inflammatory mechanisms in IBD-associated SpAs, and is essential for disease research and the future of 3D modelling.

Acknowledgements

Research funding: Medical Research Council

References

[1] Marleen G. van de Sande., Dominique L. Baeten. Immunopathology of synovitis: from histology to molecular pathways. *Rheumatology 2016;* volume 55 issue 4; pages 599-606.

[2] Renjian Xie., Vaibhav Pal., Yanrong Yu., et al., A comprehensive review on 3D tissue models: Biofabrication technologies and preclinical applications. *Biomaterials 2024*; 304; 122408.

[3] Amelia Heslington., Catharien M.U. Hilkens, Ana Marina Ferreira, Priscila Melo. Functional synovium-based 3D models in the context of human disease and inflammation. *Advanced NanoBiomed Research 2025;* volume 5 issue 7; 2500029.

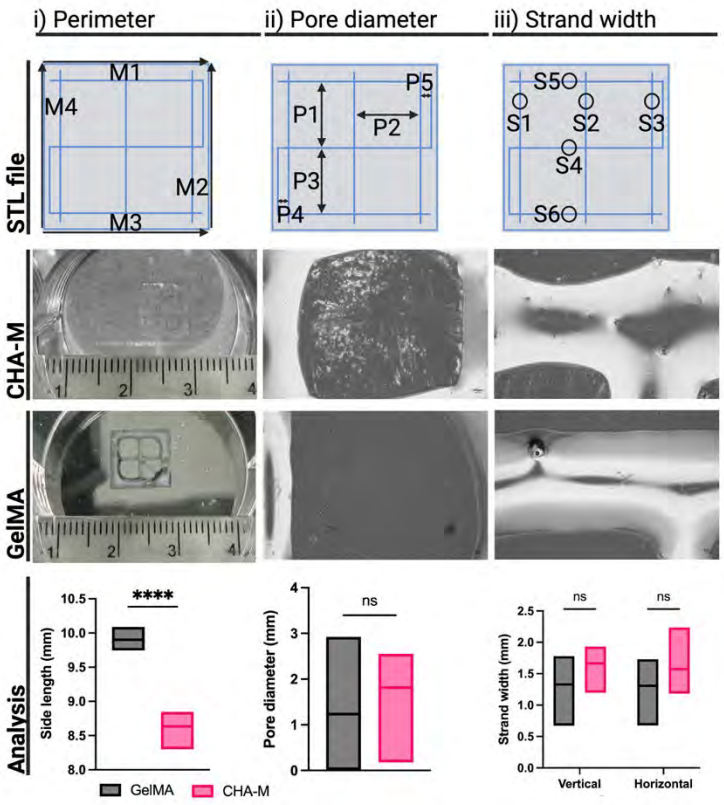

Figure 1. Printing CHA-M: resolution on a macro- and micro-scale. Dimensionality printing trials comparing CHA-M to well-established bioink GelMA, including an analysis of (i) geometry perimeter, (ii) pore diameter and (iii) strand width. i) One-way ANOVA with Tukey HSD (**** P<0.0001), (ii/iii) two-way ANOVA with Šídák multiple correction.

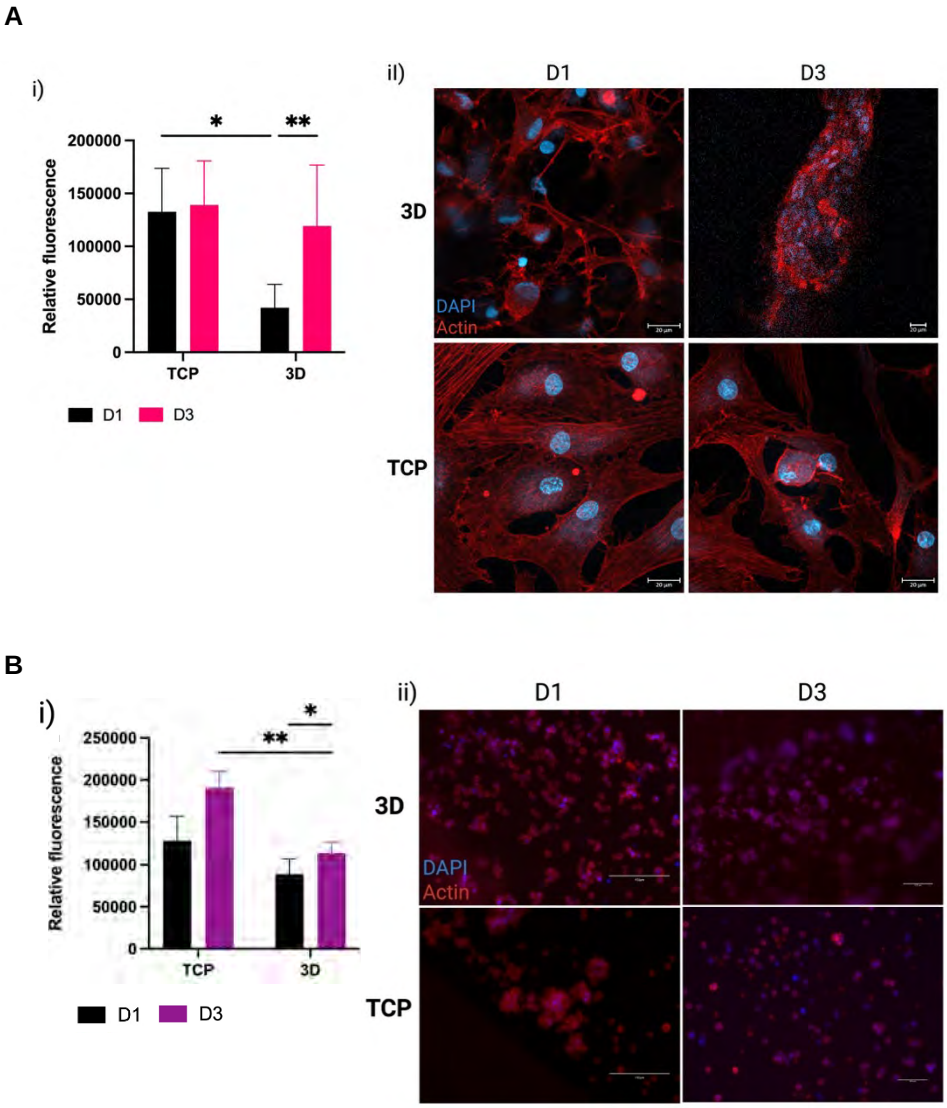

Figure 2. CHA-M cytocompatibility analyses. A) FLS i) cellular viability across timepoints by Prestoblue™ cell viability assay. Data analysed by two-way ANOVA, with multiple comparisons performed using Fisher's LSD test (* P<0.05, ** P<0.005). ii) Morphological characterisation of 3D and TCP FLS samples, across timepoints D1-D3, with cell nuclei shown in blue (DAPI) and the actin cytoskeleton in red (Phalloidin). Scale bar set to 20µm. B) THP-1 i) cellular viability across timepoints by Prestoblue™ cell viability assay. Data analysed by two-way ANOVA, with multiple comparisons performed using Fisher's LSD test (* P<0.05, ** P<0.005). ii) Morphological characterisation of 3D and TCP THP-1 samples, across timepoints D1-D3, with cell nuclei shown in blue (DAPI) and the actin cytoskeleton in red (Phalloidin). Scale bar set to 150 μm.

S45 – O5

Novel xeno-free hPLMA/dECM-MA biomaterial for 3D DLP bioprinting

Silvério S.[1,2], Santos S.C.[1], Mano J.F.[2], Custódio C.A.[1,2]
[1]Metatissue, Edifício Central, PCI, Creative Science Park Aveiro Region, Ílhavo; [2]Dept. of Chemistry, CICECO, Aveiro Institute of Materials, University of Aveiro, Portugal

Introduction

Over the years, Digital Light Processing (DLP)-based 3D bioprinting has emerged as a promising technology to develop platforms that accurately mimic native human tissues.[1,2]A fundamental factor in bioprinting techniques is the bioink's composition and properties. Recently developed photopolymerizable biomaterials of human origin – human methacryloyl platelet lysates (hPLMA) and methacrylated decellularized extracellular matrix (dECM-MA) – offer appealing options for light-based bioprinting.[3,4]In this work we combined hPLMA with dECM-MA to create a novel xeno-free bioink for DLP bioprinting.

Materials and Methods

Precursor solutions of hPLMA and dECM-MA were prepared at 15% and 1%(w/v), respectively, in a photoinitiator solution. The final ink was prepared by combining equal parts of the precursors with a photoabsorber. Its photorheological properties were evaluated, and both printed and non-printed hydrogels were characterized through compression testing and SEM. Stem cells were encapsulated in hPLMA/dECM-MA hydrogels and printed constructs, and after 7 days of culture hydrogels were stained to assess cell viability (live/dead) and cytoskeletal organization (nuclei/actin filaments).

Results

Simple structures were printed, demonstrating high shape fidelity, resolution, structural stability and reproducibility (Figure 1). Live/dead and nuclei/actin filaments staining images revealed good cell viability and proliferation, including in the bioprinted hydrogels, and bioprinted constructs demonstrated evenly distributed cells (Figure 2A). The hydrogel characterization tests revealed that by modulating the biomaterials' concentrations and/or proportions, their mechanical and structural properties can be finely tuned to meet specific TE requirements (Figure 2B).

Conclusion

The tunability of the herein developed bioink, combined with its human origin and inherent content of bioactive and structural proteins, positions it as a highly translational bioink for the fabrication of physiologically-relevant, stable scaffolds supporting long-term in vitro cell culture and potential clinical applications.

Acknowledgements

This work was developed within the scope of the project CICECO-Aveiro Institute of Materials, UID/50011/2025(DOI:10.54499/UID/50011/2025),LA/P/0006/2020(DOI:10.54499/LA/P/0006/2020)& COMPETE2030-FEDER-00836800(doi.org/10.54499/2023.17280.ICDT), financed by national funds through the FCT/MCTES (PIDDAC).

References

[1]Yu Y.,Wang Q.,Wang C.,Shang L.Living Materials for Regenerative Medicine.*Engineered Regeneration 2021*;2;96–104.
[2]Li H.,Dai J.,Wang Z.,Zheng H.,Li W.,Wang M.,Cheng F.Digital Light Processing (DLP)-Based (Bio)printing Strategies for Tissue Modeling and Regeneration.*Aggregate 2023*;4;e270.
[3]Santos S.C.,Custódio C.A.,Mano J.F.Photopolymerizable Platelet Lysate Hydrogels for Customizable 3D Cell Culture Platforms.*Advanced Healthcare Materials 2018*;7;1800849.
[4]Deus I.A.,Santos S.C.,Custódio C.A.,Mano J.F.Designing Highly Customizable Human-Based Platforms for Cell Culture Using Proteins from the Amniotic Membrane.*Biomaterials Advances 2022*;134;112574.

Figures

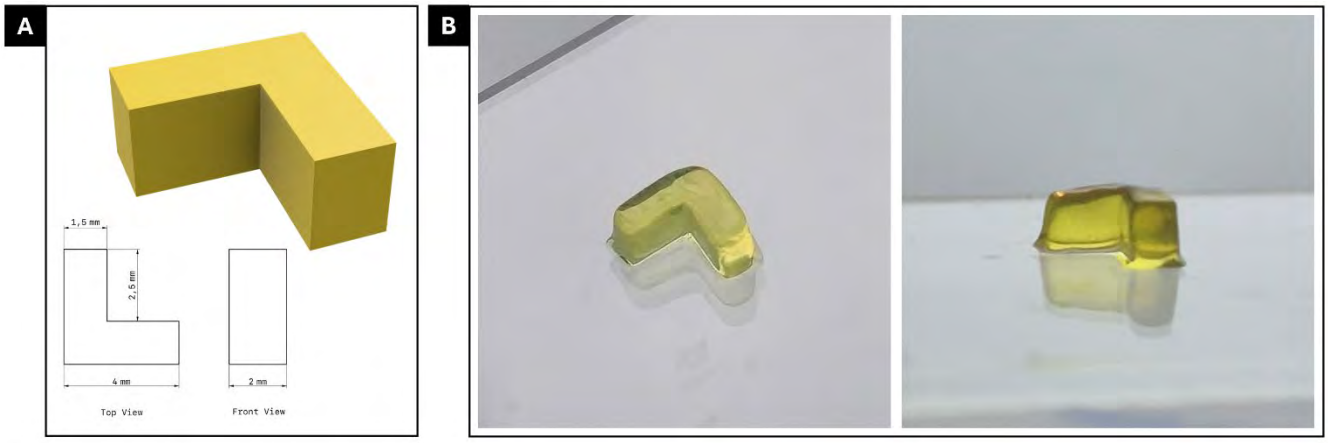

Figure 1 – (A) “L” shape 3D model. (B) Images of the "L" shape model 3D printed with a hPLMA/dECM-MA/Photoabsorber ink.

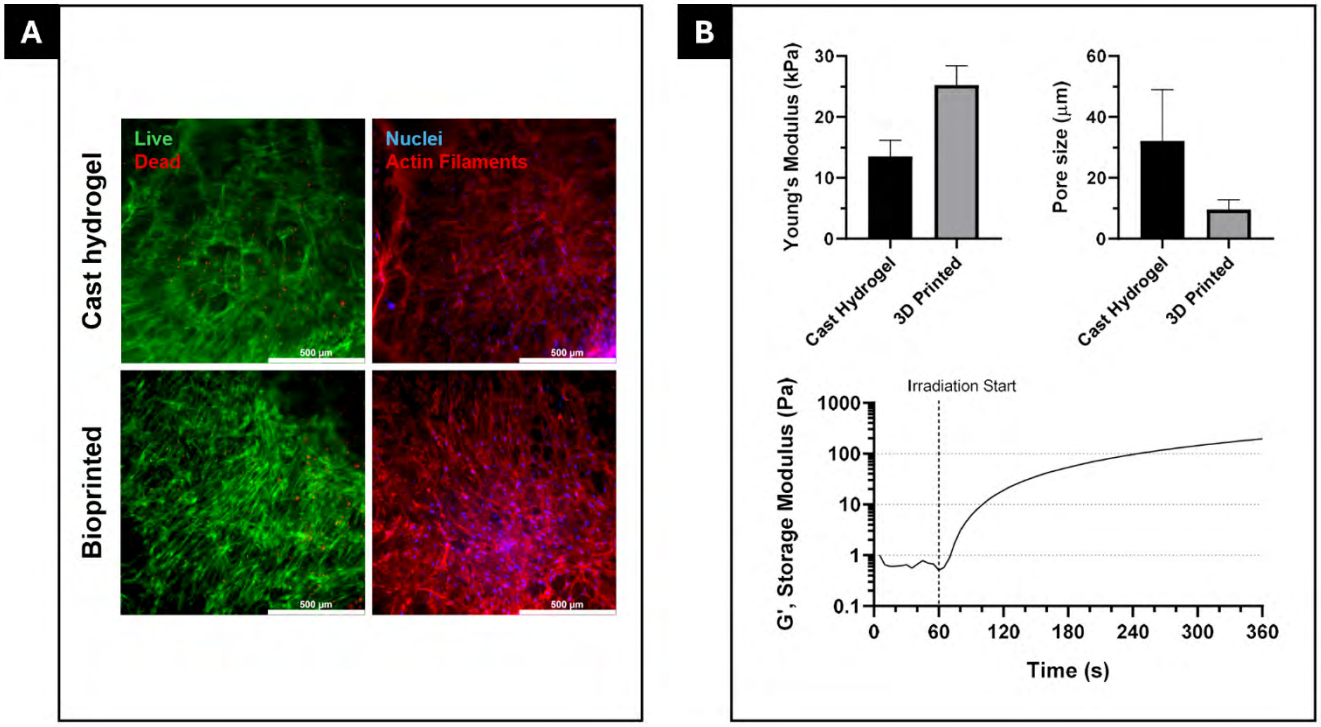

Figure 2 - (A) Images of Live/Dead and Nuclei/Actin Filaments staining of ASCs encapsulated in cast and bioprinted hydrogels, after 7 days of culture (Scale bar: 500 µm). (B) Mechanical characterization of hydrogels (cast and 3D printed), including elastic moduli from compression tests (upper left), pore size measurements (upper right) and photorheological results (bottom).

S45 – O6

Anti-thrombotic and decalcifying dECM embedded grafts for vascular tissue engineering

Hood R.M.[1], Claeyssens F.[1,2], Green N.H.[1,2]
[1]School of Chemical, Materials and Biological Engineering, University of Sheffield; [2]Insigneo Institute for In-silico Medicine, University of Sheffield, UK

Introduction

640 million people worldwide live with cardiovascular disease [1]. Autografts remain gold standard for vascular replacement, but some patients lack harvestable vessels necessitating synthetic alternatives [2]. However, these fail at smaller diameters due to acute thrombosis and poor reendothelialization. Tissue engineered vascular grafts (TEVG) are aimed to provide off-the-shelf biomimetic alternatives. Citric acid, a naturally occurring reagent, possesses the ability to chelate Ca^{2+} which aims to prevent platelet adhesion and thrombosis. It also aims to decalcify atherosclerotic deposits [3], [4]. This work aims to create a bilayer vascular graft composed of a citrate-eluting inner layer and an outer layer of decellularised extracellular matrix (dECM) embedded porous scaffold. Through extended cell culture and decellularization, a biomimetic TEVG will be created that not only contains native dECM but possesses the potential for in situ treatment.

Materials and Methods

Here we functionalised poly(glycerol sebacate) (PGS) with different molar ratios of citric acid. The polymers were characterised before electrospun mats were produced and studied for mechanical properties, cytotoxicity and hemocompatibility. The outer layer was synthesised from porous scaffolds of PGS- methacrylate and optimised for pore size and interconnectivity to encourage infiltration. Fibroblasts were cultured for 28 days to deposit ECM before decellularisation was completed to produce non-immunogenic scaffolds.

Results

FTIR, NMR and GPC confirmed the production of different compositions of PGS-citrate. Altering the proportions of citrate leads to tunability of the tensile strength, degradation and biocompatibility. Cytotoxicity testing highlighted a favourable composition of PGSC, and platelet adhesion showed a 7-fold reduction. For the outer layer, histological and immunofluorescence staining highlighted thorough infiltration and deposition of ECM. Optimisation of a decellularisation protocol led to DNA content of below the 50 ng/mg threshold. Immunofluorescence and hydroxyproline assay confirmed the retention of ECM components alongside the removal of nuclei. Reseeding with primary cells shows increased proliferation in the presence of the dECM.

Conclusion

Both layers of the vascular graft have been synthesised and studied to confirm their desired properties. PGSC scaffolds show a 7-fold reduction in platelet adhesion providing promise for the prevention of acute thrombosis. An investigation into the decalcification with PGSC will be completed and aims to break down atherosclerotic plaques *in vivo*. The outer layer contains vital proteins to encourage cell infiltration, and the increased rate of proliferation shows promise for rapid endothelialisation. Incorporation of a dynamic bioreactor culture aims to boost ECM production and cell proliferation to create more robust biomimetic scaffolds.

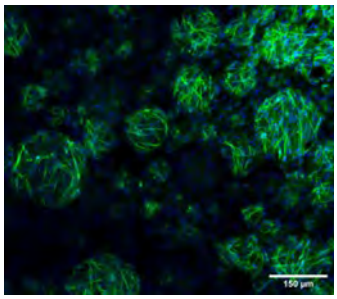

Figure 1: Confocal microscopy image showing cells stained with DAPI and Phalloidin FITC growing inside the porous scaffold and filling the voids.

S46
Modular biofabrication approaches for tissue engineering

S46 - K1
Modular tissue biofabrication

Zhang Y.S.[1]
[1]Division of Engineering in Medicine, Dept. of Medicine, Brigham and Women's Hospital, Harvad Medical School, Cambridge, USA

Introduction
Over the last decades, the field of three-dimensional (3D) printing, or additive manufacturing, has witnessed tremendous progress. 3D printing enables precise control over the composition, spatial distribution, and architecture of the printed constructs facilitating the recapitulation of the delicate shapes and structures of target patterns. More recently it has been further combined with cells and cell-laden biomaterials to offer the versatility to fabricate biomimetic volumetric tissues that are both structurally and functionally relevant. Nevertheless, conventional 3D printing and bioprinting techniques are limited in certain aspects.

Results
This presentation will discuss our recent efforts in developing a series of advanced additive (bio)manufacturing strategies that take unconventional approaches to tackle some of these problems and improve their capacities towards diverse applications in biomedicine with a focus on regenerative medicine. The focus will be placed on modular tissue biofabrication.

Conclusion
These platform technologies will likely provide new opportunities in areas from constructing functional tissues and microtissue models for promoting personalizable medicine, all the way to minimally invasive surgical implications.

S46 – O1

Volumetric bioprinting of perfusable and fully endothelialized vessels model

Zanoni G.[1,2], Größbacher G.[1,2,3], Boudia F.[4], Robin C.[2,4], Levato R.[1,2,3]
[1]Dept. Orthopaedics, University Medical Center Utrecht; [2]Regenerative Medicine Center Utrecht; [3]Dept. of Clinical Sciences, Faculty of Veterinary Medicine, Utrecht University; [4]Hubrecht Institute-KNAW & University Medical Center Utrecht, The Netherlands

Introduction

Vessel morphology and blood flow-derived mechanical forces regulate endothelial cell behavior and signaling, yet reproducing native vascular structure and physiological flow in vitro remains challenging. Current models rely on microfluidic systems with small (<300µm), rigid channels that preclude matrix remodeling. Such platforms are limited in capturing vessels where flow patterns, pulsatility, and geometry driven shear stresses dominate endothelial function. Access to perfusable vessel models in this regime would enable systematic dissection of geometry dependent mechanotransduction and flow pattern dependent cell responses. Here, we investigate volumetric bioprinting (VBP) as a rapid and scalable strategy to generate complex, perfusable vascular architectures to probe endothelial responses to mechanical cues.

Materials and Methods

We developed a channel-in-hydrogel construct integrated into a modular 3D-printed perfusion chamber capable of sustained pulsatile flow and controlled shear stress. Gelatin methacryloyl was used as resin for VBP, and as a platform for further biofunctionalization. To achieve endothelialization, we screened coatings with bioactive molecules (Fibronectin, FBS, peptides) and optimized a HUVEC seeding protocol that enables monolayer formation under flow. After overnight coating, cells were seeded and the chamber rotated 180° every hour for 6 hours to allow attachment. The chamber was connected to perfusion with fresh media, and cells were cultured under flow for 6 days (6-200 µL/min).

Results

The perfusion chamber (Figure A) supports leak free, dynamic perfusion for at least 21 days. Confocal imaging on day 6 revealed a tight endothelial monolayer and CD31 expression showed functional cell-cell junctions (Figure B). Monolayer formation was observed for a range of diameters (0.5 to 2 mm) in straight channels and for geometries with VBPs design freedom like bifurcations and gyroids. Experiments were executed under dynamic flow conditions.

Conclusion

These results establish a perfusion platform using VBP with high design freedom for endothelial vessel engineering with the potential to study flow and matrix dependent regulation of endothelial cell specification and function. Future work will incorporate endothelial cells from different developmental stages (including iPSC-derived cells), mural cells, and tissue-specific vascular subtypes.

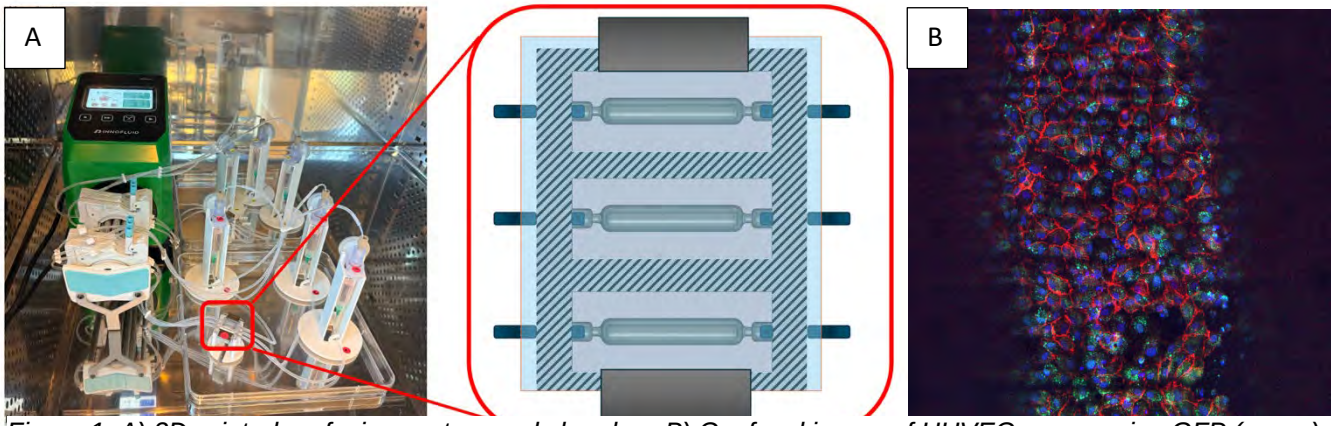

Figure 1. A) 3D-printed perfusion system and chamber. B) Confocal image of HUVECs expressing GFP (green), immunostained for CD31 (red) and counterstained with Hoechst (blue). Scale bar: 100um.

S46 – O2

A vascularized osteosarcoma-on-a-chip to model endothelial barrier and study drug transport

Lipreri M.V.[1], Totaro M.T. [2], Baldini N.[1,2], Avnet S.[2]
[1]Biomedical Science, Technologies, and Nanobiotechnology Lab, IRCCS Istituto Ortopedico Rizzoli, Bologna; [2]Dept. of Biomedical and Neuromotor Sciences, University of Bologna, Italy

Introduction

The microvasculature is fundamental to human pathophysiology and plays a central role in disease progression and therapeutic delivery. In cancer, treatment efficacy strongly depends on transport across endothelial barriers and through the three-dimensional tumor microenvironment, and vasculature systems critically influence the pharmacokinetics and pharmacodynamics of anti-cancer therapeutic agents. However, conventional in vitro models fail to adequately recapitulate these interactions, limiting their predictive value for clinical therapeutic response. This limitation is especially relevant in osteosarcoma (OS), an aggressive malignancy with poor prognosis and a lack of predictive preclinical models. In this context, microfluidic platforms offer a promising strategy to reproduce vascular architecture, physiologically relevant flow and shear-stress, and the complex organization of the different cells of the tumor microenvironment.

Aim

This work aimed to develop an osteosarcoma-on-a-chip model integrating a vascular-like endothelial barrier with a three-dimensional tumor structure to study drug transport under physiologically relevant conditions and controlled shear stress.

Materials and Methods

The platform consists of a two-layer PDMS microfluidic device with two perfused chambers separated by a microporous PET membrane. In the upper chamber, endothelial cells were co-cultured with mesenchymal stromal cells (MSCs) to establish a vascular-like barrier. In the lower compartment, MG63 OS spheroids were generated in situ within a hydrogel-based microwell array. Spheroid formation was assessed in terms of size and viability, while barrier formation was evaluated by immunofluorescence staining for VE-cadherin. Transport studies were performed using fluorescent dextrans of different molecular weights and the chemotherapeutic agent doxorubicin.

Results

MSCs enhanced endothelial barrier integrity, as shown by a stronger and more continuous VE-cadherin staining compared with endothelial monocultures.In addition, MSCs organized into elongated bundles surrounding the endothelial layer, resembling the perivascular arrangement observed in vivo. In the lower chamber, MG63 cells formed uniform spheroids within six hours, reaching an average diameter of approximately 200 µm and maintaining stable morphology for at least seven days with high viability. Permeability assays demonstrated size-dependent dextran diffusion and regulated doxorubicin transport across the endothelial interface, dependent on barrier maturation. Furthermore, we observed that the endothelial barrier was strongly influenced by the presence of OS spheroids, showing a higher proliferation rate in respect to the condition in the absence of tumor cells.

Conclusion

This microfluidic OS-on-a-chip model integrates a vascular-like barrier with tumor spheroids in a physiologically relevant microenvironment. The platform highlights the role of stromal–tumor interactions and vascular perfusion in modulating drug penetration and therapeutic response, and provides a valuable tool for prediction of human relevant pharmacokinetics/pharmacodinamics behavior, offering a promising platform to study drug delivery and drug screening.

Acknowledgements

The work was supported by Italian Association for Cancer Research (AIRC IG 2018 — project ID 21403).

S46 – O3

Convergence of extrusion-based bioprinting of microgel-microtissue composite bioinks and melt-electrowriting for cartilage regeneration

Dechant L.[1,2], Tomás Rodrigues C.[1,2], Grasselli S.[1,2], Kara Özenler A.[1,2], Kechagias S.[3], Sobreiro-Almeida R.[4], Mano J.[4], Daniel J.K.[3], Malda J.[1,2,5]

[1]Dept. of Orthopaedics, University Medical Center Utrecht, The Netherlands; [2]Regenerative Medicine Center Utrecht, The Netherlands; [3]Trinity Centre for Biomedical Engineering, Trinity Biomedical Sciences Institute, Trinity College Dublin, Ireland; [4]Dept. of Chemistry, CICECO, Aveiro Institute of Materials, University of Aveiro, Campus Universitário de Santiago, Portugal [5]Dept. of Clinical Sciences, Faculty of Veterinary Medicine, Utrecht University, The Netherlands

Introduction

Clinical translation of cartilage grafts engineered from microtissue building blocks requires biomaterials that are bioactive, xenofree, and patient-specific. Platelet lysate (PL) and its methacrylated derivative (PLMA) fulfill these criteria, yet their rheological properties make them unsuitable for extrusion-based bioprinting. Formulating PL-PLMA as granular microgels recently enabled shear-thinning, extrudable bioinks that maintain cell viability and shape fidelity post-printing.[1] The inherent microporosity of microgel constructs further supports cell-cell interaction, microtissue fusion, and tissue maturation. However, these constructs lack the mechanical properties required for load-bearing cartilage applications. Melt electrowriting (MEW) fiber reinforcement is an established strategy to address this in bulk hydrogel-based cartilage grafts, yet its effect on microgels remains uncharacterized.

Aim

To converge microgel-microtissue extrusion bioprinting with MEW fiber scaffolds on a single biofabrication platform for mechanically reinforced cartilage grafts.

Materials and Methods

PL-PLMA microgels were fabricated as previously described[1] and mixed at 2:1 ratio with equine articular chondroprogenitor cell microtissues (Fig. 1A). The bioink was cast and printed using a 22GA nozzle within a RegenHU bioprinter and microtissue distribution and printability were assessed. For converged scaffolds, polycaprolactone was melt-electrowritten and converged with microgel-microtissue bioink extrusion. Samples were cultured up to 28 days in chondrogenic medium and analyzed by live-dead staining, biochemistry, histology, and mechanical testing.

Results

Biochemistry and histology confirmed that cartilage microtissues exhibited abundant chondrogenic differentiation and cartilage-specific ECM production after 28 days when encapsulated in PL-PLMA microgels (Fig. 1A). The composite bioink was successfully printed with good shape fidelity and homogenous microtissue distribution within the bioink (Fig. 1C). Live-dead staining showed cells remained viable post-printing (Fig. 1C), and their potency for chondrogenic differentiation was confirmed by histology. Extrusion-based bioprinting of microgel-microtissue bioinks was successfully converged with MEW, enabling the precise patterning of microgel bioinks with spatial resolution of individual MEW boxes (Fig. 1D). The reinforcing effect of MEW scaffold on bulk hydrogels and microgels was demonstrated by compression testing, which increased the modulus for reinforced microgels by 600%.

Conclusion

This study presents the first convergence of microgel-microtissue extrusion bioprinting with MEW on a single biofabrication platform, enabling mechanical reinforcement and spatial patterning. Given the inherent modularity of microgel-based bioinks, this platform opens possibilities for automated biofabrication of gradient and anisotropic constructs, advancing cartilage tissue engineering toward clinical translation.

Acknowledgements

Funded by the European Union (m2M; Grant agreement: 101191729).

References

[1]Ribeiro, LS, et al. Nozzle Jamming Granularized Blood-Derived Proteins for Bioprinting Cell-Instructive Architectures. *Aggregate 2025;* 6(7); e70041.

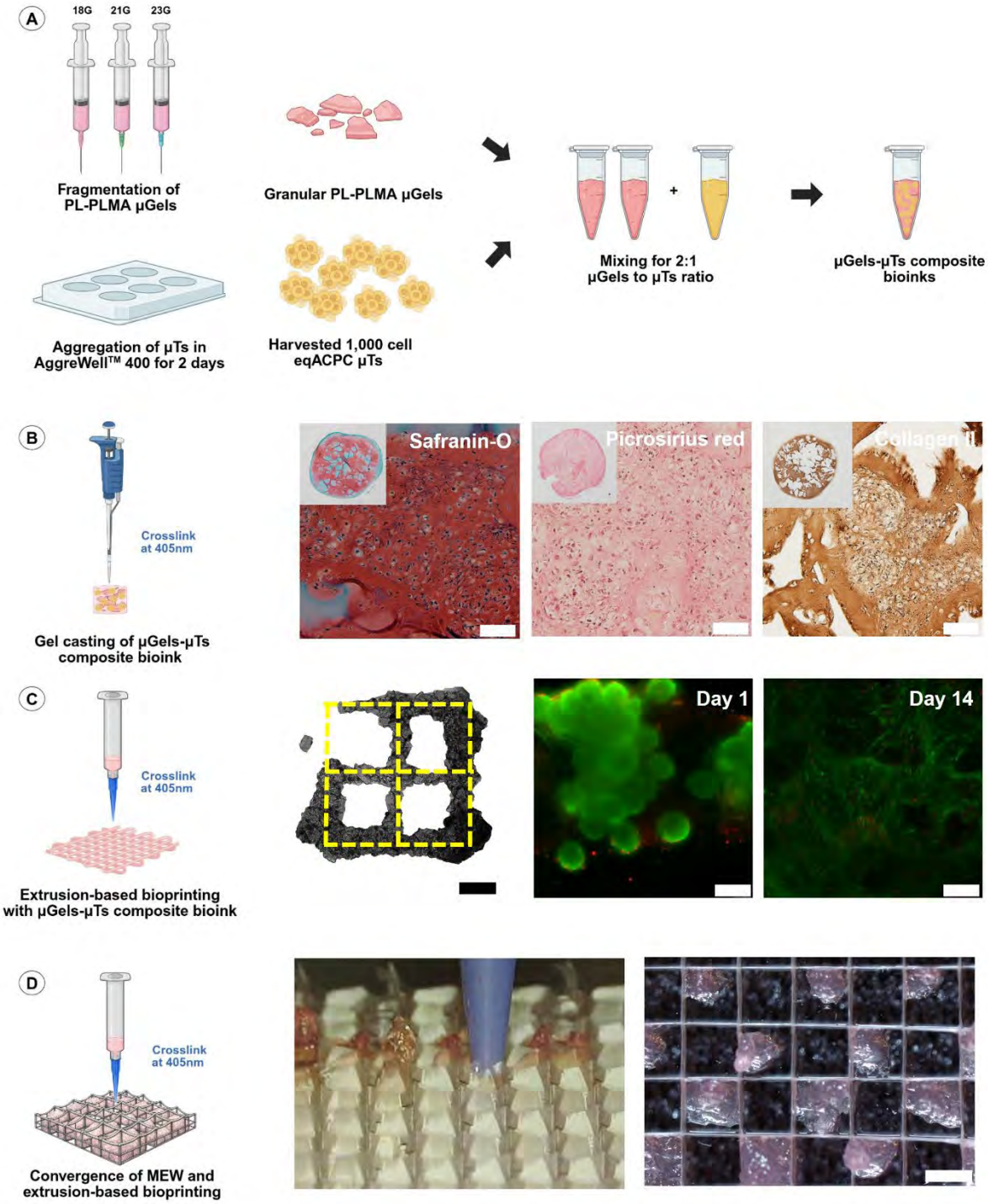

Figure 1. A) Bulk PL-PLMA microgels are fragmented and mixed at a 2:1 ratio with eqACPC microtissues to obtain microgel-microtissue composite bioinks. B) Gel casted microgel-microtissue composite bioinks differentiated for 28 days show abundent chondrogenic differentiation. Scale bar is 250 µm. C) Extrusion-based bioprinting of microgel-microtissue composite bioinks results in scaffolds with high shape fidelity and cell viability. D) Convergence of extrusion-based bioprinting with PL-PLMA microgels and melt-electrowriting enables spatial patterning in individual MEW boxes. Scale bar is 1mm.

S46 – O4

Remote magnetic actuation enhances maturation and assembly of cartilage microtissues

Demri N.S.[1], Pueyo-Moliner A.[1], Dechant L.B.[1], Rodrigues C.[1], Malda J.[1]
[1]University Medical Center Utrecht, The Netherlands

Introduction

Cartilage repair remains a major challenge due to its limited self-regeneration. While tissue engineering has advanced, recreating native cartilage architecture is still hindered by an incomplete understanding of the mechanical cues driving tissue formation.

Aim

In this study, we present a magnetic bioreactor platform to stimulate and assemble magnetically labeled cartilage microtissues, applying controlled mechanical cues to enhance chondrogenesis.

Materials and Methods

Equine articular progenitor cells (ACPCs) were labeled with 2 mM iron oxide nanoparticles 30 min per day for three days, enabling their magnetization and later their magnetic actuation. Labeled cells were compacted into spheroids and differentiated for 1 or 2 weeks before magnetic stimulation. Individual spheroids were actuated via magnets placed below the culture plate, either statically or dynamically, applying cyclical compression or horizontal sliding to induce shear stress, thanks to a system of automated actuators. Similar actuations were also performed on groups of spheroids to promote their fusion, including through magnetic levitation. After one month of differentiation, tissues underwent mechanical testing (DMA), biochemical assays (DMMB, PicoGreen, hydroxyproline), and histology (Safranin-O, Picrosirius Red, Perls').

Results

Sequential magnetic labeling enabled efficient iron uptake by ACPCs (Fig. 1A) without affecting viability or preventing differentiation, evidenced by proteoglycan and glycosaminoglycans deposition (Fig. 1B–C). Magnetically labeled spheroids could be remotely actuated by an adjacent magnet, inducing alignment of iron within the microscopic structure of the tissues (Fig. 1D) and overall tissue compaction (Fig. 1E–F). Shear stress could also be applied to tissues, as they could be cyclically slid by horizontal magnet motion (Fig. 1G). Magnetic stimulation did not impact cell viability but led to cell migration towards the magnet after two weeks (Fig. 2A). Importantly, after one month of differentiation, dynamic stimulation doubled tissue stiffness (Fig. 2B). This could be explained by matrix reorganization (Fig. 2C–D) and increased collagen and glycosaminoglycan deposition (Fig. 2E–F), particularly under cyclical sliding compression. Not only did dynamic stimulation enhance chondrogenesis in spheroid assemblies too, but magnetic cues also promoted their fusion, producing arch-like patterns and robust matrix deposition reminiscent of native cartilage (Fig. 2G-H).

Conclusion

These results further confirm that dynamic, multidirectional mechanical cues markedly enhance chondrogenesis. Moreover, magnetic actuation provides a powerful, non-contact platform to stimulate and assemble living tissues, enabling improved replication of the complex mechanical environment of native cartilage formation.

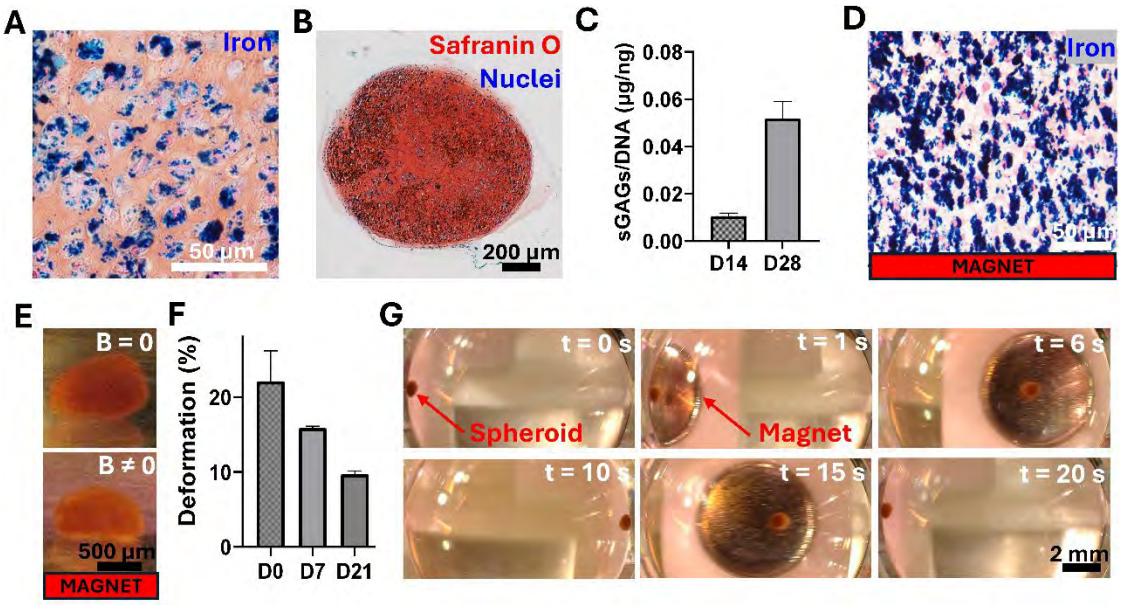

Figure 1. Magnetic actuation of magnetically labeled cartilage tissues. (A) Perls' Prussian iron blue staining counterstained with Safranin-O of a 14-day-old magnetically labeled tissue, showing iron uptake. (B) Safranin-O staining of proteoglycans and glycosaminoglycans (GAGs), counterstained with Nuclear Fast Blue, in a 28-day-old magnetically labeled tissue. (C) Ratio of sulfated GAGs (sGAGs) per DNA in 14- and 28-day-old magnetically labeled samples. (D) Perls' Prussian blue staining of 14-day-old tissues placed on a magnet for one week, showing iron alignment. (E) Side view of a 7-day-old tissue without (top) and with (bottom) a magnet below the culture plate. (F) Tissue deformation between before and after a magnet was placed below at days 0, 7 and 21. (G) Time-lapse of one cycle showing a spheroid being dragged back and forth across a culture well by a motorized magnet, sliding horizontally, to induce shear stress on the spheroid.

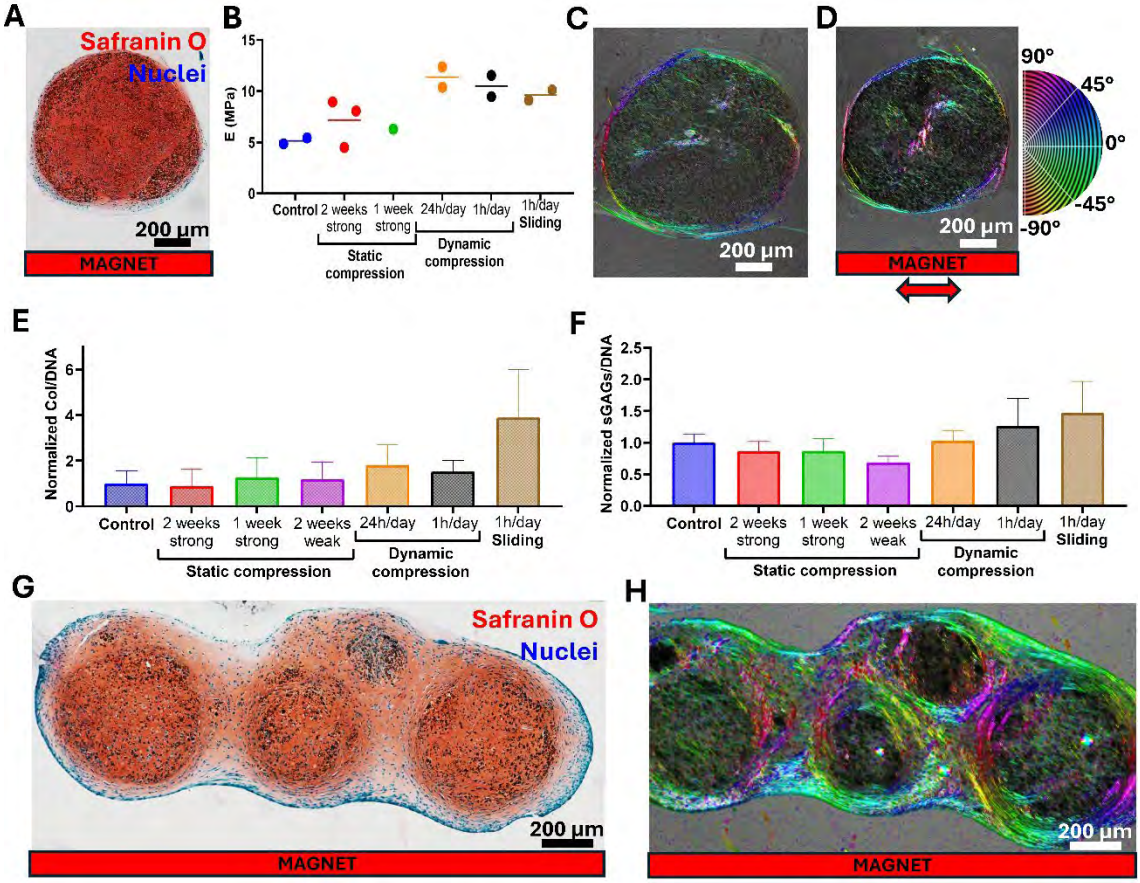

Figure 2. Magnetic stimulation and assembly improve chondrogenesis. (A) Safranin-O staining counterstained with Nuclear Fast Blue in a 28-day-old magnetically labeled tissue, compressed by a magnet since day 14. (B) Young's moduli of 28-day-old magnetically stimulated tissues. Orientation maps of collagen fibers (stained with Picrosirius Red and imaged with polarized light microscopy) in 28-day-old tissues (C) without stimulation and (D) with a horizontal magnet sliding cyclically 1h/day since day 14. Fiber orientation is indicated by the adjacent color wheel. (E) Collagen per DNA and (F) sGAGs per DNA ratios (both normalized to control) in 28-day-old magnetically stimulated tissues. Magnetic stimulations include static compression (under a strong or weak field from day 14 to day 28, or under a strong field from day 14 to day 21), dynamic cyclical compression (with 6s-long cycles and a speed of 2mm/s, applied all day or only 1h per day, from day 14 to day 28) or dynamic sliding (with 20s-long cycles and a speed of 2mm/s, over 1h per day, from day 14 to day 28). (G) Safranin-O staining counterstained with Nuclear Fast Blue and (H) corresponding orientation map of collagen fibers (stained with Picrosirius Red and imaged with polarized light microscopy) of a 28-day-old microtissue resulting from the assembly of spheroids under magnetic compression since day 14.

S46 – O5

In-situ 3D reconstruction and non-planar trajectory generation for colorectal bioprinting

Bilancia E.[1], Chiesa I. [2], Fortunato G. M.[3], De Maria C. [4], Vozzi G.[5]
[1]University of Pisa, Italy

Introduction

Colorectal diseases (CD) are a cohort of pathologies that affect the mucosa and submucosa layers of the anus, rectum, and colon of more than 2 million individuals in the European Union. CDs could benefit from the removal of the intestinal mucosa and submucosa; however, currently, no strategies exist for their replacement. In this context, the EU funded projects “TENTACLE” envisions a new strategy for the surgical treatment of CDs, by developing an innovative in situ colonoscopic bioprinting strategy for the extrusion-based bioprinting of constructs directly inside the patient rectum/colon. The TENTACLE bioprinting strategy starts with the image-based 3D registration of the patient intestinal wall, and the subsequential trajectory generation, thus allowing to deposit the desired biomaterials following the patient-specific anatomy.

Materials and Methods

The TENTACLE colonoscopic bioprinter toolhead was enriched with a 4 mm diameter side view endoscopic camera with an illumination system, to acquire images of the intestinal wall. In this study, the camera explores the intestinal lumen through a helical trajectory with fixed radius and pitch, capturing images with an overlap of approximately 80%. The intestinal wall was simulated by a customized phantom, with clinically relevant vasculature (Fig.1A). Once the images were acquired by the camera, a photogrammetry-based algorithm, based on the Structure-from-Motion workflow (COLMAP software [1]), was used to reconstruct the intestinal wall 3D model, thus defining the printing substrate. Then, the 3D model of the bioconstruct to be printed was designed with the 3D computer graphics software Blender, projected onto the reconstructed surface, and the non-planar slicing procedure was performed using a previously developed non-planar slicing algorithm2, thus generating the final trajectories. Finally, the TENTACLE bioprinter was used to bioprint the desired bioconstruct on the phantom following the planned trajectories.

Results

The photogrammetric 3D reconstruction achieves high geometric fidelity, accurately capturing the complex and confined morphology of the intestinal lumen (Fig.1B). The non-planar slicer generated stable trajectories (Fig.1C), enabling the direct and precise deposition of material onto the scanned substrate (Fig.1D).

Conclusion

The presented workflow validates the feasibility of integrating miniaturized sensing and robotic control for in-situ bioprinting in complex anatomical environments, such as the intestinal wall. The described approach lays the groundwork for future minimally invasive surgical applications, enabling the accurate bioprinting directly onto patient-specific internal geometries.

Acknowledgment

Funded by the European Union, GA:101191747.

S46 – O6

Technical pen integration for advanced additive manufacturing of biologics

Carou Senra P.[1], Rial C.[2,3], Richter A.[2], W. Basit A.[2,4], Alvarez Lorenzo C.[1], Goyanes A.[1,2,3,4]
[1]Dept. de Farmacología, Farmacia y Tecnología Farmacéutica, I+D FarmaFacultad de Farmacia, Instituto de Materiales (iMATUS) and Health Research Institute of Santiago de Compostela (IDIS), Universidade de Santiago de Compostela, Spain; [2]FABRX Ltd., London, UK; [3]FABRX Artificial Intelligence, Santiago de Compostela, Spain; [4]Dept. of Pharmaceutics, UCL School of Pharmacy, University College London,UK.

Introduction

Personalized medicine is transforming healthcare, with additive manufacturing (AM) enabling on-demand production of customized dosage forms. Although 3D printing offers versatility, 2D methods such as inkjet printing provide higher precision for low-dose deposition but remain complex for clinical implementation. Technical pens offer a simpler alternative, delivering ink consistently without thermal or electrical stress, making them suitable for sensitive biologics. **Aim.** This study aims to develop and integrate a novel technical pen-based printhead into a pharmaceutical printer to enable precise fabrication of personalized oral films loaded with a biological compound, along with a custom interface for real-time control of key printing parameters.

Materials and Methods

A pharma-ink containing 8 mg/mL desmopressin acetate (EtOH:PG 70:30 v/v) was prepared. Printing was performed with a Rotring Isograph technical pen onto 0.3 mm thick potato-starch edible paper. The M3DIMAKER 2 pharmaceutical printer was equipped with a custom modular printhead, engineered to securely mount the technical pen and allow easy integration or replacement of modular adapters. A dedicated control interface within M3DIMAKER Studio software enabled real-time adjustment of critical parameters, including printing speed, layer number, tip width, and deposition area. Rectangular patterns (2 × 4 cm) with up to four layers per design were printed.

Results

The technical pen was successfully adapted as a novel printhead for pharmaceutical 3D printing, enabling fabrication of oral films containing a biological compound. Printed desmopressin doses ranged from 33 to 134 µg, with high accuracy (99.5–100.2%), demonstrating precise and flexible dosing. Films exhibited rapid release, with over 50% of desmopressin dissolved within 10 minutes. Moreover, after one month, dose accuracy and drug content remained near 100%, demonstrating stable, precise, on-demand printing suitable for practical applications.

Conclusion

A technical pen was successfully integrated as a modular printhead in a pharmaceutical 3D printer, enabling precise, flexible, low-dose desmopressin deposition. Its gravity-driven mechanism avoided temperature, pressure, or electrical stress, potentially minimized stress on sensitive compounds, while ensuring consistent deposition, material efficiency, and cost-effectiveness, demonstrating its potential as a high-precision tool for on-demand drug delivery and additive manufacturing.

Acknowledgements

PCS acknowledges a Predoctoral Fellowship [ED481A-2023-168] from Xunta de Galicia co-funded by the EU
Funding: Spain Ministerio de Ciencia, Innovación y Universidades
MICIU/AEI/https://doi.org/10.13039/501100011033 [PID2023-149544OB-C22; PID2023-150422OB-I00], ERDF
A way of making Europe, cofunded by the European Union, Xunta de Galicia [ED431C 2024/09].

S46 – O7

4D printing of advanced tubular constructs towards artificial tendon sheaths

Fichter E. [1], Msallem B. [2], Antek N. [2], Bernhardt A. [1], Gelinsky M. [1], Dragu A. [2], Von Witzleben M.[1]
[1]Centre for Translational Bone, Joint and Soft Tissue Research, Faculty of Medicine & University Hospital, TU Dresden, Germany, [2]Dept. of Plastic and Hand Surgery University Center for Orthopedics, Trauma, and Plastic Surgery, Faculty of Medicine & University Hospital, TU Dresden, Germany

Introduction

Surgical repair of hand tendons frequently neglects reconstruction of the tendon sheath, a structure essential for low-friction gliding of the tendon. Without a functional sheath, tendon adhesion occurs in approximately 30% of cases during immobilization, leading to long-term impairment of joint mobility. An artificial substitute must therefore be tubular, thin enough to conform to the tendon anatomy, and capable of reducing gliding friction while remaining surgically handleable. 4D printing addresses the challenge of fabricating such delicate tubular membranes by adding a temporal dimension to additive manufacturing: flat constructs undergo controlled shape morphing into tubular geometries upon exposure to an external stimulus, enabling self-wrapping around the tendon.

Aim

This study targets a thin tubular membrane based on a synergistic multilayered construct of melt electrowritten, melt electrospun fiber scaffolds and a lubricious hydrogel that is surgically suturable and cytocompatible yet resists cell adhesion, mimicking key structural properties of the native tendon sheath.

Materials and Methods

Flat multilayered constructs were fabricated on a single 3D printing platform (GeSiM mbH, Germany) using sequential deposition: (1) a melt electrowritten (MEW) polycaprolactone (PCL) scaffold, (2) a dense chaotic melt electrospun layer, (3) a dense extrusion-plotted alginate-methylcellulose (AlgMC) layer, (4) a second MEW layer and (5) additional AlgMC strands with defined distances. After (3), the AlgMC dried prior to further deposition. The flat constructs were then immersed in 100 mM $CaCl_2$ to induce ionic crosslinking and trigger shape morphing into tubular geometries. Following lyophilization, the tubular structures were subjected to mechanical testing, clinical suturability evaluation, and biological assessment using synovial fibroblasts.

Results

Reproducibility of the 4D printing process was identified as a critical bottleneck. Systematic investigation of varying material compositions combined with different sterilization protocols enabled significant process optimization, allowing a precise control of printability and structural fidelity while increasing the freedom of design. The resulting tubular constructs exhibited adequate mechanical resilience under both laboratory and clinically relevant loading conditions. Biological evaluation with synovial fibroblasts confirmed favorable cytocompatibility without promoting undesired cell adhesion.

Conclusion

A millimeter-thin, shape-morphing membrane was developed that meets clinical and biological requirements for tendon sheath reconstruction. The construct demonstrated surgical handleability, suturability, and adequate mechanical performance, offering a promising strategy to reduce post-operative tendon adhesion.

Acknowledgements

The project is funded by the Federal Ministry for Economic Affairs and Climate Action following a resolution by the German Bundestag (ArtiSs, grant number: 01 IF23398N).

S47
Modular microbiomaterials for bottom-up tissue engineering

S47 – K1
Building life like LEGO: Modular microbiomaterials for bottom-up tissue engineering

Tahmasebi Birgani N.
Department of Complex Tissue Regeneration, MERLN Institute for Technology-Inspired Regenerative Medicine, Maastricht University, Maastricht, The Netherlands

Bottom-up tissue engineering aims to construct tissues from their fundamental building blocks through self- or guided assembly, enabling precise spatial organization and biomimicry of the hierarchical architecture of native tissues. While many bottom-up approaches primarily rely on assembly of cells or cell aggregates, this strategy is often insufficient for engineering extracellular matrix (ECM)-rich tissues such as bone, cartilage, tendon, and their interfaces. Recent advances in biomaterials science have enabled the development of modular microscale biomaterials, i.e., microbiomaterials, including microparticles and microgels, that can function as ECM-inspired building blocks in bottom-up tissue engineering approaches. This keynote will present strategies for designing such microbiomaterials using biomimetic chemistries and advanced precision manufacturing approaches, including droplet microfluidics, lithography, micromolding, and nanoimprinting. Droplet microfluidics enables high-throughput production of monodisperse microbiomaterial building blocks, while lithography and micromolding produce shape-defined microparticles, and nanoimprinting allows the introduction of surface micro- and nanotopographies that provide additional instructive cues to cells. Together, these methods provide precise control over chemistry, geometry, and surface topography across a broad range of biomaterial systems, including hydrogels, synthetic polymers, and hybrid composites. In addition, in this research, different approaches are explored for integrating microbiomaterials with cells to form hybrid microtissues, including co-assembly of cells and ECM-mimicking microbiomaterials in non-adherent environments to generate spheroidal microtissues, and direct cell encapsulation during microbiomaterial fabrication. Finally, strategies for assembling these microtissues into larger tissue constructs through proximity-driven fusion, geometric recognition or external stimuli, will be highlighted. By incorporating biochemical, mechanical, and topographical cues at the microscale, microbiomaterials enable controlled cell organization and differentiation, and ECM formation, providing new opportunities for engineering complex, matrix-rich tissues and graded interfaces.

Acknowledgements
This research was financially supported by the Dutch Research Council's (NWO) Incentive Grant for Women in STEM (Biotetris Project) and Gravitation Program (Materials-Driven Regeneration Project), the European Union Interreg Vlaanderen-Nederland (BIOMAT on microfluidic chip Project), the Dutch Province of Limburg (Link2.0 Project), the China Scholarship Council (CSC) from the Ministry of Education of P.R. China and the Study Abroad Program of the Turkish Ministry of Higher Education.

S47 – K2
Engineering protein-fibers and protein-sheets

Patchornik G.
Ariel University, Israel

Abstract
We present a simple and versatile method for generating protein-sheets and fibers. The assemblies are formed from doubly $(His)_6$-tagged proteins coordinated by up to equimolar concentrations of Zn^{2+} or Ni^{2+} ions, which stably bridge at least two $(His)_6$ tags. Using this strategy, five unrelated proteins: Ubiquitin (UB), tandem Z-domain of Protein A (ZZ), alkaline phosphatase (AP), Cas9, and mCherry, were successfully assembled while retaining their structure. Functional properties, including antibody binding and fluorescence, were also preserved when relevant. This platform provides a broadly applicable strategy for constructing functional protein-based materials with potential applications in basic research and medicine. As a 1st example we show that target proteins can be detected at the 50 Zepto-molar concentration (50 x 10-21 M) using protein-assemblies comprised of a doubly (His)6-tagged alkaline phosphatase and a doubly (His)6-tagged ZZ-domain, conjugated by Zn2+ thereby eliminating the use of any sophisticated instrumentation.

S47 – O1

Creating modular tubular networks with tomographic volumetric additive manufacturing for branched small diameter vascular models

Bartolf-Kopp M.[1], Gergely C.[1], Geroneit I.[1], Moser F.[1], Galaba L.[1], Chicaiza Cabezas N.[1], Priebe V.[1], Jungst T.[1]
[1]Dept. for Functional Materials in Medicine and Dentistry, University Würzburg, Germany

Introduction

Tomographic volumetric additive manufacturing (tVAM) is a powerful tool to create complex geometrical structures for biomedical applications. The system lends itself ideally for the recreation of complex tissue structures. An application of tVAM is the use of patient data to create faithful disease models that recreate the pathology of for example stenosed blood vessels. Due to limitations in effective light penetration within the photoresin, vat size and by that maximal construct size is restricted. This limits the fabrication of complex branched tubular systems for small diameter blood vessel models that could be used as *in vitro* flow perfusion or stent deployment models.

Aim

To harness the capabilities of tVAM for the creation of branched vascular trees, we established a new straightforward way to use tVAM to fabricate a modular building block system. By connecting these modules, it would be possible to create large tubular structures with branches, windings and stenoses.

Materials and Methods

Polyethylene glycol diacrylate was blended with cellulose nanofibers as rheological modifier as main resin for tVAM. CAD models of different tubular modules consisting of multiple geometries including straight pipes, bypass branches, y-branches and spirals were designed and evaluated for printability. After parameters were adjusted, modules were printed and attached to each other to create larger tubular networks. To enable cell seeding, gelatin methacryloyl (GelMA) was used as resin matrix. Cell seeding of the module lumen was done with human umbilical vein endothelial cells (HUVEC).

Results

Tube modules could be created with several different geometries, also beyond conventional pipes like star shaped lumen or stenosed tubes. By attaching them at the end points by gluing it was possible to create leak tight connections and build networks consisting of up to seven different modules (Fig 1). Flow simulations of a stenosed bypass model could be recreated experimentally. A tubular system with seven modules was created with one stenosed module into which a stent could be deployed by balloon catheter though the network. Using GelMA as resin, several modules were created and pre-seeded with HUVECs. Combining these modules to a tree enabled a high monolayer coverage compared to a pre-assembled and post seeded module network.

Conclusion

We showed that by creating single moules with tVAM, it is possible to create large tubular networks beyond the build volume limitation of commercially available systems that can be used as models for flow study or endothelialisation

S44 keynote spreker zijn abstract staat niet in de map

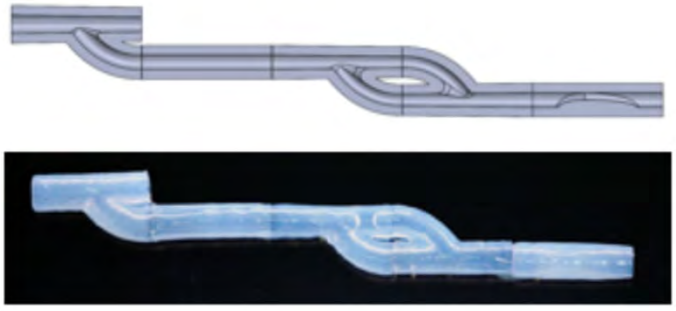

Fig. 1: CAD design (top) and printed (bottom) PEGDA modules via tVAM assembled into a branched tubular network with a stenosis module.

S47 – O2

Callus organoid-derived extracellular matrix as a modular building block for bone regeneration

Bai J.[1,2], Svitina H.[1,2], Decoene I.[1,2], Papantoniou I.[1,2]
[1]Prometheus Division of Skeletal Tissue Engineering; [2]Dept. of Development and Regeneration, Skeletal Biology and Engineering Research Center, Leuven, Belgium

Introduction

Bone fractures are common injuries, with 178 million cases worldwide in 2019.[1] Bone defects remain challenging and often result in non-unions. Callus organoids (COs) recapitulate early endochondral ossification, providing a blueprint for bone repair.[2] Nevertheless, such living implants face hurdles in preservation, transportation and allogeneic allogeneic use due to immunogenicity. One solution is to remove cells while retain extracellular matrix (ECM) as ready-to-use biomaterials.[3] Cartilaginous ECM has been studied for bone regeneration,[4] but using functionally preserved callus organoid-derived ECM as micromaterials remains unexplored. Thus, we compared decellularization and devitalization methods for COs, evaluating morphology, biochemical composition and bioactivity. We assessed osteogenic potential subcutaneously in mice and further interpreted results using proteomics. Our aim is to provide a novel off-the-shelf biomaterial for treating bone defects.

Materials and Methods

As shown in Figure 1 of the experimental design, human periosteum-derived cells were cultured in microwells with chondrogenic medium for 14 days to form COs. Various treatments, including lyophilization, freeze-thaw, detergent and enzyme exposure, were then applied to generate decellularized or devitalized ECM modules (dECMs). Followed morphological and biochemical characterization, dECMs were compared to COs by in vitro functional evaluation, proteomic analysis and *in vivo* validation ectopically in immunocompromised mice.

Results

All methods preserved the overall CO structure, with only slight shrinkage. Decellularization effectively removed >99% of DNA, as confirmed by Hoechst staining and DNA quantification (Figure 2A). After recellularization with human periosteum-derived cells, lyophilization-derived dECM most effectively supported chondrogenic and hypertrophic differentiation, based on histology and qRT-PCR (Figure 2B). Subcutaneous implantation for 8 weeks resulted in mineralized ossicle formation with cortex, trabeculae and marrow-like compartments in all groups, confirming retained bone-forming potential after processing (microCT, histology) (Figure 2C). Proteomic analysis further showed preservation of key Matrisome components, particularly in lyophilization- and detergent-treated groups, helping explain their superior functional performance (Figure 2D).

Conclusion

These findings demonstrate that decellularized and devitalized CO-derived ECM modules retain essential structural integrity, key Matrisome proteins and bone-forming capacity, serving as a potent off-the-shelf modular building block toward future translation in bone defect regeneration.

References

[1]GBD 2019 Fracture Collaborators. Global, regional, and national burden of bone fractures in 204 countries and territories, 1990-2019: a systematic analysis from the Global Burden of Disease Study 2019. Lancet Healthy Longev. 2021;2(9):e580-e592.
[2]Nilsson Hall G., Freitas L., Papantoniou I., et al. Developmentally engineered callus organoid bioassemblies exhibit predictive in vivo long bone healing. Adv Sci (Weinh). 2020;7(2):1902295-1902295.
[3]Seif-Naraghi S.B., Singelyn J.M., Salvatore M.A., et al. Safety and efficacy of an injectable extracellular matrix hydrogel for treating myocardial infarction. *Sci Transl Med. 2013*;5(173):173ra25-173ra25.
[4]Garcia Garcia A., Prithiviraj S., Raina D.B. Engineered and decellularized human cartilage graft exhibits intrinsic immunosuppressive properties and full skeletal repair capacity. *Proc Natl Acad Sci U S A. 2026*;123(2):e2507185123.

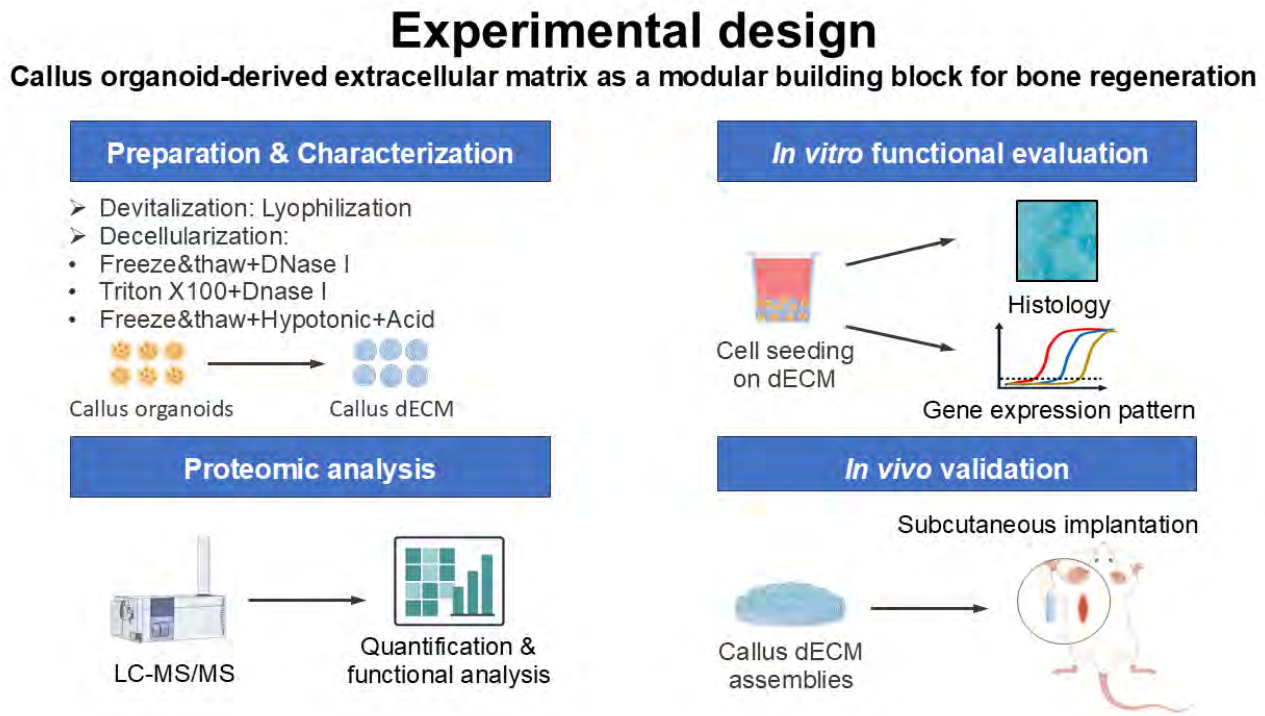

Figure 1. Overview of the experimental design. Callus organoids were processed into dECM by devitalization and decellularization, followed by morphological and biochemical characterization, *in vitro* functional evaluation, proteomic analysis and *in vivo* validation after subcutaneous implantation.

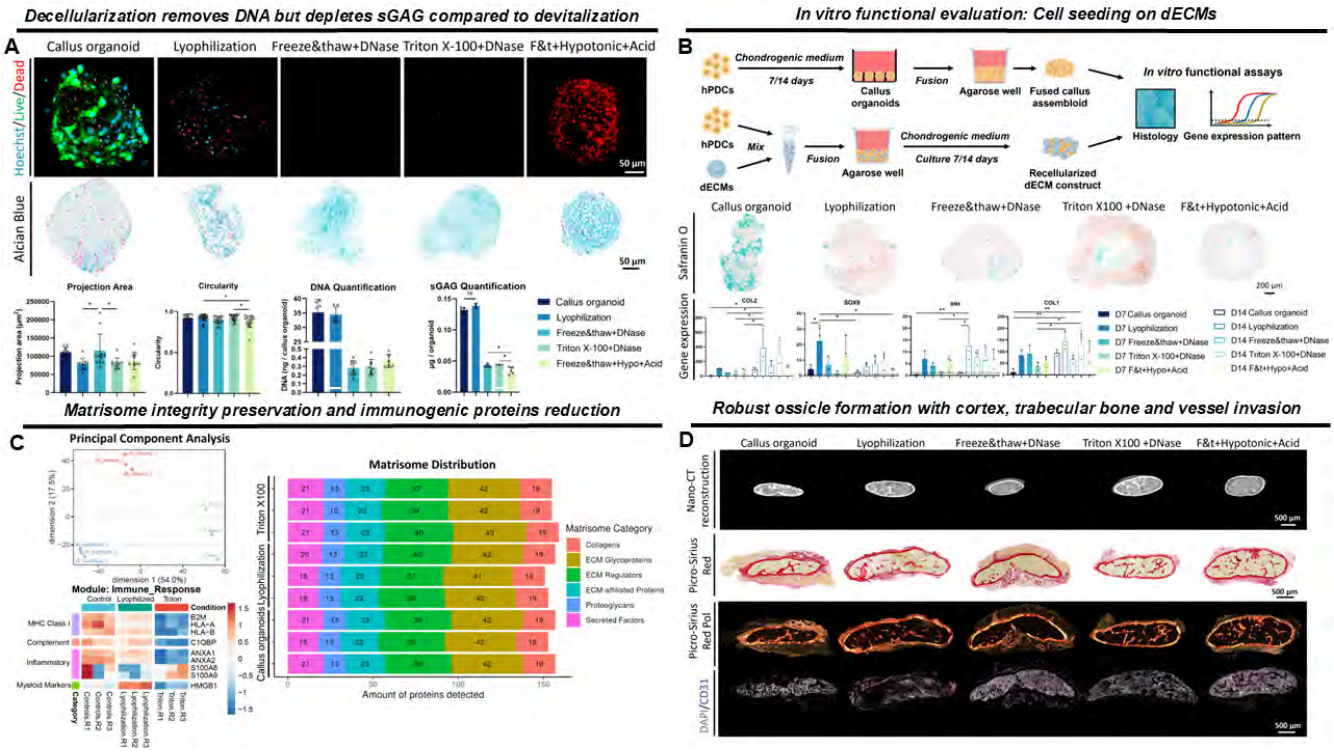

Figure 2. Overview of the main results obtained from callus organoid-derived dECMs.

S47 – O3

Hyaluronan-based transcript activated matrices and biomaterial inks for bone tissue engineering

van der Heide D.[1,5], del Toro Runzer C.[2], Della Bella E.[1], Plank C.[3], van Griensven M.[2], Balmayor E.R.[4], Stoddart M.J.[1], D'Este M.[1]
[1]AO Research Institute Davos, Davos, Switzerland; [2]Dept. of Cell Biology-Inspired Tissue Engineering, MERLN, Maastricht University, Netherlands; [3]Ethris GmbH, Planegg, Germany; [4]Experimental Orthopaedics and Trauma Surgery, RWTH Aachen University Hospital, Germany; [5]Dept. of Health Science and Technology, ETH Zürich, Switzerland

Introduction

Hyaluronan and its derivatives, when combined with matrix proteins, form essential building blocks for advanced functional biomaterials. Chemically modified RNA (cmRNA) is emerging as a promising alternative to protein delivery and DNA-based gene therapies. However, effective translation of this technology for bone regeneration requires a suitable biomaterial that can act simultaneously as a scaffold and delivery platform. To address this need, we investigated semisynthetic derivatives of hyaluronan and collagen formulated as microgels.
Aim: This study introduces a 3D-printable granular hydrogel composed of hyaluronic acid and collagen (THA-Col) designed for the delivery of bone morphogenetic protein-7 (BMP-7) cmRNA. The goal is to create a transcript activated matrix promoting bone healing.

Materials and Methods

The tyramine derivative of hyaluronic (THA) acid was crosslinked in presence of type-I collagen to form a brittle gel, then mechanically ground with multiple passages through a 100 µm metallic mesh. Printability was assessed via rheology and shape fidelity tests after printing. Cytocompatibility of microgels was tested with both fibroblasts and mesenchymal stromal cells (MSCs). MSCs were transfected with BMP-7 or metridia luciferase cmRNA by lipofectamine, either in 2D or in THA-Col bulk gels vs microgels, followed by induction of osteogenic differentiation.

Results

Microgels showed shear thinning and elastic recovery (Figure 1 A+B), confirmed by shape fidelity quantification after 3D printing. Overall, MSCs showed higher viability in the microgels (Figure 1 C), likely due to enhanced cell attachment on microgels and improved nutrition through the interstitial spaces. Unsurprisingly, cmRNA transfection impacted cell viability in all conditions, likely due to the choice of lipid-based delivery vehicles. Both bulk and microgels supported transfection of the luciferase (used as reporter) and BMP-7, but microgels samples showed the highest ALP activity (Figure 1 D).
Significance: Direct on-material transfection offers clear translational advantages as it eliminates the need for a preliminary surgery to harvest patient cells and circumvents the requirement for cmRNA transfection under GLP conditions. This simplifies the workflow, reduces procedural complexity, and ultimately decreases associated costs.

Conclusion

This study presents 3D-printable THA-Col microgels as activated matrices capable of delivering BMP-7 cmRNA to hMSCs to stimulate osteogenic differentiation. Compared with bulk hydrogels, THA-Col microgels supported higher cell viability, enabled efficient BMP-7 cmRNA transfection, and promoted osteogenic commitment of hMSCs in vitro. Together, these findings highlight the promise and practical applicability of cmRNA-based strategies for bone regeneration.

Acknowledgements

The AO Foundation and EU h2020 under grant agreement No 874790 (cmRNAbone).

ESB 2026

Figure 1

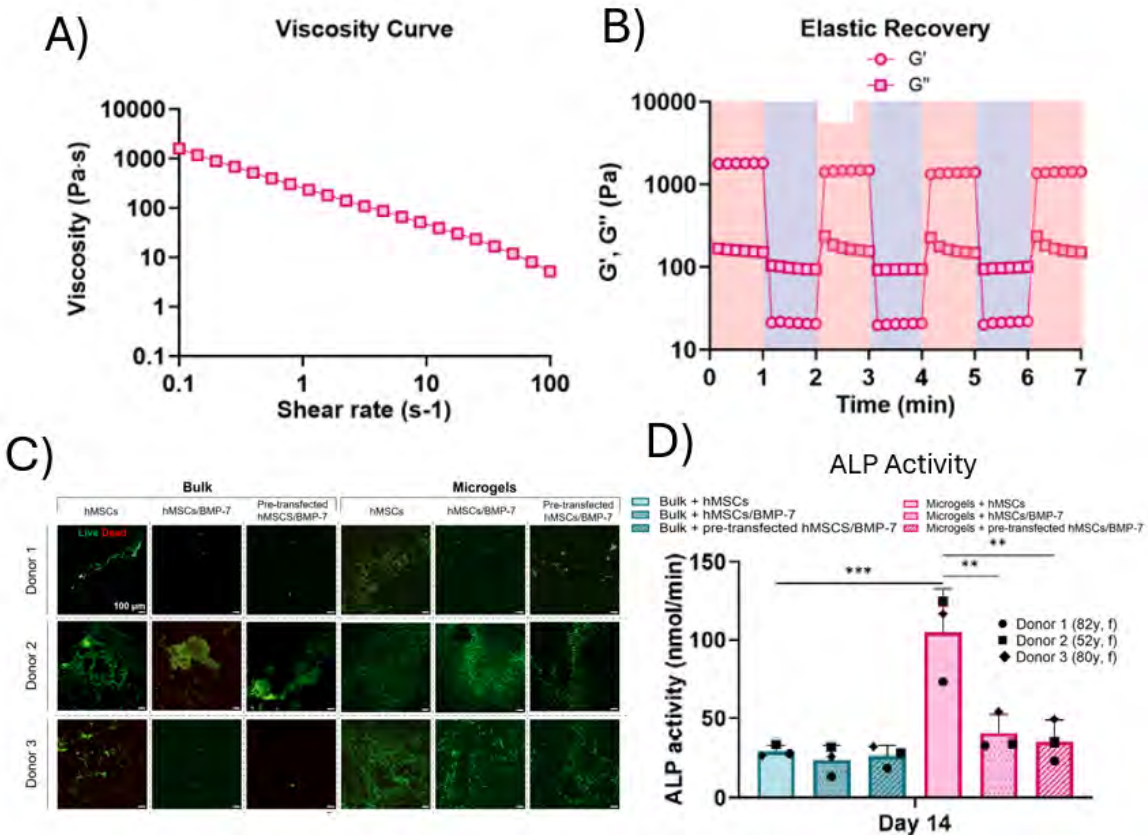

S47 – O4

Tuning the crosslinking and void fraction of highly flowable microparticles directs cell infiltration and multicellular organization

Vaziri A.S.[1], Agresti L.[2], Decarli M.C.[3], van Kooten T.[4], Shahbazi M.A.[5], Sjollema J.[6], Santos H.A.[7]
[1]Dept. of Biomaterials and Biomedical Technology, The Personalized Medicine Research Institute (PRECISION), University Medical Center Groningen (UMCG), University of Groningen, The Netherlands

Introduction

Microparticle hydrogels (MHs) are an emerging class of microporous, injectable biomaterials assembled from annealable microgels that enhance cell survival, function, infiltration and migration through their interconnected cell-scale void spaces[1]. Engineering microparticle assembly to tailor regenerative and therapeutic properties is a common goal in modulating these bottom-up platforms[2]. Towards this goal, here we aimed to understand how balancing inter- and intra-particle interactions, alongside interstitial matrix composition, influences the flowability and cellular responses of MHs.

Methods

We engineered enzymatically annealed microgels from tyramine-functionalized polymers via mechanical fragmentation, followed by a secondary photopolymerization step (**Figure 1a**). Rheology, mechanics, printability and cytotoxicity were thoroughly assessed to optimize the balance between intra- and inter-particle crosslinking. The effect of microparticles packing ratio was investigated by incorporating an interstitial matrix at varying ratios (10-40 vol.%). *In vitro* biological performance, including cell morphology, proliferation, adhesion and migration was studied using L929 fibroblasts.

Results

By fine-tuning the enzymatic- and photo-crosslinking ratios, we obtained structurally stable MHs, with a compressive modulus of 29-39 kPa and a porosity of 6.8-18.6%. Low-packing MHs led to a higher microporosity degree and enhanced *in vitro* cellular performance compared to medium- and high-packing counterparts, albeit with an expected trade-off in printability and mechanical stability (**Figure 1b, c**). Up to 3-fold increase in cell migration into medium-packing MHs is yielded over a 3-day period, compared to the bulk hydrogels (**Figure 1d**). In response to spatial confinement in void spaces, embedded cells adopted an elongated morphology and the formation of multicellular organizations after 7 days, demonstrating a correlation between microporosity and cellular network formation (**Figure 1e, f**).

Conclusion

By precisely engineering microarchitecture through controlled microporosity, this platform holds significant potential for developing self-organized cellular structures, which may open new opportunities for organ models and tissue engineering.

Acknowledgements

UMCG Research Funds.

References

[1] Claxton, N.L. *et al. 2024* “Engineering Granular Hydrogels without Interparticle Cross-Linking to Support Multicellular Organization,” *ACS Biomater. Sci. Eng.*, 10, 7594–7605.
[2] Vaziri, A. *et al.* 2025“Granular Hydrogels as Modular Biomaterials: From Structural Design to Biological Responses,” *Adv. Healthc. Mater*, 15(3), e02462.

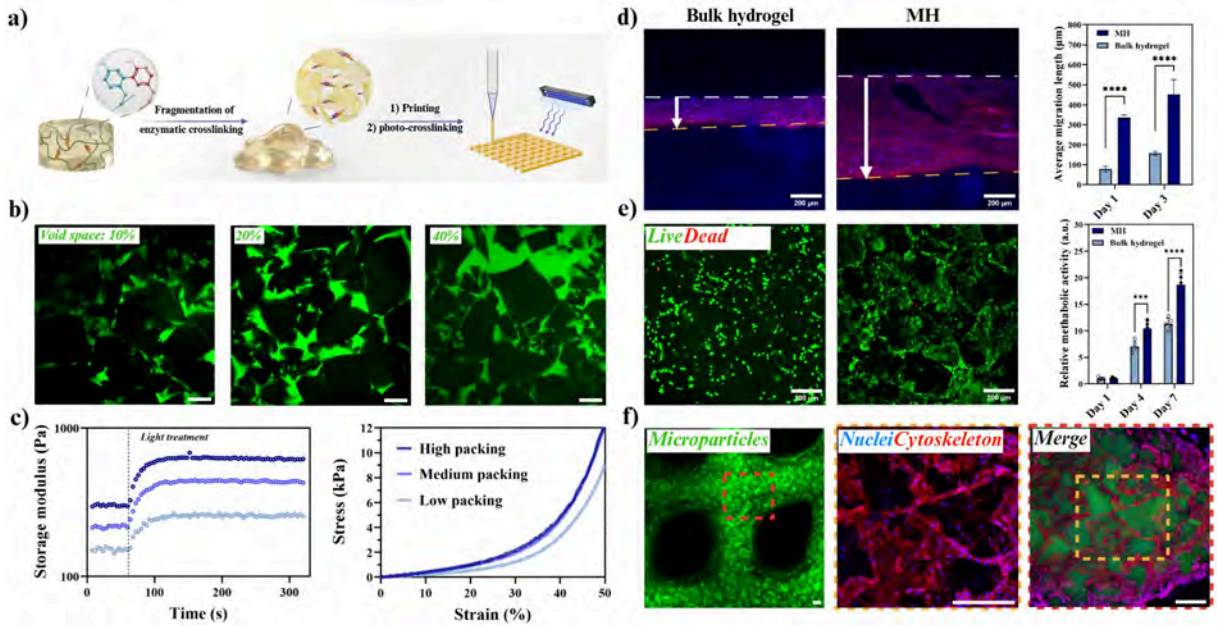

Figure 1. Engineering modular microparticle hydrogel (**a**). Effect of various packing degrees (**b**) on rheology and mechanics (**c**). Effect of microarchitecture on cell migration (**d**), viability, and proliferation (**e**), and bio-printed constructs at day 7, Scale bar=200 µm (**f**).

S47 – O5

Screening and combinatorial optimization of bioactive ions for multi-phase bone regeneration

Bianco N.[1], Truckenmüller R.[1], Tahmasebi Birgani N.[1]
[1]Dept CTR, MERLN Institute, Maastricht University, The Netherlands

Introduction

Bone healing proceeds through overlapping phases of inflammation, vascularization and mineralization, each orchestrated by distinct cell populations. To improve regeneration in large bone defects, regenerative strategies must modulate these coordinated biological events. Bioactive inorganic ions are compelling given their roles in bone metabolism, angiogenesis and immune regulation, combined with superior stability and scalability compared to growth factors. However, current studies typically evaluate ions in isolation against a single cell type, overlooking concentration-dependent and combinatorial effects across the full cellular landscape of bone repair.

Aim

This study identifies optimal ion types, concentrations and combinations across the key stages of bone healing through a systematic screening approach.

Materials and Methods

Human mesenchymal stem cells (hMSCs), human umbilical vein endothelial cells (HUVECs) and monocyte-derived macrophages (MDMs) were exposed to three concentrations (High (H), Medium (M), and Low (L)) of nine bioactive ions (Ca^{2+}, Sr^{2+}, Cu^{2+}, Zn^{2+}, Mn^{2+}, Mg^{2+}, Co^{2+}, phosphate, silicate), to assess effects on osteogenesis, angiogenesis and immunomodulation, respectively. hMSC osteogenic differentiation was assessed via alkaline phosphatase (ALP) activity and immunocytochemical analysis (ICC) of RUNX2, osteocalcin and osterix at days 7, 14 and 28. HUVEC responses at day 1, 3 and 5 were evaluated through ICC of CD144, CD31 and VEGFR2. MDM polarization was assessed at days 1, 3 and 5 via ICC of CD68 and CD206. Top-performing ion–concentration pairs from the screening will be carried into a Design of Experiments (DoE) combinatorial optimization to identify synergistic multi-ion formulations.

Results

ALP activity screening revealed concentration- and time-dependent effects across all nine ions (Fig. 1). At the highest tested concentrations, Co^{2+}, Mn^{2+}, Ca^{2+}, Sr^{2+} and Cu^{2+} consistently suppressed ALP activity, indicating dose-dependent inhibition of osteogenic commitment. Conversely, low-concentration Co^{2+} sustained elevated ALP across all timepoints, while medium-concentration Mn^{2+} and Ca^{2+} exhibited a marked late-stage increase at day 28, suggesting sustained osteogenic activity beyond the typical ALP peak. Preliminary ICC of HUVECs reveals ion-dependent differences in endothelial marker expression (Fig. 2).

Conclusion

This multi-cell-type screening approach provides a rational framework for selecting ion formulations tailored to the distinct phases of bone healing. Once complete, the ICC and polarization data will complement the ALP results and define the conditions for the combinatorial optimization stage. The resulting multi-ion formulations will inform the sequential loading and release strategy of a heterogeneous granular hydrogel developed for bone regeneration.

Acknowledgements

This research was financially supported by the LINK2.0 project funded by Maastricht University and Academic Hospital Maastricht.

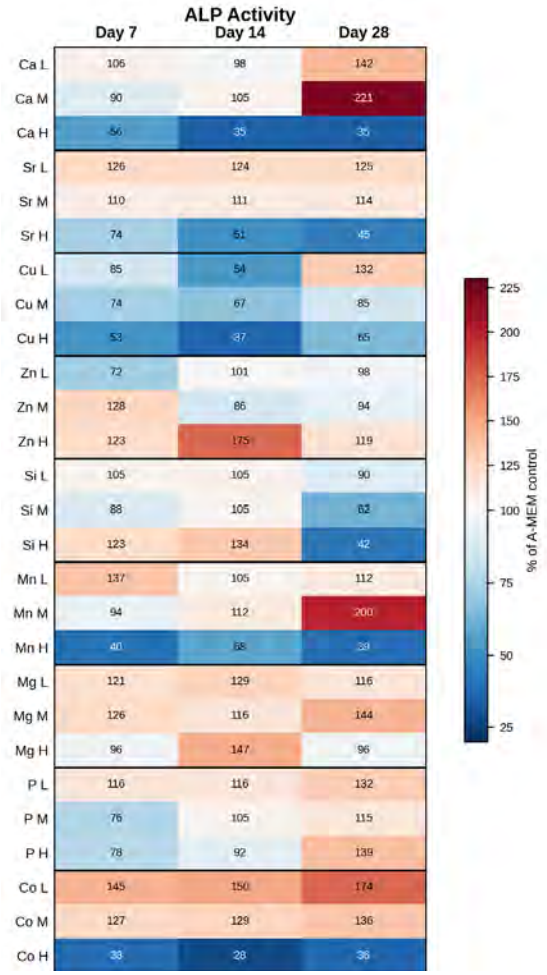

Figure 2: ***ALP activity levels of hMSCs relative to α-MEM osteogenic control. H, M, L denote high, medium and low ion concentrations, respectively. White corresponds to control level (100%).***

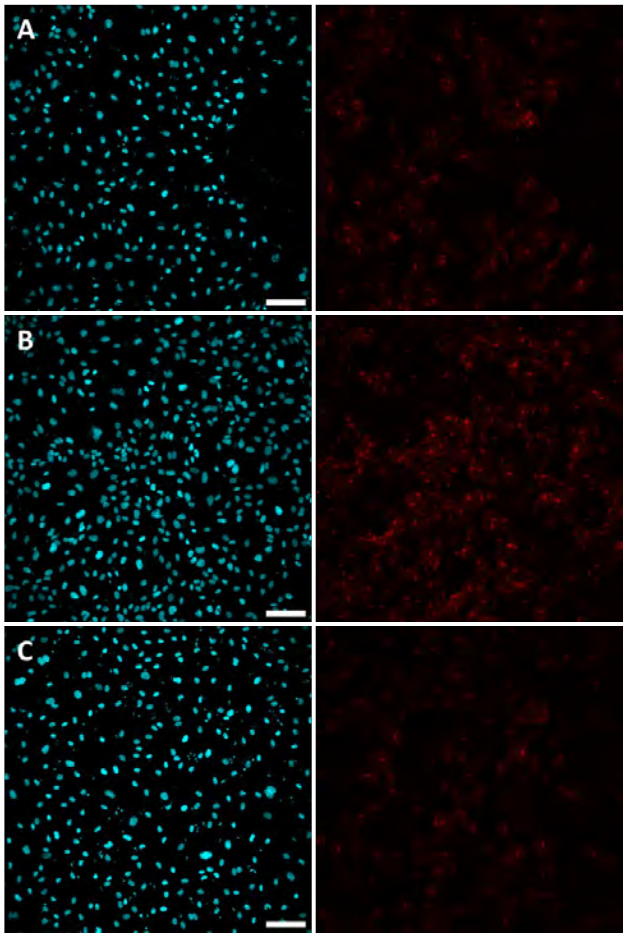

Figure 3: ***Representative ICC images of HUVECs showing DAPI (cyan) and VEGFR2 (red). (A) EGM-2 control, (B) Co^{2+} medium concentration (10 µM), (C) Mg^{2+} high concentration (5 mM). Scale bar = 100 µm.***

S47 – O6

Self-growing biohybrid engineered living matter with multiscale mechanics using mechanically programmable synthetic cells

Willemen N.G.A.[1], van Iterson R.[2], Johnbosco C.[1], Porsul I.[1], Meteling M.[1], Veenstra G-J.[2], Leijten J.[1]
[1]Leijten Laboratory, Dept. of BioEngineering Technologies, Technical Medical Centre, Faculty of Science and Technology, University of Twente, Enschede; [2]Dept. of Molecular Developmental Biology, Radboud Institute for Molecular Life Sciences, Faculty of Science, Radboud University, Nijmegen, The Netherlands

Introduction

Naïve human induced pluripotent stem cells (hiPSCs) cannot be encapsulated in fully elastic biomaterials, as they require rapid stress relaxation for survival [1]. Consequently, hiPSCs demand a limited set of biomaterials, organoid formation prior to encapsulation, or extensive in vitro pre-differentiation, all of which limit impact and applications. We hypothesized that the required stress relaxation can be encoded into engineered tissues by using cells as a biological glue. To this end, we developed mechanically programmable synthetic cells (MPSCs) that naturally self-assemble with hiPSCs into 3D engineered living microtissues (ELMs) via programmable cell-material bonding. We here introduce this approach and demonstrate that it is feasible and accelerates tissue production by steering lineage commitment and tissue deposition of hiPSCs.

Materials and Methods

MPSC synthesis: Hydrogel precursor droplets composed of 10% (w/v) Dextran-Tyramine-Biotin (DexTAB) and horseradish peroxidase in phosphate buffered saline were emulsified in 2% (w/w) Pico Surf 1 containing Novec 7500 using a microfluidic droplet generator, followed by hydrogen peroxide crosslinking [2].
ELM engineering & analysis: ELMs were formed by self-assembling MPSCs with hiPSCs into 3% (w/v) agarose microwell arrays [3]. Microgel amount, stiffness, and seeding time-points were varied. Newly formed ELMs were analysed for formation efficiency, stress relaxation, pluripotency, proliferation, and viability.
Steering hiPSC fate: hiPSCs within ELMs were steered towards a chondrogenic phenotype using a differentiation protocol [4] and different MPSCs stiffnesses (no MPSC, soft, stiff). Differentiation was analysed using histology, immunochemical staining, mechanical analysis, RNA-seq, and spatial transcriptomics.

Results

While conventional encapsulation of hiPSCs in fully elastic hydrogels resulted in cell death within three days, self-assembled ELMs exhibited sustained viability, proliferation, and pluripotency for all tested MPSCs over prolonged culture (Figure 1A). Characterization of self-assembly revealed that the process is governed by hiPSCs in a liquid-like solid manner. Moreover, providing ELMs with MPSCs over time allowed controlled tissue growth while maintaining the desired cell-material ratio. All ELMs exhibited rapid stress relaxation, independent of MPSC stiffness and quantity. This created a microenvironment conducive to hiPSC viability, metabolic activity, proliferation, and pluripotency. Finally, ELMs significantly improved hiPSC chondrogenic differentiation by accelerating lineage commitment and chondrocyte phenotype in a MPSC stiffness-dependent manner, as evidenced by genomics and proteomics data (Figure 1B).

Conclusion

Collectively, our study introduces the self-assembly of cell-like micromaterials with hiPSCs to create ELMs with programmable behaviour. We anticipate that this approach has potential to improve tissue functionality in a scalable manner, representing an essential step towards viable hiPSC-based therapies.

References:

1. D. Indana *et al*, *Nature Mat. 2021*, 33, 2101966.
2. T. Kamperman *et al.*, *Adv. Mat. 2021*, 33.
3. N. Willemen *et al, Adv. Sci. 2023*, 10, 2205487.
4. S. Lamandé *et al, PNAS 2023*, 120 (19).

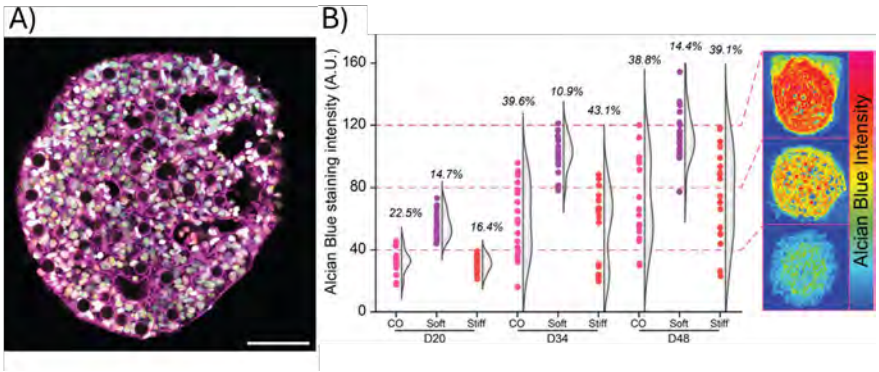

Figure 1: *A) Sox2 and Oct3/4 pluripotency staining of hiPSC within ELM. B) Quantification Alcian Blue staining of ELMs with various MPSC stiffnesses after chondrogenic differentiation.*

S48
Nanomedicine and biomaterials converging platforms for next-generation therapies

S48 – K1
Nanomedicine and biomaterials in Europe: Making convergence work for patients
From nano-enabled health technologies and advanced materials to clinical translation

Ceccaldi A.
European Technology Platform of Nanomedicine (ETPN) - France

"Nanomedicine and biomaterials are increasingly converging. By combining nanoscale design with biomaterials, advanced materials and delivery systems, this convergence is opening new possibilities, notably in oncology, targeted delivery, imaging and regenerative medicine. Yet good science alone is not enough to turn these innovations into meaningful improvements in patients' lives. Characterisation, reproducibility, safety, scalable manufacturing, regulatory strategy, clinical relevance and industrial adoption must be addressed together.
This opening talk will provide a concise overview of how nanomedicine is evolving, how it connects with biomaterials and advanced materials, and why their convergence matters for patients. It will also explain what ETPN does at European level to connect scientific, clinical and industrial communities, support innovators through translation, and contribute to shared research and innovation priorities. The experience developed through ETPN could also benefit the biomaterials community and create natural opportunities for closer links with ESB.
Europe has the scientific excellence needed to lead in these fields, but sustainable leadership cannot be built through isolated national or disciplinary efforts. The preparation of FP10, the proposed Horizon Europe programme for 2028 to 2034, creates an important opportunity to connect nanomedicine, biomaterials and advanced materials more effectively across research, translation and industrial development. What would it take to turn this convergence into better outcomes for patients while enabling the European researchers and innovators behind the best ideas to develop them in Europe?"

S48 – O1

Mesoporous silica nanocarriers for miRNA-mediated osteogenic and myogenic differentiation

Stassen N.[1], Joris V.[2], van Griensven M.[2], van Tienen F.H.J.[3], van Rijt S.H.[1]
[1]Dept. of Instructive Biomaterials Engineering, MERLN Institute for Technology-Inspired Regenerative Medicine, Maastricht University; [2]Dept. of Cell Biology-Inspired Tissue Engineering, MERLN Institute for Technology-Inspired Regenerative Medicine, Maastricht University; [3]Dept. of Translational Genomics, Mental Health and Neurosciences Research Institute (MHeNS), Maastricht University, The Netherlands

Introduction

MicroRNAs (miRNAs) regulate gene expression and direct cellular differentiation relevant to musculoskeletal tissue regeneration. However, their therapeutic use is limited by poor stability, inefficient cellular uptake and rapid degradation. Nanoparticle-based delivery systems may help overcome these limitations. Mesoporous silica nanoparticles (MSNs) are promising carriers due to their high loading capacity, tunable pore, core and surface chemistry and biocompatibility. Here, redox-responsive large-pore MSNs (LPMSNs) incorporating disulfide linkages are developed as degradable carriers for therapeutic oligonucleotides, with the additional possibility for ion doping. Using this platform, we explore miRNA delivery strategies to induce osteogenic differentiation in human mesenchymal stem cells and myogenic differentiation in human mesoangioblasts.

Materials and Methods

Disulfide-bridged LPMSNs were synthesized and amine-functionalized to enable electrostatic oligonucleotide loading. Nanoparticles were characterized for particle size, morphology and surface charge, and were *in situ* doped with osteogenic ions. Fluorescently labeled ssDNA oligonucleotide served as model cargo to evaluate loading efficiency, release behavior under reductive conditions and intracellular delivery. The platform is being further explored for delivery of lineage-specific miRNAs to influence osteogenic and myogenic differentiation, assessed through miRNA expression, downstream gene expression and differentiation-related assays.

Results

The synthesized LPMSNs exhibited uniform particle size and large pore architecture enabling efficient oligonucleotide loading. Incorporation of disulfide linkages provides a strategy for redox-responsive degradation under intracellular conditions. Fluorescence imaging demonstrated effective nanoparticle uptake and intracellular delivery of the model ssDNA oligonucleotide. These findings indicate that LPMSNs can function as effective carriers for intracellular delivery of osteogenic and myogenic miRNAs.

Conclusion

Disulfide-bridged LPMSNs represent a promising degradable nanocarrier platform for intracellular oligonucleotide delivery. This system provides a foundation for future studies aimed at delivering therapeutic miRNAs to direct stem cell differentiation for musculoskeletal regenerative medicine and to explore potential synergistic effects of osteogenic ion-doped silica nanocarriers.

Acknowledgements

This study was funded by the European Research Council (ERC CoG Nano4Bone, van Rijt).

S48 – O2

Magnetically driven cyclodextrin nanoplatforms for site-specific osteosarcoma treatment

Coria Gutiérrez A.L.[1], Sukur S.[2], Mountford J.[3], Saqawa M.[1,4], Ozel-Okcu S.[5], Ranc V.[2], Heymann D.[3], Montesi M.[4], Terán F. J.[5], Scala A.[1], Puskás I.[6], Piperno A.[1]

[1]Dept. Chemical, Biological, Pharmaceutical, and Environmental Sciences, Messina University, Messina, Italy; [2] Institute of Molecular and Translational Medicine (IMTM), Faculty of Medicine and Dentistry, Palacký University Olomouc, Czech Republic; [3]Institut de Cancérologie de l'Ouest, "Tumor Heterogeneity and Precision Medicine" Laboratory, Saint-Herblain, France; [4]Cell/Material Interaction lab, Institute of Science and Technology for Ceramics (CNR-ISSMC), Faenza, Italy; [5]NanoTech Solutions, Research and Development, Villacastín, Spain; [5]CycloLab Cyclodextrin Research and Development Laboratory Ltd., Budapest, Hungary

Introduction

Osteosarcoma (OS) is the most common primary malignant bone tumor in children and adolescents, characterized by aggressive behavior, high relapse rates, and the development of chemoresistance. Conventional chemotherapy is often limited by systemic toxicity and poor drug penetration within the tumor microenvironment. Iron oxide magnetic nanoparticles (MNPs) have attracted significant interest as promising platforms for OS therapy due to their unique physicochemical properties. Their superparamagnetic behavior, high biocompatibility, and responsiveness to external magnetic fields provide opportunities to address several key challenges in current treatment strategies. However, their clinical translation is hindered by a tendency to aggregate and oxidize.

Aim

This work aims to develop and evaluate MagnetoCyclodextrins (MNP-CDs), a novel class of magnetic materials obtained by combining MNPs with cyclodextrins (CDs). This hybrid system integrates the advantages of both components: CDs provide encapsulation capability and enhanced water solubility, while MNPs impart magnetic properties that can be utilized as tracers in magnetic particle imaging or as heating agents in magnetic hyperthermia. Furthermore, the unique bucket-shaped structure of CDs enables them to host drugs within their cavity, protecting them from hydrolysis, oxidation, and radiative or thermal degradation.

Materials and Methods

Commercial and home-made oleic acid-coated iron oxide MNPs were functionalized with the γ-cyclodextrin derivative Sugammadex (SGX, BRIDION®) to obtain MagnetoSugammadex (MNP@SGX; MS) assemblies. The chemotherapeutic drug Doxorubicin (DOX) was encapsulated at different molar ratios to form NanoTher (NT) platforms. MS assemblies were comprehensively characterized by thermogravimetric analysis (TGA), FT-IR, ζ-potential, SEM, DLS, Raman spectroscopy, and AC magnetometry. The NT were fully characterized in terms of hydrodynamic sizes, zeta potential, drug loading, encapsulation efficiency, and drug release profile.

Results

MS assemblies demonstrated enhanced dispersion stability, reduced toxicity, and successful drug loading. The NT exhibited comparable or slightly higher IC_{50} values than free DOX when tested in OS cell lines (U-2 OS, MG63, 143B, MOS-J, and KHOS). The formulations maintained stability and responsiveness to magnetic fields, suggesting their suitability for targeted applications.

Conclusion

The MagnetoSugammadex nanoplatform represents a versatile system for magnetically guided drug delivery in osteosarcoma. The evaluation of NanoTher in 3D models, such as spheroid and scaffold systems, is currently ongoing, and the results will be used to design the *in vivo* test using the osteosarcoma mouse model.

Acknowledgements

This work received funding from the European Union's HORIZON-MSCA-2021-DN-01. STRIKE-101072462.

S48 – O3

Nanozyme-functionalized 3D-bioprinted hydrogel for temporally programmed neurovascularized bone regeneration

Zeng Q.J.[1,2], Chen S.S.[1,2], Zhou Z.L.[1], Li Z.A.[1,2,3,]

[1]Dept. of Biomedical Engineering, The Chinese University of Hong Kong; [2]InnoHK Center for Neuromusculoskeletal Restorative Medicine, Hong Kong Science Park; [3]Peter Hung Pain Research Institute, The Chinese University of Hong Kong, China

Introduction

Functional bone regeneration requires coordinated neuro-vascularization for integration, yet current scaffolds lack dynamic, stage-specific regulation. We designed a core-shell nanozyme (NZ) with multi-enzyme-like activity and integrated it into a 3D-bioprinted hydrogel scaffold (Gel-NZ) to achieve temporally modulated healing.

Aim. This study aims to achieve temporally modulated neurovascularized bone regeneration through the rational design of a core-shell nanozyme within a 3D-bioprinted scaffold.

Materials and Methods

A core-shell NZ was synthesized by sequentially coating hydroxyapatite with poly(lactic-co-glycolic acid), polydopamine, and manganese-cobalt oxide. The NZ, together with bone marrow stromal cells (BMSCs), were incorporated into a photocrosslinkable bioink for 3D bioprinting. Gene expression levels were evaluated over time. The scaffold was implanted into rabbit cranial defects, with bone formation, vascularization, and innervation analyzed at 6 and 12 weeks via micro-CT, histology, and immunohistochemistry.

Results

The synthesized NZ exhibited sustained ROS-scavenging activity and ion release (**Fig. 1a-d**). *In vitro*, BMSC osteogenesis followed a distinct temporal sequence: an early-stage (day 7) characterized by the upregulation of HIF-1α and neurotrophic factors (BDNF, NGF); a mid-stage (day 14) marked by peak expression of osteogenic markers (OCN) and the angiogenic stabilizer ANGPT1; and a late-stage (day 21) featuring a coupled peak of VEGF and neurotrophic factors, facilitating advanced neuro-vascular integration (**Fig. 1e**). *In vivo*, micro-CT images confirmed that this scaffold effectively promoted bone regeneration (**Fig. 1f**).

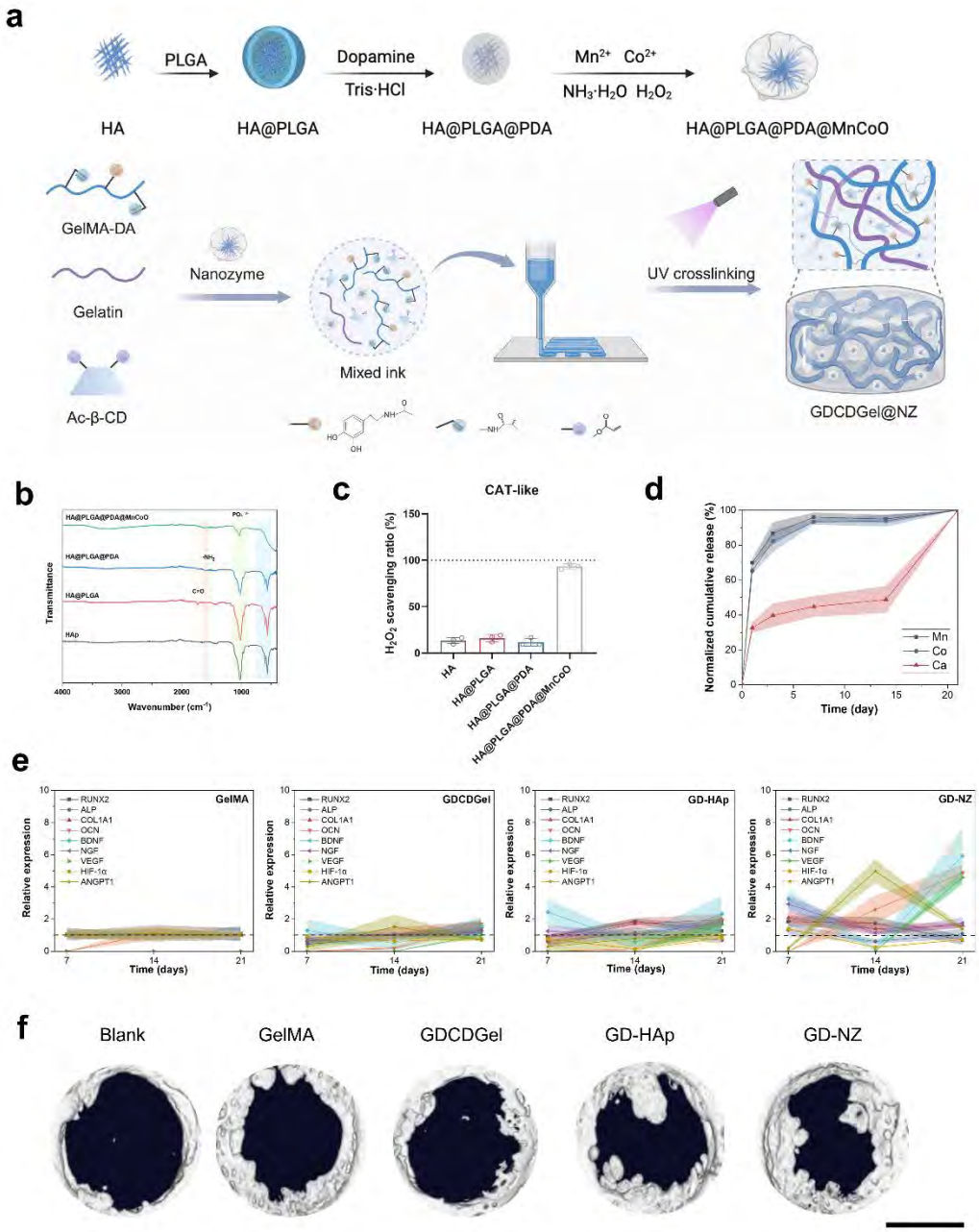

Fig. 1. Evaluation of a 3D-bioprinted nanozyme-hydrogel. (a) Synthesis and 3D bioprinting of the scaffold. (b) FTIR spectra of nanozymes. (c) CAT-like activity. (d) Cumulative ion release from Gel-NZ. (e) Temporal gene expression in BMSCs (days 7, 14, 21). (f) Micro-CT images of bone defects at 6 weeks. Scale bar: 4 mm.

Conclusions

This nanozyme-functionalized 3D-bioprinted hydrogel successfully orchestrates a coordinated sequence of cellular events, mimicking natural bone healing. It demonstrates significant potential for the reconstruction of complex, functional bone by actively promoting temporally regulated neuro-vascularized regeneration.

Acknowledgements

InnoHK Center for Neuromusculoskeletal Restorative Medicine, CUHK Shun Hing institute of Advanced Engineering (Project #BME-p224).

S48 – O4

Biomimetic hybrid liposomes derived from brain metastatic cells: A novel platform for targeted cns delivery

Patrucco M.[1], Ieva F.[1], Negre E.[3], Mangolini A.[2], Sesana S.[1], Raimondo F.[1], Bedoni M.[2], Mir M.[3], Nicolini G.[1], Re F.[1]

[1]Dept. Medicine and Surgery, University of Milano-Bicocca, Monza, Italy; [2]IRCCS Fondazione Don Carlo Gnocchi Onlus, Milano, Italy; [3]Institute for Bioengineering of Catalonia, Barcelona, Spain

Introduction

The blood-brain barrier (BBB) is a highly selective multicellular interface that restricts the delivery of therapeutics to the central nervous system. This represents a major challenge for the treatment of CNS diseases, including melanoma brain metastases, as the BBB prevents many therapeutic agents from reaching effective concentrations in the brain. While liposomes are versatile delivery platforms, efficient BBB penetration remains a significant obstacle. To address this, we developed a biomimetic strategy inspired by brain metastatic cells (BMCs), which naturally traverse the BBB by leveraging specific membrane proteins and lipids.

Aim

By incorporating melanoma BMC membrane fragments into synthetic bilayers, we harness their innate interaction with brain endothelial cells (ECs) and BBB translocation mechanisms to engineer metastatic-derived hybrid liposomes (MDHLs). We present a reproducible step-by-step characterization of the synthetic-biological integration and demonstrate that MDHLs superiorly penetrate the BBB compared to conventional liposomes using two distinct, highly reproducible human *in vitro* models: transwell and multicellular BBB-on-a-chip.

Materials and Methods

A reproducible cell membrane (CM) centrifuge-based extraction was validated with immunoblot, followed by MDHL assembly through mechanically tuned procedures. Förster resonance energy transfer assay and Raman spectroscopy confirmed the CM-synthetic lipid hybridization, while dynamic light scattering monitored physical characterization and stability. After confirming biocompatibility, fluorescently-labelled MDHLs were used to measure endothelial permeability (EP) after BBB crossing in both *in vitro* models. Finally, Trametinib-loaded MDHLs were prepared and characterized for encapsulation efficiency, targeting, and therapeutic efficacy against melanoma cells post-BBB crossing.

Results

Immunoblot confirmed CM extraction with an 80% enrichment of membrane-related proteins. MDHLs remained stable for 20 days, maintaining a size of ~130 nm, PDI <0.2, and a negative surface charge. An 8.8% reduction in FRET efficiency demonstrated efficient CM integration (Figure 1), while Raman spectroscopy confirmed the preservation of the native protein fingerprint. Notably, MDHLs exhibited significantly higher EP compared to conventional liposomes in the presented *in vitro* models (Figure 2). Trametinib-loaded MDHLs (encapsulation efficiency: 34.3%) demonstrated high targeting precision and significantly decreased the metabolic activity of metastatic melanoma cells after crossing the BBB, confirming the platform's therapeutic potential.

Conclusion

Using advanced *in vitro* models, we characterized a biomimetic nanosystem capable of efficient BBB crossing, paving the way for tailored, well-characterized platforms for precision brain drug delivery.

Figure 1 Characterization of metastatic-derived hybrid liposomes (MDHL) via FRET assay to evaluate cell membrane integration and cell membrane to lipid ratio

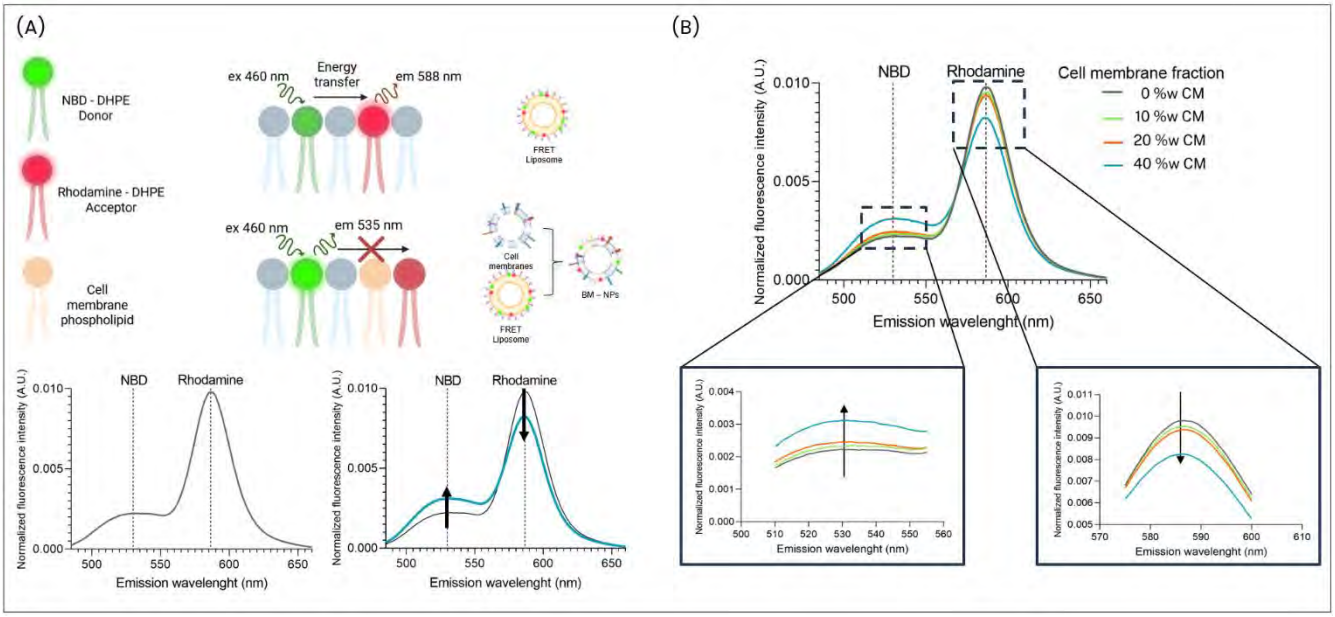

Figure 2 Schematic representation of the experimental setup used to evaluate the permeability of metastatic-derived hybrid liposomes (MDHL) across an in-vitro blood–brain barrier model

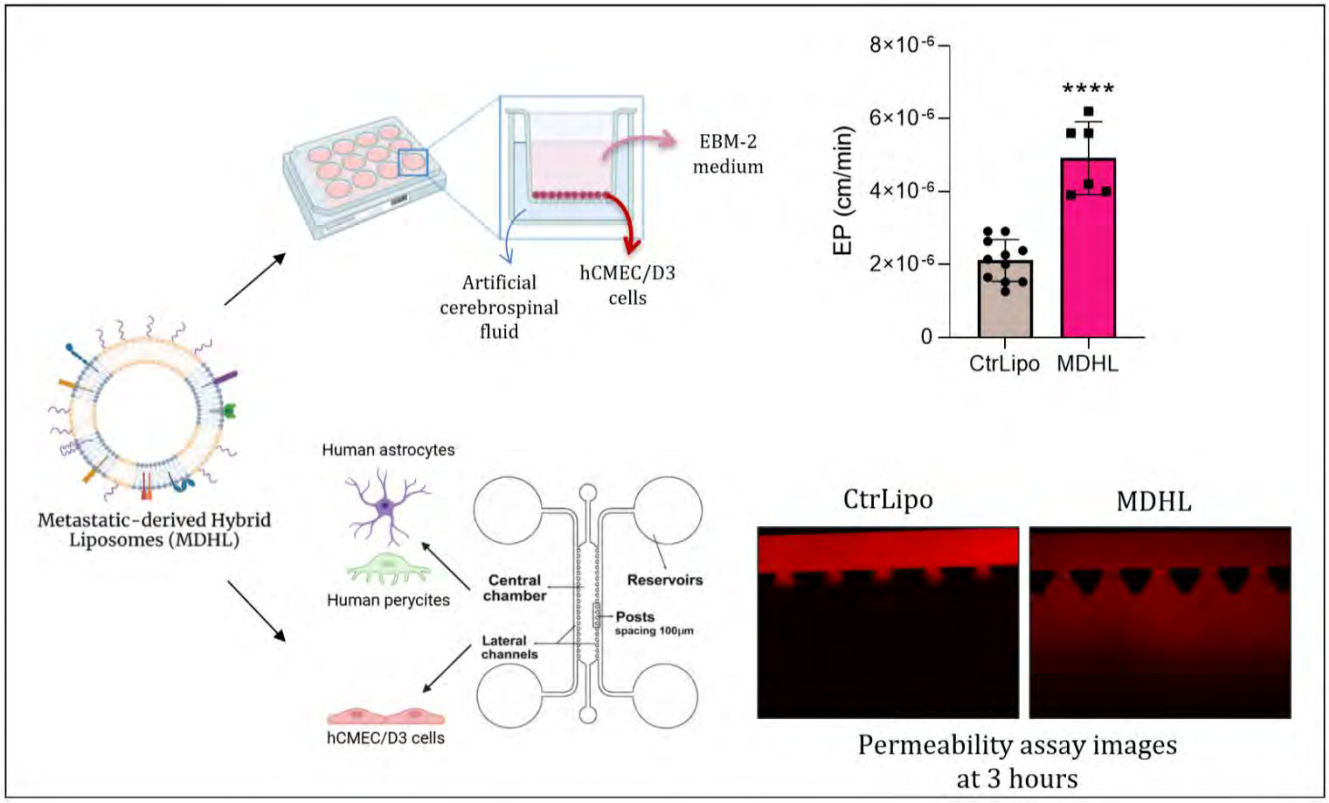

S48 – O5

Engineering ultrasound-responsive therapeutic antibubbles for glioblastoma therapy

Zengin A.[1], Sevciuc A.[1], Poortinga A.[2], Zuhorn I.[1], van Rijn P.[1]
[1]Dept.of Biomaterials and Biomedical Technology, University Medical Center Groningen; [2]Dept. of Mechanical Engineering and Polymer Technology, University of Eindhoven, The Netherlands

Introduction

Glioblastoma is one of the most aggressive brain tumors, with limited treatment options largely due to poor drug penetration across the blood–brain barrier and the absence of effective local delivery strategies.[1] Addressing these challenges requires innovative approaches; ultrasound-responsive carriers have emerged as promising platforms for targeted, on-demand drug release.[2] While gas-filled microbubbles have been extensively studied, their low drug-loading capacity and short-lived stability restrict their clinical utility. Antibubbles—micron-sized bubbles encapsulating liquid droplets—offer superior encapsulation efficiency and enhanced structural robustness, making them strong candidates for controlled, localized drug delivery.[3] In this work, we present the development of biodegradable, nanoparticle-stabilized antibubbles for ultrasound-triggered delivery of the chemotherapeutic agent Temozolomide (TMZ) to treat glioblastoma (Fig. 1A).

Materials and Methods

Biodegradable nanoparticles, with and without fluorescent dye, were fabricated using the nanoprecipitation method. The hydrodynamic diameter and zeta potential of the nanoparticles were measured by dynamic light scattering, while their morphology was characterized using transmission and scanning electron microscopy (TEM and SEM). Antibubbles were generated using the Pickering double-emulsion method. The concentration and size distribution of the antibubbles were determined using a Coulter counter. Cargo-loaded antibubbles (dye or drug) were visualized using confocal microscopy, fluorescence microscopy, and SEM. Ultrasound imaging capabilities were evaluated using a clinical ultrasound system equipped with a 5.5 MHz transducer. Drug release experiments were performed by ultrasound-mediated destruction of antibubbles (mechanical index, MI = 1.3), and the released drug was quantified using high-performance liquid chromatography.

Results

The polymeric nanoparticles (~150 nm diameter, zeta potential −18 mV) enabled the formation of highly stable antibubbles, with more than 99% of the population exhibiting diameters below 10 µm. Confocal imaging confirmed efficient encapsulation of the model dye Rhodamine B within the internal core of the antibubbles (Fig. 1B). Under clinically relevant ultrasound conditions, the antibubbles generated strong acoustic contrast and could be selectively disrupted at mechanical indices (MI) ≥ 0.6 (Fig. 1C). Furthermore, ultrasound exposure at a higher acoustic pressure (MI = 1.3) triggered TMZ release by destroying the antibubble structure. Quantification by HPLC revealed a TMZ loading efficiency of 79%, demonstrating the potential of these antibubbles as ultrasound-responsive carriers for controlled drug delivery.

Conclusion

Overall, polymeric nanoparticle-stabilized antibubbles exhibited high structural stability, strong acoustic responsiveness, and efficient ultrasound-triggered drug release. These findings highlight their potential as next-generation ultrasound-responsive theranostic platforms for glioblastoma treatment.

References

1. Singh, S., Dey, D., Barik, D., Mohapatra, I., Kim, S., Sharma, M., Prasad, S., Wang, P., Singh, A., and Singh, G. Glioblastoma at the crossroads: current understanding and future therapeutic horizons. *Signal transduction and targeted therapy 2025, 10*(1), p.213.
2. Siebenmorgen, C., Poortinga, A. and van Rijn, P. Sono-processes: Emerging systems and their applicability within the (bio-) medical field. Ultrasonics sonochemistry, *2023*, *100*, p.106630.
3. Moreno-Gomez N, Athanassiadis AG, Poortinga AT, Fischer P. Antibubbles enable tunable payload release with low-intensity ultrasound. Advanced Materials, *2023,* 35(48), p.2305296.

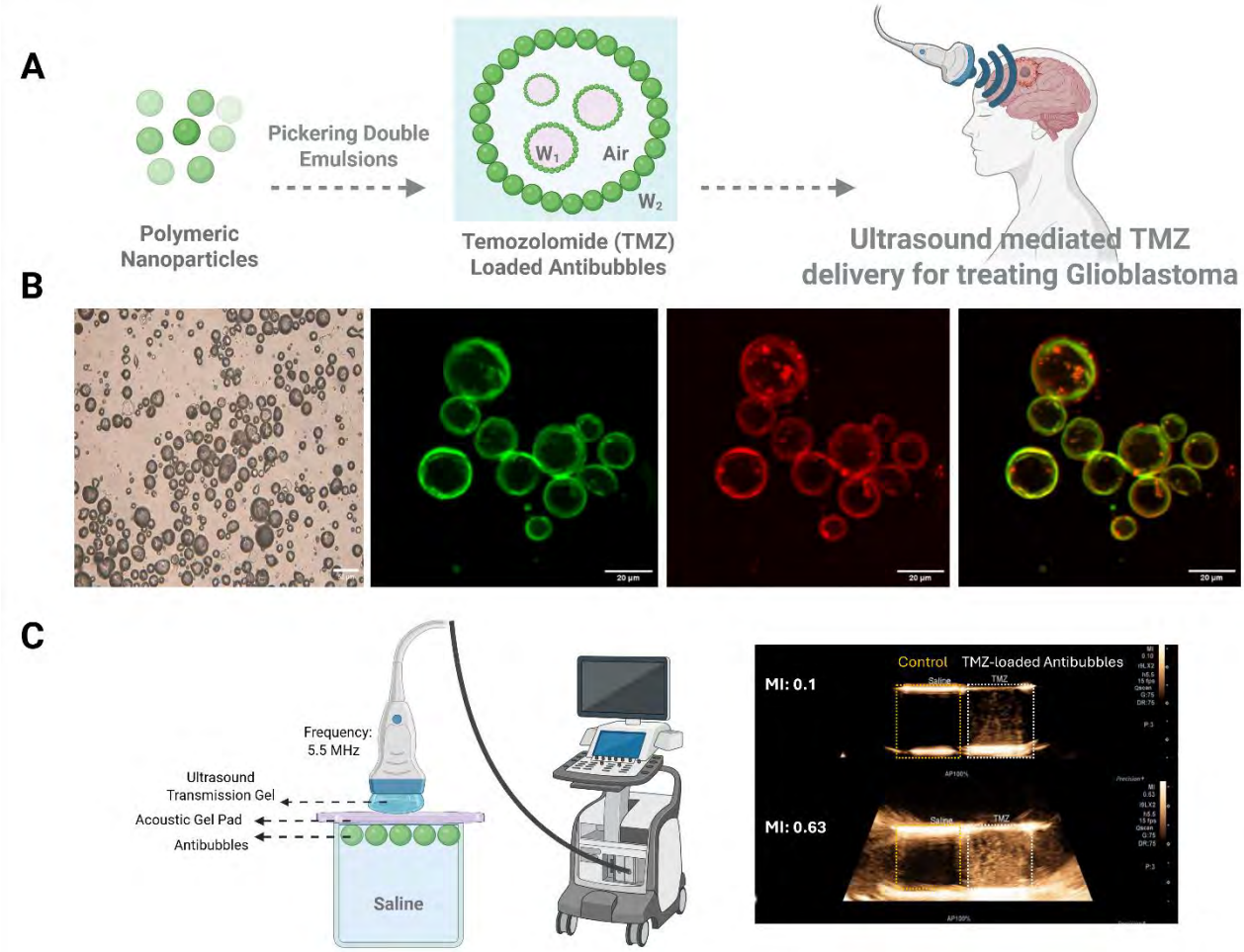
A
Pickering Double Emulsions
Polymeric Nanoparticles
W1
Air
W2
Temozolomide (TMZ) Loaded Antibubbles
Ultrasound mediated TMZ delivery for treating Glioblastoma
B
20 µm
C
Frequency: 5.5 MHz
Ultrasound Transmission Gel
Acoustic Gel Pad
Antibubbles
Saline
Control
TMZ-loaded Antibubbles
MI: 0.1
MI: 0.63

Fig. 1

S48 – O6

Engineering metal nanoclusters for targeting amyloid-β pathology in Alzheimer's disease

Jayasree R.S.[1], Resmi A.N.[2]
[1]Sree Chitra Thirunal Institute for Medical Sciences and Technology, Trivandrum, India

Introduction

Developing safe and effective therapeutic agents for Alzheimer's disease (AD) that can cross the blood–brain barrier (BBB) without compromising its integrity remains a formidable challenge in biomedical research. AD is primarily characterized by the extracellular aggregation of amyloid-beta (Aβ) plaques, which is the hallmark pathological feature of the disease. A promising therapeutic strategy is to disrupt the aggregation of these plaques.

Methods

In this context, we present a proof of concept using specifically designed metal nanoclusters as potential therapeutic agents capable of disintegrating/inhibiting Aβ plaques. Integration of brain targeting moieties like L-Dopa as a BBB crossing ligand to the metal clusters enables the clusters to cross the BBB efficiently without impairing its structural integrity. This study comprises a comprehensive behavioural assessment and detailed neuropathological evaluation of the intervention of atomically precise engineered gold nanoclusters in the streptozotocin (STZ)-induced mice model of AD.

Results

The results highlight the therapeutic benefits of these clusters, supported by additional *in vitro* investigations. Collectively, these findings underscore the potential of metal nanoclusters as a multifunctional nanoplatform for AD therapy and provide a preliminary and strong directive for their future clinical translation.

References

1. Resmi, A. N.; Sivaselvam, S.; Rekha, C. R.; Papasouli, E.; Jibin, K.; Praveen, C. S.; Koukaras, E. N.; Rerat, M.; Karamanis, P.; Jayasree
2. R. S. Nanoarchitectonics of Fluorescent Gold Nanoclusters: A Platform for Image-Guided Photodynamic Therapy of Hypoxic Tumor. Appl. Mater. Today 2024, 39, 102273.
3. Resmi, A. N.; Rekha, C. R.; Dhushyandhun, M. E.; Elangovan, S.; Shenoy, S. J.; Gulia, K. K.; Jayasree, R. S. Bifunctional Cysteine Gold Nanoclusters for β-Amyloid Fibril Inhibition and Fluorescence Imaging: A Distinctive Approach to Manage Alzheimer's Disease. J. Mater. Chem. B 2023, 11 (16), 4715–4724.
4. Santhakumar, H.; Nair, R. V.; Govindachar, D. M.; Periyasamy, G.; Jayasree, R. S. Engineering of Tripeptide-Stabilized Gold Nanoclusters with Inherent Photosensitizing Property for Bioimaging and Photodynamic Therapy. ACS Sustainable Chem. Eng. 2023, 11 (6), 2102–2114.
5. E Sarathkumar, K Jibin, S Sivaselvam, A Selva Sharma, V Alexandar, AN Resmi, P Velswamy, RS Jayasree, Enhancing chemical signal transformation in lateral flow assays using aptamer-architectured plasmonic nanozymes and para-phenylenediamine, Nanoscale, 2025, 17(5), 2469-2479

S48 – O7

Erythromycin conjugated to polyanhydride matrix for controlled topical delivery

Kwiecień K.[1], Kusibab A.[1] Marecik S.[1], Mielczarek P.[2], Ochońska D.[3], Niewolik D.[4], Jaszcz K.[4], Brzychczy-Włoch M.[3], Pamuła E.[1]

[1]Dept. of Biomaterials and Composites, Faculty of Materials Science and Ceramics, AGH University of Krakow, Poland; [2]Dept. of Analytical Chemistry and Biochemistry, Faculty of Materials Science and Ceramics, AGH University of Krakow, Poland; [3]Dept. of Molecular Medical Microbiology, Faculty of Medicine, Chair of Microbiology, Jagiellonian University, Dept. of Physical Chemistry and Technology of Polymers, Faculty of Chemistry, Silesian University of Technology

Introduction

Acne vulgaris is a prevalent chronic inflammatory disorder characterized by follicular hyperkeratinization, excessive sebum production, and bacterial colonization, with *Cutibacterium acnes* playing a central role. The increasing resistance to macrolide antibiotics, including erythromycin (ERC), combined with its poor solubility and instability, limits therapeutic efficacy and necessitates improved delivery strategies. Nanoparticle-based systems can enhance drug stability, skin deposition, and controlled release; however, most rely on lipid carriers or bulk-eroding polymers, restricting precise control over release kinetics. Polyanhydrides, which undergo surface erosion and predictable degradation, offer an attractive alternative and enable covalent drug incorporation into the polymer backbone for tunable release. Additionally, hydrogels such as gellan gum may improve topical retention and sustain drug delivery. Therefore, this study aimed to develop ERC–poly(sebacic anhydride) (PSA) conjugate nanoparticles, incorporate them into gellan gum hydrogels, and evaluate their physicochemical properties, antibacterial activity, and cytocompatibility.

Materials and Methods

PSA was synthesized via melt polycondensation and characterized using DSC, NMR, and GPC. ERC-loaded and unloaded nanoparticles were prepared by an oil-in-water emulsification–solvent evaporation method using poly(vinyl alcohol) as a stabilizer. Particle size and zeta potential were measured by laser diffraction and electrophoretic mobility, respectively. Encapsulation efficiency and drug loading were quantified by mass spectrometry, while PSA–high-resolution MS and fragmentation analysis confirmed the formation of ERC conjugates. Nanoparticles were incorporated into ionically crosslinked gellan gum hydrogels. The systems were characterized by SEM, in vitro drug release, antibacterial activity against C. acnes and Staphylococcus aureus, and cytocompatibility using L929 fibroblasts.

Results

The polymer synthesis and nanoparticle fabrication were successful. The nanoparticles were spherical, smooth, and exhibited a size range from 500 nm to several micrometers, with a negative surface charge and high encapsulation efficiency (>80%). Mass spectrometry confirmed the formation of PSA–ERC conjugates, with no detectable free ERC. Nanoparticles were homogeneously distributed within the hydrogel matrix. The formulation enabled sustained release of chemically intact ERC over 48 h in aqueous conditions. Both nanoparticles and nanoparticle-loaded hydrogels demonstrated strong antibacterial activity against C. acnes and moderate activity against S. aureus, while showing no cytotoxicity toward L929 fibroblasts.

Conclusion

This study presents a proof-of-concept polyanhydride-based nanoparticle system forming drug–polymer conjugates that preserve ERC integrity upon release. The combination of controlled degradation, sustained release, homogeneous hydrogel incorporation, and antibacterial efficacy with good cytocompatibility highlights its potential for prolonged topical delivery of erythromycin in acne treatment.

Acknowledgements

This study was supported by the Polish National Science Centre Project no. 2024/53/N/ST5/03127

S49
New horizons in antimicrobial surfaces

S49 – K1
Antimicrobial surface engineering: Recent advances in bioactive coatings, nanomaterials and peptide-based biomaterials

Stamboulis A.
University of Birmingham – UK

S49 – K2

From current to cure: New horizons in antimicrobial strategies for dental implants. The NOMAD approach to preventing peri-implant infections

Braem A.
KU Leuven, Department of Material Engineering - Belgium

S49 – O1

Immobilisation of antimicrobial peptides on titanium alloy surfaces enhances antimicrobial activity

Adak A.,[1] Stamboulis A.[1]
[1]School of Metallurgy and Materials, University of Birmingham, UK

Introduction

Implant-associated infections remain a major challenge in orthopaedic and biomedical implants due to increasing bacterial resistance to conventional antibiotics. Antimicrobial peptides (AMPs) have emerged as promising alternatives owing to their broad-spectrum antibacterial activity and low propensity for resistance development. In this study, we investigate the antimicrobial performance of titanium surfaces functionalised with newly designed antimicrobial peptides and their modified analogues.

Materials and Methods

A library of antimicrobial peptides was designed using molecular docking simulations with bacterial membrane models to optimise peptide-membrane interactions and antibacterial activity (Fig. 1a,1b). Based on binding energy analysis, the best candidates were synthesised using solid-phase peptide synthesis, followed by purification by reverse-phase HPLC and characterisation by mass spectrometry and analytical HPLC. Antimicrobial activity was evaluated using minimum inhibitory concentration (MIC) and minimum bactericidal concentration (MBC) assays against both Gram-positive and Gram-negative bacterial strains. Titanium surfaces were first silanised and subsequently functionalised with the peptides. The antibacterial activity of the peptide-coated surfaces was assessed against *Escherichia coli* and *Staphylococcus aureus*. Cytocompatibility was evaluated using a cell viability assay with NIH-3T3 fibroblast cells.

Results

The lead peptide demonstrated significant antimicrobial activity in MIC and MBC assays, showing effective bactericidal activity against the tested strains. Peptide-functionalised titanium surfaces exhibited strong antibacterial performance, with inhibition ratios exceeding 94% against *E. coli* and 96% against *S. aureus* (Fig. 1c,1d). These results indicate that immobilised antimicrobial peptides effectively inhibit bacterial adhesion and colonisation on titanium surfaces. The enhanced antibacterial activity is likely associated with sustained peptide availability at the implant surface. Furthermore, cell viability assays confirmed that the peptide-coated surfaces were non-cytotoxic toward fibroblast cells, indicating good biocompatibility.

Conclusion

The immobilisation of designed antimicrobial peptides on titanium surfaces significantly enhances antibacterial activity while maintaining cytocompatibility. These findings highlight the potential of peptide-functionalised titanium coatings as a promising strategy for preventing implant-associated infections in orthopaedic applications.

Acknowledgements

This work is supported by funding from the UKRI – Horizon Europe Grant.

Results Figure 1 (a, b) Molecular docking study between antimicrobial peptide and bacterial membrane, (c) Assessment of the antimicrobial activity on the *E. coli* upon the Polished titanium surface (P-Ti), Silanized titanium surface (Si-Ti), KR12 peptide-coated Titanium surface (Ti-KR12), peptide-coated Titanium surface (Ti-KR13). (d) Assessment of the antimicrobial activity on the *S. aureus* upon the Polished titanium surface (P-Ti), Silanized titanium surface (Si-Ti), KR12 peptide-coated Titanium surface (Ti-KR12), peptide-coated Titanium surface (Ti-KR13). Graph showing % of growth inhibition ratio. The P-Ti sample was considered as a control, showing a 0.00% inhibition ratio.

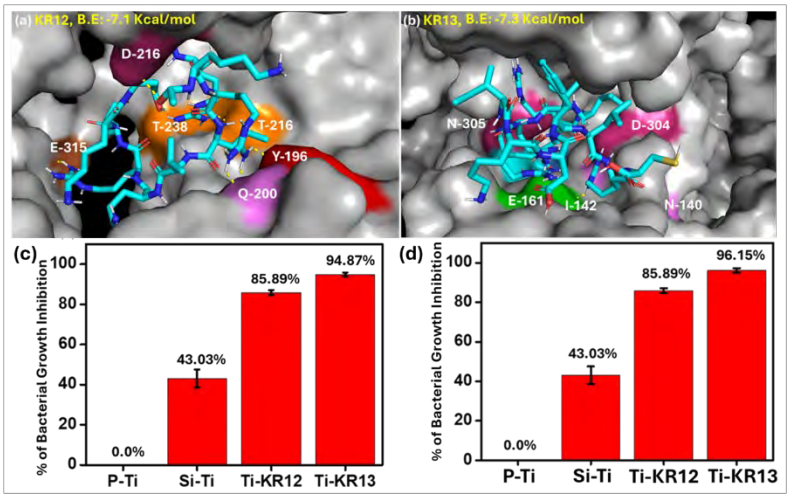

S49 – O2

Bioinspired calcium phosphate nanoneedle arrays as antibacterial surfaces for infection-resistant bone grafts

Fusacchia C.[1,2], Torres Mansilla A.[1], Degli Esposti L.[3], Kovtun A.[4], Manicone E.[5,6], Altamura D.[5], Giannini C.[5], Mariotti M.[7], Squitieri D.[7], Bugli F.[7,8], Iafisco M.[9]
[1]Istituto di Scienze, Tecnologia e Sostenibilità per lo Sviluppo dei Materiali Ceramici (ISSMC), Consiglio Nazionale delle Ricerche (CNR), Faenza; [2]Dept. di Scienze Matematiche, Fisiche e Informatiche, Università di Parma; [3]Dept. di Chimica e Chimica Industriale, Università di Genova, Italy; 4Istituto per la sintesi organica e la fotoreattività (ISOF), CNR, Bologna; [5]Istituto di Cristallografia (IC), CNR, Bari, Italy; 6Dept. di Chimica, Università di Bari; [7]Dept. di Scienze Biotecnologiche di Base, Cliniche Intensivologiche e Perioperatorie, Università Cattolica del Sacro Cuore, Roma; [8]Dept. di Scienze di Laboratorio e Infettivologiche, Fondazione Policlinico A. Gemelli, Roma; [9]Istituto per lo Studio dei Materiali Nanostrutturati (ISMN), CNR, Bologna, Italy

Introduction

Antibiotic resistance is a major threat to public health, especially in bone infections. Antibacterial nanostructured surfaces (ANSs) offer a promising alternative to conventional antibiotics. These surfaces, featuring ordered arrays of nanostructures, can eradicate bacteria upon contact. However, currently developed ANSs are typically made of bioinert materials, which lack the bioactivity necessary to promote tissue regeneration, particularly in the context of bone infections. This study builds on our previous work [1], further investigating the fabrication and characterization of bioinspired ANSs composed of calcium phosphate (CaP) nanocrystals by modulating their morphology and chemistry through the use of organic molecules in the growth solution and by ion doping.

Materials and Methods

ANSs based on CaP nano-needle arrays were prepared using a bottom-up approach inspired by biomineralization processes [1]. The nano-topography was modulated by adding citrate or hydroxycitrate at different concentrations to the growth solution. The nanocrystals were also doped with Zn ions via ionic exchange. Samples were characterized using XPS, XRD, GIWAXS, FTIR and SEM. The antimicrobial activity was evaluated against clinically relevant antibiotic-resistant strains of P. aeruginosa and S. aureus. Bacterial adhesion, viability, and morphology were investigated to correlate the antibacterial properties with the nanostructure. The induction of oxidative stress in bacterial cells was analysed, along with RNA isolation and gene expression analysis. In vitro cytocompatibility of the ANS was assessed with mammalian cells by analyzing cell viability, adhesion, and morphology.

Results

The morphology of CaP nanoneedle arrays was modulated by citrate and hydroxycitrate added during growth, with hydroxycitrate showing a stronger inhibiting effect, producing concentration-dependent changes in needle thickness, length, orientation, and crystallinity. Zinc incorporation did not alter the morphology or structure of the preformed ANSs, while XPS analyses confirmed surface Zn incorporation. Microbiological tests revealed species-dependent interactions with Zn-doped ANSs: S. aureus preferentially adhered to the surfaces, whereas P. aeruginosa remained mainly planktonic. Zn^{2+} incorporation enhanced antibacterial activity particularly against S. aureus. Both doped and undoped ANSs increased ROS production and triggered species-specific stress responses genes. Zn-doped ANSs preserved VERO cell viability and morphology, confirming cytocompatibility.

Conclusion

The ANSs introduced in this work have the potential to serve as a foundation for developing bone graft materials capable of eradicating site infections while simultaneously promoting bone regeneration.

Acknowledgements

This project was funded by the EU-NextGenerationEU, Mission 4 Component 1 CUP: B53D2300875006, Project "CHANCE" PRIN 2022 Research Grant 2022CCN7WM. Support was granted with “Potentiating the Italian Capacity for Structural Biology Services in Instruct-ERIC”, acronym “ITACA.SB” (Project No.IR0000009, CUPB53C22001790006), funded by EU’s NextGenerationEU under MUR call 3264/2021 PNRRM4/C2/L3.1.1.

References

[1]Degli Esposti L., et al., Bioinspired oriented calcium phosphate nanocrystal arrays with bactericidal and osteogenic properties. *Acta Biomaterialia* 2024; 186, 470-488.

S49 – O3

Cohesion and mechanical stability of biofilms compromised by small molecules with aromatic residue through disassembly and inhibition of functional amyloids

Igbokwe V.C.[1], Champion M.[1], Granger I.[1], Mathieu E.[1], Vidal L.[2], Hardouin J.[3], Jouenne T.[3], Wallart L.[3], Chaumont A.[4], Ball V.[1], Nardin C.[5], Ploux L.[1]
[1]Inserm UMR_S 1121, Universite de Strasbourg, Biomaterials and Bioengineering, Centre de Recherche en Biomédecine de Strasbourg, Strasbourg; [2]CNRS UMR 7361 IS2M, Universite de Haute-Alsace, Mulhouse ; [3] Polymers, Biopolymers, Surfaces Laboratory, Normandie Universite, Rouen ; [4]Laboratoire de Modélisation et Simulations Moléculaires, UMR 7140 - Chimie de la Matiere Complexe, CNRS-University, Strasbourg ; [5]Universite de Pau et des Pays de l'Adour, Pau, France

Introduction

Functional amyloids such as curli play a central role in biofilm organization and have become essential targets to inhibit biofilm formation without affecting bacterial growth. We examined whether disassembling the CsgA amyloid, the main subunit of *Escherichia coli* curli, with anti-amyloid molecules inhibits *E. coli* biofilm formation. In this original approach, amyloids are targeted directly without any interactions with the biological machinery of the amyloid biosynthesis (figure 1).

Materials and Methods

We started by identifying small molecules capable of disassembling R5T, the most amyloidogenic sequence in CsgA, and evaluated the molecules' anti-amyloid and anti-biofilm activities against *E. coli* PHL628 biofilms. The test molecules tested were lawsone (LWS), juglone (JUG), 1,8-dihydroxynaphthalene (DHN), and phenyl-β,D-glucopyranoside (PBDG).

Results

We established that LWS, JUG and DHN have a > 50 % amyloid disassembly activity. In *E. coli* PHL628 biofilms, all three molecules reduced biofilm amyloid content, yet this did not result in a corresponding reduction in biofilm biomass. Despite this, amyloid-depleted biofilms exhibited altered architecture and reduced mechanical stability, with molecule-dependent differences in compaction and surface retention under shear stress. These effects occurred without changes in planktonic growth or biofilm-associated cell abundance, indicating that amyloid targeting primarily compromises biofilm integrity.

Conclusion

These findings indicate that directly targeting bacterial functional amyloids is a promising strategy for combating bacterial biofilms without any action on vital, biological structure, thus strongly reducing the risk of resistance emergence.

Acknowledgements

The authors thank the French research agency ANR (Agence Nationale de la Recherche) for their financial support (project BABE n° ANR-22-CE19-0005).

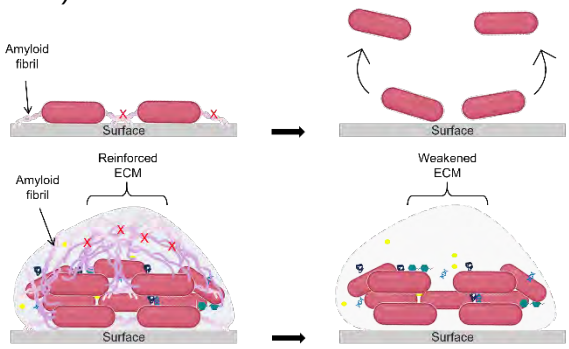

Figure 1: anti-amyloid strategy on biofilms

S49 – O4

Antimicrobial peptide functionalization of high-entropy alloy surfaces for infection-resistant osteosynthesis implants

Groult E.[1], Monasson O.[2], Pappalardo G.[3], Sabatino G.[3] , Hocini A.[4], Dirras G.[4], Boissière M.[1], Peroni E.[2], Seyer D.
[1]CY Cergy Paris Université, Laboratoire ERRMECe, Cergy Pontoise, France; [2]CY Cergy Paris Université, CNRS, BioCIS UMR 8076, Cergy Pontoise, France ; [3]Institute of Crystallography, National Research Council Italy, Catania ; [4]Université Sorbonne Paris Nord, LSPM, CNRS-UPR 3407, Villetaneuse France

Introduction

As the aging population increases and bone diseases become more common, the need for durable and reliable implantable osteosynthesis materials (1) also grows. However, the risk of infection associated with these materials remains a significant challenge, often leading to serious complications for patients. Our proposal aims to develop a new generation of antimicrobial biomaterials that combine functionality with antimicrobial features, providing a safer and more effective solution. This approach is based on the concept of multiple principal element alloys (MPEA) (2), produced through additive manufacturing using Laser Powder Bed Fusion (L-PBF) technology, along with surface biofunctionalization with antimicrobial peptides. The goal is to create a promising synergy between physicochemical properties (such as Young's modulus, corrosion resistance, fatigue
life) and the alloy's antibacterial effect.

Materials and Methods

The peptides are synthesized via microwave-assisted solid-phase synthesis (MW-SPPS), and peptide functionalization of the alloy surface is achieved through thiol-metal interactions. The peptides are previously modified with a short spacer and a cysteine residue introduced at the N-terminus of the antimicrobial peptide to enable surface grafting. To enable simple and rapid characterization, a fluorescent probe is added to the peptide, allowing visualization on the surface using microscopy.
Several antimicrobial peptides were synthesized and tested in solution using MIC and MBC assays against S. *aureus*, S.*epidermidis*, E.*coli*, and P.*aeruginosa*, as well as antibiofilm assays against S. *aureus*. Additionally, peptide combinations were examined to explore potential synergistic effects. Based on these results, two candidates were chosen: the I7R(3) sequence, known for its antimicrobial activity, and Citropin 1.1, (4) which showed promising antimicrobial and antibiofilm properties in preliminary tests. These peptides are now being studied after covalent attachment to MPEA surfaces to study their antimicrobial mechanisms, including anti-adhesive, growth-inhibitory, and bactericidal effects.

Results

Thiol metal reaction was investigated as a strategy for covalently grafting antimicrobial peptides onto MPEA surfaces (Figure 1). Initial solution-based assays identified a promising peptide pair, I7R and Citropin 1.1. These peptides showed potential synergistic effects against S.a*ureus* biofilm formation. At 50 mg/mL, I7R reduced biofilm formation by 47.4%, Citropin P1 by 89.7%, while an equimolar mixture of both peptides achieved a 95.7% reduction.

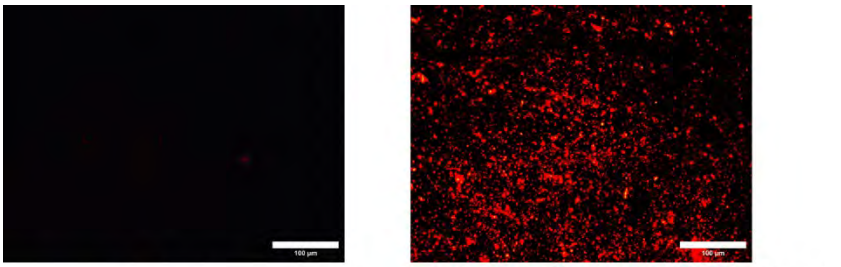

Figure 1: Epifluorescence microscopy (absorption 555 nm emission 580 - 590 nm): A uniform fluorescent coating was observed on the alloy surface, indicating that the surface functionalization strategy based on thiol interactions is effectively grafts peptides onto the substrate.

References

[1]Papin, P., Berthonnaud, E. Incidence of osteosynthesis of members in France. *International Orthopaedics 2017* 41, 1501–1506.
[2]Farzin Arjmand, Adrien Mourgout, Alima Chali, Madjid Djemai, Credson-Yannick Langueh, Olivier Monasson, Elisa Peroni, Michel Boissiere, Souad Ammar-Merah, Guy Dirras; L-PBF processing and characterization of a Ti35Nb30Zr29Mo3Ta3 multiprincipal element alloy for medical implants. *Appl. Phys. Lett. 2024*; 125 (4): 041904.
[3]Mishra B, Lushnikova T, Golla RM, Wang X, Wang G. Design and surface immobilization of short anti-biofilm peptides. Acta Biomater. 2017 Feb;49:316-328.
[4]Rodrigues de Almeida N, Catazaro J, Krishnaiah M, Singh Chhonker Y, Murry DJ, Powers R, Conda-Sheridan M. Understanding interactions of Citropin 1.1 analogues with model membranes and their influence on biological activity. *Peptides. 2019* Sep;119:170119.

S49 – O5

Light-activated photodynamic polymer biomaterials as antibiotic-independent strategies to combat antimicrobial resistance

Brooker C.[1,2], Tronci G.[1,2]
[1]Clothworkers' Centre for Textile Materials Innovation for Healthcare (CCTMIH), School of Design, University of Leeds; [2]School of Dentistry, St. James's University Hospital, University of Leeds, UK

Introduction

The global rise of antimicrobial resistance (AMR) is reducing the effectiveness of conventional antibiotics and creating an urgent need for alternative infection control strategies. Antimicrobial photodynamic therapy (APDT) offers a promising antibiotic-free approach by generating reactive oxygen species (ROS) on-demand through light exposure of a photosensitiser. Generated ROS induce rapid oxidative damage to microbial cells through multi-target mechanisms, enabling broad antimicrobial effects with limited risks of resistance development. However, many photodynamic systems rely on diffusible photosensitisers that suffer from leaching, tissue staining, cytotoxicity, and poor integration with scalable biomaterial processing. In this work, we present a staining-free photodynamic mesh of covalently functionalised poly(vinyl alcohol) (PVA) designed to provide stable, light-activated antimicrobial functionality while maintaining compatibility with fibre-based biomaterial fabrication.

Materials and Methods

A functionalised PVA derivative was synthesised via tosylation-mediated conjugation of a phenothiazine photosensitiser together with methacrylate groups enabling UV-induced crosslinking. In addition to previously developed films and wet-spun fibres, the material was fabricated into electrospun fibrous meshes from an aqueous solution suitable for antimicrobial biomedical interfaces. ROS generation under visible light irradiation was assessed using 2′,7′-dichlorodihydrofluorescein diacetate and 1,3-diphenylisobenzofuran, while cytocompatibility was evaluated using L929 mammalian fibroblast cultures.

Results

Electrospinning produced continuous nanofibrous meshes, increasing surface area and enabling efficient light-mediated ROS generation. The functionalised PVA meshes showed stable incorporation of the photosensitiser with minimal release (~3%) during aqueous incubation for 96 h, confirming covalent immobilisation within the polymer network. Upon visible light exposure, the materials produced detectable ROS within minutes, demonstrating rapid activation. Importantly, the crosslinked biomaterials maintained cytocompatibility with L929 mammalian fibroblasts, supporting their potential for biomedical applications.

Conclusion

This work presents a photodynamic polymer platform with broad material processability and capable of generating antimicrobial ROS without relying on antibiotic release. By combining covalent photosensitiser immobilisation, rapid light-triggered antimicrobial activity, and scalable fibre-based fabrication, the system represents a promising biomaterial strategy to address infections while mitigating the development of antimicrobial resistance. These properties highlight the potential of photodynamic biomaterials as next-generation infection-resistant materials for healthcare applications.

Acknowledgements

The authors gratefully acknowledge financial support from the Leeds Institute of Textiles and Colour (LITAC), the Clothworkers' Centre for Textile Materials Innovation for Healthcare (CCTMIH), and the Clothworkers' Company (London, UK).

S50
New materials and applications for volumetric bioprinting

S50 – K1
Advanced tomographic 3D printing: Fundamentals and recent developments

Madrid-Wolff J., Zhang Q., Sahli J., Pham T., Kangur T., Delrot P.
Ready3D SA – Switzeland

Tomographic Volumetric Additive Manufacturing (TVAM) is a light-based, layer-free 3D printing technology that solidifies an entire object within a photoresin-filled vial in a single step, typically within seconds. Rather than building parts layer-by-layer, VAM projects a time-varying sequence of two-dimensional light patterns from multiple angular directions into a rotating vial, so that the three-dimensional light dose accumulated at each point of the volume matches a target dose distribution computed from an inverse Radon transform. This talk reviews the principles underlying tomographic printing and the phenomena that limit its performance, the strategies used to overcome them, and our effort to scale it up towards larger, clinically relevant constructs.

TVAM is consolidating as a versatile tool in biofabrication and fast additive manufacturing, enabling the rapid production of cm-scale free form structures within seconds. By projecting a precise 3D light dose into photocurable materials, this method facilitates the creation of complex structures across a diverse array of materials, ranging from soft hydrogels to robust ceramics. This technology has been widely adopted by life scientists as it is especially gentle on living cells: printing times are short (< 30 s), photoinitiator concentrations can be kept low (< 0.1 w/v%), and sheer stress is avoided, all of which ensure a biocompatible environment and high cellular viability (> 90%).

Our work focuses on various technical challenges encountered in tomographic volumetric 3D printing. Aspects of photopolymerization kinetics, light distortion, light diffraction and light scattering will be covered, as well as the software and hardware tools we have developed to overcome these challenges and account for their impact in volumetric 3D printing to notably scale up the printing build volume up to 40 mm in diameter, a roughly five-fold increase in build volume (from 12 to close to 60 cm^3) at unchanged printing speeds (under 60 s).

Acknowledgments
This project has received funding from the Eurostars-3 joint programme (E!6780-PREPPER) with co-funding from the European Union's Horizon Europe research and innovation programme. Eurostars is part of the European Partnership on Innovative SMEs.

S50 – O1

Volumetric bioprinting of cell-laden GelMA biomaterials for biomimetic modelling of vulnerable atherosclerotic plaques

Kaliannagounder Krishnamoorthi V.[1], Cahya R.[2], Booth P.[2], White S.[2], Dalgarno K.[1]
[1]School of Engineering, Newcastle University; [2]Translational and Clinical Research Institute, Newcastle University, UK

Introduction

Atherosclerosis continues to be a leading cause of cardiovascular illness and death worldwide, mainly caused by plaque formation and rupture within arterial walls. Current experimental models largely depend on animal systems or simplified two-dimensional cultures, which fail to adequately mimic the structural and mechanical complexity of human vascular disease. Three-dimensional (3D) bioprinting provides a promising platform for creating physiologically relevant in vitro disease models that allow detailed study of plaque biomechanics and cellular interactions. In particular, volumetric bioprinting technologies enable rapid fabrication of cell-laden atherosclerotic constructs with high spatial accuracy and excellent cell viability.

Materials and Methods

Gelatin methacryloyl (GelMA) hydrogels were synthesised and optimised as bioinks for volumetric bioprinting using a tomographic illumination-based bioprinter (Tomolite, Readily3D). Multiple GelMA batches were prepared to optimise polymerisation behaviour and printing parameters, including UV light dose, light intensity, exposure time, and rotational projection settings. Simplified disc constructs (8 mm diameter, 2-3 mm thickness) were fabricated to facilitate mechanical characterisation. Human fibroblasts were incorporated into GelMA bioinks at a density of 1.5×10^5 cells mL^{-1} prior to printing. Mechanical properties were evaluated using compression testing (CellScale), while cell viability and proliferation were assessed via live/dead fluorescence imaging over a 14-day culture period.

Results

Optimising GelMA synthesis considerably decreased the UV dose needed for polymerisation, enhancing printing reliability while ensuring cell compatibility. Volumetric bioprinting allowed fast production of hydrogel constructs with uniform shape and mechanical stability. Compression tests showed Young's modulus values within the natural stiffness range of arterial tissue (around 6-43 kPa). Cell-embedded constructs exhibited excellent cytocompatibility, with viability consistently recorded between 80-98% over the two-week culture period. Quantitative analysis revealed significant increases in cell numbers from day 1 to day 14, indicating ongoing proliferation within the hydrogel matrix. Mechanical measurements confirmed that the stiffness of the constructs remained stable during culture, supporting the structural integrity of the printed matrix.

Conclusion

This study demonstrates the feasibility of developing an atherosclerotic model through volumetric bioprinting of cell-laden GelMA constructs as a platform for modelling atherosclerotic plaque environments in vitro. The printed hydrogels exhibited physiologically relevant stiffness and supported long-term cell viability and proliferation. These findings lay a foundation for developing more complex vascular plaque models that include endothelial and smooth muscle cells, enabling future studies of plaque erosion mechanisms and haemodynamic interactions within perfusion bioreactor systems.

S50 – O2

One-step spatial photo-programming of cell alignment in 3D patterned hydrogels via grayscale light-sheet volumetric bioprinting

Cedillo-Servin G.[1], Schimmenti F.[2,3], van Hattem T.[1], Frascella F.[2], Roppolo I.[2], Castilho M.[1]
[1]Dept. Biomedical Engineering, Eindhoven University of Technology, The Netherlands; [2]Dept. Applied Science & Technology, Politecnico di Torino, Turin, Italy; [3]Dept. Chemistry, Biology and Biotechnology, University of Perugia, Italy

Introduction

Guiding cell organization in 3D remains challenging for the engineering of highly anisotropic tissues. Current 3D-printing approaches often use simple stiffness gradients that lack local mechanical control and spatial freedom, hindering fabrication of centimeter-scale hydrogels with complex native-like cell organizations. Conventional volumetric bioprinting (VBP) techniques still lack the ability to either program local hydrogel (visco)elasticity without post-processing steps —e.g. tomographic VBP— or encode mechanical heterogeneities with full 3D freedom —e.g. filamented light. We recently introduced light-sheet VBP, a promising approach that creates 3D hydrogels with micro-resolved spatial control over stiffness in a single step, but its impact on cell behavior remains unexplored[(1)].

Aim

Here, we introduce grayscale light-sheet volumetric bioprinting as a one-step VBP approach to encode topological defect-inspired 3D stiffness patterns into nutrient-rich hydrogels that guide cells into user-defined organization profiles.

Materials and Methods

Gelatin and PEG-based resins with different degrees of substitution (DS) and dual-color photoinitiator were supplemented with nutrient mixes to enhance cell viability, followed by xolography printing at the intersection of a moving blue-light sheet (405 nm) and grayscaled visible-light projections with printing rates >0.4 mL/min. Grayvalues (25–100% visible-light intensity) were correlated to monomer conversion, hydrogel porosity, and (visco)elastic properties. To visualize contrast in local crosslinking density, resins were grafted *in situ* during printing with mScarlet for fluorescence imaging. C2C12 myoblasts, hMSC, and HUVEC were encapsulated at 1–2x10^6 cells/mL in nutrient-rich hydrogels with grayscale motifs based on tissue-inspired topological defects (radial, circumferential, branching) to assess a) DS and grayvalue effect on viability and ROS production, and b) motif topology and size effect on cell orientation.

Results

Dual-color photo-rheology revealed higher DS enhanced resin crosslinking, while nutrient supplementation did not severely impact light absorption (Figure 1). Grayscale-patterned hydrogels demonstrated zonal differences in porosity and a tunable stiffness range, with up to 6.4-fold increase between 25% and 100% light-dose. Unreacted monomers in low-grayvalue regions remained available for secondary crosslinking and time-resolved hydrogel stiffening, but this second step was not required to create high stiffness contrast. 3D stiffness gradients with diverse topological configurations were photo-encoded in hydrogels via grayscale motifs, which differentially guided alignment of the actin cytoskeleton in a cell-type and topology-dependent manner, primarily for motifs <200 µm with high stiffness contrast.

Conclusion

Grayscale light-sheet VBP modulated light-dose at the voxel level, leading to precise one-step control over hydrogel stiffness with full 3D freedom, while remaining compatible with post-printing stiffening. Mechanical photo-programming enabled complex cellular organization profiles, providing a powerful tool to model mechano-instructive 3D microenvironments that bridge biofabrication with mechanobiology and multicellular dynamics.

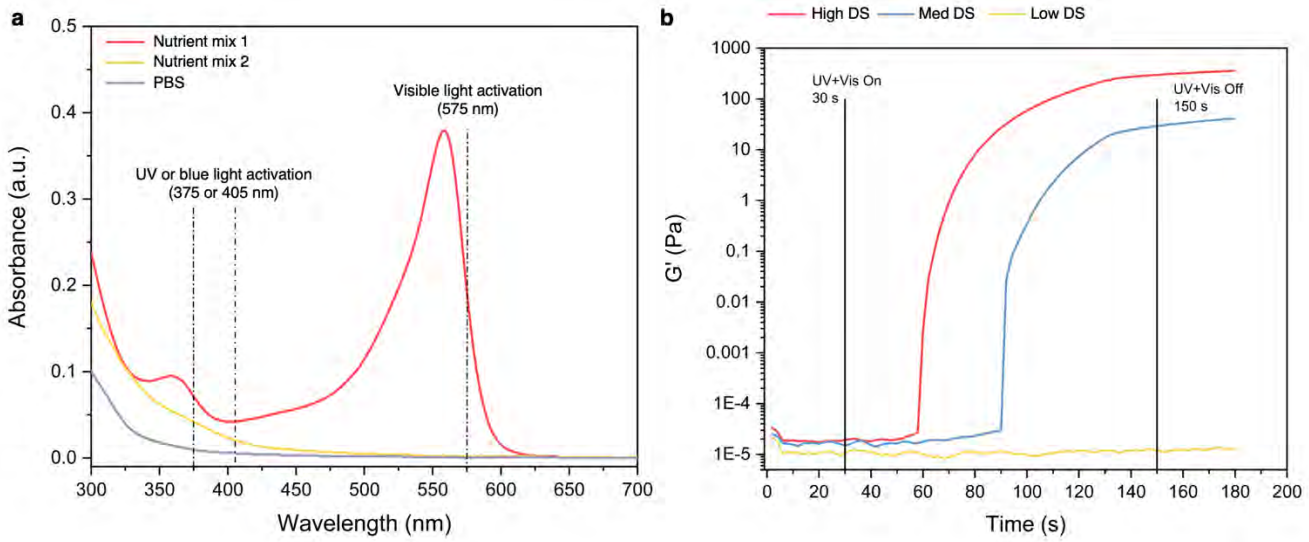

Figure 1. a) Absorption spectroscopy of nutrient supplements to enhance cell viability within bioresins; Nutrient mix 2 shows lower absorption in the UV-blue and yellow range. b) Dual-color photo-rheology of gelatin/PEG resins with different degree of substitution (DS), showing that medium or high DS are needed for photo-crosslinking.

References

[1]Stoecker L., Cedillo-Servin G., König N.F., de Graaf F.V., García-Jiménez M., Hofmann S., Ito K., Wentzel A.S., Castilho M. Xolography for Biomedical Applications: Dual-Color Light-Sheet Printing of Hydrogels With Local Control Over Shape and Stiffness. *Advanced Materials 2025*; 37(10): 2410292.

S50 – O3

Filamented light 3D bioprinting enables anisotropic stiffness gradients for controlled vascularisation

Prados-Martin L.[1], Robinson T.[1], Lim K.S.[1]
[1]School of Medical Sciences, University of Sydney, Australia

Introduction

The lack of functional vascularisation remains a major bottleneck limiting the survival and complexity of engineered tissues. The mechanical properties of biomaterials play a central role in regulating cellular organisation and tissue architecture, with matrix stiffness acting as a key driver of vascular morphogenesis. In this study, we used Filamented Light 3D Bioprinting (FLight) - a light based technique that introduces filaments into 3D-matrices - to generate controlled stiffness gradients containing anisotropic architecture. Hence, using this platform, we aim to systematically investigate the synergistic effect of mechanobiological cues and cell alignment in regulating microvessel formation. We further apply these principles to the generation of vascularised cardiac tissue constructs.

Materials and Methods

GelMA hydrogel constructs were fabricated using Filamented Light 3D Bioprinting (FLight) with a Ruthenium/Sodium Persulfate (Ru/SPS) photocrosslinking system. By projecting filamented light from a single side of the construct, we exploited Ru absorbance and cell induced light scattering to spatially modulate light exposure, generating filamented architectures with progressively decreasing stiffness along the print axis. Human mesenchymal stem cells (hMSCs) and human umbilical vein endothelial cells (HUVECs) were encapsulated within these anisotropic scaffolds. Cellular alignment and vascular network formation in response to spatial mechanical cues were quantified using confocal microscopy and image based analysis. Building on these findings, we extended the approach to high density cardiac tissue fabrication using human induced pluripotent stem cell–derived cardiomyocytes and HUVECs, assessing how graded stiffness and anisotropy jointly regulate functional tissue maturation, including contractility and vascularisation.

Results

FLight enabled the fabrication of filamented scaffolds with well defined stiffness gradients (Figure 1 a-b). Encapsulated hMSCs rapidly aligned across the constructs, demonstrating strong sensitivity to the anisotropic microarchitecture. However, HUVECs showed a pronounced gradient-dependent response (Fig. 1-c). In the stiffer (highly irradiated regions), where hMSCs-mediated remodelling was limited, endothelial cells aligned consistently but formed fewer vascular networks. In contrast, in softer distal regions, HUVEC alignment decreased while interconnected vessel formation was more pronounced. Vascularised cardiac tissue models exhibited analogous spatial responses (Fig. 1-d). In the stiffer frontal region, cells showed pronounced directional alignment and contractile activity along the FLight-defined axis, whereas the softer distal region displayed reduced alignment but enhanced vascularisation.

Conclusion

FLight enables precise engineering of stiffness gradients within hydrogel scaffolds, providing a means to balance mechanical cues for both cellular alignment and functional vascularisation. This gradient-based approach supports the fabrication of spatially organised, multicellular tissues and offers significant potential for regenerative medicine applications requiring vascularised and mechanically heterogeneous constructs.

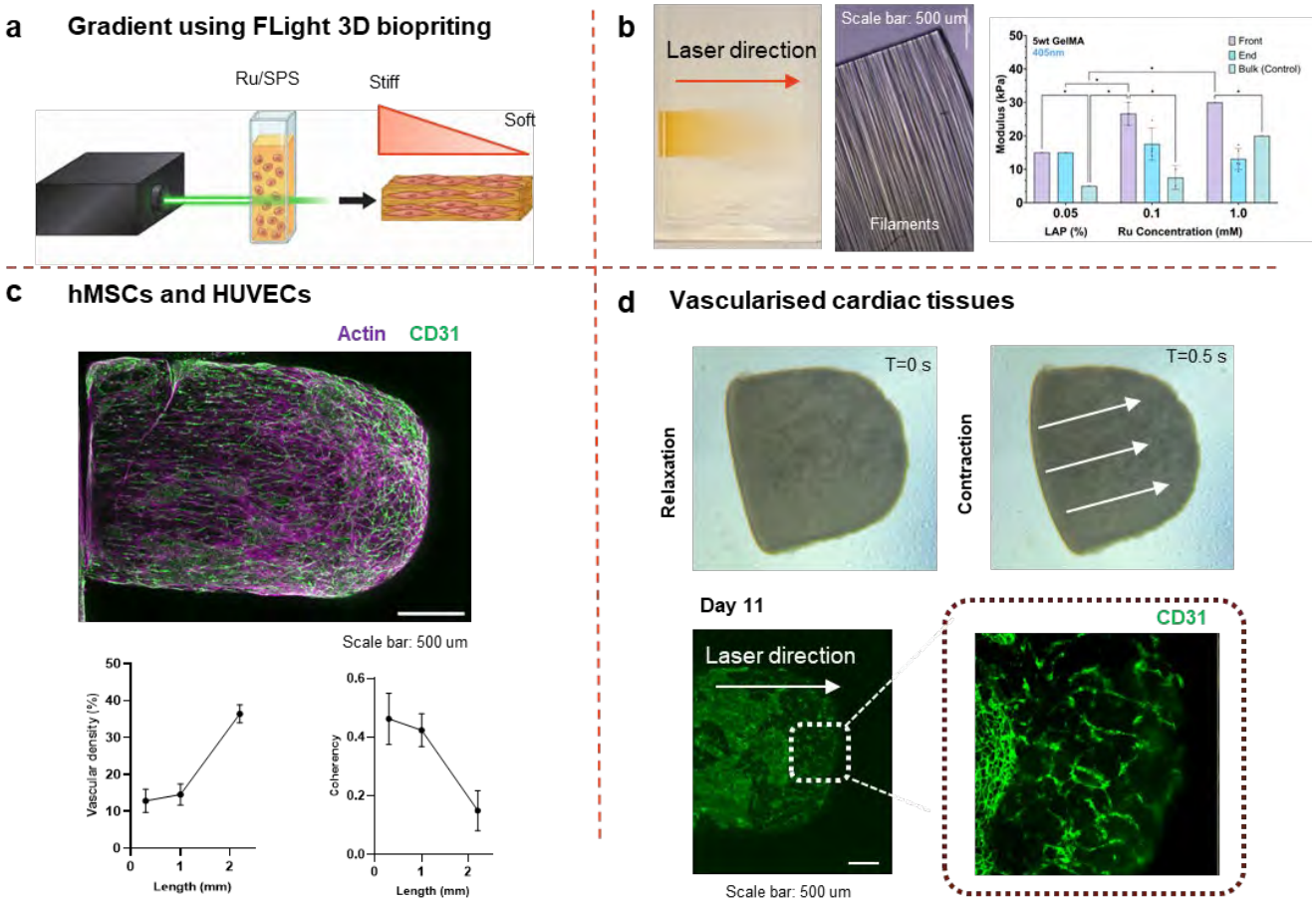

Figure 1. (a) Schematic illustration of the Filamented Light (FLight) bioprinting method, in which spatially patterned light exposure generates filamented crosslinking and stiffness gradients within a 3D construct. (b) Acellular characterisation of FLight-fabricated GelMA constructs, demonstrating filamented architectures and a graded stiffness profile along the print axis. (c) Confocal images of FLight-printed hMSC–HUVEC constructs stained for actin (magenta) and CD31 (green). Quantitative actin filament orientation analysis reveals a spatial gradient of decreasing cellular alignment from the proximal (stiffer) to the distal (softer) region. Vascular density analysis shows enhanced vascularisation in distal regions, corresponding to reduced vessel alignment (lower coherency). (d) Directional contraction of a vascularised cardiac construct, with white arrows indicating the axis of FLight exposure and the resulting contractile motion. Confocal imaging of CD31 (green) demonstrates spatially patterned vascularisation, with the magnified view highlighting enhanced microvasculature in the softer distal region.

S50 – O4

Chemically modified gelatin-based hydrogels for the volumetric printing of stents for mucosa regeneration

Santos Silva R.P.[1], Benoot T.[2], Groll J.[3], Vozzi G.[4], Chiesa I.[4], Arezzo A.[5], Barontini F.[5], Brovarone C.V.[6], Bal-Öztürk A.[7], Bernkop-Schnurch A.[8], Vicini I.[9], Laukens D. [2], Pien N.[1], Van Vlierberghe S.[1]
[1]Dept. of Organic and Macromolecular Chemistry, Ghent University, Belgium; [2]Dept. of Internal Medicine and Pediatrics, Ghent University, Belgium; [3]Dept. of Functional Materials in Medicine and Dentistry, University of Würzburg, Germany; [4]Dept. of Bioengineering and Robotics Research, University of Pisa, Italy; [5]Dept. of Surgical Sciences, University of Torino, Italy; [6]Dept. of Applied Science and Technology, Politecnico di Torino, Italy; [7]AdBioInk Biosystem Technology, Turkey; [8]Dept. of R&D,Thiomatrix, Austria; [9]Dept. of European Funding Development, Bewarrant, Belgium

Introduction

Colorectal diseases (CRDs), encompassing inflammatory, hereditary, or neoplastic forms, affect millions of people worldwide [1]. Familial adenomatous polyposis and Ulcerative colitis are two of the most common conditions and often require ileal pouch-anal anastomosis (IPAA) or total proctocolectomy, a procedure associated with significant morbidity [1]. Although surgery may provide temporary solutions, it often compromises patient's quality of life and fails to restore the colon's natural functions [2].

Aim

In this study, conducted within the EU-funded TENTACLE project, a 3D gelatin-based stent is being developed to mimic the native mechanical properties of the colon while actively promoting tissue regeneration. Functionalized gelatins will serve as starting material; different combinations of gel-methacrylate (GelMA), gel-norbornene (GelNB) with thiolated gel (GelSH) combined with thiolated cyclodextrins and ureidopyrimidinone derivates are being explored [4].

Materials and Methods

Rheology was performed to assess crosslinking under 405 nm irradiation at 20 mW•cm^{-2}, as well as viscosity profiles and mechanical stability following hydrogel formation. The target properties include a viscosity of approximately 10^4 Pa·s, a yield strength of around 1 MPa, and a stiffness in the range of 10–50 kPa, which are essential to ensure stent stability during intestinal peristaltic movements [3]. In addition, the biocompatibility of the developed materials was assessed, targeting a cell viability above 70%, in accordance with the ISO 10993-5:2009 standard. *In vitro* epithelial regeneration was further evaluated through transepithelial electrical resistance (TEER) measurements, aiming to achieve values between 200 and 400 Ω·cm² by using co-cultures of epithelial cells and fibroblasts [5].

Results

GelMA, GelNB and GelSH exhibited the expected modifications, as confirmed by NMR[6], and ortho-phthalaldehyde assay, respectively. Rheological tests on hydrogels showed an increase in storage modulus with increasing polymer (w/v)%, as well as when using gelatins with a higher degree of substitution. In contrast, when comparing different cyclodextrins, formulations with lower thiol content resulted in higher storage modulus values. Encapsulated fibroblasts in 6% (w/v) hydrogels maintained high viability and preserved their characteristic spindle-shaped morphology, as confirmed by brightfield and confocal imaging.

Conclusion

These results demonstrate that chemically modified gelatin-based hydrogels are promising candidates for the development of volumetrically printed intestinal stents. The studied formulations showed suitable chemical functionalization, tunable mechanical properties, and good cytocompatibility, supporting their potential for mimicking colonic tissue and promoting mucosal regeneration.

Acknowledgements

HORIZON-HLTH-2024-TOOL-11-02

References

1. Paiva, N. M., et al. *Scientific Reports 2018.*
2. Koerdt, S., et al. *International Journal of Colorectal Disease.*
3. Nuñez Bernal, P., et al. *Advanced Materials 2019.*
4. Carpentier, N., et al. *Biomacromolecules 2024.*
5. Howard, R. L., et al. *Biophysical Journal 2021.*
6. Van Hoorick, J., et al. *Macromolecular Rapid Communications 2018.*

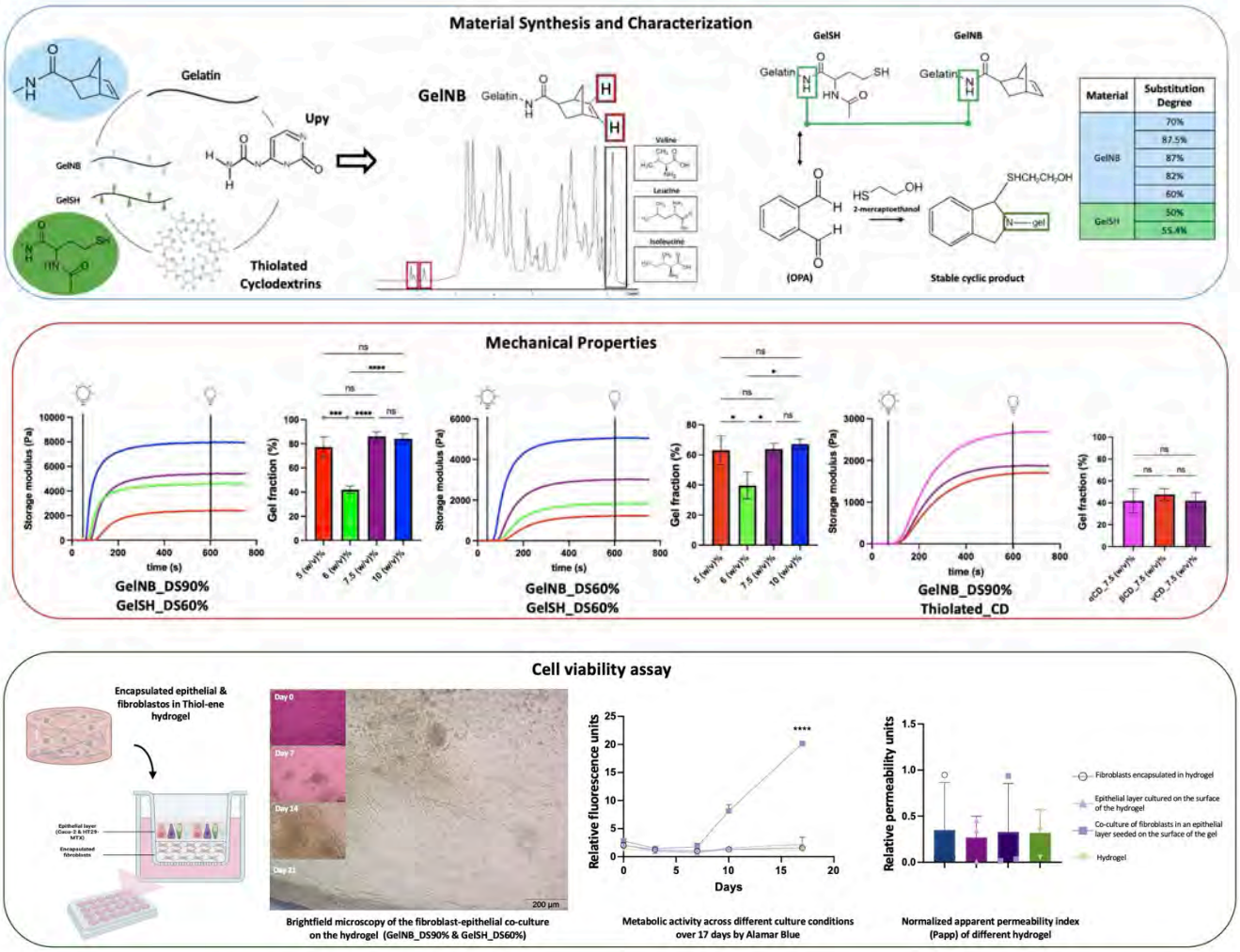

S50 – O5

Radiopaque volumetrically printed PCL scaffolds for real-time *in vivo* degradation monitoring

Quaak A.[1], Van Durme B.[1], Van Damme L.[1], Nazzi E.[1], Groborz O.[2,3], Vanhove C.[4], Thijssen Q.[1], Kolouchova K.[1], Van Vlierberghe S.[1]

[1]Polymer Chemistry and Biomaterials Group, Ghent University, Belgium; [2]Institute of Biophysics and Informatics, Charles University, Prague, Czech Republic; [3]Institute of Organic Chemistry and Biochemistry, Prague, Czech Republic; [4]Dept. of Electronics and Information Systems, Ghent University, Belgium

Introduction

Poly(ε-caprolactone) (PCL) is widely used for hard tissue engineering due to its biocompatibility and biodegradability. However, non-invasive long-term monitoring of implant degradation *in vivo* remains challenging. Radiopaque scaffolds that allow real-time imaging could provide valuable insights into implant performance and tissue regeneration dynamics.

Materials and Methods

Radiopaque PCL scaffolds were developed by covalently incorporating the iodinated contrast agent 5-acrylamido-2,4,6-triiodoisophthalic acid (AATIPA) into a photo-crosslinkable thiol–ene PCL network. This strategy ensured stable radiopacity while preventing contrast agent leaching. Scaffolds were fabricated using volumetric additive manufacturing (VAM), a light-based 3D-printing technique that enables the rapid fabrication of complex three-dimensional structures in a single step through the projection of dynamic 2D light patterns into a rotating resin volume (Figure 1). Compared to conventional layer-by-layer approaches such as stereolithography (SLA), digital light processing (DLP) and two-photon polymerization (2PP), VAM significantly reduces fabrication time while maintaining high resolution and architectural freedom.

Results

The volumetrically printed scaffolds exhibited high structural fidelity and persistent radiopacity, enabling true longitudinal µCT monitoring *in vivo*. Quantitative imaging of the same implants over a period of up to 9 months revealed progressive and continuous scaffold volume reduction. Despite ongoing mass loss, three-dimensional reconstructions demonstrated preservation of overall scaffold architecture and pore morphology throughout the monitoring period. Analysis of radiodensity evolution suggested predominantly surface-driven degradation at lower contrast content and a transition towards mixed surface–bulk degradation behaviour at higher AATIPA incorporation. Histological evaluation confirmed favourable tissue response, showing gradual thinning of the fibrous capsule, increasing vascularization, and progressive adipose tissue infiltration without signs of excessive inflammation or systemic toxicity.

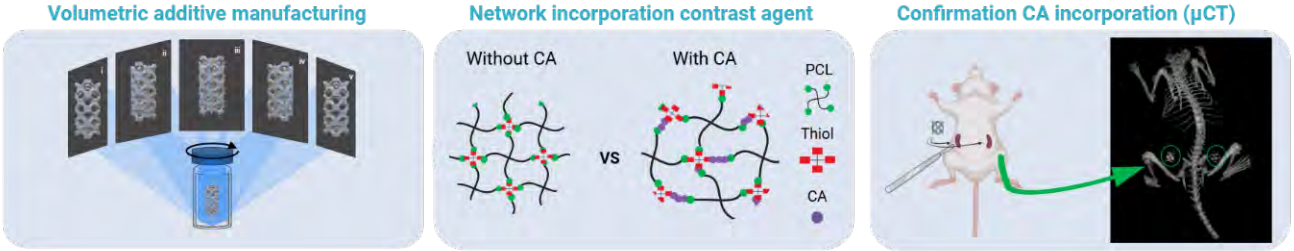

Figure 1: VAM-printing of radiopaque PCL scaffolds, enabling µ-CT-based in vivo degradation tracking.

Conclusion

This work presents a combined material and manufacturing strategy enabling ultrafast fabrication of radiopaque biodegradable scaffolds suitable for long-term *in vivo* monitoring. The ability to non-invasively track implant degradation and tissue interaction over extended periods offers new opportunities for optimizing scaffold design and advancing clinically translatable regenerative therapies.

Acknowledgements

A. Quaak gratefully acknowledges funding from the Research Foundation Flanders (FWO, 1SHDP24N).

References

1. Q. Thijssen, A. Quaak et al “Volumetric Printing of Thiol-Ene Photo-Cross-Linkable Poly(ε-caprolactone): a Tunable Material Platform for Biomedical Applications”, *Advanced Materials, 2023,* 35 (19), 2210136.
2. A. Quaak et al “Exploiting the Network Architecture of Thiol–Ene Photo-Crosslinked Poly(ε-caprolactone) towards Tailorable Materials for Light-Based 3D-Printing”, *Polymer Chemistry, 2023*, 14 (29), 3392-3403.
3. K. Kolouchova et al “Next-Gen Poly(ε-Caprolactone) Scaffolds: Non-Destructive In Vivo Monitoring and Accelerated Biodegradation”, *Adv. Health. Mat., 2025,* 14 (1), 2402256.

S50 – O6

Origami-inspired shape-memory stents fabricated via volumetric 3D printing of poly(δ-valerolactone)

Jaén-Ortega A.[1,2], Quaak A.[1], Pien N.[1], Thijssen Q.[1], Van Vlierberghe S.[1]
[1]Dept. of Organic and Macromolecular Chemistry, Polymer Chemistry and Biomaterials Group, Centre of Macromolecular Chemistry, Ghent University, Belgium; [2]Research Group in Design, Manufacturing and Materials (DM + M), School of Mechanical Engineering, Universidad Tecnológica de Panamá, Panama City, Panama

Introduction

Shape-memory stents capable of self-expansion offer a promising route toward minimally invasive implantation, as they can be delivered in a compact temporary configuration and subsequently recover their functional geometry in response to thermal stimulation. Volumetric 3D printing enables the rapid fabrication of complex geometries within seconds, making it an attractive approach for deployable biomedical devices[(1,2)]. In this work, an origami-inspired stent concept was fabricated by volumetric 3D printing using poly(δ-valerolactone) (PVL), enabling thermally triggered deployment upon exposure to body temperature (Fig. 1)[(3,4)].

Materials and Methods

A four-arm PVL was synthesized through ring-opening polymerization of δ-valerolactone, with a number-average molecular mass of 6 800 g mol^{-1} and dispersity of 1.2. The polymer was subsequently functionalized with norbornene (degree of substitution = 100%) end groups to enable rapid crosslinking via thiol–ene chemistry using pentaerythritol tetrakis(3-mercaptopropionate) as the crosslinker. The resulting resin, formulated with diphenyl(2,4,6-trimethylbenzoyl)phosphine oxide as photo-initiator and TEMPO as inhibitor, was processed by tomographic volumetric 3D printing into origami-inspired stent geometries. Thermal behavior and actuation were assessed by differential scanning calorimetry (DSC) and thermo-mechanical deployment tests. Cytocompatibility was evaluated by direct-contact Live/Dead assays using human umbilical vein endothelial cells (HUVECs).

Results

Volumetric 3D printing enabled the rapid fabrication of origami-inspired stent structures with reproducible unfolding behavior and successful recovery from the programmed temporary shape to a predefined permanent shape. The PVL-based material exhibited a melting temperature (T_m) of 35 °C (Fig. 2), enabling shape-memory activation at body temperature and enhancing its relevance for self-deployable vascular devices. Direct-contact HUVEC assays indicated no cytotoxic response, as quantitative analysis confirmed cell viability consistently above the 70 % threshold defined in ISO 10993-5:2009.

Conclusion

These results show that PVL-based thiol–ene networks can be processed by volumetric 3D printing, enabling the fabrication of origami-inspired shape-memory stents with an activation window suited to body temperature. The demonstrated endothelial cytocompatibility supports the potential of this material for minimally invasive, self-expanding implants.

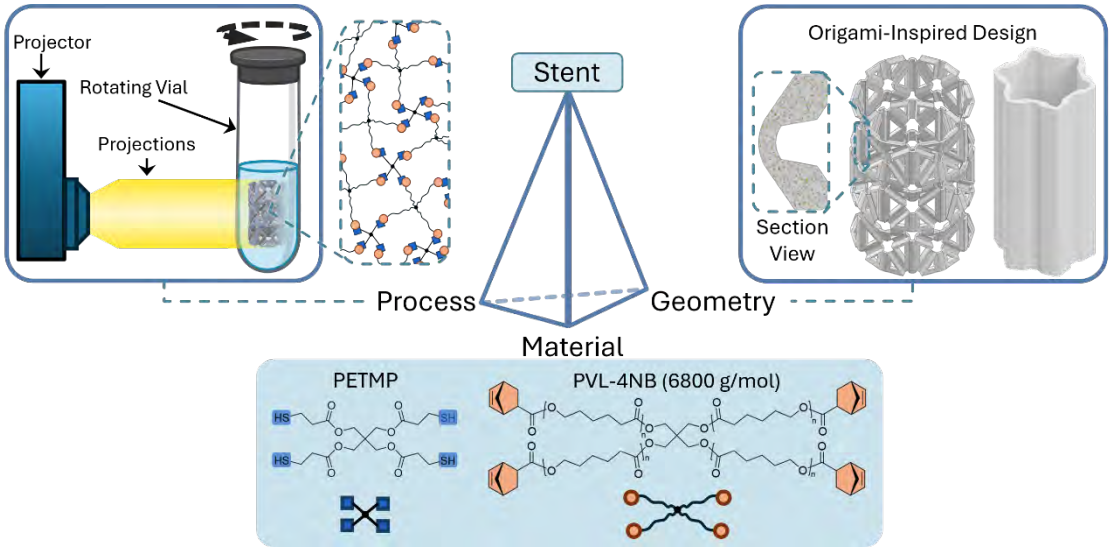

Figure 1. Overview of the volumetric 3D printing workflow using PVL as the base material and the origami-inspired stent design.

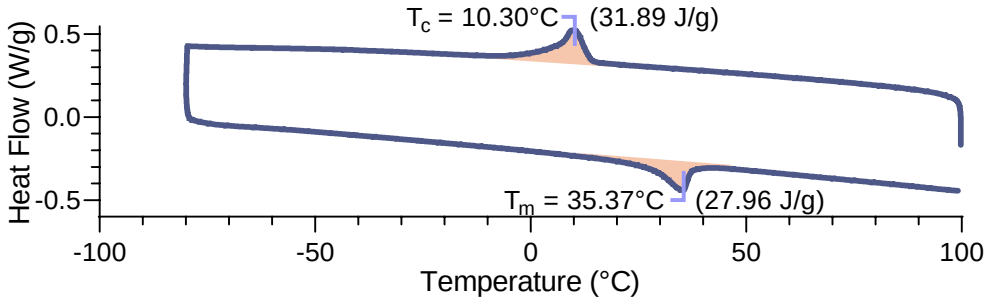

Figure 2. DSC analysis of the crosslinked PVL showing a melting temperature (T_m) below body temperature.

Acknowledgements

Q.T. acknowledges the Research Foundation – Flanders (FWO) for a doctoral fellowship (grant number 1SA2323N) and a junior postdoctoral fellowship (grant number 1201125N). S.V.V. acknowledges the Research Foundation – Flanders (FWO) for a Hercules grant (grant number I003922N). A.Q. acknowledges the Research Foundation – Flanders (FWO) for a doctoral fellowship (grant number 1SHDP24N). A.J.-O. acknowledges support from the Instituto para la Formación y Aprovechamiento de Recursos Humanos (IFARHU) and the Secretaría Nacional de Ciencia, Tecnología e Innovación (SENACYT), Republic of Panama, through the IFARHU–SENACYT scholarship program (grant number 270-2023-010)

References

1. Thijssen Q., Toombs J., Li C.C., Taylor H., Van Vlierberghe S. From pixels to voxels: A mechanistic perspective on volumetric 3D-printing. *Progress in Polymer Science* 2023;147:101755.
2. Thijssen Q., Jaén Ortega A., Vieira R.P., Van Vlierberghe S. Radical inhibition in tomographic volumetric 3D printing for thiol-ene photoresists: From photorheology to printability. *Reactive and Functional Polymers* 2024;205:106096.
3. Thijssen Q., Quaak A., Toombs J., De Vlieghere E., Parmentier L., Taylor H., et al. Volumetric printing of thiol-ene photo-cross-linkable poly(ε-caprolactone): A tunable material platform serving biomedical applications. *Advanced Materials* 2023;35(19):2210136.
4. Zhao W., Li N., Liu L., Leng J., Liu Y. Origami derived self-assembly stents fabricated via 4D printing. *Composite Structures* 2022;293:115669.

S50 – O7

Volumetric bioprinting of gelatin-based inks for osteochondral tissue engineering

Agten H.[1,2,3], Aksu D.[3], Salehi S.[3], Arslan A.[3], Van Hoorick J.[3], Bloemen V.[1,2]
[1]Skeletal Biology and Engineering Research Center KU Leuven; [2]Surface and Interface Engineered Materials, KU Leuven; [3]BIO INX BV, Zwijnaarde, Belgium

Introduction

Tissue engineering strategies for the treatment of (osteo)chondral defects involve the fabrication of living implants, a combination of cells and supporting materials, to facilitate tissue regeneration. In particular, cell-laden hydrogels offer versatility and are suitable for automated fabrication techniques, such as bioprinting. Volumetric bioprinting allows the fabrication of complex designs in a matter of seconds, with high resolution. In this work we characterized GMP-ready, gelatin-based materials, for their use in volumetric bioprinting, with the aim of developing an osteochondral implant.

Materials and Methods

Multiple gelatin-based hydrogels were characterized with photorheology (Anton Paar MCR 702) to determine photo-crosslinking kinetics. The volumetric printing procedure was optimized, by defining the reference dose as well as optimal dose using a Tomolite volumetric bioprinter (Readily3D). To optimize post-printing curing time, swelling tests as well as gel fractions tests were performed on printed structures. To assess resolution, CAD files of a triangle (negative resolution: hole diameters 0.1–0.8 mm) and the triangle's width at each tip (positive resolution) were printed using optimal exposure settings. All features were analyzed using light microscopy (EVOS XL Core), with resolution determined by the smallest feature resolved in triplicate. For cytocompatibility testing, human osteoblasts were encapsulated at a cell density of 10^6 cells/mL and a PrestoBlue assay was performed on day 1, 3 and 7 of *in vitro* culture.

Results

Photorheology revealed an equilibrium storage modulus of 23 kPa. Printing resolution was around 100 µm (positive) and 150 µm (negative). A CAD/CAM mimicry was calculated based on weighted averages, amounting to 78% (positive) and 125% (negative). Post-printing curing times were established at 15 seconds, resulting in gel fractions of 97%. When osteoblasts were encapsulated, bioprinted constructs showed maintained metabolic activity up to 7 days after fabrication. Follow-up experiments involve the encapsulation of human articular chondrocytes and an extended *in vitro* culture period (21 days) in differentiation medium.

Conclusion

Gelatin-based hydrogels are potent materials for volumetric bioprinting of living constructs. The ink is now being further evaluated in combination with human articular chondrocytes to assess cartilage tissue formation *in vitro* and *in vivo*.

Acknowledgements

This project is funded by VLAIO, Flanders innovation & entrepreneurship, mandate HBC.2023.0697.

S51
Next-generation biomaterials and bioengineering strategies against antimicrobial resistance development

S51 – K1
Reactive nanosized/nanostructured inorganic and hybrid systems for the prevention of infection

Drouet C.
Univ. Toulouse, France

Drouet C[1], Scarabelli R[1,2], Cianflone E[1], Guerin M[1,3], Choimet M[1], Al-Kattan A[1,2], Brouillet F[1], Tourrette-Diallo A[1], Oh J-M[4], Dewi Ana I[5], Grossin D[1], Subra G[3], Soulie J[1]
[1]Univ. Toulouse, Toulouse INP, CNRS, CIRIMAT, France; [2]LP3, Univ. Aix Marseille, France; [3]IBMM, Univ. Montpellier, France; [4]Dept. Energy and Materials Engineering, Dongguk University, Seoul, South Korea; [5]Faculty of Dentistry, Universitas Gadjah Mada, Jogyakarta, Indonesia

Introduction
In the context of rising antibiotic resistance and persistent threat of implant-associated infections, preventing bacterial colonization and biofilm formation on biomaterials has become as critical as treating established infections. Antimicrobial biomaterials offer a proactive solution to this dual challenge, addressing both the prevention of potential bacterial adhesion and the eradication of existing infections. These innovations are particularly relevant for orthopedic, dental, and dermatological applications. The development of bioinspired apatite-based systems and layered double hydroxides (LDHs) of diverse compositions provides multifunctional platforms that inherently resist microbial colonization while enabling the delivery of targeted therapeutic or bioactive agents to support tissue repair.

Aim
The aim of this work is to highlight how advanced biomaterial designs and fabrication strategies can shift the paradigm from reactive treatment to proactive prevention, offering personalized, infection-resistant solutions for both hard and soft tissue applications.

Materials and Methods
The study leverages nanocrystalline apatites and LDHs as core materials, functionalized to achieve antimicrobial and bioactive properties. Spray-dried core-shell microparticles were engineered from nanocrystalline apatites to enable sequential release of bioactive ions, such as antibacterial followed by pro-osteogenic agents. Additionally, 3D porous LDH/alginate composite scaffolds were fabricated using low-temperature processing techniques, including freeze-casting and cold sintering, to create structures with enhanced mechanical stability and controlled release capabilities. For dermatological applications, colloidal apatite nanoparticles were developed as smart drug carriers, with surface modifications such as peptides or phytotherapeutics to enable localized, enzyme-triggered release of antimicrobial compounds. Electrospun polymeric nanofibers were combined with laser-ablated nanoparticles (e.g., Si-, Ag-, Zn-, or apatite-based) to form non-woven mats, designed to reduce bacterial adhesion and biofilm formation in wound dressings.

Results
Advanced fabrication strategies were employed to integrate ionic or molecular antimicrobial agents into dressings, bone cements, and porous scaffolds, ensuring localized and sustained therapeutic efficacy. The engineered core-shell microparticles[1] demonstrated the ability to achieve sequential ion release, aiming to provide targeted antibacterial effects followed by pro-osteogenic properties, thus enabling bone substitutes to simultaneously prevent infection and promote bone regeneration. 3D porous LDH/alginate scaffolds[2] exhibited enhanced mechanical stability and porous architectures, suitable for the controlled release of bioactive agents such as antimicrobials, making them effective for infection-resistant bone repair and beyond, such as membranes and 3D dressings for dermatological applications. In this latter domain, colloidal apatite nanoparticles successfully enabled localized – possibly enzyme-triggered – positioning/release of bioactive agents such as antibacterial ions or peptides[3], to potentially prevent bacterial spreading. Electrospun nanofiber mats combined with laser-ablated nanoparticles[4] also showed promise for bioactive wound dressings, with adaptable and bioresponsive properties that reduce the risk of bacterial adhesion and biofilm formation.

Conclusion

These innovations highlight the potential of antimicrobial biomaterials to shift the paradigm from reactive treatment to proactive prevention, offering personalized, infection-resistant solutions for both hard and soft tissue applications. By integrating advanced materials and fabrication strategies, these systems provide localized and sustained therapeutic efficacy, paving the way for next-generation biomaterials in orthopedic, dental, and dermatological fields.

Acknowledgements

Authors thank the EU Horizon 2020 under the Marie Skłodowska-Curie grant agreement No. 861138 (AIMed project) as well as DGA-AID, Campus France, Korean NSF (PHC STAR project), and the Institut Carnot Chimie Balard CIRIMAT for partial fundings.

References

[1]Cianflone E., Brouillet F., Grossin D., Soulie J., Josse C., Vig S., Fernandes M.H., Tenailleau C., Duployer B., Thouron C., Drouet C. Toward smart biomimetic apatite-based bone scaffolds with spatially controlled ion substitutions. *Nanomaterials* 2023; 13(3); 519; doi: 10.3390/nano13030519.

[2]Lagarrigue L., Oh J.M., Xie J., Tenailleau C., Duployer B., Cazalbou S., Poquillon D., Drouet C., Soulie J. Freeze-cast Mg-Fe-CO3 nano-layered double hydroxide/alginate composite scaffolds for biomedical applications: porous architecture and mechanical properties. *Next Materials* 2024; 3; 100147; doi: 10.1016/j.nxmate.2024.100147.

[3]Guérin M., Lebrun A., Kuhn L., Azaïs T., Laurent G., Marsan O., Drouet C., Subra G. One-Pot Synthesis of Bioinspired Peptide-Decorated Apatite Nanoparticles for Nanomedicine. *Small* 2023; e2306358; doi: 10.1002/smll.202306358.

[4]Scarabelli R., Gary-Bobo M., Nguyen C., Durand D., Esvan J., Aufray M., Drouet C., Al-Kattan A. Combination of laser-generated silicon NPs and electrospun-nanofibres for the development of new-generation bioactive wound dressings. *RSC Avdances* 2026; 16; 604-616, doi: 10.1039/d5ra09481j.

S51 – O1

Contact-based functionalized gold nanoparticles for broad-spectrum antimicrobial activity

Žabčić M.[1,2], Filipić A.[3], Kogovšek P.[3], Rak M.[4], Mioč V.[5], Steyer A.[5], Gorgieva S.[6], Podlogar M.[7], Spreitzer M.[1], Vukomanović M.[1]

[1]Dept. Advanced Materials, Jožef Stefan Institute, Ljubljana; [2]Jožef Stefan International Postgraduate School, Ljubljana; [3]Dept. of Biotechnology and Systems Biology, National Institute of Biology, Ljubljana; [4]Dept. Medical Microbiology, National Laboratory of Health, Environment and Food, Koper; [5]Dept. Public Health Microbiology, National Laboratory of Health, Environment and Food, Ljubljana; [6]Faculty of Mechanical Engineering, University of Maribor; [7]Dept. for Nanostructured Materials, Jožef Stefan Institute, Ljubljana, Slovenia

Introduction

Surface-functionalized gold nanoparticles (AuNPs) with cationic amino acids exhibit strong antibacterial activity through non-specific contact-based interactions between guanidinium groups on the nanoparticle surface and phosphate groups in the bacterial envelope[1]. Such systems represent a promising strategy to combat antimicrobial resistance. As microbial resistance to existing antimicrobial compounds continues to increase worldwide, there is an urgent need for new antimicrobial agents, particularly in medicine, where infections pose a significant risk during treatment. To address this challenge, we synthesized functionalized AuNPs with mixtures of cationic amino acids and β-CD on different templates (Fig. 1a). These nanoparticles operate via a contact-based antimicrobial mechanism and show high activity against a broad range of clinical bacteria, including antibiotic resistant strains, viruses, and fungi, while limiting the ability of microorganisms to develop resistance[2].

Materials and Methods

AuNPs were synthesized using a sonochemical method. The obtained materials were characterized by XRD, XPS, UV–Vis spectroscopy, ICP and TEM. Antimicrobial activity was evaluated using disk diffusion test, a microdilution assay to monitor the growth kinetics, and a contact test to determine log reduction. It was evaluated against enveloped and non-enveloped viruses, Candida strains, and ten clinical bacterial isolates, including both Gram-positive and Gram-negative, as well as multidrug-resistant strains. The mechanism of action was further investigated by SEM and TEM analysis of microbial morphology.

Results

Functionalization was confirmed by the applied characterization techniques, verifying the presence of amino acids, gold, and the template, while nanoparticle morphology was confirmed by TEM analysis. The synthesized AuNPs exhibited strong antibacterial activity against a range of clinical bacterial isolates, including resistant and multidrug-resistant strains. Notably, no difference in activity was observed between resistant and non-resistant *Enterococcus* strains (Fig. 1b), indicating the absence of the selectivity typically associated with conventional antibiotics. Furthermore, bacteria did not develop resistance after forced incubation with AuNPs for 15 days, highlighting an additional advantage of these materials. High antiviral activity was also observed against both enveloped (phi6) and non-enveloped (MS2) viruses, as well as antifungal activity against *C.parapsilosis*, with the same mechanism of action confirmed by SEM and TEM analyses (Fig.1c).

Conclusion

These results demonstrate that functionalized AuNPs represent a promising broad-spectrum antimicrobial platform with high activity against bacteria, viruses, and fungi. Their contact-based mechanism and the absence of resistance development highlight their potential as alternative antimicrobial agents for combating antimicrobial resistance.

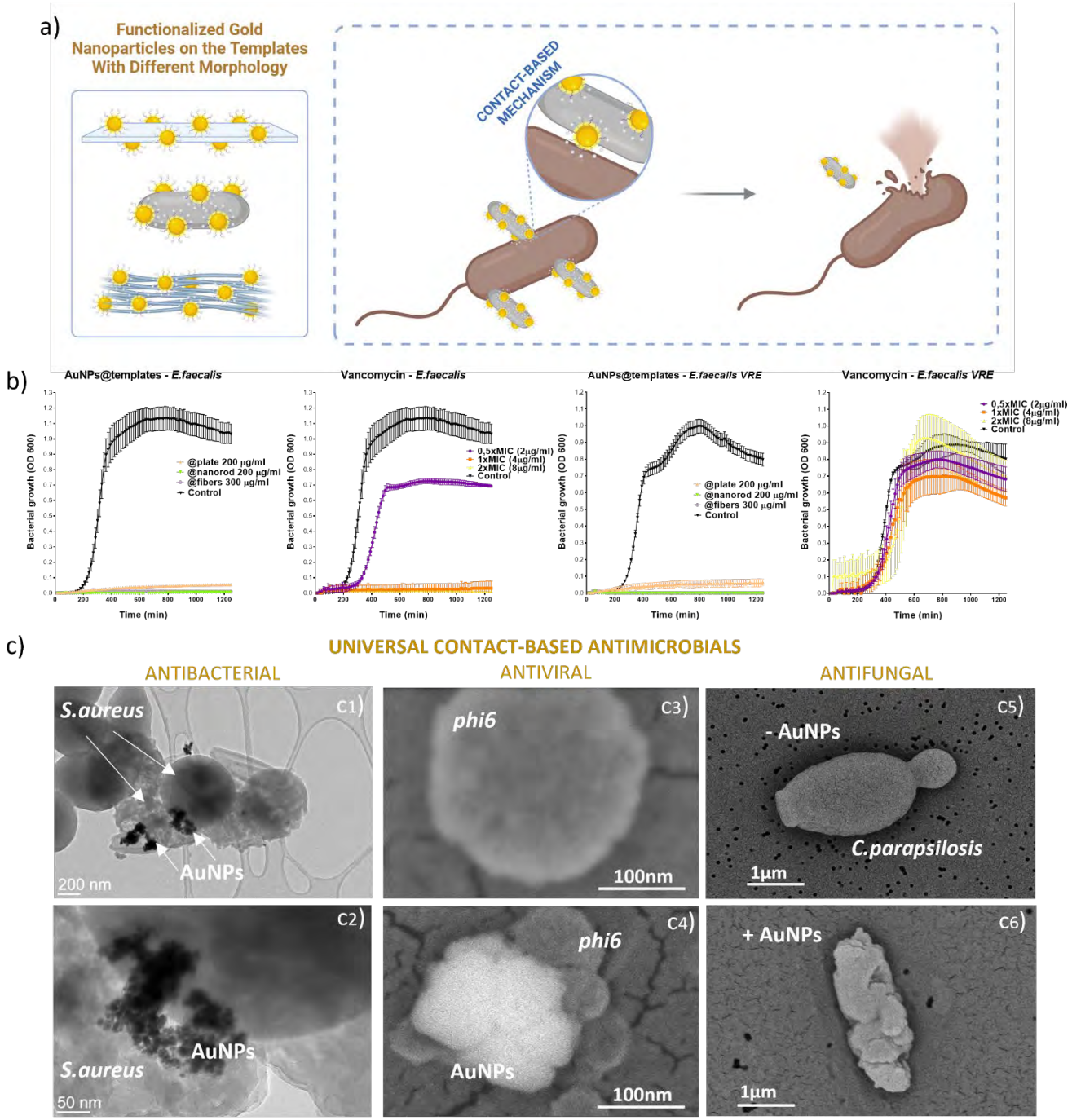

Figure 1. Contact-based mechanism of functionalized AuNPs on different templates (a); antibacterial activity of AuNPs against *E.faecalis* and *E.faecalis VRE* compared to vancomycin (b); observed TEM and SEM interactions between antimicrobials and AuNPs (c): TEM of *S.aureus* vs AuNPs (c_{1-2}), SEM of phi6 vs AuNPs (c_{3-4}) and SEM morphology of *C.parapsilosis* with and without incubation with AuNPs (c_{6-7}).

Acknowledgements

This research was funded by Slovenian Research and Innovation Agency within grants, J3-4531, PR-12591 and P2-0091 and Regenesis project No. PR-13605.

References

[1] Vukomanović M., Škapin S.D., Suvorov D. Functionalized hydroxyapatite/gold composites as "green" materials with antibacterial activity and the process for preparing and use thereof. European patent office 2018; EP2863751A1.
[2] Vukomanović M., Žabčić M, Gazvoda L., Spreitzer M., Podlogar M., Georgieva S., Jančić.U.. A contact-based antimicrobial preparation, methods for the preparation of said antimicrobial preparation and uses thereof. European patent office 2025; patent application EP25218520.2.

S51 – O2

Sustainable lignin nanoparticles empowered by gallate-oriented surface chemistry engineering for targeted antibacterial activity

Lu Z.[1], Wang X.[1,2]
[1]Dept. of Engineering and Information Technology, Laboratory of Natural Materials Technology, Åbo Akademi University; [2]Dept. of Natural and Health Sciences Pharmaceutical Sciences Laboratory, Åbo Akademi University, Turku, Finland

Introduction

Antibacterial nanomaterials provide a non-antibiotic alternative to conventional antibiotics by exploiting nanoscale physicochemical properties to promote biofilm targeting and penetration while potentially bypassing classical resistance pathways. Lignin, the most abundant aromatic biopolymer in plant biomass and widely available from biorefinery side streams, represents an attractive precursor for antibacterial nanomaterials due to its intrinsic polyphenol-derived antibacterial activity and favorable biocompatibility. Lignin nanoparticles (LigNPs) can readily form through amphiphilicity-driven self-assembly; however, their formation is governed by complex noncovalent interactions among heterogeneous lignin moieties, leading to condition-dependent assembly and limited control over surface chemistry. Thus, this constrains the translational potential of LigNPs for clinical applications, given that surface attributes are key determinants of nanoparticle-bacteria and nanoparticle-biofilm interfacial interactions. To overcome this challenge, we propose a gallate-oriented surface engineering strategy to tailor LigNP surface chemistry and enhance antibacterial and antibiofilm performance.
A benchmark library consisting of gallic acid, three alkyl gallates, and tannic acid was screened to modulate surface chemistry and amphiphilic balance in the engineered corona composition. The aim is to elucidate the relationship between surface chemistry and bactericidal activity, enabling the rational design of selective antibacterial nanomaterials from naturally derived polyphenolic biopolymers.

Materials and Methods

An alkaline lignin derived from wheat straw was used as the starting material. The synthesis to all-polyphenol NPs involves three sequential steps: (a) preparing boronated lignin by grafting aminophenylboronic acid (APBA) via amidation; (b) fabricating boronated lignin nanoparticles (BLigNPs) through antisolvent nanoprecipitation; (c) engineering the corona composition of BLigNPs with gallate derivatives (GDs) via the reversible boronate-ester formation between boronic acid and pyrogallol. *In vitro* bioassays were conducted to evaluate the antibacterial and antibiofilm activities of five types of BLigNP-GD nanoparticles. Cytocompatibility was assessed using *in vitro* cultures of normal human dermal fibroblasts, and biosafety was examined through *in vivo* acute toxicity tests in zebrafish embryos.

Results

Gallate-oriented surface engineering enabled precise modulation of BLigNP surface chemistry and bactericidal activity. Tannic-acid-functionalized nanoparticles (BLigNP-TA) showed the lowest lethal concentration against Gram-positive *S. aureus*, attributed to enriched redox-active pyrogallol groups in the corona. Propyl gallate-engineered nanoparticles (BLigNP-PG), exhibiting balanced amphiphilicity, demonstrated strong antibacterial activity against both Gram-negative *E. coli* and Gram-positive *S. aureus*. BLigNP-PG interacted effectively with distinct bacterial envelope structures through a non-specific, multi-target contact-killing mechanism and displayed enhanced association and transport within biofilms. Importantly, BLigNP-PG showed good fibroblast compatibility and negligible toxicity in zebrafish embryos, highlighting its potential as a selective broad-spectrum antibacterial nanomaterial.

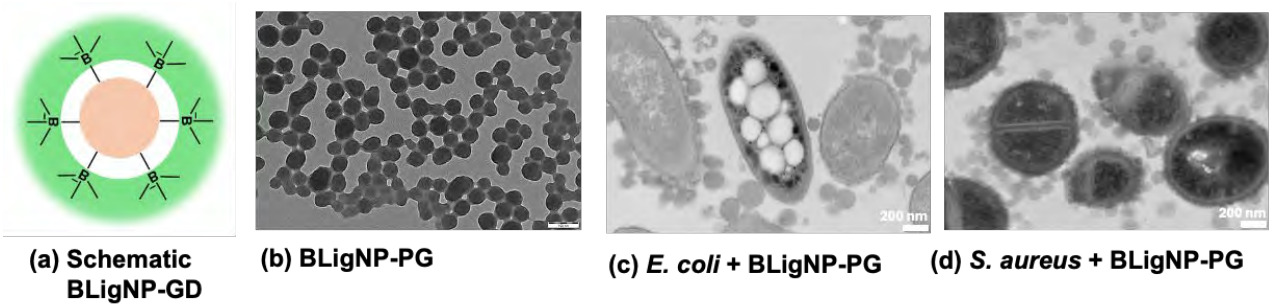

(a) Schematic BLigNP-GD **(b) BLigNP-PG** **(c) *E. coli* + BLigNP-PG** **(d) *S. aureus* + BLigNP-PG**

Figure 1: (a)Shematic structure of BLigNP-GD with lignin core and GD corona; TEM images of (b) nanoparticles of BLigNP-PG, (c) coculture of *E. coli* + BLigNP-PG, and (d) coculture of *S. aureus* + BLigNP-PG

S51 – O3

Fighting bacterial colonization of hydroxyapatite: The role of nanotopography and plasma-treated liquids

Ruiz-Sorribas A.[1,2,3], Tampieri F.[1,2], Canal C.[1,2], Ginebra M.P.[1,2,3]
[1]Biomaterials, Biomechanics and Tissue Engineering Group, Dept. of Materials Science and Engineering and Institute for Research and Innovation in Health (IRIS), Universitat Politècnica de Catalunya, Barcelona; [2]Barcelona Research Center in Multiscale Science and Engineering, Universitat Politècnica de Catalunya, Barcelona; [3]Centro de Investigación Biomédica en Red – Bioingenería, Biomateriales y Nanomedicina (CIBER-BBN), Instituto de Salud Carlos III, Madrid, Spain

Introduction

The rise of antimicrobial resistance in implant-associated infections calls for antibiotic-free preventive strategies. Firstly, we developed calcium-deficient hydroxyapatite (CDHA) materials with a high aspect ratio nanotopography, i.e. nano-needles, which impose mechanical and oxidative stress on adhering bacteria[1,2]. Second, we used cold atmospheric plasma to generate reactive oxygen and nitrogen species in the culture media, including long-lived H_2O_2 and NO_2^-, capable of inducing cellular damage[3,4].

Aim

Our objective is to combine the mechano-bactericidal properties of the CDHA nano-needle topography with the oxidative stress induced by plasma-derived RONS. The goal is to create a bioactive scaffold that simultaneously promotes bone regeneration while providing an antibiotic-free defence against implant-associated infections.

Materials and Methods

CDHA disks, either with a flat or a high-aspect-ratio nanotopography surface, were obtained by hydrolysis of alpha-tricalcium phosphate. A *Pseudomonas aeruginosa* PAO1 with constitutive green fluorescent protein (GFP) expression was cultured on the CDHA disks submerged in buffered DMEM that was either previously treated with argon plasma using a kINPen IND (Neoplas, Germany) or supplemented with H_2O_2 or $NaNO_2$. Viable attached bacteria were quantified at 24 hours with colony counting for dose-effect studies. The GFP produced was monitored during 24 hours with spectrophotometer for growth kinetics. And confocal microscopy samples were stained with propidium iodide for live/dead analyses.

Results

The antibacterial effect was dependent to the dose applied. Compared to flat disks, the combination of nanotopography and H_2O_2 resulted in a more pronounced effect at 24 hours (Fig. 1A). Plasma-treated medium delayed further the bacterial growth on nanotopography (Fig. 1B). And the confocal microscopy images show a reduced coverage of bacteria when using the nanotopography disks in combination with plasma-treated medium and H_2O_2 (Fig. 2).

Conclusion

These results highlight the potential synergy between high aspect ratio nanotopographies and plasma-treated liquids to prevent infections associated to synthetic bone grafts, while also providing a useful model to investigate their antibacterial mechanism.

Acknowledgements

European Research Council, project 101055053 (BAMBBI). Inst. Salud Carlos III and Next Generation EU funds, project IHRC22/00003 SELLO EXCEL. ISCIII-HEALTH. Maria de Maeztu CEX 2023-001300-M/AEI/10.13039/501100011033. CC and MPG acknowledge the ICREA Academia Award by the Generalitat de Catalunya.

References

1. Iglesias-Fernandez M., Buixadera-Palomero J., et al. Implementation of bactericidal topographies on biomimetic calcium phosphates and the potential effect of its reactivity. *Biomaterials Advances* 2022; 136; 212797.
2. Diez-Escudero A., Espanol M. & Ginebra M.P. High-aspect-ratio nanostructured hydroxyapatite: towards new functionalities for a classical material. *Chemical Science* 2024; 15; 55-76.
3. Labay C., Hamouda I., et al. Production of reactive species in alginate hydrogels for cold atmospheric plasma-based therapies. *Scientific Reports* 2019; 9; 16160.

4. Espona-Noguera A., Tampieri F. & Canal C. Engineering alginate-based injectable hydrogels combined with bioactive polymers for targeted plasma-derived oxidative stress delivery in osteosarcoma therapy. *International Journal of Biological Macromolecules* 2024; 257; 128841.

Figures

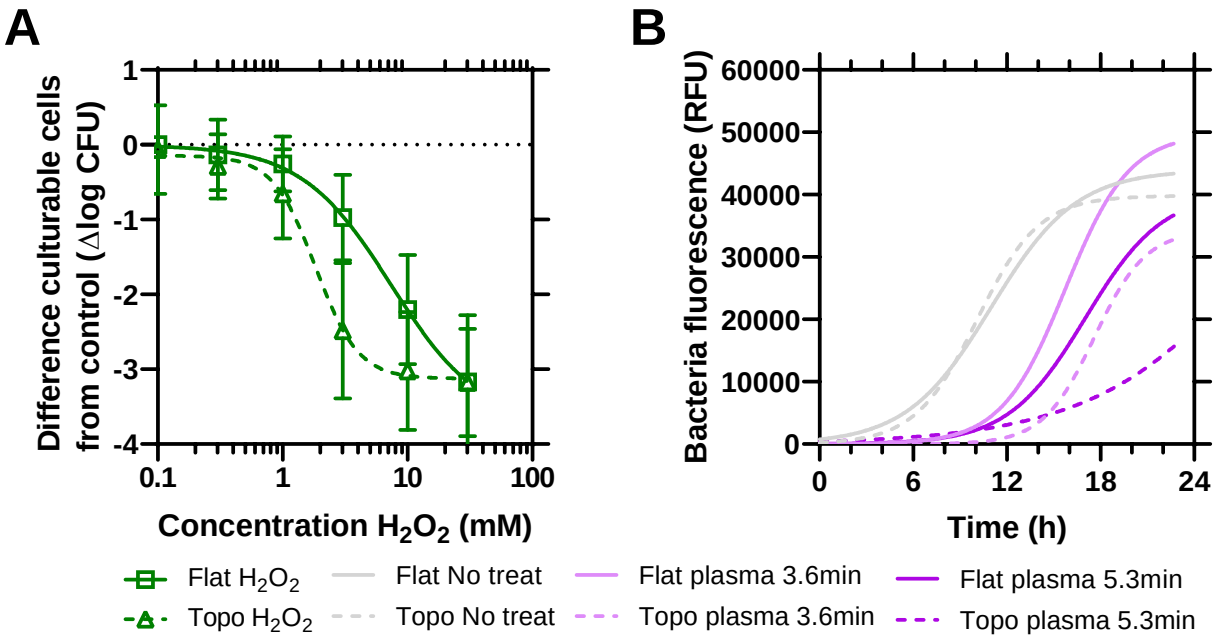

Figure 1. Dose-effect curves at 24 hours with H_2O_2 (A) and growth kinetics during 24 hours with plasma-treated medium (B) on flat (straight line) or topography (dotted line) surfaces.

Figure 2. Confocal microscopy with plasma-treated medium (A, B) or H_2O_2 (C, D) on flat (A, C) or topography (B, D) surfaces showing live (green) and dead (red) bacteria.

S51 – O5

Antimicrobial fibrinogen nanofiber scaffolds via nanoparticle integration

Dierker L.[1], Apel F.[1], Joseph J.[2], Kallepalli B.[2], Gätjen L.[3], Grunwald I.[1], Brüggemann D.[1]
[1]Hochschule Bremen - City University of Applied Sciences, Bremen; [2]University of Bremen; [3]Fraunhofer Institute for Manufacturing Technology and Advanced Materials IFAM, Bremen, Germany

Introduction

Wound infections present a significant clinical challenge, requiring advanced biomaterials with antimicrobial capabilities. Fibrinogen nanofibers have emerged as promising scaffolds for tissue engineering due to their biocompatibility and ability to support cell growth while mimicking the mechanical properties of fibrin clots [1, 2, 3]. However, fibrinogen itself does not exhibit intrinsic antibacterial properties, necessitating additional antimicrobial strategies.

Aim

We investigated how different antimicrobial metal/-oxide nanoparticles (NPs) can be incorporated into fibrinogen nanofibers to enhance their antibacterial properties against gram-positive and gram-negative bacteria.

Materials and Methods

First, the antimicrobial efficacy of aluminium oxide (Al_2O_3), copper (Cu), silver (Ag), and zinc oxide (ZnO) NPs in dispersion was evaluated via inhibition assays to identify effective concentrations for scaffold integration. Bare fibrinogen nanofibers were produced by salt-induced self-assembly [3]. Three NP integration methods were studied: co-assembly with fibrinogen and the post-treatment of fibrinogen scaffolds via the addition of NPs in droplets or in a sonication bath. Scaffold morphology and NP distribution were characterized by scanning electron microscopy (SEM). Scaffolds with evenly distributed NPs and preserved fiber architecture were used to analyze the antimicrobial activity against gram-positive *Staphylococcus cohnii* and *Bacillus subtilis*, and gram-negative *Escherichia coli.* Antimicrobial efficacy was assessed with infiltration tests, SEM imaging, an adapted ISO standard (22196), and live/dead staining.

Results

Ag NP–modified fibrinogen nanofiber scaffolds exhibited strong antibacterial activity against gram-negative *E. coli* in infiltration tests, but a negligible effect against both gram-positive bacteria. These scaffolds were successfully produced via co-assembly, yielding uniformly distributed 10 nm Ag NPs without impairing fibrinogen nanofiber assembly at concentrations of 0.01 and 0.03 mg/mL. In contrast, when Al_2O_3 and Cu NPs were used for co-assembly or post-treatments, they formed clusters, crystallized, or inhibited fiber assembly at concentrations required for bacterial growth inhibition. ZnO NPs (25 - 35 nm) were successfully incorporated via post-sonication at concentrations of 0.5 mg/mL (Fig. 1a). ZnO-modified fibrinogen scaffolds showed moderate antibacterial effects against the gram-positive bacteria *S. cohnii* and *B. subtilis* (Fig. 1b) and only a limited antibacterial effect against gram-negative *E. coli*. Results from the different assays further suggest that the antimicrobial efficacy of the studied NPs depends on environmental conditions, such as aqueous or dry surroundings.

Conclusion

This work enabled the development of fibrinogen-based scaffolds that combine biomimetic nanofiber architecture with antimicrobial functionality for wound healing applications. Future studies will focus on cytocompatibility and NP release to optimize scaffold performance.

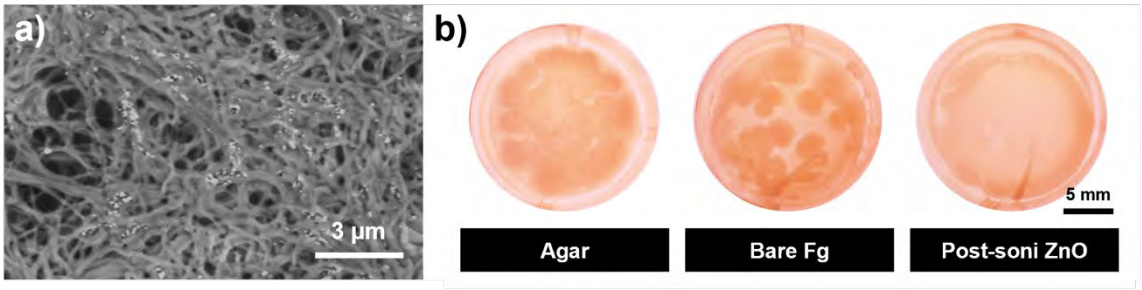

Fig. 1: Antibacterial efficacy of fibrinogen nanofibers modified with ZnO NPs. a) SEM image of ZnO-fibrinogen scaffolds prepared by post-sonication; individual NPs are visible as bright dots within the fiber network. b) Growth of *B. subtilis* colonies during the infiltration test. Colonies were observed on the control (agar only) and on bare fibrinogen (Fg) scaffolds, whereas no colonies were detected on ZnO-modified scaffolds prepared by post-sonication.

References

1. Joshi A., Nuntapramote T., Brüggemann D. Self-Assembled Fibrinogen Scaffolds Support Cocultivation of Human Dermal Fibroblasts and HaCaT Keratinocytes, *ACS Omega* 2023, 8, 9, 8650–8663
2. Kenny M., Stamboroski S., Taher R., Brüggemann D., Schoen I., Nanofiber Topographies Enhance Platelet-Fibrinogen Scaffold Interactions. *Adv. Healthcare Mater*. 2022, 11, 2200249
3. Strunk T., Joshi A., Moeinkhah M., Renzelmann T., Dierker L., Grotheer D., Graupner N., Müssig J., Brüggemann D. Structure, Properties and Degradation of Self-Assembled Fibrinogen Nanofiber Scaffolds *ACS Appl. Bio Mater.* 2024, 7, 9, 6186–6200

S51 – O5

Nano-boosted antibiotic therapy: Chitosan–cyclodextrin nanoparticles for diabetic foot treatment

Górska-Ratusznik A.[1], Czajkowski J.[1,2], Barzowska-Gogola A.[1], Budziaszek J.[1], Staniszewska-Ślęzak E.[1], Pucelik B.[1]

[1]Łukasiewicz Research Network, Kraków Institute of Technology; [2]Dept. of Biomaterials and Composites, Faculty of Materials Science and Ceramics, AGH University of Krakow, Poland

Introduction

Diabetic foot syndrome is a severe complication of diabetes mellitus, characterized by chronic wounds and an elevated risk of infection, which can result in amputation. The treatment of such infections is challenging due to limited drug penetration, impaired tissue regeneration, and increasing bacterial resistance to antibiotics. Nanotechnology-based drug delivery systems offer a promising solution, improving the stability, bioavailability, and efficacy of therapy. Chitosan nanoparticles have been shown to possess antibacterial properties and biocompatibility, while cyclodextrins have been demonstrated to enhance the solubility and encapsulation efficiency of active ingredients.

Aim

The objective of the present study was to develop and characterize chitosan–cyclodextrin nanoparticles co-loaded with an antibiotic and an adjuvant, and to evaluate their physicochemical properties, antibacterial activity, and cytotoxicity.

Materials and Methods

The preparation of Chitosan–cyclodextrin nanoparticles involved anionic gelation using sodium triphosphate, with simultaneous loading of an antibiotic and an adjuvant. The resulting systems were characterized in terms of particle size (DLS), zeta potential, morphology (TEM) and FTIR analysis. The stability of the nanoparticles over time and the release profile of the active substances were also evaluated. The antibacterial activity of the samples was assessed by determining the minimum inhibitory concentration (MIC) against a selection of bacterial strains, including *E. coli*, *P. aeruginosa*, *A. baumannii*, and *S. aureus*. Cytotoxicity was assessed using human skin cells (HaCaT cell line).

Results

The obtained results confirmed the successful synthesis of nanoparticles with an average size of approximately 50 nm, as verified by DLS and TEM. Zeta potential analysis indicated the stability of the systems, while FTIR studies confirmed the presence of interactions between the nanoparticle components. The resulting systems demonstrated stability over time and controlled release of the loaded substances. The nanoparticles demonstrated notable antibacterial activity against the tested strains, effectively impeding their growth. Concurrently, no substantial evidence of cellular toxicity was observed in the HaCaT cell line, thereby suggesting their favorable biocompatibility.

Conclusion

The development of chitosan–cyclodextrin nanoparticles co-loaded with an antibiotic and an adjuvant represents a promising drug delivery system with potential applications in the treatment of bacterial infections associated with diabetic foot. The results obtained demonstrate their high antibacterial efficacy while maintaining good biocompatibility. The proposed approach may contribute to increasing the effectiveness of therapy and serve as a basis for further research into modern treatment strategies for hard-to-heal wounds.

Acknowledgements

This work is supported by National Science Centre NCN SONATA-19 grant no. 2023/51/D/NZ7/02596

S52
Novel treatment approaches for nerve repair and functional regeneration

S52 – K1
Cell secretome and biodegradable biomaterials for nervous tissue regeneration

Salgado A.
ICVS, School of Medicine, University of Minho – Portugal
[1]Life and Health Sciences Research Institute (ICVS), School of Medicine, University of Minho, Braga; [2]ICVS/3Bs PT Associated Lab, Braga/Guimarães, Portugal

The low regeneration potential of the central nervous system (CNS) represents a challenge for the development of new therapeutic strategies. Mesenchymal stem cells (MSCs) have been proposed as a possible therapeutic tool for CNS disorders, namely due to the beneficial actions of their secretome. Indeed, the latter possesses a broad range of neuroregulatory factors that promote an increase in neurogenesis, inhibition of apoptosis/glial scar, immunomodulation, angiogenesis, neuronal and glial cell survival, as well as relevant neuroprotective actions into different pathophysiological contexts. Considering their protective action in lesioned sites, MSCs, and their secretome, might also improve the integration of local progenitor cells in neuroregeneration processes. In this sense their use could represent an important vehicle for the establishment of future CNS regenerative therapies. Previously we have shown that the administration of MSCs secretome in pre-clinical models of spinal cord injury (SCI) and Parkinson's Disease (PD) led to important motor and histological improvements. In order to further improve this, in the present talk we will discuss and present the outcomes of the combinatory use of MSCs secretome and biodegrable biomaterials, particularly self-assembling peptides, lypossomes and hydrogels in in vitro and in vivo models of SCI and PD.

S52 – O1
Bioengineering hope: Emerging technologies for nerve gap regeneration

Madduri. S
[1]University of Gevena, Bioengineering and Neuro-regeneration, Dept. of Surgery, Faculty of Medicine

Repairing nerves and regenerating axo-glial tissues remain critical yet challenging, often leading to functional impairment and pain. Axonal growth and guidance are influenced by a variety of factors, including neurotrophic agents, topographical cues, cellular components, and the surrounding tissue microenvironment. Developing effective therapies for neuro-muscular tissue regeneration demands innovative and integrative strategies. This lecture will present evidence supporting bioengineering approaches that combine these critical factors to enhance axonal growth and guidance, ultimately achieving functional restoration of neuromuscular tissue and paving the way for advanced therapeutic medicinal products

S52 – O2
In vivo validation of a 3D ex vivo nerve Injury model

Taylor C.S.[1], Field J.[2], Behbehani M.[1], Haycock J.W. [1], Boissonade F.M.[2], Claeyssens F.[1]
[1]School of Chemical, Materials and Biological Engineering, University of Sheffield; [2]School of Clinical Dentistry, University of Sheffield, UK

Introduction
Animal models have long been the cornerstone of peripheral nerve regeneration research, providing critical insights into repair mechanisms and the evaluation of biomaterials for nerve guidance conduits (NGCs). However, animal testing raises ethical and physiological concerns. In light of recent legislation, there is a clinical need for more New Approach Methodologies (NAMs), that reduce and replace the use of animal testing in research. Here, we present a three-dimensional *ex vivo* model of nerve regeneration, validated *in vivo*, to reduce the numbers of animals used in NGC research.

Methods
Polycaprolactone (PCL) (80,000 g/mol) was manufactured into fibres using electrospinning. NGCs were also produced from PCL using microstereolithography. Fibres were modified using air plasma, and modification was confirmed via XPS. Chick Dorsal Root Ganglion (DRG) bodies were extracted and explanted whole on to the ends of a 3D fibre testing method and labelled for β III tubulin, and S100β after culture. Fibre-filled conduits, modified and unmodified, were implanted into 3 mm common fibular nerve injury gaps in YFP+ mice models. Regenerated nerves were harvested an imaged to quantify sprouting index.

Results
PCL fibres, produced via electrospinning, were manufactured into a range of fibre diameters for testing. Aligned fibres were successfully threaded into 3D printed NGCs, in which fibre alignment, and density, through conduits was confirmed via microCT. Fibres were modified with air plasma successfully. Ex vivo studies confirmed the most efficient fibre diameter, promoting DRG axonal outgrowth, was 10 µm, most optimum density was 20% and that air plasma modification significantly improved neuronal cell outgrowth. Plasma-treated fibre-filled conduits supported nerve regeneration and achieved a higher success rate of regeneration compared to the other graft repairs.

Conclusions
Aligned fibre scaffolds fibres are very promising in aiding nerve regeneration after injury. They also provide an ideal scaffold for developing nerve injury models. A 3D chick DRG *ex vivo* model, offers many advantages as a nerve injury model, such as high throughput of testing materials and therapies for nerve repair. This study highlights the importance of plasma treatment on fibres for nerve regeneration *in vivo*, but confirms the validation of the *ex vivo* model developed.

S52 – O3

iPSC neural differentiation on biostable sulfuric acid-treated PEDOT: PSS under electrical stimulation

Garrudo F.F.[1,2,3,4], Rodrigues C.A.V.[2,3], Resina L.[5,6], Vaz S.[7], Estrany F.[5,6], ES Nogueira D.[2,3], Alemán C.[5,6,8], Cabral J.M.S.[2,3], Morgado J.[1], Ferreira F.C.[2,3]
[1]Dept. of Bioengineering, Instituto Superior Técnico, Universidade de Lisboa and Instituto de Telecomunicações, Portugal; [2]Dept. of Bioengineering and iBB, Institute for Bioengineering and Biosciences, Instituto Superior Técnico, Universidade de Lisboa, Portugal; [3]Associate Laboratory i4HB, Institute for Health and Bioeconomy, Portugal; [4]Dept. of Brain and Cognitive Sciences, Picower Institute for Learning and Memory, Massachusetts Institute of Technology, USA: [5]IMEM-BRT Group, Dept. d'Enginyeria Química, EEBE, Universitat Politècnica de Catalunya, Barcelona, Spain; [6]Barcelona Research Center in Multiscale Science and Engineering, Universitat Politècnica de Catalunya, Barcelona, Spain; [7]Instituto de Medicina Molecular João Lobo Antunes & Instituto de Farmacologia e Neurociências, Faculdade de Medicina, Universidade de Lisboa, Portugal; [8]Institute for Bioengineering of Catalonia (IBEC), The Barcelona Institute of Science and Technology, Spain

Introduction

There is a need to produce reliable in vitro models to fuel the transition away from in vivo models for drug screening. We can create reliable in vitro models by combining iPSCs, electroconductive polymers (e.g. poly(ethylenedioxythiophene):poly(styrene sulfonate)(PEDOT:PSS) and electrical stimulation (ES). Nevertheless, the effects of ES on iPSC neural differentiation remain unclear.

Aim

Develop highly electroconductive and biostable PEDOT:PSS substrates to study the effects of ES on iPSC neural differentiation, focusing on days 1-17 (early stage) and 18-50 (late stage).

Materials and Methods

Two formulations containing different ratios of PEDOT:PSS (Clevios™ PH 1000 and CleviosTM P VP AI 4083) were used to prepare thin films by spin-coating (samples PH1000 and AI4083). Samples were treated with sulfuric acid to remove PSS and induce the formation of a highly crystalline PEDOT-rich film. The obtained films' physico-chemical properties were evaluated, including stability when incubated in PBS at 37 ºC and 5 % CO_2; loss of electroactivity (LEA) and adsorption of the adhesion protein laminin (LN). The biocompatibility was evaluated through a proliferation assay with iPSCs, followed by 5 consecutive passages and an EB assay for sample PH1000+ES. Sample PH1000 was used to study the effect of 4 different ES protocols (1 V cm^{-1}, 100 Hz, every 12 h) on early stage neural differentiation. An optimized protocol was used to study late stage neural differentiation.

Results

We obtained highly electroconductive films, with electroconductivity values ranging between 338 – 1,076 S cm^{-1} for sample PH1000 and 0.8 – 4.0 S cm^{-1} for sample AI4083. We found no changes in the electroconductivity of sample PH1000 when incubated for 30 days in pseudo-physiological conditions, unlike sample PH1000. We also found sample PH1000 to be the most electrochemically stable (14.9 ± 1.7 % loss after 200 cycles vs 47.6 ± 1.9 % for AI4083). Finally, both samples AI4083 and PH1000 allowed extensive LN adsorption when compared with pristine glass. Cultured iPSCs on PH1000 (without and with ES) kept their pluripotency potential after 7 days and 3 passages. Further evaluation of initial neural differentiation (days 0 to 17) showed a positive effect of ES when applied between days 1 and 12, by improving neurite/axon extension, increasing neural rosette number, and maintaining the anterior/forebrain lineage. The final evaluation of long-term neural differentiation (days 0 to 50) showed a synergistic effect of ES and BrainPhys media on neuronal differentiation and functionality.

Conclusion

The results obtained complement the current understanding of the effect of ES on neuronal fate/differentiation, and direct the path for new hypotheses and studies aimed at neural regeneration and/or the design of reliable in vitro models to study, for example, neurodegenerative diseases.

Acknowledgements
The authors acknowledge dedicated funding from Fundação para a Ciência e a Tecnologia (FCT) through project BioMaterARISES (EXPL/CTM-CTM/0995/2021, DOI: 10.54499/EXPL/CTM-CTM/0995/2021). The authors also acknowledge funding provided by FCT through IT (UIDB/50008/2025, doi.org/10.54499/UID/50008/2025), iBB (UID/BIO/04565/2026), *Laboratório -Associado* I4HB (LA/P/0140/2020). FFFG also acknowledges the support of *Fundación "la Caixa"* through an individual fellowship. LR, FE and CA thank the PID2021-125767OB-I00 project, as well as the Maria de Maeztu Units of Excellence Programme CEX2023-001300-M, both funded by MCIN/AEI /10.13039/501100011033. Support for the research of C.A. was also received through the prize "ICREA Academia" for excellence in research funded by the Generalitat de Catalunya.

Target topics:

- Polymeric Biomaterials – Synthetic
- Smart and Stimuli-Responsive Biomaterials
- Biomaterial-Engineered Microphysiological Systems for Disease Modeling and Regeneration
- Stimuli-Responsive Biomaterials and Direct Biophysical Stimulation for Regenerative Medicine

S52 – O4

Dynamic alginate-based hydrogels for modulating neural cell function

Mariano A.[1], . Raucci M.G.[2], Gomez d'Ayala G.[3], Lazzarini C.[3], Benfenati V.[1], Ambrosio L.
[1]Institute of Polymers, Composites and Biomaterials, National Research Council of Italy (IPCB-CNR), Naples; [2]Institute of Polymers, Composites and Biomaterials, National Research Council of Italy (IPCB-CNR), Pozzuoli; [3]Institute for Organic Synthesis and Photoreactivity, National Research Council of Italy (ISOF-CNR), Bologna, Italy

Introduction

Hydrogels based on natural polysaccharides are widely explored as biomimetic systems for neurological applications due to their similarity to the extracellular matrix. Their physicochemical properties—such as wettability, surface charge, and stiffness regulate protein adsorption and, consequently, cell adhesion, proliferation, and differentiation. In this work, alginate-based hydrogels were tuned by varying crosslinking time and alginate/gelatin ratios to modulate their chemical–mechanical properties. Understanding these effects plays a key role in developing advanced *in vitro* models and biomaterials for neurodegenerative disease research and neural tissue engineering.

Materials and Methods

Alginate-based hydrogels were prepared as 2D substrates via solvent casting and ionically crosslinked with $CaCl_2$ or $ZnCl_2$/$MgCl_2$ at different incubation times (15, 30, and 45 min) to modulate network structure and stiffness. In parallel, alginate–gelatin type B blends (100/0, 75/25, 50/50, 25/75) were chemically crosslinked using EDC/NHS, enabling comparison between ionic and covalent systems. Hydrogels were characterized for physicochemical (FTIR-ATR, TGA, swelling, degradation, contact angle), mechanical (tensile, rheological), and morphological (AFM, SEM) properties. Biological response was evaluated using SH-SY5Y cells and primary astrocytes, focusing on adhesion, proliferation, differentiation, and functional behavior, with particular attention to astrocyte responses to matrix cues.

Results

Alginate hydrogels crosslinked with divalent ions (Ca^{2+}, Zn^{2+}, Mg^{2+}) showed tunable physicochemical and mechanical properties. Calcium-crosslinked hydrogels (AlgCa) enhanced astrocyte viability and calcium signaling. FTIR confirmed Na^{+}/Ca^{2+} exchange, while increased crosslinking reduced swelling and increased stiffness, with AlgCa45 exhibiting the highest Young's modulus and storage modulus (G′). All substrates remained stable (<10% degradation). Biologically, AlgCa supported astrocyte and SH-SY5Y adhesion and proliferation. Greater crosslinking and surface roughness promoted integrin clustering, cytoskeletal reorganization, and accelerated astrocyte differentiation, with early GFAP upregulation on AlgCa45. Neuronal differentiation was also enhanced, with the formation of neurite-like extensions and β-tubulin expression. Alginate–gelatin blends further modulated topography and cell response. Gelatin increased roughness, while intermediate compositions (Alg50–Alg75) promoted earlier astrocyte differentiation and maturation, underscoring the combined role of crosslinking density and matrix composition in regulating neural cell behavior.

Conclusions

Alginate-based hydrogels provide tunable platforms for neural applications, where crosslinking and composition regulate cell behavior. Calcium-crosslinked systems, particularly AlgCa45, and alginate–gelatin blends enhance astrocyte differentiation and neuronal maturation, highlighting the role of matrix properties in neural tissue engineering and neurodegenerative applications.

Acknowledgements

This study was supported by AFOSR (USA Air Force Office of Scientific Research) through the project ASTROSENSE – "Astrocytes neural network multiscale response to extracellular sensing cues" (G.A. nr. FA9550-25-1-0001).

S52 – O5

Multifunctional chitosan/cellulose neural interfaces with tunable electrochemical properties

Alex M.[1], Al Othman[2], AlSayah[3], Nashash[4]
[1]Biosciences & Bioengineering Graduate Program; [2]Dept. of Chemical & Biology Engineering B.; [3]Dept. of Biology, Chemistry & Environmental Sciences; [3]Dept. of Electrical Engineering, American University of Sharjah, Sharjah, UAE

Introduction

Many existing conventional neural electrodes are rigid, expensive, and often mechanically and biologically incompatible with soft tissue for implantable applications. Therefore, there exists a high demand for flexible, sustainable, and biocompatible alternatives, particularly for neural interfacing applications. Although, to some extent, conductive polymers like PEDOT and PANI have demonstrated considerable electromechanical properties suitable for these kinds of applications, they may also induce cytotoxicity and mechanical incompatibility. Thus, in recent years, alternative materials derived from natural polymers have been used to synthesize flexible bioelectrodes, including polymers, nanomaterials, carbon-based materials, natural biopolymers, and hydrogels. The rising demand for greener, cost-effective alternatives, such as cellulose, lignin, and chitosan, offers high biocompatibility, tissue conformability, and flexibility but often lacks electrical conductivity. Therefore, developing flexible, conductive, and biocompatible polymer-based bioelectrodes is essential for seamless integration with biological systems. In this study, we propose a hydrogel-based bioelectrode that integrates cellulose and chitosan to form a flexible, functional, and self-healing conductive network. In the proposed study, a simple one-pot fabrication protocol has been used to develop a hydrogel from cellulose and chitosan.

Aim

The main purpose of this study is to develop a multifunctional chitosan/cellulose-based neural interface with tunable electrochemical behavior.

Materials and Methods

A natural polymer-based hydrogel network was developed by combining the oppositely charged natural polymers cellulose and chitosan to form an ionically conductive structure. The design focuses on imparting mechanical integrity, ionic conductivity, and biocompatibility.

The fabrication method included physically crosslinking cellulose and chitosan at a temperature. Aqueous nanocellulose solution (3 wt.%) was mixed with alpha cellulose powder and glycerol. This solid mix was then combined with a chitosan solution prepared by dissolving chitosan in 5% acetic acid with KCl. The gel formed was heat-stirred at 60 °C for about 20 minutes. Then, degassing was performed to remove the air bubbles. Finally, the gel was poured into predefined molds and cured at room temperature for about 72 hours. Thus, forming an ionically conductive cellulose/chitosan hydrogel.

Results

In previous early-stage studies assessing the electrochemical characteristics of natural polymer-based bioelectrodes, promising results were obtained with natural polymers such as cellulose and chitosan. In the first study, we synthesized 8 different compositions of polydimethylsiloxane (PDMS), glycerol, and α-cellulose using PDMS as the substrate. The optimal composition, consisting of 30% cellulose, 64% PDMS, and 6% glycerol, exhibited the highest conductivity of 0.0193 S m−1 and a charge storage capacity of 4.626 mC m^{-2}. To further enhance conductivity and functionalize natural polymers for flexible electrode applications, a gelatin/α-cellulose hydrogel was investigated, inspired by previous studies based on gelatin/PDMS. Overall, the electrical characterization of the hydrogel showed a considerable ionic conductivity with the cellulose/chitosan hydrogel network.

Table-1 Comparison of the electrochemical properties of the current study with the literature

Sample material	Conductivity	Ref.
α-cellulose/nanocellulose/Chitosan	*5.75±1.25 Sm^{-1}*	*This work*
PEDOT: PSS/PAA	*247 Scm^{-1}*	*[1]*

Sulfobetaine-methacrylate/methacrylic acid/TEMPO-oxidized cellulose nanofibers/ sodium alginate, LiCl	*0.49 ± 0.05 S m^{-1}*	*[2]*
Nanocellulose-Polypyrrole	*2.4 ± 1.5 S/cm*	*[3]*
PEDOT: PSS/PVA/PAA-NHS/CTS	*9 Sm^{-1}*	*[4]*

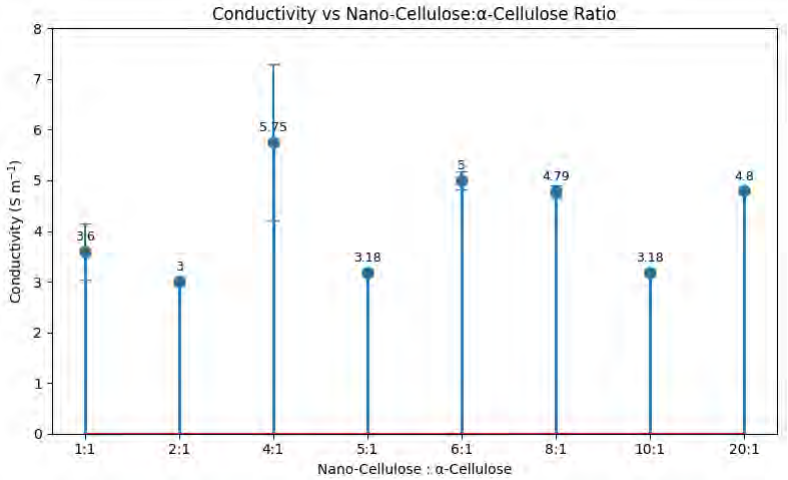

Figure 1. Conductivity in Sm^{-1} across different proportions of Nanocellulose: Alpha Cellulose

Conclusion

In this study, a novel, low-cost hydrogel bioelectrode composed of cellulose and chitosan for neural interface applications is presented. Preliminary analysis of the electrochemical behavior of the developed material indicates results consistent with previous studies on similar implantable applications using synthetic polymers. The results indicated that a nanocellulose-to-alpha-cellulose weight ratio of 4:1 provides optimal mechanical integrity, electrical conductivity, and self-healing properties. Thus, the current findings indicate the potential feasibility of developing flexible, conductive bioelectrodes from sustainable natural polymers for electrophysiological monitoring and stimulation.

References

1. J. Chong et al., “Highly conductive tissue-like hydrogel interface through template-directed assembly,” *Nat*. *Commun 2023.*, vol. 14, no. 1.
2. F. Han et al., “High-Conductivity, Self-Healing, and Adhesive Ionic Hydrogels for Health Monitoring and Human-Machine Interactions Under Extreme Cold Conditions,” *Advanced Science 2025*., vol. 12, no. 16,
3. S. Y. Srinivasan et al., “Conductive Bacterial Nanocellulose-Polypyrrole Patches Promote Cardiomyocyte Differentiation,” *ACS Appl. Bio Mater 2023*., vol. 6, no. 7.
4. F. Wang et al., “3D Printed Implantable Hydrogel Bioelectronics for Electrophysiological Monitoring and Electrical Modulation,” *Adv. Funct. Mater 2024*, vol. 34, no. 21.

S52 – O6

Using natural crosslinker alternatives to modulate bone-ECM hydrogel characteristics

Jones J.N.[1], Lee I.-N.[1], Rialas A.[1], Parmenter C.[1,2], White L.J.[1]
[1]School of Pharmacy, University of Nottingham, Nottingham, U.K.; [2]Nanoscale and Microscale Research Centre, University of Nottingham, Nottingham, U.K.

Introduction

The extracellular matrix (ECM) confers bioactive architectural and functional support to mammalian tissues, with cellular interaction facilitating constructive remodelling during tissue regeneration. Decellularization produces ECM-derived biomaterials which are already used clinically as powders and sheets, with hydrogel formats undergoing clinical trials. However, the amorphous nature of hydrogels restricts application in mechanically demanding or high-friction sites including nerves and tendons. Chemical crosslinking can overcome this by generating bonds within the ECM architecture, increasing strength.

Aim

We investigated the effects of glutaraldehyde (GA) and two naturally derived reagents, genipin (GP) and proanthocyanidins (PA), on bone-derived ECM (bECM) hydrogels.

Materials and Methods

Bovine tibiae were demineralised, delipidated, and enzymatically decellularized. bECM was digested with pepsin and neutralised to produce gels of 8 mg/mL bECM. Gels were immersed in GA, GP or PA solutions at 1 and 10 mM (DMSO/PBS mixture) for 2 hours, followed by PBS washes. Characterisation included microscopic imaging, rheology, swelling analysis and enzymatic degradation. Cytocompatibility testing used gel-conditioned media on SH-SY5Y, L929, and primary tenocytes; assessed according to the ISO-10993 70% toxicity threshold.

Results

All crosslinkers improved hydrogel robustness compared with non-crosslinked (NC) and DMSO controls. Microscopy revealed reduced porosity, pore size and fibre thickening (Figure 1a). Rheological testing showed significant increases in shear modulus, with the largest in PA10 (327-fold), followed by PA1 (61-fold), GA10 (33-fold), GA1 (9-fold) and GP10 (7-fold) (Figure 1b). GA1, GA10 and GP10 significantly reduced swelling ratios while PA10 increased, relative to NC gels, indicating increased stability Figure 1c). Control and GP1 gels rapidly degraded in collagenase, with resistance increasing in the order GP10, PA1, GA1, GA10 and PA10 (Figure 1d). Conditioned media testing showed cytotoxicity for GA10, PA1 and PA10 in SH-SY5Y cells (Figure 2a). Using filtered PA solutions reduced toxicity, with only PA10 affecting L929 cells (Figure 2b) and none affecting primary tenocytes (Figure 2c).

Conclusion

Crosslinking enhanced the strength and stability of bECM hydrogels. Use of PA demonstrated strongest mechanical reinforcement and degradation resistance; however concentration dependent cytotoxicity was observed. These findings demonstrate that use of GP and PA provides a toolkit for manipulation of bECM hydrogel properties to further expand utility.

Acknowledgements

This work was funded by EPSRC and MRC grants.

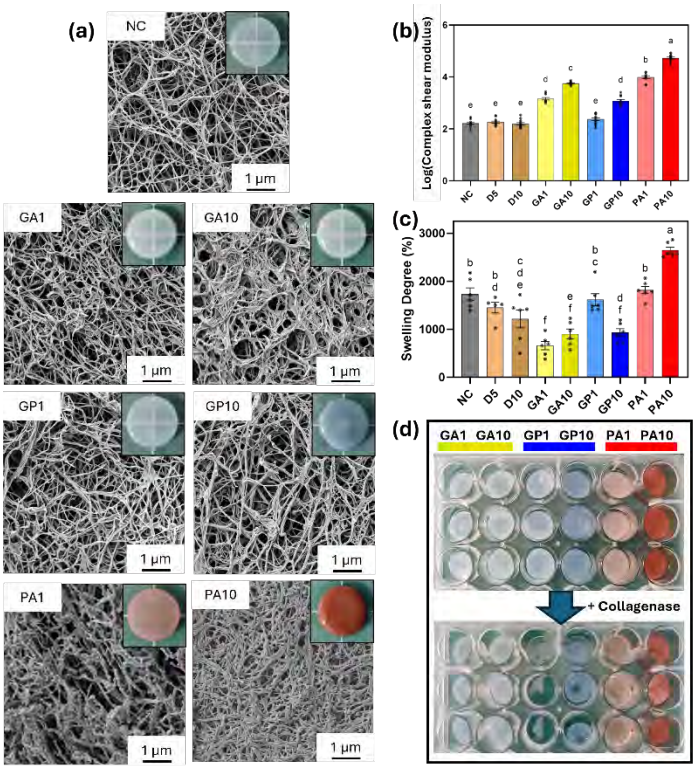

Figure 1: (a) Macro and SEM imaging of crosslinked bECM hydrogels demonstrating changes in morphology and porosity. (b) Complex shear modulus was significantly increased for all crosslinkers except GP1. Share lettering denotes no statistical difference. (c) Changes in swelling degree of crosslinked bECM hydrogels. Shared lettering denotes no statistical differences. (d) Collagenase degradation of crosslinked hydrogels

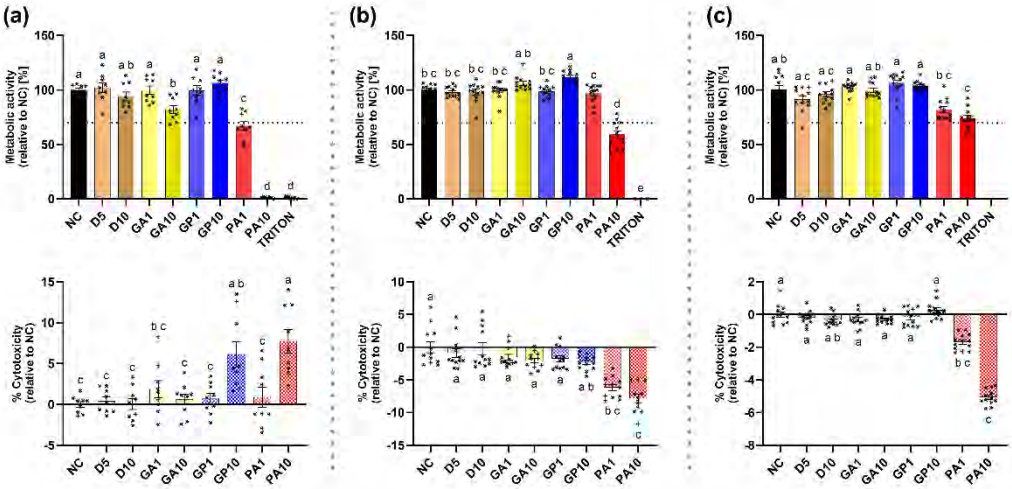

Figure 2: Assessment of gel conditioned media through metabolic activity and LDH assay for SH-SY5Y (a), L929 (b) and primary tenocytes (c).

S53
Implants in orthopaedics

S53 - K1
PEEK based implants in orthopaedics

Cameron R.E.[1]
[1]Dept. of Materials Science and Metallurgy, University of Cambridge, UK

Introduction
Polyetheretherketone (PEEK) is a high-performance polymer used in medical implants for its biocompatibility, chemical stability, low density, radiolucency, and mechanical properties that align with those of bone. Applications include joint replacement, spinal and dental implants, and trauma fixation.
While solid PEEK components have been a feature of the medical landscape for a number of years, there is growing interest in porous PEEK structures and the opportunities afforded by additive manufacturing in implant design. Architectures such as gyroid lattices offer the possibility of tailored load-bearing performance and new strategies for biological integration.
This talk will explore the challenges and opportunities of 3D printing PEEK for medical applications, focusing on design strategies, manufacturing considerations, and the potential impact of porous architectures on implant functionality.

Acknowledgements
Funding is gratefully acknowledged from the EPSRC Prosperity Partnership grant “PEEK-OPTIMA as a Platform for Natural Total Knee Replacement”, Project Reference EP/X025101/1.

S53 – O1

Mapping the effects of chamber and extruder temperatures on PEEK sheet gyroid lattice properties for medical implants

Nandakumar A.[1], Best S.M.[1], Cameron R.E.[1]
[1]Materials Science & Metallurgy, University of Cambridge, UK

Introduction

Conventional load bearing metal-based implants can induce stress shielding, shifting load away from bone. Aseptic loosening may then follow, leading to implant failure and the need for revision surgery. Implants with interconnected porous architectures can address this by matching the modulus of bone and providing space for bone ingrowth. Triply Periodic Minimal Surface (TPMS) structures provide smooth, continuous topology that imparts a more uniform stress distribution and reduce stress concentrations, compared with lattices with sharp nodes. The sheet gyroid is a popular TPMS geometry choice for use in medical implants since it provides a good combination of stiffness and permeability. Polyetheretherketone (PEEK) is a bioinert, radiolucent polymer that can be used to produce porous implants and can be imaged using conventional techniques. Fused Filament Fabrication (FFF) is a relatively inexpensive additive manufacturing technique to produce complex TPMS-based PEEK implants. Previous studies have examined the impact individual design parameters have on FFF-derived PEEK TPMS structures; in this study we report comprehensive void and failure mechanism analyses for systematic variations in chamber and extruder temperatures.

Materials and Methods

An Orion A150 FFF 3D printer was used to produce cylindrical lattice samples using 1.75 mm LT1 PEEK-Optima™ (provided by Invibio Limited). Optical imaging was used to assess the surface finish. X-ray Micro-computed Tomography (µCT) was used to scan samples, and NRecon (Bruker) software was used to generate reconstructed images. CT-Analyser (Bruker) and Dragonfly 3D World (Comet Technologies) were used to analyse void properties from reconstruction data. X-ray Diffraction and Differential Scanning Calorimetry were used to determine samples' degree of crystallinity. Uniaxial compression testing was undertaken to obtain force-displacement data. Post-failure samples were analysed using µCT, and Scanning Electron Microscopy.

Results

The relationship between the mechanical properties and void measurements were determined for the examined extruder-chamber temperature window (Figure 1), and failure mode (Figure 2). There was no significant change in the degree of crystallinity of samples, lending credence to a purely layer adhesion driven failure mechanism. All samples were demonstrated to be safe up to the elastic limit, suggesting a predictable, safe operating stress-strain regime that is desirable for orthopaedic implant applications.

Acknowledgements

Funding for this project was provided by the EPSRC (Project Reference: EP/Y528924/1, Studentship Project Reference: 2936166).

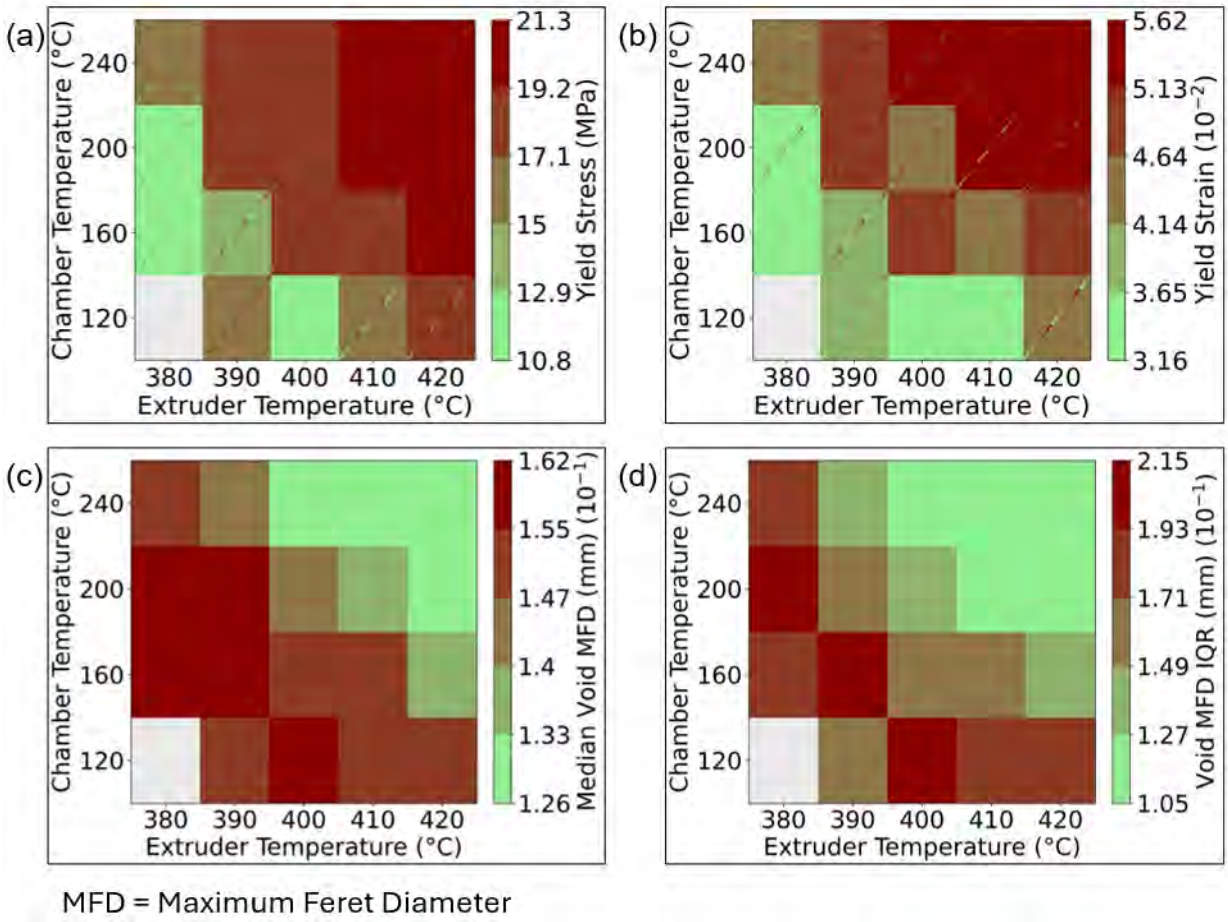

Figure 1: Extruder-chamber temperature heatmaps depicting (a) yield stress (b) yield strain (c) the median of the maximum feret diameter of the identified 3D void distribution (d) Interquartile range of the maximum feret diameter of the identified 3D void distribution

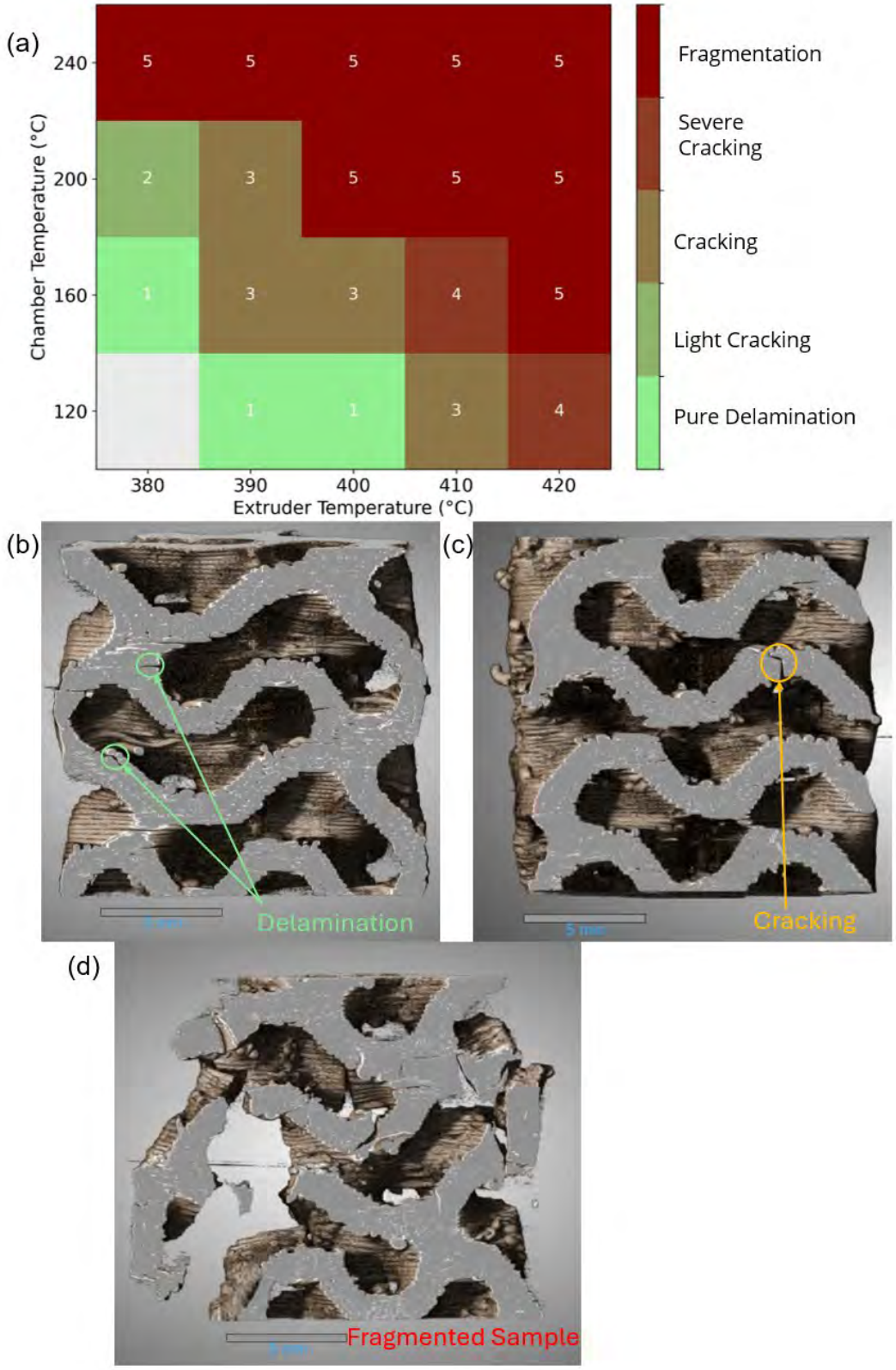

Figure 2: (a) Heatmap depicting the most severe observed failure for given extruder-chamber temperature combinations. Clipped 3D rendering of sample that experienced (b) delamination (c) cracking (d) fragmentation.

S53 – O2

A finite element study on the primary fixation of a cementless PEEK tibial component in total knee arthroplasty using a gyroid porous metaphyseal stem

Zhang H.L.[1], Best S.M.[1], Cameron R.E.[1]
[1]Dept. Materials Science and Metallurgy, University of Cambridge, UK

Introduction

Polyether ether ketone (PEEK-OPTIMA™, hereafter PEEK) has mechanical properties closer to natural bone than many conventional orthopaedic implant metals, such as titanium (Ti) and cobalt–chromium (CoCr). This mechanical similarity helps reduce stress shielding[1]. In total knee arthroplasty (TKA), tibial components are commonly fixed using polymethyl methacrylate (PMMA) bone cement; however, cemented fixation can be prone to aseptic loosening, leading to pain and revision surgery. To improve biological fixation, there is increasing interest in introducing controlled porosity at selected implant locations to increase surface roughness and promote bone ongrowth and/or ingrowth.

Aim

This study investigated an alternative cementless fixation strategy located at the metaphyseal stem, rather than focusing solely on porous features beneath the tibial baseplate. A novel gyroid porous stem design was proposed and evaluated under standard walking conditions. The objectives were to assess the primary fixation, the mechanical stability, and the stress shielding in bone.

Materials and Methods

Finite element analysis (FEA) was used to compare implant configurations and materials. A tibial component featuring a gyroid porous metaphyseal stem was modelled and assessed under different load distributions and bone material properties. Outputs included stress distributions within the implant and surrounding bone, and micromotion at the bone–implant interface as an indicator of primary fixation stability. Stress shielding was evaluated by comparing load transfer to bone for Ti versus PEEK.

Results

The gyroid stem design did not compromise overall mechanical stability with the 99.9th maximum stress within the plasticity limit for PEEK. The predicted micromotion at the bone-implant interface remained low, with the 95th maximum micromotion falling within the commonly cited thresholds for osseointegration. As shown in Figure 1, variations in bone material properties had a noticeable but mild influence on predictions, whereas load distribution had a substantial influence. The localised force at the centre of the baseplate led to the highest micromotion and stress for this porous stem design. Material-dependent differences in bone loading were observed, as demonstrated in Figure 2. Stress shielding beneath the baseplate was more pronounced for Ti, whereas PEEK showed reduced stress shielding, consistent with its closer elastic compatibility with bone.

Conclusion

A gyroid porous metaphyseal stem is a promising alternative location for cementless fixation in TKA tibial components. FEA results suggest that this design can maintain mechanical stability while keeping micromotion within a range supportive of osseointegration. In addition, PEEK reduced stress shielding beneath the baseplate compared with Ti, indicating potential advantages for long-term bone preservation and fixation performance.

Acknowledgements

This study is funded by EPSRC Prosperity Partnership Grant No. EP/X025101/1.

References

1. Zhao G., Luo J., Ma J., Wang J. Decreased stress shielding with poly-ether-ether-ketone tibial implant for total knee arthroplasty – A preliminary study using finite element analysis. Heliyon; 2024; 10(5); e27204.
2. Post, C.E.; Bitter, T.; Briscoe, A.; van Langen, I.; Fluit, R.; Verdonschot, N.; Janssen, D. The Effect of Patient-Related Factors on the Primary Fixation of PEEK and Titanium Tibial Components: A Population-Based FE Study. Bioengineering 2024, 11, 116.
3. Keyak J.H., Kaneko T.S., Tehranzadeh J., Skinner H.B. Predicting proximal femoral strength using structural engineering models. Clin Orthop Relat Res. 2005 ;(437):219-28.

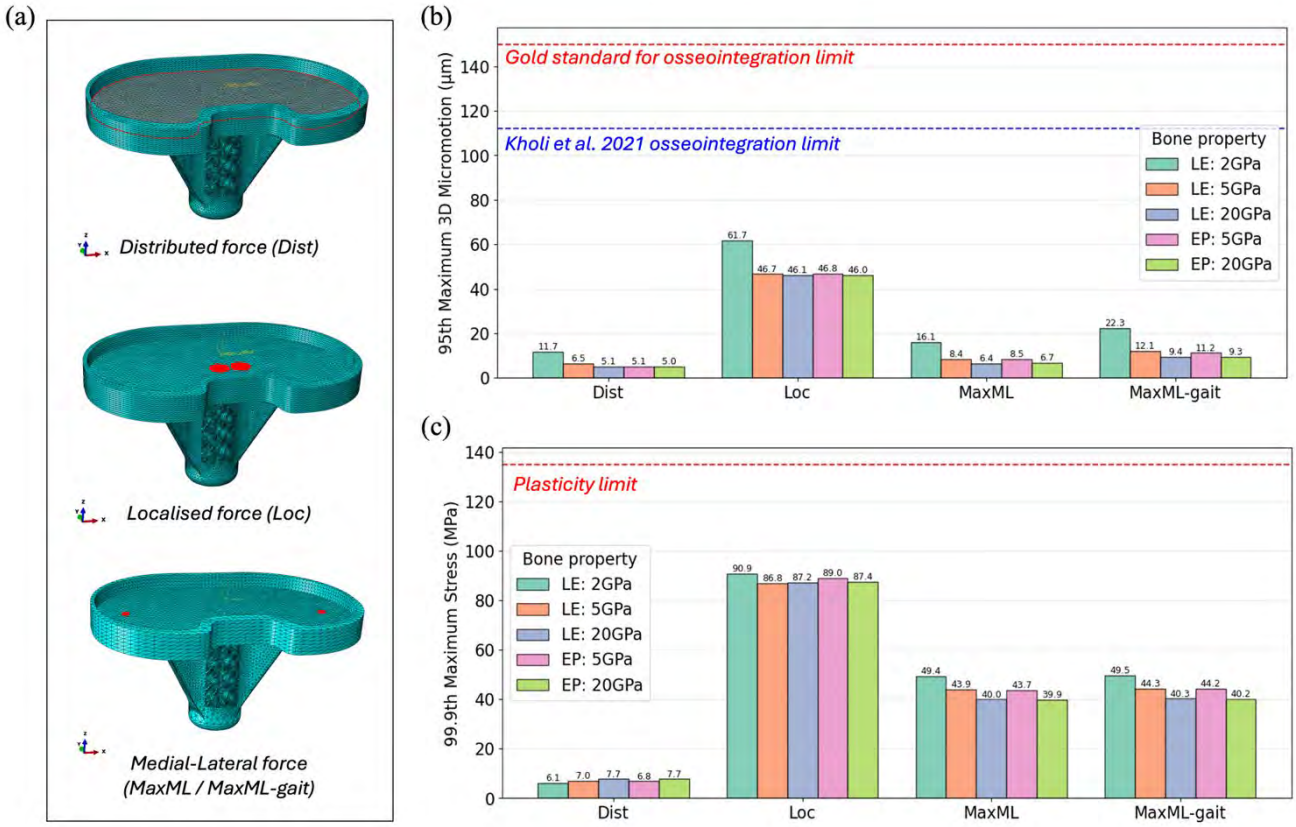

Figure 1. (a) Load distributions on the tibial baseplate: distributed force, localised force at the baseplate centre, and medial-lateral force[2]. (b) The 95th maximum micromotion at the bone-implant interface and (c) the 99.9th maximum stress in the PEEK tibial component under different load distributions and bone material properties. LE represents linear-elastic bone; EP represents elastic-plastic bone[3]. Elastic modulus is listed for each bone group.

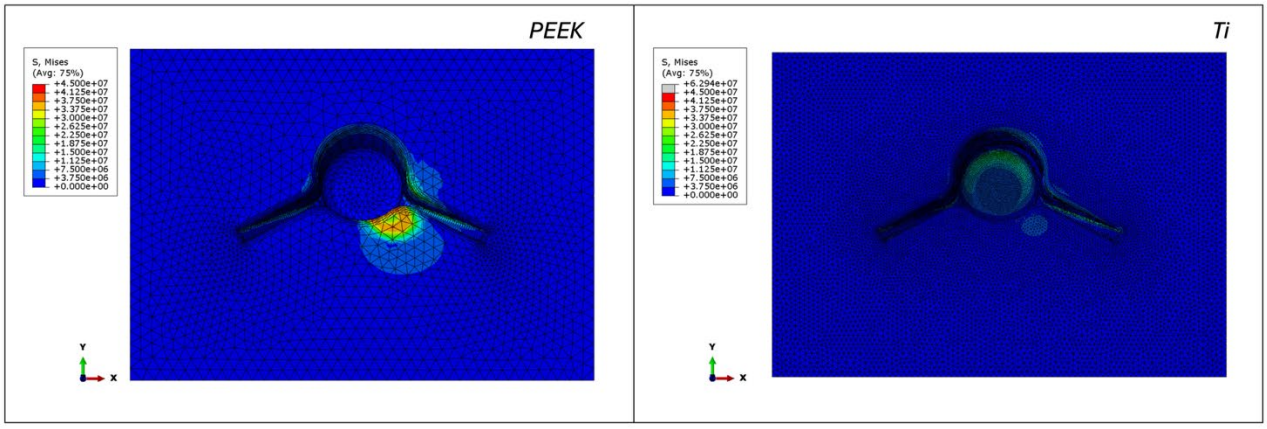

Figure 2. Stress distribution in the supporting bone for PEEK versus Ti tibial components.

S53 – O3

Wear performance of an all-polymer total knee replacement

Cowie R.M.[1], Briscoe A.[2], Jennings L.M.[1]
[1]Institute of Medical and Biological Engineering, University of Leeds; [2]Invibio Biomaterials Solutions, Thornton Cleveleys, UK

Introduction

Total knee replacement is a highly successful procedure with >90% survivorship at 10 years however, approximately 20% of patients are dissatisfied by their replacement joint so there is a clinical need to explore new materials. PEEK-OPTIMA™ (a trademark of Invibio Ltd.) is a high-performance polymer under investigation as an alternative to cobalt chrome (CoCr) in the femoral component of total knee replacements (Figure 1) due to its biocompatibility, low weight and low modulus.

Aim

The aim of this study was to assess the wear of UHMWPE in the tibiofemoral and patellofemoral joints of an all-polymer total knee replacement and to compare the wear to that of conventional materials (CoCr-on-UHMWPE).

Materials and Methods

For tibiofemoral wear simulation, 6 PEEK-OPTIMA and 6 CoCr femoral components of similar initial surface topography and geometry were paired with all-polyethylene tibial components; for the patellofemoral wear simulation, 6 additional PEEK and 6 CoCr femoral components were tested against 25 mm diameter UHMWPE patellae. Both joints were tested for 5 million cycles of wear simulation under kinematics representative of a walking gait using 25% bovine serum as a lubricant (Figure 1). Every 1 million cycles, the simulators were stopped, the UHMWPE components removed, cleaned and weighed. Loss in mass of the components determined gravimetrically was converted to a wear volume and subsequently to a wear rate. Statistical analysis was carried out to compare the wear rates of UHMWPE against the different femoral component materials using ANOVA ($p<0.05$).

Results

The wear of UHMWPE in both the tibiofemoral and patellofemoral joints was low, <5 mm^3/MC and <1 mm^3/MC respectively (Figure 2). There was no significant difference in the wear performance of the UHMWPE components when articulating against the different femoral component materials, $p=0.27$ and $p=0.38$ for the tibiofemoral and patellofemoral joints respectively. Linear scratching was observed on the surface of the PEEK femoral components however, this did not influence the wear rate which remained linear over the duration of the study.

Conclusion

Experimental wear simulation of both tibiofemoral and patellofemoral joints showed an equivalent rate of wear of UHMWPE against PEEK-OPTIMA™ and cobalt chrome femoral components. These studies show PEEK-OPTIMA™ to have promise as an alternative to cobalt chrome in the femoral component of total knee replacements.

Acknowledgements

This work was supported by Invibio Knees Ltd and the Medical Technologies Innovation and Knowledge Centre Phase 2 Regenerative Devices EP/N00941X/1 EPSRC.

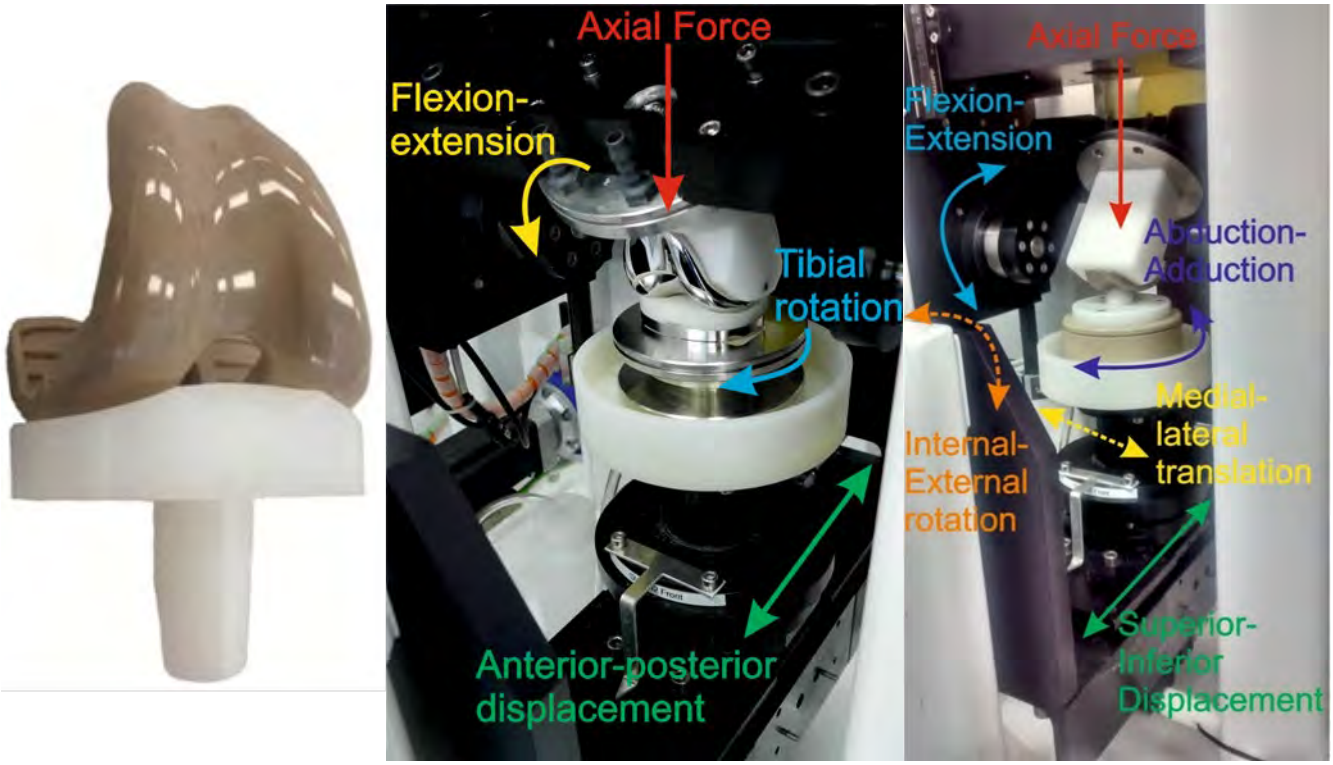

Figure 1: Left: All-polymer total knee replacement compromising a PEEK femoral component articulating against an all-polyethylene tibial component. Centre: A 6-axis electromechanical knee simulator for testing the tibiofemoral joint, driven axes shown. Right: Patellofemoral joint simulation with driven axes shown with solid lines and unconstrained axes shown by dashed lines. Note: during testing, joints are immersed in a lubricant compromising 25% bovine serum + 0.03% sodium azide solution.

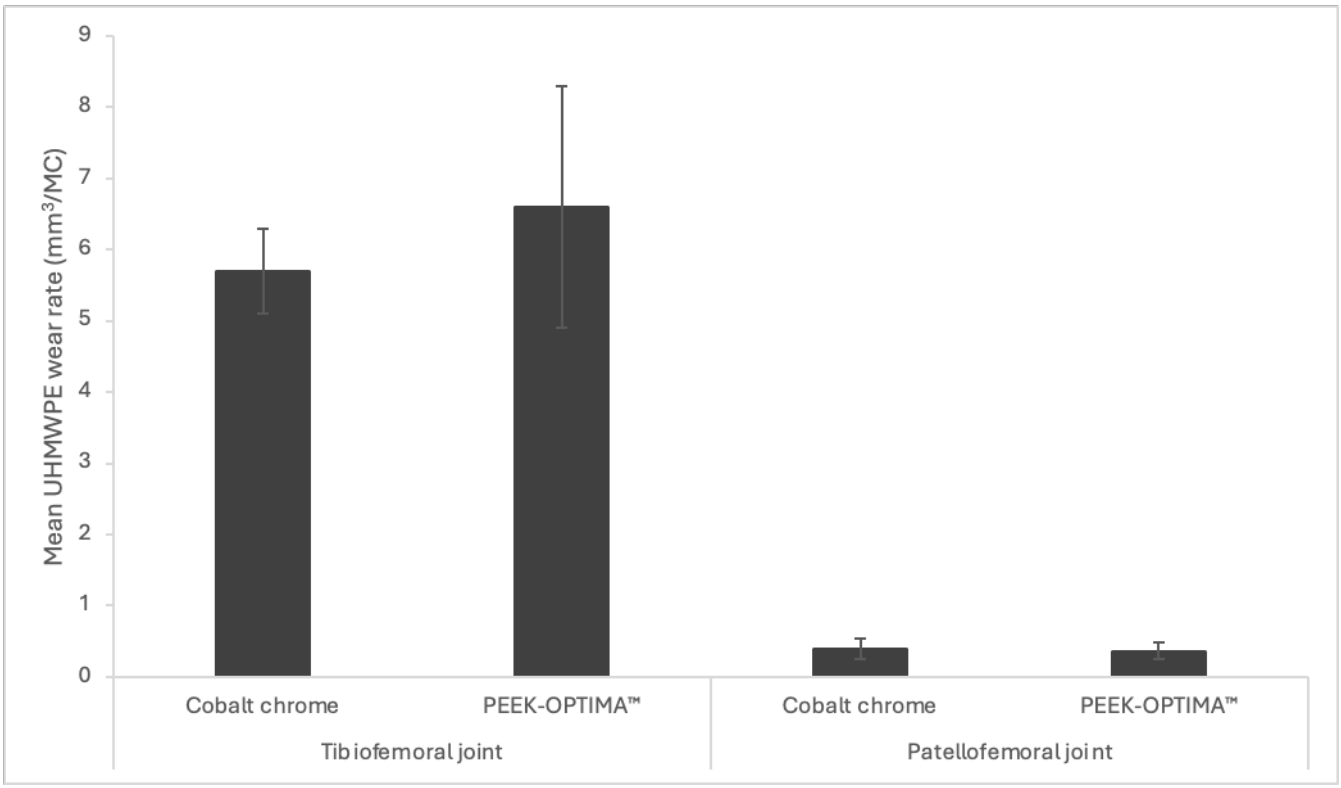

Figure 2: Mean wear rate of UHMWPE tibial components and UHMWPE patellae after 5 million cycles wear simulation articulating against the different femoral component materials (N=6).

S53 – O4

Gravimetric determination of peek-optima™ wear

Dipholo T.[1], Cowie R.M.[1], Briscoe A.[2], Jennings L.M.[1]
[1]Institute of Medical and Biological Engineering, University of Leeds; [2]Invibio Ltd, Thornton-Cleveleys, UK

Introduction

PEEK-OPTIMA™ (a trademark of Invibio Ltd) is currently under investigation as a femoral component in an all-polymer knee replacement. Studies to date have shown the wear of the UHMWPE tibial components to be comparable when articulating against PEEK or cobalt chrome femoral components[1]. The gold standard technique for measuring UHMWPE wear is gravimetric analysis. Mass changes during experimental wear simulation are due to both wear and moisture uptake by polymers, so to minimise influence of moisture uptake in wear calculations, components are soaked pre-test to saturation. Assessing the wear of PEEK-OPTIMA™ using gravimetric techniques has been difficult likely due to inconsistent fluid absorption and stabilisation challenges.

Aim

The aim of this study was to understand the influence of different parameters (e.g. lubricant, temperature, stabilisation method) on the fluid absorption and stabilisation of PEEK, then to assess the wear of PEEK in an UHMWPE-on-PEEK bearing couple in simple geometry.

Material and Methods

This study was conducted to investigate the effect of soaking fluid (bovine serum or water), stabilisation methods (vacuum desiccation or Leeds 48 hour drying) and temperature (room or 40°C) on moisture uptake of PEEK-OPTIMA™ and UHMWPE during pre-test soaking (Figure 1). Saturated PEEK-OPTIMA™ plates (N=3) and dry (non-soaked) plates (N=3) were subsequently tested against UHMWPE pins in a 6-station pin on plate rig. 25% bovine serum was used as a lubricant, test conditions were chosen to replicate knee joint kinematics, and the study was carried out for 2 million cycles. The wear of plates was assessed gravimetrically using the vacuum-desiccation method, with soak controls used to compensate for moisture uptake. A student's t-test statistical analysis was used for the PEEK plates wear factors.

Results

Saturation of PEEK typically took 50 days and the protocol with the most fluid taken up by PEEK, was soaking in sterile water at 40°C and stabilised with the vacuum-desiccation method (Figure 1). Figure 2 shows the wear factor of the PEEK-OPTIMA™ plates. There was a significant difference between the wear factors of the saturated and non-saturated PEEK plates ($p=0.03$). Plates that were not soaked to saturation have negative wear factors indicating continued fluid absorption during wear simulation; soaking plates enabled the wear of PEEK to be measurable.

Conclusion

A protocol for the saturation and stabilisation of PEEK was developed and application of this protocol allowed wear of PEEK to be measured in an UHMWPE-on-PEEK bearing couple.

Acknowledgements

PEEK-OPTIMA™ plates used in the study were provided by Invibio Ltd. Dipholo T is a PhD student co funded by EPSRC and Invibio Ltd through a Full-Time EPSRC CASE studentship.

References

[1]Cowie RM, et al. JOEIM 230, 2016 (11):1008-1015

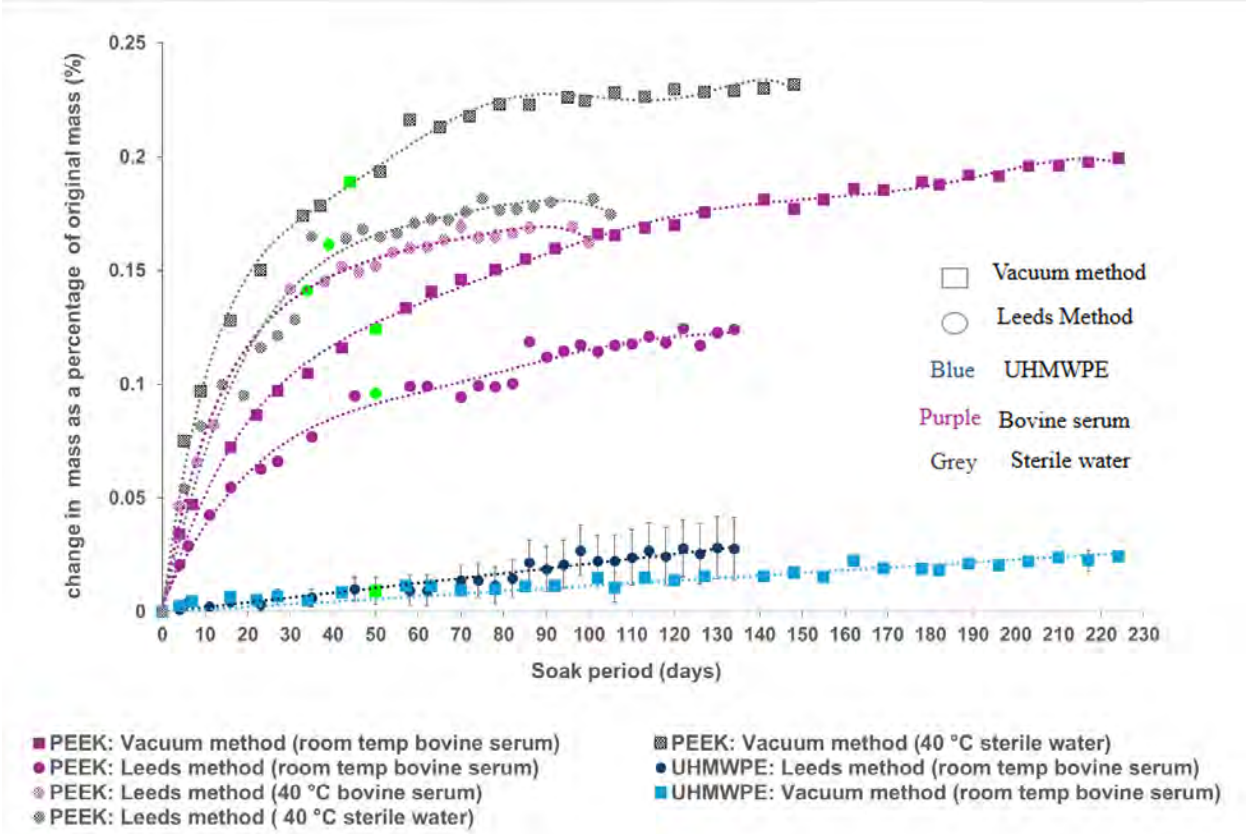

Figure 1: Percentage change in mass (mean ± 95 % confidence interval) of PEEK and UHMWPE under different soaking conditions. Green fill shows the first time point at which the saturation requirement is reached.

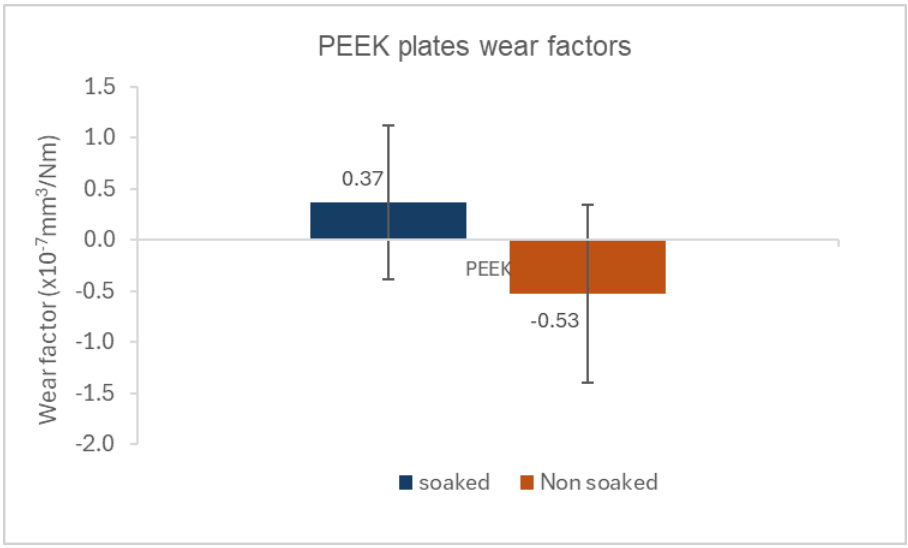

Figure 2: Wear factors of PEEK plates (mean ± 95% confidence Interval)

S53 – O5

Bioactive scaffolds for optimizing the soft tissue–prosthesis interface

Sergio, I.[1,2,3], Sercia, L.[1,2,3], Gigli, G.[1,2,4], Gervaso, F.[1,2], Polini, A.[1,2], Scalera, F.[1,2]
[1]CNR NANOTEC,Institute of Nanotechnology, c/o Campus Ecotekne; [2]Tecnomed Puglia Technopole for Precision Medicine (Biotech Lecce Hub), c/o Campus Ecotekne; [3]Dept. of Innovation Engineering, University of Salento; [4]Dept. of Experimental Medicine, University of Salento, Lecce, Italy

Introduction

Percutaneous osseointegrated prosthetic systems enable direct skeletal anchorage through a transcutaneous implant, but their long-term success is limited by inadequate soft tissue integration at the skin–implant interface. The disruption of the epidermal barrier predisposes the site to infection, inflammation, epithelial downgrowth, and bacterial colonization, highlighting the need for biomaterial strategies capable of restoring a stable biological seal.

Aim

To address this unmet need, we developed a bioactive bilayer scaffold designed to improve sealing and soft tissue integration around transcutaneous prosthetic abutment.

Materials and Methods

The system (fig. a) combines an elastic sealing layer, specifically engineered to interface with the metallic prosthetic component, forming a low-permeability barrier at the implant surface, and a porous bioactive layer, intended to interface with the surrounding soft tissue to promote cellular infiltration and tissue ingrowth. An optimized intermediate adhesive layer ensures stable bonding between the two components. The sealing layer was fabricated from a PVA/glycerol hydrogel obtained via thermal treatment and repeated freeze–thaw cycles. The bioactive layer was produced as a GelMA/PEGDA/HAMA hydrogel, photo-crosslinked using LAP. An intermediate PVA/GelMA/glycerol layer was introduced and photo-crosslinked in situ to prevent delamination and preserve mechanical integrity. The compact morphology of the sealing layer and the interconnected porous architecture of the bioactive layer were confirmed by scanning electron microscopy (SEM). Scaffold stability was investigated under physiological conditions (PBS, 37 °C). Biocompatibility was evaluated using fibroblasts (3T3) and keratinocytes (HaCaT) through direct and indirect cytotoxicity assays, as well as adhesion and proliferation studies. Mechanical properties were assessed by tensile and compressive testing.

Results

The sealing layer exhibited high stretchability (elongation at break ~445%), soft tissue–compliant elasticity (~30 kPa), mechanical robustness, and biologically inert behavior. The bioactive layer showed tissue-like mechanical properties (compressive modulus ~10–12 kPa) and supported adhesion and proliferation of both fibroblasts and keratinocytes. The bilayer scaffold remained mechanically and structurally stable for up to 60 days in vitro. Overall, the bilayer remained mechanically and structurally stable for up to 60 days in vitro, maintaining robustness in aqueous conditions and ensuring high cell viability (~95% for both fibroblasts and keratinocytes) for up to 7 days (fig. b).

Conclusion

Preliminary results demonstrate structural stability, tissue-compliant mechanical properties, and good cytocompatibility. Ongoing in vitro studies are designed to investigate the interaction between the scaffold and the surrounding tissue under physiologically relevant conditions, using a three-dimensional vascularized skin model.

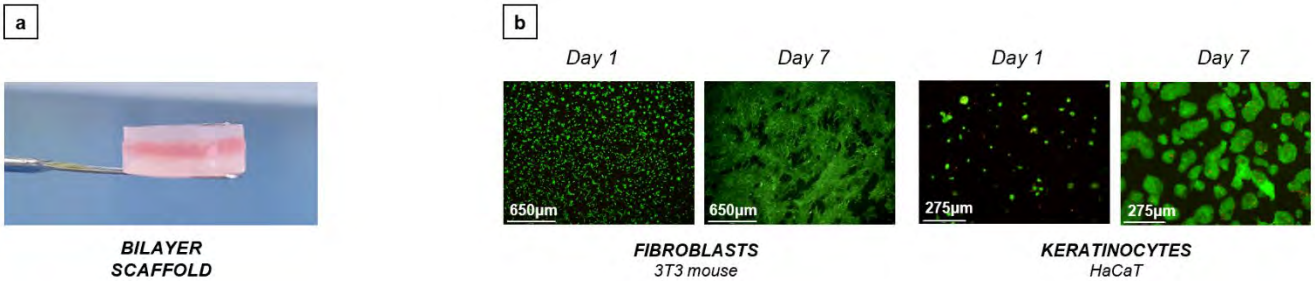

Acknowledgements
This work was supported by the Italian Ministry of University and Research (MUR) through the complementary actions to the NRRP “Fit4MedRob” Grant (PNC0000007, CUP B53C22006960001) and by Regione Puglia through the “Tecnopolo per la medicina di precisione” (TecnoMed Puglia) program (DGR n. 2117, 21/11/2018; CUP B84I18000540002).

S54
Piezoelectric biomaterials from design to functional interfaces in tissue engineering

S54 - K1
Biodegradable nanopiezoelectrics fo body healing

Nguyen, T.D.[1]
[1]Dept. of Biomedical Engineering, Institute of Materials Science, Polymer Program, University of Connecticut School of Engineering, Storrs, USA

Piezoelectric materials, a type of “smart” material that generates electricity while deforming and vice versa, have been used extensively for many important implantable medical devices such as sensors, transducers, and actuators. However, commonly utilized piezoelectric materials are either toxic or nondegradable. Thus, implanted devices employing these materials raise a significant concern in terms of safety issues and often require an invasive removal surgery, which can damage directly interfaced tissues/organs.
Here, we present a strategy for materials processing, device assembly, and electronic integration to 1) create biodegradable and biocompatible piezoelectric nanofibers with a highly controllable, efficient, and stable piezoelectric performance, and 2) demonstrate device applications of this nanomaterial, including a highly sensitive biodegradable pressure sensor for monitoring vital physiological pressures and a biodegradable ultrasonic transducer for blood–brain barrier opening that can be used to facilitate the delivery of drugs into the brain.
These significant applications, which have not been achieved so far by conventional piezoelectric materials demonstrate the achieved biodegradable nanofibers as a powerful material platform that offers a profound impact on various medical fields including drug delivery, tissue engineering, and implanted medical devices.

S54 – O1

Piezoelectric KNN ceramics: Synthesis-driven optimization for enhanced osteoblast response

Staehlke S.[1], Guzzo C.M.[2], Rebl H.[1], Glaum J.[2]
[1]Institute of Cell Biology, Rostock University Medical Centre, Germany; [2]Dept. of Materials Science and Engineering, Norwegian University of Science and Technology (NTNU), Trondheim, Norway

Introduction

Piezoelectric ceramics such as potassium sodium niobate ($K0.5Na0.5NbO_3$, KNN) are promising electrically active biomaterials for bone repair and regeneration 1. Their electromechanical properties may enable direct cellular stimulation to improve the healing of bone defects at implant sites. However, the microstructural stability and biological performance of KNN strongly depend on precursor chemistry and synthesis conditions. This study focused on how stoichiometric modifications and processing routes influence material stability, piezoelectric functionality, in vitro cytocompatibility, and cellular effects on bone-related cells. The objective was to evaluate synthesis-driven material optimization and its impact on osteoblast behavior.

Materials and Methods

Chemically undoped KNN ceramics subjected to deliberate stoichiometric adjustments (stoichiometric, S-KNN; 0.2 mol% alkali-excess, A-KNN), and hybrid-atmosphere sintering (H-KNN) [1]. KNN pellets (10 mm ⌀) were poled via corona discharge (30 kV, 30 min, 2.3 cm electrode spacing). All KNN compositions were characterized regarding surface microstructure, ion release, and piezoelectric stability in culture medium. Cell biological evaluation was performed using MG-63 human osteoblasts [2] cultured on unpolarized and polarized KNN for 24 h. Cell adhesion, spreading, morphology, cytoskeletal organization, metabolic activity, and reactive oxygen species (ROS) generation were analyzed. Titanium alloy served as reference material.

Results

Synthesis-driven modification significantly affected material stability and cell response: A- and H-KNN ceramics demonstrated enhanced aqueous stability compared to S-KNN, primarily due to suppression of hygroscopic secondary phases. All KNN compositions retained measurable piezoelectric response during 14 days under physiological conditions. KNN ceramics maintain the viability of MG-63 cells, highlighting the material´s favorable biocompatibility profile. KNN microstructures ensure functional stability and affect cell behavior. Polarization resulted in modest but reproducible improvements in osteoblast spreading, actin filament formation, and metabolic activity, accompanied by increased ROS level (see Figure).

Conclusion

Optimized KNN ceramics exhibit reliable *in vitro* cellular behavior, supporting osteoblast viability and adhesion comparable to those of clinically established titanium alloys. Polarization-induced surface charges further enhance cell spreading and motility. These findings provide a platform for the development of KNN-based piezoelectric biomaterials for bone regeneration in tissue engineering.

Acknowledgements

This work was funded by the DFG (SFB 1270/1,2, 299150580) and the Research Council of Norway (EPIC, 301020; NorFab, 349807).

References

[1]Thu M., Guzzo C.M., Glaum J. et al. Potential for medico-biological applications of potassium sodium niobate: A review. *Progress in Materials Science* 2025;152:101448.
[2]Staehlke S., Rebl H., Nebe B. Phenotypic stability of the human MG-63 osteoblastic cell line at different passages. *Cell Biol Int.* 2019;43(1):22-32.

ESB
2026

S54 – O2

Cell-specific activation of cytoskeleton regulators and voltage-gated ion channels mediated by piezoelectric $K_{0.8}Na_{0.2}NbO_3$ nanoparticles and low-intensity pulsed ultrasound

Trucco D.[1,2,3], Parlanti P.[4], Vannozzi L.[1,2], Pucci C.[1,2], Turini C.[1,2], Gemmi M.[4], Jost C.[5], Fedutik Y.[5], Campanella B.[6], Onor M.[6], Pustovalov V.[7], Gruppioni E.[8], Pané S.[7], Ricotti L.[1,2]
[1]The BioRobotics Institute, Scuola Superiore Sant'Anna, Pisa, Italy; [2]Dept. of Excellence in Robotics & AI, Scuola Superiore Sant'Anna, Pisa, Italy; [3]Institute for Bioengineering and Biosciences and Dept. of Bioengineering, Instituto Superior Técnico, Universidade de Lisboa, Portugal; [4]Center for Materials Interfaces, Electron Cristallography, Istituto Italiano di Tecnologia, Pontedera, Italy; [5]PlasmaChem GmbH, Berlin, Germany; [6]Istituto di Chimica dei Composti Organometallici, Consiglio Nazionale delle Ricerche (CNR), Pisa, Italy; [7]Multi-Scale Robotics Lab (MSRL), Institute of Robotics and Intelligent Systems (IRIS), ETH Zurich, Switzerland; [8]Centro Protesi INAIL, Bologna, Italy

Introduction

Piezoelectric nanomaterials activated by low-intensity pulsed ultrasound (LIPUS) can convert acoustic stimulation into a localized electrical field. These signals may modulate intracellular mechanotransduction pathways, including cytoskeletal regulators and voltage-gated ion channels, which are central to musculoskeletal cell function. In this study, potassium sodium niobate ($K_{0.8}Na_{0.2}NbO_3$) nanoparticles (KNN_NPs) were deeply characterized and evaluated as lead-free piezoelectric nanomaterials for ultrasound-mediated wireless modulation of human chondrocytes and C2C12 myoblasts.

Materials and Methods

KNN_NPs were synthesized via a sol–gel method. Morphology was analyzed by Trasmission Electron Microscopy (TEM), while piezoelectric properties were measured using Piezoresponse Force Microscopy (PFM). Degradation was evaluated in water for up to 3 months, and ion release was quantified by Inductively Coupled Plasma-Mass Spectrometry (ICP-MS). KNN_NPs were subsequently coated with propylene glycol alginate (PGA-KNN_NPs) to improve colloidal stability and cytocompatibility. Human chondrocytes and C2C12 myoblasts were seeded in culture and exposed to PGA-KNN_NPs at 100 $\mu g.mL^{-1}$ for 24 h to allow cellular internalization. Cells were then stimulated using a custom LIPUS setup previously developed by our group, designed to ensure controlled acoustic transmission and minimize undesired reflections (frequency 1 MHz, intensity 250 $mW.cm^{-2}$, duty cycle 20%). Pathway-focused gene expression analyses targeting cytoskeleton regulators and voltage-gated ion channels were performed one day after stimulation.

Results

KNN_NPs exhibited an orthorhombic perovskite structure with an average size of ~20 nm (Fig.1a) and a strong piezoelectric response ($d_{33} \approx 88$ pm V^{-1}) (Fig.1b). Degradation studies revealed a controlled ion-release profile ($K^+ > Na^+ \gg Nb^{5+}$) under physiological-like conditions (Fig.1c). PGA functionalization improved colloidal stability, cellular uptake, and cytocompatibility, with no adverse effects observed up to 100 $\mu g.mL^{-1}$ (Fig.1d). Gene expression analyses revealed cell-specific responses to the combined PGA-KNN_NPs internalization and LIPUS stimulation. In human chondrocytes, enhanced Ca^{2+} signaling and increased expression of mechanosensitive ion channels (PIEZO1, TRPV4) were observed together with downregulation of several actin-regulating genes (Fig. 1e). In C2C12 myoblasts, upregulation of contractility and polarity regulators (*Mylk2, Mark2*) (Fig. 1f) and several voltage-gated Na^+, K^+, and Ca^{2+} channels.

Conclusion

These findings indicate that PGA-KNN_NPs represent a biocompatible piezoelectric platform capable of enabling wireless, ultrasound-mediated electromechanical stimulation of musculoskeletal cells. Upon LIPUS activation, internalized nanoparticles generate localized electrical cues that induce lineage-specific transcriptional responses. This approach can provide a strategy to modulate cell behavior without implanted electrodes while maintaining the potential for partial material resorption over time.

Acknowledgements

This work was funded by MioPRO^2 project (INAL, PR23-CR-P1), BRIEF project (NextGenerationEU, IR0000036), and SPORA project (HORIZON-MSCA-2025-PF-01-01, 101284586).

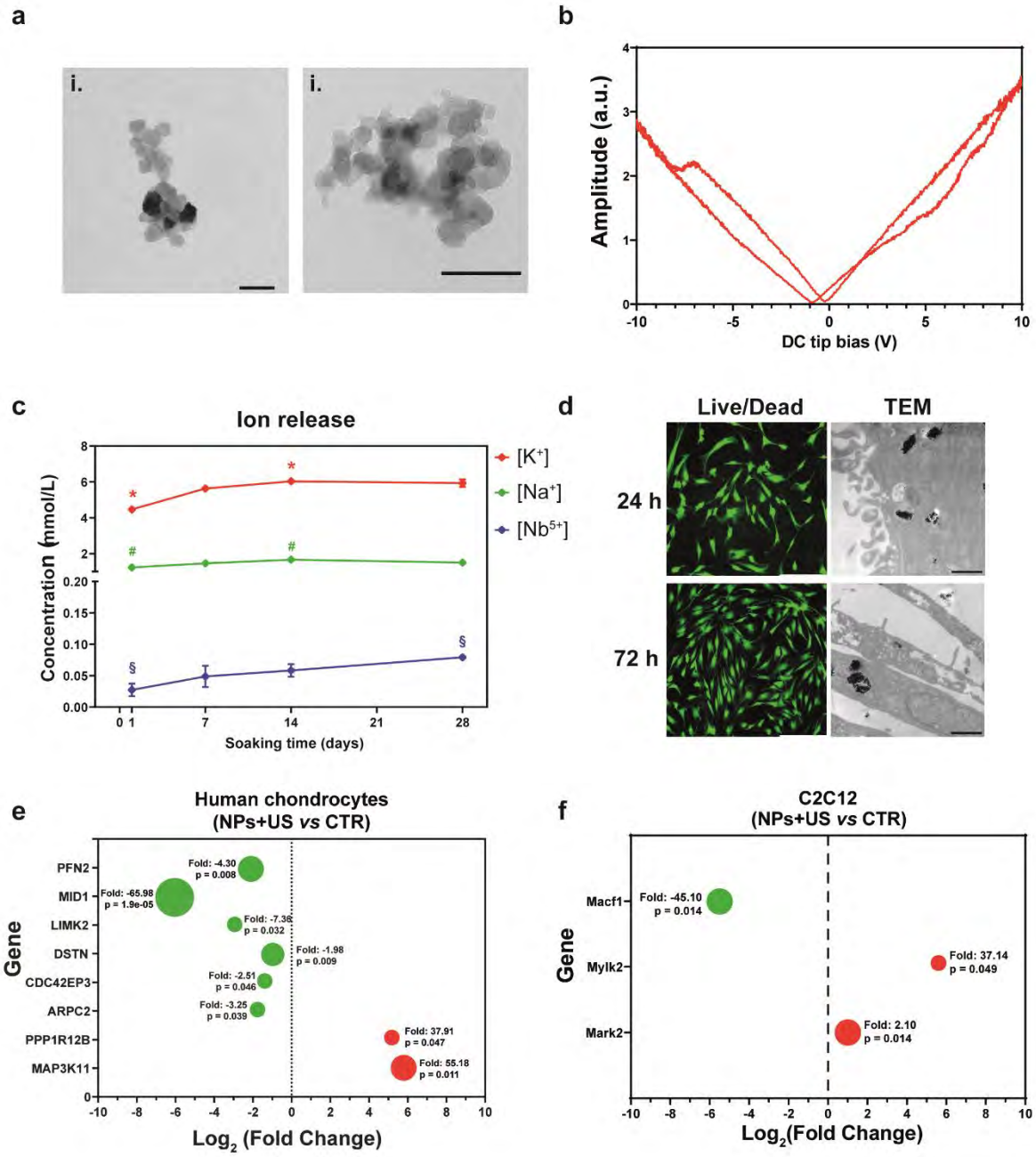

Fig. 1. (a) TEM images of (i) KNN NPs and (ii) PGA-KNN NPs. (b) Piezoelectric amplitude loops measured under DC bias (−10 to +10 V). (c) Time-dependent release of K^+, Na^+, and Nb^{5+} ions up to 28 days. (d) Cytocompatibility and cellular uptake of PGA-KNN NPs in human chondrocytes. Differential gene expression in the NPs+US group versus control (CTR) for (e) human chondrocytes and (f) C2C12 myoblasts (red: upregulated; green: downregulated).

S54 – O3

Active tunning of protein distribution and conformation on magnetoactive composites

Rodriguez-Lejarraga P.[1], Fernández Maestu J.[1], Petrenko V.[1,2], Silván U.[1,2], Lanceros-Mendez S.[1,2]
[1]BCMaterials, Basque Center for Materials, Applications and Nanostructures, 48940 Leioa, Spain; [2]Ikerbasque, Basque Foundation for Science, Bilbao, Spain

Introduction

Stimuli-responsive materials are essential for properly mimicking the dynamics of tissue microenvironment. Since protein adsorption determines the biological activity of biomaterials, developing surfaces that control protein layer organization is crucial. Magnetoactive composites enable non-invasive, remote control of surface properties, providing a unique platform to regulate the protein interface and subsequent biological activity.
In this context, since protein adsorption critically determines the biological activity of biomaterials, developing surfaces capable of steering protein layer organization is crucial. To address this, magnetoactive composites enable non-invasive, remote control of surface properties, providing a unique platform to regulate the protein interface and subsequent biological activity.

Aim

This study reports on the development of poly(vinylidene fluoride)-cobalt ferrite (PVDF-CFO) magnetoactive composites and the influence of alternating (AC) magnetic fields on the adsorption of fibronectin and collagen type I proteins.

Materials and Methods

PVDF-CFO films (20 wt.% CFO) were prepared via doctor blade and annealing at 210 °C. Composite characterization was performed using different experimental techniques, including infrared spectroscopy, differential scanning calorimetry, mechanical, electrical and magnetic. Films were functionalized with fibronectin (10 µg/ml) or collagen type I (300 µg/ml) for 1 hour. During adsorption, an AC magnetic field (4.3 Hz) was applied via a rotating N42 neodymium magnet, obtaining a magnetic flux density of ±100 mT at the sample surface, while non-stimulated samples served as controls. Finally, samples were rinsed and fixed, and their supramolecular organization was analyzed by atomic force microscopy.

Results

Characterization confirmed a high electroactive β-phase content (81 ± 10%) and a robust piezoelectric response (d_{33} = 23 pm/V) of the PVDF-CFO composite, with low surface roughness (S_a = 1.5 ± 0.1 nm). Under the AC magnetic field stimulation, the supramolecular organization of the protein interface was significantly modulated. For fibronectin, the magnetic stimulation decreased the protein layer homogeneity, doubling the area of protein-free "pockets" while decreasing their density (Figure 1a). On the other hand, collagen type I showed reduced fibril compactness and altered height profiles compared to non-stimulated substrates (Figure 1b). These structural changes suggest that magnetostrictive strain from CFO nanoparticles triggers a piezoelectric response in the PVDF matrix, dynamically altering the surface electric potential.

Conclusion

This study demonstrates the potential of magnetoactive PVDF-CFO composites for the on-demand modulation of protein interfaces. These findings represent a first step toward developing smart biomaterials capable of dynamically tuning the protein organization, offering a new path to direct cellular responses and enhance functional tissue regeneration.

Figure 1: Representative atomic force microscopy topographical images of a) fibronectin and b) collagen-coated PVDF-CFO composites without, and with the AC magnetic field stimulation. Scale bars represent 200 nm.

S54 – O4

Multiscale modeling of PVDF piezoelectric ultrafine fiber meshes for cochlear applications

Sestini M.[1,2], Montorsi M.[3,4], Milazzo M.[2], Berrettini S.[1,5], Labardi M.[3], Danti S.[2]
[1]U.O. Otorinolaringoiatria, Audiologia e Foniatria, Azienda Ospedaliero-Universitaria Pisana, Pisa, Italy; [2]Dept. of Civil and Industrial Engineering, University of Pisa, Italy; [3]Institute for Chemical-Physical Processes, Council of National researches, Pisa, Italy; [4]College of Physics and Optoelectronic Engineering, Shenzhen University, China; [5]Dept. of Surgical, Medical, Molecular Pathology and Emergency Medicine, University of Pisa, Italy

Introduction

Ultrafine piezoelectric fiber meshes represent a promising strategy for the treatment of sensorineural hearing loss, by replacing the native function of damaged hair cells of the cochlea. These materials enable self-powered mechanical-to-electrical transduction, converting acoustic-induced mechanical vibrations into electrical signals. However, the multiscale nature of these structures — from fiber-level electromechanical coupling to membrane-scale acoustic response — makes their direct numerical modelling computationally demanding.
In this work, a homogenized numerical framework was developed to represent the microstructure of aligned poly(vinylidene fluoride) (PVDF) fiber meshes and investigate their mechano-electrical behaviour. Moreover, the mechano-acoustic response of a basilar membrane-inspired structure was modeled in a macrofluidic reactor.

Materials and Methods

COMSOL Multiphysics and SolidWorks were used for finite element modeling (FEM) simulations and computer assisted design (CAD), respectively. At the microstructural level, aligned PVDF fibers were represented through a geometrically parametrized 3D periodic cell (Figure 1A). Structural mechanics was coupled with the piezoelectricity module to account for mechano-electrical coupling. Independent mechanical loads were applied to derive homogenized elasticity tensors and piezoelectric stress–charge coefficients. A sensitivity analysis was performed by varying fiber density, alignment, diameter and inter-fiber connection strength. In parallel, a macroscopic mechano-acoustic FEM model was implemented by coupling a thin elastic membrane immersed in water through acoustic-structure interaction to reproduce a scaled-up cochlear tube.

Results

The homogenized model enabled systematic evaluation of microstructural parameter influence on mechanical stress distribution and electric polarization generated under deformation. Variations in fiber density, alignment and inter-fiber connectivity significantly affected the predicted piezoelectric response and the extracted homogenized tensors. Changing the fiber alignment from 10° to 80° produced a non-linear increase in the e_{31}, while e_{32} and e_{36} piezoelectric coefficients reached a maximum for 45° and 60° fiber orientation, respectively (Figure 1B). At the macroscopic scale, acoustic simulations revealed frequency-dependent displacement peaks along the membrane length under harmonic excitation (Figure 1C), consistent with the expected tonotopic behaviour of cochlear structures.

Conclusion

This work provides a framework for interpreting experimental measurements of piezoelectric fibrous meshes, quantifying the mechanical properties and the electrical signal generated by the piezoelectric fibrous mesh. It represents a step towards the characterization of a multifunctional experimental platform capable of evaluating acousto-mechanic behaviour, piezoelectric signal generation and, possibly, cell response under acoustically induced mechanical simulation.

Acknowledgements

Funded by the European Union–Next Generation EU via the Italian Ministry of University and Research (MUR), PRIN 2022 program (PROMISE project, Prot. 2022JYHMPF CUP: I53D23004700006).

Figure 1.

S54 – O5

Auxetic cardiac patches combining mechanical support and piezoelectric stimulation for myocardial repair

Marino S.[1,2], Roy K.[3], Saini D.[3], Galizia P.[4], Zhang Q.[5], Rodriguez B.[5], Panseri S.[4], Tofail S. A.[3], Monaghan M. G.[1,2,6]

[1]Discipline of Mechanical, Manufacturing and Biomedical Engineering, Trinity College Dublin, Ireland; [2]Trinity Centre for Biomedical Engineering, Trinity Biomedical Science Institute, Trinity College Dublin, Ireland; [3]Dept. of Physics and Bernal Institute, University of Limerick, Ireland; [4]CNR-ISSMC, National Research Council of Italy Institute of Science, Technology and Sustainability for Ceramics, Faenza, Italy; [5]School of Physics and Conway Institute of Biomolecular and Biomedical Research, University College Dublin, Ireland; [6]CÚRAM, Research Ireland Centre for Medical Devices, University of Galway, Ireland

Introduction

Myocardial infarction remains a leading cause of morbidity and mortality worldwide. It results from interrupted coronary blood flow, leading to cardiomyocyte loss and scar tissue formation. Current treatments mainly restore perfusion but do not actively promote myocardial repair. Engineered cardiac patches represent a promising strategy; however, most designs fail to simultaneously provide mechanical support and restore the heart's electrical activity.

Aim

To address this limitation, we aim to develop a cardiac patch integrating bioinspired auxetic architectures with piezoelectric polymers. Auxetic geometries expand laterally when stretched, enabling improved adaptation to the heart's multidirectional motion, while piezoelectric materials generate electrical signals in response to cyclic strain.

Materials and Methods

Auxetic piezoelectric patches were fabricated via melt electrowriting (MEW) using polyvinylidene fluoride (PVDF) and its copolymers. A lozenge-truss geometry was designed to achieve auxetic behaviour through rotational deformation at the nodes. Polymer melts were processed using a custom-built heated collector (>120 °C) and low collector speeds to ensure stable fibre deposition. Printing fidelity and mechanical properties were evaluated by SEM and uniaxial tensile testing, respectively. Poisson's ratio was calculated using MATLAB-based video tracking. The patches were subsequently corona-poled to maximize their piezoelectric response. Local piezoelectric activity was characterized by piezoresponse force microscopy (PFM). Cytocompatibility was assessed through live/dead assays using iPSC-derived cardiac fibroblasts and cardiomyocytes. Cell morphology and attachment were further examined by immunofluorescence staining of the cytoskeleton and cardiac-specific markers.

Results

Stable MEW printing was achieved for both PVDF and PVDF-TrFE, producing well-defined lozenge-truss architectures. PVDF showed a wider processing window, enabling patches with fibre diameters below 20 µm and stacks exceeding 40 layers. Mechanical testing and Poisson's ratio calculations confirmed reproducible stress-strain behaviour and clear auxetic deformation within physiologically relevant strain ranges. PVDF-TrFE exhibited a stronger piezoelectric response in PFM measurements due to its fully all-trans conformation. Live/dead assays demonstrated high viability of iPSC-derived cardiac fibroblasts and cardiomyocytes on both patch types, while immunofluorescence confirmed cell attachment and cytoskeletal organization, with cardiomyocytes displaying characteristic cardiac marker expression.

Conclusion

MEW-fabricated auxetic patches exhibited robust mechanical behaviour, tunable early-strain response, and pronounced auxeticity within physiologically relevant strain ranges. Together with their measurable piezoelectric properties and cytocompatibility with cardiac cells, these results highlight the potential of auxetic piezoelectric architectures to couple mechanical deformation with local electrical stimulation, opening new opportunities for advanced cardiac patch design.

Acknowledgements

This work is funded by the ERC-2023-COG program under the HORIZON-ERC (European Research Council) grant No. 101125153.

S54 – O6

3D-Printed piezoelectric scaffolds coupled with ultrasound stimulation synergistically promote the osteogenic differentiation of mesenchymal stem cells for bone tissue engineering

Barbosa F.[1,2], Miguel F.[1,2], Santos M.[1,2], Marcelino P.[1,2,3], Ferreira F.[1,2], Silva J.[1,2]
[1]Dept. of Bioengineering and iBB - Institute for Bioengineering and Biosciences, Instituto Superior Técnico, Lisboa; [2]Associate Laboratory i4HB – Institute for Health and Bioeconomy, Lisboa; [3]CDRSP, Polytechnic of Leiria, Marinha Grande, Portugal

Introduction and Aim

The rising incidence of trauma- and osteoporosis-related non-union fractures in an aging population has increased the clinical need for effective bone substitutes, driving growing interest in bone tissue engineering (BTE) strategies. Among these, the development of biomimetic scaffolds represents a promising approach, as they can provide structural support while simultaneously promoting bone regeneration. Bone maintenance and repair are strongly linked to its intrinsic piezoelectric properties, mainly arising from type I collagen and the hydroxyapatite-rich extracellular matrix. Additive manufacturing techniques such as Fused Deposition Modelling (FDM) enable the reproducible fabrication of scaffolds with controlled architecture, microporosity and mechanical properties. In this context, combining piezoelectric scaffolds with ultrasound (US) stimulation offers a novel approach to deliver localized electrical cues to cells and enhance bone regeneration.
In this study, 3D-printed porous scaffolds were fabricated using different piezoelectric filaments—poly-L-lactic acid (PLLA), polyvinylidene fluoride (PVDF), and conductive PVDF—to compare their physicochemical properties and evaluate their osteogenic potential with or without wireless US stimulation.

Materials and Methods

The produced 3D porous piezoelectric scaffolds were characterized in terms of their structural (SEM and µ-CT), chemical (FTIR), hydrophilicity (contact angle), piezoelectric charge coefficient (d33) and mechanical properties (compressive tests). The scaffolds were seeded with human bone-marrow mesenchymal stem/stromal cells (hBMSCs) and cultured for 21 days under osteogenic induction and exposed to a previously optimized US stimulation protocol (Figure 1). At the culture endpoint, the osteogenic potential of the different experimental groups was assessed in terms of cell proliferation (Alamar Blue assay) and bone-specific gene/protein expression (RT-qPCR and immunohistochemical analyses).

Results

SEM and µ-CT analyses confirmed that all scaffolds exhibited a homogeneous morphology and high printing fidelity (Figure 2a), with minimal defects and pore sizes consistent with the CAD design. All scaffolds, except PLLA, displayed hydrophobic behavior, while PLLA showed mechanical properties closer to those of native trabecular bone. Conductive PVDF scaffolds exhibited a significantly higher piezoelectric charge coefficient compared to the other materials (Figure 2b). Importantly, the application of the US stimulation protocol enhanced significantly the proliferation (Figure 2c) and the osteogenic differentiation of hBMSCs, particularly in PLLA scaffolds, as demonstrated by increased alkaline phosphatase (ALP) activity (Figure 2d) and significant upregulation of osteogenic markers (*Runx2*, *COL1A1*, *Piezo2*).

Conclusion

Overall, our findings demonstrate a clear synergy between the 3D scaffolds' piezoelectric features and US stimulation on the enhancement of the osteogenic differentiation of hBMSCs, highlighting this strategy high potential for improved BTE strategies.

Acknowledgements

The authors acknowledge dedicated funding from FCT through iBB (UID/04565/2025), I4HB (LA/P/0140/2020), and Assistant Researcher FCT Tenure contract (iBB_U5_SCERG_FCT TENURE (121) iBB) awarded to JS. This work was also funded by ELECTROBONE project through the seed funding initiative of the European University Alliance Unite! – University Network for Innovation, Technology and Engineering. Views and opinions expressed are however those of the authors only and do not necessary reflect those of the Unite! Alliance.

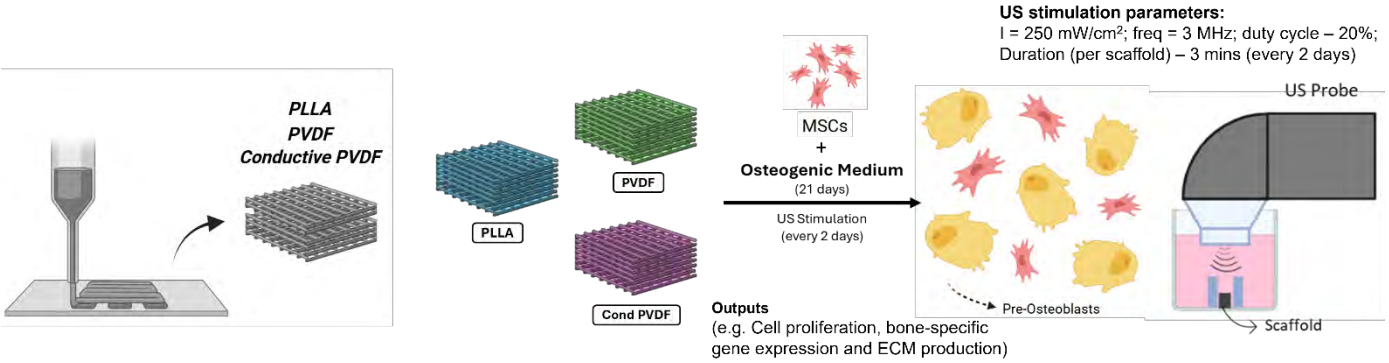

Figure 1 Schematic representation of the US stimulation protocol for the culture of hBMSCs on the different 3D printed piezoelectric scaffolds.

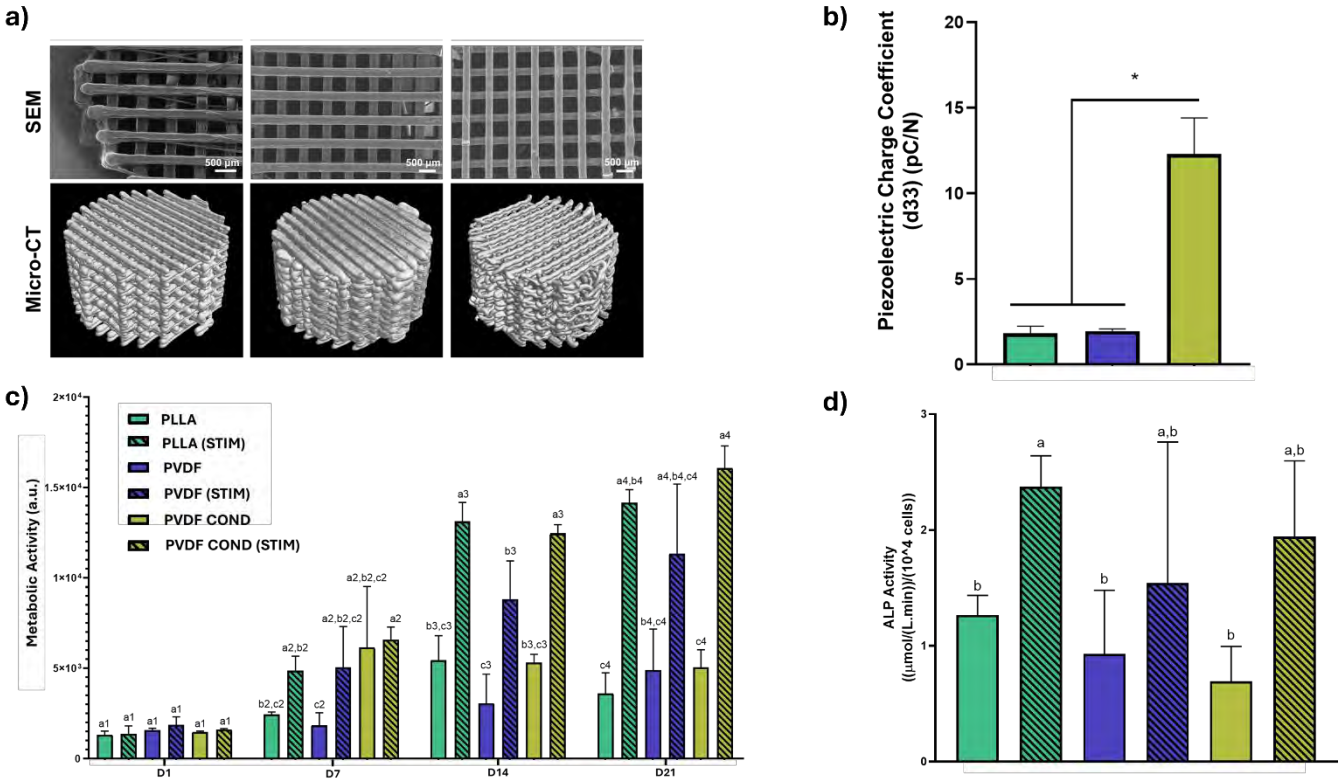

Figure 2 (a) SEM and µ-CT 3D reconstruction images of the different 3D-printed piezoelectric scaffolds; (b) Piezoeletric charge coefficient (d33) of the 3D-printed piezoelectric scaffolds. N=5, *p<0.05; (c) Cell proliferation (AlamarBlue assay) of hBMSCs cultured on piezoelectric PLLA, PVDF and conductive PVDF 3D-printed scaffolds with and without ultrasound stimulation, N=3; p<0.05; (d) ALP activity quantification hBMSCs cultured for 21 days on the different piezoelectric scaffolds with and without US stimulation. N=4, p<0.05. Note: Letters are used to represent statistical significance. Groups that share the same letter do not display statistically significant differences between them (Tukey/homogenous groups).

S54 – O7

Remotely and non-invasively activated piezoelectric scaffolds for electromechanical tissue regeneration

Kim D.[1], Banerjee H.[1]. Kim J.K.[2], Kim M.[3], Kim S.-W.[4], and Kar-Narayan S.[1]
[1]Materials Systems Engineering, Max Planck Institute for Dynamics of Complex Technical Systems, Magdeburg, Germany; [2]Dept. of Orthopedic Surgery, Asan Medical Center, University of Ulsan College of Medicine, Seoul, Republic of Korea; [3]Dept. of Mechanical Engineering, Korea Advanced Institute of Science and Technology, Daejeon, Republic of Korea; [4]Dept. of Materials Science and Engineering, Yonsei University, Seoul, Republic of Korea

Introduction

Electromechanical stimulation plays an important role in the regeneration of electrically responsive tissues such as nerve and bone. Piezoelectric biomaterials have recently emerged as promising candidates because they can convert mechanical deformation into electrical signals that mimic endogenous bioelectrical cues. However, conventional electrical stimulation strategies often rely on implanted electrodes or wired systems, which can limit long-term stability and increase the risk of tissue damage. Remotely activated biomaterials offer an attractive alternative by enabling non-invasive and spatiotemporally controllable stimulation through external energy sources. However, strategies enabling remote activation of piezoelectric scaffolds while maintaining mechanical compatibility with biological tissues remain limited. This study aims to develop remotely activated piezoelectric scaffolds capable of generating electromechanical stimulation for tissue regeneration.

Materials and Methods

For remotely activated electromechanical stimulation, two piezoelectric scaffold systems were developed targeting nerve and bone regeneration. For peripheral nerve regeneration, electrospun scaffolds composed of poly(ethylene glycol) (PEG) and poly(L-lactic acid) (PLLA) were fabricated to exploit the intrinsic piezoelectric properties of PLLA. PEG was incorporated to introduce hydrophilicity and mechanical softness, improving the biological compatibility of the fibrous scaffold, while PLLA provides piezoelectric functionality. The aligned fibrous architecture provides topographical guidance for axonal growth while enabling mechanical deformation of the scaffold under ultrasound stimulation. Ultrasound-induced vibration of the fibrous matrix generates localized piezoelectric signals within the scaffold, thereby providing electromechanical cues that support neuronal regeneration.

For bone regeneration, a stimuli-responsive scaffold was designed using a liquid crystal elastomer (LCE) matrix incorporating photothermal metal-organic frameworks (MOFs). To enhance the functionality of the LCE system, a dual-mesogen strategy combining RM257 and RM82 was employed. While RM257 forms relatively stiff networks that provide structural stability, the incorporation of RM82 introduces increased mechanical adaptability, enabling dynamic actuation of the scaffold. Upon near-infrared (NIR) irradiation, photothermal conversion within the MOF induces reversible deformation of the LCE scaffold. Piezoelectric layers composed of PLLA were integrated through a layer-by-layer architecture to convert the actuation-induced mechanical deformation into electrical stimulation, providing electromechanical signals that can promote bone regeneration.

Results

Ultrasound stimulation of the electrospun PEG/PLLA scaffold generated measurable piezoelectric signals and promoted neurite extension along the aligned fibrous structure. The electromechanical stimulation provided by the scaffold enhanced neuronal guidance and supported nerve regeneration across injured regions approaching autograft performance.

In the NIR-responsive system, photothermal heating of MOF particles induced reversible deformation of the LCE scaffold under NIR irradiation. The repetitive actuation generated dynamic mechanical strain within the multilayer structure, which was converted into electrical signals by the piezoelectric layers. This electromechanical stimulation provided cues that support osteogenic activity.

Together, these results demonstrate that remotely applied physical stimuli can be effectively translated into localized piezoelectric signals through engineered scaffold systems, providing electromechanical cues that promote regenerative responses across different tissue types.

Conclusion

These results demonstrate the potential of remotely activated piezoelectric biomaterials to convert externally applied energy into localized electromechanical stimulation for tissue regeneration. By integrating stimulus responsive scaffold systems with PLLA-based piezoelectric layers, the proposed platform enables the generation of bioelectrical cues through ultrasound- or light-induced mechanical deformation. This strategy highlights a versatile approach for delivering programmable electromechanical signals to support regenerative processes in multiple tissues.

Acknowledgements

The authors gratefully acknowledge financial support from the Department of Materials Systems Engineering at the Max Planck Institute for Dynamics of Complex Technical Systems, Germany

S55
Precision polymer chemistry as a tool to modulate biological and biomedical functions

S55 – K1
Mechanical control of molecular recognition and bioactivity in of Peptide Rotaxanes and Polyrotaxanes

Schaufelberger F.[1,2]
[1]University of Warwick – UK, [2]KTH Royal Institute of Technology, Department of Chemistry – Sweden

Introduction
Mechanically interlocked molecules (MIMs) feature mechanical bonds, which link multiple distinct components together and allow free movement between them without dissociation. Over the last decades, MIMs have been applied in diverse areas from switchable catalysis to smart materials. However, they have found limited use in biomedicine and biomaterials, due to the often lengthy synthesis and poor solubility in biological media.[1] Directly addressing these challenges, here we use Nature's own building blocks (i.e. peptides)[2] to construct stimuli-responsive interlocked molecules and materials for bioapplications in a rapid and highly efficient manner.

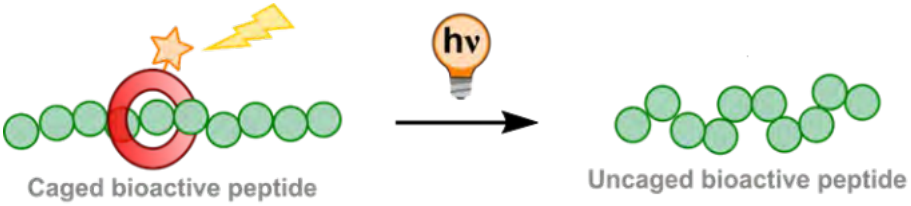

***Figure 1**. Conceptual overview of the supramolecular approach to precision biomaterials.*

Aim
We will use bioactive native peptides as the rotaxane axle, and show that the bioactivity can be silenced via obstruction of an encircled stimuli-responsive macrocycle,[3] which acts as "protective armour" and stabilises the peptide (Figure 1). Upon application of a stimulus, self-immolative cleavage of the macrocycle occurs, liberating the free peptide.

Materials and methods
All systems where synthesised with solution-phase peptide synthesis and analysed with NMR spectroscopy, HRMS and HPLC.

Results
In this talk, I will present our development of the peptide rotaxane platform and its application to precision biomaterials synthesis, in particular for the synthesis of enzyme sequence recognition elements, for precise control of peptide self-assembly and for making responsive hydrogels. As proof-of-concept, we use matrix metalloproteinase 2-responsive peptide sequences (PLGLAG) and cage these with macrocycles to form peptide rotaxanes (Figure 2a). Application of appropriate stimuli (here fluoride ions) cleaves the macrocycle, enabling recognition by biomacromolecules. Molecular modelling confirms the mechanical silencing effect (Figure 2b), and I will further present several examples of where we can leverage this precision control to turn biorecognition on *in situ*. A particular example is our development of rotaxanated peptide pre-gelators, where macrocycle cleavage turns on gelation ability (Figure 2c).

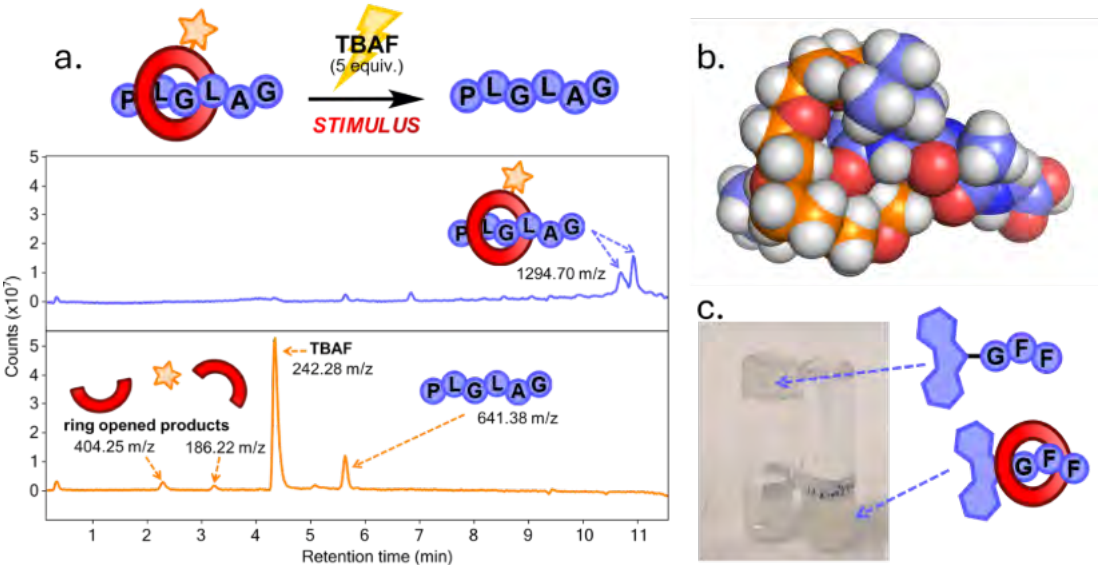

Figure 2. Example data. a) Mechanical uncaging of enzyme-active peptide sequences via stimuli. b) Modelling studies illustrating the immense silencing effect of the supramolecular elements. c) Proof-of-concepts studies showing control of peptide self-assembly using the rotaxane approach.

Conclusion

Here I will present our efforts over the last years to develop a platform approach to cage peptides with bulky protecting elements that can be opened swiftly and efficiently using a wide range of stimuli. We envision wide applications of this technology in biomaterials and chemical biology, firmly demonstrating that the mechanical bond is a versatile and generally useful tool for precision biomaterials development.

References

1. S. R. Beeren, C. T. McTernan and F. Schaufelberger, *Chem*, **2023**, *9*, 1378–1412.
2. P.-L. Wang, P. Chen, R. Yang, D. J. Tetlow, Z.-H. Zhang, J. Han, S. D. P. Fielden, P. Howlader, L. Zhang and D. A. Leigh, Angew. Chem. Int. Ed., **2025**, *64*, e202513115.
3. A. Saady, G. K. Malcolm, M. P. Fitzpatrick, N. Pairault, G. J. Tizzard, S. Mohammed, A. Tavassoli and S. M. Goldup, *Angew. Chem. Int. Ed.* **2024***, 63*, e202400344.

S55 – O1

Interactive endothelium-mimicking nanocoatings enable anticoagulation-free hemocompatibility in artificial placenta systems

Kasapgil E.[1,2], Englert J.[1,3], Witzdam L.[1,3], Rodriguez-Emmenegger C.[1,3,4]
[1]Institute for Bioengineering of Catalonia (IBEC), Barcelona, Spain; [2]Biomedical Engineering Dept., Izmir Bakircay University, Turkey; [3]DWI, Leibniz Institute for Interactive Materials e.V., Aachen, Germany; [4]Catalan Institution for Research and Advanced Studies (ICREA), Barcelona, Spain

Introduction

Preterm birth affects approximately 15 million infants annually and remains the leading cause of death in children under five, accounting for over one million deaths each year. Artificial placenta (AP) systems aim to replicate *in utero* oxygenation for extremely premature infants; however, their translation is limited by poor hemocompatibility and the need for systemic anticoagulation. Current extracorporeal membrane oxygenation (ECMO) devices are highly thrombogenic, increasing the risk of life-threatening bleeding. Here, we introduce interactive endothelium-mimicking nanocoatings that enable anticoagulation-free hemocompatibility by integrating antifouling, coagulation modulation, and on-demand fibrinolysis.

Materials and Methods

A multilevel endothelium-mimicking nanocoating was engineered using ultrathin hydrophilic polymer networks (poly(CBMAA-*co*-BPMAA); CBMAA: carboxybetaine methacrylamide; BPMAA: benzophenone methacrylamide) to create a hydrated antifouling interface. The coating was functionalized with components enabling (i) nitric oxide (NO)-mediated suppression of platelet activation (iNOS), (ii) local modulation of coagulation via inhibitors of FXIIa, FXa, and kallikrein, and (iii) on-demand fibrinolysis through immobilized tissue plasminogen activator (tPA). Coatings were applied to flat substrates and hollow fiber membranes. Hemocompatibility was assessed using human blood under dynamic conditions (37°C, 2 h), including mini-oxygenator flow models. Surface morphology and thrombus formation were analyzed by SEM, while oxygen transfer performance was evaluated.

Results

The nanocoatings formed stable ultrathin interfaces that reduced protein adsorption by up to 98% while preserving antifouling properties after biofunctionalization. The coatings enabled localized regulation of coagulation, generating nitric oxide (NO) at physiological levels and selectively capturing activated coagulation factors (FXIIa, FXa, and kallikrein). Immobilized tissue plasminogen activator (tPA) remained active and induced fibrinolysis, leading to digestion of macroscopic fibrin clots within hours. Under dynamic blood flow in mini-oxygenator models, uncoated membranes showed extensive thrombus formation, whereas coated membranes remained free of clot deposition across multiple donors, as confirmed by SEM after 2 h blood exposure. Importantly, oxygenation was preserved, with no impairment in gas transfer.

Conclusion

We present an interactive, endothelium-mimicking nanocoating that enables anticoagulation-free hemocompatibility by integrating antifouling, coagulation modulation, and fibrinolysis. This strategy prevents and resolves thrombosis while preserving oxygenation, addressing a key limitation of artificial placenta technologies. Our approach provides a pathway toward safer extracorporeal life support systems.

Acknowledgements

The authors acknowledge financial support from the German Federal Ministry of Education and Research (BMBF; 031B1153A, 031B1154B), the HemoRecap project supported by AiF (IGF-No. 22647 N), the Deutsche Forschungsgemeinschaft (DFG, 346972946), and the European Union's Horizon Europe research and innovation programme under the Marie Skłodowska-Curie Grant Agreement number 101211437.

S55 – O2

Engineered polymer carriers integrated with lab-on-fiber photonics for light-controlled locoregional drug delivery

Caputo T.M.[1,2], Berruti G.M.[1], Mulè C.[1], Cusano A.M.[2], Romanelli A.M.[3], Giaquinto M.[3], Micco A.[2], Consales M.[1], Ricciardi A.[1], Aliberti A.[1,2], Cusano A.[1,2]
[1]Optoelectronics Group, Dept. of Engineering, University of Sannio, Benevento; [2]CeRICT scarl, Benevento; [3]Dept. of Information and Electrical Engineering and Applied Mathematics, University of Salerno Fisciano (Sa), Italy

Introduction

Rational design of polymer carriers with controlled composition and network architecture enables precise modulation of drug loading, stability, and release kinetics. However, systemic chemotherapy still suffers from poor tumor selectivity and dose-limiting toxicity, highlighting the need for polymer-based delivery systems enabling localized and externally controlled drug release. Among emerging strategies, light-triggered platforms combined with optical fiber technologies offer spatially and temporally controlled drug delivery through remote light activation in minimally invasive devices.

Aim

Development of light-activated locoregional drug delivery systems by integrating engineered polymer carriers with Lab-on-Fiber photonic devices.

Materials and Methods

Thermoresponsive microgels were synthesized via free-radical copolymerization of N-isopropylmethacrylamide-based monomers, forming crosslinked networks with hydrodynamic diameters of ~600 nm in the swollen state. The optimized formulation showed encapsulation efficiency (EE) of ~74% and drug loading (DL) up to 130% for doxorubicin, with a volume phase transition temperature above physiological conditions (~42–45 °C). Microgels were covalently immobilized onto a fiber-optic heater (FOH) based on a single-mode optical fiber coated with a 150 nm-thick gold layer, enabling photothermal conversion (~12 °C per 100 mW). In parallel, sorafenib-loaded poly(lactic-co-glycolic acid) (PLGA) nanoparticles were synthesized via optimized emulsion–solvent evaporation. The particles exhibited mean diameters of ~248 nm, EE up to ~90%, and DL of ~8.9%. They were immobilized on side-emitting optical fibers through photocleavable linkers enabling light-triggered carrier detachment. Biological validations were performed using breast (MCF7) and liver (HepG2) cancer cell models.

Results

Thermoresponsive microgels showed negligible drug leakage under physiological conditions. Optical activation of the FOH generated localized heating up to ~55 °C, inducing microgel collapse and doxorubicin release. Up to ~200 ng of drug was delivered within minutes, reaching concentrations of ~1.3 µg mL^{-1} and exceeding passive diffusion from non-activated controls. *In vitro* experiments confirmed that optically released doxorubicin retained its biological activity, reducing MCF7 cell viability to ~20% in 2D cultures, with comparable effects between fiber-released and free drug at equivalent concentrations.
PLGA nanoparticles displayed strong drug retention, with only ~3–4% passive release over 9 days. Compared with free sorafenib, the nanoparticle formulation significantly enhanced cytotoxic efficacy in HepG2 cells: treatment with sorafenib-loaded nanoparticles at 7.5 µM reduced cell viability to ~17% after 168 h, whereas the free drug maintained ~50% viability.

Conclusion

Engineered polymer carriers integrated with lab-on-fiber photonic devices enable externally triggered, spatially controlled drug delivery. Thermoresponsive microgels and biodegradable PLGA nanoparticles demonstrate how rational polymer design can regulate drug release and modulate therapeutic response in locoregional cancer therapy.

ESB 2026

Engineered polymer carriers integrated with Lab-on-Fiber photonics for light-controlled locoregional drug delivery

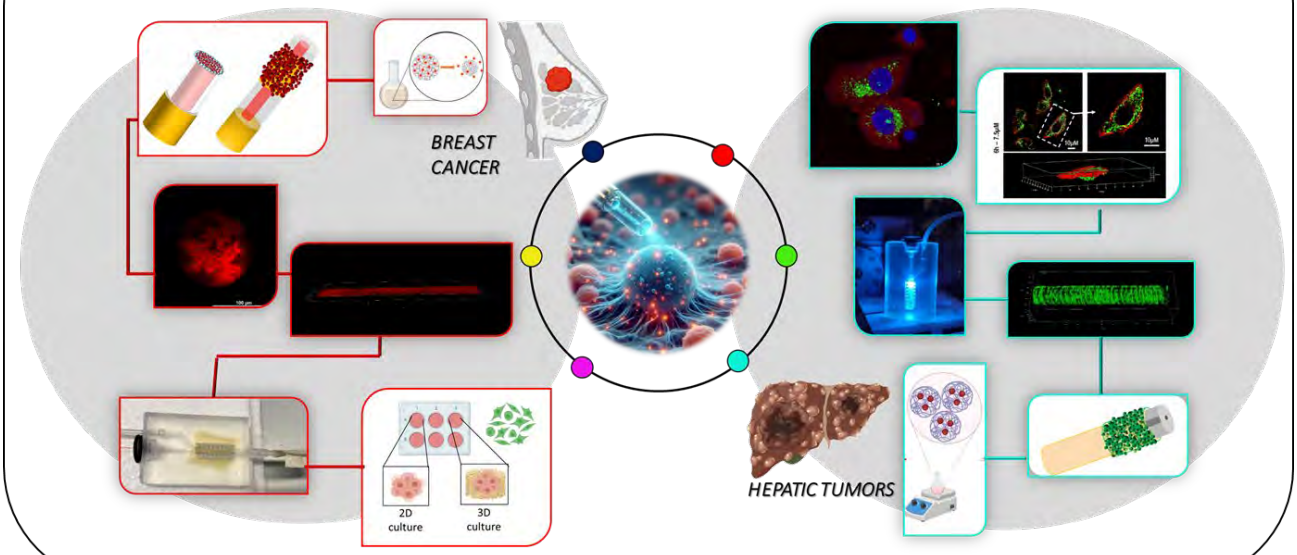

S55 – O3

A vascular heart-on-chip model for studying accelerated aging in space

Van Hoorick J.[1], Rehnberg E.[2,3], Dobos A.[1], Aksu D.[1], Arslan A.[1], Surdo L.[4], Stenuit H.[4], Sonnaert M.[5], Wackers G.[5], Reniers M.[6], Baatout S.[3], Tabury K.[3]
[1]BIO INX, Ghent; [2]Dept. of Molecular Biotechnology, Ghent University; [3]SCK CEN, Radiobiology Unit, Belgian Nuclear Research Center, Mol; [4]Space Applications Services, Zaventem; [5]Antleron, Leuven; [6]Quality by Design, Wilrijk, Belgium

Introduction

Age-related variations in cardiac structure and function increase sensitivity to cardiovascular diseases (CVDs), which continue to be the most prevalent cause of mortality worldwide (1). There is a lack of physiologically relevant human in vitro models of cardiac aging, as many models cannot replicate mature heart tissue and its microenvironment. This constraint is crucial in severe circumstances such as spaceflight, where microgravity and cosmic radiation accelerate cellular aging. This accelerated aging presents a chance to study age-related pathophysiological mechanisms and explore possible treatments earlier than would be feasible on Earth (2).

Aim

The goal of this project is to develop a vascularized human-derived heart-on-a-chip model to assess the effects of cardiac aging in space and recognize potential acceleration.

Materials and Methods

Human induced pluripotent stem cell (iPSC) derived cardiomyocyte organoids were encapsulated in a printed microstructure with specified perfusion channels using the commercial gelatin-based bioink (HYDROBIO INX U200, BIO INX) (Figure 1A). Multiphoton lithography (MPL) (UPNANO NanoOne; 150 mW, 750 mm/s, 5× objective) was employed to generate high-resolution channel networks, and the constructs were incubated for six weeks. A Presto Blue assay was employed to assess cellular metabolic activity, while live-dead staining via laser scanning microscopy was used to determine cell viability. Non-encapsulated organoids were utilized as controls.

Results

During the six-week culture period, considerable levels of cellular viability and metabolic activity were shown by live/dead staining and CellTiter-Glo 3D analysis (Figure 1B and C). Immunofluorescent imaging demonstrated a high cardiomyocyte composition (~77%) and an organized endothelial cell lining (~6.4%) (data not shown). Endothelial cell alignment along MPL-printed channels was induced by VEGF-mediated preconditioning, resulting in the formation of perfusable vascular networks. Organoids showed continuous rhythmic beating throughout the six-week culture period.

Conclusion

The organoid viability and organization were enhanced by the printed vascularized microstructures, which subsequently allowed in vivo-like perfusion and assessment under microgravity and radiation during the 2026 ISS mission. This platform supports cardiac aging research, evaluates preventative measures in space, and enables real-time evaluation of human heart tissue for pharmaceutical and personalized medicine on Earth.

Acknowledgements

The AstroCardia project is funded by VLAIO / EU RRF (HBC.2022.0569).

References

[1]Skardal A., Shupe T., Atala A. Organoid-on-a-chip and body-on-a-chip systems for drug screening and disease modeling. *Drug Discovery Today. 2016*; 21(9): 1399–1411

[2]Tabury K., Rehnberg E., Baselet B., Baatout S., Moroni L. Bioprinting of cardiac tissue in space: where are we? *Advanced Healthcare Materials. 2023*; 12(23): 2203338.

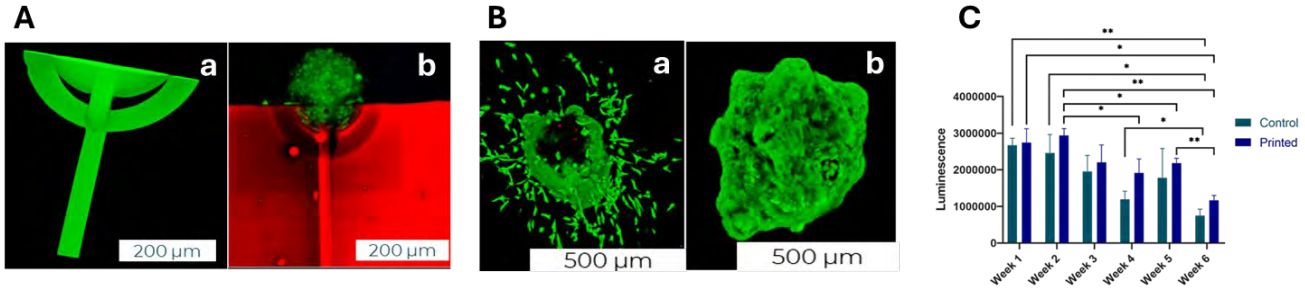

Figure 1 A) Printed structure of half of the design that was injected with the FITC-dextran (a), and organoids labelled with green fluorescent protein (GFP) were captured and positioned centrally within the structure (b) (Scale bars: 200 µm); **B)** Live/Dead staining of organoids cultured for 6 weeks. Organoids encapsulated in 3D-printed vascular structures using HYDROBIO INX U200 (a); organoids cultured without printed structures (control) (b) (Scale bars: 500 µm); **C)** Long-term metabolic activity of organoids cultured without printed structures (control, green) and organoids encapsulated in 3D-printed vascular structures (blue) measured using the CellTiter-Glo 3D assay over six weeks. Statistical significance was determined between time points (*$p < 0.05$, **$p < 0.01$).

S55 – O4

Electrospun P3HB fibers functionalized with hesperidin for skin regeneration

Coccia E.[1], Mula E.[1,2], Sessini V.[2], Paolucci M.[1]
[1]Dept. of Sciences and Technologies, University of Sannio, Benevento, Italy; [2]Dept. of Organic and Inorganic Chemistry, Alcalá de Henares, Madrid, Spain

Introduction

Chronic and acute skin wounds remain a major clinical challenge. Effective wound healing requires biomaterials capable of providing structural support, guiding cellular organization, and modulating the inflammatory microenvironment that governs tissue regeneration. Bacterial polyhydroxyalkanoates have attracted increasing interest in regenerative medicine due to their biocompatibility, biodegradability, and processability into biomimetic structures. Among them, poly(3-hydroxybutyrate) (P3HB) can be processed by electrospinning to produce fibrous matrices that closely resemble the architecture of the extracellular matrix, making them promising candidates for skin tissue engineering and wound healing applications.

Materials and Methods

Electrospun P3HB fibrous mats were investigated as three-dimensional scaffolds for wound healing applications. The cytocompatibility of the bacterial P3HB material was assessed by culturing murine fibroblasts (L929) directly on the scaffolds. Cell viability and proliferation were evaluated at 1, 3, and 5 days using LDH and MTT assays. To enhance the scaffold's biological functionality, P3HB fibers were functionalized with 4% hesperidin (P3HB-4H), a citrus-derived flavanone reported for its antioxidant, anti-inflammatory, and regenerative properties. To explore the potential anti-inflammatory properties of this system, the P3HB-4H scaffold was evaluated by analyzing inflammatory responses in human keratinocytes (HaCaT) under basal and TNF-α-induced pro-inflammatory conditions, using the inflammatory marker COX-2.

Results

LDH measurements confirmed the non-toxic nature of the material compared to the control, and MTT analysis revealed a progressive increase in metabolic activity over time relative to control cultures, indicating sustained cell viability and proliferation on the scaffolds, consistent with the three-dimensional architecture of electrospun matrices.

Immunofluorescence analysis of COX-2 showed increased immunopositivity in TNF-α-stimulated control cultures and in TNF-α-stimulated cells cultured on P3HB fibers, indicating expected inflammatory activation. In contrast, keratinocytes cultured on P3HB-4H scaffolds displayed a markedly reduced COX-2 signal under the same conditions, suggesting a potential anti-inflammatory effect mediated by the bioactive compound.

Conclusion

Complementary cellular models involving keratinocytes and fibroblast–keratinocyte interactions are being used to better reproduce the complexity of the skin microenvironment and to further investigate wound healing processes in vitro. Collectively, these findings demonstrate how the precise functionalization of electrospun P3HB fibers with hesperidin enables the development of bioactive scaffolds capable of modulating inflammatory responses and promoting skin regeneration, highlighting their promise as next-generation wound healing patches.

S55 – O5

Starch-hydroxyapatite composite biomaterials with hierarchical porosity

Bouras H.[1], Buwalda S.[1], Tillier Y.[1], Roscelli A.[1,2], Nedelec J.-M.[3], Corinus A.[2], Luton F.[2], Pradille C.[1], Marchat D.[4], Budtova T.[1]

[1]Mines Paris, PSL Research University, Center for Materials Forming, UMR CNRS 7635, Sophia Antipolis; [2]Université Côte d'Azur, CNRS UMR7275, Inserm U1323, Institut de Pharmacologie Moléculaire et Cellulaire, Sophia-Antipolis; [3]Université Clermont Auvergne, Clermont Auvergne INP, CNRS, ICCF, Clermond-Ferrand; [4]Mines Saint-Etienne, Université Jean Monnet, Etablissement Français du Sang, INSERM, U1059 Sainbiose, Saint-Etienne, France

Introduction

Porous starches are an interesting class of bio-based materials with significant potential in various biomedical applications, ranging from tissue engineering scaffolds to drug carriers. To ensure their effectiveness, e.g. as substitutes for cancellous bone, controlling morphology and porosity is essential. In this contribution, the preparation of starch-based composite materials with hierarchical porosity and the establishment of processing-structure-properties correlations are highlighted.

Materials and Methods

Porous potato starch-based materials were prepared starting from starch dissolution in water at 95 °C and retrogradation. Starch aerogels were obtained by replacing water in hydrogels with non-solvent (ethanol or acetone, resulting in organogels), followed by drying with supercritical CO_2; xerogels were produced via evaporative drying of organogels under low vacuum. To enhance material potential for bone regeneration, hydroxyapatite beads (HA) were added to the starch solution, leading to porous starch-HA composites. The influence of processing parameters (starch and HA concentration, retrogradation time, type of non-solvent and drying method) on the material properties (e.g. morphology, density, specific surface area, stiffness) was systematically studied.

Results

The porous starches possessed low density (0.25 - 0.55 g/cm^3) and specific surface area up to 120 m^2/g. The drying method did not significantly influence the properties of the final materials, suggesting that evaporative vacuum drying of an organogel constitutes a cost-effective way of making porous starch biomaterials. The incorporation of HA beads in the starch matrix resulted in material densification and a corresponding reduction in specific surface area. All materials were highly porous, nanostructured and with interconnected pores. Microtomography and SEM images revealed homogeneous dispersion of HA within the porous starch phase. Structures with hierarchical porosity were produced by 3D printing, with pores' walls based on starch-HA composite xerogels.

Conclusion

The combination of straightforward preparation, tunable hierarchical porosity and biocompatibility makes 3D-printed starch-HA xerogels promising for use as e.g. bioactive scaffolds. These materials combine large pores of controlled dimensions, obtained via 3D printing, which should facilitate cell proliferation and vascularization, with intrinsic porosity and sub-micron size pores in the pore walls, which should support cellular activity.

Acknowledgements

We are grateful to CARNOT M.I.N.E.S. (CARINGS program) for funding, Roquette for providing starch and Région Sud-Provence-Alpes-Côte d'Azur for support in the acquisition of the MAIA 3 SEM (Research Call 2019). We also acknowledge Prof. D. Eglin (Mines Saint-Etienne), Dr. J. Jaxel (PERSEE, Mines Paris), G. Corvec, Dr. F. Georgi and C. Collin (CEMEF, Mines Paris) for scientific advice and technical assistance.

S55 – O6

Protein nanofiber resins for 2pp fabrication of immunostimulatory microswimmers

Jermyn S.[1,2], Hayati L.[1,2], Carr A.[1,2], Ali J.[1,2]
[1]Dept. Chemical & Biomedical Engineering, FAMU-FSU College of Engineering; [2]National High Magnetic Field Laboratory, Tallahassee, FL. USA

Introduction

There is increasing desire to improve current therapeutics by enhancing stability, increasing circulation time, adding targeting capabilities and minimizing off-target effects. One solution under increasing investigation is the employment of self-assembled peptides, and protein or lipid-based structures. These have shown to be highly biocompatible, easily standardized and produced, and capable of enhancing the performance or delivery of therapeutics such as vaccines and anti-cancer drugs [1]. A specific protein, flagellin, has been shown to promote pro-inflammatory cytokine production, enhance antigen-specific adaptive immune responses, and trigger generalized immune cell recruitment to secondary lymphoid sites. Cytokines have also been shown to incite immune activation that can aid in restoring tumor-specific cytotoxic T-cells enabling reinvigorated tumor-antigen recognition and tumor growth inhibition [2], [3]. Here we describe the creation of a novel 2PP flagella based microswimmer capable of precise targeting to enhance and prolong local immune response and deliver anti-cancer compounds *in vitro*.

Materials and Methods

Salmonella *typhimurium* was cultured in modified LB broth and cultured at 37 °C under moderate agitation for 12-16 hours until late log phase. A concentrated solution of flagella was obtained through vortexing and 3 rounds of centrifugation. Eosin Y (1% w/w) was implemented as a type II photoinitiator to facilitate 2 Photon Polymerization between flagellar filaments using the UpNano NanoOne system. Ideal printing power and speed were determined over the ranges of 40mW-180mW and 0.2-2mm/s. Iron Oxide nanoparticles were incorporated into the material using a Thinky mixer to impart actuation capabilities. Particles were actuated using a 20mT rotating magnetic field generated with the MiniMag MagnebotiX system.

Results

Ideal Flagella resin printing parameters were determined to be between 100-140 mW at speeds of 0.2-0.4 mm/s, with overall printing performance shown in Figure 1. Magnetic nanoparticles were successfully incorporated into the resin prior to 2PP fabrication of structures, and printed geometries were actuated in a 20mT rotating magnetic field as seen in Figure 2.

Conclusion

Flagella were successfully isolated and implemented in conjugation with Eosin Y to create a new protein based 2PP resin for fabrication of magnetic microswimmers. Printing parameters were optimized and magnetic nanoparticles incorporated. For future investigation the optimization of magnetic nanoparticle loading and investigation into immunostimulatory properties and drug delivery kinetics is critical for practical development.

Acknowledgements

This work was funded by the National Science Foundation (No. EES-2306449, EES-2219558, EES-2000202) and supported by the NSF FAMU CREST Center award (No. EES-2514451). This material is also based upon work supported by the Air Force Office of Scientific Research under award numbers FA9550-22-1-0247 and FA9550-23-1-0662. Some of the work was performed at the National High Magnetic Field Laboratory, which is supported by National Science Foundation Cooperative Agreement No. DMR-2128556 and the State of Florida. Any opinions, findings, and conclusions or recommendations expressed in this material are those of the author(s) and do not necessarily reflect the views of the United States Air Force. Research was also sponsored by the Army Research Office and was accomplished under Grant Number W911NF26-1-A016. The views and conclusions contained in this document are those of the authors and should not be interpreted as representing the official policies, either expressed or implied, of the Army Research Office or the U.S. Government. The U.S. Government is authorized to reproduce and distribute reprints for Government purposes notwithstanding any copyright notation herein.

References

1. S. Zhang et al., Potential Application of Self-Assembled Peptides and Proteins in Breast Cancer and Cervical Cancer. Int. J. Mol. Sci., 2023; vol. 24, no. 23, p. 17056
2. M. M. Rahman, I. D. Grice, G. C. Ulett, and M. Q. Wei Advances in Bacterial Lysate Immunotherapy for Infectious Diseases and Cancer. J. Immunol. Res. 2024; 4312908
3. Y. Zhao et al., The NLRC4 inflammasome receptors for bacterial flagellin and type III secretion apparatus. Nature 2011; vol. 477, no. 7366; pp. 596–600

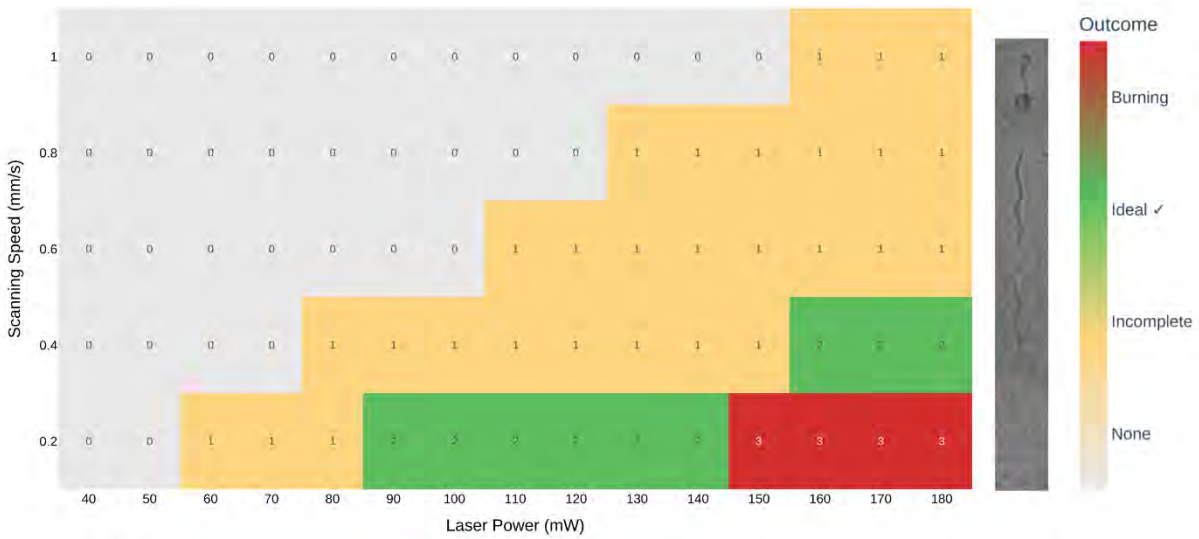

Figure 1) Printing power and speed using UpNano's 10X objective (NA 0.4) were varied to identify the optimal printing parameters for flagella-based resin as depicted by the qualitative scale shown on the right.

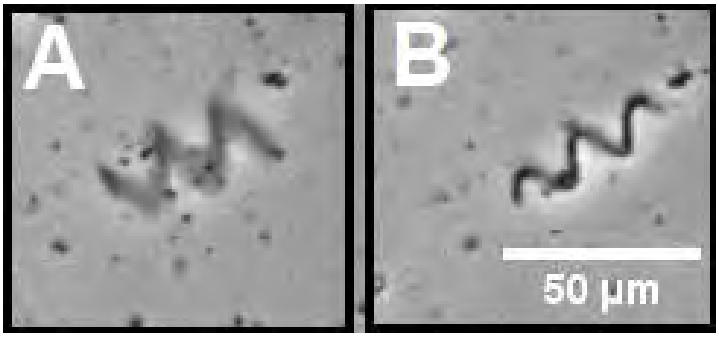

Figure 2) 2PP fabricated flagella-based helices with iron oxide nanoparticles embedded within the print material. Shape anisotropy can be observed in the microswimmer as shown in the comparison of 2A and 2B, in which the microswimmer has been rotated 90 degrees around its long axis via magnetic field actuation.

S56
RSC biomaterials chemistry interest group symposium injectable hydrogels for TERM applications

S56 – K1
Injectable Laponite® crosslinked pNIPAM hydrogels for use as biologically instructive scaffolds

Sammon C[1]
[1]School of Engineering and Built Environment, Sheffield Hallam University, Sheffield, UK

Introduction
Laponite® crosslinked pNIPAM hydrogels (L-pNIPAM) are a highly versatile platform for tissue engineering, demonstrating efficacy across musculoskeletal, cartilaginous and soft-tissue systems.

Aim
This paper describes the development and characterisation of a suite of L-pNIPAM hydrogel formulations capable of supporting cell viability, differentiation, and tissue-specific matrix formation across multiple regenerative applications with the objective of evaluating them as minimally invasive, injectable scaffolds for restoring structure and function in diverse tissues including intervertebral disc, bone and intestinal epithelium.

Materials and Methods
A general materials and methods workflow across the studies involved synthesising L-pNIPAM hydrogels, preparing cell or tissue samples and evaluating biological and mechanical outcomes. All hydrogel formulations (L-pNIPAM, L-pNIPIMA-co-DMAc and L-NIPAM-co-HPMA) were polymerised at 80 °C, mixed with cells (e.g., MSCs or intestinal crypts), injected via fine-gauge needles, cultured under controlled conditions (hypoxia/normoxia/dynamic culture) and assessed using histology, immunohistochemistry, SEM and mechanical testing.

Results
Modification of the crosslink density and/or the nature of the copolymer facilitated the manufacture of fully injectable hydrogels with a range of mechanical properties (0.2-24.3 MPa) and varied interconnected porous networks (visualised using SEM). This resulted in materials capable of being used across a range of tissue engineering applications. In the intervertebral disc (IVD), L-pNIPAM-based formulations integrate with native nucleus pulposus tissue, support mesenchymal stem cell (MSC) differentiation, resist extrusion under dynamic loading and restore mechanical function. Similarly, in bone regeneration, L-pNIPAM-co-DMAc hydrogels, especially when combined with hydroxyapatite nanoparticles, promote osteogenic differentiation without added growth factors, enhance matrix deposition and integrate with surrounding bone while enabling minimally invasive delivery. Within the gastrointestinal tract, L-pNIPAM supports intestinal crypt and Lgr5+ stem-cell culture, facilitating long-term maintenance and differentiation into multiple epithelial lineages under dynamic culture conditions.

Conclusion
Collectively, these studies highlight the adaptability of L-pNIPAM hydrogels as injectable, mechanically supportive and biologically instructive scaffolds capable of tailoring cellular behaviour across diverse tissues including IVD, bone, and gut, positioning them as promising candidates for next-generation regenerative therapies. The system enables minimally invasive, clinically relevant delivery, maintaining low viscosity for needle injection, gelling *in situ* and avoiding toxic crosslinkers while remaining biocompatible.

Acknowledgements
The author gratefully acknowledges financial support from Versus Arthritis, Research England, the Medical Research Council (MR/P026796/1), the H2020 iPSpine Project (Grant Agreement 825925) and MedTech.

S56 – K2

Injectable aggrecan-mimicking peptide–CS hydrogels for early-stage cartilage repair

Warren J.P.[1], Ingham E.[2], Fisher J.[2], Warriner S.L.[3], Fermor H.L.[2]
[1] Department of Materials, The University of Manchester, Manchester, UK, [2] Institute of Medical & Biological Engineering, University of Leeds, Leeds, UK, [3] School of Chemistry, University of Leeds, Leeds, UK.

Introduction

Osteoarthritis is characterised by progressive loss of articular cartilage, leading to pain and impaired joint mechanics; surgical options for late disease are unsuitable for many younger, active patients. Loss of cartilage glycosaminoglycans (GAGs) correlates with reductions in compressive stiffness. We therefore propose covalently GAG-functionalised, self-assembling peptide (SAP) hydrogels, capable of penetrating cartilage and assembling *in situ,* to restore resistance to deformation in early disease.

Aim

The aim of this work was to design, synthesise, and characterise self-assembling peptide–CS conjugated hydrogels, and then assess the effect of treating GAG-depleted cartilage with these hydrogels

Materials and Methods

P_{11}-4/P_{11}-8 were prepared by Fmoc-SPPS and azide-terminated; chondroitin sulfate (CS) was alkyne-functionalised. Conjugation used copper-based azide–alkyne click chemistry; products were purified (dialysis) and confirmed by ^{1}H NMR, SEC-MALLS and LC-MS. Hydrogels were assessed by negative staining TEM and small-amplitude oscillatory rheology at 37 °C (plate–plate 25 mm; 0.033 mm gap); amplitude sweeps (1, 20 Hz) defined the LVER, followed by frequency sweeps (1–20 Hz) at the selected strain to obtain G′. For tissue testing, porcine femoral condyles were GAG-depleted using 0.1% SDS/PBS and validated by Safranin-O/Fast Green, CS-56 and DMMB (severe depletion). Materials were injected via 30 G needle; after equilibration, creep indentation (2.54 N, 1 h; 2.5 mm indenter) quantified deformation. FRAP evaluated *in situ* network mobility.

Results

The depletion protocol removed 76 ± 2 % GAG (mean ± S.D; n = 6); histology and immunolabelling confirmed GAG loss with preserved tissue architecture. TEM showed that covalently tethering CS reorganised peptide-only tapes into longer, thicker and denser fibrillar networks, exceeding the effects of SAP + free CS and indicating stabilisation of higher-order assembly. Rheology (G′) demonstrated high gel stiffness for the conjugates: P_{11}-4–CS reached 434.6 ± 51.3 kPa; P_{11}-8–CS reached 153.7 ± 15.4 kPa (37 °C). Creep indentation showed increased deformation in depleted versus native tissue ($p < 0.005$) and significant reduction ($p<0.005$) after treatment (mean ± 95 % S.D; n = 3 per treatment). P_{11}-8–CS demonstrated 80.3 ± 0.9 % restoration; whilst P_{11}-4–CS resulted in 68.2 ± 2.5 % restoration (Figure 1). FRAP showed no fluorescence recovery within injected regions, confirming stable, in-tissue self-assembled networks. Collectively, maximal stiffness (P_{11}-4–CS) did not equate to maximal restoration (P_{11}-8–CS), implicating intratissue transport/penetration as a key driver of efficacy.

Conclusion

Covalently CS-functionalised SAP hydrogels assembled within cartilage, delivered high G′ and restored tissue-level resistance after severe GAG loss. The less stiff P_{11}-8–CS restored function most effectively, suggesting that compliance-driven penetration and integration are critical design parameters for minimally invasive early-stage repair.

Acknowledgements

This work was supported by funding from the EPSRC DTC-TERM (EP/L014823/1).

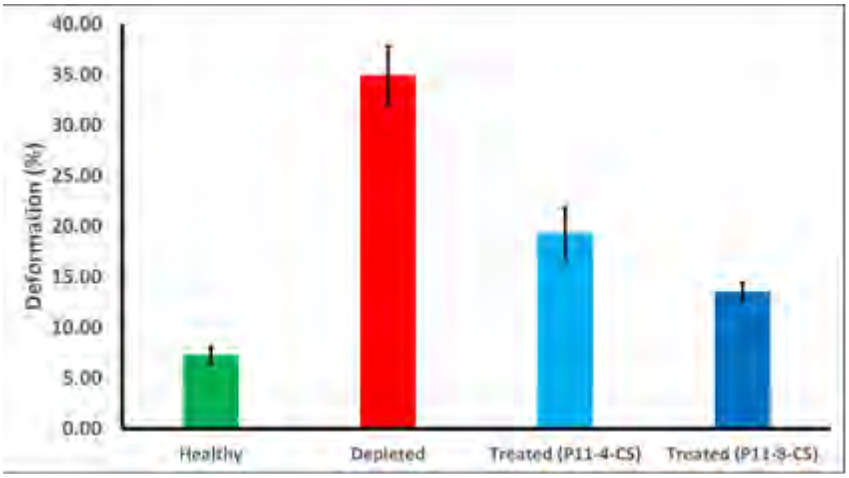

Figure 1: Normalised percentage deformation of different femoral cartilage states for each sample's cartilage thickness (n=3, error bars = mean ± S.D)

S56 – O2

Injectable hyaluronic acid/collagen type II/silk fibroin composite hydrogels for mechanically reinforced nucleus pulposus regeneration under dynamic loading

Torabi Rahvar P.[1], Kumar A.[1], Wöltje M.[2], Gantenbein B.[1,3]
[1]Tissue Engineering for Orthopaedics and Mechanobiology, Bone and Joint Program, Dept. for BioMedical Research (DBMR) of the Medical Faculty, University of Bern, Switzerland; [2]Institute of Textile Machinery and High-Performance Material Technology, TUD University of Technology, Dresden, Germany; [3]Dept. of Orthopaedic Surgery and Traumatology, Inselspital, Bern University Hospital, Medical Faculty, University of Bern, Switzerland

Introduction

Chronic low back pain is frequently associated with degeneration of the intervertebral disc (IVD), affecting over 500 million people worldwide. Degeneration typically initiates in the nucleus pulposus (NP), where progressive cell loss and extracellular matrix (ECM) degradation compromise both mechanical function and biochemical homeostasis. Effective regenerative strategies must therefore restore mechanical integrity while recreating a supportive microenvironment for cells.

Aim

This study aims to enhance the mechanical performance of hyaluronic acid (HA) and collagen type II (COLII) – based hydrogels for IVD regeneration by incorporating silk fibroin (SF) microfibers and evaluating their behavior under dynamic loading conditions.

Materials and Methods

Bone marrow–derived mesenchymal stromal cells (BMSCs) were encapsulated within HA/COLII and HA/COLII/SF hydrogels (Figure 1a), and cytocompatibility was assessed using calcein AM/ethidium homodimer-1 staining. Constructs were subjected to dynamic compression (10% strain, 1.5 Hz, 1 h/day) using a custom mini-bioreactor (Figure 1d) with specially designed flower-shaped chambers (Figure 1e). Degenerated bovine IVD explants were generated via papain injection and subsequently treated with the hydrogels.

Results

Live/dead staining confirmed high cell viability in both hydrogel formulations (Figure 1b), demonstrating good cytocompatibility; the red appearance of SF fibers was attributed to nonspecific binding of ethidium homodimer-1. Macroscopic evaluation of treated explants showed improved tissue integrity and mechanical stability compared to degenerated controls (Figure 2a). Magnetic resonance imaging (MRI) further revealed that hydrogel-treated IVDs retained hydration and disc height under dynamic loading, whereas papain-treated controls exhibited pronounced degeneration (Figures 2b, 2c).

Conclusion

The developed HA/COLII/SF injectable hydrogel provides a mechanically reinforced and biologically supportive platform for NP regeneration. Its ability to maintain cell viability and improve structural properties under physiologically relevant loading conditions highlights its potential as a minimally invasive therapeutic strategy for IVD degeneration. Furthermore, this system represents a valuable platform for investigating mechano-responsive regenerative therapies for degenerative disc disease.

Acknowledgements

This work was supported by the SNSF Weave Grant (#320030E_224175) and the DFG (#437213841). We thank Wolf-Dieter Zech, Julia Bruenig, and Andrina Auderset for their assistance with magnetic resonance imaging.

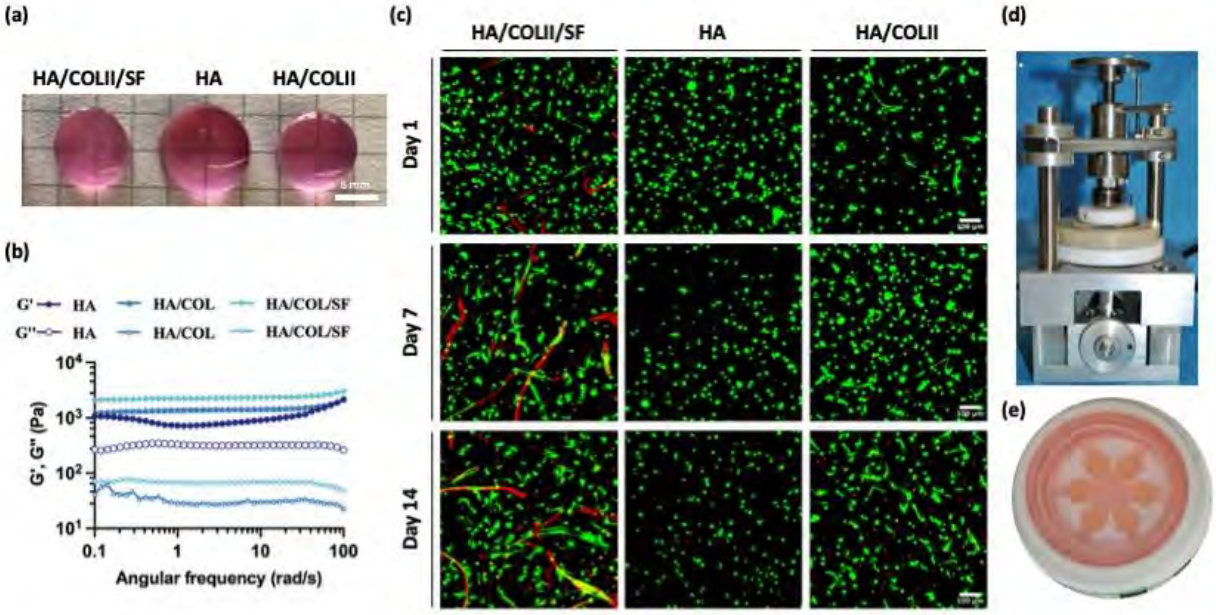

Figure 1. (a) Hydrogels composed of hyaluronic acid (HA), type II collagen (COL II), and silk fibroin (SF). (b) Storage modulus (G') and loss modulus (G") of hydrogels with different compositions. (c) Live/dead assay of human mesenchymal stem cells (hMSCs) encapsulated within the various hydrogel formulations. (d) Mini bioreactor used for mechanical loading of cell-laden hydrogels. (e) Flower-shaped chambers designed for hydrogel placement and mechanical loading under sterile conditions.

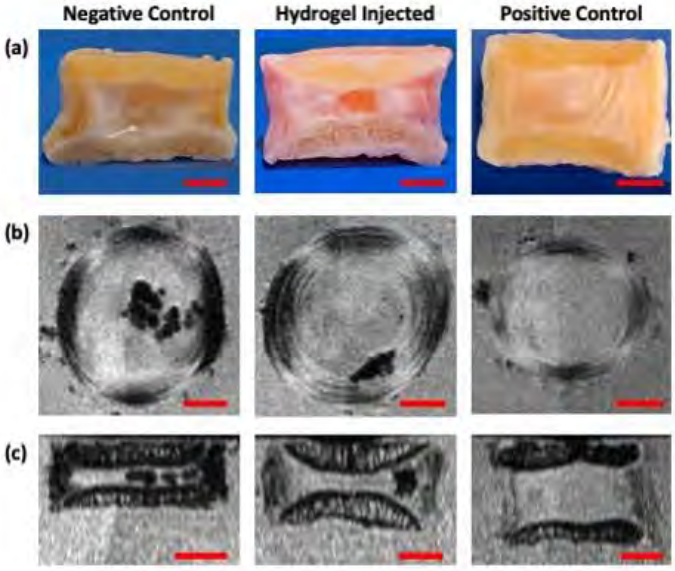

Figure 2. (a) Macroscopic and (b,c)magnetic resonance imaging (MRI) assessment of intervertebral disc (IVD) explants following dynamic culture, demonstrating improved disc hydration and height in hydrogel-treated samples. Scale bars: 5 mm.

S56 – O3

Design of customized injectable hydrogels relying on Schiff-base and supramolecular interactions as potential antibiotic-free therapeutic platforms

Pappalardo R.[1,2], Boffito M.[1], Cassino C.[3], Laurano R.[1], Ceresa C.[4], Fracchia L.[4], Ciardelli G.[1,2]
[1]Dept. of Mechanical and Aerospace Engineering, Politecnico di Torino, Turin; [2]Institute for Chemical-Physical Processes IPCF-CNR, Pisa; [3]Dept. of Science and Technological Innovation and Magnetic Resonance Platform (PRISMA-UPO), Università del Piemonte Orientale "A. Avogadro", Alessandria; [4]Dept. of Pharmaceutical Sciences, Università del Piemonte Orientale "A. Avogadro", Novara, Italy

Introduction

Schiff-base and supramolecular chemistries offer versatile strategies to engineer hydrogels through dynamic covalent and reversible non-covalent interactions, respectively, enabling control over their physicochemical and rheological properties. Owing to their mild gelation, injectability, and self-healing ability, they represent promising platforms for drug delivery.

Aim

In this work, double crosslinked hydrogels were developed, relying on Schiff-base bonds between poly(ether urethane) (PEU) chains and the physical assembly of poly(pseudo)rotaxanes (PPRs) resulting from α-cyclodextrins (α-CDs) threading along polymer chains. Moreover, thymol (Thy) was encapsulated as antimicrobial compound by exploiting the inclusion complex formation with β-CDs.

Materials and Methods

Poly(ethylene glycol)-based PEUs exposing primary amines (SHE3350) or aldehyde-end groups (AHE1500) were synthesized and their ability to form inclusion complexes with α-CDs was characterized by nuclear magnetic resonance (NMR) spectroscopy and X-Ray powder diffraction (XRD) analysis. Double crosslinked hydrogels were prepared by mixing SHE3350, AHE1500 and α-CD aqueous solutions. Schiff-base (SHE3350-AHE1500) and double crosslinked (SHE3350-AHE1500-CD) hydrogels were compared to assess their physico-chemical and rheological properties. In parallel, inclusion complexes of β-CDs and Thy (βCD/Thy) were prepared and their cytocompatibility, antioxidant and antibacterial properties were assessed. Lastly, βCD/Thy-loaded SHE3350-AHE1500-CD gels were formulated, and the release was quantified for 10 days in physiological-like conditions.

Results

SHE3350 (24 kDa and polydispersity index D 1.7) and AHE1500 (4 kDa, D 1.5) were able to form physically assembled PPRs when mixed with α-CDs. Due to the concurrent formation of supramolecular interactions and Schiff-base bonds, SHE3350-AHE1500-CD underwent faster gelation than SHE3350-AHE1500 and showed superior mechanical properties (E=7 kPa vs. 2.4 kPa) and enhanced self-healing ability. In parallel, the successful βCD/Thy formation was confirmed (71% encapsulation efficacy). βCD/Thy exhibited enhanced cell viability and a lower minimum inhibitory concentration (MIC) against *S. aureus* compared to free Thy (0.1 mg/mL *vs.* 0.25 mg/mL), while the ROS scavenging activity was not altered upon complexation. Moreover, βCD/THY complexes were released from SHE3350-AHE1500-CD gel in 10 days in a controlled and sustained manner. Lastly, the therapeutic platform showed high cytocompatibility (ca. 75% cell viability).

Conclusion

This work highlighted the potential of tailored hydrogels as injectable antibiotic-free platforms for the effective delivery of antibacterial compounds.

Acknowledgements

This research received funding from the European Union - NextGenerationEU through MUR under PNRR - M4C2-I1.3 Project PE_00000019 "HEAL ITALIA". The abstract content reflects only the authors' view and opinion. Neither the European Union nor the European Commission can be held responsible for them. The authors also thank the ATTITUDE project titled "vAlorization of wasTe products for the fabrication of sustainable paTient-personallzed paTches targeting different phases of the woUnD hEaling cascade", which was financed by Fondazione Pisa (Italy) Call 2022 "Scientific and Technological Research" in macroarea of Biomedicine.

S56 – O4

Resistance-suppressing antibacterial ε-polylysine/hyaluronic acid injectable hydrogels for treating wound infections

Sceglovs A.[1,2], Siverino C.[3], Skadins I.[4], Moriarty T.F.[3], Kroica J.[4], Salma-Ancane K.[1,2]
[1]Institute of Biomaterials and Bioengineering at Riga Technical University, Latvia; [2]Baltic Biomaterials Centre of Excellence, Headquarters at Riga Technical University, Latvia; [3]AO Research Institute Davos, Switzerland; [4]Dept. of Biology and Microbiology, Riga Stradins University, Latvia

Introduction

The growing threat of antimicrobial resistance has created an urgent demand for non-antibiotic biomaterials capable of preventing infections without promoting bacterial resistance. In this study, we developed injectable, covalently cross-linked hydrogels composed of ε-poly-l-lysine (ε-PL) and hyaluronic acid (HA) for localized wound infection treatment.

Materials and Methods

ε-PL/HA hydrogels were synthesised using chemical cross-linking approach at varying mass ratios. The resulting hydrogel formulations were comparatively analyzed through comprehensive characterization such as molecular structure, surface morphology and topology, stability and biodegradation studies, autoclavability, release kinetics, and rheological studies. *In vitro* evaluation comprised advanced antibacterial testing against both reference and clinically isolated bacterial strains, including multidrug-resistant strains (*MRSA* and *ESBL*), as well as biocompatibility assessment using direct and indirect assays with human/animal fibroblast cell lines.

Results

The chemical cross-linking strategy employed in this study resulted in the formation of a stable biopolymeric matrix. The hydrogels demonstrated required for proposed tissue engineering application properties, such as autoclavability, macroporosity (60–200 μm), and high antibacterial/antibiofilm activity. Rheological analysis revealed hydrogels viscoelastic properties: stiffness (10–15 kPa), injectability, recovery capability (up to 98%), and gelation time (up to 50 min). Swelling capacity, zeta potential, ε-PL release kinetics, bactericidal activity, and biocompatibility across different fibroblast cell lines were found to be dependent on the ε-PL mass ratio within the hydrogel composition.

Conclusion

This study reports the development of covalently cross-linked ε-polylysine/hyaluronic acid hydrogels with tunable ε-PL content. Rheological analysis confirmed injectability for minimally invasive, syringe-based delivery. The hydrogels exhibited broad-spectrum antibacterial and antibiofilm activity against clinically relevant, including multidrug-resistant, bacteria, with sustained efficacy over time. Cytocompatibility studies revealed a dose-dependent fibroblast response to ε-PL, emphasizing its role in modulating cell viability. Overall, these injectable ε-PL/HA hydrogels combine favorable rheological properties, potent antibacterial performance, and biocompatibility, representing a promising non-antibiotic strategy for localized treatment of bacterial wound infections.

Acknowledgements

The authors acknowledge financial support from the “Biomedical and Photonics Research Platform for the Development of Innovative Products (Project No IVPP-EM-Innovation-2024/1-0002 "Biomedical and Photonics Research Platform for Innovative Products (BioPhot))” project No. OSI_PIP_BioPhoT-2025/2-0071 “Injectable Hydrogel for Antimicrobial and Regenerative Therapy of Fracture-Related Bone Infections (BoneART)” and access to the infrastructure and expertise from Horizon 2020 project No. 857287 (BBCE – Baltic Biomaterials Centre of Excellence).

S56 – O5

Injectable multifunctional nanoengineered strontium-based laponite® hydrogels accelerates bone regeneration via favorable physiochemical properties and promoting osteo-/anticlastogenic effects

Abuhamdan R.M.[1,2,], Xu Z.[3], Cavanagh B.[4], Boccaccini A.R.[3], Murphy C.M.[2,5,6], Kaur K.[1,2]
[1]School of Pharmacy and Biomolecular Sciences, RCSI, Dublin, Ireland; [2] Tissue Engineering Research Group, Dept. of Anatomy & Regenerative Medicine, RCSI, Dublin, Ireland; [3]Institute of Biomaterials, University of Erlangen-Nuremberg, Erlangen, Germany; [4]Cellular and Molecular Imaging Core, RCSI, Dublin, Ireland; [5]Advanced Materials and Bioengineering Research Centre, RCSI and TCD, Dublin, Ireland; Trinity Centre for Biomedical Engineering, Trinity College Dublin (TCD), Ireland

Introduction

In osteoporotic conditions, the activity of the osteoclasts (OCs) outweighs that of osteoblasts (OBs)[1]. This loss of homeostasis between OC-mediated bone resorption and OB-mediated bone formation leads to a decreased bone mass and density, resulting in bone fragility and a higher risk of fractures, particularly vertebral ones. Current gold-standard treatments, vertebroplasty/kyphoplasty, involve the injection of bone cement. They, however, fail to restore bone homeostasis or promote bone-repair and regeneration[2]. To address these limitations, we used Strontium (Sr), a calcium analogue, and Laponite®-2D nanodisks to leverage the synergistic effects of both components when encapsulated within chitosan/collagen hydrogels to develop a mechanically robust injectable system with favourable structural/biological properties. This makes it a promising drug free therapeutic strategy.

Aim

To develop injectable hydrogels capable of enhancing bone regeneration by simultaneously promoting osteogenesis and inhibiting osteoclastogenesis for osteoporosis treatment.

Materials and Methods

Strontium phosphate nanoparticles (SrPO) were preprepared by one pot synthesis method. Thermoresponsive hydrogels nanoengineered with Laponite® (0-0.25%w/v) and SrPO(0.15-1%w/v) were prepared by mixing acid solubilized chitosan with collagen in the presence of β-glycerophosphate, a gelling agent at pH~7.4. The structural properties of prepared hydrogels were characterised in detail. To determine biocompatibility and the bone regeneration capacity of hydrogels on mesenchymal stem cells (MSCs) and osteoclast (RAW 264.7), *in vitro* cell proliferation and osteogenic differentiation were assessed via Alamar Blue™, PicoGreen™ and calcium mineralization, while osteoclastogenesis was evaluated using tartrate resistant acid phosphatase (TRAP) activity and staining of large multinucleated cells in the presence of RANK-L.

Results

Mechanically robust nanoengineered injectable hydrogels were successfully prepared. It was found that increasing nanofiller (Laponite® and SrPO) concentration enhanced gel stiffness, crosslinking density, swelling while reducing degradation (*Figure 1*), key factors for their structural stability and therapeutic effectiveness. MSCs exhibited strong proliferation on the hydrogels (*Figure 2a&b*), and their osteogenic differentiation resulted in significantly higher calcium deposition compared to control hydrogels. Importantly, SrPO nanoparticles were non-toxic to osteoclasts at concentrations up to 250 µg/mL (*Figure 2c&d*), yet they effectively inhibited cellular differentiation, demonstrating their dual role in promoting bone formation while suppressing bone resorption.

Conclusion

Hydrogels containing nanofillers showed superior structural, osteogenic and anti-osteoclastogenic properties compared to hydrogels without these components. The synergistic effect of the SrPO with Laponite® in promoting bone regeneration while inhibiting bone resorption highlights their potential as a drug-free strategy for the treatment of osteoporosis.

References

[1]*The Lancet 2011* 377,1276–1287.
[2]*Journal of Bone and Mineral Research* 2019, 34,3–21.

Figures

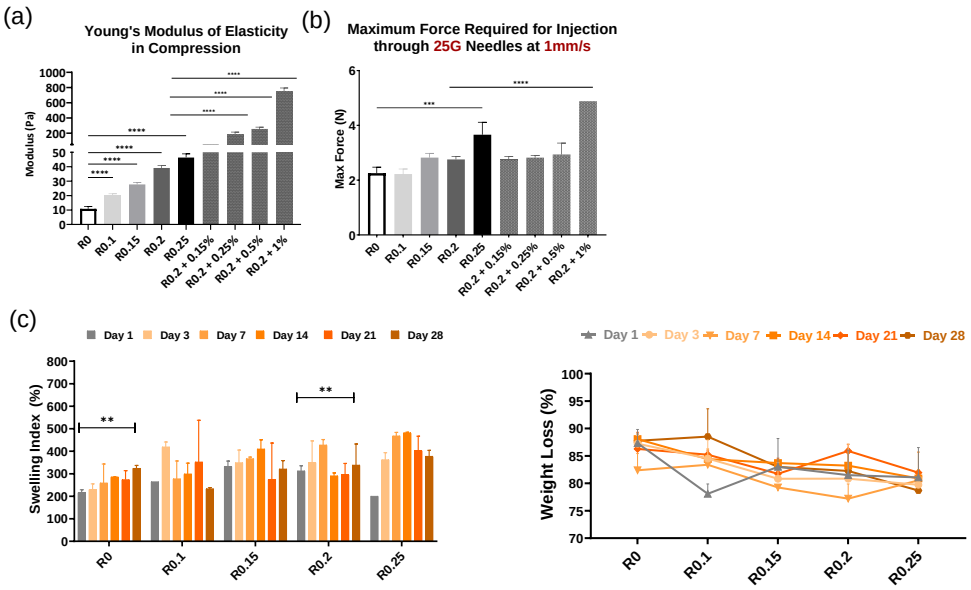

Figure 1. *Mechanical elasticity of produced hydrogels (a) and the maximum force required for injection of the hydrogel solutions through 25-gauge needles at a speed of 1 mm/sec (b). Bars designate means and error bars indicate ± SD, (n=3). The swelling index % (c) and the weight loss % (d) of Laponite® loaded hydrogels in phosphate buffered saline (PBS) at pH=4.5. Bars designate means and error bars indicate ± SD, (n=2).*

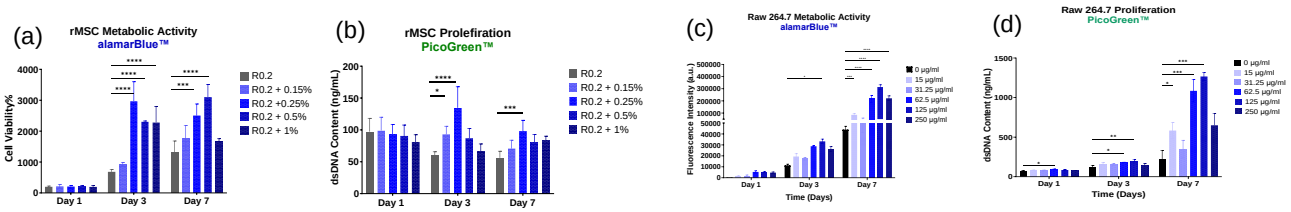

Figure 2. *Metabolic activity (a) of rMSCs cultured on Laponite® and SrPO hydrogels at days 1, 3, and 7, and the proliferation (b) of the rMSCs cells. Metabolic activity (c) of Raw 264.7 cells cultured on the surface of 12 well plates at days 1, 3, and 7, and the proliferation (d) of the Raw 264.7 cells. Bars designate means and error bars indicate ± SD, (n=4).*

S56 – O6

Injectable hyaluronic acid hydrogel-enabled mesenchymal stem cell therapy for diabetic chronic wound repair

Song R.[1], Tai H.[2], Wang W.[1]
[1] Charles Institute of Dermatology, School of Medicine, University College Dublin, Dublin, Ireland; [2] Bláfar Ltd., Cherrywood Business Park, Dublin, Ireland

Introduction

Diabetic chronic wounds remain difficult to treat because persistent inflammation, oxidative stress, poor angiogenesis, and impaired tissue regeneration compromise the local healing microenvironment. Previous studies have shown that injectable hydrogels can enhance stem cell retention and improve wound repair, while in situ forming HA-based hydrogels can support sustained local therapeutic delivery in chronic wound settings. [1-3] Building on this foundation, we developed an injectable hyaluronic acid (HA)-based hydrogel system for in situ mesenchymal stem cell (MSC) encapsulation and delivery, aiming to improve stem cell function and remodel the diabetic wound microenvironment toward regeneration.

Materials and Methods

The hydrogel was formed by mixing acrylated HA (HA-A) and thiolated HA (HA-SH), enabling rapid in situ gelation through a mild thiol–Michael addition reaction. MSCs were encapsulated within the precursor solution before gelation to generate a cell-laden injectable HA hydrogel. The system was evaluated for injectability, in situ gelation, and its ability to support MSC viability and organization. Biological effects relevant to chronic wound repair were assessed by examining cell-related regenerative functions and wound microenvironment modulation, including macrophage polarization, growth factor secretion, fibroblast migration, endothelial tube formation, and overall wound healing response.

Results

The overall therapeutic design and proposed mechanism of the MSC-loaded injectable HA hydrogel are summarized in Figure 1. The HA-based injectable hydrogel enabled local MSC encapsulation with rapid in situ gelation and provided a supportive three-dimensional microenvironment for cell delivery. Encapsulated MSCs maintained viability and showed enhanced spheroid-like organization within the hydrogel. Functionally, the MSC-loaded hydrogel supported a more regenerative wound microenvironment, with evidence of enhanced M2 macrophage polarization, paracrine activity, fibroblast migration, and endothelial tube formation. These effects were associated with reduced inflammation and oxidative stress, improved angiogenic potential, and enhanced tissue regeneration in diabetic chronic wounds. Collectively, the results indicate that the injectable HA hydrogel not only serves as a delivery vehicle but also acts as a microenvironment-regulating scaffold that amplifies MSC-mediated repair.

Conclusion

This study demonstrates that an injectable HA hydrogel can enhance MSC-based therapy for diabetic chronic wounds by improving local cell delivery and promoting regenerative microenvironment modulation. Beyond this specific wound-healing application, the work highlights the broader translational potential of injectable HA hydrogels as adaptable platforms for cell-based regenerative therapies.

Acknowledgements

The authors acknowledge the support of University College Dublin and Bláfar Ltd. for research and platform development. The authors gratefully acknowledge Shenzhen Beike Biotechnology for providing human umbilical cord-derived mesenchymal stem cells used in this study.

References

[1]Xu Q., A S., Gao Y., Guo L., Creagh-Flynn J., Zhou D., Greiser U., Dong Y., Wang F., Tai H., Liu W., Wang W., Wang W. A hybrid injectable hydrogel from hyperbranched PEG macromer as a stem cell delivery and retention platform for diabetic wound healing. *Acta Biomaterialia* 2018; 75; 63-74.
[2]Dong Y., A S., Rodrigues M., Li X., Kwon S.H., Kosaric N., Khong S., Gao Y., Wang W., Gurtner G.C. Injectable and tunable gelatin hydrogels enhance stem cell retention and improve cutaneous wound healing. *Advanced Functional Materials* 2017; 27; 1606619.
[3]Yu H., Zhang J., Yang L., Tian Y., Milne C., Jin P., Li Q., Song R., Wang W. MSC-derived exosomes injectable hyaluronic acid hydrogel for enhanced chronic wound healing. *Journal of Controlled Release* 2025; 385; 113985.

Figure 1. Therapeutic rationale for the current hydrogel-enabled MSC system. HA-A and HA-SH are mixed with MSCs to form an injectable HA hydrogel by thiol-Michael addition, enabling rapid in situ gelation after local administration to diabetic chronic wounds. Within this 3D niche, MSCs undergo in situ spheroid formation, maintain viability and stemness, and enhance wound-relevant functions including growth-factor secretion, M2 macrophage polarization, fibroblast migration and endothelial support. These effects are proposed to shift the diabetic wound bed from a chronic inflammatory, poorly regenerative state toward a pro-healing microenvironment.

S57

Scaffolds for advanced cell models of disease including tumour microenvironments

S57 – K1

Exploring cell-matrix interactions in health & desease using precision biomaterials

Ashworth J.C.[1]
[1]Biodiscovery Institute, University of Nottingham, Nottingham, UK

Advanced cell models of living tissues are gaining attention as possible alternatives to *in vivo* preclinical models. There is, however, a current paradox between these highly specialized cell models, derived from patient tissue or from stem cells, and the one-size-fits-all biomaterials often used to grow them. These biomaterials do not typically represent tissue-specific extracellular matrix (ECM), despite its known importance in regulating many biological processes.

This talk will explore the combination of ECM analysis and biomaterials design to generate improved *in vitro* mimics of human tissues. By combined control over key features such as mechanical environment, biomolecular composition, and structural patterning, novel biomaterials may be designed to match tissue- and disease-specific ECM. I will describe my lab's research into spatially patterned 3D matrix organization, incorporating independent control over ECM composition and multiscale mechanical properties. To inform model design, we are developing workflows for 2D and 3D tissue imaging, incorporating compositional analysis (e.g. via the Nottingham GlycoAnalytics hub) and structural characterisation by multiphoton and second harmonic generation (SHG) microscopy. The resulting multimodal image data provides the blueprints for our tissue-specific models, generated using a range of biomaterial fabrication methods from hydrogel design to ice-templating. By combining these defined biomaterials with complex cell models for 3D culture, this approach allows us to uncover how cell-matrix interactions influence the processes involved in tissue homeostasis and/or disease progression.

Focussing on breast cancer as proof-of-concept, we are developing this approach to probe ECM regulation of tissue organization in a patient-realistic setting. Primary breast organoids cultured within defined ECM mimetics display high viability, branching morphology, and cellular heterogeneity, with collagen fibre patterning directing the invasion of patient-derived breast cancer cells. By reproducing tissue-realistic ECM organization, these "precision biomaterials" recreate cell-matrix interactions specific to the target tissue. This approach is providing novel insights into the mechanisms of tissue regulation, with future potential to uncover a new realm of previously undiscovered therapeutics targeting the role of the ECM.

Acknowledgements
This work was supported by: University of Nottingham, UK; Henry Royce Institute for advanced materials Equipment Access Scheme (Cambridge 3D Bioelectronics Facility: Cambridge Royce facilities grant EP/P024947/1, Sir Henry Royce Institute recurrent grant EP/R00661X/1); Academy of Medical Sciences (Springboard Award: [REF: SBF0010\1065]); Animal Free Research UK (Grant number: 194). Animal Free Research UK does not support or fund any experiments involving animals, animal tissue, animal cells or cell lines, or animal-derived products.

S57 – K2

Mapping patient-specific prostate cancer stroma interactions in a three-dimensional bioengineered tumour microenvironment

Low Jun Wei J.[1], Skowronek K.[1], Noronha M.[1], Garside A.[1], Niranjan B.[3,] Risbridger G.[3,5], Lawrence M.[3,5], Taubenberger A.[1,2]

[1]Center for Molecular and Cellular Bioengineering (CMCB), BIOTEC, TUD, Dresden University of Technology, Germany; [2]Leibniz-Institute of Polymer Research Dresden (IPF), Max Bergmann Center of Biomaterials, Dresden, Germany; [3]Melbourne Urological Research Alliance, Biomedicine Discovery Institute, Monash University, Clayton, Victoria, Australia; [4]Peter MacCallum Cancer Centre, Melbourne, Victoria, Australia; [5]Sir Peter MacCallum Dept. of Oncology, The University of Melbourne, Victoria, Australia; [6]Cabrini Institute, Cabrini Health, Malvern, Victoria, Australia.

Introduction

Prostate cancer (PCa) is the 2nd leading cause of cancer death among males in Germany. Although multiple treatment options are available, advanced prostate cancer is currently considered incurable. Thus it is important to dissect mechanisms contributing to disease progression and also to better predict patient outcome. Among other factors, tumour-stromal interactions have been recognised as important contributors to cancer progression and therapy resistance. These cellular interactions, however, are complex and not well characterized using conventional 2D PCa *in vitro* models.

Aim

In our study we set out to develop a bioengineered 3D model to study tumour stroma interactions of the primary PCa niche.

Materials and Methods

To emulate cellular interactions with the extracellular matrix, we embedded PCa cell lines (BPH-1, PC-3 cells) and patient-derived cancer associated fibroblasts (CAFs) or normal fibroblasts (NPFs) into mechanically tuneable gelatin methacryloyl (GelMa) hydrogels. We then characterised cellular crosstalk via morphological, molecular and mechanical readouts, e.g. quantitative imaging analysis of fluorescently labelled cells, Brillouin microscopy, as well as metabolic characterisations.

Results

Here we have developed a 3D bioengineered model, consisting of epithelial PCa cells and patient-derived prostatic fibroblasts. Fibroblast morphology and cellular network formation were found to be sensitive to the hydrogels' mechanical properties. While soft hydrogels (elastic modulus <1kPa) allowed for the formation of vital cellular networks of CAFs, poorer cell growth and negligible network formation were seen in stiffer hydrogels. NPF cultures generally displayed lower viability, with less extended cell bodies and no network formation. In co-cultures with epithelial cancer spheroids, CAFs derived from different patient donors promoted cancer cell invasion to varying degrees.

Conclusions

In summary, we have established a 3D *in vitro* platform that allows for the study of tumour-stromal interactions in a patient-specific manner, which in extension can also be used to study effects of anti-cancer drugs. Ongoing work evaluates whether complex cell behaviours that are observable *in vitro* tumour model can predict patient outcome.

S57 – O1

Evaluating nanoparticle penetration in tumor-like matrices using a volumetrically 3D printed model

Abrishami A.[1], Faurès M.[1], Shavandi A.[1]
[1]3BIO-BioMatter, École polytechnique de Bruxelles, Université libre de Bruxelles (ULB), Belgium

Introduction

Limited penetration of therapeutic nanoparticles into solid tumors remains a major challenge in cancer nanomedicine. The dense extracellular matrix (ECM), heterogeneous pore structure, and elevated interstitial pressure of the tumor microenvironment significantly restrict nanoparticle transport. Consequently, reliable in vitro platforms capable of reproducing ECM barriers are essential for quantitatively evaluating nanoparticle diffusibility before in vivo studies.

Aim

This work aims to establish a volumetrically printed tumor model that enables systematic investigation of nanoparticle diffusion through ECM-mimicking hydrogels and to quantify the transport behavior of fluorescent probes with different hydrodynamic sizes.

Materials and Methods

Tumor-like models were fabricated using volumetric 3D printing of a photocurable GelMA–PEGDA hydrogel resin containing a central core and perfusable channels to mimic tumor architecture. The hydrogel matrix was characterized in terms of density, porosity, swelling behavior, and compressive mechanical properties. Hydrated samples stained with fluorescent dyes were analyzed by confocal microscopy to observe pore structure in the native wet state, while freeze-dried samples were examined using micro-computed tomography (micro-CT) and scanning electron microscopy (SEM) to assess internal morphology. Biocompatibility and cell adhesion of the constructs were assessed by culturing HT-29 colorectal cancer cells within the hydrogel matrices. Diffusion studies were performed using fluorescent probes with increasing hydrodynamic size, including Dextran-FITC and phospholipid-stabilized quantum dots (PL@QDs). Transport was investigated under two conditions, including static diffusion from a central core and dynamic perfusion with a physiological flow rate through printed channels to simulate flow-driven transport.

Results

The printed GelMA–PEGDA hydrogels exhibited ECM-like characteristics with high water content (>80%) (Fig. 1). Confocal microscopy and SEM revealed pore diameters ranging from approximately 10–100 µm. Mechanical testing showed compressive moduli of ~10–30 kPa, while swelling analysis demonstrated a mean swelling ratio of 8.86 ± 0.40 after 7 days. HT-29 cells maintained high viability (>70%) within the constructs, confirming biocompatibility after 7 days. Static diffusion of Dextran-FITC reached approximately 60% relative diffusion after 4 h, indicating partial penetration into the hydrogel matrix (Fig. 2). In contrast, dynamic perfusion of PL@QDs through the printed channels significantly enhanced transport, reaching ~100% relative diffusion after 4 h. Fluorescence microscopy further confirmed nanoparticle delivery and accumulation in the cell-seeded core region of the tumor model.

Conclusion

This study presents a volumetrically printed GelMA–PEGDA hydrogel tumor model. The platform enabled evaluation of macromolecule and nanoparticle transport under static and perfusion conditions, revealing size-dependent diffusion and improved distribution under flow. These results highlight the utility of the model for studying nanoparticle transport in tumor-like environments, although further studies are needed to validate and expand its applications.

Acknowledgements

The author acknowledges the support of Université Libre de Bruxelles and the FNRS ASP (60231).
A.S. acknowledges support from the FNRS under the CDR grant J.0188.24.
The authors further acknowledge the Walloon Region for financing, in whole or in part, the equipment used in this study through the Technology Platforms of Excellence, *Alternative to animal experimentation,* and *Biogreen*.

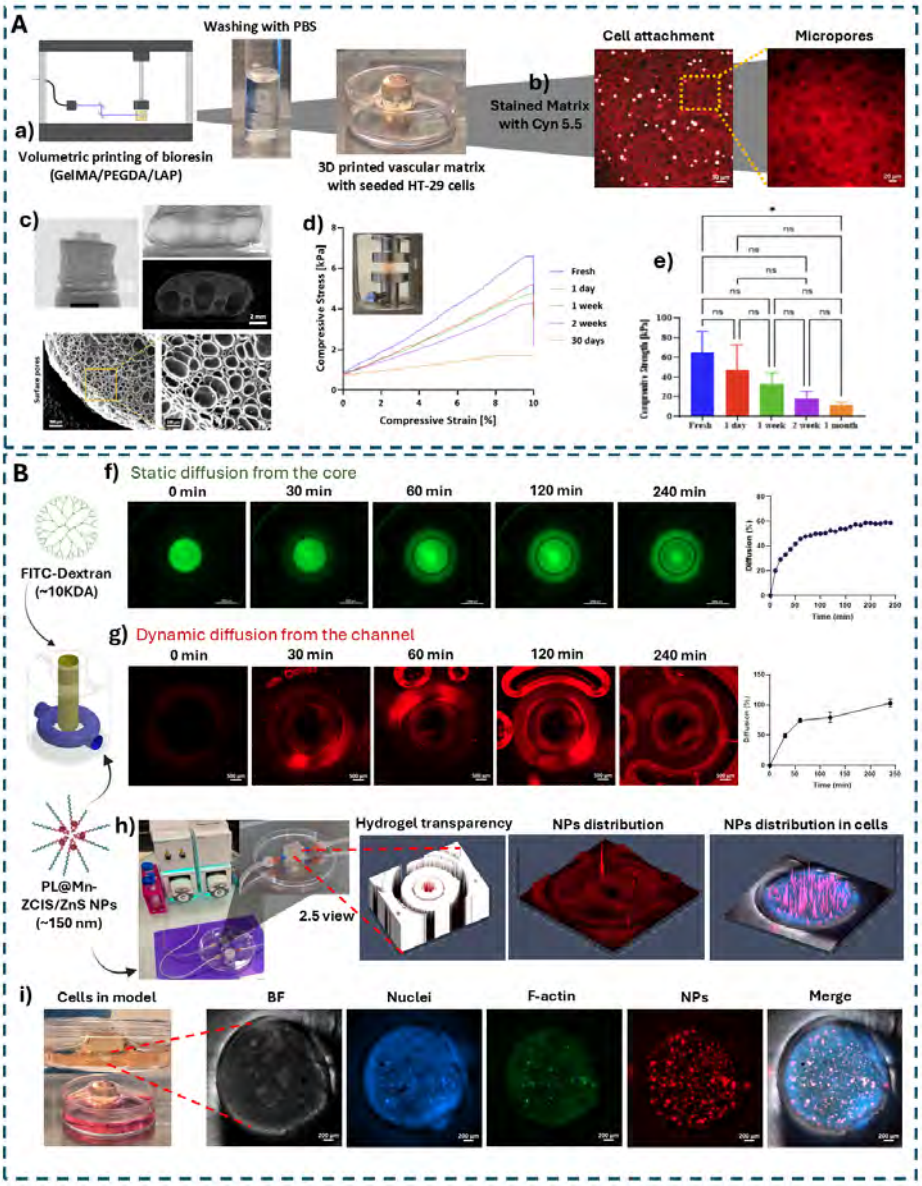

Figures A and B. a) Volumetric 3D printing setup and fabrication workflow of the GelMA–PEGDA tumor model; b) microporous hydrogel structure visualized by confocal microscopy (hydrated samples) and c) micro-CT and SEM (freeze-dried samples); d) compressive mechanical characterization; e) Compressive strength at different incubation times; f) static diffusion from the core using Dextran-FITC; g) dynamic diffusion from the channel using PL@QDs; h) experimental setup of the perfusion system and printed model with cells; i) fluorescence microscopy showing nanoparticle delivery and accumulation in the cell-seeded tumor core.

S57 – O2

Engineering 3d bone organotypic models of dormant breast cancer metastasis to study cell-extracellular matrix crosstalk

Mitxelena-Iribarren O.[1], Heras U.[1,2], Aiastui A.[3,4], Cipitria A.[1,5]
[1]Group of Bioengineering in Regeneration and Cancer, Biogipuzkoa Health Research Institute, Donostia/San Sebastian; [2]Dept. of Cell Biology and Histology, Faculty of Medicine and Nursing, University of the Basque Country EHU, Leioa; [3]Multidisciplinary 3D Printing Platform, Biogipuzkoa Health Research Institute, Donostia/San Sebastian; [4]ISCIII Platform of Biobanks and Biomodels, Instituto de Salud Carlos III (ISCIII), Madrid; [5]IKERBASQUE, Basque Foundation for Science, Bilbao, Spain

Introduction

Early detection of disseminated cancer cells (DCCs) in metastatic niches such as the bone marrow is a complex challenge. DCCs leaving the primary tumor tend to enter a dormant state once they reach this metastatic site.

Aim

To mimic the 3D microenvironment of dormant breast cancer (BC) cells with engineered 3D bone organotypic models to investigate mechanisms of dormancy and to test new drugs.

Materials and Methods

3D bone organotypic in vitro models were developed based on microCT scans of human bone[1], segmented using self-developed deep learning models with ORS-Dragonfly and 3D printed by stereolithography. Scaffolds were treated with NaOH and coated with calcium phosphate, to create an osteoinductive microenvironment. After sterilization, human mesenchymal stromal cells (hMSC) were seeded and cultured for 21 days with either normal cell growth media (bone marrow mimicking niche) or osteogenic media (endosteal niche). hTERT-HUVECs were co-cultured to obtain a perivascular niche. Then, two BC cell lines modified with the FUCCI-2 cell cycle reporter were added to the niches in order to analyze their crosstalk with the cell-derived matrix. These cells included MCF7 (oestrogen receptor-positive luminal BC cells) and MDA-MB-231 (triple-negative BC cells). Interaction between BC cells and the hMSC-derived matrix was characterised using immunofluorescence and confocal imaging, and quantified with self-developed deep learning models in ORS-Dragonfly.

Results

hMSC-derived 3D matrix in bone marrow mimicking and endosteal niches was composed of fibronectin, osteocalcein, collagen I & III and α-SMA and its volume and density increased with time (Figure 1). In addition, when seeding MCF-7 of MDA-MB-231 BC cells in the niches, a significant increase in the amount of fibronectin, osteocalcein and collagen I&III was observed. Moreover, fibers showed less alignment and less organised structure when BC cells were cultured in the niches, demonstrating that BC cells altered the ECM microarchitecture (Figure 2). Similarly, we found a correlation between the BC cell cycle and properties of the hMSC-derived niche: MCF-7 cell population decreased, with more growth arrested cells, while a higher population of MDA-MB-231 cells remained proliferative in both niches, demonstrating how the bone microenvironment affects the dormant or proliferative state of the DCCs.

Conclusion

3D bone organotypic models allow improved understanding of cell-ECM interaction at early stages of metastasis, which could have applications in the development of new therapeutic strategies targeting these cells and their microenvironment.

Acknowledgements

We acknowledge financial support from Fundación Científica Asociación Española Contra el Cáncer, (grant numbers POSTD234723MITX, PRYCO247223GOMI and LABAE223466CIPI); the Gipuzkoa Provincial Council (2025-CIE4-000015-01), the Spanish Ministry of Science and Innovation (PID2021-123013OB-I00 funded by MCIN/AEI/10.13039/501100011033/FEDER, UE); the Basque Government Department of Education (PRE_2024_2_0005 and PRE_2025_2_0097) and the European Research Council Consolidator Grant (DORMATRIX, 101123883), IKERBASQUE Basque Foundation for Science.

References

[1] Moreno-Jiménez I., Heining S., Heras U., et al. 3D osteocyte lacunar morphometry of human bone biopsies with high resolution microCT: From monoclonal gammopathy to newly diagnosed multiple myeloma. *Bone* 2024; 189; 117236.

Figures

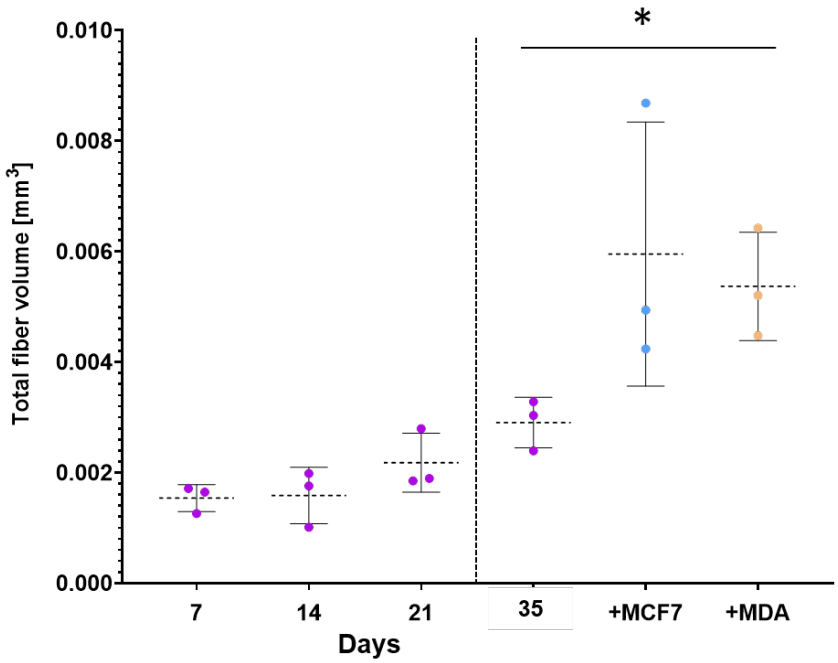

Figure 1: Quantification of hMSC derived ECM evolution over time and under the co-culture of BC cells.

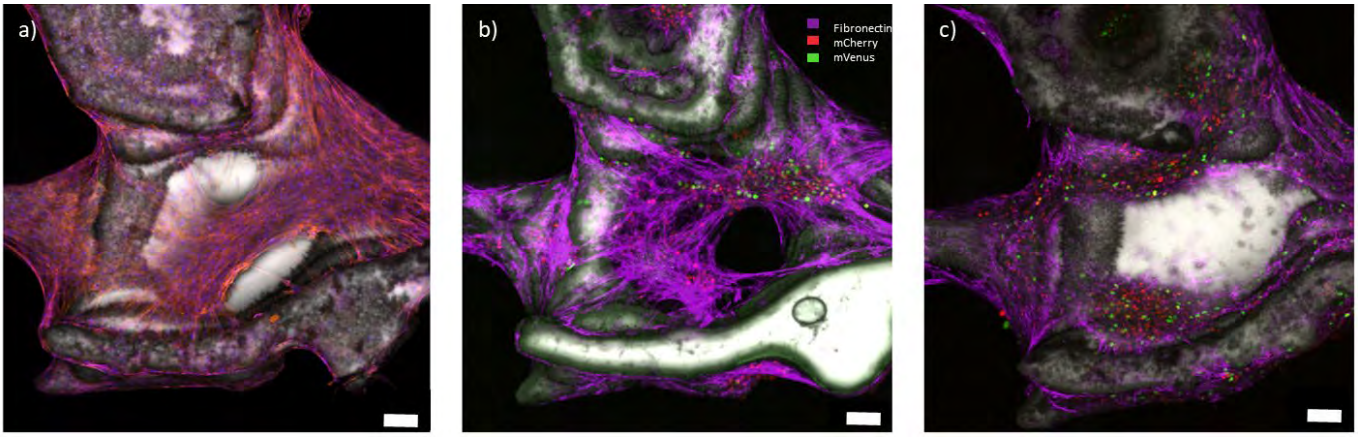

Figure 2: Immunofluorescence images of the bone organotypic niches at day 35, having a) hMSC only and in co-culture with b) MCF-7 or c) MDA-MB-231 BC cells for two weeks. Scale bar 100 µm.

S57 – O3

Monitoring 3D printed disease models: Tools and strategies

Mateo A. M[1], Perin F. [1], Troncoso-Afonso L. [2], García-Astrain C.[1,3]
[1]POLYMAT, Applied Chemistry Department, Faculty of Chemistry, University of the Basque Country UPV/EHU, Donostia−San Sebastián; [2]CICbiomaGUNE, Basque Research and Technology Alliance (BRTA), Donostia-San Sebastián; [3]IKERBASQUE-Basque Foundation for Science, Bilbao, Spain

Introduction

The transition from traditional two-dimensional (2D) cell cultures to three-dimensional (3D) cell models has emerged as a pivotal bridge between in vitro research outcomes and their clinical applications. Unlike 2D cultures, 3D models more accurately replicate the complexity of in vivo cellular microenvironments, providing deeper insights into cell behavior, disease monitoring, and drug testing. However, the shift to 3D models necessitates the development of sensing technologies capable of monitoring cellular processes within these intricate environments. One promising solution lies in the integration of sensors into the materials used to construct 3D cell models. By incorporating sensors into (bio)ink formulations for (bio)printing, we unlock new possibilities for creating more realistic models that can monitor disease progression and facilitate high-throughput drug screening.

Aim

The goal of this work is to develop sensing strategies that can be incorporated into 3D cell models for in-situ monitoring of cell behaviour and disease progression

Materials and Methods

For the preparation of the models, we developed different (bio)inks using biopolymers, synthetic polymers, and decellularized extracellular matrix-based hydrogels, incorporating plasmonic nanoparticles (NPs) or conjugated polymers (CPs) for in vitro sensing. Bare gold nanoparticles (NPs) are employed to detect cell-secreted metabolites using Surface Enhanced Raman Spectroscopy (SERS), while CPs enable colorimetric and fluorescence reading.

Results

In this work, we explored different configurations of 3D cell models. Plasmonic scaffolds containing gold nanorods (AuNRs) were designed to support cancer cell growth and enable monitoring of chemotherapeutic drug consumption using SERS, revealing differences in drug uptake among different cell types. On the other hand, CPs were incorporated into bioink formulations to track pH variations through colorimetric and fluorescent responses, enabling the detection of disease-related processes and the development of infection models.

Conclusion

The integration of sensors within (bio)inks offers a promising strategy for developing smart tissue models that can provide valuable insights into disease mechanisms and therapeutic responses.

Acknowledgements

Financial support was provided by the Spanish MICIU PID2024-162567OA-I00 and a 2025 Leonardo Grant for Scientific Research and Cultural Creation from the BBVA Foundation. We acknowledge support from the María de Maeztu Excellence Unit CEX2023-001303-M funded by MCIN/AEI/10.13039/501100011033.

S57 – O4

Alginate-based hydrogels to quantify ECM viscoelasticity

Kay R.[1], Tsigkou O.[2], Tirella A.[3]
[1]Dept. Pharmacy and Optometry, UoM, Manchester, UK; [2]Dept. Materials, UoM, Manchester, UK; [3]Dept. Industrial Engineering, UniTn, Trento, Italy

Introduction

The extracellular matrix (ECM) provides physical and biochemical signals to cells, directing many biological mechanisms. ECM viscoelasticity has been widely identified as a key mechanical property involved in these cell-substrate interactions, however, a standardised approach to precisely quantifying the key viscoelastic parameters of both human tissues and biomaterials is lacking. Novel testing methods are key to developing in-vitro models able to recapitulate ECM-cell signals of normal and diseased states, hence, enabling investigation of their effects on cells. Here, we report a testing method able to directly compare viscoelastic properties of human tissue samples and hydrogels.

Materials and Methods

Creep-relaxation cycles were optimised and used in combination with a mathematical model to identify viscoelastic parameters of highly hydrated materials (hydrogels). The developed mathematical model combines Maxwell and Kelvin models (springs, dashpots) to map the elastic, viscous, and time-dependant responses independently. Creep-relaxation cycles were performed through rheology and compression, adapting the mathematical model accordingly. Specifically, the relaxation time is utilised to compare hydrogels as an important viscoelastic parameter. As cell-substrate interactions take place over short time periods (~1s), the energy released immediately after removal of the applied stress was used to quantify viscoelasticity. Selected alginate-based hydrogel formulations were used to validate the model.

Results

A small library of alginate-based hydrogels (conjugation with PEG varying in MW) with tuneable viscoelasticity varying independently of other mechanical properties (e.g. Young's modulus) was created. The model returned viscoelastic parameters capable of mimicking a wide range of biological tissues (compared to literature). Between 0.01% and 0.5% strain energy is released within the first 0.5s in either shear or compression, in line with values from human tissues. The lower the energy released, the more viscous the material. Increasing the molecular weight of PEG increases viscosity, while increasing calcium crosslinking increases elasticity.

Conclusion

The developed protocol for testing highly hydrated materials informs on their viscoelastic properties. The model was assessed using alginate-based hydrogels, and precise identification of key viscoelastic parameters in biological processes, e.g. relaxation time, could aid in deciphering cell-substrate interactions. This platform offers a unique perspective in testing biomaterials for the development of new technologies towards personalised applications and to better study the effect of substrate mechanical properties on cellular adhesion, migration, proliferation, and differentiation.

Acknowledgements

The authors would like to thank the EPSRC funded Centre for Doctoral Training in Advanced Biomedical Materials (grant reference EP/S022201/1) for funding this work.

S58
Smart biomaterials and bio-adhesives to combat pathogenic microbes

S58 – K1
Assembling peptides: A chemical toolbox for the design of bioactive nanomaterials

Elsawy M.A.[1]
[1]Division of Pharmacy and Optometry, University of Manchester, Manchester, UK

Molecular self-assembly has been exploited in Nature to develop the complex higher macromolecular structures of both the genome and proteome. Our work focuses on understanding the fundamentals behind self-assembly of protein structures and learning lessons from those biomacromolecules for the design of de novo ultra-short, constrained peptides that self-assemble into bio-inspired fibril structures. Using chemical toolbox of amino acid building blocks, we adopt a bottom-up engineering approach for the rational design of our peptides, where the primary sequence dictates the resulting self-assembled nanostructure [1-4].
We have manipulated those peptide-based nanostructures for the innovation of novel stable, responsive and functional bionanomaterials with various potential pharmaceutical, biomedical and biotechnological applications. Recently, we have started exploring the antimicrobial activity of our peptide nanofibrous hydrogels, in an attempt to overcome Antimicrobial Resistance in infected wounds. In this talk we will focus on the bactericidal and antibiofilm activity of our peptide nanofibrous hydrogels, which could be topically used for hydration and treatment of infected acute wounds (e.g. in treatment of calcinosis associated with myositis) and chronic ulcerated ones (e.g. diabetic foot ulcers).

Acknowledgements
This work is partially funded by the Myositis UK (Myositis Small Grant; 016_SG_MyositisUK_ME) and the UK Research and Innovation (UKRI) Cross Research Council Responsive Mode grant (UKRI3713)

References
[1] Khedr A., Soliman M., Elsawy M. **(2023).** 'Chapter 1: Design rules for de novo self-assembling peptide nanostructures', in Elsawy M. ***Peptide Bionanomaterials: From Design to Application*.** Gewerbestrasse, Switzerland: Springer Nature (ISBN 978-3-031-29359-7). DOI: 10.1007/978-3-031-29360-3_1
[2] Wychowaniec J., Patel R., Leach J., Mathomes R., Chhabria V., Patil-Sen Y., Hidalgo-Bastida A., Forbes R., Hayes J., Elsawy M. Aromatic stacking facilitated self-assembly of ultra-short ionic complementary peptide sequence: β-sheet nanofibres with remarkable gelation and interfacial properties, ***Biomacromolecules* 2020;** *21*: 2670-2680. DOI: 10.1021/acs.biomac.0c00366
[3] Soliman M., Khedr A., Sahota T., Armitage R., Allan R., Laird K., Allcock N., Ghuloum F., Amer M., Alazragi R., Edwards-Gayle C., Wychowaniec J., Vargiu A., Elsawy M. Unraveling the Atomistic Mechanism of Electrostatic Lateral Association of Peptide β-Sheet Structures and Its Role in Nanofiber Growth and Hydrogelation, ***Small* 2025;** *21*: 2408213. DOI: 10.1002/smll.202408213
[4] Khedr A., Soliman M., Corrigan A., Sahota T., Armitage R., Allcock N., Jegadeesan J., Amer M., Alazragi R., Ahmad Z., Wychowaniec J., Elsawy M. Charge Directed Selective Co-Assembly of Ionic Complementary Peptide Binary Mixtures, ***Small* 2026**; *22*: e13140. DOI: 10.1002/smll.202513140

S58 – K2

Multifunctional albumin and bioactive glass-based bio-adhesives for bone regeneration and antimicrobial applications

Gera S.[1], Jones J.R.[1]
[1]Dept. of Materials, Royal School of Mines, Imperial College London, London, UK

Introduction

The fixing of fractured bone remains challenging for not having suitable biomaterial which are bioactive, scaffold support for fixation and anti-infective against pathogens. Current therapy using non-biodegradable metal screws/plates/nails is susceptible to infections, and requires re-surgery for removal, and are not suitable for fixing small fragments. Conventional polymethyl methacrylate cements are non-biodegradable, non-bioactive, poor adhesion in wet conditions and cytotoxic. Therefore, there is urgent need for developing safe and effective biomaterial for the bone fracture. Hence, we aimed to fabricate mussel inspired multifunctional bio adhesive hydrogel made up of bioglass, polydopamine, and bovine serum albumin (BSA).

Materials and methods

Comparatively two multifunctional hydrogels have been fabricated, 1) polydopamine-bioglass-Bovine serum albumin crosslinked by EDC/NHS 2) polydopamine-bioglass-photo-crosslinked BSA methacrylate. Crosslinking chemistry was used to synthesise each component as i) PDA by polycondensation of dopamine, ii) bio-glass (BG) nanoparticles by sol-gel process and iii) Photo-crosslinked BSA methacrylate with Polyethylene Glycol Diacrylate (PEGDA) and photo-initiator Lithium phenyl- 2,4,6- trimethylbenzoylphosphinate (LAP). Hydrogel fabrication — These hydrogels were prepared of different BG conc. (1-20% w/v). Then characterised by Circular Dichroism for BSA structure, rheology for storage and loss modulus, scanning electron microscopy for morphology Fig 1a, adhesion to collagen membrane by Dynamic Mechanical Analysis, lap shear strength by Instron tensile tester, compared to fibrin glue. Further, ion release in phosphate buffer saline quantified by Inductive Coupled Plasma Mass spectroscopy and hydroxyapatite formation by X-Ray. The biocompatibility was tested in osteoblast cells (SaOS2) by MTT and live-dead assay Fig 1b, c. Additionally, osteogenesis by alkaline phosphatase assay (ALP), mineralisation by Alizarin red Fig1d, RUNX2 expression by immunostaining, antioxidant activity by Dichlorodihydrofluorescein Diacetate. Finally, antimicrobial activity was evaluated against the resistant bacteria

Results

- Hydrogel was characterized for structure, morphology, crosslinking by tools as described above.
- The PDA, BG concentration had significant effect on adhesion, mechanical properties, as demonstrated by variations in gelation time and storage modulus.
- Both chemically, photo crosslinked hydrogels exhibit higher lap shear strength compared to fibrin glue.
- Exhibited biocompatibility on osteoblast cells and antioxidant potential.
- Observed constant Ca, Si release indicating osteogenic effect as upregulated ALP, mineralisation, RUNX2 expression.
- Promising antimicrobial activity was noted.

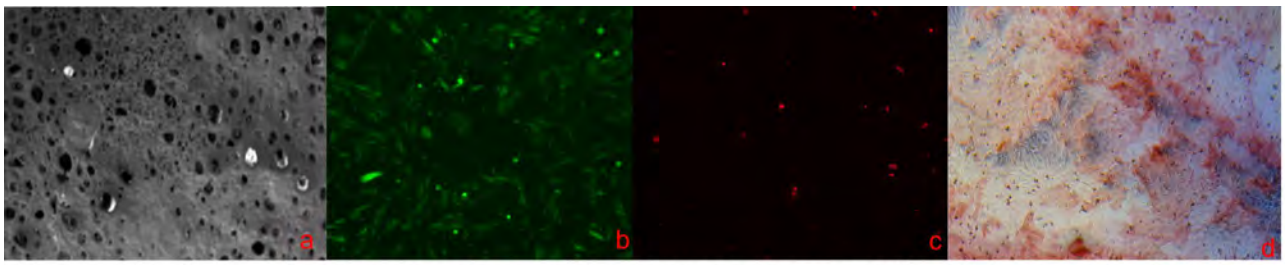

Figure 1. (a) Surface morphology, (b,c) Hydrogel biocompatibility by Live/dead staining assay; (d) Mineralisation observed in osteoblast cells

Conclusion

The developed multifunctional hydrogel is biocompatible with simultaneous tissue adhesion, bioactive for bone repair, anti-infective, thus offering a promising alternative to fibrin glue for surgical applications.

Acknowledgements
Authors gratefully acknowledge funding from UKRI and the European Commission for FIX-heal project (EP/Z002443/1) under MSCA/PF-2023.

S58 – O1

KR-12 functionalised collagen as an antimicrobial biomaterial ink for bone regeneration

Echeverri E.[1], Palo-Nieto C.[2], Muhammad T.[3], Mourkas E.[4], Kontakis M.G.[1], Leliopoulos C.[5], Andersson B.[1], Järhult J.D.[4], Göransson U.[3], Hailer N.P.[1]
[1]OrthoLab, Department of Surgical Sciences/Orthopaedics, Uppsala University, Uppsala, Sweden; [2]Dpto. Ciencia de los Materiales, I. M. y Q. I., IMEYMAT, Facultad de Ciencias, Universidad de Cádiz, Cádiz, Spain; [3]Pharmacognosy, Department of Pharmaceutical Biosciences, Uppsala University, Uppsala, Sweden; [4]Zoonosis Science Center, Department of Medical Sciences, Uppsala University, Uppsala, Sweden; [5]Dept. of Macromolecular Chemistry, Uppsala University, Uppsala, Sweden

Introduction

Critical-size bone defects remain a major clinical challenge where additive manufacturing offers promising solutions through patient-specific implants replicating native bone architecture. Collagen is widely used in bone tissue engineering but requires chemical modification to overcome its limited mechanical strength. Implant-associated infection is a serious orthopedic complication, making materials with intrinsic antimicrobial properties highly desirable. Antimicrobial peptides (AMPs) offer broad-spectrum activity, low risk of resistance development, and good biocompatibility, making them attractive candidates for this purpose.

Aim

This study aims to develop 3D-printable collagen scaffolds incorporating KR-12 AMP derivatives with intrinsic antibacterial function for bone regeneration.

Materials and Methods

Two conjugation strategies were employed to covalently bind KR-12 derivatives to type I collagen using EDC/NHS carbodiimide coupling and thiol-ene maleimide chemistry. Peptide incorporation was quantified using a HABA/Avidin assay following biotin labeling of the derivatives. Printing optimization of the resulting biomaterial inks was performed by varying polymer concentration and extrusion parameters to achieve suitable flow properties for direct ink writing with an open-source bioprinter. Printed scaffolds were characterized structurally by electron microscopy and enzymatic degradation was assessed in 0.01 U/mL collagenase solution over two weeks. *In vitro* biological evaluation included confocal imaging of human osteoblasts (hOB), metabolic activity, and alkaline phosphatase (ALP) activity, complemented by antimicrobial testing against *Staphylococcus aureus.*

Results

KR-12 derivatives were successfully incorporated into collagen, achieving 60–80 mg peptide/g dry material. Scaffolds exhibited highly porous architecture with randomly oriented open pores, and visible collagen fibrils indicating intricate 3D interconnectivity, favorable for cell attachment and nutrient diffusion. In the degradation assay, the samples demonstrated good short-term stability, retaining over 80% mass at 24 h, with 60–74% mass remaining after two weeks. Antimicrobial testing demonstrated that the KR-12 functionalised collagen scaffold significantly reduced bacterial counts at 24 h. Confocal imaging confirmed hOB growth on the scaffolds, with cells displaying high metabolic and ALP activity, indicative of good osteoblast function.

Conclusion

We present the first 3D-printable collagen-based biomaterial ink incorporating an AMP, demonstrating effective printability and antibacterial activity. Covalent integration of a stabilized KR-12 derivative highlighted the critical role of conjugation method in determining peptide loading and bioavailability. The KR-12 functionalised collagen sample showed activity against *S. aureus*, a key pathogen in fracture-related infection, alongside favorable biocompatibility and rheological properties suitable for extrusion-based 3D printing. This resorbable collagen-KR12 scaffold represents a promising candidate for bone tissue engineering where infection prevention is essential.

S58 – O2

Mesoporous bioactive glasses as carrier systems for local bacteriophage delivery in implant-associated infections

Vater C.[1], Richter R.F.[1], Kopelmann F.[1], Uggeri E.[1], Lode A.[1]
[1]Centre for Translational Bone, Joint and Soft Tissue Research, Faculty of Medicine of Dresden University of Technology, Germany

Introduction

Bacteriophages, viruses that infect and kill bacteria with high specificity, are a promising addition to antibiotic therapy of implant-associated infections, especially when the effectiveness of antibiotics is compromised by multidrug-resistant bacteria. Their local administration is considered beneficial; with the use of biomaterials as carriers, bacteriophages should be immobilized at the site of infection and released over time.

Aim

This work explored the general applicability of mesoporous bioactive glasses (MBG) as delivery system for bacteriophages. In addition to developing a procedure for efficient loading, the influence of the MBG composition on binding and release of active bacteriophages as well as the release of active bacteriophages from injectable MBG-hydrogel composites were investigated.

Materials and Methods

MBG microparticles of a molar ratio of Si/X/P of 80:15:5, with X = Ca, Na or La, were produced by a sol-gel method with Pluronic P123 as sacrificial template material. T4 bacteriophages against *Escherichia coli* were used as model strain. To investigate the release of active bacteriophages, the T4-loaded MBG microparticles were incubated in human plasma-like medium at 37 °C; the medium was changed at defined time points and the supernatants were tested for their effectiveness against *E. coli* using growth curve analysis and plaque formation assay. For application as an injectable delivery system, T4-loaded Ca-MBG microparticles were mixed with alginate- or fibrin-based hydrogels.

Results

All MBG microparticles could be loaded with an efficiency of >95% by incubation in a bacteriophage suspension for just 5-10 minutes. The release of active bacteriophages depended on the bacteriophage titer used for loading and on the MBG composition. After loading with a comparatively low titer (10^6 plaque forming units), Ca-MBG and La-MBG released active phages over at least 14 days, whereas Na-MBG showed nearly no release. This observation can be correlated with the zeta potential which was significantly lower for Na-MBG, indicating a very strong binding of the bacteriophages with their positively charged tail. By combining loaded Ca-MBG with the hydrogels, injectable composite materials were created which released active bacteriophages over a long period of time.

Conclusion

MBG microparticles enable sustained local bacteriophage delivery. Due to their bioactivity and associated stimulation of bone regeneration, bacteriophage-loaded MBG appear particularly promising for treatment of bone implant-associated infections. The combination of MBG with hydrogels not only allows for easy application, but also enables the development of dual release systems.

Acknowledgements

This work was funded by the German Research Foundation (DFG; Project No. 536226074).

S58 – O3

Cellulose nanofibers as a platform for 3D-printed scaffolds for tissue engineering and Zn-functionalized wound dressings with antibacterial activity

Pita-Vilar M.[1], Castro-Rodriguez M.[1], Alvarez-Lorenzo C.[1], Chinga-Carrasco G.[2], Diaz-Gomez L.[1]
[1]Dept. de Farmacología, Farmacia y Tecnología Farmacéutica, I+D Farma Group (GI-1645), Facultad de Farmacia, Instituto de Materiales (iMATUS) and Health Research Institute of Santiago de Compostela (IDIS), Universidade de Santiago de Compostela, Spain; [2]RISE PFI, Trondheim, Norway

Introduction

Cellulose nanofibers (CNFs) are sustainable biomaterials that mimic the extracellular matrix by reproducing its nano- and microscale fibrous network, similar to collagen fibers, thereby supporting cell organization. Lignin-containing pulps offer a cost-effective alternative to bleached pulps, although residual lignin may influence oxidation efficiency, fibrillation, scaffold structure, and cellular responses.

Aim

This study aimed to develop and evaluate 3D-printed CNF scaffolds from pulps with different lignin contents and assess Zn^{2+} functionalization to obtain biocompatible antibacterial scaffolds for wound dressing applications.

Materials and Methods

CNFs were produced from bleached and unbleached kraft pulps through TEMPO-mediated oxidation followed by mechanical fibrillation, and characterized for surface chemistry, morphology, and rheology. Dispersions (2-2.5% w/w) were extrusion-printed into scaffolds with aligned fiber orientation. Structural and mechanical properties were evaluated by SEM, micro-CT, and mechanical testing, and antioxidant activity was assessed. Biocompatibility and cell proliferation were studied using fibroblasts, while inflammatory response was analyzed with murine macrophages. For antibacterial functionality, scaffolds were functionalized with Zn^{2+} and evaluated for loading and release behavior, cytocompatibility, hemocompatibility, and antibacterial and antibiofilm activity.

Results

TEMPO oxidation introduced carboxyl groups in both CNFs, with higher functionalization in bleached pulps, suggesting partial interference of residual lignin with oxidation. Increased carboxylation improved nanofibrillation, producing smoother morphology, smaller fibril diameters, and improved thixotropic recovery. Inks at 2-2.5% enabled reliable printing of highly porous (>90%) interconnected scaffolds with random or aligned architectures defined by extrusion direction. Higher CNF concentration and aligned structures reduced collapse and improved mechanical properties, reaching stiffness and tensile strength values comparable to native skin. Both CNF types supported fibroblast proliferation, confirming cytocompatibility. Macrophage assays showed a transient increase in TNF-α and moderate IL-6, consistent with early healing activation, while IL-4 and IL-10 remained low, indicating a balanced immune response. Zn-functionalization preserved cell viability but reduced fibroblast adhesion, which may facilitate painless dressing removal. All scaffolds were hemocompatible, and Zn incorporation significantly enhanced antibacterial and antibiofilm activity against *S. aureus* and *P. aeruginosa*.

Conclusion

3D-printed CNF scaffolds exhibit high porosity, controlled fiber alignment, and mechanical properties suitable for wound dressings. Although lignin content affects oxidation and fibrillation, cytocompatibility and balanced inflammatory responses are maintained. Zn^{2+} functionalization provides antibacterial activity, highlighting CNFs as a promising platform for advanced wound dressings.

Acknowledgements

Supported by Spanish Ministerio de Ciencia e Innovación (MCIN/AEI/PID2023-150422OB-I00; CNS2023-145568), Xunta de Galicia (ED431C 2024/09; M.P.V. predoctoral contract ED481A-2023-164), FEDER, and the Norwegian Research Council.

S59
Soft material-based integrated platforms for biomedical applications

S59 – K1
Elastin-like proteins containing heparin-binding domains for injectable hydrogels in cardiac tissue engineering

Geysmans N.[1], Vastmans L.[2], Bito V.[2], Graulus G.-J.[1]
[1]UHasselt, Institute for Materials Research (IUMAT), Biomolecule Design Group; [2]UHasselt, Biomedical Research Institute, CARDIOLab, Diepenbeek, Belgium;

Introduction
A heart attack leads to irreversible damage to the heart muscle. Current treatment methods primarily focus on preventing secondary infarcts but do not address the sustained tissue damage. Consequently, a myocardial infarction often initiates an unfortunate chain of events leading to the development of cardiac arrhythmias and ultimately heart failure. New stem cell therapies are under development, but their effectiveness is limited by the poor retention of these cells at the infarct site. As a result, most injected cells do not have sufficient time to differentiate into functional cardiomyocytes. Injectable hydrogels provide an effective approach to enhancing stem cell retention. Elastin-like proteins (ELPs) have a long history in this field due to their intrinsic lower critical solution temperature (LCST). In this contribution, we describe the design and biotechnological production of recombinant ELPs incorporating heparin-binding domains (HBDs).

Materials and Methods
Three tetrameric ELPs with constructs containing either only RGD (RRRR), only HBD (HHHH) or an equal mix of the two cell adhesion domains (RHHR) were genetically engineered and expressed in *E. coli* (BLR (DE3) and BL21 (DE3) pLysS) using the pET28a plasmid. Following cell lysis, the fusion proteins were purified with inverse transition cycling (ITC) and characterised with SDS-PAGE, western blotting (WB) and mass spectrometry (MS). Biocompatibility assays were performed using human umbilical vein endothelial cells (HUVECs). The ELPs were mixed with oxidised hyaluronic acid (HA_{ox}), forming dynamic imine bonds. The resulting hydrogels were characterised and their adhesive properties evaluated via lap-shear tests.

Results
The ELPs were successfully expressed and purified by ITC yielding more than 50 mg/L of culture. The ELPs were subsequently used to yield dynamic hydrogels via reaction with HAox, and their biocompatibility was validated using HUVECs. The injectability and adhesive properties of the hybrid HAox-ELP gels were demonstrated using a universal mechanical analyser.

Conclusion
In this contribution, the expression of HBD-containing ELPs and their biocompatibility assessment are described. The ELPs' interactions with negatively charged ECM components were studied using lap-shear tests as an in vitro model for tissue integration.

Acknowledgements
This work was supported by the Special Research Fund (BOF) of Hasselt University under project R-13370.

S59 – O1

Programmable pH-responsive hydrogels for soft actuation and targeted lower-GI tract drug delivery

Cerdan K.[1], Gorissen B.[2], Mignon A.[1]
[1]Dept. of Materials Engineering, Surface and Interface Engineered Materials (SIEM), KU Leuven, Group T Leuven Campus; [2]Dept. of Mechanical Engineering, Robotics, Automation and Mechatronics (RAM), KU Leuven, Belgium

Introduction

Targeted drug delivery to the lower gastrointestinal (GI) tract remains a major challenge in the treatment of inflammatory bowel diseases (IBD). Since most drug vehicles are administered orally, the therapeutic cargo is often released prematurely, mainly in the stomach, where it undergoes acidic degradation and early dissolution. This contributes to systemic exposure, dose escalation, and increased adverse effects. With estimates suggesting that more than 7 million people in Europe and the United States will be affected by IBD-related conditions by 2030, developing scalable strategies capable of delivering drugs precisely to the large intestine is a time-pressing need for the raising number of affected patients.

Materials and Methods

To address this challenge, we introduce a versatile platform of pH-responsive hydrogels designed for integration into soft robotic drug carriers as illustrated in Figure 1. These hydrogels are based on a ternary mixture of poly(ethylene glycol) diacrylate (PEGDA), acrylic acid (AA), and poly(ethylene glycol) methyl ether acrylate (PEGMEA), offering orthogonal control over key material properties: PEGDA adjusts crosslink density and mechanical stiffness; AA provides ionizable groups that yield pH-responsiveness; and PEGMEA acts as a flexible spacer that enhances deformability and further expands property modulation. Together, these components allow the fabrication of hydrogels with highly tunable properties by simply adjusting monomer ratios, precursor concentration, and photo-processing conditions. While similar pH-responsive systems have been previously explored, our ternary formulation offers significant advantages in synthetic simplicity, modularity, and scalability.

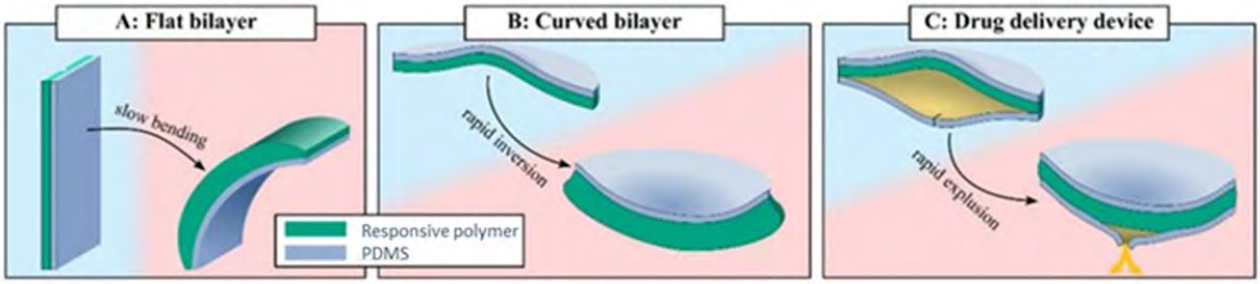

Figure 1. Schematic representation of a composite pH-responsive actuator assembled as a A: Flat bilayer, B: Curved bilayer, and C: Drug delivery vehicle.

Results/ Conclusion

In this regard, we performed a systematic characterization of swelling behavior, mechanical performance, and structural morphology (via x-ray scattering) to map compositions of interest across a wide material library. From this library, selected hydrogels are fabricated into diverse geometries and integrated into hybrid silicone-hydrogel constructs capable of complex actuation driven exclusively by environmental pH shifts. By controlling the degree of swelling and swelling kinetics through compositional design, we demonstrate programmable motions that can be leveraged to regulate drug release profiles.

Acknowledgements

This research is supported by the Research Foundation – Flanders (FWO) for the project funding G007825N.

S59 – O2

Dynamics of spontaneous particle folding induced by cells

Martins R.[1], Esteves H.[2,3], Dias C.[3] Araújo N. [2,3], Oliveira M. [1], Mano J[1]
[1]Dept. Chemistry, Aveiro University; [2]Dept. Physics, Faculty of Sciences of the University of Lisbon; [3]Center for Theoretical and Computational Physics, Faculty of Sciences of the University of Lisbon, Portugal

Introduction

The interaction between cells and materials opens possibilities for tailoring biological and therapeutic properties, enabling cellular response to be tuned according to the physical and chemical characteristics of substrates. This study explores the use of flexible polymeric slender materials as platforms that can be shaped by the autonomous action of mesenchymal stem cells (MSCs).

Aim

We aim to determine whether cells actively build mechanically instructive microenvironments through their own contractile forces and explore whether these will favour differentiation into the phenotype that is programmed for the cells.

Materials and Methods

Thin polymeric membranes of nanometric (is it really nanometric? Sub-millimetric sounds more accurate) thickness and 500 µm lateral size were prepared in different shapes. MSCs were adhered onto the prepared particles in suspension, and both particle deformability and the overall development of the hybrid cell-biomaterials systems were assessed over 14 days. The effect of cell seeding density was assessed, and specific cellular features were correlated with the particles' bending capability. Numerical simulations were performed using a coarse-grained model for flexible membranes, accounting for bending and stretching to study the mechanical response of the membranes to cellular traction.

Results

Cell-induced folding of PCL microparticles is governed by the interplay between geometry, matrix stiffness and cell density. Square particles with intermediate stiffness (2.5% PCL) supported maximal proliferation and exhibited density-dependent bending (Fig.1), whereas softer (2%) matrices deformed rapidly and stiffer (3%) matrices resisted remodelling. Increased stiffness shifted the active folding zone toward the particle centre and imposed progressively aligned, near-perpendicular cellular orientation, indicating higher contractile thresholds. Notably, polymer concentration rather than geometry determined edge thickening, reinforcing peripheral stiffness heterogeneity and tuning long-term deformability without markedly altering overall shape. Numerical simulations elucidated how folding requires a collective torque to overcome the membrane's bending resistance**.** While individual cell work is enough to locally deform the membrane; multiple cells are required for these deformations to merge into a folded structure.

Conclusion

Changes in particle geometry and flexural stiffness had a direct impact on particles morphology and overall organization of the later-formed 3D hybrid structures. Inhibition of cellular contractility resulted in a significant reduction in the overall ability of cells to deform the substates. Numerical simulations, corroborate the experimental results and allow to characterize, in a systematic way, how the hybrid structures depend on the interplay between cell's traction forces and particle's geometry and stiffness.
Overall, our results contribute to a better understanding of the mechanisms of cellular autonomous activity towards thin substrates, with putative application in future therapeutic approaches that rely on the localised fine control of cellular response.

Acknowledgements

This work was financially supported by the European Research Council grant agreement ERC-2019-ADG-883370 (project REBORN, DOI: 10.3030/883370) It was developed within the scope of the project CICECO – Aveiro Institute of Materials, UID/50011/2025 & LA/P/0006/2020 (DOI 10.54499/LA/P/0006/2020), financed by national funds through the FCT/MCTES (PIDDAC) and was supported by FCT - Fundação para a Ciência e Tecnologia, I.P. by UID/00618/2025, 2023.00754.BD and https://doi.org/10.54499/2023.00754.BD.

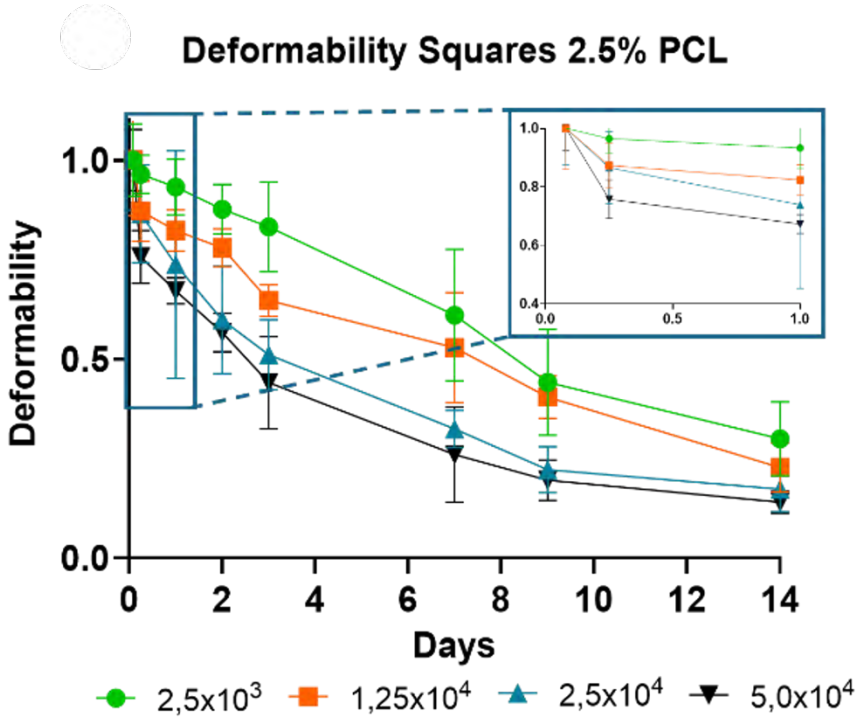

Fig1. Time-dependent deformability of PCL particles for 14 days. The inset highlights early time points, revealing subtle differences between conditions during the initial phase. Square 2.5% PCL particles cultured at different initial cell seeding densities (2.5×10^3, 1.25×10^4, 2.5×10^4 and 5.0×10^4 cells cm^{-2}).

S59 – O3

A hydrogel system to support mechanically induced chondrogenesis

Cuahtecontzi Delint R.[1], Rigou I.[1], Day G.J.[1], Tsimbouri P.M.[1], Childs P.G.[2], Meek D.[3], Reid S.[2], Salmeron-Sanchez M.[4], Dalby M.J.[1]

[1]Centre for the Cellular Microenvironment, University of Glasgow, UK; [2]Centre for the Cellular Microenvironment, University of Strathclyde, Glasgow, UK; [3]Queen Elizabeth University Hospital, Glasgow, UK; [4]Institució Catalana de Recerca i Estudis Avançats (ICREA), IBEC, Barcelona, Spain

Introduction

Cartilage is an avascular tissue with minimal capacity for self-healing. Unattended cartilage damage results in osteoarthritis (OA), the most prevalent chronic pathology of joints. With OA costing the UK approximately $300B annually, including substantial indirect costs, novel strategies to stimulate or enhance cartilage regeneration is a critical research priority.(1) Current clinical approaches, namely autologous chondrocyte implantation or matrix-assisted (MACI), have been the focus of cartilage regeneration for >25 years. Their success is limited because cultured chondrocytes require transforming growth factor beta (TGFb) to regain phenotype. However, this growth factor drives differentiation toward an undesirable deep cartilage phenotype (collagen X-rich) rather than the desired hyaline phenotype (collagen II-rich), even when driving chondrogenesis from mesenchymal stromal cells (MSCs), highlighting a need for non-biochemical approaches and a supportive matrix to ensure delivery.

Aim

Building on previous work using nanovibration as a mechanotransduction cue to direct MSCs differentiation into bone cells(2), this study explores its potential in guiding MSCs toward chondrocytes to produce a hyaline cartilage matrix without the use of exogenous biochemical growth factors, and supportive a hydrogel-based delivery system.

Materials and Methods

We seed the MSCs as a micromass to simulate 3D conditions and subject them to nanovibration, demonstrating the feasibility of a mechanical stimulus to encourage chondrogenesis in MSC without supplementing with exogenous growth factors. Additionally, a viscoelastic polyethylene injectable hydrogel was developed to integrate and support the chondrogenic phenotype of these primed MSCs and facilitate their delivery to the damaged cartilage.

Results

These hydrogels were engineered with tunable mechanical properties to mimic native hyaline cartilage microenvironment to support maintenance of the chondrogenic phenotype. Furthermore, viability and chondrogenic key markers were quantified at gene (qPCR) and protein expression levels (immunofluorescence) such as SRY-box transcription factor (SOX9), collagen II, collagen X, and aggrecan, alongside matrix production through histological staining.

Conclusion

We developed an approach to commit MSCs into high quality chondrocytes using nanovibration. This integrated strategy provides an attractive route towards minimally invasive delivery of committed MSCs to chondrogenesis to address the prevalence of OA.

Acknowledgements

EPSRC EP/X013057/1. Prof.Richard Oreffo.

References

1. Elridge S, Barawi A, Wang H. Agrin induces long term osteochondral regeneration by supporting repair morphogenesis. Science translational medicine, 12, 559
2. Tsimbouri PM, Childs PG, Pemberton, GD. Stimulation of £D osteogenesis by mensenchymal stem cells using a nanovibrational bioreactor. Nat Biomeg Eng. 12, 1004.

S59 – O4

Design and characterization of animal-free scaffold for fat cultured food ingredients production

Sottini B.[1], Fiorati A.[1, 2], De Nardo L.[1, 2], Altomare L.[1, 2]
[1]Dept. of Chemistry, Materials, and Chemical Engineering "G. Natta", Politecnico di Milano; [2]INSTM Local unit, Politecnico di Milano, Italy

Introduction

Cultivated ingredients represent a promising alternatives to conventional meat products. Despite the good performances of animal-derived scaffolds (e.g. gelatin), their use conflicts with cultured meat research challenge to reduce animal component. Cell adhesion and tissue supporting properties of plant-based scaffold should be improved, for example by incorporating vegetal protein.
This work aims to develop mushroom based acid-free chitosan films, enriched with soybean peptone and yeast extracts, as animal-free scaffold with improved biological properties suitable for cultured fat production.

Materials and Methods

Mushroom based chitosan films are obtained following Casalini et al.[1] procedure. Chitosan is initially dissolved in acidic environment and subsequently neutralized to form a hydrogel, which is re-dissolved through carbon dioxide (CO_2) injection. Soybean peptone (CSP20) and yeast extracts (CSY20) are incorporated at 20% $w/w_{chitosan}$. The rheological properties of the formulations and the stability in aqueous environment of films obtained via solvent casting are tested. 3T3-L1 preadipocytes are seeded onto 15mm diameter samples, and induced to differentiate up to 10 days. Cell viability, differentiation capacity, and morphology are assessed and compared to evaluate the additives effect.

Results

The proposed method enables the production of acid-free mushroom chitosan films, through simple process based on reversibility of water carbonation. All formulations exhibit a shear thinning behavior, indicating suitability for extrusion-based applications. Films result stable in aqueous environment, reaching a swelling ratio plateau below 140% after 48 hours.
Indirect cytotoxicity test shows cell viability above 70%, confirming effective removal of acid residues during scaffolds preparation.
Alamar Blue assay reveals preadipocytes progressive and good proliferation over time, further confirmed by Live/Dead staining prior to differentiation (Figure 1). Hoechst and phalloidin staining assess the effects of plant-based protein additives on cell adhesion and morphology. Differentiated cells seeded on pure chitosan samples tend to aggregate into circular structures, reflecting the limited cell adhesion. In contrast, differentiated cells on CSP20 and CSY20 films, exhibit a more spread morphology, indicating enhanced substrate adhesion, likely due to the presence of amino acids adhesion motifs (Figure 2a). Oil Red O staining confirms this trend, with a wider lipid droplets distribution in CSP20 and CY20 samples (Figure 2b).

Conclusion

This work demonstrates an innovative method for producing food-safe mushroom chitosan scaffold. The incorporation of plant-derived protein additives enhances cell adhesion and functionality, supporting chitosan films application as animal-free scaffold in cultured fat production. Further study will investigate textural properties of the final product, long-term and larger-scale cell culture.

Acknowledgements

"Food for Future: 3D plant-derived structures to produce adipose tissue as innovative food ingredient for cultured meat", PRIN 2022, 2022APBX8X.

References

[1]Casalini R., Ghisoni F., Bonetti L., Fiorati, A., De Nardo, L. Development of acid-free chitosan films in food coating applications: Provolone cheese as a case study. *Carbohydrate Polymers* 2024, 331, 121842.

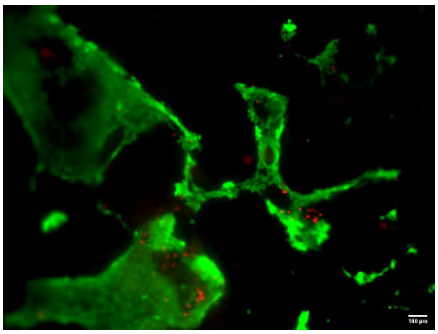

Figure 2. Live/Dead staining at day 10 prior cell differentiation (live cells: green spots, dead cells: red spots)

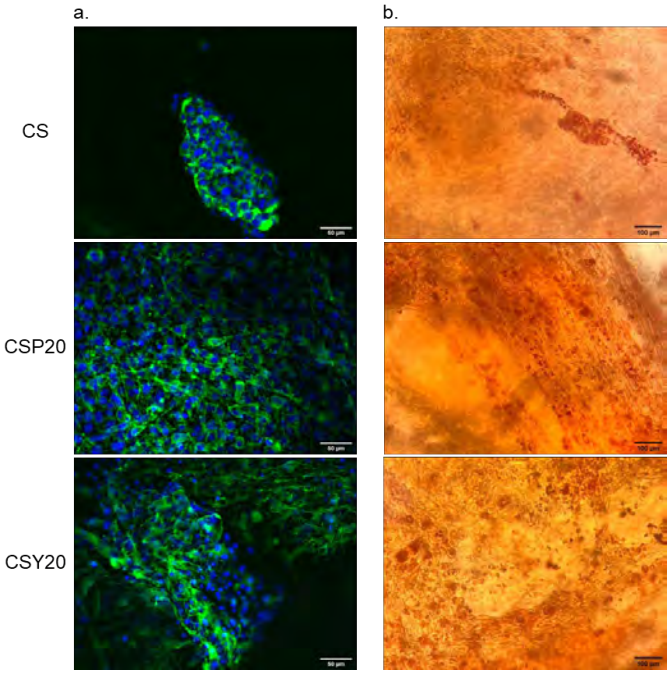

Figure 1. a. Fluorescence microscopy staining of differentiated cells (cell nuclei: blue spots, Hoechst staining; cell cytoskeleton: green spots, Phalloidin staining). **b.** Optical microscopy staining of differentiated cells (lipid droplets: red spots, Oil Red O staining)

S59 – O5

Development of a HAWC–mRNA nanoparticle platform for topical nanogel delivery in junctional epidermoylis bullosa

Dunne T., Buckley N., McCarthy H.O.
[1]School of Pharmacy, Queen's University, Belfast, Northern Ireland

Introduction

Junctional epidermolysis bullosa (JEB) is an autosomal recessive skin-fragility disorder resulting from pathogenic variants in LAMB3 and COL17A1, encoding laminin-332 and type XVII collagen, respectively. Viral gene-replacement therapies can restore dermal-epidermal adhesion but are limited by manufacturing complexity, repeated dosing, and poor compatibility with fragile skin. A topical, non-viral mRNA delivery system targeting keratinocytes and dermal fibroblasts offers a promising alternative for local gene replacement in JEB.

Aim

To establish a cell-penetrating peptide (HAWC)-mRNA nanoparticle platform, define its critical quality attributes (CQAs), and identify transfection conditions supporting efficient, cytocompatible delivery for initial steps to incorporate into a polymer-based topical nanogel.

Materials and Methods

GFP-mRNA was synthesised by *in vitro* transcription (IVT) from a SapI-linearised, T7-driven eGFP plasmid and capped co-transcriptionally using CleanCap; integrity and purity were confirmed by agarose gel electrophoresis and UV-Vis spectroscopy. HAWC-GFP-mRNA nanoparticles were prepared by electrostatic complexation at N:P ratios 6-20 and characterised by dynamic light scattering (hydrodynamic diameter, polydispersity index), electrophoretic light scattering (zeta potential) and RiboGreen encapsulation assays (Figure 1). A two-level factorial Design of Experiments (DoE) in HaCaT keratinocytes and human dermal fibroblasts assessed impact of N:P ratio, GFP-mRNA dose, cell density, and incubation time on transfection efficiency (GFP-positive cells by flow cytometry) and viability (propidium iodide staining; Figure 2). Plasmids encoding LAMB3 and COL17A1 were similarly transcribed and formulated with HAWC and characterised via physicochemical assays (Figure 1).

Results

IVT-generated GFP-mRNA produced the expected size with absorbance ratios and minimal contamination. HAWC-GFP-mRNA nanoparticles exhibited hydrodynamic diameters ≤150nm, positive zeta potentials ≥+10mV, polydispersity indices ≤0.3, and encapsulation efficiencies ≥90% across all N:P ratios (Figure 1A-C). DoE analysis identified GFP-mRNA dose ($p=0.0002$; contributing effect=43.30%) as the principal determinant of transfection, with additional contributions from N:P ratio ($p=0.0099$; contributing effect=15.95%) and their interaction ($p=0.0145$; contributing effect=13.96%). Optimal conditions (N:P 6, 1.5 µg GFP-mRNA, 20,000 cells/well, 4-8 h incubation) achieved 23-26% GFP-positive cells with 93-96% viability (Figure 2). Dose-response studies confirmed model predictions and stability of CQAs. Formulations containing LAMB3 and COL17A1 mRNA also achieved >90% encapsulation and remained within defined CQA parameters (Figure 1D-E), with N:P-dependent shifts in size and zeta potential consistent with their longer transcript lengths.

Conclusion

This study establishes a peptide-mRNA nanoparticle platform with defined CQAs and transfection window balancing efficiency and cytocompatibility in keratinocytes and dermal fibroblasts. Extending the platform from GFP-mRNA to LAMB3- and COL17A1-mRNA supports its relevance to JEB-relevant cargos and underpins subsequent incorporation of HAWC-mRNA nanoparticles into a polymer-based nanogel for topical delivery and functional evaluation in JEB models.

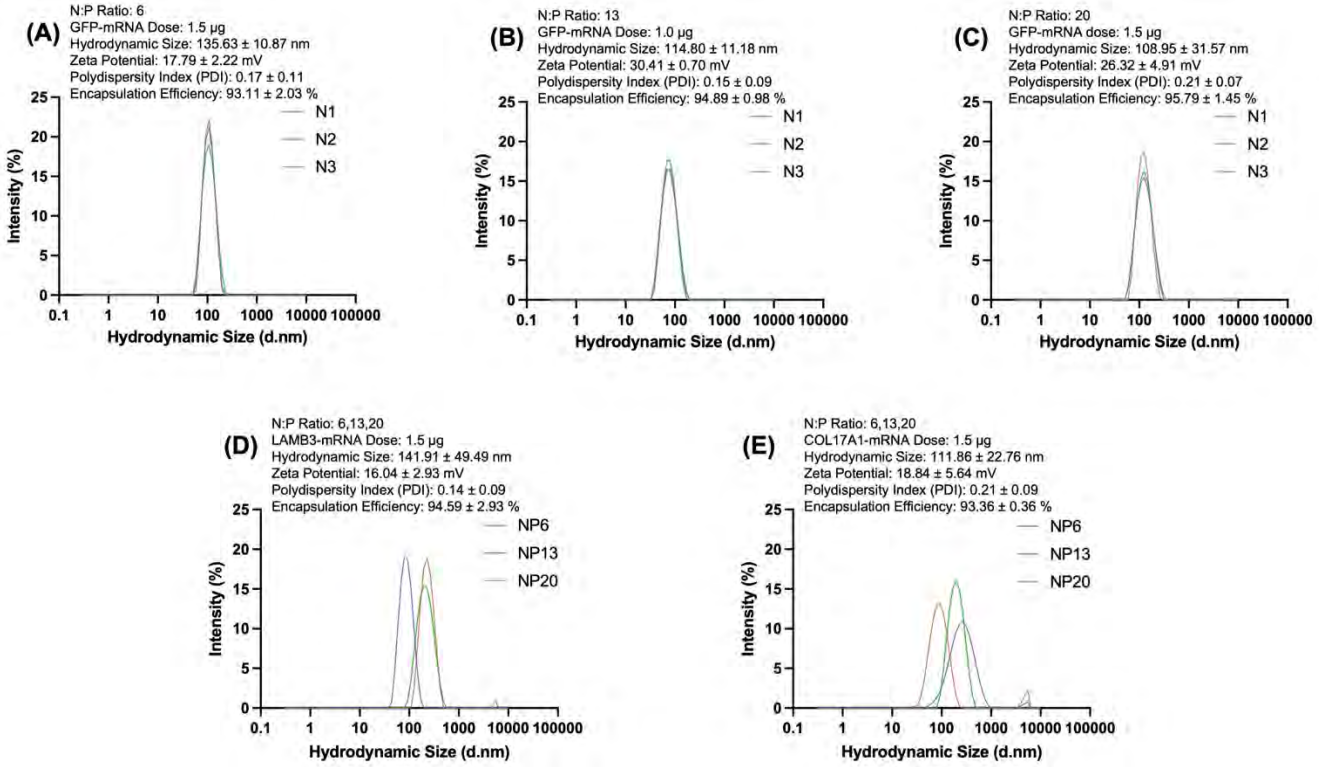

Figure 1: Physicochemical properties of freshly prepared GFP-mRNA/HAWC nanoparticles used in the Design of Experiments to optimise the transfection protocol for the HaCaT cells. Representative DLS intensity distributions of freshly prepared GFP-mRNA/HAWC nanoparticles as a function of N:P ratio and GFP-mRNA dose, which were measured with a Zetasizer Ultra (Malvern Panalytical, UK). (A) N:P ratio 6 and GFP-mRNA dose of 1.5 µg, (B) N:P ratio 13 and GFP-mRNA dose of 1.0 µg, (C) N:P ratio 20 and GFP-mRNA dose of 1.5 µg, (D) N:P ratio 6,13,20 and LAMB3-mRNA dose of 1.5 µg, (E) N:P ratio 6,13,20 and COL17A1-mRNA dose of 1.5 µg. Data from three independent formulations (n = 3).

(A)

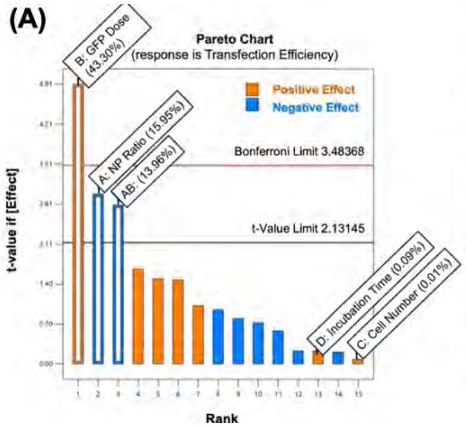

(B)

Response	Experimental (Mean ± SD)	Predicted (Mean)	Error (%)
Control	0.70 ± 0.14%	-	-
TE_4 hours	23.70 ± 2.19%	24.40%	2.87
TE_6 hours	22.73 ± 1.63%	25.90%	12.23
TE_8 hours	26.03 ± 1.56%	29.50%	11.75
Control	96.09 ± 0.57%	-	-
CV_4 hours	94.80 ± 1.55%	93.90%	0.96
CV_6 hours	93.07 ± 1.69%	87.90%	5.88
CV_8 hours	93.10 ± 1.06%	81.20%	14.66

Figure 2: (A) Pareto chart of the standardised effects and percentage contributions on transfection efficiency for the optimisation of the HaCaT cell transfection protocol using the two-level factorial DoE approach. and (B) transfection efficiency (TE) and cell viability (CV) experimental and predicted data with percentage error based on the optimal parameters determined using the two-level factorial DoE approach to optimise the HaCaT transfection protocol as a function of incubation time of HaCaT cells following transfection with freshly prepared GFP-mRNA/HAWC nanoparticles.

Acknowledgements

Four-Year PhD Research Programme sponsored by

debra

THE BUTTERFLY SKIN CHARITY

S59 – O6

PVA-based wound dressing films incorporating quercetin-loaded chitosan nanoparticles

Özer, B.[1], Ülker Turan, C.[1]
[1]Gebze Technical University, Dept. of Bioengineering, Kocaeli, Türkiye

Introduction

Drug delivery systems provide controlled release, improve drug stability and enhance therapeutic efficacy[1]. Wound dressings benefit from such systems by addressing bacterial infection and oxidative stress, which can delay healing process[2]. Incorporating bioactive compounds into polymeric films has emerged a promising approach. Quercetin is a natural flavonoid with antioxidant and antibacterial properties, chitosan nanoparticles act as biocompatible carriers, and polyvinyl alcohol (PVA) provides a flexible, hydrophilic, and biocompatible matrix suitable for wound dressing applications[3,4].

Aim

This study aimed to develop a PVA-based wound dressing film incorporating quercetin-loaded chitosan nanoparticles and to investigate its potential for wound healing applications.

Materials and Methods

Quercetin-loaded chitosan nanoparticles (Q-CSNPs) were prepared via ionic gelation and incorporated into PVA (Q-CSNP-PVA) to produce wound dressing films by solvent casting. PVA films with free quercetin (Q-PVA) were also prepared for comparison. The films were characterized for structural, thermal, and physicochemical properties using various analytical techniques. Quercetin release was studied at pH 7.4 and 5.6, and antioxidant activity was evaluated by DPPH assay. Antibacterial activity against *S. aureus* and *E. coli* was assessed via colony count, and cytotoxicity was tested on L929 fibroblasts using the MTT assay.

Results

Structural analyses confirmed the successful incorporation of quercetin and chitosan nanoparticles into the PVA matrix. *In vitro* release studies demonstrated that Q-PVA films released 43% and 45% of quercetin at pH 7.4 and 5.6 after 24 h, respectively, whereas Q-CSNP-PVA films exhibited a more controlled release profile, releasing 33% and 30% under the same conditions. Both formulations showed a significant antibacterial activity; Q-PVA reduced *S. aureus* and *E. coli* colonies by approximately 54–55% and Q-CSNP-PVA films achieved a reduction of about 44–45% compared with the control. The films also displayed strong antioxidant activity in the DPPH assay. Q-PVA films exhibited radical scavenging activity of 41.6-91.2% at concentrations of 0.5-10 mg/mL, whereas Q-CSNP-PVA films showed activities ranging from 32.3-90.1% within the same range. MTT assay results confirmed that all tested concentrations of both film formulations were non-toxic to L929 fibroblasts, maintaining cell viability above above 70% at 48 h.

Conclusion

Q-PVA and Q-CSNP-PVA films demonstrated controlled quercetin release, significant antibacterial and antioxidant activities, and good cytocompatibility, highlighting their potential as effective polymeric wound dressings for enhanced healing.

Acknowledgements

This study was supported by the Scientific and Technological Research Council of Türkiye (TÜBİTAK) under Project No: 224M366. The authors gratefully acknowledge TUBITAK for supporting scientific mobility through the 2224-A Grant Program.

References

[1] Adepu S., Ramakrishna, S. Controlled drug delivery systems: Current status and future directions. *Molecules* 2021; 26; 5905.
[2] Peng W., Li D., Dai K., Wang Y., Song P., Li H., Tang P., Zhang Z., Li Z., Zhou Y., Zhou C. Recent progress of collagen, chitosan, alginate and other hydrogels in skin repair and wound dressing applications. *International Journal of Biological Macromolecules* 2022; 208; 400–408.
[3] Gherman S.P., Biliuță G., Bele A., Ipate A.M., Baron R.I., Ochiuz L., Șpac A.F., Zavastin D.E. Biomaterials Based on Chitosan and Polyvinyl Alcohol as a Drug Delivery System with Wound-Healing Effects. *Gels* 2023; 9; 122.
[4] Li X., Yang X., Wang Z., Liu Y., Guo J., Zhu Y., Shao J., Li J., Wang L., Wang K. Antibacterial, antioxidant and biocompatible nanosized quercetin-PVA xerogel films for wound dressing. *Colloids and Surfaces B: Biointerfaces* 2022; 209; 112175.

S59 – O7

Physicochemical-informed bayesian machine learning for the optimization of alginate methacrylation

Ferri P.[1], Durà-Hernández M.[1], Sánchez-García D.[1], Reinal-Ferre I.[2], Alba-Pérez A.[2], Calderón-García P.[2], Gallego-Ferrer G.[2,3], Gentile P.[2,3], García-Gómez J.M.[1,3]
[1]Biomedical Data Science Lab, Universitat Politècnica de València; [2]Centro de Biomateriales e Ingeniería Tisular, Universitat Politècnica de València; [3]Biomedical Research Networking Centre on Bioengineering, Biomaterials and Nanomedicine (CIBER-BBN), Carlos III Health Institute, Valencia, Spain

Introduction

Sodium alginate (NaAlg) forms hydrogels via ionic crosslinking; however, while biocompatible, this mechanism lacks the tunability required for precision bioengineering. Methacrylation addresses this by enabling photocrosslinking, which forms stable covalent bonds. Achieving a specific degree of substitution (DS) depends on parameters like NaAlg concentration, methacrylic anhydride concentration and reaction time. Traditional Design of Experiments (DoE) evaluates these using general quadratic models, but this approach commits to static experimental runs and ignores underlying physicochemical phenomena. Therefore, the aim of this study was to develop a physicochemical-informed Bayesian formulation optimization model to efficiently predict and target a specific DS during NaAlg methacrylation.

Materials and Methods

A target-oriented Bayesian optimizer was developed using wet-lab formulation data of NaAlg (PRONOVA UP LVG) modified with methacrylic anhydride (MA). The dataset was systematically cleaned to include only samples where double-dialysis acted effectively to remove unreacted compounds, a condition supported by ^{1}H-NMR estimation of guluronic acid protons. To ground the machine learning predictions in reality, the model incorporated a pseudo-first-order kinetic law representing the reaction of hydroxyl groups on the alginate backbone with MA. Specifically, the model accounts for concentration dependencies and time. The algorithm's utility function was designed to maximize proximity to the target DS, which in our case was 60%, while heavily weighting prediction uncertainty to promote formulation exploration. Furthermore, a diversity penalty was introduced to prevent the algorithm from selecting highly similar formulation points in the search space.

Results

The physicochemical-informed model successfully fitted the filtered experimental dataset. The fit was validated using Bayesian inference, calculating parameter covariance and estimating predictive uncertainty via the Delta method. By evaluating the utility function across a virtual search grid, the model generated a prioritized batch of novel formulation configurations predicted to hit the ~60% DS target. This informed approach demonstrated superior sample efficiency and extrapolation capabilities compared to traditional DoE. This improvement is structurally justified: the model dynamically adapts to outcomes through its acquisition function, bypassing the mathematically mandated, rigid regional sampling of orthogonal DoE models. It explicitly minimizes the distance to the target DS while rigorously accounting for spatial uncertainty.

Conclusion

Incorporating physical and chemical laws into a Bayesian optimization framework significantly enhances the formulation of methacrylated hydrogels. This AI-driven approach mitigates the effects of poor data quality and reduces experimental burden, offering a highly efficient pathway for designing tunable biomaterials.

Acknowledgements

This research is part of the EU-funded HYDROHEAL project (101178398, HORIZON Innovation Actions programme).

ESB 2026

Physicochemical-informed Bayesian machine learning for the optimization of alginate methacrylation

Sodium alginate methacrylation

$$\text{Alg-OH} + \text{MA} \xrightarrow{k_{sub}} \text{Alg-MA} + \text{Methacrylic Acid}$$

Data curation

Double dyalisis + ^{1}H-NMR

Design of experiments approach

$$y = \beta_0 + \sum_{i=1}^{k} \beta_i x_i + \sum_{i=1}^{k} \beta_{ii} x_i^2 + \sum_{i=1}^{k-1} \sum_{j=i+1}^{k} \beta_{ij} x_i x_j + \epsilon$$

- Lacks physicochemical knowledge
- Static design wastes samples in ineffective regions

Proposed approach

$$U(\mathbf{x}) = -|\hat{y}(\mathbf{x}) - y_{\text{target}}| + \kappa \cdot \sigma_y(\mathbf{x})$$

$$\hat{y}(\mathbf{x}) = f(\mathbf{x}; \boldsymbol{\theta}) = \alpha \cdot [\text{MA}] \cdot [\text{Alg}]^{\beta} \cdot (1 - e^{-k \cdot t})$$

$$\sigma_y^2(\mathbf{x}) \approx \nabla f(\mathbf{x})^T \cdot \Sigma_\theta \cdot \nabla f(\mathbf{x})$$

$$\text{Score}_{\text{final}}(\mathbf{x}) = U(\mathbf{x}) \times \prod_{\mathbf{p} \in \text{Batch}} \left(1 - e^{-\lambda \cdot \|\mathbf{x} - \mathbf{p}\|}\right)$$

- Integrates physicochemical knowledge
- Sample efficient

HYDROHEAL

S60
Stimuli-responsive biomaterials and direct biophysical stimulation for regenerative medicine

S60 - K1
Ultrasound and Bioinstructive Biomaterials for Mechanobiological Control in Regenerative Medicine

Ricotti L.[1]
[1]The BioRobotics Institute, Scuola Superiore Sant'Anna, Pisa, Italy

This keynote lecture will explore the compelling synergy between remotely applied forces, primarily ultrasound, delivered in a controllable and repeatable manner, and smart biomaterials as innovative tools to modulate mechanobiological pathways for cell and tissue engineering. The talk will span mechanistic in-vitro studies elucidating the pathways activated by remote forces and biomaterial cues, preclinical in-vivo models demonstrating tissue repair, and emerging clinical applications and device developments.
Highlighted examples will include the synergistic effects of ultrasound and bioinstructive hydrogels in enhancing the chondrogenic differentiation of human adipose-derived mesenchymal stromal cells and modulating inflammation, paving the way for new therapeutic strategies for osteoarthritis. Additional preclinical and clinical case studies will illustrate how ultrasound can be employed to modulate mechanobiological responses related to fibroblast and keratinocyte proliferation for wound healing, as well as its use in non-invasive (liquid) biopsy of intestinal cells to support personalized treatment of ulcerative colitis.

Acknowledgements
This work received financial and technical support from INAIL, project MioPRO2, grant n.PR23-CR-P1, and project WOUND, grant n.PR23-CR-P2

S60 - K2

A novel wireless nanobioelectronic systems to modulate breast cancer cells bioelectricity

Jones CF [1,2], Matias D [3,4], Mastrantuono E [3,4], Graça L [3,4], Ferreira FC [1,2], Esteves T [1,2], Sanjuan-Alberte[1,2]
[1] Dept. of Bioengineering and Institute for Bioengineering and Biosciences, Instituto Superior Técnico, Universidade de Lisboa, Lisbon, Portugal, [2] Associate Laboratory i4HB—Institute for Health and Bioeconomy, Instituto Superior Técnico, Universidade de Lisboa, Lisbon, Portugal, [3] Gulbenkian Institute for Molecular Medicine (GIMM), Lisboa, Portugal, [4] Faculdade de Medicina, Universidade de Lisboa, Lisboa, Portugal

Introduction

Cancer cells exhibit unique bioelectrical properties that influence their tumorigenic potential and therapeutic strategies targeting these remain underexplored.

Aim

A wireless nanobioelectronic system to modulate cancer cell bioelectricity based on piezoelectric and conductive nanoparticles (BTO@PEDOT-NPs) was developed and activated by ultrasound (US) in vitro on two human breast cancer cell lines (MCF-7, MDA-MB-231) and healthy fibroblasts (HMF), and validated their efficacy in vivo using the 4T1 murine breast cancer model.

Materials and Methods

BTO@PEDOT-NPs consisted of a barium titanate (BTO) core and poly(3,4-ethylenedioxythiophene) (PEDOT) shell. Physico-chemical characterisation and biocompatibility of these was performed. Cells were treated with 200 µg/mL of BTO@PEDOT-NP and stimulated by US. Intracellular reactive oxygen species (ROS), calcium levels and cell membrane potential were measured. For in vivo studies, 4T1 cells were injected into the mammary gland of C57BL/6 mice, divided into three groups: control, NPs, and NPs+US. 100 µl of NPs (600 µg/ml) were injected every 2 days starting day 7 and US was applied at the tumor site at an intensity of 0.4 W/cm2 for 150 sec a cycle, (3 cycles at day 7; 2 cycles/day from day 8 to 12). Tumor growth was monitored until day 15, followed by postmortem analysis.

Results

Following US stimulation, cell viability decreased significantly in breast cancer cells treated with BTO@PEDOT-NPs, reducing to 31% (MCF-7) and 24% (MDA-MB-231), while HMF cells remained unaffected. Mechanistic studies revealed that nanoparticle activation increased ROS and intracellular calcium concentrations, disrupting the cancer cells' bioelectronic homeostasis. Membrane polarisation halted cell cycle progression in cancer cells, while HMF polarisation did not affect viability nor cell cycle, suggesting a direct interference with their tumorigenic circuitry. In vivo, the NPs+US group showed remarkable efficacy in inhibiting tumor growth in the 4T1 murine breast cancer model. Other test groups showed no significant differences, confirming the synergistic efficacy of the combined treatment.

Conclusion

BTO@PEDOT-NPs activated by US can selectively modulate the bioelectricity of breast cancer cells without affecting healthy cells. The system's ability to polarise cancer cell membranes and halt their proliferation was further validated in an aggressive in vivo murine model, where tumor growth was significantly inhibited by the NP+US treatment. These findings highlight bioelectricity as a critical target for future cancer interventions, paving the way for innovative strategies to combat tumor progression.

Acknowledgements

Funding from FCT—Portuguese Foundation for Science and Technology BIOMIMIC-CRC(2023.13896.PEX), iBB(UID/04565/2025) and i4HB(LA/P/0140/2020); and “la Caixa” Foundation(ID100010434) through projects LCF/BQ/PI22/11910025 and LCF/BQ/P122/11910009. Thanks to Senentxus Lanceros-Mendez, Paula Rodriguez-Lejarraga, Akhil Jain, Filipa Pires and Prof Morgado for valuable contributions on discussions and materials characterization of this work.

S60 – O1

Innovative biophotonic fibers with red upconversion emission for post-surgical light therapy and deep tissue stimulation

Gobbo V.A.[1], Ojha N.[1], Vakkada Ramachandran A.[1], Ressler A.[1], Nasser K.[1], Närhi M.[1], Boussard-Plédel C.[2], Massera J.[3], Petit L.[1]
[1]Faculty of Engineering and Natural Sciences, Tampere University, Finland, [2]CNRS ISCR, University of Rennes, France, [3]Faculty of Medicine and Health Technology, Tampere University, Finland

Introduction

Bioactive glass fibers have been developed for biomedical applications, including biosensing and light therapy. However, after their implantation in human body, the poor penetration of visible light through the skin strongly limits post-surgical phototherapy and imaging.

Aim

Herein, bioactive glass-based fibers are doped with upconverter crystals emitting red light under near infrared (NIR) stimulation, guaranteeing deep tissue penetration and conversion of the NIR to red light, triggering fiber applicability in photostimulation.

Materials and Methods

Upconverter crystals ($(Y_{1-x}Er_xTi)_2O_7$, x=28at%) were prepared using solid state reaction at 1500°C for 4h (heating rate 10°C/min) and successively grounded. Glass preforms ($26.93SiO_2$–$26.93B_2O_3$–$22.66Na_2O$–$21.77CaO$–$1.72P_2O_5$ mol%), doped with 1%wt crystals, were drawn at 680°C with preform descent speed of 2 mm/min and drawing speed of 4.7 m/min. The fibers were characterized by XRD and micro-luminescence/micro-Raman spectroscopy, and upconversion spectra upon 980nm pumping were acquired. The fiber dissolution and bioactivity were evaluated upon immersion in aCSF and SBF, up to 14 days.

Results

The crystals were successfully prepared showing no secondary phase (XRD), and dispersed in the glass preform. 200µm-diameter fibers were drawn from preform without undesired glass crystallization. The fibers showed a strong red-light emission under 980nm pumping (Fig.1A)), as also confirmed by the acquisition of the upconversion spectra (Fig.1(B)), presenting two main bands at around 650-700nm and 550nm, respectively attributed to $^3H_4 \rightarrow {}^3H_6$ and $^1G_4 \rightarrow {}^3H_6$ transitions of Er^{3+}. Soaking the fibers (Fig.1(C)) in aCSF and SBF led to the formation of a reactive layer on which tricalcium phosphate (Ca/P=1.50, Fig.1(D)) and hydroxyapatite ((Ca+Mg)/P=1.66, Fig.1(E)) precipitated. Tricalcium phosphate exfoliated over time, while the thickness of the hydroxyapatite layer increased progressively, reducing the diameter of the fiber core.

Conclusion

Luminescent fibers were successfully drawn from bioactive glass with embedded upconverter crystals, emitting red light under near infrared pumping. It was demonstrated that the doping process did not affect the bioactivity of the glass. Immersion in aCSF triggered the formation of tricalcium phosphate, whose gradual dissolution helped sustain the intensity of the upconverted signal over time. This study clearly demonstrated the potential of composite fiber for biomedical applications.

Acknowledgements

The study was funded by Research Council of Finland (MAXheal project – 361160&361159).

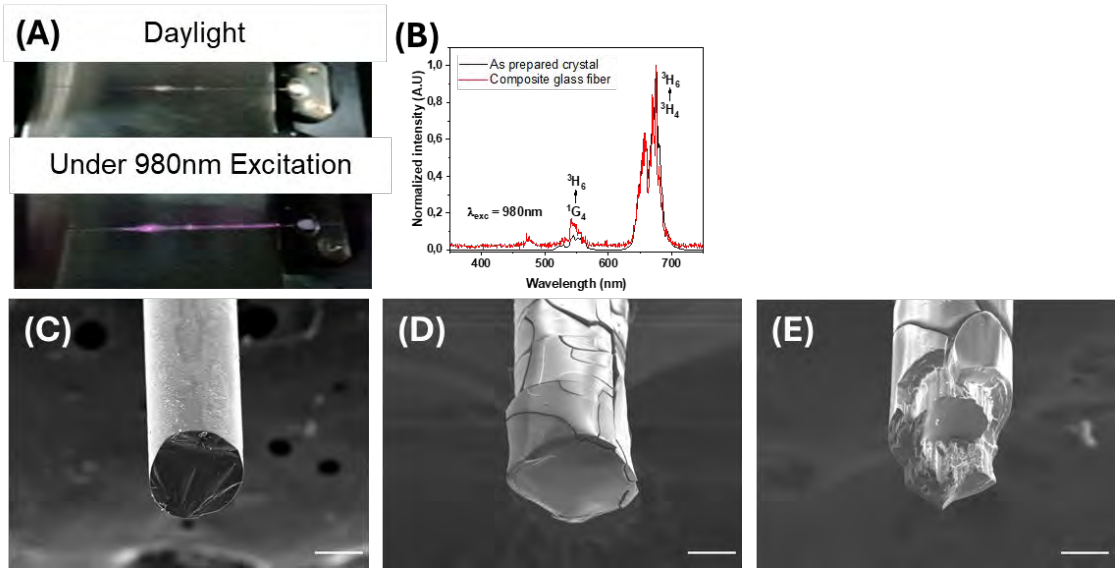

Figure 1. (A) Doped preform, fibers in daylight and 980nm excitation, and (B) upconversion spectra. SEM images of the fibers (C) as drawn, and upon 14 days immersion in (D) aCSF and (E) SBF; scalebar is 100 µm.

S60 – O2

Correlating magnetically targeted and physiological mechanostimulation to map functional domains of PIEZO channels

Teixeira S. P. B.[1], Marques F. L.[1,2], García-Lojo, D.[1], Domingues, R. M. A.[1]
[1]International Iberian Nanotechnology Laboratory (INL), Braga, Portugal, [2]Dept. Ceramics and Materials Engineering, University of Aveiro (UA), Portugal

Introduction

Cells rely on mechanotransduction to couple physical forces to biochemical signaling. PIEZO channels, widely expressed across different tissues, mediate this conversion for diverse inputs including shear, membrane tension, and pressure. However, how different force types engage specific channel regions to shape downstream signaling remains difficult to resolve due to the lack of tools that can interrogate PIEZO at submolecular precision. Here, we introduce an approach that systematically correlates responses evoked by targeted magnetic actuation with those produced by physiological stimuli (shear flow and cyclic strain), enabling direct, domain-level comparison of input-output relationships in PIEZO function.

Materials and Methods

PIEZO1-targeting nanoswitches (PINS) were designed to bind preselected PIEZO1 epitopes and magnetically stimulate discrete channel regions on-demand. PINS were produced via molecular imprinting against two *in silico*-selected peptides to achieve high recognition specificity for two functional domains (extracellular Cap and Blade). Superparamagnetic iron oxide nanoparticles were incorporated to grant magnetic responsiveness. Comprehensive physicochemical profiling (morphology, size and ζ-potential distribution, composition, and target affinity) identified optimal formulations for cellular response interrogation. Applying these, we performed side-by-side analyses in wild-type and PIEZO1-deficient cells, quantifying gene and protein expression programs triggered by epitope-specific actuation and benchmarking them against response signatures elicited by microfluidic shear and substrate stretching.

Results

Both Cap- and Blade-targeting PINS showed spherical morphologies and narrow size distributions, with mean hydrodynamic diameters of 150.3±2.1 nm (Blade) and 146.4±1.3 nm (Cap), and slightly negative ζ-potentials, indicating that epitope imprinting did not influence core physicochemical features. Endothelial cells exposed to oscillating magnetic fields in the presence of PINS exhibited upregulation of *PIEZO1* and *VEGF* markers in an epitope-dependent manner, revealing distinct modes of function for each domain. This was significantly decreased by PIEZO1-knockdown, confirming specificity of PINS-mediated actuation. In parallel, cells subjected to venous-range shear (3.6 dyn/cm², above PIEZO1 gating threshold) or pulsatile stretch (5% strain) provided physiological comparators. Ongoing gene-expression and protein analyses focus on canonical PIEZO1-dependent markers (e.g., Ca^{2+}-responsive pathways, angiogenesis) to quantify overlap between responses induced by each stimulus.

Conclusion

This comparative framework, aligning domain-targeted magnetomechanical inputs with canonical force paradigms, enables assignment of functional force-transduction roles to specific PIEZO regions and clarifies how distinct mechanical contexts are decoded into divergent signaling cascades. Collectively, the study provides a correlation-driven map linking PIEZO domain engagement to force sensing-selectivity, advancing mechanistic understanding of channel versatility and opening avenues for precise, modular control of mechanotransduction in tissue-engineering and regenerative contexts.

Acknowledgements

European Research Council (ERC) under the EU's Horizon Europe research and innovation programme (Grant No. 101171765 – FORTIFy); Portuguese Foundation for Science and Technology (FCT – DOI: 10.54499/2022.05526.PTDC).

S60 – O3

Sustainable cellulose nanofibrils as ultrasound-driven piezoelectric interfaces for wireless neuromodulation

Klompmaker K.K.[1], Chen M.[1], Zhang Y.[2], Athanassiadis A.[3], Fischer P.[3]
[1]Aarhus University, Denmark, [2]INANO, Aarhus University, Denmark, [3]Heidelberg University / MPI, Germany

Introduction

Wireless bioelectronic stimulation is emerging as a key strategy for guiding neuronal regeneration, yet current systems rely predominantly on rigid inorganic piezoceramics that limit biocompatibility and sustainability. Cellulose nanofibrils (CNF) are renewable, biodegradable, and intrinsically piezoelectric, offering a fully organic alternative for ultrasound-mediated neuromodulation.

Aim This study aims to evaluate phosphorylated cellulose nanofibrils (pCNF) as sustainable, ultrasound-responsive piezoelectric biointerfaces capable of converting acoustic stimulation into biologically relevant neuronal activation.

Materials and Methods

Phosphorylated cellulose nanofibrils (pCNF) were engineered to enhance surface charge and dispersion under physiological conditions. Nanoscale piezoelectricity was characterized using piezoelectric force microscopy, while ultrasound delivery was calibrated via hydrophone and laser vibrometry. Cytocompatibility and biointerface properties were evaluated in fibroblast and neuronal cultures. Functional responses were assessed in SH-SY5Y neuroblasts and primary dorsal root ganglion (DRG) neurons using intracellular calcium and reactive oxygen species (ROS) imaging.

Results

pCNF exhibited pronounced piezoelectric phase contrast and ultrasound-dependent electrical output, confirming robust electromechanical activity. The nanofibrils formed a tight interface with cell membranes while maintaining excellent cytocompatibility. Upon ultrasound stimulation, pCNF significantly amplified neuronal activation compared to ultrasound alone, including up to ten-fold increases in calcium transient amplitudes in DRG neurons and elevated intracellular ROS signalling. Importantly, systematic pharmacological inhibition studies in SH-SY5Y cells revealed a multimodal activation mechanism, where selective blockade of mechanosensitive ion channels, voltage-gated sodium channels, intracellular Ca^{2+} release, and redox signalling pathways differentially modulated the response, indicating coordinated contributions from membrane excitability and intracellular signalling cascades.

Conclusion

These findings establish pCNF as a sustainable, fully organic platform for ultrasound-driven neuromodulation. Beyond planar systems, this material is highly suited for integration into 3D biofabrication strategies such as extrusion printing and electrospinning, where controlled fibril alignment may enhance piezoelectric output. This approach opens new opportunities for engineering aligned ultrasound-responsive nerve guide conduits that combine topographical guidance with on-demand electrical stimulation for neural regeneration.

S60 – O4

Independent control of elasticity and viscosity in an ELR-based hydrogel

Lorenzo S[1], Acosta S[1], Quintanilla L[1], Alonso M[1], Rodríguez-Cabello J.C.[1]
[1] Bioforge Lab, LADIS, CIBER-BBN, University of Valladolid, Valladolid, Spain

Introduction

The mechanical properties of the extracellular matrix play a key role in regulating cellular functions. Beyond stiffness, viscoelasticity, namely, the ability to dissipate energy and relax stress, also critically influences fundamental processes such as cell migration, proliferation, and differentiation. However, because elasticity and viscosity are often intrinsically coupled, the development of materials that enable their independent tuning is essential to better understand cellular mechanobiological responses.

Materials and Methods

In this study, we developed a hydrogel platform composed of three elastin-like recombinamers (ELRs), designed to modulate elastic and viscous contributions through the combination of orthogonal covalent crosslinking and liquid-liquid phase separation. Two ELRs form the solid polymeric network and are crosslinked via strain-promoted azide-alkyne cycloaddition (SPAAC) [1], whereas a third thermoresponsive ELR generates an additional coacervate phase at 37 °C. The mechanical behaviour of the resulting hydrogels was evaluated by rheological and stress-relaxation assays. Human mesenchymal stem cells (hMSCs) were cultured on the hydrogels to assess cell viability and morphology.

Results

Rheological analyses showed that the incorporation of the coacervate phase increased the loss modulus (G'') by up to one order of magnitude while maintaining the storage modulus of the hydrogel, indicating that viscous and elastic components can be selectively tuned within the studied system. In addition, hydrogels containing the coacervate phase exhibited slower stress relaxation than the corresponding purely elastic matrices, suggesting prolonged retention of internal stresses. hMSCs cultured on these more viscoelastic hydrogels maintained viability above 95%, but exhibited reduced spreading and a more rounded morphology compared with cells cultured on matrices lacking the coacervate phase. These observations suggest altered cell-matrix mechanical coupling in response to changes in the viscoelastic properties of the substrate.

Conclusion

Overall, this ELR-based hydrogel platform enables the selective tuning of elastic and viscous components and provides a useful tool to investigate how time-dependent mechanical cues influence cell behaviour. Its versatility makes it a promising system for mechanobiology studies and for the design of viscoelastic scaffolds for tissue engineering and regenerative medicine.

Acknowledgements

Supported by the Spanish Government (grants PID2021-122444OB-100 and PID2022-137484OB-I00 funded by MCIN/AEI/ 10.13039/501100011033 and by ERDF, EU), from the Department of Education, Junta de Castilla y León (grant VA188P23 and CLU-2023-1-05 cofunded by ERDF) and from Centro en Red de Medicina Regenerativa y Terapia Celular de Castilla y León.

References

[1.] González de Torre, I., et al. Acta Biomaterialia 10, 2495–2505 (2014).

S60 – O5

Electroactive biodegradable PHBV/SF patches for mechanically stimulated skin regeneration

Bogas, D.[1,2], Lanceros-Mendez, S.[1,3,4,5], Ribeiro, C.[1,3]
[1]Physics Centre of Minho and Porto Universities (CF-UM-UP), University of Minho, Braga, Portugal, [2]IB-S – Institute for Research and Innovation on Bio-Sustainability, University of Minho, Braga, Portugal, [3]LaPMET - Laboratory of Physics for Materials and Emergent Technologies, University of Minho, Braga, Portugal, [4]BCMaterials, Basque Centre for Materials and Applications, UPV/EHU Science Park, Leioa, Spain, [5]Ikerbasque, Basque Foundation for Science, Bilbao, Spain

Introduction

Skin regeneration remains a major challenge due to the limited ability of damaged tissue to restore its structure and functionality. In this context, electroactive biomaterials capable of converting mechanical stimuli into electrical signals offer promising strategies to promote cell activity and tissue repair.
Electroactive, biocompatible, and biodegradable polymers, such as poly(3-hydroxybutyrate-co-3-hydroxyvalerate) (PHBV) and silk fibroin (SF), are attracting increasing interest for the development of active scaffolds in tissue engineering applications.

Materials and Methods

Films and fibrous samples with different PHBV/SF ratios were produced by solvent casting and electrospinning, respectively. The materials were subjected to physicochemical characterization to evaluate their structural and functional properties. Their biological performance was evaluated using HaCat keratinocyte cells as an *in vitro* skin model. To investigate the influence of an active microenvironment, mechanical stimulation was applied to the electroactive materials to induce an electrical response through the piezoelectric properties of the samples. Additionally, cell differentiation assays were performed for up to 14 days under both static and dynamic conditions. The antimicrobial activity of the developed materials was also evaluated against *E. coli* and *S. aureus*.

Results

The developed PHBV/SF materials showed no cytotoxicity and promoted the proliferation of HaCat cells over 7 days of culture. Furthermore, mechanoelectrical stimulation appears to enhance keratinocyte proliferation, particularly in samples with higher SF content (Figure 1). These results indicate that the electroactive microenvironment generated by the materials can positively influence keratinocyte behaviour. Preliminary results showed that the developed materials have antimicrobial properties against both strains.

Conclusion

This study shows promising results for the development of active patches for skin regeneration.

Acknowledgements

The authors also thank the FCT for financial support under grant UI/BD/154698/2023, contract under the Stimulus of Scientific Employment, Individual Support, doi.org/10.54499/2020.04163.CEECIND/CP1600/CT0019, through the strategic funding of CF-UM-UP (doi.org/10.54499/UID/04650/2025)

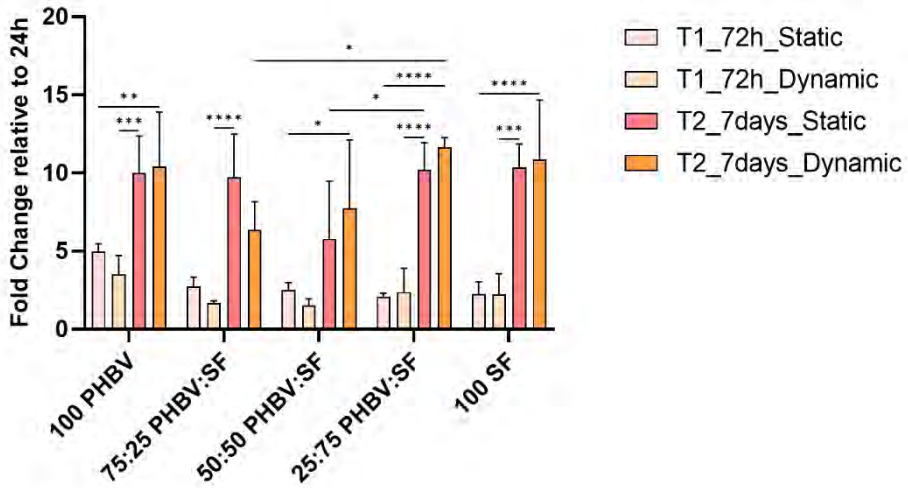

Figure 1: Cell proliferation of HaCat keratinocyte culture up to 7 days under static and dynamic conditions. The cell proliferation values were determined regarding the cells adhered on the material after 24h adhesion. The results are expressed as the mean ± SD.

S62
Engineering functional tubular tissues: From urethral reconstruction to vascularized biofabricated grafts

S62 – K1
Clinical perspective on tissue engineering for urethral reconstructive surgery

De Graaf, P.[1], Martinier I.C.[1], De Kort L.M.O[1] Pennisi, C.P.[2]
[1]Dept. of Urology, University Medical Center Utrecht, Utrecht, the Netherlands; [2]Department of Health Science and Technology, Aalborg University, Denmark

Introduction
The urogenital tract is vulnerable to a wide range of congenital and acquired disorders across all age groups, many of which significantly impair quality of life. Although the bladder was among the first organs engineered in the laboratory and transplanted to patients[1], tissue engineering (TE) in urology has yet to become a clinical reality.

This lecture focuses on the clinical need for TE in urethral reconstruction. Urethral disease is common, and demand for urinary tract reconstruction continues to rise due to increased use of intraurethral instrumentation and radiotherapy, an aging population, and the growing number of individuals with gender dysphoria. Augmentation urethroplasty—currently the most effective treatment for urethral stricture—relies on oral mucosa grafts. However, this approach is limited by the availability of donor tissue and its inability to replace the surrounding vascularized tissue (corpus spongiosum), leading to complications (urethral fistulas, recurrence).

As with most organs, adequate vascular support is essential for urethral function and long term graft survival. Insights from autologous grafts and clinical experience must therefore inform TE strategies. Because TE is inherently multidisciplinary—uniting clinicians, biologists, and materials scientists—future solutions should recognize and integrate clinical need, the patients voice, and the technological advancements[2].

A major limitation in early attempts to apply TE to urethral reconstruction is the integration of regulatory bodies. In the current Advanced Therapy Medicinal Products (ATMP) landscape these regulatory bodies are essential to to advance TE based urethral reconstruction toward clinical application.

Conclusion
Clinically relevant urethral grafts can only be developed through a truly multidisciplinary consortium.

Acknowledgements
This work was supported by the STRONG-UR European consortium, a project funding from the Horizon Europe program under grant agreement No 101191695.

References
[1]Atala A, Bauer SB, Soker S, Yoo JJ, Retik AB. Tissue-engineered autologous bladders for patients needing cystoplasty. *Lancet.* 2006;367:1241-1246.
[2]Juul N, Chamorro CI, Broekhuijsen K, Ekerhult TO, Fossum M, Guler Z, de Kort L, Kouwer P, van Poelgeest-Pomfret ML, Soria F, van Steenbeek F, Withagen M, de Graaf P. Lessons Learned from Tissue Engineering in Urethral Reconstruction and Pelvic Organ Prolapse. *Tissue Eng Part B Rev*. 2025 doi: 10.1177/19373341251363635.

S62 – K2

Coordinated epithelial–stromal regeneration for urethral repair using advanced polymeric scaffolds

Miettinen Susanna[1], Kurki Alma[1], Dixit Kartikeya[1], Sartoneva Reetta[1]
[1]Adult Stem Cell Group, Faculty of Medicine and Health Technology. Tampere University, Finland

Introduction

Reconstruction of extensive urothelial and urethral defects remains clinically challenging, as current approaches relying on autologous grafts are limited by donor-site morbidity, insufficient tissue availability, and complications. Importantly, functional urethral regeneration requires not only restoration of a continuous urothelial epithelium but also regeneration of the underlying stroma. The stromal compartment provides mechanical support, enables vascularization, and contributes to smooth muscle function, all of which are essential for long-term urethral patency and prevention of fibrosis or stricture formation. The aim of this work was to evaluate polymer-based biomaterials combined with human urothelial cells (hUCs) and human adipose-derived stromal/stem cells (hASCs) for integrated urethral tissue regeneration, with emphasis on stromal functionality and epithelial–stromal interactions.

Materials and Methods

Biodegradable polymeric biomaterials were investigated, including polylactide (PLA) blended with polybutylene succinate (PBSu), poly(trimethylene carbonate) (PTMC), poly(L-lactide-co-ε-caprolactone) (PLCL) membranes with varying surface topographies, and ascorbic acid 2-phosphate (A2P)-releasing supercritical CO_2-foamed PLCL scaffolds. Materials were assessed using hUC and hASC mono- and cocultures. Cell viability, proliferation, morphology, and phenotype maintenance were analyzed, alongside stromal functionality via smooth muscle differentiation markers and extracellular matrix production. Selected materials were further evaluated in vivo in urethral defect models to assess tissue integration, epithelial continuity, inflammation, and fibrosis.

Results

PBSu-containing materials supported hUC viability and proliferation while promoting hASC attachment, proliferation, and early smooth muscle marker expression, indicating preserved stromal differentiation. PLCL membranes supported hUC attachment and phenotype maintenance, with textured variants showing favorable mechanical compliance. A2P-releasing PLCL scaffolds significantly enhanced hASC proliferation and collagen deposition while maintaining stable hUC phenotype in mono- and coculture, suggesting improved epithelial–stromal interaction. In vivo, both PLCL and PTMC membranes supported urethral repair, with restoration of epithelial integrity, minimal fibrosis, and low inflammatory response.

Conclusion

Polymeric biomaterials combined with hUCs and hASCs provide a promising platform for coordinated urethral epithelial and stromal regeneration. Supporting stromal regeneration alongside epithelial repair is essential for functional outcomes. Future work should integrate these systems into advanced in vitro models: bioprinting enables spatial organization of epithelial and stromal compartments, while microfluidic platforms recapitulate physiological flow and mechanical cues. These approaches will support mechanistic studies and accelerate development of clinically translatable therapies.

S62 – O1

From Donor Tissue to Graft: decellularization of Human Urethra for Organ-specific Reconstruction

Sueters J.J.[1], Chabaud S.[1], Bolduc S[1,2]
[1]LOEX/Regenerative Medicine Division, CHU de Québec-Université Laval Research Center, Quebec, Canada, [2]Dept. of Surgery, Université Laval, Quebec, Canada.

Introduction

Current surgical methods for urethral reconstruction and repair generally rely on the use of autologous buccal mucosa or dermal flaps. However, lack of sufficient tissue, inherent tissue differences and surgical risks have led clinicians towards new solutions, such as tissue engineering. An organ-specific acellular matrix offers great potential due to their identical architecture and matrix composition without risk of immunorejection.

Aim. Create a sterile and clinically-suitable acellular urethral matrix from healthy human tissue.

Materials and Methods

The authors developed a chemical decellularization protocol for human urethral tissue. Resected penectomy tissue from 13 healthy transgender patients was used. Successful decellularization was confirmed by applying established acellular criteria (DNA <50 ng and <200 bp). Matrix preservation was histologically evaluated using a 7-point Likert scale for holes in the ECM, rupture and thinning of the matrix, in combination with quantitative proteomics. Suitability as a tissue-mimicking scaffold for urethral reconstruction was determined by the protein preservation (proteomics), biomechanical properties (uniaxial tensile test), and surgical handling (suturability). The cytotoxicity of non-sterilized matrices was investigated and compared to matrices sterilized with ethanol + antibiotics or PAA, by recording proliferation (MTT) and growth inhibition (Alamar Blue) of seeded fibroblasts and urothelial cells for 20 days.

Results

The produced human decellularized urethral matrices satisfied acellular criteria with 4.1 ng DNA/mg ECM (5.3%, $P<0.001$) of <200 bp in length. Histology demonstrated ECM preservation without holes, ruptures or thinning (rarely/never). Qualitative proteomics showed a predominantly preserved composition of the core matrisome, consisting of collagens, glycoproteins, and proteoglycans. In accordance to our previous work on human decellularized vagina[1], the peak load, strain at rupture, and elastic modulus were significantly reduced. Despite significant contraction (36%, $P<0.0001$) and slight swelling (8%, NS), the decellularized urethral matrices were rated good/very good in terms of suturability. Non-sterilized and sterilized urethral matrices did not cause cytotoxicity, but biomechanical properties of the urethral matrices were reduced by both sterilization methods.

Conclusion

Our study provides insight in how decellularization and sterilization effect the physical properties and clinical suitability of human urethral tissue. Human decellularized urethral matrix showed safe, biocompatible and had sufficient mechanical strength to allow surgical manipulation and in vivo functionality. We conclude that human decellularized urethra is a promising tissue-engineered material for urethral reconstruction, which may improve long-term patients' quality of life and could offer a great future alternative to current treatments.

Acknowledgements

This research received financial support from Amsterdam University Funds and the Canadian Institute of Health Research (CIHR).

[1]Sueters J.J., Xiao F., Roovers J.P.R.W., Bouman M.B., Groenman, F.A., Maas H., Huirne J.A.F., Smit T.H. Creation of a decellularized vaginal matrix from healthy human vaginal tissue for potential vagina reconstruction: experimental studies. *International Journal of Surgery* 2023; 109(12); 3905-3918.

ESB 2026

References

S62 – O2

Material extrusion-based additive manufacturing of gelatin-based hydrogels for urethral tissue engineering

Dixit K. [1,2], Ala Mononen K. [1,2], Sartoneva R. [1,2], Pien N. [3], Eeckman N.[4], Pennisi P.[5], Van Vlierberghe S [3], Miettinen S.[1,2]

[1] Adult Stem Cell Group, Faculty of Medicine & Health Technology, Tampere University, Tampere, Finland, [2] Tays Research Services, Wellbeing Services County of Pirkanmaa, Tampere University Hospital, Tampere, Finland, [3]Polymer Chemistry and Biomaterials Group, Centre of Macromolecular Chemistry (CMaC), Ghent University, Ghent, Belgium, [4]4Tissue, Zwijnaarde, Belgium, [5]Aalborg Universitet, Gistrup, Denmark

Introduction

Urethral stricture disease represents a significant clinical challenge, with current reconstructive strategies including buccal mucosa grafting limited by donor site morbidity, graft failure, and the inability to restore the complex multicellular architecture of native urethral tissue. Tissue-engineered constructs fabricated via material extrusion-based additive manufacturing offer a viable route toward anatomically relevant, cell-laden scaffolds capable of recapitulating the urothelial, stromal, and vascular compartments of the urethra. Gelatin-based hydrogels, specifically methacrylated gelatin (GelMA) and thiol–norbornene crosslinked gelatin (GelSH-GelNB), are promising bioink candidates owing to their tunable mechanical properties, photocrosslinkability, and inherent bioactivity derived from the extracellular matrix. However, a systematic comparative assessment of their printability and cytocompatibility across the relevant cell populations remains lacking.

Materials and Methods

10% (w/v) GelMA and GelSH-GelNB hydrogels were formulated and additively manufactured using PNEUMAHEAT tool via BRINTER CORE 3D printer into two-layer mesh constructs with a 0°/90° fibre orientation to assess printability in terms of filament continuity, pore geometry fidelity, and dimensional accuracy. Cytocompatibility was evaluated in two experimental configurations: (i) two-dimensional (2D) monoculture, in which human adipose-derived stromal cells (hASCs), human umbilical vein endothelial cells (HUVECs) and human urothelial cells (hUCs) were seeded onto hydrogel surfaces, and (ii) three-dimensional (3D) encapsulation, in which the hASCs and HUVECs populations were embedded within the hydrogel matrix. Cell viability and proliferative activity were assessed at days 1, 3, and 7 post-culture using a Live/Dead fluorescence assay, CyQuant proliferation assay, and DAPI/Phalloidin immunofluorescence staining for morphology.

Results

Both 10% (w/v) GelMA and GelSH-GelNB demonstrated consistent filament deposition and well-defined pore architecture under the evaluated printing parameters, confirming their processability via extrusion based additive manufacturing. In 2D monoculture, both cell types hASCs and HUVECs exhibited sustained viability and progressive proliferation across the 7-day observation period on both hydrogel formulations. Under 3D encapsulation conditions, hASCs maintained proliferative capacity over time, whereas HUVECs displayed comparatively attenuated proliferation, suggesting differential sensitivity to the three-dimensional hydrogel microenvironment. In case of hUCs, it was observed that morphology of the cells remained spherical throughout the culture period indicating improper attachment of the cells on the hydrogel surface warranting further optimisation and investigation. These findings establish a preliminary cytocompatibility profile for both bioinks in the context of multilayered multicellular urethral tissue constructs and inform subsequent optimisation of bioink composition and printing parameters.

Conclusion

In sum, these results demonstrate that both GelMA and GelSH-GelNB hydrogels are processable via material extrusion-based additive manufacturing and they initially support viability and growth of hASCs, HUVECs and hUCs, establishing a foundation for their future development into bioprinted urethral constructs.

Acknowledgements
STRONG-UR is a project funded by the European Union and has received funding from the Horizon Europe programme under grant agreement No 101191695. Views and opinions expressed are however those of the author(s) only and do not necessarily reflect those of the European Union or HaDEA. Neither the European Union nor the granting authority can be held responsible for them.

S62 – O3

Creating modular tubular networks with tomographic volumetric additive manufacturing for branched small diameter vascular models

Bartolf-Kopp M[1], Gergely C[1], Geroneit I[1], Moser F[1], Galaba L[1], Chicaiza Cabezas N[1], Priebe V[1], Jungst T[1]
[1] Dept. for Functional Materials in Medicine and Dentistry, University Würzburg, Germany

Introduction

Tomographic volumetric additive manufacturing (tVAM) is a powerful tool to create complex geometrical structures for biomedical applications. The system lends itself ideally for the recreation of complex tissue structures. An application of tVAM is the use of patient data to create faithful disease models that recreate the pathology of for example stenosed blood vessels. Due to limitations in effective light penetration within the photoresin, vat size and by that maximal construct size is restricted. This limits the fabrication of complex branched tubular systems for small diameter blood vessel models that could be used as *in vitro* flow perfusion or stent deployment models.

Aim

To harness the capabilities of tVAM for the creation of branched vascular trees, we established a new straightforward way to use tVAM to fabricate a modular building block system. By connecting these modules, it would be possible to create large tubular structures with branches, windings and stenoses.

Materials and Methods

Polyethylene glycol diacrylate was blended with cellulose nanofibers as rheological modifier as main resin for tVAM. CAD models of different tubular modules consisting of multiple geometries including straight pipes, bypass branches, y-branches and spirals were designed and evaluated for printability. After parameters were adjusted, modules were printed and attached to each other to create larger tubular networks. To enable cell seeding, gelatin methacryloyl (GelMA) was used as resin matrix. Cell seeding of the module lumen was done with human umbilical vein endothelial cells (HUVEC).

Results

Tube modules could be created with several different geometries, also beyond conventional pipes like star shaped lumen or stenosed tubes. By attaching them at the end points by gluing it was possible to create leak tight connections and build networks consisting of up to seven different modules (Fig 1). Flow simulations of a stenosed bypass model could be recreated experimentally. A tubular system with seven modules was created with one stenosed module into which a stent could be deployed by balloon catheter though the network. Using GelMA as resin, several modules were created and pre-seeded with HUVECs. Combining these modules to a tree enabled a high monolayer coverage compared to a pre-assembled and post seeded module network.

Conclusion

We showed that by creating single moules with tVAM, it is possible to create large tubular networks beyond the build volume limitation of commercially available systems that can be used as models for flow study or endothelialisation

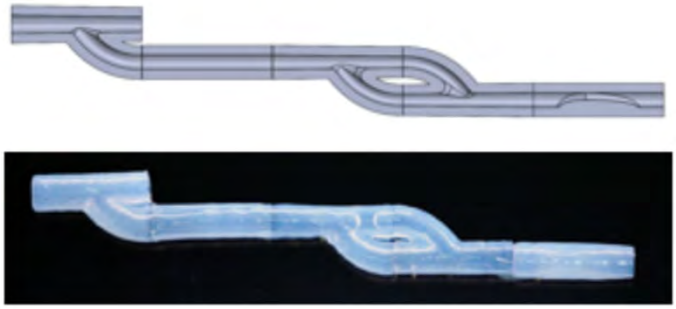

Fig. 1: CAD design (top) and printed (bottom) PEGDA modules via tVAM assembled into a branched tubular network with a stenosis module.

S62 – O4

Matrix architecture governs urethral organoid fate: phenotypic responses across soft, stiff, and porous collagen type I substrates

Martinier, I, Cómitre-Andersen, L.S, Nijhuis, J, de Kort, L, de Graaf, P
Dept. of Urology - Regenerative Medicine Utrecht, University Medical Center Utrecht, The Netherlands

Introduction

Understanding urethral epithelium biology and interactions with the surrounding tissue is limited by the lack of accurate models. Several urogenital and male reproductive organs have already been miniaturised using organoids, including the prostate, the testis, and the bladder. However, because the urethral epithelium differs from those models, they cannot be transposed to the urethra, limiting our comprehension of physiological phenomena and their relevance for urethral treatment. Beyond the lack of urethral organoids, current methods of culturing organoids rely on tumorigenic and chemically undefined hydrogels such as basement membrane extract (BME), which cannot be translated to the clinic. Considering this, there is an urge to replace BME with more relevant support that mimics the native cellular microenvironment. *In vivo*, type I collagen is the main building block of the extracellular matrix, making it a particularly interesting alternative to BME.

Aim

Our goal is to generate urethral models and to explore organoid-material interactions under physiological conditions, using a set of collagen substrates with controlled architecture and mechanical properties.

Materials and Methods

Epithelial cells derived from patient tissue were first grown in BME with tailored medium. We then explored organoid-collagen interactions by growing cells in weak hydrogels of various concentrations (1-8 $mg.mL^{-1}$), as well as on stiff porous and non-porous collagenous substrates. These new materials are composed solely of type I collagen, elaborated in non-denaturing conditions, at physiological concentrations of 100-200 $mg.mL^{-1}$ and up to pathological concentrations of 400-900 $mg.mL^{-1}$. Non-porous collagen matrices were fabricated via evaporation followed by fibrillogenesis, i.e. by inducing the self-assembly of collagen molecules into fibrils upon osmotic pressure increase. Porous matrices were fabricated via controlled freezing of collagen solutions, followed by topotactic fibrillogenesis.

Results

Urethral organoids display typical cytokeratin markers and a hollow shape in BME (Fig.1-A and B1). In contrast, in weak collagen hydrogels, organoids form more slowly and exhibit a less spherical morphology (Fig.1-B2). Denser substrates, with a stiffness ranging from 20 to 1400 kPa, promote the formation of organoid-like structures capable of remodelling and exerting traction on collagen fibrils (Fig.1-B4); a capacity absent in single cells.

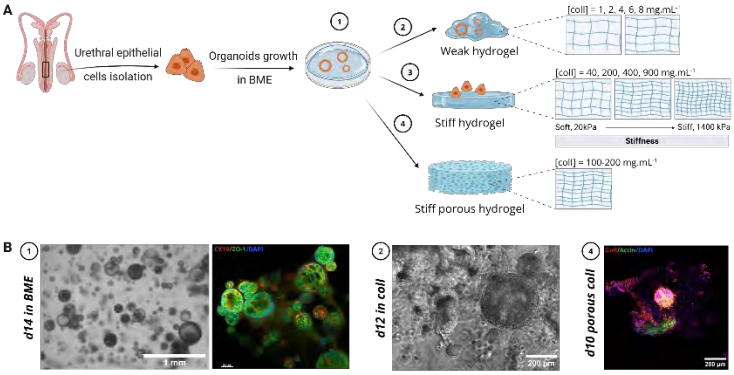

Figure 1. Urethral organoids establishment and interactions with collagenous substrates.

Conclusion

Our approach informs on organoid-material interactions, focusing here on urethral epithelial organoids and type I collagen substrates, which are clinically translatable and closely mimic biological tissues.

Acknowledgements

I.Martinier acknowledges the STRONG-UR consortium for funding, a project funded by the Horizon Europe programme under grant agreement No 101191695.

S62 – O5

Dual vascularization: engineering a 3D perfusable vascular model integrating blood and lymphatic vessels

Vonna E.[1], Huang X. [1], Simon-Yarza T.[1]

[1]Laboratory for Vascular Translational Science (LVTS), INSERM U1148, Université Paris Cité, Université Sorbonne Paris Nord, France

Introduction

Human vasculature is composed of two vessel networks that coordinate to maintain tissue homeostasis: the blood vasculature distributes oxygen, nutrients, signaling molecules to tissues, while the lymphatic vasculature returns interstitial fluid to the bloodstream and plays a major role in the transport of lipids and immune cells. Disruptions in the balance between these two networks, particularly impaired lymphatic drainage, have been associated with diseases, such as lymphedema, tumor metastasis, atherosclerosis and obesity. Perfusable vessels-on-chip rarely include the lymphatic network, which remains less studied and understood than the blood vasculature. Besides, incorporating hydrogels that replicate the properties of the native extracellular matrix in vessel-on-chip models contributes to better mimic the physiological environment compared to traditional polydimethylsiloxane (PDMS)-based platforms. **Aim.** To address these limitations, we propose a double-network polysaccharide hydrogel as a 3D matrix to engineer blood and lymphatic vessels in a fluidic platform to mimic physiological flow conditions.

Materials and Methods

Micromolding was used to form two parallel microchannels within the polysaccharide hydrogel (see Figure, graphical abstract – Part A). Primary blood endothelial cells and smooth muscle cells were seeded in one channel (ca. 300 mm) to engineer a small artery, while primary lymphatic endothelial cells were seeded in the other channel (ca. 100 mm) to form a lymphatic capillary (see Figure, graphical abstract – Part C). Besides, a tailor-made fluidic platform was designed using computer-aided design (CAD) and manufactured by 3D printing. This chamber allowed to connect the microchannels to peristaltic pumps to independently perfuse the vessels by applying two different intraluminal flows, along with a reservoir to mimic the interstitial flow that is crucial for vessel maturation (see Figure, graphical abstract – Part B).

Results

Results showed that, the double-network hydrogel had sufficient mechanical strength to withstand connection to rigid fluidic ports while supporting cell culture of blood and lymphatic cells. The platform enabled the application of physiologically relevant shear stress within the blood microchannel, as well as an appropriate drainage rate in the lymphatic microchannel. Moreover, following *in situ* seeding of the cells into the microchannels, both blood and lymphatic endothelial cells successfully adhered to the gel walls to form monolayers along their respective microchannels, mimicking vessel-like structures.

Conclusion

This dual-vascularized and perfusable *in vitro* model is pioneer in integrating lymphatics in arterial models and will provide unprecedent possibilities to investigate interactions between the arterial and lymphatic compartments in vascular-related diseases, such as atherosclerosis, under physiologically relevant conditions.

GRAPHICAL ABSTRACT

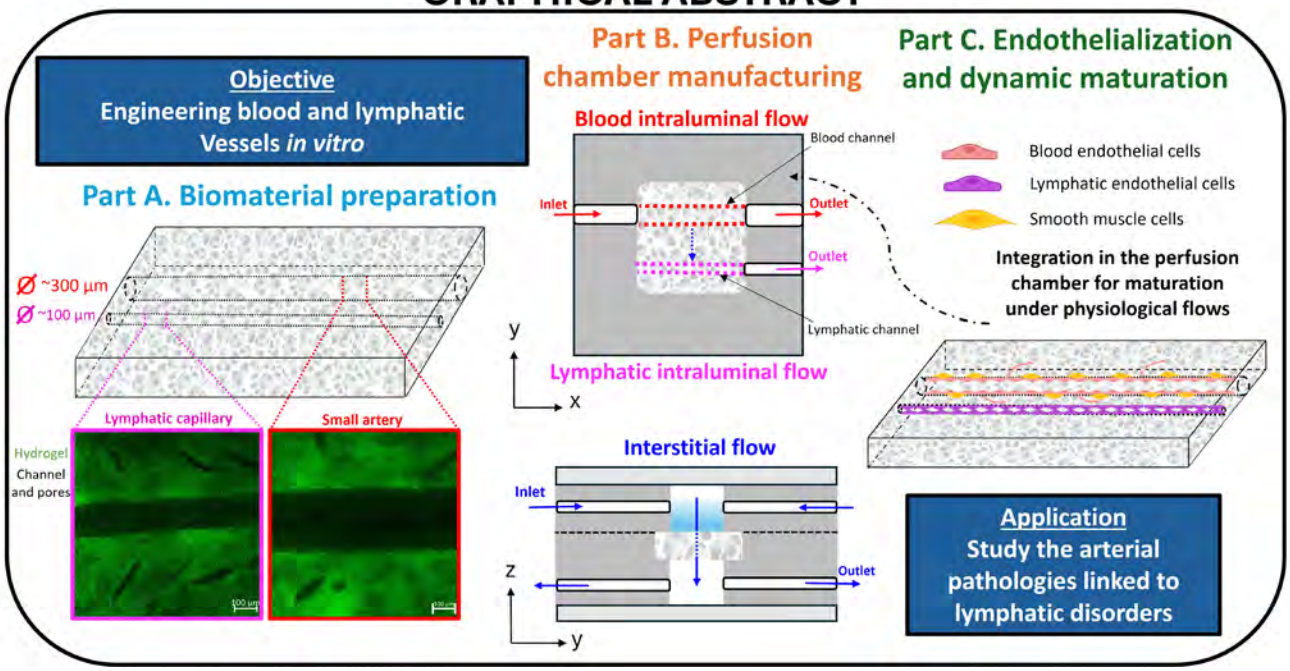

S63 – O1

Women Leading Innovation: Bridging Science, Career, and Equity across Continents in Biomaterials

This symposium aims to celebrate and amplify the contributions of women in biomaterials science across continents, while addressing critical challenges in career development and gender equity. The session will feature cutting-edge research led by female scientists, spanning advanced biomaterials for tissue engineering, neural repair, and surface engineering. Confirmed speakers include: **Geetha Manivasagam (India)**, **Ana Paula Rosifini (Brazil)** and **Ana Paula Pêgo (Portugal)**, representing diverse scientific expertise and geographical perspectives.

Beyond scientific excellence, the symposium will foster dialogue on work-life balance, mentorship, and strategies for professional growth at different career stages. Talks will also explore policies and institutional approaches to dismantle systemic biases and close the gender gap in STEM. **While highlighting women's experiences, the themes of equity, career sustainability, and inclusive practices are universally relevant and will benefit all scientists navigating demanding careers in STEM.**

By combining research presentations with interactive discussions, this session will provide actionable insights for creating inclusive environments that empower biomaterial scientists globally. Aligned with ESB2026's mission to promote multidisciplinary collaboration and diversity, this symposium offers a unique platform to advance both scientific innovation and societal impact in biomaterials research.

Chairs

- **Ana Paula Pêgo** (Research Coordinator, Portugal)
- **Ana Paula Rosifini** (Brazil)

Keynote Speakers:

Geetha Manivasagam

Vellore Institute Of Technology, India

geethamanivasagam@vit.ac.in

Ana Paula Rosifini

São Paulo University State University, Brazil

paula.rosifini@unesp.br

Ana Paula Pêgo

Instituto de Investigação e Inovação da Universidade do Porto, Portugal

apego@i3s.up.pt

S65
Biodegradation, stability, and Long-Term performance

S65 – K1
Tailoring the structure of polyphosphoester networks for the design of functional scaffolds for tissue engineering

Jérôme Christine[1]
[1]CERM, CESAM RU, University of Liege, Belgium

Introduction
Polyphosphoesters (PPEs) are emerging as versatile polymer platforms for biomedical applications owing to their tunable chemical structure, hydrolytic degradability, and potential biocompatibility. Their properties can be finely adjusted through the choice of monomers, copolymer composition, and macromolecular architecture, providing control over hydrophilicity, degradation behavior, and mechanical properties. Furthermore, the incorporation of reactive functionalities offers opportunities for the introduction of bioactive molecules and the formation of covalently crosslinked networks. These features make PPEs particularly attractive for the development of temporary biomaterials whose properties can be tailored to specific tissue engineering requirements.

Aim
This work aims to investigate how the molecular and network architecture of degradable polyphosphoesters can be tailored to develop functional scaffolds with controlled mechanical and structural properties. Two complementary strategies were explored. First, the network architecture was designed to increase the extensibility of PPE-based elastomers and thereby expand their accessible mechanical properties. Second, High Internal Phase Emulsion (HIPE) templating was investigated as a strategy to generate highly porous, interconnected PPE scaffolds suitable for cell culture.

Materials and Methods
Polyphosphoester copolymers with different macromolecular architectures and pendant unsaturated functionalities were synthesized by organocatalyzed ring-opening polymerization. The resulting polymers were subsequently converted into covalently crosslinked elastomeric networks by photopolymerization. For scaffold fabrication, PPE-based formulations were processed using HIPE templating, followed by polymerization to generate interconnected porous matrices.

Results
The architecture of the precursor copolymers was found to have a pronounced effect on the mechanical behavior of the resulting networks. In particular, photo-crosslinked PPEs with a blocky architecture displayed substantially enhanced extensibility compared with previously reported random copolymer networks, reaching elongations at break of up to **180%**. Clear correlations between polymer microstructure and macroscopic properties, including Young's modulus and elongation at break, were established, demonstrating the critical role of network architecture in controlling the mechanical response of PPE-based elastomers.
In parallel, HIPE templating enabled the successful fabrication of degradable PPE scaffolds with an interconnected porous morphology. Modifying the structure of the polyphosphoester allowed the preparation of a series of porous matrices with tunable characteristics. These scaffolds provide a promising platform for cell culture and further investigation toward tissue engineering applications.

Conclusion
This work demonstrates that controlling polyphosphoester architecture at the molecular and network levels provides an effective means of tailoring both the mechanical behavior and three-dimensional structure of degradable scaffolds. The combination of enhanced elastomeric properties and interconnected porosity highlights the potential of PPEs as versatile, degradable platforms for the development of functional biomaterials for tissue engineering and regenerative medicine.

Acknowledgements
This research was supported by the FRS-FNRS through the HIPE-PEPS project and the O. Rabaux FRIA grant, and by the European Interreg MR programme within the framework of the PolyDREAM project.

S65 – O1

Biodegradable phosphoroamidate photopolymers with tunable mechanical properties and controlled degradation for additive manufacturing

Mostofizadeh M.[1], Teasdale I.[1]
[1] Institute of Polymer Chemistry, Johannes Kepler University, Austria

Introduction

Additive manufacturing (AM) enables fabrication of complex 3D biomaterials for applications such as drug delivery systems and tissue engineering scaffolds. Many AM technologies rely on UV-curable resins due to their high resolution and rapid processing. However, widely used acrylate-based photopolymers may generate cytotoxic residual monomers and form non-degradable carbon backbones, limiting biomedical use. Recently introduced amino acid phosphoroamidate (APA) photomonomers[1] provide a promising platform for degradable photopolymers. These monomers contain hydrolytically cleavable phosphorus–nitrogen bonds that degrade under physiological conditions into biocompatible phosphates and amino acids.

Aim. The aim of this work is to develop biodegradable APA-based photopolymers with tunable mechanical properties and controlled degradation behaviour for photochemical 3D printing by systematically varying amino acid substituents and comonomer composition.

Materials and Methods

APA photomonomers were synthesized by coupling selected amino acids to a phosphorus core to obtain monomers containing hydrolytically cleavable phosphorus–nitrogen bonds. The monomers were functionalized with vinyl or propargyl groups to enable photocuring. Polymer formulations were prepared using multifunctional thiols, crosslinkers, and selected comonomers to control network architecture and crosslink density. Copolymerization with thiols enabled network formation via thiol-based photopolymerization[2], while vinyl ester and carbonate derivatives allowed the preparation of single-component photopolymerizable resins[3]. The resulting formulations were processed using photochemical 3D printing techniques and characterized regarding their thermomechanical properties and degradation behaviour.

Results

APA-based formulations enabled materials with tunable mechanical properties and degradation behaviour. By varying amino acid substituents and comonomer composition, polymer networks ranging from stiff materials to elastic elastomers were obtained. Degradation was evaluated by monitoring mass loss at pH 7.4 and 37 °C. In contrast to polyester systems such as PLGA, APA formulations exhibited pronounced hydrolytic degradation. Several systems showed a near-linear mass decrease, indicating a surface-erosion-dominated mechanism. The degradation rate depended on amino acid structure, hydrophilicity, and crosslink density. Optical observations revealed progressive surface roughening and dimensional reduction without catastrophic fragmentation, confirming erosion from the exterior inward.

Conclusion

APA-based photopolymers represent a versatile platform for biodegradable UV-curable resins for additive manufacturing. By varying amino acid substituents and comonomer composition, materials with a broad range of mechanical properties, from stiff polymers to elastomers, can be obtained with tunable degradation rates. This strategy enables predictable degradation behaviour and provides promising materials for drug delivery and biomedical applications.

Acknowledgements

The authors gratefully acknowledge funding by the ACCURE project under Project ID ATCZ00083.

References

[1]Haudum S., Lenhart S., Müller S.M., Tupe D., Naderer C., et al. Amino acid-based polyphosphorodiamidates with hydrolytically labile bonds for degradation-tuned photopolymers. *ACS Macro Letters 2023*; 12; 673–678.
[2]Mostofizadeh M., Kainz M., Alihosseini F., Haudum S., Youssefi M., Bauer P., et al. Phosphoramide hydrogels as biodegradable matrices for inkjet printing and their nano-hydroxyapatite composites. *ACS Applied Materials & Interfaces 2024*; 16; 52902–52910.

[3]Haudum S., Demirdögen B., Müller-Müchler L., Döttl S.C., Müller S.M., Naderer C., et al. Biodegradable resins for photochemical 3D printing via vinyl ester and vinyl carbonate functionalized amino acid-phosphoramidates. *European Polymer Journal 2024*; 211; 113037.

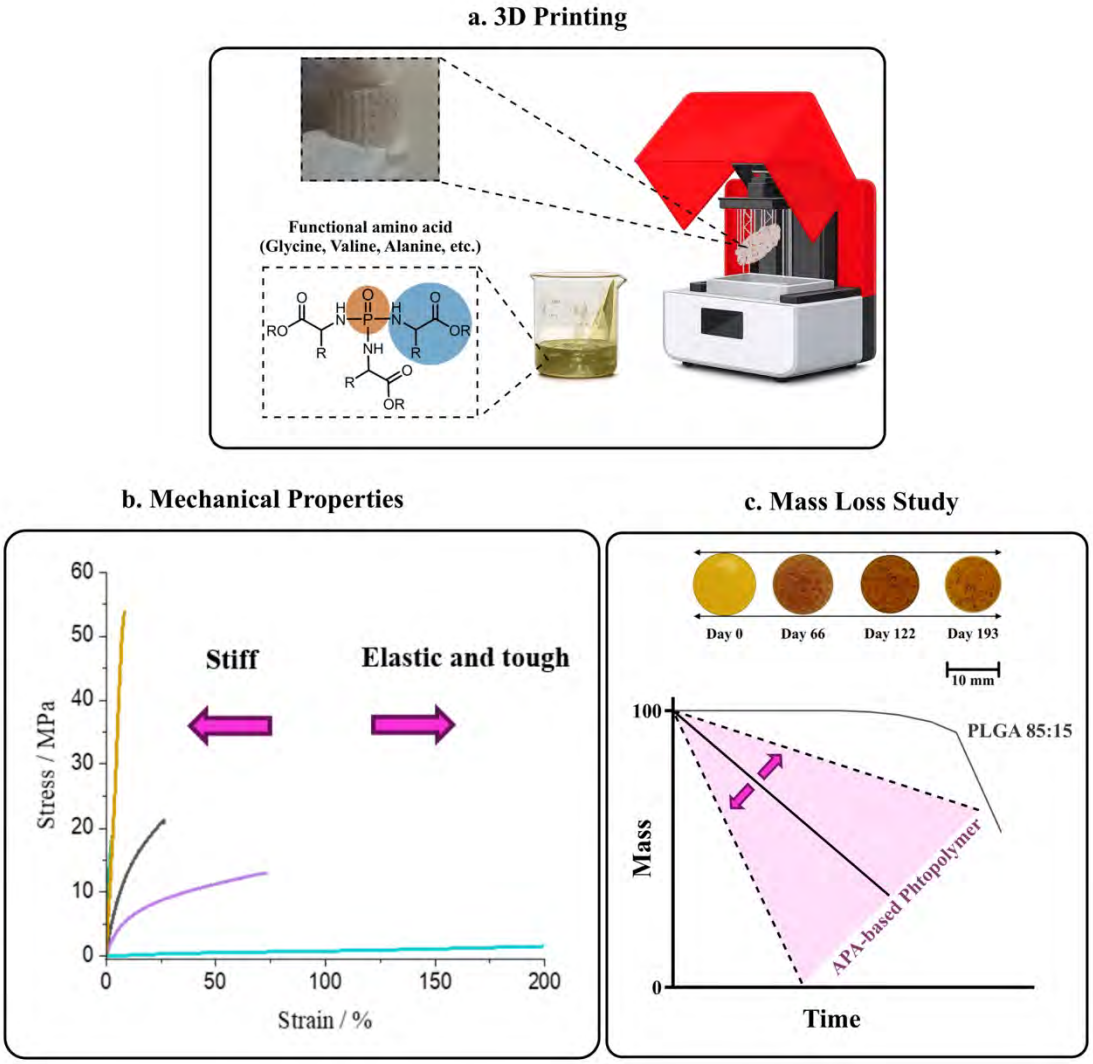

S65 – O2

From sea to scaffold: barnacle materials actively promote bone regeneration through multiple pathways

Chang L.[1], Wen Z.H.[1,2,3]
[1]Institute of BioPharmaceutical Sciences, National Sun Yat-sen University, Kaohsiung, Taiwan, [2]Dept. of Marine Biotechnology and Resources, National Sun Yat-sen University, Kaohsiung, Taiwan, [3]National Museum of Marine Biology & Aquarium, Pingtung, Taiwan

Introduction

Building upon our previous work on coral bone graft material[1], this study further investigates their capacity to regulate the osteo–immuno–angiogenic microenvironment during bone regeneration. Conventional grafts primarily provide passive osteoconduction but lack active immunomodulatory and angiogenic functions[2,3]. Here, we evaluated whether sintered barnacle materials can overcome these limitations and actively promote the healing of critical-sized bone defects.

Materials and Methods

Exoskeletons of *Megabalanus tintinnabulum* (MT) and *Tetraclita japonica formosana* (TJF) were sintered at high temperatures to remove organics while preserving the calcium carbonate skeleton. *In vitro* osteogenic potential was evaluated using preosteoblast differentiation assays, complemented by Correlative Light and Electron Microscopy (CLEM) to visualize cell distribution on the materials. Immunocompatibility responses were assessed in RAW264.7 macrophages, and angiogenic potential was assessed using HUVEC migration and tube formation assays. *In vivo* efficacy was tested in a rat critical-sized calvarial defect model for up to five months, with tissue–material interfaces analyzed using micro-CT and multiphoton confocal Second Harmonic Generation (SHG) imaging.

Results

Sintered MT and TJF materials demonstrated osteogenic potential *in vitro*. MC3T3-E1 cells cultured on barnacle materials showed enhanced differentiation. CLEM visualized preosteoblast attachment and differentiation. Macrophages exposed to MT and TJF extracts maintained minimal M1 marker expression, indicating immunocompatibility. Extracts also enhanced endothelial migration and angiogenic activity, accelerating HUVEC tube formation via pro-angiogenic pathways. *In vivo*, micro-CT revealed greater new bone formation compared with the commercial xenograft. Multiphoton SHG imaging confirmed distributed cells and mineralized collagen deep within barnacle material cavities.

Conclusion

These findings demonstrate that sintered MT and TJF barnacle exoskeletons are bioactive materials with excellent immunocompatibility and promote angiogenesis and osteogenesis, highlighting MT and TJF materials as sustainable and superior alternatives to conventional coral bone grafts for bone tissue engineering.

Acknowledgements

This study was supported by the National Science and Technology Council of Taiwan (114-2313-B-291 -001 -MY3).

References

[1]Chang, L., et al., Cultivated Pocillopora acuta coral as a sustainable and effective biomaterial: enhanced osteogenic potential and structural integrity. Materials & Design, 2025. 258: p. 114610.
[2]Einhorn, T., Gerstenfeld, L. Fracture healing: mechanisms and interventions. Nat Rev Rheumatol 11, 45–54 (2015).

S65 – O3

Effect of supercritical CO_2 on the structure and degradation of PLA surgical meshes

Cédric Bossard[1,2,3], Safa Ouerghemmi[1], Nicolas Blanchemain[2], Bernard Martel[3]
[1]Cousin Surgery, Wervicq-Sud, France, [2]INSERM U1365, Université de Lille, Lille, France, [3]UMET, Université de Lille, Villeneuve-d'Ascq, France

Introduction

Implantable textile meshes are widely used for abdominal hernia repair, providing temporary mechanical support during tissue healing. In mesh manufacturing, yarns are typically coated with sizing agents that enable them to withstand the mechanical stresses of weaving. The coating is subsequently removed, typically with organic solvents. The company COUSIN Surgery previously employed diethyl ether for this purpose but has recently replaced it with supercritical CO_2 ($scCO_2$), which offers several advantages including low toxicity and reduced environmental impact. However, the ability of $scCO_2$ to diffuse into polymer matrices may also induce structural modifications, for instance changes in crystallinity.

Aim

This study investigates the impact of $scCO_2$ treatment on the properties of polylactic acid (PLA), a bio-based and biodegradable polymer used in COUSIN Surgery's meshes.

Materials and Methods

PLA meshes were provided by COUSIN Surgery. They were treated by static $scCO_2$ at various temperatures (40 to 80 °C) and pressures (80 to 320 bar) for 1 h. Changes in crystalline structure were determined by DSC. Ethanol extracts of meshes (0.3 g/mL, 36 h at 50 °C) were analysed by GC-MS. Tensile testing was performed on 3 x 2 mm meshes at 10 mm/min. Accelerated hydrolytic degradation was conducted in PBS at 50 °C and the molecular weight was monitored by GPC-SEC in chloroform.

Results

DSC showed that the initial PLA mesh exhibits a high crystallinity (56 ± 4%). At pressures above 240 bar, $scCO_2$ led to a narrower melting peak, indicating a more uniform lamellar structure. Variations in crystallinity were not statistically significant due to the inherent variability of industrial PLA meshes. GC–MS analysis revealed that $scCO_2$ extracted residual monomers and oligomers entrapped in the polymer matrix. Extraction strongly depended on the temperature and pressure used for scCO2. Removal of these monomers was associated with an increase in uniaxial tensile stiffness, likely due to reduced internal plasticization. At 40°C and 160 bar, $scCO_2$ significantly delayed hydrolytic degradation: Mn decreased from 120,000 to 70,000 g/mol after 12 weeks of immersion, compared to 5 weeks for untreated meshes.

Conclusion

In addition to cleaning, $scCO_2$ can significantly delay the degradation of PLA meshes. This effect may partly result from the extraction of lactic acid monomers, which are known to catalyse ester bond hydrolysis.

Acknowledgements

This work is funded by the Métropole Européenne de Lille and by l'Initiative d'Excellence de l'Université de Lille in the frame of the Industrial Research Chair REGFI.

S65 – O4

Electrocompaction vs. Mechanical Compaction - Production of Stable (Fibre Reinforced) Collagen Gels

Schyra P[1], Feldgiebel L[1], Cherif C[1], Wöltje M[1]

[1] Institute of Textile Machinery and High Performance Material Technology (ITM), TUD Dresden University of Technology, Dresden, Germany

Collagen-based materials have emerged as critical components in the development of biomaterials for tissue engineering and regenerative medicine due to their biocompatibility and structural similarity to native extracellular matrices. However, the stability and mechanical properties of collagen hydrogels remain key challenges for their application in load-bearing environments. To address this, we compare two innovative compaction methods electrocompaction and mechanical compaction for the production of stable, fibre-reinforced collagen gels.

Electrocompaction is a novel technique that employs an external electric field to align and condense collagen fibrils, resulting in anisotropic, denser structures. Conversely, mechanical compaction relies on physical loading to compress hydrogels, enhancing their density and mechanical strength. Both methods aim to improve the structural and functional properties of collagen gels, but the underlying mechanisms and resulting material characteristics differ significantly.

In this study, we systematically evaluated the effects of electrocompaction and mechanical compaction on the morphology, mechanical properties, and stability of collagen gels, both with and without fibre reinforcement. Collagen gels were prepared at physiological pH and subjected to either electrocompaction using a custom-designed apparatus or mechanical compaction via uniaxial compression. Fibre reinforcement was achieved by the incorporation of aligned wet-spun collagen or chitosan fibres during the gelation process.

Characterization techniques, including scanning electron microscopy (SEM), tensile testing, and differential scanning calorimetry (DSC), were employed to assess fibril alignment, mechanical performance, and thermal resistance. Electrocompacted gels exhibited highly aligned fibril structures, superior tensile strength, and greater anisotropy compared to mechanically compacted gels. Fibre-reinforced collagen gels displayed further improvements in mechanical properties, with electrocompaction producing a more uniform integration of fibres and collagen fibrils. These findings highlight the potential of electrocompaction for producing collagen-based biomaterials with tunable anisotropy and improved mechanical stability, which are crucial for applications in soft tissue engineering.

In conclusion, this work provides a comprehensive comparison of electrocompaction and mechanical compaction as strategies for producing stable, fibre-reinforced collagen gels. The results underscore the promise of electrocompaction in advancing the design of next-generation biomaterials for biomedical applications.

Acknowledgements

The acid-soluble collagen was kindly provided by Michèle Lindner from GfN & Selco (Wald-Michelbach, Germany)

S65 – O5

Heating of dental composites: the crucial role of the silane coupling agent on the consistency change

Grob B., Nad P., Catel Y.
Ivoclar Vivadent AG, Schaan, Liechtenstein

Introduction

Methacrylate-based composites are widely used in restorative dentistry owing to their excellent esthetic and mechanical properties. These dental composites mainly consist of dimethacrylate monomers and functionalized inorganic particles. To ensure a good compatibility of the inorganic filler particles with organic resin matrix and to covalently incorporate the particles in the polymer network during the polymerization, the filler surface is functionalized with coupling agents such as methacrylate based silanes. Besides the previously mentioned properties, these silanes affect the consistency of the dental composite as well. To ease the filling of tooth cavities with composites exhibiting a hard consistency, such composites are often preheated to reduce their consistency. Unfortunately, the preheating of typical composites does not result in a flowable consistency.

Aim

We envisioned to improve the drop in consistency upon heating by optimizing the filler surface/ monomer mixture interaction.

Material and Methods

The consistency of the uncured composites was determined at various temperatures (23 °C, 30 °C and 60 °C) using a texture analyzer. The flexural strength and modulus of the cured composites were assessed according to ISO 4049.

Results

Several silane coupling agents were synthesized and used to functionalize glass fillers. The resulting particles were evaluated in dental composites in diverse concentrations. It was shown that the nature of the silane has a strong influence on the consistency at various temperatures, double bond conversion and flexural strength and modulus of the corresponding composites.

Conclusion

The functionalization of particles with tailored silanes represents a promising technology for the development of dental composites exhibiting an adaptive consistency upon heating.

S65 – O6

Enzymatically crosslinked alginate-nanocellulose inks for 3D printing and tissue engineering scaffolds

Mohan T.[1], Zeller M.[1], Kargl R.[1], Stana Kleinschek K.[1]
[1]Institute of Chemistry and Technology of Biobased Systems, Graz University of Technology, Graz, Austria

Introduction

The incorporation of biopolymers in 3D printing, particularly polysaccharide based hydrogels, has significantly advanced tissue engineering and regenerative medicine. This work addresses the need for mechanically robust yet adaptable hydrogel scaffolds that can be crosslinked without the addition of external solutions, thereby improving print fidelity and processability for biomedical applications

Aim

This study aims to develop and characterize enzyme crosslinked 3D printed bioinks based on alginate tyramide (Alg-TA, see **Scheme 1**), nanofibrillated cellulose (NFC), glucose, and calcium carbonate ($CaCO_3$), using a dual enzyme system of glucose oxidase (GOx) and horseradish peroxidase (HRP) to achieve combined ionic and covalent crosslinking. The goal is to elucidate how crosslinking conditions influence mechanical performance, shape fidelity, and suitability of the resulting scaffolds for regenerative medicine applications.

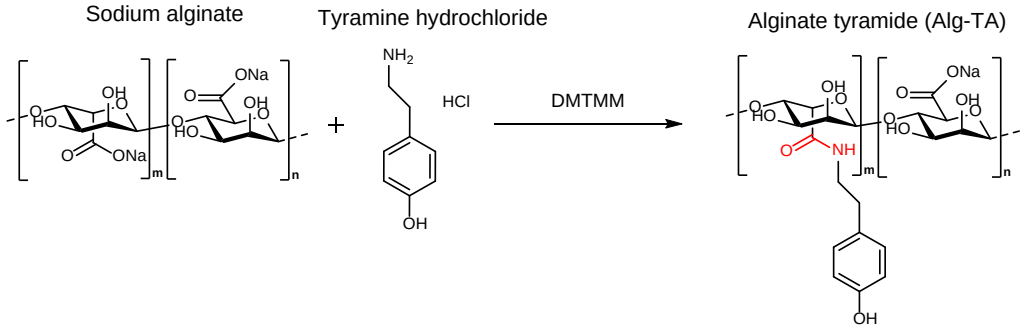

Scheme 1: Synthesis of alginate tyramide in aqueous condition.

Materials and Methods

Alginate was chemically modified to alginate tyramide (Alg-TA) and blended with NFC to formulate printable hydrogels containing glucose, $CaCO_3$, GOx, and HRP. In this dual enzyme system, GOx catalyzes in situ generation of H_2O_2 from glucose, which then drives HRP mediated covalent crosslinking of phenolic groups in Alg-TA, while $CaCO_3$ provides Ca^{2+} ions for ionic crosslinking. A systematic variation of pH, glucose and enzyme concentrations, $CaCO_3$ content, and atmospheric conditions was performed to study their influence on gelation, printability, and scaffold formation. 3D constructs were printed and mechanically tested in tension to determine tensile strength and elongation at break, and their shape fidelity and dimensional stability were qualitatively and quantitatively assessed after printing and incubation.

Results

The dual crosslinking strategy enabled solution free gelation, yielding 3D printed scaffolds with excellent shape fidelity, mechanical integrity, and dimensional stability. Scaffolds containing $CaCO_3$ exhibited a tensile strength of 0.13 ± 0.02 N/mm² and an elongation at break of 77 ± 4%, indicating high flexibility, whereas scaffolds without $CaCO_3$ showed higher tensile strength (0.26 ± 0.04 N/mm²) but reduced elongation (36 ± 3%), reflecting a stiffness–flexibility trade off governed by ionic crosslinking density. A detailed analysis of the crosslinking parameters revealed a complex interplay between pH, glucose and enzyme concentrations, and oxygen availability, which collectively controlled gelation kinetics, network architecture, and final scaffold performance.

Conclusion

The developed Alg TA/NFC bioinks, crosslinked via an in situ GOx/HRP driven covalent network combined with $CaCO_3$ mediated ionic crosslinking, offer a versatile platform for fabricating strong and adaptable 3D printed

hydrogel scaffolds. The tunable mechanical properties and high shape fidelity highlight their potential for tailoring constructs to specific tissue engineering and regenerative medicine applications.

S66
Bioinspired and biomimetic materials

S66 – K1
Collagen Rope Trick: Cell-Laden Collagen Fibre Assembly at Liquid Interfaces

Matsusaki M.
Graduate School of Engineering, The University of Osaka, Suita, Osaka, Japan

Fibrous tissues in mammals—including skeletal muscle, cardiac muscle, tendons, and nerves—exhibit hierarchical, centimeter-scale architectures composed of micrometer-scale, anisotropically aligned extracellular matrix (ECM) fibres and cells. Replicating these structures in vitro remains a longstanding challenge in bioengineering. An ideal scaffold should support diverse cell types, maintain stable cell–ECM interactions, and promote topographical alignment of adherent cells under cytocompatible conditions. Recently developed approaches include melt electrowriting of fibre bundles, twisting cell sheets, chemically crosslinking recombinant elastin, microfabrication techniques using microfluidics and filamented light patterning enabled the formation of cell-laden constructs. However, these strategies remain limited in scalability, precise cell–ECM alignment, cytocompatibility, and mechanical robustness, and cells typically attach only to material surfaces. These challenges highlight the need for new strategies to engineer hierarchical fibrous scaffolds that faithfully mimic native tissue architecture and functionality.
We recently developed a simple method to fabricate cell-laden viscous matrices by mixing collagen, heparin, and cells in Tris-HCl buffer (pH 7.4) for just 1 min, enabling the formation of three-dimensional (3D) cancer–stromal or hepatocyte tissue constructs[1,2]. Microscope observation of the resulting matrix in the absence of cells revealed micro- to millimeter-scale random fibrous structures. Based on this observation, we hypothesized that nanometer-scale collagen assembly could be accelerated through interactions with polyanions, as heparin is a typical strong polyelectrolyte. To test this, we optimized collagen and heparin concentrations, the composition of polyanion components, and the contact conditions between collagen and polyanions.
Here, we present a liquid–liquid interfacial spinning method to produce highly uniaxially aligned, centimeter-scale collagen fibres (**Fig. 1**). The dried fibres exhibit exceptional mechanical properties, with fracture strength of 280 MPa, Young's modulus of 6 GPa, and toughness of 17 MJ m^{-3}, comparable to spider silk and tendon collagens.
Incorporating living cells into the collagen solution yielded centimeter-scale, cell-laden aligned fibres, with densely adherent, uniaxially aligned cells and over 80% viability. Interfacial collagen assembly further enables fabrication of dimension-controlled constructs, like 2D sheets, 0D capsules, and 1D tubes, thus providing modular building blocks for centimeter-scale 3D tissues and organ-like structures. This approach offers a versatile platform to engineer mechanically robust, cell-laden tissues with controlled hierarchical architecture.

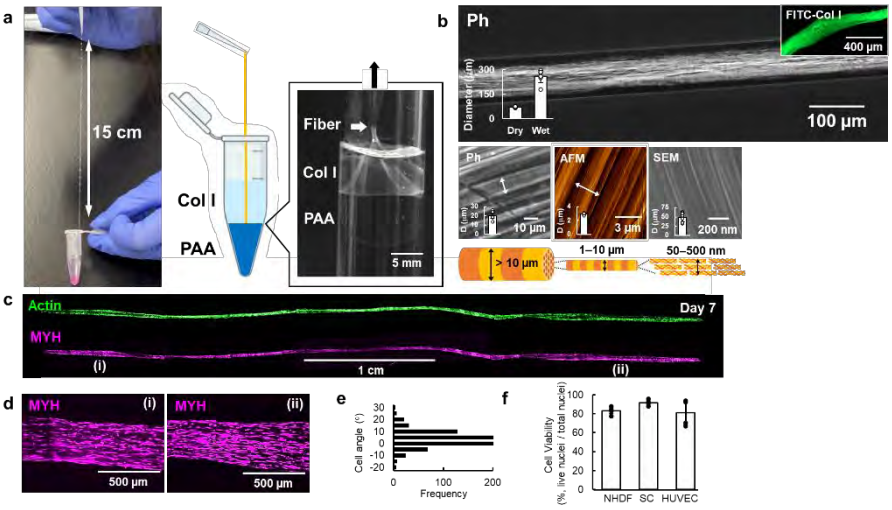

Fig. 1. Interfacial spinning process of collagen fibres. Photographs and microscope images of collagen fibres (a,b). Immunofluorescence images (c,d), cell alignment (e) and viability (f) of the obtained cell-laden fibres.

References

1. Takahashi, Y. *et al., Acta Biomaterialia* **183**, 111–129 (2024).
2. Naito, Y. *et al., Acta Biomaterialia* **140**, 275–288 (2022).

S66 – O1

Engineering the Spleen: Photocrosslinkable Hydrogels for Volumetric Bioprinting of a Red Pulp–Inspired 3D Microenvironment

Magalhães, MV[1,2], Bonhomme C[3], Florczack S[3], Araújo M[1], Sousa IV[1,2], Maia A[1], Levato R[3,4,*], Barrias CC[1,*]

[1]Institute for Research and Innovation in Health, Porto University, Porto, Portugal; [2]Faculty of Engineering, Porto University, Porto, Portugal; [3]Dept. Clinical Sciences, Faculty of Veterinary Medicine, Utrecht University, Utrecht, The Netherlands; [4]Dept.Orthopedics, University Medical Center Utrecht, Utrecht, The Netherlands
*Corresponding authors

Introduction

Abdominal trauma is frequent and often involves the spleen, one of the most injured organs. Although spleen-preserving strategies have improved, splenectomy remains common in severe injury being associated with lifelong risks, including overwhelming infection. Despite this clinical need, spleen bioengineering remains largely underexplored, with existing approaches relying on oversimplified scaffolds and poorly defined cellular mixtures, with limited translational potential. The splenic red pulp (RP, ~80% of the organ) is a unique microenvironment where fibroblasts, extracellular matrix (ECM), and vascular structures coordinate central blood-filtering and immune functions. Previous studies suggest that stromal compartments can guide organ regeneration by recruiting immune components upon transplantation, supporting the concept that a RP-like niche may restore essential splenic functions. However, current strategies fail to capture the multicellular organisation and structural complexity of the RP, underscoring the need for biomimetic scaffolds/cells combined with scalable biofabrication approaches capable of generating hierarchical, vascularised constructs.

Aim

To address this, we explored volumetric bioprinting (VBP) as a strategy to enable rapid fabrication of structurally complex constructs, developing VBP-compatible photocrosslinkable sdECM-based bioresins and incorporating spleen-derived vascular units (S-VUs) as building blocks to support stromal organisation and hierarchical microvascular self-assembly toward RP-like 3D-constructs.

Materials and Methods

Hydrogels were generated via visible-light di-tyrosine photocrosslinking. sdECM was combined with tyramine-modified gelatin (GEL-T) and/or alginate (ALG-T) to improve cell-matrix interactions and structural stability, respectively. Formulations were screened by varying composition/crosslinking conditions and characterised for sol-gel fraction/swelling/mechanical properties. For biocompatibility assessment, hydrogels were tested as matrices for human splenic fibroblasts (HSF) 3D-culture. Selected formulations were evaluated for VBP-printability. S-VUs were generated by co-assembling endothelial-colony-forming cells (ECFCs) with HSF and embedded within hydrogels to assess vascularized tissue formation.

Results

All formulations enabled rapid/homogeneous photocrosslinking (<30s) with adequate light penetration for VBP. Adding ALG-T consistently increased stiffness (~3.5-fold, compressive modulus) and slightly decreased hydrogel's sol-fraction/swelling, suggesting a more efficient crosslinking. sdECM/GEL-T hydrogels supported fibroblast spreading and multicellular network formation but exhibited pronounced contraction (Fig.1). Addition of ALG-T significantly reduced contraction, improved structural stability, while preserving cell compatibility. Selected sdECM/GEL-T/ALG-T formulations also supported VBP of 3D-constructs with defined architecture. S-VUs showed stable assembly, with optimal endothelial retention and angiogenic potential observed at 1:5 ECFC/HSF ratio (Fig.2). Upon hydrogel embedding, S-VUs formed capillary-like structures supported by fibroblast-rich networks, with variable organisation across formulations.

Conclusion

Photocrosslinkable sdECM-based hydrogels support HSF organisation and microvascular self-assembly from spleen VUs, establishing a VBP-compatible platform as a first step toward engineering RP-like tissue constructs.

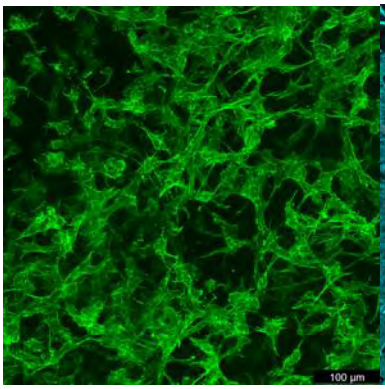

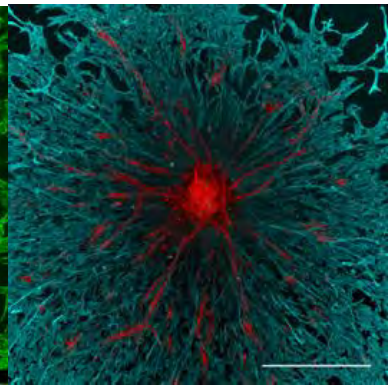

Figure 1(left). 3D culture of HSF within sdECM/GEL-T hydrogels after 7 days. **Figure 2(right).** S-VU culture within sdECM hydrogel after 7 days.

S66 – O2

From Quince Seeds to Osteo-Dental Regeneration: QSM/nHAp Scaffolds for Mandibular Repair

Yilmaz-Dagdeviren H.D.[1], Cetin Genc C.[2], Arslan Y.E.[3], Derkus B.[4], Deniz Y.[5], Degirmenci A[5]

[1]Dept. of Bioengineering, Faculty of Engineering, Izmir Institute of Technology, Izmir, Turkey; [2]Dept. of Oral and Maxillofacial Surgery, Faculty of Dentistry, Canakkale Onsekiz Mart University, Canakkale, Turkey; [3]Regenerative Biomaterials Laboratory, Dept. of Bioengineering, Canakkale Onsekiz Mart University, Canakkale, Turkey; [4]Stem Cell Research Laboratory, Dept. of Chemistry, Ankara University, Ankara, Turkey; [5]Dept. Of Oral and Maxillofacial Radiology, Faculty of Dentistry, Canakkale Onsekiz Mart University, Canakkale, Turkey;

Introduction

Complications associated with autografting procedures in maxillofacial regeneration have directed increasing attention toward tissue-engineered scaffolds as alternative therapeutic strategies. In this context, composite scaffolds designed to mimic the native extracellular matrix (ECM) have emerged as promising candidates for implantation[1,2]. In this study, the regenerative capacity of quince seed mucilage–nano hydroxyapatite (QSM/nHAp) composite scaffolds were investigated using a rabbit mandibular defect model. Previous *in vitro* studies demonstrated that the QSM/nHAp scaffold promotes cellular spheroid formation and supports osteogenic differentiation. Therefore, the introduction of this composite biomaterial into an *in vivo* model may provide a plant-based, sustainable, biocompatible, and regenerative scaffold for mandibular bone repair [1]. **The aim of this study** was to evaluate the *in vivo* bone regeneration potential of QSM/nHAp composite scaffolds in a rabbit mandibular defect model by assessing their capacity to support new bone formation, tissue integration, and overall healing performance within the defect site.

Materials and Methods

Following the water-based extraction of QSM, composite scaffolds were fabricated by incorporating nano-hydroxyapatite (nHAp) particles into the QSM polymer at a 1:1 (v/v) ratio. The resulting blend was subsequently crosslinked using EDC–NHS chemistry, lyophilized, and sterilized to obtain porous scaffolds. These scaffolds were then implanted into the right side of bilaterally created critical-sized mandibular defects in New Zealand rabbits (n = 36). Mini-plate fixation was applied to stabilize the defect area, support the surrounding tissue, and prevent further fracture propagation. Mandibular regeneration was evaluated using histochemical analyses and micro-computed tomography (µCT) imaging.

Results

According to the obtained results, all QSM/nHAp-implanted samples demonstrated favorable cellular infiltration without any signs of adverse immune or inflammatory reactions. The scaffolds exhibited gradual biodegradation over time, which facilitated the controlled release of nHAp particles and consequently enhanced the bone regeneration process within the defect area. Interestingly, a simultaneous development of both dental and bone tissues was observed in all QSM/nHAp-treated groups. The emergence of dental roots accompanied by de novo bone formation became clearly visible in µCT images as early as day 21, indicating the strong regenerative potential of the composite scaffold.

Conclusion

Overall, these findings highlight QSM/nHAp composite scaffolds as a sustainable plant-based biomaterial capable of simultaneously promoting bone and dental regeneration. Such scaffolds may represent a promising next-generation strategy for maxillofacial tissue engineering and osteo-dental regenerative therapies.

Acknowledgements

This study is financially supported from Çanakkale Onsekiz Mart University Scientific Research Projects Coordination Unit (Project ID: TSA-2022-4022).

References

1 Cetin Genc C., Yılmaz-Dagdeviren H.D., Deniz Y., Derkus B., Degirmenci A., Arslan Y.E. Unveiling bone and dental regeneration potential of quince seed mucilage-nanohydroxyapatite scaffolds in rabbit mandibles. Journal of Biomedical Materials Research Part B: Applied Biomaterials 2025; 113; e35570.
2 Cetin Genc C., Yilmaz H.D., Karaca B., Kiran F., Arslan Y.E. Nano-hydroxyapatite incorporated quince seed mucilage bioscaffolds for osteogenic differentiation of human adipose-derived mesenchymal stem cells. International Journal of Biological Macromolecules 2022; 195; 492–505.

S66 – O3

Recombinant spider silk-enriched alginate scaffolds for long-term bovine mesenchymal stem cell expansion

Cohen S[1], Rottenberg Fromm M[1], Sklan E[2], Tavor Re'em T[1],
[1]Dept. of Pharmaceutical Engineering, Azrieli College of Engineering, Jerusalem, Israel; [2]Seevix Material Sciences Ltd., Hadassah Ein-Karem Jerusalem, Israel

Introduction

Harnessing the potential of bovine mesenchymal stem cells (bMSCs) for cultured meat production requires the design of new scaffolds that support cell growth and tissue formation. Alginate, a biocompatible polysaccharide, is commonly used for scaffolding due to its biocompatibility and ability to mimic the extracellular matrix. However, it has limited mechanical properties, such as strength and stability. Recombinant spider silk biopolymer (SVX, Seevix) is biocompatible, highly porous, and has previously been shown to enhance alginate bioinks for cell bioprinting, due to its strength and elasticity. This study aims to develop edible, alginate-based scaffolds for cultured meat by incorporating SVX particles to enhance mechanical properties and cell functionality.

Materials and Methods

SVX particles were produced using an E. coli expression system (Seevix). bMSCs were evaluated in a stepwise platform progression including spontaneously formed spheroids, bioprinted ring-shaped constructs, bulk edible alginate hydrogels, and macroporous freeze-dried edible scaffolds. Bioprinting was performed using the Allevi 2 bioprinter. Scaffold mechanical properties were evaluated using a tensiometer, while cell viability was assessed using a CellTiter-Glo assay. Large-scale edible scaffolds with an approximate diameter of 5 cm were fabricated, and cell distribution was assessed by spatial biopsies.

Results

SVX supplementation (0.02%) supported viable bMSC spheroid formation, improved long-term viability in bioprinted ring constructs (Figure 1 A), and enhanced the mechanical performance of both research-grade and food-grade alginate hydrogels. In 1.5 cm-diameter freeze-dried macroporous scaffolds, cultured for 29 days, SVX-alginate demonstrated improved long-term cell viability (Figure 1 B-C). The large-scale edible scaffold remained culture-compatible for more than 31 days and achieved an approximately 19-fold expansion, with an estimated final yield of approximately 3.16 × 10^7 viable cells per scaffold based on five spatial biopsies used to assess uniformity.

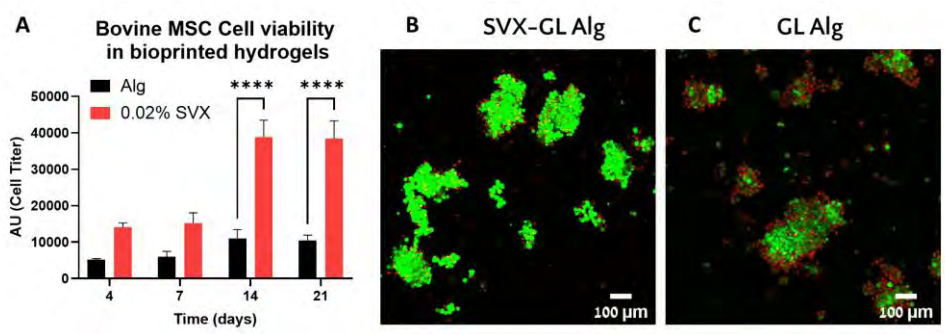

Figure 1: Enhanced bMSC cell viability in SVX-enriched alginate models in bioprinted models, assessed by CellTiter-Glo (A), and in SVX-enriched edible GL alginate macroporous scaffolds, by confocal live/dead imaging on day 29 (Calcein-AM – green; propidium iodide – red)

Conclusion

These findings identify SVX-alginate as an edible, mechanically reinforced scaffold strategy for prolonged bMSC culture across scales. By improving both handling robustness and long-term cell support, this platform addresses practical bottlenecks in scalable 3D cultivated-meat manufacturing and highlights recombinant spider-silk-like particles as promising functional additives for next-generation food biomaterials.

Acknowledgements

We thank Dr. Sharon Shelezinger, the Hebrew University of Jerusalem, for providing the bMSCs, and the Israeli Cultivated Meat Consortium, and the Azrieli College of Engineering, Jerusalem for their financial support.

S66 – O4

Nanostructured bioceramic surfaces potentiate antibiotic efficacy against *P. aeruginosa*

Grzelak J.[1,2,3], Iglesias-Fernández M.[1,2,3], Thompson T.P.[4], Biscaut C.[1,2], Ceccarelli L.[1,2], Gilmore B.F.[4], Ginebra M.P.[1,2,3]

[1]Biomaterials, Biomechanics and Tissue Engineering Group, Department of Materials Science and Engineering and Institute for Research and Innovation in Health (IRIS), Universitat Politècnica de Catalunya – BarcelonaTech, Barcelona, Spain; [2]Barcelona Research Centre in Multiscale Science and Engineering, Universitat Politècnica de Catalunya · BarcelonaTech, Barcelona, Spain; [3]Centro de Investigación Biomédica en Red de Bioingeniería, Biomateriales y Nanomedicina (CIBER-BBN), Instituto de Salud Carlos III, Spain; [4]Biofilm Research Group, School of Pharmacy, Queen's University Belfast, Medical Biology Centre, Belfast, UK.

Introduction

Bone grafting materials, which may be derived from natural sources or engineered synthetically, are designed to treat bone defects, restoring both the structural and functional integrity of the affected bone. However, infections at the surgical site can compromise bone regeneration and lead to graft failure.

Nanotopographies, inspired by the surface of cicada wings, have shown strong bactericidal properties by mechanical rupture of bacterial envelope. Recently we have reported the synthesis of nanotopographies on calcium-deficient hydroxyapatite (CDHA), a bioactive ceramic with composition and structure closely mimicking natural bone mineral and highly relevant in the field of bone regeneration.

The objective of this work was to determine the capacity of nanostructured CDHA surfaces to potentiate the activity of commonly used antibiotics against *Pseudomonas aeruginosa*, a highly adaptable opportunistic pathogen frequently responsible for bone infections.

Materials and Methods

Calcium phosphate nanotopographies (Fig. 1A) were formed by the hydrolysis of α-tricalcium phosphate (α-TCP) to CDHA. α-TCP discs were immersed in distilled water at 60 °C for 60 h. Flat discs used as control were fabricated by compacting CDHA powder. The material was characterized by XRD and SEM. Flat and nanostructured discs were then incubated with *P. aeruginosa* (NCIMB 10548) inocula in Mueller-Hinton broth with increasing concentrations of antibiotic (gentamicin or meropenem). The synergistic effect of antibiotic and nanotopography on bacteria viability and vitality was studied by optical density measurements, CFU counting, confocal microscopy, SEM, as well as PrestoBlue and BacTiter-Glo assays.

Results

We observed a decrease of Minimum Inhibitory Concentration for bacteria incubated on nanostructured surfaces compared to flat surfaces, as indicated by a decrease in viability (Fig. 1C) and metabolic activity (Fig. 1D). Bacteria with disrupted membranes were observed on nanotopographies at all antibiotic concentrations, while on flat surfaces only the highest concentrations induced damage (Fig. 1B).

Conclusion

Our work establishes that nanostructured bioceramic surfaces can potentiate antibiotic efficacy, offering a potent synergistic strategy against *P. aeruginosa* infections. By lowering the threshold for bacterial eradication, these surfaces facilitate a reduction in clinical antibiotic loads, potentially mitigating side effects and resistance while providing a bioactive scaffold for bone regeneration.

Acknowledgements

This work was financially supported by the European Union - ERC grant (BAMBBI; 101055053, doi: 10.3030/101055053). The research group is part of Maria de Maeztu Units of Excellence Programme CEX2023-001300-M/funded by MCIN/AEI/10.13039/501100011033, Spanish Ministry of Science and Innovation.

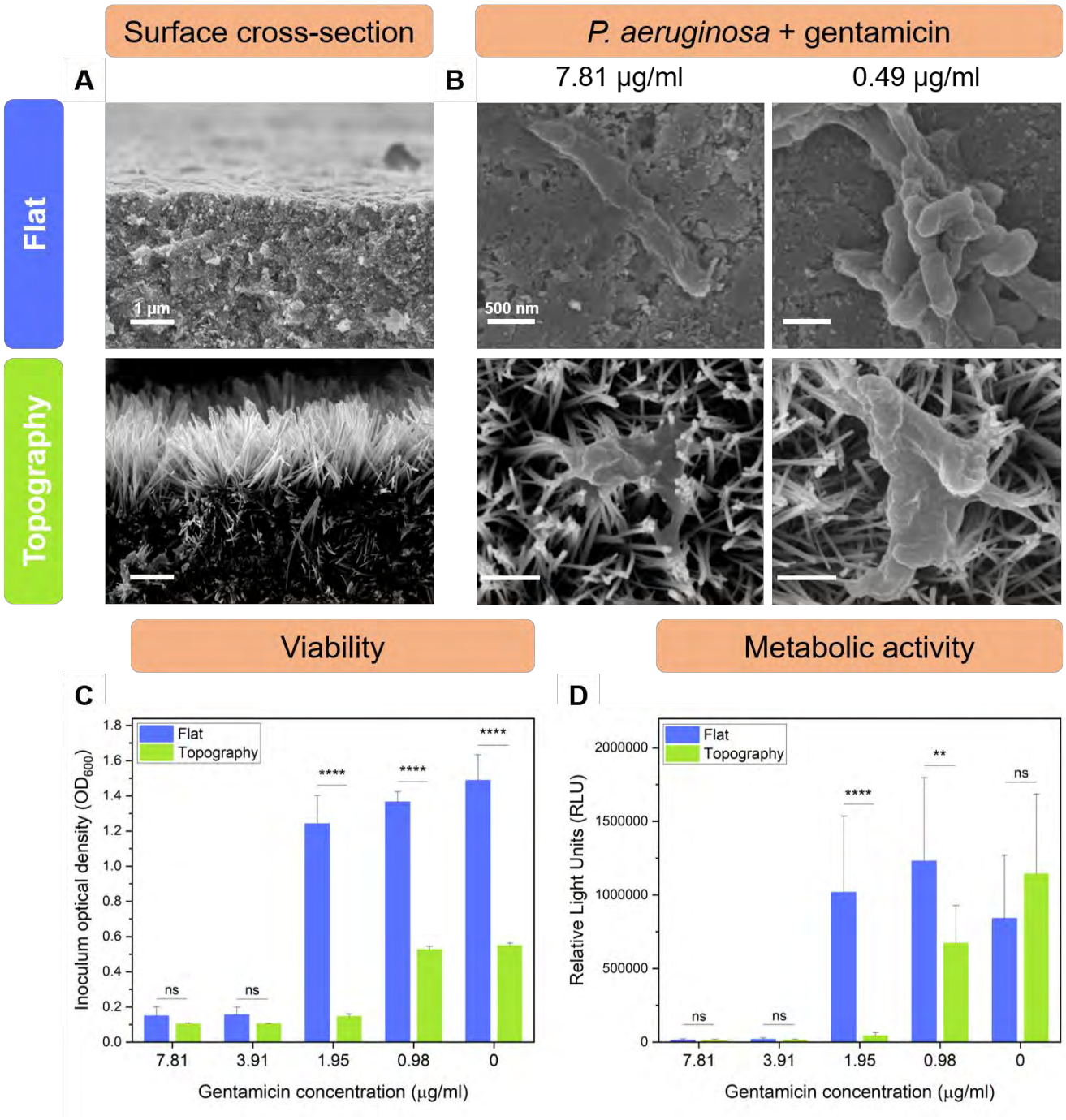

Figure 2. A) SEM cross-section images of flat and nanostructured CDHA surfaces. B) SEM micrographs showing P. aeruginosa *incubated on flat and nanostructured samples with two distinct concentrations of gentamicin at 16 h. C) Optical density of* P. aeruginosa *inocula collected from the flat and nanostructured CDHA surfaces with varying concentrations of gentamicin after 16 h of incubation. Statistical significance was considered at $p < 0.05$. D) Metabolic activity of* P. aeruginosa *incubated on flat and nanostructured CDHA surfaces with gentamicin at 16 h, measured using BacTiter-Glo assay. Statistical significance was considered at $p < 0.05$.*

S66 – O5

Bio-Mechano-Compatible Electrospun Scaffold as External Support to Prevent Autograft Dilatation in the Ross Procedure

Reis, M. S.[1,2], Rosadas, M.[1], Ho, C. I.[1], Pazmino, C. A.[1], Costa, J. B.[1], Vervenne, T.[2], Mignon, A.[2], Oliveira, A. L.[1], Ribeiro, V. P[1]

[1]*Universidade Católica Portuguesa, CBQF - Centro de Biotecnologia e Química Fina – Laboratório Associado, Escola Superior de Biotecnologia, Rua Diogo Botelho 1327, 4169-005 Porto, Portugal*
[2]*Smart Polymeric Biomaterials Research Group – Department of Materials Engineering, Campus Group T, KU Leuven, Belgium*

Introduction

The Ross procedure is a surgical intervention that replaces a diseased aortic valve with the patient's own pulmonary valve [1]. Despite its advantages, associated with the adaptative growth and biocompatibility, the dilatation of the autograft due to high systemic pressure remains a concern [1]. This study aims at producing a scaffold to prevent autograft dilatation combining mechanical resilience and controlled biodegradability with bioactive cues to improve biocompatibility, avoiding the low-porosity and stiffness of the current solutions.

Materials and Methods

Tubular scaffolds of 2.5 mm inner diameter were electrospun using PCL (Mn ≈ 81.6 kg/mol), bovine elastin, and porcine aortic decellularized extracellular matrix (dECM) (19:0.5:0.5 w/v% ratio) (Fig. 1A). The results were compared to PCL and PCL:Elastin without dECM. Characterization included scanning electron microscopy (SEM) morphology, tensile testing, swelling, and accelerated hydrolytic degradation (0.2M NaOH). Cytocompatibility was assessed via conditioned medium and direct human dermal fibroblast (hDF) seeding on the tube lumen. Metabolic activity and DNA were quantified, while cellular morphology and attachment were visualized using SEM and 4',6-diamidino-2-phenylindole (DAPI) staining.

Results

The incorporation of elastin and dECM into the scaffold provided consistent fibers ($1 - 2\ \mu m$) (Fig. 1B) leading to a reduction in the stiffness, as compared to pure PCL. Under physiological pressures, The tri-blend scaffold withstood failure, exhibiting supraphysiological burst pressures (Fig. 1C). Physicochemical analysis showed minimal swelling after 24h (3 ± 3%) and controlled weight loss, demonstrating superior structural stability compared to the faster degradation of PCL and PCL:elastin (Fig. 1D). *In vitro*, live/dead staining showed no harmful byproducts released by the tri-blend scaffolds, with hDFs maintaining a healthy phenotype (Fig. 1E), confirmed by cytocompatibility levels over 95% after 72h (Fig. 1F). Direct contact studies demonstrated successful scaffold colonization, with the tri-blend supporting robust hDF adhesion, viability, and proliferation over 14 days (Fig. 1G).

Conclusion

PCL:Elastin:dECM electrospun scaffolds balanced mechanical reinforcement with biological functionality, avoiding the excessive rigidity of pure synthetic polymers. The blend promoted robust hDF adhesion and proliferation on the tube lumen. Since fibroblasts dominate the aortic adventitial layer, the interface for external supports, this bioactive scaffold offers a promising strategy for reinforcing pulmonary autografts in the Ross procedure.

Acknowledgements

BE@T – Bioeconomia para Têxtil e Vestuário, investimento TC-C12-i01 – Bioeconomia Sustentável" – Programa de Recuperação e Resiliência (PRR). Project IBEROS+ (0072_IBEROS_MAIS_1_E)-Instituto de Biofabricación en Red para El Envejecimiento Saludable, funded by "Interreg VI A España – Portugal (POCTEP) 2021-2027. Fundação para a Ciência e Tecnologia (FCT) contract 2023.07374.CEECIND and scholarship 2025.04247.BDANA.

References

[1]Chauvette, Vincent et al. A review of pulmonary autograft external support in the Ross procedure. Expert Rev Med Devices. (2019)

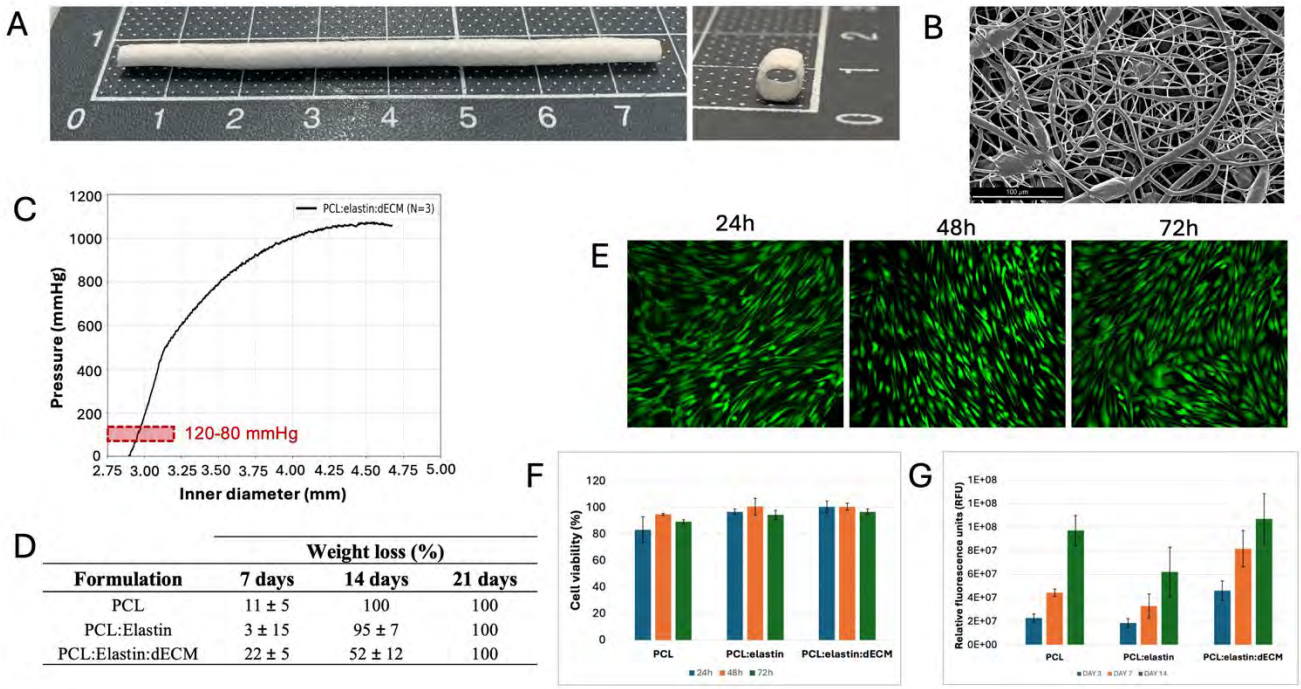

D

	Weight loss (%)		
Formulation	**7 days**	**14 days**	**21 days**
PCL	11 ± 5	100	100
PCL:Elastin	3 ± 15	95 ± 7	100
PCL:Elastin:dECM	22 ± 5	52 ± 12	100

Figure 1 – A. Electrospun tubular structure; B.SEM micrograph of the inner surface of the PCL:Elastin:dECM scaffold; C. Pressure-diameter curve of the PCL:Elastin:dECM scaffold; D. Weight loss percentage of PCL, PCL:Elastin and PCL:Elastin:dECM scaffolds during accelerated hydrolytic degradation. E. Live/Dead fluorescence microscopy of hDFs after 72h exposure to PCL:Elastin:dECM scaffold leachates; F. Cell viability of hDFs after 72h exposure to different scaffold leachates; G. Metabolic activity of hDFs seeded in the different scaffolds after 14 days of culture.

S66 – O6

Elastin-Like Polypeptide Extracellular Matrix Mimics for Artificial Skin Models

Rodriguez M.,1 Belaidi J-P.,2 Garanger E.1 and Lecommandoux S. 1

1 Univ. Bordeaux, CNRS, Bordeaux INP, LCPO, UMR 5629, Pessac F-33600, France
2 L'Oréal Recherche Avancée, 93600 Aulnay-sous-Bois, France

Introduction

Artificial skin models have emerged in the late 20th century to meet the need for ethical and reproducible alternatives to animal testing. Initially developed for wound healing and burn treatment, they have evolved into sophisticated three-dimensional systems that mimic the structure and function of human skin.[1] A wide range of biomaterials has been explored to reconstruct the extracellular matrix (ECM) of human skin. Natural polymers like collagen and hyaluronic acid, as well as synthetic ones such as poly(ethylene glycol), are commonly used in tissue engineering. However, they present limitations in reproducing the complexity of a stable and biocompatible ECM. Recently, biomimetic systems based on recombinant macromolecules, including elastin-like polypeptides (ELPs), have been developed to optimize biological functionality and mechanical performance. [2] ELPs are promising biocompatible, protein-like polymers because their sequences and molar mass can be precisely controlled using recombinant DNA and protein engineering approaches. ELPs are derived from the hydrophobic domain of elastin, a key ECM protein that provides resilience and elasticity to different tissues including skin, making them very attractive in tissue engineering applications.[3]

Materials and Methods

In this work, we used a universal polypeptide backbone with the exact protein sequence MW[VPGVGVPGMG(VPGVG)$_2$]$_{20}$, which was chemically modified onto methionine residues' side chain to incorporate acrylate functions.[4] The latter were subsequently reacted with thiol containing groups to introduce the cell adhesion peptide GRGDS and phenol groups that were used to enzymatically cross-link polypeptide chains as depicted in the *Figure*.

Results

NMR analyses evidenced the efficient grafting of acrylate functions onto the ELP as well as the incorporation of GRGDS and phenol groups. The remaining acrylate functions were neutralized into carboxylic groups. The final ELP[M(*GRGDS-phenol*)$_1$V$_3$-80] was found to be biocompatible as assessed by cytotoxicity assays at 5 mg/mL on HDFs. Physico-chemical and mechanical properties of the hydrogel were measured by different techniques (*e.g.*, rheology, microscopy) and the viability of HDFs in 3D culture was monitored over one week to assess the biocompatibility of this new hydrogel.

Conclusion

/The present work proposes a new biomaterial based on bioactive ELPs that can be crosslinked in mild conditions to form a hydrogel for ECM mimics applications.

References

[1] Quizel, C. *et al. Journal of Investigative Dermatology*. **2024,** *144*, 2650
[2] Rodríguez-Cabello, J C. *et al. Adv. Funct. Mater.* **2020**, *30*, 1909050
[3] Garanger, E., Lecommandoux, S. *Adv. Drug Deliv. Rev.* **2022**, *191*, 114589
[4] Dai, M. *et al. Biomacromolecules.* **2021,** *22,* 4956

S67
Biomaterial responses in a pathological environment

S67 – K1
Bioprinted interfacial complex constructs for advanced healthcare applications

Chatzinikolaidou M.[1,2]
[1]Dept. Materials Science and Engineering, Heraklion, Greece; [2]Foundation for Research and Technology Hellas (FORTH), Heraklion, Greece

This paper reports on the biofabrication of functional, mechanoactive composite bioinks with encapsulated living cells (bone, adipose and Wharton jelly derived mesenchymal stem cells) via extrusion bioprinting for interfacial tissue engineering including vascularized bone and osteochondral grafts. We report on the design and fabrication of bioinks containing an elastic, extrudable polymeric network matrix comprising biomimetic biomaterials including gelatin, elastin, gellan gum, methylcellulose combined with inorganic osteoinductive materials such as nanohydroxyapatite, functionalized bioactive glass, and laponite.

The developed hydrogel-based inks were examined for their printability, rheological properties, thermal behavior, crystallinity, water uptake and degradation rate. The cell-containing constructs were assessed biologically in vitro for their osteogenic, osteoclastogenic, angiogenic and chondrogenic capacity, as well as for their antibacterial activity. The multifunctional bioprinted constructs indicate printing accuracy values of up to 75%, with the composite bioinks being higher. The bioinks demonstrate excellent capability regarding extrusion printability at extrusion pressures of 30-100 kPa, favoring high cell survival rates. Rheological analysis of the bioinks reveals >90% viscosity recovery. The gene expression of relevant osteogenic, osteoclastogenic, angiogenic and chondrogenic markers, as well as the biochemical markers and the extracellular matrix collagen and glycosaminoglycans were significantly elevated in the composite bioinks. Mechanical stimulation of the cell-encapsulated constructs by means of a bioreactor demonstrated significantly increased cell activity, particularly towards osteogenesis, angiogenesis and antiosteoclastogenesis. The bioprinted constructs were implanted in a subcutaneous mouse model for two weeks, indicating the absence of adverse immunological reactions.

S67 – O1

In situ targeted electrode formation based on enzymatic polymerization fueled by altered metabolic pathways in epileptic brain microenvironment

De Roos F.[1,2], Cornuéjols R.[2], Vergaelen M.[1], K.C. D.[3], Drakopoulou S.[3], Abrahamsson T.[2], Simon D.[2], Berggren M.[2], Spyropoulos G.[3], Uguz I.[4], Raedt R.[1], Strakosas X.[2]
1 4BRAIN, Dept. of Head and Skin, Ghent University, Ghent, Belgium, [2] Laboratory of Organic Electronics, Dept. of Science and Technology, Linköping University, Norrköping, Sweden, [3] Dept. of Information Technology, Ghent University, Ghent, Belgium, [4] Dept. of Biomedical Engineering, Stevens Institute of Technology, Hoboken, New Jersey, United States

Introduction

Epilepsy affects over 60 million people worldwide, and one-third of patients suffer from drug-resistant epilepsy. Deep brain stimulation (DBS) provides an alternative therapy but often fails due to mechanical mismatch between rigid electrodes and soft brain tissue. Moreover, current pre-fabricated implants cannot adapt to the dynamic biochemical environment of the epileptic brain. We present a glucose-responsive hydrogel precursor that polymerizes *in situ* into soft, organic conductive electrodes in hyperexcitable conditions, characterized by increased extracellular glucose. This formulation integrates glucose oxidase (GOx) and horseradish peroxidase (HRP) with an EDOT/thiophene-based monomer (ETE-COONa), leveraging the elevated glucose levels occurring during epileptic activity to drive localized oxidative polymerization. The resulting electrodes are electrically conductive, biodegradable, and naturally cleared over time, thus minimizing chronic tissue response while enabling adaptive and reversible neural interfacing.

Materials and Methods

Five hydrogel matrices (GelMA, PVA, gelatin, HA, alginate) were compared using GOx/HRP systems triggered by physiological vs elevated glucose concentrations. Upon polymerization, the ETE-COONa monomer exhibits blue coloration, indicating polymer formation. Hydrogel precursor formulations were systematically optimized by varying GOx, HRP, and ETE-COONa concentrations to maximize conductivity contrast between high- and low-glucose conditions. This electrochemical characterization was done using current-voltage (I-V) measurements and electrochemical impedance spectroscopy (EIS).

Results

Alginate was selected for its optimal polymerization response and dual responsiveness to both glucose and elevated calcium levels observed during seizures. Optimized alginate-GOx/HRP formulation (1% alginate, GOx 180U/mL, HRP 360U/mL, ETE-COONa 48mg/mL) demonstrated robust selectivity for elevated glucose levels. Visual assessment showed minimal blue coloration under normal glucose conditions versus intense polymerization under epileptic-like conditions. Current-voltage measurements showed a 26-fold conductivity contrast after 60 min (210 µA high glucose vs. 8 µA low glucose). Electrochemical impedance spectroscopy confirmed time-dependent impedance reduction only in high-glucose conditions, indicating progressive conductive polymer network formation at the electrode interface, while low-glucose controls remained stable and non-conductive.

Conclusion

This glucose-responsive alginate hydrogel enables intrinsic, site-specific electrode formation triggered by elevation of glucose levels, typical for seizure conditions. The soft, biodegradable material minimizes foreign body response while supporting electrical stimulation, representing a major advantage towards closed-loop, adaptive DBS for drug-resistant epilepsy.

Acknowledgements

This work was supported by internal funding from the BOF (Bijzondere Onderzoeks-Fonds) at Ghent University.

S67 – O2

A mechano-modulatory 3D hydrogel platform to dissect fibroblast fate and matrix remodelling in skin fibrosis

Presa R[1,2], Granja L P[1], Chaudhuri O[3], Pereira R F[1,2]
[1]Instituto de Investigação e Inovação em Saúde, Porto, Portugal, [2]Instituto Ciências Biomédicas Abel Salazar, Porto, Portugal, [3] Dept. of Mechanical Engineering, Stanford, USA

Introduction

Fibrosis is characterized by excessive extracellular matrix (ECM) deposition, persistent fibroblast activation and progressive tissue stiffening. In the skin, it often arises after burns or surgical injury, leading to replacement of healthy tissue by pathological ECM. Despite its clinical impact, antifibrotic drug discovery still relies on animal models that poorly recapitulate human pathophysiology and in vitro systems that fail to reproduce key features of the fibrotic niche. Fibroblasts integrate biochemical signals such as transforming growth factor-β (TGF-β) with biophysical cues from matrix mechanics, yet most current models rely on 2D substrates or 3D hydrogels with limited mechanical control, leading to inaccurate fibroblast responses and high failure rates in clinical trials.

Aim

The goal of this work was to engineer a patient-informed, mechano-modulatory 3D hydrogel platform recapitulating ECM mechanical changes during skin fibrosis to uncover how mechanical and biochemical signals regulate fibroblast activation and ECM remodelling.

Materials and Methods

Mechanically tuneable hydrogels were developed using an RGD-containing pectin-derived macromer by combining ionic gelation and Diels–Alder chemistry to control network architecture. Hydrogels' mechanical properties were assessed by rheology. Healthy primary human dermal neonatal fibroblasts were encapsulated (10 M cells/mL) within hydrogels and cultured under either basal conditions or TGF-β1 (10 ng/mL) stimulation for 14 days. Cell behaviour and ECM composition were assessed by confocal microscopy and proteomic analysis, respectively.

Results

Double-crosslinked hydrogels were optimized to match the stiffness of healthy (G' = 1.9 ± 0.2 kPa) and fibrotic-like (G' = 5.0 ± 0.7 kPa) human skin. Over 14 days, fibroblasts remained viable and proliferative within the gels and progressively formed dense, interconnected cellular networks. Moreover, cells displayed comparable spreading and morphology regardless the stiffness, suggesting robust adaptation to the 3D environment. Notably, proteomic analysis revealed that while TGF-β1 induced a fibrotic programme in both soft and stiff hydrogels, stiff gels amplified and diversified this response by upregulating ECM, metabolic, and mechanosensitive proteins.

Conclusion

The developed mechano-modulatory 3D hydrogel provides a human-relevant platform for modelling skin fibrosis and studying how dermal fibroblasts integrate biochemical and mechanical signals in 3D. Using this system, we uncovered a synergistic interplay between matrix mechanics and biochemical cues that amplifies fibroblast activation and ECM remodelling. Overall, our findings contribute to develop more physiologically relevant in vitro models for fibrosis research and therapeutic screening.

Acknowledgements

This work was supported by projects 2022.06048.PTDC and 2024.16796.PEX, and the fellowship 2022.13383.BD funded by the Portuguese Foundation for Science and Technology.

S67 – O3

Tunable gelatin-chitosan hydrogels for lymph node-inspired 3D models in cancer immunotherapy

Fajardo-García A[1,2,3], Guasch J[3], Garcia-Torres J[1,2,4]
[1]Dept. of Materials Science and Engineering and Institute for Research and Innovation in Health, Universitat Politècnica de Catalunya-BarcelonaTech, Barcelona, Spain, [2]Barcelona Research Center in Multiscale Science and Engineering, Universitat Politècnica de Catalunya-BarcelonaTech, Barcelona, Spain, [3]Institute of Materials Science of Barcelona (ICMAB-CSIC), Barcelona, Spain, [4]Centro de Investigación Biomédica en Red de Bioingeniería, Biomateriales y Nanomedicina (CIBER-BBN), Instituto de Salud Carlos III, Madrid, Spain

Introduction

Cancer remains one of the leading causes of death worldwide, and its progression and response to therapy are strongly influenced by the tumor microenvironment (TME), a dynamic milieu comprising cancer cells, stromal cells, immune cells and extracellular matrix (ECM). However, conventional in vitro models poorly reproduce the three-dimensional and biomechanical complexity of native tissues. In this context, lymph node-inspired hydrogels are promising platforms for physiologically relevant 3D models to study immune-related processes and evaluate immunotherapeutic strategies. Among natural polymers, gelatin and chitosan are attractive candidates due to their biocompatibility and biodegradability, with gelatin providing cell-adhesive motifs and chitosan contributing structural tunability.

Aim. This work aims to engineer and optimize gelatin-chitosan hydrogels with tunable properties to mimic lymph node-like microenvironments, with the final goal of generating 3D platforms for the study of cancer immunotherapy.

Materials and Methods

Gelatin-chitosan hydrogels were prepared by dissolving gelatin in deionized water and chitosan in 1% v/v acetic acid, followed by mixing, casting in a Petri dish, cooling overnight at -4 °C, and immersion in NaOH. Gelatin gelation was temperature-induced, while chitosan gelation occurred via pH change. Different chitosan:gelatin precursor concentrations (2.0:2.7, 2.75:3.71, and 3.5:4.73 % w/v) and NaOH concentrations (0.25, 0.75, and 2 M) were investigated. Hydrogel morphology, chemistry, porosity and pore interconnectivity were assessed by environmental scanning electron microscopy (ESEM), Fourier transform infrared spectroscopy (FTIR) and micro-computed tomography (micro-CT). Swelling and biodegradation tests were conducted as part of the initial physicochemical characterization, while mechanical properties were assessed through compression testing. Cellular responses were studied by confocal microscopy and flow cytometry.

Results

The resulting hydrogels exhibited composition-dependent physicochemical and mechanical properties. Swelling assays in deionized water, PBS, and complete RPMI medium (RPMI + 10% FBS + 1% P/S) showed reduced water uptake with increasing biopolymer content, while NaOH concentration had the strongest influence, significantly reducing swelling in all media. Compression testing revealed that higher polymer content increased hydrogel stiffness, whereas increasing NaOH concentration within a given formulation decreased stiffness and promoted a more elastic-like response. Young's modulus values ranged from 4.91 to 20.9 kPa, placing these hydrogels within a mechanically relevant range for lymph node-mimicking applications. Preliminary results suggest that cell behavior can be influenced by the physicochemical and mechanical properties of the hydrogels.

Conclusion

These results show that gelatin-chitosan hydrogels provide physicochemical and mechanical properties within the relevant range of lymph node tissues, therefore representing promising candidates for the development of lymph node-inspired 3D microenvironments to study tumor–immune interactions and support evaluation of emerging immunotherapeutic strategies.

Acknowledgements

Authors acknowledge funding from MCIU/AEI /10.13039/501100011033 / FEDER, UE (CNS2022-136109, CNS2023-144236, PID2022-141120OB-I00, PID2024-159041OB-I00, CEX2023-001300-M, and CEX2023-001263-S) and Agència de Gestió d'Ajuts Universitaris i de Recerca de Catalunya (AGAUR) (2021-SGR-01368) for financial support.

S67 – O4

An infection-responsive collagen-based wet-spun textile fibre for wound monitoring

Gorman, J[1,2], Brooker, C[1,2], Li, X[1], Tronci, G[1,2]
[1]Clothworkers Centre for Textile Materials Innovation for Healthcare (CCTMIH), Leeds Institute of Textiles and Colour (LITAC), University of Leeds, United Kingdom, [2]Division of Oral Biology, St. James's University Hospital, School of Dentistry, University of Leeds, United Kingdom

Introduction

Commercial wound dressings are made from textile fibres due to their inherent flexibility and mechanical strength; by embedding responsive elements directly into fibres, smart textiles can provide real-time feedback on wound status while maintaining breathability and a close interface with the wound bed. However, current wound monitoring strategies still rely on specialist imaging software or an algorithm, which is costly, time-consuming and which requires patient visit at the clinic. With the unsustainable costs associated with wound care globally, there is an urgent need for simple, cost-effective, smart wound dressings enabling remote wound monitoring. One biomarker of wound infection is the pH, whereby healthy skin exhibits an acidic environment (pH £6), whereas infected wounds exhibit a raise in pH in the alkaline region (pH>7). We hypothesised that this infection associated pH shift could be leveraged to achieve textile wound dressings with pH-responsive colour change enabling visual warning of wound infection. Bromothymol Blue (BTB) was employed as commercially available halochromic dye that shifts colour from yellow to blue upon contact with solutions of increasing alkalinity.

Materials and Methods

Rat tail collagen functionalised with 4-vinyl benzyl chloride (4VBC) was wet spun into fibres and then UV cured to produce 4VBC* fibres for use as building block of wound dressings Fig.1). Fibres were gravimetrically loaded via drop casting a known amount of BTB onto dehydrated wet spun fibres. Release profiles in pH 5 and pH 8 were measured via UV-Vis spectroscopy to represent healthy and infected wounds, respectively. Degradation of 4VBC* fibres in a collagenase rich media (pH 7.4, 37°C, 2 CDU) was recorded by measuring the relative mass (wt.%) of dry fibres collected after 24, 48 and 72 hours of enzymatic incubation with respect to the initial dry mass. Tensile tests were performed on hydrated individual fibres (5 N load cell, Instron 5544, Massachusetts, USA).

Results

4VBC* collagen fibres exhibited a loading efficiency of 99±3 wt.% together with high retention of BTB (88 wt.%) after 48-hr incubation in acidic environments. The dry fibres demonstrated controlled swelling in aqueous environments (up to 5-fold increase in weight), remarkable wet-state Ultimate Tensile Strength (UTS: 12±3— 15±7 MPa), and up to ~30 wt.% mass retention after 24 hours in a collagenase-rich buffer.

Conclusion

Fibres demonstrated mechanical integrity in hydrated states, whilst maintaining the ability to degrade in the presence of collagenase, allowing for varying wound healing applications such as woven dressings and resorbable sutures. Fibres also successfully displayed a rapid, reversible, visual colour change under acidic and basic conditions displaying their effective capabilities of signalling wound infection without the need for specialist equipment or algorithm.

Acknowledgements

The authors gratefully acknowledge financial support from the Clothworkers' Company, LITAC and the Institution of Mechanical Engineers (through IMechE Whitworth Senior Scholarship Award to JG).

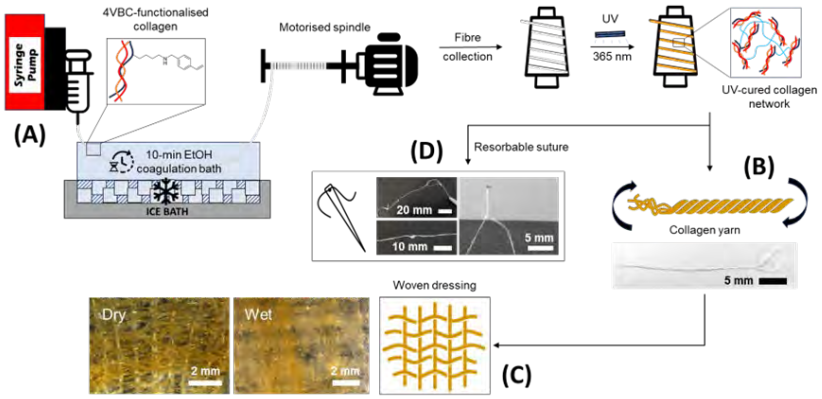

Figure 1. Schematic of wet spinning apparatus and production of functionalised collagen fibres into either woven dressings or resorbable sutures.

S67 – O5

Chitosan and citric acid – cyclodextrin polymer hydrogel for drug delivery: relationship between rheological characteristics and release properties

Chijcheapaza-Flores H [1,2], Tabary N [2], Cazaux F [2], Staelens JN [2], Blanchemain N [1], Nicot R [1,3], Garcia Fernández MJ [1], Martel B [2]

[1] University of Lille, INSERM, U1365 - Advanced Drug Delivery Systems, France, [2] University of Lille, CNRS, INRAE, Centrale Lille, UMR 8207 – UMET – Unité Matériaux et transformations, France, [3] University of Lille, CHU Lille, Dept. of Oral and Maxillofacial Surgery, France

Introduction

Hydrogels are widely used in drug delivery and tissue engineering due to their capacity to mimic the extracellular matrix and enable the controlled release of active pharmaceutical ingredients (API). Chitosan (CHT) is one of the most commonly used cationic polymers for hydrogel preparation and can be combined with a wide range of anionic polymers, such as a citric acid polymer of cyclodextrin developed by Martel *et al.* (1), which can form host-guest complexes with APIs.

Aim. This study investigates the relationship between the rheological properties of CHT/PCD hydrogels, including their soluble and insoluble fractions, and the release of sodium naproxen from these systems to clarify how CHT and PCD contribute to viscoelastic behavior and drug release properties.

Materials and Methods

Powder mixes without the API were prepared by mixing CHT (Sigma Aldrich, 80% DDA, high molecular weight) with soluble PCD (PCDs) or insoluble PCD (PCDi) using a Mixer Mill MM400 (Retsch®). The API-loaded mix was obtained by prior wet granulation of PCDs/PCDi with NaNX (Thermo Fisher, 1% w/w). CH/PCDs/PCDi hydrogels were formed using an interconnected syringe system (Figure 1), as previously described by Chijcheapaza-Flores *et al*. (2). The formulations were initially screened by assessing the viscoelastic properties of several CHT/PCDs and CHT/PCDs/PCDi concentrations using an HR 10 rheometer (TA Instruments). In the second stage, the formation of the cyclodextrin (CD)/NaNX inclusion complex using PCD was confirmed by ^{1}H NMR, and NaNX release was assessed using a USP I dissolution apparatus (Agilent) in PBS at 37 °C and 50 rpm.

Results

The results indicate that PCDs have a greater impact than PCDi on the viscoelastic properties of the CHT/PCDs/PCDi hydrogels. In contrast, when PCDi was present, no significant difference in viscoelastic properties was observed ($p<0.05$). The release kinetics study showed that CHT/PCDs slowed the release of NaNX compared with the CHT solution and hyaluronic acid (HA), which is commonly used in intra-articular medical devices. Finally, the formulations containing PCDi showed only partial release of NaNX.

Conclusion

In conclusion, for a fixed concentration, an increasing PCDs concentration exhibited an increased hydrogel elasticity and slowed down the NaNX release, while PCDi retained NaNX inside the hydrogel. These findings could be attributed to the trapping of NaNX within the PCDi network (highly crosslinked).

Acknowledgements

This project was funded by the French National Research Association (ANR, JCJC contract) under the code ANR-21-CE19-0012 CHITOGEL.

References

1. Martel B et al. J Appl Polym Sci (2005) 97:433–442. doi:10.1002/app.21391
2. Chijcheapaza-Flores et al., Gels (2023) 9(3):262. doi:10.3390/gels9030262

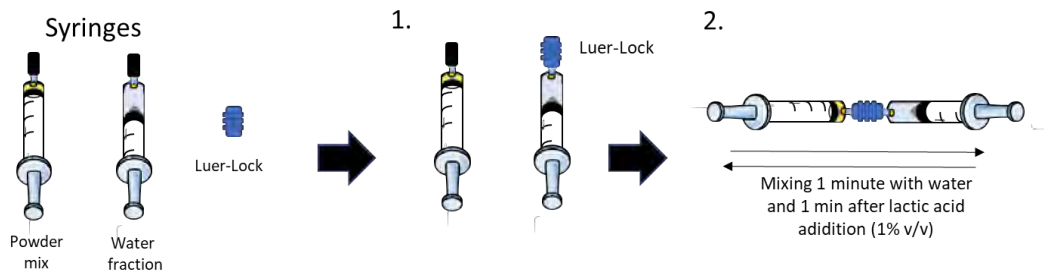

Figure 1: Preparation of CHT/PCD hydrogels using an interconnected syringe system

S67 – O6

Aesthetic Dental Materials: Photoactive anti-infective Fluorapatite Coatings

Dawkins L[1,2], Daskalakis E[1], Jha A[1]
[1]School of Chemical and Process Engineering, University of Leeds, United Kingdom; [2]School of dentistry, University of Leeds, United Kingdom

Introduction

AMR is an increasing threat for healthcare systems worldwide as a result many antimicrobials becoming less effective for treating infection. Antibiotics are used as a preventative measure for surgical wounds. The development of anti-infective dental materials can help with repression of the infection. Using pro-angiogenic and pro-osteogenic materials can also promote enhanced wound healing, improving initial stability and increased implant success rates.

Materials and Methods

Sol-gel synthesis was used to solubilise cerium (Ce^{3+}) and europium (Eu^{3+}) into strontium fluorapatite nanoparticles. This leads to rare earth elements becoming cationically substituted into the fluorapatite structure enabling fluorescence (photoluminescence spectroscopy) when excited with specific laser wavelengths. SEM and confocal microscopy have been used to investigate topographical properties of fluorapatite thin film on Ti6Al4V discs (possibility of coating applications), along with EDX for analysis of ion distribution. Cytotoxicity and Microbiological characterization have been performed to investigate the biological properties.

Results

The fluorescence emission was measured using various UV and visible excitation sources, 395nm (figure 1), 405n and 450nm, with characteristic Eu^{3+} peaks being identified. Profilometry analysis revealed that PLD provides an ultra-thin coating, with desired micro-roughness for cell adhesion, creating a desirable environment for cell proliferation and differentiation. Dip coating results in non-uniform coatings, but still resulting in good cell viability. The outcome of cell culture experiment shows that at low weight percentage concentrations of Ce^{3+} and Eu^{3+} there is no negative influence on cell viability (figure 2). Cerium containing biomaterials have also been found to enhance antimicrobial activity, acting as a natural deterrent for bacterial infection. Microbiological characterization has been performed to confirm these properties.

Conclusion

Materials characterization of the doped fluorapatite confirms the composition and structure of the particles. Fluorescence spectroscopy has shown that the material fluoresces when excited using appropriate laser wavelengths. Biological characterisation has confirmed the doped FA is safe for cells and exhibits antibacterial properties. The inclusion of these materials can lead to improved wound healing and shorter recover times. Fluorapatite nanoparticles doped with Eu^{3+}/Ce^{3+} can serve in place of antibiotics for dental implant care. Further research would include their biofunctionalization as biosensing devices due to their fluorescent properties.

Acknowledgements

We give thanks to the EPSRC for the award of project funding and studentship to Miss Lydia Dawkins.
Thank you to LEMAS and the Bragg Centre for the use of facilities and equipment.

Figures

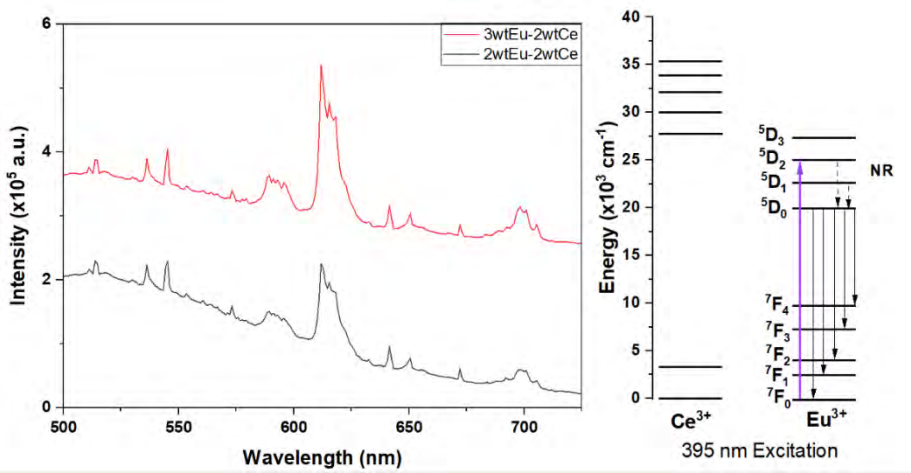

Figure 1: photoluminescence spectra of 3wt%Eu2wt%Ce doped 2wt%Sr FA and 2wt%Eu2wt%Ce doped 2wt%Sr FA using 395nm excitation laser. Notable peak at 614nm. Energy Level Diagram to demonstrate the excitation and relaxation which is occurring within the ions. Ce^{3+} ions are not excited by this wavelength.

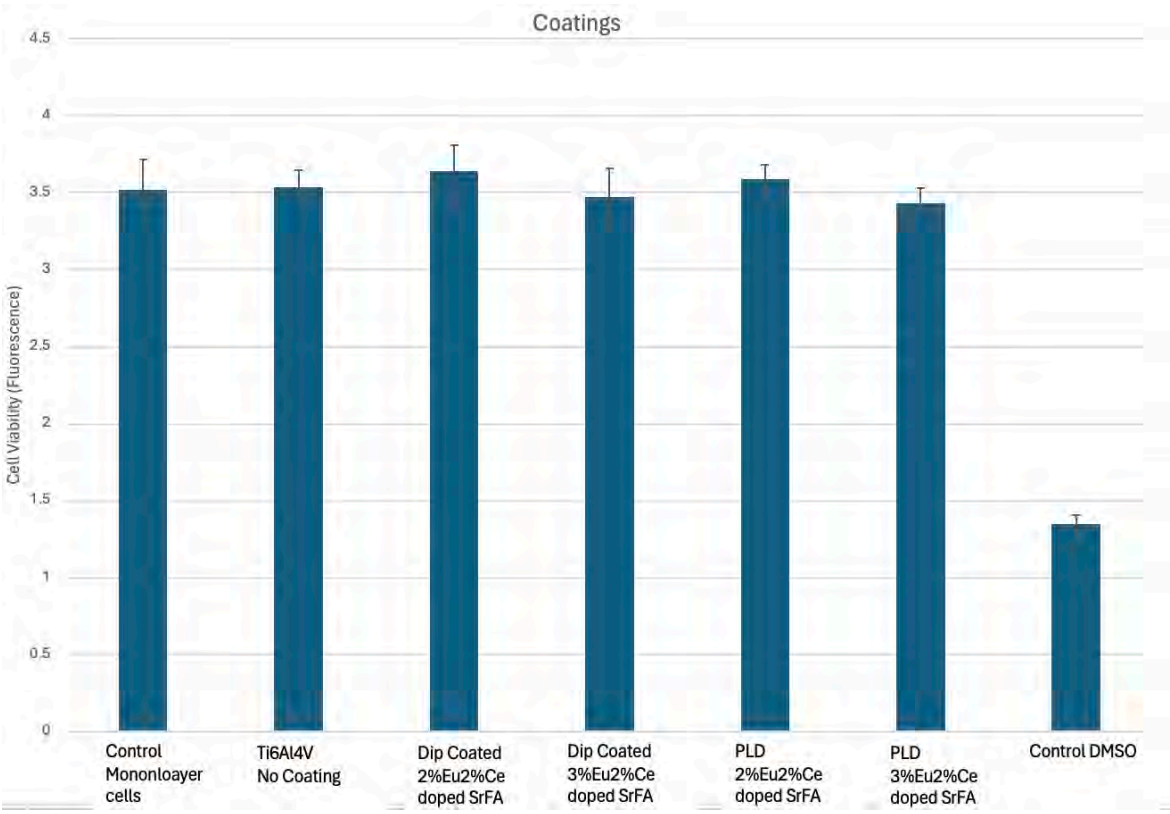

Figure 2: Cytotoxicity Live/Dead data for 3wt%Eu2wt%Ce doped 2wt%Sr FA and 2wt%Eu2wt%Ce doped 2wt%Sr FA using G292 osteosarcoma cell line. Comparison of Monolayer cell control with Ti6Al4V uncoated discs, dip coated discs using 3% and 2% compositions, and PLD coated discs using 3% and 2% compositions. No significant difference ($p>0.05$) based on independent T-test signifying material is non-toxic.

S67 – K1
Bioprinted interfacial complex constructs for advanced healthcare applications

Chatzinikolaidou M.[1,2]
[1]Dept. Materials Science and Engineering, Heraklion, Greece; [2]Foundation for Research and Technology Hellas (FORTH), Heraklion, Greece

This paper reports on the biofabrication of functional, mechanoactive composite bioinks with encapsulated living cells (bone, adipose and Wharton jelly derived mesenchymal stem cells) via extrusion bioprinting for interfacial tissue engineering including vascularized bone and osteochondral grafts. We report on the design and fabrication of bioinks containing an elastic, extrudable polymeric network matrix comprising biomimetic biomaterials including gelatin, elastin, gellan gum, methylcellulose combined with inorganic osteoinductive materials such as nanohydroxyapatite, functionalized bioactive glass, and laponite.

The developed hydrogel-based inks were examined for their printability, rheological properties, thermal behavior, crystallinity, water uptake and degradation rate. The cell-containing constructs were assessed biologically in vitro for their osteogenic, osteoclastogenic, angiogenic and chondrogenic capacity, as well as for their antibacterial activity. The multifunctional bioprinted constructs indicate printing accuracy values of up to 75%, with the composite bioinks being higher. The bioinks demonstrate excellent capability regarding extrusion printability at extrusion pressures of 30-100 kPa, favoring high cell survival rates. Rheological analysis of the bioinks reveals >90% viscosity recovery. The gene expression of relevant osteogenic, osteoclastogenic, angiogenic and chondrogenic markers, as well as the biochemical markers and the extracellular matrix collagen and glycosaminoglycans were significantly elevated in the composite bioinks. Mechanical stimulation of the cell-encapsulated constructs by means of a bioreactor demonstrated significantly increased cell activity, particularly towards osteogenesis, angiogenesis and antiosteoclastogenesis. The bioprinted constructs were implanted in a subcutaneous mouse model for two weeks, indicating the absence of adverse immunological reactions.

S67 – O1

In situ targeted electrode formation based on enzymatic polymerization fueled by altered metabolic pathways in epileptic brain microenvironment

De Roos F.[1,2], Cornuéjols R.[2], Vergaelen M.[1], K.C. D.[3], Drakopoulou S.[3], Abrahamsson T.[2], Simon D.[2], Berggren M.[2], Spyropoulos G.[3], Uguz I.[4], Raedt R.[1], Strakosas X.[2]
1 4BRAIN, Dept. of Head and Skin, Ghent University, Ghent, Belgium, [2] Laboratory of Organic Electronics, Dept. of Science and Technology, Linköping University, Norrköping, Sweden, [3] Dept. of Information Technology, Ghent University, Ghent, Belgium, [4] Dept. of Biomedical Engineering, Stevens Institute of Technology, Hoboken, New Jersey, United States

Introduction

Epilepsy affects over 60 million people worldwide, and one-third of patients suffer from drug-resistant epilepsy. Deep brain stimulation (DBS) provides an alternative therapy but often fails due to mechanical mismatch between rigid electrodes and soft brain tissue. Moreover, current pre-fabricated implants cannot adapt to the dynamic biochemical environment of the epileptic brain. We present a glucose-responsive hydrogel precursor that polymerizes *in situ* into soft, organic conductive electrodes in hyperexcitable conditions, characterized by increased extracellular glucose. This formulation integrates glucose oxidase (GOx) and horseradish peroxidase (HRP) with an EDOT/thiophene-based monomer (ETE-COONa), leveraging the elevated glucose levels occurring during epileptic activity to drive localized oxidative polymerization. The resulting electrodes are electrically conductive, biodegradable, and naturally cleared over time, thus minimizing chronic tissue response while enabling adaptive and reversible neural interfacing.

Materials and Methods

Five hydrogel matrices (GelMA, PVA, gelatin, HA, alginate) were compared using GOx/HRP systems triggered by physiological vs elevated glucose concentrations. Upon polymerization, the ETE-COONa monomer exhibits blue coloration, indicating polymer formation. Hydrogel precursor formulations were systematically optimized by varying GOx, HRP, and ETE-COONa concentrations to maximize conductivity contrast between high- and low-glucose conditions. This electrochemical characterization was done using current-voltage (I-V) measurements and electrochemical impedance spectroscopy (EIS).

Results

Alginate was selected for its optimal polymerization response and dual responsiveness to both glucose and elevated calcium levels observed during seizures. Optimized alginate-GOx/HRP formulation (1% alginate, GOx 180U/mL, HRP 360U/mL, ETE-COONa 48mg/mL) demonstrated robust selectivity for elevated glucose levels. Visual assessment showed minimal blue coloration under normal glucose conditions versus intense polymerization under epileptic-like conditions. Current-voltage measurements showed a 26-fold conductivity contrast after 60 min (210 µA high glucose vs. 8 µA low glucose). Electrochemical impedance spectroscopy confirmed time-dependent impedance reduction only in high-glucose conditions, indicating progressive conductive polymer network formation at the electrode interface, while low-glucose controls remained stable and non-conductive.

Conclusion

This glucose-responsive alginate hydrogel enables intrinsic, site-specific electrode formation triggered by elevation of glucose levels, typical for seizure conditions. The soft, biodegradable material minimizes foreign body response while supporting electrical stimulation, representing a major advantage towards closed-loop, adaptive DBS for drug-resistant epilepsy.

Acknowledgements

This work was supported by internal funding from the BOF (Bijzondere Onderzoeks-Fonds) at Ghent University.

S67 – O2

A mechano-modulatory 3D hydrogel platform to dissect fibroblast fate and matrix remodelling in skin fibrosis

Presa R[1,2], Granja L P[1], Chaudhuri O[3], Pereira R F[1,2]
[1]Instituto de Investigação e Inovação em Saúde, Porto, Portugal, [2]Instituto Ciências Biomédicas Abel Salazar, Porto, Portugal, [3] Dept. of Mechanical Engineering, Stanford, USA

Introduction

Fibrosis is characterized by excessive extracellular matrix (ECM) deposition, persistent fibroblast activation and progressive tissue stiffening. In the skin, it often arises after burns or surgical injury, leading to replacement of healthy tissue by pathological ECM. Despite its clinical impact, antifibrotic drug discovery still relies on animal models that poorly recapitulate human pathophysiology and in vitro systems that fail to reproduce key features of the fibrotic niche. Fibroblasts integrate biochemical signals such as transforming growth factor-β (TGF-β) with biophysical cues from matrix mechanics, yet most current models rely on 2D substrates or 3D hydrogels with limited mechanical control, leading to inaccurate fibroblast responses and high failure rates in clinical trials.

Aim

The goal of this work was to engineer a patient-informed, mechano-modulatory 3D hydrogel platform recapitulating ECM mechanical changes during skin fibrosis to uncover how mechanical and biochemical signals regulate fibroblast activation and ECM remodelling.

Materials and Methods

Mechanically tuneable hydrogels were developed using an RGD-containing pectin-derived macromer by combining ionic gelation and Diels–Alder chemistry to control network architecture. Hydrogels' mechanical properties were assessed by rheology. Healthy primary human dermal neonatal fibroblasts were encapsulated (10 M cells/mL) within hydrogels and cultured under either basal conditions or TGF-β1 (10 ng/mL) stimulation for 14 days. Cell behaviour and ECM composition were assessed by confocal microscopy and proteomic analysis, respectively.

Results

Double-crosslinked hydrogels were optimized to match the stiffness of healthy (G' = 1.9 ± 0.2 kPa) and fibrotic-like (G' = 5.0 ± 0.7 kPa) human skin. Over 14 days, fibroblasts remained viable and proliferative within the gels and progressively formed dense, interconnected cellular networks. Moreover, cells displayed comparable spreading and morphology regardless the stiffness, suggesting robust adaptation to the 3D environment. Notably, proteomic analysis revealed that while TGF-β1 induced a fibrotic programme in both soft and stiff hydrogels, stiff gels amplified and diversified this response by upregulating ECM, metabolic, and mechanosensitive proteins.

Conclusion

The developed mechano-modulatory 3D hydrogel provides a human-relevant platform for modelling skin fibrosis and studying how dermal fibroblasts integrate biochemical and mechanical signals in 3D. Using this system, we uncovered a synergistic interplay between matrix mechanics and biochemical cues that amplifies fibroblast activation and ECM remodelling. Overall, our findings contribute to develop more physiologically relevant in vitro models for fibrosis research and therapeutic screening.

Acknowledgements

This work was supported by projects 2022.06048.PTDC and 2024.16796.PEX, and the fellowship 2022.13383.BD funded by the Portuguese Foundation for Science and Technology.

S67 – O3

Tunable gelatin-chitosan hydrogels for lymph node-inspired 3D models in cancer immunotherapy

Fajardo-García A[1,2,3], Guasch J[3], Garcia-Torres J[1,2,4]
[1]Dept. of Materials Science and Engineering and Institute for Research and Innovation in Health, Universitat Politècnica de Catalunya-BarcelonaTech, Barcelona, Spain, [2]Barcelona Research Center in Multiscale Science and Engineering, Universitat Politècnica de Catalunya-BarcelonaTech, Barcelona, Spain, [3]Institute of Materials Science of Barcelona (ICMAB-CSIC), Barcelona, Spain, [4]Centro de Investigación Biomédica en Red de Bioingeniería, Biomateriales y Nanomedicina (CIBER-BBN), Instituto de Salud Carlos III, Madrid, Spain

Introduction

Cancer remains one of the leading causes of death worldwide, and its progression and response to therapy are strongly influenced by the tumor microenvironment (TME), a dynamic milieu comprising cancer cells, stromal cells, immune cells and extracellular matrix (ECM). However, conventional in vitro models poorly reproduce the three-dimensional and biomechanical complexity of native tissues. In this context, lymph node-inspired hydrogels are promising platforms for physiologically relevant 3D models to study immune-related processes and evaluate immunotherapeutic strategies. Among natural polymers, gelatin and chitosan are attractive candidates due to their biocompatibility and biodegradability, with gelatin providing cell-adhesive motifs and chitosan contributing structural tunability.

Aim. This work aims to engineer and optimize gelatin-chitosan hydrogels with tunable properties to mimic lymph node-like microenvironments, with the final goal of generating 3D platforms for the study of cancer immunotherapy.

Materials and Methods

Gelatin-chitosan hydrogels were prepared by dissolving gelatin in deionized water and chitosan in 1% v/v acetic acid, followed by mixing, casting in a Petri dish, cooling overnight at -4 °C, and immersion in NaOH. Gelatin gelation was temperature-induced, while chitosan gelation occurred via pH change. Different chitosan:gelatin precursor concentrations (2.0:2.7, 2.75:3.71, and 3.5:4.73 % w/v) and NaOH concentrations (0.25, 0.75, and 2 M) were investigated. Hydrogel morphology, chemistry, porosity and pore interconnectivity were assessed by environmental scanning electron microscopy (ESEM), Fourier transform infrared spectroscopy (FTIR) and micro-computed tomography (micro-CT). Swelling and biodegradation tests were conducted as part of the initial physicochemical characterization, while mechanical properties were assessed through compression testing. Cellular responses were studied by confocal microscopy and flow cytometry.

Results

The resulting hydrogels exhibited composition-dependent physicochemical and mechanical properties. Swelling assays in deionized water, PBS, and complete RPMI medium (RPMI + 10% FBS + 1% P/S) showed reduced water uptake with increasing biopolymer content, while NaOH concentration had the strongest influence, significantly reducing swelling in all media. Compression testing revealed that higher polymer content increased hydrogel stiffness, whereas increasing NaOH concentration within a given formulation decreased stiffness and promoted a more elastic-like response. Young's modulus values ranged from 4.91 to 20.9 kPa, placing these hydrogels within a mechanically relevant range for lymph node-mimicking applications. Preliminary results suggest that cell behavior can be influenced by the physicochemical and mechanical properties of the hydrogels.

Conclusion

These results show that gelatin-chitosan hydrogels provide physicochemical and mechanical properties within the relevant range of lymph node tissues, therefore representing promising candidates for the development of lymph node-inspired 3D microenvironments to study tumor–immune interactions and support evaluation of emerging immunotherapeutic strategies.

Acknowledgements

Authors acknowledge funding from MCIU/AEI /10.13039/501100011033 / FEDER, UE (CNS2022-136109, CNS2023-144236, PID2022-141120OB-I00, PID2024-159041OB-I00, CEX2023-001300-M, and CEX2023-001263-S) and Agència de Gestió d'Ajuts Universitaris i de Recerca de Catalunya (AGAUR) (2021-SGR-01368) for financial support.

S67 – O4

An infection-responsive collagen-based wet-spun textile fibre for wound monitoring

Gorman, J[1,2], Brooker, C[1,2], Li, X[1], Tronci, G[1,2]
[1]Clothworkers Centre for Textile Materials Innovation for Healthcare (CCTMIH), Leeds Institute of Textiles and Colour (LITAC), University of Leeds, United Kingdom, [2]Division of Oral Biology, St. James's University Hospital, School of Dentistry, University of Leeds, United Kingdom

Introduction

Commercial wound dressings are made from textile fibres due to their inherent flexibility and mechanical strength; by embedding responsive elements directly into fibres, smart textiles can provide real-time feedback on wound status while maintaining breathability and a close interface with the wound bed. However, current wound monitoring strategies still rely on specialist imaging software or an algorithm, which is costly, time-consuming and which requires patient visit at the clinic. With the unsustainable costs associated with wound care globally, there is an urgent need for simple, cost-effective, smart wound dressings enabling remote wound monitoring. One biomarker of wound infection is the pH, whereby healthy skin exhibits an acidic environment (pH £6), whereas infected wounds exhibit a raise in pH in the alkaline region (pH>7). We hypothesised that this infection associated pH shift could be leveraged to achieve textile wound dressings with pH-responsive colour change enabling visual warning of wound infection. Bromothymol Blue (BTB) was employed as commercially available halochromic dye that shifts colour from yellow to blue upon contact with solutions of increasing alkalinity.

Materials and Methods

Rat tail collagen functionalised with 4-vinyl benzyl chloride (4VBC) was wet spun into fibres and then UV cured to produce 4VBC* fibres for use as building block of wound dressings Fig.1). Fibres were gravimetrically loaded via drop casting a known amount of BTB onto dehydrated wet spun fibres. Release profiles in pH 5 and pH 8 were measured via UV-Vis spectroscopy to represent healthy and infected wounds, respectively. Degradation of 4VBC* fibres in a collagenase rich media (pH 7.4, 37°C, 2 CDU) was recorded by measuring the relative mass (wt.%) of dry fibres collected after 24, 48 and 72 hours of enzymatic incubation with respect to the initial dry mass. Tensile tests were performed on hydrated individual fibres (5 N load cell, Instron 5544, Massachusetts, USA).

Results

4VBC* collagen fibres exhibited a loading efficiency of 99±3 wt.% together with high retention of BTB (88 wt.%) after 48-hr incubation in acidic environments. The dry fibres demonstrated controlled swelling in aqueous environments (up to 5-fold increase in weight), remarkable wet-state Ultimate Tensile Strength (UTS: 12±3— 15±7 MPa), and up to ~30 wt.% mass retention after 24 hours in a collagenase-rich buffer.

Conclusion

Fibres demonstrated mechanical integrity in hydrated states, whilst maintaining the ability to degrade in the presence of collagenase, allowing for varying wound healing applications such as woven dressings and resorbable sutures. Fibres also successfully displayed a rapid, reversible, visual colour change under acidic and basic conditions displaying their effective capabilities of signalling wound infection without the need for specialist equipment or algorithm.

Acknowledgements

The authors gratefully acknowledge financial support from the Clothworkers' Company, LITAC and the Institution of Mechanical Engineers (through IMechE Whitworth Senior Scholarship Award to JG).

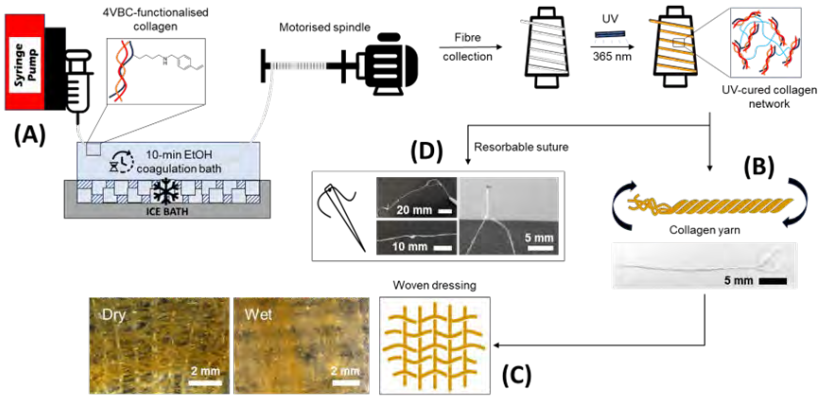

Figure 1. Schematic of wet spinning apparatus and production of functionalised collagen fibres into either woven dressings or resorbable sutures.

S67 – O5

Chitosan and citric acid – cyclodextrin polymer hydrogel for drug delivery: relationship between rheological characteristics and release properties

Chijcheapaza-Flores H [1,2], Tabary N [2], Cazaux F [2], Staelens JN [2], Blanchemain N [1], Nicot R [1,3], Garcia Fernández MJ [1], Martel B [2]

[1] University of Lille, INSERM, U1365 - Advanced Drug Delivery Systems, France, [2] University of Lille, CNRS, INRAE, Centrale Lille, UMR 8207 – UMET – Unité Matériaux et transformations, France, [3] University of Lille, CHU Lille, Dept. of Oral and Maxillofacial Surgery, France

Introduction

Hydrogels are widely used in drug delivery and tissue engineering due to their capacity to mimic the extracellular matrix and enable the controlled release of active pharmaceutical ingredients (API). Chitosan (CHT) is one of the most commonly used cationic polymers for hydrogel preparation and can be combined with a wide range of anionic polymers, such as a citric acid polymer of cyclodextrin developed by Martel *et al.* (1), which can form host-guest complexes with APIs.

Aim. This study investigates the relationship between the rheological properties of CHT/PCD hydrogels, including their soluble and insoluble fractions, and the release of sodium naproxen from these systems to clarify how CHT and PCD contribute to viscoelastic behavior and drug release properties.

Materials and Methods

Powder mixes without the API were prepared by mixing CHT (Sigma Aldrich, 80% DDA, high molecular weight) with soluble PCD (PCDs) or insoluble PCD (PCDi) using a Mixer Mill MM400 (Retsch®). The API-loaded mix was obtained by prior wet granulation of PCDs/PCDi with NaNX (Thermo Fisher, 1% w/w). CH/PCDs/PCDi hydrogels were formed using an interconnected syringe system (Figure 1), as previously described by Chijcheapaza-Flores *et al*. (2). The formulations were initially screened by assessing the viscoelastic properties of several CHT/PCDs and CHT/PCDs/PCDi concentrations using an HR 10 rheometer (TA Instruments). In the second stage, the formation of the cyclodextrin (CD)/NaNX inclusion complex using PCD was confirmed by ^{1}H NMR, and NaNX release was assessed using a USP I dissolution apparatus (Agilent) in PBS at 37 °C and 50 rpm.

Results

The results indicate that PCDs have a greater impact than PCDi on the viscoelastic properties of the CHT/PCDs/PCDi hydrogels. In contrast, when PCDi was present, no significant difference in viscoelastic properties was observed ($p<0.05$). The release kinetics study showed that CHT/PCDs slowed the release of NaNX compared with the CHT solution and hyaluronic acid (HA), which is commonly used in intra-articular medical devices. Finally, the formulations containing PCDi showed only partial release of NaNX.

Conclusion

In conclusion, for a fixed concentration, an increasing PCDs concentration exhibited an increased hydrogel elasticity and slowed down the NaNX release, while PCDi retained NaNX inside the hydrogel. These findings could be attributed to the trapping of NaNX within the PCDi network (highly crosslinked).

Acknowledgements

This project was funded by the French National Research Association (ANR, JCJC contract) under the code ANR-21-CE19-0012 CHITOGEL.

References

1. Martel B et al. J Appl Polym Sci (2005) 97:433–442. doi:10.1002/app.21391
2. Chijcheapaza-Flores et al., Gels (2023) 9(3):262. doi:10.3390/gels9030262

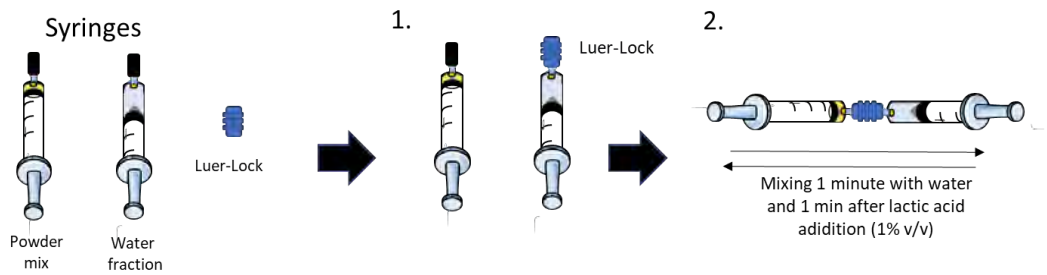

Figure 1: Preparation of CHT/PCD hydrogels using an interconnected syringe system

S67 – O6

Aesthetic Dental Materials: Photoactive anti-infective Fluorapatite Coatings

Dawkins L[1,2], Daskalakis E[1], Jha A[1]
[1]School of Chemical and Process Engineering, University of Leeds, United Kingdom; [2]School of dentistry, University of Leeds, United Kingdom

Introduction

AMR is an increasing threat for healthcare systems worldwide as a result many antimicrobials becoming less effective for treating infection. Antibiotics are used as a preventative measure for surgical wounds. The development of anti-infective dental materials can help with repression of the infection. Using pro-angiogenic and pro-osteogenic materials can also promote enhanced wound healing, improving initial stability and increased implant success rates.

Materials and Methods

Sol-gel synthesis was used to solubilise cerium (Ce^{3+}) and europium (Eu^{3+}) into strontium fluorapatite nanoparticles. This leads to rare earth elements becoming cationically substituted into the fluorapatite structure enabling fluorescence (photoluminescence spectroscopy) when excited with specific laser wavelengths. SEM and confocal microscopy have been used to investigate topographical properties of fluorapatite thin film on Ti6Al4V discs (possibility of coating applications), along with EDX for analysis of ion distribution. Cytotoxicity and Microbiological characterization have been performed to investigate the biological properties.

Results

The fluorescence emission was measured using various UV and visible excitation sources, 395nm (figure 1), 405n and 450nm, with characteristic Eu^{3+} peaks being identified. Profilometry analysis revealed that PLD provides an ultra-thin coating, with desired micro-roughness for cell adhesion, creating a desirable environment for cell proliferation and differentiation. Dip coating results in non-uniform coatings, but still resulting in good cell viability. The outcome of cell culture experiment shows that at low weight percentage concentrations of Ce^{3+} and Eu^{3+} there is no negative influence on cell viability (figure 2). Cerium containing biomaterials have also been found to enhance antimicrobial activity, acting as a natural deterrent for bacterial infection. Microbiological characterization has been performed to confirm these properties.

Conclusion

Materials characterization of the doped fluorapatite confirms the composition and structure of the particles. Fluorescence spectroscopy has shown that the material fluoresces when excited using appropriate laser wavelengths. Biological characterisation has confirmed the doped FA is safe for cells and exhibits antibacterial properties. The inclusion of these materials can lead to improved wound healing and shorter recover times. Fluorapatite nanoparticles doped with Eu^{3+}/Ce^{3+} can serve in place of antibiotics for dental implant care. Further research would include their biofunctionalization as biosensing devices due to their fluorescent properties.

Acknowledgements

We give thanks to the EPSRC for the award of project funding and studentship to Miss Lydia Dawkins.
Thank you to LEMAS and the Bragg Centre for the use of facilities and equipment.

Figures

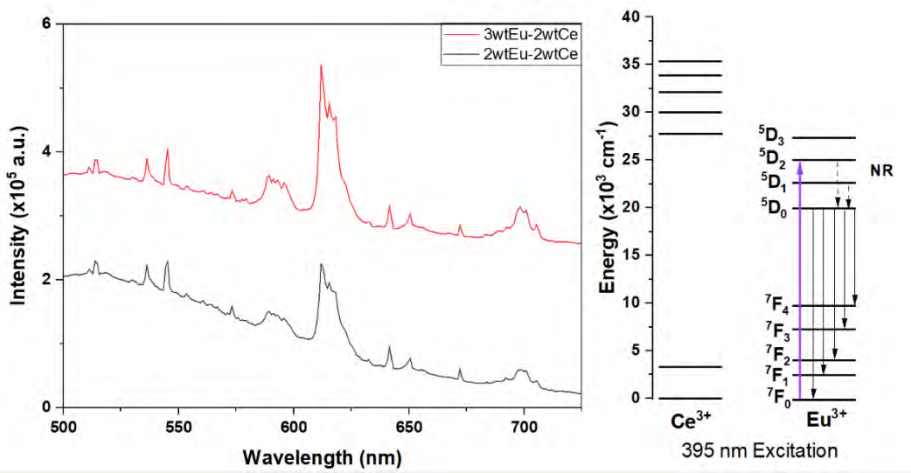

Figure 1: photoluminescence spectra of 3wt%Eu2wt%Ce doped 2wt%Sr FA and 2wt%Eu2wt%Ce doped 2wt%Sr FA using 395nm excitation laser. Notable peak at 614nm. Energy Level Diagram to demonstrate the excitation and relaxation which is occurring within the ions. Ce^{3+} ions are not excited by this wavelength.

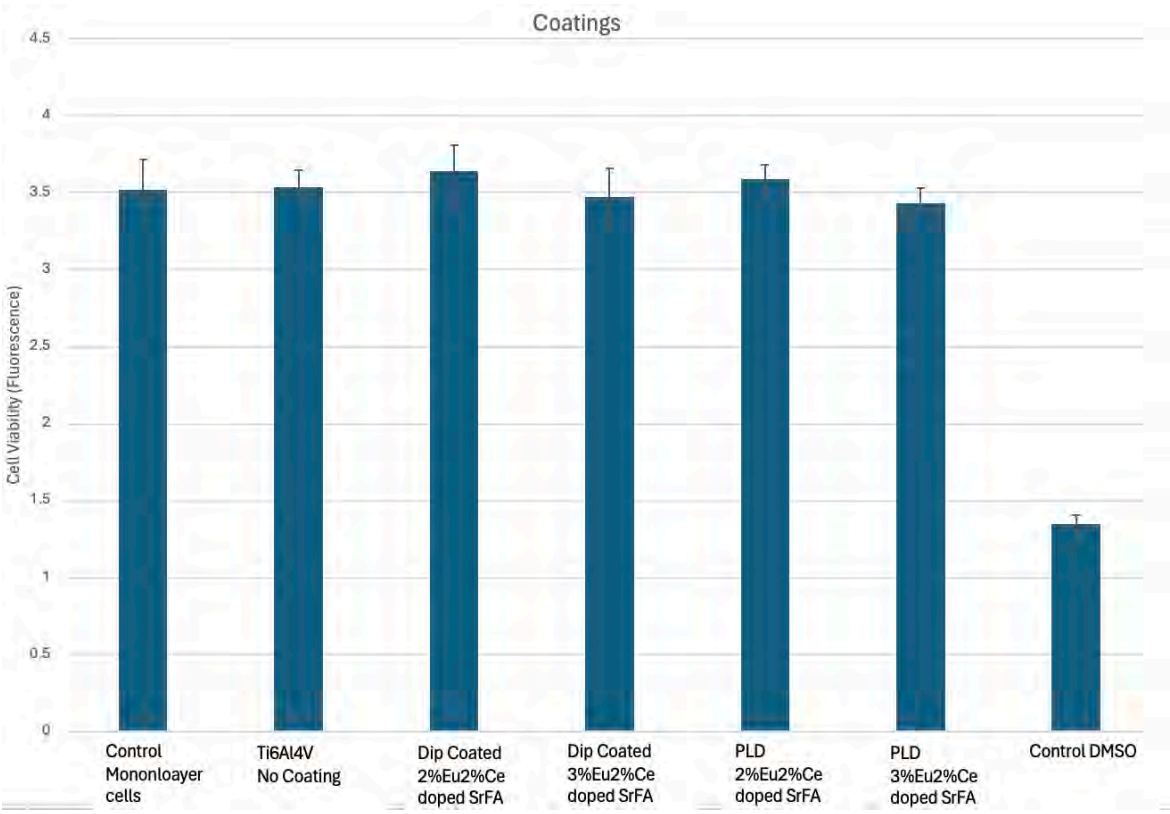

Figure 2: Cytotoxicity Live/Dead data for 3wt%Eu2wt%Ce doped 2wt%Sr FA and 2wt%Eu2wt%Ce doped 2wt%Sr FA using G292 osteosarcoma cell line. Comparison of Monolayer cell control with Ti6Al4V uncoated discs, dip coated discs using 3% and 2% compositions, and PLD coated discs using 3% and 2% compositions. No significant difference ($p>0.05$) based on independent T-test signifying material is non-toxic.

S68 - Biomaterial-driven tissue regeneration and aging

S68 – K1
Programming physical cues to direct cellular function

Khoon S. Lim

S68 – O1

3D printed Ti6Al4V TPMS bone-analogues: bridging mechanical asymmetry and in vivo osseointegration

Karali B.K.[1], Basu B.[2]
[1]Laboratory of Biomaterials Science and Translational Research, Materials Research Centre, IISc Bangalore, Bengaluru, India, [2]CSIR-CGCRI, Kolkata, India.

Introduction

Complex bone defects impose conflicting biological and mechanical requirements. Even within long bones, cortical and cancellous regions prefer different pore sizes, stiffness ranges, and vascularization kinetics. Addressing these multifaceted demands requires implants that go beyond simple porosity to actively mimic the heterogeneous nature of natural bone tissue.

Aim

This study aims to investigate the mechano-biological performance of laser powder bed fusion (L-PBF) printed Ti6Al4V Schwarz diamond triply periodic minimal surface (SDW-TPMS) structures. We evaluate how tuning 3D pore topology can achieve a clinically relevant tension-compression asymmetry mimicking natural cortical bone and determine its effect on in vitro pre-osteoblast maturation and in vivo 3D osseointegration compared to conventional plasma-coated Ti bulk implants.

Materials and Methods

Ti6Al4V SDW-TPMS structures (2.5-3.0 mm unit cell size) were fabricated via L-PBF. Mechanical properties were assessed under uniaxial tension and compression, correlating with micro-computed tomography (Micro-CT) pore network modeling. Following in vitro pre-osteoblast (MC3T3-E1) assays, an optimized 3.0 mm design (~48% porosity) was implanted into a rabbit femoral condyle defect model. Osseointegration was benchmarked against an industrial standard Ti plasma-coated bulk Ti6Al4V control using Micro-CT over 12 weeks.

Results

The SDW-TPMS architectures exhibited a pronounced tension-compression asymmetry. Compressive elastic modulus (14-20 GPa) and strength (413-547 MPa) contrasted starkly with tensile modulus (38-55 GPa) and strength (325-475 MPa). This asymmetry is governed by distinct failure mechanisms: compressive failure demonstrated stable, progressive strut buckling, whereas tensile failure was abrupt and defect-driven. Biologically, the interconnected porous network promoted robust in vitro pre-osteoblast maturation (Figure 1). In vivo, the interconnected pores in the SDW-TPMS structures facilitated rapid 3D bone ingrowth deep within the network, significantly outperforming the slow 2D surface ongrowth of the bulk control (Figure 2).

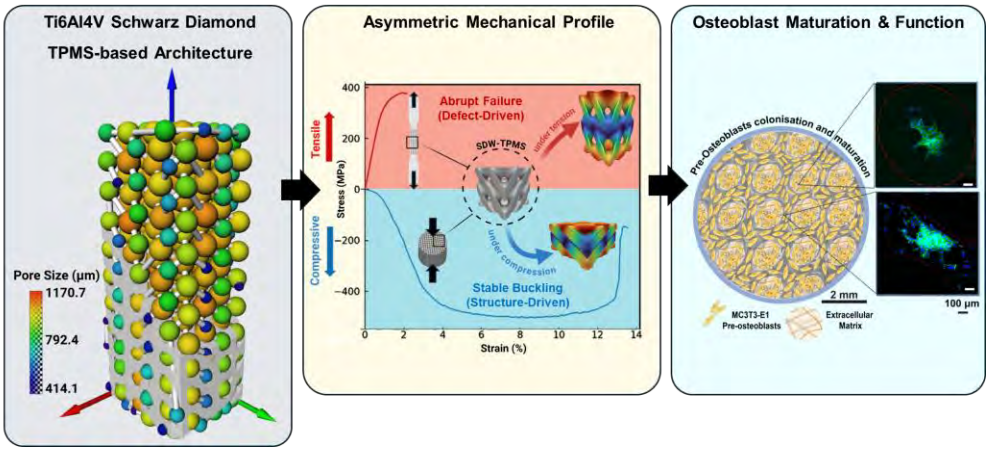

Fig 1: Evaluation of the Ti6Al4V SDW-TPMS structure (left to right): 3D pore network model; stress-strain curves highlighting tension-compression asymmetry; fluorescence microscopy of MC3T3-E1 cell adhesion on the SDW-TPMS architecture over 7 days.

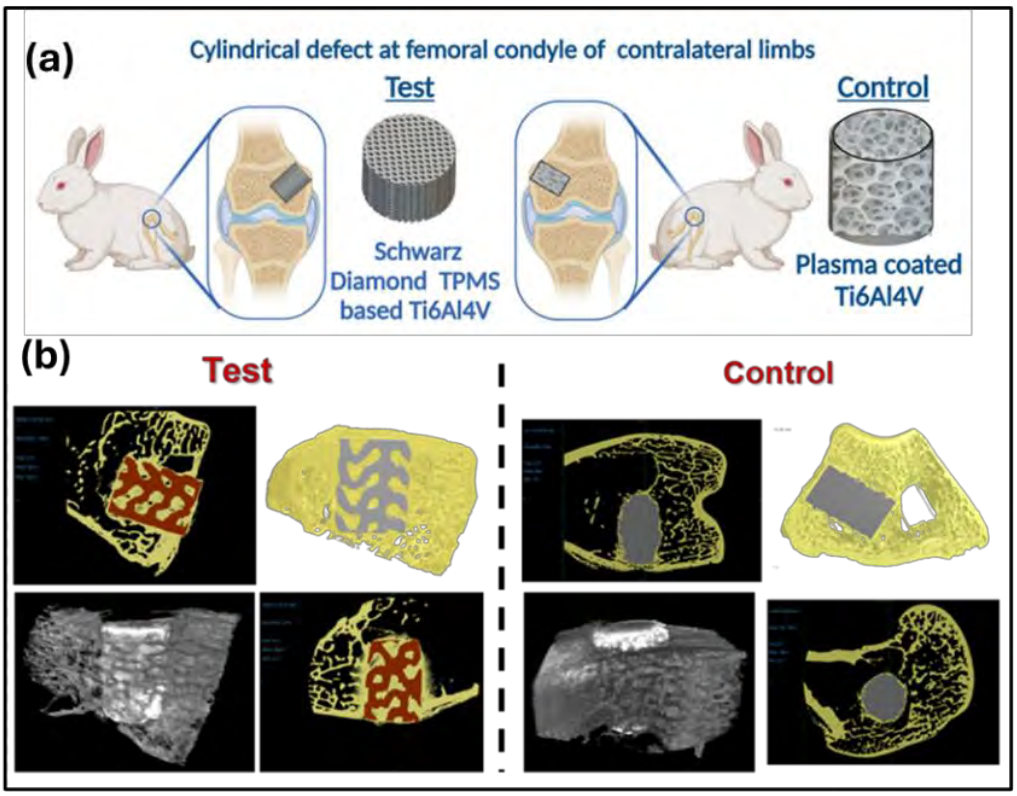

Fig 2: (a) Osseointegration study of L-PBF printed Ti6Al4V TPMS in rabbit model, (b) 3D reconstructions at 84 days (12 weeks) demonstrating profound 3D bone ingrowth deep throughout the test implant's porous network, contrasting with the limited 2D surface ongrowth of the bulk control)

Conclusion

These findings validate SDW-TPMS structures for the development of improved load bearing orthopedic implants by linking pore topology to in-vivo performance.

Acknowledgements
Support from the Core Research Grant of the SERB, Government of India (CRG/2020/001145), the Abdul Kalam National Technological Innovation Fellowship (INAE/121/AKF), and industrial collaboration with Orthotech India Pvt. Ltd. is acknowledged.

References

[1] Bijay Kumar Karali, Suresh Suthar, Sushant Banerji, Bikramjit Basu, Asymmetric mechanical behavior and pre-osteoblast differentiation in 3D printed Ti6Al4V-based triply periodic minimal surface bone-analogues: the role of pore topology, Acta Biomaterialia, Volume 207, 2025, Pages 633-652.
[2] Hua-Jie Mao, Wei Lei, Qian-Hai Ding, Han-Xiao Zhu and Jun-Gang Xu, A Review on Janus Biomaterials: Asymmetric Design for Advanced Bone Regeneration, Materials Today Communications, (2026).

S68 – O2

3D-Printed photoactive pectin–silk fibroin film for skin wound healing

Joaquinito A. S.[1,7], Pinto M.T.[2], Hackbarth S.[3], Isreb A.[4], Almeida A.[5], Guerreiro S.G.[2,6], Giuntini F.[7], Faustino, M.A.F.[1]

[1]LAQV-Requimte and Dept. of Chemistry, University of Aveiro, Portugal, [2]Instituto de Investigação e Inovação em Saúde, Universidade do Porto, Portugal, [3]Photobiophysics, Institute of Physics, Humboldt University of Berlin, Berlin, Germany, [4]Dept. of Clinical Sciences, Liverpool John Moores University, Liverpool, UK, [5] CESAM, Dept. of Biology, University of Aveiro, Portugal, [6]Dept. of Biomedicine, Biochemistry Unit, Faculty of Medicine University of Porto, Portugal, [7]School of Pharmacy and Biomolecular Sciences, Liverpool John Moores University, Liverpool, UK

Introduction

Biomedical research has leapt to great heights of scientific development over the years, yet something as simple as skin wound dressings becomes somewhat stagnated, especially when we consider the world of personalized medicine. In cases of severe, infected, chronic or diabetic wounds it is especially important to provide an adequate environment for healing. A major unmet need in skin wound care lies in improving tissue regeneration after debridement through smart dressings designed to modulate the wound microenvironment. By combining structural support with bioactive matrix functions, these systems can foster cellular repair, reduce microbial persistence and antimicrobial resistance, minimise fibrotic healing, and stimulate neovascularization towards higher-quality skin regeneration. Antimicrobial photodynamic therapy (aPDT) has gained considerable attention in wound healing applications, offering a non-invasive strategy to control microbial bioburden while promoting tissue regeneration.

Aim

Considering this, we propose a porphyrin-embedded pectin and silk fibroin-based formulation which is 3D-printable to be used for wound healing purposes through photodynamic action.

Materials and Methods

A printable Pectin-Silk Fibroin- Porphyrin (PSP) ink was obtained and subject to characterization by rheometry, thermogravimetric analysis, differential scanning calorimetry, surface fluorescence, FTIR and SEM. The 3D-printed film was tested for its *in vitro* biocompatibility in human dermal fibroblasts (HDF): viability assay and migration assay. For *in vivo* assays, Chorioallantoic Membrane (CAM) assay was used. Cell viability and migration of HDF was investigated after light irradiation with PSP films, while *in vivo* CAM assay provided clues regarding the angiogenic properties, inflammation and fibrosis triggered by treatment with PSP material. Antibacterial activity of PSP films was also investigated against methicillin-resistant *S. aureus* (MRSA).

Results

The PSP ink was found to be shear-thinning and printable. 3D-printed PSP film exhibited high fluorescence, insolubility in aqueous environments, and thermal stability. Biocompatibility in dark conditions was assured in all human cell line, bacteria and chicken embryo. PSP films exhibited antibacterial activity against MRSA as well as angiogenic potential in chicken embryos after appropriate light irradiation.

Conclusion

PSP films under light irradiation were able to inactivate MRSA, demonstrating potential to disinfect a wound site. They have also influenced an increased angiogenesis in the CAM of treated chicken embryos without fibrosis. Neovascularization was improved in the treated area with PSP which in turn favors healing. Overall, the PSP ink is printable, opening possibilities to personalized wound dressings, and the printed films show potential for wound healing under appropriate light conditions, especially in cases of infected injuries.

Acknowledgements and Funding
The authors thank the University of Aveiro and FCT/MECI for the financial support provided to UID/50006 - Laboratório Associado para a Química Verde - Tecnologias e Processos Limpos, UID/50006/2025 DOI 10.54499/UID/50006/2025). The authors also thank to the DAAD-FCT mobility project 2021.09774.CBM and Royal Society International Exchange 2023 Round 1. Grant number IES/R1/231205. AS Joaquinito also thanks FCT/MCTES for her PhD grant (2021.06854.BD).

S68 – O3

Exploring bioactive scaffolds in Spinal Cord Injury rat models: targeting neuroinflammation and regeneration

Martínez-Ramírez, J.[1], Benayas, E.[1], Hernández-Martín, Y.[2,3], Caz, J. V.[1], Madroñero-Mariscal, R.[2,3,4], López-Dolado, E.[2,3,4], Serrano, M. C.[1,*]
[1]Materials for Medicine and Biotechnology Group, Instituto de Ciencia de Materiales de Madrid, CSIC, Madrid, Spain, [2]Laboratory of Interfaces for Neural Repair, Hospital Nacional de Parapléjicos, SESCAM, Toledo, Spain
[3]Instituto de Investigación Sanitaria de Castilla-La Mancha (IDISCAM), Toledo, Spain, [4]Design and development of biomaterials for neural regeneration, HNP, Associated Unit to CSIC through ICMM, Toledo, Spain

Introduction

Spinal Cord Injury (SCI) triggers a cascade of inflammation and inhibitory scarring that severely limits axonal regeneration and functional recovery. In the context of the Piezo4Spine project, we have developed multifunctional reduced graphene oxide (rGO) scaffolds integrating nanocarriers functionalized with immunomodulatory and/or gene regulating molecules to modulate the lesion microenvironment after SCI *in vivo*.

Materials and Methods

rGO scaffolds were fabricated by freeze-casting and loaded with nanocarriers previously functionalized with immunomodulatory (cytokines) and/or gene therapies (RNAs). The physicochemical properties of the individual components and their combination were carefully characterized using dynamic light scattering, thermogravimetric analysis, and transmission and scanning microscopies, among other techniques. Release of bioactive cargos was quantified by ELISA and RiboGreen assays, respectively. The biocompatibility and bioactivity of the materials were confirmed *in vitro* by using relevant neural and immune cells, prior to *in vivo* studies. A C6 right hemisection was performed on adult male Wistar rats, and the scaffolds were implanted immediately after injury. Animals were monitored for up to 120 days post-injury. A representative selection of inflammatory, vascular and neural markers was assessed (*e.g.*, vimentin, ED-1, GFAP, MAP-2, βIII-tubulin, GAP-43) to evaluate inflammation, glial scarring, vascularization, and neural tissue regeneration within and around the scaffold in the spinal tissue. Functional recovery was assessed by using open field, asymmetry and grooming tests to quantify spontaneous behavior and forelimb function recovery.

Results

Implantation of these bioactive scaffolds mechanically supported the lesion site resulting in improved locomotor performance compared to the SCI-alone group. Furthermore, histological analysis showed that neural components were preserved with respect to injured rats not carrying scaffolds and, in some cases, significantly increased. ED-1, GFAP and vimentin were typically reduced in comparison with the SCI-alone group, suggesting a reduction in inflammation and fibroglial scarring. We also observed enhanced vascularization within the lesion side in animals implanted with these scaffolds.

Conclusion

These findings demonstrate that rGO-based scaffolds combined with targeted nanocarrier delivery can simultaneously provide structural guidance and immunomodulatory and neuroregenerative properties in the context of experimental SCI. Our research supports the concept that a combined approach involving several therapeutic elements is a promising pathway to enhance neural repair and functional recovery after SCI. Finally, it opens new avenues for the design of translationally relevant neurotherapeutics for the central nervous system.

Acknowledgements

This work has received funding from the European Union's Horizon Europe research and Innovation Programme under grant agreement No. 101098597 (Piezo4Spine). It has been also supported by grant PID2023-150170OB-I00 funded by MICIU/AEI/10.13039/501100011033 and FEDER, UE.

S68 – O4

An elastic and degradable blood vessel graft to regenerate damaged arteries

Shiraev T*[,1,2,3,4], Bocking WJ*[,1,2,4], Wang Z[2,5], Li M[6], Seth L[1,2,4], Partel L[7], Wise IK[8], Tran AH[2,4], Zhang M[2,5], Roohani I[9], Rnjak-Kovacina J[10], Mithieux S[2,5], Paterson H[11], O'Sullivan J[1,2,4,12], Lal S[1,2,4,12], Weiss AS[2,5], Bannon P[1,11,13,14], Hume RD[1,2,4]

The Baird Institute for Applied Heart and Lung Research, Newtown, New South Wales, Australia, [2]Charles Perkins Centre, University of Sydney, Sydney, New South Wales, Australia, [3]Dept. of Vascular Surgery, Royal Prince Alfred Hospital, Camperdown, New South Wales, Australia, [4]School of Medical Sciences, Faculty of Medicine and Health, University of Sydney, Sydney, New South Wales, Australia, [5]School of Life and Environmental Sciences, Faculty of Science, University of Sydney, Sydney, New South Wales, Australia, [6]Walter and Eliza Hall Institute of Medical Research, Melbourne, Victoria, Australia, [7]Sydney Imaging, Core Research Facilities, The University of Sydney, Sydney, New South Wales, Australia, [8]Laboratory Animal Services, Core Research Facilities, The University of Sydney, Sydney, New South Wales, Australia, [9]School of Biomedical Engineering, University of Technology Sydney, Sydney, Australia, [10]Graduate School of Biomedical Engineering, University of New South Wales, Sydney, Australia, [11]Central Clinical School Surgery, Faculty of Medicine and Health, The University of Sydney, Sydney, New South Wales, Australia, [12]Dept. of Cardiology, Royal Prince Alfred Hospital, Camperdown, New South Wales, Australia, [13]Institute of Academic Surgery, Royal Prince Alfred Hospital, Sydney, New South Wales, Australia, [14]Dept. of Cardiothoracic Surgery, Royal Prince Alfred Hospital, Sydney, New South Wales, Australia.

Introduction

Multiple genetic and acquired diseases can cause irreversible damage to arteries and can be life-threating. A common treatment is to replace damaged arteries with synthetic grafts. Unfortunately, these are made from rigid materials that cause abnormal blood flow and can form potentially fatal thrombosis (blood clots), causing the artery to occlude (block). To address these failings, we developed grafts synthesised from tropoelastin-polyglycerol sebacate (TE-PGS); two elastic materials with a similar stiffness to healthy arteries. These grafts are also degradable; encouraging new healthy tissue to regenerate and replace the graft as it degrades. Although promising, our previous study was in mice, which are approximately 3000 times smaller than humans. Thus, for clinical translation, we have upscaled our grafts (Fig 1a) and implanted them into sheep (Fig 1b).

Materials and Methods

We surgically resected a 3cm section of sheep carotid arteries and implanted either: 1) 4mm diameter TE-PGS elastic degradable grafts, 2) 4mm diameter clinical-grade expanded polytetrafluorethylene (ePTFE aka GORE-TEX) control grafts or 3) sham surgeries, whereby the artery was ressected and re-anastomosed. We then periodically analysed blood flow and 'graft-to-neoartery' remodelling using computed tomography (CT) angiography and ultrasound imaging, every 2 months for 8 months. Following neoartery removal, we performed proteomics, multiplexed immunohistochemistry (IHC), 3D IHC and mechanical testing analyses.

Results

TE-PGS grafts showed a significantly increased patency rate of 66.7% versus 12.5% for ePTFE control grafts (Fig 1c,d,e, reduced blockages/occlusions). Additionally, TE-PGS grafts successfully remodelled *in vivo* into a 'neoartery' (Fig 1f), expanding from 4mm to 5.5mm diameter, closer to native artery diameter of 6mm, with subsequent reduced stenosis and improved blood flow. In contrast, clinical-standard ePTFE control grafts maintained a 4mm diameter throughout, exhibiting increased stenosis and abnormal blood flow. Additionally, *ex vivo* multiplexed IHC and 3D IHC showed *de novo* elastin fibre formation, smooth muscle cell infiltration and ongoing immune cell remodelling in TE-PGS 'neoarteries'.

Conclusion

ePTFE is the gold-standard synthetic material used in the clinic, that often occludes (blocks), leading to repeat surgeries, amputations and death. Our large animal study shows TE-PGS degradable grafts outperform ePTFE and encourages vessel regeneration via 'neoartery' formation. If successfully translated, these grafts could treat a wide range of artery diseases and significantly improve millions of patients' lives.

Acknowledgements
This study was supported by a Heart Foundation Vanguard Grant (#107321-2023) and The Baird Institute for Applied Heart and Lung Research.

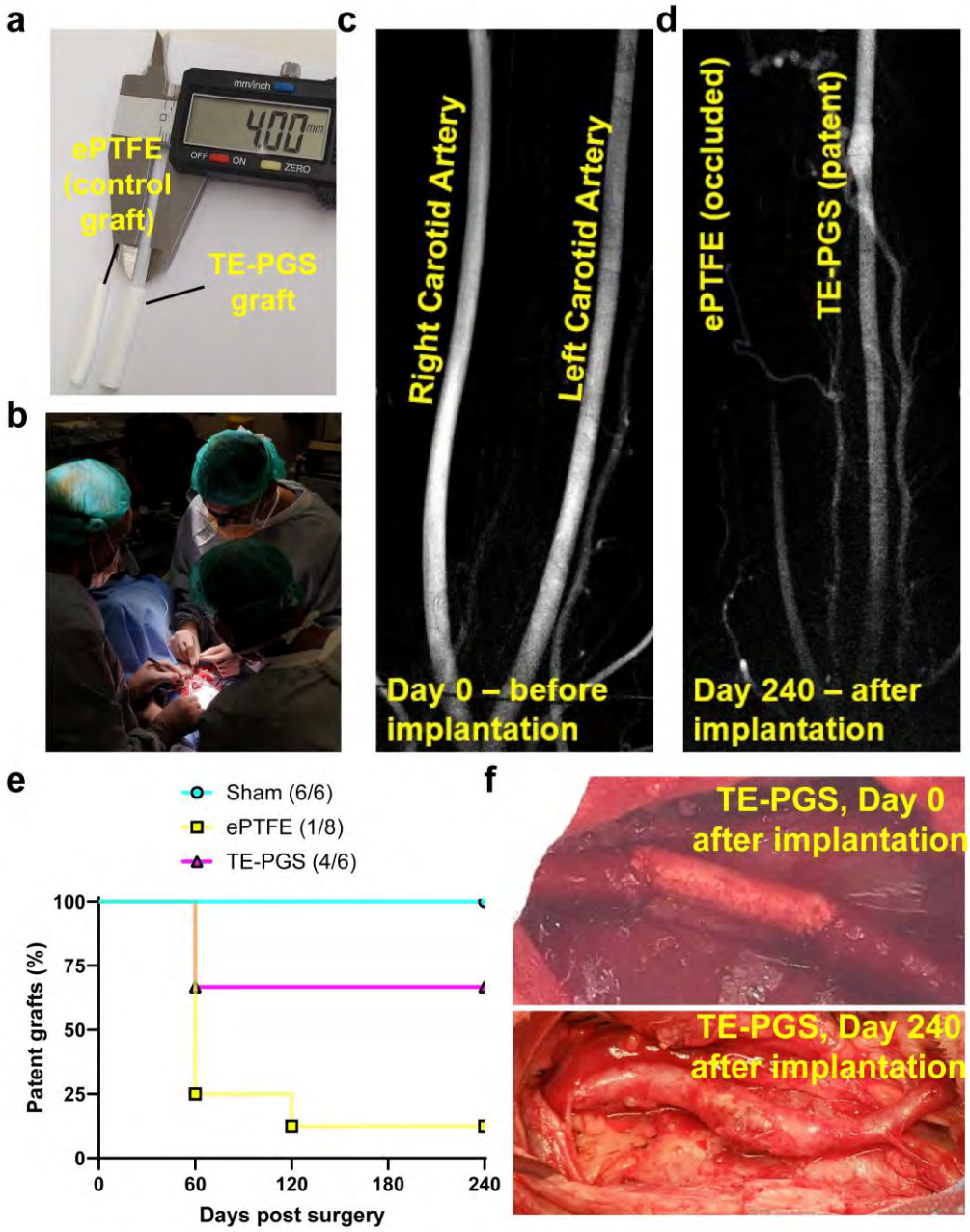

Figure 1 - Elastic and degradable tropoelastin-polyglycerol sebacate (TE-PGS) blood vessel graft to regenerate damaged arteries – a) Photo of TE-PGS and clinical-standard expanded polytetrafluoroethylene (ePTFE) control 4mm artery grafts, b) Photo of sheep carotid artery graft implantation surgery, c) Sheep carotid artery angiogram before surgery, d) Sheep carotid artery angiogram 8 months post-surgery, showing occluded ePTFE graft, e) Graft patency over 8 months post-surgery, f) TE-PGS graft immediately following implantation and 8 months post-surgery.

S68 – O5

Lytamer-containing layer-by-layer constructs enhance the migratory capacity of fibroblasts from aged diabetic patients

Soares da Costa D[1,2], Brito A[1,2], Costa R[1,2], Díaz A[3], Pazó A[3], Reis RL[1,2], Pashkuleva I[1,2]
[13]B's Research Group, I3Bs – Research Institute on Biomaterials, Biodegradables and Biomimetics, University of Minho, Portugal, [3]Lincbiotech, Poligono Parque Tecnoloxico Galicia, Spain

Introduction

Diabetic foot ulcers (DFUs) are a major complication of diabetes. Despite their high prevalence, DFUs remain unmet clinical condition with no effective treatment. To address this clinical need, we investigated lysosome-targeting chimeras (LYTACs) in combination with hyaluronan (HA) - a major extracellular component that is dysregulated in DFU and contributes to the chronic, non-healing state.

Materials and Methods

LYTACs are emerging therapeutic platforms that promote the degradation of extracellular proteins by redirecting them to lysosome-shuttling receptors, thus, enabling the removal of pathogenic proteins that cannot be targeted by conventional methods. We engineered a lytamer comprising a LYTAC motif coupled to an MMP9 antibody (Lytac-abMMP9) to targeted the extracellular MMP9 in DFU. For controlled delivery of Lytac-abMMP9, we developed HA/chitosan(CHIT) membranes using layer-by-layer assembly and investigated the effect of the Lytac-abMMP9 loading method/storage on the release profile as well as on the viability, morphology, and migratory capacity of fibroblasts derived from non-diabetic and diabetic patients. The capacity of the construct to absorb protein exudate was also assessed using simulated wound fluid.

Results

We observed a sustained release of Lytac-abMMP9 with a minimal amount after 1 day (~1–3nM, no difference between wet and stored, dry samples) and a marked increase after 2 days (~15–20nM). The results demonstrated that the membrane drying after loading does not compromise the Lytac-abMMP9 activity, suggesting that it can be used for the processing of on-shelf products. Wound closure was assessed after 1 and 3 days to distinguish early migratory responses from later proliferative effects. Scratch size decreased significantly over time in all groups (Fig.1), confirming progressive closure. At Day 1, control cultures showed impaired gap closure in aged non-diabetic (AND) and aged diabetic (AD) fibroblasts compared with non-aged non-diabetic (NAND) cells, demonstrating that aging reduces migratory capacity. HA/CHIT membranes, both loaded and unloaded, significantly enhanced early closure, indicating stimulation of cell motility and adhesion-related processes. HA/CHIT membranes improved wound closure in NAND and AND cells but not in AD cells. For AD cells, Lytac-abMMP9 was essential and only membranes loaded with Lytac-abMMP9 enhanced significantly the migratory capacity of aged diabetic fibroblasts. Additionally, all membranes increased absorption of protein from artificial wound exudate (***$p = 0.0004$).

Conclusion

The developed membranes exhibited sustained Lytac-abMMP9 release, efficient exudate adsorption and promoted early wound closure by enhancing fibroblast migration. Lytac-abMMP9 incorporation is crucial for restoring migratory capacity in aged diabetic cells.

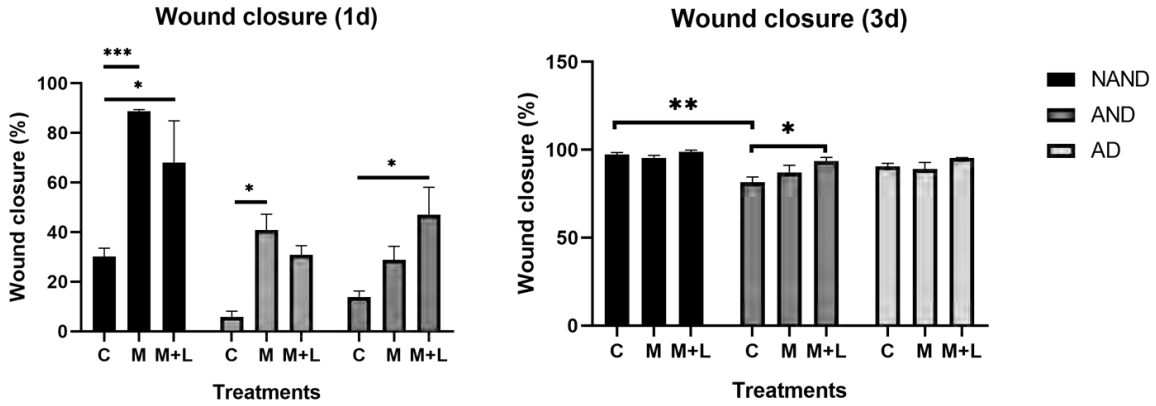

Figure 1 – Data obtained from scratch assay using cells from non-aged non-diabetic patients (NAND), aged non-diabetic (AND), and aged diabetic patients (AD). C- controls on tissue culture polystyrene, M- only LbL membranes, M+L- membranes loaded with Lytac-abMMP9

Acknowledgements
Portuguese Fundação para a Ciência e Tecnologia (FCT, grants 2022.03823.CEECIND/CP1718 /CT0003, 2022.00764.CEECIND/CP1718/CT0020), EC (EIC Pathfinder “Aptadegrad” HORIZON-EIC-2022-PATHFINDEROPEN-01-101099063).

S68 – O6

Biodegradable Wound Dressing Using a Synergistic Micro- and Nano-Architecture of Silica Gel and Poly(3-hydroxybutyrate) for Tissue Regeneration, as a platform technology for hydrophobic drugs: evaluation in a 3D In Vitro Full Thickness Skin Model

Nadler K.[1], Weigel T. [1], Şensözlüler S.[2], Soylu N.B.[2], Kozan S.[3], Kars M. D.[3], Kars G.[2], Probst J.[1], Dembski S.[1], Christ B.[1]

[1]Translational Center Regenerative Therapies TLC-RT, Fraunhofer Institute for Silicate Research ISC, Würzburg, Germany, [2]Faculty of Science, Dept. of Molecular Biology and Genetics, Necmettin Erbakan University, Konya, Türkiye, [3]Faculty of Engineering, Dept. of Biomedical Engineering, Necmettin Erbakan University, Konya, Türkiye

Introduction

Chronic wounds, affecting 1-2% of the population in industrialized countries, represent a significant healthcare burden, leading to continuous treatment needs, immobility, and pain.[1] Effective wound healing is critical, as disruptions can impede recovery and lead to chronicity. This study explores biodegradable wound dressings, combining silica-based fibers (RENACER®) that degrade to *ortho*-silicic acid (oSA) with electrospun poly(3-hydroxybutyrate) (PHB) fibers. This bilayer wound dressing is designed to address deep wound defects providing support through *µ*-structures while facilitating efficient cell migration via *sub-µ*-structures. Additionally, the scaffold serves as a platform for encapsulating hydrophobic active ingredients. Using human wounded *in vitro* full-thickness skin models (wFTSM) based on a synthetic membrane[2], this study evaluates healing efficacy, thereby addressing the lack for standardized testing systems in the management of deep wounds.

Materials and Methods

The wound dressing was developed by alternating layers of sol-gel-based, pressure-spun *µ*-silica fibers and electrospun *sub-µ*-PHB fibers (with and without carotenoids). The individual components (silica and PHB fibers) underwent material science and biological assessments, including gravimetric degradation, *in vitro* cytotoxicity tests, structural analysis, and mechanical testing. Then, the bilayered scaffold was evaluated using a quantitative collagen assay and cell migration behavior analysis. Wound healing was examined using a wFTSM with HE and IF staining and quantitative wound parameters.

Results

The properties of silica-based fleece were tunable for flexibility and cross-linking. oSA was identified as the degradation product that exhibited no cytotoxicity. Carotenoids were successfully incorporated into PHB fibers, achieving over 80% cell viability and 50% of ascorbic acid's antioxidant properties. A bilayered scaffold was produced that significantly increased collagen production and enhanced cell migration. *In vitro* wound healing experiments revealed that the bilayered scaffold promotes dermal wound regeneration and collagen production in the wound site.

Conclusion

The scaffold's efficiency in the wound model relies on an open-meshed silica structure integrated with ECM-like PHB *sub-µ*-fibers that support dermal healing. The incorporation of hydrophobic bacterial carotenoids acts as a ROS scavenger. Additionally, the dressing enhances collagen synthesis through silica degradation and the fibers' ECM-like properties. This combination of oSA-releasing *µ*-fibers and ECM-like *sub-µ*-structures shows significant potential for chronic wound management without the need of dressing changes. Future research should focus on addressing infections in chronic wounds by incorporating antifungals or antibiotics, evolving the dressing into a comprehensive drug delivery system for clinical applications.

Acknowledgements

This study was supported by the EU project REGENEU (no. 101079123) funded by Horizon Europe.

References

[1] Falanga V., et al. *Chronic wounds*. Nature reviews 2022, 8; 50.

[2] Weigel T. et al. Fully Synthetic 3D Fibrous Scaffolds for Stromal Tissues-Replacement of Animal-Derived Scaffold Materials Demonstrated by Multilayered Skin. *Advanced materials 2022*, 34, 10.

S69
Biomaterials across tissues and diseases

S69 – K1
Light-based bioprinting to pattern materials and guide cell behavior

Levato R.
Utrecht University, The Netherlands

S69 – O1

Non-vascularized abdominal rectus fascia as a natural biomaterial for cross-disciplinary soft-tissue reconstruction

Muylle E.[1], Van De Winkel N.[2], De Hertogh G.[3], da Cunha M.[1], Thorrez L.[4], Nafteux Ph.[1], De Leyn P.[1], D´Hoore A.[2], Pirenne J.[5], Ceulemans L.J.[1]

[1]Thoracic Surgery, KU/UZ Leuven, Belgium, [2]Abdominal Surgery, KU/UZ Leuven, Belgium, [3] Pathology, KU/UZ Leuven, Belgium, [4]Dept. of Development and Regeneration, KU Leuven Kulak, Kortrijk, Belgium, [5]Abdominal Transplant Surgery, KU/UZ Leuven, Belgium.

Introduction

Reconstruction of complex soft-tissue defects remains challenging due to the limitations of current synthetic and biologic biomaterials, which are prone to infection, degradation, and mechanical failure. Non-vascularized abdominal rectus fascia allotransplantation (NVRF-Tx) offers a native, unprocessed, three-layer scaffold comprising anterior and posterior rectus sheaths with peritoneum of a donor, after removal of the abdominal rectus muscles (Fig.1). Initially introduced in intestinal-Tx, where it achieved durable abdominal closure with low herniation rates, NVRF-Tx has demonstrated notable immune tolerance, supported by allogeneic animal models showing successful integration without immunosuppression. Since 2020, our center has expanded its application to diverse reconstructions in both immunocompetent and immunosuppressed patients. **Aim.** This study evaluates NVRF-Tx as a natural biomaterial, focusing on clinical scaffold performance, host integration, and immune response.

Materials and Methods

This single-center prospective study included all consecutive NVRF-Tx procedures between 09/2020-09/2025 at our centre. Donor fascia was preserved after procurement in Institut-George-Lopez-1 solution with gentamicin at 2°C. No ABO or human-leukocyte-antigen matching was performed. Primary outcomes were closure durability and hernia occurrence. Secondary endpoints included donor-specific antibody (DSA) formation and histological remodeling. Descriptive statistics were used, with results reported as median (IQR) or counts (%).

Results

A total of 47 NVRF-Tx (48 donors) procedures were performed in 41 patients for abdominal and chest wall reconstruction, as well as perineal, pericardial, and diaphragmatic defects (Table 1). During a median follow-up of 149 days (79–294), no clinical or radiological herniation occurred. No fascia-related complications were noted. One graft required replacement following repeated surgery for bowel leakage; three grafts were removed due to pancreatic leakage; and one was replaced during repeat multivisceral-Tx. No NVRF-related mortality occurred. Histology demonstrated neovascularization, fibroblast infiltration, and collagen deposition (Fig.1). DSA developed in 16 of 32 evaluable cases, without clinical impact. Eight deaths occurred, all unrelated to NVRF-Tx.

Conclusion

NVRF-Tx represents a natural biomaterial for reconstruction of complex defects. Its combination of mechanical strength, and capacity for host-driven remodeling positions it as a robust biomaterial with cross-disciplinary applicability.

Figure 1: Non-vascularized abdominal rectus fascia allotransplantation.

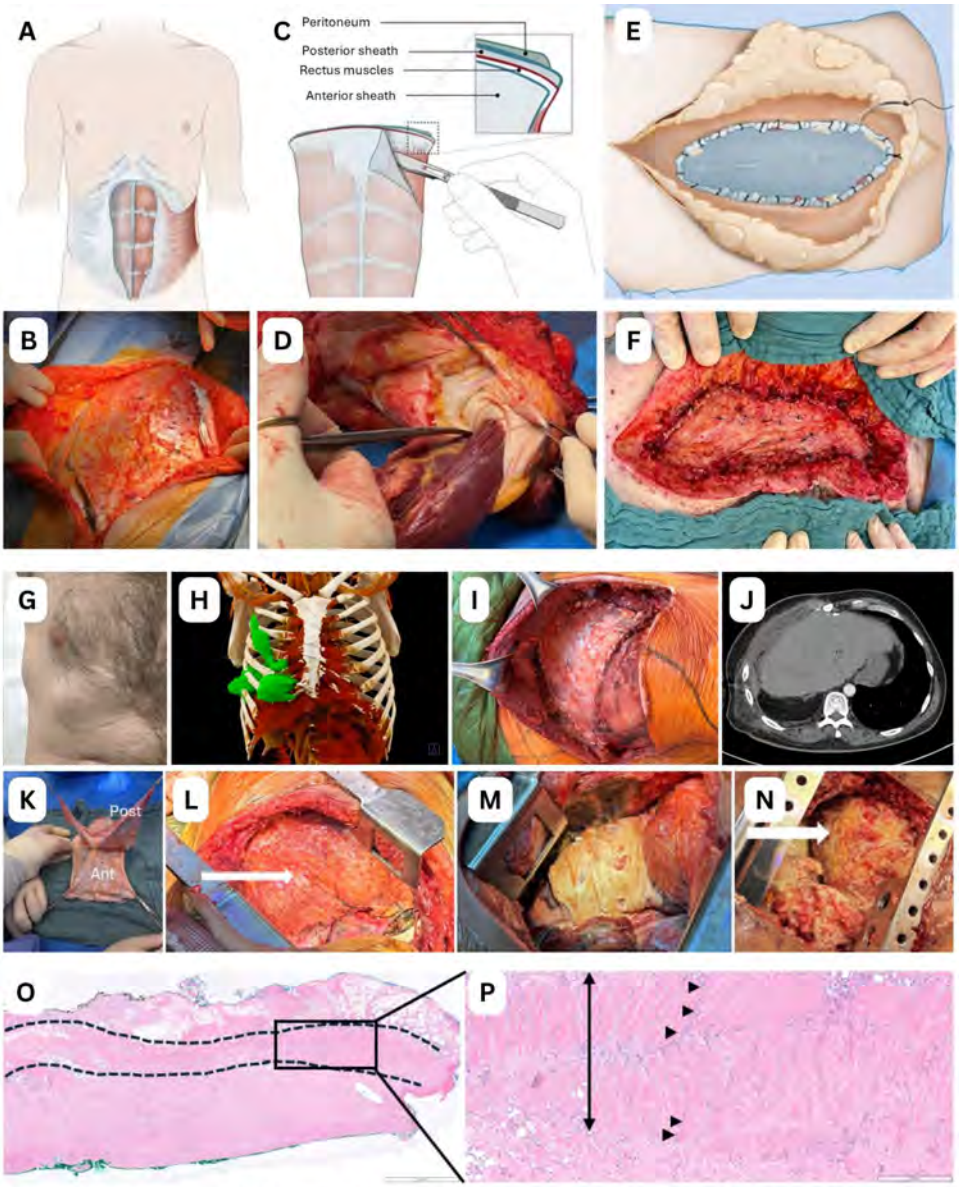

Figure 1. Non-vascularized abdominal rectus fascia allotransplantation (NVRF-Tx). A–B. Anatomical position of the rectus muscles in situ. After incision to the level of the anterior rectus fascia, lateral dissection is performed to fully expose the rectus compartment. **C–D.** Following procurement of the rectus block from the donor site, the rectus muscles are removed on the bench, leaving only the anterior and posterior rectus fascial sheaths with attached peritoneum. **E–F.** The NVRF graft is typically sutured as an inlay patch using a running Prolene suture. **G.** Preoperative clinical image showing palpable echinococcal masses located inframammary and along the right lateral thoracic wall. **H.** Three-dimensional reconstruction of a preoperative CT scan demonstrating echinococcal cysts located paracardially and in the right preperitoneal region, with invasion of the thoracic wall and the diaphragmatic dome both laterally and ventrally. **I.** Intraoperative image of the NVRF allograft covering the defect after excision of the echinococcal cysts, including resection of four ribs. **J.** CT scan 3 months after NVRF transplantation demonstrating an intact thoracic wall. **K.** Splitting of the anterior (Ant) and posterior (Post) rectus fascia sheaths on the back table. **L.** Intraoperative image showing reconstruction of the right hemidiaphragm using the anterior rectus fascia sheath (white arrow) after extended pleurectomy/decortication for disseminated thymoma; the anterior rectus fascia sheath is sutured to the ribs using non-absorbable braided polyester sutures (Ethibond® 0). **M.** For pericardial reconstruction, the posterior rectus fascia sheath is positioned with the peritoneal surface facing the heart and sutured circumferentially with non-absorbable monofilament polypropylene sutures (Prolene® 2/0) to restore pericardial continuity. **N.** Intraoperative image of the NVRF-allograft one month after diaphragmatic reconstruction during reintervention for persistent air leakage demonstrating a solid, well-integrated, and macroscopically neovascularized graft (white arrow). **O.** Hematoxylin and eosin (H&E) staining of a biopsy obtained 1 month after diaphragmatic reconstruction. The two dotted lines indicate the borders of the rectus fascia allograft. The green ink marks the peritoneal side, while the blue/black ink marks the thoracic side. On both sides of the allograft, newly formed, highly fibrotic tissue is present, with more pronounced deposition on the peritoneal side. **P.** Higher magnification detail (H&E) of the NVRF-allograft shown in panel M. The double black arrow indicate the NVRF-allograft, visible as discrete precipitated collagen fibers. Between these fragments, newly formed, highly cellular fibrotic host tissue is infiltrating the graft. Blood vessels within this tissue are observed; two vessels are indicated by black arrow heads.

Table 1: Donor and recipient characteristics.

DONOR CHARACTERSTICS (n=48)			
Donor type	DBD: 43/48 (89.6%) DCD: 5/48 (10.4%)	**Median age (years) (IQR)**	50 (35 – 63)
Sex	Female: 26/48 (54.2%) Male: 22/48 (45.8%)	**Median BMI (kg/m^2)**	24 (22 - 26)
Median preservation time of NVRF allograft (days) (IQR)	6 (2 - 16)	**Microbiological culture of NVRF allograft**	Positive: 7/47 (14.9%) Negative: 40/47 (85.1%) NR: 1/48
RECIPIENT CHARACTERISTICS (n=41)			
	Immunosuppressed patients		**Immunocompetent patients**
	Simultaneous NVRF-Tx with SOT (n=8)	Elective NVRF-Tx after SOT (n=9)	(n=24)
Median age (years) (IQR)	47 (42 - 50)	65 (60 - 74)	63 (53 - 69)
Sex	Female: 4/8 (50.0%) Male: 4/8 (50.0%)	Female: 3/9 (33.3%) Male: 6/9 (66.7%)	Female: 8/24 (33.3%) Male: 16/24 (66.7%)
Median BMI (kg/m^2)	20 (19 - 22)	25.4 (24.2 – 27.9)	24.2 (21.8 – 26.6)
Oncological setting	Yes: 0/8 (0.0%) No: 8/8 (100.0%)	Yes: 1/9 (11.1%) No: 8/9 (88.9%)	Yes: 12/24 (50.0%) No: 12/24 (50.0%)
Contaminated field	Yes: 0/8 (0.0%) No: 8/8 (100.0%)	Yes: 3/9 (33.3%) No: 6/9 (66.6%)	Yes: 12/24 (50.0%) No: 12/24 (50.0%)
Median length of total hospitalization (days) (IQR)	86 (72 - 111)	10 (7 - 16)	18 (13 - 31)
Median follow-up (days) (IQR)	241 (132 - 403)	225 (124 - 337)	121 (47 - 258)
Herniation (radiographic/ clinical)	Yes: 0/8 (0.0%) No: 8/8 (100.0%)	Yes: 0/9 (0.0%) No: 9/9 (100.0%)	Yes: 0/24 (0.0%) No: 24/24 (100.0%)
NVRF allograft removal	Yes: 4/12 (33.3%)* No: 8/12 (66.7%)*	Yes: 0/12 (0.0%)* No: 12/12 (100.0%)*	Yes: 1/26 (3.8%)* No: 25/26 (96.2%)*
DSA against NVRF allograft donor	Yes: 2/4 (50.0%) No: 2/4 (50.0%) NA/NR: 4/8	Yes: 1/7 (14.3%) No: 6/7 (85.7%) NA/NR: 2/9	Yes: 13/21 (61.9%) No: 8/21 (38.1%) NA/NR: 3/24
Patient survival	Yes: 4/8 (50.0%) No: 4/8 (50.0%)	Yes: 9/9 (100.0%) No: 0/9 (0.0%)	Yes: 20/24 (83.3%) No: 4/24 (16.7%)

*The total number does not equal the number of recipients, as some recipients received more than one fascia graft, and in some cases fascia from a single donor was used for multiple transplant procedures. DBD, donation after brain death; DCD donation after cardiac death; NVRF(-Tx), non-vascularized rectus fascia (transplantation); SOT, solid organ transplantation; IQR, interquartile range; BMI, body mass index; DSA, donor-specific antibodies; NA, non applicable; NR, not reported.

S69 – O2

Modulation of oxidative stress in cardiac fibrosis through chitosan hydrogels

Zoso A.[1], Cutietta G.[1], Hamouda I.[2], Montembault A.[2], Chiono V.[1]
[1]Dept. of Mechanical and Aerospace Engineering, Politecnico di Torino, Torino, Italy, [2]Ingénierie des Matériaux Polymères Laboratory, Villeurbanne, France

Introduction

Cardiac fibrosis is characterized by a state of oxidative stress, which contributes to disruption of cell homeostasis and inflammation through excessive production of reactive oxygen species (ROS) [1]. Chitosan, a biocompatible polysaccharide, has been reported to exhibit ROS scavenging activity depending on its molecular weight and degree of deacetylation [2].

Aim.

This work examines chitosan hydrogels as active biomaterials designed to modulate oxidative and inflammatory stresses in cardiac tissue.

Materials and Methods

Chitosan hydrogels (4-38% deacetylation degree, DA) were synthesized at varying concentrations. Oxidative stress conditions were reproduced in physiological medium by controlled ROS generation using an atmospheric pressure plasma jet (APPJ). Hydrogels antioxidant capacity was assessed by monitoring ROS depletion in APPJ-treated medium over 4 days through UV–Vis analysis. The ability of chitosan hydrogels to reduce cell oxidative stress was assessed on human cardiac fibroblasts (HCFs, Promocell) by measuring cell viability, and the expression of α-smooth muscle actin (α-SMA), Hypoxia-Inducible Factor 1-alpha (HIF-1) and extracellular matrix proteins involved in fibrotic transition (Collagen I, Fibronectin) through immunofluorescence. Ongoing studies are investigating hydrogels anti-inflammatory potential on murine macrophages (RAW 264.7, ATCC), analyzing their viability and CD86 expression after ROS stimulus with and without chitosan hydrogels.

Results

Chitosan hydrogels exhibited DA-dependent ROS neutralization, with intermediate DA values showing the highest activity. Under oxidative conditions, HCFs displayed reduced viability and increased expression of fibrotic markers (α-SMA, collagen I, fibronectin). Treatment with chitosan hydrogels preserved cell viability and significantly reduced the expression of these markers.
HIF-1α expression induced by ROS was also decreased in the presence of chitosan hydrogels. Preliminary results in macrophages support their potential anti-inflammatory effect, showing increased cell viability and reduced CD86 expression.

Conclusion

These results demonstrate the antifibrotic effect of chitosan hydrogels through the mitigation of oxidative and inflammatory stresses. Further investigation will unfold chitosan hydrogels potential in cardiac regenerative medicine.

Acknowledgements

This work was conducted within the EU project PACGEL (Grant No. 101067882).

References

[1] Y. E. Kim and J. Kim, ACS Appl. Mater. *Interfaces 2022*, 14, 23002−23021.
[2]A. Kim S. International Journal of Polymer Science. *Vol. 2018*, 2018.

S69 – O3

Dual-detectable nanoparticles for tracking cell fate in autoimmune diseases

García-Fernández L[1,2], García Hernández R[3], Nakal-Chidiac A[1], Palao-Suay R[1,2], Martín-Saldaña S[1,2], García-Grande A[4], Coronado MJ[5], Zamora Cañadas C[3], Martín-Saavedra F[2,6], Escudero-Duch C[3,6], Sánchez-Casanova S[3,6], Vilaboa N[3,6], Cussó L[7,8,9], Salinas B[7,8,9], Desco M[7,8,9], Sánchez-López AJ[3,10], Aguilar MR[1,2]
[1]Instituto de Ciencia y Tecnología de Polímeros (ICTP), CSIC, Madrid, Spain, [2]Centro de Investigación Biomédica en Red de Bioingeniería, Biomateriales y Nanomedicina (CIBER-BBN), Instituto de Salud Carlos III, Spain, [3]Neuroimmunology Unit, Madrid, Spain, [4]Flow Cytometry Core Facility, Madrid, Spain, [5]Confocal Microscopy Facility, Madrid, Spain, [6]Instituto de Investigación Hospital Universitario La Paz (IdiPAZ), Madrid, Spain, [7]Unidad de Medicina y Cirugía Experimental, Hospital General Universitario Gregorio Marañón, Instituto de Investigación Sanitaria Gregorio Marañón (IiSGM), Madrid, Spain, [8]Departamento de Bioingeniería, Universidad Carlos III, Madrid, Spain, [9]CIBER de Salud Mental, Instituto de Salud Carlos III, Madrid, Spain, [10]Biobank, Hospital Universitario Puerta de Hierro Majadahonda/Instituto de Investigación Sanitaria Puerta de Hierro-Segovia de Arana, Madrid, Spain

Introduction

This study aimed to develop a multimodal imaging system using polymeric nanoparticles to track disease-related cells. Multimodal imaging combines techniques like near-infrared (NIR) optical imaging and magnetic resonance imaging (MRI) to leverage their respective strengths for enhanced diagnostic accuracy and treatment monitoring.

Polymeric nanoparticles, particularly those based on biocompatible materials like chitosan, are ideal for such applications due to their versatility and ability to encapsulate both imaging agents and therapeutic compounds. To enable NIR imaging, IR-820 fluorescent probe was used as ionic crosslinker of chitosan-palmitic acid nanoparticles, as encapsulation can improve the dye's biocompatibility and stability. For MRI tracking, they incorporated an alginate-based magnetic ferrofluid into the same nanoparticles.

The specific goal was to monitor the circulation pattern of encephalitogenic cells (EC), which are autoimmune T-cells that infiltrate the central nervous system and drive multiple sclerosis (MS) pathology. By loading these nanoparticles into ECs before injecting them into an adoptive transfer experimental autoimmune encephalomyelitis (at-EAE) mouse model in orderto understand disease mechanisms and potentially guide future therapies for MS.

Materials and Methods

Dual-detectable NP were synthesized by ionic gelation, incorporating the fluorescent probe IR-820 and magnetic ferrofluid (A-FF). NP were incubated with EC to allow NP internalization and were visualized by NIR and MRI. The tocicity of the NPs and the capacity to promote MS on NP-loaded EC was studied *in vitro. In vivo* cell fate was monitored using MRI and NIR in a at-EAE model

Results and Conclusion

A multimodal tracking system was successfully developed using chitosan-palmitic acid NP crosslinked with IR820 and loaded with alginate stabilized magnetic ferrofluid. The engineered NP were endocyted by EC NPs produced a slight decrease in cell metabolic activity, but it was maintained over 75% at all tested concentrations (Figure 1a), allowing tracking of the EC by both MRI and NIR imaging (Figure 1b). When tested *in vivo*, the NP did not interfere with the onset of at-EAE, thereby confirming its suitability for monitoring EC distribution without compromising the induction or progression of the disease (Figure 1c).

The MRI signal from NP was appreciated in the peritoneal cavity immediately after the inoculation, and no signal changes with respect to baseline images were detected afterwards. The developed NP enabled efficiency *ex vivo* tracking of EC fate post-inoculation using NIR. Dual-imaging that combined NIR fluorescence from IR820 and reflection imaging from A-FF was validated through *ex vivo* analyses (Figure 1d). The *ex vivo* analysis demonstrated that NP-labelled EC can cross the blood-brain barrier within the first 24 h.

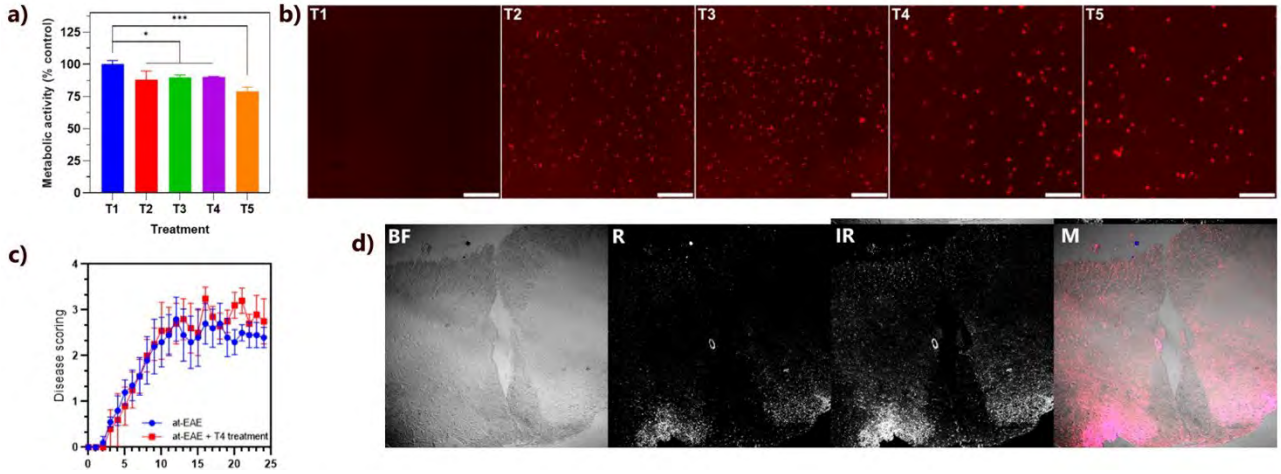

Figure 1. Evaluation of NP-labeled EC with different NP treatments (T1: EC without NP; T2: EC incubated with a 1:50 dilution of NP loaded with 2.5 µg/mL A-FF; T3: EC incubated with a 1:100 dilution of NP loaded with 2.5 µg/mL A-FF; T4: EC incubated with a 1:50 dilution of NP loaded with 25 µg/mL A-FF and T5: EC incubated with a 1:100 dilution of NP loaded with 25 µg/mL A-FF. **a)** Relative metabolic activity of EC incubated for 72 h. Data are presented as mean ± standard deviation (n=3). Statistical analyses were performed using one-way analysis of variance (ANOVA) and Bonferroni's multiple comparison test to determine statistically significant differences: $*p < 0.05$; $**p < 0.01$ and $***p < 0.005$. **b)** Confocal pictures of EC loaded with the different treatments. Scale bars: 20µm. **c)** Disease scoring of animals treated with unlabeled EC or EC incubated with T4 treatment. Data are presented as mean ± standard deviation (n=5). **d)** Confocal microscopy (20x) of cryostat sections of the spinal cord with T4-labeled EC. BF: Bright-field image of the tissue. R: Reflectance confocal microscopy image. IR: Infrared confocal image. M: Merge showing the presence of iron (blue) and IR-820 (red). Scale bars: 10µm

This work provides a deeper understanding of the EC trafficking, including kinetics and targeted tissues, and will enhance the knowledge of disease processes and support the development of innovative therapies aimed at modulating cell migration into the CNS.

Acknowledgements

This work was supported by:

- Spanish Ministry of Science, Innovation, and Universities: grants PID2023-149301OB-I00, PID2023-149734NB-C21 and PID2021-126325OB-I00 funded by MICIU/AEI (DOI: 10.13039/501100011033) and by ERDF/EU
- Instituto de Salud Carlos III (ISCIII): Project PT23/00027, co-funded by the European Union.
- Comunidad de Madrid: Projects S2022/BMD-7406 (RADIOPROTECT-CM) and S2022/BMD-7403 (RENIM-CM)
- Centro de Investigación Biomédica en Red, Instituto de Salud Carlos III. (Refs. CB06/01/0013 and CB06/01/0008).

This research was performed within the framework of the Nanomedicine CSIC HUB (Ref. 202180E048).

S69 – O4

Next-Generation Gelatin-Alginate Cryogels Coated with Dopamine and Combined with TGF-β and FAK Inhibitors for Effective Hypertrophic Scar Management

Giol E-D, Cecoltan S, Șerbănescu A-D, Tofan V-C, Țucureanu C, Ionescu I-E, Caragheorgheopol R, Stăvaru C, Caraș I
Cantacuzino National Military Medical Institute for Research and Development, Romania

Introduction

An abnormal response to injury may lead to the formation of aberrant scars, such as keloid and hypertrophic scars (HTS), a phenomenon characterized by excessive fibrosis formation and an often complications in burn, trauma and surgery. World-wide, wound and scar treatments bear a significant financial burden on the healthcare system, with billions of dollars spent and multiple patients suffering pain, itching, stiffness, loss of sensation or loss of joint mobility. Current prophylaxis and treatments focus on approaches interfering with pathologically disorganized wound healing processes (scar reduction therapies), nonetheless, there is a lack of topical dressings customized for pathological needs that arise during the wound healing process, such as haemostasis, inflammation, proliferation and remodeling - the four main stages that occur during healing.

Aim

Herein, we propose a novel approach based on gelatin-alginate cryogels coated with dopamine, to act as haemostatic agent, and contain scarless tissue formation promoters (TGF-ß and FAK inhibitors) known to reduce myofibroblast transdifferentiation and consequently fibrosis.

Materials and Methods

Gelatin-alginate (GEL-ALG) cryogels were obtained by crosslinking a mixture of 10% GEL solution with 2% ALG solution. Calcium-based or EDC/NHS – based crosslinking agents were used as such or together to crosslink under subzero conditions. Subsequently, a pDA-coating was applied using Messersmith's protocol and various incubation times (3h and 24h) to fine-tune haemostatic and adhesion properties. APTT values were determined using a StagoMax coagulometer and swelling capacity, dimensional stability and release profiles were investigated under relevant physiological conditions (37◦C, PBS or cell culture medium). In vitro cytotoxicity and scratch assay was performed on HaCaT cells.

Results

To address the current limitations in HTS treatments cryogels obtained from biocompatible polymers (GEL-ALG), highly used and applied in biomedical applications, with well-known reported-protocols for modification, crosslinking and processing, were coated with dopamine, an emerging haemostatic agent, and combined with a mixture of TGF-β and FAK-inhibitors. Non-cytotoxic cryogels, up to 1000% swelling degrees and aPTT values lower than poor-platelet-plasma and manufacturer normal conditions' control. Scratch assays proved the biological activity of the released SB-431542 and PF-562271 inhibitors.

Conclusion

In vitro experiments showed promising results for designed cryogels as candidates for reducing hypertrophic scar formation and in vivo testing is scheduled in the near future.

Acknowledgements

This work was supported by a grant of the Ministry of Research, Innovation and Digitization, CCCDI - UEFISCDI, project number PN-IV-P7-7.1-PED-2024-1578, SCARSTOP, within PNCDI IV.

S69 – O5

Zwitterionically modified guar gum for 3D bioprinting of anti-biofouling cell-laden biomaterials

Swilem A.[1,2,3], Hartley A.[1], Xie F.[1,4], Leese H. S.[1,3]
[1]Dept. of Chemical Engineering, University of Bath, UK, [2]Dept. of Chemistry, Ain Shams University, Cairo, Egypt, [3]Centre for Bioengineering and Biomedical Technologies (CBio), University of Bath, UK, [4]Chongqing Key Laboratory of Speciality Food Co-Built by Sichuan and Chongqing, College of Food Science, Southwest University, Chongqing, China

Introduction

Advances in 3D bioprinting now allow fabrication of cell-laden biomaterials for tissue engineering,[1] yet bioink development remains constrained by the limited range of biomaterials that can be reliably printed into complex 3D-structures. Functions of implanted bioprinted constructs is further hindered by biofouling and foreign body reaction, which can trigger cellular overgrowth, fibrosis, and reduced nutrient and oxygen transport to encapsulated cells. To tackle this challenge, zwitterionic polymers, which form super-hydrated, charge-balanced surfaces, have emerged as promising candidates for creating ultra-low-fouling biomaterials.[2]

Aim

This work aims to develop zwitterionic guar gum-based bioinks that resist biofouling while maintaining suitable printability.

Materials and Methods

Zwitterionic guar gum (ZGG) was synthesised by reacting guar gum (GG) with 3-((3-chloropropyl)dimethylammonio)propane-1-sulfonate in an isopropanol/water mixture using KOH. To enable photocrosslinking, ZGG was functionalised with methacryloyl groups via methacrylic anhydride, yielding ZGGMA. Gelatin methacryloyl (GelMA) was prepared following standard protocols. Chemical structures, degree of substitution (DS) and molecular weight (M_w) were confirmed by ^{1}H NMR and GPC. Biocompatibility was assessed using C2C12 cells. Rheological properties, including shear-thinning, amplitude sweep and recoverability, were measured. Bioinks were formulated in PBS with LAP photoinitiator (0.1% w/v) and photocured under 365 nm UV light. An open-source extrusion bioprinter was assembled for printability studies.[3] Mechanical properties and morphology of crosslinked hydrogels were examined. Antifouling behaviour was evaluated via adsorption of fluorescein-labelled albumin. Printability was assessed through filament formation and collapse tests with microscopic imaging.

Results

^{1}H NMR confirmed successful synthesis of ZGGMA with a DS of 0.1 (Fig. 1a). Zwitterionic modification reduced the viscosity of GG due to increased hydrophilicity and partial degradation (Fig. 1b); therefore, rheological properties were tuned by blending ZGGMA with GGMA (Fig. 1c). Cytotoxicity assays showed good biocompatibility. ZGGMA hydrogels reduced non-specific protein adsorption by ca. 50% compared with GGMA (Fig. 2b). Mechanical testing for ZGGMA6% hydrogels showed compressive moduli around 40 kPa (Fig. 2a), but this can be modulated through crosslinking density and formulation to match the mechanical range of various tissues.[4] Bioinks demonstrated good printability through optimisation of polymer concentration, composition, and printing parameters (Fig. 2c-e). Cryo-SEM revealed a microporous network (1.4 µm) (Fig. 2f). A coaxial bioprinting setup was developed to produce core–shell constructs using GelMA-encapsulated cells as the core.

Conclusion

Developed ZGGMA-based bioinks exhibited antifouling behaviour, biocompatibility, and mechanical properties suitable for soft tissue engineering, showing strong potential for cell-encapsulation therapies.

Acknowledgements

EPSRC (EP/Z00201X/1); Imaging facility team at the University of Bath

References

[1] Jeon J., Park H., Leach J.K., Alsberg E. Biofabrication of engineered tissues by 3D bioprinting of tissue specific high cell-density bioinks. *Materials Today* 2025; 86; 172-182.

[2] Liu Q., Chiu A., Wang L.H. et al. Zwitterionically modified alginates mitigate cellular overgrowth for cell encapsulation. *Nature Communications* 2019; 10; 5262.
[3] https://www.instructables.com/OPEN-SOURCE-BIOPRINTER/
[4] Cox T.R., Erler J.T. Remodeling and homeostasis of the extracellular matrix: implications for fibrotic diseases and cancer. *Dis Models Mechanisms* 2011; 4; 165-178.

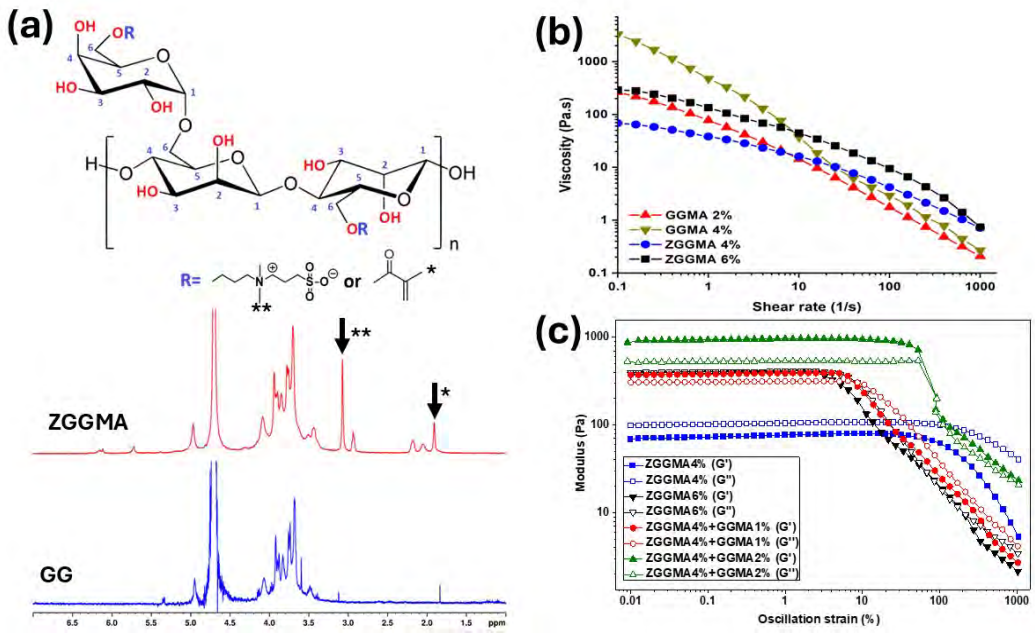

Fig. 1. (a) chemical structure of ZGGMA and ^{1}H NMR spectra; (b) shear-thinning behaviour of ZGGMA and GGMA; (c) amplitude sweep for ZGGMA and ZGGMA/GGMA blends

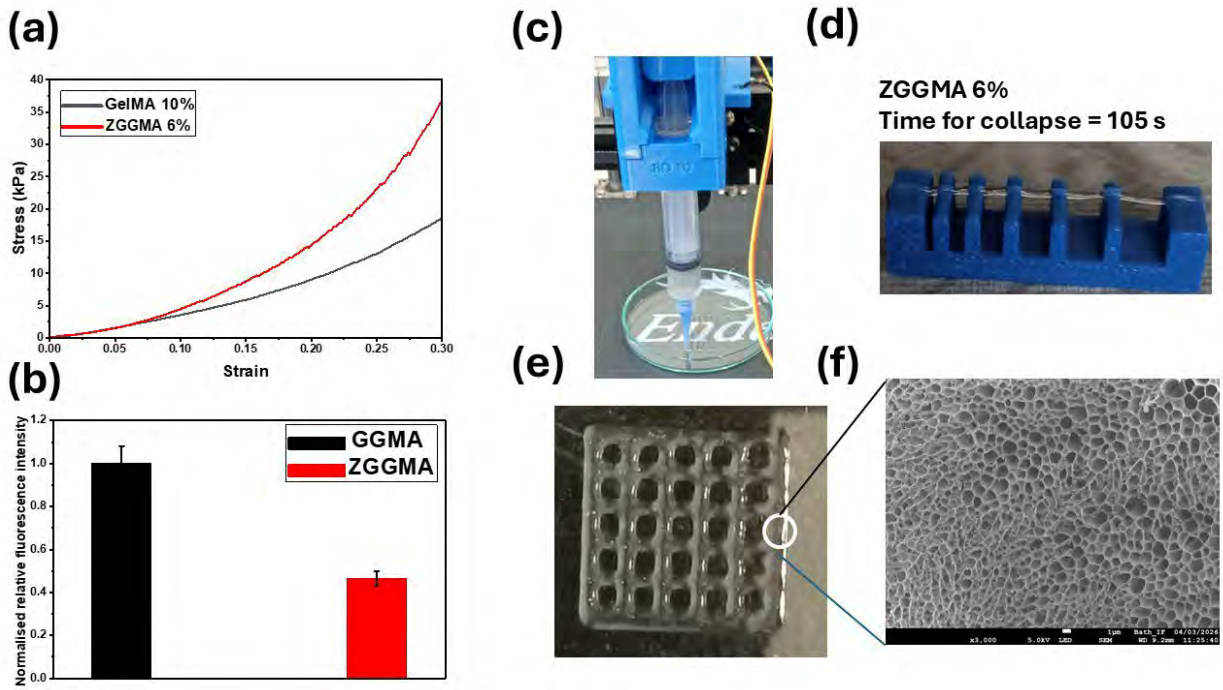

Fig. 2. (a) Stress-strain curves for ZGGMA 6% and GelMA 10%; (b) normalised anti-fouling behaviour of ZGGMA compared with GGMA (n=3); (c) open-source bioprinter; (d) filament collapse test for ZGGMA 6%; (e) and (f) a photographic and cryo-SEM images of bioprinted ZGGMA 6% in PBS solution after curing with UV light for 2 min., respectively

S69 – O6

Recreating the Liver Microenvironment with Human-Derived Biomaterials

Lobo M.C [1,2], Rufino A.T.[1], Mano J.F.[2], Custódio C.[1,2]
[1]Metatissue – Biosolutions, Lda, PCI- Creative Park Aveiro Region, Ílhavo, Portugal, [2]Dept. of Chemistry, CICECO, University of Aveiro, Campus Universitário de Santiago, Portugal

Introduction

Drug development remains lengthy and inefficient, with approval timelines often exceeding ten years and success rates from Phase I to market launch below 10%. Drug-induced liver injury (DILI) accounts for 18–30% of drug withdrawals, highlighting the need for improved preclinical hepatotoxicity prediction. Conventional animal models poorly replicate human liver physiology and metabolism, limiting their translational relevance. Consequently, there is growing interest in human-relevant three-dimensional (3D) *in vitro* models that better mimic the hepatic microenvironment while reducing animal use. Biomaterial-based systems that reproduce the extracellular matrix (ECM) are particularly promising, as they provide structural, biochemical, and mechanical cues essential for hepatocyte function.

Aim

This work aims to develop a biomimetic human liver model using protein-based biomaterials within a xeno-free culture system.

Materials and Methods

A xeno-free culture system for HepG2 hepatocyte-like cells was established by comparing conventional culture medium supplemented with fetal bovine serum (FBS) and with human platelet lysates (hPL). Cell proliferation and metabolic activity were evaluated, and hepatic functionality was assessed through urea synthesis and cytochrome P450 (CYP450) activity. To recreate the liver microenvironment, HepG2 cells were encapsulated in photocrosslinkable hydrogels composed of methacryloyl-modified human platelet lysates (hPLMA) and methacryloyl-modified decellularized ECM (dECM-MA). Different formulations were evaluated to optimize hydrogel composition and cell density. For validation, a hepatotoxicity evaluation was performed using DILI concern drugs (acetaminophen, ibufenac, busulfan) and evaluating their effect in the metabolic activity and functionality of HepG2 cells encapsulated in the hydrogels.

Results

hPL supplementation supported cell proliferation and metabolic activity comparable to FBS, while maintaining hepatic functionality, including urea synthesis, and CYP450 activity. Encapsulation studies revealed that hydrogels containing 10% hPLMA and 0.7% dECM-MA (1:1) with a cell density of 10×10^6 cells/mL generated a soft ECM-rich matrix with mechanical properties like native liver tissue and promoted high cell viability and sustained metabolic activity. Furthermore, a metabolic dose-response curve of the DILI concern drugs was established for the encapsulated cells, demonstrating the permeability of the hydrogel matrix.

Conclusion

The integration of hPLMA and dECM-MA enables the development of a human-derived, xeno-free 3D culture platform capable of sustaining hepatocyte-like cell function. This biomimetic system provides physiologically relevant biochemical and mechanical cues, representing a promising strategy to improve hepatotoxicity prediction and support more reliable preclinical drug screening.

Acknowledgements

This work was developed within the scope of the project CICECO Aveiro Institute of Materials, UID/50011/2025(DOI 10.54499/UID/50011/2025) & LA/P/0006/2020(DOI 10.54499/LA/P/0006/2020), financed by national funds through the FCT/MCTES (PIDDAC). MCL thanks FCT through PDQI for her PhD grant ref. 2024.03688.BDANA.

S69 – O7
From Scientific Innovation to a Viable Product

Trappenburg D.
Smart Biomaterials Center (SBMC)

Biomaterials are increasingly applied across a broad range of tissues and diseases, from orthopaedic and cardiovascular applications to wound healing and regenerative medicine. They can function as stand-alone medical devices, as carriers or delivery systems for pharmaceuticals, or as scaffolds and matrices in combination with cells. While a growing number of biomaterial-based products have successfully reached patients, many new technologies are still being developed by start-ups, industry and academic research groups.
This presentation provides an overview of the biomaterials landscape, highlighting companies that have successfully brought biomaterial-based products to the market as well as companies developing the next generation of biomaterial applications. By comparing applications across indications and product concepts, it illustrates both the breadth of opportunities and the different development routes biomaterials can follow.
However, translating a promising biomaterial from academic research into a viable healthcare product requires considerably more than demonstrating scientific performance. Academic development often focuses on mode of action, formulation optimisation, laboratory studies, animal studies and publications. Successful product development additionally requires early consideration of reproducibility, intellectual property, scalability, manufacturing, sterilisation, quality management and regulatory strategy.
The intended indication and clinical setting are equally important. Understanding the target patient population, who provides and pays for the treatment, and which stakeholders influence adoption determines requirements for production volumes, manufacturing processes, costs and implementation in the healthcare system.
Using practical observations from working with biomaterial innovators, this presentation discusses common gaps in academic business and product development plans and demonstrates why regulatory strategy, quality management, process engineering, analytical development and financing should be considered early rather than sequentially at the end of R&D.
The key message is that successful biomaterial innovation requires parallel development of the science, the product, the manufacturing process and the business case. Bringing these perspectives together early can reduce development risks, prevent costly redesign and improve the pathway from promising research to clinical application.

S70
Biomaterials combined with cells (Cell-Instructive materials)

S70 – K1
Chain-selective presentation of RGD in static and dynamic double-network hydrogels modulates hMSC mechanotransduction and secretome

Baker, M.
Maastricht University, The Netherlands

S70 – K1

Włodarczyk-Biegun, M.,
University of Groningen/Silesian University of Technology, The Netherlands

S70 – O1

Engineered cell-laden hemostatic hydrogels for all-round rapid repair of diabetic wounds and liver bleeding

Malay Nayak[1], Sudip Mukherjee*[1]
[1]Cell Therapy Laboratory, School of Biomedical Engineering, Indian Institute of Technology, Banaras Hindu University, IIT (BHU), Varanasi, UP, India

Introduction

The complex microenvironment of diabetic wounds, characterized by persistent inflammation, impaired angiogenesis, and compromised hemostasis, severely delays healing and presents a significant clinical challenge. Current therapies often lack the multi-faceted approach required to address these interwoven pathologies effectively.

Aim

In this work, we aim to develop an engineered cell based hemostatic hydrogel secreting multimodal therapeutic factors targeting blood clotting, reducing inflammation and all-round rapid healing of diabetic chronic wounds.

Materials and Methods

Herein, we present a novel cell-based therapeutic platform: precision-engineered human embryonic kidney (HEK 293T) cells encapsulated within alginate hydrogels, designed for diabetic wound repair and liver hemostasis. HEK 293T cells are stably engineered via a PiggyBac transposon system to co-express pro-angiogenic human Vascular Endothelial Growth Factor A (hVEGFA), hemostatic Factor VIII (hFVIII), and immunomodulatory Interleukin-10 (hIL10), ensuring sustained secretion of these therapeutic factors.

Results

In vitro studies confirmed hVEGFA-mediated elevation of cell migration and wound closure, hFVIII stimulated acceleration of blood clotting, and hIL10's role as a potent anti-inflammation reducing oxidative stress. A synergistic combination of hVEGFA, hFVIII, and hIL10 notably achieved superior *in vitro* and *in vivo* wound healing (Figure 1). In a diabetic rat full-thickness excisional wound model, administration of these engineered cell-laden hydrogels significantly accelerated wound closure within 2 weeks. Furthermore, cell-secreted hFVIII demonstrated remarkable hemostatic efficacy when mixed with human blood *ex vivo* and in a liver puncture model, reducing blood loss and clotting time *in vivo*.

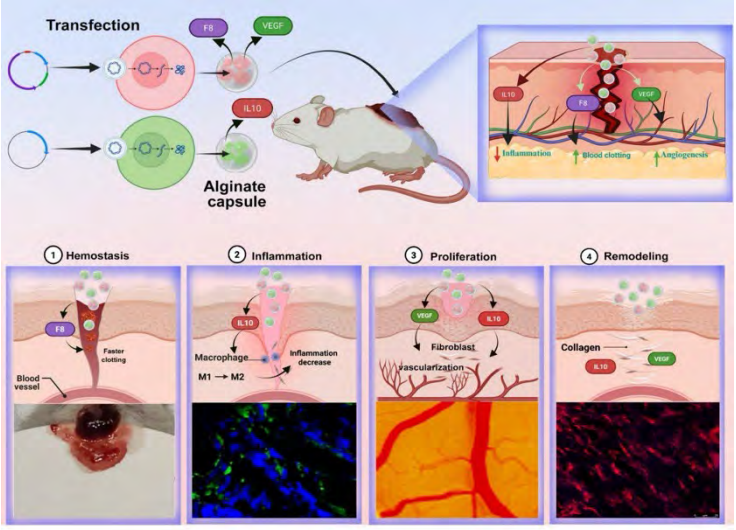

Figure 1: Overall schematic diagram developing an engineered cell laden hemostatic hydrogel for rapid healing of diabetic wound

Conclusion

This multi-functional cell-based hydrogel system offers a comprehensive and promising platform for rapid attenuation of homeostasis for rapid diabetic wound healing. Although some ethical considerations are there, we will target this therapy for a clinical trial in the near future.

S70 – O2

Engineering an Immuno-instructive Mucus for Inflammatory Bowel Disease

Blacklock L[1], Moran G[1], Mata A[2], Ghaemmaghami A[1]
[1]Faculty of Medicine & Health Sciences, University of Nottingham, Nottingham, UK, [2] Faculty of Science, University of Nottingham, Nottingham, UK

Introduction

Inflammatory Bowel Disease (IBD) is a chronic disease with no cure that causes stomach cramps, diarrhoea and bloody stools, severely impacting patients' quality of life. Usually, a mucus layer separates gut commensal bacteria from the epithelial cells in the intestines. In IBD, due to genetic and environmental predisposition, the epithelial cell tight junction connections breakdown so mucus production and quality are reduced. This results in a loss of cellular protection by the mucus which creates bacterial dysbiosis and continual activation of the intestinal immune system, that causes chronic inflammation and wounding of the gut lining. Current IBD treatments have many side effects. To address this, we aim to restore gut homeostasis using immuno-instructive biomaterials based on peptide amphiphiles, that are synthetically derived amphiphilic molecules that self-assemble into hydrogels in aqueous environments.

Aim

To engineer specific peptide amphiphile sequences with pro-healing and anti-inflammatory properties that form a hydrogel within the intestinal mucus layer, and to show efficacy in restoring epithelial barrier integrity in an *in vitro* IBD model.

Materials and Methods

Peptide amphiphiles were generated using solid phase peptide synthesis and endowed with an immuno-instructive epitope known as DGEA, designed to repolarise macrophages to an anti-inflammatory M2 phenotype[1]. Hydrogels were cultured with intestinal cell lines Caco-2 and HT29-MTX-E12 that secrete mucus to recapitulate the epithelial lining of the intestines and to test the integration with the native mucus layer. Hydrogels were cultured with the monocytic cell line THP-1 to identify an immuno-instructive response by measuring cytokine release via enzyme-linked immunosorbent assay.

Results

Figure 1 shows cytokine expression of naïve THP-1 derived macrophages (M0) in the presence of the immuno-instructive hydrogel DGEA or with additional IL-4, compared to cells polarised to pro-inflammatory (M1-like) or anti-inflammatory (M2-like) phenotypes. The results demonstrate that the DGEA hydrogel suppresses TNF-α and IFN-γ expression, signature pro-inflammatory cytokines while not seeming to suppress anti-inflammatory cytokines TGF-β and IL-1 receptor antagonist. Figure 2 shows a scanning electron micrograph of heterogenous fibre network formed when the hydrogels were assembled upon mucus-producing cell lines and incubated under standard cell culture conditions overnight.

Fig 1.

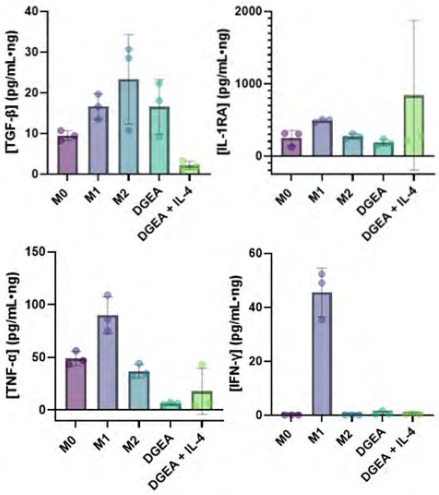

Fig 2.

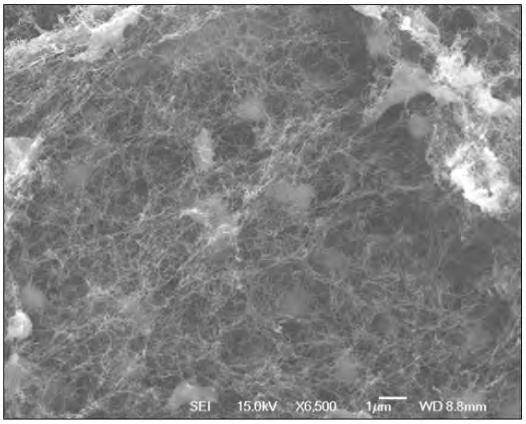

Conclusion

The peptide amphiphile hydrogels demonstrate immuno-instructive capacity to reduce pro-inflammatory cytokine expression as well as to integrate within the native cellular mucus. Future projections are to further probe the immuno-instructive capacity of the hydrogels using an immunocompetent intestinal cell model and to better define the gel properties of the cellular mucus-hydrogel system.

Acknowledgements

Authors would like to acknowledge funding from the Medical Research Council, Wellcome Trust and Innovate UK [MIMIC Cluster. Grant No: UKRI3162]. The work was financially supported by the NIHR Nottingham Biomedical Research Centre at University of Nottingham, Nottingham, UK; the project AOCMF-21-04S from the AO Foundation, AO CMF. The AO CMF is a clinical division of the AO Foundation — an independent medically guided not-for-profit organisation; and La Caixa, HR25-00392: Loco-radiolysed Treatment for Glioblastoma Self-Enhanced Chemotherapy and Targeted RNA Delivery.

References

[1]Byung-Hyun Cha., Su Ryon Shin., Jeroen Leijten., Yi-Chen Li., Sonali Singh., Julie C. Liu., Nasim Annabi., Reza Abdi., Mehmet Dokmeci., Nihal Engin Vrana., Amir M. Ghaemmaghami., Ali Khademhosseini. Integrin-Mediated Interactions Control Macrophage Polarization in 3D Hydrogels. *Advanced Healthcare Materials* 2017; 2192-2640.

S70 – O3

Beyond conductivity: conductive polymers as local regulators of electrical and redox microenvironments

Humpolíček P[1], Vícha J[1], Vašíček O[2], Muchová M[1], Valášková K[1]
[1] Tomas Bata University in Zlín, Zlín, Czech Republic, [2] Institute of Biophysics of the Czech Academy of Sciences, Brno, Czech Republic

Introduction

Conductive polymers, particularly polypyrrole (PPy), have long been regarded primarily as electrically active materials in biomedical engineering. However, our group has demonstrated that their biological relevance extends far beyond conductivity. PPy and its composites exhibit intrinsic reactive oxygen species (ROS)-scavenging activity, making them potent modulators of oxidative stress and, consequently, of immune cell behaviour and downstream inflammatory signalling.

Aim

This work aims to connect a validated hydrogel platform for small intestine tissue models with the concept of PPy-based conductive, ROS-scavenging domains. We outline how a layered, ECM-inspired scaffold with crypt–villus architecture can serve as a host in which PPy-containing regions may be positioned to achieve spatially local control over the electrical and redox microenvironment.

Materials and Methods

Layered hydrogel scaffolds were prepared from interpenetrating networks of collagen I and thiolated hyaluronan (HA-SH) and cast into cell culture inserts with a permeable membrane. Gelation at physiological pH and temperature yielded thin layers whose composition could be tuned to adjust mechanical properties. Crypt–villus-like topography was created by imprinting precisely 3D-printed forms into the pre-gel solution and keeping them in place during swelling, resulting in stable crypt-like depressions. These COL/HA-SH scaffolds were used to assess basic cytocompatibility and epithelial response using Caco-2 cells, and to correlate layer composition with stiffness and architecture via rheology and microscopy.

Results

Scaffolds could be reproducibly patterned into crypt-like geometries that remained stable after swelling and supported Caco-2 adhesion on the surface and within the depressions. Adjusting HA-SH content allowed systematic tuning of scaffold elasticity, providing physiologically relevant stiffness ranges between layers. This validates the COL/HA-SH system as a structurally and mechanically controllable host for more complex intestinal models. Within this framework, PPy-based composites, combining electrical conductivity and ROS-scavenging activity, are identified as candidate phases to be locally integrated into selected regions to co-shape electrical and redox conditions.

Conclusion

Data demonstrate a robust, patterned COL/HA-SH hydrogel platform that mimics key features of the small intestine and supports epithelial growth in crypt-like structures. Building on this foundation, locally positioned PPy-based conductive, ROS-scavenging domains could in next steps transform conductive polymers from passive conductors into dual-function regulators of the intestinal microenvironment, enabling spatially targeted modulation of both electrical and oxidative cues.

Acknowledgements

This work was supported by the Czech Science Foundation (grant 25-17718S) and by the Ministry of Education, Youth and Sports of the Czech Republic – DKRVO (RP/CPS/2022/001).

S70 – O4

Engineered recombinant strategies to organohydrogel design for tissue engineering

Lee TY[1], Gautrot JE[1]
[1]School of Engineering and Materials Science, Queen Mary, University of London, UK

Introduction

Cell-instructive hydrogels have emerged as promising biomaterials for tissue engineering. However, synthetic cell-instructive, for example, based on PEG or hyaluronic acid hydrogels often suffer from weak mechanical properties and are inherently nanoporous, requiring cell-mediated degradation and/or high degree of stress relaxation in order to promote cell spreading. In contrast, 3D cell spreading in fibrin or collagen gels is fast and enables rapid cell migration. However, synthetic hydrogels enabling the control of microporosity have been challenging to achieve. To address these pitfalls, we propose cell-instructive colloidal gels composed of microdroplets that enable the control of porosity and tunable mechanical properties. We apply the resulting organohydrogels to mimic adipose tissues for the regulation of stem cell phenotypes for tissue engineering.

Materials and Methods

Oil-in-water microdroplets stabilised by engineered protein nanosheets displaying peptides for supramolecular crosslinking (e.g. fibrin binding, phenylalanine/cucurbituril, zinc binding) were generated via homogenisation. Subsequent incubation with complementary motifs resulted in dynamic colloidal networks. The schematic of the organohydrogels is illustrated in Figure 1. For protein engineering, peptides were coupled onto albumins via thiol-ene reaction. Rheological measurements were conducted to characterise mechanical properties of resulting organohydrogels. Bioactive motifs were incorporated into the protein through recombinant expression. The recombinant proteins were used to prepare the organohydrogels for cell culturing. Bone marrow-derived mesenchymal stem cells (MSCs) were cultured on the organohydrogels to evaluate cytocompatibility and further characterised via confocal microscopy and flow cytometry.

Results

Three peptides based on different supramolecular interactions were designed and coupled to the proteins to generate corresponding organohydrogels. Storage moduli between 100 and 1000 Pascal were achieved with different formulations. The resulting soft organohydrogels demonstrated shear-thinning properties. Yeasts were transformed to express proteins with bioactive peptides. The conditions for producing and extracting the recombinant proteins were optimised. The obtained proteins were used to prepare emulsions for MSC culture. Various formulations were used in cell cultures to examine cell adhesion and spreading with the organohydrogels generated. MSCs rapidly adhered to the surface of microdroplets and proliferated in these materials to comparable levels to cells adhering to 2D tissue culture plastic, as shown in Figure 2.

Conclusion

The results demonstrate that supramolecular crosslinking of engineered microdroplets is an efficient strategy to form organhohydrogels based on colloidal networks. This can generate dynamic and tunable colloidal cell-instructive materials that support stem cell maintenance and proliferation.

Acknowledgements

Funding from the ERC (ProLiCell, 772462) and BBSRC (LIDo, BB/T008709/8) is gratefully acknowledged.

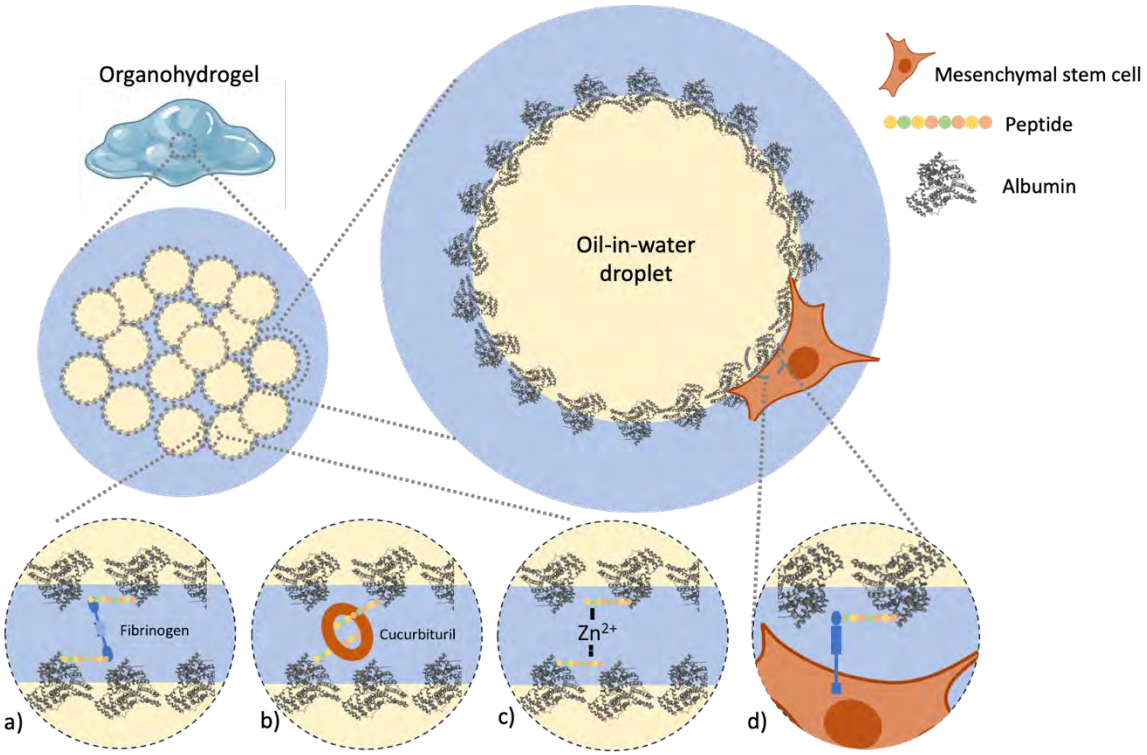

Figure 1. Schematic of organohydrogel formed with a colloidal network of oil-in-water microdroplets. The droplets are crosslinked with different supramolecular interactions facilitated by peptides: a) fibrin binding, b) phenylalanine/cucurbituril and c) zinc binding. d) Bioactive peptides interact with cells to promote cell adhesion.

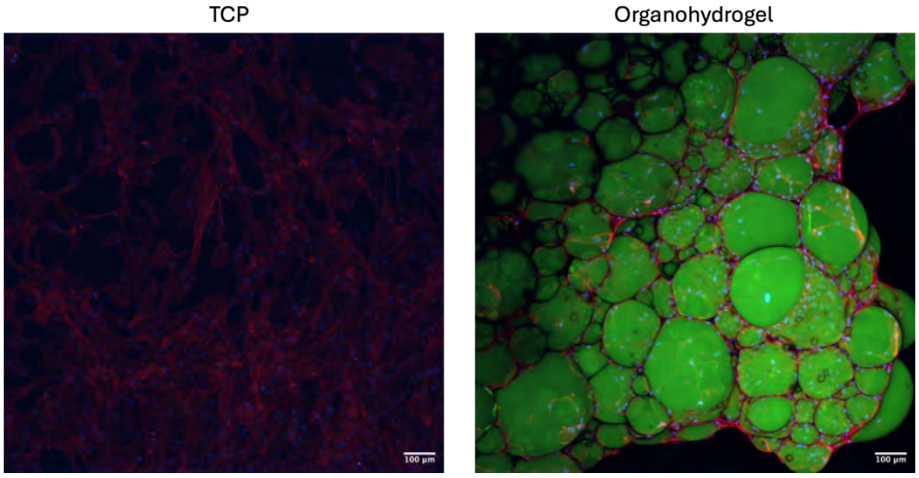

Figure 2. Confocal images of MSC cultures after 7 days on a) tissue culture plastic (TCP) and b) organohydrogels (blue, DAPI; red, phalloidin; green, BODIPY 493/503).

ESB 2026

Building a gradient scaffold to support enthesis repair using SHED cells

R. Wandless[1], D.Y.S. Chau[1], H.W. Kim[2,3], J.C. Knowles[1,2]
[1] Division of Biomaterials and Tissue Engineering, UCL Eastman Dental Institute, University College London, Royal Free Hospital, Rowland Hill Street, London, NW3 2PF, UK [2] Eastman-Korea Dental Medicine Innovation Centre, Dankook University, Cheonan, 31116, South Korea [3] Institute of Tissue Regenerative Engineering (ITREN), Dankook University, Cheonan 330-715, Republic of Korea

Introduction

The tendon-to-bone enthesis is a transition zone with mineralisation and stiffness gradients that allow force transmission from muscle to bone without damage. Examples include the periodontal ligament (PDL) and the Achilles tendon insertions, which are regularly damaged by excessive force or inflammatory disease[1]. Current research focuses on bone marrow or tendon stem cells, but limitations include low availability and invasive harvesting[2]. Stem cells from human exfoliated deciduous teeth (SHED) offer a potential alternative because they are obtained non-invasively, differentiate into multiple cell types, and have immunomodulatory properties that reduce fibrosis.

Aim: This project aims to develop a collagen scaffold with a mechanical stiffness gradient that mimics the tendon-to-bone enthesis. The scaffold will support differentiation of stem cells into bone, cartilage, and tendon within a single structure and investigate stem cell behaviour in environments with different mechanical stiffness.

Materials and Methods

SHED cells (IX Cells Biotechnologies, USA) were cultured in StemFIT 3D well inserts (MicroFIT, Republic of Korea) to form spheroids. After 24 hours, the media was replaced with neutralised Rat Tail Collagen (First link, UK). The stiffness of the hydrogel was altered in 3 ways: increasing the collagen concentration, genipin crosslinking and compression. Collagen stiffness was assessed by DMA, and the fibre arrangement was visualised through SEM and AFM. Differentiation of SHED was induced with the addition of 100mM dexamethasone, 10mM sodium BGP and 1ug/ml ascorbic acid (bone), 10ng/ml TFG-B (cartilage) and TGF-B and 100ng/ml CTGF (tendon) to DMEM media and incubated for 28 days. Differentiation was determined by PCR and IHC imaging.

Results

DMA showed increased Young's modulus from 0.2 kPa up to 2.7 kPa with higher collagen concentration, 2.2 kPa with genipin crosslinking, and up to 80 kPa with compression (fig. 1). Encapsulation of SHED cells in collagen hydrogels show migration of SHED cells as they branch from the spheroids after 24 hours, with less contraction of the hydorgel compared to ADSC. Differentiation of SHED cells was shown through IHC staining and PCR analysis with an increase of differentiation markers by day 28 (fig. 2).

Conclusion

SHED cells show promising potential for use in enthesis repair. They have significant advantage over other stem cell types in building larger tissue constructs due to less invasive harvesting techniques, high differentiation capacity, migratory ability with less contraction and immunomodulatory properties. The stiffness of collagen hydrogels can be manipulated to support differentiation of SHED cells into multiple cell types to be used in the construction of larger tissue constructs.

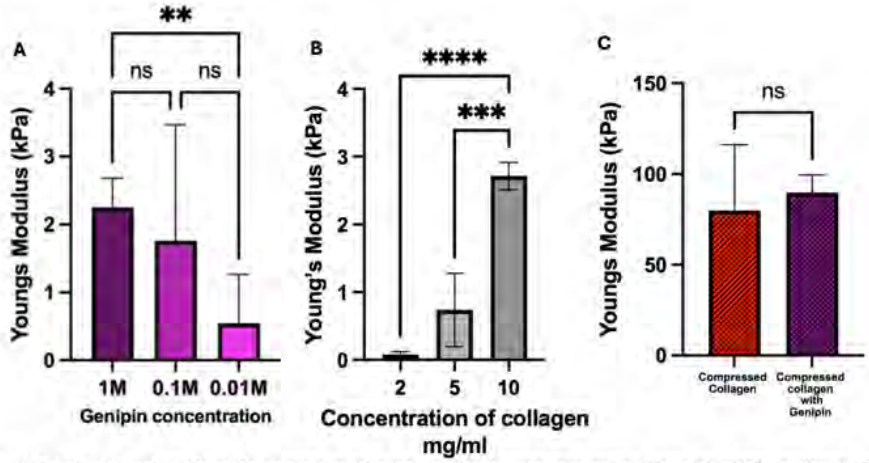

Fig 1: Graphs showing Young's modulus of collagen hydrogels assessed through DMA analysis. The stiffness of the collagen was altered through genipin crosslinking (A), increasing the concentration of collagen (B) and compression (c)

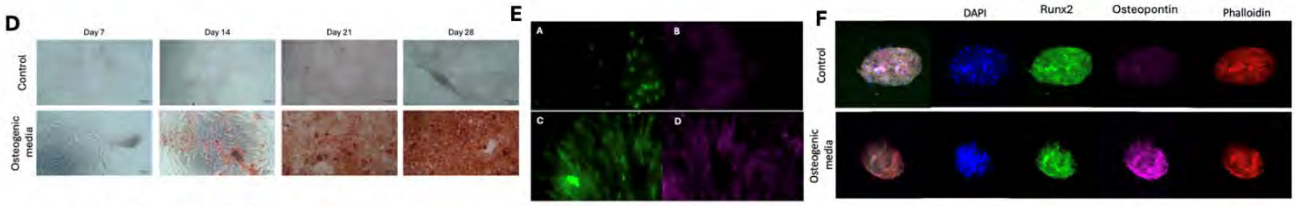

Fig 2: D: Alizarin red staining showing mineralization of SHED cells in 2D culture in control and osteogenic media. E: IHC staining and confocal imaging of SHED cells grow in control media (EA/EB) and osteogenic media (EC/ED) with RUNX2 (green) and Osteopontin staining at day 28. F: confocal images of RUNX2 and Osteopontin staining at day 21 in 3D spheroid culture

References

1.Killian, M. L. Growth and mechanobiology of the tendon-bone enthesis. *Semin. Cell Dev. Biol.* **123**, 64–73 (2022).
2.Wang, L. *et al.* Comparative effect of skeletal stem cells versus bone marrow mesenchymal stem cells on rotator cuff tendon-bone healing. *J. Orthop. Transl.* **47**, 87–96 (2024)

S71
Biomaterials for bone and cartilage regeneration

S71 – K1
Engineering cartilage with structured light

Zenobi-Wong, M.
ETH Zurich, Switzerland

Human tissues are permeated by physiological spaces at the organ, tissue, cellular, and molecular levels. These spaces provide critical means of transport, communication, signal propagation, morphogen diffusion, cellular crosstalk, and localized biochemical reactions. Given their omnipresent nature, structuring hydrogels to contain tissue-specific "void" spaces becomes a critical factor in scaffold design.

In this presentation, I describe how structured hydrogels can promote the formation of zonally organized articular cartilage, particularly using filamented light (FLight) biofabrication. This technique can reproduce the orthogonal arrangement of collagen fibers in the deep and superficial layers. We also show that patterning the hydrogel with macroscopic channels improves the histological and mechanical properties of cartilage. Finally, when light is applied through an image-guided fiber, it becomes possible to fill ex vivo cartilage lesions with structured hydrogels.

S71 – K2

Human protein-based ultrathin membranes toward the development of self-assembled cell aggregates for osteo differentiation.

Pires-Santos M.[1], Monteiro C.F.[1], Mano J.F.[1]
[1]CICECO - Aveiro Institute of Materials, Department of Chemistry, University of Aveiro, Portugal.

Introduction

Tissue engineering has increasingly focused on developing scaffolds that support intrinsic cell behavior and promote microenvironments resembling native tissue. Yet many current approaches rely on predefined architectures that passively host cells. Here, we present a fully human-derived system in which cells actively remodel their substrate, autonomously sculpting dynamic three-dimensional (3D) microenvironments.

Materials and Methods

Ultrathin membranes were produced by solvent casting of amyloid-like nanofibrils formed from human platelet lysate methacryloyl (hPLMA) in the presence of the ionic liquid cholinium tosylate.[1] To modulate the membrane properties, the fibrillar network was produced by varying the concentration of hPLMA, yielding membranes with distinct thicknesses. Bone marrow mesenchymal stem cells (BM-MSCs) were seeded on top of the membranes. The viability, metabolic activity, 3D self-organization, and osteogenic differentiation were assessed through confocal imaging, ALP activity assays, ELISA, RT-qPCR, and Proteomics. Morphometric parameters (area and circularity) were used to characterize cell-driven folding.

Results

Both membrane formulations supported cell adhesion and proliferation. However, hPLMA concentration directly influenced thickness and thus folding capacity. Membranes with higher hPLMA content exhibited increased thickness, resulting in reduced folding efficiency and larger, less compact aggregates. Under osteogenic stimulation medium, constructs exhibited increased circularity and upregulation of osteogenic markers (OSP, ALPL, RUNX2, COL1A1, DCN) while maintaining increased viability without necrotic core formation (Figure 1).

Conclusion

This system provides a bioactive and tunable platform where cells shape their 3D microenvironment according to their needs, offering a promising and novel strategy for osteoregenerative tissue engineering.

Acknowledgements

This work was developed within the scope of the project CICECO Aveiro Institute of Materials, UID/50011/2025 (DOI 10.54499/UID/50011/2025) & LA/P/0006/2020 (DOI 10.54499/LA/P/0006/2020), financed by national funds through the FCT/MCTES (PIDDAC). Manuel Pires-Santos acknowledge the Portuguese Foundation for Science and Technology for the doctoral grant 2024.01120.BD. This work was financed by the European Research Council Advanced Grant “REBORN” (ERC-2019-ADG-883370).

References

[1]Monteiro, C. F., et al. ACS Nano (2024). 18 (24).

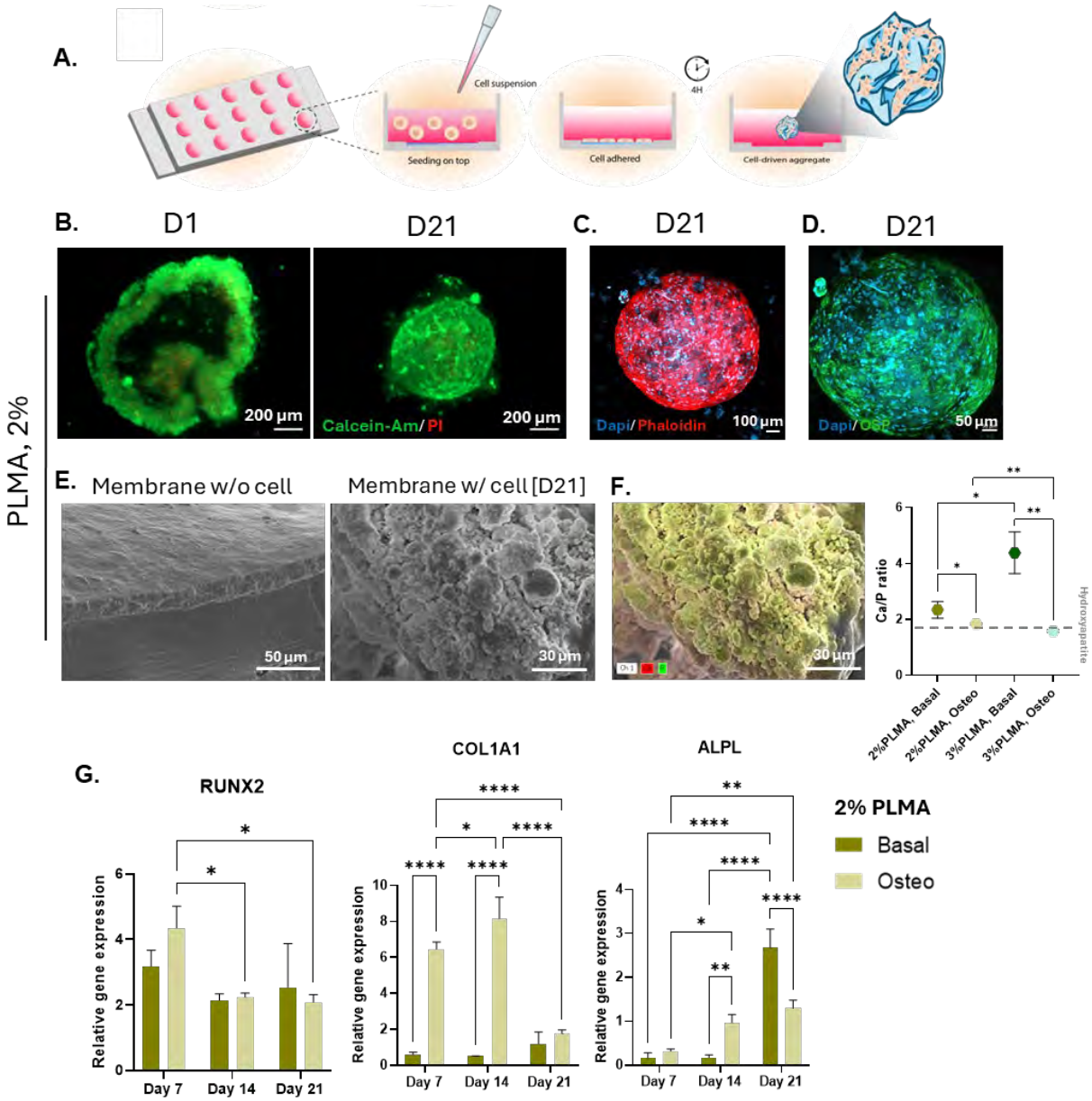

Figure 1. Human protein-based ultrathin membranes toward the development of self-assembled cell aggregates for osteo differentiation. (A) Schematic representation of the cell-driven folding process of human protein–based ultrathin membranes leading to the formation of cell–membrane aggregates. (B) Live/dead viability assay of cell–membrane aggregates throughout 21 days of culture. (C) Cellular organization and distribution within the aggregates at day 21, assessed by DAPI/phalloidin staining. (D) Immunofluorescence staining of osteopontin in cell–membrane aggregates after 21 days of culture. (E) Scanning electron microscopy (SEM) images of the membrane before and after cell seeding. (F) SEM-EDS analysis of cell–membrane aggregates after 21 days of culture showing the calcium/phosphate ratio. (G) RT-qPCR analysis of osteogenic gene expression (RUNX2, COL1A1, and ALPL) in basal and osteogenic conditions over time.

S71 – O1

The promoting effect of *Balanus albicostatus* cement protein 19k (Balcp19k)

Biru Hu, Jing Wang
College of Science, National University of Defense Technology, Changsha city, Hunan Province, China

The high incidence of skin wounds remains a significant challenge in clinical settings. Dressing materials, infused with bioactive components, are essential and extensively utilized in specific circumstances. According to traditional Chinese medicine therapeutic regimens, powders made of the flesh/shells of *Balanus albicostatus* were used to treat sores due to their ability to alleviate inflammatory responses. Nevertheless, information is scarce regarding the effective components and the pharmacological mechanisms involved. In this work, purified *Balanus albicostatus* cement protein 19k (Balcp19k) was obtained as a single-component material via an *E. coli*-based heterologous expression system. It had the potential to promote fibroblast proliferation and migration, which were crucial for wound healing.

Immunofluorescence revealed that Balcp19k treatment promoted M2 macrophage transformation in wound tissues. Correspondingly, the expression of inflammation-related genes (e.g., IL-6, TNF-α, and IFN-γ) was significantly reduced ($p < 0.05$). Moreover, histological examination indicated that this treatment accelerated skin-wound healing by promoting collagen fiber deposition and angiogenesis, and restraining inflammatory cell infiltration in the full-thickness skin of mice. In conclusion, Balcp19k is a biocompatible, effective constituent found in *Balanus albicostatus*. This bioactive protein could be novel therapeutic material for wound healing, with ability to regulate fibroblast migration, alleviate early-stage inflammatory responses, and enhance collagen fiber deposition and angiogenesis.

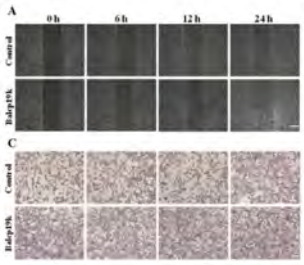

Fig.1 Effect of Balcp19k on NIH 3T3 cell migration

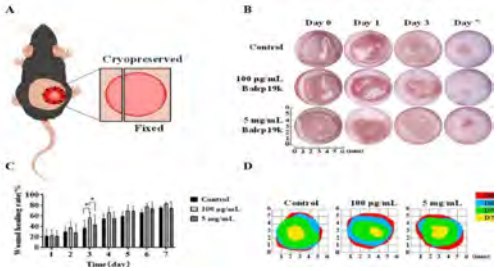

Fig.**2** Effects of Balcp19k with different concentrations on wound healing in mice

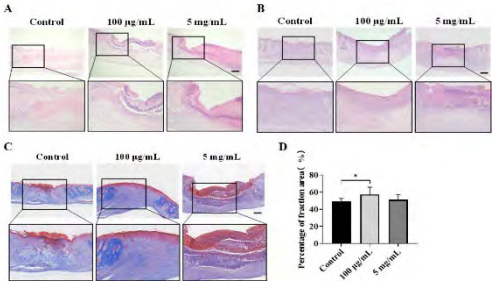

Fig.3 Histological evaluation of Balcp19k in the wound treatment.

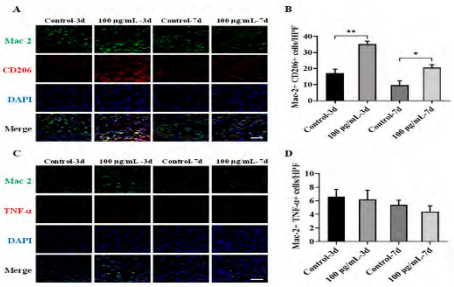

Fig.4 Immunofluorescence assay for macrophage polarization.

1] Liang Chao, Li Yunqiu, Liu Zhiming, Wu Wenjian and Hu Biru. Protein Aggregation Formed by Recombinant cp19k Homologue of Balanus albicostatus Combined with an 18 kDa N-Terminus Encoded by pET-32a(+) Plasmid Having Adhesion Strength Comparable to Several Commercial Glues. PLoS One 2015, 10, e0136493.

[2] Junyi Song , Ling Zeng , Zijian Ye , Peng Lu , Chengyu Jing , Biru Hu, Hao He, The promoting effect of Balanus albicostatus cement protein 19k (Balcp19k) on wound healing by regulating fibroblast migration and relievingearly-stage inflammation responses, International Journal of Biological Macromolecules, 289 (2025) 138781

Materials and Methods

Firstly, highly purified Balcp19k was prepared using the E. coli-based heterologous expression system and chromatography. Secondly, treatment with 100 μg/ mL Balcp19k significantly facilitated fibroblast proliferation and migration in vitro cell assays. Then Balcp19k was applied to full-thickness skin wounds in mouse models. Finally, inflammation-related biomarkers were quantitatively analyzed using immune-fluorescence and real-time PCR

Results

purified Balanus albicostatus cement protein 19k (Balcp19k) was obtained as a single-component material via an E. coli-based heterologous expression system. It had the potential to promote fibroblast proliferation and migration, which were crucial for wound healing. Immunofluorescence revealed that Balcp19k treatment promoted M2 macrophage transformation in wound tissues. Correspondingly, the expression of inflammation-related genes (e.g., IL-6, TNF-α, and IFN-γ) was significantly reduced ($p < 0.05$). Moreover, histological examination indicated that this treatment accelerated skin-wound healing by promoting collagen fiber deposition and angiogenesis, and restraining inflammatory cell infiltration in the full-thickness skin of mice.

S71 – O2

Biomimetic modification of hyaluronic acid – adipic acid hydrazide hydrogels with chondroitin sulfate and collagen

Walczak K.[1], Reczyńska-Kolman K.[1], Pamuła E.[1]
[1]Dept. of Biomaterials and Composites, Faculty of Materials Science and Ceramics, AGH University of Krakow, Krakow, Poland

Introduction

Hyaluronic acid (HA)-based hydrogels crosslinked with adipic acid dihydrazide (ADH) are promising biomaterials for tissue engineering due to their biocompatibility and tunable properties. However, their limited bioactivity and structural complexity restrict their ability to fully mimic the extracellular matrix (ECM)[1]. To overcome these limitations, incorporation of chondroitin sulfate (CS) and collagen is investigated. CS enhances hydration and regulates cell signaling, while collagen provides structural support and cell adhesion sites[2]. Such modifications are expected to improve the biological performance of HA-ADH hydrogels and better replicate the native tissue microenvironment.

Aim

The aim of this study is to modify HA-ADH hydrogels through the incorporation of chondroitin sulfate and collagen, and to comprehensively evaluate their physicochemical properties and biological performance in order to assess their potential for biomimetic tissue engineering applications.

Materials and Methods

Oxidized hyaluronic acid (oxi-HA) was prepared by reacting HA with sodium periodate ($NaIO_4$) for 24 h in the dark, followed by quenching with ethylene glycol, dialysis (5 days), and freeze-drying. For hydrogel formation, oxi-HA and adipic acid dihydrazide (ADH) were dissolved in distilled water at 4 °C and mixed at a 4:1 volume ratio to form a crosslinked network. Oxidized chondroitin sulfate (oxi-CS), prepared via periodate oxidation, was incorporated as an additional aldehyde source to enhance crosslinking and bioactivity, while recombinant human collagen was introduced as a fibrillar phase forming an interpenetrating network (IPN). Self-healing was evaluated by sample cutting and recovery time measurement. Microstructure was analyzed using optical microscopy and SEM. Swelling and mass changes were assessed in PBS, while FTIR confirmed chemical modifications. Biological properties were evaluated on L929 fibroblasts using Live/Dead staining, and AlamarBlue assay.

Results

Modifications with chondroitin sulfate and collagen improved the biological response of the hydrogels on L929 fibroblasts, while FTIR spectra confirmed successful chemical functionalization. In particular, FTIR analysis of oxi-HA indicated the formation of aldehyde groups, whereas spectra of oxi-HA/ADH hydrogels confirmed the presence of newly formed N–H bonds, evidencing crosslinking. The hydrogels exhibited self-healing properties, with structural recovery observed within 30 minutes after cutting. Microscopic analysis revealed a porous microstructure. Additionally, the materials demonstrated high water uptake capacity, with rapid swelling observed within the first 24 hours of incubation in PBS, indicating their potential for biomedical applications.

Conclusion

The developed system represents a promising biomaterial, and this study enabled the identification of the most suitable formulations for further development of ECM-mimetic hydrogels in the form of microgels.

Acknowledgements

This study was supported from the subsidy (No 16.16.160.557) and by the Program „Excellence initiative – research university" for the AGH University of Krakow.

References

[1] Wang L., Zhang H., Wu J., Li Y. Advances in hyaluronic acid-based biomaterials for biomedical applications. *Biomaterials Science* 2025; 13; 1021–1045.
[2]Nguyen B.B., Chiu K.L., Arun V., Panitch A., Carney R.P. Chondroitin sulfate/hyaluronic acid-blended hydrogels suppress chondrocyte inflammation under pro-inflammatory conditions. *ACS Biomaterials Science & Engineering* 2024; 10; 3242–3254

S71 – O3

Microfluidic Wet-Spinning of Aligned Collagen–GAG Fibers for Cartilage Repair

Wagner K. N.[1], Roger Y.[2,3], Pykacz E.[4,5], Plettenburg O.[4,5], Hoffmann A.[2,3], Brüggemann D.[1]
[1] Biophysics and Applied Biomaterials, Hochschule Bremen - City University of Applied Sciences, Germany
[2] Biological Basics for Biohybrid Implants, Dept. of Orthopedic Surgery Hospital, Hannover Medical School, Germany, [3] Lower Saxony Center for Biomedical Engineering, Implant Research and Development (NIFE), Hannover, Germany, [4] Medical Chemistry, Institute of Organic Chemistry, Leibniz University Hannover, Germany
[5] Institute of Medicinal Chemistry, Molecular Targets and Therapeutics Center, Helmholtz Zentrum München (GmbH), Germany

Introduction

The superficial zone of articular cartilage is the first region affected by osteoarthritis and consists of densely packed, horizontally aligned collagen fibers and glycosaminoglycans (GAGs) like chondroitin sulfate (CS) and hyaluronic acid (HA). Due to the limited self-healing capacity of cartilage, new scaffold materials that mimic the mechanical and biological properties of native cartilage tissue are required. Wet-spinning via microfluidic systems is frequently used to generate aligned collagen fiber scaffolds. However, this technique requires high collagen concentrations of up to 30 mg/mL, limiting resource efficiency and scalability. Moreover, the fabrication of GAG-containing collagen fibers using microfluidic wet-spinning has not yet been reported.

Aim

This study aims to establish a microfluidic wet-spinning process to produce aligned collagen fibers at low protein concentrations, while enabling the addition of GAGs.

Material and Methods

Collagen type I spinning solutions were analyzed by turbidity measurements after mixing with polyethylene glycol (PEG) and GAGs in acidic medium. A microfluidic chip was designed to enable wet-spinning of aligned fibers from collagen-PEG solutions. Fibers were collected in a PBS bath and subsequently cross-linked. Fiber morphology and composition were analyzed by scanning electron microscopy (SEM) and attenuated total reflection-Fourier-transform-infrared (ATR-FTIR) spectroscopy, respectively. Biocompatibility was evaluated using human bone marrow–derived mesenchymal stem cells.

Results

Mixing collagen type I with PEG in acetic acid resulted in nanofibrous structures with diameters of 31 ± 11 nm, that remained below the detection limit of turbidity measurements. The addition of CS promoted collagen fiber assembly, as indicated by increased absorbance values and confirmed by SEM analysis of dried fibers. The designed microfluidic chip enabled continuous flow conditions, resulting in the fabrication of aligned fibers at collagen concentrations as low as 1 mg/mL, with an alignment degree of 30 ± 10% (Figure 1A and 1B). SEM analysis confirmed the presence of characteristic D-banding patterns in wet-spun collagen fibers, indicating preservation of the native fibrillar structure (Figure 1C). ATR-FTIR measurements verified the absence of PEG in wet-spun fibers, confirming efficient removal of the crowding agent during fiber formation. Subsequent cell culture experiments on self-assembled collagen nanofibers demonstrated good proliferation and typical mesenchymal stem cell morphology, indicating good cytocompatibility of the scaffolds.

Conclusion

Microfluidic wet-spinning combined with molecular crowding enabled the fabrication of aligned collagen–GAG nanofibers from low protein concentrations, with GAG addition promoting collagen self-assembly. This strategy represents a resource-efficient route to fabricate scalable cartilage-mimetic fiber scaffolds.

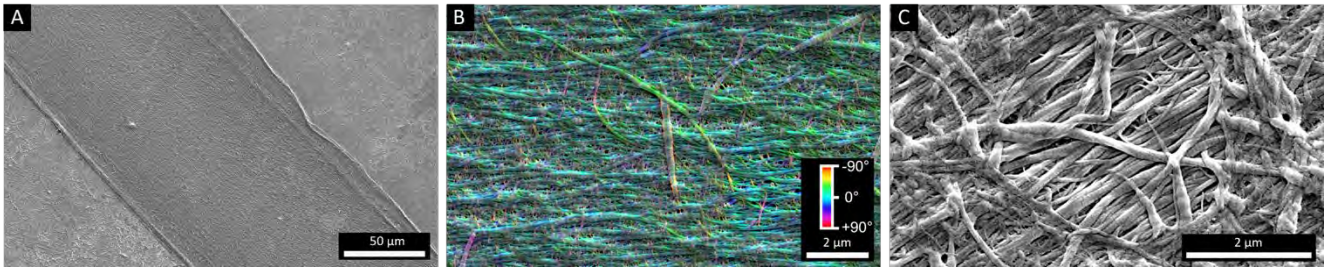

Figure 1: SEM images of wet-spun collagen fibers. (A) Wet-spun collagen microfiber on glass comprised of aligned nanofibers. (B) Orientation analysis of collagen nanofibers using OrientationJ (ImageJ plugin). Color map represents the angle with the horizontal axis. (C) D-banding patterns in aligned, wet-spun collagen nanofibers.

S71 – O4

Mechanically induced bactericidal effects of nanostructured hydroxyapatite and titanium surfaces under static and dynamic conditions for bone tissue engineering

Menarbazari A.A.[1,2], Grzelak J.[1,2,3], Ginebra M.P.[1,2,3]

[1] Biomaterials, Biomechanics and Tissue Engineering Group, Dept. of Materials Science and Engineering and Institute for Research and Innovation in Health (IRIS), Universitat Politècnica de Catalunya - BarcelonaTech, Barcelona, Spain, [2] Barcelona Research Centre in Multiscale Science and Engineering, Universitat Politècnica de Catalunya · BarcelonaTech (UPC), Barcelona, Spain, [3] Centro de Investigación Biomédica en Red de Bioingeniería, Biomateriales y Nanomedicina (CIBER-BBN), Instituto de Salud Carlos III, Madrid, Spain

Introduction

Bone infections trigger progressive tissue destruction. This calls for the development of advanced biomaterials capable of simultaneously inhibiting bacterial colonization and fostering bone regeneration. The development of high-aspect-ratio surface nanotopographies has emerged as a promising strategy to provide bactericidal properties to biomaterials relevant for bone tissue engineering, particularly titanium and calcium phosphates. However, their antibacterial performance is mainly evaluated under static conditions, which do not reflect the physiological environment. Here, we evaluate the antibacterial performance of nanostructured calcium deficient hydroxyapatite (CDHA) and titanium (Ti), compared to their flat counterparts, under both static and dynamic conditions.

Materials and Methods

Flat and nanoneedle-structured surfaces of Ti and CDHA were fabricated and assessed for their antibacterial performance against *Escherichia coli*, a gram-negative model, including bacterial adhesion and viability. Experiments were performed under static conditions and two controlled shear stress levels (~1 and 2 dyne/cm²) using an orbital shaker, designed to mimic physiologically relevant fluid flow environments. Bacterial mortality and surface coverage were quantified using confocal Live/Dead imaging, complemented by scanning electron microscopy (SEM).

Results

Nanoneedle-structured Ti and CDHA surfaces exhibited significantly higher bactericidal activity compared to their flat counterparts across all conditions (Fig. 1A,B). Under dynamic conditions, bactericidal efficiency of nanostructured surfaces increased markedly, reaching up to 84 ± 15% mortality after 16 h. Notably, nanostructured CDHA surfaces outperformed both flat surfaces and Ti controls.

Shear flow further enhanced bacterial killing compared to static conditions, suggesting that fluid-induced interactions increase bacteria–surface contact and promote bactericidal effects. In parallel, nanostructured CDHA surfaces significantly reduced bacterial adhesion, showing the lowest surface coverage among all groups after 3 h (Fig. 1C,D).

SEM analysis (Fig. 1E) revealed pronounced morphological deformation and membrane disruption of bacteria on nanoneedle surfaces, supporting a mechanically induced bactericidal mechanism.

Conclusion

Nanostructured CDHA surfaces demonstrate a dual antibacterial effect by simultaneously reducing bacterial adhesion and inducing mechanobactericidal activity, particularly under dynamic conditions. These findings highlight the potential of topography-driven, antibiotic-free strategies for the design of next-generation bone grafts.

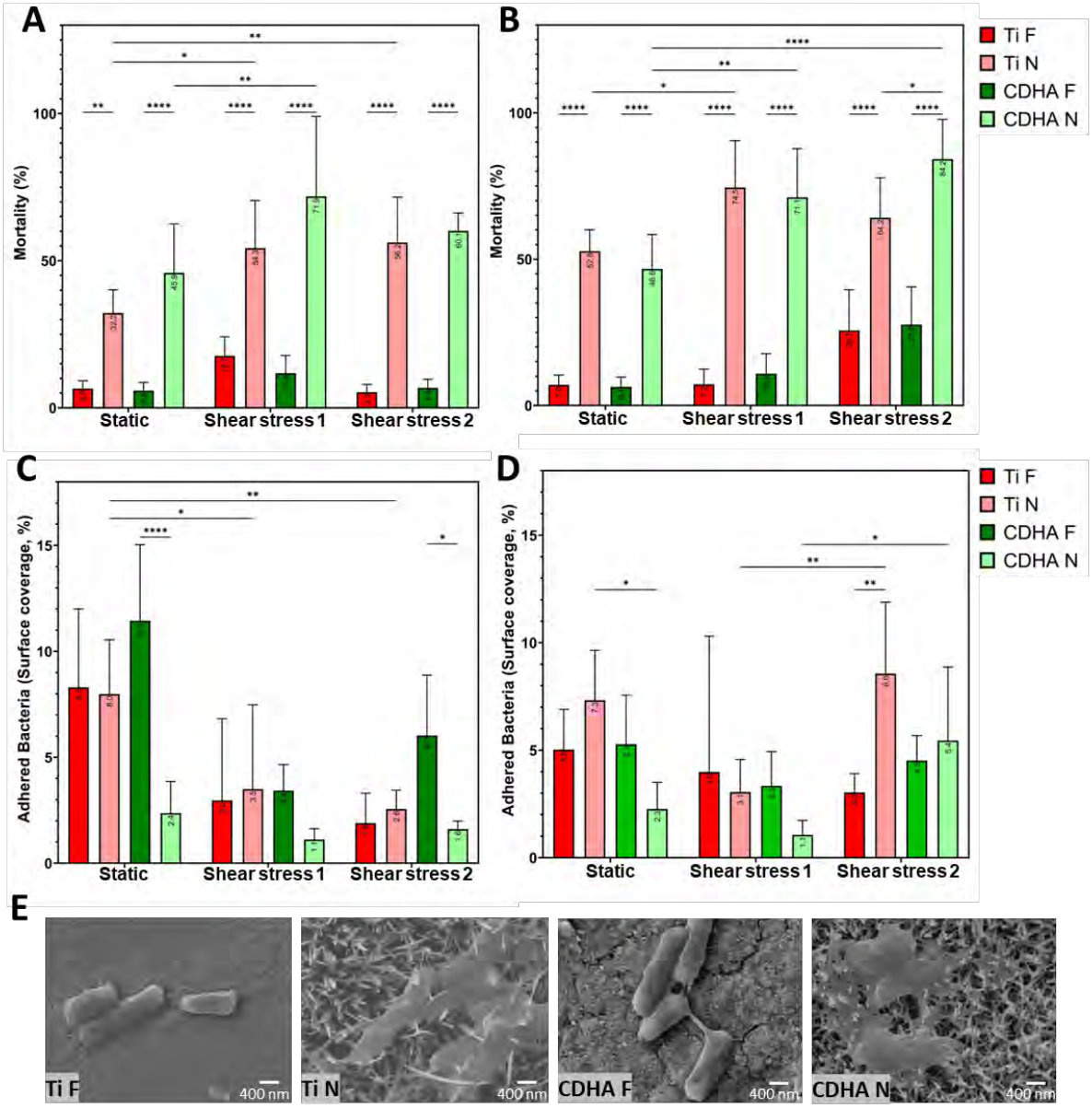

Figure 1
Quantification of bacterial mortality (%) derived from Live/Dead BacLight staining and confocal microscopy at (A) 3 h and (B) 16 h. Corresponding quantification of surface-associated bacterial adhesion at (C) 3 h and (D) 16 h. Statistical significance was considered at $p < 0.05$. (E) SEM images of flat and needle-structured surfaces after 16 h of static incubation with *Escherichia coli*, demonstrating differences in bacterial adhesion and surface–bacteria interactions across materials and topographies.

Acknowledgements
This work was financially supported by the European Union - ERC grant (BAMBBI; 101055053). The research is part of Maria de Maeztu Units of Excellence Programme CEX2023-001300-M/funded by MCIN/AEI/10.13039/501100011033, Spanish Ministry of Science and Innovation.

S71 – O5

Mineralized Himalayan Sheep Wool Based Composite 3D Printed Scaffolds with Curcumin for Osteosarcoma Management

Diwan H.[1], Murab S.[1]
[1]School of Biosciences and Bioengineering, Indian Institute of Technology Mandi, India

Introduction

Osteosarcoma is an aggressive primary bone malignancy that frequently results in pulmonary metastasis and large bone defects following surgical resection. Effective repair of these defects requires biomaterials capable of providing structural support while promoting bone regeneration and suppressing residual tumor activity. Three-dimensional printing (3DP) enables precise control over scaffold architecture, allowing fabrication of constructs that mimic native bone structure. However, conventional thermoplastic scaffolds such as polycaprolactone (PCL) lack intrinsic bioactivity, limiting effective cell–material interactions. Himalayan sheep wool contains bioactive cell-binding motifs (RGD, LDV, LDS, and EDS) that enhance cellular adhesion and tissue integration. In this study, wool fibers were mineralized with hydroxyapatite to create a biomimetic scaffold, while curcumin-encapsulated nanoliposomes were incorporated to provide localized anticancer delivery and improved bioavailability. The resulting multifunctional 3DP scaffolds aim to support bone regeneration following tumor resection.

Aim

The aim of this study was to develop a curcumin-loaded nanoliposomal delivery system incorporated within a three-dimensional printed (3DP) scaffold containing mineralized wool fibers to enhance curcumin bioavailability while promoting bone regeneration and preventing implant-associated infections following osteosarcoma tumor resection.

Materials and Methods

Mineralized wool fibers were synthesized *via in situ* hydroxyapatite mineralization and incorporated into polycaprolactone (PCL) to fabricate 3D printed composite scaffolds. Curcumin-encapsulated nanoliposomes were prepared using a thin-film hydration method and integrated into the scaffolds. Antibacterial efficacy was evaluated against Escherichia coli and Staphylococcus aureus. Anticancer efficacy toward MG63 osteosarcoma cells and osteogenic potential toward osteoblasts were assessed using Live/Dead staining, Alamar Blue assay, FE-SEM imaging, cytoskeletal staining, and Alizarin Red mineralization analysis.

Results

CW3DP scaffolds showed strong antibacterial activity with only 16% *E. coli* survival, while MW3DP exhibited moderate inhibition (32%). CW3DP significantly reduced MG63 viability and disrupted cytoskeletal organization due to sustained curcumin release (Figure 1.). In contrast, MW3DP supported enhanced cell attachment and mineralization. Both mineralized scaffolds promoted osteoblast proliferation and calcium deposition compared to PCL controls, indicating improved osteogenic potential (Figure 2.).

Figure 1. Anticancerous efficacy of 3DP scaffolds

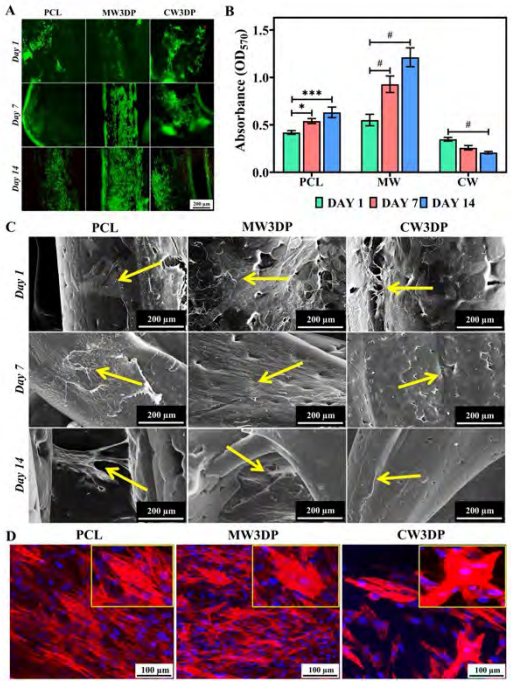

Figure 2. Osteogenic efficacy of 3DP scaffolds

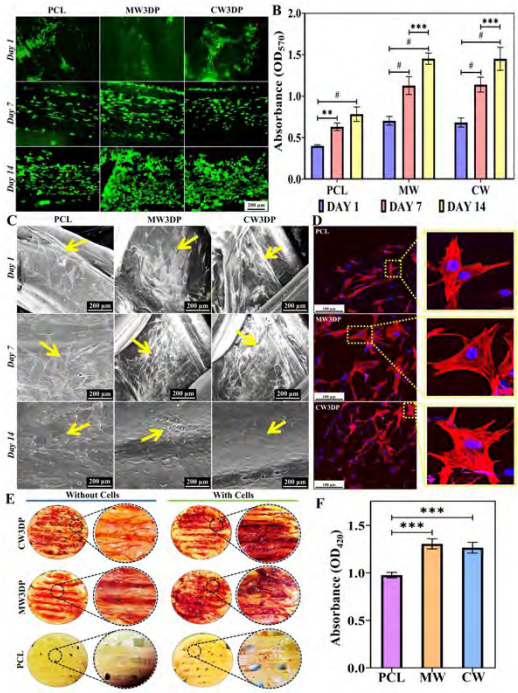

Conclusion

The developed curcumin-encapsulated nanoliposomal 3DP scaffolds reinforced with mineralized wool fibers represents a promising multifunctional platform for post-tumor bone defect repair. By combining sustained drug delivery with structural support, the scaffold has the potential to enhance bone regeneration while simultaneously preventing implant-associated infections and inhibiting osteosarcoma progression.

Acknowledgements
SM acknowledges the funding support from IIT Mandi (IITM/SG/SUM/88), Anusandhan National Research Foundation (ANRF, India) (SRG/2023/002182), IIT Mandi iHub and HCI Foundation (IIT MANDI iHub/RD/2023/012), and DST-FIST (SR/FST/LS-II/2022/950). HD acknowledge the scholarship support from MoE, Govt. of India.

References

[1]Sarkar N., Bose S. Liposome-Encapsulated Curcumin-Loaded 3D Printed Scaffold for Bone Tissue Engineering. *ACS Applied Materials & Interfaces 2019*; 11; 17184–17192.

S71 – O6

Albucol: uVA/Riboflavin-stabilized Albumin-Collagen Composite Scaffold Enabling Vascularized Bone Organoid Formation

Klink.M[1,2], Fan.L[1], Beurton.J[3], Lavalle.P[3], Xiong.X[1]
[1]NMI Natural and Medical Sciences Institute at the University of Tübingen, Reutlingen, Germany, [2]Dept. of Biology, Faculty of Science, University of Tübingen, Germany, [3]Biomaterials and Bioengineering, Centre de Recherche en Biomédecine de Strasbourg, Université de Strasbourg, France

Introduction

Engineering bone substitutes that combine mechanical stability and biologically instructive cues remains a challenge in biomaterials design. Albumin-based scaffolds provide structural stability but lack extracellular matrix (ECM) signals required for efficient cellular organization and vascularization. To address this limitation, we developed a protein-based composite scaffold platform, termed Albucol, with collagen stabilized on albumin scaffolds via UVA/riboflavin crosslinking to create a robust ECM-mimicking microenvironment for vascularized bone organoid formation.

Aim

This study aimed to develop Albucol scaffolds, in which collagen is stabilized on albumin scaffolds via UVA/riboflavin crosslinking, and to evaluate whether this approach preserves scaffold mechanics while enabling osteogenic and vascular organization for bone organoid formation.

Materials and Methods

Porous albumin scaffolds were fabricated and functionalized with collagen by bulk incorporation or surface coating. In Albucol scaffolds, surface collagen was stabilized using UVA/riboflavin crosslinking. Scaffold morphology and collagen distribution were analyzed by scanning electron microscopy (SEM), while mechanical and viscoelastic properties were assessed by rheology and differential scanning calorimetry (DSC). Degradation was monitored for 28 days. Biological performance was evaluated using co-culture with human mesenchymal stromal cells (hMSCs) and human umbilical vein endothelial cells (HUVECs). Vascular organization was assessed by immunofluorescence (CD31, VE-cadherin), network analysis, and RT-qPCR. Osteogenic differentiation and mineralization were evaluated by ALP, Alizarin Red S/von Kossa staining, calcium quantification, and histological analysis.

Results

Albucol scaffolds preserved the mechanical characteristics of albumin constructs while providing a stabilized collagen interface. In co-culture, optimal hMSC:HUVEC ratios promoted endothelial self-organization, with enhanced $CD31^+$/VE-$cadherin^+$ network formation compared to unmodified albumin scaffolds.

Conclusion

UVA/riboflavin-mediated collagen stabilization enables Albucol scaffolds that combine mechanical robustness with ECM-like bioactivity, supporting coordinated osteogenic and vascular responses for vascularized bone organoid engineering.

Acknowledgements

This research was carried out within the framework of the ALBUCOL Consortium and was co-financed through the Offensive Science initiative by the European Union's Interreg Upper Rhine program, with additional support from the Grand Est Region, the Ministry of Science, Research and the Arts of Baden-Württemberg, the Ministry of Science and Health of Rhineland-Palatinate, the Cantons of Basel-Landschaft and Basel-Stadt, and the Swiss Confederation.

References

[1]Fan L., Jung O., Herrmann M., Shirokikh M. et al. Deciphering UVA/Riboflavin Collagen Crosslinking: A Pathway to Improve Biomedical Materials. *Advanced Functional Materials 2024*; 34; 2401742.
[2]Fan L., Ren Y., Burkhardt C., Jung O., Schnettler R., Barbeck M., Xiong X. Evaluation of Injectable Composite Material Comprising Biphasic Bone Substitutes and Crosslinked Collagen. *Advanced Engineering Materials 2023*; 25; 2300508.
[3]Aloui E., Beurton J. et al. Salt-Compact Albumin as a New Pure Protein-based Biomaterials: From Design to In Vivo Studies. *Advanced*

Healthcare Materials 2025; 14; 2403385.

S72
Biomaterials for combination therapies (Drug–Device, Drug–Cell)

S72 – K1

Diaz-Rodriguez, P.
University of Santiago de Compostela, Spain

S72 – K2
Engineering Biofunctional Scaffolds for Multimodal CNS Regeneration

Sing Yian Chew
Nanyang Technological University, Singapore

Central nervous system (CNS) repair remains a major challenge, shaped by complex biophysical and biochemical cues that regulate cell fate, host responses, and injury microenvironment remodelling. The extracellular matrix is a key regulator of these processes, and replicating its structural and signalling properties in engineered constructs offers a promising route to functional regeneration.

Our research focuses on developing biofunctional scaffolds that recapitulate the key aspects of extracellular matrix architecture and molecular signalling to modulate cell-host interactions and promote regeneration after CNS injury. These platforms include fiber-based constructs that mimic the dimensions and organization of extracellular matrix networks, as well as 3D-printed scaffolds offering customisable, application-specific geometries. Together, they serve as vehicles for the delivery of nucleic acid therapeutics, including RNA interference approaches to promote nerve regeneration and remyelination, as well as human spinal cord progenitor cells for spinal cord injury repair.

In this talk, I shall share our recent advances in scaffold engineering and therapeutic integration and describe how machine learning is being applied to gain deeper insights into cell therapy and tissue regeneration outcomes. By integrating biomaterial-guided signalling with targeted cell and gene therapies, and data-driven approaches, we seek to establish more predictive and adaptive strategies for next-generation neuroregenerative medicine.

S72 – O1

Hydrogel Microneedle Patches with SERS Detection for Rheumatoid Arthritis Treatment

Liu L, Jin L, He H Y*
Dept. of Materials Science and Engineering, East China University of Science and Technology, Shanghai, China

Introduction

Rheumatoid arthritis (RA) is a highly disabling autoimmune disease, and clinical systemic administration suffers from severe side effects and low patient compliance. This study aims to develop a multifunctional hydrogel microneedle patch loaded with melittin/chondroitin sulfate (MEL/CS) complexes, combined with surface-enhanced Raman scattering (SERS) microneedles, to achieve localized anti-inflammatory treatment and real-time inflammation monitoring for RA.

Materials and Methods

MEL/CS complexes were prepared via electrostatic complexation with optimized mass ratio. Methacrylated CS (CSMA) was synthesized as the matrix to fabricate paw-adapted CSMA-based cryo-microneedle patches, and MEL/CS complexes were incorporated for controlled release. RA rat models were established, and in vitro/vivo experiments were performed to evaluate the anti-inflammatory effects, biocompatibility, and therapeutic efficacy. SERS microneedles were utilized for in-situ detection of dynamic changes in ankle pH and reactive oxygen species (ROS) in RA rats.

Results

The optimal MEL:CS mass ratio was 1:3, which significantly alleviated MEL's acute cytotoxicity, inhibited fibroblast-like synoviocyte (FLS) migration and M1 macrophage polarization, and promoted chondrocyte Col II expression. The cryo-microneedle patches effectively penetrated the stratum corneum, alleviated paw swelling, reduced inflammatory factors (IL-1β, TNF-α, MMP-3) in joint tissues and blood, and avoided systemic organ damage caused by injection administration. SERS microneedles achieved accurate real-time tracking of RA inflammation progression via pH and ROS detection.

Conclusion

The multifunctional MEL/CS-loaded cryo-microneedle patches realize localized anti-inflammatory treatment and real-time inflammation monitoring for RA, with high biocompatibility and low toxicity.

S72 – O2

A Smart Ingestible Capsule for Targeted Sampling of Intestinal Microbiota

Hamoud-Michel H.[1,2], Prattico C. [3], King I.[3,4,5], Maurice C. F. [3,4], Ahmadi, A. [1,2]
[1]Dept. of Mechanical Engineering, École de technologie supérieure, Montreal, Canada; University of Montreal Hospital Research Center (CRCHUM), Montreal, Canada; [3]Dept. of Microbiology and Immunology, McGill University, Montreal, Canada; [4]McGill Centre for Microbiome Research, Montreal, Canada; [4]McGill University Health Centre Research Institute, Montreal, Canada.

Introduction

The gut microbiota plays a central role in gastrointestinal (GI) diseases, yet its spatial organization remains poorly understood. Current sampling approaches are limited: stool samples reflect only distal colonic contents, while biopsies are invasive and can perturb the native microbiota. Ingestible capsules have emerged as a promising alternative for region-specific sampling of the GI tract. However, existing designs often rely on complex electronic components or external actuation, limiting their scalability and robustness. Passive systems offer a simpler alternative but typically depend on absorbent materials, resulting in slow uptake and incomplete sample recovery. Therefore, there is a need for simple, passive ingestible systems enabling rapid, precise fluid collection with minimal loss.

Aim. To develop a passive ingestible capsule that enables targeted sampling of the small intestine through pH-triggered activation and rapid fluid capture within an isolated chamber for efficient recovery.

Materials and Methods

The capsule (Ø7.7 × L16.25 mm) consists of a 3D-printed housing (Biomed Clear, Formlabs) coated with pH-sensitive Eudragit L100-55 (1–2 layers, 25 µL each) (Figure 1a). Fluid enters an isolated chamber and is recovered via pipette (135 ± 20 µL). A polyacrylamide hydrogel-based swelling mechanism (45% w/v acrylamide, 1% w/v ammonium persulfate, and 0.5–2.0% w/v N,N′-methylenebisacrylamide) seals the capsule via volumetric expansion. Coating performance was evaluated in pH-adjusted phosphate-buffered saline via sequential submersion (2 h at pH 1.5, then 4h at pH 6.8). Leakage was assessed using dye and 1 µm polystyrene fluorescent microparticles. Viable *Escherichia coli* recovery was evaluated by sampling inoculated BHI media over 3 h, followed by plating

Results

The capsule enabled targeted sampling and retention within an isolated chamber (Figure 1b). Bacteria were collected and remained viable post-sampling, confirming effective sampling (Figure 1c). No leakage of dye or fluorescent microparticles was observed over 24 h, with absorbance near baseline, demonstrating robust containment (Figure 1d). The capsule exhibited selective activation, with no fluid uptake in gastric conditions and efficient sampling at intestinal pH, confirming pH-responsive coating functionality (Figure 1e). Fluid entry kinetics were modulated by coating thickness, with additional Eudragit layers delaying activation (Figure 2a). Sealing time varied with crosslinker concentration and hydrogel length without a clear trend (Figure 2b). Hydrogels (1.0–2.0% w/v) generated sufficient swelling-induced force to ensure reliable closure (Figure 2c).

Conclusion

Ultimately, this capsule enables targeted sampling of the small intestine with rapid and efficient sample recovery, providing a non-invasive platform for investigating GI microbial communities and their effect on health.

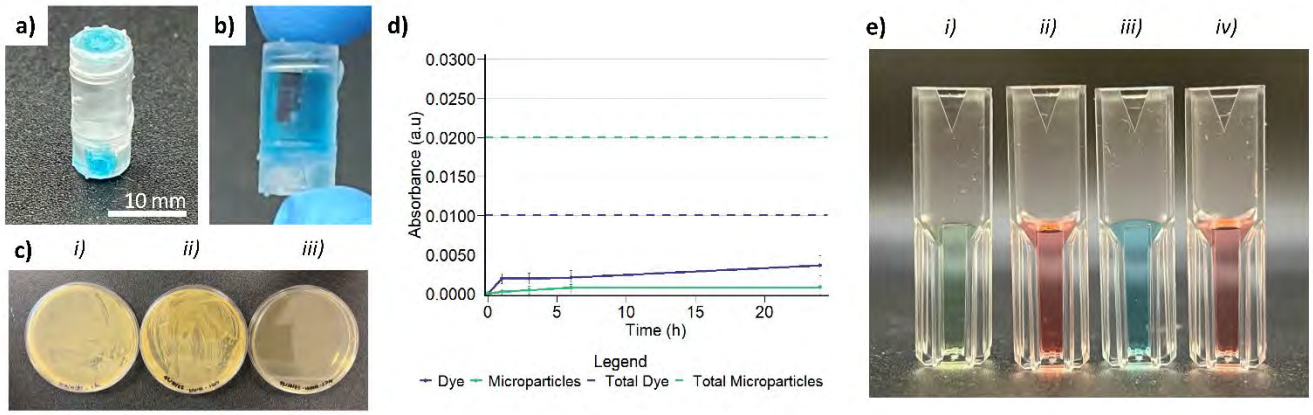

Figure 1. a) Assembled ingestible capsule coated with the pH-sensitive polymer Eudragit L100-55; b) Capsule following sampling, showing dyed fluid captured within an isolated internal chamber; c) *In vitro* sampling of *E. Coli* showing: i) culture recovered within capsule, ii) culture media, iii) negative control; d) Evaluation of leakage over 24 h using dye and 1 µm fluorescent microparticles, with absorbance indicating negligible release in comparison to capsules with leakage (dashed lines); e) Comparison of capsule response in simulated GI fluids: i) gastric, ii) small intestinal, iii) large intestinal, and iv) recovered sample from the capsule.

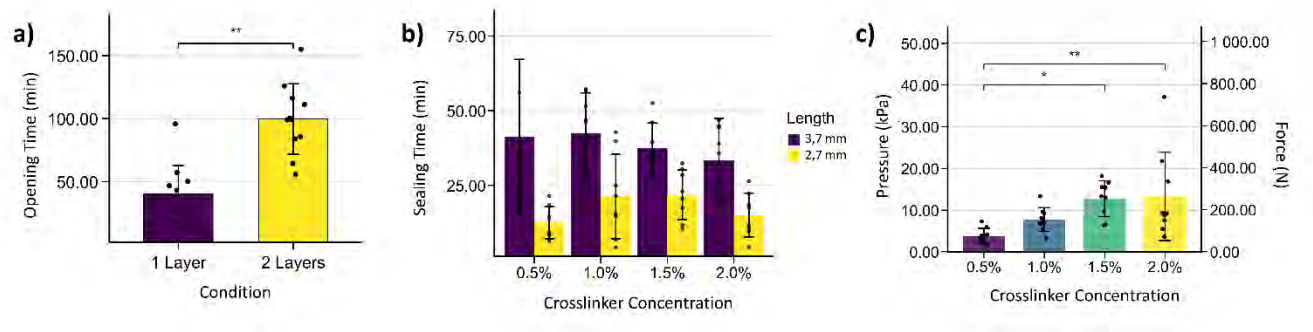

Figure 2. (a) Fluid entry time following exposure to target pH for capsules with one or two layers of Eudragit L100-55; (b) Sealing time, defined as the time required for hydrogel swelling to fully close the capsule openings, for varying crosslinker concentrations and hydrogel lengths; (c) Swelling-induced force and corresponding pressure generated by hydrogels, demonstrating sufficient sealing capacity.

S72 – O3

GelMA-based delivery system of stable induced regulatory T cells for local immunomodulation

Ricciardi C.[1,2], Nasello G.[2,3], Borgiani E.[2,3], Dederen A.[2,3], Epasto G.[1], Geris L.[2,3,4]
[1]Dept. of Engineering, University of Messina, Messina, Italy, [2]Skeletal Biology and Engineering Research Center, KU Leuven, Leuven, Belgium, [3]Prometheus, Division of Skeletal Tissue Engineering, KU Leuven, Leuven, Belgium, [4]Biomechanics Research Unit, GIGA, University of Liège, Liège, Belgium

Introduction

Regulatory T cells (Tregs) are pivotal for immune homeostasis and tissue regeneration. Local administration of natural Tregs (nTregs) has shown potential in bone healing[1], yet clinical translation is hampered by limited *in vivo* persistence and *in vitro* expansion. Induced Tregs (iTregs) represent an attractive alternative, though maintaining stability comparable to nTregs remains challenging[2].

Aim

This study develops a gelatin methacryloyl (GelMA) hydrogel platform for localized delivery of viable, phenotypically stable iTregs for immunomodulation.

Materials and Methods

Naïve $CD4^+$ T cells were isolated from murine spleens and lymph nodes via negative magnetic selection. Differentiation into iTregs was induced using Transforming Growth Factor-β (TGF-β) and interleukin-2 (IL-2), with plate-bound anti-CD3 alone or together with anti-CD28. Cells were split at day2 and TGF-β removed at day3 to initiate a resting phase with IL-2 only either in 2D or in 5% w/v GelMA hydrogels (2×10^5 cells/gel). Hydrogels were prepared with or without encapsulated IL-2; the former were washed and maintained in IL-2-free medium, while the latter in IL-2-supplemented medium. Viability and Foxp3 expression of retrieved cells were evaluated at D7 by flow cytometry and Live/Dead confocal imaging and compared to 2D controls.

Results

Stimulation with anti-CD3 alone prevented overstimulation and showed improved iTreg viability compared with conventional anti-CD3/CD28 activation (Fig. 1a). Furthermore, removing TGF-β at D3 while maintaining IL-2 sustained high viability until D10 (Fig. 1b), identifying D3 as the optimal timepoint for encapsulation, as iTreg viability and phenotype were maintained without further TGF-β or anti-CD3 stimulation. Washes of IL-2-containing gels caused massive cell death at D7 (Fig. 2a, b), indicating minimal non-specific binding of IL-2 to the GelMA matrix. In contrast, cells remained viable when IL-2 was supplied in the medium. Importantly, flow cytometry confirmed that iTregs within GelMA maintained Foxp3 expression at all timepoints (Fig. 2c).

Conclusion

The results establish a robust protocol for generating stable iTregs and encapsulating them in GelMA. Identifying D3 as the ideal encapsulation point and showing that IL-2 rapidly leaches without covalent tethering highlights the need for localized, covalent IL-2 binding to ensure long-term iTreg viability and function in regenerative medicine.

References

[1]Nayer B., Tan J.L., Alshoubaki Y.K., Lu Y.Z., Legrand J.M.D., Lau S. *et al.* Local administration of regulatory T cells promotes tissue healing. *Nature Communications* 2024; 15; 1–19.
[2]Mikami N., Kawakami R., Sugimoto A., Arai M., Sakaguchi S. Generating functionally stable and antigen-specific Treg cells from effector T cells for cell therapy of inflammatory diseases. *Sci Transl Med* 2025; 17; 1–16.

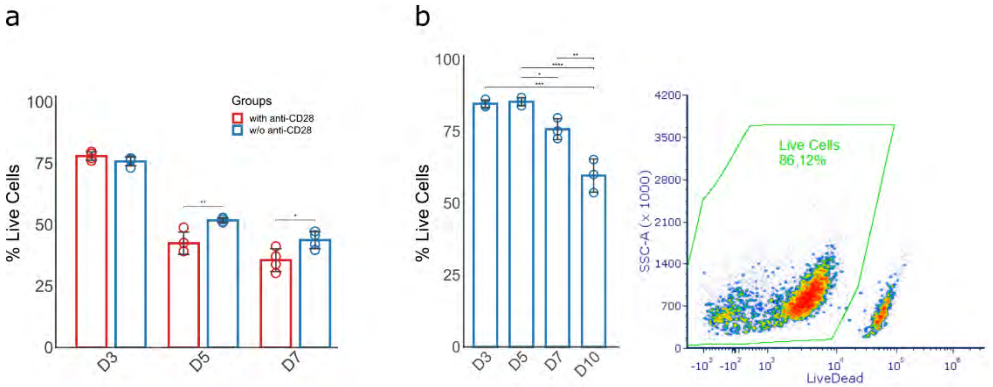

Figure 1

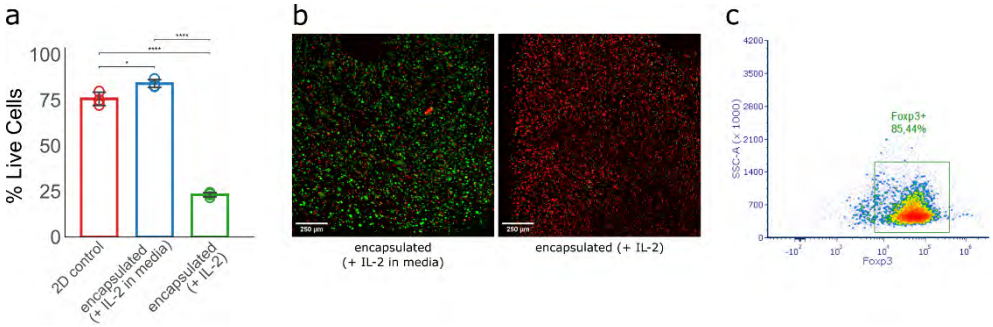

Figure 2

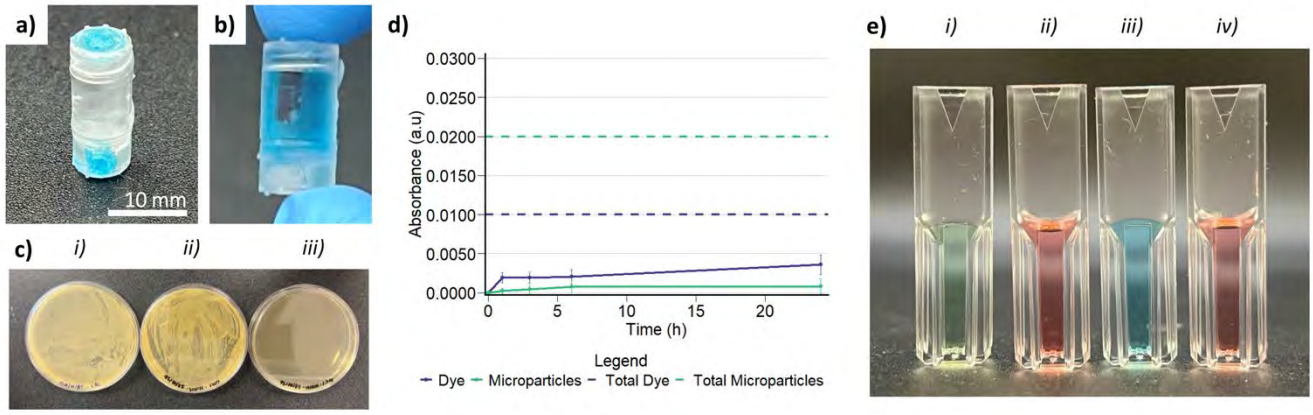

Figure 1. a) Assembled ingestible capsule coated with the pH-sensitive polymer Eudragit L100-55; b) Capsule following sampling, showing dyed fluid captured within an isolated internal chamber; c) *In vitro* sampling of *E. Coli* showing: i) culture recovered within capsule, ii) culture media, iii) negative control; d) Evaluation of leakage over 24 h using dye and 1 µm fluorescent microparticles, with absorbance indicating negligible release in comparison to capsules with leakage (dashed lines); e) Comparison of capsule response in simulated GI fluids: i) gastric, ii) small intestinal, iii) large intestinal, and iv) recovered sample from the capsule.

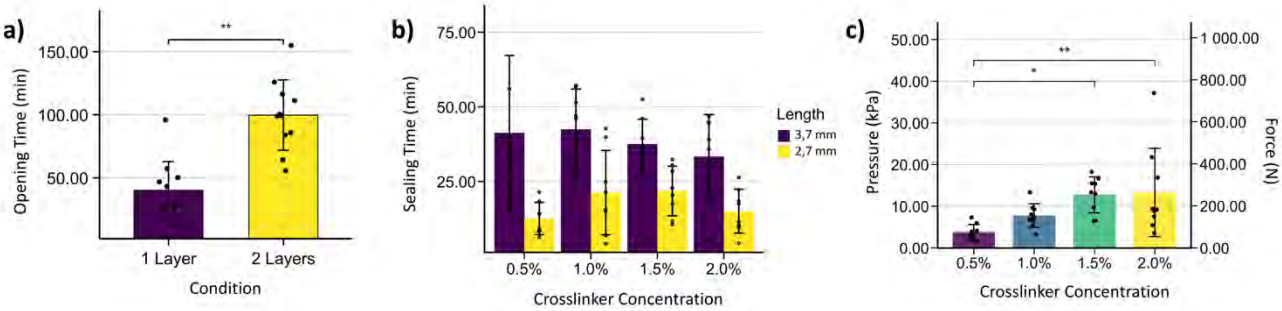

Figure 2. (a) Fluid entry time following exposure to target pH for capsules with one or two layers of Eudragit L100-55; (b) Sealing time, defined as the time required for hydrogel swelling to fully close the capsule openings, for varying crosslinker concentrations and hydrogel lengths; (c) Swelling-induced force and corresponding pressure generated by hydrogels, demonstrating sufficient sealing capacity.

S72 – O4

Multifunctional calcium phosphate systems for simultaneous infection control and bone regeneration

Loca D.[1,2], Oselska E.[1,2] and Sceglovs A.[1,2]
[1]Institute of Biomaterials and Bioengineering, Riga Technical University, [2] Baltic Biomaterials Centre of Excellence, Headquarters at Riga Technical University

Introduction

Bone implant-associated infections remain a major complication due to biofilm formation and poor penetration of systemic antibiotics. Local delivery systems that provide sustained antibacterial activity while supporting bone regeneration are therefore essential. Calcium phosphates (CaP) offer this dual functionality through tunable drug loading, controlled release at the implant site, and intrinsic osteoconductivity. This study explores CaP-based systems for the delivery of gentamicin and vancomycin at varying concentrations, alongside phase tuning to modulate bone regeneration rates.

Materials and Methods

Calcium phosphate (CaP) systems were prepared using α-tricalcium phosphate-based formulations with varying phase compositions to tailor physicochemical properties. Gentamicin sulfate and vancomycin hydrochloride were incorporated into CaP formulations at concentrations of 1–10 wt%. The materials were characterized by X-ray diffraction (XRD) for phase composition, Brunauer–Emmett–Teller (BET) analysis for specific surface area, helium pycnometry and Archimedes' method for porosity determination, and scanning electron microscopy (SEM) for morphology. Drug release profiles were assessed in phosphate-buffered saline at 37 °C using UV–Vis spectroscopy. Cytocompatibility was evaluated using MC3T3-E1 preosteoblast cells, while antibacterial activity was tested against *Staphylococcus aureus* (ATCC 25923).

Results

Gentamicin-loaded CaP systems provided sustained antibacterial concentrations exceeding MIC values (>0.5–8 µg/mL) for up to several weeks, and in some cases up to 6 months, while maintaining >80% cell viability and supporting osteogenic cell proliferation. Vancomycin-loaded CaPs demonstrated strong antibacterial efficacy, with all compositions releasing sufficient drug to achieve complete eradication of high bacterial loads (initial concentration OD 0.015, ~10^7 CFU/mL) at each evaluated time point (24, 48, and 72 h), even after repeated bacterial reintroduction.

Conclusion

Calcium phosphate-based systems enable effective local delivery of gentamicin and vancomycin, combining sustained antibacterial activity with osteoconductive properties. These materials provide both prolonged infection control and rapid bacterial eradication while maintaining cytocompatibility. Future work will focus on tuning CaP composition and exploring alternative antimicrobial agents, such as plant-derived secondary metabolites, to reduce antibiotic resistance and enhance regenerative outcomes.

Acknowledgements

The authors acknowledge financial support from the **"**Biomedical and Photonics Research Platform for the Development of Innovative Products (BioPhoT, IVPP-EM-Inovācija-2024/1-0002)" project No. OSI_PIP_BioPhoT-2025/1-0048 "BIOmaterials for infection COntrol and fast bone tissue REgeneration (BIOCORE)" and access to the infrastructure and expertise from Horizon 2020 project No. 857287 (BBCE – Baltic Biomaterials Centre of Excellence).

S73
Biomaterials for drug delivery systems

S73 – K1
Doubly reversibly crosslinked bioinks

J. Maurice Pütz[1], Ekaterina Takmakova[1], Kelsey R. de Graaf[2], Andrew Kerr[1], Nikita Durandin[2], Robert Luxenhofer[1]
[1] Dept. of Chemistry, and Helsinki Institute of Sustainability Science, Faculty of Science, University of Helsinki, Finland, [2] Faculty of Engineering and Natural Sciences, Tampere University, Finland

Bioinks typically hydrogels as key components to ensure printability and structural stability in biofabrication. In this regard, we previously demonstrated the suitability of thermogelling diblock copolymers comprising poly(2-methyl-2-oxazoline) and thermoresponsive poly(2-n-propyl-2-oxazine) for bioink formulations.[1] However, since this bioink was only weakly physically cross-linked, long term cell culture was not possible without modifications. Later modification with furan and maleimide functionalities allowed rapid and convenient covalent cross-linking, which in principle is reversible via the retro-Diels-Alder reaction, however, this is not feasible under physiological conditions.[2]

In contrast, modification of shear-thinning thermogelling polymers with lipoic acid allows a very straightforward doubly reversible crosslinking. Furthermore, the functionality enables flexibility in (de-)polymerization methods via radical, UV, thiolate or reductive mechanisms. In addition, the new bioinks have interesting properties for applications in wound care and drug delivery systems.

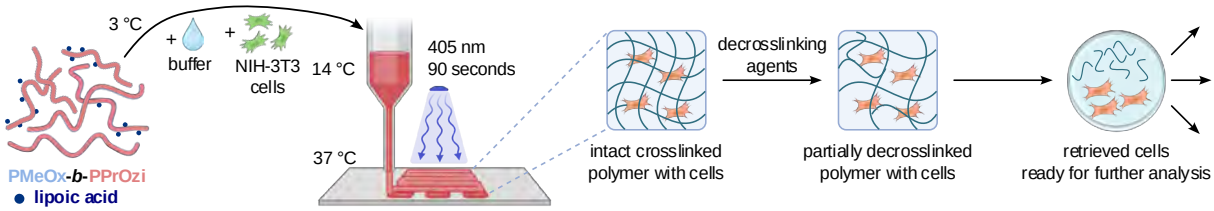

Figure 1. Preparation steps for novel bioink. Dithiolane functionalized copolymer is mixed with water/media and cells. Then added into a 3D bioprinter. Printed structures are cured by UV-light. After the targeted maturation cultivation, the bioink is decrosslinked and cells can be retrieved.

We present a straightforward two-step post-polymerization modification to synthesize crosslinkable and extrusion printable copolymers. These copolymers form stable and durable hydrogels with thermogelling properties, underlining their suitability for 3D-printing applications.
The printed structures exhibit excellent shape fidelity and resolution, with crosslinking achieved by radical, UV and thiolate mechanisms. The resulting hydrogels are soft, durable, and elastic. Cytocompatibility tests conducted post-printing and crosslinking confirmed the bioink's viability, highlighting its potential for biofabrication.

References
[1] T. Lorson, S. Jaksch, M. Lübtow, T. Jüngst, J. Groll, T. Lühmann, R. Luxenhofer, *Biomacromolecules* **2017**, *18*, 2161-2171.
[2] L. Hahn, M. Beudert, M. Gutmann, L. Keßler, P. Stahlhut, L. Fischer, T. Lorson, I. Thievessen, T. Lühmann, R. Luxenhofer. *Macromol. Biosci.* **2021**, *21*, 10, 2100122

S73 – O1

Niosomal film-forming gel for topical delivery of colchicine: formulation, characterization, and controlled release performance

Shekari T[1], Maboudi A[2], Amani N[1], Akrami-Hasan-Kohal M[3], Ostad S.N.[4], Hosseinzadeh Ardakani Y[5], Akbari Javar H*[1]

[1]Dept. of Pharmaceutics, Faculty of Pharmacy, Tehran University of Medical Sciences (TUMS), Iran, [2]Dept. of Pharmaceutics, School of Pharmacy, Zanjan University of Medical Sciences, Zanjan, Iran, [3]Polymers, Biopolymers, Surfaces Laboratory (PBS, UMR CNRS 6270), University of Rouen Normandy, Mont-Saint-Aignan, France, [4]Toxicology and Poisoning Research Centre, Dept. of Toxicology and Pharmacology, Faculty of Pharmacy, Tehran University of Medical Sciences, Iran, [5]Biopharmaceutics and Pharmacokinetic Division, Dept. of Pharmaceutics, Faculty of Pharmacy, Tehran University of Medical Sciences, Iran

Introduction

Colchicine is widely used in the management of acute gout, but oral administration is limited by dose-related gastrointestinal side effects and a narrow therapeutic window. Topical delivery systems offer a promising alternative by enhancing localized therapeutic action while minimizing systemic exposure and associated toxicity.

Aim

This study aimed to develop a niosome-loaded film-forming gel for topical colchicine delivery to enable sustained release and prolonged residence on the skin.

Materials and Methods

Colchicine-loaded niosomes were prepared using the thin-film hydration method and incorporated into a film-forming gel matrix. The formulation was characterized for particle size, polydispersity index, zeta potential, entrapment efficiency, drug content, pH, and rheological behavior. In vitro drug release was evaluated using a Franz diffusion cell, and drug content was quantified using a validated UV–visible spectrophotometric method. Dermal irritation and sensitization studies were performed to assess biocompatibility.

Results

The optimized formulation showed a mean niosome size of 155.1 ± 70.0 nm, an entrapment efficiency of 68.24 ± 1.36%, and shear-thinning rheological behavior suitable for topical application. In vitro release studies demonstrated sustained release, with approximately 80% cumulative drug release over 24 h, compared with the rapid release observed for the film-only formulation. Kinetic modeling indicated that release from the niosome-in-film system was best described by the Korsmeyer–Peppas model. No observable adverse dermal responses were detected in the irritation or sensitization studies in the tested animal models.

Conclusion

These findings suggest that the colchicine-loaded niosomal film-forming gel is a promising topical drug delivery system for sustained drug release, with potential to reduce systemic side effects associated with oral administration.

Acknowledgements

This research was financially supported by Tehran University of Medical Sciences (TUMS) under Grant Code IR.TUMS.AEC.1404.043.

S73 – O2

Elaboration of photothermal hydrogels triggering the release of therapeutics from connected wound dressings

Bouhamad R.[1], Defrançois S.[2], Maton M.[2], Hildebrand F.[2], Staelens J.N.[1], Blanchemain N.[2], Martel B.[1], Zobrist C.[1], Tabary N.[1], Lyskawa J.[1]
[1] Univ. Lille, CNRS, INRAE, Centrale Lille, UMET Unité Matériaux et Transformations, France, [2] Univ. Lille, INSERM, France

Introduction

Diabetes foot infection (DFI) represents one of the most common and severe complications of diabetes, with 20% of cases requiring amputations, thereby reducing quality of life and increasing the risk of death. In this context, the European project DIAMOND, funded by the Interreg France-Wallonie-Vlaanderen program, aims to develop a connected wound dressing able to monitor the wound condition in real time, thanks to integrated sensors, and to release antibiotics on demand through a photo-responsive hydrogel. In our part, we focus on the elaboration of the photothermal hydrogel loaded with antibiotics.

Materials and Methods

The viscoelastic hydrogel was prepared by mixing chitosan (CHT), a cationic polymer with an anionic polycyclodextrin citrate polymer (PCD) in acidic medium, using an interconnected syringe system developed by Chijcheapaza et al.[1]
The photothermal responsiveness was provided by incorporating polydopamine nanoparticles (nPDA) synthesized via an auto-polymerization process from dopamine hydrochloride in basic oxidizing conditions.
Rifampicin (RFP) and ciprofloxacin (CFX) were loaded onto the nPDA in batches and spread in the hydrogel. Drug loading rates and release were assessed by UV spectrophotometry at 334 nm for RFP and 271 nm for CFX.
A near-infrared (980 nm) laser was used to irradiate the hydrogel. The irradiation was performed for four cycles of 1 min at 0.13 W/cm², separated by 1 min intervals. The temperature of the hydrogel was monitored using a thermal imaging camera (Optris PI 640i).

Results

During the irradiation cycles, the hydrogel containing nPDA consistently reheated to approximately 45°C, while the control hydrogel without nPDA revealed no significant temperature increase (Figure1).
Antibiotics were loaded onto the nPDA, reaching 0.4 and 0.6 mg/g of nPDA for RFP and CFX respectively.
The release studies in PBS (37°C, 80 rpm) (Figure2) have demonstrated that the hydrogel retains 96-99% of the total loaded rifampicin content at 20, 37 and 50°C within 2 days, displaying sequestration and low passive diffusion of the antibiotics in the absence of photo-stimulation.

Conclusion

A photothermal hydrogel with high responsiveness based on CHT and PCD containing nPDA loaded with two antibiotics was elaborated. Preliminary tests displayed a low passive diffusion and sequestrating effect toward drugs in absence of laser light stimulation.

Further work will focus on the antibiotic release upon near-infrared irradiation in order to confirm the expected triggering effect. The cytotoxicity as well as the coating of the hydrogel on the wound dressing will also be investigated.

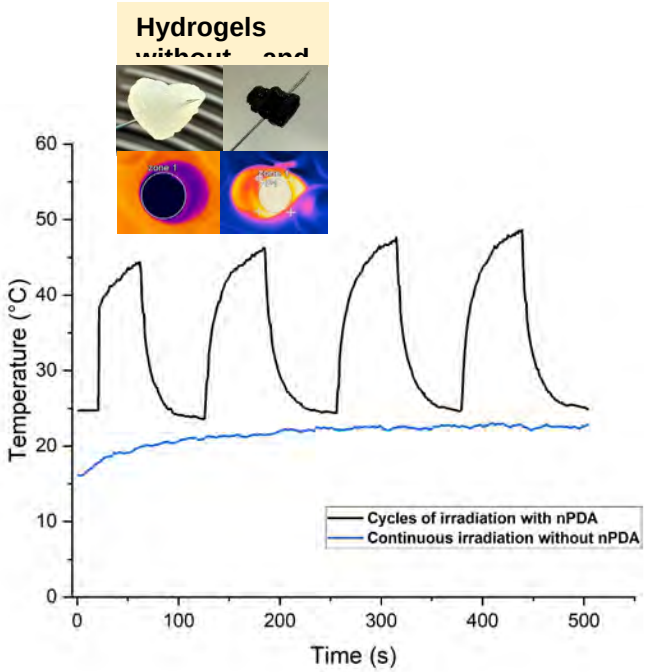

Figure 2. Irradiation of hydrogels at 0.13 W/cm²

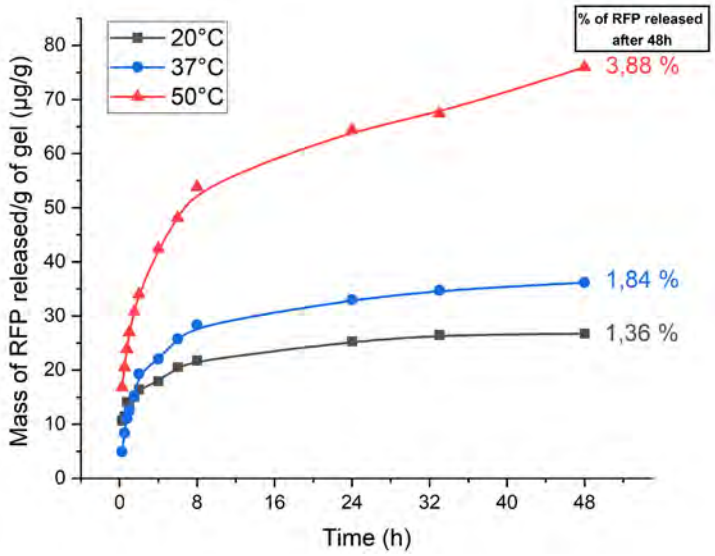

Figure 1. Release study of rifampicin without photo-stimulation

References

[1] Chijcheapaza-Flores, H. et al. *Gels 2023*, *9* (3), 262.

S73 – O3

Design and preclinical–clinical evaluation of drug-eluting osteosynthesis plates for the prevention of bone infections

J Dartus[1, 2,3], F Chai[1], O Carpentier [3], S Putman[2], N Blanchemain[1], F Monchau[3]
[1]Université de Lille, France, [2]CHU Lille, Université de Lille France, [3]Université d'Artois, Béthune, France

Introduction

Postoperative infections remain a major complication in orthopedic trauma surgery, particularly in cases requiring internal fixation. Osteomyelitis and implant-associated infections may impair fracture healing, increase morbidity, and necessitate revision surgery. Conventional osteosynthesis plates provide mechanical stabilization but do not actively prevent microbial colonization. Local delivery of antibiotics directly from the implant surface represents a promising strategy to reduce infection risk while maintaining the mechanical integrity required for bone fixation.
The objective of this study was to design and evaluate innovative osteosynthesis plates capable of incorporating therapeutic agents, particularly antibiotics, for local drug delivery. The study combined computer-aided design, additive manufacturing, mechanical characterization, and in vivo evaluation to assess the feasibility, mechanical reliability, and biological performance of these drug-eluting implants.

Materials and Methods

Two osteosynthesis plates incorporating internal reservoirs intended for drug loading were designed using three computer-aided design (CAD) software platforms: Blender, FreeCAD, and SolidWorks. The implants were fabricated using additive manufacturing (3D printing, Trumpf, Germany) technologies. Two metallic materials were selected depending on the experimental model and clinical application.
A titanium plate was produced for implantation in a rat model presenting a femoral diaphyseal fracture. In parallel, a stainless steel 316L plate was manufactured for veterinary clinical use in dogs undergoing tibial plateau leveling osteotomy (TPLO).
Mechanical performance was evaluated through compression and three-point bending tests using a Shimadzu AGS universal testing machine equipped with a 10 kN load cell. These experiments aimed to verify that the modified implant geometry maintained sufficient structural resistance despite the presence of drug-loading cavities. In addition, computational modeling was performed to simulate torsional loading conditions and predict implant behavior under rotational stresses.
Biological evaluation included in vivo implantation in rats to assess tissue response and implant biocompatibility over a three-month period. Clinical performance was also investigated in canine patients undergoing TPLO surgery, with postoperative monitoring focusing on implant stability, fracture healing, and potential complications.

Results

Mechanical testing demonstrated that the developed plates maintained satisfactory resistance to compressive and bending loads, consistent with the mechanical requirements for orthopedic fixation devices. Computational simulations further indicated adequate torsional stability despite the internal structural modifications required for drug incorporation.
In the preclinical rat model, the titanium implants exhibited excellent biocompatibility after three months of implantation. No adverse inflammatory response, implant rejection, or abnormal tissue reaction was observed, and bone healing progressed normally at the fracture site.
Clinical evaluation in canine patients undergoing TPLO surgery demonstrated favorable surgical outcomes. At three months of follow-up, all treated animals showed satisfactory functional recovery and stable fixation, resulting in a success rate of 100%, with no postoperative infections or implant-related complications reported.

Conclusion

This study demonstrates the feasibility of designing and manufacturing osteosynthesis plates capable of incorporating drugs while maintaining adequate mechanical performance. CAD-based design, 3D printing, and biomechanical validation enabled the development of next-generation implants.
The encouraging preclinical and veterinary clinical outcomes highlight the potential of such devices to reduce implant-associated infections and improve fracture management. Further studies will be required to optimize drug delivery strategies and evaluate long-term performance before translation to broader clinical use.

Acknowledgements
SATT, Eurasanté, …

References

[1]Brevet Artois

S73 – O4

Eliciting systemic antitumor immunity and remodeling the microenvironment with a dual-targeting in situ nanovaccine

Lin ZK[1], Lee W[2], Chiang CS[2], Chen SY[1]
[1]Dept. of Materials Science and Engineering, National Yang Ming Chiao Tung University, Hsinchu, Taiwan, Republic of China, [2]Cell Therapy Center, China Medical University Hospital, Taichung, Taiwan, Republic of China

Introduction

In recent years, therapeutic cancer vaccines have gained significant attention following breakthroughs in personalized cancer vaccines (PSVs) from companies like Moderna and BioNTech. However, PSVs face critical hurdles, including tumor heterogeneity, high costs, and complex manufacturing. While in situ cancer vaccines (ISVs) present a compelling strategy to overcome these issues by generating a broad-spectrum antigen response—thereby mitigating the risk of antigen escape under selective pressure—they primarily act locally within the tumor microenvironment (TME) and fail to modulate lymphoid organs essential for T cell priming. Thus, there is an urgent need for strategies that can bridge this gap: eliciting systemic immunity while simultaneously reprogramming the immunosuppressive TME.

In this context, we have developed NanoFig: a systemic, real-time in situ nanovaccine. NanoFig utilizes an ionizable PBAE core to co-deliver the chemotherapeutic docetaxel (DTX) and the immunoadjuvant CpG. Crucially, it is surface-functionalized with fucoidan to target both cancer cells and antigen-presenting cells (APCs). This dual-targeting approach facilitates the in situ generation of tumor-associated antigens (TAAs). By engaging lymphoid organs to activate robust and diverse T cell responses, NanoFig effectively translates local antigen release into a potent systemic defense, ultimately remodeling the TME (Figure 1).

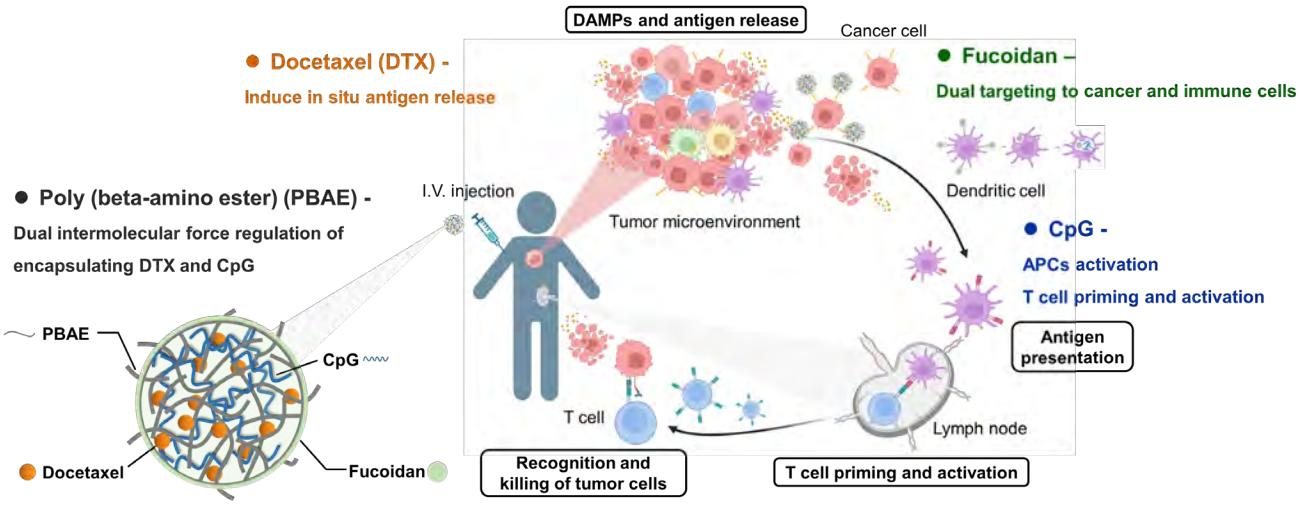

Figure 1. Schematic illustration of NanoFig as a real-time in situ cancer vaccine.

Materials and Methods

NanoFig was prepared by co-encapsulating DTX and CpG within a PBAE core using microfluidic mixing, followed by fucoidan surface coating. Subsequent experiments evaluated its physicochemical properties, targeting affinity for cancer cells and APCs, and capacity to elicit systemic immunity *in vivo*.

Results

NanoFig exhibited a mean particle size of 167.7 nm (Figure 2a). Following surface coating with negatively charged fucoidan, a distinctive charge reversal was observed (Figure 2b). SEM and TEM images revealed a unique, fig-like core-shell structure, which inspired the name "NanoFig" (Figure 2c). In animal studies, NanoFig effectively targeted both cancer and immune cells (Figure 2d) and demonstrated potent tumor suppression. By reducing tumor volume nearly 2-fold compared with the free-drug group, this result highlights the critical advantage of

targeted delivery (Figure 2e). Furthermore, systemic in vivo immune activation was confirmed: the cytotoxic $CD8^+$ T cell population expanded (Figure 2f) with significantly elevated $CD107a^+$ and granzyme B expression (Figure 2g, h). Concurrently, a marked reduction in immunosuppressive regulatory T cells (T_{reg}) was achieved (Figure 2i).

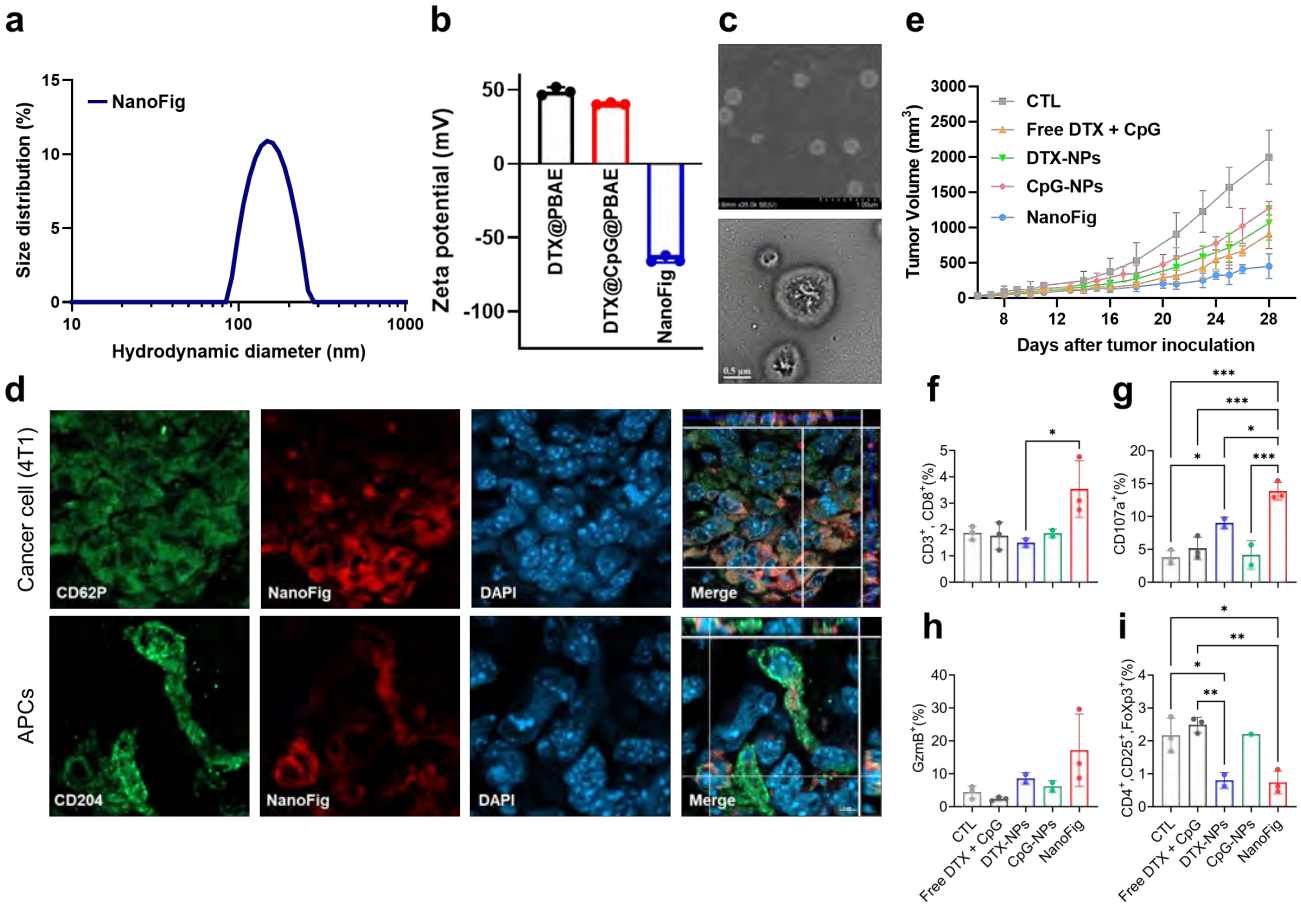

Figure 2. Characterization and in vivo evaluation of NanoFig.
(a-c) Physicochemical properties including size, zeta potential, and morphology. (d) Confocal imaging confirms in vivo targeting function. (e) NanoFig demonstrates superior tumor growth inhibition. (f-i) NanoFig led to increased CD8 T cell expression and decreased the proportion of immunosuppressive T cells.

Conclusion

In conclusion, we have simplified the preparation process of cancer vaccines, transforming it into a real-time, in situ cancer vaccine. By utilizing a dual-targeting strategy to simultaneously modulate tumor and peripheral immunity, we have achieved a potent, synergistic cancer vaccine.

Acknowledgements

This project is funded by the National Science and Technology Council (NSTC) (NSTC 114-2223-E-A49-005).

S73 – O5

Estrogen-embedded bone-seeking polymers to inhibit osteoporotic bone resorption

Iwasaki Y.[1,2], Takai S.[3], Okuno Y.[1,2]

[1]Dept. Chem. Mater. Eng., Kansai University, Osaka, Kansai University, Osaka, Japan, [3]Grad. Sch. Sci. Eng., Kansai University, Osaka, Japan

Introduction

Several symptoms including central nervous system-related disorders; metabolic, weight, cardiovascular and musculoskeletal changes; urogenital and skin atrophy; and sexual dysfunction have been experienced by woman at menopause, and these symptoms are related with estrogen deficiency. To moderate these symptoms, estrogen replacement therapy (ERT) has been used. However, its use specifically for osteoporosis treatment is restricted due to concerns about various side effects, such as breast cancer and cardiovascular disease. To facilitate targeted estrogen delivery to the bone tissue, we have synthesized an E_2V-embedded polyphosphodiester (E_2VP_n. Fig.1) with various degrees of polymerization (DP) and the optimal structure to present ideal functions were clarified.

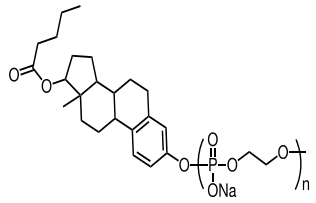

Fig. 1 Chemical structure of E_2VP_n.

Materials and Methods

Estradiol valerate (E_2V) served as the initiator for the ring-opening polymerization of 2-methoxy-2-oxo-1,3,2-dioxaphosphorane (MP) using a DBU catalyst. The resulting polymers were demethylated with trimethylamine and neutralized to yield water-soluble E_2VP_n. For tracking, fluorescently labeled variants (fE_2VP_n) were synthesized by incorporating 2-(but-3-yn-1-yloxy)-2-oxo-1,3,2-dioxaphospholane (BYP) followed by Cy5-azide conjugation via "click" chemistry. Bone marrow mononuclear cells were isolated from mice and cultivated in the differentiation medium. Following a 4-day incubation with E_2VP_n or estrogen-free controls (P_n), cells were analyzed via TRAP staining and Rhodamine phalloidin to quantify multinucleated osteoclasts. Additionally, qPCR was performed to evaluate the expression of key differentiation markers and transcription factors. Pharmacokinetics were assessed in ICR mice via tail vein injection of fE_2VP_n. Blood clearance and area under the curve were determined by plasma fluorescence over 72 hours, while cryosections of the femur were analyzed to confirm bone localization. The therapeutic potential was evaluated using an ovariectomized (OVX) mouse model. Mice received bi-weekly injections of E_2VP_n over six weeks. Bone density and microarchitecture were quantified using micro-CT.

Results

In vitro, E_2VP_n completely suppressed osteoclast differentiation and actin ring formation. Although the polymer with a lower degree of polymerization (DP) (E2VP10) showed stronger suppression of osteoclast marker gene expression, presumably due to reduced steric hindrance upon binding to the estrogen receptor, the results in vivo favored the chain with the higher molecular weight. In vivo distribution studies using fluorescently labeled E2VPn revealed that affinity for bone depends on DP. High-molecular-weight fE_2VP_{150} exhibited superior blood circulation and significant accumulation in bone tissue, whereas low-molecular-weight fE_2VP_{10} was rapidly cleared by the kidneys. In ovariectomized (OVX) mice, micro-CT analysis confirmed that E_2VP_{150} most effectively prevented bone resorption. Although smaller polymers possess higher receptor affinity, the enhanced pharmacokinetic profile and bone-targeting capability of the larger polymers are essential for in vivo therapeutic success. This underscores that optimizing molecular weight is critical for the systemic delivery of bone-targeting minerals.

Fig. 2 2D micro-CT images of distal femur.

Conclusion

The E_2VP_n platform represents a promising "bone-seeking" delivery system, highlighting that macromolecular architecture is a primary driver of therapeutic success in living systems.

Acknowledgements

This work was supported by KAKENHI from the Japan Society for the Promotion of Science (#23H03750).

References

[1]Iwasaki Y., Fukaura S., Mabuchi S, Okuno Y., Yokota A., Neo M. Suppression of bone resorption in ovariectomized mice using estrogen-immobilized polyphosphodiesters. *Materialia* 2024; 36; 102166.

S73 – O6

Tunable Thermosensitive Chitosan/β-Glycerophosphate Hydrogels for Local Irinotecan Delivery

Piotrowska U.[1], Orzechowska K.[2], Laskowska A.[3], Sobczak M.[1]
[1]Dept. of Pharmaceutical Chemistry and Biomaterials, Medical University of Warsaw, Poland, [2]Students Scientific Group BIOMAT, Medical University of Warsaw, Poland, [3]Dept. of Pharmaceutical Microbiology and Bioanalysis, Medical University of Warsaw, Poland

Introduction

Thermosensitive chitosan (CS) hydrogels formed in the presence of β-glycerophosphate (β-GP) have attracted increasing attention as injectable biomaterials for local drug delivery. These systems undergo sol-gel transition at physiological temperature, enabling minimally invasive administration and in situ gel formation [1-2]. However, a major challenge of CS/β-GP systems is the balance between gelation kinetics, mechanical stability and drug release behaviour. Small-molecule additives may provide a strategy to tune hydrogel structure and transport properties [3].

Aim

The aim of this study was to investigate the influence of selected inorganic and organic modifiers on the physicochemical properties and release behaviour of thermosensitive CS/β-GP hydrogels loaded with irinotecan (CPT-11), a clinically relevant chemotherapeutic used in colorectal cancer therapy.

Materials and Methods

Thermosensitive hydrogels were prepared from CS solutions neutralised with β-GP under cooling conditions. Sodium bicarbonate ($NaHCO_3$) was used as an inorganic modifier, while glucose and glycerol were introduced as organic additives. Gelation behaviour was evaluated using the tube inversion method. Structural properties were characterised by FTIR spectroscopy. Swelling behaviour was determined gravimetrically in PBS (pH 7.4). In vitro release of CPT-11 was assessed at 37 °C and analysed using Weibull modelling. Biological response was evaluated using extract-based cytotoxicity assays (ISO 10993-5) on BALB/3T3 fibroblasts and HCT-116 colorectal carcinoma cells, complemented by direct-contact observations with HCT-116 and CCD-18Co cells.

Results

All CS/β-GP formulations exhibited temperature-induced sol-gel transition at 37 °C, with gelation time strongly dependent on formulation composition. $NaHCO_3$ significantly accelerated gelation, producing rapidly stabilising hydrogels, whereas glucose and glycerol generated more gradual gelation behaviour. Release studies revealed biphasic CPT-11 profiles characterised by an initial burst phase followed by slower diffusion-controlled release. The extent of drug release correlated with hydrogel hydration and microstructure, with glucose-modified hydrogels showing the highest cumulative release. Weibull analysis confirmed formulation-dependent transport mechanisms. Cytotoxicity assays demonstrated good biocompatibility of drug-free hydrogels, while CPT-11-loaded formulations reduced viability of HCT-116 cells. Direct-contact observations further revealed hydrogel-mediated formation of multicellular spheroids by HCT-116 cells in soft, non-adhesive environments.

Conclusion

The results demonstrate that small-molecule modifiers enable effective tuning of gelation kinetics, hydrogel structure and drug release behaviour in CS/β-GP systems. Such thermosensitive hydrogels represent adaptable biomaterial platforms for local drug delivery and biointerface studies relevant to colorectal applications.

Acknowledgements

This research was funded in whole or in part by National Science Centre, Poland [2022/47/D/NZ7/01403].

References

[1] Li X., Fan D., Ma X., Zhu C., Luo Y., Liu B., Chen L., A novel injectable pH/temperature sensitive CS-HLC/β-GP hydrogel: the gelation mechanism and its properties. *Soft Materials* 2014; 12; 1-11.
[2] Jarry C., Leroux J.-C., Haeck J., Chaput C., Irradiating or autoclaving chitosan/polyol solutions: effect on thermogelling chitosan-β-glycerophosphate systems. *Chemical and pharmaceutical bulletin* 2002; 50; 1335-1340.
[3] Deng A., Kang X., Zhang J., Yang Y., Yang S., Enhanced gelation of chitosan/β-sodium glycerophosphate thermosensitive hydrogel with sodium bicarbonate and biocompatibility evaluated. *Materials Science and Engineering: C* 2017; 78; 1147-1154.

S73 – O7

Non-viral CRISPR/Cas9-based nanoformulation to gene editing aged cells

Barrera A[1,2], Tomatis F[2], Pitrez P[2], Santos S[2,3], Nobre R[2,4], Simões S[1,2], Ferreira L[1,2,5]
[1]Faculty of Medicine, University of Coimbra, Coimbra, Portugal, [2]CiBB - Centre for Innovative Biomedicine and Biotechnology, University of Coimbra, Coimbra, Portugal, [1]University of Coimbra, Institute for Interdisciplinary Research, Doctoral Programme in Experimental Biology and Biomedicine (PDBEB), Coimbra, Portugal, [4]ViraVector, University of Coimbra, Coimbra, Portugal, [5]CoLAB4Ageing, Biocant Park, Coimbra, Portugal.

Introduction

Gene editing technologies have emerged as promising therapeutic tools for treating age-related diseases. Viral delivery of CRISPR/Cas9 remains widely used but they pose several challenges, including immunogenicity, limited packaging capacity, and off-target effects, which restrict their safety and clinical applicability. Non-viral delivery systems offer a safer alternative; however, their efficiency remains low in non-dividing cells typical of aged tissues.

Aim

This work aims to develop an effective non-viral CRISPR-based formulation for gene editing in aged cells. The system was validated using cells derived from patients with Hutchinson-Gilford Progeria Syndrome (HGPS).

Materials and Methods

The nanoparticle (NP) design was optimized through a screen of branched polymers. The NPs results from interaction between the polymer and CRISPR ribonucleoprotein (RNP) complexes. The NPs were physicochemical characterized and validated using cells derived from patients with HGPS, a rare-accelerated aging disorder caused by a mutation in the LMNA gene. The NPs-RNP was used to induce knockout of the mutated LMNA gene (progerin) in HGPS-derived fibroblasts, smooth muscle cells (HGPS-iPSC-SMCs), and endothelial cells (HGPS-iPSC-ECs), all differentiated from patient-specific iPSCs. A lentivirus (LV) was used as a control. The NPs uptake, viability and endosomal damage were evaluated in HGPS fibroblasts using WT fibroblasts as controls. To evaluate the mechanism of NPs interaction with aged cells, the glucose uptake, GLUT1 expression and ATP were evaluated in WT and HGPS cells.

Results

The NPs-PNPs demonstrated to have higher internalization in aged cells when compared with proliferative cells and were able to activate at higher levels GLUT1 transporter (glucose transporter) which enhanced cell glycolysis and finally enhanced cellular endocytosis. It is important to note that this activation already leverages from the higher expression of a cellular transporter in aged (HGPS and senescent) as compared to proliferative cells. Cells were incubated with NPs-RNPs targeting LMNA for 24 h, and total RNA was harvested after 4 days. Digital droplet PCR revealed progerin transcript reduction of 38%, 51.7%, and 47.2% in HGPS-fibroblasts, HGPS-iPSC-SMCs, and HGPS-iPSC-ECs, respectively. Additionally, progerin protein levels in HGPS-fibroblasts decreased 78% after 10 days. This efficiency of NPs-RNPs was comparable with the capability of LV to knockout the LMNA gene and to reduce the progeria protein levels, demonstrate the potential of NP-RNPs.

Conclusion

In conclusion, our findings demonstrate that our non-viral nanoparticle system offers a safe and effective platform for CRISPR/Cas9 delivery in hard-to-transfect aged cells, with significant potential for therapeutic applications in HGPS and other age-related diseases.

Acknowledgements

The authors acknowledge the COMPETE2020, the EIC Project REGENERAR (Ref. 101129812), EIC Project CHANgeing (Ref. 101087071) and FCT program TREATABLE (2022.07615.PTDC), RETORNA (project no 15977) and mFIBRO (2023.12846.PEX). PRR project HfPT (Ref. 02/C05-i01.01/2022.PC644937233-00000047). SS acknowledge to FCT for the funding (2024.11680.CEECIN).

S74
Biomaterials for localized and targeted therapies

S74 – K1
Engineering Spatial Microenvironments for Brain–Interface Applications

Catalina Vallejo Giraldo C.
College of Science and Engineering, College of Medicine, Nursing & Health Sciences, Rinn Medical Devices, Research Ireland Centre for Medical Devices, University of Galway, Ireland

Glioblastoma multiforme (GB) is an aggressive form of brain cancer with a global incidence of approximately 250,000 new cases per year and a 5-year survival rate below 2%. The current standard-of-care—surgical resection followed by radiotherapy and temozolomide (TMZ) chemotherapy—aims to induce cancer cell death [1]. However, resistance to TMZ and radiation often develops rapidly due to intrinsic DNA repair mechanisms. Space, stiffness, and geometry are well-established regulators of cellular behaviour across diverse biological systems [2]. Yet, the potential of spatial modulation to guide cell–material interactions for brain-specific applications, such as cancer therapy, remains underexplored.

In my talk, I will present cellular and biomaterial strategies we have developed that incorporate spatial cues to advance glioblastoma research through two complementary therapeutic approaches. The first directly targets cancer cells by disrupting their DNA repair pathways, physically confining brain cells within defined 3D geometries to modulate their behaviour. The second focuses on remodelling the tumour microenvironment to enhance the effectiveness of current treatments and increase cancer cell susceptibility.
Collectively, these findings demonstrate how engineered spatial microenvironments can be leveraged to develop more effective cellular therapies and improve the integration of biomaterials with brain tissue.

References
[1] A. C. Tan, D. M. Ashley, G. Y. López, M. Malinzak, H. S. Friedman, M. Khasraw, CA Cancer J Clin 2020, 70, 299.
[2] C. M. Denais, R. M. Gilbert, P. Isermann, A. L. McGregor, M. Te Lindert, B. Weigelin, P. M. Davidson, P. Friedl, K. Wolf, J. Lammerding, Science 2016, 352, 353.

S74 – O1

Investigating the role of a plant-derived polysaccharide in chemoresistance in acute myeloid leukaemia

Lee R.L.[1], Tsimbouri M.[1], Berry C.[1], Gonzalez-Garcia C.[1]
[1]Centre for the Cellular Microenvironment (CeMi), Advanced Research Centre, University of Glasgow, UK

Introduction

The poor prognosis of acute myeloid leukaemia (AML) is partly driven by chemoresistance arising from interactions between leukaemic cells, stromal cells, and the surrounding microenvironment. Acemannan (ACE), traditionally used for dermatological applications, has recently demonstrated pro-haematopoietic, anti-cancer, and adjuvant properties in several animal models. However, its mechanism of action and efficacy in cancer, particularly AML, remain unclear.

Aim

This project aims to characterise the role of ACE in AML using a three-dimensional bone marrow microenvironment (BMME) model that better represents the AML niche.

Materials and Methods

To investigate ACE in a physiologically relevant setting, we developed a collagen-based hydrogel that mimics the BMME. Rat tail collagen type I hydrogels containing 0, 1, or 2 mg/mL ACE were fabricated using fibrillogenesis. The hydrogel model was mechanically characterised using rheology, and a chemoresistive niche was optimised. Human mesenchymal stem cells (MSCs) and the human AML cell line MOLM-13 were encapsulated in mono- and co-cultures. Cell viability and response to cytarabine, a first-line AML chemotherapy, were assessed to determine whether ACE exerts adjuvant or modulatory effects on chemoprotection conferred by MSCs.

Results

Rheological characterisation confirmed the hydrogel model fell within the BMME niche stiffness range (Young's modulus ~ 360 Pa), and a chemoresistive niche was optimised using a co-culture of spheroid MSCs and MOLM-13.

High viability and cell retention of MOLM-13 and spheroid MSCs were confirmed in ACE-free hydrogels, validating the hydrogel as a BMME model. ACE treatment reduced MOLM-13 cell counts in both mono- and co-cultures, while increasing MSC cell counts. In co-cultures, ACE enhanced MOLM-13 sensitivity to cytarabine and independently reduced MOLM-13 survival in the absence of cytarabine.

To explore potential mechanisms, a Human Cytokine Array was performed on supernatants from MSC-only hydrogels (0 and 2 mg/mL ACE). ACE reduced secretion of cytokines and chemokines associated with AML chemoresistance (GDF-15, IGFBP-3, and osteopontin), supporting a role for ACE in modulating the microenvironment to counteract stromal-mediated drug resistance.

Conclusion

Overall, these findings suggest that ACE may have adjunctive therapeutic potential in AML by suppressing leukaemic cell survival, enhancing the efficacy of cytarabine, altering MSC-derived secretory profiles, and supporting MSC growth. Further investigations, including macrophages in our BMME model, may help clarify the pathways through which ACE exerts its anti-cancer and adjuvant effects.

Acknowledgements

This work is supported by the EPSRC-NIA (EP/T000457/1). Advice from Dr Lluis Oliver Cervello, Dr Xinyu Li, Dr Euan Urquhart, Dr Lauren Hope and Dr Lydia-Styliani Marinou.

S74 – O2

New hydrogel vehicles for reactive oxygen and nitrogen target tumorigenesis and liver damage *in vivo*

Albert Caballeria-Casals[1], Giulia Fornabaio[2,3], Albert Espona-Noguera[2], Francisco Sanus[1], Carmen Peralta[1], Cristina Canal[2,3]
Barcelona, Spain, [2]Biomaterials, Biomechanics and Tissue Engineering Group, Universitat Politècnica de Catalunya, Barcelona, Spain, [3]Barcelona Research Centre in Multiscale Science and Engineering, UPC, Spain

Introduction

Hepatocellular carcinoma (HCC) is strongly associated with cirrhosis and presents high mortality rates, with limited therapeutic options. The aim of this study was to assess the therapeutic potential of reactive oxygen and nitrogen species (RONS) derived from cold atmospheric gas plasma (CAP) technology. In particular we developed novel hydrogel-based vehicles (Plasma-treated hydrogel - PTH) for RONS as an intraoperative asset to improve outcomes in cirrhotic, tumour-bearing livers, a context in which this has not previously been explored.

Materials and Methods

We compared the effects of CAP treatment and/or plasma-treated hydrogels, in a diseased tissue *in vivo*. A new rat model of concomitant cirrhosis and HCC was developed and a specific surgical technique was applied prior to different CAP and/or PTH based interventions.

Results

An alginate-based injectable PTH was developed, including optimized crosslinking and CAP-reactivity to maximize RONS concentrations. It was characterized in terms of concentration of RONS, pH and to ensure adhesion to the treated tissue *in vivo* (Fig 1 bottom). The tissue area and penetration of RONS during CAP treatment was determined employing tissue surrogates (Fig. 1 top).

Pronounced benefits were obtained with different doses for each of the individual therapies, as well as the combined treatment groups. Interestingly the positive effects observed with shorter treatments with CAP compare to those with long treatment of PTH, and they are related to the hormetic effects ascribed to RONS. Among the in vivo effects observed, this work will discuss the improved post-operative survival, reduced tumor burden, enhanced tissue regeneration, and reductions in tissue damage, inflammation, and tumour marker expression.

Figure 1. CAP and PTH application on the liver of a HCC-induced rat

Conclusion

Our findings demonstrate that the novel RONS vehicles developed and CAP-based strategies significantly reduced tumour burden, attenuate both surgical and disease-related hepatic injury, and diminished fibrosis in the cirrhotic liver. Thus, CAP and PTH appear as a promising tool in advanced liver therapy, with potential applications in both oncology and chronic liver diseases with impaired hepatic functions.

Acknowledgements

Project PID2022-141120OB-I00 funded by MCIU /AEI /10.13039/501100011033 / FEDER, UE and Red PlaSPAIN RED2024-153647-T. GF and CC belong to the SGR2022-1368.

S74 – O3

Nanotherapy Approaches to Combat Helicobacter pylori: tiny Particles, Big Impact

Parreira P[1,2], Pinho AS[1,3], Fonseca D[1], Chitas R[1], Martins MCL[1,2,3]
[1]i3S – Instituto de Investigação e Inovação em Saúde, University of Porto, Portugal, [2]INEB – Instituto de Engenharia Biomédica, Porto, Portugal, [3]ICBAS – Instituto de Ciências Biomédicas Abel Salazar, University of Porto, Portugal

Introduction

Helicobacter pylori infection is the main risk factor for the development of various gastrointestinal diseases, ranging from chronic gastritis to gastric cancer. In fact, nearly 90% of gastric cancer cases are linked to this Gram-negative pathogen, the only bacterium classified as carcinogenic by the International Agency for Research on Cancer (IARC). *H. pylori* colonizes the gastric mucosa of over 50% of the global population. The current treatment consists of a combination of two to three broad-spectrum antibiotics and a proton pump inhibitor. However, antibiotic-based therapy still fails in 10 to 40% of infected patients[1].

Aim

This presentation will highlight different bioengineering strategies explored by our group using nanoparticles (NPs) as alternatives to conventional antibiotics for *H. pylori* eradication, namely: i) Lipid NPs; ii) Cholesterol coated gold NPs, that specifically target *H. pylori* by exploiting its auxotrophic dependence of cholesterol; iii) Antimicrobial peptide (AMP) coated chitosan NPs, developed using a simple and efficient microfluidic device, which enables the bioconjugation of AMPs onto chitosan NPs during their formation via thiol-norbornene (TNPC) "photoclick" chemistry.

Materials and Methods

Lipid-NPs, Cholesterol-NPs & AMP-NPs were designed, optimized and evaluated against *H. pylori* strains according to references [2,3,4], respectively.

Results

Lipid NPs were able to target and kill *H. pylori* both *in vitro* (Fig. 1) and *in vivo*, without affecting other bacteria in the gut microbiome. Cholesterol NPs specifically kill *H. pylori* supporting the development of a “trojan horse” therapeutic strategy based on *H. pylori* cholesterol autotrophy. AMP-NPs, although not specific to *H. pylori*, can effectively kill the bacterium upon contact.

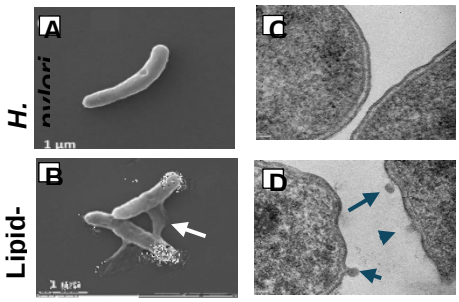

Fig. 1. SEM (left; scale bars: 1µm) and TEM (right; scale bars: 50nm) micrographs of H. pylori J99 (A, C) after Lipid NPs exposure (B, D).

Conclusion

All developed NPs kill *H. pylori* by disrupting its membrane, as observed by scanning electron microscopy (SEM) and/or transmission electron microscopy (TEM).

Acknowledgements

MOBILIsE_Plus project, co-funded by the European Union through the NORTE 2030 Regional Program of the European Regional Development Fund (FEDER), under the operation with the code NORTE2030-FEDER-01801000. FCT for the 2023.07672.CEECIND contract.

References

[1]Chitas, *et al.*Targeted nanotherapeutics for the treatment of *Helicobacter pylori* infection. Journal of Biomedical Science;2024; 31;78

[2]Seabra CL, *et al.* Paving the way for a non-antibiotic and microbiota friendly therapy for *Helicobacter pylori*: In vitro and in vivo
performance of lipid nanoparticles. Helicobacter, 2024, 29, e13050
[3] Pinho AS, *et al.* Cholesterol functionalized nanoparticles are effective against Helicobacter pylori, the gastric bug: a proof-of-concept
study. Advanced Healthcare Materials, 2025, 14(10)**:** 2404065
[4] Fonseca D, *et al.* One-pot microfluidics to engineer chitosan nanoparticles conjugated with antimicrobial peptides using “photoclick” chemistry: validation using the gastric bacterium Helicobacter pylori. ACS Applied Materials & Interfaces, 2024, 16(12) 14533

S74 – O4

Perivascular biodegradable mesh for extending vein graft patency for delivery of glucocortcosteroid

Kasi(S)[1], Shepherd(J)[2], Zakkar(M)[3]
[1]School of engineering, University of Leicester, UK, [2]School of engineering, University of Leicester, UK, [3]Dept. of cardiovascular science, University of Leicester, Glenfield hospitals, UK

Introduction

The Long saphenous vein (LSV) is the most used conduit to achieve revascularisation in ischemic heart disease. However arterial hemodynamics in the vein triggers a proinflammatory state which ultimately leads to a chain of events that contribute to vein graft failure (VGF). With failure of the vein graft revision surgery is required. Patency of vein grafts can be extended by a range of means including pharmacological treatment of several precursor conditions of VGF. Zakkar et al found that the venous endothelial cells arterialised in vein grafts when pretreated with dexamethasone which could improve graft patency.

Aim

To fabricate a biodegradable unidirectional drug releasing perivascular conduit to target early inflammation and thereby improve patency rates in vein grafts.

Materials and Methods

Insoluble type 1 collagen isolated from bovine achilles tendon was swollen in acetic acid for 48 hours and homogenised to prepare collagen slurry. 1 wt% collagen was frozen for 1 hour (-20°C) and then dexamethasone containing collagen slurry poured on top prior to lyophilisation (VirTis AdVantage Freezedryer). Optimisation of drug release was considered by loading various drug doses in various densities of collagen (0.5 wt%,1wt% and 2wt%) to help understand drug release kinetics. In vitro degradation test and UV visible spectrophotometry were used to quantify drug release. Sterilisation was carried out using UV B of wavelength 302nm. Non porous collagen was fabricated by air drying 1wt% collagen. Fabrication of tubular perivascular conduits was a multi step process involving lyophilisation. Fourier transformation infrared spectroscopy and scanning electron microscopy were used for physiochemical analysis. Drug uptake by vein segments from the collagen constructs was also investigated in in culture models.

Results

Dual layer collagen constructs achieved desired drug release profile to tackle early inflammation. The volume of collagen construct was further reduced to achieve neutral pH conditions and cater to fabrication for all types of grafts. UV sterilisation of collagen constructs was successful and did not alter drug release profile. Moreover, unidirectional drug release was clearly observed. Fabrication of perivascular conduits were also successful exhibiting good integration with barrier film for up to 28 days as shown in figure1. Finally quantification of dexamethasone uptake in vein explants in in vitro culture models showed steady drug uptake between day 1 and 7.

Conclusion

Tubular perivascular, drug-loaded collagen-based conduits were successfully produced. Drug release was shown to be both unidirectional and at a rate hypothesised to be optimal for treatment of early inflammation, with uptake measured in vein segments as shown in figure 2.

Acknowledgements

This work was funded by University of Leicester future 100 scholarship and MRC CiC grant from UKRI.

Figure 1 showing fabricated perivascular drug delivery conduit.

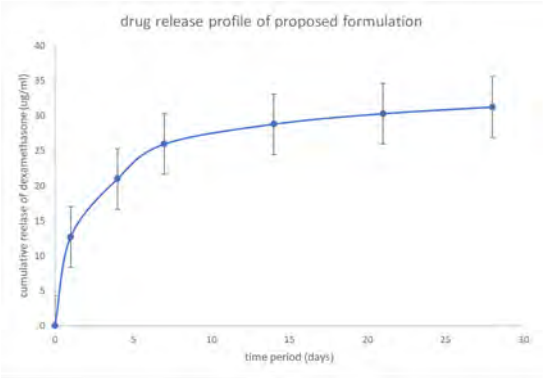

Figure 2 showing drug release profile of the proposed formulation to tackle early inflammation.

S74 – O5

Metals against Leishmaniasis: a study on biodegradable metal nanoparticles against *Leishmania* infection

Gomes-Ribeiro, B. F.[1,2], Bernardo, L.[3,4], Terrón, M. C.[5], Sanchez, F. D.[5], Díaz, S. B.[5], Carrillo, E.[3,4], Moreno, J.[3,4], Echeverry-Rendon, M.[1], Llorca, J.[1]

[1] IMDEA Materials Institute, Getafe-Madrid, Spain, [2] Malopolska Center of Biotechnology, Jagiellonian University, Cracow, Poland (current affiliation), [3] WHO Collaborating Centre for Leishmaniasis, Instituto de Salud Carlos III, Majadahonda-Madrid, Spain, [4] Centro de Investigación Biomédica en Red de Enfermedades Infecciosas (CIBERINFEC), Instituto de Salud Carlos III, Majadahonda-Madrid, Spain, 5 Electron Microscopy Unit, Instituto de Salud Carlos III, Majadahonda-Madrid, Spain

Introduction

Mg and Zn biodegradable nanoparticles (BNPs) have potential as therapeutics against leishmaniasis (Figure1). This vector-borne disease is caused by protozoan *Leishmania* spp. parasites, which infect cells of the immune system, such as macrophages, and thrive in the acidic environment of the lysosome. As a result, the immune acitivity of these cells is deregulated, leading to a variety of symptoms ranging from the destruction of epidermis and mucosal membrane (cutaneous leishmaniasis, mucocutaneus leishmaniasis), to their accumulation in organs such as spleen, liver or the bone marrow (life threatening visceral leishmaniasis). There is no known cure and treatments are based on pentavalent antimonial compounds, which present severe toxicity and adverse effects for the patient. A new effective treatment is urgently needed.[1]

Figure 1

Aim

To characterize the anti-leishmanial activity of BNPs. Through their degradation, they can increase the pH of the physiological media[2]:

$Mg+2H_2O \rightarrow Mg(OH)_2+H_2$
$Zn+2H_2O \rightarrow Zn(OH)_2+H_2$

Thus, upon reaching the lysosome of an infected macrophage, these BNPs can increase the pH of the environment killing the intracellular parasite.

Materials and Methods

Zn and Mg NPs were functionalized with 3-aminopropyltriethoxysilane (APTES), to increase dispersibility in physiological media, and were characterized by electron microscopy, nanosight for coloidal stability and inductively coupled plasma-optical emission spectroscopy. Their cytotoxicity was assessed at 24h, 48h and 72h against THP-1 derived macrophages. Similarly, the IC_{50} against *Leishmania* parasites was determined, and effective concentrations were established and tested against infected macrophages. Lastly, the mechanism of action of these particles was assessed. BNPs internalization by infected macrophages was studied through TEM. Expression of markers for ROS production, M1/M2 macrophage polarization, in infected and non-infected macrophages, both before and after treatment with BNPs, were determined.

Results
A significant reduction of infection was observed when infected macrophages were treated with BNPs (Figure2). TEM analysis and markers for ROS production and M1/M2 macrophage polarization allowed the establishment of a comprehensive model of the cellular uptake and metabolic pathways that result in the anti-*Leishmania* mechanism.

Figure 2

Conclusion
Mg and Zn-based NPs have substantial potential for the treatment of leishmaniasis.

Acknowledgements
This project received funding from the European Union's Horizon 2020 research and innovation programme under the Marie Sklodowska-Curie grant agreement No. 101110142

References
[1]Georgiadou, S P., *et al.* Leishmaniasis revisited: Current aspects on epidemiology, diagnosis and treatment. *Journal of Translational Internal Medicine* 2015; 2; 43-50.
[2]Echeverry-Rendón, M., *et al.* Cytotoxicity Assessment of Surface-Modified Magnesium Hydroxide Nanoparticles, *ACS Omega* 2022; 21, 17528 – 17537.

S74 – O6

Fabrication and Characterization of 3D-Printed Alginate Micro-Implants for Sustained Faricimab Delivery

Farokh A[1,2], Bogdan C.L.[1,3,4], Khalili H.[1,3,4], Zolgharni M.[1,2]
[1]THRIVE Centre, University of West London, UK, [2]School of Computing and Engineering, University of West London, UK, [3]School of Medicine and Biosciences, University of West London, UK, [4]School of Pharmacy, University College London, UK

Introduction

Age-related macular degeneration (AMD) continues to be a major cause of permanent vision loss globally. The neovascular form of the disease often requires regular intravitreal injections of anti-VEGF biologic therapies to keep the condition under control. Although Faricimab, a bispecific antibody that targets both VEGF-A and Angiopoietin-2, allows for longer intervals between treatments than earlier therapies, repeated dosing is still required because the eye clears drugs quickly and biologics have limited bioavailability. Sustained-release ocular implants have shown clinical success for small-molecule medications, but there are currently few well-established systems for the controlled delivery of antibody-based treatments in AMD care.

Aim

The aim of this study is to develop and evaluate a 3D-printed alginate-based intravitreal implant designed for prolonged release of biologics.

Materials and Methods

Alginate was selected as the primary biomaterial due to its biocompatibility, biodegradability, and mild ionic crosslinking mechanism, which supports protein stability. To improve mechanical integrity and modulate release kinetics, composite formulations incorporating in situ polymerised collagen and hyaluronic acid methacrylate were developed. Extrusion-based 3D bioprinting enabled the fabrication of micro-scale implants with geometries approximating clinically approved ocular implants, ensuring compatibility with established injection protocols. Release kinetics, structural stability, and degradation behaviour were evaluated using an ocular rig model designed to replicate physiological aqueous humour turnover.

Results

The results demonstrate the successful fabrication of ocular-scale micro-implants loaded with antibody therapeutics using extrusion-based 3D bioprinting and alginate-based composite biomaterials. The printed implants maintained structural stability and enabled sustained release of Faricimab for over 80 days. Notably, the alginate matrix provided a protective microenvironment that preserved the structural integrity of the antibody. Stability studies showed that Faricimab in solution rapidly aggregated and degraded within 24 hours at 37 °C, whereas encapsulation within the alginate hydrogel significantly reduced aggregation and maintained protein stability during short-term stability studies.

Conclusion

These findings highlight the dual function of the 3D-printed alginate implant as both a drug delivery platform and a protein-stabilising matrix. This work therefore presents a novel strategy for the fabrication of injectable micro-scale ocular implants capable of delivering biologic therapeutics, offering a promising approach to reduce injection frequency and improve long-term treatment outcomes for patients with age-related macular degeneration.

S75
Biomaterials for soft tissue and organ regeneration

S75 – K1
Lessons Learned and Critical Challenges in Advancing Adipose Tissue Engineering

Kluger P.
Institute of Interfacial Process Engineering and Plasma Technology, University of Stuttgart, Germany

S75 – O1
DLP-Based 4D Printed Hydrogel for Soft Tissue Engineering

Tadge T[1], Raichur A[1]
[1]Dept. of Materials Engineering, Indian Institute of Science, Bangalore, India

Introduction

Digital Light Processing based 4D printing has emerged as a transformative technology in biomedical engineering, enabling the fabrication of smart, stimuli-responsive biomaterials with high spatial resolution. Hydrogels are widely used in soft tissue engineering due to their biocompatibility, high water content, and tunable mechanical properties. When combined with 4D printing strategies, these materials can be engineered to dynamically change shape in response to environmental stimuli, providing new opportunities for developing adaptive tissue scaffolds.

Aim

This study aims to develop a DLP-based 4D printed hydrogels tailored for soft tissue engineering applications. The hydrogel formulation incorporates biocompatible, photo-crosslinkable polymers with shape-morphing capabilities triggered by physiological stimuli such as water.

Materials and Methods

A glycoprotein was first methacrylated to introduce photocrosslinkable functional groups. Subsequently, a biomaterial ink was prepared by combining the methacrylated glycoprotein with lithium phenyl-2,4,6-trimethylbenzoylphosphinate (LAP) as the photoinitiator and tartrazine as the photoblocker to enable controlled photopolymerization during DLP printing. The methacrylation efficiency of the glycoprotein and the printability of the formulated bio-ink were evaluated prior to fabrication. Hydrogel constructs with controlled architectures were then fabricated using a DLP printing system. Gradient crosslinking was introduced during the printing process to generate differential swelling behavior across hydrogel layers, enabling programmed shape transformation. The printed hydrogels were characterized for swelling, morphology, and porosity. Mechanical properties were evaluated by measuring the Young's modulus of the hydrogels. In vitro studies were further performed to assess cytocompatibility and cell adhesion on the printed hydrogel scaffolds.

Results

The glycoprotein-based biomaterial ink showed successful methacrylation and excellent printability using the DLP technique. The introduction of gradient crosslinking during printing produced differential swelling within the layered structures, resulting in shape-morphing behavior. Upon exposure to water, the initially printed flat sheets transformed into tube-like structures (Fig. 1.1). Morphological analysis and swelling studies confirmed a lesser swelling, lower pore size and higher stiffness of higher crosslinked layer than less crosslinked layer (Fig. 1.2, 1.3, 1.4). In vitro studies further demonstrated that the hydrogels were cytocompatible and supported cell adhesion (Fig.1.5, 1.6).

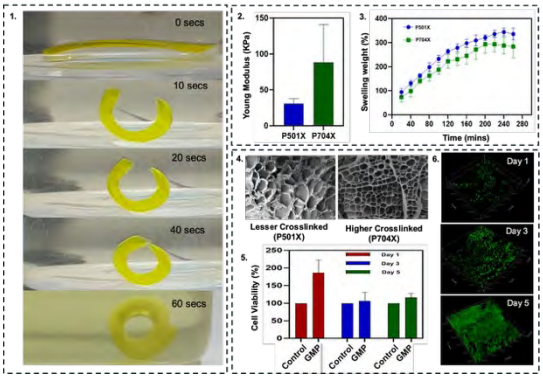

Conclusion

The developed DLP-based 4D printed glycoprotein hydrogels exhibit high printability, tunable mechanical properties, and programmable shape-morphing behavior triggered by water. Their porous architecture and cytocompatibility highlight their potential as dynamic scaffolds for soft tissue engineering

Acknowledgements

Authors are thankful to the Department of Materials Engineering, Indian Institute of Science Bangalore, and Hindustan Unilever for providing financial assistance for this project.

S75 – O2

Engineering Regenerative Niches for Intestinal Therapy via Encapsulation of iPSC-Derived Mesenchymal Stem Cells in Synthetic Degradable Microgels

Mora-Boza A.[1, 2], Rodríguez-Alonso P.[2], Lyu J.[2], Ahmedin Z.[3], Liu A.[4], García A. J.[3], Pandit A.[2]
[1]School of Life Sciences, Technical University of Munich, Freising, Germany, [2]CÚRAM, Research Ireland Centre for Medical Devices, University of Galway, Ireland, [3]George W. Woodruff School of Mechanical Engineering, Georgia Institute of Technology, Atlanta, GA, USA, [4]Optics11, Boston, MA, USA

Introduction

Intestinal mesenchymal stem cells (IMSCs) are critical stromal cells that promote epithelial regeneration through Wnt/BMP signaling and support immune tolerance, making them promising candidates for intestinal therapies[1]. Despite this potential, their regenerative capabilities remain largely unexplored. Although IMSCs can be derived from human iPSC-derived intestinal organoids (HIOs), this process currently depends on tumorigenic and poorly defined Matrigel®, limiting translational applications[2]. Here, we introduce a synthetic platform of protease-degradable polyethylene glycol norbornene (PEG-NB) microgels, fabricated via microfluidics, to deliver IMSCs for the treatment of inflammatory bowel disease.

Materials and Methods

HIOs were derived from iPSCs and, once mature, dissociated into single cells and sorted by magnetic-activated cell sorting into $EpCAM^+$ and $EpCAM^-$ IMSCs, followed by immunostaining for vimentin, collagen I, and α-SMA. IMSCs were encapsulated in PEG-NB microgels using a flow-focusing microfluidic device with *in situ* photopolymerization[3]. Microgels were fabricated at 4, 6, and 10 wt% and functionalized with a protease-sensitive linker (VPM) and adhesion peptide (RGD). Microgel stiffness was measured by nanoindentation. Encapsulated cells were monitored by live/dead fluorescent imaging over 21 days, and secretomes from naïve and IFN-γ-stimulated IMSCs were quantified using LEGENDplex™. Conditioned media were applied to HIOs for RNA-seq analysis to assess transcriptomic responses.

Results

$EpCAM^+$ HIOs displayed heterogeneous epithelial lineages, whereas IMSCs expressed a Col-I/Vimentin/α-SMA. PEG-NB microgels (6, 8, and 10 wt%) were fabricated, showing effective Young's moduli of 78.3±21.0, 158.3±68.1, and 301.8±53.5 Pa, respectively with a homogeneous size distribution (~350 µm), and supporting IMSCs viability over 21 days for all microgels formulations. IFN-γ increased inflammatory cytokine secretion, mitigated by higher stiffness. RNAseq of HIOs treated with IMSC-conditioned media revealed a pro-regenerative signature associated with epithelial proliferation and stemness, while modulating immune-related processes. Data deconvolution using XCell2, indicated a higher enrichment of Transit-Amplifying cells in HIOs exposed to secretomes from IFN-γ-conditioned microgels, positively correlated with increasing stiffness.

Conclusion

Synthetic PEG-NB microgels provide a versatile platform for stem cell–based intestinal therapies. IMSCs remained highly viable within the microgels, and increasing microgel stiffness suppressed proinflammatory responses. Their secretome further promoted epithelial regeneration in a stiffness-dependent manner, emphasizing the potential of IMSCs for regenerative medicine applications.

Acknowledgements

RI&EU (Grants:13/RC/2073_P2,101126640); MSCA Postdoctoral Fellowship (Grant: 101028216); Research Ireland (Grant: 13/RC/2073_P2)

References

[1] Helen E. Abud, et al, Cellular and Molecular Gastroenterology and Hepatology 17, 5 (2024).
[2] Tian, C. M. et al. Cell Death Discov. 9, *255 (2023*).
[3] A. Mora-Boza, et al. Adv. Healthcare Mater. 12, *2300942 (2023*).

S75 – O3

Therapeutic ion releasing fluorophosphate glass for ischemic wound care

Balasubramanian M.[1], Ganesan S.M.[1], Kandaswamy R.[1], Sankaralingam P.[2], Thangavel V.C.[2]
[1]Dept. of Rubber and Plastics Technology, Madras Institute of Technology Campus, Anna University, Chromepet, Chennai, Tamil Nadu, India, [2]Bone Substitutes, Madurai, Tamil Nadu, India

Introduction

Ischemic wounds, including burns and chronic ulcers, remain a major challenge in regenerative medicine due to poor vascularization, limited oxygen supply, and delayed cellular proliferation. Biomaterials capable of releasing therapeutic ions have emerged as promising strategies to stimulate angiogenesis and accelerate tissue regeneration. Fluorophosphate (FP) bioactive glasses provide controlled ion release and tunable degradation, while metal oxide doping can further enhance biological responses[1]. However, their application in topical wound healing systems remains largely unexplored.

Aim

This study aimed to develop multifunctional metal oxide doped fluorophosphate glass nanoparticle based topical formulations and evaluate their ability to promote angiogenesis and accelerate ischemic wound healing.

Materials and Methods

Silver, zinc, and magnesium doped fluorophosphate glass nanopowders were synthesized via melt quenching and incorporated into polymeric carriers (PEG, and PPG) to formulate bioactive topical systems[2]. Cytocompatibility was assessed using HDF, HEK, and HUVEC cell lines. Fibroblast migration was evaluated using scratch assays, while angiogenic potential was analyzed using the chorioallantoic membrane (CAM) assay. Growth factor expression (FGF, EGF, VEGF) was quantified through Western blot analysis. The therapeutic performance of optimized formulations was further validated in vivo using rat cut and burn wound models, followed by histopathological and immunohistochemical analyses.

Results

Among the formulations tested, MgFP incorporated within a PPG carrier exhibited the most favorable biological response. The system demonstrated high cytocompatibility and significantly enhanced fibroblast migration and angiogenesis. Western blot analysis revealed substantial growth factor upregulation, with MgFP-PPG inducing a 9.8-fold increase in EGF expression, while AgFP-PPG produced a 4.2-fold increase in VEGF secretion. In vivo studies confirmed accelerated wound repair (Figure 1), with MgFP-PPG achieving 73% wound contraction by day 7 compared with 46% in untreated controls (Table 1). Histological evaluation further indicated enhanced granulation tissue formation, collagen deposition, and neovascularization.

Conclusion

Ion releasing metal oxide doped fluorophosphate glass topical formulations represent a promising biomaterial platform for ischemic wound healing. The MgFP-PPG formulation demonstrated optimal cytocompatibility, angiogenic stimulation, and accelerated wound repair, highlighting its potential as a next generation therapeutic strategy for chronic wound management.

Acknowledgements

The research was fully supported by Bone Substitutes, Madurai 625014, India. The authors are much grateful to the PAMC Hospital, Madurai, and the Department of Rubber and Plastics Technology, MIT campus, Anna University, Chennai-600044.

References

[1]Sankaralingam P., Sakthivel P., Subbiah A., Periyasamy A., Rahumathullah J.B., Thangavel V.C. Fluorophosphate bio-glass for bone tissue engineering: in vitro and in vivo study. *Bioinspired Biomimetic Nanobiomaterials 2021*; 10; 123-131

[2]Balasubramanian M., Ganesan S.M., Sankaralingam P., Thangavel V.C., Kandaswamy R. Multifunctional metal oxide-doped nanofluorophosphate glass: a bioactive topical formulation for ischemic wound repair. *ACS Biomaterials Science & Engineering 2025*; 11; 6195-6215.

Table 1. Quantitative analysis of wound contraction in rat cut wound models on Day 14 post treatment

Treatment Group	Wound Contraction (%) on day 14
PPG-MgFP	73%
PPG-AgFP	63%
PPG-ZnFP	72%
Untreated group	46%

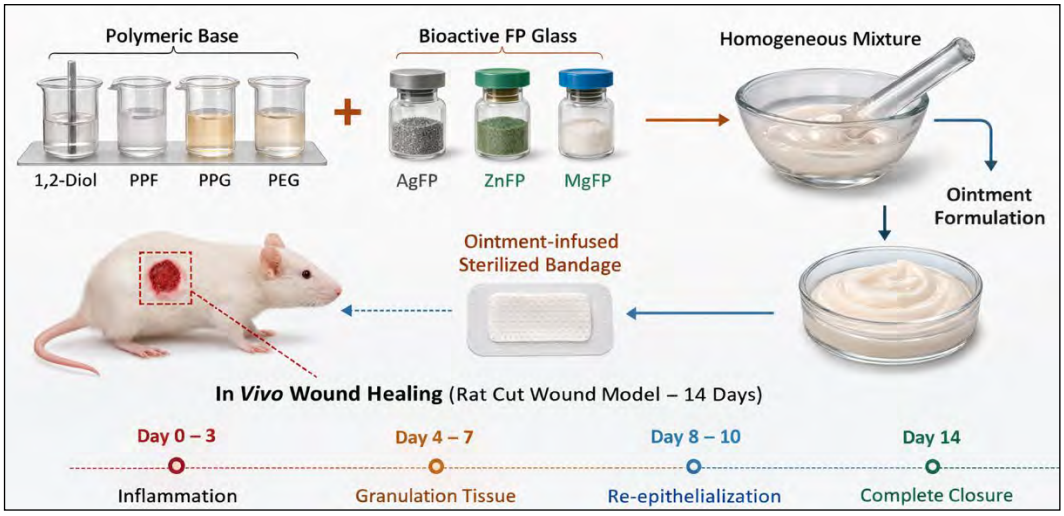

Figure 1. Schematic illustration of fluorophosphate glass nanoparticle based topical formulation and its in vivo evaluation in rat wound models showing progressive healing over 14 days

S75 – O4
Towards semi-synthetic liver-like tissues

De Dios Andres P.[1], Stadler B.[1]
[1]Interdisciplinary Nanoscience Center (iNANO), Aarhus University, Aarhus, Denmark

Introduction

Integrating biomaterials with living cells remains a major challenge in tissue engineering and regenerative medicine. For example, alginate microgels encapsulating catalase and coated with poly(L-lysine) have been co-cultured with hepatocytes to provide supportive detoxification functions.[1] However, these microreactors remained active for only 24 h and showed limited integration with HepG2 cells due to their simplistic interface design.
Here, we developed semi-synthetic liver-like tissues by combining alginate microgels with hepatocytes. Microgels were camouflaged with cell membrane vesicles and functionalized with a small-molecule antioxidant to protect HepG2 cells from reactive oxygen species in semi-synthetic aggregates.[2] In addition, we used 3D bioprinting to fabricate centimeter-scale tissues composed of HepaRG cells and functionalized microgels. The HepaRG cells differentiated into hepatocyte and biliary cells resembling native liver tissue, while antioxidant-loaded microgels reduced oxidative stress in steatotic tissues[3] (Figure 1).

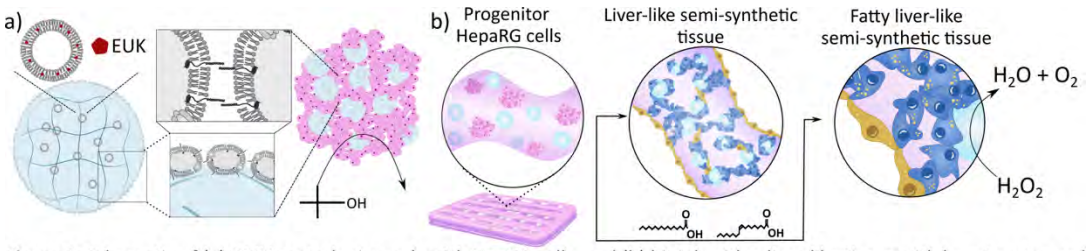

Figure 1. Schematic of (a) CMV-coated microgels with HepG2 cells, and (b) bioink with a liver-like tissue with hepatocytes and biliary cells.

Materials and Methods

Alginate microgels were fabricated using an Encapsulator, optionally incorporating artificial enzymes. Cell membrane vesicles (CMVs) were purified from HepG2 cells and used to coat microgels that were co-cultured with HepG2 cells in 96-well plates with an ultralow attachment surface in different cell-to-microgel ratios. Cell aggregates of HepaRG cells were cultured for 24 hours before being suspended in a bio-ink mixture containing alginate, gelatin methacryloyl (GelMA), and microgels. This composite ink was then 3D-bioprinted and maintained in culture for up to 35 days. Cellular proliferation was assessed via dsDNA quantification and LIVE/DEAD staining. Expression of relevant hepatic markers was evaluated using RT-qPCR. To model liver steatosis, differentiated HepaRG cell-based tissues were treated with free fatty acids for two weeks and analyzed for lipid accumulation through fat staining techniques.

Results

CMV-camouflaged microgels showed improved integration with proliferating HepG2 cells compared to PLL-coated microgels. Encapsulation of a ROS-scavenging artificial enzyme enhanced protection against tBuOOH-induced stress, improving HepG2 cell viability, proliferation, and mitochondrial health in semi-synthetic aggregates. HepaRG aggregates were successfully incorporated into 3D-bioprinted constructs using an alginate/GelMA–microgel composite ink and remained viable during a 35-day culture. Differentiation initiated at day 14 led to increased expression of hepatocyte and biliary markers by day 28. A steatotic tissue model induced by fatty acid incubation displayed lipid accumulation and elevated ROS levels. Functional assays using hydrogen peroxide revealed reduced oxidative stress in steatotic tissues in the presence of catalytic microgels.

Conclusion

Taken together, these 3D semi-synthetic aggregates and tissues where the microgels supported their biological counterparts within a tissue-mimicking milieu, exhibited augmented hepatocyte-like functions, and constitute a step toward developing a minimal liver model.

References

[1]Y. Zhang, et al., Planar and Cell Aggregate-Like Assemblies Consisting of Microreactors and HepG2 Cells. *ACS Omega*, 2017, 2, 7085-7095
[2]P. de Dios Andres et al., Cell Membrane Vesicle Camouflaged Artificial Cells. *Adv. Funct. Mater.* 2025, 35, 2424504.
[3]P. de Dios Andres et al. (in preparation)

S75 – O5

Alginate/gelatin/silk fibroin-containing patches protect against myocardial infarction-mediated reduction in cardiac function in a murine model

Vettori L.,[1,2], Matthee A.,[1,2], Matthews N.,[1,2], Gentile C.,[1,2],
[1]School of Biomedical Engineering, University of Technology Sydney, Australia, [2]Cardiovascular Regeneration Group, Heart Research Institute, Sydney, Australia.

Introduction

Cardiovascular disease, including myocardial infarction (MI) and heart failure (HF), remains a major cause of death globally. The irreversible and progressive damage of a failing heart is due to its limited regenerative capacity, and a heart transplant remains the gold-standard treatment for end-stage HF patients. A heart transplant is available to only a few patients due to its risks and its limited compatibility. Our team has recently demonstrated that the transplantation of alginate (Alg) and gelatin (Gel) bioprinted patches represents a promising approach to improve cardiac function *in vivo* using a murine MI model. Additionally, we showed that CT and MRI scans can be used to generate patient-specific bioprinted patches that can be folded and delivered *via* a keyhole procedure, which means faster recovery for patients compared to the current open-heart surgery required for a heart transplant. More recently, we demonstrated that the addition of silk fibroin (SF, a natural polymer used for its strength and elastic properties) to Alg/Gel hydrogels can improve the contractile function of *in vitro* vascularised cardiac spheroids. The aim of this study was to evaluate whether the addition of SF to Alg/Gel hydrogels could improve the performance of the transplanted patch following MI *in vivo*, therefore protecting against HF.

Materials and Methods

Alg/Gel/SF hydrogels were used to generate patches to be transplanted in a permanent model of left anterior descending (LAD) ligation in Rag1 mice. Mice were divided into four experimental groups: *i*) sham (non-MI); *ii*) MI; *iii*) MI with the transplanted Alg/Gel patches; and *iv*) MI with the transplanted Alg/Gel/SF patches. Ultrasound imaging was performed to measure the left ventricular ejection fraction % (LVEF%) at baseline (before MI), as well as at 14 and 28 days post-MI. At 28 days, the heart was excised and sectioned for downstream analyses.

Results

The transplantation of Alg/Gel/SF patches improved the LVEF% by ~20% compared to the one in MI animals. Histological analyses showed that AlgGelSF patches reduced fibrosis in infarcted animals, while bulk RNAseq analyses demonstrated that they improved the expression of genes regulating tissue-repairing processes, fibrosis, cell proliferation, and tissue homeostasis in MI mice.

Conclusion

Altogether, our findings demonstrate that AlgGelSF hydrogels can be used to protect against the reduction in LVEF% following MI, with the potential to be used as a safer and personalised alternative to heart transplant in HF patients.

S75 – O6

Sustainable acellular fish skin biomaterial with preserved lipid reservoirs

Botelho, C.M.[1,2], Barbosa, M.A.[1,2]
[1] ICBAS - Instituto de Ciências Biomédicas Abel Salazar, Universidade do Porto, Portugal, [2] i3S - Instituto de Investigação e Inovação em Saúde, Universidade do Porto, Portugal

Introduction

Decellularization is extensively used to produce immune-compatible biomaterials, but most matrices are sourced from mammalian tissues, which pose risks of disease transmission and immune rejection. Fish by-products offer a sustainable alternative, with negligible zoonotic concerns and low immunogenicity. Decellularization commonly relies on surfactants and enzymes to remove cellular material, although it disrupts tissue ultrastructure, removes glycosaminoglycans and lipids, and leaves residues that impair host integration.

Aim

The present study aimed to produce a tissue-engineered graft from fresh mackerel skin using a surfactant- and enzyme-free decellularization method designed to retain native architecture and composition, both essential for cell recruitment and tissue regeneration.

Materials and Methods

Atlantic mackerel (*S. scombrus*) skins were obtained fresh from a local restaurant. Following flesh removal, skins (N=9) were transported on ice, washed, and processed using a surfactant- and enzyme-free treatment based on hypertonic buffers and high concentrations of sodium chloride (NaCl). A Triton X-100 protocol served as control. Decellularized skins were analyzed for DNA content and major extracellular matrix (ECM) components, including collagens, elastin, glycosaminoglycans, and lipids. Structural preservation was assessed by histological staining and high-resolution imaging (AFM, SEM, TEM). Mechanical properties were analyzed by uniaxial tensile testing and viscoelastic measurements. Cytocompatibility was evaluated by direct and indirect assays using stromal and endothelial cells (HDFs and HUVECs, respectively).

Results

Both protocols removed cellular and nuclear material while retaining the 3D protein network. The surfactant-free method better preserved glycosaminoglycans and lipids (Figure 1). These components are prone to leaching but are crucial for modulating inflammation and tissue repair. Histological and structural analyses revealed an intact epidermis, a fibrillar dermis, and a porous hypodermis, with an interconnected ECM favorable for cell infiltration. Mechanical testing showed comparable viscoelastic behavior between groups, with increased stiffness following decellularization. All experimental groups demonstrated excellent cytocompatibility, with low cytotoxicity and high metabolic activity in both HDFs and HUVECs cultures. Cells showed a spindle-shaped morphology and robust proliferation, therefore confirming the overall safety of decellularized skin for healthcare applications.

Conclusion

The surfactant- and enzyme-free decellularization protocol generated a 3D fish skin-derived tissue construct with preserved architecture, enhanced retention of bioactive components, and optimal mechanical behavior. Given its structural and compositional complexity, this biomaterial represents a promising platform for delivering intrinsic anti-inflammatory and pro-regenerative cues.

Acknowledgements

This work was supported by Fundação para a Ciência e a Tecnologia (Grant 2024.00876.BD) and the Molecular and Cellular Biotechnology Applied to Health Sciences Doctoral Program (BiotechHealth).

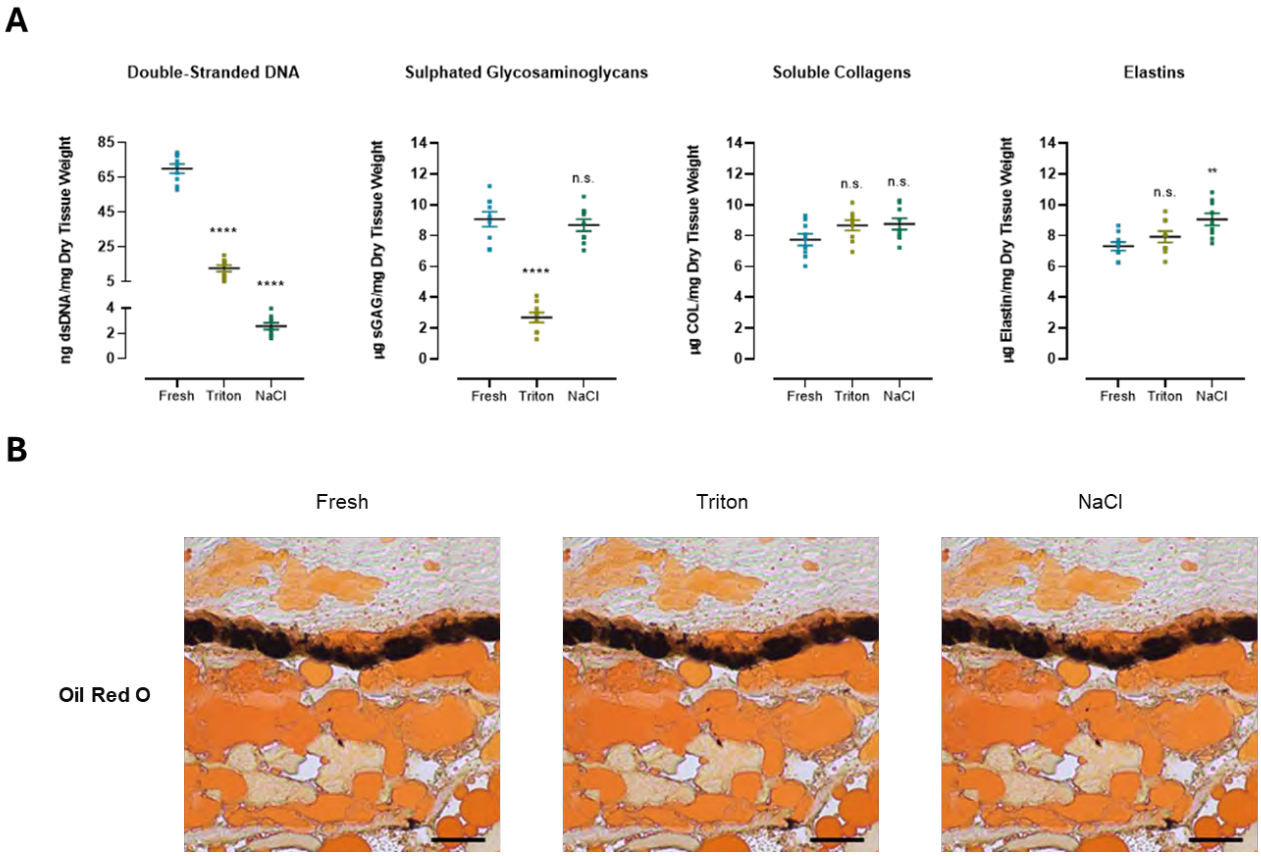

Figure 1. (A) Molecular quantification of double-stranded DNA, glycosaminoglycans, collagens, and elastins (N = 9). Mean ± SEM. One-way ANOVA. Sidak's Multiple Comparison Test. ****$p < 0.0001$. (B) Oil Red O histological staining of neutral lipids. Scale bar: 50 µm.

S75 – O7

Multifunctional Plasmonic Hydrogels as Tunable Biomaterials for Mechanobiology of Myogenic Cells

P. Peng[1], F. Guo[1], O. Deschaume[1], H. Declercq[2], W. Thielemans[3] and C. Bartic[1]
[1]Dept. of Physics and Astronomy, KU Leuven, Belgium, [2]Dept. of Development and Regeneration, KU Leuven, Kortrijk, Belgium, [3]Dept. of Chemical Engineering, KU Leuven, Kortrijk, Belgium

Introduction

Plasmonic hydrogel-based systems can provide biomimetic and dynamic microenvironments for tissue engineering. By integrating soft extracellular matrix materials with light-addressable nanoparticles, we can obtain externally controlled non-invasive cell mechanical actuation, and localized functional sensing. This allows for the investigation of cell-substrate interactions under dynamic conditions. Such systems are particularly relevant for exploring how external cues influence cellular mechanics, cytoskeletal remodeling, and mechanotransduction.

Aim

Establish a multifunctional plasmonic hydrogel-based system for investigating biomechanical responses in myogenic cells. Specifically, we aimed to assess the effect of cyclic stress application on the cell stiffness before and after stimulation by means of atomic force microscopy (AFM) and to relate these mechanical changes to cytoskeletal organization and mechanosensing.

Materials and Methods

A multifunctional gold nanorods (GNRs) containing gelatin methacryloyl (GelMA) based plasmonic hydrogel system was prepared. Fluorescence nanosensors were incorporated to monitor localized temperature and oxygen related changes in the microenvironment during stimulation. Myogenic cells cultured on the gels were examined before and after stimulation using AFM to assess cell stiffness, while cytoskeletal and Yes-associated protein (YAP) stainings were performed to evaluate the morphological features.

Results

Bulk rheology and AFM showed that GNR incorporation modifies the photopolymerization kinetics and changes the local surface mechanics and topography, while the hydrogel remains primarily elastic (which is important for the reversible cyclic stimulation of cells). NIR stimulation protocols can induce micrometer-scale deformations and short stimulation cycles (10 min) can induce significant changes in Young's modulus as quantified by AFM. Furthermore, a significant increase in the YAP N/C ratio indicates an active cellular response to mechanical tension. These findings were accompanied by cytoskeletal reorganization, indicating structural adaptation to the applied cues.

Conclusion

These findings demonstrate that plasmonic hydrogel-based systems can combine localized microenvironmental sensing with the analysis of stimulation-associated biomechanical responses in myogenic cells. The combined observation of altered cell mechanics, cytoskeletal remodeling, and YAP nuclear localization highlights the utility of this biomaterial approach for studying dynamic cell-material interactions and mechanotransduction in vitro.

Acknowledgements

P.P., O.D., W.T., H.D. and C.B. acknowledge the KU Leuven BOF funding (grant C14/23/093).
O.D. and C.B. acknowledge the FWO infrastructure grant I000624N.

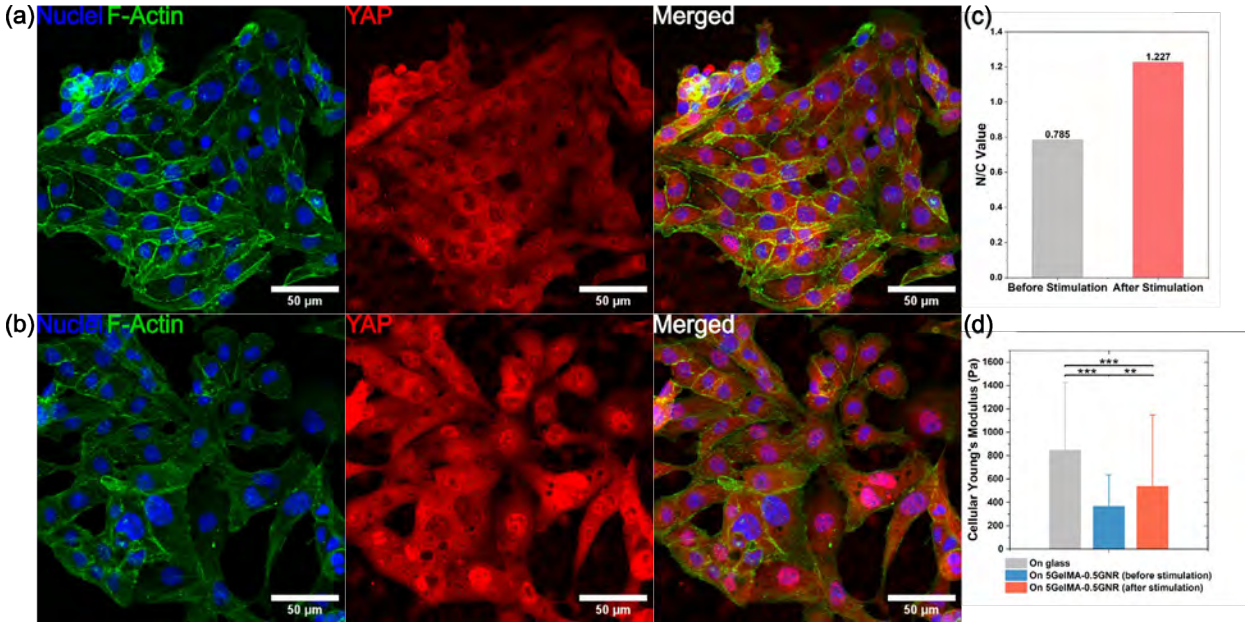

Figure 1. Effect of NIR stimulation on YAP nuclear localization and stiffness of cells cultured on hydrogel. Representative confocal images before (a) and after (b) 30 min NIR stimulation, showing nuclei (blue), F-actin (green), and YAP (red) stainings. (c) Quantification of the YAP nuclear to cytoplasmic ratio (N/C ratio) before and after NIR stimulation. (d) Cellular Young's modulus measured by AFM for cells cultured on glass and on hydrogel before and after NIR stimulation (cells on glass, n=112; cells on hydrogel, n=127; *** $p < 0.001$, ** $p < 0.01$).

S77 Biomaterials translated to the clinic

S77 – K1

Polymeric Platforms Tailored to Pathological Microenvironments: Strategies for Inflammation and Skin Repair

Rosa Aguilar M. [1,2], Luis Echevarria-Torres P.[1,2], Domingo-Lopez D.[1,2], Palao-Suay R.[1,2], Benito-Martínez S.[2,3,4], Lorena Benito Garzón[5], Martin-Saldaña S.[1,2], Calvo Montalvo C.[1], Pascual G.[2,3,4], García-Fernández L.[1,2], Rojo L.[1,2].

[1] Instituto de Ciencia y Tecnología de Polímeros (ICTP), CSIC, 28006, Madrid, España,[2] CIBER de Bioingeniería, Biomateriales y Nanomedicina, Instituto de Salud Carlos III. (CIBER-BBN, ISCIII), 28029, Madrid, España., [3] Dept. de Medicina y Especialidades Médicas, Facultad de Medicina y Ciencias de la Salud, Universidad de Alcalá, 28805, Alcalá de Henares, España, [4] Instituto Ramón y Cajal de Investigación Sanitaria (IRYCIS), 28050, Madrid, España, [5] Dept. de Anatomía e Histología Humanas, Facultad de Medicina, Universidad de Salamanca, 37007, Salamanca, España.

Introduction

Inflammation is a fundamental biological response involved in a wide spectrum of pathological conditions, ranging from cancer to chronic wounds. Its molecular complexity, characterized by excessive production of reactive oxygen species (ROS), altered pH, immune dysregulation and degradation of the extracellular matrix, creates microenvironments that profoundly affect the efficacy of therapeutic interventions. Over the last years, our group has been dedicated to the design of smart polymeric systems capable of responding to such pathological cues, with early developments focused on targeted cancer treatments and controlled drug release. In recent years, this expertise has converged toward the creation of biomaterials tailored to inflammatory microenvironments, where stimulus-responsive degradation and controlled delivery can offer precise, on-demand therapeutic action.
Within the field of dermatology, inflammation plays a central role in conditions such as radiodermatitis and burn injuries. These injuries are defined by extreme oxidative stress, compromised barrier function and impaired cell proliferation, posing significant clinical challenges. Therefore, polymeric nanoparticles delivering bioactive compounds and smart hydrogels capable of responding to ROS or acidic pH, emerge as powerful strategies to address the multifactorial nature of these lesions. This keynote will present representative advances from our group in the development of such systems and their application to inflammatory skin disorders.

Materials and Methods

Polymeric nanoparticles were synthesized using microfluidic methods to achieve precise control over particle size, composition and encapsulation efficiency. Their antioxidant, antimicrobial and regenerative potential was assessed in *ex vivo* human burn models and in radiated skin generated with the T-Skin Human Full Thickness model. In parallel, ROS- and pH-responsive hydrogels incorporating thioketal or phenylboronic groups were fabricated and characterized. Hybrid nanoparticle-hydrogel constructs were also explored.

Results

Microfluidic nanoparticles showed high stability, very low polydispersity and the ability to deliver bioactive molecules relevant for modulating oxidative stress and promoting tissue regeneration. Selected formulations improved epithelial recovery and enhanced expression of key differentiation and proliferation markers in burn and radiated skin models. Responsive hydrogels exhibited selective degradation under inflammatory conditions, enabling controlled release and antioxidant activity. Integrated systems demonstrated complementary and potentially synergistic behavior.

Conclusion

Smart polymeric nanoparticles and inflammation-responsive hydrogels represent versatile and powerful platforms for addressing complex inflammatory conditions. Their adaptability, targeted action and regenerative potential place them as promising tools for treating radiodermatitis, burns and a broader range of inflammation-driven pathologies.

Acknowledgements
Grant PID2023 149301OB I00 (MICIU/AEI/10.13039/501100011033 and ERDF/EU). Grant S2022/BMD 7406 (Community of Madrid). MSCA PF grant 101153515.

S77 – O1

mRNA polyplexes for tackling fibrosis in the context of spinal cord injury

Carvalho LS[1,2], Félix P[2,3], Simões S[2,3], Serrano, MC[4], Ferreira, L[2,3],
[1]University of Coimbra, Institute for Interdisciplinary Research, Doctoral Programme in Experimental Biology and Biomedicine (PDBEB), Coimbra, Portugal, [2]CiBB - Centre for Innovative Biomedicine and Biotechnology, University of Coimbra, Coimbra, Portugal, [3]Faculty of Medicine, University of Coimbra, Coimbra, Portugal, [4]Instituto de Ciencia de Materiales de Madrid (ICMM), Consejo Superior de Investigaciones Científicas (CSIC), Madrid, Spain

Introduction

Spinal cord injury (SCI) disrupts the communication between the brain and peripheral body, causing loss of motor, sensory, and autonomic functions. Current therapies remain symptomatic. A major barrier to regeneration is the activation of fibroblasts, driving extracellular matrix deposition and a fibrotic scar that inhibits neuronal repair. mRNA therapies offer a versatile way to induce strong, transient, and programmable expression of therapeutic anti-fibrotic proteins, yet remain underexplored in SCI. Developing suitable delivery systems, along with efficient models for formulation screening, is essential for advancing mRNA therapies for SCI.

Aim

To develop a nanoformulation targeting fibroblasts for mRNA delivery, using a spinal cord (SC) organotypic model as a physiologically relevant *in vitro* platform.

Materials and Methods

A polymeric nanoparticle (PNP) with fibroblast tropism was previously identified through a polymer-library screening[1]. The mRNA-loaded PNPs were physiochemically characterized. PNPs were evaluated in relevant cell cultures (meningeal fibroblasts, embryonic neurons, and glial cells) and in a SC organotypic slice model. Rat SC slices were maintained in an air–liquid interface, treated with PNPs loaded with GFP mRNA as a reporter, and GFP^+ cells were analyzed. An acute injury was established via a stab lesion at the grey matter to evaluate nanoparticle tropism in the injured microenvironment. Results were compared to the commercial transfection reagent DharmaFECT (DF).

Results

A robust SC organotypic model was established, maintaining high viability up to 14 DIV and supporting its use as a relevant platform for SC therapy evaluation. The PNPs (~270 nm, >+20 mV) showed ~100% mRNA-loading efficiency. They achieved uniform transfection across slices with efficient penetration (**Fig1**). Around 40% and 45% of GFP^+ cells co-expressed PDGFR-α and vimentin, respectively (fibroblast markers), compared to ~10% and 20% with DF. In contrast, only ~10% of GFP^+ cells co-stained for astrocytes (GFAP) or microglia (IBA1). All GFP^+/PDGFR-$α^+$ cells expressed α-SMA, indicating selective transfection of activated, pro-fibrotic fibroblasts. In the injury model, cell death peaked at 6 hours, and PNP treatment generated a distinct GFP^+ interface around the stab lesion (absent in GFP-DF slices) (**Fig2**), highlighting a selective, formulation-dependent response within the injured microenvironment.

Conclusion

Using our organotypic platform, we demonstrated selective tropism of mRNA-PNPs toward fibroblasts within the SCI microenvironment, highlighting a promising strategy for antifibrotic mRNA interventions after SCI.

Acknowledgements

EIC Project Piezo4Spine (GA101098597); FCT mFIBRO project (2023.12846.PEX); PRR project HfPT - Health from Portugal (02/C05-i01.01/2022.PC644937233-00000047); Provas de Conceito UC by Santander (PT0054.B.06.D); FCT fellowship UI/BD/154204/2022.

References

[1]Rodrigues A.F., Rebelo C., Simões S., Paulo C., Pinho S., Francisco V., Ferreira L. A Polymeric Nanoparticle Formulation for Targeted mRNA Delivery to Fibroblasts. *Advanced Science 2023*; 10: 2205475.

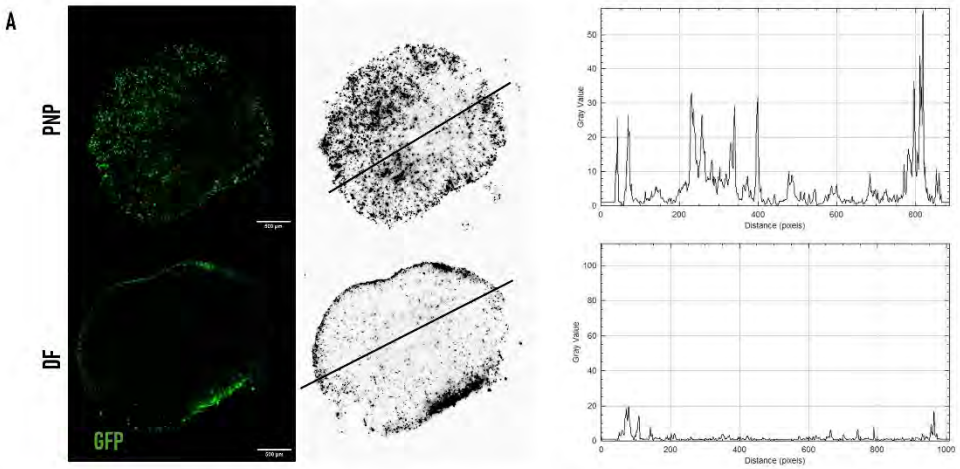

Figure 1. Transfection efficiency and spatial distribution of the polymeric formulation in rat spinal cord organotypic cultures (SCOC). (A) Representative fluorescence images of SCOCs treated with GFP-PNP or GFP-DF, showing GFP expression throughout the slices. A corresponding intensity profile (gray value histogram) along the indicated black line illustrates the distribution of GFP signal across the tissue of both formulations.Scale bars = 500 µm.

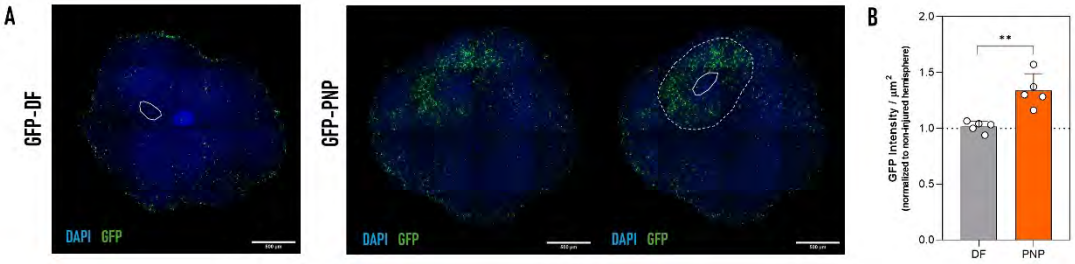

Figure 2. Accumulation and retention of the polymeric formulation in injured spinal cord organotypic cultures (SCOCs). (A) Representative fluorescence images of SCOCs treated for 24 h with GFP-DF or GFP-PNP, administered 1 h post-injury. The lesion core is delineated by a solid line, and the peri-lesional interface is indicated by a dashed line. (B) Quantification of GFP fluorescence intensity per µm² in the injured hemisphere, normalized to the contralateral non-injured hemisphere. Scale bars = 500 µm. n= 5.

S77 – O2

Multiphasic electrospun and film-based dural substitute: cell-specific layer selection, watertight membrane engineering and in vivo biocompatibility

Tosiani J-P.[1], Baudequin T.[1]
[1]Université de technologie de Compiègne, CNRS, Biomechanics and Bioengineering, Compiègne, France.

Introduction

Native dura mater is an interface between bone and the other meninges, requiring hydrostatic resistance and side-specific cellular support. Cerebrospinal fluid leakage after dural repair can cause infections, pain and delayed healing. Current substitutes rarely combine durable watertightness with dura-like mechanics and biological integration. We hypothesized that a multiphasic substitute integrating electrospun cell-promotive layers with an ultrathin watertight membrane could reconcile these requirements.

Materials and Methods

Electrospun PCL-based scaffolds (± silk fibroin, ± nano-hydroxyapatite; random or aligned fibers) were assessed for biomimetic tensile behavior by measuring elastic modulus, ultimate tensile strength and strain at failure, then cultured with human dural fibroblasts (HDuFs) and adipose-derived stem cells (ADSCs). Cell viability at day 7 was assessed by Live/Dead staining and MTS metabolic assay. Gene expression at day 25 was quantified by RT-qPCR to guide layer selection. Watertight membranes (electrospun or solvent-casted PCL) were evaluated in tension and under hydrostatic pressure. Selected layers were assembled into a multiphasic substitute, tested in dry and wet conditions and under hydrostatic loading, then implanted subcutaneously in rats for 28 days for histological assessment of overall biocompatibility.

Results

All electrospun scaffolds were cytocompatible (>160–310% metabolic activity vs day 1). PCL/nano-hydroxyapatite (random) induced the strongest osteogenic signature in ADSCs (COL1A1 and SPARC upregulation; SPP1 detected). HDuFs showed consistent dura-like expression on PCL (random) and PCL/silk fibroin (aligned), including increased COL1A1 with GJA1 and MGP. Selection of the meningeal-facing layer was based on combined biological and mechanical criteria: PCL (random) showed suitable gene expression but inadequate mechanics, whereas PCL/silk fibroin (aligned) met both requirements and was selected. Among barrier candidates, a solvent-casted PCL film formed a homogeneous ultrathin membrane with a hydrostatic resistance of ~400 mmHg, well above physiological intracranial pressure (~4–18 mmHg, up to ~100 mmHg in extreme conditions), in contrast to the explored electrospinning-based approaches (~40 mmHg), and was therefore selected for the final prototype. The final construct incorporating this film, resisted very high pressures (>1200 mmHg (Figure 1). In vivo, the complete multiphasic substitute showed uncomplicated healing, limited fibrosis and no evident inflammatory infiltrate at 28 days (Figure 2).

Conclusion

Layer-by-layer screening enabled rational selection of an osteogenic bone-facing phase and a HDuFs–supportive meningeal phase. Coupling these with an ultrathin solvent-cast barrier produced a multiphasic dural substitute combining dura-range mechanics with robust watertightness and preliminary in vivo biocompatibility. This substitute candidate will therefore undergo further preclinical evaluation in orthotopic dural repair models.

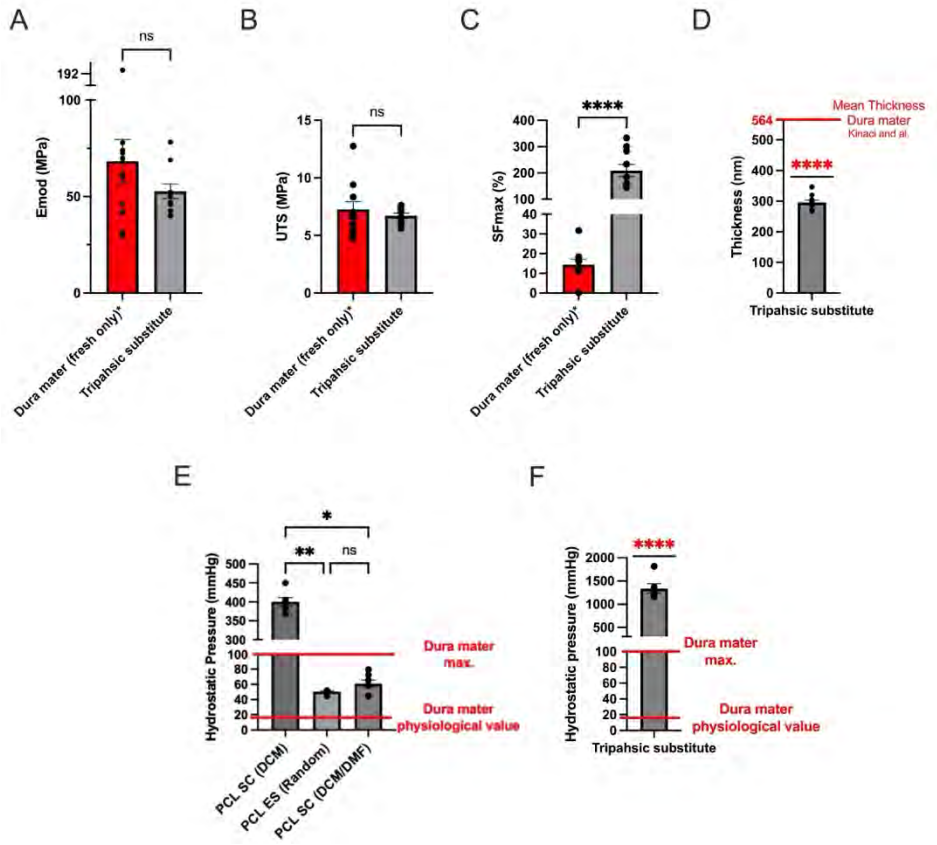

Figure 1: Mechanical and hydrostatic performance of the barrier layer and the triphasic substitute. (A) Elastic modulus (E_{mod}) of the substitute compared with dura mater reference values (N = 10). (B) Ultimate tensile strength (UTS) (N = 10). (C) Strain at failure (SF_{max}(%)) (N = 10). (D) Thickness measurement (N=10). (E-F) Hydrostatic pressure resistance of the barrier layer or the triphasic substitute (N = 6). Red lines indicate physiological cerebrospinal fluid pressure (4–18 mmHg) and the maximal rupture threshold of native dura mater (~100 mmHg). Statistical significance is indicated as *p < 0.05, **p < 0.01, ***p < 0.001, ****p < 0.0001. Bars represent mean ± SEM (Kruskal-Wallis, ANOVA or t test, Mann-Whitney or Wilcoxon t test).

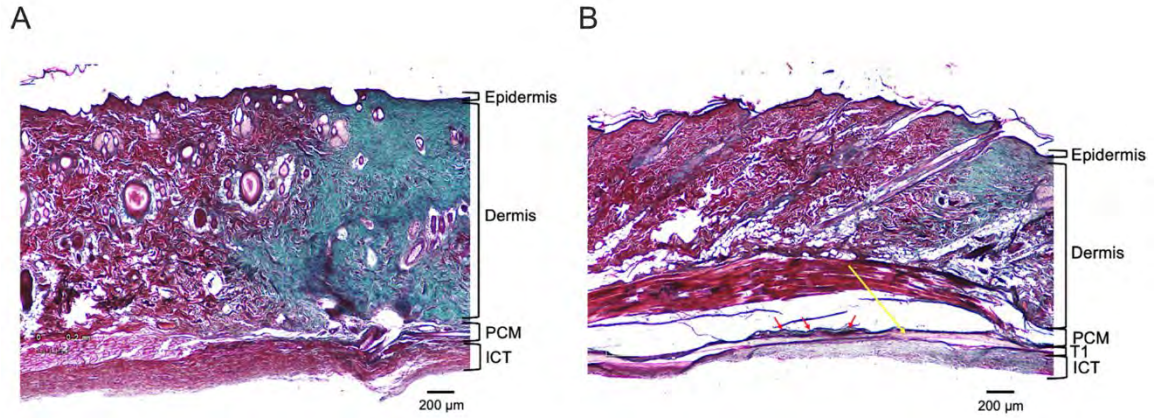

Figure 2: Masson's trichrome staining of SD rat skin at 1 month reveals limited fibrotic encapsulation around the implanted material. A) Sham condition (control). B) Triphasic substitute (T1) implant section. (magnification ×6, scale bar = 200 µm). Red arrows: collagen capsule; Yellow arrow: Triphasic substitute. Macroscope Leica DMS 1000. PCM: panniculus carnosus; ICT: interstitial connective tissue.

S77 – O3

Development of a hydrogel-based sustained ocular drug delivery system for vitreous replacement in proliferative vitreoretinopathy

Junge V.[1], Pröhl F.[1], Luyken A.K.[1], Schaub F.[1], Fuchsluger T.A.[1], Schulz A.[1,2]
[1] Dept. of Ophthalmology, Rostock University Medical Center, Rostock, Germany
[2] Dept. of Life, Light & Matter, University of Rostock, Rostock, Germany

Introduction

Proliferative vitreoretinopathy (PVR) is a complication of retinal detachment characterized by pathological cellular proliferation and contractile membrane formation that can lead to recurrent retinal detachment and vision loss. Antimetabolites, such as methotrexate (MTX), currently examined as intravitreal injections at doses typically ranging from 100-400 µg per injection, have shown potential to inhibit cell proliferation and reduce PVR progression. However, their clinical application remains limited by the requirement for repeated intraocular injections, as the drug is rapidly cleared from the vitreous cavity, requiring prolonged therapeutic exposure.

Aim

This study aims to develop a hydrogel-based vitreous substitute capable of sustained antimetabolite release, combining structural vitreous replacement with localized drug delivery for improved PVR therapy.

Materials and Methods

Hyaluronic acid solved in phosphate buffered-saline was methacrylated and then photopolymerized for 20 min at room temperature by UV-light (365 nm) with N-vinyl-pyrrolidone serving as crosslinker and Irgacure 2959 serving as photoinitiater. MTX was incorporated into poly(lactic-co-glycolic) acid (PLGA) microparticles, which were subsequently injected into the gels prior to crosslinking. PLGA particles were synthesized via W/O/W double emulsion solvent evaporation technique using ethyl acetate as the organic phase and polyvinyl alcohol as stabilizer, followed by solvent removal and particle recovery by centrifugation. The release of MTX from gels with and without particle incorporation with various MTX concentrations (80 µg/ml, 160 µg/ml, 320 µg/ml) was analyzed via UV-Vis spectroscopy for up to two weeks.

Results

MTX encapsulated in PLGA microparticles (diameter: 23,7 µm ± 8,1 µm) were integrated into hydrogels that are optically transparent (transmission: >90%; refractive index: 1.3353) and viscoelastic ($G' = 191 \pm 8.98$ Pa; $G'' = 35.2 \pm 0.99$ Pa). Without encapsulation into hydrogel, up to 60% of MTX was released as a burst in the first three hours. Following encapsulation, only minimal, but sustained release of MTX was observed for two weeks towards therapeutically relevant concentrations of 5 µg/ml.

Conclusion

Hyaluronic acid–based hydrogel vitreous substitutes incorporating MTX-loaded PLGA microparticles enabled sustained and prolonged drug release compared to free MTX. Ongoing studies are evaluating release over six weeks and investigating higher drug loading, smaller particle size, and direct exposure of PVR cells to the hydrogel-based delivery system.

S77 – O4

Injectable Zeolite Nanocrystals for Tumor Oxygenation and MRI Imaging

Abdallah Amedlous[1], Charly Hélaine[2], Francesco Dalena[1], Clément Anfray[2], Thomas Ménard[2], Isis Blanchard[2], Jérôme Toutain[2], Samuel Valable[2*], Svetlana Mintova[1*]
[1]Université de Caen Normandie, ENSICAEN, CNRS, LCS, Caen, France
[2]ISTCT UMR6030, Université de Caen Normandie, CNRS, Normandie Université, GIP CYCERON, Caen, France

A reliable and biocompatible synthesis route is essential for translating zeolite nanomaterials into biomedical applications. Here, we report the synthesis of nanosized faujasite zeolite crystals (PBS-Na-FAU) using clinical-grade phosphate-buffered saline (PBS) as the reaction medium. The use of PBS enables the formation of highly crystalline zeolite nanocrystals while preserving microporosity and ensuring excellent colloidal stability under physiologically relevant conditions.
This synthesis strategy yields uniform nanosized crystals without compromising structural integrity, demonstrating that buffered saline environments are compatible with zeolite crystallization. Post-synthetic ion exchange was employed to introduce gadolinium (Gd^{3+}) into the framework, replacing monovalent cations (Na^+/K^+) to form PBS-Gd-FAU. This controlled ion-exchange process preserves the zeolite structure while enhancing functional properties.
In situ FTIR measurements showed that Gd incorporation increases oxygen adsorption by ~23% at 20 kPa compared to the parent material. The nanocrystals exhibit a high oxygen storage capacity with a controlled release of 2.68 $mg \cdot L^{-1}$ under hypoxic conditions. T_1 relaxometry at 7 T revealed a relaxation rate of 9.254 $mM^{-1} \cdot s^{-1}$, approximately twice that of conventional Gd-based contrast agents.
Biological evaluations confirmed the absence of toxicity in vitro, ex vivo, and in vivo. MRI studies further demonstrated effective oxygen delivery within brain tumors, validating the functionality of the synthesized nanoplatform.

S77 – O5

Injection-Moldable Medical-Grade UHMWPE-Based Synthetic Biomaterials for Orthopedic Applications

Sablaniya D[1, 2], Basu B[1, 2]*
[1, 2]Laboratory for Biomaterials Science and Translational Research, Materials Research Centre, Indian Institute of Science, Bangalore, India
[2]Centre of Excellence for Dental and Orthopedic Applications, Material Research Centre, Indian Institute of Science, Bangalore, India

Introduction

Ultra-high molecular weight polyethylene (UHMWPE) is the widely used biomaterial for articulating components in total joint arthroplasty due to its excellent biocompatibility and mechanical durability[1]. However, its extremely high molecular weight leads to very high melt viscosity, which severely limits its processability using conventional injection molding. Consequently, orthopedic components are fabricated via extrusion or compression molding followed by extensive machining, resulting in substantial material waste, high manufacturing cost, and limited design flexibility. long-term clinical performance of UHMWPE implants is influenced by biological responses to wear debris, including inflammatory signalling, and osteolysis[1]. Therefore, developing injection-processable[2] UHMWPE biomaterials while maintaining their mechanical and biological performance remains a critical challenge for scalable orthopedic implant manufacturing.

Aim

This study aims to engineer an injection-moldable UHMWPE-based biomaterial through polymer blend design and processing optimization, enabling scalable manufacturing of orthopaedic implant without compromising the mechanical, tribological, and biocompatibility performance compared with commercially available medical-grade UHMWPE (GUR 1050).

Materials and Methods

Medical-grade UHMWPE (GUR 1050) was blended (1–5 wt% mPE) with short-chain maleated polyethylene (mPE) via melt compounding, subsequently processed using injection molding. Physiochemical and rheological properties were characterised using FTIR, XRD, DSC, TGA, and a rheometer. Mechanical performance was evaluated using ASTM D638 tensile testing. Dimensional integrity and internal defects of injection-molded acetabular liner prototypes were examined using micro-computed tomography (µCT). Cytocompatibility of the optimized 4 wt% mPE blend was evaluated using MC3T3 pre-osteoblast cells. Injection-molded acetabular liners were further tested in a hip joint simulator up to 2 million cycles, and cellular responses of wear debris were investigated using RAW264.7 and MC3T3 co-culture.

Results

Incorporation of short-chain mPE improved the processability of UHMWPE. The melt flow index increased from 6.2 to 8.2 g/10 min, while viscosity decreased from 18.83 to 12.30 kPa·s. The optimized 4 wt% mPE blend exhibited improved tensile strength increasing from 27.5 to 31.4 MPa and elongation increasing from 46.4% to 77.7%. Injection molding produced defect-free (confirmed by µCT) acetabular liner prototypes with dimensional tolerances within orthopedic standards (shrinkage 2.1–2.4%, ovality 0.06–0.09 mm). Cytocompatibility comparable to medical-grade UHMWPE was observed, while hip simulator testing generated wear debris consistent with clinically reported UHMWPE particles.

Conclusion

Polymer blend engineering using mPE enables injection moldability of UHMWPE while preserving mechanical performance and cytocompatibility. This biomaterial provides a viable route towards scalable, near-net-shape manufacturing of UHMWPE orthopedic components and supports the development of cost-effective polymeric implants for total joint arthroplasty.

References

[1]Kurtz, S. M. *UHMWPE Biomaterials Handbook: Ultra High Molecular Weight Polyethylene in Total Joint Replacement and Medical Devices: Third Edition* (2015). doi:10.1016/C2013-0-16083-7

[2]Sablaniya, D., Vignesh, R., Abhilash, S. P. T. & Basu, B. Impact of Short- Chain Maleated Polyethylene Addition on Viscosity , Moldability , and Strength – Ductility Combination of UHMWPE Blends for Commercial Scale Manufacturing of Acetabular Liner. (2025) doi:10.1002/app.56917

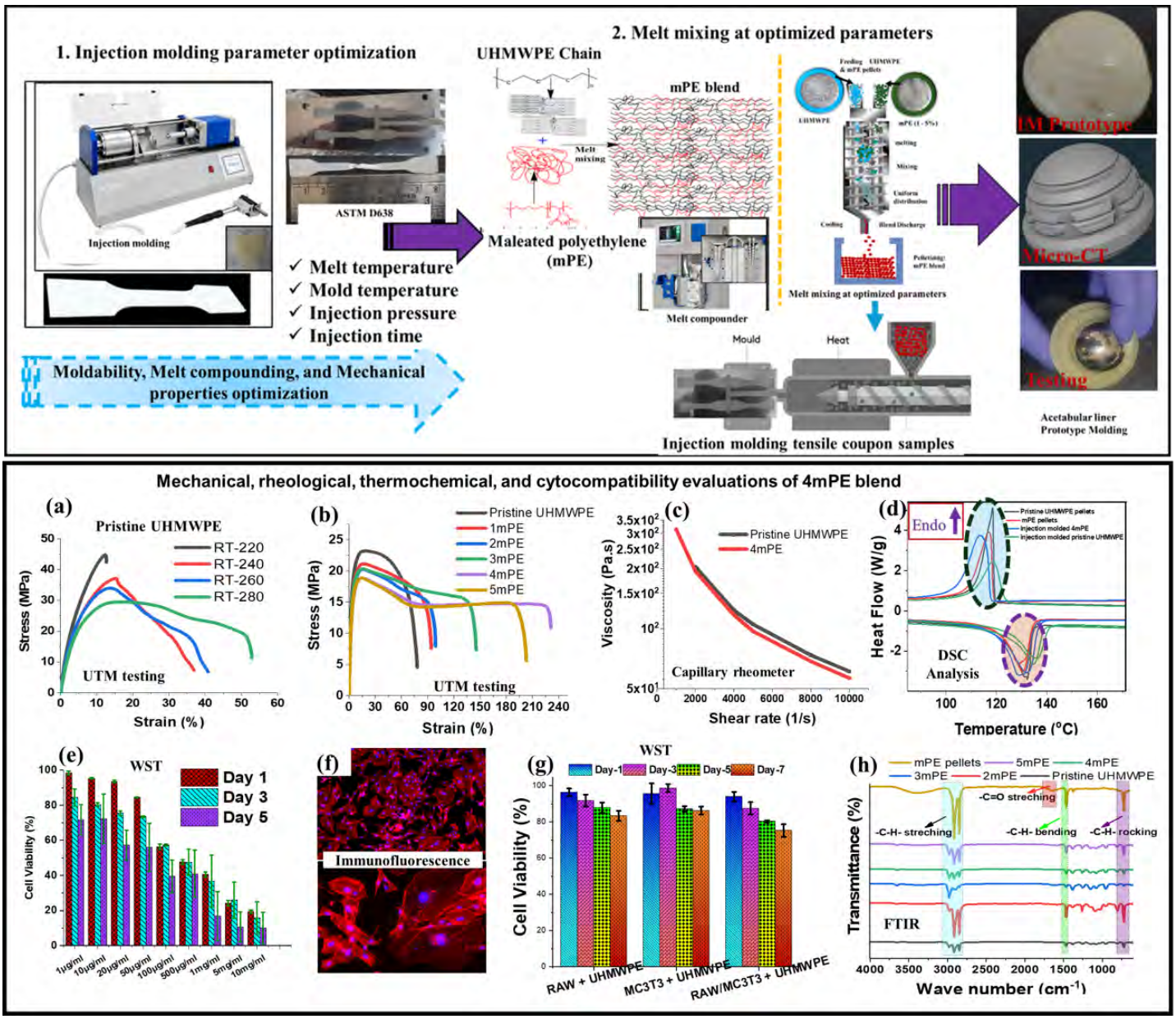

Figure 1. Overview of polymer blend engineering and characterization of injection-moldable UHMWPE biomaterials. (Top) Optimization of injection molding parameters and melt compounding of UHMWPE with maleated polyethylene (mPE) to fabricate acetabular liner prototypes. (Bottom) Mechanical, rheological, thermal, and chemical characterization together with in vitro cytocompatibility studies demonstrating the performance of the optimized 4 wt% mPE blend.

accelerating translational research and improving clinical outcomes.

S77 – O6

Bench-to-bedside translation of Self-Healing colloidal hydrogels as Next generation design of Flowable Hemostatic Matrix: from Preclinical evaluation to Human Clinical Trials

Kaiwen Chen 1, Qiwei Ying 1, Huanan Wang1,*
MOE Key Laboratory of Bio-Intelligent Manufacturing, Dalian Key Laboratory of Artificial Organ and Regenerative Medicine, School of Bioengineering, Dalian University of Technology, Dalian, P. R. China

(s)
Self-healing materials represent a paradigm shift in designing functional biomedical devices for drug delivery, tissue regeneration, and 3D bioprinting. However, their clinical translation remains limited by challenges such as insufficient mechanical strength, potential cytotoxicity from chemical modifications, and complex activation requirements. Here, we report the development of a self-healing colloidal gelatin hydrogel engineered as a flowable hemostatic matrix, and successfully demonstrate its bench-to-bedside translation into a biomedical device (Colloidose®). Specifically, amphoteric gelatin sub-microparticles self-assemble into an integrated gel network exhibiting a high storage modulus (G'>15 kPa) and a healing efficiency exceeding 95%, enabling rapid in situ solidification to accelerate blood clot formation. By benchmarking against conventional flowable matrices composed of coarse hundreds micrometer-sized gelatin granules, we demonstrate that Colloidose® offers superior hemostatic efficacy in anatomically challenging or pressure-intolerant sites (e.g., hepatobiliary, otorhinolaryngologic, and gynecologic surgeries). Supported by comprehensive preclinical studies and over 300 clinical cases, Colloidose® exemplifies the successful translation of an advanced self-healing biomaterial, establishing its role as a next-generation hemostat and opening new avenues for injectable and moldable biomedical devices.

Acknowledgements
This work was supported by the National Natural Science Foundation of China (No.52273102).

S78 Bioprinting and additive manufacturing

S78 – K1
Emerging Fabrication Technologies to Drive the Next Era of Innovation in 3D Printing

Dalton P.
University of Oregon, US

S78 – K2

Light-based 3D-printing of tunable photo-crosslinkable gelatins for urethral repair

Pien N.[1], Bogaert B.[1], Willemarck R.[1], Lapere A.[1], Pokholenko I.[1], Dixit K.[2], Eeckman N.[3], Shajahan A.[4], Miettinen S.[2], Porsborg S.[4], Pennisi P.[4], Van Vlierberghe S.[1]
[1]Polymer Chemistry and Biomaterials Group, Centre of Macromolecular Chemistry (CMaC), Ghent University, Ghent, Belgium; [2]Tampere University, Finland; [3]4Tissue, Zwijnaarde, Belgium; [4]Aalborg Universitet, Gistrup, Denmark

Introduction

Urethral stricture disease remains a persistent clinical challenge due to limited autologous graft options and risk of re-stricture. Here, we developed a gelatin-based bioink toolbox for light-based biofabrication of soft tissue-like constructs using volumetric additive manufacturing (VAM) and digital light processing (DLP).[1] Gelatin was functionalized as (i) gelatin-methacryloyl (GelMA), (ii) a thiol-ene pair consisting of gelatin-norbornene and thiolated gelatin (GelNB/GelSH), and (iii) a bifunctional methacryloyl-norbornene derivative (GelMANB) enabling orthogonal crosslinking with various thiol-crosslinkers to tune network density (Fig.1).

Materials and Methods

Photocrosslinkable gelatin derivatives were synthesized with varying degrees of substitution (DS) and formulated at 5-10%(w/v) using different thiol crosslinkers, photoinitiator, and photoabsorber systems. Resin printability and photocrosslinking behaviour were evaluated for both VAM and DLP. Hydrogels and printed constructs were characterized for gel fraction, swelling, and (photo)rheological properties. Cytocompatibility was evaluated on selected resin formulations using human adipose-derived stromal, umbilical vein endothelial and urothelial cells (day 1, 3 and 7), while fibroblast-based biofabrication studies are ongoing.

Results

Across all gelatin chemistries, physico-chemical properties were broadly tuneable by DS, polymer concentration (5-10%(w/v)), and crosslinking strategy. GelMA formulations (DS 34-96%) reached storage moduli (G′) of 0.5-15 kPa and swelling ratios of 25-55. GelNB/GelSH (DS 39-63%) formulations showed G′ values of 2-12 kPa, while swelling ratios decreased from 60 to 20 with increasing crosslink density. GelMANB (DS MA41-66%, NB24%) hydrogels exhibited tuneable G′ values of 1-16 kPa, swelling ratios of 10-20, and gel fractions >95%, depending on concentration and thiol-crosslinker.

For VAM, selected resins enabled reproducible fabrication of stable 3D constructs. VAM-printed (7.5%(w/v)) GelNB/GelSH reached a compressive modulus of 0.27±0.05 kPa, while corresponding values for GelMA96 and GelMANB were 0.22±0.05 kPa and 0.15±0.03 kPa (GelMA41NB25/DTT) and 0.10±0.03 kPa (GelMA41NB25/GelSH), respectively. For DLP, GelMA and GelMANB were successfully processed after optimization of photoinitiator concentration, photoabsorber concentration, and layer exposure time, yielding tubular constructs with excellent CAD/CAM fidelity. Selected resin formulations supported excellent viability.

Conclusion

This gelatin-based light-driven biofabrication platform enables rapid fabrication of lumenized scaffolds with tunable physico-chemical properties, supporting further development toward urethral tissue engineering.

Acknowledgements

STRONG-UR is a project funded by the European Union and has received funding from the Horizon Europe programme under grant agreement No 101191695. Views and opinions expressed are however those of the author(s) only and do not necessarily reflect those of the European Union or HaDEA. Neither the European Union nor the granting authority can be held responsible for them.

References

[1] N. Pien et al. Exploring the Impact of Volumetric Additive Manufacturing of Photo-crosslinkable Gelatin on Mesenchymal Stromal Cell Behavior and Differentiation, Addit Manuf (2025). https://doi.org/10.1101/2025.02.17.638591.

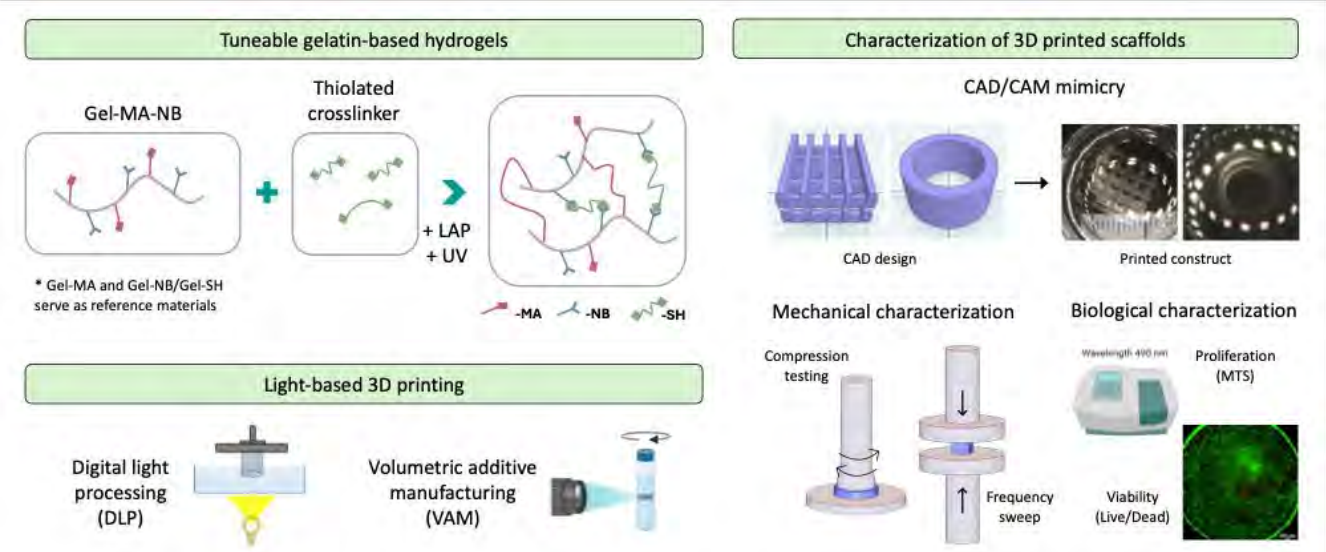

Figure 1. Schematic overview of (A) synthesis of tunable photo-crosslinkable gelatin-based hydrogels, (B) material processing using light-based 3D printing techniques, and (C) characterization of the 3D printed scaffolds

S78 – O1

Lab-on-a-chip platform with controlled oxygen release systems to promote osteochondral system survival

Sérgio Scalzo[1,3],Fabio Caixeta Nunes[2,3] ,David Rendón[3],Sushila Maharjan[3], Thiago Stocco[3,4], Yu Shrike Zhang[3], Anderson Lobo[4]

[1]Dept. of physiology and biophysics, Federal University of Minas Gerais, Brazil, [2]Dept. of Biosystems Engineering, University of São Paulo, Brazil, [3]Dept. of Medicine, Harvard Medical School, BWH, USA, [4]Dept. of Bioengineering, Brazil University, Brazil [5]Dept. of Materials Engineering, Federal University of Piauí, Brazil

Introduction

Engineering biomaterials and microphysiological systems that recapitulate osteochondral tissue remains a major challenge in regenerative medicine, particularly due to the need to sustain cell viability and reproduce the coupled biochemical and mechanical cues of a partially avascular microenvironment. Building upon these, the present project seeks to develop and optimize a lab-on-a-chip platform to achieve a more precise and sustained oxygen release over time through a microengineered bioreactor. To accomplish this goal, we developed a microfluidic-based system integrated with an oxygen modulation module capable of dynamically regulating oxygen levels within the cellular microenvironment. Materials and Methods: Three microfluidic platforms were fabricated (PDMS, resin, and hybrid PDMS-resin-PMMA), incorporating optimized channel geometries, hydrogel-anchoring pillars, laminar flow control, and pneumatic membranes for mechanical compression. These features allow simultaneous perfusion and controlled mechanical stimulation, mimicking osteochondral mechanobiology. Results: To achieve precise and dynamic oxygen modulation without direct chemical interference in the culture chamber, we developed an integrated microfluidic oxygen control system combining an oxygen generator and an oxygen scavenger module. The oxygen generator, based on gas diffusion through PDMS membranes, allowed controlled oxygenation up to normoxic levels (21% O_2). Oxygen removal was achieved using a $Na_2SO_3/CoSO_4$ redox system physically isolated from the cell compartment by a PDMS membrane, enabling rapid and tunable deoxygenation. Two independent configurations, an active pump-driven system and a passive reservoir-based system, enabled reproducible oxygen modulation ranging from physiological (5–21%) to severe hypoxic conditions (<1%). Human mesenchymal stem cells (hMSCs) encapsulated in 5% GelMA demonstrated sustained viability (>85%) within the chip after seven days, comparable to conventional 2D cultures. Morphological progression confirmed cellular adaptation to the 3D microenvironment. Conclusion: Collectively, these results establish a versatile organ-on-a-chip platform capable of integrating perfusion, mechanical stimulation, and precise oxygen control. This system provides a robust microphysiological model for studying oxygen-dependent differentiation, mechanotransduction, and osteochondral tissue engineering, advancing translational regenerative medicine strategies.

S78 – O2

3D bioprinting of animal-free perfusable Blood Vessel using adipose-derived stem cell-derived vascular cells

Sushma Priya[1], Vishwanie Mahadeo[2], Deepak kalaskar[1]

[1]UCL Division of Surgery and Interventional Science, Royal Free Hospital, London, UK

[2]UCL Institute of Cardiovascular Science, Pre-clinical and Fundamental Science Dept., London, UK

Introduction

The development of physiologically relevant vascular models is essential for tissue engineering, disease modelling and drug screening. However, conventional vascular constructs frequently rely on primary vascular cells and animal-derived culture supplements or biomaterials, limiting reproducibility, scalability and translation towards fully human-relevant experimental systems. This study developed an animal-free 3D bioprinted vascular construct using human adipose-derived stem cells (ADSCs) as a single cell source for generating endothelial-like and smooth muscle-like vascular cells.

Materials and Methods

Human ADSCs were differentiated into endothelial-like cells (dECs) and smooth muscle-like cells (dSMCs) using animal-free culture conditions. Phenotypic differentiation was assessed using vascular lineage markers. Bilayered blood vessel were fabricated by coaxial extrusion bioprinting using VascuBiomatrix™, with dSMCs incorporated within the vessel wall and dECs subsequently establishing the luminal endothelial lining. Constructs were maintained under static or dynamic perfusion culture for up to 14 days. Biological maturation was evaluated by immunofluorescence analysis of endothelial, smooth muscle and extracellular matrix markers. Vessel functionality was further assessed by permeability,and angiogenic response**.**

Results

ADSCs successfully differentiated into vascular phenotypes, with dECs exhibiting CD31, vWF expression and dSMCs expressing α-smooth muscle actin and myosin heavy chain. Bioprinted constructs maintained a continuous tubular architecture and developed spatially organised endothelial and smooth muscle layers. Dynamic perfusion enhanced vascular maturation and extracellular matrix deposition compared with static culture. Endothelialised vessels showed improved barrier function, with approximately 50% lower 70-kDa dextran diffusion under dynamic culture. The constructs also demonstrated enhanced angiogenic activity in the chorioallantoic membrane assay.

Conclusion

This study demonstrates a fully animal-free strategy for engineering perfusable blood vessel by combining ADSC-derived vascular cells with extrusion bioprinting and dynamic maturation. The platform provides a human-relevant and scalable vascular model for vascular tissue engineering and potentially for disease modelling and preclinical screening.

Acknowledgements

This work was supported by the Humane Research Trust, UK. The authors gratefully acknowledge their financial support for this research.

S78 – O3

3D Printing of Ultra-High-Resolution Biocompatible Photopolymers for Bone Implants via µ-DLP

Siapera M.1, Mohammed A.2, Moderau N.3, Lampret B., Myant C.1
[1]Dyson School of Design Engineering, Imperial College London, London, United Kingdom
[2]School of Design, Royal College of Art, London, United Kingdom
[3]Dept. of Surgery and Cancer, Imperial College London, London, United Kingdom

Introduction

The restoration of skeletal integrity for critical-sized bone defects remains a significant clinical challenge. While 3D printing, specifically vat photopolymerisation (VPP), offers the spatial resolution required to fabricate intricate, bone-mimicking metamaterial lattices, clinical translation is frequently hindered by a "biocompatibility gap". Most existing materials fail to simultaneously provide the mechanical rigor required for high-load applications and the biological safety necessary for permanent integration. This research addresses this disparity through two integrated innovations: the development of a novel biocompatible, high-stiffness material system and the creation of an in-house micro-Digital Light Projection (µ-DLP) 3D printer.

Materials and Methods

A bespoke µ-DLP 3D printing system was developed to achieve feature sizes as fine as 5 µm. In parallel, a library of novel biocompatible photopolymers was formulated, utilising high-stiffness monomers specifically tailored for the µ-DLP system. Biological performance was evaluated using both direct-contact and extract-based cytotoxicity assays over 52 hours with the HB2 epithelial cell line. Mechanical properties were assessed via uniaxial compression testing in accordance with ASTM D695-23 standards. For the optimisation of the printing process the resin's curing kinetics were quantified by generating a Jacobs working curve, which allowed for the empirical determination of resin specific optical constants including critical exposure energy and penetration depth.

Results

Preliminary biological assessments demonstrated high cell viability, validating the material's safety for potential clinical applications. Mechanically, the materials exhibited a compressive modulus exceeding 2 GPa, representing some of the highest reported values for biocompatible polymers in VPP additive manufacturing. When structured into complex metamaterial lattices, the compressive

modulus aligns with the mechanical range of vertebral trabecular bone, typically between 100-500 MPa. Optical characterisation enabled precise determination of resin-specific curing parameters, with extracted critical exposure energy and penetration depth allowing accurate prediction of the curing behaviour. This facilitated the integration of the material system with the µ-DLP platform which enabled the fabrication of complex lattice geometries with feature sizes as small as 5 µm (Figure 1).

***Figure 1**. Parts imaged using SEM. Egg-beater shaped lattice structures exhibiting strut resolutions of 5µm. Left: Top-down view. Right: Lateral view. Scale bars 50 µm.*

Conclusion

The integration of a novel material system and the µ-DLP fabrication process establishes a powerful platform for producing biocompatible, ultra-detailed, load-bearing metamaterial implants. This approach successfully addresses the mechanical and biological requirements necessary for the permanent integration of bone-mimicking structures.

S78 – O4

Melt electrowriting of medium-chain-length polyhydroxyalkanoates: from processing to structures

Weber L[1], Domingos M[1], Roy I[2], Peach C[3]

[1]Dept. of Mechanical and Aerospace Engineering & The Henry Royce Institute, The University of Manchester, UK, [2]Dept. of Materials Science and Engineering, University of Sheffield, UK, [3]Manchester Shoulder and Elbow Unit, Manchester University Foundation NHS Trust, Manchester, UK

Introduction

Bacterial polyhydroxyalkanoates (PHAs) are sustainable, biocompatible, and bioresorbable polymers with increasing relevance for biomedical applications. However, their use in high-resolution biofabrication techniques such as melt electrowriting (MEW) remains limited, particularly due to insufficient understanding of their processing behaviour compared to established materials such as polycaprolactone (PCL).

Aim

This study investigates the suitability of a medium-chain-length PHA (mcl-PHA) for MEW by linking its thermal and rheological properties to processing behaviour, structural fidelity, and biological response.

Materials and Methods

mcl-PHA was synthesised via microbial fermentation and characterised using thermogravimetric analysis (TGA), differential scanning calorimetry (DSC), and oscillatory rheology. This data was used to define a MEW processing window. Due to the narrow processability range, parameter optimisation was constrained and primarily guided by voltage and feed rate adjustments, with fibre morphology assessed by scanning electron microscopy.
Melt electrowritten architectures were evaluated using fibroblasts to assess cell viability and alignment via LIVE/DEAD™ fluorescence staining.

Results

mcl-PHA exhibited low crystallinity, a negative glass transition temperature (~−40 °C), and low melt viscosities (300–550 Pa·s), enabling MEW processing at reduced pressures (0.1–0.3 MPa) and temperatures (40–50 °C) well below degradation thresholds. A defined processing window was established, with a critical translation speed of 4–5 mm s^{-1} and stable fibre deposition at 10–15 mm s^{-1}. Fibre diameters down to ~20 µm and multilayered structures were achieved (
Figure 1).
However, delayed solidification limited shape fidelity, leading to fibre fusion and reduced structural stability at higher layer counts (> 10 layers). This behaviour constrained parameter exploration and required mitigation through reduced processing temperatures including substrate pre-cooling.
Fibroblasts showed high viability and aligned along parallel fibre architectures, with alignment increasing at smaller fibre spacings, indicating geometry-driven contact guidance.

Conclusion

mcl-PHA enables low-temperature MEW processing and the fabrication of fine, cell-guiding architectures but is characterised by solidification-limited fidelity that requires adapted processing strategies. These findings establish a distinct processing–structure relationship compared to PCL and position mcl-PHA for applications prioritising sustainable sourcing, mild processing, and biological guidance over mechanical robustness.

Acknowledgements

The authors would like to thank the EPSRC-funded Centre for Doctoral Training in Advanced Biomedical Materials grant EP/S022201/1 and the Henry Royce Institute EPSRC grants EP/R00661X/1, EP/S019367/1, EP/P025021/1, and EP/P025498/1.

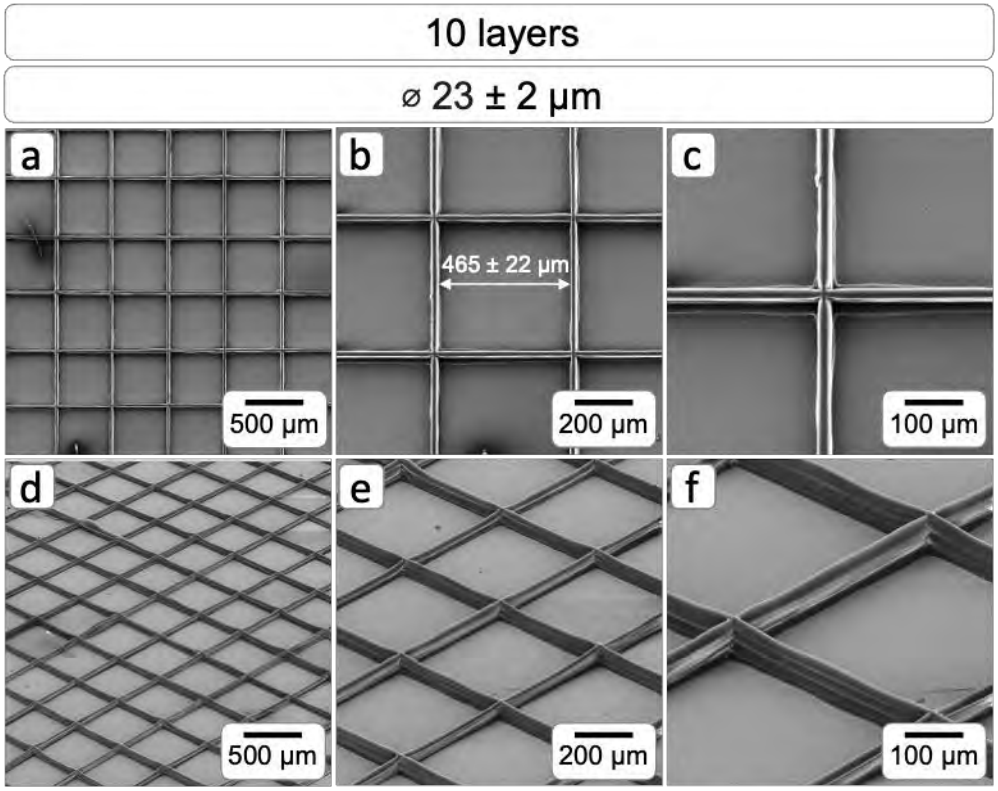

***Figure 1**: Scanning electron microscope images in top (a–c) and side view (d–f) of a grid pattern melt electrowritten with mcl-PHA. Line spacing is 500 µm and layer count is 10 by design.*

S79
Cell–Material interactions and biointerfaces

S79 – K1

Camarero-Espinosa S.
POLYMAT - Basque Center for Macromolecular Design and Engineering, Spain

S79 – O1

Interplay between stiffness and mineralization in collagen constructs regulates osteoclastogenesis

Bressan M.[1,2], van Alphen T.L.[1], Wentzel A.S.[1,2,3], Ito K.[2,4], Hofmann S.[2,3], Castilho M.[1,2]
[1] Biomaterial Engineering & Biofabrication Group, Dept. of Biomedical Engineering, Eindhoven University of Technology, Eindhoven, The Netherlands, [2] Institute for Complex Molecular System, Eindhoven University of Technology, Eindhoven, The Netherlands, [3] Bioengineering Bone Group, Dept. of Biomedical Engineering, Eindhoven University of Technology, Eindhoven, The Netherlands, [4] Orthopaedic Biomechanics Group, Dept. of Biomedical Engineering, Eindhoven University of Technology, Eindhoven, The Netherlands

Introduction

Bone is a dynamic tissue that is continuously remodeled through the coordinated activity of osteoclasts and osteoblasts. Osteoclast differentiation and activity are strongly influenced by properties of the bone matrix. While the mineral presence has been shown to promote sealing zone formation over other podosome superstructures[1], recent studies culturing osteoclasts on biomineralized type I collagen substrates reported only minimal activity[2]. This suggests that mineral presence alone might be insufficient to drive osteoclastogenesis. We hypothesize that both matrix stiffness and composition are prerequisites for osteoclastogenesis and sealing zone formation.

Aim

To investigate how matrix stiffness and composition influence osteoclastogenesis and sealing zone formation using engineered biomineralized type I collagen constructs with controlled stiffness.

Materials and Methods

Collagen constructs were prepared as casted 2D films or 3D extrusion-printed scaffolds (square lattices, 300x300µm pore size), biomineralized via the polymer-induced liquid precursor method (PILP), and characterized structural-wise by micro-computed tomography (µCT) and stiffness by uniaxial compression. Human monocytes were cultured on (non-)mineralized constructs for 16 days with and without osteoclastogenic supplements, and osteoclast differentiation and morphology were assessed by a tartrate-resistant acid phosphatase (TRAP) assay, electron microscopy, and fluorescent staining for TRAP.

Results

Mineralized collagen 2D films exhibited very low stiffness and limited mineralization, and these films did not support TRAP-positive cells (Fig 1A, 1C). In 3D, the apparent stiffness of collagen scaffolds was successfully optimized, increasing it by ~150-fold after mineralization (0.26kPa vs 40.67kPa). The optimized and mineralized collagen scaffolds, printed with a macromolecular crowder, supported TRAP-positive cells (Fig 1B) with a morphology comparable to that of osteoclasts found in literature (Fig 1D). No significant difference was found in TRAP expression, immunofluorescence staining, or cell morphology between mineralized collagen scaffolds cultured with or without osteoclastic supplements, implying the possibility of material-driven osteoclastogenesis.

Conclusion

Overall, our findings demonstrate that mineralized collagen constructs can support osteoclastogenesis, but as hypothesized, this is dependent on stiffness This highlights the critical interplay of matrix properties in regulating osteoclastogenesis and the challenge of isolating single-factor effects. It also underscores the critical role of these parameters for biomaterial design in bone healing.

References

[1] Blangy A. The osteoclast cytoskeleton, Current understanding and therapeutic perspectives for osteoporosis. *Journal of Cell Science* 2020;133(13).
[2] de Melo Pereira D. Cobalt-containing calcium phosphate induces resorption of biomineralized collagen by human osteoclasts. *Biomaterial Research* 2021; 25(1);1–13.

S79 – O2

Microfluidic electrochemical biosensing platform for continuous, non-invasive monitoring of cardiac biomarkers in engineered tissues

Silva C[1,2], Rezaei Z[1], Alarcon A[1], Lozada R[1], Vásquez E[1], Fernandes MM[2], Ock J[3], Ha C[3], Bae N[3], Lee H[3], Shin SR[1]

[1]Division of Engineering in Medicine, Dept. of Medicine, Harvard Medical School, Brigham and Women's Hospital, Cambridge, MA, USA, [2]Center for MicroElectromechanical Systems (CMEMS-UMinho), University of Minho, Campus de Azurém, Guimarães, Portugal, [3]Korea Additive Manufacturing Innovation Center (KAMIC), Korea Institute of Industrial Technology (KITECH), Siheung, Republic of Korea

Introduction

In the United States, heart disease remains the leading cause of death, with one death occurring every 34 seconds and associated healthcare costs exceeding $168 billion (2021–2022). These statistics highlight the urgent need for improved diagnostic and monitoring strategies. Cardiac biomarkers, endogenous molecules released during myocardial stress or damage, offer a promising route for early detection and longitudinal monitoring.

Aim

This work aims to develop a scalable, non-invasive microfluidic–electrochemical platform for continuous monitoring of cardiac biomarkers secreted from cardiac tissues.

Materials and Methods

The platform integrates electrochemical impedance spectroscopy (EIS)-based biosensors with a modular microfluidic chip for automated sampling. The sensing interface comprises semiconductor-fabricated Ti/Pd/Au planar electrodes produced via wafer-scale manufacturing, enabling low-cost and reproducible fabrication of over 1,000 devices. Gold working electrodes were functionalized with antibodies targeting Creatine Kinase–Myocardial Band (CK-MB) and C–C motif chemokine ligand 2 (CCL-2). Detection was performed using ferricyanide-mediated impedance measurements, where antigen binding increased charge-transfer resistance. The system was validated using cell culture media collected from cardiomyocytes over a 14-day period.

Results

The biosensor demonstrated sensitive detection of CK-MB and CCL-2 across pg/mL to ng/mL concentrations. A limit of detection of 0.3054 pg/mL was achieved for CCL-2, with a linear dynamic range extending to 1 ng/mL. The platform enabled time-resolved monitoring of biomarker secretion during tissue maturation. The microfluidic module supported automated media extraction, solution exchange, and seamless integration with the sensing unit.

Conclusion

This study presents a scalable and sensitive platform for real-time monitoring of cardiac biomarkers in engineered tissues. The integration of microfluidics with EIS-based biosensing supports automated operation and high reproducibility, providing a foundation for multiplexed and point-of-care-compatible organ-on-chip diagnostic systems.

Acknowledgements

Silva C. acknowledges the FCT (Fundação para Ciência e Tecnologia) for its individual grant (2023.02782.BD).
This work was supported by the National NanoFab Center (NNFC) grant funded by the Korea government (MSIT) (No. RS-2024-00440903) and by European commission for VINNY project (ID:101130039).

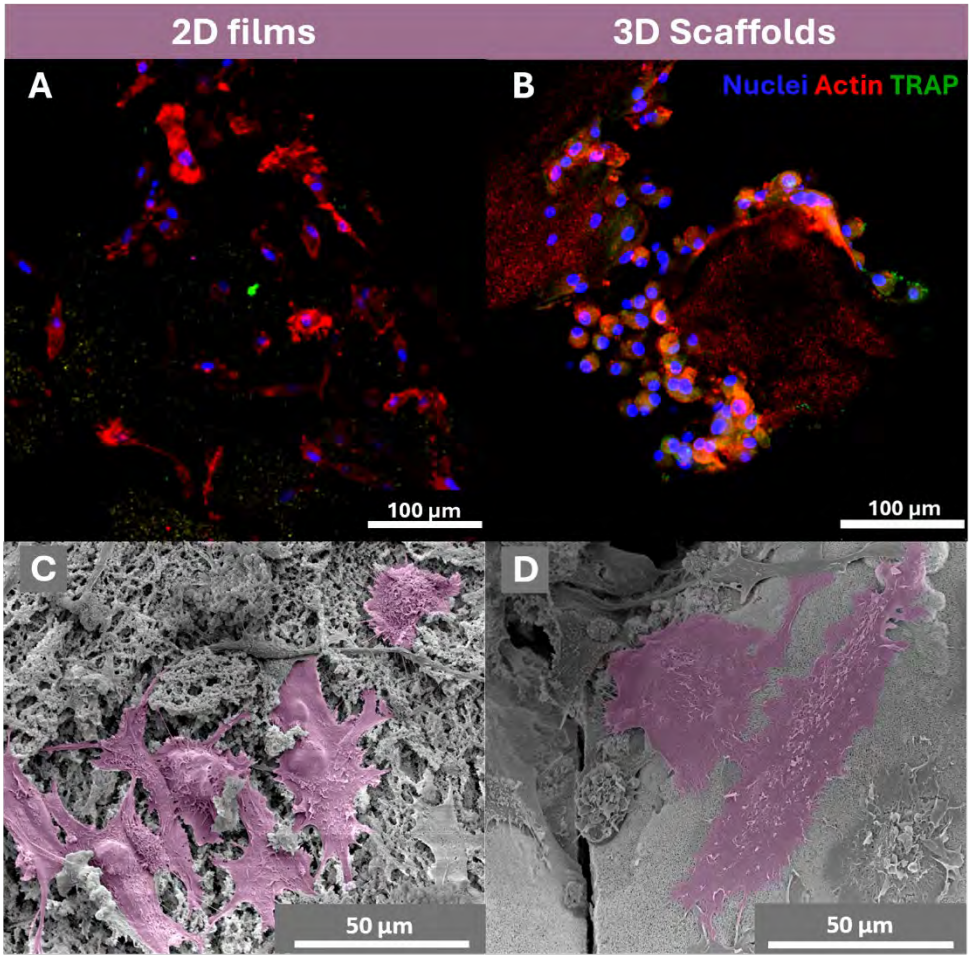

Figure 1. Confocal and SEM imaging of osteoclasts on mCOL substrates. [A] TRAP- cells on mCOL 2D films; [B] TRAP+ cells on mCOL 3D scaffolds; [C] cells on mCOL 2D films; [D] osteoclast-like cells on mCOL 3D scaffolds. Abbreviations: mCOL: mineralized collagen; TRAP: Tartrate-resistant acid phosphatase.

S79 – O3

Engineering a fully bone organ with active remodeling and vascularization on biphasic calcium phosphate scaffolds

Hammad M[1], Chavanas S[1], Naji A[1,2], Layrolle P[1]
[1]INSERM/Toulouse University UMR 1214, Toulouse Neuro Imaging Center (ToNIC), CHU Toulouse Purpan, Toulouse, France, [2]Dept. of Environmental Medicine, Research and Education Faculty, Medicine Science Cluster, Kochi Prefecture, Japan

Introduction

Reproducing the dynamic interplay between bone-forming osteoblasts, bone-resorbing osteoclasts, and vascular networks remains one of the biggest challenges in bone tissue engineering. Current *in vitro* bone models do not simultaneously recapitulate osteogenesis, osteoclast-mediated resorption, and vascular network formation, limiting their physiological and translational relevance. Here, we report the development of a human bone organ exhibiting bone formation, resorption, and early vascular network formation through the integration of primary cells and induced pluripotent stem cells (iPSCs) on biphasic calcium phosphate (BCP) scaffolds.

Materials and Methods

Human bone marrow derived mesenchymal stem cells (hBMSC), human umbilical vein endothelial cells (HUVEC) and peripheral blood-derived monocytes (PBMC) were seeded on BCP granules. Cultures were maintained for six weeks in osteogenic medium to mimic physiological conditions. Undifferentiated iPSCs were subsequently added to the matured tri-dimensional (3D) complex. Cell ratios were optimized to maximize matrix mineralization, vascular network formation and osteoclast activity. Osteogenic and resorptive activities were quantified via ALP and TRAP assays, qPCR (RUNX2, OCN, OPN), and confocal imaging for matrix mineralization and vascular formation.

Results

The tri-culture system generated a self-organizing, viable bone tissue. hBMSCs exhibited robust osteogenesis, depositing abundant mineralized matrix, while sclerostin expression indicated osteocyte maturation. HUVECs formed interconnected microvascular networks integrated with mineralized regions. Multinucleated osteoclasts actively resorbed the matrix, demonstrating functional remodeling. Post-integration iPSCs further enhanced the construct by increasing microvascular branching and increasing osteogenic potential. SEM, nano-tomography, and histological analyses revealed dense, collagen-mineralized tissue with trabecular-like organization, establishing a mature, physiologically relevant bone-like architecture.

Conclusion

Combining human primary cells with BCP scaffolds successfully generated an *in vitro* bone organ that recapitulates remodeling and early vascular organization. Incorporating iPSCs further enhanced vascular complexity and osteogenic performance, yielding a promising human model for studying bone physiology and regenerative therapies.

Acknowledgements

Funded by the European Commission ORTHO ALLO UNION

S79 – O4

A changing world: matrix viscoelasticity and degradability synergize to govern stem cell mechanobiology differentially in 3D vs 2D

Luo Z.[1],Pringle E.W.[1],Gourdon D.[1],Gonzalez-Garcia C.[1],Cantini M.[1]
[1]Centre for the Cellular Microenvironment, University of Glasgow, Glasgow, United of Kingdom.

Introduction

Native extracellular matrices (ECMs) are viscoelastic and degradable environments. Cells sense and respond to these biophysical and biochemical cues through mechanotransductive and matrix remodelling processes: an interplay that regulates not only key cellular functions, such as migration and differentiation, but also tissue homeostasis and pathology. While significant progress has been made in understanding these mechanobiological phenomena, several key questions remain unresolved, hindering progress in biomaterial design for regenerative medicine and tissue models. Indeed, the contributions of viscoelasticity and degradability to the modulation of cell mechanobiological behaviours remain unresolved; this is also exacerbated by the complexity of current hydrogel systems. This work aims to engineer a simple polyethylene-glycol (PEG)-based hydrogel platform with tuneable viscoelasticity and degradability, where the interplay between mechanotransduction and ECM remodelling in the mechanobiology of human mesenchymal stem cells (hMSCs) can be comprehensively studied.

Materials and Methods

We engineered and characterised pairs of soft (~1kPa) and rigid (~10 kPa) 2D and 3D PEG-Maleimide hydrogels, each containing an elastic ($\tan\delta \approx 0.1$) and a more viscous counterpart ($\tan\delta \approx 0.15$), functionalised with fibronectin-derived adhesive ligand RGD and crosslinked with matrix metalloproteinases-cleavable peptide VPM or a scrambled counterpart. We then examined hMSCs behaviour through immunofluorescence.

Results

We found that the mechanoresponse of hMSCs to viscoelasticity depends on hydrogel stiffness, dimensionality, and degradability. In 2D environments, viscoelasticity dominated cellular responses, promoting adhesion on soft hydrogels but not inducing YAP nuclear translocation, while hindering mechanotransduction on rigid substrates. Degradability, although promoting spreading on softer surfaces, did not significantly affect YAP mechanoactivation. When cells were encapsulated in 3D matrices, both viscoelasticity and degradability influenced the mechanoresponse. In stiffer environments, degradability was essential for cells to overcome mechanical confinement and enable YAP translocation, whereas viscous cues alone were sufficient to rescue YAP mechanoactivation in softer niches (Fig.1).

Furthermore, we observed a correlation between these mechanotransductive responses and ECM remodelling, as evidenced by deposition and reorganisation of fibronectin and collagen I. Indeed, on 2D substrates early fibronectin remodelling was mainly regulated by viscoelasticity, with fibrils associating with cell spreading and focal adhesion formation. Instead, degradability was essential for fibronectin remodelling within 3D matrices (Fig.2). These early responses governed later ECM remodelling, including collagen I.

Conclusion

We engineered a robust, yet simple, hydrogel platform with tuneable viscoelasticity and degradability, dissecting the roles of these cues in stem cell mechanobiology. These mechanobiological platform will also inform the design of advanced biomaterials and tissue models.

Figures

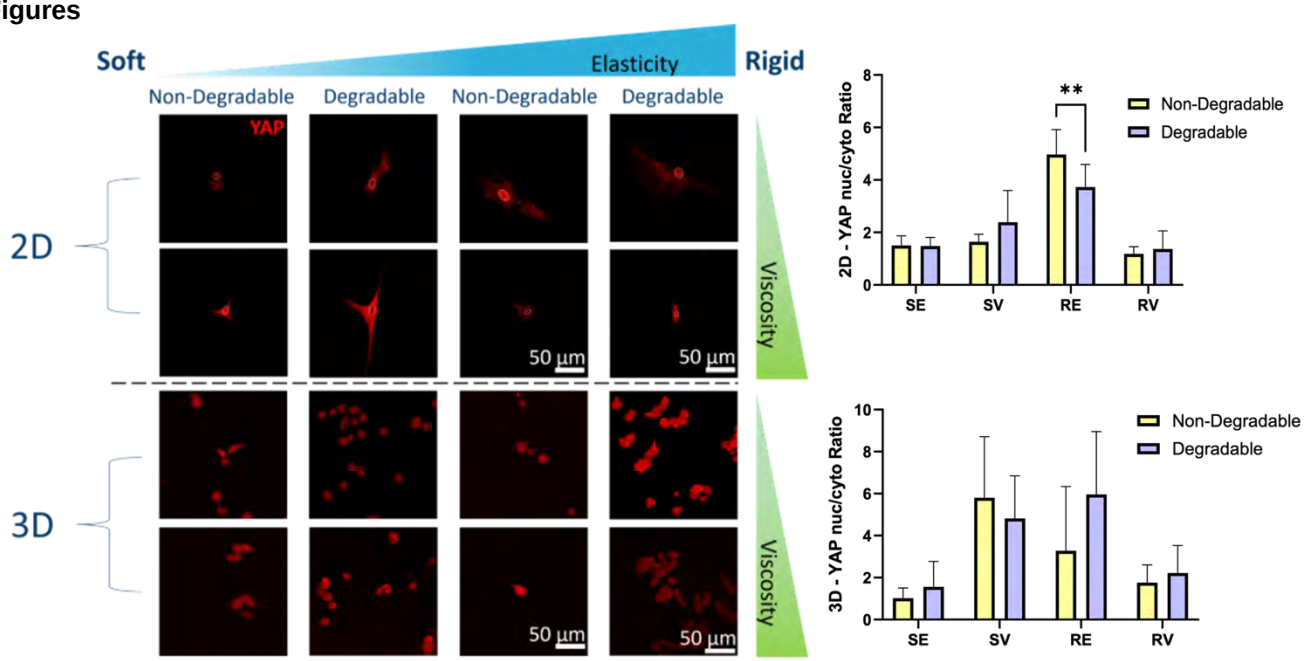

Figure 1:
Fluorescent Microscopy Images of hMSCs YAP Localisation on Non-degradable & Degradable PEG-MAL Hydrogels with Different Extents of Viscoelasticity 3 Days After Seeding. Hydrogels were functionalised with RGD. Cell seeding density: 5,000 cells/cm^2 (2D) and 2,000,000 cells/mL (3D). White dotted line indicates the area of nucleus. Scale bar = 50 µm (n = 30).

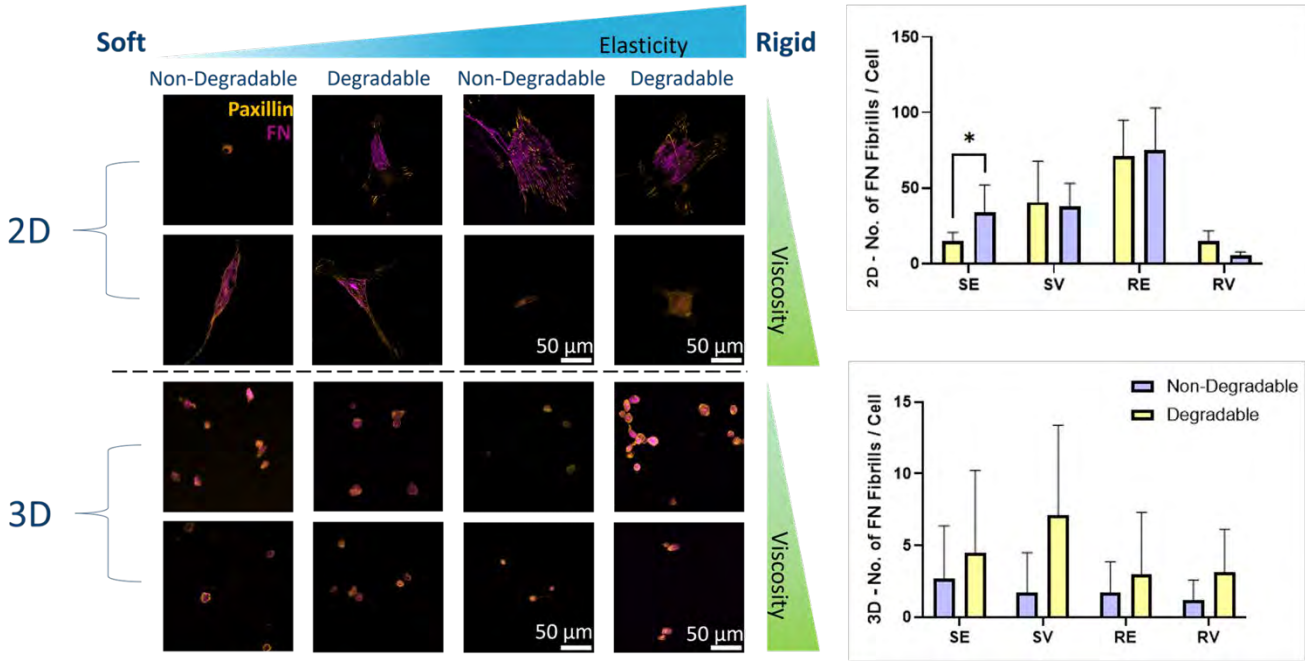

Figure 2:
Fluorescent Microscopy Images of hMSCs Focal Adhesion Formation (Yellow) and ECM Deposition (Magenta) on Non-degradable & Degradable PEG-MAL Hydrogels with Different Extents of Viscoelasticity 3 Days After Seeding. Hydrogels were functionalised with RGD. Cell seeding density: 5,000 cells/cm^2 (2D) and 2,000,000 cells/mL (3D). Scale bar = 50 µm (n = 30).

S79 – O5

Development of plant growth-promoting bacteria with artificial humic acids capsules for enhanced agricultural sustainability

Robert Guiu-Sans[1,2], Bartosz Tylkowski[1], Magdalena Jopek[3], Krzysztof Ambroziak[3], Paweł Trzciński[4], Svitlana Filonenko[5], Nataliia Doskaliuk[5], Ricard Garcia-Valls[2], Joseph J. Richardson[6], Magdalena Olkiewicz[1]
[1]Eurecat, Centre Tecnològic de Catalunya, Chemical Technologies Unit, Spain, [2]Dept. of Chemical Engineering, Universitat Rovira i Virgili, Spain, [3]Intermag sp. z o.o., Poland, [4]Instytut Ogrodnictwa - Państwowy Instytut Badawczy, Zakład Mikrobiologii i Ryzosfery, Poland, [5]Humify GmbH, Germany, [6]Dept. of Chemical and Environmental Engineering, School of Engineering, RMIT University, Australia

Massive agricultural production is required to feed the increasing global population. However, the current extensive use of agrochemicals pollutes the environment.[1] Therefore, new crop performance enhancers need to be developed. In their design, plant biostimulants become essential.
Plant biostimulants are substances or microorganisms applied to plants to enhance their growth, regardless of their nutrient content.[2] A promising subset is humic substances, which are constituent fractions of soil organic matter and are biologically active.[3] Another strong candidate is plant growth-promoting bacteria (PGPB), an important biological alternative with the capacity to increase crop yield.[3]
Encapsulation of the biostimulants aims to protect and deliver them efficiently, minimising environmental disruption and loss of costs, while displaying synergistic effects. Nevertheless, current encapsulation techniques in agriculture often involve the use of non-biodegradable materials,[4] and costly processes.[5]
In this study, sustainable biostimulant capsules, based on biodegradable polymer (alginate), loaded with artificial humic acids (AHAs) and different species of PGPB, are prepared by ionic gelation. Once obtained, the formulations will be tested in field trials to evaluate their efficacy.

References

[1]Indira Devi, P.; Manjula, M.; Bhavani, R.V. *Annu Rev. Environ. Resour.* 2022, *47*, 399–421.
[2]du Jardin, P. *Sci. Hortic.* 2015, *196*, 3-14.
[3]da Silva M. S. R. de A.; dos Santos B. de M. S.; da Silva, C. S. R. de A.; da Silva, C. S. R. de A.; Antunes L. F. de S.; dos Santos, R. M.; Santos, C. H. B.; Rigobelo, E. C. *Front. Microbiol.* 2021, *12*, 719653.
[4]Katsumi, N.; Kusube, T.; Nagao, S.; Okochi, H. *Chemosphere* 2021, *47*, 129185.
[5]Bhatia, M. *Encapsulation of Active Molecules and Their Delivery System Chapter 8* 2024, 131-140.

Robert Guiu Sans is a fellow of Eurecat’s "Vicente López" PhD grant program.

The authors acknowledge financial support from the European Union’s Horizon Europe research and innovation programme under grant agreement 101157265.

S79 – O6

Intra/extra-cellular functions of inorganic nanozymes for anticancer treatments

Naganuma T[1]
[1] Research Centre for Macromolecules and Biomaterials, National Institute for Materials Science (NIMS), Tsukuba, Japan

Introduction

Nano-biomaterials with enzyme-mimetic activities (nanozymes: NZs) have been expanding in therapeutic applications, including anticancer therapy. In general, *internalized* NZs produce and/or scavenge harmful reactive oxygen species (ROS), leading to cancer cell death and/or normal cell protection against the side effects of conventional anticancer therapies. However, the pro-oxidant activities of NZs in tumour cels are limited due to a high cancer antioxidant capacity. In addition, the functions of *extracellular* NZs on a surface of tumour cells are still veiled. Cerium oxide nanoparticle (CNP)-based nanozymes (CNZs) have a capability to possess excellent anti/pro-oxidant activities. Moreover, our previous studies have revealed that extracellular CNPs regulate normal cell proliferation dependent on different cerium valence states (Ce^{3+}/Ce^{4+});[1] while those with both Ce valence states inhibit the proliferation of specific tumour cells without generating intracellular ROS.[2] The interaction of extracellular CNZs with tumour cells, therefore, may serve to further enhance the anticancer efficiency.

Aim

This study demonstrates that intracellular CNZs selectively regulate ROS in normal/tumour cells, while extracellular CNZs on the surface of tumour cells play a role in enhancing the anticancer efficacy.

Materials and Methods

Ultrasmall CNZs were synthesized by a room temperature synthesis method form cerium (III) nitrate hexahydrate, [3] and their characteristics were evaluated by transmission electron microscopy, zeta potential analyser and X-ray diffraction. To increase a residence time of CNZs on a cell surface, their nanoclusters (CNZ-NCs) were formed. Subsequently, cellular responses to intra/extra-cellular CNZ-NCs in normal/tumour cells were investigated (*e.g.* cell viability/proliferation, intracellular ROS levels, and protein expression).

Results

At the physiological condition, intracellular CNZ-NCs increased normal cell proliferation by scavenging intracellular ROS, but they had no impact on tumour cell proliferation. However, the intracellular CNZ-NCs reduced tumour cell viability dependent on the features of tumour microenvironment (TME), such as weakly-acid pH and high H_2O_2 levels. Interestingly, even at the physiological condition, extracellular CNZ-NCs affect tumour cell viability in combination chemotherapy. In this presentation, we will discuss the intra/extra-cellular functions of CNZ-CNs for enhancing the anticancer efficiency.

Conclusion

This study demonstrated that intracellular CNZ-NCs act as anti/pro-oxidants in normal/tumour cells in environmental dependency. Furthermore, extracellular CNZ-NCs on the surface of tumour cells play an important role in anticancer chemotherapy. These findings suggest the therapeutic potential of extracellular CNZ-NCs in TME for anticancer treatment.

References

[1]Naganuma T., Traversa E., The effect of cerium valence states at cerium oxide nanoparticle surfaces on cell proliferation. *Biomaterials* 2014; 35; 15; 4441-4453.
[2]Naganuma T, Selective inhibition of partial EMT-induced tumour cell growth by cerium valence states of extracellular ceria nanoparticles for anticancer treatment. *Colloids Surf B Biointerfaces* 2024; 236;113794.
[3]Naganuma T, Shape design of cerium oxide nanoparticles for enhancement of enzyme mimetic activity in therapeutic applications" *Nano Research* 2017; 10;1; 199-217.

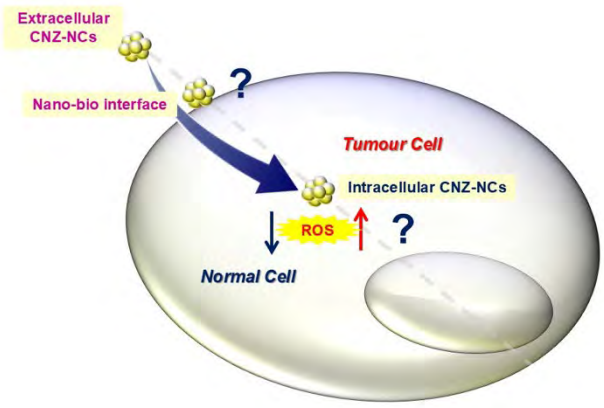

Fig. 1 Schematic drawing of the potential functions of intra/extra-cellular CNZ-NCs for anticancer treatments.

S79 – O7

A Microengineered Platform for Geometrical Confinement and Dorsoventral Patterning of Human Spinal Cord Organoids

Grimalt-Mirada R[1], Barceló X[1], Sáez FM[1], Ortega JA[2,3], Álvarez Z[1,4,5]
[1]Biomaterials for Neural Regeneration, Institute for Bioengineering of Catalonia (IBEC), Barcelona, Spain, [2]Dept. of Pathology and Experimental Therapeutics, Institute of Neurosciences, University of Barcelona, L'Hospitalet de Llobregat, Spain, [3]Institut d'Investigació Biomèdica de Bellvitge (IDIBELL), L'Hospitalet de Llobregat, Spain, [4]CIBER en Bioingeniería, Biomateriales y Nanomedicina, CIBER-BBN, Madrid, Spain, [5]Center for Regenerative Medicine (CRN), Northwestern University, Chicago, USA

Introduction

Human spinal cord organoids (hSCOs) are powerful models to study development and disease, but current systems rely on stochastic self-organization, often generating multiple neural tube–like structures and lacking a central canal, a key developmental organizer. Here, we aim to develop a microengineered platform that guides hiPSC self-assembly into toroidal microarchitectures to improve structural organization and enable dorsoventral patterning reminiscent of the early neural tube.

Materials and Methods

We used 2-Photon Polymerization (2PP) 3D printing to fabricate high-resolution platforms containing arrays of microwells with a central pillar, around which hiPSCs self-assembled into toroidal structures. Once continuous rings formed, cells were differentiated towards neural lineage following standard hSCO differentiation protocols. The 2PP printing technology also enabled spatially controlled biochemical functionalization of the central pillar to further guide dorsoventral patterning in the toroids.

Results

The platform supported the formation of continuous 3D rings surrounding the central pillar, which developed into tube-like structures that overgrew the pillar after 12 days in culture. Cell viability within the platform was confirmed, and seeding conditions were optimized both manually and using inkjet bioprinting. The resulting tubular structures displayed a defined lumen and expressed key neural markers (SOX2, TUJ1, Ki67), indicating successful neural induction (Figure 1).

Conclusion

By combining high-resolution microfabrication with stem cell technology, we promoted single-lumen organization and tube-like cytoarchitecture reminiscent of early neural tube development in hSCOs. This shift from conventional organoid self-aggregation to geometry-guided morphogenesis represents a key step toward generating biomimetic hSCOs with improved structural fidelity. Ultimately, this system provides a robust platform for studying human spinal cord development, injury, and regeneration.

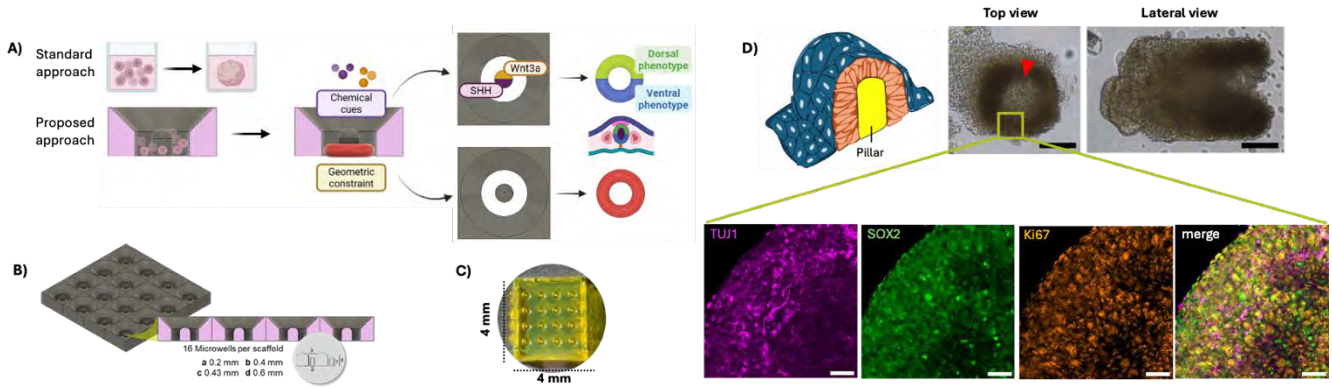

Figure 1
A) Graphical abstract. B) Platform design containing an array of 16 microwells. C) 2PP 3D printed platform. D) Top: tube-like structures extracted from the platform on day 12 after seeding. Arrowhead points at the central lumen. Scale bars: 100 um. Bottom: Immunohistochemistry of relevant neural markers (TUJ1, SOX2 and Ki67). Images were obtained by confocal microscopy. Scale bars: 50 um.

Acknowledgements
We acknowledge financial support from the fellowship 2025 STEP 00182, funded by Generalitat de Catalunya and co-funded by the European Union. The project leading to these results has received funding from “la Caixa” Foundation under the project code LCF/PR/HR25/52450044. This study was also supported by grant RYC2020-028732-I funded by MICIU/AEI/10.13039/501100011033 and by “ESF Investing in your future”. Z. Álvarez and J.A. Ortega are currently Ramón y Cajal investigators.

S80
Ceramic and glass biomaterials

S80 – K1
Scaling Nanostructured Materials for Advanced 3D Tissue Biofabrication and Therapeutic Applications

Oscar Castaño Linares
University of Barcelona (UB), Spain

S80 – O1

Magnetic mesoporous bioactive glass nanoparticles co-doped with cobalt and boron for angiogenic and osteogenic stimulation

Michálek M.[1], Vitázková M.[1], Vargas Z.[1], Šoltýsová A.[2]
[1]FunGlass, A. Dubček University of Trenčín, Slovakia, [2]Dept. of Molecular Biology, Faculty of Natural Sciences, Comenius University in Bratislava, Slovakia

Introduction

Mesoporous bioactive glass nanoparticles (MBGNPs) show exceptional promise in bone regeneration due to their high surface area, controlled ion release, and biodegradability. Therapeutic ion incorporation, particularly boron and cobalt, can enhance angiogenesis and osteogenesis, critical processes for bone healing [1]. Cobalt mimics hypoxia by stabilizing HIF-1α, promoting VEGF expression and blood vessel formation, while boron enhances osteoblast differentiation and VEGF secretion. Integration of superparamagnetic iron oxide nanoparticles (SPIONs) enables magnetic targeting and potential imaging capabilities. This study developed multifunctional nanocomposites combining Co and B co-doped MBGNPs with SPIONs, protected by silica shells, for controlled therapeutic ion delivery and enhanced bone tissue regeneration.

Materials and Methods

MBGNPs with compositions SiO_2-CaO, doped with 3 mol% B (3B), 3 mol% Co (3Co), and 3 mol% B + 3 mol% Co (3B3Co) were synthesized via microemulsion-assisted sol-gel method using CTAB, ethyl acetate, ammonia, TEOS, and calcium nitrate, followed by calcination at 650°C. Nanocomposites were prepared by coating 3B3Co MBGNPs with silica shells (CoBT) and conjugating SPIONs via co-precipitation (CoBTSp) shown in Fig.1. Characterization included TEM, SEM, XRD, FTIR, BET, ICP-OES, and magnetic measurements. In vitro bioactivity was assessed in simulated body fluid (SBF) and Tris buffer. Biocompatibility was evaluated using MG-63 osteosarcoma cells, MC3T3-E1 preosteoblasts, and HDFa fibroblasts. Cell viability (MTT assay), LDH activity, VEGF secretion (ELISA), DNA fragmentation, gene expression (RT-qPCR for VEGF-A, HIF-1α, FGF2, RUNX2, COL18A1, TP53), and mineralization (Alizarin Red S staining after 7 and 21 days) were assessed at concentrations ranging from 25-100 µg/mL.

Results

MBGNPs displayed spherical-to-ellipsoidal morphology (aspect ratio 1.3-1.6), with specific surface areas of 189.8-260.4 m^2/g and slit-shaped mesopores. XRD and FTIR confirmed amorphous silica structure with incorporated dopants. All MBGNPs demonstrated excellent bioactivity, forming hydroxyapatite layers in SBF within 14 days. Ion release studies showed sustained release of Si, Ca, B, and Co over 21 days, with higher reactivity in doped samples. Cell viability exceeded 100% at concentrations ≥100 µg/mL for all formulations. Co-doped samples (3B3Co) significantly enhanced VEGF secretion (130% increase vs. reference) without cytotoxicity or increased LDH activity. Silica-coated nanocomposites (CoBT, CoBTSp) exhibited reduced ion release, maintaining biocompatibility up to 400 µg/mL with no genotoxicity. RT-qPCR revealed significant upregulation of VEGF-A (up to 6-fold), HIF-1α (up to 4-fold), and RUNX2 (up to 8-fold) in CoBTSp-treated cells at 25-100 µg/mL after 3-7 days. Alizarin Red S quantification showed significantly higher mineralization in CoBTSp samples (up to 3-fold increase) after 21 days compared to control. Magnetic characterization confirmed superparamagnetic behavior with saturation magnetization of 22 emu/g.

Conclusion

Multifunctional magnetic nanocomposites combining Co and B co-doped MBGNPs with SPIONs were successfully developed, demonstrating dual angiogenic and osteogenic properties suitable for bone regeneration applications. The silica coating provided controlled ion release while maintaining excellent biocompatibility. The nanocomposites significantly enhanced VEGF-A and RUNX2 expression and promoted mineralization, indicating strong potential for magnetically targeted bone tissue engineering and theranostic applications [2,3].

Acknowledgements

This work has received funding from the European Innovation Council (EIC) under the project no. 101186758. Views and opinions expressed are, however, those of the author(s) only and do not necessarily reflect those of the European Union or the European Research Executive Agency (REA). Neither the European Union nor the

granting authority can be held responsible for them. Financial support for this work was granted also by the APVV-23-0097.

References

1. Sharifi, E. et al. Mesoporous Bioactive Glasses in Cancer Diagnosis and Therapy: Stimuli-Responsive, Toxicity, Immunogenicity, and Clinical Translation. *Advanced Science* vol. 9 Preprint at https://doi.org/10.1002/advs.202102678 (2022).
2. Vitázková, M. et al. High VEGF Secretion Using Co and B Co-doped Bioactive Mesoporous Glass Nanoparticles for Enhanced Angiogenesis. ACS Omega https://doi.org/10.1021/acsomega.5c00874 (2025) doi:10.1021/acsomega.5c00874.
3. Vitázková, M. et al. Magnetic Mesoporous Bioactive Glass Nanocomposite for Enhanced Osteogenesis and Angiogenesis in Bone Tissue Engineering. *ACS Appl. Bio Mater.* **8**, 7145 – 7160 (2025).

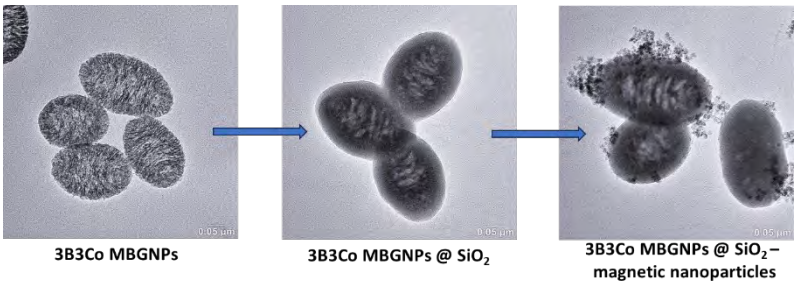

Fig.1: TEM images of the developed MBGNPs+SPIONs composites.

S80 – O3

Cytotoxicity Reduction of Iron Nitride Particles via Oxidation

Usuki S.[1], Ogawa T.[2], Yokoi T.[3], Ogura S.[3], Hori M.[3], Matsumoto A.[3], Miyakawa M.[4], Majima Y.[4], Kawashita M.[3]
[1]Graduate School of Medical and Dental Sciences, Institute of Science Tokyo, Tokyo, Japan, [2]Graduate School of Engineering, Tohoku University, Sendai, Japan, [3]Laboratory for Biomaterials and Bioengineering, Institute of Integrated Research, Institute of Science Tokyo, Tokyo, Japan, [3]Materials and Structures Laboratory, Institute of Integrated Research, Institute of Science Tokyo, Kanagawa, Japan

Introduction

The development and modification of magnetic particles have expanded their use in biomedical applications, such as magnetic hyperthermia for cancer treatment. Iron nitride has been suggested as a candidate material for this treatment[1,2]. However, while iron nitride particles generate heat to induce anticancer effects, they show cytotoxicity in fibroblast (L929) cell lines due to increased pH levels and the release of iron ions[2]. Thus, we aimed to develop novel particles that maintain superior heat-generation properties while exhibiting improved cytocompatibility. In this study, the iron nitride particles were oxidized, and their structures, heat-generating properties, and cytotoxicity, were investigated.

Materials and Methods

Iron nitride particles were synthesized from hematite and sodium amide at 250 ºC for 12 h[1], then oxidized at 50–200 ºC for 1h in air. Samples oxidized at 50, 100, and 200 ºC were named FN50, FN100, and FN200, respectively, where FN represents the sample without oxidation treatment. The crystalline phases of the samples were determined by X-ray diffraction (XRD). The heat-generating properties of the samples were investigated under an alternating magnetic field (100 kHz, 125 Oe) for 10 minutes. The cytotoxicity of the particles was assessed by exposing the L929 cell line to the samples for 24 h. Cytotoxicity was evaluated by calculating the IC_{50} (i.e., half-maximal inhibitory concentration) from the cell viability. Iron uptake by cells was quantified 3 h after exposure to the samples by normalizing FerroOrange fluorescence to Hoechst.

Results

According to the XRD patterns, iron nitride and iron oxide were coexisting in the sampes when oxidized above 100 ºC, and the diffraction peak intensity of iron oxide increased with higher oxidizing temperatures. The heat-generation properties decreased as the oxidizing temperature increased; meanwhile, the oxidized samples showed low cytotoxicity compared to the unoxidized sample (Table 1). An analysis of the factors contributing to the reduced cytotoxicity revealed that iron uptake by cell decreased as the oxidation temperature increased (Fig. 1).

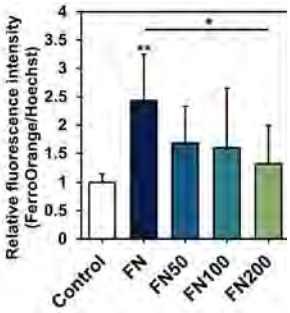

Fig. 1. FerroOrange fluorescence intensity normalized by Hoechst fluorescence intensity (Tukey's test, $^{**}P < 0.01$ and $^{*}P < 0.05$; $n = 4$).

Conclusion

The oxidation is an effective strategy for reducing the cytotoxicity of iron nitride; however, to maintain superior heat generation properties effective for cancer treatment while achieving cytocompatibility, further surface modification of iron nitride particles is necessary.

Table 1. Temperature increase (ΔT) of agar phantom with samples and IC_{50} of samples.

Sample	ΔT (ºC)	IC_{50} (μg/mL)
FN	23.4	65.3
FN50	18	106
FN100	11.7	533
FN200	1.7	2036

Acknowledgements

We acknowledge financial support from JSPS KAKENHI, grant nos. JP22H03949 and JP25K03460; JST SPRING, grant no. JPMJSP2180; and by a grant from MEXT (DEJI²MA).

References

[1]Usuki S., Ogawa T., Shimabukuro M., Yokoi T., and Kawashita M. Synthesis of ε-$Fe_{2-3}N$ Particles for Magnetic Hyperthermia. *J. Funct. Biomater.* 2025; 16(3); 203.
[2]Shibata M., Ogawa T., and Kawashita M. Synthesis of Iron Nitride Nanoparticles from Magnetite Nanoparticles of Different Sizes for Application to Magnetic Hyperthermia. *Ceram. Int.* 2019; 45(17); 23707-23714.

[3]Usuki S., Ogawa T., Shimabukuro M., Yokoi T., and Kawashita M. Synthesis and Cytotoxicity Evaluation of Iron Nitride Nanoparticles for Magnetic Hyperthermia. *The 45th Annual Meeting of Japanese Society for Biomaterials* 2023; 381.

S80 – O4

In-solution manufacturing of versatile porous phosphate-based glasses for hard and soft tissue regeneration

Berry C.[1], Zhao H.[2], Smales G. J.[3], Felipe-Sotelo M.[1], Wilkinson H. N.[4,5], Hardman M. J.[4,5], Carta D.[1]
[1]School of Chemistry and Chemical Engineering, University of Surrey, United Kingdom, [2]School of Bioscience and Medicine, University of Surrey, United Kingdom, [3]Institute for Inorganic Chemistry, Graz University of Technology, Graz, Austria, [4]Centre for Biomedicine, Hull York Medical School, Hull, United Kingdom, [5]Skin Research Centre, Hull York Medical School, Hull, United Kingdom.

Introduction

The combination of supramolecular templating with in-solution methods such as sol-gel (SG) and coacervation (COA) has received increased interest for the synthesis of highly porous phosphate-based glasses (PGs) for biomedical applications.[1] PGs are bioresorbable and release therapeutic ions upon dissolution, stimulating cellular proliferation and differentiation. Introducing porosity increases surface area and enables pore geometries that promote cell attachment and tissue ingrowth, therefore enhancing bioactivity.[2] Incorporation of therapeutic ions such as Ti^{4+} promotes osteogenesis and improves the thermal and mechanical stability of PGs, allowing greater control over dissolution behaviour, which is critical in biomaterial design. Additional ions, including Cu^{2+} and Ga^{3+}, impart antibacterial properties and enhancement of wound closure.[3]

Aim

To manufacture highly porous PGs loaded with Cu, Ga and Ti ions and asses their tissue regeneration capabilities.

Materials and Methods

Porous PGs were synthesised *via* SG and COA routes. SG glasses in the P_2O_5-CaO-Na_2O system were prepared using *n*-butyl phosphate, calcium methoxyethoxide and sodium methoxide and were loaded with therapeutic metallic ions. Pluronic-type surfactants (P123 and F108) were used to enhance textural properties.
Glasses in the P_2O_5-CaO-Na_2O-TiO_2 system were also prepared by COA using sodium polyphosphate, calcium nitrate tetrahydrate and titanium isopropoxide.

Results

Porous PGs were characterised using complementary techniques of X-ray diffraction, Fourier-transform infrared spectroscopy and thermal analysis. Porosity was investigated using small angle X-ray scattering, N_2 adsorption-desorption analysis at 77 K and scanning electron microscopy (SEM).
SEM imaging of SG-derived PGs exhibited extended porosity following surfactant removal (**Figure 1)**, while COA-derived Ti-PGs displayed macroporosity across the surface. Ion release analysis using microwave plasma atomic emission spectroscopy shows that therapeutic ion release directly correlates to loading.
Indirect contact cell studies of Ti-PGs with osteoblasts (MC3T3-E1) and keratinocytes (HaCaTs) demonstrated continued proliferation for up to 14 days. Cu-loaded PGs exhibited significant antibacterial activity against *S.aureus* (Gram-positive) and *E. coli* (Gram-negative) bacteria, while Ga-loaded samples showed activity against *S. aureus*. Assessment using a human *ex vivo* model showed excellent wound healing capabilities, with Cu- and Ga-loaded PGs achieving up to 93 % and 97 % wound closure, respectively (**Figure 2**).

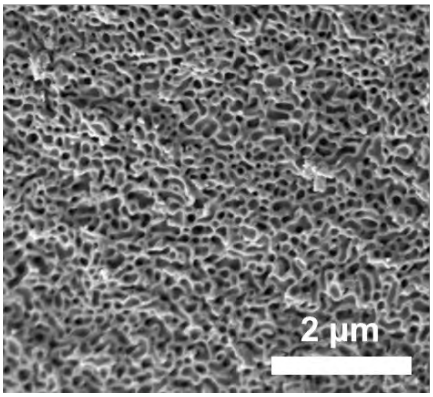

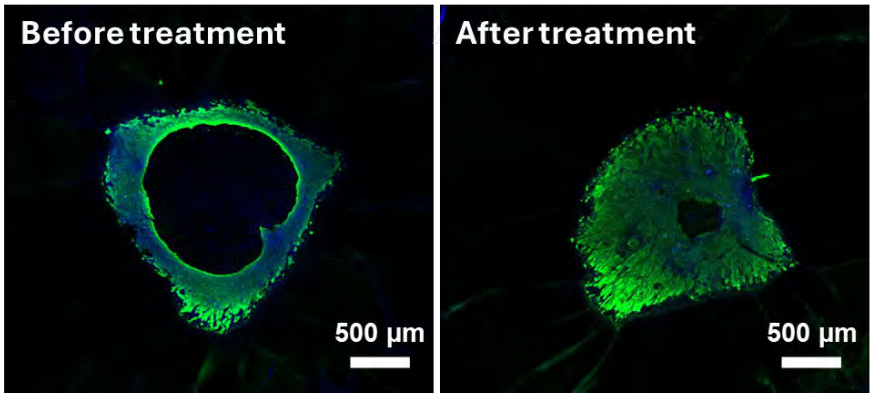

Figure 1. SEM image of Ga-PPG

Figure 2. Wound healing effect of Cu-PPG treatment

Conclusion

This study demonstrates that porous phosphate glasses can be successfully synthesised using SG and COA routes. Cu- and Ga-containing PGs exhibit promising antibacterial activity and significant wound healing potential, while Ti-containing PGs show promising properties for hard tissue regeneration.

References

[1]Foroutan F., Kyffin B. A., Abrahams I., Corrias A., Gupta P., Velliou E., Knowles J. C., Carta D. Mesoporous Phosphate-Based Glasses Prepared via Sol-Gel. *ACS Biomaterials Science & Engineering*, 2020; 6; 1428-1437.

[2]Izquierdo-Barba I., Vallet-Regi M. Mesoporous bioactive glasses: Relevance of their porous structure compared to that of classical bioglasses. *Biomedical Glasses*, 2015; 1; 140-150.

[3]Berry C. A., Reinart K., Smales G. J., Wilkinson H. N., Hardman M. J., Marchesini S., Lee W., Nery E. T., Moghaddam Z., Hoxha A., Felipe Sotelo M., Gutierrez-Merino J., Carta. D. Hierarchically porous copper and gallium loaded sol-gel phosphate glasses for enhancement of wound closure. *Journal of Materials Chemistry B*, 2025; 13; 15662-15677.

S80 – O5

Molybdenum-copper co-doped mesoporous bioactive glass nanoparticle-coated PCL scaffolds for osteomyelitis treatment and bone regeneration

Andrade Pinto J.C.[1,2] , Mahmoudifard M.[1], Xin Y.[1], Jung C.[1], Fredel M.C.[2], Hotza D.[2], Boccaccini A.R.[1]
[1]Institute of Biomaterials, Dept. of Materials Science and Engineering, Friedrich-Alexander-Universität Erlangen-Nürnberg (FAU), Erlangen, Germany
[2]Federal University of Santa Catarina (UFSC), Florianópolis, Brazil

Introduction

Chronic osteomyelitis is a persistent bone infection, frequently associated with Staphylococcus aureus, poor local vascularization, prolonged inflammation, and impaired bone regeneration. These features reduce the effectiveness of systemic antibiotic therapy and contribute to recurrence and bone destruction. Multifunctional scaffolds capable of locally combining antibacterial, pro-regenerative, and immunomodulatory effects are therefore highly attractive. Mesoporous bioactive glass nanoparticles (MBGNs) are promising for this purpose because of their high surface area, tunable composition, and controllable ion release. In particular, molybdenum has been associated with osteogenic and inflammation-modulating effects, whereas copper is relevant for antibacterial activity and angiogenic stimulation. In the present work, we extend a previously established PCL-MBGN scaffold platform toward Mo/Cu co-doped systems designed for osteomyelitis treatment.

Materials and Methods

MBGNs were synthesized by a sol-gel/micro-emulsion route and incorporated as surface coatings onto FDM-printed PCL scaffolds. The study design included five groups: PCL, PCL + plain MBGNs, PCL + Cu-MBGNs, PCL + Mo-MBGNs, and PCL + MoCu-MBGNs. The materials were characterized by SEM/EDX, FTIR, XRD, and ion-release analysis, while scaffold bioactivity was assessed in simulated body fluid. Early biological screening was designed to include pre-osteoblast viability on scaffolds and antibacterial testing relevant to osteomyelitis applications. The present system builds on the group's previously published PCL/MBGN coating strategy, while introducing dual-ion functionalization directed toward infection-associated bone defects.

Results

Preliminary characterization of the current Mo/Cu-based system indicated successful preparation of doped MBGNs, with spectral features consistent with Cu-O and Mo-containing species, and coated scaffolds showing surface-associated particle deposition. Early SBF results suggested hydroxyapatite-forming ability after short-term immersion. These findings are supported by the previously reported group platform, in which PCL scaffolds coated with ion-doped MBGNs exhibited well-defined interconnected pore architecture (~550 µm), improved hydrophilicity after surface treatment/coating, clear apatite formation during SBF immersion, burst silicon release within the first 48 h, and cumulative release of therapeutic ions over 7 days. That platform also showed significantly improved MC3T3-E1 viability and more favorable cell spreading on MBGN-containing scaffolds compared with bare PCL. Taken together, these results support the feasibility of extending the platform toward Mo/Cu co-doping for combined antibacterial and bone-regenerative action.

Conclusion

Mo/Cu co-doped MBGN-coated PCL scaffolds represent a promising multifunctional strategy for osteomyelitis treatment by integrating scaffold-guided bone regeneration with ion-mediated antibacterial and pro-healing effects. The preliminary results, together with the previously validated group platform, support further biological evaluation of this system as a local therapeutic scaffold for infection-related bone defects.

Acknowledgements

The authors acknowledge the PROBAL/CAPES-DAAD collaboration and the institutional support of FAU, UFSC, and ITA.

S82
Composite and hybrid biomaterials

S82 – K1
Multiphoton lithography for bioinspired composite and hybrid biomaterials: From architecture to function

Charitaki M.
Foundation for Research and Technology – Hellas, Greece

Multiphoton lithography (MPL) provides a powerful approach for the fabrication of three-dimensional tructures with precise control over their microscale architecture. Its combination with natural, hybrid, and composite materials offers opportunities to tailor not only the geometry of the fabricated structures, but also their physicochemical and biological properties.

Our work explores the development of multifunctional biomaterials through a range of material and structural approaches. Biopolymer-based hybrid hydrogels combining gelatin methacryloyl (GelMA) and chitosan derivatives have demonstrated their potential to support cell proliferation and biomineralization. The role of architecture has also been investigated through the fabrication of three-dimensional auxetic structures, demonstrating how microscale geometry can be used to tailor mechanical behaviour and influence cell–material interactions.

More recent work focuses on the incorporation of bioactive and functional components directly into materials suitable for multiphoton fabrication. Curcumin-containing GelMA systems are being investigated to combine high-resolution structuring with natural-based antimicrobial functionality, while the addition of bioactive inorganic components provides a route towards organic–inorganic composite scaffolds with bone-mimetic properties. In parallel, protein-based and nanocomposite microstructures with stimuli-responsive behaviour are being explored as platforms whose properties can respond to changes in the surrounding environment.

In conclusion, this work aims to develop biomaterial systems in which material composition, structural design, and biological functionality are considered together. MPL provides the flexibility to combine these elements within precisely defined three-dimensional architectures, supporting the development of bioactive, responsive, and multifunctional materials for tissue engineering and regenerative medicine.

S82 – O1

Inorganic-organic hybrid coatings with siderophore-like activity

Matlak T.[1], Kyzioł K.[1], Widziołek M.[2], Rarata K.[2,3], Sebastian V.[4, 5], Kyzioł A.[6]
[1]Faculty of Materials Science and Ceramics, AGH University of Krakow, Poland; [2]Institute of Zoology and Biomedical Research, Jagiellonian University, Kraków, Poland; [3]Doctoral School of Exact and Natural Sciences, Jagiellonian University, Kraków, Poland; [4]Instituto de Nanociencia y Materials de Aragón (INMA), CSIC-Universidad de Zaragoza, Spain; [5]Dept. of Chemical Engineering and Environmental Technologies, University of Zaragoza, Spain; [6]Faculty of Chemistry, Jagiellonian University, Krakow, Poland

Introduction

Reducing peri-implant complications, particularly those related to biofilm formation and inflamed tooth supporting tissues of periodontal patients, remains a paramount challenge in modern biomedical engineering. Inorganic-organic hybrid materials are at the forefront of research interest due to their unique physicochemical properties. The application of novel colloidal systems based on metal-polyphenol networks modifying the surface of silver or copper nanoparticles facilitates a synergistic effect, combining the excellent mechanical properties of titanium substrates with the broad-spectrum antimicrobial activities of silver nanoparticles and metal ions. Furthermore, such functional materials offer a viable response to the global crisis of antimicrobial resistance (AMR).

Materials and Methods

The designed system comprises antimicrobial coatings deposited on Ti Grade 2 alloy using sequential dip-coating or immersion methods. Prior to deposition, the alloy undergoes mechanical polishing followed by RF (Radio Frequency) glow-discharge plasmochemical treatment. This process is intended to remove native titanium oxides and environmental contaminants. The use of argon-oxygen plasma promotes the formation of a controlled oxide layer and efficient surface activation. Subsequently, coatings are fabricated using silver nanoparticles (AgNPs). The synthesis is achieved via the reduction of silver(I) nitrate with tannic acid (TA), where free phenolic groups on the nanoparticle surfaces are subsequently complexed with iron(III) or copper(II) ions (Ag@TA_Fe(III), Ag@TA_Cu(II)).

Results

The synthesized nanoparticles were characterized in terms of morphology, stability, and biological activities. TEM imaging revealed a uniform spherical morphology with an average primary particle size of approximately 20 nm. Colloidal stability was confirmed via Zeta potential measurements (DLS), with values ranging from -30 to -25 mV. Antioxidant activity, determined by DPPH and FRAP assays, was significantly enhanced by the incorporation of metal ions into the surface polyphenolic layers . This reactivity was closely correlated with the antimicrobial activity of the colloids. Consequently, the Ag@TA_Cu(II) colloid was utilized to functionalize the Ti Grade 2 surface. The resulting hybrid layers were characterized to assess deposition efficiency, microstructure, and chemical composition using SEM-EDS analysis.

Conclusion

The study demonstrated that incorporating Cu(II) ions into Ag-tannic acid networks markedly enhances both antioxidant and antimicrobial activities. Plasmochemical activation of Ti Grade 2 enabled the robust deposition of the resulting hybrid coatings. These multifunctional systems offer a promising strategy for mitigating periodontal and peri-implant infections addressing the global challenge of antimicrobial resistance.

Acknowledgements

This work was supported by the National Science Center within project OPUS 22 (2021/43/B/ST4/02833).

S82 – O2

Polysaccharide-based dressing enriched with zinc oxide nanoparticles and bacitracin for infected wound treatment

Kusibab A.[1], Macyk A.[1], Ochońska D.[2], Brzychczy-Włoch M.[2], Reczyńska-Kolman K.[1], Pamuła E.[1]
[1]Department of Biomaterials and Composites, AGH University of Krakow, Krakow, Poland; [2]Department of Molecular Medical Microbiology, Jagiellonian University Medical College, Krakow, Poland

Introduction

Treatment of infected and highly exuding wounds requires advanced dressings capable of absorbing large amounts of exudate while providing effective antibacterial action. Polysaccharide-based hydrogels are promising candidates due to their biocompatibility and ability to maintain a moist environment[1].
This study aimed to develop and characterize highly porous gellan gum/sodium alginate (GG/Alg) dressings enriched with zinc oxide nanoparticles (ZnO(n)) and bacitracin (BAC) to enhance antibacterial performance while reducing antibiotic dosage.

Materials and Methods

ZnO(n) were characterized in terms of size, surface area, and antimicrobial activity. Four types of hydrogels (GG/Alg, GG/Alg+ZnO, GG/Alg+BAC, GG/Alg+ZnO+BAC) were prepared and freeze-dried to obtain porous matrices. Materials were evaluated in terms of morphology (SEM), swelling capacity, BAC release profile, cytotoxicity using L929 fibroblasts (AlamarBlue and live/dead staining), and antibacterial activity against *Staphylococcus aureus*, *Staphylococcus epidermidis*, and *Streptococcus pyogenes*.

Results

ZnO(n) exhibited a mean size of 26 ± 4 nm and a high specific surface area of 39.16 m^2/g, supporting their potential antibacterial performance. All freeze-dried samples showed a highly porous structure and excellent swelling capacity exceeding 4000%, corresponding to the ability to absorb more than 40 times their dry weight. BAC release studies revealed a burst release profile, with approximately 90% of the drug released within the first 2 h. Cytotoxicity studies demonstrated good biocompatibility of GG/Alg and GG/Alg+BAC samples, while ZnO-containing samples showed reduced cell viability under extract conditions. Antibacterial studies confirmed that BAC-containing samples exhibited strong activity against all strains tested, with enhanced effects observed in GG/Alg+ZnO+BAC, indicating a potential cooperative antibacterial effect.

Conclusion

The developed GG/Alg+ZnO+BAC dressing shows great potential as a dressing for infected and exuding wounds due to its high absorbency and enhanced antibacterial activity. However, further optimization of ZnO(n) concentration is required to balance antibacterial efficacy and cytotoxicity. The results provide a basis for the development of advanced multifunctional wound dressings.

Acknowledgements

This research was funded by the Ministry of Science and Higher Education, Poland, from the Program “Excellence Initiative – Research University” for the AGH University of Krakow and the National Science Center, Poland (2025/57/B/ST5/01898).

References

[1]Zhu, T.; Mao, J.; Cheng, Y.; Liu, H.; Lv, L.; Ge, M.; Li, S.; Huang, J.; Chen, Z.; Li, H. Recent Progress of Polysaccharide-Based Hydrogel Interfaces for Wound Healing and Tissue Engineering. *Adv. Mater. Interfaces* **2019**, *6*, 1900761.

S82 – O3

Plasmonic granular hydrogels for 3D printing breast cancer models and monitor cell behaviour by Surface-Enhanced Raman Spectroscopy (SERS)

Troncoso-Afonso, L.[1,2,3] Fernandes, M.[4] Marchena, F.S.J. [4] Włodarczyk-Biegun, M.K. [4,5] García-Astrain, C.[6,7] and Liz-Marzán, L.M.[1,3,6,7]

[1]CIC BiomaGUNE, Basque Research and Technology Alliance (BRTA), 20001 Donostia-San Sebastián, Spain.[2]Department of Applied Chemistry, University of the Basque Country, 20018, Donostia-San Sebastián, Gipuzkoa, Spain.[3]Centro de Investigación Biomédica en Red de Bioingeniería Biomateriales, y Nanomedicina (CIBER-BBN), Paseo de Miramón 182, 20014 Donostia-San Sebastián, Spain. [4]Zernike Institute for Advanced Materials, University of Groningen, Groningen, the Netherlands.[5]Biotechnology Centre, The Silesian University of Technology, Gliwice, Poland. [6]POLYMAT and Department of Applied Chemistry, Faculty of Chemistry, University of the Basque Country UPV/EHU, Paseo Manuel Lardizábal 3, 20018 Donostia-San Sebastián, Spain.[7]Ikerbasque Basque Foundation for Science, 48013 Bilbao, Spain.
ltroncoso@cicbiomagune.es

Introduction

In vitro cancer models are essential for studying the mechanisms that drive tumor development and therapeutic response.[1] Granular hydrogels-formed by jamming microgels-offer a versatile platform to mimic this heterogeneity due to their tunable mechanics, interconnected porosity, and ability to support nutrient and oxygen exchange.[2] These materials can be 3D-printed to generate controlled multiscale architectures with precise spatial control.[3] Moreover, plasmonic nanoparticles can be incorporated into the microgels, yielding printable materials that support cell growth while enabling metabolite detection via surface-enhanced Raman spectroscopy (SERS).[4] This work aims to develop granular plasmonic hydrogels to build 3D breast cancer models while monitoring tumor progression and therapeutic response.

Materials and Methods

Gelatin methacryloyl (GelMA) microgels were synthesized on chip using LAP as a UV-crosslinking photoinitiator. Gold nanorods (AuNRs) were incorporated into the microgel precursors, and their optical properties were analyzed by UV-Vis spectroscopy. Granular inks were produced by centrifugation, removing excess PBS, and subsequently characterized using rheology, confocal fluorescence microscopy, two-photon emission luminescence (2-PEL), SERS, and scanning electron microscopy. These inks were then 3D-printed into square-mesh scaffolds using a 3D Discovery RegenHU bioprinter.

Results

GelMA-AuNR microgels displayed an average diameter of 82.58 ± 13.05 µm. AuNR incorporation enabled efficient 2-PEL imaging. After jamming, the granular ink showed stable rheological properties between 20-40 °C, though decreases in G′ and G″ at 40 °C suggested physical contribution to the crosslinking of GelMA microgels. Photo-rheology confirmed further crosslinking upon LAP supplementation. Square-shaped scaffolds were successfully 3D-printed. The material was incubated with different analytes, which were successfully detected by Surface-Enhanced Raman Spectroscopy, **demonstrating the capability of the material to monitor the culture environment.** Finally, square-shaped scaffolds were successfully fabricated by 3D printing.

Conclusion

We have successfully prepared GelMA-AuNRs which can be used to obtain granular inks suitable for 3D bioprinting and SERS monitoring of cell metabolites. These plasmonic granular hydrogels can be used to build advanced 3D breast cancer models while enabling real-time monitoring of cellular activity within a complex tissue-like environment.

Acknowledgements

Financial support was provided by the European Research Council (ERC-2017-AdG #787510 4DBIOSERS and ERC-2024-Stg #101161716 JAM2PRINT) and by the Spanish MICIU/AEI/10.13039/501100011033. L.T.A. thanks

the Spanish Ministry of Universities for a Formación de Profesorado Universitario Fellowship (FPU21-05867) and (EST25/00274). L.T.A. thanks the CIBER-BBN for the Ayuda de Movilidad fellowship.

References

[1] L. Hutchinson *et al.*, Nat. Rev. Clin. Oncol., 2011, 8, 189-190.
[2] A. C. Daly, Adv. Healthcare Mater. 2023, 2301388.
[3] V.G. Muir, J.A. Burdick, Chem. Rev. 2021, 121, 18.
[4] L. Troncoso-Afonso *et al.*, Chem. Soc. Rev., 2024, 53, 5118-5148.

S82 – O4

Magnetoelectric GelMA-Graphene Hydrogels for Remote Cardiac Stimulation and Sensing

Viteri A.[1,2], Colombi S.[2,3], Resina L.[2,3], Ginebra M.-P.[1,2,4,5], Engel E.[1,2,4,5], Alemán C.[2,3,4], García-Torres J.[1,2,5]
[1]Dept. of Materials Science and Engineering and Institute for Research and Innovation in Health, Universitat Politècnica de Catalunya-BarcelonaTech, Barcelona; [2]Barcelona Research Center in Multiscale Science and Engineering, Universitat Politècnica de Catalunya-BarcelonaTech, Barcelona; [3]Dept. of Chemical Engineering, Universitat Politècnica de Catalunya-BarcelonaTech, Barcelona; [4]Institute for Bioengineering of Catalonia (IBEC), Barcelona Institute of Science and Technology (BIST), Barcelona; [5]Centro de Investigación Biomédica en Red de Bioingeniería, Biomateriales y Nanomedicina (CIBER-BBN), Instituto de Salud Carlos III, Madrid, Spain

Introduction

Multifunctional biomaterials capable of integrating sensing, actuation, and biological compatibility are highly attractive for next-generation bioelectronic interfaces. In this work, we developed a hybrid hydrogel based on gelatin methacryloyl (GelMA) incorporating magnetoelectric nanoparticles (MENPs) and graphene flakes to obtain a soft, conductive, and magnetically responsive biomaterial. MENPs enable the conversion of external magnetic stimuli into local electric signals, while graphene enhances the electrical conductivity of the hydrogel network. This composite hydrogel is designed to provide a bioactive matrix capable of supporting cardiac cells while enabling wireless electrical stimulation and simultaneous electrical recording.

Aim

Development of magnetoelectric GelMA-Graphene hydrogels for remote cardiac stimulation and simultaneous bioelectronic sensing.

Materials and Methods

GelMA was synthesized through gelatin methacrylation and photo-crosslinked via UV-initiated free-radical polymerization. MENPs consisting of a magnetostrictive $CoFe_2O_4$ core and a piezoelectric $BiTiO_3$ shell were synthesized by a hydrothermal method and characterized using HRTEM, XPS, XRD, and magnetometry. MENPs and graphene flakes were dispersed in the GelMA prepolymer solution prior to crosslinking to obtain composite hydrogels. The resulting materials were characterized in terms of morphology, mechanical properties, electrical and electrochemical behavior, and magnetic responsiveness. Cell viability and proliferation were performed using H9c2 rat cardiac myoblasts by live/dead staining and PrestoBlue assays, respectively.

Results

Core-shell MENPs were successfully synthesized and structurally confirmed by TEM, HRTEM, XPS, and XRD analyses, while magnetic measurements verified the formation of an interface between $CoFe_2O_4$ core and $BiTiO_3$ shell (Figure 1a). Their incorporation, together with graphene flakes, within the GelMA matrix produced porous hydrogel networks with tunable stiffness and improved electrical conductivity (Figure 1b). The composite biomaterials supported high cardiac cell viability after seven days in culture, demonstrating good cytocompatibility. Importantly, cardiac cells embedded within the hydrogels showed enhanced proliferation when an external magnetic field was applied, indicating that the MENPs within the biomaterial effectively generated local electrical cues (Figure 1c). Moreover, the nanocomposite hydrogel allowed simultaneously recording the electrical changes. These results highlight the potential of multifunctional GelMA-based biomaterials for wireless bioelectronic interfaces and for the development of soft, implantable systems capable of remotely regulating and sensing cellular behavior.

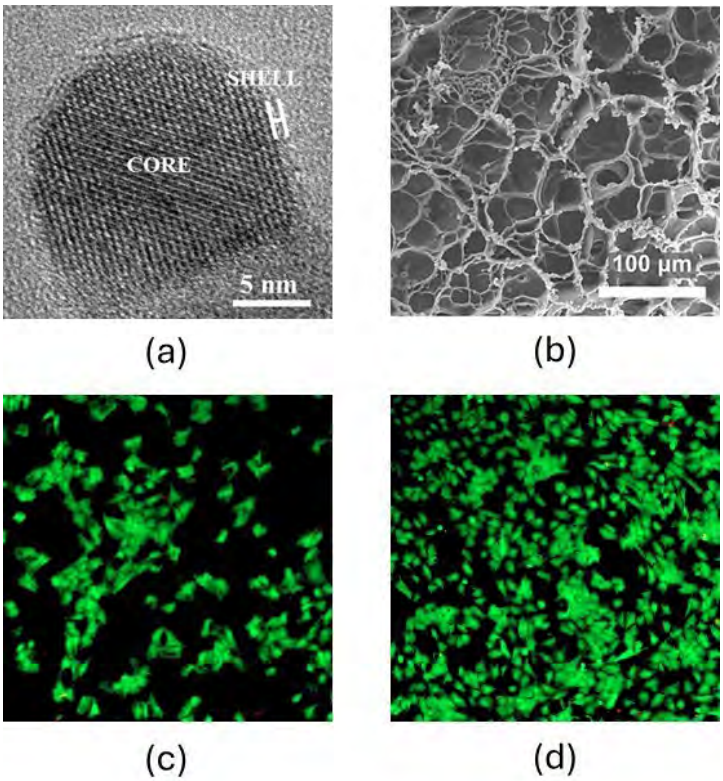

Figure 1. (a) HRTEM image of MENPs. (b) SEM image of GelMA-based hydrogels. Confocal images of GelMA-based hydrogels (c) without and (d) with magnetic stimulation.

Conclusion

A novel GelMA-based hydrogel incorporating MENPs and graphene exhibits magnetically induced electrical output, and enhanced conductivity for simultaneous sensing while maintaining biocompatibility. This multifunctional material platform holds significant potential for wireless stimulation of cardiac cells and the design of soft, flexible bioelectronic interfaces.

Acknowledgements

Authors acknowledge funding from MCIU/AEI /10.13039/501100011033 / FEDER, UE (CNS2022-136109, PID2024-157506OB-I00, PID2022-141120OB-I00, CEX2023-001300-M) and Agència de Gestió d'Ajuts Universitaris i de Recerca de Catalunya (AGAUR) (2021-SGR-01368, 2021-SGR-00387) for financial support.

S82 – O5

Development of hybrid nanodevices based on Chitosan/Hyaluronic acid/Folic acid-Carbon Dots for the treatment of lung infections

Della Sala F.[1†], Marino G.[1,2†], Barretta M.[1,2], di Gennaro M.[1], Longobardo G.[1], Paradiso R.[3], Del Sorbo L.[3], Borriello G.[3], Borzacchiello A.[1]
[1]Institute of Polymers, Composites and Biomaterials, National Research Council (IPCB-CNR), Naples, Italy;
[2]Department of Environmental, Biological and Pharmaceutical Sciences and Technologies (DiSTABiF), University of Campania "L. Vanvitelli", Caserta, Italy;
[3]Istituto Zooprofilattico Sperimentale del Mezzogiorno (IZSM), Naples, Italy.

Introduction

Bacterial infections represent a critical challenge in the management of pulmonary diseases, specifically in chronic obstructive pulmonary disease (COPD) and acute respiratory distress syndrome (ARDS). These infections frequently trigger acute exacerbations, accelerating the decline of pulmonary function. The efficacy of traditional antimicrobial therapies is increasingly compromised by the global rise of multidrug resistance (MDR) and a lack of new antibiotics[1]. Consequently, there is an urgent need for innovative therapeutic strategies that utilize novel mechanisms of action to circumvent current resistance patterns. Biocompatible nanosystems have emerged as a promising approach to bypass pathogen defense mechanisms[2]. Among them, nanogels (NGs) made by chitosan (CS) and hyaluronic acid (HA), natural polysaccharides with inherent antimicrobial properties, and folic-acid carbon dots[3] (FA-CDs), nanostructured carbon-based materials which offer intrinsic antibacterial activity and high tunability, have gained increasing attention.

Aim. The aim of this work is the design, fabrication and characterization of the hybrid nanogels (CS/HA-FACDs hybrid NGs) as an innovative therapeutic strategy for the treatment of bacterial infections.

Materials and Methods

Hybrid NGs were obtained by the single-step ionic gelation method with an accurate pH control. Hydrodynamic size, size distribution, ζ-potential and stability over time measurements were conducted by means of Dynamic Light Scattering. Nanoparticles morphology was investigated through Transmission Electron Microscopy. Chemical composition and intermolecular interactions were investigated using UV-Vis absorbance, Fourier Transform Infrared and Raman spectroscopies. Furthermore, cell viability was assessed via AlamarBlue assay and cell morphology was validated through Confocal Laser Scanning Microscopy imaging. Finally, antimicrobial tests were carried out.

Results

CS/HA-FACDs hybrid NGs exhibited an average hydrodynamic diameter of ~ 160 nm, a positive ζ-potential of ~ +20 mV and a good colloidal stability over a period of 15 days. The morphological investigation showed quasi-spherical, well-dispersed, non-agglomerated nanoparticles. Spectroscopic measurements confirmed the encapsulation of FA-CDs in the nanohybrid structure (Figure 1,2) and that the fabrication method leads to electrostatic interactions between the precursors without chemical reactions. AlamarBlue assay on human lung fibroblast cells for biocompatibility evaluation showed good viability up to 72 hours. Antimicrobial tests demonstrated a bactericidal effect, especially for pathogens involved in lung bacterial infections, such as *Staphylococcus aureus* and *Pseudomonas aeruginosa*.

Conclusion

This study presented the fabrication of stable nanohybrids via a single-step ionic gelation process. The chemical-physical characterization showed good features, including nanoscale size, positive surface charge and colloidal stability, which are critical for lung delivery and antimicrobial efficacy. Biological characterization revealed excellent cytocompatibility and significant reduction in bacterial viability.

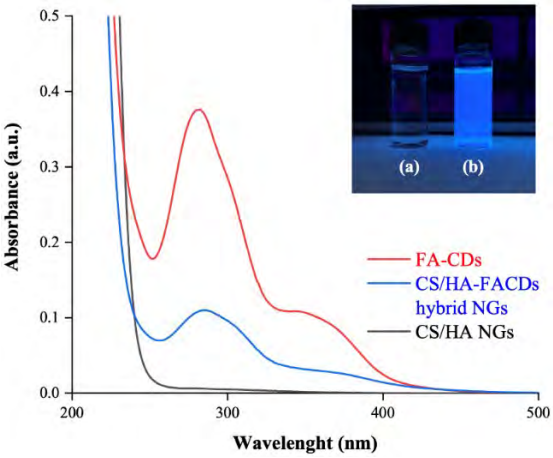

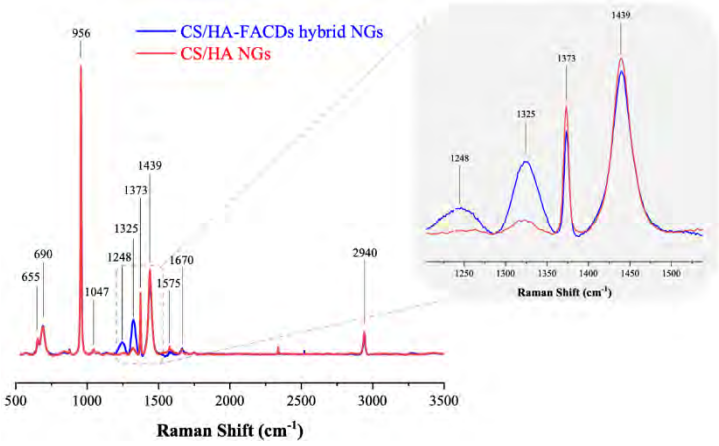

Figure 1. UV-Vis absorbance spectra (200-500 nm) of FA-CDs, CS/HA-FACDs hybrid NGs and CS/HA NGs. Inset refers to a photograph of aqueous dispersion of (a) CS/HA NGs and (b) CS/HA-FACDs hybrid NGs under UV light.

Figure 2. Raman spectra of CS/HA NGs and CS/HA-FACDs hybrid NGs. On the right side, it is reported a zoomed.

Acknowledgements

The authors acknowledge the research project “One Health Basic and Translational Research Actions addressing Unmet Needs on Emerging Infectious Diseases” – INF-ACT, CUP B53C20040570005”. This research has been supported by EU funding within the NextGenerationEU-MUR PNRR Extended Partnership initiative on Emerging Infectious Diseases (Project no. PE00000007, INF-ACT). Francesca Della Sala was recipient of an INF-ACT Foundation Early-Career Award (INF-ACT/ECA/2024).

References

[1] Mancuso, G.; Midiri, A.; Gerace, E.; Biondo, C. Bacterial antibiotic resistance: the most critical pathogens. *Pathogens* 2021, 10 (10), 1310.

[2] León-Buitimea, A.; Garza-Cárdenas, C. R.; Román-García, M. F.; Ramírez-Díaz, C. A.; Ulloa-Ramírez, M.; Morones-Ramírez, J. R. Nanomaterials-Based Combinatorial Therapy as a Strategy to Combat Antibiotic Resistance. *Antibiotics* 2022, 11 (6), 794.

[3] Yu, M.; Guo, X.; Lu, H.; Li, P.; Huang, R.; Xu, C.; Gong, X.; Xiao, Y.; Xing, X. Carbon dots derived from folic acid as an ultra-succinct smart antimicrobial nanosystem for selective killing of S. aureus and biofilm eradication. *Carbon 2022*, 199, 395-406.

S82 – O6

In situ mineralized decellularized extracellular matrix (DCM)-alginate based bioink for bone 3D-bioprinting

Handa S.[1], Dagar P.[1], Behera S.S.[1], Stoffer J.[2], Espinal A.[2], Snyder A.[2], Whitlock P.W.[2], Murab S.[1]
[1]School of Biosciences and Bioengineering, Indian Institute of Technology Mandi, Mandi, India; [2]Division of Pediatric Orthopaedic Surgery, Cincinnati Children's Hospital Medical Center, Cincinnati, Ohio, USA

Introduction

Critical-sized bone defects (CSDs) remain a major clinical challenge as they can't heal spontaneously. They are commonly caused by trauma, tumor resection, infection, or congenital abnormalities. Conventional treatments, including metallic implants, autografts, and allografts, suffer from limitations such as poor osteointegration, donor site morbidity, limited availability, and infection risk. Tissue engineering has therefore emerged as a promising strategy for bone regeneration. Three-dimensional (3D) printing enables fabrication of defect-specific scaffolds with controlled architecture; however, commonly used thermoplastics such as polylactic acid (PLA) and polycaprolactone (PCL) are bioinert and lack biological cues required for cell attachment and mineralization. In contrast, 3D bioprinting allows incorporation of cells and bioactive biomolecules to better mimic the extracellular matrix (ECM). Decellularized extracellular matrix (DCM) retains native biochemical components but exhibits limited mechanical strength for load-bearing applications. Incorporation of hydroxyapatite (HA) can improve osteoconductivity and mechanical properties, although direct addition may compromise printability and cell viability. This study therefore developed a biomimetic HA-DCM-alginate bioink through controlled *in situ* mineralization of bone-derived DCM and evaluated its physicochemical, rheological, and biological performance following 3D bioprinting.

Materials and Methods

Goat bones were decellularized using sequential chemical treatments and characterized by biochemical assays, LC-MS/MS, and histology. The DCM was pepsin-digested and subjected to *in situ* HA mineralization on DCM and alginate. Resulting matrices were analyzed by SEM-EDX, FTIR, XRD, and AFM. Alginate, DCM-alginate, and HA-DCM-alginate bioinks were formulated and evaluated for rheological, mechanical, swelling, degradation, and printability properties. 3D-bioprinted scaffolds were assessed for mineralization, MG-63 cell viability and proliferation, and mechanical performance in an *ex vivo* goat bone defect model.

Results

Decellularization effectively removed cellular components while preserving collagen and glycosaminoglycans (GAGs), confirmed by significantly reduced DNA levels ($p < 0.001$) and histological staining showing loss of nuclei with retained ECM proteins (Figure-1). Proteomic analysis revealed a dense ECM protein network including annexins and collagen, associated with metabolic and matrix regulatory functions. *In situ* mineralization showed needle-like HA crystals on DCM, whereas alginate showed limited deposition. EDX confirmed higher Ca-P content in DCM, with Ca/P = 1.74 indicating HA. FTIR, XRD, and AFM verified carbonate-containing HA formation, increased crystallinity, and roughness. HA-DCM-alginate showed superior rheology, compressive strength, printability, stability, mineralization, cell proliferation (Figure-2), and restored mechanical competence in an *ex vivo* bone defect model.

Conclusion

A stiff biomimetic HA-DCM-alginate bioink mimicking the organic-inorganic composition of native bone exhibited favourable rheology, improved compressive strength, and supported enhanced cell proliferation, mineralization, and restoration of mechanical integrity in an *ex vivo* bone defect model, demonstrating potential for bone tissue engineering.

Acknowledgements

SM acknowledges the funding support from IIT Mandi (IITM/SG/SUM/88), Anusandhan National Research Foundation (ANRF, India) (SRG/2023/002182), IIT Mandi iHub and HCI Foundation (IIT MANDI iHub/RD/2023/012), and DST-FIST (SR/FST/LS-II/2022/950). SH, PD, SSB acknowledge the scholarship support from MoE, Govt. of India.

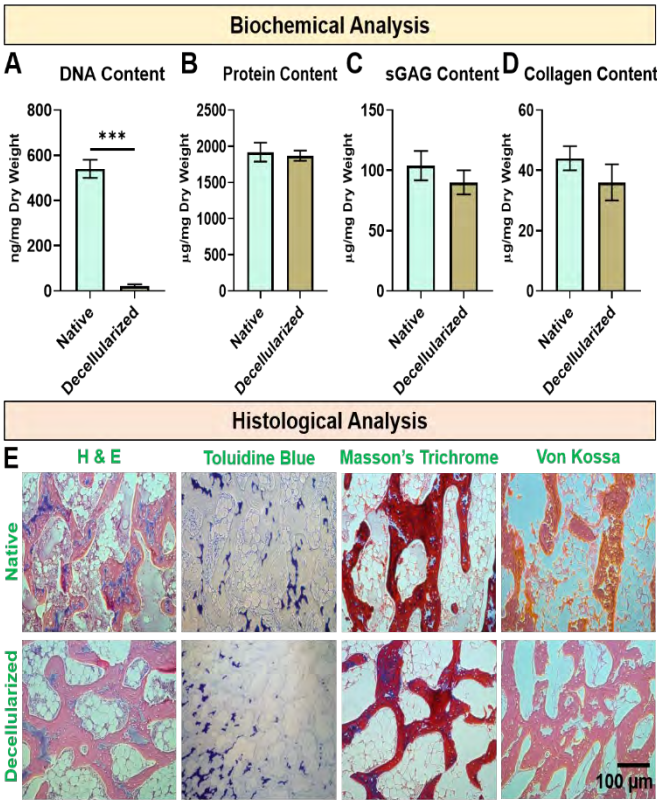

Figure-1: Biochemical and histological characterization of native and decellularized goat bone tissue (***p < 0.001)

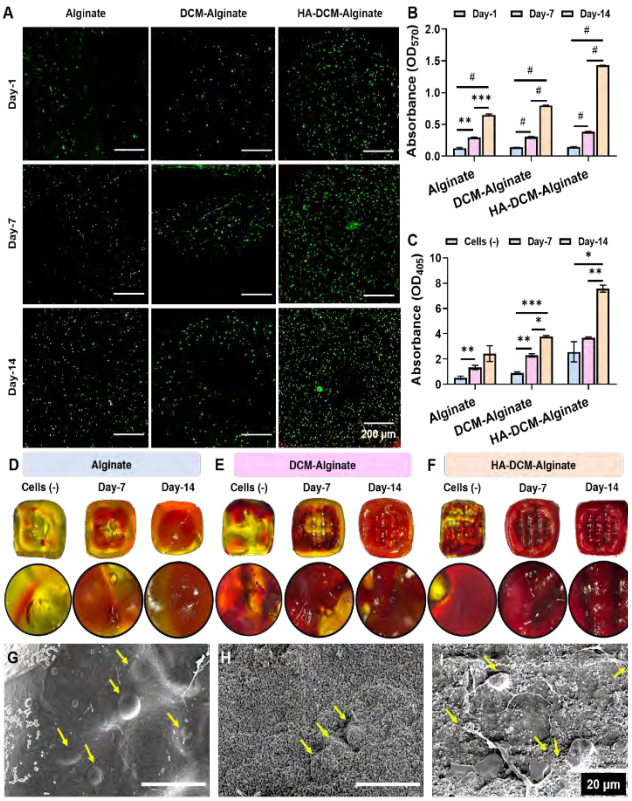

Figure-2: *In vitro* studies and evaluation of osteogenic potential of 3D bioprinted scaffolds (*p < 0.05, **p < 0.01, ***p < 0.001, #p < 0.0001)

S82 – O7

Warp-knitted spacer fabrics as reinforcement for hydrogels in tissue engineering

Hoffmann L.A.[1], Flock H.[1], Becker L.A.[1], Emonts C.[1], Gries T.[1]
[1]Institut für Textiltechnik of RWTH Aachen University, Aachen, Germany

Introduction

End-stage liver failure is primarily treated by liver transplantation, but the shortage of donor organs limits its availability. Tissue engineering offers a promising alternative through the development of artificial liver tissue. Scaffolds play a crucial role in this context, as they provide structural support and influence the mechanical environment of cells. Warp-knitted spacer fabrics are of particular interest due to their adjustable and voluminous architecture and wide range of mechanical properties.

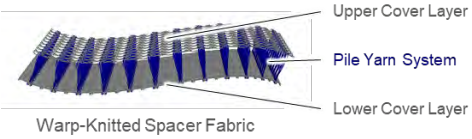

Aim

The aim of this study is to evaluate the suitability of warp-knitted spacer fabrics as scaffold materials for liver tissue engineering with regard to their compression properties. Focus lies on the investigation of the pile yarn system.

Materials and Methods

The compression properties of the spacer fabrics were characterized using unconfined compression of a circular sample (diameter 22 mm, hight 6 mm). The effects of the factors pile yarn fineness (80 dtex and 100 dtex) and pile yarn cross-sectional shape (round and snowflake-shaped) were analyzed using a 2^2 factorial design. Hydrogel concentration was varied in an 1-factor experiment design in combination with a spacer fabric with 80 dtex round pile yarns to determine the effect of the reinforcement on different concentrations.

Results

The results show significant effects of pile yarn fineness ($p < 0.001$) and pile yarn cross-sectional shape ($p = 0.004$) on the compression force at a compression to half the sample hight, a residual distance of 3 mm.
Pure gelatin hydrogels exhibit compression forces from 0.73 N (SD = 0.08 N) at 2.5 % concentration up to 6.29 N (SD = 1.42 N) at 10 % concentration. Reinforced with spacer-fabric the 2.5 % gelatin hydrogel reached a compression force almost 5 times more than without reinforcement.

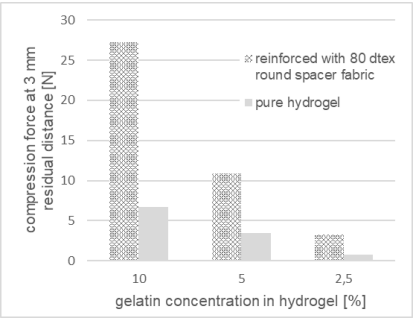

Conclusion

Warp-knitted spacer fabrics can be used easily to reinforce hydrogels for tissue engineering. The composite exhibits mechanical properties that are considerably closer to those of human liver tissue than pure gelatin hydrogel. These findings indicate that warp-knitted spacer fabrics are promising scaffold materials for applications in tissue engineering and represent a potential approach for the development of biomimetic liver constructs.

Acknowledgements

This project is funded by the DFG (German Research Foundation) in cooperation with the Institute of Printing Science and Technology (Darmstadt). Reference number: 527466060

S83
Computational modeling, digital twins, and in silico testing

S83 – K1
Exploring the role of optical depth of field in volumetric, light-based additive manufacturing

Hayden Taylor, UC Berkeley, Keynote talk, ESB, September 2026

Volumetric additive manufacturing is appealing for bioprinting because of its ability to define geometries within complex volumes of heterogeneous material. The technique is increasingly being used in experiments involving very low-modulus (sub-kPa) hydrogels, dispersions of cells, and multi-material substrates. Controlling the penetration of light through these volumes of materials must consider absorption, scattering, and occlusion; on all these topics, significant progress has been made recently. Additionally, the depth of field of the light patterns projected into the material may, in some cases, be smaller than the diameter of the target printing volume, necessitating more sophisticated planning of the light dosing strategy than in a conventional approach in which the light patterns are approximated as prismatic. This talk will discuss some considerations around depth of field from the perspective of delivered dose contrast, achievable spatial resolution, and computational complexity during light dose planning.

S83 - O1

Mechanical diversity of binding interactions improves robustness in soft biomaterials

Papafilippou E.[1], Bonfanti A.[2], Baldauf L.[3], Charras G.[3,4], Kabla A.[3]
[1]Dept. of Engineering, University of Cambridge, Cambridge, UK; [2]Dept. of Civil and Environmental Engineering, Politecnico di Milano, Milan, Italy; [3]London Centre for Nanotechnology, University College London, London, UK; [4]Dept. of Cell and Developmental Biology, University College London, London, UK

Introduction

Cell–cell junctions in epithelial tissues must withstand dynamic mechanical stresses while maintaining cohesion. Adhesion proteins display distinct force-dependent binding behaviours [1], yet how such mechanical diversity contributes to junction stability remains unclear.

Aim

How does mechanical diversity in adhesion units influence intercellular junction resilience?

Materials and Methods

We have developed a theoretical model based on Bell's model of force-dependent bond dissociation [2,3], describing two populations of reversible slip bonds. The populations are mechanically coupled through shared tension. Association rates are assumed constant, while dissociation rates increase exponentially with force. We analyse the dynamics of bond fractions, equilibrium states, and system stability under constant and cyclic loading. Analytical and stochastic simulations are used to compare mixed and single-population junctions, focusing on stability, time to equilibrium, and failure behaviour.

Results

Mixed population junctions exhibit enhanced stability compared to single-population systems. Under load, force-mediated interactions lead to cross-recruitment between weak and strong bonds, increasing overall bond occupancy. Weak bonds transiently absorb mechanical load, shielding stronger bonds and delaying their rupture. Under cyclic loading, mixed bond populations display greater robustness, maintaining higher bond fractions and resisting failure over extended times. Phase-space analysis reveals enlarged stable regimes, indicating improved tolerance to fluctuations in force and bond composition, compared to single population junctions. Mechanical diversity further enables decoupling between force sensing and structural robustness: weak bonds provide rapid responsiveness to tension changes, while strong bonds ensure long-term stability.

Conclusion

Mechanical diversity in adhesion proteins enhances junction resilience by promoting cooperative dynamics between bond populations. By enabling load sharing and delaying failure, mixed systems outperform homogeneous ones under both constant and cyclic loading. These results highlight protein diversity as a key design principle in living tissues, allowing independent tuning of mechanical sensing and structural integrity.

References

[1]Charras G., Yap A. Tensile forces and mechanotransduction at cell–cell junctions. *Current Biology* 2018; *28*(8); R445-R457.
[2] Bell G.I. Models for the specific adhesion of cells to cells: a theoretical framework for adhesion mediated by reversible bonds between cell surface molecules. *Science* 1978; 200(4342) ; 618-627.
[3] Papafilippou E., Bonfanti A., Charras G., Kabla A. Emergent Tissue Stability from Intercellular Bond Dynamics during Cyclic Mechanical Loading. *bioRxiv* 2025.

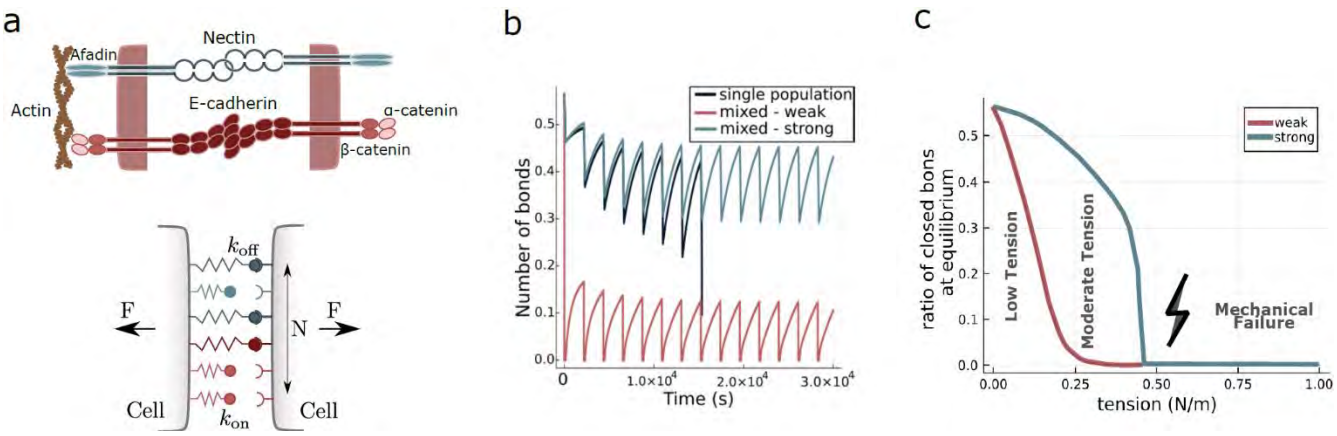

Figure 1: (a) Schematic of epithelial cell–cell junctions illustrating distinct adhesion complexes (e.g. nectin and E-cadherin) and their cytoskeletal anchoring. Bottom: theoretical model of two populations of reversible adhesion units (weak and strong slip bonds) coupled through shared tension. Bonds form with a constant association rate (k_{on}) and dissociate with a force-dependent rate (k_{off}) following Bell's model. (b) Dynamics of bond occupancy under cyclic loading. A mixed population (weak and strong bonds) maintains higher overall bond numbers compared to a single-population system. Weak bonds exhibit rapid turnover, while strong bonds sustain load, resulting in enhanced stability over time. (c) Equilibrium fraction of closed bonds as a function of applied tension. Weak bonds dominate at low tension but rapidly unbind, whereas strong bonds remain stable up to higher tensions. Mechanical diversity extends the stable regime and delays catastrophic failure under increasing load.

S83 – O2

De novo discovery of LLPS-prone short peptides: Mechanistically interpretable generative modelling and coarse-grained molecular dynamics

Ghalandari B., Patra H. K.
Centre for Advanced Materials in Clinical and Experimental Medicine, Dept. of Surgical Biotechnology, University College London, London, UK

Introduction

Liquid–liquid phase separation (LLPS) is a fundamental natural process where biomolecules (e.g., proteins, RNA) spontaneously condense into membraneless droplets including organelles. Short peptides represent promising minimal building blocks for artificial biosynthetic condensates. However, predicting LLPS behaviour from primary sequence remains challenging, largely due to complex interactions among charge, aromatic residues, side chain hydrophobicity, and conformational disorder.

Aim

To develop a computational discovery workflow for short peptides (length 10-12 amino acids) with LLPS capacity and evaluate their phase behaviour using molecular simulations.

Materials and Methods

A computational pipeline was developed using AI-driven peptide design to generate LLPS-prone sequences. Generative models based on RNN and transformer architectures were used to produce a peptide library (10^8). The generated sequences were analysed using a feature extraction framework calculating descriptors including net charge per residue, aromatic content, hydropathy, and disorder propensity. Selected candidates were subsequently evaluated using coarse-grained molecular dynamics simulations up to 5000 ns under different salt concentrations (1, 10, 100, 300, 500, and 1000 mM).

Results

Dimensionality reduction revealed that selected peptides cluster within a confined region of feature space distinct from the broader generated library, indicating enrichment for LLPS-compatible features. Three representative peptides were investigated using coarse-grained molecular dynamics simulations. Under favourable conditions, peptides assembled into condensate-like structure with reduced radius of gyration values of approximately 2–3 nm and volume fraction values exceeding 0.30. Pronounced backbone radial distribution function peaks near 3 nm indicated strong local ordering. Cluster analysis showed the emergence of single dominant aggregates, while diffusion coefficients decreased across systems, confirming stronger intermolecular interactions. Multiple structural (e.g., radial distribution functions) and dynamical (e.g., diffusion coefficients) metrics consistently supported the formation of dense peptide assemblies across simulation study conditions. Simulation trajectories confirmed progressive self-assembly from dispersed peptides into compact condensates (Figure 1). These results demonstrate the ability of the computational framework to identify peptide sequences capable of robust LLPS-like self-assembly behaviour.

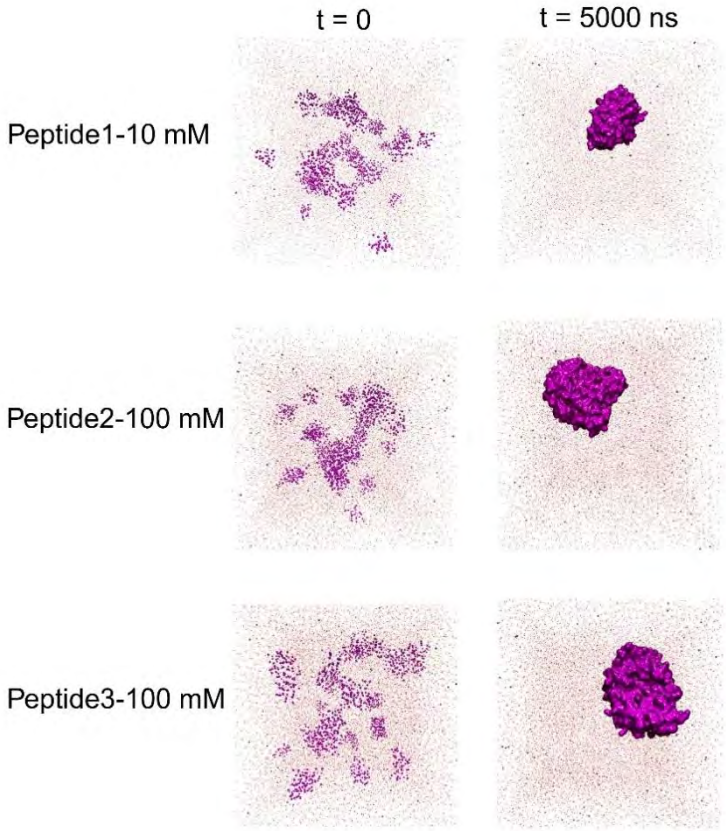

Figure 1. Time-resolved snapshots showing condensate formation by selected peptides.

Conclusion

We report a computational framework for discovering LLPS-prone peptides and evaluating their in silico phase behaviour through integrating generative modelling, feature-based screening, and molecular dynamics simulations.

S83 – O3

Gyroid printing using robocasting for bone regeneration: Influence of induced anisotropy on printability and mechanical properties

Biscaccianti V., Vézier J., Delplace V., Charbonnier B.
Nantes Université, Oniris, Univ Angers, INSERM, Regenerative Medicine and Skeleton, RMeS, Nantes, France

Introduction

Gyroid structures are increasingly used in bone applications, with growing evidence of their biological and mechanical performance. Although widespread with light-based additive manufacturing, their fabrication via robocasting is still very limited. Their 3D tortuous geometry is highly challenging for viscoelastic pastes extrusion printing, and process-specific strategies remain underexplored. This work presents a geometry-focused approach to improve gyroid printability using robocasting, notably through anisotropic modifications to reduce overhangs and gaps bridging while preserving the intended features of the macroporous network, such as the percentage of porosity. Our aim is to enable more biologically relevant robocasted architectures while preserving material freedom.

Materials and Methods

Anisotropic gyroid 3D surfaces were generated in a custom workflow. Toolpaths and GCode files were generated directly from surfaces in the modeling software. The influence of the unit cell size (UCS, i.e. 3D dimensions of one gyroid period) and anisotropy factor (i.e. ratio of UCS height over width and length) on the gyroid's printability were analyzed in silico through the overall percentage and average length of bridging trajectories. To confront simulation with actual printing, samples were printed with a control bone cement (alpha-tricalcium phosphate / Pluronic F127). The influence of selected parameters, especially anisotropic elongation, was evaluated on compressive and flexural properties.

Results

In order to assess the influence of geometrical modifications on theoretical printability, we first analyzed the overhangs (i.e. angulation from vertical axis) of the 3D surfaces. Standard gyroids presented highly overhanging regions, with an average angulation of 33°, independently of UCS. Increasing the anisotropy factor allowed to reduce overhangs from 33° to 18°, improving printability overall. When generating the toolpath, theoretical printability can be improved by minimizing bridging percentage and average length. In this context, reducing UCS from 4.0 mm to 1.0 mm decreased the average bridging length from 0.46 mm to 0.14 mm but reduced the calculated percentage of porosity from 85% to 40% and increased print duration by 290%. While this constitutes an improvement of printability, the consequences on porosity and print duration strongly limit this strategy. In contrast, increasing anisotropy from 1.0x to 2.0x (with 2 mm UCS) did not affect porosity and print duration while it improved printability by reducing the percentage (from 20.4% to 7.1%) and average length (from 0.28 mm to 0.17 mm) of bridging. As a proof of concept, gyroid samples with 2 mm UCS and anisotropy factor of 1.0x, 1.5x and 2.0x were successfully printed, with an average porosity measured between 45.9% and 47.3% across conditions. Mechanical assays revealed an increase in maximum compressive strength (from 3.2 ± 1.02 MPa to 4.6 ± 0.9 MPa) linked with anisotropic elongation, further supporting this strategy.

Conclusion

Overall, a comprehensive tool was developed for generating, analyzing and optimizing robocasting toolpaths of gyroid architectures, allowing their successful printing with bone cement. We provided evidences that anisotropic elongation improved printability and compressive properties of the structures while preserving their porosity, opening new possibilities for robocasted gyroid structures in bone regeneration.

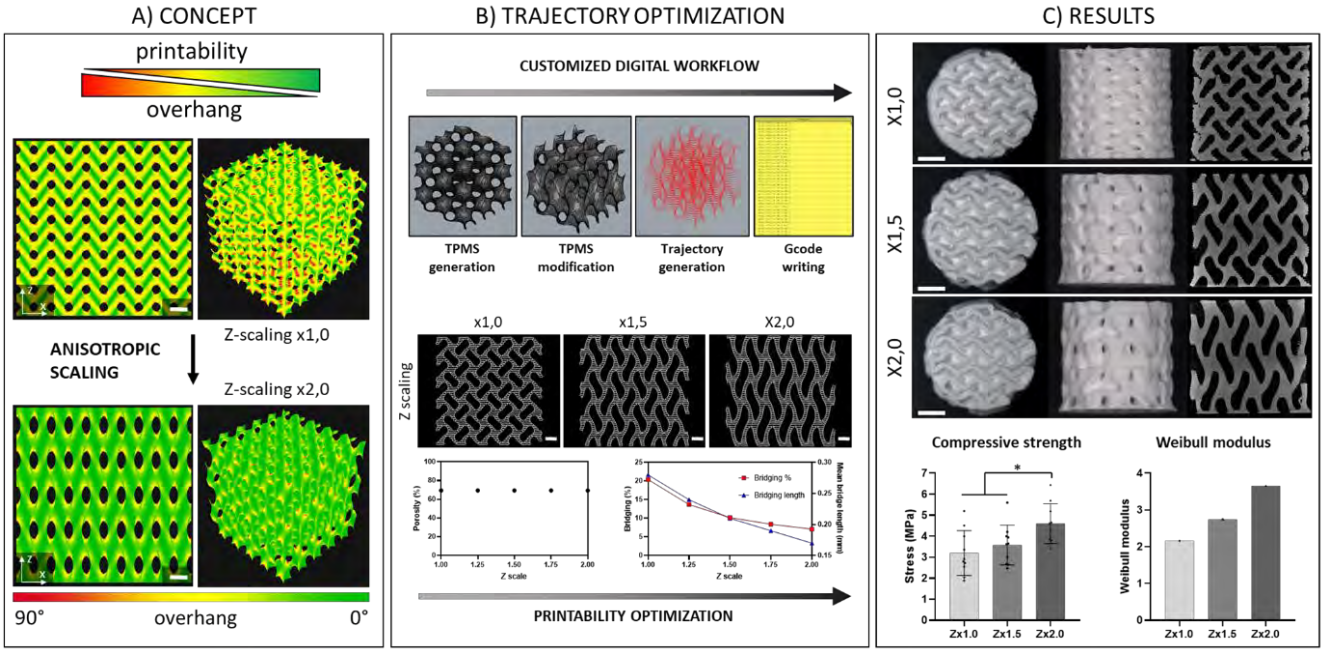

Figure 1 : Graphical Abstract. A) Preliminary concept: A common rule in extrusion printing is that reducing overhangs (angle between a surface and the vertical axis) improves printability. As shown here on the overhang mapping of gyroid structures, vertical anisotropic scaling reduces the overall inclination of the surface. B) Trajectory generation and optimization: in order to apply the previous concept, customized trajectories were generated in Rhino 3D Grasshopper, resulting as expected in fewer and shorter bridging trajectories (i.e. printing in mid-air over gaps) while maintaining porosity. C) Print results: samples were printed using robocasting. Measured porosity was consistently between 42% and 52% throughout samples of 1.0, 1.5 and 2.0 Z scaling. Print quality was visually improved in elongated samples. Compressive properties were enhanced in elongated samples (N=10). Scale bars = 1 mm.

S83 – O4

Multiphysics computational model of doxorubicin diffusion in scaffold-engineered fibrotic tumor microenvironments within an avian CAM model

Bocconi A., Conci C.[1], Cherubin L., Martinelli C., Mainieri G., Vigneri M., Jacchetti E., Raimondi M.T.
Department of Chemistry, Materials and Chemical Engineering "Giulio Natta", Politecnico di Milano, Milan, Italy

Introduction

Breast cancer progression is tightly coupled to collagen-driven matrix stiffening, which creates physical barriers to drug delivery and therapeutic efficacy. We developed a chick embryo chorioallantoic membrane (CAM) model implanted with three distinct two-photon-polymerized SZ2080 scaffolds, each with a different pore size, as a biomaterial-based experimental platform to recapitulate distinct degrees of fibrosis-associated transport barriers in cancer pathology[1]. Here, we present a predictive multiphysics computational model calibrated on this platform to determine how scaffold microarchitecture shapes fibrosis-associated transport barriers and modulates doxorubicin distribution.

Materials and Methods

COMSOL Multiphysics simulations coupled the Transport of Diluted Species and fluid dynamics modules to predict doxorubicin diffusion within two-photon-polymerized SZ2080 scaffolds with square pores of 10 × 10, 30 × 30, and 50 × 50 μm², used as engineered templates of fibrosis-associated transport barriers. For each scaffold, scaffold-specific CAM vascular geometric parameters were extracted from experimental data obtained by two-photon intravital microscopy, including vessel diameter, inter-vessel spacing, bifurcation density, vessel length, and surface density. Blood flow velocities were derived from in vivo tracking of red blood cells. Fibrotic capsule architecture, including collagen density and fiber orientation, was quantified by second-harmonic generation imaging. Doxorubicin transport coefficients were experimentally determined in CAM tissue.

Results

These experimental analyses defined scaffold-specific vascular, fibrotic, and transport parameters used as model geometrical inputs and boundary conditions. Simulations predicted doxorubicin concentration profiles over 120 minutes post-injection using a measured diffusion coefficient of 7×10^{-11} m²/s in CAM tissue. Pore size modulated predicted drug accumulation: 50 × 50 μm² scaffolds showed 1.5-fold higher accumulation than 30 × 30 μm² scaffolds, whereas 10 × 10 μm² scaffolds showed the lowest predicted accumulation. Spatial concentration gradients of doxorubicin within the fibrotic compartment revealed geometry-dependent diffusive resistance.

Conclusion

This integrated computational-experimental approach shows that scaffold geometry is associated with distinct vascularization and collagen organization patterns that determine doxorubicin distribution in this CAM tumor model. By integrating intravital microscopy, SHG imaging, and experimentally measured transport coefficients into a calibrated multiphysics model, this biomaterial-based disease platform provides a predictive in vivo-in silico framework linking scaffold microarchitecture to fibrosis-associated transport barriers and drug penetration.

Acknowledgements

ERC, project BEACONSANDEGG, G.A. 101053122.

References

[1]Conci C. et al. In vivo label-free tissue histology through a microstructured imaging window. *APL Bioengineering* 2024; 8; 016102.

S83 – O5

Biomimetic Hypoxic Microenvironment for Glioblastoma Using Organ-on-Chip

Sercia L.[1,2,3], Corallo G.[2,3], De Giorgi A.[2,3], Scalera F.[2,3], Portone A.[2,3], Franco P.[4], Stoppelli M.P.[4,5], Gigli G.[2,3,6], Polini A.[2,3], and Gervaso F.[2,3]

[1]Dipartimento di Ingegneria dell'Innovazione, University of Salento, Lecce, Italy; [2]Institute of Nanotechnology, National Research Council (CNR-NANOTEC), Lecce, Italy; [3]Tecnomed Puglia – Technopole for Precision Medicine (Biotech Lecce Hub), Lecce, Italy; [4]Institute of Genetics and Biophysics "A. Buzzati Traverso" (CNR-IGB), National Research Council, Naples, Italy; [5]UniCamillus-Saint Camillus International University of Health Sciences, Departmental Faculty of Medicine and Surgery, Rome, Italy; [6]Dipartimento di Medicina Sperimentale, University of Salento, Lecce, Italy.

Introduction

Glioblastoma (GBM) is the most aggressive primary brain tumor, characterized by rapid progression, therapeutic resistance, and poor prognosis. A hallmark of GBM is severe intratumoral hypoxia, which drives tumor growth, invasion, and resistance to therapy. Conventional two-dimensional cultures and many animal models fail to reproduce the spatial and temporal oxygen heterogeneity of the tumor microenvironment, limiting their predictive value. Organ-on-chip technologies enable the recreation of physiologically relevant microenvironments through controlled fluid dynamics and mass transport. The aim of this study was to develop a microfluidic GBM-on-Chip platform capable of generating controllable, pathophysiologically relevant hypoxic conditions in vitro.

Materials and Methods

A custom microfluidic device was fabricated using digital light processing (DLP) to support dynamic cell culture under controlled perfusion. GBM cells and astrocytes were cultured within a chitosan-based matrix inside the device. A computational model was developed to simulate fluid dynamics and oxygen transport coupled to cellular consumption, incorporating flow velocity, diffusion coefficients, and oxygen uptake rates. This model was used to predict spatiotemporal oxygen distributions and guide optimization of perfusion protocols and device geometry. Experimental measurements of the hypoxia marker HIF-1α were performed to validate model predictions.

Results

Two culture strategies were investigated to engineer controllable hypoxia: 4 days of static culture followed by 4 days of perfusion (4S+4D) and 8 days of continuous perfusion from seeding (8D), both at 100 µL/h. Simulations revealed markedly different oxygen dynamics between protocols. In the 4S+4D condition, the device remained open during the static phase, maintaining near-atmospheric oxygen (~21%), followed by a progressive decline after sealing and initiating perfusion, reaching 1.09% pO_2 at day 8. In contrast, the 8D protocol induced immediate oxygen depletion, resulting in a lower final pO_2 of 0.65% and prolonged hypoxic exposure. Thus, hypoxia severity could be tuned by protocol without modifying device architecture. HIF-1α immunostaining confirmed significantly higher hypoxia under continuous perfusion, supporting model predictions. These results demonstrate a reproducible system capable of generating controlled hypoxic microenvironments relevant to GBM pathology.

Conclusion

This microfluidic GBM-on-Chip platform reliably reproduces key hypoxia-driven features of the tumor microenvironment in vitro. Integration of computational modeling with experimental validation enabled rational optimization of operating conditions to achieve physiologically relevant oxygen levels. The ability to modulate hypoxia through perfusion protocols alone provides a powerful tool for studying tumor biology and may enhance the predictive value of preclinical models for drug testing and therapeutic development.

Acknowledgements

The authors acknowledge the Italian Ministry of Research (MUR) under the complementary actions to the NRRP "D34 Health" Grant (# PNC0000001). The study was supported also by the "Tecnopolo per la medicina di precisione" (TecnoMed Puglia) - Regione Puglia DGR n.2117 of 21/11/2018, CUP: B84I18000540002.

S83 – O7

Patient-specific screw and plate configuration design for femoral fractures: A digital twins and machine learning approach

Lorente O.L. [1], Gómez J. [2], Bono A.[3], Martín del Brío B.[3], Salceda J.[4], Albareda J.[2], Puértolas S.[1]
[1]Dept. Mechanical Engineering, University of Zaragoza, Spain; [2]Orthopedic Surgery and Traumatology, University Hospital Lozano Blesa, Zaragoza, Spain; [3]Dept. of Electronic Engineering and Communications, University of Zaragoza, Spain; [4]Radiology Department, University Hospital Lozano Blesa, Zaragoza, Spain

Introduction

Lateral plate fixation is widely used for complex and distal femoral fractures. Plate osteosynthesis is versatile and adaptable to different fracture configurations; however, variations in femoral geometry, bone quality, and fracture morphology complicate selection of the optimal plate and screw configuration [1,2]. Patient-specific computational models enable preoperative evaluation of fixation strategies and personalized surgical planning, although real-time application is often limited by the high computational cost of biomechanical simulations.

Materials and Methods

A patient-specific digital twin is generated from a reference femur model obtained from computed tomography (CT) data and parameterized to the patient's anthropometry [3] using measurements extracted from standard clinical X-ray images. Different fracture types are then generated on the digital twin, and the fixation plate is virtually positioned with various locking screw configurations, producing three-dimensional osteosynthesis models. These models are analyzed using the Finite Element Method (FEM), where material properties, physiological loads, contact interactions, and boundary conditions are defined.

The simulation results are processed to generate a structured dataset for distal femoral fractures (Wiss zones 3, 4, and 5). The resulting input–output vectors are used to train an artificial intelligence system based on Multilayer Perceptron (MLP) neural networks. Input variables include anthropometric and clinical parameters such as anatomical size and morphology, patient weight, bone quality, fracture location, and degree of comminution (Figure 1). The system outputs the plate length and screw configuration most appropriate for each case.

Results

The proposed framework enables rapid parametric generation of digital osteosynthesis models. FEM simulations provide stresses, strains, displacements, and interfragmentary micromotion to evaluate the biomechanical conditions at the fracture site, implant, and bone for each fixation system and to assess their compatibility with fracture healing.

The trained machine learning system reproduces FEM-derived biomechanical indicators with a deviation below 2%, enabling real-time evaluation of osteosynthesis options and recommending the most appropriate configuration for each case.

Conclusion

The integration of patient-specific digital twins, computational biomechanics, and machine learning provides an effective tool for personalized surgical planning in distal femoral fractures treated with lateral plates, enabling rapid prediction of mechanical behavior and optimization of the fixation strategy.

Acknowledgements

This work was supported by the Spanish Ministry of Science and Innovation and the European Union under Grant PID2022-140539OB-I00.

References

[1]Canton, G., Giraldi, G., Dussi, M., Ratti, C., & Murena, L. (2019). Osteoporotic distal femur fractures in the elderly: Peculiarities and treatment strategies. Acta Biomedica, 90, 25–32.
[2]Toro, G., Calabrò, G., Toro, A., De Sire, A., & Iolascon, G. (2015). Locking plate fixation of distal femoral fractures is a challenging technique: A retrospective review. Clinical Cases in Mineral and Bone Metabolism, 12, 55–58.
[3]Chen, X., He, K., Chen, Z., & Wang, L. (2016). A parametric approach to construct femur models and their fixation plates. Biotechnology and Biotechnological Equipment, 30(3), 529–537.

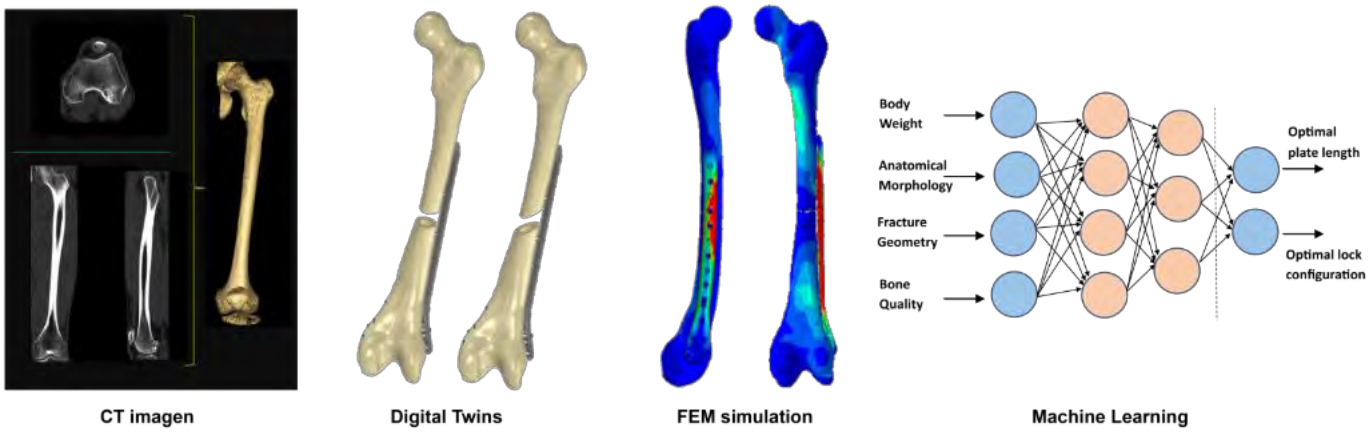

Figure 1. Stepwise definition of the process: Computational Tomography CT - Digital Twin - FEM simulation - IA

S84
Controlled and sustained release technologies

S84 – K1
Tailorable photo-curable polymeric inks for 3D-printed bioactive materials

Catalani L.H.
Institute of Chemistry, University of São Paulo – Brazil

Tissue engineering increasingly demands safe, biodegradable functional polymers able to sustain the complex architectures needed for tissue regeneration. Developing biomaterials tailored to the specific requirements of target tissues remains a persistent challenge despite rapid advances in bioengineering, given how intricate biological tissues are. Light-based biofabrication techniques — 2D micropatterning, photo-curable coatings and films, in situ photo-crosslinking of injectable systems, dynamic biomaterials, and stereolithography-based 3D printing — have driven the development of an increasingly diverse set of photosensitive materials. Few, however, combine bioactivity with ready processability. Our laboratory has pursued functional materials for 3D-printing inks along two lines: functionalizing printed surfaces with protein-based bioactives and producing inks from prodrug polymers. Panthenol (provitamin B5), a precursor of coenzyme A and a cofactor central to a myriad of biosynthetic pathways, gave rise to a series of 3D ink formulations. Globalide-derived polymers formed the second line of work: crosslinked films were post-functionalized with N-acetylcysteine via thiol-ene coupling of the native globalide double bonds, opening a route to decorate printed structures with cysteine-bearing peptides. Our aim was not to target a single tissue but to build versatile systems — photo-curable formulations adaptable across biomedical applications — expanding the toolbox available for medical use.

S84 – O1

Collagen microspheres for localized antiinflammatory delivery in chronic skin lesions

Gallo N.[1,2], Kodra C.[1,2], Nito A.[3], Salvatore S.[2], Quarta A.[3], Sannino A.[4]
[1]Dept. Engineering for Innovation, University of Salento, Lecce, Italy; [2]Typeone Biomaterials Srl, Calimera, Italy; Institute of Nanotechnology, CNR, Lecce, Italy; [4]Dept. Experimental Medicine, University of Salento, Lecce, Italy

Introduction

Chronic wounds represent a major clinical burden, characterized by persistent inflammation that stalls the natural healing process. While non-steroidal anti-inflammatory drugs (NSAIDs) are effective in modulating this inflammatory response, their systemic administration often leads to significant adverse effects. To overcome these limitations, localized and controlled delivery systems are required to maintain a therapeutic microenvironment at the wound site. Gelatin-based carriers are ideal candidates due to their biocompatibility, biodegradability, and ease of modification.

Aim. The objective of this study was to develop and optimize gelatin-based microspheres crosslinked with tannic acid for the sustained topical delivery of ketoprofen, aimed at locally treating chronic skin lesions.

Materials and Methods

The microspheres were synthesized using a single water-in-oil (W/O) emulsification process. Optimization was achieved by systematically varying homogenization speeds, crosslinking durations, and molar ratios of the components. The resulting system underwent comprehensive characterization, including morphological analysis, physicochemical, functional testing, and biological evaluation. Specifically, cyclooxygenase (COX) inhibition assays were used to verify drug activity, while bioadhesion and cytocompatibility were tested on wound models.

Results

The optimized formulation produced spherical microspheres with diameters ranging from 5 to 35 µm. These particles exhibited high crosslinking efficiency and a stable, controlled drug release profile over time. Functional assays confirmed that ketoprofen retained its pharmacological activity (COX inhibition) after encapsulation. Furthermore, the microspheres demonstrated excellent bioadhesive properties and were found to be cytocompatible.

Conclusion

Tannic acid-crosslinked gelatin microspheres serve as a biocompatible and effective platform for the localized delivery of ketoprofen. By providing controlled release and maintaining drug bioactivity, this system represents a promising strategy for managing inflammation in chronic wounds and enhancing tissue repair.

S84 – O2

Tunable Hyaluronic Acid-Based Injectable Hydrogels for Sustained and Bioactive Delivery of Sodium Channel Blockers in Neuropathic Pain

Jackson S[1], Sathi Devi L[1], Casadidio C[1] and Censi R[1]
[1]School of Pharmacy, University of Camerino, ChIP Chemistry Interdisciplinary Project Research Centre, Via Madonna Delle Carceri, 62032, Camerino, MC, Italy

Introduction

Chronic neuropathic pain remains a major clinical challenge, often requiring repeated dosing of sodium channel blockers such as lidocaine and crobenetine, with limited duration of action and systemic side effects. Injectable hydrogels based on hyaluronic acid (HA) offer a promising strategy for localized and sustained drug delivery.

Aim. In this study, thermo-responsive and disulfide-crosslinked HA-based hydrogels were developed to enable controlled release of lidocaine and crobenetine. We hypothesized that ionic interactions between the cationic drugs and negatively charged HA significantly influence drug release and can be tuned by varying the degree of substitution (DS) of thiolated HA.

Materials and Methods

Vinyl sulfonated ABA triblock copolymer (10% DS) and thiolated HA (DS 30%, 64%, 87%) were synthesized and characterized by ^{1}H-NMR. Two hydrogel systems were prepared: (i) Michael addition-crosslinked hydrogels formed by reacting vinyl sulfone-functionalized triblock copolymer with thiolated HA, and (ii) disulfide-crosslinked HA hydrogels formed via oxidation of thiol groups. Lidocaine hydrochloride and crobenetine were incorporated during gel preparation. Swelling and in vitro release studies were conducted in PBS (37°C), and drug quantification was performed by HPLC. Rheological characterization (oscillatory shear measurements) was performed to determine storage (G′) and loss (G″) moduli and assess network stiffness as a function of HA DS. Therapeutic efficacy was evaluated in SH-SY5Y neuronal cells using the CoronaGreen sodium influx assay. Sodium channel blocking activity of released drugs was compared with free drug and placebo controls. Statistical analysis was performed, and significance was defined relative to placebo.

Results

All the hydrogel systems formed stable injectable depots. Rheological analysis demonstrated that increasing HA DS significantly increased G′, indicating higher crosslink density and reduced network mesh size. This correlated with reduced swelling capacity at higher DS. Additionally, frequency sweep measurements confirmed the predominance of elastic behavior (G′>G″) across all formulations, indicating the formation of stable and mechanically robust networks suitable for injectable applications. The correlation between rheological strength and release kinetics further supports that modulation of HA degree of substitution enables precise control over hydrogel network architecture and, consequently, drug diffusion behavior. Drug release profiles showed that HA DS strongly influenced release kinetics. For lidocaine, release was slower in formulations with higher HA content, consistent with increased ionic interactions. For crobenetine, release was markedly prolonged in HA-rich formulations, and incomplete release was observed in disulfide-crosslinked systems, confirming strong drug–polymer affinity. Overall, tuning HA DS enabled modulation of release duration.

CoronaGreen assays demonstrated that both lidocaine and crobenetine significantly reduced sodium influx compared to placebo (*$p<0.05$). Importantly, drug released from hydrogels preserved sodium channel blocking efficacy comparable to free drug, indicating maintained bioactivity after encapsulation and release (Fig.1).

Conclusion

Injectable HA-based hydrogels enable tunable and sustained delivery of lidocaine and crobenetine through controlled crosslink density and ionic interactions. Rheological and release studies confirmed that HA DS governs network structure and drug release kinetics. Released drugs retained therapeutic efficacy in neuronal cells, highlighting the potential of these hydrogels as localized delivery platforms for neuropathic pain management.

Acknowledgements

This research was funded by European Union's Horizon 2020 Research and Innovation Programme under the Marie Skłodowska-Curie Actions (MSCA), Innovative Training Network (ITN) "PIANO", grant agreement No. 956477.

S84 – O3

Hydrogels mediated delivery of human serum albumin enhances penetration and uptake in Liver spheroid Model

Ahmed Sana*[1], Broering Dieter [1], Assiri Abdallah[1], Mir Tanveer Ahmad*[1]
[1]Transplant Research and Innovation, Organ Transplant center of Excellence (OTCoE), King Faisal Specialist Hospital and Research Center, Riyadh, Saudi Arabia

Introduction

Three-dimensional (3D) Spheroid models provide physiologically relevant platforms that better recapitulate cell-cell interactions and tissue environments compared with traditional two-dimensional cultures. However efficient delivery of biomacromolecules into spheroids structures remains challenging to diffuse barriers and dense cellular organization. Biomaterials based delivery systems, particularly hydrogels, offers promising strategies to improve controlled release and penetration of therapeutic proteins. In this study, we investigated a synthetic natural polymer hydrogel system composed of polyvinyl alcohol (PVA), polyvinyl pyrrolidone (PVP) and chitosan for enhanced delivery of human serum albumin into liver spheroid models.

Materials and Methods

Liver spheroids were generated using hepatocyte derived cells under controlled 3D culture conditions. A composite PVA/PVP-Chitosan hydrogels were fabricated to encapsulate HAS as a model therapeutic protein. The hydrogel formulation was optimized to achieved sustained protein release and improved diffusion into the spheroid structure. Spheroids were exposed to HSA loaded hydrogel systems and compared with conventional protein incubation control. Protein penetration and intracellular uptake were assessed using fluorescence microscopy and quantitative image analysis. Spheroid viability and morphology were evaluated using Live/Dead staining and histology analysis.

Results

The hydrogel-mediated delivery system significantly enhanced HSA penetration into liver spheroid compared with direct protein incubation. Fluorescence imaging demonstrated deeper and more uniform distribution of HSA throughout the spheroid structure, including the inner core regions. Quantitative image analysis indicated substantially increase intracellular protein uptake in hydrogel- treated spheroids. Importantly, the hydrogel system-maintained spheroid viability and structural integrity, confirming good cytocompatibility of the biomaterials formulation.

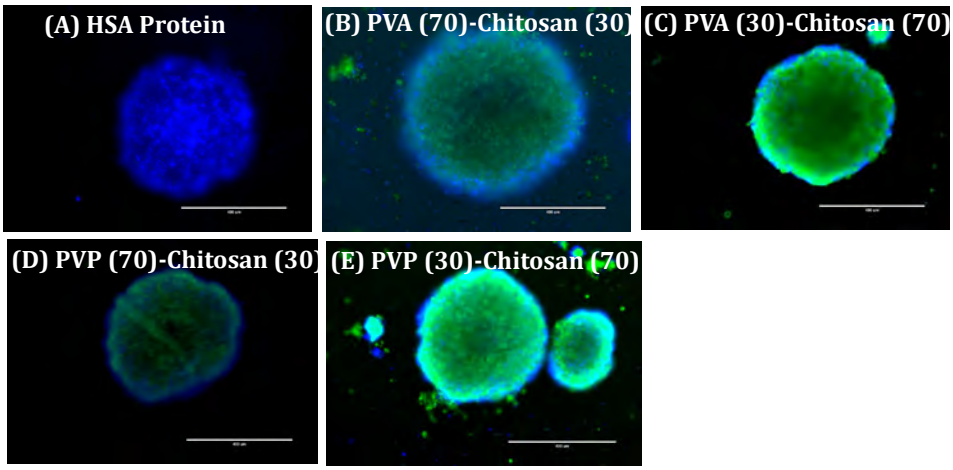

Figure 1: Fluorescence images showing internalization of human serum albumin (HSA) into spheroids mediated by PVA and PVP-chitosan composite hydrogels. (A) Spheroids treated with HSA alone. (B, C) Spheroids treated with HSA delivered via PVA(70)-chitosan(30) and PVA(30)-chitosan(70) hydrogels, respectively. (D, E) Spheroids treated with HSA delivered via PVP(70)-chitosan(30) and PVP(30)-chitosan(70) hydrogels, respectively. Enhanced green fluorescence within the spheroids indicates improved protein internalization compared to HSA alone. Scale bars as indicated.

Conclusion

The PVA/PVP- Chitosan hydrogel platform effectively improves biomacromolecules delivery into complex 3D liver spheroid models. This biomaterial-assisted strategy may provide a versatile approach for enhancing therapeutic protein delivery in tissue engineering, drug screening and regenerative medicine applications.

S84 – O4

Green-Synthesized MnO_2@INU-g-bPEI Nanoparticles for Layer-by-Layer siRNA Delivery and MRI-Guided Theranostics

Scoppetta G[1], Auriemma G[1], Funicello N[2], Del Gaudio P[1], Sardo C[1], Aquino RP[1]
[1]Dept. of Pharmacy (DIFARMA), University of Salerno, Fisciano (SA), Italy; [2]Dept. of Physics, University of Salerno, Fisciano (SA), Italy

Introduction

Organic/inorganic MnO_2-based nanocarriers for nucleic acid delivery and theranostics combine MRI visibility and tumor-responsive catalytic activity, but their clinical translation requires improved colloidal stability and controlled Mn^{2+} release.

Materials and Methods

Hybrid MnO_2/INU nanoparticles were synthesized through a mild aqueous redox reaction between $KMnO_4$ and inulin, which acted as reducing, stabilizing, and templating agent. The $KMnO_4$/INU molar ratio was optimized to control morphology and composition. Physicochemical characterization included UHR-SEM/STEM, DLS, ELS, FTIR, UV–Vis, EDX, and ICP-OES. MRI relaxometry was evaluated in agarose gel phantoms at pH 7.4. Nanoparticles were sequentially coated by layer-by-layer deposition of INU-bPEI2 and INU-bPEI4 polycations[1] to generate charged templates for siRNA stratification.

Results

An optimized $KMnO_4$/INU ratio of 5 (R5) yielded uniform spherical nanoparticles (≈ 150 nm) with narrow size distribution and negative ζ-potential (~−50 mV). Relaxometric studies at physiological pH showed negligible T_1 effects and a clear T_2 response, with $r_2 = 4.47\ s^{-1}\cdot mM^{-1}$, confirming suitability as T_2-weighted contrast agents.
Subsequent layer-by-layer functionalization with INU-bPEI2 and INU-bPEI4 successfully reversed surface charge and enabled layering of negatively charged siRNA. All the steps were optimized, yielding colloidally stable nanoparticles in water with preserved nucleic acid retention. Moreover, the coating didn't affect the typical peroxidase-like activity of MnO2 NPs.

Conclusion

Overall, the present results identify MnO_2@INU-g-bPEI-based multilayer nanoparticles as a promising theranostic nanoplatform integrating structural stability, siRNA stratification capability, preserved nanozyme-like activity, and T_2 MRI visibility. The combination of green synthesis, modular layer-by-layer functionalization, and imaging potential highlights the translational value of these hybrid nanosystems for the development of stimuli-responsive, trackable siRNA delivery systems in oncology.

Acknowledgement

The authors gratefully acknowledge Dr. Chiara Amante for SEM acquisitions and Prof. Tonino Caruso for elemental analysis. The authors also acknowledge the support of the PhD Program in RNA and Gene Therapy.

Reference

[1] Mazzacano et al., *Engineering a library of inulin based polyplexes and core-shell nanoparticles: Inside the targeted siRNA delivery to colorectal cancer cells*, Material Today Advances 2025, 28, 100645.

S84 – O5

Proteinosomes as a delivery system to enhance hydrogel scaffold bioactivity in tissue engineering applications

Nifosì M.[1,2], Maghin E.[1,3], Confalonieri M.[1], Piccoli M.[1], Valente S.[3], Braidotti N.[3], Gobbo P.[3,4], Pavan P.G.[1,2], Todros S.[2]

[1]Fondazione Istituto di Ricerca Pediatrica Città della Speranza, Padova, Italy; [2]Dept. of Industrial Engineering, University of Padova, Italy; [3]Department of Chemical and Pharmaceutical Sciences, University of Trieste, Italy; [4]National Interuniversity Consortium of Materials Science and Technology, Unit of Trieste, Italy

Introduction

Developing functional scaffolds for skeletal muscle tissue engineering remains a challenge. Although several natural and synthetic hydrogels have been investigated, many conventional formulations lack sustained bioactivity and do not provide the cues required for myoblast proliferation and myogenic differentiation. To address these limitations, we propose the integration of semipermeable protein–polymer microcapsules called *proteinosomes*, as cargo delivery systems within hydrogel scaffolds, allowing for the controlled release of bioactive molecules. Proteinosomes can be filled with different internal synthetic polymer networks and loaded with cytokines that can be delivered to tailor specific cellular responses.

Materials and Methods

Proteinosomes were produced using the Pickering emulsion technique by vortexing the aqueous phase, composed of two bio-orthogonal amphiphilic protein/polymer nanoconjugates, two structural scaffold polymers, and loaded molecules, such as dextran or insulin-like growth factor 1 (prt-IGF1), in 2-ethyl-1-hexanol. The microcapsules were transferred from oil to aqueous solution using an optimized centrifugation-based protocol. Proteinosomes' morphology was characterized through microscopy analyses. After loading proteinosomes with different AlexaFluor488-labeled dextran isoforms, the release kinetic was investigated by time-course fluorescence measurements. The bioactivity of prt-IGF1 was initially validated in 2D myoblast culture, where cell growth and proliferation were quantified. Finally, prt-IGF1 were integrated within 3D myoblast-laden hydrogel scaffolds to investigate their capacity to enhance cellular proliferation.

Results

Proteinosome populations were characterized by optical microscopy (Figure 1A). All tested formulations preserved their morphology throughout the transfer process. Time-course fluorescence measurements showed that low-molecular-weight dextran was released more rapidly than higher-molecular-weight species (Figure 1B), and increasing the concentration of the internal polymeric network progressively slowed the molecule release kinetics (Figure 1C). In vitro analyses evidenced that, in the presence of prt-IGF1, cell growth occurred at an intermediate rate between control samples in which the cytokine was added or not to the culture medium (Figure 2A, B). Consistently, in both soluble and encapsulated IGF1 conditions, the percentage of proliferating cells was significantly higher compared to cultures without the cytokine's addition (Figure 2C, D).

Conclusion

Proteinosomes represent a promising delivery system for the sustained and controlled release of bioactive molecules to enhance the biological properties of hydrogel scaffolds.

Acknowledgements

This work was supported by the National Recovery and Resilience Plan, Mission 4, Component 2, Investment 1.1, by the Italian Ministry of University and Research, funded by the European Union Next Generation EU – Project Title "Novel visible light-degradable hydrogels embedded with cell-laden proteinosomes for the 3D bioprinting of diaphragm-like muscle tissues (3D-L-INKED)" (CUP C53D23008360001).

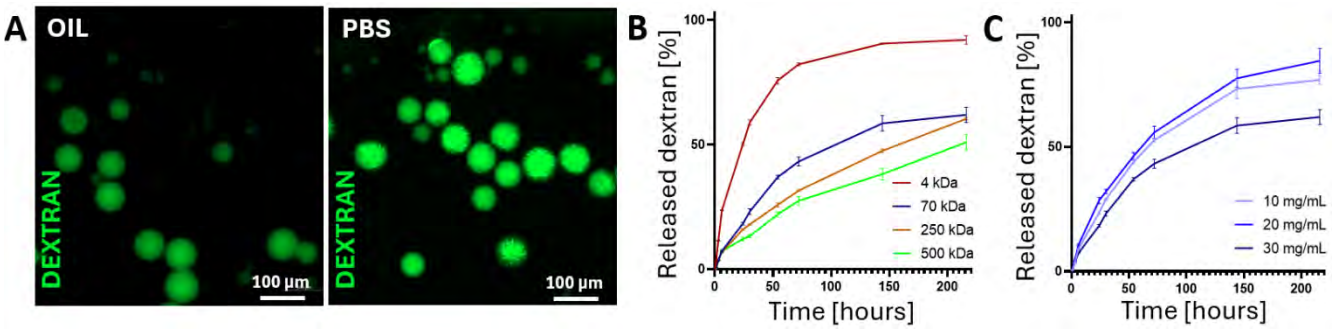

Figure 1: (A) Fluorescence images of proteinosomes loaded with dextran in oil and in PBS 1X. (B) Release kinetics of different dextran isoforms encapsulated within proteinosomes formulated with a polymeric proto-cytoskeleton concentration of 30 mg/mL. (C) Release kinetics of 70 kDa dextran isoform encapsulated within proteinosomes formulated with different synthetic polymeric network concentrations.

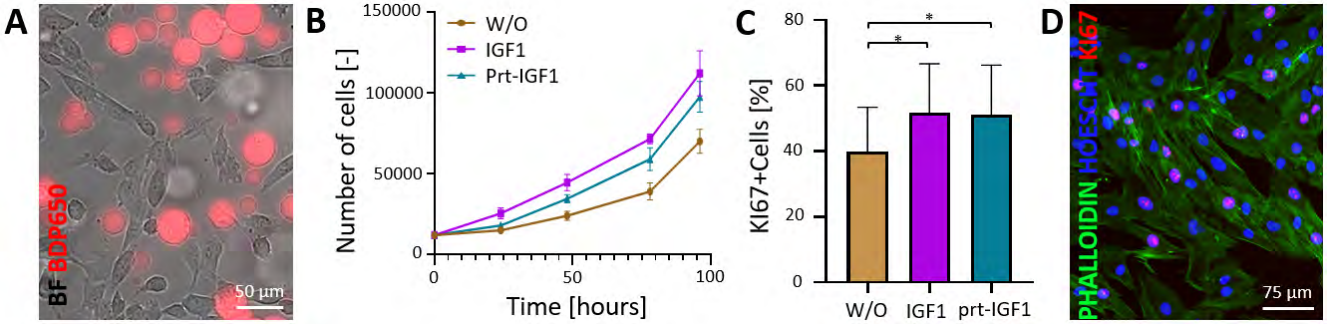

Figure 2: (A) Image of BDP650-tagged IGF1-loaded proteinosomes and myoblasts in 2D culture. (B) Four-day growth curve of cells cultured with medium alone, with culture medium supplemented with soluble IGF1, and with culture medium containing prt-IGF1. (C) Percentage of proliferating cells relative to the total cell population after 2 days of culture with medium alone, with culture medium supplemented with soluble IGF1, and with culture medium containing prt-IGF1. (D) Fluorescence image of cells after 2 days of culture with culture medium containing prt-IGF1. Hoechst was used for nuclear staining, phalloidin for cytoskeletal visualization, and Ki67 as a proliferation marker.

S84 – O6

Polyelectrolyte complexes as nanocarriers for growth factors

Kubies D.[1], García-Briones G.S.[1], Matiyani M.[1], Sivkova R.[1], Filipová M.[1], Podhorská N.[1], Filová E.[2], Kříž J.[3]
[1]Institute of Macromolecular Chemistry CAS, Prague, Czech Republic; [2]Institute of Physiology CAS, Prague, Czech Republic; [3]Dept. of Diabetes, Institute for Clinical and Experimental Medicine, Prague, Czech Republic

Introduction

Controlled delivery of growth factors (GFs), regulating cell migration, differentiation, and proliferation, is essential for successful regenerative and therapeutic strategies in biomedical applications. However, direct administration of GFs is often limited by their short half-life, rapid diffusion from the target site, and possible loss of bioactivity. Polyelectrolyte complexes (PECs), formed under mild aqueous conditions, represent a promising strategy for encapsulating GFs without disrupting protein structure while maintaining their biological activity. Nevertheless, the high toxicity commonly associated with fully charged polycations remains a major limitation for their biomedical applications.

Aim

This work aimed to develop PEC-based nanocarriers for GF delivery using polycations with either reduced charge density or time-dependent charge decrease, thereby lowering carrier cytotoxicity while maintaining efficient complexation with heparin, a polyanionic component with high bioaffinity for various GFs, and high protein-loading capacity.

Materials and Methods

Nanocarriers were prepared by controlled complexation of heparin with polycations under physiological conditions. Two types of PEC systems were investigated: i) NPs composed of pegylated quaternized dextran with a degree of substitution by ammonium groups ranging from 60% to 120% (Peg-QDex), and ii) ultrathin layer-by-layer (LbL) film coatings formed from charge-shifting poly(dimethylaminoethyl acrylate) containing from 50% to 100% charged monomer units (PDMAEA) and quaternized chitosan (QCH). Hep served as a reservoir of bioactive proteins (VEGF, FGF-2, TGF-β1, or CXCL12). NPs were characterized for particle size, zeta potential (ZP), and stability. LbL films were analyzed for film build-up by surface plasmon resonance and for thickness by spectroscopic ellipsometry. Protein release was quantified by ELISA, while carrier cytotoxicity and GF bioactivity were evaluated using several in vitro cellular assays.

Results

PEG-QDex block copolymers provided effective steric stabilization of polycation/Hep NPs (~200 nm), enabling NP preparation, storage, and redispersion without cryoprotectants. Optimized deposition conditions allowed the fabrication of LbL films composed of PDMAEA or QCH with reduced charge density while maintaining high protein loading. Pre-complexation of GFs with Hep before carrier fabrication significantly increased loading efficiency (up to ~85%) and maintained the bioactivity of the released GFs. Carrier cytotoxicity was primarily governed by polycation charge density and, in the case of NPs, also by ZP values. The polycations bearing about 70% of charged units represented a good compromise between stable complexation and acceptable cytocompatibility. A gradual charge loss in charge-shifting PDMAEA polycations also influenced carrier stability and modulated GF release. The released proteins retained their biological activity and effectively stimulated cellular responses (e.g., HUVECs, ASCs, and MSCs) at carrier concentrations below toxic levels.

Conclusion

PEC systems based on heparin and heparin-binding proteins represent a versatile platform for the preparation of nanocarriers with controlled GF delivery. Importantly, the use of charge-shifting polycations allows the fabrication of PEC nanocarriers with improved cytocompatibility and sustained bioactivity.

Acknowledgements

The research was supported by the Ministry of Health of the Czech Republic in cooperation with the Czech Health Research Council (project No. NW25-01-00221) and the Ministry of Education, Youth and Sport of the Czech Republic (the project “National Institute for Cancer Research, Programme EXCELES, ID Project No. LX22NPO5102).

S85
Enabling technologies for improved biomaterial research: From biomaterial design to regenerative medicine

S85 – K1
Extracellular matrix (ECM) as a powerful biomaterial for regenerative medicine applications

Boccafoschi F.[1], Di Francesco D.[2]
[1]Dept. of Health Sciences, University of Piemonte Orientale, 28100 Novara, Italy; [2]Tissuegraft srl, 28100 Novara, Italy

Introduction
The use of biological materials in tissue engineering and regenerative medicine is significantly increasing due to their excellent regenerative properties. In particular, materials derived from decellularized tissues (dECM) resulted of particular interest as their intrinsic bioactivity is preserved.1 In fact, regenerative medicine is based on three main pillars: i) the ability to maintain the cell phenotype allowing a functional regeneration; ii) the ability to sustain the neovascularization of the formed tissue; iii) guiding the immunomodulatory potential towards tissue regeneration.

Aim
To characterize the regenerative ability of the decellularized bovine pericardium-derived hydrogel and related matrix bound nanovesicles (MBV) with respect to their potential use as injectable materials for tissue engineering applications.

Materials and Methods
Hydrogel and MBV derived from decellularized bovine pericardium have been characterized in terms of chemical-physical properties. To verify the regenerative ability for different applications, cytocompatibility has been tested using varied cell lines (fibroblasts, endothelial cells, corneal epithelial cells, chondrocytes, osteoblasts, neuronal cells, etc.). The immunomodulatory potential has been evaluated through macrophage polarization marker expression using human monocytes from peripheral blood.

The angiogenic potential was assessed in vitro by immunofluorescence staining, eNOS expression, angiogenic cytokine release and tube formation assay, ex vivo with aortic ring assay, and in vivo with a hind limb ischemia (HLI) model. Wound healing potential was also validated in vivo.

Results
Hydrogel and MBV derived from decellularized pericardium showed excellent regenerative potential. Cytocompatibility of both materials was confirmed for all cells lines, with increase in cell viability, maintenance of cell morphology and significant enhancement of cell specific phenotype markers. The immunomodulatory potential indicated the ability of the hydrogel and MBV of guiding macrophage polarization toward the expression of a regenerative (M2) phenotype. The angiogenic potential has been extensively demonstrated in all the conditions (in vivo, ex vivo and in vivo). The histological observation of HLI test is represented in Figure 1, in which presence of neovascularization in hydrogel and MBV injection site 1 month after ischemic damage can be appreciated.

Prevention of necrosis and revascularization also showed ability of both hydrogel and MBV to induce in vivo healing and functional regeneration in ischemic conditions.

Conclusion
Biological matrices from decellularized tissues and related products represent an innovative and versatile material for regenerative medicine and tissue engineering applications.

Acknowledgements
Authors thanks Tissuegraft srl for the unconditioned financial support.

References
[1]Brown M, Li J, Moraes C, Tabrizian M, Li-Jessen NYK. Decellularized extracellular matrix: New promising and challenging biomaterials for regenerative medicine. *Biomaterials* 2022; 289; 121786.

S85 – O1

Standardized evaluation of compound–material interactions and antimicrobial activity against BSL-3 pathogens using the ClicKit-Well platform

Feldmann N.[1], Kurz S.[1], Hoffmann E.[2], Gaudin C.[2], Ndjogou D.[3], Baulard A.[2], Spohn J.[1]
[1]Fraunhofer-Institute for Ceramic Technologies and Systems (IKTS), Leipzig, Germany; [2]Institute Pasteur Lille, Center for Infection and Immunity (CIIL), Lille, France; [3]Institute Pasteur Lille, UMR1177 – Drugs and Molecules for Living Systems, Lille, France

Introduction

In drug development, reliable *in vitro* assays are essential for characterizing novel antimicrobial compounds and studying their activity in host-pathogen environments. However, many experimental systems used in infection biology rely on conventional cell culture plastics, where uncontrolled compound adsorption and variable material interactions can influence experimental outcomes and may lead to misinterpretation of compound efficacy. These effects are particularly critical in high-containment laboratories, where experimental reproducibility and standardized evaluation of antimicrobial activity are essential.

The patented Fraunhofer ClicKit-Well (1) is a versatile laboratory platform enabling standardized testing directly on different material surfaces in cell biology, while maintaining the geometry and characteristics of conventional multi-well plates. The system has previously been validated for the use under biosafety level 1 (BSL-1) and BSL-2 conditions and is currently being evaluated for its applicability in BSL-3 laboratories. Here, we investigate its use for cultures of *Mycobacterium tuberculosis* (*Mtb*), an important human BSL-3 pathogen, and for assessment of anti-*Mtb* compounds and their interactions with different plastic surfaces relevant in preclinical drug discovery.

Materials and Methods

The ClicKit-Well system consists of a modular assembly forming fluid-tight wells on flat material samples using an elastic receiving element and a mechanical closure. This configuration allows controlled exposure of cells, microorganisms or compounds to defined material surfaces while maintaining compatibility with standard incubator conditions.

Proof-of-concept studies using *Mtb* cultures exposed to known antimicrobial compounds were conducted over extended cultivation periods. Key parameters evaluated included reliable fluid-tight sealing, safe handling under BSL-3 containment conditions, robust cultivation performance and drug stability. In parallel, adsorption studies were performed to investigate interactions between selected compounds and four commonly used cell culture plastic materials. These experiments support the quantification of potential compound loss due to material adsorption and enable standardized comparison of compound-material interactions.

Results

Initial findings indicate that the system design allows reliable sealing and stable cultivation conditions comparable to standard bacterial culture formats including under BSL-3 conditions. Ongoing experiments further evaluate the test system performance and assess reproducibility of compound exposure across different plastic substrates. Compounds with known anti-*Mtb* activity and low affinity to the tested plastic materials showed high efficacy and significantly reduced the bacterial load, whereas other compounds displayed limited efficacy due to adsorption to specific plastic surfaces.

Conclusion

Our study showed that the ClicKit-Well platform enables standardized investigation of compound-material interactions in infection biology and provides a robust *in vitro* framework for antimicrobial drug evaluation with demonstrated applicability from BSL-1 to BSL-3 laboratory conditions.

References:

[1]Issleib C., et al. Arrangement For Performing In Vitro Biocompatibility Tests. *Patent* 2020; DE102018221415.

S85 – O2

A robotic wound care patient for surgical site infection research

Shlomo Y.[1], Orlov A.[1], Kreychman I.[1], Gefen A.[1,2,3]
[1]School of Biomedical Engineering, Tel Aviv University, Tel Aviv, Israel; [2]Dept. of Public Health and Primary Care, Ghent University, Ghent, Belgium; [3]Dept. of Mathematics, Statistics and Data Science Institute, Hasselt University, Hasselt, Belgium

Introduction

Surgical site infections (SSIs) remain common postoperative complications causing substantial morbidity and healthcare burden. Existing preclinical models lack physiological realism and quantitative evaluation under controlled conditions, particularly bacterial colonization and adaptation within the wound microenvironment, including pH variations. There is a need for a standardized, reproducible platform integrating biomechanical simulation with microbiological analysis to enable objective evaluation of bacterial responses under SSI-relevant conditions.

Materials and Methods

A life-sized robotic wound care patient (RWCP) was developed to simulate SSI under controlled conditions. The system incorporates soft tissue simulants, a laparotomy incision, controlled exudate delivery, respiration simulation, and temperature control (Figure 1). Simulated wound fluid (SWF) inoculated with *Lactobacillus delbrueckii* subsp. *bulgaricus*, a non-pathogenic bacterial simulant, was delivered at a clinically relevant flow rate.

Two SWF conditions (three independent replicates each) were tested: pH 5.8 (lower) and pH 6.8 (higher), spanning clinically reported acidic and more neutral wound environments. After 24 hours of flow, dressings applied over the incision were collected for analysis.

Scanning electron microscopy (SEM) images of wound dressings (≥20 per replicate) were processed through a validated computational workflow comprising supervised deep learning-based segmentation (Cellpose), batch morphometric quantification in FIJI, and custom Python-based topology analysis for automated chain detection.

Results

At pH 5.8 bacterial counts increased by 45% compared to pH 6.8 ($p = 0.02$), while area coverage did not differ significantly. Bacteria exhibited significant elongation, reflected by reduced circularity and roundness ($p = 0.004$) and increased aspect ratio ($p = 0.02$) (Figure 2). Topological analysis revealed nearly fourfold more chains ($p = 0.01$) and a 1.4-fold increase in bacteria per chain ($p = 0.02$), indicating enhanced aggregation.

Conclusion

To our knowledge, this is the first robotic wound care platform integrating biomechanical simulation with automated quantitative microbiological analysis. The RWCP provides a physiologically relevant and reproducible framework for controlled SSI modeling, enabling standardized preclinical benchmarking of biomaterials and wound care technologies, and supporting evidence-based SSI prevention strategies.

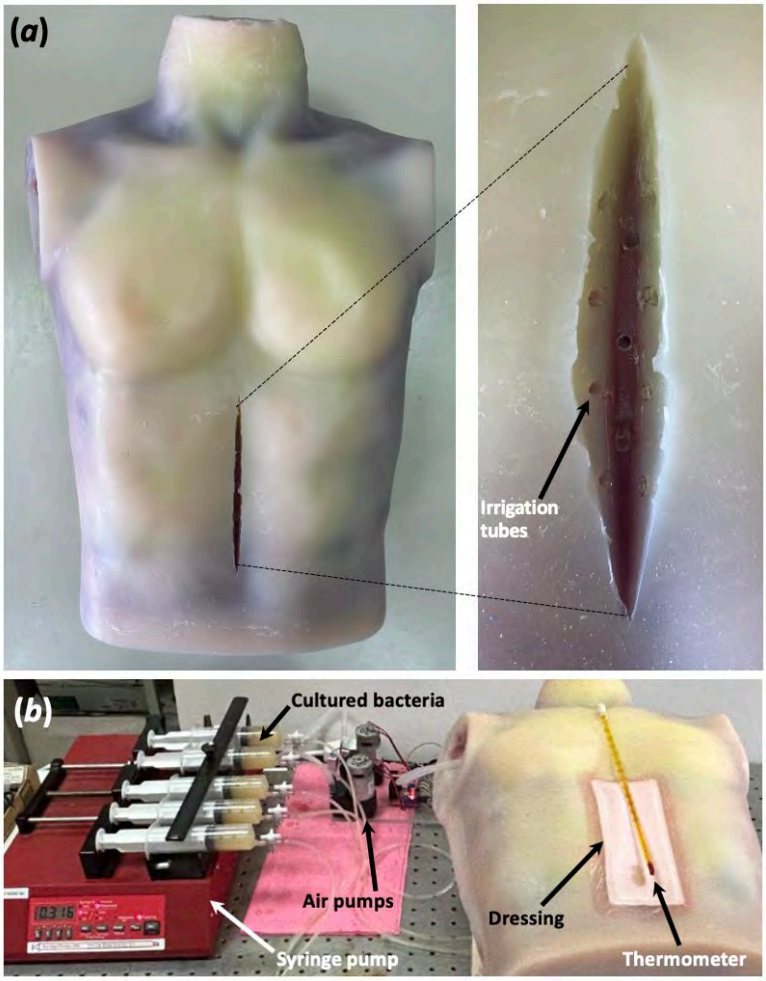

Figure 1. RWCP for SSI simulation. (a) RWCP with laparotomy incision. (b) Experimental setup.

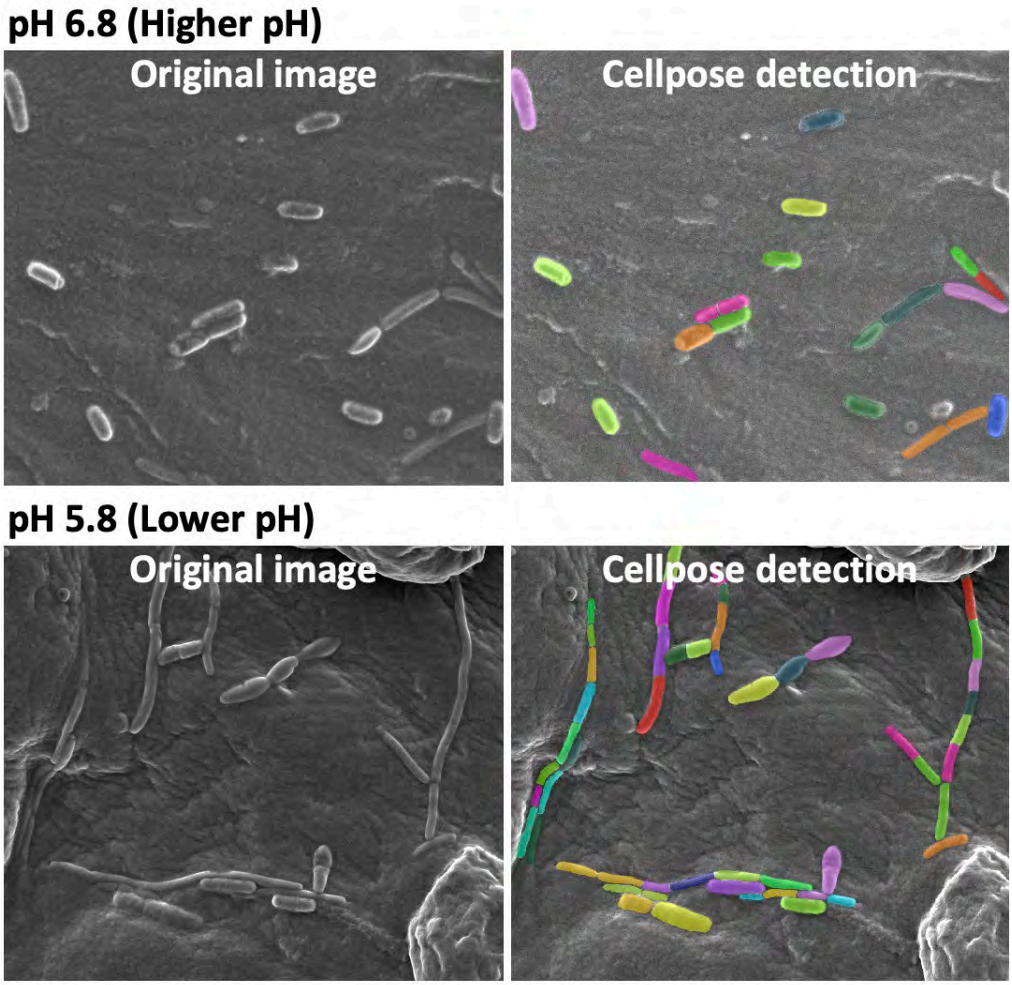

Figure 2. SEM images of bacteria on wound dressings and automated segmentation at higher and lower pH.

S85 – O3

Application of double-shot pyrolysis GC-MS for the chemical characterization of dental thermoplastics

Li Q.[1], Turkalj M.[1], Sun W.[1], Trullemans L.[2], Van Meerbeek B.[1], Vanoirbeek J.[3], Sels B.[2], Van Landuyt K.L.[1]
[1]Dept. of Oral Health Sciences, KU Leuven; [2]Dept. of Microbial and Molecular Systems, KU Leuven, Leuven, Belgium; [3]Dept. of Public Health and Primary Care, KU Leuven, Leuven, Belgium

Introduction

Thermoplastic materials are widely used in dentistry for clear aligners, retainers, and mouthguards. Because these devices are worn in the oral cavity for long periods, identifying their exact chemical composition is an essential step for biological risk assessment. Traditional extraction-based analytical methods often target predefined lists of chemicals and can miss certain trace compounds. Pyrolysis-gas chromatography-mass spectrometry (Py-GC/MS) combined with evolved gas analysis-mass spectrometry (EGA-MS) is an established tool for analyzing complex plastics, but it is rarely utilized for dental materials.

Aim

To introduce Py-GC/MS and EGA-MS to the dental field to directly map polymer networks and identify organic additives in commercial thermoplastic sheets.

Materials and Methods

Nine kinds of commercial dental thermoplastic sheets were analyzed. Solid samples (50-300 µg) were prepared and tested directly without solvent extraction. First, EGA-MS (PY-3030D, Frontier Laboratories, Fukushima, Japan; ISQ 7000, Thermo Fisher Scientific, Waltham, MA, USA) was used to record the thermal degradation profile of each material from 75°C to 800°C. Based on these thermal profiles, double-shot Py-GC/MS (TRACE 1610 GC, Thermo Fisher Scientific, Waltham, MA, USA) was performed. This involved a thermal desorption (TD) stage to release and identify low-molecular-weight additives, followed by a flash pyrolysis (FP) stage at higher temperatures to fragment and identify the main polymer backbone. The resulting mass spectra were compared with F-Search libraries for chemical identification.

Results

The combined approach successfully determined the composition of all materials. EGA-MS and FP identified primary polymer groups: polyolefins, styrenic copolymers, ethylene-vinyl acetate, and cyclohexanedimethanol (CHDM) copolyesters. The technique was particularly effective in revealing that clear aligners have a complex multilayer structure, consisting of a polyurethane core and a CHDM-copolyester outer shell. During the TD stage, the method detected various small molecules. These included processing residues like tetrahydrofuran, aldehyde-based clarifiers, and specific hindered phenolic antioxidants like 2,4-di-tert-butylphenol.

Conclusion

Double-shot Py-GC/MS combined with EGA-MS is a highly effective, direct analytical method for the chemical characterization of dental thermoplastics. It successfully screens both the main polymer backbones, including hidden multilayer structures, and trace organic additives in a single workflow. Introducing this robust technique to dental biomaterials research provides a more complete understanding of their composition, which facilitates accurate subsequent quantification and biocompatibility evaluations.

Acknowledgements

This research was supported by the KU Leuven (C24E/19/078). We gratefully acknowledge the dental manufacturers for providing the thermoplastic materials, and we also thank Interscience and Kris Steenwegen for their generous support and contributions to this work. Qianpeng Li was supported by CSC grant No. 202507650005.

S85 – O4

A magnetically navigated microfluidic platform for controlled in vitro assessment of microrobot performance

Garcia-Lizarribar A.[1], Vera C.[1], Ajeeb R.[2], Medina-Sanchez M.[2 3,4], Ibarlucea B.[1]
[1]TECNALIA, Basque Research and Technology Alliance (BRTA). San Sebastián, Spain; [2]CIC nanoGUNE. San Sebastián, Spain; [3]IKERBASQUE. Basque Foundation for Science. Bilbao, Spain; [4]Chair of Micro- and Nano Biosystems, Center for Molecular Bioengineering (B CUBE), Dresden University of Technology. Dresden, Germany

Introduction

Magnetically actuated microrobots hold significant promise for targeted therapeutic delivery, especially in applications such as guided immunotherapies. Despite their potential, the in vitro evaluation of magnetically driven systems remains limited by the constraints of current microfluidic platforms. Existing devices often rely on bulky electromagnetic assemblies, complex multi-coil configurations, or external robotic actuation stages, reducing flexibility and complicating routine use. Many microfluidic chips are still fabricated from PDMS, a material that requires labour-intensive and time-consuming soft-lithography processes, hindering rapid and reproducible production of large batches. Although stereolithography (SLA)-based additive manufacturing offers a faster and more direct route for creating microfluidic structures, most commercially available SLA resins exhibit poor biocompatibility or leach cytotoxic components, limiting their suitability for cell-based assays. Together, these limitations impede accurate physiological modelling and restrict the systematic evaluation of magnetic-based therapeutic strategies.

Here, we use additive manufacturing methods to develop an accessible, biocompatible, and optically compatible microfluidic platform incorporating a simple and compact magnetic navigation system, enabling efficient and reliable in vitro testing of magnetically driven microrobots for advanced therapeutic applications such as CAR-T-based cancer treatments. The magnetic system will enable precise control over the exact localization of the microrobots and their directed motion along the microfluidic platform, facilitating the study of therapeutic release on in vitro configurations.

Materials and Methods

To address these limitations, we designed and produced a microfluidic platform using stereolithography (SLA) and integrated it with a compact, manually operated magnetic navigation system. This actuation module is small, user-friendly, and does not require complex electromagnetic setups or external robotic devices. It allows intuitive operator-controlled positioning and steering of magnetically responsive micro- and nano-robots directly within the microchannels. The platform supports both continuous-flow operation, suitable for mimicking dynamic physiological environments, and batch mode, ideal for localized manipulation or endpoint analysis. The microfluidic chips were manufactured and post-processed to obtain highly biocompatible, optically transparent materials, making them compatible with cell culture and enabling continuous, high-resolution monitoring using confocal microscopy.

Results

The platform was employed to evaluate the efficacy of magnetically driven microrobots designed for guided cancer therapy based on CAR-T cell mechanisms. Using the integrated magnetic navigation system, microrobots were accurately steered toward target cell populations cultured within the microfluidic chambers (Figure 1). The system enabled quantification of navigation with precision, microrobot–cell interactions and localised therapeutic outcomes under controlled microenvironmental conditions.

Figure 1. A) SLA-based microfluidic prototype with integrated magnetic navigation. B) Cells stained with calcein and ethidium homodimer cultured on the device showing 100% viability.

Conclusion

We present a versatile, biocompatible, and user-friendly microfluidic–magnetic platform that overcomes key limitations of current microfluidic systems for magnetic microrobotics research. Its compact manual navigation system eliminates the need for complex magnetic infrastructures, while SLA-enabled fabrication ensures rapid, reproducible chip production. Compatibility with confocal microscopy and cell culture further enhances its value for biological studies. Overall, this platform expands experimental capabilities for evaluating magnetic microrobots and supports the development of advanced cell-based therapies such as CAR-T-guided cancer treatments.

Acknowledgements

This research was funded by the ELKARTEK program (Basque Government), project nG25, grant KK-2025/00001.

S85 – O5
Imaging cell-matrix interactions: From synthetic fibrous hydrogels to molecular tension sensing

Roch S.
KU Leuven, Belgium

Introduction
Cells actively deform and reorganize their surrounding matrix. Understanding how synthetic biomaterials respond to these forces is important for designing systems that better mimic native extracellular environments. Fibrous hydrogels based on polyisocyanides (PIC) reproduce many mechanical features of natural ECM, making them a useful platform to examine how cells generate long range deformations and matrix remodeling. To better interpret these behaviours, we also explored how to measure the molecular forces that cells transmit through adhesion proteins.

Aim
Our goals were to (i) characterise how cells remodel synthetic PIC hydrogels, (ii) relate these matrix scale deformations to forces generated at focal adhesions, and (iii) evaluate FRET based tension sensor designs to identify reliable probes for future studies.

Materials and Methods
PIC hydrogels were used as a synthetic ECM model due to their fibrous structure and strain stiffening behaviour. Cell induced deformation and remodeling were quantified using 3D displacement microscopy to capture densification, stiffening and long range force propagation in a bead free manner.1
To examine adhesion level forces, we expressed FRET based vinculin tension sensors in cells on polyacrylamide substrates and measured vinculin tension together with traction forces using traction force microscopy (TFM).2
To address limitations observed in these experiments, we performed a systematic comparison of multiple FRET sensor variants on glass under identical FLIM FRET conditions, assessing fluorophore pairs, mechanical modules and circular permutations.3

Results
Cells in PIC hydrogels generated clear fiber densification and matrix stiffening, together with long range deformations extending up to ~100 µm. Both reversible responses and slower plastic remodeling were observed, showing that PIC hydrogels capture essential emergent behaviours of fibrous ECM materials.
TFM–FRET measurements revealed that vinculin tension increased with substrate stiffness and aligned with traction hotspots at focal adhesions, supporting a link between adhesion level forces and matrix engagement.
The systematic evaluation of FRET tension sensors showed that green–red fluorophore pairs (e.g., Clover mScarletI) and binary response mechanical modules provided the most robust and interpretable force readouts, while circular permutations influenced their sensitivity.

Conclusion
PIC hydrogels offer a robust synthetic platform to study how cells deform fibrous matrices and how matrix mechanics influence long range mechanical responses. The combination of TFM with molecular tension sensors provides complementary insight into adhesion level forces, while the systematic evaluation of sensor architectures offers practical guidelines for selecting reliable probes for future biomaterial based mechanotransduction studies.

S85 – O6

PEG-nitrosothiols as kinetic regulators of thiol-maleimide crosslinking for homogeneous and compositionally diverse hydrogels

Serna J.A.[1], Iwohn M.J.[1], Seifermann M.[1], Dopp F.[2], Muhle-Goll C.[2], Levkin P.A.[1,3]
[1]Institute of Biological and Chemical Systems-Functional Molecular Systems (IBCS-FMS), Karlsruhe Institute of Technology (KIT); [2]Institute for Biological Interfaces 4 (IBG-4), Karlsruhe Institute of Technology (KIT); [3]Institute of Organic Chemistry (IOC), Karlsruhe Institute of Technology (KIT), Karlsruhe, Germany

Introduction

The thiol-maleimide Michael-type addition chemistry is acknowledged as a long-standing approach for bioconjugation, hydrogel crosslinking and functionalization of advanced materials. In hydrogel design for tissue engineering, it is praised for its very high efficiency and selectivity as well as its compatibility with physiological conditions. However, its reaction kinetics are often too fast for practical use: when thiol-modified crosslinkers and maleimide-functionalized biomaterials are combined, gelation outpaces mixing, yielding heterogeneous networks. This limitation has been recognized for over a decade, yet existing solutions (acidic pH, pKa-tuned peptide linkers, or photoactivatable protecting groups) each introduce constraints that limit compositional freedom or biocompatibility.

Aim

In this work, we address this challenge by introducing PEG-nitrosothiols (PEGSNO) as a new class of dormant crosslinkers that decouple precursor mixing from network formation. By utilizing mild, cell-compatible nucleophiles, such as sodium ascorbate (SA) or sodium thiosulfate (STS), we trigger the on-demand regeneration of free thiols via transnitrosation. This approach enables the controlled formation of homogeneous hydrogels across diverse biomaterial compositions.

Materials and Methods

PEGSNO was synthesized by S-nitrosylation of thiol-terminated PEG and characterized by UV-Vis spectroscopy, ^{1}H-NMR, ^{15}N-NMR, and Ellman's assay. The decomposition of PEGSNO in the presence of two nucleophiles (SA or STS) was characterized by UV-Vis spectroscopy and thiol regeneration was confirmed by Ellman's assay. The compositional crosslinking window, defined as the range of PEG-RSNO and nucleophile concentrations yielding stable, homogeneous gels, was mapped in a high-throughput fashion using a droplet microarray (DMA) platform, in which hydrogel precursors were dispensed in the nanoliter range across 80 or 320 independent spots. Network homogeneity was assessed by fluorescence microscopy, and bulk mechanical properties and gelation kinetics were characterized by oscillatory rheology. NO release was quantified by Griess assay, and cytocompatibility of the system was studied in fibroblasts and epithelial cells using metabolic activity assays and Live/Dead staining.

Results

PEGSNO exhibited stable S-nitroso functionalization and released free thiol upon nucleophile addition in a concentration-dependent manner. The delayed thiol availability expanded the crosslinking window sufficiently to allow complete mixing prior to network formation, yielding homogeneous hydrogels across all tested maleimide-functionalized biomaterials — PEG, fish gelatin and hyaluronic acid. High-throughput screening on the DMA resolved the crosslinking window across nucleophile type and concentration in a single experiment. Rheological properties of PEGSNO hydrogels were comparable to PEG-thiol controls, confirming that kinetic regulation does not compromise final network mechanics. NO co-release was detected at concentrations that impaired cell viability in some formulations, identifying it as the primary remaining challenge; ongoing work investigates NO scavenging strategies to decouple structural control from oxidative stress.

Conclusion

PEG nitrosothiols offer a chemically straightforward and compositionally flexible route to solving a long-standing structural problem in maleimide-thiol hydrogel engineering. Transnitrosation-triggered thiol release gives access to a crosslinking window that conventional PEG-thiol chemistry lacks, and miniaturized high-throughput screening provides the analytical resolution to map and exploit it efficiently. Together, these tools establish a new framework for the rational design of homogeneous biomaterial hydrogels.

Acknowledgements
We thankfully acknowledge funding from the German Academic Exchange Service (Deutsche Akademische Austauschdienst, DAAD) and Germany's Excellence Strategy 2082/-1-390761711 (Excellence Cluster “3DMM2O”).

S87
Hydrogels for tissue engineering and regeneration

S87 – K1
Bioinspired materials for intervertebral disc regeneration: Design principles and translational perspectives

Le Visage C.
Regenerative Medicine and Skeleton, RMeS, Nantes, France

Intervertebral disc degeneration is a leading cause of chronic low back pain, imposing significant socioeconomic and healthcare burdens worldwide. Conventional clinical interventions, such as spinal fusion and artificial disc replacement, are often associated with long-term complications and fail to replicate the complex structural, mechanical, and biological functions of the native disc. Recent advances in biomaterials science offer a promising avenue for regenerative therapies that aim to restore disc function through bioinspired design principles.

This talk will explore the development of next-generation biomaterials, emphasizing the hierarchical architecture and multifunctionality of the native disc, the integration of tissue-specific mechanical properties, and cellular microenvironments conducive to disc regeneration. We will examine current strategies in scaffold design, including composite hydrogels, electrospun fibrous networks, and 3D-bioprinted constructs. Additionally, the talk will highlight incorporating bioactive components, such as GDF-5 or TGF-beta growth factors, extracellular vesicles, and adult stem cells, into scaffold designs to enhance regenerative outcomes and restore disc functionality. Through an interdisciplinary lens, this talk will highlight the translational potential of bioinspired materials and the challenges that remain in their clinical application.

S87 – O1

Tuning alginate matrix viscoelasticity reveals mechanoregulation of microglial inflammation

Morais M.R.G.[1,2,3], Coelho R.[1,2,4], Faria M.[1,2,4], Carvalho E.D.[1,2], Athanasopoulou G.[1,2,3], Pêgo A.P.[1,2,3]
[1]Institute for Research and Innovation in Health (i3S), University of Porto; [2]Instituto Nacional de Engenharia Biomédica (INEB), University of Porto; [3]School of Medicine and Biomedical Sciences (ICBAS), University of Porto; [4]Instituto Superior de Engenharia do Porto (ISEP), Porto, Portugal

Introduction

Neurodegenerative disorders impose a growing socioeconomic burden as life expectancy increases. Many of these conditions are associated with alterations in tissue mechanical properties. It is increasingly accepted that microglia, the primary immune cells of the CNS, are mechanosensitive, and that their function may be closely tied to mechanotransduction pathways. However, the impact of matrix rheological properties on microglial responses remains largely unknown.

Aim

In this study, we are developing a 3D tissue-engineered model to investigate how microglial activation is shaped by the mechanical properties of their surrounding extracellular environment.

Materials and Methods

Alginate-based matrices with distinct viscoelastic profiles were produced by varying alginate concentration (1 or 2% w/v) and oxidation degree (60 or 30%). All formulations included RGD adhesion motifs and the MMP-sensitive peptide PVGLIG to better mimic brain ECM. The hydrogels, mechanical properties were characterized by bulk rheology, and diffusion coefficients of fluorescent dextran (20 and 70 kDa) were quantified by FRAP. Primary rat microglia were encapsulated within these 3D environments and stimulated with LPS. Metabolic activity, nitrite release, and gene expression levels were subsequently assessed.

Results

Modulating alginate concentration and degree of oxidation yielded matrices with distinct viscoelastic behaviors, all within the physiological stiffness range of the brain parenchyma (0.1–1 kPa). Diffusion properties were comparable across formulations. Microglial metabolic activity remained stable regardless of matrix composition and LPS treatment. Upon LPS stimulation, microglia cultured within the softer 1% alginate hydrogels showed significantly increased nitrite production and elevated expression of *NOS2*, *IL-6*, and *CD14*, indicating a heightened pro-inflammatory phenotype. Conversely, 2% alginate matrices led to reduced expression of *TLR4* and *Siglec5*, suggesting dampened responsiveness to inflammatory cues.

Conclusion

We successfully tuned matrix viscoelasticity while maintaining a consistent biochemical environment. Microglia remained viable and responsive within these 3D systems. Our findings demonstrate that mechanical properties of the extracellular matrix modulate microglial responses to inflammatory stimulation. This work contributes to understanding how brain tissue mechanics shape neuroinflammatory processes and may support the identification of new therapeutic targets for neurodegenerative disease management.

Acknowledgements

Air Force Office of Scientific Research, USA (Awards FA9550-20-1-0417 and FA9550-23-1-0599). Portuguese Foundation for Science and Technology (SFRH/BD/140363/2018; 2022.13353.BD) and ASTROTECH 956325-ASTROTECH-H2020-MSCA-ITN-2020.

S87 – O2

Post-Ischemic remodeling: Elastin-like recombinamer hydrogel in ST-elevated myocardial infarction (STEMI)

Malli S.E.[1], Costa M.D.[1], Zigmantaitė V.[2], Valantinas R.[2], Karčiauskas D.[2,], Krivickienė A.[2], Cabello J.C.R.[3], Dockery P.[4], Pandit A.[1]
[1]CÚRAM, Research Ireland Centre for Medical Devices, University of Galway; [2]Lithuanian University of Health Sciences; [3]Technical Proteins Nanobiotechnology, Universidad de Valladolid; [4]Anatomy, School of Medicine, University of Galway

Introduction

Myocardial infarction (MI) arises when there is an abrupt decrease or cessation of blood supply to the cardiac muscle, which results in damage to the tissue. Despite advances in treatment, MI remains a major cause of mortality worldwide. Current therapies primarily focus on restoring blood flow but often do not fully address long-term cardiac tissue damage and remodelling. Recently, biomaterial-based strategies have emerged as promising tools for cardiac repair. The objective of this study was to evaluate the potential of an elastin-like recombinamer hydrogel (ELR) to reduce infarct size and collagen deposition while promoting cardiac tissue repair following transmural MI (STEMI) in an ovine model.

Materials and Methods

ELR-hydrogel was synthesized via catalyst-free click chemistry and subsequently characterized using matrix-assisted laser desorption/ionization–time-of-flight, sodium dodecyl sulfate polyacrylamide gel electrophoresis, and fourier transform infrared spectroscopy. The mechanical and thermal characteristics were examined using rheological, thermogravimetric, and differential scanning calorimetry analyses. Swelling studies were conducted to determine the stability of the hydrogel. Cellular compatibility was assessed by evaluating the metabolic activity and viability of cardiac fibroblast cells. In a preclinical setting, a STEMI ovine model was developed, and the hydrogel was injected into the infarcted myocardium. Subsequent evaluations were carried out using a randomized ovine model (n=8/timepoint), which comprised both male and female subjects. Subjects were systematically categorized into four distinct experimental cohorts: Sham, MI-induced, PBS-treated, and ELR-hydrogel treated. Evaluations were conducted at multiple timepoints (Day 0, 7, 28, and 90), with n = 8 per timepoint/group. Cardiac function was assessed using echocardiography and electrocardiogram, complemented by blood biomarkers such as troponin-I. A comprehensive suite of analyses, including histology, immunohistochemistry, scanning and transmission electron microscopy, and omics studies, was employed to determine the hydrogel's efficacy and safety in promoting cardiac functional recovery, encouraging positive ventricular remodeling, and reducing fibrosis and infarct size.

Results

In this study, an ELR-hydrogel formulation was optimized, and its physicochemical properties were meticulously characterized. The results demonstrated an increased storage modulus with a transition temperature 12 °C and thermal degradation of the hydrogel around 270 °C (Fig1.a-c). FTIR spectroscopy revealed the presence of a secondary structure of the ELR within the spectral range of 1500–1700 cm^{-1} (Fig1.d). In vitro assessments showed an increased metabolic activity and viability of cardiac fibroblasts cells treated with hydrogel compared with control group only cells (Fig1.e-f). In a STEMI ovine model, extensive myocardial damage and structural disruption was noticed in the D28MI group compared to the control (Sham) (Fig2.a), significant ST-segment elevation confirming acute ischemic injury (Fig2.b), increased troponin levels were markedly in the MI group providing biochemical evidence of myocardial injury (Fig2.c), and a decrease in left ventricular ejection fraction from D0 to D28 reflecting impaired cardiac functionality (Fig2.d). Finally, the hydrogel was administered to MI animals, and cardiac functionality was modulated.

Acknowledgements

Hardiman Scholarship 2022, EU- Grant Number 101091766, Research Ireland- Grant Number 13/RC/2073_P2

Reference

[1]Contessotto, P., Orbanić, D., Da Costa, M., Jin, C., Owens, P., Chantepie, S., ... & Pandit, A. (2021). Elastin-like recombinamers-based hydrogel modulates post-ischemic remodeling in a non-transmural myocardial infarction in sheep. *Science Translational Medicine*, *13*(581), eaaz5380.

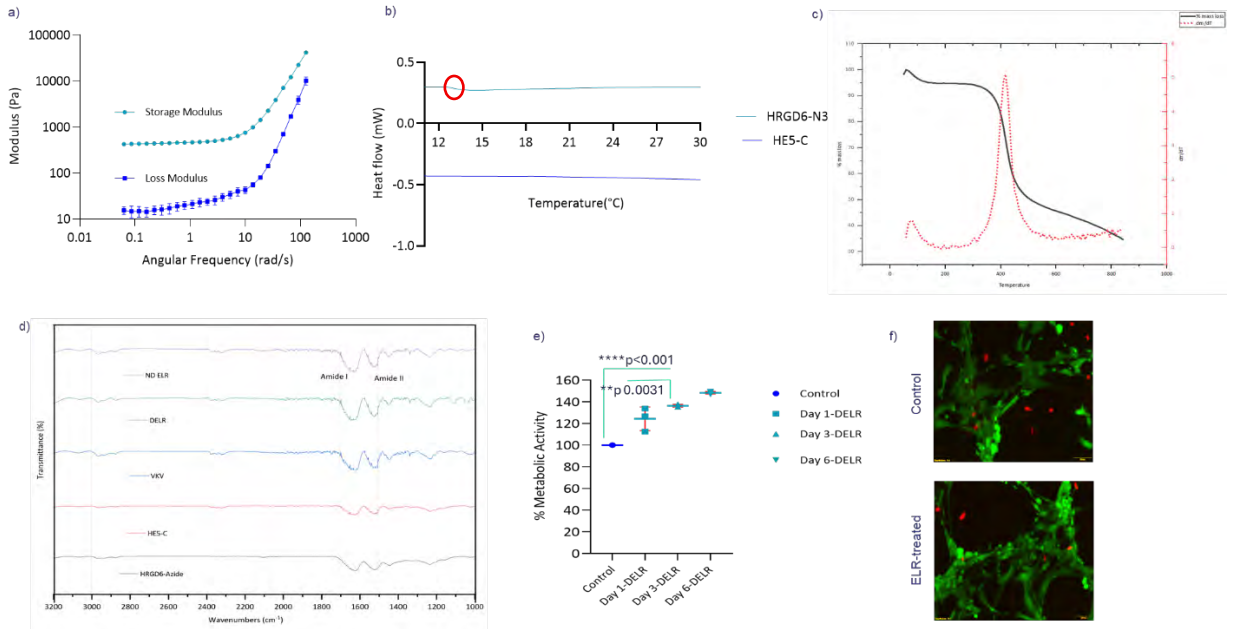

Figure1 Physico-chemical characterization: a) Rheological assessment of the hydrogels b) Transition temperature c) Thermal degradation d) Functional group assessment e) Metabolic activity of cardiac fibroblast cells treated with hydrogel f) Cell viability of cardiac fibroblast cells treated with hydrogel

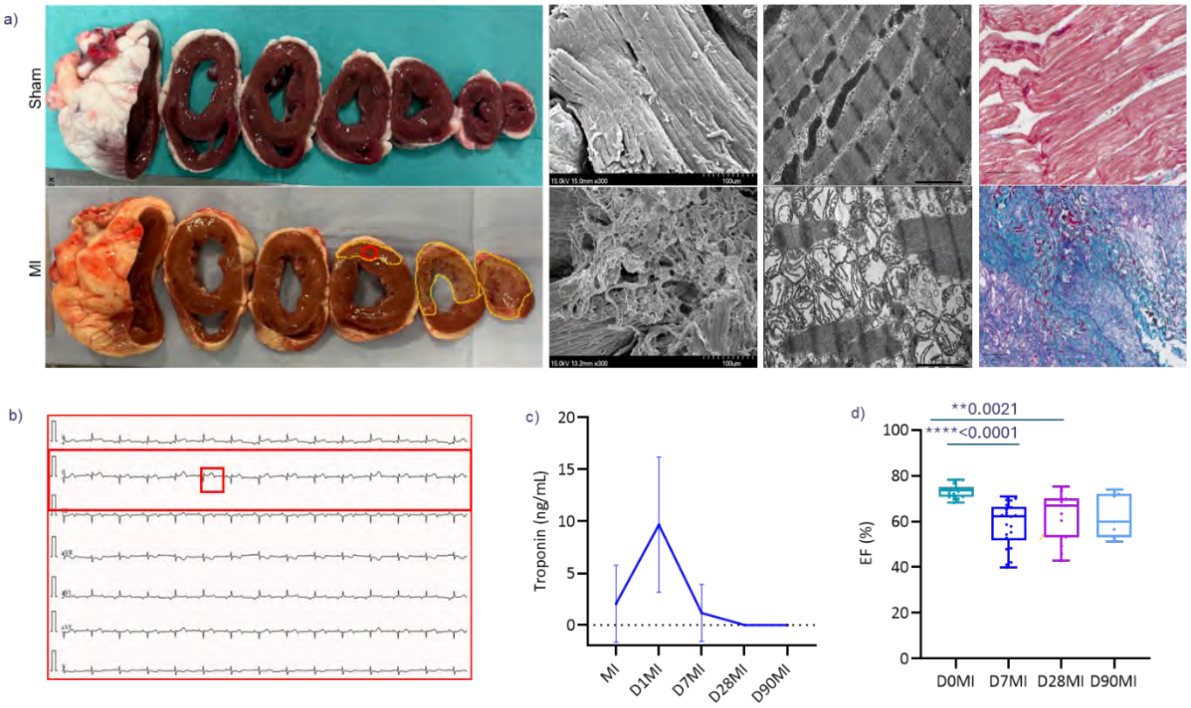

Figure 2 STEMI ovine model: a) Representative cardiac tissue sections showing the difference in myocardial damage between the control (sham) and MI groups b) Electrocardiographic evidence of ST-segment elevation following MI induction c) Increase in circulating troponin levels after MI, confirming myocardial injury d) Reduction in left ventricular ejection fraction observed after MI induction, indicating impaired cardiac function.

S87 – O3

High-throughput screening of biomaterials - A new methodology for screening of hydrogels for the organ-on-chip applications

Pishva B.[1,2,3], Le Blon D.[1,2], Koppen C.[1,2], Dupont C.[3], Van Meenen J.[1,2]
[1]Dept. Ophthalmology, University of Antwerp, Wilrijk; [2]Dept. Ophthalmology, Antwerp University Hospital, Edegem, Belgium; [3]Dept. Bio and Soft Matter (BSMA), University of Catholic the Louvain, Louvain-la-Neuve, Belgium

Introduction

Recent progress in tissue engineering and organ-on-chip technologies has increased the need for reliable biomaterials that can support proper cell attachment and growth. In the development of cornea-on-chip model, selecting an appropriate substrate that resembles the natural stromal environment of the cornea is particularly important. The material used as a sublayer must allow corneal epithelial cells to attach, proliferate, and maintain their normal phenotype. In this study, we established a new methodology to quantify the attachment and proliferation of human corneal epithelial cell line (HCET) on several coatings and different types of hydrogels to identify suitable candidates for future cornea-on-chip model.

Materials and Methods

This study compared HCET cell behavior on standard coatings, including gelatin, collagen II, laminin, and FNC, along with several hydrogels. These included enzymatically crosslinked gelatin and photo-crosslinkable gelatin-based hydrogels such as GelMA. To enable consistent imaging and accurate analysis, the hydrogels were prepared as flat layers in 96-well plates without forming a meniscus using a specific centrifugation method. Cells were monitored at different time points using time-lapse imaging with an in-house confocal microscope (Cell Discoverer 7). A staining protocol was optimized to ensure low toxicity and signal stability for up to three days while minimizing background autofluorescence from the hydrogels. Images were analyzed using ImageJ together with custom scripts that are currently being developed on GitHub. In addition, RNA extraction from the same samples was carried out at the final stage, allowing further investigation of cellular responses while reducing experimental variability.

Results

The imaging and analysis revealed clear differences in cell growth depending on the substrate. Some coatings promoted strong cell attachment and spreading, whereas certain hydrogels led to altered cell behavior compared with the tissue culture plastic control. An interesting observation was seen with GelMA hydrogel which HCET cells showed limited spreading and lower proliferation rates on it. Instead of forming a uniform monolayer, cells migrated toward each other and gradually formed spheroid-like clusters. The imaging workflow and staining strategy allowed accurate quantification of these differences, while successful RNA extraction made it possible to further explore the biological mechanisms involved.

Conclusion

Overall, this study provides useful insights into how different coatings and hydrogels influence corneal epithelial cell behavior. The findings help identify promising biomaterial candidates that could mimic the corneal stroma and support epithelial cell growth. These results represent an important step toward developing a more reliable cornea-on-chip model.

S87 – O4

Low-temperature gelation of norbornene-functionalized gelatin and PEG-thiol hydrogel

Vänskä H.[1], Parihar V.S.[2], Björninen M.[3], Kellomäki M.[4]
Faculty of Medicine and Health Technology, Tampere University, Tampere, Finland

Introduction

Using thermal crosslinking, chemical initiators that are often harmful for the cells, can be avoided. However, it is rarely used in cell-compatible hydrogels because thermally initiating reactions typically require temperatures detrimental for cells. In this study, a compromise strategy was explored exploiting highly reactive thiol-norbornene chemistry of the polymer backbones with low concentrations of thermal initiator. It was hypothesized that room temperature (RT) would be sufficient for initiation and hydrogel formation.

Aim

The aim of this work was to determine whether spontaneous radical formation of ammoniumpersulfate (APS) at RT can initiate thiol-ene crosslinking between gelatin-norbornene (Gel-NB) and 4-arm-thiolated poly(ethylene glycol) (4-arm-PEG-thiol).

Materials and Methods

Gelatin was functionalized with norbornene (~40%) using EDC coupling chemistry to obtain Gel-NB. Functionalization was verified by ^{1}H-NMR spectroscopy and quantified using UV-Vis spectroscopy. Precursor solutions containing Gel-NB and commercial 4-arm-PEG-thiol were prepared in DI-water or DPBS at a total polymer concentration of 5 w/v-%. Hydrogels were formed by adding APS at either 0.25 or 0.5 w/v-% and incubating mixtures at 21 or 37 °C (Fig.1). Gelation was assessed via tube-tilt tests and time-sweep rheology. Hydrogels were further characterized with frequency- and amplitude-sweeps. Preliminary swelling degree and stress-relaxation studies were conducted. Cytocompatibility was evaluated by culturing WI-38 human fibroblasts on the hydrogel surface. Positive control was polystyrene wellplate.

Results

Mixing APS with precursors induced hydrogel formation, producing clear hydrogels (Fig. 1). Gelation behaviour depended on APS concentration and crosslinking temperature. With lower concentration (0.25 w/v-%) the gelation happened slower, and it also took longer time to reach full crosslinking compared to 0.5 w/v-% (Fig. 2). The gelation began faster when the temperature was increased from 21 °C to 37 °C. It also resulted in earlier full crosslinking. In frequency-sweeps the hydrogels behaved independently of the APS concentration or gelation temperature, whereas amplitude-sweeps indicated that hydrogels formed at 37 °C had extended linear viscoelastic regions. Preliminary swelling tests showed no excessive swelling, and stress-relaxation measurements indicated limited stress-relaxation capacity. Cell study showed that fibroblasts that were in direct contact with hydrogels, but adhered to the wellplate plastic, showed high viability and typical morphology (Fig. 2).

Conclusion

In this study, Gel-NB and 4-arm-PEG-thiol were successfully crosslinked into hydrogels using spontaneous radical formation from APS at RT. The gelation rate could be tuned by varying the APS concentration or the crosslinking temperature. This approach offers a simple and accessible hydrogel fabrication method that is suitable for cell-culture applications.

Acknowledgements

The authors thank the Centre of Excellence in Body-on-Chip Research (CoEBoC) by Academy of Finland and Doctoral School of Tampere University

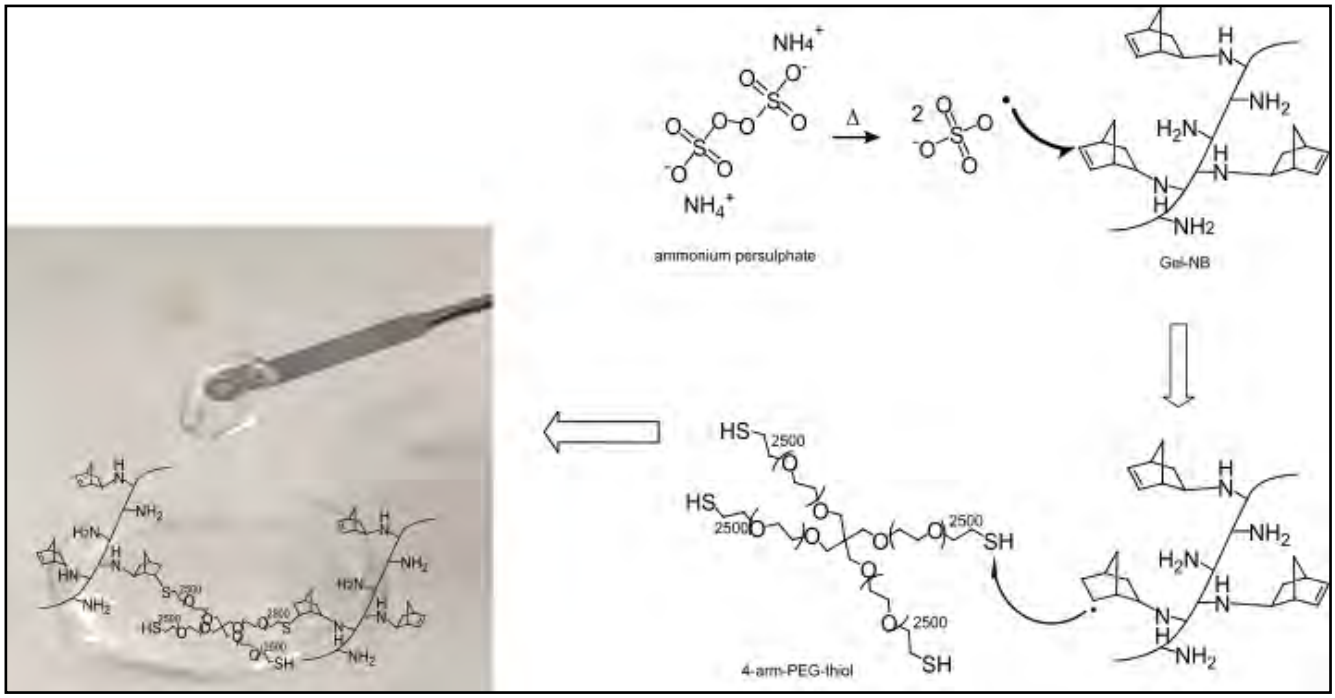

Figure 1 Spontaneous radical formation from ammoniumpersulfate (APS) at RT or 37 °C initiated crosslinking between Gel-NB and 4-arm-PEG-thiol leading to formation of clear hydrogel.

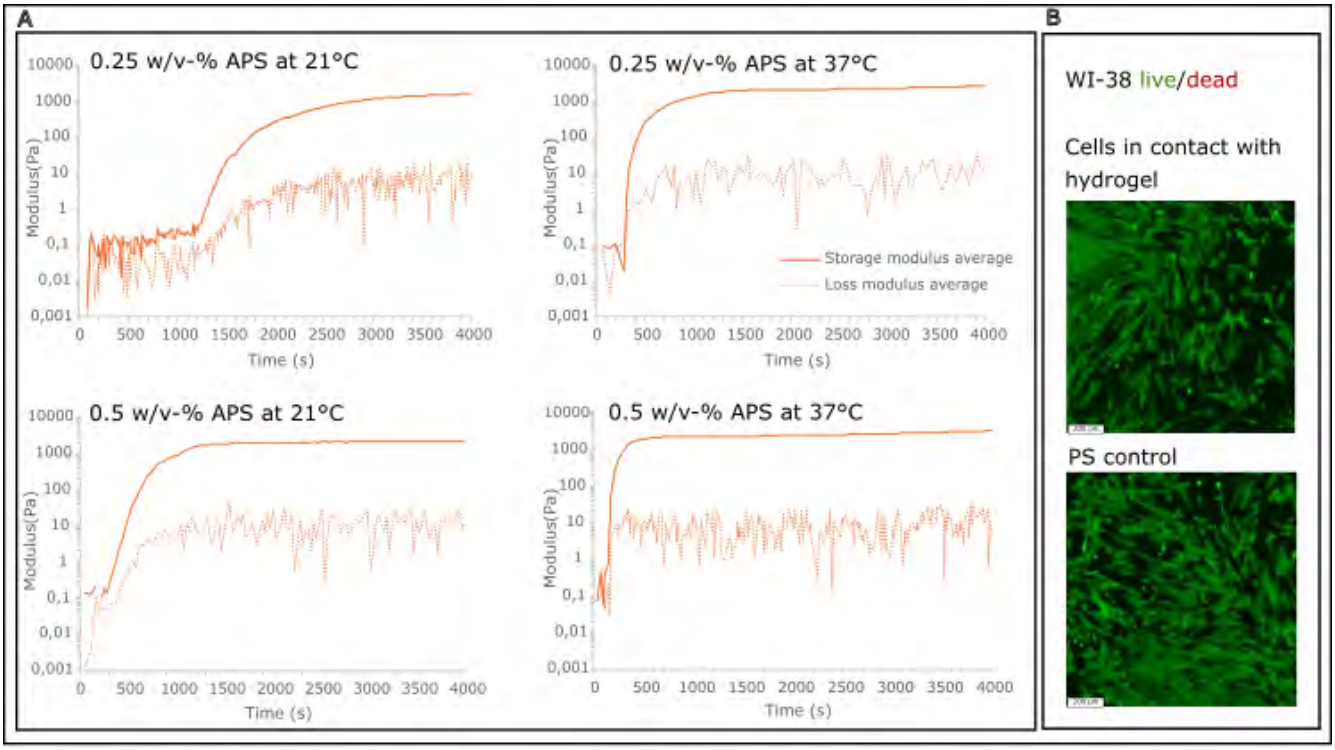

Figure 2 A) Time-weep rheology illustrating the hydrogel gelation with 0.25 or 0.5 w/v-% APS concentration at 21 °C or 37 °C. B) Cytocompatibility assessment showed aligned and viable cells growing on the wells in contact with hydrogel but adhered on the wellplate plastic.

S87 – O5

Human corneal epithelial cell transfer on biosynthetic scaffolds grown in 3D printed cell seeding devices to treat persistent corneal epithelial defects

Robinson D.E., Moreiras H., Menassa N., Williams R., Kearns V., and Levis H.J.
Dept. of Eye and Vision Science, The University of Liverpool, Liverpool, UK

Introduction

Persistent corneal epithelial defects (PCED), are wounds at increased risk of corneal ulceration, infection, perforation, neovascularisation, and scarring, often leading to pain, discomfort, and vision loss. Typically, the epithelium does not heal within 14 days even with standard clinical interventions, such as lubricating gel application, creating, significant ophthalmological challenges to clinicians. We are developing a novel hydrogel-based cell bandage designed to deliver allogeneic human corneal epithelial cells (hCEpCs) directly to the ocular surface for the treatment of PCED.

Materials and Methods

We have developed a novel methacrylated (MA) poly-epsilon-lysine (PeK) based hydrogel to culture hCEpCs. PeK was methacrylated to allow cross linking under UV. An array of co-polymer hydrogels, and double network gels, produced with NHS chemistry were characterised. The hydrogels strength, flexibility, transparency and ability to sustain epithelial cells was determined. The gels were sterilised using supercritical CO2 (scCO2). A device to allow cell seeding and culture on hydrogels was created using Formlabs 4, 3D printing technology. Human corneal epithelial cell line HCE-T and hCEpCs were used to investigate cell/gel compatibility. Indirect and direct cytotoxicity was measured using resazurin assays. Transfer of hCEpCs directly onto an ocular surface model using deepithelialised human corneal buttons was also achieved.

Results

ScCO2 sterilisation significantly altered the stiffness of some hydrogel formulations, though cells still attached. The hydrogels showed sufficient mechanical strength and flexibility to be handled for transfer. The hydrogels had a max stress of 0.4 MPa and a stiffness of 2.5 MPa. The hydrogels allowed attachment and maintenance of hCEpCs with appropriate morphology and expression of (p63) or absence (CK12) of key epithelial markers. Normal metabolic activity was seen in 70% of cells and approximately 60% of cells were transferred to the surface of the human corneal buttons after the hydrogel had been in contact with the ocular surface for 2 days.

Conclusion

The production of a hydrogel carrier for the delivery of hCEpCs to the corneal surface has been achieved. This work has developed a promising cell-based therapy in PCED, with possible clinical applications. Future studies will focus on in vivo safety tests in rabbits to assess the potential of our approach.

Acknowledgements

We would like to thank our funding body, MRC DPFS.

S87 – O6

Combined thermal and rheological characterization of polyvinyl alcohol hydrogels using a freeze-thaw technique

Yang Y.[1], Strasser C.[2], Küspert S.[2], Marsh S.[3], Rummel F.[2]
[1]NETZSCH Instruments, Shanghai, China; [2]NETZSCH-Gerätebau GmbH, Selb, Germany; [3]NETZSCH Thermal Instruments, Wolverhampton, UK

Introduction

Polyvinyl alcohol (PVA) hydrogels are promising materials for biomedical applications like articular cartilage restoration due to their biocompatibility, tunable mechanical properties, and water-holding capacity. PVA hydrogels can be obtained by chemical or physical crosslinking[1]. Freeze-thaw processing enables physical crosslinking through crystalline regions acting as network junctions.

The aim of this study is to develop an experimental method for preparing PVA hydrogels for biotribological model testing while simultaneously detecting crystallization during freeze-thaw cycling. This approach enables production of specimens with suitable rheological and tribological properties for artificial cartilage applications.

Materials and Methods

15%w/w PVA solutions were prepared by dissolving PVA (molecular weight 61,000) in deionized water at 80 °C for 40 minutes under stirring. The solution was transferred to a cylindrical sample holder in a rotational rheometer equipped with Peltier modules for freeze-thaw cycling (five cycles from 10 °C to -20 °C, heating/cooling rate 1 K min^{-1}, with 30 min isothermal phases). A Pt100 sensor was positioned near the sample for direct temperature measurement.

Complementary differential scanning calorimetry (DSC) measurements were performed using a DSC equipped with a USB camera to observe structural changes during freeze-thaw processing.

Rheological measurements were carried out on a rotational rheometer using parallel-plate geometries. Tribological testing was conducted using a 3-ball-on-disc setup with PVA hydrogel specimens and bovine-serum-based artificial synovial fluid.

Results

Combined freeze-thaw and DSC measurements indicate exothermic processes occurring at approximately -10 °C. Synchronized DSC camera recordings support this observation. A decrease in the exothermic peak over successive freeze-thaw cycles is discussed.

Rheological characterization of the hydrogels was performed using amplitude, frequency and temperature sweeps, allowing correlation between rheological behavior and thermal events. Changes in the phase angle during oscillatory shear are compared with the exothermal peak observed in the DSC measurements.

The suitability of the hydrogels for cartilage applications is evaluated using tribological data presented as Stribeck curves.

Conclusion

Combining rheological and thermal characterization during freeze-thaw processing provides insight into PVA hydrogel formation. This approach enables improved control of physical crosslinking and supports the optimization of hydrogels with defined mechanical and tribological properties for biomedical applications.

References

[1]Zhong Y., et al. Construction methods and biomedical applications of PVA-based hydrogels. *Frontiers in Chemistry* 2024; 12; 1-21.

S87 – O7

Design and mechanistic investigation of colloid-assembled self-healing (CASH) gels

Chen K.[1], Dou Z.[1], Ying Q. [1], Wang H.[1]
MOE Key Laboratory of Bio-Intelligent Manufacturing, Dalian Key Laboratory of Artificial Organ and Regenerative Medicine, School of Bioengineering, Dalian University of Technology, Dalian, 116023, P. R. China

Colloid-assembled self-healing (CASH) hydrogel materials represent a promising design strategy for self-healing materials, which have been widely applied in engineering fields due to their characteristic shear-thinning and self-healing properties. In particular, they enable injectable, moldable, and printable biomaterials for applications such as tissue repair, drug delivery, and 3D printing. This study first focuses on the design of CASH hydrogels and proposes an innovative cross-scale nano-colloidal network structure design strategy of "nanosphere building blocks—reversible bonding—self-healing network construction". By leveraging the synergistic effect of nano-size effect and reversible bonds, a dense and dynamically re-constructable three-dimensional network is constructed, thereby overcoming the long-standing trade-off between mechanical strength and self-healing efficiency in conventional hydrogel. Further, focusing on the common scientific problem of the self-healing mechanism of colloidal hydrogels, a photo-controlled imaging platform to rapidly arrest the colloidal network at specific stages of shear deformation and recovery, realizing three-dimensional reconstruction of the hydrogel network at single-particle resolution. Based on this, we establish a cross-scale structure-activity relationship linking nanoparticle network topology to macroscopic elasticity, and the dynamic reconstruction law of particle-assembled networks and the self-healing mechanism of "shear-induced coarsening-hardening effect" are revealed, providing important theoretical support for the design of mechanically stable self-healing colloidal materials.

Acknowledgements
This work was supported by the National Natural Science Foundation of China (No.52273102).

S88
Immunomodulatory and immuno-instructive biomaterials

S88 – K1
Immunomodulatory multifunctional biomaterials for tissue regeneration

Shin H.[1], Jeong H.[1]
[1]Dept. Bioengineering, Hanyang University, Seoul, Republic of Korea

Introduction
Tissue regeneration is a complex, multi-stage process encompassing inflammation, vascularization, matrix formation, and remodeling. As each stage is governed by distinct biological demands, effective biomaterial design requires careful selection of bioactive cues and equally careful consideration of how they are delivered. In this regard, inorganic metallic ions have emerged as particularly attractive candidates, capable of simultaneously engaging multiple regenerative pathways, including immunomodulation, angiogenesis, stem cell differentiation, and cell recruitment, through a single material platform. Polyphenols such as tannic acid and EGCG further complement this approach, contributing anti-inflammatory, antioxidant, and ROS-scavenging properties. However, both ions and polyphenols are subject to dose-dependent toxicity and exhibit context-dependent biological responses, underscoring the importance of a well-designed delivery system. Their intrinsic ability to form stable coordinative bonds with one another gives rise to metal-phenolic networks (MPNs), providing a versatile framework for their co-delivery in a structurally controlled manner. Importantly, the design of the carrier, including its architecture and resulting release kinetics, offers an additional degree of freedom for aligning bioactive output with the evolving needs of the regenerative microenvironment. This presentation introduces a series of MPN-based biomaterial platforms developed for multifunctional tissue regeneration. By systematically varying the ionic composition, spanning Ca^{2+}, Mg^{2+}, Zn^{2+}, and Sr^{2+}, and engineering the carrier architecture accordingly, these systems were tailored to address the biological requirements of diverse tissue targets, demonstrating efficacy in both soft (e.g., skin) and hard (e.g., bone) regeneration. Across these platforms, macrophage polarization from M1 to M2, enhanced angiogenesis, osteogenic differentiation, and/or improved cell recruitment and proliferation could be observed, with the polyphenol's antioxidant activity providing an additional anti-inflammatory contribution. Collectively, these findings underscore the potential of ion- and polyphenol-based platforms as adaptable, multifunctional tools for tissue regeneration.

Acknowledgements
This work was supported by the Engineering Research Center (RS-2025-02263336) from the National Research Foundation of Korea (NRF), funded by the Korean government.

S88 – K2

Hydrogel activating regulatory T cells in vivo regenerates bone defects

Nasello G.[1,2,3], Lafuente Gómez N.[1,2], Geris L.[3,4], Mooney D.[1,2]
[1]Harvard University, Cambridge, MA; [2]Wyss Institute, Boston, MA; [3]KU Leuven, Leuven, Belgium, [4]Université de Liège, Liège, Belgium

Introduction

Successful bone repair relies on a rapid transition from early inflammation to regeneration1. Regulatory T cells (Tregs) play a key role in this transition2, but direct delivery of these cells often results in poor persistence3. A biomaterial-based approach that activates endogenous Tregs at the injury site could provide a localized alternative. This study evaluated collagen-based hydrogels engineered for sustained release of AS2863619, a cyclin dependent kinase inhibitor that induces Foxp3 expression in T cells4. The goal was to create a material-driven strategy that maintains local drug exposure during the early repair window, increases Treg accumulation and promotes bone regeneration.

Materials and Methods

Collagen hydrogels were loaded with AS2863619 either below (20 µg) or above (100 µg) its solubility threshold to generate diffusion-based or dissolution-controlled release. Laponite nanoparticles were incorporated to introduce electrostatic retention. Drug release was quantified under sink conditions into PBS, and collected samples were tested for biological activity. In vitro immune profiling examined the effects of different AS2863619 concentrations on T cells, macrophages, and dendritic cells. In vivo evaluation used 4 mm calvarial defects in C57BL6J mice treated with blank hydrogels or hydrogels containing AS2863619 with or without laponite. T cell subsets and macrophage phenotypes were analyzed on days 3, 7, 8, 9, and 10. Bone regeneration was measured by µCT and histology at weeks 4 and 8.

Results

Drug loading above solubility reduced burst release from 74±5% to 26±2% and extended release duration to 11 days. Incorporation of laponite further reduced burst release to 19±2% and maintained residual drug within the hydrogel for more than 2 weeks. Released AS2863619 remained fully active in Foxp3 induction assays. Low drug concentrations, such as 0.1 µM, increased Foxp3 expression with minor effects on innate cells. In vivo, AS2863619 hydrogels increased the Treg percentage within $CD4^+$ T cells from 5±1% in blank gels to 17±10% with the 1000 µg load (n=8-9). Circulating Tregs in blood remained near 5% across groups, and other systemic T cell subsets were unchanged (n=8-9). Higher local drug doses also reduced the fraction of $CD11b^+CD206^-CD80^+$ macrophages. At 28 days, hydrogels containing both AS2863619 and laponite significantly reduced defect size and achieved complete bridging in 2 of 5 animals.

Conclusion

Sustained delivery of AS2863619 from collagen hydrogels creates a localized tolerogenic niche that enhances Treg activity and accelerates bone regeneration. This biomaterial platform provides a practical and targeted alternative to cell based immunotherapies for non healing defects.

References

[1]Duda G.N., et al. N*at Rev Rheumatol* 2023; 19; 78–95.
[2]Nayer B., et al. *Nat Commun* 2024; 15; 7863.
[3]Ho P., et al. *Sci. Transl. Med.* 2024; 16; eadm8859.
[4]Akamatsu M., et al. *Sci. Immunol.* 2019; 4; eaaw2707.

S88 – O1

Immunomodulatory potential of polydopamine coatings in drug delivery patches targeting chronic inflammation

Macartney R.A.[1], Budharaju H.[2], Roy I.[2,3], Knowles J.C. [1]
[1]Division of Biomaterials and Tissue Engineering, University College London Eastman Dental Institute, London, UK; [2]School of Chemical, Materials & Biological Engineering, Faculty of Engineering, University of Sheffield, Sheffield, United Kingdom; [3]Insigneo Institute, University of Sheffield, Sheffield, United Kingdom

Introduction

Chronic oral inflammatory diseases result in persistent pain and discomfort leading to significantly altered quality of life for afflicted patients. Following investigations into the development of drug loaded patches as potential treatments we have sought to enhance the mucoadhesive properties of such patches using a mussel inspired polydopamine coating. Polydopamine coatings have been extensively investigated in relation to nanoparticles for drug delivery applications, showing potential to enhance mucoadhesion and immunomodulation. Here, we aim to investigate the potential translation of these coatings to drug-eluting patch materials of different geometries.

Materials and Methods

Patches were fabricated from polyhydroxyalkanoates via 3 different methods, solvent casting, electrospinning and 3D-printing. Following fabrication, samples were coated with the polydopamine via self-polymerisation of dopamine hydrochloride using 2 methods: a traditional immersion coating and a fast spray coating. Sample properties were assessed using SEM and FTIR to confirm the presence of the coatings. Adhesive properties were studied using porcine mucosae in a reverse compression test. Cytocompatibility was assessed using oral epithelial cells (MOE-1a) whilst immunomodulatory properties were assessed using RAW-264.7 macrophages.

Results

Polydopamine coatings could be successfully deposited on samples using both coating methods as confirmed by increases in FTIR spectrum intensity at 1478-1678 cm^{-1} and 3000-3700 cm^{-1} indicating the presence of N-H bonding in the polydopamine structure (Figure 1). Comparable results were obtained in terms of mucosal adhesion achieved between the traditional and spray coating methods (Figure 2). All polydopamine coated samples showed reactive oxygen species scavenging ability using the 2,2-diphenyl-1-picrylhydrazyl (DPPH) assay. Polydopamine coated samples showed enhanced oral epithelial cell viability, perhaps owing to the significant increases seen in surface free energy following applications of coatings from 33.33-33.94 to 68.45-88.83 mN/m depending on sample geometry. The ability of the polydopamine coated samples to quench intracellular reactive oxygen species production has been confirmed using the DCFH-DA detector with subsequent fluorescent imaging and spectrophotometric analysis.

Conclusion

Polydopamine coatings show good potential for use as immunomodulatory additions to biomaterial structures beyond nanoparticles. Mechanisms contributing to the immunomodulatory properties include reactive oxygen species scavenging abilities and potential to polarise macrophages. Additionally, the proven potential for these coatings to enhance the mucoadhesive properties of materials highlights their potential in aiding with drug delivery films targeting chronic inflammatory conditions such as stomatitis.

Acknowledgements

We acknowledge the funding obtained from Engineering and Physical Science Research Council (EPSRC) [grant number EP/X022196/1, EP/X026108/1].

Figure 1) FTIR spectra showing the increase in intensity within expected wave-ranges for N-H bonding present in the polydopamine coatings depositing on electrospun samples via the traditional immersion coating technique (ES-PD) or the fast spray coating method (ES-SC_2) compared with baseline signal observed for control electrospun samples (ES).

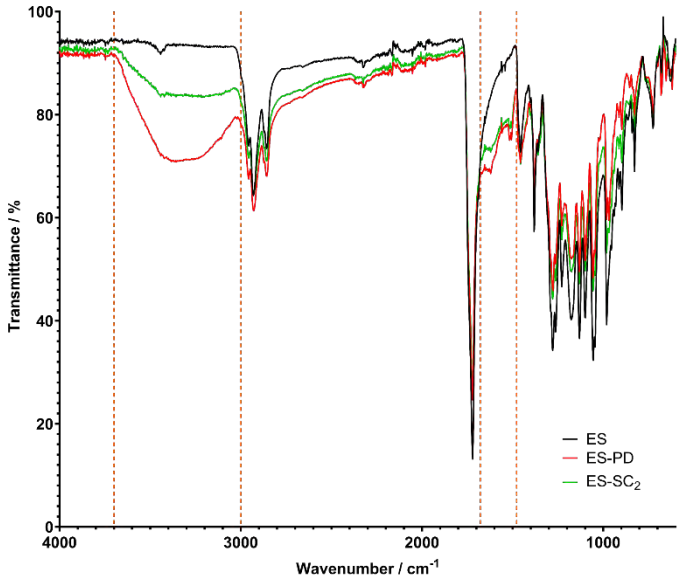

Figure 2) Adhesion force measurements taken using the reverse compression method under mucin-soaked conditions for control electrospun samples (ES), traditional immersion coated samples (ES-PD) or the fast spray coated sample (ES-SC_2).

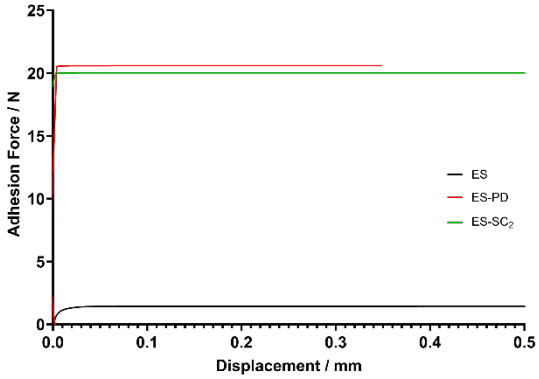

S88 – O2

Immunomodulatory Effects of Chromium-Doped Nanoparticles on Macrophage Polarization for Osteoporotic Bone Repair and Remodelling

Yusuf A.S.[1,2], Kaur K.[1,2]

[1]School of Pharmacy and Biomolecular Sciences, Royal College of Surgeons in Ireland (RCSI); [2]Tissue Engineering Research Group, Dept. of Anatomy & Regenerative Medicine, RCSI, Dublin, Ireland

Introduction

Osteoporosis is characterized by an imbalance between osteoclast-mediated bone resorption and osteoblast-mediated bone formation.[1] Recent advances in osteoimmunology have highlighted the contribution of pro-inflammatory M1 macrophages to bone resorption and in pathogenesis of osteoporosis. However, when these macrophages are polarised to M2, they inhibit bone resorption and promote osteogenesis.[1] This polarization of macrophages from M1 to M2 is mediated by cytokine signaling. Chromium (III), Cr^{3+}, is an essential trace element with important roles in human health.[2] Although Cr^{3+} has been reported to contribute to the treatment of diabetes and obesity and to improve liver and kidney function.[2] However, its role in bone regeneration and immune modulation remains unclear.

Aim

This work is aimed to investigate the potential of Cr^{3+} doped hydroxyapatite nanoparticles (Cr-nHAp) for immunomodulation and bone regeneration in osteoporotic conditions.

Materials and Methods

Cr-nHAp was prepared via co-precipitation with varying Cr^{3+} concentrations (0, 1, 3 and 5 mol%).[3] Their physicochemical properties were characterized in detail. Cell cytotoxicity, proliferation and differentiation including matrix mineralization and gene expression was measured using Alamar Blue, Pico Green, calcium assay and RT-qPCR respectively. Cellular Interaction and uptake of Cr-nHAP was assessed using confocal microscopy and flow cytometry. Anti-inflammatory effects on macrophage polarisation (M1 to M2) were evaluated using ELISA, flow cytometry, and fluorescence microscopy. A co-culture bone model was used to investigate Cr-nHAp's immunomodulatory impact on THP-1 macrophages and its effect on osteoblast-mediated bone regeneration.

Results

Cr-nHAp samples exhibited a pure crystalline phase with rod-shaped morphology (Figure 1). They exhibited high biocompatibility up to 62.5 µg/mL. Substituting 5mol% of calcium with Cr in nHAp significantly enhanced osteoblast activity while inhibiting osteoclast differentiation. Cellular Interaction and uptake by THP-1 macrophages was confirmed by confocal microscopy and flow cytometry. Cr-nHAp significantly reduced the secretion of pro-inflammatory (M1) cytokines (TNF-α, IL-8, and IL-1β) and increased anti-inflammatory (M2) cytokines (IL-10 and IL-22), indicating a phenotypic shift from M1 to a tissue-repair–associated phenotype M2. Flow cytometry and immunofluorescence staining, further confirmed increased CD163+ M2 and decreased CD80+ M1 macrophages in treated groups (Figure 2).

Conclusion

This study shows the immunomodulatory potential of Cr-nHAp in restoring osteoblast-osteoclast balance via cytokine signalling in osteoporosis. Overall, this study presents a pioneering advance in osteoimmune modulation strategy for bone regenerative applications.

References

[1]Wang, W., Liu, H., Liu, T., Yang, H. and He, F. Insights into the role of macrophage polarization in the pathogenesis of osteoporosis. *Oxidative medicine and cellular longevity* 2022; p.2485959.

[2]Swaroop, A., Bagchi, M., Preuss, H. G., Zafra-Stone, S., Ahmad, T., & Bagchi, D. Benefits of chromium (III) complexes in animal and human health. *The nutritional biochemistry of chromium (III)* 2019; 251-278.

[3]Hu, W., Ma, J., Wang, J. and Zhang, S. Fine structure study on low concentration zinc substituted hydroxyapatite nanoparticles. *Materials Science and Engineering C* 2012; 2404-2410

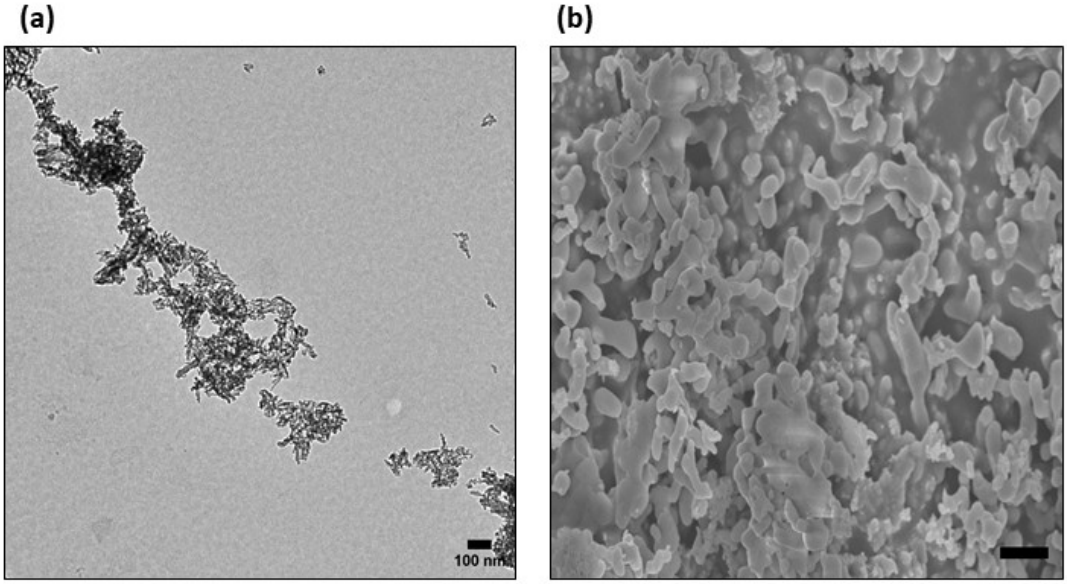

Figure 1: Representative (a) transmission electron microscopy, and (b) scanning electron microscopy images showing rod-shaped Cr-nHAp

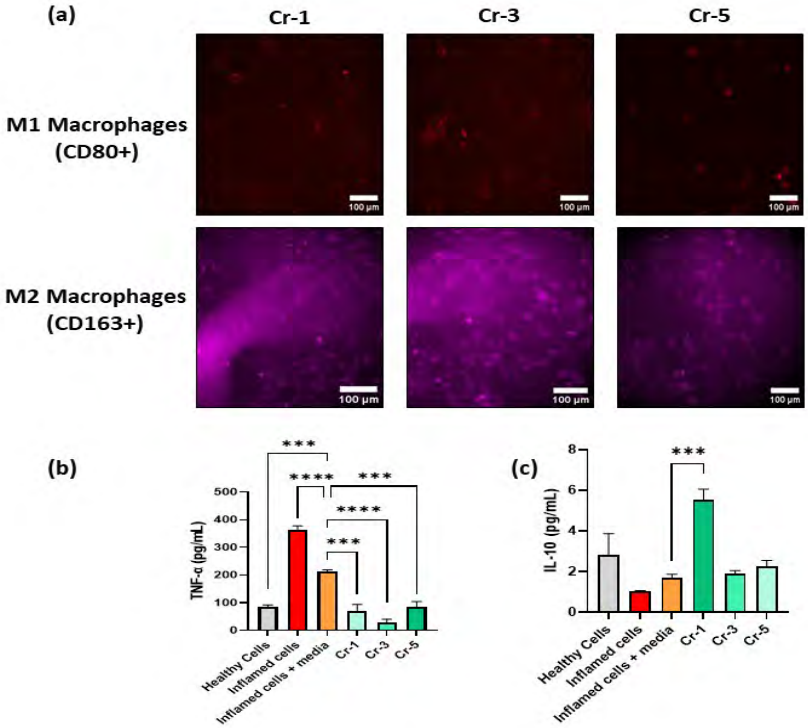

Figure 2: (a) Representative fluorescence microscopy image showing few M1 macrophages compared to polarized M2 macrophages after treatment with Cr-nHAp, (b) Reduction in secretion of a key pro-inflammatory cytokine (TNF-α) by THP-1 macrophages was observed following treatment with Cr-nHAp, indicating a shift away from the M1 macrophage phenotype, (c) Increase in secretion of a key anti-inflammatory cytokine (IL-10) was observed in THP-1 macrophages following treatment with Cr-nHAp, indicating a shift toward an M2 macrophage phenotype

S88 – O3

Praseodymium-Nanocarriers for Immunomodulation and Bone Regeneration in Osteoporosis

Raju L.[1,2], Ferreira A.[1], Kaur K.[1, 2], Murphy C.M.[1, 3]
[1]Tissue Engineering Research Group (TERG), Royal College of Surgeons in Ireland; [2]School of Pharmacy and Biomolecular Sciences, Royal College of Surgeons in Ireland; [3]Trinity Centre for Biomedical Engineering, Trinity College Dublin, Dublin, Ireland

Introduction

Reactive oxygen species (ROS) and chronic inflammation drive osteoporosis by disrupting the bone homeostasis. Elevated ROS levels induce the release of pro-inflammatory cytokines, which, in turn, stimulate ROS generation, forming a vicious cycle that accelerates bone loss. Targeting this ROS-inflammatory axis therefore a promising therapeutic strategy for the treatment of osteoporosis.

Praseodymium (Pr), a rare earth element, can partially substitute calcium due to its similar binding behaviour. Its antioxidant and pro-angiogenic properties may benefit bone repair, yet its role in bone remodelling is not well understood. We hypothesise that Pr's antioxidant activity could modulate bone inflammation and, together with its pro-angiogenic effects, enhance regeneration.

Aim. To develop Pr-functionalised nanoparticles that can modulate the anti-oxidant and anti-inflammatory axis, thereby directing macrophage polarisation and inhibiting osteoclast activity for osteoporotic fracture repair

Materials and Methods

Nanohydroxyapatite (nHAp) is functionalised with a range of Pr ions (0.05 mol% - 0.5 mol%) by co-precipitation method and characterised by SEM, FTIR, XRD and nanoparticle tracking analysis (NTA). The biocompatibility was assessed with monocytes (RAW264.7) using quantitative assays such as Alamar Blue™ and PicoGreen™.

The monocytes were treated with osteoclast differentiation media (50 ng/ml RANKL + nanoparticles) for 10 days, and differentiation activity was assessed by cytoskeleton staining with Alexa Fluor™ 546 phalloidin.

Results

The nHAp and Pr-nHAp nanoparticles were successfully synthesised and characterised (Figure 1). They exhibited a crystalline, rod-shaped morphology, unaffected by Pr incorporation. The nanoparticles showed a broad particle size distribution, with the mean size being around 50nm and a surface charge ranging from -7 to -10 mV. The FTIR spectra confirmed the Pr substitution in the nHAp lattice, as indicated by a decrease in the intensity of OH^- band vibration at 632 cm^{-1} with increasing Pr concentration.

Biocompatibility studies showed that Pr-nHAp supports cell proliferation with the higher concentrations (0.2% and 0.5%) significantly enhanced proliferation by Day 7. Preliminary studies on osteoclast differentiation showed that nHAp and Pr-nHAp initially promote osteoclastogenesis; however, at later stages, they induce osteoclast toxicity, characterised by premature cell death and disruption of actin ring formation (Figure 2), reducing overall osteoclast function.

Conclusion

These findings suggest that Pr-nHAp can suppress osteoclast activity by disrupting cytoskeletal organisation. The ongoing evaluation of anti-oxidant and macrophage polarisation is expected to provide further insights into the mechanistic pathways involved. Collectively, this study supports the potential application of Pr-nHAp as therapeutic agent for the treatment of osteoporosis.

Acknowledgements

This work is supported by the European Research Council Consolidator Grant under agreement GAP-101125820 (RESTORE)

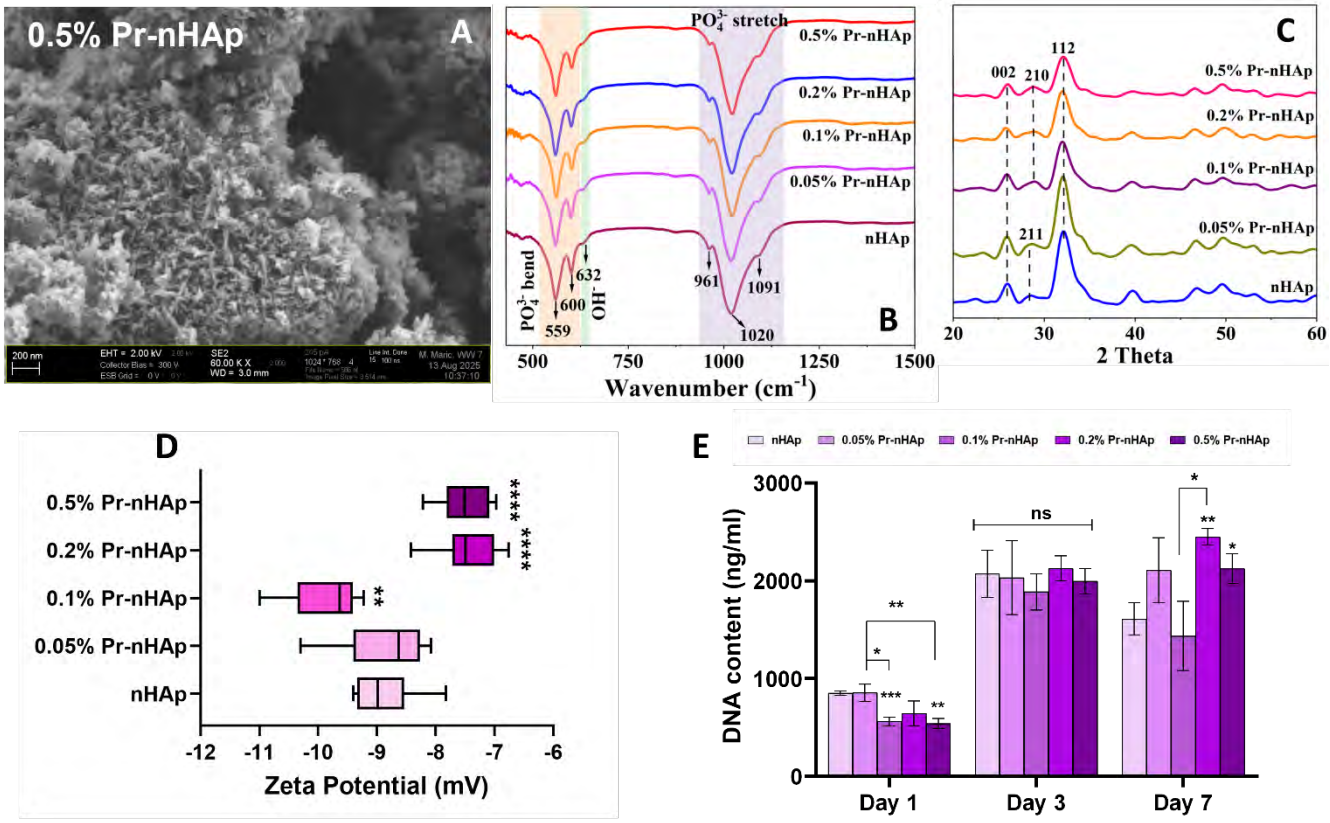

Figure 1. Physicochemical and biological characterisation of nHAp and Pr-nHAP. (A) Representative SEM image of 0.5% Pr-nHAp. (B) FTIR spectra (C) XRD pattern (D) Zeta potential and (E) Biocompatibility against RAW 264.7 of nHAp and Pr-nHAp.

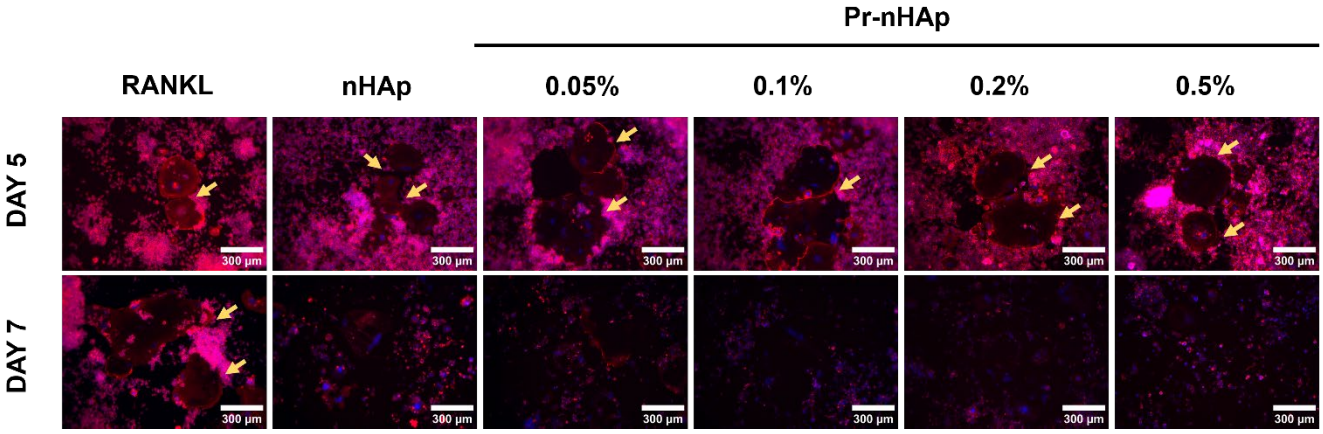

Figure 2. Effect of nHAp and Pr-nHAp (0.05 mol% - 0.5 mol%) on F-actin ring formation in RANKL-induced RAW 264.7 cells. (mag. 10x; scale bar=300 µm).

S88 – O4

Macrophage-targeted and reprogrammed exosome-functionalized fibrous scaffold promote heterogeneous tissue regeneration

Jin S.[1]
[1]Dept. of Orthopedics, Southwest Hospital, Army Medical University, Chongqing 400038, China

Introduction

Bone defects caused by trauma, infection, or tumor removal are often combined with soft tissue injury. This creates a major clinical problem because there are no effective methods to repair both hard and soft tissues at the same time.

Aim

This study presents a strategy that combines physical and biological signals based on materiobiology and immune-guided regeneration.

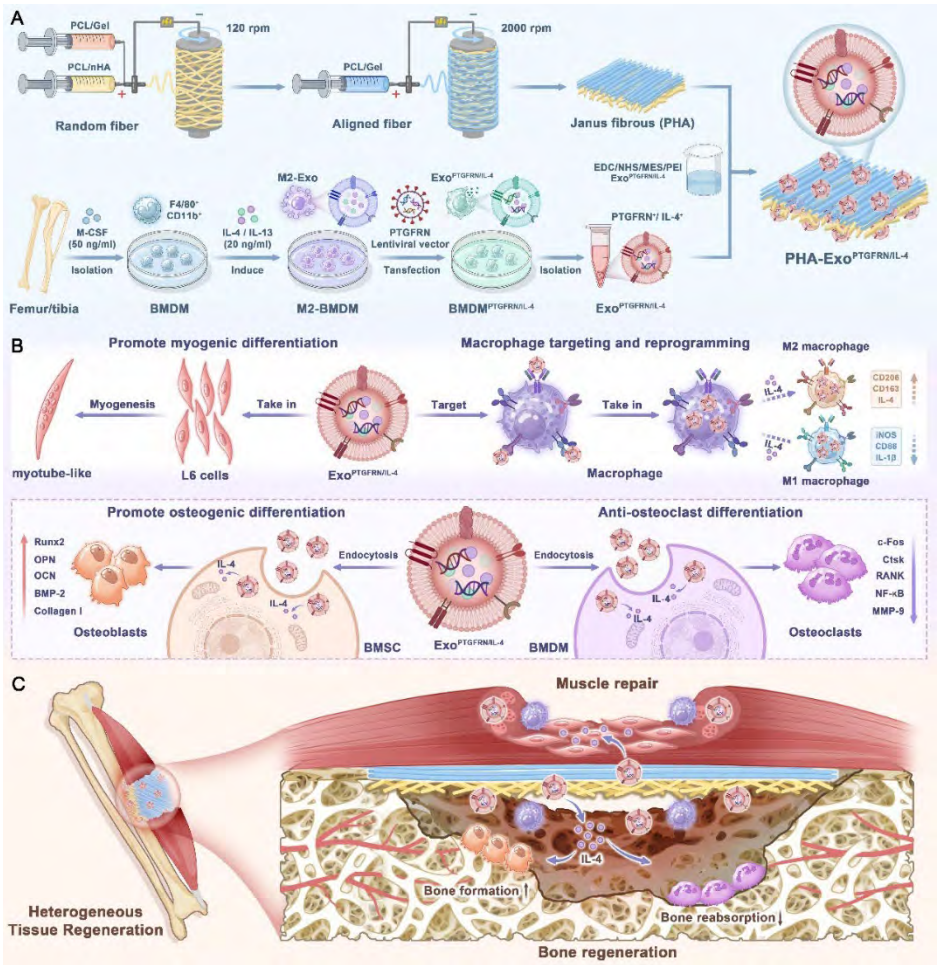

Figure 1. Schematic illustration depicting the fabrication process of the Exo$^{PTGFRN/IL-4}$-functionalized Janus fibrous scaffold (PHA-Exo$^{PTGFRN/IL-4}$) and its proposed mechanism for orchestrating cellular behaviors and guiding heterogeneous tissue regeneration.

Materials and Methods

An asymmetric fibrous scaffold (PHA) was fabricated by sequential electrospinning, with an aligned-fiber layer on the top and a random-fiber layer on the bottom. Bone marrow–derived macrophages were isolated and co-stimulated with IL-4 and IL-13 to induce M2 polarization, followed by lentiviral transduction to overexpress

PTGFRN, yielding exosomes that concomitantly overexpress PTGFRN and IL-4 ($Exo^{PTGFRN/IL-4}$). These exosomes were then further immobilized onto the surface of the asymmetric fibrous scaffold to fabricate PHA-$Exo^{PTGFRN/IL-4}$.

Results

Exosomes derived from macrophages and modified with PTGFRN and IL-4 have two main roles: targeting and reprogramming of macrophages. Evaluation of the foreign body response showed that the scaffold did not cause long-term inflammation or systemic toxicity. It also regulated fibrosis, angiogenesis, and macrophage polarization. *In vitro* experiments and *in vivo* models, including muscle injury, calvarial bone defect, and mandibular defect models, showed that $Exo^{PTGFRN/IL-4}$ promoted myogenic and osteogenic differentiation while suppressing osteoclastogenesis. This led to effective soft tissue repair and bone regeneration. A comprehensive *in vivo* evaluation confirmed its favorable biocompatibility profile throughout the foreign body response timeline and demonstrated its efficacy in guiding the functional regeneration of calvarial bone, mandibular bone, and skeletal muscle.

Conclusion

In summary, the PHA-$Exo^{PTGFRN/IL-4}$ scaffold integrates both physical and biochemical cues, presenting a promising therapeutic strategy for heterogeneous tissue regeneration. By addressing the distinct requirements ("heterogeneity") and shared principles ("commonality") of different tissue types, this study engineered a mechanically robust Janus scaffold functionalized with $Exo^{PTGFRN/IL-4}$ to confer macrophage targeting and reprogramming capabilities. The PHA-$Exo^{PTGFRN/IL-4}$ scaffold system establishes a novel paradigm for complex tissue repair, bridging a critical gap between foundational biomaterial research and translational medical applications.

Acknowledgements

This work was supported by the National Natural Science Foundation of China (32401132) and the China Postdoctoral Science Foundation (2022TQ0224).

S88 – O5

Modulating immune responses of superparamagnetic iron oxide nanoparticles by smart biopolymer coatings

Pournoori N.[1], Sarlus H.[2], Sjöström D.J.[3], Hytönen V. P.[1], Harris R.A.[2], Nilsson P.H.[3], Oommen O.P.[4]
[1]Fac. Medicine and Health Technologies, Tampere University, Tampere, Finland; [2]Dept. Clinical Neuroscience, Karolinska Institutet, Stockholm, Sweden; [3]Dept. Chemistry and Biomedicine, Linnaeus University, Kalmar, Sweden; [4]Sch. Pharmacy and Pharmaceutical Sciences, Cardiff University, Cardiff, UK

Introduction

Nanoparticles hold significant promise as drug delivery platforms; however, adsorption of serum proteins onto their surfaces critically influences biodistribution and can trigger adverse immunological responses. Surface modification with biopolymers can impart stealth properties that reduce immune reactions while enabling controlled targeting and modulation of biological responses. Among clinically used biopolymers, heparin (HP) and dextran sulfate (DS) are widely employed for thrombotic complications. HP is well known for its anticoagulant activity, but its anti-inflammatory and immunomodulatory properties remain comparatively underexplored. Although HP has been investigated for inflammatory conditions such as asthma, inflammatory bowel disease, and acute coronary syndrome, its broader application is limited by bleeding risks and complications including heparin-induced thrombocytopenia. DS, a semi-synthetic polyanionic polysaccharide with a higher sulfate density and flexible branched structure, has been proposed as an alternative, offering similar therapeutic potential while potentially mitigating some adverse effects. DS can interact with scavenger receptors on immune cells, enabling modulation of macrophages and dendritic cells. Despite these promising features, comparative studies examining the immunological properties of HP and DS, particularly in nanoparticle-based drug delivery systems, remain limited. In this study, we fabricated HP- and DS-coated superparamagnetic iron oxide nanoparticles (SPIONs) and systematically compared their physicochemical characteristics and immunological responses.[1] The nanoparticles were evaluated using human whole blood assays, primary immune cells, endothelial cell models, and animal studies. This work aims to elucidate the relative immunomodulatory properties of HP and DS coatings and assess their potential applications in anticancer therapy and regenerative medicine.

Methodology and Results

SPIONs were synthesized using a modified co-precipitation method and characterized physicochemically, revealing monodisperse quasi-spherical nanoparticles with hydrodynamic sizes of 78 nm and 93 nm for DS-SPIONs and HP-SPIONs, respectively. Stability was assessed over time via size and zeta potential in PBS. Although both formulations inhibited key complement cascade markers, they exhibited opposing immunological profiles. HP-SPIONs triggered monocyte and endothelial cell activation and promoted a pro-inflammatory, M1-like macrophage response. In contrast, DS-SPIONs suppressed endothelial activation, showed enhanced myeloid cell uptake, and induced an immunosuppressive, pro-healing phenotype in murine and human macrophages. Magnetic resonance imaging (MRI) was used to monitor *in vivo* biodistribution and organ accumulation. While both formulations were cleared from the reticuloendothelial system within 24 hours, HP-SPIONs showed higher initial hepatic accumulation and delayed splenic uptake compared to DS-SPIONs. Consistent with imaging data, DS-SPIONs induced a subtle expansion of splenic immune cells, suggesting a more robust early engagement with the mononuclear phagocyte system.

Conclusion

These findings highlight Surface Modification and sulfated functionalization of SPIONs as promising, biocompatible strategies for targeted drug delivery, with potential applications in regenerative medicine and anticancer immunomodulation.

Acknowledgements

The authors acknowledge financial support from the Tampere University Foundation sr.

References

[1] Pournoori N., Sarlus H., Sjöström D. J., Pavan Parvathaneni R. Varghese O. P., Hytönen V. P., Harris R. A., Nilsson P. H., Oommen O. P.; Reprogramming Immunogenicity of Iron Oxide Nanoparticles through Sulfated Glycan Presentation. *Small 2026*; *22* (11); e08613.

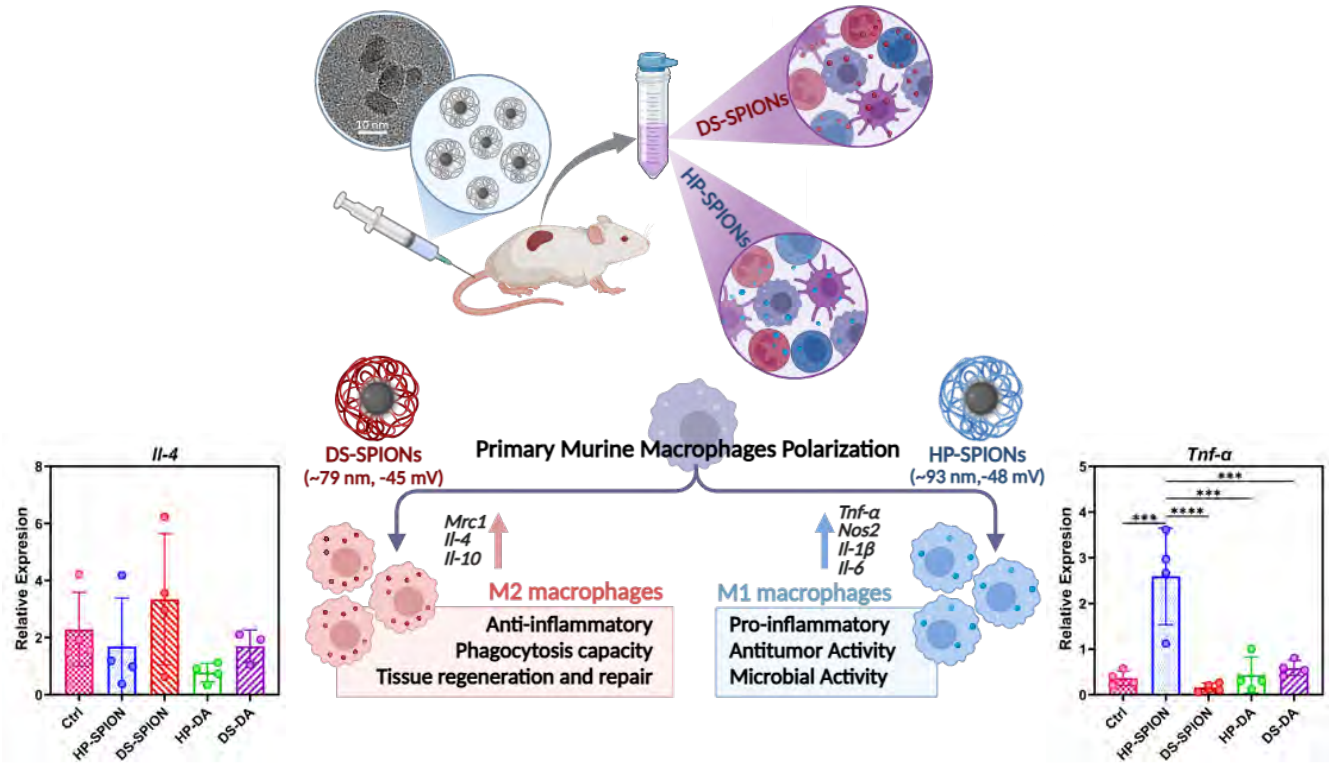

Figure 1. Summary of procedure and outcomes of this study. (Adapted from [1])

S89
In vitro, in vivo, and preclinical evaluation of biomaterials

S89 – K1
A cell-centric perspective on biomaterials: From cellular diversity to in vitro tendon models

De Schauwer C.
Veterinary Stem Cell Research Unit, Dep. of Translational Physiology, Infectiology and Public Health, Faculty of Veterinary Medicine, Ghent University, Belgium

Introduction
Biomaterials provide structural, mechanical and biochemical cues that profoundly influence cellular behaviour. At the same time, cells differ in their intrinsic characteristics and actively respond to and remodel their surrounding microenvironment. Consequently, cellular responses to biomaterials emerge from a complex interplay between biological variability, material properties, scaffold architecture, processing conditions and environmental cues. This lecture will explore how a cell-centric perspective can complement biomaterial development by considering not only how materials influence cells, but also how cell identity, tissue source, functional state and culture history contribute to biological outcomes.

Materials and Methods
Examples from our research on mesenchymal stromal cells (MSCs), cell–biomaterial interactions and tissue-specific in vitro models will illustrate this interplay. Donor- and tissue source-dependent variation in cellular characteristics and function will be considered alongside studies examining how biomaterial formulation, crosslinking, scaffold architecture and biofabrication influence cellular behaviour. The impact of culture history and environmental conditions will also be addressed, including how cellular adaptation to changes in the microenvironment may affect experimental outcomes. Finally, in vitro tendon models will serve as tissue-specific case studies integrating biomaterial properties, cellular function and mechanical cues.

Results
Our findings illustrate that cellular outcome is shaped at multiple, interconnected levels. Donor characteristics influence MSC proliferation, phenotype and differentiation potential, while MSCs from different tissue sources display distinct expansion profiles and functional properties. Cellular state, culture history and environmental conditions may further modulate biological responses, suggesting that cellular adaptation and experimental context should be considered when interpreting cell–biomaterial interactions. In turn, biomaterial composition, mechanics and architecture influence cell morphology and lineage-specific differentiation, while processing and crosslinking add further complexity. In tendon-specific models, matrix properties and mechanical cues influence tenocyte morphology, alignment, extracellular matrix deposition and remodelling. Together, these examples highlight the reciprocal nature of cell–biomaterial interactions and the value of evaluating biomaterials within their biological, physical and environmental context.

Conclusion
Integrating cellular diversity with biomaterial characterisation may provide a more comprehensive understanding of material performance and improve the physiological relevance and reproducibility of tissue engineering strategies. A cell-centric perspective complements biomaterial design by recognising that biological outcomes arise from interactions between material properties and cells with a particular identity, source, functional state and culture history. Considering these interacting variables, including how cells adapt to changing environments, may support the development of more informative in vitro models and the rational evaluation of biomaterials for regenerative medicine.

Acknowledgements
This research was funded by the Research Foundation - Flanders (FWO) (S002821N; 12E4523N; 1S02822/24N) and the Industrial Research Fund of Ghent University (IOF-StarTT/039).

ESB
2026

S89 - K2

From Stem Cells to Ocular Repair: Biomaterials for Differentiation, 3D Bioprinting and Clinical Translation

Heli Skottman[1]
[1]Faculty of Medicine and Health Technology, Tampere University, Finland

Introduction

Corneal blindness is the third leading cause of blindness worldwide, affecting millions of patients and creating a substantial unmet clinical need due to the severe shortage of donor corneas. Stem cell-based therapies hold great promise for treating ocular surface diseases such as bilateral limbal stem cell deficiency (LSCD) and corneal endothelial disorders. However, successful translation of these therapies relies on biomaterials that can mimic native stem cell niches, guide cell differentiation, and support tissue regeneration. Our research focuses on developing biomaterial-based strategies for ophthalmic regenerative medicine by investigating how biomaterials influence stem cell differentiation, recreate key features of the stem cell niche, and support corneal tissue regeneration. In parallel, we are developing bioinks and 3D bioprinting approaches to generate functional corneal tissues and advance the translation of stem cell-based therapies for ocular diseases.

Materials and Methods

Human pluripotent stem cells (hPSCs) are differentiated into corneal limbal stem cells (LSCs), corneal endothelial cells (CECs), and corneal keratocytes (iCKs). Biomaterial-based culture systems are utilized to investigate cell–matrix interactions and to elucidate the role of the limbal niche in regulating stem cell fate and function. Molecular and functional characterization of stem cell-derived corneal cells is performed using established phenotypic, transcriptomic, and functional analyses. In parallel, advanced bioinks are developed for corneal tissue engineering and are being integrated into the Horizon Europe KeratOPrinter project, which aims to generate full-thickness corneal grafts through 3D bioprinting of stem cell-derived corneal cells.

Results

Current studies demonstrate that biomaterial-guided differentiation supports the generation of corneal cell populations exhibiting key molecular, phenotypic, and functional characteristics of native cells. Investigations of limbal niche-inspired biomaterials are providing new insights into the mechanisms regulating stem cell maintenance, differentiation, and regenerative capacity. Ongoing biofabrication studies indicate that stem cell-derived corneal cells can be successfully combined with printable biomaterials to create increasingly complex corneal tissue constructs. Within the KeratOPrinter project, stem cell technologies, biomaterials, and GMP-compatible manufacturing approaches are being integrated to establish scalable processes for the production of bioengineered corneal grafts.

Conclusion

Biomaterials are a key enablers of ocular repair by supporting stem cell differentiation, recreating regenerative microenvironments, and facilitating the fabrication of clinically relevant tissue substitutes. Ongoing advances at the interface of stem cell biology, biomaterials science, and 3D bioprinting are accelerating the development of ophthalmic therapies and bringing bioengineered corneal grafts closer to clinical translation.

Acknowledgements

Our work has been funded by Research Council Finland, Jane and Aatos Erkko Foundation and the European Union's Horizon Europe research and innovation programme under grant agreement No 101191726.

S89 – K2

From Stem Cells to Ocular Repair: Biomaterials for Differentiation, 3D Bioprinting and Clinical Translation

Skottman H.
Faculty of Medicine and Health Technology, Tampere University, Finland

Introduction

Corneal blindness is the third leading cause of blindness worldwide, affecting millions of patients and creating a substantial unmet clinical need due to the severe shortage of donor corneas. Stem cell-based therapies hold great promise for treating ocular surface diseases such as bilateral limbal stem cell deficiency (LSCD) and corneal endothelial disorders. However, successful translation of these therapies relies on biomaterials that can mimic native stem cell niches, guide cell differentiation, and support tissue regeneration. Our research focuses on developing biomaterial-based strategies for ophthalmic regenerative medicine by investigating how biomaterials influence stem cell differentiation, recreate key features of the stem cell niche, and support corneal tissue regeneration. In parallel, we are developing bioinks and 3D bioprinting approaches to generate functional corneal tissues and advance the translation of stem cell-based therapies for ocular diseases.

Materials and Methods

Human pluripotent stem cells (hPSCs) are differentiated into corneal limbal stem cells (LSCs), corneal endothelial cells (CECs), and corneal keratocytes (iCKs). Biomaterial-based culture systems are utilized to investigate cell–matrix interactions and to elucidate the role of the limbal niche in regulating stem cell fate and function. Molecular and functional characterization of stem cell-derived corneal cells is performed using established phenotypic, transcriptomic, and functional analyses. In parallel, advanced bioinks are developed for corneal tissue engineering and are being integrated into the Horizon Europe KeratOPrinter project, which aims to generate full-thickness corneal grafts through 3D bioprinting of stem cell-derived corneal cells.

Results

Current studies demonstrate that biomaterial-guided differentiation supports the generation of corneal cell populations exhibiting key molecular, phenotypic, and functional characteristics of native cells. Investigations of limbal niche-inspired biomaterials are providing new insights into the mechanisms regulating stem cell maintenance, differentiation, and regenerative capacity. Ongoing biofabrication studies indicate that stem cell-derived corneal cells can be successfully combined with printable biomaterials to create increasingly complex corneal tissue constructs. Within the KeratOPrinter project, stem cell technologies, biomaterials, and GMP-compatible manufacturing approaches are being integrated to establish scalable processes for the production of bioengineered corneal grafts.

Conclusion

Biomaterials are a key enablers of ocular repair by supporting stem cell differentiation, recreating regenerative microenvironments, and facilitating the fabrication of clinically relevant tissue substitutes. Ongoing advances at the interface of stem cell biology, biomaterials science, and 3D bioprinting are accelerating the development of ophthalmic therapies and bringing bioengineered corneal grafts closer to clinical translation.

Acknowledgements

Our work has been funded by Research Council Finland, Jane and Aatos Erkko Foundation and the European Union’s Horizon Europe research and innovation programme under grant agreement No 101191726.

S89 – O1

A Resorbable and Biomimetic 3D-Printed Hydrogel Scaffold Driving Large-Volume Soft Tissue Repair: Evidence from a Large Animal Study

Cherblanc A.[1], Frobert P.[2], Despert H.[2], Gleizes M.[1], Livret C.[1], Dos Santos M.[1], Thepot A.[1], and Durand C.[1]

[1]Healshape SAS, Lyon, France; [2]Centre Léon Bérard, Lyon, France

Introduction

Breast cancer is the most common cancer in women and often requires total mastectomy. Despite numerous available techniques, many patients decline breast reconstruction due to concerns about postoperative sequelae, multiple surgeries, and the use of synthetic implants. Recent advances in 3D printing and regenerative medicine have paved the way for a novel approach: 3D-printed scaffolds designed to promote autologous tissue ingrowth. Our team has developed a 3D-printed biomimetic prosthesis composed of a hydrogel of sodium alginate and gelatine, both naturally derived biomaterials. This scaffold temporarily provides volume and structural support to soft tissue while promoting cellular infiltration. Its functional properties were evaluated *in vivo*.

Materials and Methods

Subcutaneous implantation studies of scaffolds ranging from 1 to 300 cc were performed in rat and ovine models, with a follow-up period up to 8 months. The biocompatibility profile, tissue response, resorption kinetics, degradation mechanisms, and regenerative properties of the scaffold were assessed through macroscopic observations, imaging (ultrasound and CT scan), blood analysis, and histopathology.

Results

Scaffold volumes up to 300 cc were successfully implanted in both small and large animal models and followed for up to 8 months. Long-term and scale-up studies demonstrated that the implant maintains its softness and mechanical integrity while showing a favourable biocompatibility profile. A moderate postoperative inflammatory response that decreased over time was observed. No necrosis was detected, and a thin capsule formation (< 1 mm) around the prosthesis was noted. Central host tissue colonisation with complete colonisation of the scaffold porosity was observed from day 30. A newly formed mature fibroconnective tissue, with extracellular matrix deposition and aligned collagen fibres, was observed at 243 days (Figure 1). Progressive resorption kinetics (with approximately 50% of resorption at 243 days) and several biomaterial degradation mechanisms were identified, including cellular phagocytosis and hydrolysis. Vascular infiltration towards the centre of the scaffold was observed, with blood vessels reaching diameters of up to 100 µm and a density of 34 ± 6 vessels/mm^2 at 243 days (Figure 2), indicating regeneration of functional tissue.

Conclusion

This 3D-printed bioprosthesis represents a promising biomimetic and safe alternative for breast reconstruction by promoting natural tissue regeneration. The scaffold gradually resorbs over time and demonstrates a favourable tolerance profile without major complications. These results support its potential for future clinical applications.

Figure 1: Histological evaluation of the implanted scaffold 243 days after subcutaneous implantation in an ovine model. A: HE&S sub-gross view of the implantation site showing complete host tissue ingrowth within the scaffold; B: Higher magnification illustrating homogeneous cell infiltration throughout the scaffold pores; C: Masson's trichrome staining demonstrating mature tissue regeneration with extracellular matrix deposition and aligned collagen fibres.

Figure 2: Macroscopic and histological appearance of the implantation site 243 days after subcutaneous implantation in an ovine model. A: Representative macroscopic view showing good integration of the scaffold within surrounding soft tissue; B: Representative histopathological image with CD31 immunostaining of endothelial cells (brown) highlighting a dense vascular network within the regenerated tissue.

S89 – O2

A multifunctional millifluidic imaging window for intravital biomaterial validation in living chicken embryos

Cherubin L.[1], Cama A.[1], Laganà M.[2], Nardini A.[3], Bocconi A.[1], Cortesi C[1]., Martinelli C.[1], Mauri E.[1], Martínez Vázquez R.[3], Cerullo G.[4], Osellame R,[3], Jacchetti E.[1], Conci C.[1], Raimondi M.T.[1]
[1]Department of Chemistry, Materials and Chemical Engineering 'Giulio Natta', Politecnico di Milano, Milano, Italy; [2]Gemma Prototipi, Erba, Italy; [3]Istituto di Fotonica e Nanotecnologie (IFN)-CNR, Milano, Italy; [4]Department of Physics, Politecnico di Milano, Milano, Italy

Introduction

The chicken embryo chorioallantoic membrane (CAM) assay is a well-established *in vivo* model for biomaterials validation. Building on a previously developed miniaturized imaging window for intravital biomaterial assessment in the CAM[1], here we present an evolved platform integrating a millifluidic channel and a drug-permeable PDMS membrane within the Eggs&Beacon synthetic eggshell (Fig.1a). Our device enables simultaneous real-time intravital monitoring and spatially controlled, dose-defined drug administration at the biomaterial-tissue interface, allowing direct correlation between local compound concentration and host tissue response.

Materials and Methods

Our imaging window (Fig.1b) consists of a silicone core with a 100µm-high millifluidic channel, sealed by plasma bonding a 100µm-thick PDMS membrane and a 170µm-thick glass coverslip (Ø20mm). Two side ports enable drug delivery and index-matching fluid perfusion. Atop the PDMS membrane, 3D-microscaffolds[1] (180×180×80µm³) were fabricated via two-photon polymerization to host the biomaterial under investigation in direct contact with the CAM. To assess optical accessibility, the device was placed on the CAM and intravital imaging of the vascularized tissue was performed by two-photon microscopy. Platform delivery validation was performed by perfusing Rhodamine B (C_{inlet}=1mM) at 5–10µL/min. Spectrophotometric quantification of Rhodamine concentration across the membrane and fluorescence imaging of intracellular accumulation in MDA-MB-231 cells seeded on the membrane were supported by a CFD model of transmembrane diffusion kinetics.

Results

Intravital two-photon microscopy confirmed optical access to the CAM vascularized tissue, enabling visualization of vascular network and blood flow quantification by two-photon excitation microscopy and Soret band fluorescence, respectively, as well as fibrillar collagen by second harmonic generation. CFD modeling predicted a delivery rate of 3ng/min at 10µL/min, confirmed experimentally by spectrophotometric quantification at the membrane outlet, achieving 2.2±0.32ng/min. Fluorescence imaging of MDA-MB-231 cells before (Fig.2a) and 30 minutes after (Fig.2b) Rhodamine B perfusion showed progressive intracellular accumulation of the compound further confirming delivery capability of the system.

Conclusion

By providing optical access and controlled local delivery to biomaterials in direct contact with the CAM, our platform enables longitudinal quantitative assessment of the local host tissue response. We validated PDMS-membrane permeability and imaging capability using Rhodamine B as a model compound. Future work will focus on implanting 3D-microscaffolds loaded with biomaterials of interest on the CAM and perfusing bioactive compounds through the millifluidic channel enabling real-time intravital monitoring of the dose-dependent inflammatory and angiogenic response elicited by the hosted biomaterial.

Acknowledgements

ERC, project BEACONSANDEGG,G.A.101053122.

References

[1] Conci C. et al. Adv. Optical Mater. 2022, 10, 2101103.

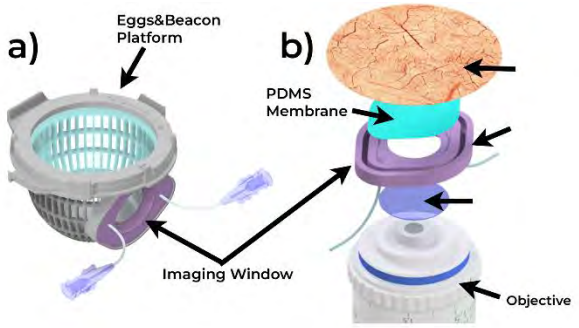

Figure 1. a) CAD design of the Eggs&Beacon platform. b) Exploded view of the imaging window and its components.

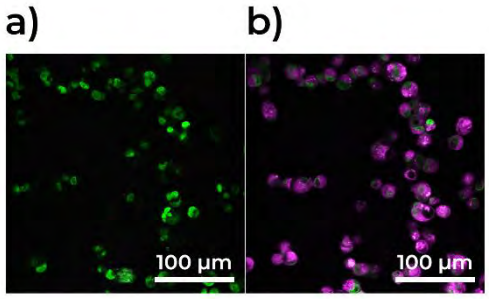

Figure 2. Confocal microscopy (GREEN, Cell Nuclei; MAGENTA, Rhodamine B) of MDA-MB-231 cells a) before and b) 30 minutes after Rhodamine B perfusion through the millifluidic channel.

S89 – O3

A Paper-Based Platform for Skin-on-Chip Modeling of Psoriasis

Beyerstedt S[1], Janss D R[1], Städler B M[1]
[1]Interdisciplinary Nanoscience Center (iNANO), Aarhus University, Aarhus, Denmark

Introduction

The identification of optimal therapies for psoriasis remains largely dependent on trial-and-error approaches, resulting in increased healthcare costs and reduced patient quality of life. While antibody-based biologics are highly effective, their use is often restricted to later treatment lines due to cost and potential side effects. Finding the right treatment for an affected individual remains a challenge, highlighting the need for predictive in vitro platforms capable of replicating human skin physiology and disease-specific responses.

Aim

In this study, we present a paper-based skin-on-chip platform designed to model psoriatic skin and evaluate therapeutic responses. Specifically, we aim to investigate cytokine-mediated interactions between dermal and epidermal layers and assess the efficacy of antibody-based treatments in reverting the psoriatic phenotype.

Materials and Methods

The platform is based on a paper scaffold, where the intrinsic porous network of cellulose fibers serves as a biomimetic three-dimensional extracellular matrix. The device is fabricated using inkjet printing with a water-based ink, followed by autoclaving to define hydrophobic and hydrophilic regions, enabling passive fluid control and air–liquid interface culture conditions. To reconstruct the skin microenvironment, fibroblasts are incorporated within the paper scaffold to form a dermal compartment, while keratinocytes are seeded on the surface to generate a differentiated epidermal layer. This co-culture system enables physiologically relevant dermal–epidermal crosstalk. A psoriatic phenotype is induced using a cytokine cocktail (IL-17A, IL-22, and TNF-α).

Results

The platform supports the co-culture of fibroblasts and keratinocytes within a structured three-dimensional environment and enables air–liquid interface conditions required for epidermal differentiation[1]. The incorporation of a cytokine cocktail establishes an inflammatory microenvironment suitable for modeling psoriasis-related processes. The system provides a controlled setting to study dermal–epidermal interactions under disease-relevant conditions.

Conclusion

This study presents a reproducible, low-complexity paper-based skin-on-chip model for inflammatory skin disease research. The platform lays the groundwork for future studies investigating disease mechanisms and evaluating therapeutic interventions, including antibody-based treatments, in a controlled and potentially patient-specific manner.

Acknowledgements

Independent Research Fund Denmark and Sino-Danish Collaboration.

References

[1] de Dios Andres P, Städler B. Micromotor-Assisted Keratinocytes Migration in a Floating Paper Chip. Small. 2023;19(13):e2201251

S90
Medical device design and engineering

S90 – K1
Supramolecular hydrogels: from biomedical applications to unpredicted phenomena
Dankers P.

S90 – O1

Electrospun polyhydroxyalkanoate membranes for transcutaneous luminescent gas sensing

Akpo E.[1,2,3], Thong Khong M.[3], Schneider L.[4], Lemechko P.[5], Bruzaud S.[4], Rousier R.[2], Darcos V.[3], Rolere S.[1], Texier I.[2], Ricoul F.[2]

[1]CEA, Liten, Univ. Grenoble Alpes, Grenoble; [2]CEA, Leti, Univ. Grenoble Alpes, Grenoble; [3]IBMM, Univ. Montpellier, CNRS, ENSCM, Montpellier; [4]IRDL, UMR CNRS 6027, Univ. Bretagne Sud, Lorient; [5]UBSIDE, Ploemeur, France

Introduction

Quantifying the physiological distribution and real-time dynamics of transcutaneous gases, such as O_2 and CO_2, is essential for understanding mechanisms underlying normal and pathological conditions[1]. Recently, polymeric membranes, such as polystyrene membranes, functionalized with platinum(II)octaethylporphyrin and 8-hydroxypyrene-1,3,6-trisulfonate have emerged as powerful tools for O_2 and CO_2 monitoring[2,3]. These technologies offer painless alternative to invasive methods like arterial blood gas analysis and provide precise detection ranges until 100 hPa for CO_2 and 200 hPa for O_2[4]. However, most of these sensing systems are manufactured using toxic solvents, including dimethylformamide and halogenated solvents.

Aim

This study aims to demonstrate that poly(hydroxyalkanoates) (PHAs) combined with luminescent probes are promising materials for designing biocompatible transcutaneous sensors via electrospinning under green conditions.

Materials and Methods

PHAs such as PHBV (poly(3-hydroxybutyrate-*co*-3-hydroxyvalerate)) and PHO-*g*-PEG (PHA with pendant poly(ethylene glycol) chains) were obtained through biosynthesis and chemical approaches, and extensively characterized (SEC, NMR, DSC). Electrospun membranes containing gas-sensitive probes were fabricated using either conventional toxic solvents or REACH-compliant green solvents. Their sensing performance was evaluated on a dedicated experimental setup.

Results

Combining biosynthesis and chemical approaches, such as Huisgen cycloaddition, allowed access to original PHA structures. The tailored polymers enabled electrospinning under green conditions using environmentally friendly solvents, such as ethanol and ethyl acetate, which are better suited for biomedical applications. In addition, polymer blending strategies enabled better control of the electrospinning process and improved fiber morphology (1 to 4 µm diameter). Finally, oxygen sensors were successfully obtained by incorporating luminescent probes, such as porphyrins, into the electrospun membranes without altering their structure (Fig. 1).

Conclusion

Thanks to our hybrid synthesis approach that offers PHA structural versatility, we obtained through safer manufacturing processes highly promising optically active electrospun membranes for transcutaneous gas detection, potentially enabling enhanced patient safety and comfort.

Acknowledgements

This work has received funding from the French National Research Agency (ANR) under the grant agreement ANR-23-ce06-0005.

References

[1]Lim C.-J. et *al.* Wearable, Luminescent Oxygen Sensor for Transcutaneous Oxygen Monitoring. *ACS Appl. Mater. Interfaces;* 2018; 10; 41026.

[2]Ludačka P. et *al.* Luminescent Oxygen Sensor with Self-Sterilization Properties Based on Platinum(II)octaethylporphyrin in Polymeric Nanofibers. *ACS Mater. Au;* 2025; 5; 331.

[3]Chu C.-S. et *al.*, Optical sensor for dual sensing of oxygen and carbon dioxide based on sensing films coated on filter paper. *Appl. Opt.;* 2017; 56; 1225.

[4] Bernasconi S. et *al.* Recent Technologies for Transcutaneous Oxygen and Carbon Dioxide Monitoring. *Diagnostics;* 2024; 14; 785.

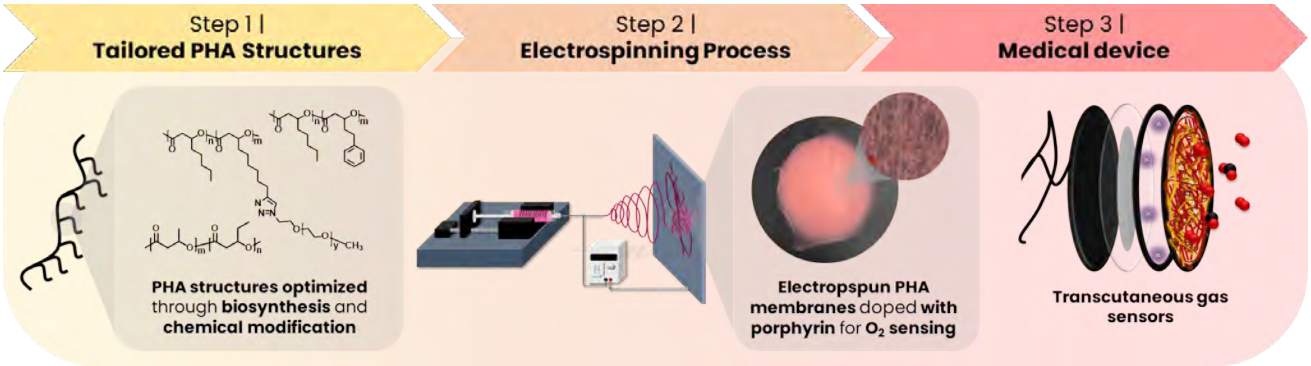

Figure 1. The strategy for designing PHA optical sensors for transcutaneous gas sensing.

S90 – O2

Prototype Development: Phononic Material for Focused Electromechanical Neuromodulation

Bhattarai. P[1], Biggs. M[1]
[1]CÚRAM Research Ireland Centre for Medical Devices, Galway, Ireland

Introduction

A low-intensity focused ultrasound (FUS) operates by directing ultrasonic energy to a targeted brain region, concentrating acoustic power at the focal point while sparing surrounding tissue along the propagation path. This feature enables precise, non-invasive stimulation of deep brain structures, extending beyond the reach of other conventional methods. Despite these advantages, the spatial resolution of FUS decreases at lower frequencies, which limits its utility for fine-scale cortical neuromodulation [1]. To overcome this limitation, we aim to establish a tunable and spatially precise FUS prototype capable of selectively stimulating neuronal and glial cells for the treatment of Parkinson's disease non-invasively.

Materials and Methods

A Fresnel acoustic lens was designed to achieve a focal length of 30 mm with a lateral spatial resolution of 0.5 mm in COMSOL Multiphysics. Lens parameters were iteratively optimized to achieve maximal acoustic focus and intensity. The finalized lens design was fabricated using a stereolithographic Formslab 3D printer. For experimental validation, a single-element piezoelectric transducer was driven by a function generator through a radiofrequency (RF) power amplifier. Acoustic pressure fields were recorded using a calibrated needle hydrophone, mounted on a three-axis motorized positioning system. Spatial pressure maps were acquired using a digital oscilloscope, controlled via BenchVue software for semi-automated scanning. To monitor thermal effects, a negative temperature coefficient (NTC) thermistor was placed at the focal region and interfaced with a microcontroller for real-time temperature acquisition. A 3D printed skull model was integrated with the lens to measure focal intensity in a transcranial neuromodulation setting.

Results

An integrated FUS prototype was developed by coupling the optimized 3D-printed acoustic Fresnel lens with a water-immersed 2.25 MHz ultrasound transducer (Fig1a). Numerical simulations demonstrated that the FUS configuration produced a ten-fold increase in peak acoustic pressure at a focal distance of 30 mm compared to a non-focused ultrasound (nFUS) configuration at the same frequency (Fig1b). The lateral spatial resolution at the focal point was estimated to be approximately 1.25 mm. Experimental measurements using a needle hydrophone confirmed the simulation results (Fig1c). In the XZ plane, a distinct high-intensity focal region was observed at approx. 31mm from the lens, corresponding to the zone of constructive interference. In the XY plane, the focal spot exhibited a lateral spatial resolution of 1.46 mm (Fig1d). Thermal effects at the focus were characterized using a thermistor placed at the focal region. Both continuous and pulsed ultrasound sequences were evaluated. The temperature rise was found to be tunable by adjusting input parameters, including the transducer's driving voltage, pulse repetition frequency (PRF), and burst count (Fig. 2b). Using a peak-to-peak input voltage of 500 mV, the temperature elevation at the focus remained below 5°C, thereby avoiding thermal damage and preserving safe operational thresholds for neuromodulation applications.

Conclusion

In this study, we developed and validated a low-cost, and customizable FUS prototype incorporating an optimized 3D-printed Fresnel acoustic lens for non-invasive neuromodulation in Parkinson's disease.

Acknowledgements

Taighde Éireann – Research Ireland, under Grant number 13/RC/2073_P2.

References

[1]Matt E, Radjenovic S, Mitterwallner M and Beisteiner R. Current state of clinical ultrasound neuromodulation. Front. Neurosci. 18:1420255; 2024

S90 – O3

Kink-resistant, compliant textile grafts for peripheral arterial occlusion disease

Schneider K. Becker F., Riedl P., Wienen D., Schlinkmann R., Gries T.
[1]Institut für Textiltechnik, RWTH Aachen University, Aachen, Germany

Introduction

About 20 % of over 70-year-olds in Germany suffer from peripheral arterial disease (PAD). Without treatment the symptoms range from resting pain, losing the ability to walk, tissue necrosis, to amputation of the affected extremity. Treatment of PAD involves bypassing the affected artery either with an autologous or a textile graft. The current textile grafts however suffer from a low patency rate due to issues such as compliance mismatch, i.e., the inability to radially expand like native arteries.

Aim

We aim to develop a textile graft for over-the-knee applications. Such a graft needs to be kink-resistant due to the flexion and extension of the knee, blood-tight, and have native-like compliance. To obtain native-like compliance over the entire physiological pressure range we use both thermoplastic polyurethane (TPU) and polyethylene terephthalate (PET) as weft yarn during round weaving of the textile graft. The elastic properties of TPU enable native-like compliance at low pressures, while stiff PET provides the needed reduction in compliance at higher pressures. A helical reinforcing fiber with a high bending stiffness, in the shape of a hollow TPU fiber, provides the necessary kink-resistance while maintaining compliance through a low axial stiffness. The hollow structure enables the optimization of the ratio of bending stiffness to axial stiffness through the variation of the wall thickness. An electrospun TPU coating provides the necessary blood impermeability and improves biocompatibility for the textile graft.

Materials and Methods

We investigated the spinnability of fine multifilament TPU and of hollow fiber TPU on a melt spinning machine (single-screw spinning plant, Fourné Maschinenbau GmbH, Germany). The effects of the process parameters, such as the spin finish concentration, draw ratio, temperature and quench rate on the mechanical properties of the resulting fibers were analysed.

Results

We successfully demonstrated the spinnability of hollow fiber TPU with optimized axial to bending stiffnesses. Furthermore, fine multifilament fibers of 50 dtex and 80 dtex were produced with an elongation of >70% and a tenacity of > 15cN/tex. Increasing the spin finish concentration from 10 % to 20 % resulted in a significant increase in fiber cohesion during relaxation, thus increasing processability during weaving.

Conclusion

The developed fine multifilament TPU combined with the hollow fiber reinforcing fibers offer a promising stepping stone for the development of kink-resistant textile grafts with native-like compliance for over-the-knee applications.

Acknowledgements

This project is supported by the Federal Ministry for Economic Affairs and Energy (BMWE) on the basis of a decision by the German Bundestag.

S90 – O4

An electrospun PLGA-hyaluronic acid symatix® platform for consistent and scalable soft tissue regeneration

Ghorbani F.[1], Cirstea M.[1], Behbehani M.[2], McKean R.[1]
[1]The Electrospinning Company Limited, Harwell Science and Innovation Campus, Oxfordshire; [2]Scope Ophthalmics Ltd, Unit 4 Amberley Court, Whitworth Road, County Oak Way, Crawley, West Sussex, RH11 7XL, UK

Introduction

Biological membranes such as collagen matrices and human amniotic membrane are widely used to modulate healing in regenerative medicine. However, their clinical performance can be limited by donor variability, inconsistent material properties, and supply constraints, which affect reproducibility and translational scalability. To address these limitations, a biosynthetic platform has been developed. The design integrates a fibrous architecture, providing a hydrated and mechanically supportive interface for epithelial repair while enabling scalable manufacturing.

Materials and Methods

Electrospun Symatix® PLGA-HA membranes were fabricated by the Electrospinning Company. The platform was evaluated using human epithelial cell models, focusing on ocular surface regeneration. Cellular responses were assessed using wound closure assays, proliferation analysis, immunostaining of epithelial markers, and morphological evaluation. Ex-vivo handling tests were also performed to evaluate suturability, adhesive compatibility, and structural stability under hydrated conditions.

Results

In-vitro studies demonstrated accelerated wound closure and enhanced epithelial cell proliferation on electrospun PLGA-HA matrices. Cells showed improved stratification and organisation, with immunostaining confirming expression of corneal epithelial markers and tight junction proteins indicative of functional barrier restoration. Morphological analysis revealed uniform polygonal cell morphology and continuous surface coverage within three days. Ex-vivo handling assessments demonstrated that membranes could be sutured or applied with tissue adhesive without tearing, maintaining structural stability under hydrated conditions.

Conclusion

These findings suggest that electrospun PLGA-HA membranes promote rapid re-epithelialisation by providing a permissive microenvironment for cell attachment, migration, and differentiation. The fibrous architecture supports cell spreading and spatial organisation. Overall, electrospun PLGA-HA membranes demonstrate improved performance comparable to biological materials while offering promoted manufacturing scalability for clinical translation. Although initial validation focused on ocular surface repair, the underlying design principles are applicable to broader applications, including wound healing, barrier membranes, and mucosal regeneration.

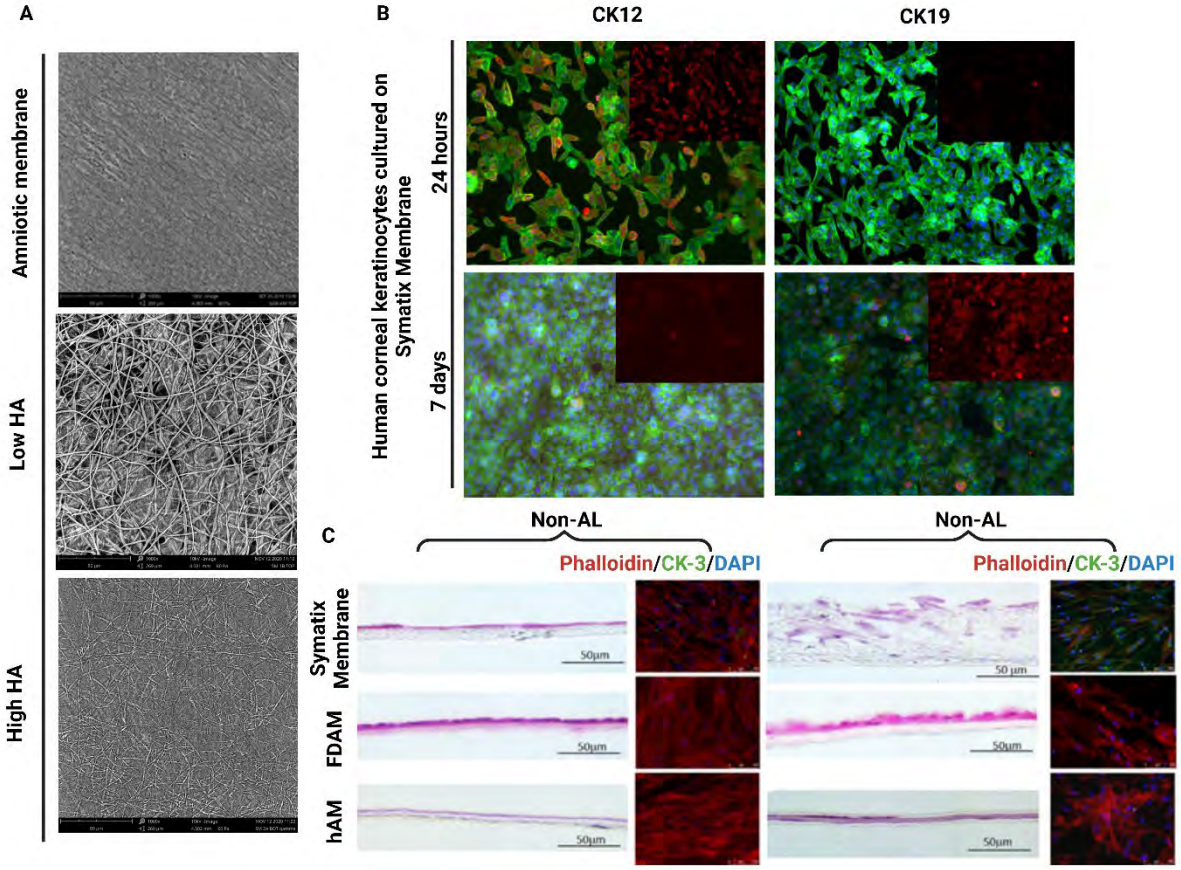

Fig1. Characterisation of the electrospun Symatix® membrane. (A) SEM images of amniotic membrane and electrospun membranes with low and high HA content. (B) Human corneal keratinocytes cultured on Symatix® for 24 h and 7 days showing CK12 and CK19 expression. (C) Histology and immunofluorescence of epithelial layers on Symatix®, freeze-dried amniotic membrane (FDAM), and human amniotic membrane (hAM) under non-air-liquid conditions.

S90 – O5

Reducing dose, enhancing contrast: Biodegradable dendrimers for CT stroke imaging

Silva D.[1,2], Torrado M.[1,3], Gomez-Lázaro M.[1], Pêgo A.P.[1,3], Leiro V.[1]
[1]i3S – Instituto de Investigação e Inovação em Saúde, Universidade do Porto; [3]FCUP – Faculdade de Ciências da Universidade do Porto, Universidade do Porto; [3]ICBAS-UP – Instituto de Ciências Biomédicas Abel Salazar, Universidade do Porto, Porto, Portugal

Introduction

Stroke affects around ¼ of the population throughout their lifetime, being the 2nd leading cause of death worldwide. The Central Nervous System is extremely sensitive, so time is of the essence to apply treatment. This makes an effective and fast diagnosis the utmost priority to reduce the chance of disability or death.
Computed Tomography (CT) can offer excellent image quality and early diagnosis, as well as being inexpensive and widely available. Thus, CT is considered a gold standard for stroke diagnosis, especially when using iodinated contrast agents (CAs) that allow unrivaled microvasculature visualization.
Despite its advantages, current CAs are rapidly cleared by the kidneys, demanding high doses or multiple administrations. These doses are often a burden to patients, especially those already suffering from kidney dysfunction[2].
These drawbacks can be overcome by using proprietary biodegradable dendrimers[2], functionalized with iodinated CAs available clinically, leading to advanced dendritic contrast agents (DCAs). Their intrinsic characteristics (nanosize, globular, highly branched, low-disperse structure) allow for increased tunability and iodine content. Thus, the proposed DCAs are suited to brain CT imaging while reducing dosage[3,4].

Materials and Methods

Our proprietary dendrimers were synthesized until generation 3 and functionalized with an EMA-approved chemically modified CA to obtain our DCA, characterized by NMR, DLS, and TEM. Iodine content was quantified by micro-CT. DCA biocompatibility was verified at different concentrations on neuronal and epithelial cell lines, as well as in mouse cortical neurons through resazurin/LDH release, and live-dead assays. Hemolysis and clotting assays were performed on human red blood cells and recalcified plasma. SLICK mice were injected with a final concentration of ~9 mg I/mL of both EMA-CA and DCA. Image contrast was assessed using a micro-CT scan.

Results

The DCA was successfully synthesized in very good yields and characterized by NMR. It displayed 25x increased contrast in when compared to clinical triiodinated CA at the same concentration (Figure 1).
In all tested cells, DCA was completely biocompatible. There were no significant changes in cell metabolic activity nor cytotoxicity when incubated with our DCA. Additionally, hemocompatibility was further evidenced by hemolysis and clotting assays, showing to be non-hemolytic and non-thrombogenic.
Through initial *in vivo* tests, we observe that DCA at the same timepoint as EMA-CA appears to remain in the body of mice longer, suggesting increased circulation time (Figure 2).

Conclusion

The results obtained show the developed DCA to be a promising candidate for CT stroke diagnosis, as well as great potential for future translation to the clinic.

Acknowledgements

LaCaixa Foundation(CI23-10022); FCT(2024.04832.BDANA); 2021.00472.CEECIND.

References

[1]Davenport, M.S. et al. “Use of Intravenous Iodinated Contrast Media in Patients with Kidney Disease: Consensus Statements from the American College of Radiology and the National Kidney Foundation.” *Radiology* 2020; 294,3; 660-668.
[2]Pêgo, AP, Leiro, V et al. "Biodegradable dendritic structure, methods and uses thereof." U.S. Patent No. 10,858,484. 8 Dec. 2020.
[3]Torrado, M. et al. “DETOX: An innovative dendritic nanosystem for the delivery of BoNT/A LC domain to ischemic neurons” *Biomaterials* 2026; 326.
[4]Leiro, V. et al. “Versatile fully biodegradable dendritic nanotherapeutics” *Biomaterials* 2022; 281.

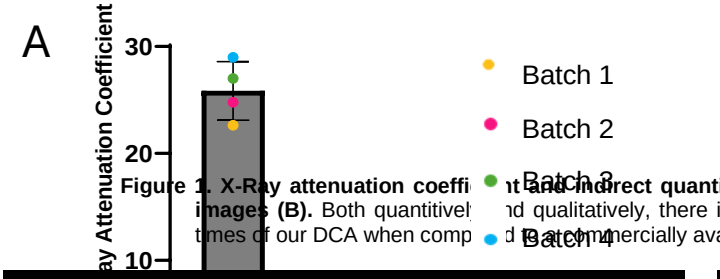

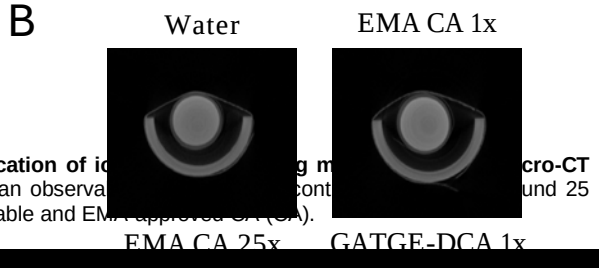

Figure 1. X-Ray attenuation coeffi nt and indirect quantification of io g m cro-CT images (B). Both quantitivel nd qualitatively, there is an observa cont und 25 times of our DCA when comp d to commercially available and EMA approved CA (CA).

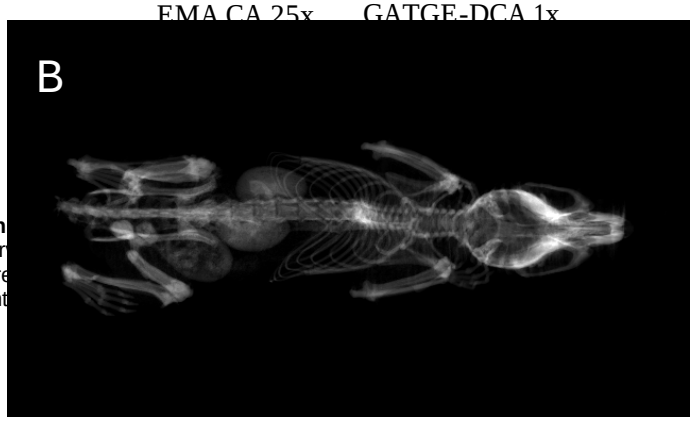

an
ser
here
oint

S91 - K1

Bioactive materials interacting with cells and tissue through surfaces: The role of processes, linking arms and biomolecules

Mantovani D., PhD, FBSE, FASM, FAIMBE, FCAE

Laboratory for Biomaterials and Bioengineering, Canada Research Chair I in Biomaterials and Bioengineering for the Innovation in Surgery, Dept of Min-Met-Materials Engineering & Research Center, Quebec University Hospital, Laval University, Québec City, Canada

Over the last 50 years, biomaterials, prostheses and implants saved and prolonged the life of millions of humans around the globe. The main clinical complications for current biomaterials and artificial organs still reside in an interfacial mismatch between the synthetic surface and the natural living tissue surrounding it. This is particularly true on metallic biomaterials. In fact, despite several works addressed and advanced, the challenge that the interface represents, clinical complications are often observed.

Today, additive manufacturing, nanotechnology, nanomaterials and surface modifications provide new insight to bring effective advances to the current problem of clinical complications and even allow us to envisage strategies for organ shortage. Advanced technologies from materials science, merged with new biological paths towards the development of functional solutions for clinical applications, open new doors for conferring properties to metallic biomaterials that a decade ago were unthinkable. In this talk, the potential of merging 1) novel processes from surface science allowing grafting of biologically active molecules, with 2) advanced processes for metals showing extreme properties and controlled composition to provide engineering solutions to clinical challenged will be depicted.

Focus will be on how additive manufacturing might or might not fulfill the expectations for personalized medicine, on how nanostructures might or might not answer to the demand of metals-by-design implants, and how surface modifications might or might not confer what is required for the metal to interface and integrate the surrounding tissue and cells. The intrinsic goal of this talk is to present an extremely personal look at how the next generation of biodegradable and not-biodegradable metals can impact clinics and surgery, and how the resulting unique properties allowed biomedical functional applications to progress, from their introduction to the promising future that metals may or may not continue to hold for improving the quality of the life of millions worldwide.

S91 - O1

Metal-coordinated surface for stem cell fate control in bone tissue engineering

Moreno R.[1], Zibarov A.[1], Rémy M.[1], Vellutini L.[2], Buffeteau T.[2], Durrieu M.-C [1]
[1]CBMN (UMR 5248), Univ. Bordeaux, Pessac; [2] ISM (UMR 5255), Univ. Bordeaux, Talence, France

Introduction

In tissue engineering, controlling the differentiation of human mesenchymal stem cells (hMSCs) in vitro is crucial to obtain cells differentiated to a desired lineage. This requires the design of biomaterials that support cell growth while providing bioactive signals to guide differentiation. **This project aims** to develop innovative strategies to direct hMSC differentiation toward the osteogenic lineage. One approach involves immobilizing metal ions on surfaces to create a localized and controlled bioactive signal. The initial focus is on zinc, known for its positive effect on osteogenic differentiation in solution and in zinc-doped bioactive glasses through ion release. However, the impact of immobilized zinc on cell differentiation remains unexplored.

Materials and Methods

This project introduces the original concept of zinc immobilization using dipicolylamine-bearing dendrons, capable of coordinating different metal ions, such as Zn^{2+} (Complex C4, Fig. 2). The synthesis of these dendrons has been optimized, and grafted onto silicon substrates using a novel spin-coating silanization method with a phthalimide-terminated silylated coupling agent (Alk-Phtha)[1], providing an efficient alternative to conventional techniques. Surfaces are characterized by colorimetric assays (Coomassie Blue), Water Contact Angle (WCA), X-ray Photoelectron Spectroscopy (XPS), Time-of-Flight Secondary Ion Mass Spectrometry (ToF-SIMS), and Polarization-Modulation Infrared Reflection Absorption Spectroscopy (PM-IRRAS). Cell culture experiments are conducted to evaluate the effects of these functionalized surfaces on hMSC behavior. Osteogenic differentiation is assessed by immunocytochemical fluorescence staining of markers associated with different stages, including RUNX2 and osteopontin (OPN) for osteoblast differentiation, and E11 for early osteocytes. Furthermore, cell viability and proliferation were evaluated by the CCK-8 colorimetric assay.

Results

Surface characterization confirms successful functionalization and metal immobilization. Colorimetric assays quantify amine group density (0.7 NH_2/nm^2), while ToF-SIMS reveals a homogeneous distribution of organic moieties prevenient from the immobilized dendrons. XPS confirms the presence of zinc, WCA shows increased surface complexity leads to higher hydrophobicity, and PM-IRRAS provides insight into the compactness of the grafted layer. hMSCs cultured on these surfaces show enhanced expression of osteogenic markers at early stages, indicating a positive effect of immobilized zinc on differentiation. Complementary qPCR analyses are currently in progress to further quantify gene expression levels.

Conclusion

Future work will explore immobilization of additional metal ions and their combinations to achieve synergistic and antibacterial effects. This approach develops multifunctional surfaces that promote differentiation and prevent infection. Overall, this strategy provides a versatile platform for immobilizing metal complexes, helping elucidate signaling pathways and opening new perspectives in biomaterials design.

References

[1]Kosovari M., Buffeteau T., Thomas L., Guay Bégin A.A.,et al. Silanization Strategies for Tailoring Peptide Functionalization on Silicon Surfaces: Implications for Enhancing Stem Cell Adhesion. *ACS Applied Materials & Interfaces* 2024; 16; 29770–29782.

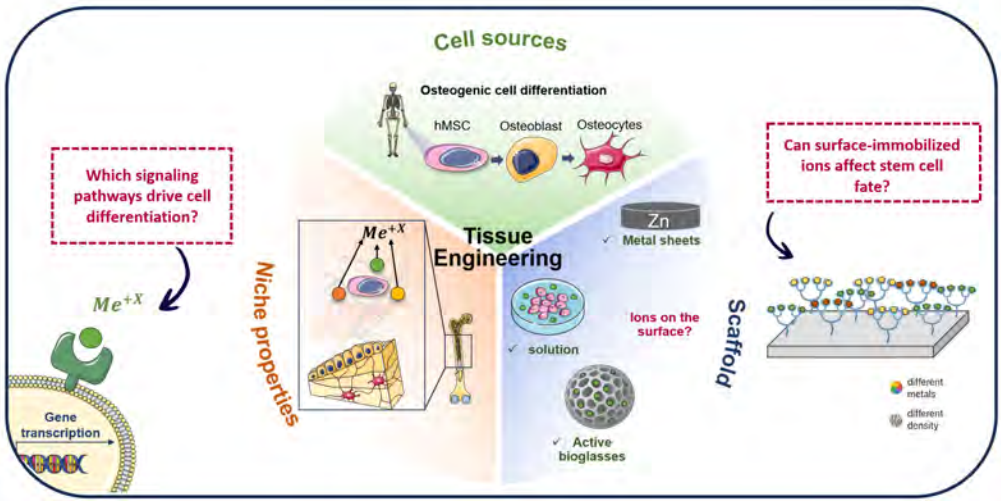

Fig 1. Graphical representation of bone tissue engineering components, showing that this project will study hMSC osteogenic differentiation driven by metal ion-engineered niches, highlighting established scaffolds (MBGs, metal surfaces, and ionic solutions), and introducing the novel concept of surface-immobilized combinatorial metal ions for cell differentiation, as well as probing signaling pathways.

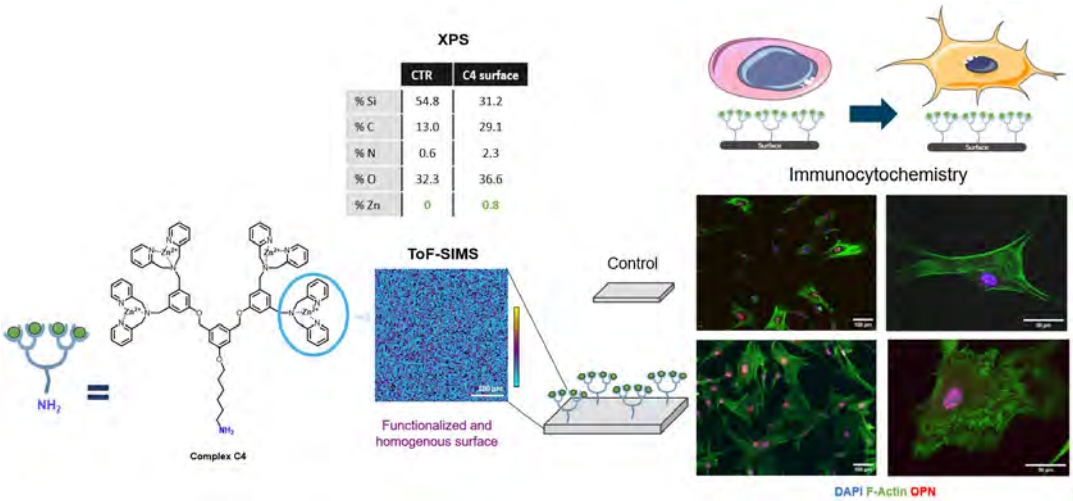

Fig 2. XPS, ToF-SIMS, and immunocytochemistry analyses of C4-functionalized surfaces reveal surface composition, homogeneity, and their influence on hMSC adhesion, cytoskeletal organization, and early osteogenic differentiation.

S91 – O2

Comparative fatigue performance and microstructural characterization of Ti-6Al-4V biomaterial fabricated via advanced manufacturing techniques

Rishad A.R.[1,2], Suwas S.[1,2], Basu B.[2,3]
[1]Dept. of Design and Manufacturing, Indian Institute of Science; [2]Dept. of Materials Engineering, Indian Institute of Science; [3]Materials Research Centre, Indian Institute of Science, Bangalore, India

Introduction

Ti6Al4V is the premier choice for load-bearing orthopaedic implants due to its superior specific strength and biocompatibility. However, the adoption of advanced manufacturing techniques such as Metal Injection Moulding (MIM) and Selective Laser Melting (SLM) introduces unique microstructural challenges, notably internal porosity, which can significantly compromise fatigue life. Establishing a multi-scale correlation between processing-induced defects and long-term mechanical reliability is essential to ensure these advanced manufacturing routes meet stringent clinical standards.

Aim

This study aims to provide a rigorous comparative evaluation of the fatigue behaviour of Ti6Al4V produced through three distinct routes: MIM, conventional wrought processing, and SLM. The objective is to benchmark fatigue limits and identify the specific failure mechanisms associated with each manufacturing pathway.

Materials and Methods

Ti6Al4V specimens were fabricated using MIM, SLM, and by conventional wrought processing. High-cycle fatigue testing was conducted to generate S-N (Stress-Number of cycles) curves for each group. Defect analysis was performed using micro-computed tomography (micro-CT) to quantify internal porosity. Failure mechanisms and crack initiation sites were investigated via Scanning Electron Microscopy (SEM) fractography. These characterisation methods allow for a direct correlation between internal defects and the resulting fatigue life.

Results

Initial comparative testing identified that residual internal porosity in as-fabricated MIM samples serves as the primary driver for fatigue failure. Archimedes density measurements revealed a porosity volume fraction of approximately 5% within the MIM specimens, whereas the conventional wrought samples exhibited 100% theoretical density. SEM-based fractography confirmed that fatigue cracks predominantly initiated at sub-surface pores in the MIM group, which act as local stress concentrators. Consequently, the MIM samples demonstrated significantly lower fatigue limits compared to the dense, defect-free wrought benchmarks. Ongoing work on SLM-fabricated Ti6Al4V is evaluating the critical role of build parameters on fatigue crack propagation.

Conclusion

This research establishes a comprehensive framework for evaluating the fatigue resistance of advanced manufactured Ti6Al4V biomaterials. By correlating the 5% porosity (measured by the Archimedes method) in as-fabricated MIM components with specific failure mechanisms, the study highlights the performance gap relative to 100% dense wrought alloys. These findings provide a critical baseline for future work, which will focus on the efficacy of Hot Isostatic Pressing (HIP) to eliminate internal porosity and Surface Mechanical Attrition Treatment (SMAT) to enhance surface-level fatigue resistance. Together, these post-processing strategies aim to bridge the performance gap between advanced manufactured and conventional wrought alloys, ensuring the mechanical reliability required for next-generation orthopaedic components.

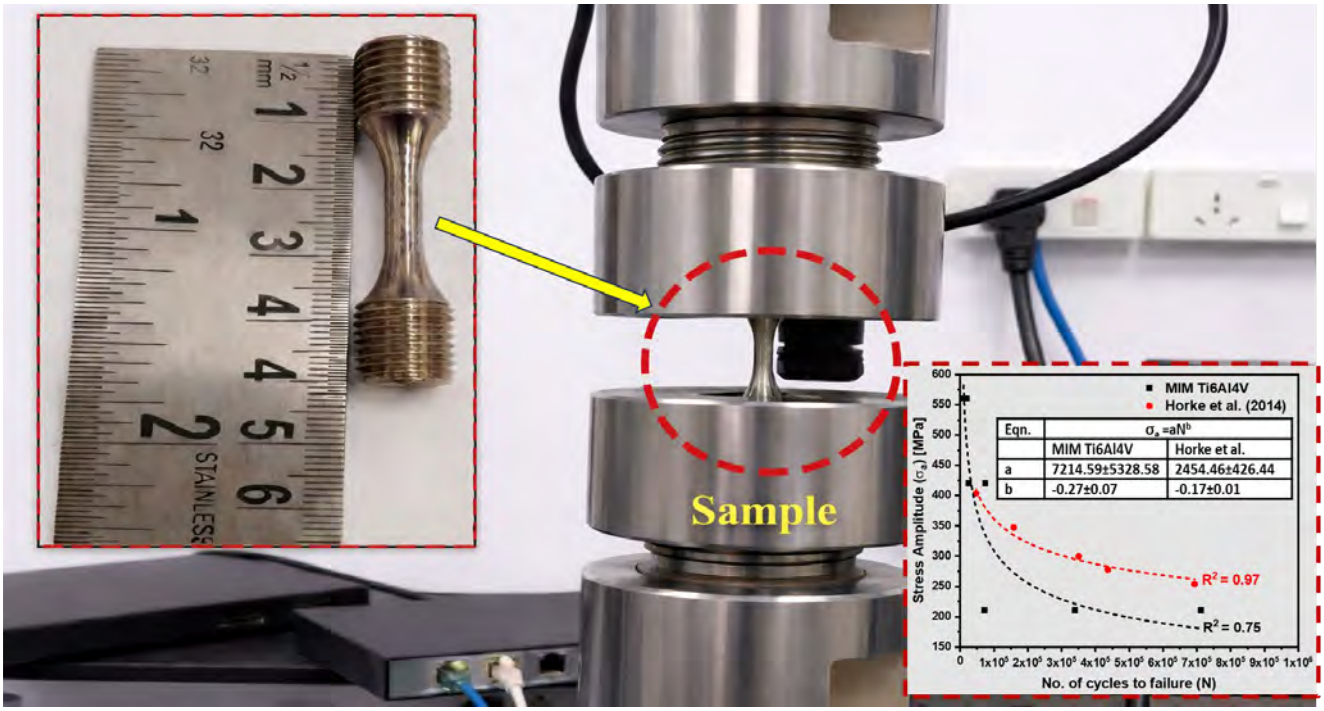

Fig 1. Ti6Al4V specimen mounted on an axial servo-hydraulic fatigue testing machine and the S-N Curve

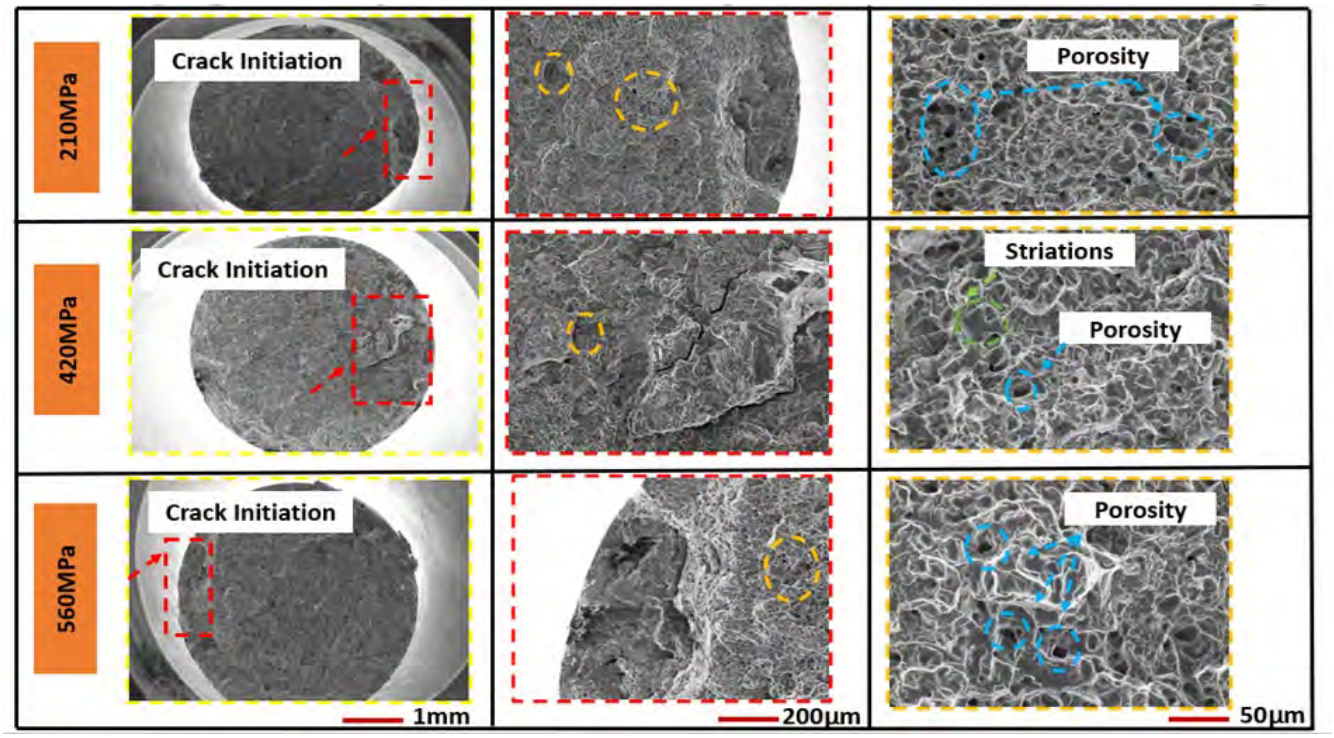

Figure 2. Fractographic analysis of Metal Injection Molded (MIM) Ti6Al4V alloy under varying fatigue stress levels. Top to bottom images represents SEM micrographs of fracture surfaces for samples tested at 210 MPa, 420 MPa, and 560 MPa, illustrating the transition in failure morphology

S91 – O3

Zinc-incorporated porous coatings on Ti-35Nb-7Zr-5Ta alloy produced by micro-arc oxidation for biomedical applications

Bartmański M.[1], Knabe A.[1,2], Ronowska A.[2], Sypniewska J.[1], Pawłowski Ł.[1], Rościszewska M.[1], Mania S.[3], Ünalan I.[4], Grünewald A.[4], Boccaccini A.R.[4]

[1]Dept. of Biomaterials Technology, Gdansk University of Technology, Gdańsk, Poland; [2]Dept. of Laboratory Medicine, Medical University of Gdansk, Gdańsk, Poland; [3]Dept. of Chemistry Technology and Biotechnology of Food, Gdansk University of Technology, Gdańsk, Poland; [4]Institute of Biomaterials, University of Erlangen-Nuremberg, Erlangen, Germany

Introduction

Titanium alloys are widely used in biomedical implants due to their high strength and biocompatibility. However, the commonly used Ti6Al4V alloy has a high elastic modulus (~110 GPa) compared to bone (10–30 GPa) and contains potentially cytotoxic elements (Al, V). The Ti35Nb7Zr5Ta alloy represents a promising alternative with a lower elastic modulus (~55 GPa) and non-toxic composition. To further enhance implant bioactivity, surface modification techniques such as micro-arc oxidation (MAO) are employed to produce porous oxide coatings.

Aim

The aim of this study was to produce and characterize a porous zinc-containing oxide coating on Ti35Nb7Zr5Ta alloy using the micro-arc oxidation (MAO) process in order to enhance its bioactivity for potential biomedical implant applications.

Materials and Methods

Surface modification of Ti-35Nb-7Zr-5Ta titanium alloy was performed by micro-arc oxidation (MAO) in an electrolyte containing glycerophosphate, calcium acetate, and zinc salts (zinc nitrate and zinc acetate). The MAO process was conducted at 300 V for 10 min with a current density of 83 mA/cm². Surface morphology and chemical composition were analyzed by SEM/EDS, while coating thickness was measured using a thickness gauge. Wettability was determined by water contact angle measurements. Corrosion behavior was evaluated in Kokubo's simulated body fluid (SBF). Zinc ion release was measured after 24 and 72 h of incubation. Biological performance was assessed using hFOB 1.19 and MG-63 cells, and antibacterial activity was tested against *Staphylococcus aureus* and *Escherichia coli*.

Results

The results indicate that the MAO process produces a porous and homogeneous coating on Ti35Nb7Zr5Ta alloy. Although pore morphology varied with modification time, coating thickness remained relatively constant (6–7 µm). EDS analysis confirmed the incorporation of calcium, phosphorus, and zinc into the coatings. The modified surfaces showed strong hydrophilicity, with the contact angle decreasing from 60° for the polished alloy to ~10° after MAO treatment. Zinc ion release into the culture medium was observed after 24 h and depended on the processing parameters. No cytotoxic effects toward human osteoblasts or MG-63 cells were detected, and the coatings exhibited antibacterial activity against both tested bacterial strains.

Conclusion

The MAO process successfully produced porous and homogeneous coatings on Ti35Nb7Zr5Ta titanium alloy with incorporated Ca, P, and Zn, resulting in highly hydrophilic surfaces. The developed coatings demonstrated good cytocompatibility and antibacterial activity, indicating their potential for biomedical implant applications.

Acknowledgements

This work was funded by the Polish National Science Centre (project no. 2023/51/D/ST11/02078, SONATA program, M.B).

S91 – O4

Tailored surface finishing of biodegradable Fe–Mn–C alloys through dual organic–inorganic acid pickling

Lucena I.[12], Paternoster C.[1], Multigner M.[2], Mantovani D.[1]
[1]Lab for Biomaterials and Bioengineering, CRC-I, Dept. of Min-Met-Materials Eng., University Hospital Research Center, Regenerative Medicine, Laval University, Québec, Canada; [2]Dept. of Applied Mathematics, Materials Science and Electronic Technology, ESCET, Universidad Rey Juan Carlos, Madrid, España

Introduction

Biodegradable metals are promising materials for temporary implants, enabling controlled degradation while supporting tissue regeneration. Among them, Fe–Mn–C alloys offer suitable mechanical properties and tunable corrosion behaviour for load-bearing applications. However, their surface condition critically governs degradation kinetics, biological response, and further surface processing. Manufacturing-induced oxide layers often introduce chemical heterogeneity and unstable corrosion behaviour. Although acid pickling is widely used for oxide removal, existing protocols are derived from permanent alloys and are not directly applicable to biodegradable systems, where excessive dissolution must be avoided. This work evaluates tailored organic, organic–inorganic, and inhibitor-assisted pickling strategies to achieve controlled oxide removal and reproducible surface states.

Materials and Methods

Hot-rolled Fe–13Mn–1.2C samples were treated using acetic (A) and formic (F) acids, alone or combined with phosphoric (P), nitric (N), or perchloric (C) acids. Inhibitor-assisted pickling was performed using 2,2′-bipyridyl. Treatments were conducted at 24 ± 0.5 °C with immersion times between 1 min and 30 min. Surface characterization included mass loss, contact angle (CA), roughness, scanning electron microscopy (SEM) and X-ray photoelectron spectroscopy (XPS). Electrochemical behaviour was assessed using open-circuit potential (OCP) and potentiodynamic polarization (PDP).

Results

Pickling performance strongly depended on acid composition. Pure organic acids showed limited oxide removal and negligible material loss, whereas organic–inorganic and inhibitor-assisted systems enabled effective descaling. Surface roughness ranged from Ra ≈ 0.4–1.8 µm, with all treatments increasing wettability; mixed systems achieved superhydrophilic behaviour (CA < 10°). SEM confirmed oxide removal and improved surface homogeneity (Fig. 1), particularly for F-based and inhibitor-assisted conditions. XPS revealed composition-dependent surface chemistry, including Fe-enriched and phosphate-modified layers. Electrochemical results followed similar trends: milder treatments showed more stable OCP and lower corrosion currents, while aggressive systems increased activity due to over-etching.

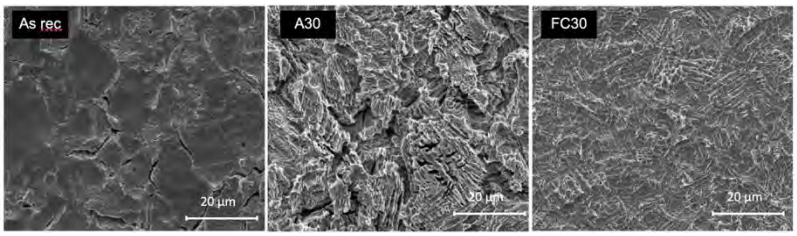

Figure 1. SEM micrographs illustrating the surface evolution of Fe–13Mn–1.2C alloys from the as-received condition, characterized by a heterogeneous and cracked oxide scale, to pickled states: A30 (partial oxide removal with residual oxide islands) and FC30 (uniform and homogeneous surface morphology).

Conclusion

Tailored organic–inorganic and inhibitor-assisted pickling enables controlled oxide removal in biodegradable Fe–Mn–C alloys while preserving substrate integrity. Optimized conditions produce uniform, hydrophilic, and chemically stable surfaces, supporting reproducible degradation and subsequent surface finishing. These findings highlight the need to adapt conventional treatments to biodegradable systems and contribute to the development of reliable surface preparation protocols for temporary implants.

Acknowledgements

LBB, NSERC Canada, Prima Quebec, and the CHU de Quebec Research Centre.

S91 – O5

Tunable bioactive hydrogels via bisphosphonate–metal coordination

Zhong L.[1], van Rijt S.[1]
[1]Dept. of Instructive Biomaterials Engineering, MERLN Institute for Technology-Inspired Regenerative Medicine, Maastricht University, Maastricht, The Netherlands

Introduction

Synthetic hydrogels are water-swollen polymer networks that mimic key features of the extracellular matrix (ECM) and provide a controllable 3D cell culture environment. However,conventional covalent hydrogels are purely elastic and fail to reproduce the dynamic behavior of native tissues. In biological tissues, reversible molecular interactions within the extracellular matrix enable continuous stress relaxation, remodeling, and adaptation to mechanical stimuli. Dynamic and self-healing hydrogels based on metal–coordination interactions introduce such adaptive behaviour, as these reversible bonds can generate networks with broadly tunable mechanical properties, ranging from stiff, covalent-like interactions to soft, supramolecular networks. However, developing cytocompatible hydrogels that combine these dynamic properties with cellular adaptability remains a significant challenge. Bisphosphonates provide a controllable ligand platform for metal coordination, allowing tuning of network dynamics and mechanics.

Aim

To develop cytocompatible hydrogels based on bisphosphonate–metal coordination with customizable mechanical and dynamic properties for bone tissue engineering applications.

Materials and Methods

Alendronic acid (ALA), a bisphosphonate, and RGD peptides were conjugated to multi-arm poly (ethylene glycol) (PEG) to generate a bifunctional polymer (PEG–ALA–RGD). Dynamic hydrogels with diverse mechanical properties were subsequently formed through coordination with various metal ions, including Mg^{2+}, Ca^{2+}, Sr^{2+}, Mn^{2+}, Fe^{2+}, Zn^{2+}, and Cu^{2+}. Cytocompatibility and cellular responses were then evaluated using mesenchymal stem cells (MSCs) cultured within these dynamic hydrogels.

Results

We developed an efficient method for synthesizing multi-arm poly (ethylene glycol) (PEG) functionalized with the bisphosphonate ligand and RGD peptides at controlled ratios. Coordination between these ligands and different metal ions generated transient hydrogel networks exhibiting diverse mechanical and dynamic behaviors, including tunable stiffness, rapid stress relaxation, and self-healing. Furthermore, the hydrogels demonstrated improved stability for long-term culture and excellent cytocompatibility, particularly for RGD-functionalized systems promoting enhanced stem cell adhesion and spreading.

Conclusion

This work establishes a universal platform for metal–coordination based hydrogels with tunable dynamic mechanical properties and excellent cytocompatibility, offering strong potential for regenerative medicine and 3D tissue culture.

Acknowledgements

This work was supported by the European Research Council (ERC) through the Consolidator Grant Nano4Bone (S. van Rijt).

S91 – O6

Detection of enzymes using a wireless, implantable, and bioresorbable device

Babin T.[1], Benamara M.[2], Jadid M.[2], Hoang A.[1], Sauter-Starace F.[1], Texier I.[1]
[1]CEA-LETI/DTIS, Univ. Grenoble Alpes, Grenoble, France; [2]CEA-LETI/DSYS, Univ. Grenoble Alpes, Grenoble, France

Introduction

Anastomotic leaks (leaks of gastric fluid through a suture) are major complications of bariatric surgery that can lead to severe outcomes, including sepsis. Their early detection is critical. The implantation of a sensor adjacent to the suture could early alert the patient and/or medical staff before the onset of clinical symptoms. However, no commercially available portable and rapid diagnostic method currently exists. To address this challenge, we have developed a wireless resorbable sensing device capable of detecting gastric enzymes whose presence outside the suture is indicative of an abnormal leak. The system operates through the enzymatic digestion of a bio-based hydrogel. This approach could enable rapid and reliable diagnosis, while allowing the device to safely degrade in situ after a few weeks of service, thereby eliminating the need for surgical retrieval.

Materials and Methods

The sensing mechanism relies on enzymatically induced modifications of the electrical properties of a gelatin hydrogel encapsulating metallic microparticles. This sensitive hydrogel was then integrated in a resorbable RLC circuit based on molybdenum conductive tracks and electrodes patterned by laser cutting, and insulated by natural candelilla wax and beeswax.

Results

First, we studied the kinetics of digestion of the modified hydrogel by digestive enzymes (trypsin) according to polymer concentration and degree of crosslinking, and metallic microparticle content of the formulation. The conductive hydrogel was then characterized using the EpsiMu method to validate the modification of its electrical parameters during digestion. Both hydrogel conductivity and dielectric permittivity were strongly influenced by the presence of metallic microparticles at frequencies compatible with wireless sensing applications.

Subsequently, the hydrogel was incorporated into the capacitive element of an RLC model circuit (Figure 1). The complete prototype of the wireless sensor was fabricated using bioresorbable materials. Its in vitro validation in representative fluids is on-going.

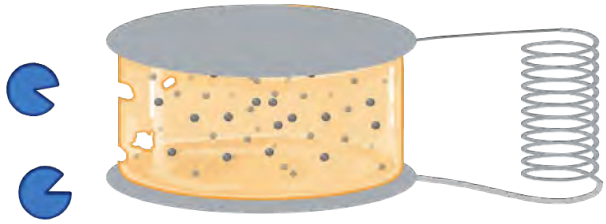

Figure1: Principle of the wireless enzyme sensor

Conclusion

We have developed a wireless sensor capable of detecting enzymatic degradation within a few hours. The device is composed entirely of bioresorbable and biocompatible materials, enabling its potential use for the early detection of anastomotic leakage through the identification of gastric enzymes, then its full resorption after its service time. More broadly, this type of device could be applied to other biomedical contexts requiring enzymatic sensing by adapting the hydrogel design to target different enzymatic environments, thereby extending the versatility of the proposed approach.

S92
Metallic Biomaterials

S91 - K1
Bioactive materials interacting with cells and tissue through surfaces: The role of processes, linking arms and biomolecules

Mantovani D., PhD, FBSE, FASM, FAIMBE, FCAE

Laboratory for Biomaterials and Bioengineering, Canada Research Chair I in Biomaterials and Bioengineering for the Innovation in Surgery, Dept of Min-Met-Materials Engineering & Research Center, Quebec University Hospital, Laval University, Québec City, Canada

Over the last 50 years, biomaterials, prostheses and implants saved and prolonged the life of millions of humans around the globe. The main clinical complications for current biomaterials and artificial organs still reside in an interfacial mismatch between the synthetic surface and the natural living tissue surrounding it. This is particularly true on metallic biomaterials. In fact, despite several works addressed and advanced, the challenge that the interface represents, clinical complications are often observed.

Today, additive manufacturing, nanotechnology, nanomaterials and surface modifications provide new insight to bring effective advances to the current problem of clinical complications and even allow us to envisage strategies for organ shortage. Advanced technologies from materials science, merged with new biological paths towards the development of functional solutions for clinical applications, open new doors for conferring properties to metallic biomaterials that a decade ago were unthinkable. In this talk, the potential of merging 1) novel processes from surface science allowing grafting of biologically active molecules, with 2) advanced processes for metals showing extreme properties and controlled composition to provide engineering solutions to clinical challenged will be depicted.

Focus will be on how additive manufacturing might or might not fulfill the expectations for personalized medicine, on how nanostructures might or might not answer to the demand of metals-by-design implants, and how surface modifications might or might not confer what is required for the metal to interface and integrate the surrounding tissue and cells. The intrinsic goal of this talk is to present an extremely personal look at how the next generation of biodegradable and not-biodegradable metals can impact clinics and surgery, and how the resulting unique properties allowed biomedical functional applications to progress, from their introduction to the promising future that metals may or may not continue to hold for improving the quality of the life of millions worldwide.

S91 - O1

Metal-coordinated surface for stem cell fate control in bone tissue engineering

Moreno R.[1], Zibarov A.[1], Rémy M.[1], Vellutini L.[2], Buffeteau T.[2], Durrieu M.-C [1]
[1]CBMN (UMR 5248), Univ. Bordeaux, Pessac; [2] ISM (UMR 5255), Univ. Bordeaux, Talence, France

Introduction

In tissue engineering, controlling the differentiation of human mesenchymal stem cells (hMSCs) in vitro is crucial to obtain cells differentiated to a desired lineage. This requires the design of biomaterials that support cell growth while providing bioactive signals to guide differentiation. **This project aims** to develop innovative strategies to direct hMSC differentiation toward the osteogenic lineage. One approach involves immobilizing metal ions on surfaces to create a localized and controlled bioactive signal. The initial focus is on zinc, known for its positive effect on osteogenic differentiation in solution and in zinc-doped bioactive glasses through ion release. However, the impact of immobilized zinc on cell differentiation remains unexplored.

Materials and Methods

This project introduces the original concept of zinc immobilization using dipicolylamine-bearing dendrons, capable of coordinating different metal ions, such as Zn^{2+} (Complex C4, Fig. 2). The synthesis of these dendrons has been optimized, and grafted onto silicon substrates using a novel spin-coating silanization method with a phthalimide-terminated silylated coupling agent (Alk-Phtha)[1], providing an efficient alternative to conventional techniques. Surfaces are characterized by colorimetric assays (Coomassie Blue), Water Contact Angle (WCA), X-ray Photoelectron Spectroscopy (XPS), Time-of-Flight Secondary Ion Mass Spectrometry (ToF-SIMS), and Polarization-Modulation Infrared Reflection Absorption Spectroscopy (PM-IRRAS). Cell culture experiments are conducted to evaluate the effects of these functionalized surfaces on hMSC behavior. Osteogenic differentiation is assessed by immunocytochemical fluorescence staining of markers associated with different stages, including RUNX2 and osteopontin (OPN) for osteoblast differentiation, and E11 for early osteocytes. Furthermore, cell viability and proliferation were evaluated by the CCK-8 colorimetric assay.

Results

Surface characterization confirms successful functionalization and metal immobilization. Colorimetric assays quantify amine group density (0.7 NH_2/nm^2), while ToF-SIMS reveals a homogeneous distribution of organic moieties prevenient from the immobilized dendrons. XPS confirms the presence of zinc, WCA shows increased surface complexity leads to higher hydrophobicity, and PM-IRRAS provides insight into the compactness of the grafted layer. hMSCs cultured on these surfaces show enhanced expression of osteogenic markers at early stages, indicating a positive effect of immobilized zinc on differentiation. Complementary qPCR analyses are currently in progress to further quantify gene expression levels.

Conclusion

Future work will explore immobilization of additional metal ions and their combinations to achieve synergistic and antibacterial effects. This approach develops multifunctional surfaces that promote differentiation and prevent infection. Overall, this strategy provides a versatile platform for immobilizing metal complexes, helping elucidate signaling pathways and opening new perspectives in biomaterials design.

References

[1]Kosovari M., Buffeteau T., Thomas L., Guay Bégin A.A.,et al. Silanization Strategies for Tailoring Peptide Functionalization on Silicon Surfaces: Implications for Enhancing Stem Cell Adhesion. *ACS Applied Materials & Interfaces* 2024; 16; 29770–29782.

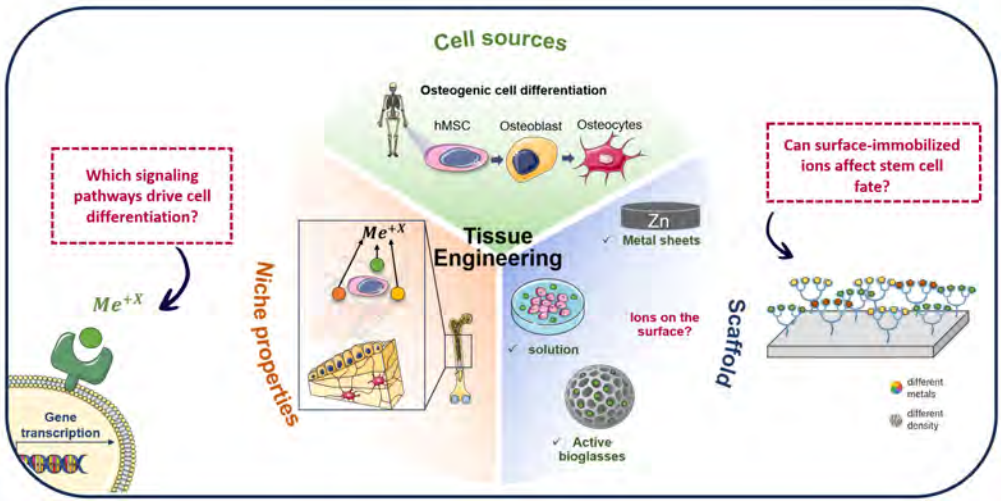

Fig 1. Graphical representation of bone tissue engineering components, showing that this project will study hMSC osteogenic differentiation driven by metal ion-engineered niches, highlighting established scaffolds (MBGs, metal surfaces, and ionic solutions), and introducing the novel concept of surface-immobilized combinatorial metal ions for cell differentiation, as well as probing signaling pathways.

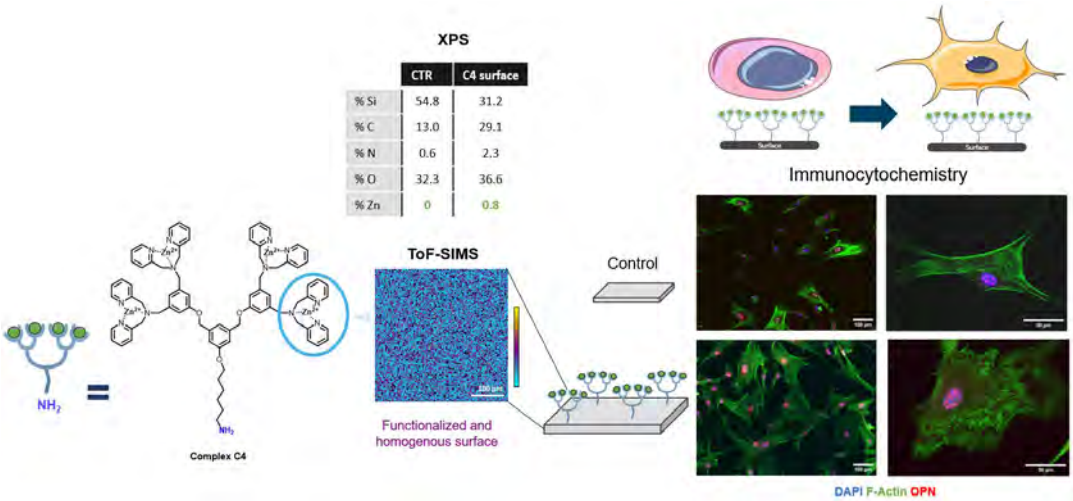

Fig 2. XPS, ToF-SIMS, and immunocytochemistry analyses of C4-functionalized surfaces reveal surface composition, homogeneity, and their influence on hMSC adhesion, cytoskeletal organization, and early osteogenic differentiation.

S91 – O2

Comparative fatigue performance and microstructural characterization of Ti-6Al-4V biomaterial fabricated via advanced manufacturing techniques

Rishad A.R.[1,2], Suwas S.[1,2], Basu B.[2,3]
[1]Dept. of Design and Manufacturing, Indian Institute of Science; [2]Dept. of Materials Engineering, Indian Institute of Science; [3]Materials Research Centre, Indian Institute of Science, Bangalore, India

Introduction

Ti6Al4V is the premier choice for load-bearing orthopaedic implants due to its superior specific strength and biocompatibility. However, the adoption of advanced manufacturing techniques such as Metal Injection Moulding (MIM) and Selective Laser Melting (SLM) introduces unique microstructural challenges, notably internal porosity, which can significantly compromise fatigue life. Establishing a multi-scale correlation between processing-induced defects and long-term mechanical reliability is essential to ensure these advanced manufacturing routes meet stringent clinical standards.

Aim

This study aims to provide a rigorous comparative evaluation of the fatigue behaviour of Ti6Al4V produced through three distinct routes: MIM, conventional wrought processing, and SLM. The objective is to benchmark fatigue limits and identify the specific failure mechanisms associated with each manufacturing pathway.

Materials and Methods

Ti6Al4V specimens were fabricated using MIM, SLM, and by conventional wrought processing. High-cycle fatigue testing was conducted to generate S-N (Stress-Number of cycles) curves for each group. Defect analysis was performed using micro-computed tomography (micro-CT) to quantify internal porosity. Failure mechanisms and crack initiation sites were investigated via Scanning Electron Microscopy (SEM) fractography. These characterisation methods allow for a direct correlation between internal defects and the resulting fatigue life.

Results

Initial comparative testing identified that residual internal porosity in as-fabricated MIM samples serves as the primary driver for fatigue failure. Archimedes density measurements revealed a porosity volume fraction of approximately 5% within the MIM specimens, whereas the conventional wrought samples exhibited 100% theoretical density. SEM-based fractography confirmed that fatigue cracks predominantly initiated at sub-surface pores in the MIM group, which act as local stress concentrators. Consequently, the MIM samples demonstrated significantly lower fatigue limits compared to the dense, defect-free wrought benchmarks. Ongoing work on SLM-fabricated Ti6Al4V is evaluating the critical role of build parameters on fatigue crack propagation.

Conclusion

This research establishes a comprehensive framework for evaluating the fatigue resistance of advanced manufactured Ti6Al4V biomaterials. By correlating the 5% porosity (measured by the Archimedes method) in as-fabricated MIM components with specific failure mechanisms, the study highlights the performance gap relative to 100% dense wrought alloys. These findings provide a critical baseline for future work, which will focus on the efficacy of Hot Isostatic Pressing (HIP) to eliminate internal porosity and Surface Mechanical Attrition Treatment (SMAT) to enhance surface-level fatigue resistance. Together, these post-processing strategies aim to bridge the performance gap between advanced manufactured and conventional wrought alloys, ensuring the mechanical reliability required for next-generation orthopaedic components.

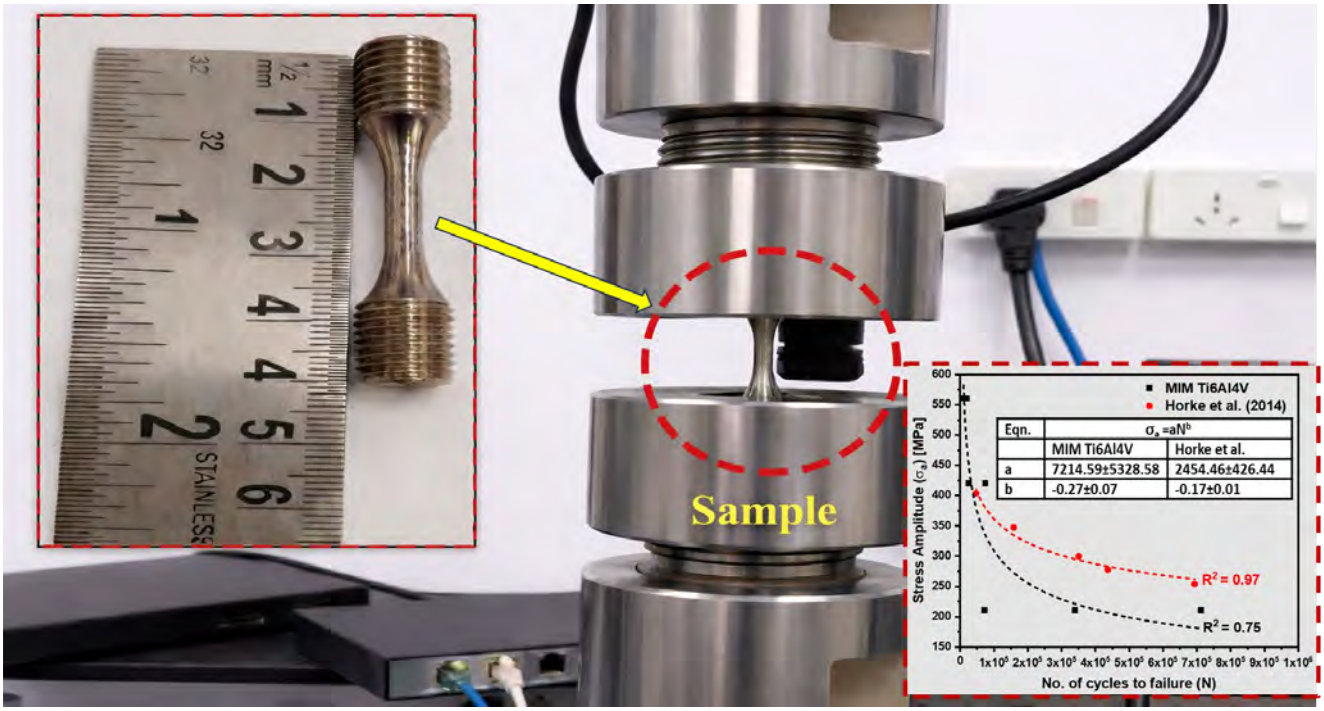

Fig 1. Ti6Al4V specimen mounted on an axial servo-hydraulic fatigue testing machine and the S-N Curve

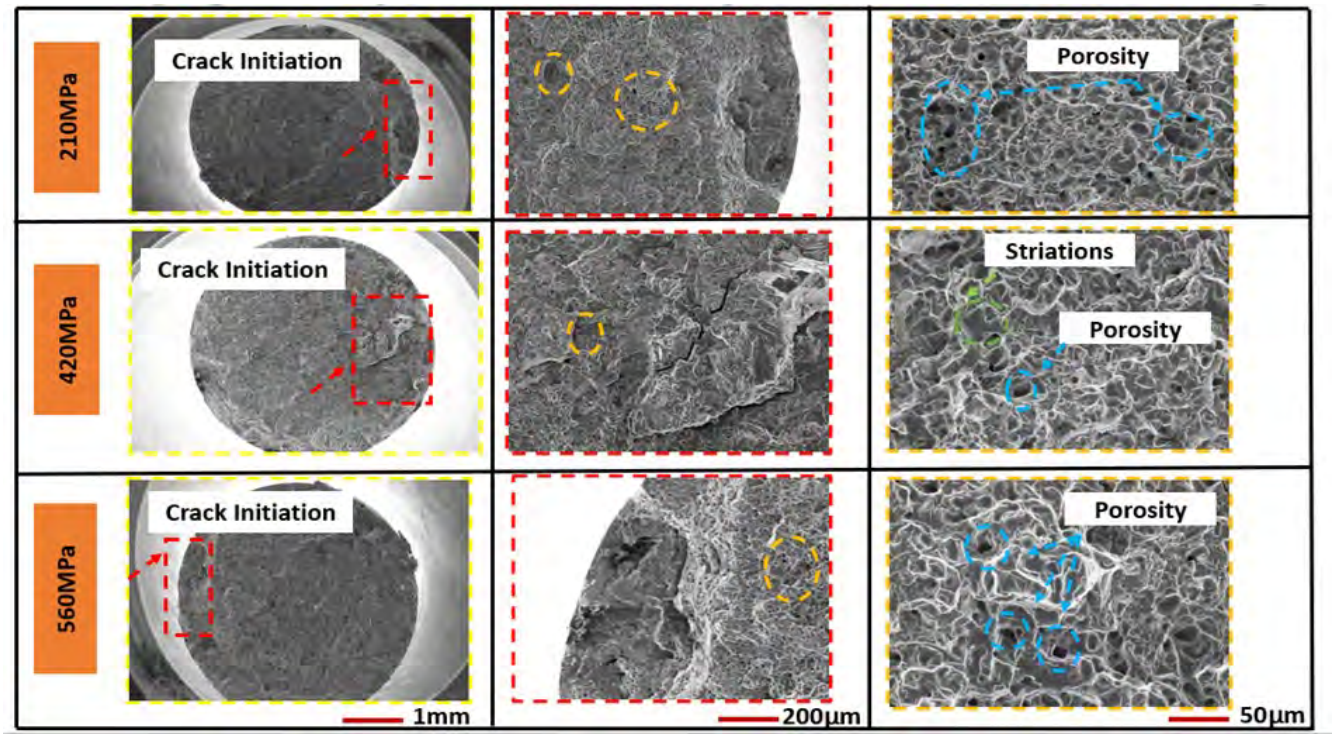

Figure 2. Fractographic analysis of Metal Injection Molded (MIM) Ti6Al4V alloy under varying fatigue stress levels. Top to bottom images represents SEM micrographs of fracture surfaces for samples tested at 210 MPa, 420 MPa, and 560 MPa, illustrating the transition in failure morphology

S91 – O3

Zinc-incorporated porous coatings on Ti-35Nb-7Zr-5Ta alloy produced by micro-arc oxidation for biomedical applications

Bartmański M.[1], Knabe A.[1,2], Ronowska A.[2], Sypniewska J.[1], Pawłowski Ł.[1], Rościszewska M.[1], Mania S.[3], Ünalan I.[4], Grünewald A.[4], Boccaccini A.R.[4]

[1]Dept. of Biomaterials Technology, Gdansk University of Technology, Gdańsk, Poland; [2]Dept. of Laboratory Medicine, Medical University of Gdansk, Gdańsk, Poland; [3]Dept. of Chemistry Technology and Biotechnology of Food, Gdansk University of Technology, Gdańsk, Poland; [4]Institute of Biomaterials, University of Erlangen-Nuremberg, Erlangen, Germany

Introduction

Titanium alloys are widely used in biomedical implants due to their high strength and biocompatibility. However, the commonly used Ti6Al4V alloy has a high elastic modulus (~110 GPa) compared to bone (10–30 GPa) and contains potentially cytotoxic elements (Al, V). The Ti35Nb7Zr5Ta alloy represents a promising alternative with a lower elastic modulus (~55 GPa) and non-toxic composition. To further enhance implant bioactivity, surface modification techniques such as micro-arc oxidation (MAO) are employed to produce porous oxide coatings.

Aim

The aim of this study was to produce and characterize a porous zinc-containing oxide coating on Ti35Nb7Zr5Ta alloy using the micro-arc oxidation (MAO) process in order to enhance its bioactivity for potential biomedical implant applications.

Materials and Methods

Surface modification of Ti-35Nb-7Zr-5Ta titanium alloy was performed by micro-arc oxidation (MAO) in an electrolyte containing glycerophosphate, calcium acetate, and zinc salts (zinc nitrate and zinc acetate). The MAO process was conducted at 300 V for 10 min with a current density of 83 mA/cm². Surface morphology and chemical composition were analyzed by SEM/EDS, while coating thickness was measured using a thickness gauge. Wettability was determined by water contact angle measurements. Corrosion behavior was evaluated in Kokubo's simulated body fluid (SBF). Zinc ion release was measured after 24 and 72 h of incubation. Biological performance was assessed using hFOB 1.19 and MG-63 cells, and antibacterial activity was tested against *Staphylococcus aureus* and *Escherichia coli*.

Results

The results indicate that the MAO process produces a porous and homogeneous coating on Ti35Nb7Zr5Ta alloy. Although pore morphology varied with modification time, coating thickness remained relatively constant (6–7 µm). EDS analysis confirmed the incorporation of calcium, phosphorus, and zinc into the coatings. The modified surfaces showed strong hydrophilicity, with the contact angle decreasing from 60° for the polished alloy to ~10° after MAO treatment. Zinc ion release into the culture medium was observed after 24 h and depended on the processing parameters. No cytotoxic effects toward human osteoblasts or MG-63 cells were detected, and the coatings exhibited antibacterial activity against both tested bacterial strains.

Conclusion

The MAO process successfully produced porous and homogeneous coatings on Ti35Nb7Zr5Ta titanium alloy with incorporated Ca, P, and Zn, resulting in highly hydrophilic surfaces. The developed coatings demonstrated good cytocompatibility and antibacterial activity, indicating their potential for biomedical implant applications.

Acknowledgements

This work was funded by the Polish National Science Centre (project no. 2023/51/D/ST11/02078, SONATA program, M.B).

S91 – O4

Tailored surface finishing of biodegradable Fe–Mn–C alloys through dual organic–inorganic acid pickling

Lucena I.[12], Paternoster C.[1], Multigner M.[2], Mantovani D.[1]
[1]Lab for Biomaterials and Bioengineering, CRC-I, Dept. of Min-Met-Materials Eng., University Hospital Research Center, Regenerative Medicine, Laval University, Québec, Canada; [2]Dept. of Applied Mathematics, Materials Science and Electronic Technology, ESCET, Universidad Rey Juan Carlos, Madrid, España

Introduction

Biodegradable metals are promising materials for temporary implants, enabling controlled degradation while supporting tissue regeneration. Among them, Fe–Mn–C alloys offer suitable mechanical properties and tunable corrosion behaviour for load-bearing applications. However, their surface condition critically governs degradation kinetics, biological response, and further surface processing. Manufacturing-induced oxide layers often introduce chemical heterogeneity and unstable corrosion behaviour. Although acid pickling is widely used for oxide removal, existing protocols are derived from permanent alloys and are not directly applicable to biodegradable systems, where excessive dissolution must be avoided. This work evaluates tailored organic, organic–inorganic, and inhibitor-assisted pickling strategies to achieve controlled oxide removal and reproducible surface states.

Materials and Methods

Hot-rolled Fe–13Mn–1.2C samples were treated using acetic (A) and formic (F) acids, alone or combined with phosphoric (P), nitric (N), or perchloric (C) acids. Inhibitor-assisted pickling was performed using 2,2′-bipyridyl. Treatments were conducted at 24 ± 0.5 °C with immersion times between 1 min and 30 min. Surface characterization included mass loss, contact angle (CA), roughness, scanning electron microscopy (SEM) and X-ray photoelectron spectroscopy (XPS). Electrochemical behaviour was assessed using open-circuit potential (OCP) and potentiodynamic polarization (PDP).

Results

Pickling performance strongly depended on acid composition. Pure organic acids showed limited oxide removal and negligible material loss, whereas organic–inorganic and inhibitor-assisted systems enabled effective descaling. Surface roughness ranged from Ra ≈ 0.4–1.8 µm, with all treatments increasing wettability; mixed systems achieved superhydrophilic behaviour (CA < 10°). SEM confirmed oxide removal and improved surface homogeneity (Fig. 1), particularly for F-based and inhibitor-assisted conditions. XPS revealed composition-dependent surface chemistry, including Fe-enriched and phosphate-modified layers. Electrochemical results followed similar trends: milder treatments showed more stable OCP and lower corrosion currents, while aggressive systems increased activity due to over-etching.

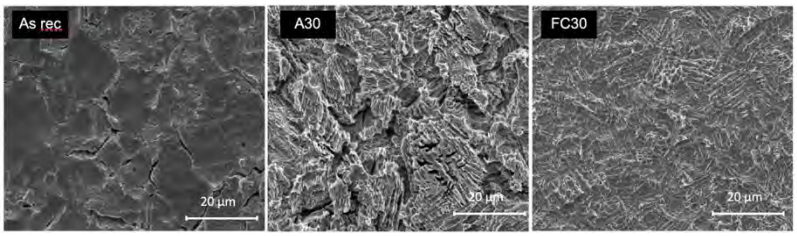

Figure 1. SEM micrographs illustrating the surface evolution of Fe–13Mn–1.2C alloys from the as-received condition, characterized by a heterogeneous and cracked oxide scale, to pickled states: A30 (partial oxide removal with residual oxide islands) and FC30 (uniform and homogeneous surface morphology).

Conclusion

Tailored organic–inorganic and inhibitor-assisted pickling enables controlled oxide removal in biodegradable Fe–Mn–C alloys while preserving substrate integrity. Optimized conditions produce uniform, hydrophilic, and chemically stable surfaces, supporting reproducible degradation and subsequent surface finishing. These findings highlight the need to adapt conventional treatments to biodegradable systems and contribute to the development of reliable surface preparation protocols for temporary implants.

Acknowledgements

LBB, NSERC Canada, Prima Quebec, and the CHU de Quebec Research Centre.

S91 – O5

Tunable bioactive hydrogels via bisphosphonate–metal coordination

Zhong L.[1], van Rijt S.[1]
[1]Dept. of Instructive Biomaterials Engineering, MERLN Institute for Technology-Inspired Regenerative Medicine, Maastricht University, Maastricht, The Netherlands

Introduction

Synthetic hydrogels are water-swollen polymer networks that mimic key features of the extracellular matrix (ECM) and provide a controllable 3D cell culture environment. However,conventional covalent hydrogels are purely elastic and fail to reproduce the dynamic behavior of native tissues. In biological tissues, reversible molecular interactions within the extracellular matrix enable continuous stress relaxation, remodeling, and adaptation to mechanical stimuli. Dynamic and self-healing hydrogels based on metal–coordination interactions introduce such adaptive behaviour, as these reversible bonds can generate networks with broadly tunable mechanical properties, ranging from stiff, covalent-like interactions to soft, supramolecular networks. However, developing cytocompatible hydrogels that combine these dynamic properties with cellular adaptability remains a significant challenge. Bisphosphonates provide a controllable ligand platform for metal coordination, allowing tuning of network dynamics and mechanics.

Aim

To develop cytocompatible hydrogels based on bisphosphonate–metal coordination with customizable mechanical and dynamic properties for bone tissue engineering applications.

Materials and Methods

Alendronic acid (ALA), a bisphosphonate, and RGD peptides were conjugated to multi-arm poly (ethylene glycol) (PEG) to generate a bifunctional polymer (PEG–ALA–RGD). Dynamic hydrogels with diverse mechanical properties were subsequently formed through coordination with various metal ions, including Mg^{2+}, Ca^{2+}, Sr^{2+}, Mn^{2+}, Fe^{2+}, Zn^{2+}, and Cu^{2+}. Cytocompatibility and cellular responses were then evaluated using mesenchymal stem cells (MSCs) cultured within these dynamic hydrogels.

Results

We developed an efficient method for synthesizing multi-arm poly (ethylene glycol) (PEG) functionalized with the bisphosphonate ligand and RGD peptides at controlled ratios. Coordination between these ligands and different metal ions generated transient hydrogel networks exhibiting diverse mechanical and dynamic behaviors, including tunable stiffness, rapid stress relaxation, and self-healing. Furthermore, the hydrogels demonstrated improved stability for long-term culture and excellent cytocompatibility, particularly for RGD-functionalized systems promoting enhanced stem cell adhesion and spreading.

Conclusion

This work establishes a universal platform for metal–coordination based hydrogels with tunable dynamic mechanical properties and excellent cytocompatibility, offering strong potential for regenerative medicine and 3D tissue culture.

Acknowledgements

This work was supported by the European Research Council (ERC) through the Consolidator Grant Nano4Bone (S. van Rijt).

S91 – O6

Detection of enzymes using a wireless, implantable, and bioresorbable device

Babin T.[1], Benamara M.[2], Jadid M.[2], Hoang A.[1], Sauter-Starace F.[1], Texier I.[1]
[1]CEA-LETI/DTIS, Univ. Grenoble Alpes, Grenoble, France; [2]CEA-LETI/DSYS, Univ. Grenoble Alpes, Grenoble, France

Introduction

Anastomotic leaks (leaks of gastric fluid through a suture) are major complications of bariatric surgery that can lead to severe outcomes, including sepsis. Their early detection is critical. The implantation of a sensor adjacent to the suture could early alert the patient and/or medical staff before the onset of clinical symptoms. However,no commercially available portable and rapid diagnostic method currently exists. To address this challenge, we have developed a wireless resorbable sensing device capable of detecting gastric enzymes whose presence outside the suture is indicative of an abnormal leak. The system operates through the enzymatic digestion of a bio-based hydrogel. This approach could enable rapid and reliable diagnosis, while allowing the device to safely degrade in situ after a few weeks of service, thereby eliminating the need for surgical retrieval.

Materials and Methods

The sensing mechanism relies on enzymatically induced modifications of the electrical properties of a gelatin hydrogel encapsulating metallic microparticles. This sensitive hydrogel was then integrated in a resorbable RLC circuit based on molybdenum conductive tracks and electrodes patterned by laser cutting, and insulated by natural candelilla wax and beeswax.

Results

First, we studied the kinetics of digestion of the modified hydrogel by digestive enzymes (trypsin) according to polymer concentration and degree of crosslinking, and metallic microparticle content of the formulation. The conductive hydrogel was then characterized using the EpsiMu method to validate the modification of its electrical parameters during digestion. Both hydrogel conductivity and dielectric permittivity were strongly influenced by the presence of metallic microparticles at frequencies compatible with wireless sensing applications.

Subsequently, the hydrogel was incorporated into the capacitive element of an RLC model circuit (Figure 1). The complete prototype of the wireless sensor was fabricated using bioresorbable materials. Its in vitro validation in representative fluids is on-going.

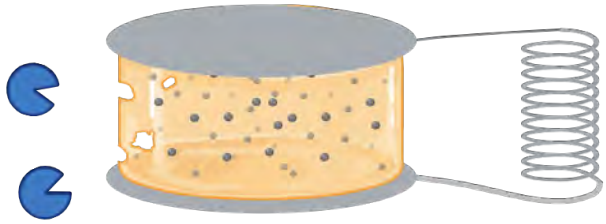

Figure1: Principle of the wireless enzyme sensor

Conclusion

We have developed a wireless sensor capable of detecting enzymatic degradation within a few hours. The device is composed entirely of bioresorbable and biocompatible materials, enabling its potential use for the early detection of anastomotic leakage through the identification of gastric enzymes, then its full resorption after its service time. More broadly, this type of device could be applied to other biomedical contexts requiring enzymatic sensing by adapting the hydrogel design to target different enzymatic environments, thereby extending the versatility of the proposed approach.

S93
Nanostructured and nanocomposite biomateriasl

S93 – K1
Engineering dynamic intervaces with 3D printing

Selhuber-Unkel C.
Heidelberg University – ISEAM – Germany

S93 – O1

Organic polydopamine nanobots for remotely controlled propulsion and targeted bio-interfacing

Battaglini M.[1], Shchori GS.[2], Carmignani A.[1], Rosenfeld D.[2,3,4], Ciofani* G.[1]

[1]Istituto Italiano di Tecnologia, Smart Bio-Interfaces, Viale Rinaldo Piaggio 34, 56025 Pontedera, Italy; [2]School of Biomedical Engineering, Faculty of Engineering, Tel Aviv University, Tel Aviv, 6997801 Israel; [3]Center for Nanoscience and NanotechnologyTel Aviv UniversityTel Aviv 6997801, Israel; [4]The Sagol School of NeuroscienceTel Aviv UniversityTel Aviv 6997801, Israel

Introduction

Most nanobots developed to date rely on inorganic nanomaterials, particularly magnetic or metallic nanoparticles, to enable remote actuation and navigation. While effective, these materials raise important concerns related to long-term toxicity, limited biodegradability, and potential immune responses, which may hinder their clinical translation. In contrast, fully organic nanobots remain largely unexplored, despite offering promising advantages in safety and biocompatibility. Polydopamine nanoparticles (PDNPs), formed through the spontaneous self-polymerization of dopamine, possess intrinsic biocompatibility, biodegradability, antioxidant properties, and strong photothermal conversion under near-infrared (NIR) light. These characteristics make PDNPs particularly attractive building blocks for the development of next-generation biohybrid or fully organic nanorobotic systems, where minimizing toxicity while maintaining functional responsiveness is essential for clinical applicability. In this work, we introduce a novel class of organic nanobots (PDA-BOTs) capable of controlled propulsion under NIR irradiation. Unlike previously reported systems that require magnetic fields or catalytic chemical reactions for motion, PDA-BOTs exploit light-induced photothermal gradients to generate propulsion in a minimally invasive and externally controllable manner. We further analyze how particle size, laser parameters, and the formation of a human plasma protein corona influence their maneuverability and evaluate their ability to accumulate within glioblastoma spheroids. Additionally, we develop a computational model to characterize and predict their propulsion dynamics.

Materials and Methods

PDNPs of four controlled sizes (100, 200, 500, and 1000 nm) were synthesized using a Stöber-based polymerization protocol (representative images in **Figure 1a**). Their physicochemical features were assessed by SEM, TEM, DLS, and zeta potential analysis. Protein corona formation was achieved by incubating PDNPs with Cy3-labelled human plasma. NIR-induced propulsion was quantified by tracking particle trajectories and speeds across varying laser power and positioning conditions. To complement experimental data, we developed a computational model of PDA-BOT movement that accounts for laser-induced thermal gradients, Brownian motion, and hydrodynamic interactions. Model predictions were compared with experimentally acquired particle trajectories. For proof-of-concept targeting, PDA-BOTs were guided toward U87 glioblastoma spheroids under NIR irradiation, and particle accumulation near spheroid borders was quantified (representative images in **Figure 1b**).

Results

PDA-BOTs exhibited NIR-driven propulsion in aqueous environments, with speed and direction tunable as a function of laser orientation, irradiation power, and PDNP diameter. The computational model accurately recapitulated experimentally observed trajectories and speed distributions, confirming that propulsion arises from localized photothermal gradients and size-dependent hydrodynamic effects. Across all tested sizes, PDA-BOTs could be remotely steered with high spatial precision. In biological assays, NIR-guided PDA-BOTs accumulated around U87 glioblastoma spheroids, confirming their suitability for targeted navigation in complex 3D microenvironments.

Conclusion

PDA-BOTs represent the first fully organic, remotely controllable nanobots based on polydopamine. Their biocompatibility, photothermal responsiveness, and steerability in both abiotic and protein-rich environments,

combined with a predictive computational model describing their propulsion dynamics, highlight their strong potential for biomedical applications, including targeted drug delivery, cancer therapy, and minimally invasive micro-manipulation.

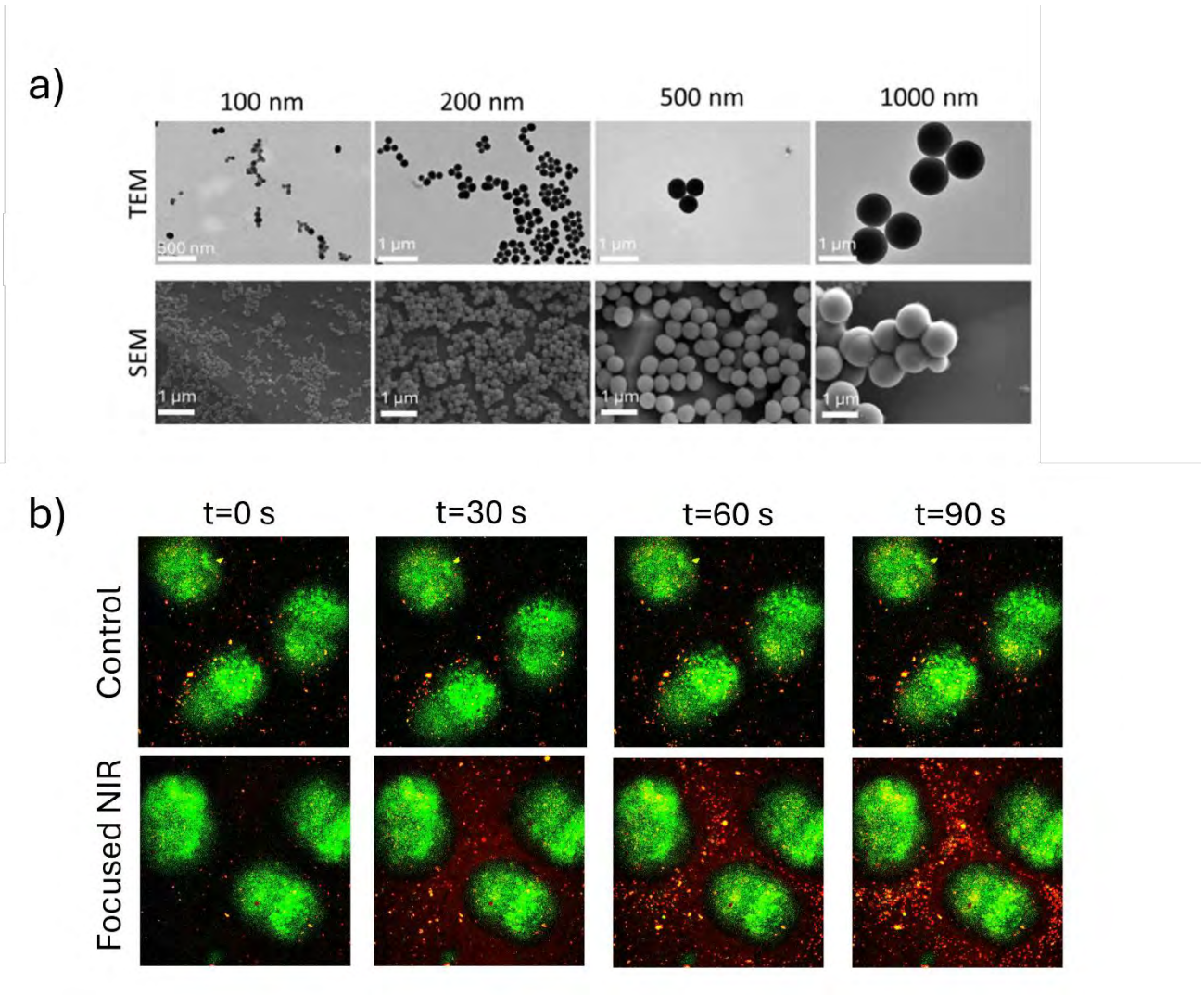

Figure 1. a) SEM (top panels) and TEM (bottom panels) of PDNPs of various diameters. b) confocal images showing the accumulation of PDNPs with and without NIR irradiation in proximity to glioblastoma spheroids at various time points (in green spheroids, in red PDNPs)

S93 – O2

Sequence-engineered Au/TiO_2 hybrid nanocomposites on diatomaceous biosilica: a green synthesis strategy for enhanced antibacterial performance

Brzozowska W.[1], Olszewska M.[1], Railean V.[2,3], Skowronski L.[1]
[1]Division of Surface Science, Faculty of Chemical Technology and Engineering, Bydgoszcz University of Science and Technology, Bydgoszcz, Poland; [2]Centre for Modern Interdisciplinary Technologies, Nicolaus Copernicus University in Toruń, Toruń, Poland; [3]Department of Infectious, Invasive Diseases and Veterinary Administration, Institute of Veterinary Medicine, Nicolaus Copernicus University in Toruń, Toruń, Poland

Introduction

The development of antimicrobial biomaterials capable of preventing bacterial colonization on medical and environmental surfaces remains a major challenge. Hybrid nanostructures combining metallic and metal-oxide phases offer a promising strategy due to their complementary antibacterial mechanisms and potential synergistic effects. In this work, environmentally sustainable Au/TiO_2 hybrid nanocomposites supported on porous diatomaceous biosilica were developed. Particular attention was devoted to the influence of nanoparticle formation sequence on nano-architecture and antibacterial performance.

Materials and Methods

Au/TiO_2/DE nano-microcomposites were synthesized using three complementary strategies differing in the sequence of nanoparticle formation: (i) reduction of Au^{3+} on diatomaceous earth followed by TiO_2 deposition via the sol–gel route (1stAu+2ndTiO$_2$), (ii) formation of TiO_2/DE followed by in situ reduction of Au^{3+} (1stTiO_2+2ndAu), and (iii) simultaneous synthesis of both components. Gold nanoparticles were obtained through green reduction using plant extracts from *Rosa canina* and *Ribes nigrum*, eliminating the need for conventional chemical reducing agents. A total of 25 materials, including reference matrices and single-component systems, were prepared. The materials were characterized using SEM, TEM, XRD, XPS and ICP-OES. Antibacterial activity was evaluated by determining minimal inhibitory concentrations (MIC) against *Escherichia coli*, *Proteus mirabilis*, *Klebsiella pneumoniae* and *Staphylococcus aureus*.

Results

Microscopy analyses confirmed successful incorporation of Au and TiO_2 nanoparticles within the hierarchical porous structure of diatomaceous biosilica. ICP-OES measurements demonstrated that nanoparticle loading strongly depended on synthesis sequence and the plant extract used.

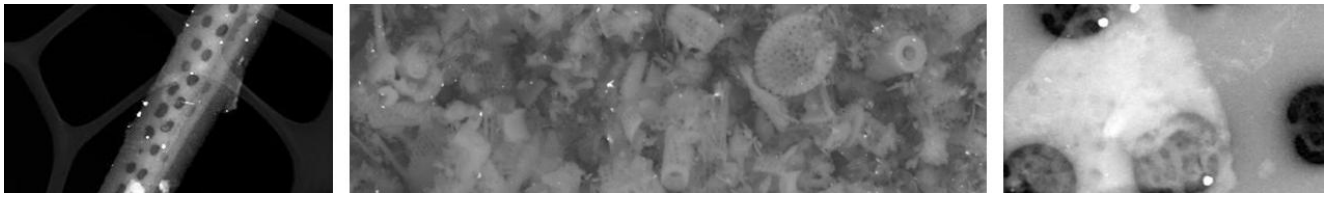

The highest Au contents (up to ~14–16 wt%) were obtained for materials synthesized via the 1stTiO_2+2ndAu route using *Ribes nigrum* extract, while sequential deposition of Au prior to TiO_2 resulted in significantly lower metal loading. Antibacterial assays revealed that reference DE and TiO_2/DE materials were inactive under dark conditions, whereas Au-containing materials exhibited measurable antimicrobial activity. Importantly, hybrid Au/TiO_2/DE composites showed enhanced antibacterial performance compared with Au/DE systems, indicating a synergistic interaction between the metallic and oxide phases. The most active materials, synthesized via the 1stTiO_2+2ndAu route, achieved MIC values of 6.25 mg mL^{-1} against *Proteus mirabilis*, corresponding to a two-fold improvement compared with Au-only systems.

Conclusion

The results demonstrate that the sequence of nanoparticle formation is a key parameter controlling nano-architecture, nanoparticle accessibility and antibacterial activity in Au/TiO_2 hybrid systems. Importantly, the study provides a rational strategy for tailoring hybrid nanostructures by controlling synthesis sequence, enabling the design of sustainable antimicrobial biomaterials based on biogenic silica matrices. The developed sequence-

engineered green synthesis approach offers a versatile platform for designing functional nanomaterials with potential applications in antimicrobial coatings and biomaterial surfaces.

Acknowledgements

This research was supported by the National Science Centre, Poland, within the MINIATURA 8 project no. 2024/08/X/ST5/00109.

S93 – O3

Effect of crosslinker molecular weight in nanogel plasticizers on the glass transition temperature of polymer matrices

Sreejith Sasidharan Lathikumari, Manju Saraswathy*
Division of Dental Products, Department of Biomaterial Science and Technology, Biomedical Technology Wing, Sree Chitra Tirunal Institute for Medical Sciences and Technology, Thiruvananthapuram, Kerala, India, PIN-695012
*Corresponding author: manjus@sctimst.ac.in

Introduction

A high amount of plasticizers is used to impart flexibility to various biomedical devices, including blood bags (30–50%), catheters (up to 80%), and denture soft-liners (40–47%). Traditionally, plasticizers are low molecular weight compounds incorporated into polymer networks to enhance softness and flexibility by reducing intermolecular and intramolecular interactions, thereby lowering the glass transition temperature (Tg). However, the use of phthalate ester plasticizers raises significant concerns due to their tendency to leach out from the material over time. This migration not only alters the mechanical properties and elasticity of the material but is also associated with health risks such as reproductive toxicity and developmental disorders. To address these issues, various strategies have been explored, including the use of high molecular weight or branched plasticizers, surface modification, and covalent incorporation of plasticizers into polymer networks. In this context, our study focuses on developing flexible polymer systems using biocompatible nanogel additives as an alternative to conventional small-molecule plasticizers.

Methods

Polyethylene glycol dimethacrylate (PEGDMA) with varying molecular weights (550 Da to 20,000 Da) was synthesized via an addition reaction between polyethylene glycol (PEG) and 2-isocyanatoethyl methacrylate (IEM), catalyzed by triethylamine. Nanogels were then prepared using tert-butyl acrylate and PEGDMA at a molar ratio of 90:10. A total of 20 mol% mercaptoethanol was used as a chain transfer agent to control the size of the nanogels. These nanogels were subsequently covalently incorporated into the parent polymer network to evaluate their plasticizing effect.

Results

The incorporation of covalently cross-linked nanogels significantly influenced the glass transition temperature (Tg) of the parent polymer matrix. The extent of Tg modulation depended on both the concentration of nanogels and the molecular weight of the PEGDMA crosslinker used in the synthesis. The findings demonstrate that nanogel-based plasticizers can effectively tune the thermal and mechanical properties of polymer systems without the drawbacks associated with conventional plasticizer migration.

Conclusion

This study highlights the potential of biocompatible nanogel additives as a novel class of plasticizers for biomedical applications. By eliminating the need for small-molecule plasticizers such as phthalates, this approach addresses toxicity and migration concerns while enabling precise control over material properties. These findings provide valuable insights for designing safer and more effective flexible polymer systems for medical use.

Acknowlegement

We sincerely acknowledge the Director and the Head, BMT Wing, SCTIMST, as well as the Department of Biotechnology, Government of India, for their financial support in conducting this study.

References

1. Erythropel et al; Leaching of the plasticizer di(2-ethylhexyl) phthalate (DEHP) from PVC medical devices. *Environmental Health Perspectives*, 2014, **122**, 593–599.
2. M. Rahman, C. S. Brazel; The plasticizer market: an assessment of traditional plasticizers and research trends to meet new challenges. *Progress in Polymer Science*, 2004, **29**, 1223–1248.

S93 – O4

Metal-oxide nanoparticles` effect on in vivo and in vitro applications

Tóth Zs.-R[1], Kovács L.[2], Dénes K.SZ.[2], Szentes S.[2], Buba E.[1,3], Páll E.[4], Dreancă A.[4], Baia L.[1,3,5], Magyari K.[1,6]
[1]Interdisciplinary Research Institute on Bio-Nano-Sciences, Babes-Bolyai University, Cluj-Napoca, Romania; [2]Babeș-Bolyai University, Faculty of Medical and Health Sciences/ICDI-SNA Research Center, Cluj-Napoca, Romania; [3]Doctoral School in Physics, Faculty of Physics, Babes-Bolyai University, Cluj-Napoca, Romania; [4]Faculty of Veterinary Medicine, University of Agricultural Science and Veterinary Medicine, Cluj-Napoca, Romania; [5]Faculty of Physics, Babes-Bolyai University, Cluj-Napoca, Romania; [6]INSPIRE Research Platform InfoBioNano4Health & Biomedical Imaging, Babeș Bolyai University, Cluj-Napoca

Introduction

Cerium oxide nanoparticles (CeO_2 NPs) are one of the metal oxides with significant potential for wound healing. CeO_2 NPs were successfully applied in the four different stages of wound healing because of their several properties (antibacterial, antifungal, cell viability, and antioxidant). In our previous study[1], we demonstrated that the morphology of the particles has a critical role in their applicability. We concluded that the specific characteristic, originating from the specific morphology, could affect the antifungal, antibacterial, and hemocompatibility of the CeO_2 NPs.

Aim Therefore, this study (Fig. 1) focuses on the differently shaped CeO_2 NPs cell viability and necrosis properties in cultured cells and antioxidant properties. We also subjected the materials to in vivo tests, examining their wound healing and antioxidant properties in paraquat induced gut leakage and Parkinson models in Drosophila.

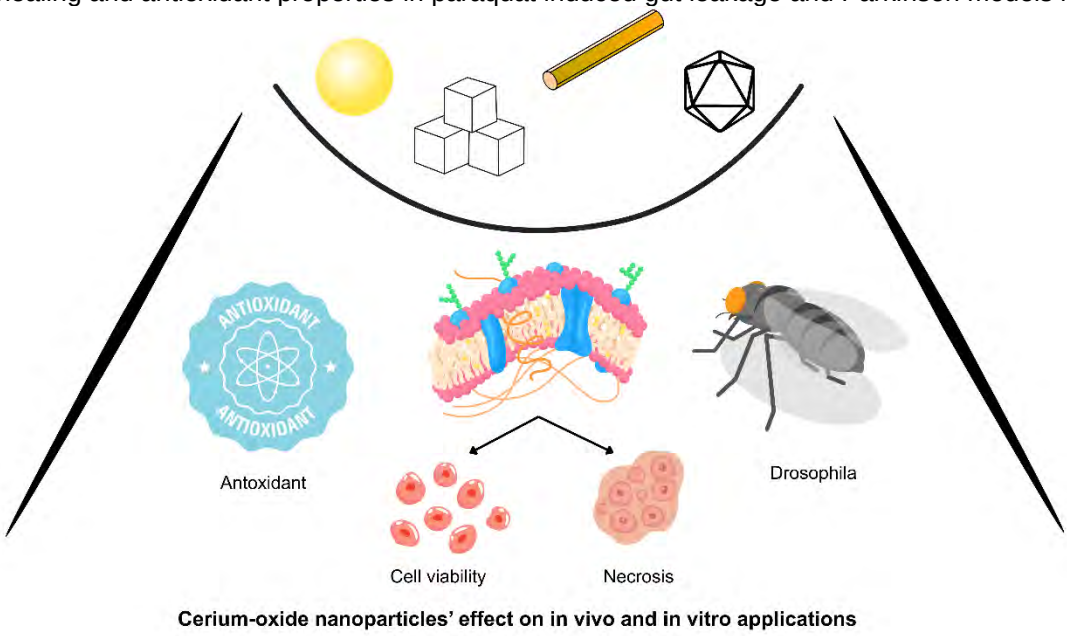

Figure 1: Graphical abstract of the study

Materials and Methods

Hydrothermal/Solvothermal synthesis methods were used to synthesise nanosphere, nanocube, nanorod and polyhedral CeO_2 NPs. The obtained particles were investigated with X-ray diffraction, transmission electron microscopy, Fourier Transform Infrared -, X-ray photoelectron - and UV-Vis Spectroscopy. The obtained nanoparticles' antioxidant character was determined by chemical method (CUPRAC method) and biologically (total antioxidant nonenzymatic capacity determination). The cell viability was investigated on Human keratinocytes cells, and the necrosis was determined on Human Umbilical Vein Endothelial Cells. The nanoparticles' effect on gut leakage and Parkinson disease was investigated using Paraquat fed Drosophila models pre-treated, co-treated and post-treated with CeO_2 by chronic oral administration.

Results

The different nanoparticles result different values of surface charge, Ce^{3+}/Ce^{4+} ion distribution, area/volume ratio, and crystallinity. Since various biological processes usually take place on the surface, the above-mentioned characters may be important for their application. It can be stated that regardless of morphology, all particles show high cell viability. Only in the case of the nanosphere particle was an antioxidant character observed. Furthermore, we noticed that necrosis was also shape-dependent. Consistent with their antioxidant potential, the administration of CeO_2 NPs was beneficial in Paraquat induced toxicity in Drosophila models. A moderate effect was observed in the gut leakage effect, however post-treatment of Paraquat induced Parkison disease model was improved considerably by chronically ingesting spherical CeO_2 nanoparticles.

Conclusion

As we have established in our preliminary study[1], the shape of the nanoparticles, like the size of the nanoparticles, affects their usability. Thus, it can be concluded that they can be safely used in vitro in terms of cell viability and in vivo (physiological effect on Drosophila). The antioxidant character cannot be achieved by using the above-mentioned forms.

Acknowledgements

This work was supported by a grant of the Ministry of Research, Innovation and Digitization, CNCS - UEFISCDI, project number PN-IV-P1-PCE-2023-1377, within PNCDI IV.

References

[1]Tóth Zs.-R., Feraru A., Saszet K., Veréb G., Vodnar D. C., Todea M., Timar-Gabor A., Sand D., Dreanca A., Magyari K., Baia L., Relation between shape-tailored CeO_2 nanoparticles morphology and hemocompatibility and antimicrobial effect, Biomaterials Advances, 171, 2025, 214229

S93 – O6

Hybrid Black Phosphorus Quantum Dots–Polydopamine Platform for Tunable Neural Activity Modulation

[1]A. Bigham, [1]A. Mariano, [1]S. Martino, [2]R. Fabbri, [2]V. Benfenati, [1]L. Ambrosio, [1]M.G. Raucci
[1]Institute of Polymers, Composites and Biomaterials, National Research Council of Italy (IPCB-CNR), Viale John Fitzgerald Kennedy 54, Mostra d'Oltremare Pad. 20, 80125 Naples, Italy.
[2]Institute for Organic Synthesis and Photoreactivity, National Research Council of Italy (ISOF-CNR), Via Piero Gobetti, 101, 40129 Bologna, Italy.

Introduction

Black phosphorus quantum dots (BPQDs) are emerging nanomaterials for biomedical applications, particularly in neural cell modulation, due to their biocompatibility, tunable electronic properties, and photothermal and photodynamic effects. They can interact with cellular membranes, regulate oxidative stress, and enable controlled drug or gene delivery.

In this study, we develop a BPQD-based nanocomposite functionalized with polydopamine to enhance antioxidant properties. The nanocomposites biofunctionality is evaluated with neuron-like cells and astrocytes, which are essential for brain homeostasis. The balance between astrocyte proliferation and differentiation plays a critical role in gliotic and inflammatory responses in neurological disorders.

We investigate the impact of the nanocomposite on cell proliferation, differentiation, and inflammation pathways. This work aims to modulate neuron–astrocyte interactions, offering new strategies for neurodegenerative disease treatment and neural tissue engineering.

Materials and Methods

Black phosphorus nanosheets (BPNSs) were purchased from XFnano and stored under oxygen-free and dark conditions to prevent oxidation. BPQDs were subsequently synthesized via a two-step microwave-assisted process, yielding homogeneous quantum dots. The BPQDs–polydopamine (BPQDs–PDA) nanocomposite was prepared via in situ polymerization of dopamine around BPQDs, driven by electrostatic interactions arising from their differing zeta potentials. Briefly, dopamine hydrochloride was added to a Tris-base solution containing BPQDs and allowed to polymerize for several hours. The resulting nanocomposite was collected, rinsed with deionized water, and dried under vacuum.

Results

BPQDs and BPQDs–PDA were characterized in terms of their physicochemical, morphological, and biological properties. Raman spectroscopy confirmed the characteristic BPQDs peaks at 360, 434, and 462 cm^{-1}, while BPQDs–PDA exhibited additional bands at 1374 and 1590 cm^{-1}, consistent with polydopamine incorporation. Transmission electron microscopy (TEM) further validated the successful synthesis and morphology of the nanostructures. Raman spectroscopy and imaging demonstrated rapid cellular uptake within a few hours. In vitro studies using SH-SY5Y cells and astrocytes revealed that BPQDs enhance cell viability, morphology, and differentiation. Notably, astrocytes displayed a well-spread morphology, indicative of active interaction with the surrounding microenvironment.

Conclusion

BPQDs and BPQDs–PDA exhibit strong potential for neural cell modulation, combining favorable physicochemical properties, efficient cellular internalization, and high biocompatibility. Their ability to enhance cell viability, morphology, and differentiation underscores their promise as multifunctional platforms for neural tissue engineering and the treatment of neurodegenerative disorders.

Acknowledgements

This study was supported by AFOSR (USA Air Force Office of Scientific Research) through the project ASTROTALK - Modulation of astrocytes as new paths to dialogue with the brain - Grant Agreement nr. FA9550-23-1-0736

References

Bigham, A., Mariano, A., Boccaccini, A. R., Ambrosio, L., & Raucci, M. G. (2026). Black phosphorus in theragenerative medicine: a multi-organ perspective on disease modulation and tissue repair. Bioactive Materials, 58, 422-471.

S93 – O7

Au-nanoparticle-doped PVA:PEG nanofibers for wound healing applications

Filova E.[1], Slepicka P.[2], Slepickova Kasalkova N.[2], Jencova V.[3], Lisnenko M.[3], Hauzerova S.[3], Lukas D.[3], Nebesarova J.[4], Rimpelova S.[5,6], Wu Y-C.[1], Bacakova L.[1]

[1]Laboratory of Biomaterials and Tissue Engineering, Institute of Physiology CAS, Prague, Czech Republic; [2]Department of Solid State Engineering, University of Chemistry and Technology Prague, Prague, Czech Republic; [3]Faculty of Science, Humanities and Education, Department of Chemistry, Technical University of Liberec, Liberec, Czech Republic; [4]Laboratory of Electron Microscopy, Faculty of Science, Charles University, Prague, Czech Republic, [5]Department of Biochemistry and Microbiology, University of Chemistry and Technology Prague, Prague, Czech Republic; [6]Department of Tissue Engineering, Institute of Experimental Medicine of the Czech Academy of Sciences, Prague, Czech Republic

Introduction

Treatment of chronic wounds is long-term and is often ineffective due to infection. Therefore, new ways of chronic wound treatment are being studied.

Aim

We aimed to develop and characterize polyvinyl alcohol-polyethylene glycol (PVA:PEG)-based nanofibers containing Au either inside the nanofibers or on their surface.

Materials and Methods

PVA:PEG nanofibers were prepared via electrospinning at different PVA:PEG ratios. Au was sputtered into the PEG solution or onto the nanofibers. Some nanofibers were heat-treated. The materials were characterized using SEM, AFM, and EDS; their cytocompatibility was analyzed *in vitro* via metabolic activity measurement and immunofluorescence staining of collagen (NHDF cells) and von Willebrand factor (HUVEC cells); antimicrobial properties of the materials were also evaluated using a drop method.

Results

Au was relatively homogeneously distributed within the material. Heat treatment affected both the surface morphology and chemistry of the prepared samples, as revealed by SEM, EDX, and AFM techniques. Metabolic activity/cell viability of cells growing with the tested nanomaterial samples was similar to that growing on the control tissue culture polystyrene surface. The HUVECs were positively stained for von Willebrand factor, and NHDFs were proven to produce collagen on day 7. Antimicrobial tests demonstrated partial inhibition of bacterial growth, as evidenced by a reduction in colony-forming units.

Conclusion

The PVA:PEG–based nanofibers with homogeneously dispersed AuNPs at different Au concentrations were successfully prepared. The materials with higher Au content appear promising for the treatment of chronic wounds with or without bacterial infection.

Acknowledgements

Supported by the Project No CZ.02.01.01/00/22_008/0004562, within the Jan Amos Komensky Operational Program of the Ministry of Education, Youth and Sports of the Czech Republic, co-funded by the European Union.

S94
Polymeric biomaterials – natural

S94 – K1

Di Meo C.[1], Calabrese L.[2], Vassallo V.[3], La Gatta A.[1], E. Bedini[2] and Schiraldi C[1].
[1]Dept. of Experimental Medicine, University of Campania "Luigi Vanvitelli", Naples, Italy; [2]Dept. of Chemical Science, University of Naples "Federico II", Naples, Italy; [3]Dept. of Life Sciences, Health and Health Professions, Link Campus University, Rome, Italy

Introduction
The development of biomimetic hydrogels that combine extracellular matrix (ECM) mimicry with injectability and printability remains a major challenge in tissue engineering (TE). Three-dimensional constructs offer unique opportunities to better recapitulate native tissue architecture and dynamic cell-matrix interactions compared to conventional two-dimensional models. In particular, there is growing interest in assessing the role of glycosaminoglycans (GAGs) in modulating cell behavior, especially within printable 3D systems.

Materials and Methods
Interpenetrating networks based on GAGs, were designed as functional biomaterials for injectable medical device, TE and advanced *in vitro* models. A comprehensive physicochemical characterization of the GAGs was performed, including molecular weight distribution and macromolecular conformation. Methacryloyl-modified gelatin (GelMA), was combined with high molecular weight hyaluronic acid and either unsulfated chondroitin (BC) or extractive chondroitin sulfate (CS), enabling a direct comparison of GAG origin and sulfation. The resulting formulations were investigated in terms of rheological properties, printability, and network stability. GAGs release was analyzed by capillary electrophoresis. Both acellular and cell-seeded constructs were fabricated using extrusion-based 3D printing and subsequently evaluated under static and dynamic culture conditions. Depending on the specific *in vitro* model, human primary or stem or cancer cells were employed. Cell viability and metabolic activity were assessed using Live/Dead staining and Alamar Blue assay, while molecular analyses were performed through RT-PCR, Western blotting, and immunofluorescence.

Results
All injectable formulations demonstrated to support cell viability also showing anti-inflammatory activity in pathological chondrocytes and synoviocytes cultures. The novel bioinks exhibited excellent injectability, enabling the fabrication of stable 3D constructs with controlled cylindrical architecture. UV-induced crosslinking produced robust and tunable networks, characterized by controlled GAGs release, stable degradation profiles and mechanical properties. Cell-laden constructs showed high viability, and sustained proliferation over time. Human fibroblast-laden scaffolds were cultivated for up to three weeks under both static and dynamic culture conditions in bioreactors. Notably, dynamic culture significantly enhanced the expression of collagen I and elastin, compared to static conditions. These effects were particularly pronounced in constructs containing BC.

Conclusion
Diverse *in vitro* models were exploited to evaluate the functional role of biofermentative chondroitin beside hyaluronan, demonstrating anti-inflammatory activity and stem cells differentiation ability. The ECM-mimetic GelMA-based systems, containing HA and BC or CS as key components, represent sustainable and versatile platforms that combine biomimicry, printability, and biological functionality. Beyond TE, these constructs are promising tools for tailored cut *in vitro* models that recapitulate ECM, within a specific microenvironment, to study pathological conditions and support drug screening.

Acknowledgment
This work was partially supported by the MIMIT project "CROSS GAG" CUP B29J24001220005 (Italy) and BioTekNet ScpA.

S94 – O1

Design of chitosan and hyaluronic acid nanoparticles able to overcome the mucus barrier for the treatment of lung infections

Della Sala F.[1], Barretta M.[1], Marino G.[1,2], di Gennaro M.[1], Paradiso R.[3], Borriello G.[3], Borzacchiello A[1].
[1]Institute of Polymers, Composites and Biomaterials, National Research Council (IPCB-CNR), Naples, Italy; [2]Department of Environmental, Biological and Pharmaceutical Sciences and Technologies (DiSTABiF), University of Campania "L. Vanvitelli", Caserta, Italy; [3]Istituto Zooprofilattico Sperimentale del Mezzogiorno (IZSM), Naples, Italy.

Introduction

Bacterial respiratory infections cause morbidity, especially in chronic obstructive pulmonary disease (COPD) and acute respiratory distress syndrome (ARDS) patients. This critical health challenge is further exacerbated by the alarming rise of multidrug-resistant (MDR) pathogens and the hypersecretion of dense lung mucus. While naturally serving as a primary defense mechanism, pathological mucus transforms into a breeding ground for bacteria and an impenetrable barrier for conventional treatments[1]. To overcome this barrier, chitosan (CS) and hyaluronic acid (HA) offer a promising biopolymeric solution. CS provides mucoadhesivity and intrinsic antimicrobial action by disrupting bacterial cell walls, while the hydrophilicity of HA facilitates mucus penetration and prevents bacterial adhesion[2].

Aim

This study presents the rational design of intrinsically bioactive, drug-free nanoparticles (NPs) using a synergistic CS and HA combination. By fine-tuning these biopolymers, a nanoplatform was developed and engineered to navigate the mucus barrier and deliver direct, localized antimicrobial effects, minimizing the reliance on conventional antibiotics.

Materials and Methods

The NPs were fabricated via the ionic gelation method, specifically engineering the use of HA by systematically modulating its molecular weight and concentration. The NP size over time, surface charge, and morphology were characterized (dynamic light scattering, microscopy), as well as chemical interactions (Fourier-transform infrared spectroscopy). Furthermore, mucoadhesion, mucus penetration, antioxidant activity (DPPH assay), and biological activity on human lung fibroblasts (HLF) were investigated. Finally, bacterial growth reduction against *Staphylococcus aureus* and *Pseudomonas aeruginosa* was evaluated.

Results

Physicochemical characterization confirmed the formation of stable, spherical nanostructures driven exclusively by electrostatic interactions. By modulating HA content and molecular weight, NP size and surface charge were successfully tuned from 75 to 210 nm and +21.8 to +33.9 mV, respectively. Formulations with the lowest HA content (2.4%) achieved an optimal balance, demonstrating strong initial mucoadhesion followed by superior mucus penetration (Figure 1), reaching approximately 250% after 24 hours. Furthermore, the nanosystems exhibited excellent cytocompatibility on both healthy and COPD HLF (viability consistently >75%, Figure 2), preserving a healthy cell morphology. The drug-free NPs also displayed a robust antioxidant capacity capable of neutralizing free radicals. Finally, NPs demonstrated effective antimicrobial activity against *Staphylococcus aureus* and *Pseudomonas aeruginosa*.

Conclusion

The engineered drug-free CS/HA NPs achieve an optimal balance of initial mucoadhesion and superior mucus penetration. Exhibiting excellent cytocompatibility with HLF and robust antioxidant capacity, this intrinsically bioactive nanoplatform offers a safe, innovative strategy to bypass the mucus barrier and treat respiratory infections without relying on conventional antibiotics.

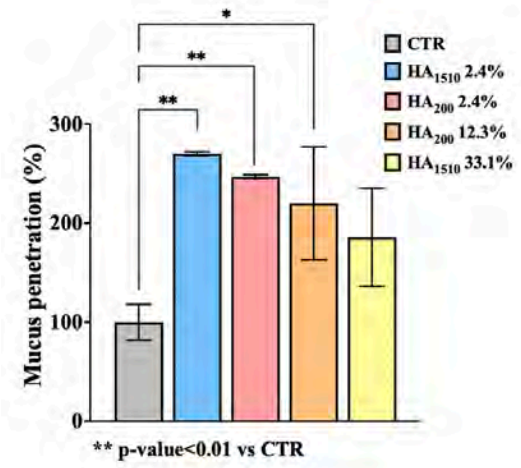

Figure 1: In vitro assessment of mucus penetration after 24 h on artificial mucus.

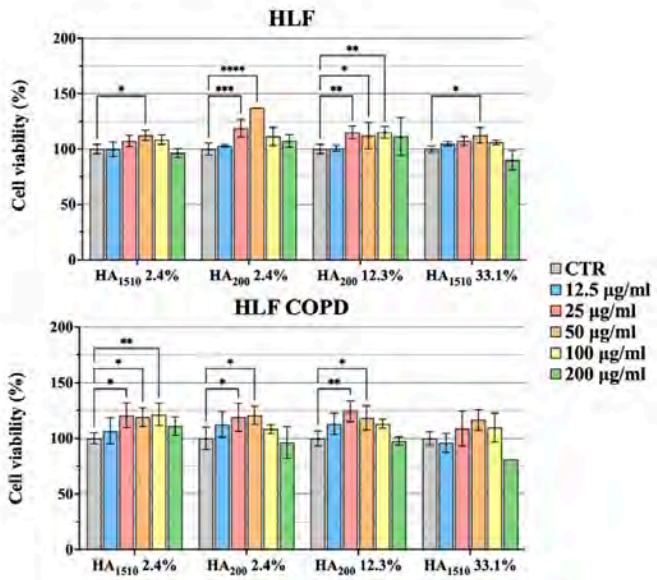

Figure 2: Percentage of cell viability of HLF and HLF COPD cells and 48 h of incubation with different NP formulations.

Acknowledgements

The authors acknowledge the research project “One Health Basic and Translational Research Actions addressing Unmet Needs on Emerging Infectious Diseases” – INF-ACT, CUP B53C20040570005”. This research has been supported by EU funding within the NextGenerationEU-MUR PNRR Extended Partnership initiative on Emerging Infectious Diseases (Project no. PE00000007, INF-ACT). Francesca Della Sala was recipient of an INF-ACT Foundation Early-Career Award (INF-ACT/ECA/2024).

References

[1]Pangeni R., Meng T., Poudel S., Sharma D., Hutsell H., Ma J., Rubin B.K., Longest W., Hindle M., Xu Q. Airway mucus in pulmonary diseases: Muco-adhesive and muco-penetrating particles to overcome the airway mucus barriers. *International Journal of Pharmaceutics*; 2023; 634; 122661.

[2]Liang Y., He Q., Duan L., Gong H., Zu M., Xie D., Xiao B. Fluorinated hyaluronates endow oral nanoparticles with mucus penetration and colonic macrophage targeting properties. *Smart Materials in Medicine*; 2021; 2; 250-259.

S94 – O2

Multifunctional antioxidant hybrid hydrogels containing cerium oxide nanocrystals for accelerated wound healing

Minsart M.[1,*], De Vos J.[2,*], Meuleman H.[1,2], Deblock L.[2], Bogaert B.[1], Van Daele L.[1], De Buysser K.[2,#], Dubruel P.[1,#]
[1]Polymer Chemistry and Biomaterials (PBM) Group, Centre of Macromolecular Chemistry (CMaC), Department of Organic and Macromolecular Chemistry, Ghent University, Belgium; [2]Sol-gel Centre for Research on Inorganic Powders and Thin films Synthesis (SCRiPTS) Group, Department of Chemistry, Ghent University, Ghent, Belgium.
* = joint first authors, # = joint last authors

Introduction

Wound management remains a critical component of modern clinical practice. The high incidence and recurrence of chronic wounds underscore the need for innovative wound healing solutions capable of accelerating tissue repair and mitigating oxidative stress.[1] In this regard, hybrid materials derived from the union of organic and inorganic substances are very promising.

Aim

This work aims to develop multifunctional nanocomposite hydrogels by incorporating cerium oxide nanocrystals (CeO_2-NCs), leveraging the reversible Ce^{3+}/Ce^{4+} redox cycling to enable ROS scavenging and accelerate the healing process. To fully realize the therapeutic potential of these systems, we explored the tailoring of the NC size and surface chemistry combined with modification of the polymer matrix to strengthen NC–polymer interactions to engineer an antioxidant wound dressing.

Materials and Methods

For the hydrogel matrix, alginate and hyaluronic acid were functionalized to create hydrogel networks and the modified polymers were characterized by NMR and FTIR. In parallel, CeO_2-NCs were synthesized via solvothermal methods and analyzed using NMR, XRD, TEM and DLS. To enhance the NC retention and strengthen the NC–polymer interactions, the NCs were surface-functionalized and the polymers further modified with (nitro)dopamine. The resulting composites were evaluated for their swelling, gel fraction, and mechanical properties. NC leaching was quantified by ICP-MS and the antioxidant activity was assessed using DPPH. The hemocompatibility, biocompatibility and healing performance were examined through *in vitro* live/dead and scratch assays.

Results

CeO_2-NCs were successfully synthesized and surface-functionalized yielding NCs compatible with aqueous polymer systems. The biopolymers were successfully modified to introduce crosslinkable functionalities as well as catechol groups to facilitate interaction with the NCs. The resulting hydrogels exhibited swelling degrees ranging from 13.8 to 34.9 g/g and gel fractions above 80 % with Young's moduli between 87.4 and 788 kPa, showing higher swelling and mechanical strength than the commercial dressing HydroTac®. The biological evaluations further supported the suitability of the developed materials for use as wound dressings. Hemocompatibility assays yielded excellent results (hemolysis degree < 1 %). The antioxidant activity was demonstrated for catechol-functionalized polymers as well as for CeO_2-NCs (separately and combined). Scratch assays combined with live/dead staining confirmed excellent cytocompatibility (viability ≥ 96.23 ± 1.55 %) for all tested materials, showing that neither the polymers nor the incorporated NCs induced adverse cellular responses (Figure 1).

Conclusion

This research highlights the potential of (nitro)dopamine-functionalized hydrogels incorporating CeO_2-NCs as next-generation wound dressings that synergistically combine structural support, accelerated healing and antioxidant protection.

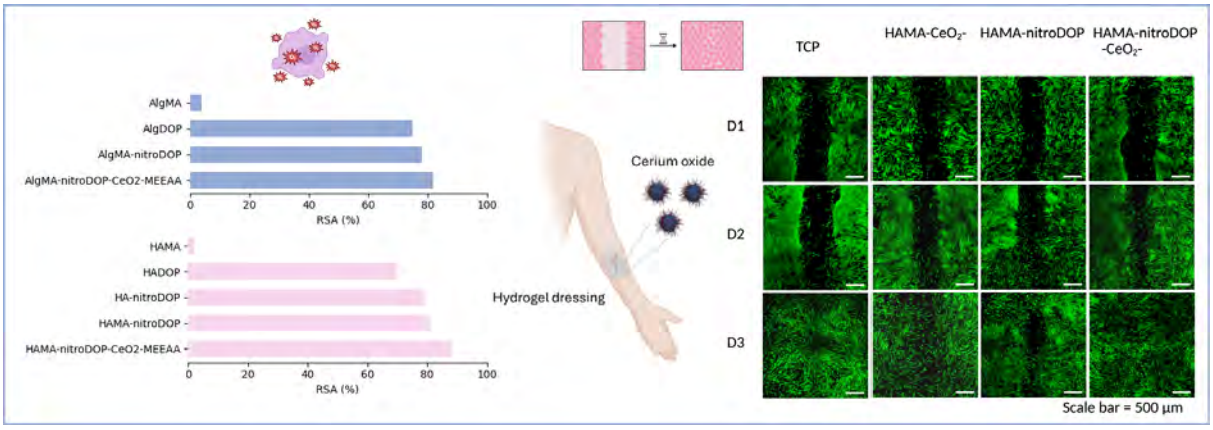

Figure 1. Highlighted results of the performed research. Partly created using BioRender.

References

[1]Dong Y., Wang Z. ROS-scavenging materials for skin wound healing: advancements and applications. *Front Bioeng Biotechnol.* 2023; 11

S94 – O3

Protease catalyzed cross-linking of peptide grafted alginate chains

Loibner, P.[1], Bučak Gasser, D.[1*], Steindorfer, T. [1], Dorn, T.[1], Wrodnigg, T.[2], Neshchadin, D. [2], Gescheidt, G.[2], Bračič, M.[3], Mohan, T.[1], Stana Kleinschek, K.[1], Kargl, R. [1]

[1]Institute of Chemistry and Technology of Biobased Systems, Graz University of Technology, Austria
[2]Institute of Physical and Theoretical Chemistry, Graz University of Technology, Austria
[3]Institute of Engineering Materials and Design, University of Maribor, Slovenia

Introduction

Bacterial peptidoglycans (PGs) are supramolecular networks of crosslinked, peptide-grafted glycan chains. PGs are crucial for the mechanical stability and resistance of bacterial cell walls. Reproducing these structures synthetically is of high interest and (pseudo-)PGs could expand our understanding of bacterial cell walls.[1] However, many semi-synthetically produced pseudo-PG-constructs involve chemical methods that are tedious and wasteful.[2] The aim of this work was to develop and investigate a new method for the chemo-enzymatic synthesis of pseudo-PGs.

Materials and Methods

Our work describes a new chemo-enzymatic approach for the synthesis of pseudo-PGs using peptide-grafted alginate (3) and glycine-based crosslinkers (red), which undergo protease-catalyzed crosslinking to yield viscoelastic gels with tunable mechanical properties (Figure 1). The enzymatic gelation processes were monitored via time- and temperature dependent oscillatory shear rheology and NMR experiments using varying crosslinker concentrations, yielding information about the kinetics of the peptide bridge formation and the viscoelasticity and stability of the pseudo-PGs.

Results and Conclusion

Peptide grafted alginate can efficiently be cross-linked through amide bonds using a protease as a catalyst. The gel-forming kinetics and density can be controlled by the temperature, and by the type and concentration of the cross-linking agent. We propose that this method is generic for peptides and polysaccharides, and has a high impact on biomaterials research, peptide delivery, testing of antibiotic efficacy or for investigating human immune cell response.

References

[1]Wolf A.J., Underhill D. M., Peptidoglycan recognition by the innate immune system. Nat. Rev. Immunol 2018; 18; 243-254.
[2]Vacariu C.M., Tanner M. E., Recent Advances in the Synthesis and Biological Applications of Peptidoglycan Fragments. Chemistry – A European Journal 2022; 28; e202200788.

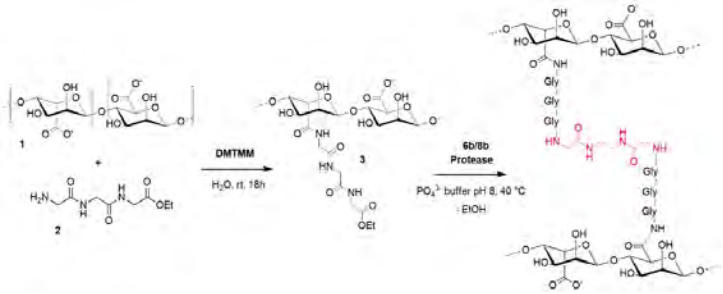

Figure 1. Strategy for pseudo-PG synthesis combining peptide conjugation with enzyme catalysis.

S94 – O4

Tensile properties of single- and multi-type mixed fibre bundles of spider silk

Promnil S.[1], Liprandi D.[1], Illing T.[2], Jani M.[1], Heinz P.[1], Wolff J.[1]
[1]Evolutionary Biomechanics, Zoological Institute and Museum, University of Greifswald, Greifswald, Germany; [2]Institute of Physics, University of Greifswald, Greifswald, Germany.

Introduction

Spider silk is a high-performance biological material whose exceptional strength, extensibility, and toughness arise from the hierarchical organisation of spidroin proteins. Spiders produce multiple silk types with distinct mechanical properties and often combine them into composite fibre bundles tailored to specific functions. While individual silk types, particularly major ampullate silk, have been extensively studied, the mechanical behaviour of naturally assembled mixed-fibre bundles remains poorly understood, especially in non-orb-weaving spiders.
Here, we investigate the mechanical properties of major ampullate, minor ampullate, and aciniform silk, as well as their natural bundles, in *Pholcus phalangioides*. By comparing single fibres, forcibly silked bundles, and naturally spun mixed threads, we assess how silk-type integration influences bundle mechanics. Our results provide new insight into how spiders use fibre-level diversity to tune thread-level mechanical performance.

Materials and Methods

Adult P. phalangioides were collected and maintained under controlled conditions. Silk threads were harvested on cardboard frames following established protocols, including naturally spun draglines, bridging lines, and gumfoot threads. Aciniform fibres and posterior median spinneret (PMS) bundles were obtained by forcible silking. Fibre number and diameter were measured using polarised light microscopy and scanning electron microscopy. Mechanical properties were determined by nano-tensile testing at a constant strain rate of 1% s^{-1}.

Results

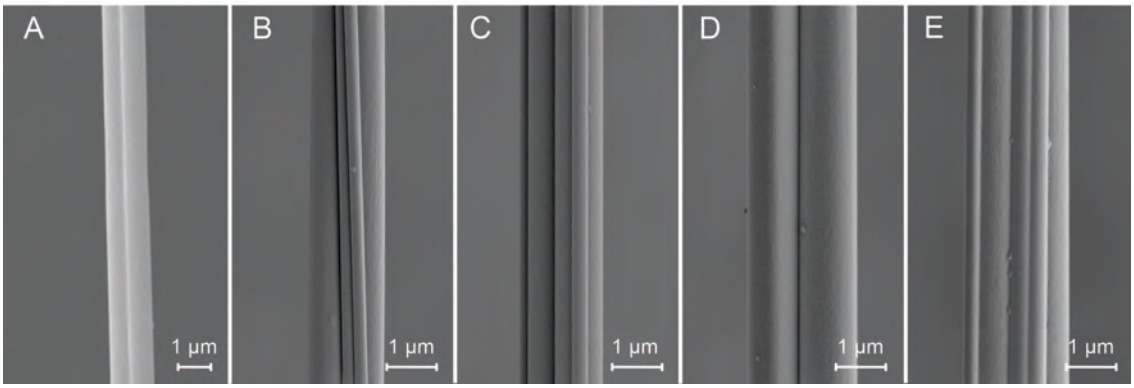

Figure 1 Scanning electron micrographs of Pholcus phalangioides silk bundles naturally spun in different behavioural contexts. (A) Two-fibre drop-down dragline (N2), (B) four-fibre drop-down dragline (N4), (C) walking dragline, (D) bridging line, and (E) gumfoot thread.

Microscopy (Figure1) confirmed that naturally spun *P.phalangioides* threads are multi-fibre bundles with thread-type-specific fibre numbers and compositions. Fibre diameter distributions indicate that different behavioural threads combine major ampullate, minor ampullate, and aciniform silks in distinct configurations, with bridging lines composed exclusively of minor ampullate fibres and gumfoot threads showing the most complex mixtures. Notably, fibre diameters varied systematically among thread types, suggesting that spiders modulate fibre size and composition in response to functional and spinning conditions[3].

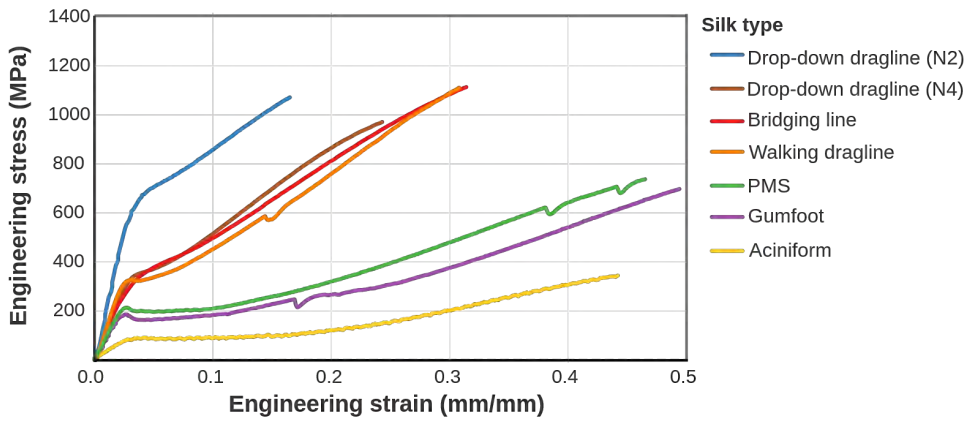

Figure 2 Comparative stress-strain curves of naturally spun P.phalangioides silk bundles (N2 two-fibre dragline, N4 four-fibre dragline, walking dragline, bridging line, and gumfoot thread) and forcibly silked samples (single aciniform fibre and posterior median spinneret fibre bundle, PMS).

Stress–strain behaviour (Figure2) was consistent with that of spider silk, with limited internal fibre failure in mixed bundles, indicating effective load sharing. Mechanical performance varied systematically with silk type and bundle composition, with N2 draglines showing the highest stiffness and yield stress, bridging lines achieving the highest load at break, and gumfoot threads, aciniform silk, and PMS bundles exhibiting greater extensibility. Notably, naturally spun mixed-fibre bundles, particularly walking draglines, bridging lines, and PMS threads, displayed higher toughness than pure aciniform silk[4], highlighting the advantages of behaviourally assembled silk composites.

Conclusion

Mechanical performance of spider silk bundles cannot be predicted solely from fibre composition or number. Instead, spiders behaviourally tune thread properties to functional demands, with two-fibre draglines optimised for stiffness and load bearing and multi-fibre bundles favouring extensibility and durability. These findings emphasise the role of natural spinning behaviour in silk mechanics and provide inspiration for biomimetic design.

Acknowledgements

This work was supported by an ERC Start Grant (101040724—SuPerSilk) under the European Union's Horizon 2020 research and innovation programme.

References

[1]Agnarsson I., Kuntner M., Blackledge T.A. Bioprospecting Finds the Toughest Biological Material: Extraordinary Silk from a Giant Riverine Orb Spider. *PLOS ONE* 2010; 5(9); e11234.

[2]Wang Q., McArdle P., Wang S.L, Wilmington R.L., et al. Protein secondary structure in spider silk nanofibrils. *Nature Communications* 2022; 4329; 13.

[3]Jani M., S. Promnil, Heinz P., Liprandi D., et al. Functional diversity and behavioural use of fibre producing silk glands in the cosmopolitan cellar spider *Pholcus phalangioides* (Fuesslin, 1775). *Journal of Experimental Biology* 2025; 228; jeb250392.

[4]Promnil S., Liprandi D., Illing T., Jani M., et al. Tensile properties of single- and multi-type mixed fibre bundles of spider silk. *Soft Matter* 2026; 22; 1455-1472.

S94 – O5

A mechanically programmable hydrogel platform for probing mechanotransduction during plant protoplast regeneration

Mukherjee A.[1], Van der Molen A.[1], Schöppl P.[2], Froeling R.[2], Pasheeva A.[1], Ragalie A.[1], Preulier P.[1], Es Sayed J.[1], Sprakel J.[2], Kamperman M.[1]

[1]Polymer Science, University of Groningen, Groningen, The Netherlands; [2]Laboratory of Biochemistry, Wageningen University and Research, Wageningen, The Netherlands

Introduction

Mechanical signals regulate cellular behavior across biological systems. In animal cells, engineered biomaterials have enabled systematic studies demonstrating that matrix mechanics can influence cell fate. In plants, however, experimental platforms capable of delivering defined mechanical cues to individual cells remain limited, hindering mechanistic investigation of how physical forces regulate dynamic processes such as regeneration and morphogenesis.

Protoplasts, generated by enzymatic digestion of plant cell walls provide a unique system to study *de novo* regeneration and cell wall assembly. However, they are typically cultured in liquid media where mechanical properties cannot be precisely controlled. Here, we address this limitation by engineering 3D hydrogel microenvironments that enable programmable mechanical control during protoplast regeneration (Figure1).

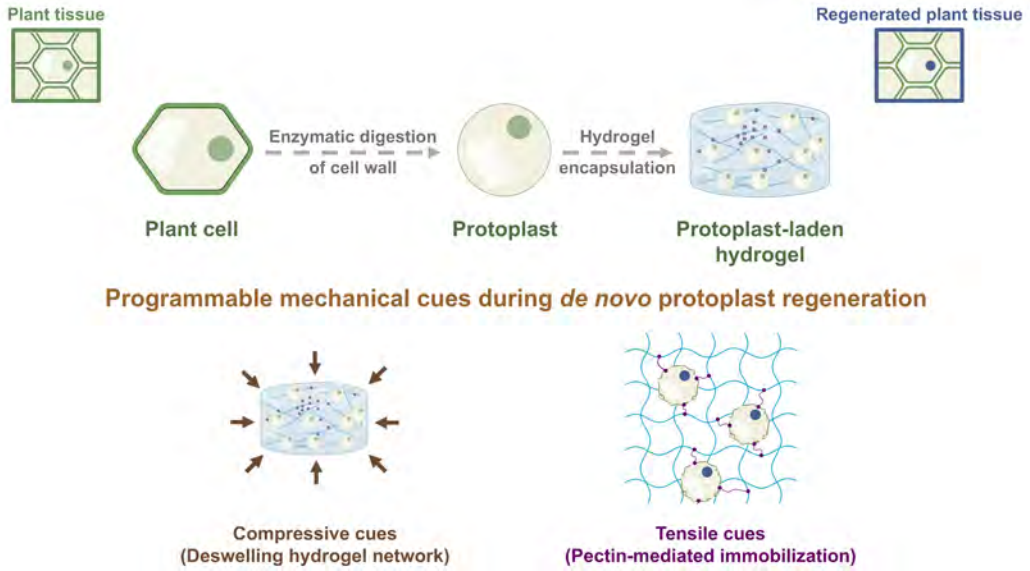

Figure 1. Mechanical control of *de novo* protoplast regeneration in 3D hydrogels

Materials and Methods

Methacrylated hyaluronic acid (HAMA) photocrosslinked hydrogels were developed for encapsulation of *Arabidopsis thaliana* protoplasts. Programmable compressive stresses were introduced by engineering deswelling HAMA networks via polyelectrolyte complexation with polycationic polymers such as poly(diallyldimethylammonium chloride) (PDADMAC), poly(L-lysine) (PLL), and polyethyleneimine (PEI). To enable transmission of tensile stresses, protoplasts were immobilized by incorporating boronic acid functional groups onto the HAMA backbone. Because protoplasts lack integrin-like adhesion proteins that mediate cell-matrix attachment in mammalian systems, dynamic covalent boronate ester bonds were used to enable attachment with the hydrogel matrix and *cis*-diols present in pectic components of the regenerating cell wall.

Results

Photocrosslinked HAMA hydrogels provided mechanically defined microenvironments for protoplast encapsulation that supported high cell viability. Hydrogel stiffness could be tuned from 10-70 kPa by varying molecular weight

and the degree of methacrylation, enabling investigation of matrix stiffness on viability. Cell wall staining experiments confirmed the regenerative potential of encapsulated protoplasts.
To apply compressive stresses to encapsulated protoplasts, polyelectrolyte complexation of the photocrosslinked polyanionic HAMA network with polycations, induced pronounced deswelling (up to 95%). The magnitude of shrinkage could be tuned through orthogonal parameters including polycation type, molecular weight, charge density, and the soft deformability of HAMA matrix.
An orthogonal strategy was implemented to transmit tensile forces to regenerating protoplasts by immobilization to HAMA matrix. Dynamic covalent boronate ester bonds characterized by ^{11}BNMR and rheology indicated fast relaxation (1.25s) indicating robust attachment without compromising the regeneration process.

Conclusion
Together, these results establish a mechanotransductive biomaterial platform capable of delivering programmable compressive and tensile cues to regenerating protoplasts. Our mechanically adaptive hydrogel platform provides a novel framework for enabling mechanical control over plant tissue engineering.

S94 – O6

3D ZnO Tetrapod-Based PLLA Biocomposite Films as Potential Antimicrobial Food Packaging Materials

Moreira J.[1,2], Mishra K.Y.[3], Fernandes M.M.[1,2]
[1]Center for Micro-Electro Mechanical Systems, University of Minho, Guimarães, Portugal; [2]LABBELS-Associate Laboratory in Biotechnology and Bioengineering and Microelectromechanical Systems, University of Minho, Braga, Portugal; [3]Mads Clausen Institute, NanoSYD, University of Southern Denmark, Sønderborg, Denmark

Introduction

Antimicrobial packaging reduces food contamination, enhancing safety and shelf life. Conventional polymers such as polyethylene, polypropylene, and polystyrene dominate due to versatility, durability, and low cost, but their persistence and contribution to microplastics drive the search for sustainable alternatives[1]. Biodegradable polymers like piezoelectric poly(L-lactic acid) (PLLA) are promising due to possibility to its electroactive properties, though limited barrier properties and lack of intrinsic antimicrobial activity at static conditions remain challenges[2]. Incorporating functional nanomaterials, such as 3D ZnO tetrapods, can enhance biodegradable films, providing antimicrobial activity and improved functionality[3]. PLLA/ZnO tetrapod biocomposites therefore represent a promising strategy for developing multifunctional, sustainable, and active food packaging systems.

Materials and Methods

PLLA-based biocomposite films were prepared by solvent casting using the doctor blade technique, with varying ZnO tetrapod concentrations. Films were characterized for morphology (SEM), chemical structure (FTIR), thermal behavior (DSC, TGA), surface wettability, optical properties, mechanical performance, and degradation. Antimicrobial activity was tested against bacterial and fungal strains under static and dynamic condition, through application of vibration cue at 4Hz (1cm amplitude) using a mechanical bioreactor. Practical applicability was evaluated in fruit packaging under real storage conditions.

Results

Biodegradable PLLA films incorporating ZnO tetrapods exhibited significant antimicrobial activity under both static and dynamic conditions, alongside enhanced UV resistance and potential piezoelectric responsiveness under mechanical stimulation. The developed films demonstrated adequate mechanical durability, biocompatibility, and tunable surface and thermal properties depending on filler concentration. These biocomposites effectively combine biodegradability with functional performance, highlighting their strong potential for sustainable and active food packaging applications.

Conclusion

PLLA/ZnO tetrapod biocomposite films successfully integrate biodegradability with potent antimicrobial activity, UV resistance, and piezoelectric responsiveness, while maintaining mechanical robustness and tunable properties. Their multifunctional performance positions them as highly promising candidates for next-generation sustainable and active food packaging, offering a practical route to safer and longer-lasting products in agriculture.

Acknowledgement

This work was supported by European commission for VINNY project (ID:101130039).

References

[1]Upadhyay P., Zubair M., Roopesh M.S., Ullah A. An overview of advanced antimicrobial food packaging: emphasizing antimicrobial agents and polymer-based films. Polymers 2024; 16; 2007.
[2]Sun T., Ren S., Hu J., Zhang J., Liu L., Du J., Dong T. Copolymerized and blended poly(L-lactic acid)-based films with potential for dairy packaging: Soil degradation behavior. Industrial Crops and Products 2025; 234; 121583.
[3]Mishra Y.K., Adelung R. ZnO tetrapod materials for functional applications. Materials Today 2018; 21; 631-651.

Functional hydrogel materials for biomedicine and biotechnology: From design to 3D-printed systems

Meyer J.[1], Kara S.[1,2]
[1]Institute of Technical Chemistry, Leibniz University Hannover, Callinstraße 5, 30167 Hannover, Germany
[2]Biocatalysis and Bioprocessing Group, Department of Biological and Chemical Engineering, Aarhus University, Gustav Wieds Vej 10, 8000 Aarhus, Denmark

Introduction

Hydrogels are versatile biomaterials with highly hydrated and tunable polymer networks, making them attractive for both biomedical and biotechnological applications.[1] Their porous structure enables the incorporation of biomolecules and enzymes while maintaining functionality. Advances in polymer chemistry and fabrication technologies, such as 3D printing, allow the development of tailored hydrogel materials for enzyme immobilization and functional biomaterials.

Materials and Methods

Functional hydrogels based on ionic liquid-derived monomers and poly(aspartic acid) were synthesized to obtain materials with tunable properties. Gelation and mechanical characteristics were analyzed by rheology and *in situ* rheology–Raman spectroscopy. Swelling behavior, biocompatibility, and antimicrobial activity were evaluated. Functionalized hydrogel particles and digital light processing (DLP) 3D-printed hydrogels were prepared and investigated as matrices for enzyme immobilization.

Results

The synthesized hydrogel systems showed tunable physicochemical properties depending on polymer composition and crosslinking density. Ionic liquid-based hydrogels exhibited equilibrium swelling degrees of up to ~900%, while maintaining stable polymer networks with storage moduli in the kilopascal range. Rheological investigations revealed rapid gelation behavior and provided insights into network formation during polymerization. The combined rheology–Raman approach enabled simultaneous monitoring of mechanical gelation and chemical conversion during crosslinking and polymerization.[2] Several hydrogel systems demonstrated favorable biocompatibility and intrinsic antimicrobial activity against representative bacterial strains. Functionalized poly(aspartic acid) hydrogel particles provided reactive groups for covalent enzyme immobilization and enabled stable enzyme incorporation within the polymer network.[3] Synthetic hydrogels were successfully processed using DLP to fabricate 3D-printed structures with defined geometries. These printed hydrogels served as immobilization matrices for enzymes, such as a peroxygenase or lipase, and enabled the integration of biocatalysts into structured materials suitable for continuous synthesis.

Conclusion

The presented overview of studies demonstrates that functional hydrogels constitute a versatile materials platform for biotechnology and biocatalysis. Through rational polymer design, advanced characterization methods, and additive manufacturing technologies, hydrogel materials tailored for mechanical properties, swelling behavior, and chemical functionality. These materials enable efficient enzyme immobilization in particle-based systems as well as in structured 3D-printed matrices. The combination of tunable hydrogel chemistry with additive manufacturing opens new opportunities to develop structured biomaterials for biotechnological and biomedical applications.

Acknowledgements

JM thanks the German Research Center (Deutsche Forschungsgemeinschaft, DFG grant no 568637738) for the financial support. SK thanks the Ministry for Science and Culture for Lower Saxony for the Holen & Halten starting grant (grant no. 12.5-76251-17-9/ 20) for financial support.

References

[1] Meyer S, Meyer L.-E., Kara S., Enzyme immobilization in hydrogels: A perfect liaison for efficient and sustainable biocatalysis. *Engineering in Life Science* 2021, 22(3-4), 106943.

[2]Lambrecht S., Biermann M., Jopp S, Kara S., Meyer J. A novel characterization technique for hydrogels – in situ Rheology-Raman spectroscopy for gelation and polymerization tracking. *Materials Advances* 2024; 5; 6957-6966.

[3]Meyer J., Meyer L.-E., Borg H., Dorfs D., Kara S. Functionalized poly(aspartic acid) hydrogel particles as a carrier for covalent enzyme immobilization. *RSC Sustainability* 2025; 3(8); 3554-3566.

S95
Polymeric biomaterials – synthetic

S95 – K1
Temperature-responsive biodegradable injectable polymer systems for biomedical applications

Ohya Y.
Dept. Chem. Mater. Eng., Kansai Univ., Suita, Osaka, Japan

Introduction

Thermo-gelling polymer systems have attracted considerable attention as injectable polymers (IPs) for biomedical applications1. Most thermo-gelling systems undergo sol-gel transitions to form hydrogels via physical cross-linking. One of the practical problems for these systems is the short duration of the gel in the body. This property is one of the obstacles to the clinical application of biodegradable IP systems. We reported biodegradable temperature-responsive IP systems forming partial covalent cross-linking via thiol-ene reactions.2 The obtained formulation showed temperature-responsive irreversible sol-gel transition and longer duration of the gel. We investigated the potential utility of the system as sustained drug-releasing systems, anti-adhesive materials, stem cell delivery devices, immunological cancer therapeutic systems.

Sustained drug-releasing (Gels 2017, 3, 38; J. Anesth. 2025, 39, 435)
We investigated the sustained release of the antidiabetic drug glucagon-like peptide-1 (GLP-1) and the local anesthetic levobupivacaine (Lev) from IP gels. Subcutaneous administration of GLP-1–loaded IP to mice maintained GLP-1 blood concentrations for prolonged periods. Furthermore, when Lev-loaded IP was locally administered in a rat nociceptive avoidance model, a long-lasting anesthetic effect was observed.

Anti-adhesive materials (ACS Appl. Bio Mater. 2021,4, 3079).
The anti-adhesion effect of IP gels was investigated using a rat postoperative adhesion model. A favorable anti-adhesion effect was observed when the IP gel was combined with a drug (chymase inhibitor).

Treatment of ischemic heart disease (Sci. Technol. Adv. Mater. 2021, 22 627)
IP containing adipose-derived stem cells (AdSCs) was locally injected into ischemic myocardial tissue in a mouse myocardial infarction model. As a result, long-term retention of AdSCs and recovery of cardiac function were observed.

Immunological cancer therapy (Adv. Therap. 2024, 7, 2300296; Int. J. Pharm. 2024, 652, 123801)
IP containing cancer antigens and an adjuvant (CpG-DNA) was administered to tumor-bearing mice. Tumor growth inhibitory effects were observed by the sustained release of antigen and adjuvant. In addition, tumor growth inhibition was confirmed with an IP formulation containing dendritic cells (DCs), cancer antigens, and CpG-DNA as a DC vaccine.

Conclusion

These results demonstrate that the IP systems developed are useful for sustained-release drug delivery systems, anti-adhesion materials applicable in endoscopic surgery, stem cell therapy for myocardial infarction, and cancer immunotherapy.

References

[1]Ohya Y. et al., *React. Funct. Polym*. 2013, 73, 979-985.
[2]Yoshida Y., Ohya Y. et al., *Biomater*. Sci. 2017, 5, 1304-1314.

S95 – K2
Poly(2-oxazoline)s as antifouling materials

Hoogenboom R.
Supramolecular Chemistry Group, Centre of Macromolecular Chemistry, Department of Organic and Macromolecular Chemistry, Ghent University, Belgium

Introduction

Despite the widespread use of poly(ethylene glycol) (PEG) to shield nanoparticle carriers, the future use of PEG is restricted by the widespread occurrence of antiPEG antibodies in the human population, which further increased after the COVID-19 vaccination campaign with PEGylated lipid nanoparticle mRNA vaccines.1,2 Unlike PEG, poly(2-oxazoline) materials often exhibit reduced immunogenicity (less antibody generation, even during challenging experiments in which PEG as reference shows strong antibody formation) and improved stability, making them promising candidates for next-generation biomaterials and therapeutics.3,4 The non-ionic hydrophilic nature of poly(2-oxazoline)s with short alkyl side chains, namely poly(2-methyl-2-oxazoline) (PMeOx) and poly(2-ethyl-2-oxazoline) (PEtOx), leads to efficient antifouling properties by suppression of interactions with proteins and cells.5 Hence, these poly(2-oxazoline)s can directly substitute PEG as antifouling coating of drug carriers and implants to shield them from the immune system. In this work we report our efforts to develop alternative poly(2-oxazoline) and poly(2-oxazine) superhydrophilic and antifouling polymers.

Materials and methods

Polymers were prepared by living cationic ring-opening polymerization of the corresponding 2-oxazoline and 2-oxazine monomers. Hydrophilicity of the polymers was evaluated by logP determination and/or reversed phase HPLC. Full details can be find in the publications that are cited in the results section.

Results

Going beyond classical poly(2-oxazoline)s we evaluated the antifouling properties of a poly(2-methyl-2-oxazine) (PMeOzi) coating, which shows similar hydration behavior as PEtOx while being less hydrophilic than PMeOx. In contrast with the general believe that more hydrophilic polymers have better antifouling properties, it was unexpectedly found that the PMeOzi coating exhibited better antifouling performance than PMeOx, PEtOx and PEG.1 This improved performance was ascribed to the higher chain segment mobility, as indicated by a lower glass transition temperature, of PMeOzi further suppressing interactions with proteins and cells. In another study we evaluated poly(2-oxazoline)s with short ether side chains as well as alkylamino side chains, revealing that poly(2-methoxymethyl-2-oxazoline had similar or slightly better hydrophilicity than PMeOx, while also poly(2-dimethylamino-2-oxazoline) was found to have a negative logP indicating high water-solubility.2,3 Finally, we recently introduced poly(2-hydroxymethyl-2-oxazoline) as most hydrophilic poly(2-oxazoline) reported to date.4 Interestingly, this polymer was found to have minimal interactions with proteins and cells in a preliminary evaluation of antifouling properties of the solubilized polymer chains.

Conclusion

Structural variation of poly(2-oxazoline) and poly(2-oxazine) structures allows the development of highly hydrophilic polymers that show better antifouling performance than the commonly used PEG, PMeOx and PEtOx.

References

[1]Hoogenboom R., Benetti E.M., et. al. Chemical design of non-ionic polymer brushes as biointerfaces: Poly (2-oxazine) s outperform both poly (2-oxazoline) s and PEG. Angew. *Chem. Int. Ed*. 2018; 57(36); 11667-11672.
[2]Sedlacek O., Hoogenboom R. et al. Straightforward Route to Superhydrophilic Poly(2-oxazoline)s via Acylation of Well-Defined Polyethylenimine. *Biomacromolecules* 2019; 20; 222-230.
[3]Sedlacek O., Hoogenboom R.et al. Poly(2-amino-2-oxazoline)s: a new class of thermoresponsive polymers. *Polym. Chem.* 2019; 10; 4683.
[4]Jana S., Hoogenboom R. et al. Poly(2-Hydroxymethyl-2-Oxazoline) as Super-Hydrophilic Antifouling Polymer. Angew. *Chem. Int. Ed.* 2025; 64(12); e202424873.

S95 – O1

Adaptive PEG hydrogels with clustered biochemical signals for tumoroids culturing

Apartsin E.[1], Richard N.[2], Meesters N.[3], dM Vivanco M.[3], Durrieu M.-C.[1]
[1]Univ. Bordeaux, CNRS, Bordeaux INP, CBMN, UMR 5248, Pessac, France; [2]Univ. Poitiers, CNRS, XLIM, UMR 7252, Futuroscope Chasseneuil, France; [3]CICbioGUNE, Bilbao, Spain

Introduction
Organoids and tumoroids are usually cultured in Matrigel, whose undefined composition, batch variability, and animal origin hamper mechanistic studies and translation toward clinically relevant models. Synthetic hydrogels offer an attractive alternative by enabling independent control of mechanical cues and biochemical functionalization. We developed a chemically defined PEG bis-dendron hydrogel platform with tunable mechanics, porosity, and controlled peptide clusterization to better support the maturation of breast cancer organoids (Figure 1).

Materials and Methods
Norbornene-bearing precursors of two distinct topologies (commercial star-shaped PEG and original PEG bis-dendrons) were cross-linked with star-shaped PEG-SH via photoinitiated thiol-ene reaction. Small- and large-amplitude oscillatory rheology and stress relaxation experiments provided elastic modulus, viscoelastic dissipation, critical strain, and relaxation parameters. Polymer chain dynamics in the hydrated state were investigated by MAS solid-state NMR. Freeze-fracture cryo-SEM was employed to visualize hydrogel ultrastructure and apparent pore architecture. Bioactivity was introduced by grafting RGD peptide; peptide clusterization within the network was assessed by confocal microscopy. Luminal B and triple-negative breast cancer spheroids were encapsulated in hydrogels upon polymerization, and their viability ad morphology were assessed through cultivating.

Results and Discussion
Bis-dendron hydrogels exhibited markedly higher swelling and larger apparent pores than star-shaped networks, consistent with lower crosslinking density and longer chains between crosslinks. Rheology and NMR jointly revealed abundant weak interchain interactions in bis-dendron networks, thus evidencing adaptive viscoelastic behavior and mobility-associated friction at high frequencies compared with star-shaped PEG gels. Terminal norbornene moieties organized into dendritic clusters acted as anchoring sites for RGD, generating spatially localized peptide-rich islands instead of homogeneous ligand distributions (Figure 2). This peptide clusterization is expected to favor multivalent integrin engagement and more physiological breast cancer cell-matrix signaling than uniformly decorated matrices with the same global peptide content. This has resulted in better maturation in breast cancer tumor organoids.

Conclusions
PEG bis-dendron hydrogels constitute a versatile, chemically defined toolbox in which stiffness, viscoelasticity, porosity, and RGD clusterization can be modulated in a predictable manner. By jointly tuning mechanical properties and bioactivity of these hydrogels, this platform is poised to enable improved maturation and functional relevance of breast cancer organoids and other tumor-derived 3D models, with potential applications in drug screening and mechanobiology.

Acknowledgements
This project is co-financed by the Interreg Atlantic Area Programme through the European Regional Development Fund. We also thank the Nouvelle-Aquitaine Regional Research Network on Recomposed and Reconstructed Humans in Health (HR2S).

Figure 1

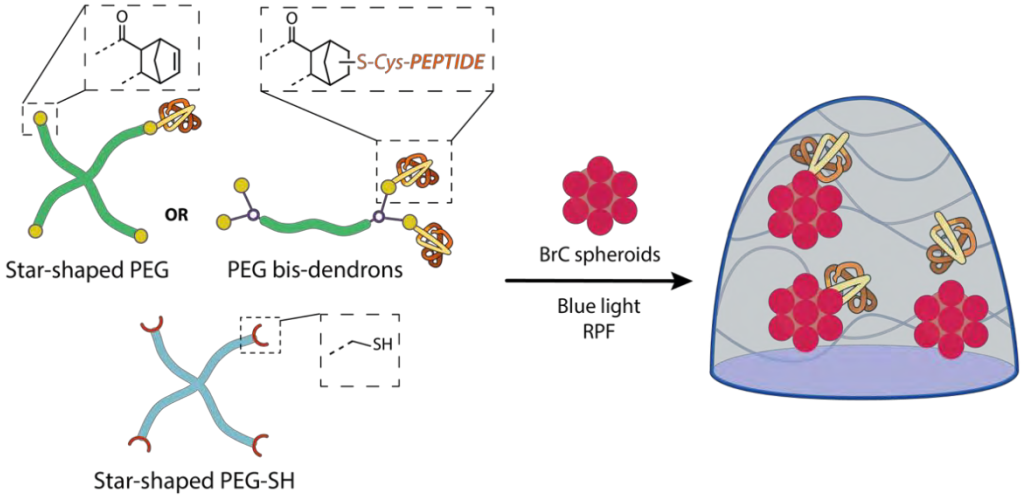

Figure 2

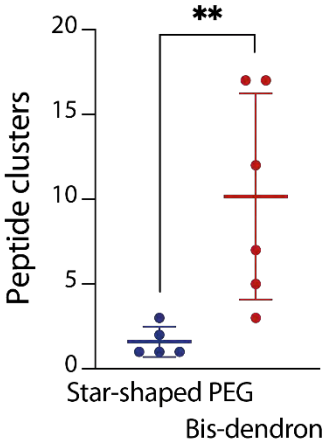

S95 – O2

Biological assessment of azithromycin-loaded poly(sebacic acid) microparticles for lung delivery: antimicrobial efficacy and response in *S. aureus*-epithelial cell coculture model

Czajkowski J.[1,3], Calderon-Jacinto R.[2], Kwiecień K.[1], Barzowska-Gogola A.[3], Pucelik B.[3], Brzychczy-Włoch M.[4], Pauthe E.[2], Pamuła E.[1]

[1]Department of Biomaterials and Composites, AGH University of Krakow, Kraków, Poland; [2]ERRMECe Laboratory, CY Cergy Paris Université, Neuville sur Oise, France; [3]Łukasiewicz Research Network – Krakow Institute of Technology, Kraków, Poland; [4]Department of Molecular Medical Microbiology, Jagiellonian University Medical College, Kraków, Poland

Introduction

Dry powder formulations for pulmonary drug delivery enable targeted treatment of the lungs, reducing systemic side effects and allowing the use of lower drug doses. Chronic respiratory infections associated with cystic fibrosis and chronic obstructive pulmonary disease are often driven by biofilm-forming bacteria such as *Staphylococcus aureus*, which exhibit increased resistance to conventional antibiotic therapies. To address this challenge, we developed poly(sebacic acid) (PSA) microparticles loaded with azithromycin, an antibiotic exhibiting antibacterial and immunomodulatory properties.

Materials and Methods

Azithromycin-loaded poly(sebacic acid) microparticles (PSA_AZ MPs) were manufactured using an oil-in-water emulsification method and characterized in terms of particle size distribution to assess their suitability for pulmonary delivery. Cytocompatibility, cellular uptake, and reactive oxygen species (ROS) production were evaluated in RAW264.7 macrophages. Antibacterial activity against *S. aureus* was determined using a minimum inhibitory concentration (MIC) assay. In addition, biofilm inhibition was assessed by colony counting and confocal microscopy. Finally, the performance of PSA_AZ MPs was investigated in a coculture model of A549 lung epithelial cells and *S. aureus* to evaluate host–pathogen interactions and therapeutic efficacy, using quantitative cell and bacterial counting alongside fluorescence microscopy imaging.

Results

PSA_AZ MPs exhibited a geometric particle size distribution promising for inhalation, with approximately 76% of particles within the optimal 1-5 µm size range. The system demonstrated good cytocompatibility up to 100 µg/mL and did not induce reactive oxygen species (ROS) production, indicating a favorable safety profile under the tested conditions. Moreover, PSA_AZ MPs showed reduced uptake by macrophages compared to unloaded particles, suggesting limited phagocytic clearance *in vitro*. The formulation showed strong antibacterial activity, significantly inhibiting *S. aureus* biofilm formation, with a 4-log reduction in bacterial count, accompanied by a marked decrease in biofilm biomass and metabolic activity. In coculture conditions, PSA_AZ MPs achieved a 3-log reduction in bacterial viability while preserving epithelial cell integrity, whereas untreated conditions resulted in extensive bacterial overgrowth and complete eradication of epithelial cells.

Conclusion

PSA_AZ MPs represent a promising inhalable drug delivery platform enabling effective *in vitro* delivery of azithromycin, resulting in antibacterial activity and modulation of host-pathogen interactions. These findings support further evaluation of this system in more advanced models.

Acknowledgements

This work was supported by the Implementation Doctorate Programme (Edition XI) funded by the Ministry of Science and Higher Education of Poland (No. DWD/9/0164/2025), the National Science Centre, Poland, and the ‘Excellence Initiative – Research University’ programme at AGH University of Krakow, Poland.

S95 – O3

Thermosensitive and photocrosslinkable PVA–PEG hydrogel as a synthetic alternative to Matrigel for organoid culture

Lemarié L.[1,2], Radix S.[3] & Sohier J.[2]
[1]SEGULA Technologies France, Nanterre, France
[2]CNRS UMR 5305, LBTI (Tissue Biology and Therapeutic Engineering Laboratory), Lyon, France
[3]UCBL1, CNRS UMR 5246 ICBMS (Institute of molecular and supramolecular Chemistry And Biochemistry), Lyon, France

Introduction

Matrigel is widely used as a matrix for organoid and stem cell culture because of its thermogelling properties and soft viscoelastic characteristics. However, its animal origin, batch variability and limited control over mechanical properties restrict its reproducibility and translational potential. Synthetic thermoresponsive polymers represent a promising alternative if they can reproduce reversible temperature-dependent self-assembly while enabling mechanical tuning. In this study, we developed a synthetic PVA–PEG copolymer designed to mimic Matrigel-like thermosensitive behaviour while incorporating methacrylate groups enabling post-gelation photocrosslinking.

Materials and Methods

Poly(vinyl alcohol) (PVA) was functionalized using a two-step graft-onto strategy mediated by toluene-2,4-diisocyanate (TDI). Poly(ethylene glycol) methacrylate (PEG500-MA) was first reacted with TDI in anhydrous DMSO at 40 °C to form PEG-isocyanate intermediates, which subsequently reacted with hydroxyl groups of PVA to generate urethane linkages. Reaction mixtures were purified by ethanol precipitation, dialysis and freeze-drying to obtain a soluble copolymer. Different formulations were synthesized by varying PEG molecular weight and degree of substitution (DS). Polymer functionalization was characterized by ^{1}H-NMR and FTIR. Thermoresponsive behaviour was evaluated by optical microscopy. Photocrosslinking capability was assessed using lithium phenyl-2,4,6-trimethylbenzoyl phosphinate (LAP) under 395 nm irradiation. Cytocompatibility was assessed using keratinocyte cell lines according to ISO 10993-5.

Results

Formulation screening revealed a strong dependence of aqueous solubility and thermosensitivity on the degree of substitution and PEG architecture. Highly substituted polymers (DS ≈ 80 %) showed poor solubility due to partial intermolecular crosslinking, whereas moderate substitution (DS ≈ 50 %) restored full solubility while maintaining thermoresponsive behaviour. ^{1}H-NMR and FTIR analyses confirmed successful grafting of PEG chains onto the PVA backbone through urethane linkages.

The optimized formulation (P16), containing PEG500-MA representing approximately 25 % of the grafted PEG fraction, exhibited a temperature-dependent self-assembly transition around 10–15 °C. Optical microscopy revealed the progressive formation of hydrophobic domains during heating from 4 °C to 25 °C, indicating structural reorganization of the polymer network (Figure 1), consistent with a temperature-induced hydrophilic–hydrophobic transition.

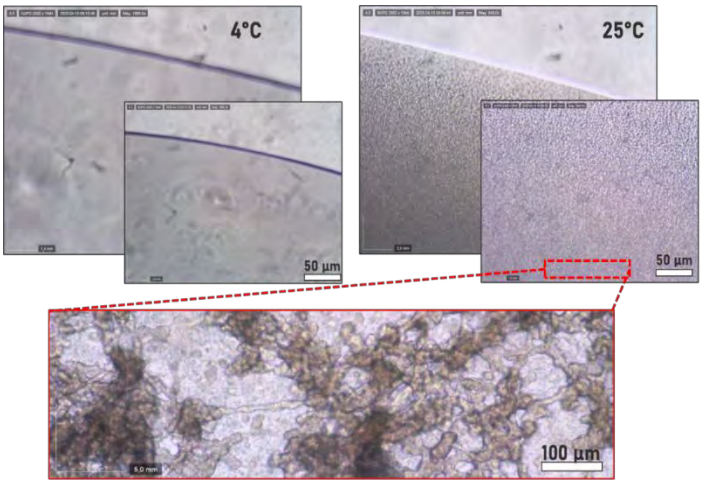

Figure 1 : Optical microscopy observation of the structural rearrangement of P16 during the thermal transition from 4 °C to 25 °C.

Photocrosslinking experiments demonstrated that the presence of methacrylate groups enables the formation of a soft and stable hydrogel upon UV exposure, confirming the ability of the system to transition from a thermosensitive solution to a mechanically stabilized network. Cytocompatibility evaluation demonstrated excellent biocompatibility after purification, with keratinocyte viability exceeding 97 % in both direct and indirect contact conditions (Figure 2), confirming efficient removal of residual cytotoxic species.

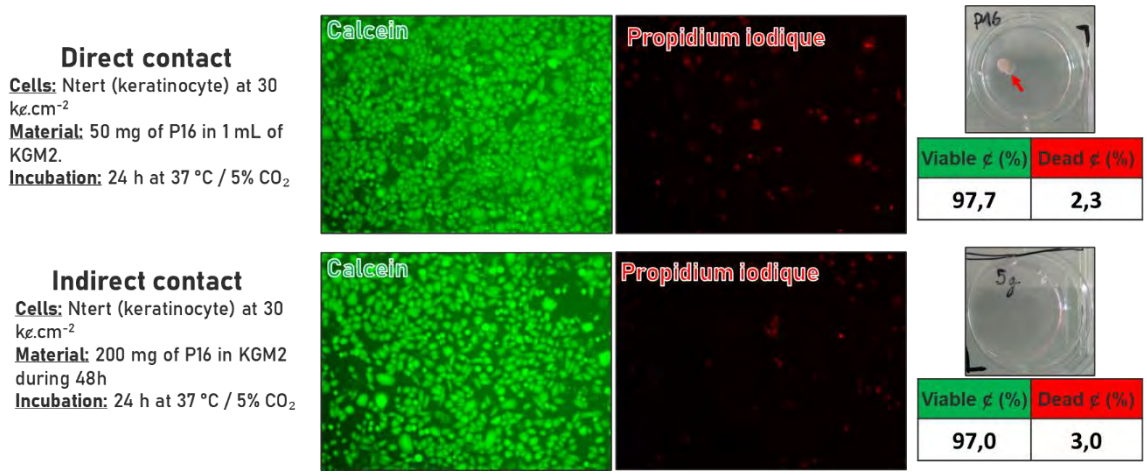

Figure 2 : Cytocompatibility of P16 after purification according to ISO 10993-5, showing high keratinocyte viability in direct and indirect contact conditions.

Conclusion

This work demonstrates a thermosensitive and photocrosslinkable PVA–PEG copolymer capable of reproducing key physical characteristics of Matrigel while enabling robust hydrogel formation via photoreticulation. Thermosensitivity has been validated as a proof of concept, while ongoing work focuses on enhancing gel formation directly from the thermally induced state and on quantifying viscoelastic properties as a function of UV exposure. This synthetic platform is expected to offer improved compositional control and reproducibility compared to natural matrices, supporting its development as a tunable alternative for organoid and stem cell culture.

S95 – O4

Development of a dual-stimuli responsive system for on-demand drug delivery and magnetic hyperthermia

Gonçalves A.[1,2], Fernandes S.N.[1], Pádua A.S.[3], Silva J.C.[3], Borges J.P.[1], Castilho M.[2], Soares P.I.P.[1]
[1]CENIMAT|i3N, Department of Materials Science, School of Science and Technology, NOVA University Lisbon, Caparica, Portugal; [2]Biomaterial Engineering & Biofabrication, Institute for Complex Molecular Systems, Eindhoven University of Technology, Eindhoven, The Netherlands; [3]CENIMAT|i3N, Department of Physics, School of Science and Technology, NOVA University Lisbon, Caparica, Portugal

Introduction

Cancer remains a major global health challenge, with conventional treatments often associated with significant systemic toxicity and limited efficacy. Innovative approaches, including drug delivery systems and magnetic hyperthermia, have attracted attention as promising alternatives for controlled, localized therapy at the tumor site. A temperature increase can remotely trigger the release of therapeutic molecules from inside a thermoresponsive matrix upon implantation in the human body. This trigger can be achieved using an alternating magnetic field (AMF), whereas the co-localization of magnetic nanoparticles (MNPs) within the thermoresponsive matrix induces localized heating, enabling on-demand drug release.

Aim. The aim of the present work is the production of a magnetic layer and thermoresponsive p(NIPAAm)- based fibers as drug delivery carriers to enable on-demand, controlled, and localized release of doxorubicin.

Materials and Methods

MNPs were produced using a combined chemical co-precipitation and hydrothermal treatment method. Complete characterization of the MNPs was performed, including physicochemical properties, stability in physiological conditions, magnetic properties, hyperthermia assays, and in vitro assays using a tumor cell line.

The synthesis of a thermoresponsive copolymer, poly(N-isopropylacrylamide-co-hydroxymethylacrylamide), p(NIPAAm-HMAAm) was performed via free radical polymerization, and the copolymers were processed by electrospinning to produce thermoresponsive fibers. Thermoresponsive membranes were submitted to degradation, swelling, drug release, and cytotoxicity assays.

Results

The hydrothermal treatment enables particle growth from 8 to 20 nm, changing from a spherical to a cubical shape, while maintaining their superparamagnetic properties at physiological temperatures. The particles exhibited good colloidal stability after 6 months of storage, with enhanced heating efficiency under an AMF. After incorporation into a commercially available resin, in vitro assays using PC3 cells demonstrated that the produced constructs significantly decreased cell viability upon exposure to an AMF.

As for the thermoresponsive membrane, the synthesized p(NIPAAm-HMAAm) polymer exhibited a lower critical solution temperature (LCST) of approximately 40 ºC and was processed into defect-free thermoresponsive fibers with an average diameter of 300 nm. Thermal crosslinking allowed the membranes to keep up to 70 % of their initial weight after 28 days in PBS, while water uptake assays indicate significant differences above and below the polymer's LCST. Drug release studies using doxorubicin show that temperature variation enabled the thermoresponsive fibers to release up to an additional 10 % of the drug after the initial burst release.

Conclusion

The proposed combination enables synergistic cancer treatment, aiming to minimize side effects on healthy tissues while enabling implantation with minimal invasion in solid tumors, thereby improving patient care.

Acknowledgements

This work is funded by National Funds through the FCT - Fundação para a Ciência e a Tecnologia, I.P., under the scope of the projects UID/50025/2020-2025 and LA/0037/2020 of the Associate Laboratory Institute of Nanostructures, Nanomodelling and Nanofabrication – i3N.

S95 – O5

Thiol-yne Mediated Covalent Conjugation-Induced Self-Assembly for Multiscale Polymeric Biomaterials

Noonan C[1], Conteh J[1], Cooke L[1], Nic Robin E[1], Tran T[1], Mai B[1,2]
[1]School of Biological and Chemical Sciences, University of Galway, Galway, Ireland
[2]CURAM – Research Ireland Center for Medical Devices, University of Galway, Ireland

Introduction

Polymeric Nanoparticles, PNPs, have emerged as a promising tool in drug delivery due to their versatility and multi-functionality. PNPs are conventionally prepared through either the self-assembly of amphiphilic block copolymers or emulsification polymerisation. However, controlling the self assembly of amphiphilic block copolymers is challenging and the use of surfactants in emulsification polymerisation is hindered by potential toxicity. Conjugation induced self assembly (COSA) is an emerging approach to prepare multi-functional PNPs. This study reported the synthesis of new water soluble and alkyne derived-polymers that undergoes the COSA based on UV-light mediated thiol-yne click chemistry. We uncovered the role of molar mass, crosslinking density and irradiation time on the formation of PNPs along with the possibility to load doxorubicin in an in-situ process.

Materials and Methods

The synthesis of the water-soluble and alkyne-derived polymers involves the Photo-ATRP of N-succinimidyl methacrylate, followed by the aminolysis reaction of the resultant PNSMA to introduce alkyne pendants. This product was characterized by using ^{1}H NMR. In the next step, the controlled formation of NPs via UV light-mediated thiol-yne click chemistry was studied using dithiothreitol (DTT) and Lithium phenyl-2,4,6-trimethylbenzoylphosphinate (LAP) as crosslinker and photo-initiator. The kinetic of thiol-yne click chemistry was studied using Raman Spectroscopy. The resultant nanoparticle was characterized using Dynamic Light Scattering (DLS) and Transmission Electron Microscopy (TEM). The possibility to post-functionalize resultant NPs using alkyne-azide click chemistry was demonstrated by the conjugation of azido-coumarin dye.

Results

The TEM images in figure 1a) confirm the formation of nanoparticles over time as by two minutes of irradiation the polymer has assembled into spherical NPs of about 200 nm with the size increasing to just under 1 µm by 5 minutes. The DLS results in figure 1b) also confirm this result. The Raman spectrum in figure 1c) shows the decrease in intensity of alkyne band as the irradiation time increases. However, the alkyne band is still present in the spectrum for the NPs indicating that functionalisation is possible.

Conclusion

We report an approach to control the formation of functional polymeric materials based on thiol-yne click chemistry. Such approach was used to prepare PNPs that can load chemotherapy in situ and be post-functionalized *via* alkyne-azide click chemistry. The developed nanoparticle platform is appealing for drug delivery and imaging.

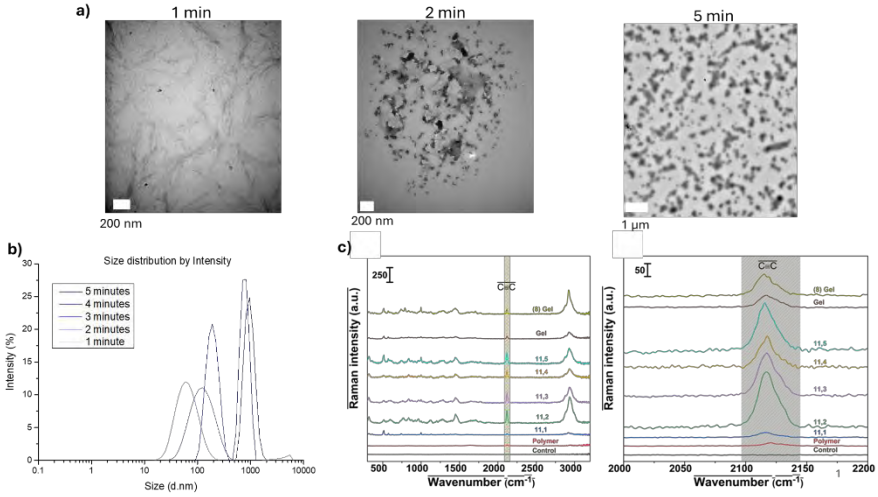

Figure 3: *a)* TEM images of the polymer forming nanoparticles as time increases, *b)* DLS size distribution by intensity as time under irradiation increases at a polymer concentration of 50 mg/ml and 50% cross linking density *c)* Raman spectrum highlighting the decrease in intensity of the alkyne bond.

Acknowledgements
This project has received funding from the European Union's Horizon Europe Excellent Science programme under the Marie Skłodowska-Curie Actions Grant Agreement [Grant Agreement No 101081457] and in part from CÚRAM Research Ireland Centre for Medical Devices [under Grant Reference 13/RC/2073_P2

S97
Scaffolding design for tissue engineering

S97 – K1
Self-feeding living materials enabled by cell responsive glycogen nanoparticles as metabolic batteries

Gurian M.[1], Willemen N.[1], Porsul I.[1], Bassous N.[2], Hiemstra J.[1], Shin S.R.[2], Leijten J.[1]
[1]Dept. Bioengineering Technologies, University Twente, Enschede, The Netherlands; [2]Dept. Medicine, Brigham and Women's Hospital, Harvard Medical School, Boston, USA

Introduction
The engineering of living tissues is considered promising for replacing, restoring, and regenerating damaged tissues and organs. Unfortunately, current applications are still limited to relatively small sizes due to restricted diffusion of oxygen and nutrients, leading to cellular necrosis and eventually implant failure. Recent strategies to overcome this limitation involve in situ metabolic support, continuously supplying oxygen or nutrients throughout the engineered tissue. While promising, these methods rely on xenogeneic enzymes, which can trigger immune responses and show reduced efficiency within the host, thus hindering their clinical translation. Here, we introduce an innovative approach utilizing glycogen, a naturally occurring nanoparticle typically found in mammalian cells for the storage and release of glucose when necessary. Specifically, we demonstrate that human mesenchymal stem cells (hMSCs) can utilize extracellular glycogen as a metabolic support system, sustaining cellular function in anoxic environments for clinically relevant time periods.

Materials and Methods
We established a culture system in which hMSC were maintained within nutrient-free DMEM containing 1% pen/strep and a single metabolite under anoxia. Cell functionality was determined by determining hMSC viability, metabolic activity and protein secretion over time. Glycogen-containing dextran-tyramine (DexTA) core-shell microgels were prepared using droplet microfluidics. Outside-in crosslinking of microgels was induced with the controlled diffusion of H2O2. These microgels were used in 2D and 3D cell culture to maintain hMSC viability and metabolic activity over time. GelMA hydrogels containing hMSCs and glycogen-loaded core shell microgels were implanted subcutaneously in mice to study their effect on cell survival and implant vascularization in vivo.

Results
Glycogen nanoparticles offer a first of its kind self-feeding metabolic support system. This system is facilitated by cell-mediated secretion of glycogen-degrading enzymes thus facilitating concentration controlled release of glucose. The use of core-shell microgels allowed for stable retention of the glycogen, while allowing free diffusion of glycogen-degrading enzymes and glucose. This approach was proved sufficient for maintaining cellular survival and function in anoxic conditions for at least a month. Moreover, glycogen incorporation enhanced the pro-angiogenic behavior of hMSCs by enhancing the secretion of numerous angiogenic factors including VEGF expression. Subcutaneous implantations in immunocompetent mice revealed that glycogen indeed drastically increased survival of implanted cells as well as facilitated full thickness vascularization of the implant. Surprisingly, we also observed a significant reduction in implant inflammation in terms of immune cell infiltration and shifting macrophage activation towards a pro-regenerative M2 phenotype.

Conclusion
Our findings demonstrate that extracellular glycogen effectively supports hMSC functionality in anoxic environments for clinically relevant periods of time by acting as metabolic batteries, which addresses a key challenge in larger tissue-engineered constructs. This approach utilizes a naturally occurring nutritional nanoparticle, potentially reducing the need for xenogeneic enzymes and enhancing the chances for clinical translation. Our findings are promising for the development of advanced metabolic support strategies to enhance the functionality of tissue-engineered constructs in clinically relevant settings.

References
[1]Willemen N., et al. *Trends in Biotech*. 2021; 39 (11). 10.1016/j.tibtech.2021.01.007
[2]Zargarzadeh M., et al. *Materials Horizons* 2022; 9 (2). 10.1039/D0MH01982H
[3]Willemen N., et al. Adv. *Healthc. Mater* 2022; 11 (13). 10.1002/adhm.202102697

[4]Van Loo B., et al. *Materials Today Bio* 2020; 6. 10.1016/j.mtbio.2020.100047

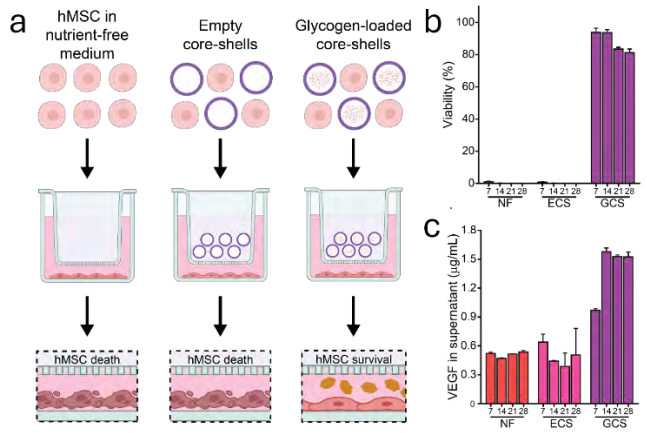

Figure 1: a) hMSCs were cultured in nutrient-free (NF) medium only, or with empty (ECS) or glycogen-loaded core-shell microgels (GCS). b) Glycogen-loaded core-shell microgels maintain hMSC viability over 28 days and c) lead to increased VEGF secretion.

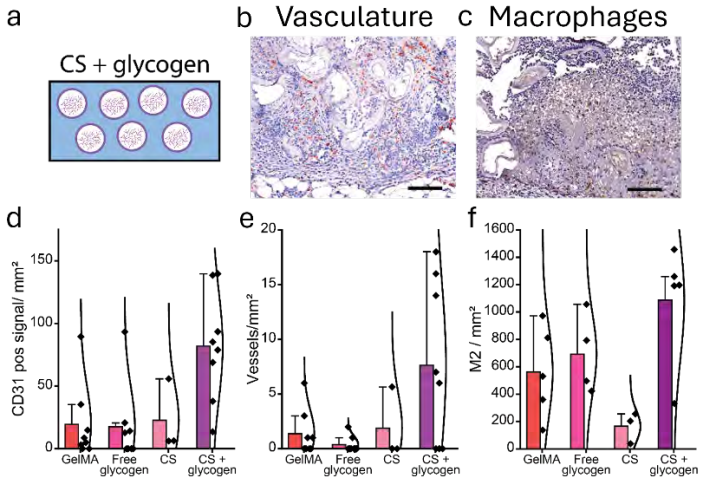

Figure 2: a) Glycogen-loaded core-shell microgels were incorporated within a GelMA hydrogel for implantation, initiating b) vasculature formation and c) presence of macrophages. Increased d) CD31 presence, e) vessel area, and f) macrophage presence was observed for gels containing glycogen-loaded core shell microgels compared to the control conditions *in vivo*. Scale bar: 100 µm.

S97 – O1

Hybrid poloxamer-gelatin bioresins for soft tissue engineering using digital light processing and volumetric additive manufacturing bioprinting

Bogaert B.[1], Van Vlierberghe H.[2], Dubruel P.[1]
[1]Polymer Chemistry and Biomaterials group, Dept. Organic and Macromolecular Chemistry, Ghent University; [2]Dept. Gastroenterology and Hepatology, UZ Ghent, Ghent, Belgium

Introduction

Light-based bioprinting techniques such as digital light processing (DLP) and volumetric printing (VAM) allow to fabricate complex, cell-laden constructs using photocrosslinkable precursors. Common examples include modified gelatin (GelMA/GelNB-GelSH), and poly(ethylene glycol) di(meth)acrylate. These materials encompass a relatively small range of physicochemical properties.

Aim

To broaden this available range, poloxamer-based precursors were prepared, and their physicochemical properties were characterized. In addition, the combination of these poloxamer precursors with modified gelatins was investigated as promising bioresins for soft tissue engineering applications.

Materials and Methods

Poloxamers (F108, F127, F68 and F87) were modified to acrylate-endcapped urethane-based precursors (AUPs) using isophorone diisocyanate and an acrylated oligoethylene (n=6) spacer. GelMA(AEMA) was prepared as a cell-interactive ligand by modification of bovine gelatin type B. All precursors were characterized by proton nuclear magnetic (^{1}H-NMR) resonance to quantify their double bond content. Furthermore, their physicochemical properties when crosslinked at different temperatures (4°C, 21°C and 37°C) were analyzed using tensile, compression, frequency sweep analysis and their cross-linking behaviour by in-situ photorheology. Processability was assessed using DLP and VAM. Optimal resins were used for bioprinting at 2M cells/mL and post-printing viability was investigated using live/dead staining and an MTS assay.

Results

^{1}H-NMR confirmed the successful modification of all precursors and was used to quantify the double bond content, showing full conversions for all poloxamers (0.13 – 0.23 mmol/g). Tensile testing (Fig. 1A) showed the lowest Young's moduli for AUPF127 (23.0 ± 1.5 kPa), and increasing with a decrease in molar mass, e.g. AUPF87 (281.6 ± 11.2 kPa). Compressive moduli (Fig. 1B) showed more dependence on the cross-linking temperature with the lowest modulus being AUPF127 (22.2 ± 2.5 kPa) and highest AUPF87 (438.4 ± 43.9). Interestingly, poloxamer solutions crosslinked at lower temperatures demonstrate more visco-elastic behaviour (tan δ: 0.2-0.5). CAD/CAM ratios of 95-97% were obtained with the smallest printable features being 50 µm in both DLP and VAM (Fig 1E and Fig. 1F). Biocompatibility essays on 3D printed samples showed viabilities >80% over a 7-day period (Fig. 1C) with a continuous increase in metabolic activity (Fig. 1D). Introduction of gelatin significantly increased cell adhesion.

Conclusion

AUP-modified poloxamers cover a wide range of physicochemical properties applicable for soft tissue engineering. Their thermogelling behaviour can be exploited to enhance compatibility with both DLP and VAM printing resulting in exceptionally high resolutions for high molar mass precursors.

Acknowledgements

The authors would like to thank FWO for the financial support (1SHE724N).

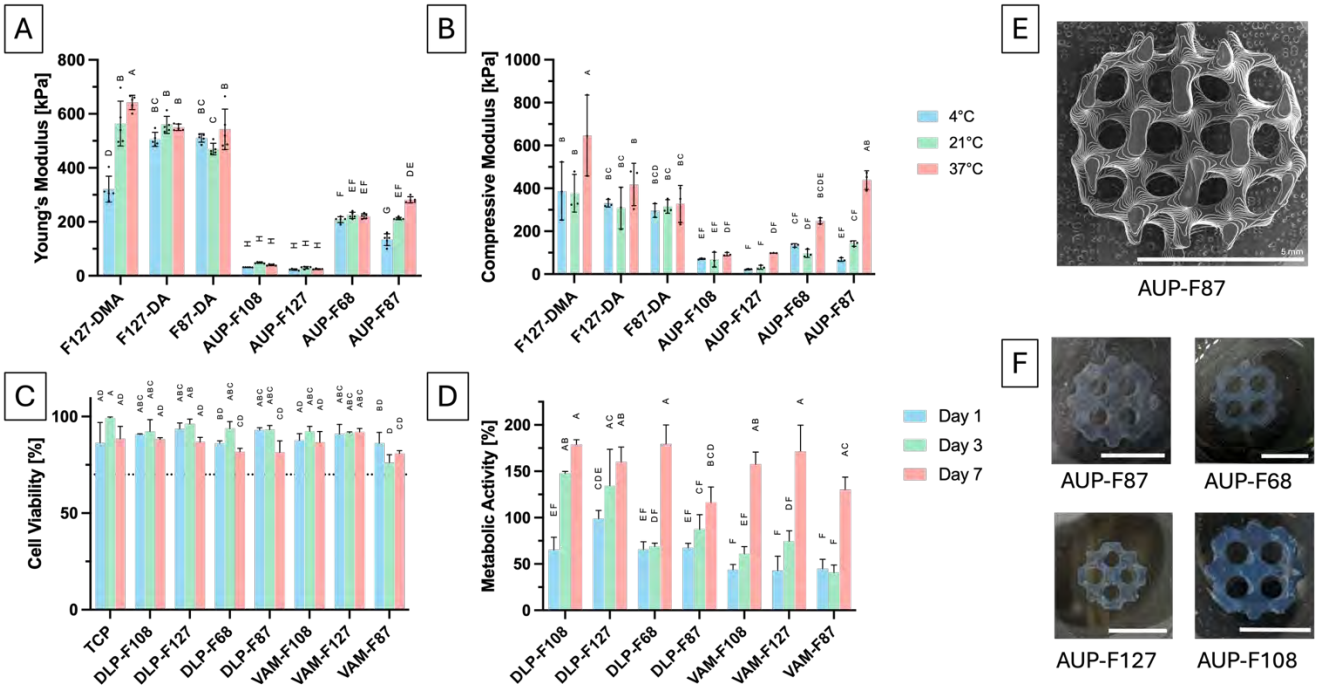

Figure 1: (A) Tensile Young's modulus of 30 %(w/w) solutions crosslinked at 4°C (blue), 21°C (green) and 37°C (red). (B) Compressive modulus of 30 %(w/w) solutions crosslinked at 4°C (blue), 21°C (green) and 37°C (red) determined by frequency sweep analysis. (C) Cell viability of HFF monolayer in direct contact with 3D printed poloxamer samples on day 1 (blue), day 3 (green) and day 7 (red). (D) Metabolic activity of HFF monolayer in direct contact with 3D printed poloxamer samples on day 1 (blue), day 3 (green) and day 7 (red). (E) SEM image of DLP-printed gyroid in AUP-F87 after drying. (scalebar = 5 mm). (F) Images of VAM-printed IWPs in different AUPs after equilibrium swelling (scalebar = 5mm).

S97 – O2

Comparison of viscoelastic behaviour in TPMS scaffolds for bone tissue engineering

Castro A.P.G.[1,2], Todescato F.[1,3], Teixeira I.[1], Ruben B.R.[4], Vena P.[5], Fernandes P.R.[1]
[1]IDMEC, Instituto Superior Técnico, Lisbon, Portugal; [2]ESTSetúbal, Instituto Politécnico de Setúbal, Setúbal, Portugal; [3]Dept. of Materials Science and Engineering Sciences, Uppsala University, Uppsala, Sweden; [4]CDRSP-ESTG, Instituto Politécnico de Leiria, Leiria, Portugal; [5]Dept. of Chemistry, Materials and Chemical Engineering, Giulio Natta, Politecnico di Milano, Milan, Italy

Introduction

The use of triply periodic minimal surfaces (TPMS) is frequently cited for scaffold design in bone tissue engineering (BTE). TPMS-based BTE scaffolds can be designed as a function of the manufacturing technology, biomaterial or application. It is widely accepted that two structures with the same porosity, but different geometries, will have different micro and macromechanical behaviours, although it is not fully understood yet how these differences can be predicted.

Aim. To understand the influence of different porosity levels and TPMS geometries on the viscoelastic response of polymeric scaffolds, to provide insight into the design of BTE scaffolds independently from the provided manufacturing technology and biomaterial.

Materials and Methods

The scaffolds were generated with LisbonTPMS-tool in six configurations: two geometries (Gyroid (SG) and Schwarz Diamond (SD)) and three porosities (60%, 70%, and 80%). The printing material used was Visijet M3 Crystal polymer, for the printer ProJet 3D MJP 3600 (3D Systems, USA). Solid samples were produced for comparison purposes. The viscoelastic response was tested with the following protocol: compression rate of 1.8 mm/min until 1.5% displacement followed by 2 hours hold to assess stress relaxation. The impact of three curing time points after production was also evaluated for solid and SD samples (70% and 80%) at weeks 2, 5, and 8. Two outputs were reported: Young's modulus (E) and relaxation stress gap (representing the decay from peak stress, correspondent to the ramp compression, to the end of the relaxation period).

Results

Figure 1 shows that both SG and SD scaffolds displayed an increase in the stress gap from 60% to 80% porosity, but SD scaffolds exhibited an intermediate reduction in the stress gap, from 60 to 70% porosity. Scaffolds are less stiff and more prone to pronounced relaxation behaviour that the solid samples. Additionally, table 1 shows that solid samples showed increasing stress gap and decreasing stiffness as the weeks progressed, contrarily to what was observed for the porous scaffolds.

Conclusion

Overall, it was observed that increasing porosity causes a decrease in stiffness and an increase in stress relaxation over the experiments duration. These findings confirm that different TPMS geometries show differences in how stress is distributed through the structure, with clear influence from the configuration and not only from the porosity. On-going studies include the parametrisation and numerical modelling of the viscoelastic behaviour of TPMS geometries, to enhance the design of BTE scaffolds.

Acknowledgements

This work was supported by Fundação para a Ciência e a Tecnologia (FCT), Portugal, through LAETA (project UID/50022/2025), CDRSP (project UID/04044/2025) and PhD Grant 2024.00399.BD, and COST Action EuroCurvoBioNet CA22153, supported by COST (European Cooperation in Science and Technology).

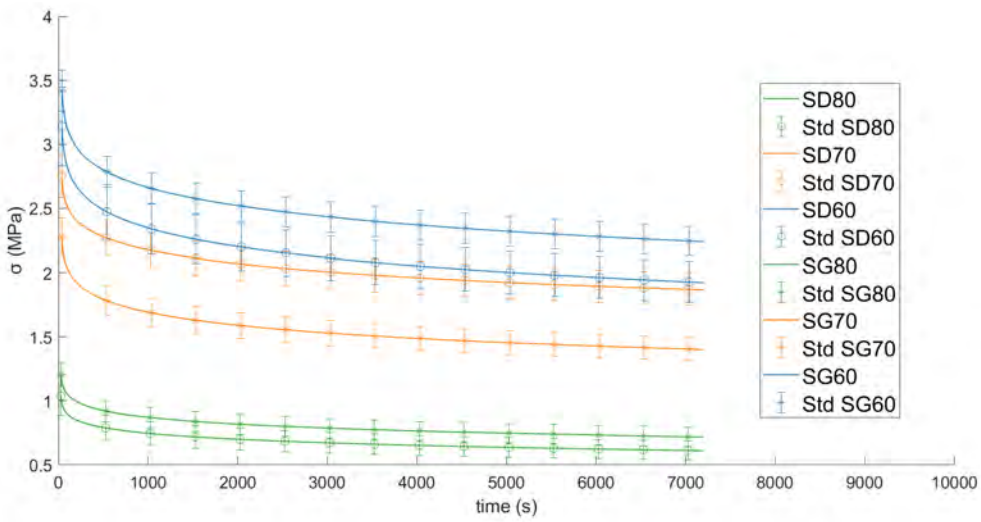

Figure 1: Stress relaxation for TPMS scaffolds.

Table 1: Young Modulus and stress gap for Solids and SD scaffolds at three curing times: Week 2, 5 and 8.

		Week 2	**Week 5**	**Week 8**
Solids	E (MPa)	2082,3	1977,3	1444,7
	Stress Gap	33,4%	30,3%	39,4%
SD70	E (MPa)	157,6	190,8	196
	Stress Gap	74,7%	49,4%	46,9%
SD80	E (MPa)	60,8	70,9	66
	Stress Gap	87,7%	75,2%	63,2%

S97 – O3

High resolution printed 3D artificial scaffolds for studying the influence of extracellular matrix biophysical cues on fibroblast migration

Arcas A.[1,2], Drobecq I.[1], Fournie V.[1], Malaquin L.[1], Ferrand A.[2], Venzac B.[1]
[1]LAAS-CNRS, Université de Toulouse, CNRS, UPR 8001, 7 avenue du colonel Roche ; [2]I2MC, Université de Toulouse, INSERM/UPS UMR 1297, 1 Av. du Professeur Jean Poulhès, 31400 Toulouse, France

Crohn's disease displays chronic inflammation of digestive tissues, with densification and rigidification of the extracellular matrix (ECM). Studying the impact of this altered matrix on fibroblasts is required to understand relapses. In this tissue, the ECM is mainly composed of rigid collagen fibers with diameters from 100 nanometers to micrometers[1]. In vitro, stiffness of usual ECM models depends on pore size for both hydrogels and 3D printed scaffolds. However, this pore size strongly influences cell behaviors, such as morphology and migration, also dependent on fiber dimensions and orientations2. While scaffolds produced by high resolution two-photon polymerization (2PP) present fibers down to 200 nm in diameter[3], they lack independent control of stiffness and fiber density. In this work, we developed new 2PP-based scaffolds to study fibroblast migration and fate in synthetic ECM, whose biophysical cues (micro-architecture, density and stiffness) replicate Crohn's disease characteristics.

Materials and Methods

Scaffolds were printed with biocompatible acrylic photoresin (E = 1.5 GPa) on a Nanoscribe GT2 printer. The manually coded patterns consist of fibers arranged in stacked cubes with or without vacancies. Cubic scaffolds measured 360 µm per side and 120 µm in height, with interfibrillar spacing of 7.5 to 24 µm, and fiber diameters of 1.3 to 2.5 µm, measured using scanning electron microscopy (SEM). Young's modulus of the scaffolds was measured using a homemade compression device. Human colon fibroblasts (CCD18-Co) were seeded onto fibronectin-coated scaffolds at 1×10^5 cells/mL, then cultured for 14 days prior to confocal microscopy or SEM.

Results

The scaffold stiffness decreased with thinner fibers and larger spacings. Young's modulus (E) down to 25 kPa was obtained, reaching soft tissue range. Adding defects allowed decoupling stiffness from the fiber density and dimensions. For example, stiffness of a scaffold decreased (spacing 7.5 µm, fiber dimension 1.2 µm) from E = 20 MPa to E = 300 kPa by adding defects.

Fibroblast behavior was studied on scaffolds. At days 1, 7 and 14 of culture, nuclei and plasma membranes were stained. Using nuclear segmentation, we analyzed morphology, orientation and distribution of cells relative to scaffold parameters. From early culture, we observed differences in cell morphology and alignment of nuclei toward scaffold centers across spacings. This suggests that the cells are migrating within the structures. The cells also showed good adhesion and survival on scaffolds.

Conclusion

Through this work, we achieved micrometric fiber dimensions with accurate control. Scaffold stiffness was drastically decreased while maintaining constant fiber density, pore size and fiber dimensions, effectively decoupling stiffness and micro-architecture. Moreover, fibroblast spreading depended on the fiber spacing. In the future, we will improve the ECM model by introducing primary fibroblasts from healthy and Crohn's patients to characterize the role of ECM biophysical cues on fibroblast phenotypes.

Acknowledgements

This work was supported by LAAS-CNRs micro and nanotechnologies platform, a member of the Renatech french national network. This work was funded by the "Agence Nationale de la Recherche" (ANR) as part of the JCJC programme.

References

[1]Naba Alexandra. 2024. Nat Rev Mol Cell Biol
[2]Loh , *et al*. 2013. *Tissue engineering.*
[3]Jing X, *et al*. 2022. *Front Bioeng Biotechnol*.

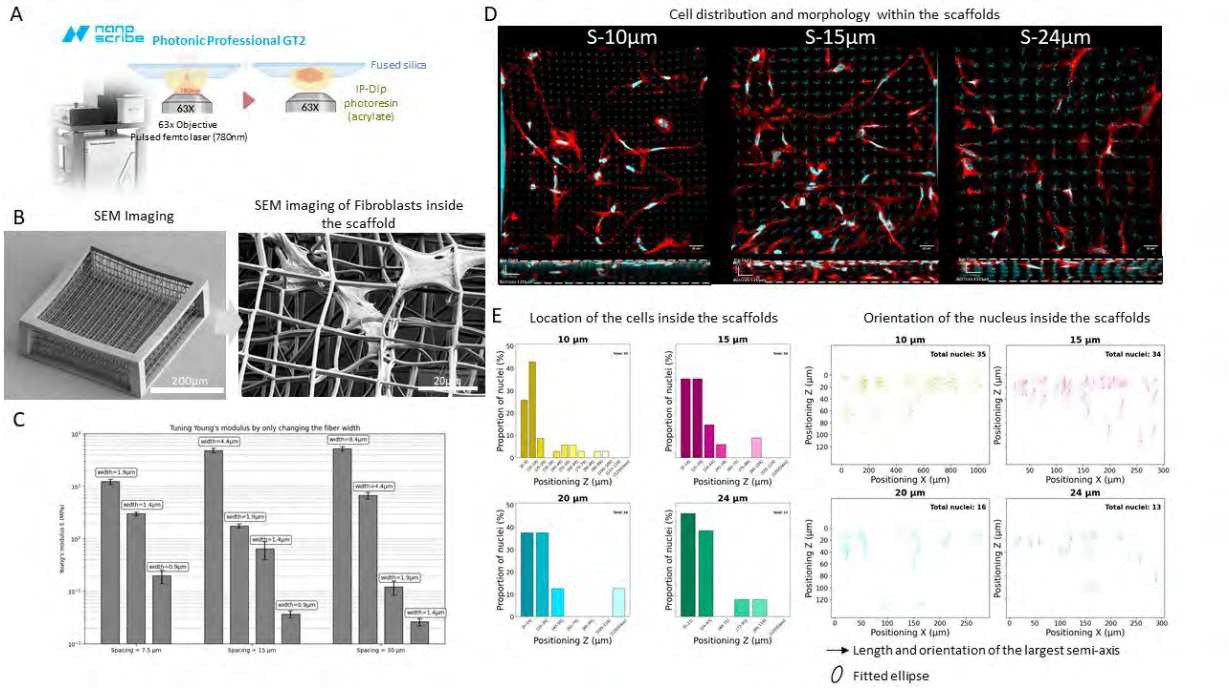

<u>High resolution printed 3D artificial scaffolds for studying the influence of extracellular matrix biophysical cues on fibroblast migration:</u> **(A)** Schematic representation of the printing process on the Nanoscribe GT2 printer. **(B)** Scanning electron microscopy (SEM) imaging was performed on a 360 x 360 x 120 µm scaffold with 24 µm spacing and 1.5 µm fibre sections. This was examined with and without cells inside, after seven days of culture, fixation, dehydration and metalisation with Au/Pd (0.1KA). **(C)** Effect of fiber section on Young's modulus at different spacings (7.5, 15 and 30 µm). **(D)** Maximum intensity projection of fibroblasts inside the scaffolds, stained with SPY-DNA for the nucleus (cyan) and CellMask for the plasma membrane (red) in the X and Z planes. **(E)** Number, positions and orientation of the nuclei inside the scaffolds on day 1 of cell culture determined by 3D segmentation of the nuclei.

S97 – O4

Digital light processing of γ-PGA (gamma-polyglutamic acid) based sol-gel hybrid biomaterials

Li Y.[1], Iqbal H.[1], Chung R.-J.[2], Jones J.R.[1]
[1]Dept.Materials, Imperial College London, London, UK; [2]Dept.Chemical Engineering and Biotechnology, National Taipei University of Technology (Taipei Tech), Taipei, Taiwan

Introduction

There is a significant clinical demand for scaffolds capable of promoting regeneration in non-union bone defects (fractures failed to heal properly with aid[1]). However, the ideal criteria for scaffolds, of combining bioactivity and ability to share load with host bone, has yet to be met. Inorganic/organic hybrids are promising candidates by offering synergy of mechanical properties, controlled degradation and bioactivity[2]. The use of digital light processing (DLP) as a 3D printing technique enables the fabrication of complex porous scaffolds that allow tissue growth while providing mechanical strength. The aim of this project is to 3D print the first γ-PGA based silica hybrids. γ-PGA, as an analogue of collagen, can be produced by bacteria fermentation. It therefore exhibits good biodegradability and biocompatibility[3]. The challenge was to impart light curability to the polymer. The final mechanical properties of the hybrids can be tailored for different bone defects accordingly.

Materials and Methods

The γ-PGA was functionalised with glycidyl methacrylate (GMA) to form γ-PGA-GMA. A co-polymer with polycaprolactone-diacrylate, PCL-DA, was synthesised to increase the hydrophobicity of the organic network. It was produced by reacting polycaprolactone-diol (PCL-diol) with acryloyl chloride.

The hybrid resin for DLP printing was prepared by adding organic component γ-PGA-GMA/PCL-DA into the pre-hydrolysed tetraethyl orthosilicate (TEOS) as the silica precursor. During the sol-gel process, the coupling agent 3-(trimethoxysilyl)propyl methacrylate (TMSPMA) was added to form covalent bonds between the organic and inorganic phases. To achieve an accurate printing process, photoinitiators and photoabsorbers were utilised.

Results

The functionalization of γ-PGA and PCL-diol were proven by ^{1}H NMR spectra. Monoliths of γ-PGA-GMA/silica and γ-PGA-GMA/PCL-DA/silica hybrids were prepared through UV curing. Gyroid scaffolds were printed via DLP. Compression test on gyroid scaffolds showed an ultimate compressive strength of around 13.5 MPa at 7% strain (Figure 1), which falls in the range of cancellous bone. Micro-CT images revealed the pore diameter of around 1.1 mm, and 3D image analysis yielded the gyroid porosity of approximately 47%, size distributions of struts and channels (Figure 2).

Conclusion

γ-PGA-GMA/silica hybrid (I/O = 20 wt%: 80 wt%) gyroid scaffolds were successfully fabricated via DLP printing and exhibited good mechanical properties. Micro-CT results demonstrated the sufficient channel size of gyroids for tissue ingrowth. The addition of PCL-DA showed promising effects in restraining the water uptake of γ-PGA-GMA/silica hybrids. Gyroids made of γ-PGA-GMA/PCL-DA/silica hybrid will be further investigated to achieve controlled printing process while possessing appropriate mechanical properties in aqueous environment for bone regeneration in real cases.

References

[1]Lasanianos NG., Kanakaris NK., Giannoudis PV. Current management of long bone large segmental defects. *Orthopaedics and Trauma* 2010; 2; 149–163.
[2]Jones JR. Review of bioactive glass: From Hench to hybrids. *Acta Biomaterialia* 2013; 1; 4457–4486.
[3]Poologasundarampillai G., Yu B., Tsigkou O., Valliant E., Yue S., Lee PD., Hamilton RW., Stevens MM., Kasuga T., Jones JR. Bioactive silica–poly(γ-glutamic acid) hybrids for bone regeneration: effect of covalent coupling on dissolution and mechanical properties and fabrication of porous scaffolds. *Soft Matter* 2012; 17; 4822-4832.

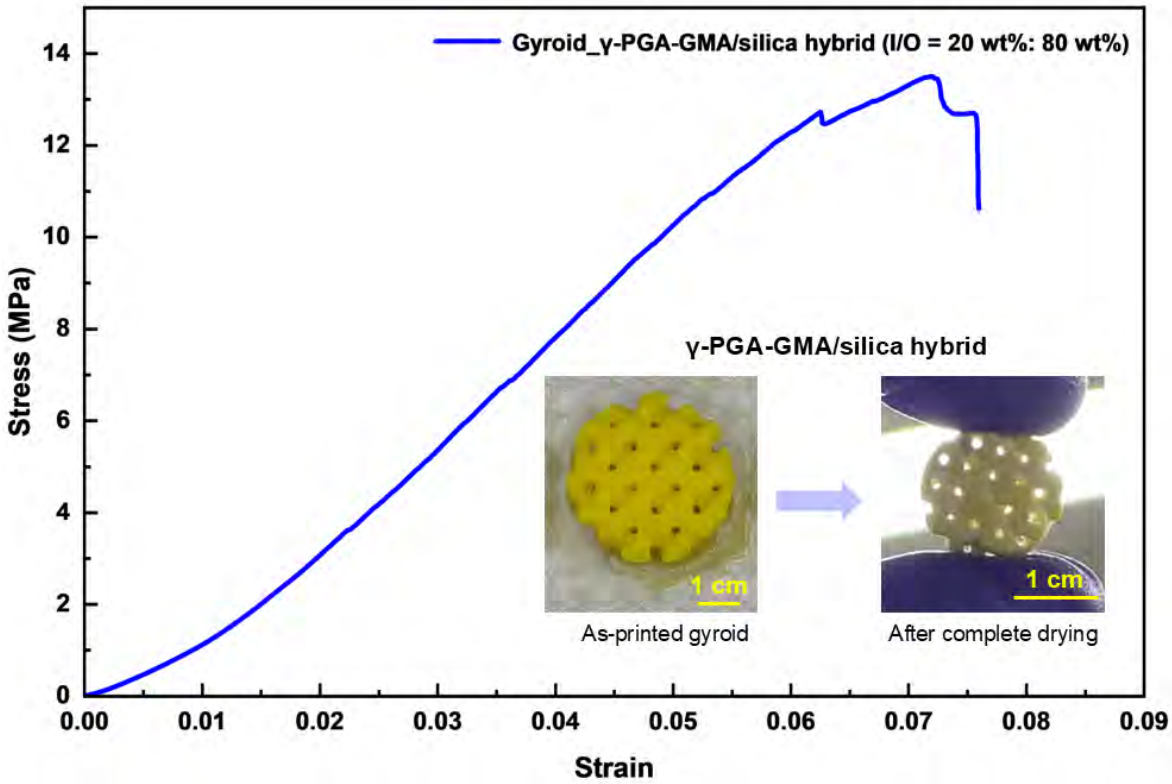

Figure 1. Stress-strain curve of dried γ-PGA-GMA/silica hybrid gyroid scaffold (I/O = 20 wt%: 80 wt%).

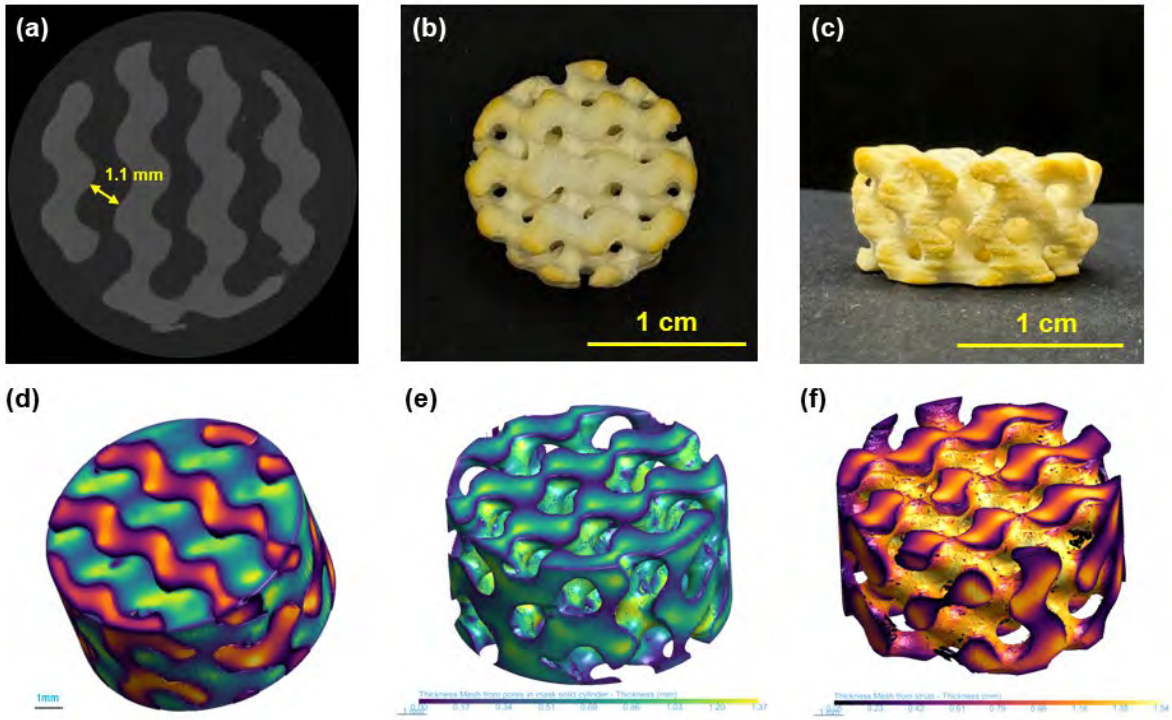

Figure 2. Micro-CT analysis and images of γ-PGA-GMA/silica hybrid gyroid scaffold (I/O = 20 wt%: 80 wt%): (a) micro-CT of one slice of the gyroid structure; (b) top view image; (c) side view image; (d) 3D rendering of the whole gyroid structure; (e) 3D rendering of the channels; (f) 3D rendering of the struts.

S97 – O5

Polymer-based honeycomb membrane on a 3D porous bioactive glass: Towards a new generation of scaffolds for bone tissue engineering

Larroudé S.[1], Calderón-Jacinto R.[2], Houaoui A.[2], Boissière M.[2], Pauthe E.[2], Massera J.[1]
[1]Faculty of Medicine and Health Technology, Tampere University, Tampere, Finland; [2]ERRMECe, CY Cergy Paris University, Neuville-sur-Oise, France

Introduction

Bone reconstruction with grafts can be impaired by soft tissue infiltration at the defect site[1]. To prevent this, polymer membranes have been developed, they are traditionally dissociated from the graft, extending clinical procedure time and complexity. Recently, we reported the deposition of a poly (L-co- D, L lactic acid) honeycomb membrane onto bioactive glass (BG) discs and assessed the impact of gamma-radiation sterilization on their physico-chemical properties[2]. Although these newly developed biphasic materials showed promise, depositing the membrane onto clinically relevant bone scaffolds remained challenging. In this study, we demonstrate the deposition of a membrane on scaffolds with a gradient of porosity. The membrane supports cell viability and proliferation while preventing cell adherence on top of the scaffold.

Materials and Methods

As explained in[2], 13-93B20 BG was synthetized using the melt-quenching technique and crushed into powder (Ø < 38 µm). A 30 wt% BG powder in 25 wt% Pluronic F127 solution was prepared and BG scaffolds were 3D printed with a gradient of porosity (dense top). After sintering, samples were conditioned in TRIS buffer (24h) and dried before membrane deposition. Honeycomb membranes were generated on the scaffolds using the breath figure method using poly (L-co-D, L lactic acid) (10 mg/mL), 1% surfactant dioleoyl phosphatidylethanolamine in chloroform. Cytocompatibility of scaffolds, membranes and assemblies was evaluated using human adipose stem cells (hADSCs), by live/dead assay and proliferation on top of the materials using CyQUANT™. Morphology of the hADSCs on top of the composites (half membrane-covered surfaces) was evaluated by DAPI/phalloidin staining.

Results

hADSCs proliferated well on conditioned bioactive glass scaffold. Cells remained viable on the membranes and assemblies, though in lower numbers. CyQUANT™ proliferation assay showed no significant difference between scaffolds and assemblies (Figure 1A). After 1 and 3 days, cells on assemblies appeared smaller and thinner on the membrane side but spread and elongated on the BG side. After 7 days, cells were elongated on both sides likely due to CaP precipitation, on top of the membrane, from scaffold ion release (Figure 1B).

Conclusion

This work investigated the possibility to generate a honeycomb membrane on top of a 3D printed BG scaffold. A controlled gradient of porosity enabled the membrane deposition. The assemblies showed great cytocompatibility and proliferation while disrupting cell attachment due to membrane's surface topography. This approach supports new biphasic materials combining the osteopromotive properties of inorganic materials with the barrier effect of HC polymer-based membranes.

References

[1]Dahlin C, Linde A, Gottlow J, Nyman S. Healing of Bone Defects by Guided Tissue Regeneration: *Plast Reconstr Surg*. 1988;81(5):672-676.
[2]Deraine A, Rebelo Calejo MT, Agniel R, et al. Polymer-Based Honeycomb Films on Bioactive Glass: Toward a Biphasic Material for Bone Tissue Engineering Applications. *ACS Appl Mater Interfaces*. 2021;13(25):29984-29995.

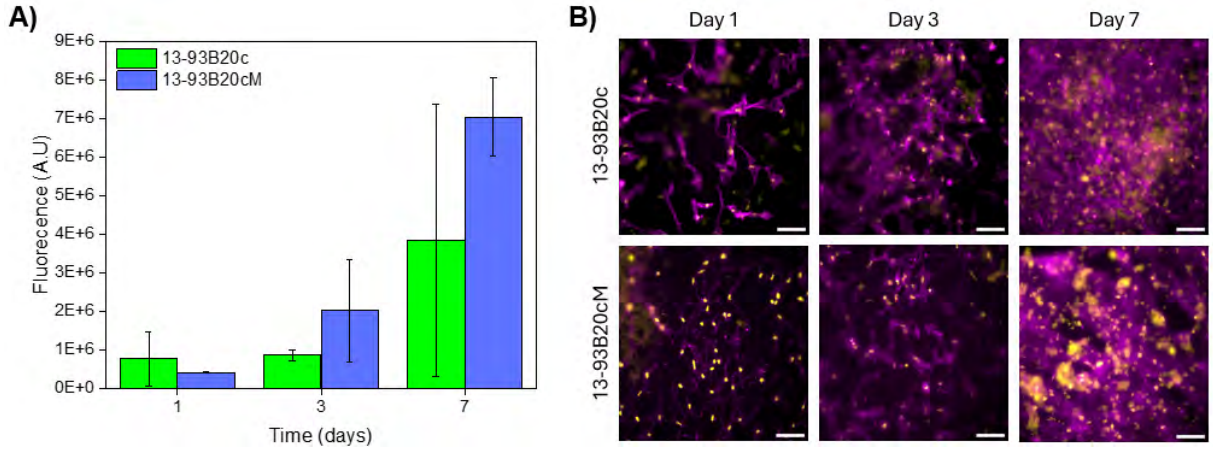

Figure 2: A) CyQUANT cell proliferation assay on the conditioned scaffold (13-93B20c) and the conditioned scaffold with a membrane (13-93B20cM); B) DAPI (yellow) and phalloidin (purple) staining on top of 13-93B20c and 13-93B20cM. Scale bar: 100 µm

S97 – O6

Thiol-guided peptide-functionalized albumin hydrogels with tunable architecture and bioactivity

Mehwish N.[1,2], Sánchez Homs J.[1,2], López-Gómez P.[1,2], Ginebra M.-P.[1,2,3,4], Mas-Moruno C.[1,2,3]
[1]Biomaterials, Biomechanics and Tissue Engineering Group, Department of Materials Science and Engineering, Escola d'Enginyeria Barcelona Est (EEBE) and Institute for Research and Innovation in Health (IRIS), Universitat Politècnica de Catalunya BarcelonaTech (UPC), Barcelona; [2]Barcelona Research Center in Multiscale Science and Engineering, Universitat Politècnica de Catalunya, Spain; [3]Centro de Investigación Biomédica en Red, Bioingeniería, Biomateriales y Nanomedicina (CIBER-BBN), Instituto de Salud Carlos III, Madrid, Spain; [4]Institute for Bioengineering of Catalonia (IBEC), Barcelona, Spain

Introduction

Balancing biological functionality with simplicity and cost remains a persistent challenge in the design of biomaterials for regenerative applications. Albumin-based hydrogels offer an appealing solution as scalable and chemically versatile protein platforms [1]; however, their lack of inherent bioactivity limits their capacity to actively engage cells. Incorporation of adhesive peptide motifs [2] such as RGDS represents a powerful strategy to overcome this limitation, yet the ultimate cellular response is governed not only by biochemical cues but also by the physicochemical characteristics established during gelation.

Aim

This study aims to engineer RGDS-functionalized albumin hydrogels via thiol-based conjugation and evaluate how peptide incorporation and gelation strategy influence their physicochemical properties and cellular response.

Materials and Methods

Bovine serum albumin (BSA) was modified to obtain thiolated (sBSA) and methacrylated (mBSA) derivatives. RGDS peptides were incorporated via thiol-maleimide and thiol-ene coupling. Hydrogels were fabricated using thermal gelation (70°C), UV crosslinking (405 nm), and cryogelation (−20°C). Hydrogels were characterized for mechanical properties, swelling, and degradation. Human bone marrow mesenchymal stem cells (hBMSCs) were used to assess cytocompatibility, adhesion, and morphology.

Results

Gelation strategy significantly influenced hydrogel architecture and performance. Macroscopic observations revealed distinct morphologies, with thermal hydrogels appearing brittle, UV-crosslinked systems more transparent and fluid-like, and cryogels exhibiting opaque and sponge-like structures (Figure 1). Cryogels displayed highly interconnected macroporous structures (100–250 µm), high swelling (>300%), and slower degradation.

RGDS functionalization enhanced cell adhesion and spreading across all systems (Figure 1). Thermal and UV hydrogels promoted planar cell morphology, while cryogels supported cell infiltration due to their porous structure. Mechanical analysis indicated that thermal gels were stiff but brittle, whereas UV gels were weaker, and cryogels provided a balance between elasticity and stability.

Conclusion

The combination of thiol-based peptide conjugation with different gelation strategies enables precise control over albumin hydrogel properties. Cryogelation offers advantageous architectures for 3D cell interactions, while RGDS incorporation enhances bioactivity. This platform represents a versatile and cost-effective approach for biomaterial design in tissue engineering.

Acknowledgements

This work was supported by Agencia Estatal de Investigación (PID2023-148538OB-I00) and Generalitat de Catalunya (AGAUR FI_B fellowship).

References

[1] Kong F., Mehwish N., Lee B.H. Emerging albumin hydrogels as personalized biomaterials. Acta Biomaterialia 2023, 157; 67-90.
[2] Oliver-Cervelló L., López-Gómez P., Martin-Gómez H., Marion M., Ginebra M.-P., Mas-Moruno C. Functionalization of alginate hydrogels with a multifunctional peptide supports mesenchymal stem cell adhesion and reduces bacterial colonization. Chemistry – A European Journal 2024; 30, e202400855.

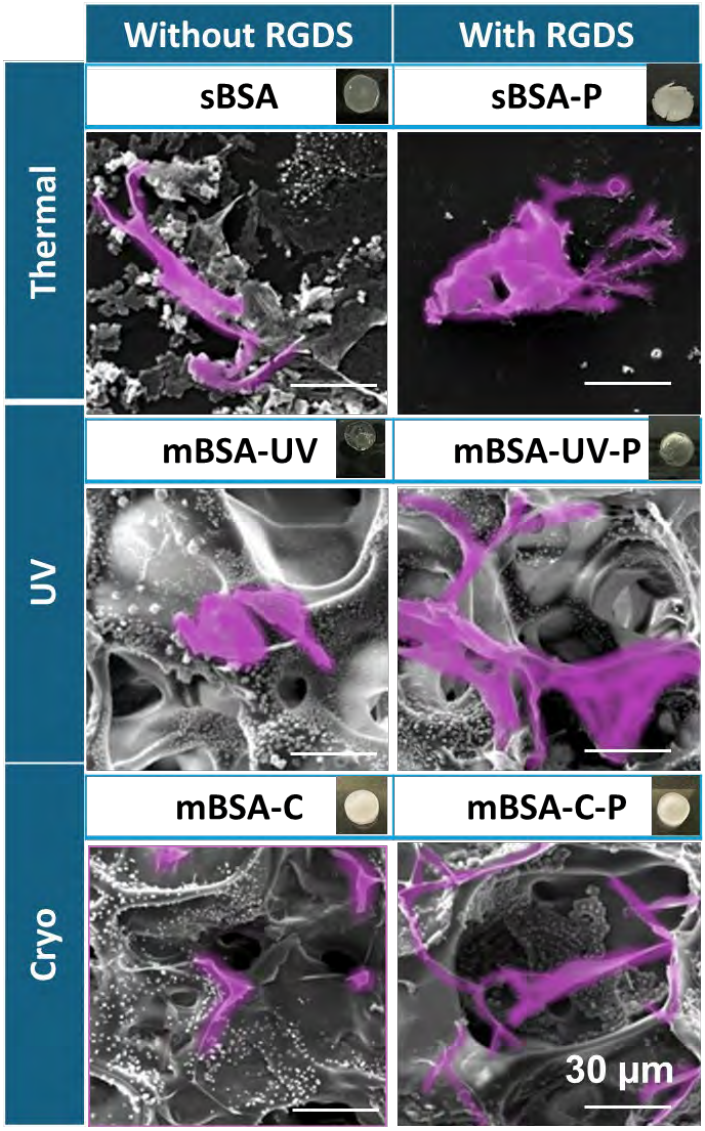

Figure 1. Representative macroscopic images of albumin hydrogels and scanning electron microscopy (SEM) images showing cell morphology and adhesion across different gelation strategies and RGDS functionalization conditions. Macroscopic scale bars: 5 mm. SEM scale bars: 30 µm.

S98
Smart and stimuli-responsive biomaterials

S98 – K1

Vermonden T.
Utrecht University,The Netherlands

S98 – K2

Programming via printing: Single-step fabrication of shape-morphing biomaterials for mechanobiology and tissue engineering

Henderson J.H.
Department of Biomedical and Chemical Engineering and BioInspired Institute, Syracuse University, Syracuse, NY, USA

Introduction

Manufacturing with shape-memory polymers (SMPs) has the potential to enable paradigm-shifting advances across biomedicine and soft robotics through the creation of devices possessing spatially varying material functionality that cannot be achieved by any current approach. Realizing this potential has been limited, however, by the reliance of conventional shape memory on separate, often complex programming steps and by gaps in fundamental understanding at the interface of materials processing and materials science.

Materials and Methods

To transcend these limitations, our group has developed programming via printing (PvP), a single-step, single-material approach in which molecular-scale tensile strain is trapped directly during extrusion and fixed by vitrification as each fiber cools, programming shape memory at the fiber level using inexpensive, off-the-shelf printers and commercially available SMPs. Because the trapped strain is set by print parameters such as nozzle temperature and layer architecture, PvP makes spatially patterned, tunable actuation an accessible, low-cost, and broadly adoptable capability. Throughout, we pair experiment with mechanics-based simulation to predict and design the mapping from print parameters to programmed shape.

Results

Recent work has extended PvP from uniaxial contraction to biaxial self-shrinking that improves cell seeding, dynamic control of surface topography through shape-memory-driven wrinkling of thin metallic and polymeric films for the study of cell mechanobiology, and spatially patterned strain trapping that yields programmable shape morphing from a single material. Most recently, we have moved beyond contraction to demonstrate parts that expand along multiple axes, broadening the geometries and soft-tissue applications that 4D-printed SMP scaffolds can address. Extending this trajectory, we are coupling PvP-programmed architectures with mechanophore-based force sensing to resolve how mechanical force is transmitted across scales, from the molecular level to the biomaterial-cell interface, and to connect programmed deformation with cell mechanotransduction.

Conclusion

Together, these advances establish PvP as an integrated, interdisciplinary route from fundamental materials processing and science to emerging biomedical applications. Here we will present this overview and discuss the opportunities and open challenges in advancing single-material 4D fabrication toward functional, stimuli-responsive devices.

Acknowledgements

This work was supported by the U.S. National Science Foundation (CMMI-2022421 and DMR-2611321).

S98 – O1
Ionomeric extracellular matrices for dynamic tissue engineering

Burgess M.K.[1], Murray R.T.[1], Lucian V.M.[1], Liu Z.[1], Cleveland R.O.[1], Beeston C.J.[1], Nair M.[1]
[1] Institute of Biomedical Engineering, Department of Engineering Science, University of Oxford, Oxford OX3 7LD, UK

Introduction

Existing biomaterials for repair are largely static, while tissues are dynamic and shaped by changing biochemical, electrical, and mechanical cues. Conventional electroactive polymers (EAPs) used in stimuli-responsive regenerative platforms often suffer from poor biocompatibility, limited degradability, and incompatible operating conditions. Electroactive biomaterials better mimic tissue environments but lack sufficient mechanical output for dynamic platforms. Here, we introduce an ionic electrochemical actuator made from bio-derived materials, termed ionomeric extracellular matrices (iECMs). This approach imparts EAP-like electroactivity enabling extracellular matrices (ECM) to translate biochemical and electromechanical signals to tissue while maintaining ECM mimetic biochemistries.

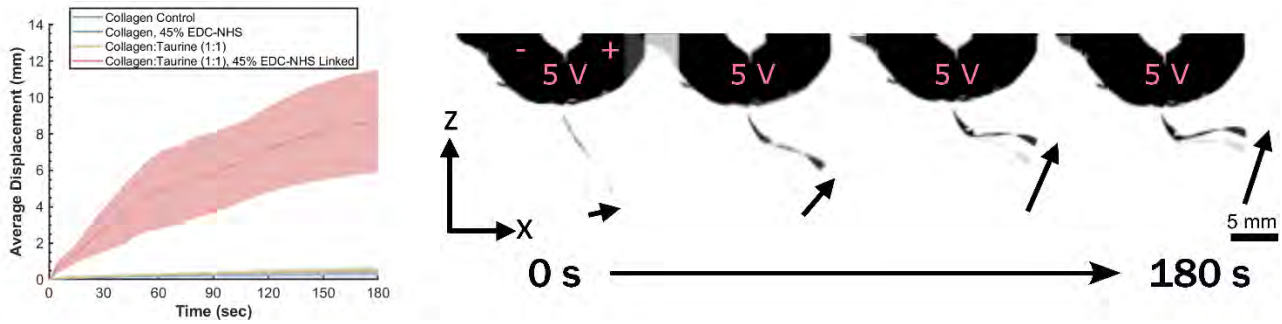

Figure 1. iECM Displacement under electrical stimulation.

Materials and Methods

iECMs were fabricated by carbodiimide (EDC/NHS) linking of taurine to collagen free carboxyls, with characterisation of functionalisation (FTIR, EDX) and charge density. Electromechanical properties of tri-layer silver-plated iECM actuators were assessed against collagen controls across several parameters (0.5–7 V, 24 hours). Biocompatibility was assessed on stimulated and unstimulated iECM-coated plates with C2C12, human dermal fibroblasts (HDFs), and human umbilical vein endothelial cells (HUVECs) against collagen controls.

Results

Our taurine functionalisation strategy increased collagen charge density 8.9-fold (Fig. 1), with functionalisation confirmed by FTIR and EDX. This was accompanied by a 19.4-fold increase in free-end deflection of tri-layer beams under 5 V, with frequency-dependent, directionally controllable actuation stable over 24 h. These iECMs supported growth of C2C12, HUVECs and HDFs. We observe comparable HDF numbers in iECMs to collagen control without stimulation1.4-fold and up to 3.6-fold increase in population when stimulated (Fig. 2).

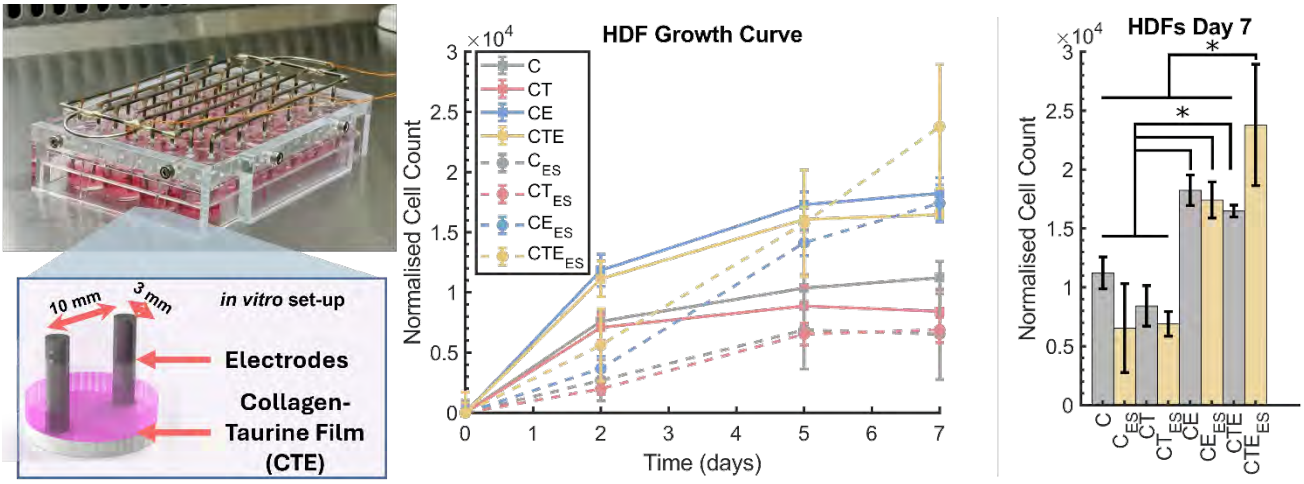

Figure 2. 7-day HDF growth on electrically stimulated (ES) and unstimulated taurine functionalised collagen (CTE), collagen (C), collagen-taurine blend (CT), and crosslinked collagen (CE)

Conclusion

This research introduces novel electroactive ECM-based materials, demonstrates electromechanical actuation, and validates biocompatibility with skin, muscle, and vascular cells, surpassing collagen in cell growth. Collectively, our results establish sulfonated collagen iECMs as a promising platform for electrically and mechanically active, tissue-mimetic constructs for applications such as wound healing and other dynamic regenerative therapies.

Acknowledgements

This work was supported by Royal Society of Chemistry (E20-8065), Engineering and Physical Science Research Council (EP/Y004434/1, EP/W524311/1), Rhodes Trust, and Emmanuel College. We thank I.N. Dyson (SEM/Tensile) and B. Bower (EDS) for technical assistance.

S98 – O2

4D bioprinting of photo-curable polymers for the fabrication of self-folding structures

Fortunato G. M.[1], Guerra A.[1], Chiesa I.[1], Montassier J.[2,3], Kvakova K.[2,3], Pinese C.[2,3], De Maria C.[1], Nottelet B.[2,3], Vozzi G.[1]

[1]Research Centre "E. Piaggio" and Dept. of Information Engineering, University of Pisa, Pisa, Italy; [2]Polymers for Health and Biomaterials, IBMM, University of Montpellier, Montpellier, France; [3]Department of Pharmacy, Nîmes University Hospital, Nimes, France.

Introduction

The ability of flat structures to self-fold in response to an external stimulus is highly valuable for engineering anatomical tubular tissues or for producing bioinspired devices. Self-folding can be achieved by combining two materials with different responses to the same stimulus, so that when the stimulus is applied (*e.g.,* temperature or humidity change), the resulting deformation mismatch generates mechanical stress that causes the structure to bend or fold. This strategy was recently successfully applied to self-rolling drug eluting patches based on PEG-PLA star copolymers[1-2], whose 3D photo-printability was then confirmed[3].

Aim. The aim of this study is to design and develop resorbable 4D-printed active structures combining two PEG-PLA materials with different hygroscopic responses, capable of producing controlled folding/bending.

Materials and Methods

Photocurable (405 nm) PEG/PLA-based copolymers were used. The hydrophilic formulation was prepared by dissolving the copolymer in propylene carbonate at a concentration of 300mg/mL, followed by the addition of lithium-phenyl-2,4,6-trimethylbenzoylphosphinate (LAP) at 2.5mg/mL. Hydrophobic formulations were prepared with the same protocol but with LAP at 5mg/mL and two copolymer concentrations: 300 and 500mg/mL.

Material properties were assessed through swelling and contact angle measurements. 4D-printing experiments were then performed using a robotic biofabrication platform (Mecademic MECA500) equipped with an extrusion-based bioprinting tool and a photocuring unit. Two configurations were investigated to identify the arrangement that maximized folding: (i) a continuous hydrophobic bottom layer with hydrophilic lines on top, and (ii) a continuous hydrophilic bottom layer with hydrophobic lines on top. The bottom layer was a 20mm sided square, while the top layer consisted of eight parallel lines. By immersion in deionized water, the analysis verified whether the curvature followed the lines direction and whether the final radius approached that of a complete cylinder (Figure 1A).

Results

Swelling and contact angle measurements are reported in Figures 1B-C. Since no significant differences were observed between the two hydrophilic materials, the 500mg/mL formulation was selected for printing. Folding tests showed that structures with a continuous hydrophobic layer and discrete hydrophilic lines on top exhibited the most effective folding behavior (Figures 2A-B), observing the same trend even with larger structures (Figure 2C). Conversely, structures with a continuous hydrophilic layer and hydrophobic lines on top did not display any folding (Figure 2D).

Conclusion

The controlled folding in 4D-printed bilayer structures depends on the spatial arrangement of materials with different hygroscopic responses and enables predictable curvature for fabricating bioinspired tubular structures and dynamic biomedical devices.

Acknowledgements

This research has been supported by the European Union's Horizon Europe research and innovation programme (grant no. 101178568, DAEDALUS)

Figure 1 A) Design of the structure and folding behavior under Hydratation. – B) Swelling values in the three dimensions for the hydrophobic (left) and hydrophilic (right) materials. - C) Contact angle measurements; t0=1h; t1=24h; t2=7d.

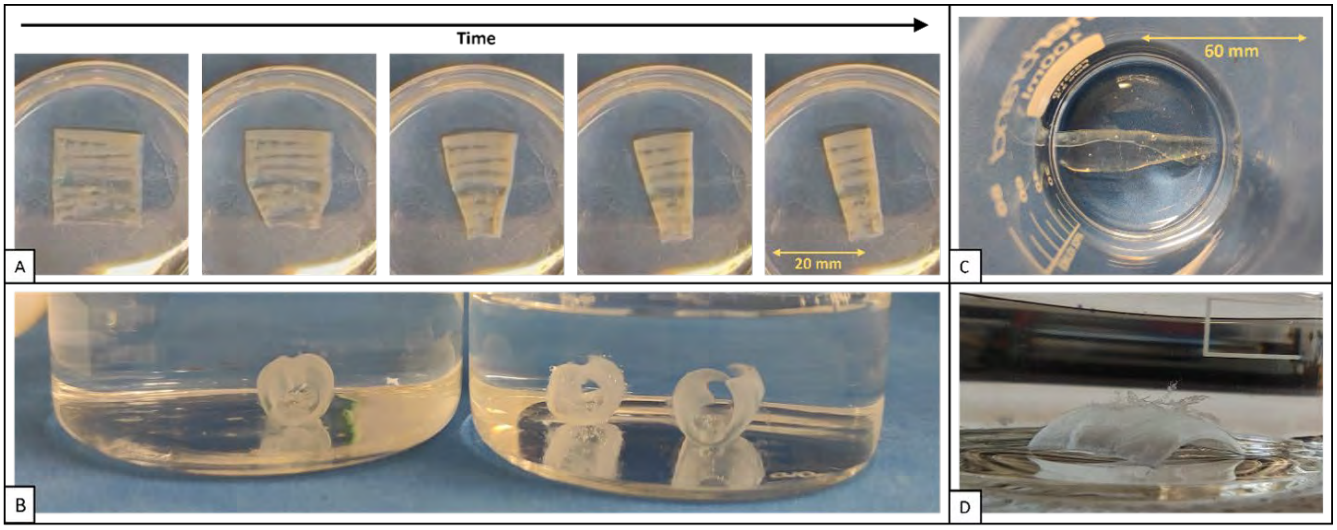

Figure 2 A) Folding process of the printed structure over time. - B) Side view of the folded structures forming a closed cylinder. - C) Folding of the structure with a size of 60 mm. - D) Absence of folding in structures printed with a continuous hydrophilic bottom layer and a hydrophobic top layer.

References

[1] Grosjean, M., Ouedraogo, S., Déjean, S., Garric, X., Luchnikov, V., Ponche, A., ... & Nottelet, B. Bioresorbable bilayered elastomer/hydrogel constructs with gradual interfaces for the fast actuation of self-rolling tubes. ACS applied materials & interfaces 2022; 14(38); 43719-43731.

[2] Ouedraogo, S., Grosjean, M., Brigaud, I., Carneiro, K., Luchnikov, V., Mathieu, N., ... & Ponche, A. Fabrication and characterization of thin self-rolling film for anti-inflammatory drug delivery. Colloids and Surfaces B: Biointerfaces 2024; 241; 114039.

[3] Grosjean, M., Schmidleithner, C., Dejean, S., Larsen, N. B., & Nottelet, B. Degradable 4D-printed hydration-driven actuators from a single family of amphiphilic star-shaped copolymers. Materials & Design 2024; 241; 112953.

S98 – O3

Electroactive polysaccharide-based hydrogels: Targeting stimuli responsive biomaterials for biotechnological applications

Pérez-Madrigal M.M.[1,2], Ramírez-Alba M.D.[1,2,3], Resina, L.[1,2], Teixidó, I.[1,2], Alemán C.[1,2,4]
[1]Chemical Eng. Dept., UPC-BarcelonaTech; [2]Barcelona Research Center in Multiscale Science and Engineering, UPC-BarcelonaTech; [3]Physics Dept., UPC-BarcelonaTech; [4]Institute for Bioengineering of Catalonia (IBEC), Barcelona, Spain

Introduction

Skin, the largest organ of the human body, acts as the primary barrier against environmental threats and pathogens. However, it is also vulnerable to trauma and disease, and its repair process is often complex and slow. Within this context, our goal is to promote the healing of challenging skin wounds by combining conductive wound dressings based on polysaccharide hydrogels with electrical stimulation (ES), following an advanced and cost-effective method. Beyond this specific application, we aim to develop multifunctional electroactive biomaterials with potential use as drug delivery, biosensing, and tissue engineering.

Materials and Methods

Hydrogels were produced from a wide range of naturally derived polysaccharides, including not only conventional matrices such as hyaluronic acid, alginate, and chitosan, but also agarose, cellulose derivatives, and laminarin. During the optimization of gelation, polysaccharide-based hydrogels were prepared by adjusting the total solid content and the weight ratio of the precursors in order to obtain robust and minimally swellable systems with sufficient internal cohesion for handling, characterization, and biological evaluation. Electroactivity was introduced by incorporating conducting polymers and other electroactive moieties through different strategies. In addition to poly(hydroxymethyl-3,4-ethylenedioxythiophene) (PEDOT-MeOH), other conducting polymers such as polypyrrole (PPy) and polyaniline (PANI), as well as other conductive particles, were integrated into the hydrogel matrices. The chemical and structural properties of the resulting electroactive hydrogels, together with their mechanical and electrochemical performance, were characterized using multiple analytical techniques. Furthermore, cytocompatibility was assessed through cell viability assays, while *in vitro* ES experiments were conducted to evaluate their ability to modulate cellular behavior.

Results

Mechanically stable systems were obtained with gelation times depending on the polysaccharide composition. The incorporation of conductive moieties generally preserved the water absorption capacity of the base hydrogels, while also influencing their mechanical properties (e.g., Young's modulus and compressive strength) and improving their electrochemical response. Importantly, the electroactive formulations exhibited good cytocompatibility, with cell viability values above 80%. Under ES conditions, the systems promoted efficient cell migration using low voltages and short stimulation periods. Notably, within 1 h after 15 min of ES, the artificial wound gap was completely closed by a homogeneous monolayer of migrated epithelial cells.

Conclusion

Beyond conductive wound dressings for skin regeneration, these systems represent a versatile platform for broader biotechnological applications, as electrically controlled drug delivery and biosensing functionalities were also demonstrated. Future studies will focus on evaluating these materials in more complex and physiologically relevant models, including 3D-printed skin constructs.

S99
Surface modification and functionalization

S99 – K1
Nanostructured Sustainable Hydrogels for Tissue Regeneration

Stancu IC[1,2]
[1]Advanced Polymer Materials Group, National University of Science and Technology POLITEHNICA Bucharest, Bucharest, Romania; [2]Faculty of Medical Engineering, National University of Science and Technology POLITEHNICA Bucharest, Bucharest, Romania

Introduction
The engineering of nanostructured hydrogels as tunable 3D extracellular environments has the potential of predefining the cellular response transforming static biomaterials into active, instructive scaffolds able to guide cell fate and accelerate functional tissue repair. The fabrication of biomimetic constructs and surfaces progressively evolved towards combining current knowledge on tissue structure, nanotechnology, natural origin biomaterials, and bio-inspired fabrication, to synergistically replicate parts of the tissue native complexity for functional tissue regeneration. Nanomaterials such as bioceramics, C-nanospecies, noble metal nanoparticles and polymer nanoparticles or nanofibrils are appealing nanophases to engineer bioactive nanocomposite hydrogels. These complex systems, although compatible with 3D-(bio)printing and suitable for tissue regenerative applications, face challenges in balancing structural integrity with cell viability and controlled long-term biodegradation.
Aim. Nanostructured hydrogels incorporating structural instructiveness and multicomponent formulations with sustainable elements used as matrices or as nano-scale regulators, hold the potential to precisely guide cellular behavior through tailored structural, topographical and biochemical cues, overcoming traditional mechanical limitations. This lecture highlights the potential and challenges of using nanofillers for the engineering of acellular and cellular scaffolds based on green and blue hydrogels, while addressing critical hurdles in tissue engineering – shape fidelity, stability, mechanical reinforcing and bioactivity, simultaneously resolving the elaboration of formulations for electrospinning and 3D (bio)printing.

Materials and Methods
Various nanomaterials including bioceramics, nanodiamond, silver nanoparticles, and nanocellulose are used as nanophases in sustainable hydrogels fabricated through electrospinning and 3D (bio)printing and in-processing or post printing stabilized. Their potential as nano-scale (bio)chemical, structural and mechanical regulators is assessed.

Results
Such 3D (bio)printed or electrospun nanostructured scaffolds with improved bioactivity and cell interactivity present challenges in managing anisotropy, hierarchical organization, component interfacial complexity and, in matching biodegradability and bioactivity relevant for tissue regeneration[1].

Conclusion
Nanostructuring of sustainable hydrogels allows for tunable bioactivity and mechanical profiles for scaffolds and tissue substitutes with regenerative potential, opening new strategies in nerve and bone regeneration, implant integration, wound healing, and antibacterial protection.

Acknowledgements
This lecture was possible through the projects ERANET-M-3-Cellu4Heal, and PED44/2025-PersOC4Reg, and in collaboration with Elena Olăreț, Carmen-Valentina Nicolae, Andrada Serafim, Ioana Maria Marinescu, Sorina Dinescu, Adriana Lungu, Alexandra Cernencu, Bogdan Vasile, Grațiela Grădișteanu, Kamal Mustafa, Kristin Syverud, Monica Sandri, Stian Kreken Almeland, Samih Mohamed-Ahmed, Esko Kankuri, Doris Steinmuller-Nethl.

References
[1]Nicolae C.V., Kadousaraei M.J., Yamada S., et al. Nanostructured multicomponent bioinks with nanodiamond and magnesium-doped nanohydroxyapatite for enhanced bone tissue engineering. *Materials & Design* 2026; 262; 115510.

S99 – O1

Immunomodulatory effects of peptide-based coatings on a 3D gingival model for peri-implantitis prevention

Mallor-Solís I[1], Perez-Amodio S[2], Moreno-Duarte D[1], Posolo-Cinel V[1], Mas-Moruno C[3], Gil J[1], Aparicio C[1,4]

[1]BOBI-Bioinspired Oral Biomaterials and Interfaces Lab, Department of Materials Science and Engineering, UPC-Universitat Politècnica de Catalunya (Barcelona-Tech), Barcelona, Spain, [2]Bioengineering institute of technology (BIT), Universitat International de Catalunya (UIC), Sant Cugat del Vallès, Spain, [3]Biomaterials, Biomechanics and Tissue Engineering Group (BBT), Department of Materials Science and Engineering, Universitat Politècnica de Catalunya – BarcelonaTech, 08019, Barcelona, Spain, [4]Catalan Institute for Research and Advanced Studies (ICREA), Barcelona, Spain

Introduction

The usage of transepithelial implants has significantly increased, leading to prevalent evidence of failure. In fact, dental implants, fail at a rate of one million per year worldwide, another example. Main reason for failure is peri-implantitis, 34% of patients. Similarly in transcutaneous osseointegrated prosthetic systems for amputees, the infections reach up to 38.3% at 24 months Peri-implantitis is defined as an irreversible inflammatory process mediated by biofilm colonization that can result in implant failure. Conventional treatments (antimicrobial strategies and mechanical debridement) do not directly address the dysregulated immune response that drives disease progression. Recent advances in biomaterials have highlighted the potential of bioactive coatings to actively modulate local immune responses and promote tissue regeneration. Ilantide, a peptide derived from the interleukin-1 receptor antagonist (IL-1Ra), has demonstrated immunomodulatory activity by selectively blocking IL-1 receptor, and therefore IL-1β cascade, which plays a central role in varied inflammatory processes. 3D gingival models recapitulate cellular heterogeneity vs. 2D cultures, better predicting in vivo immunomodulatory effects and preclinical translation. **Aim.** To evaluate the immunomodulatory effects of Ilantide peptide nanocoatings on titanium using a stimulated 3D gingival tissue model by regulating pro-inflammatory cytokines.

Materials and Methods

Ilantide peptide was covalently immobilized to titanium disks using L-3,4-dihydroxyphenylalanine (DOPA), as anchoring unit, to create bioactive nanocoatings. Controls included non-coated disks, randomized peptide sequences, soluble Ilantide peptide and IL-1Ra. A 3D gingival tissue model was developed using human oral keratinocytes, fibroblasts, and macrophages to replicate the structural and cellular complexity of the gingival tissue, facilitating the study of cell-cell in response to external stimuli. Pro-inflammatory stimuli were applied to 3D models, which were subsequently exposed to Ilantide-coated and non-coated samples. Titanium disks were placed in direct contact with the surface of the 3D tissue for a defined incubation period to ensure interaction between the tissue and the nanocoatings. ELISAs were used to analyze the levels of IL-1β and TNF-α, in the presence and absence of the pro-inflammatory stimuli. Macrophage polarization was evaluated through cytokine arrays and immunohistology using specific markers for M1 and M2 polar states. Statistical significance was determined using ANOVA and Tukey's post-hoc tests ($p<0.05$).

Results

Ilantide-coated titanium disks significantly reduced IL-1β and TNF-α secretion in lysates and supernatants compared to controls in stimulated 3D gingival models. Immunostaining revealed a notable shift towards pro-reparative M2-like macrophage polarization. Ilantide coating also downregulated pro-inflammatory pathways in keratinocytes and fibroblasts, supporting a regenerative tissue environment.

Conclusion

Ilantide peptide nanocoatings demonstrated significant immunomodulatory effects by reducing pro-inflammatory cytokine production and promoting M2-like macrophage polarization in a 3D gingival tissue model. These findings suggest that Ilantide could enhance soft tissue integration around dental implants and aid prevention of peri-implantitis, paving the way for next-generation immunomodulatory implant designs.

S99 – O2

Repurposing hair as a functional bioelectronic interface for high-resolution EEG via conductive polymer dyes

S Shweta[1], M Giobliaki[2], L Sohail[1], T Abrahamsson[2], R Cornuejols[2], M Seitanidou[2], D KC[1], S Drakopoulou[1], M Berggren[2], R Raedt[3] , X Strakosas[2], G D. Spyropoulos[1]

[1]*Department of Information Technology, Faculty of Engineering and Architecture, Ghent University, Technologiepark Zwijnaarde 126, 9052 Zwijnaarde, Belgium*

[2]*Department of Science and Technology (ITN), Laboratory of Organic Electronics (LOE), Campus Norrköping, Linköping University SE-581 83 Linköping, Sweden*

[3]*Department of Head and Skin, Faculty of Medicine and Health Sciences, Ghent University, Campus UZ Ghent, Corneel Heymanslaan 10, 9000 Gent, Belgium*

Introduction

Organic bioelectronics aim to improve the interface between electronic devices and biological tissues by leveraging mixed ionic-electronic conduction, mechanical compliance, and biocompatibility. One widely adopted application is electroencephalography (EEG), where conventional electrodes placed on the scalp are often limited by their rigidity or rely on conductive gels that can dry out over time, compromising signal stability and user comfort. A major persistent challenge in EEG is the presence of hair, which obstructs direct contact between electrodes and the scalp, leading to increased impedance and reduced signal quality. Here, we overcome this limitation by introducing a novel method that transforms hair itself into a functional bioelectronic interface through the application of dyes (e-dyes) capable of converting hair to mixed ionic-electronic conductors.

Materials and Methods

We report two complementary e-dye strategies: (i) a temporary coating based on poly(3,4-ethylenedioxythiophene):polystyrene sulfonate (PEDOT:PSS) combined with dopamine hydrochloride, applied to polydopamine-functionalized hair to promote strong adhesion; and (ii) a semi-permanent system achieved through in situ polymerization of a conductive polymer precursor molecule (carboxylated EDOT; EEE-COONa) directly on the hair shafts. Both formulations produce mechanically stable, low-impedance coatings that maintain excellent wearability. To evaluate the performance of the e-dyed hair interface, we recorded alpha rhythms during eye closure and captured eye-blink artifacts over the occipital region, confirming the system's ability to resolve characteristic neural signals. Additionally, we validated its versatility by acquiring ECG signals that clearly displayed the QRS complexes of a healthy cardiac cycle.

Results and Conclusion

This method reimagines hair as a discreet, biocompatible, and scalable bioelectronic interface, offering enhanced comfort and usability for wearable EEG applications and more. By repurposing hair as an active sensing substrate, we establish a new paradigm for non-invasive, high-resolution neurophysiological monitoring, enabling applications in neuropsychiatric diagnostics, mobile brain-computer interfaces (BCIs), and beyond.

S99 – O3

Surface modification of bioresorbable polymers for opposite thrombogenic responses in stents and coils

Cano-Morenilla M[1], Chausse V[1], Pino M[2], Díaz-Ricart M[2], Balcells M[3], Mas-Moruno C[1,4], Pegueroles M[1,4]

[1] Biomaterials, Biomechanics and Tissue Engineering Group (BBT), Department of Materials Science and Engineering, Barcelona Research Center in Multiscale Science and Engineering (CCEM) and Institute for Research and Innovation in Health (IRIS), Universitat Politècnica de Catalunya-BarcelonaTech, Barcelona, Spain.

[2] Hematopathology, Pathology Department, Centre de Diagnòstic Biomèdic, Institut d'Investigacions Biomèdiques August Pi i Sunyer, Hospital Clínic, Universitat de Barcelona, Barcelona, Spain.

[3] Institute for Medical Engineering and Science, Massachusetts Institute of Technology, Cambridge, MA, USA

[4] Centro de Investigación Biomédica en Red-Bioingeniería, Biomateriales y Nanomedicina (CIBER-BBN), Instituto de Salud Carlos III, Madrid, Spain

Introduction

Thrombogenicity at the biomaterial interface must be tailored to the specific clinical application. While cardiovascular stents require anti-thrombogenic surfaces to prevent clot formation, embolization coils rely on rapid thrombus formation for effective vessel occlusion. Surface modification strategies, such as tuning topography, wettability, and biomolecule immobilization, enable this control. These approaches modulate protein adsorption and platelet activation, allowing the design of surfaces with either hemocompatible or pro-coagulant behavior. This work highlights how tailored surface properties can meet the opposite functional requirements of stents and embolization devices.

Materials and Methods

PLCL stents were fabricated from P95 (95:05), P85 (85:15) and B70 (P85/P70, 70:30), dissolved in chloroform and processed by solvent-cast direct writing (SC-DW) using a custom DIW printer (CIM-UPC, Spain), followed by thermal treatment at 65 °C. Surface properties were tailored to modulate thrombogenicity. Linear topography was introduced by printing onto a patterned mandrel. Wettability was tuned via 2M NaOH etching or O_2 plasma. Biofunctionalization was achieved by immobilizing linear RGDS, linear YIGSR, and platform RGDS-YIGSR (PF) peptides (±CF), synthesized by Fmoc/tBu chemistry, O_2 plasma activation and EDC/NHS coupling[1]. Physicochemical and mechanical properties were characterized (OM, DSC, DMTA, XPS, compression and radial tests). Biological performance was evaluated with HCAECs and thrombogenicity assays.

Results

PLLA and PLCL bioresorbable stents were successfully 3D-printed with controlled geometry and strut thickness rangig from 150 and 230 µm, increasing with caprolactone content. Thermal analysis showed Tg values close to body temperature, particularly for B70 (Tg = 32 °C; χc = 20.3%) compared to P85 (Tg = 42 °C; χc = 26%). DMTA confirmed shape recovery at body temperature of 79% for B70, 21% for P85, and 5% for P95. Mechanically, P85 exhibited higher compression resistance at 50% deformation (0.035 N/mm vs. 0.023 N/mm for B70) and slightly greater elastic recovery (98.0% vs. 95.3%). Linear topography was successfully reproduced on the inner surface, promoting endothelial cell alignment without increasing thrombogenicity (Figure 1). Thrombogenicity was also influenced by polymer composition, increasing with lactic acid content and decreasing with caprolactone content. Peptide functionalization resulted in homogeneous coatings (>700 pmol/cm²), enhancing endothelial adhesion and proliferation while reducing platelet adhesion in all cases (Figure 2).

Conclusion

3D-printed PLCL stents with Tg close to body temperature enable controlled thrombogenicity through surface modification, supporting their potential as bioresorbable vascular devices with antithrombotic or pro-coagulant behavior.

Acknowledgements

Project PID2024-161387OB-C22 funded by MICIU/AEI/10.13039/501100011033 and by FEDER, UE. María de Maeztu CEX 2023-001300-M/AEI/10.13039/501100011033

References

[1] Chausse V. et al. Functionalization of 3D printed polymeric bioresorbable stents with a dual cell-adhesive peptidic platform combining RGDS and YIGSR sequences. Biomater. Sci., 2023, 11, 4602 (2023).

Figure 1. a) SEM image of the linear patterning obtained on the inner surface of the 3D-printed stent; b) Thrombogenicity results of 3D-printed PLCL stents with/without internal topography (T), compared to a commercial metallic stent, quantified as the red blood cell-to-total cell ratio; c) Representative images of the coagulation process after 15 min.

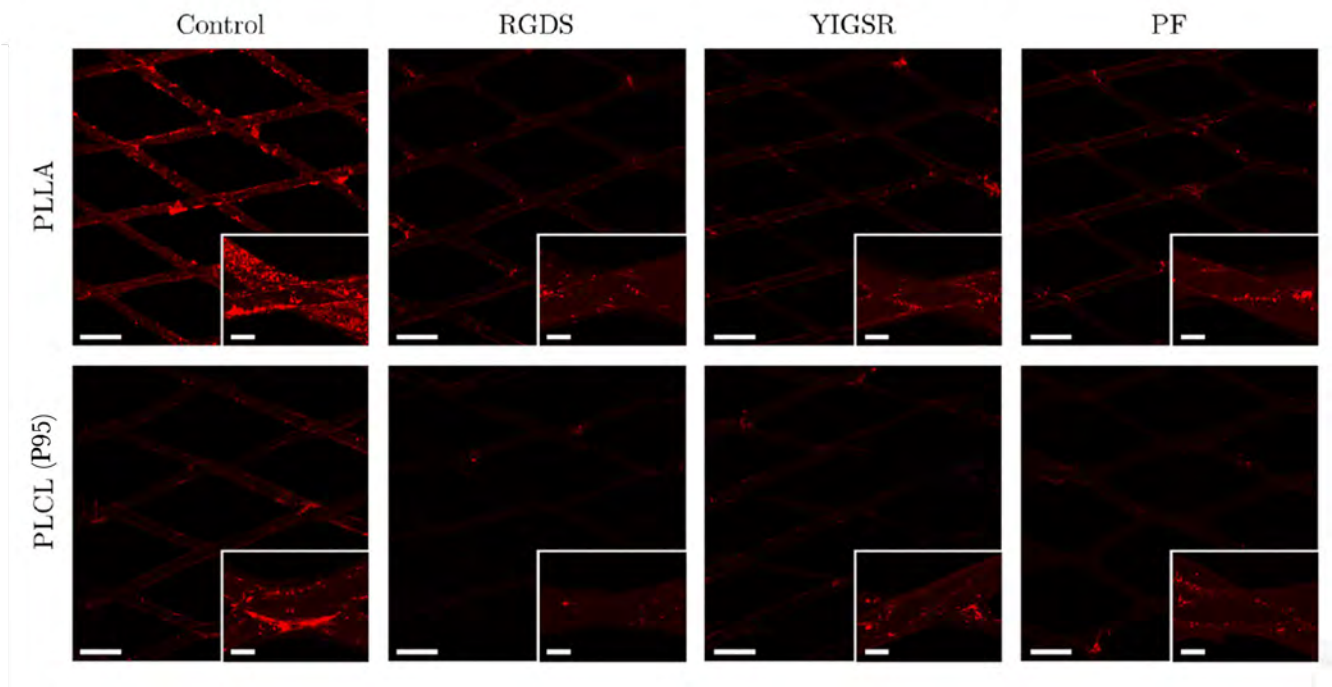

Figure 2. Platelet adhesion on control and functionalized PLLA and PLCL (P95) stents following blood perfusion in a chamber for 5 minutes at shear rate of 800 s^{-1}.

S99 – O4

Surface functionalization of PLLA-coated stainless-steel devices for hard tissue engineering through macroscopic polarization

Rocha, J.[1]; Ivanov M.[1]; Vilarinho P.[1]
[1]Department of Materials and Ceramics Engineering, CICECO – Aveiro Institute of Materials, University of Aveiro, Aveiro, Portugal

Introduction

Poly-L-lactic acid (PLLA) is an aliphatic polyester that is biocompatible, bioactive and biodegradable, with potential uses in biomedical applications. Another property that makes PLLA suitable for biomedical, specifically orthopedic uses, is associated piezoelectricity. The bio-piezoelectricity present in the bone is crucial for regeneration and vascularization and via mimicking this property the biological response of metallic implants can be enhanced where PLLA is a coating to metallic implants conferring piezoelectricity. The surface charges of materials also play a crucial role in the regeneration of bone tissue, especially in the early stages. In this work 316L stainless steel (316L SS) devices were coated with PLLA and macroscopically polarized to demonstrate the enhancement in the regeneration processes.

Materials and Methods

PLLA solution was prepared using 1,4-dioxane as solvent. 316L SS substrates were coated with a PLLA film by spin-coating.

Stainless steel devices coated with PLLA were then submitted to a thermal annealing process to improve the crystallinity, which influences the piezoelectric response. The devices were polarized through corona discharge, with a voltage of -5kV via lab-made equipment.

Samples were characterized using FTIR, XRD and SEM.

The samples were then tested in-vitro regarding its cytocompatibility (PrestoBlue™ viability assay) and osteogenic differentiation potential (Alizarin Red S (ARS) solution protocol), using human dental pulp stem cells (hDPSCs). The biocompatibility of the devices was assessed in-vivo using adult male Sprague Dawley rats.

Results

In the cytocompatibility assays, no cytotoxicity was observed in the cultured hDPSCs with any of the samples.

In the osteodifferentiation assays, it was possible to observe mineral material deposition in all samples (Figure 1.), with the polarized sample group (SS/SIL/PLLA 120 -5kV) presenting the best results.

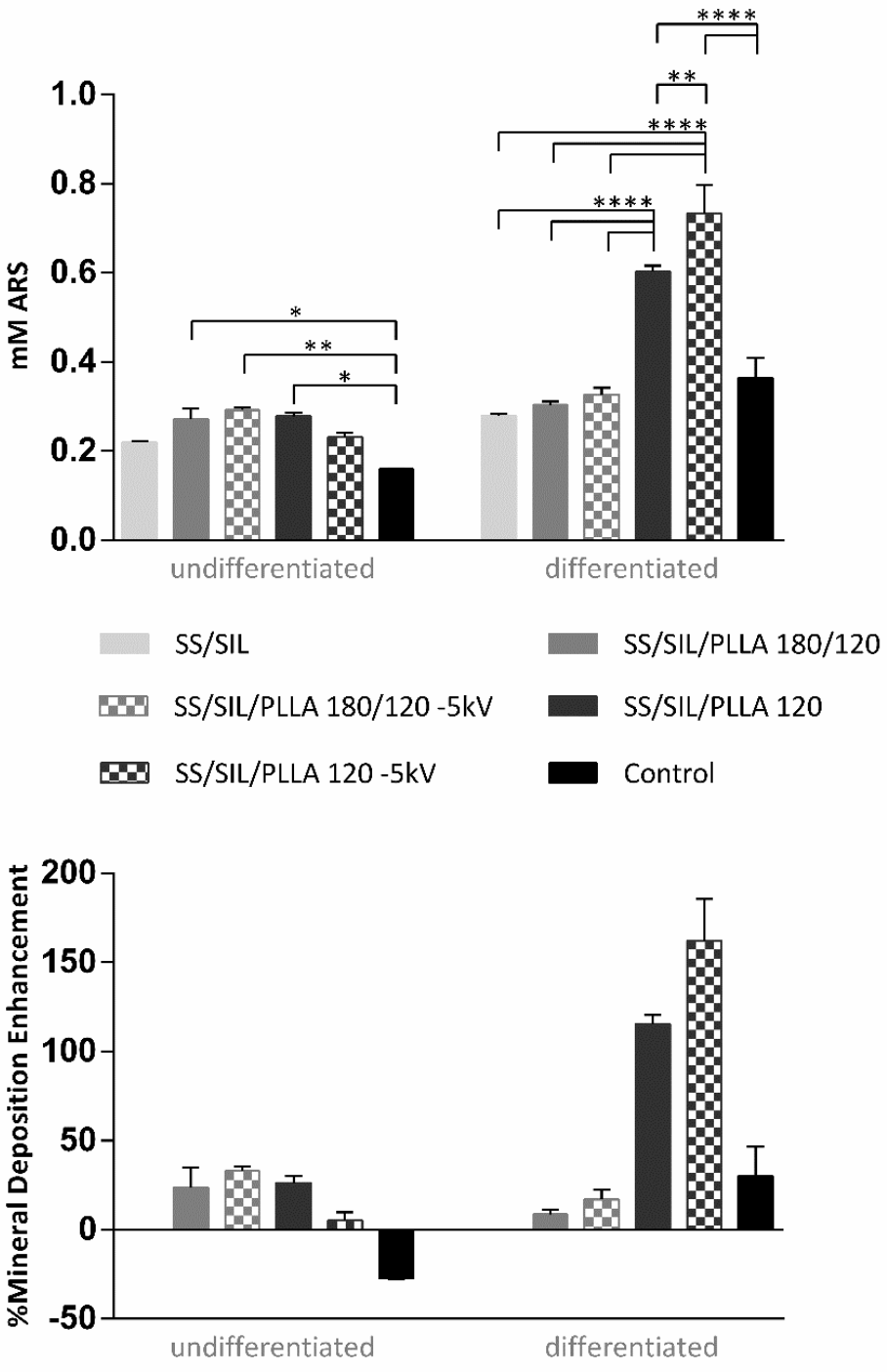

Figure 1 – Osteogenic differentiation assays results, ARS semi-quantification on top and mineral deposition enhancement on the bottom.

In the in-vivo biocompatibility assessment no significant adverse reactions were detected in the histological analysis (Figure 2.), the polarized samples (SS/SIL/PLLA 120 -5kV) presented the lowest histological reaction.

Figure 2 – Histological analysis after in-vivo tests

Conclusion

The 316SS devices coated with PLLA in this work proved suitable to be used as an implantable device in orthopedic applications. Functionalization of PLLA by conferring surface charges through corona poling proved effective, polarized samples presenting improved cytocompatibility, biocompatibility and osteogenic differentiation potential.

Acknowledgements
This work was developed within the scope of the project CICECO-Aveiro Institute of Materials, UIDB/50011/2020, UIDP/50011/2020 & LA/P/0006/2020, financed by national funds through the FCT/MCTES (PIDDAC). The authors acknowledge the FCT for the PhD grant PRT/BD/154790/2023.

S99 – O5

Angiogenesis, healing and immunomodulation studies of copper-functionalized mesoporous bioactive glass nanoparticles as a dual platform for bone regeneration and infection control

Luna-Martínez M*[1], Cicuéndez M[2,3], Colilla M[3,4], García A[3,4], González B[3,4], Jiménez-Jiménez C[3] and Izquierdo-Barba I[3,4]

[1] Departamento de Química en Ciencias Farmacéuticas, Facultad de Farmacia, Universidad Complutense de Madrid, Madrid, Spain; [2] Departamento de Química en Ciencias Farmacéuticas, Facultad de Farmacia, Universidad Complutense de Madrid, Instituto de Investigación Sanitaria del Hospital Clínico San Carlos (IdISSC), Madrid, Spain; [3] Centro de Investigación Biomédica en Red de Bioingeniería, Biomateriales y Nanomedicina (CIBER-BBN), Spain; [4] Departamento de Química en Ciencias Farmacéuticas, Facultad de Farmacia, Universidad Complutense de Madrid, Instituto de Investigación Sanitaria Hospital 12 de Octubre (i+12), Madrid, Spain.

Introduction

The alarming rise of antibiotic-resistant bacteria poses a critical challenge to global health, especially in bone infections, where pathogens severely impair tissue regeneration. There is a need to explore new alternative strategies based on multifunctional biomaterials capable of combining antimicrobial activity with regenerative potential.

Aim

To develop and evaluate a multifunctional nanoplatform based on copper-doped mesoporous bioactive glass nanoparticles, designed to promote bone regeneration by combining antimicrobial activity, angiogenic stimulation, osteogenic capacity, and modulation of the immune response.

Materials and Methods

Mesoporous bioactive glass nanoparticles were synthesized in the SiO_2-CaO system; these nanoparticles are characterized by their high specific surface area, adjustable mesoporosity, excellent biocompatibility, intrinsic bioactivity, and drug delivery capabilities[1]. The nanoparticles were functionalized with the third-generation (G3) poly(propylene imine) dendrimer via surface silanol groups, to enhance their interaction with cellular and bacterial membranes[2]. Subsequently, they were doped with Cu^{2+} ions to confer angiogenic and antimicrobial properties.
The presence of mesoporosity in the nanosystem enables a high loading capacity for therapeutic agents such as the antibiotics levofloxacin and rifampicin, which act on Gram-negative *Escherichia coli* and Gram-positive *Staphylococcus aureus* bacteria, respectively[3]. Biocompatibility and regenerative potential were evaluated in human vegetative endothelial cells (HUVECs), while immunomodulatory capacity was analyzed in RAW264.7 macrophages by studying their phenotypic polarization.

Results

The nanoparticles showed high biocompatibility and significantly promoted key processes in tissue regeneration, including accelerated wound closure, cell migration, and invasion. The presence of Cu^{2+} promoted the stimulation of angiogenic processes related to factors such as VEGF and FGF-2, which are essential for the formation of new vascularized tissue[4].
Simultaneously, the nanosystem exhibited enhanced antimicrobial activity due to the release of antibiotics, producing a synergistic effect against *S. aureus* and *E. coli*.
At the immunological level, the results indicated that the internalization of the nanoparticles modulates the macrophage response, promoting a balance between pro-inflammatory (M1) and reparative (M2) phenotypes, which is fundamental for effective bone regeneration.

Conclusion

Functionalized and copper-doped mesoporous bioactive glass nanoparticles constitute an advanced nanoplatform for regenerative medicine. Their ability to integrate osteogenic, angiogenic, antimicrobial, and immunomodulatory properties allows for the simultaneous treatment of infection and bone tissue regeneration. These results position this nanosystem as a promising strategy for the treatment of infected bone defects from a comprehensive regenerative perspective.

Acknowledgements
Thanks to Fundación Ramón Areces (FD5/22_01, *Nano4Infection*) and Ministry of Science and Innovation (PID2023-149093OBI00, *MAGEN4BONE*) for funding.

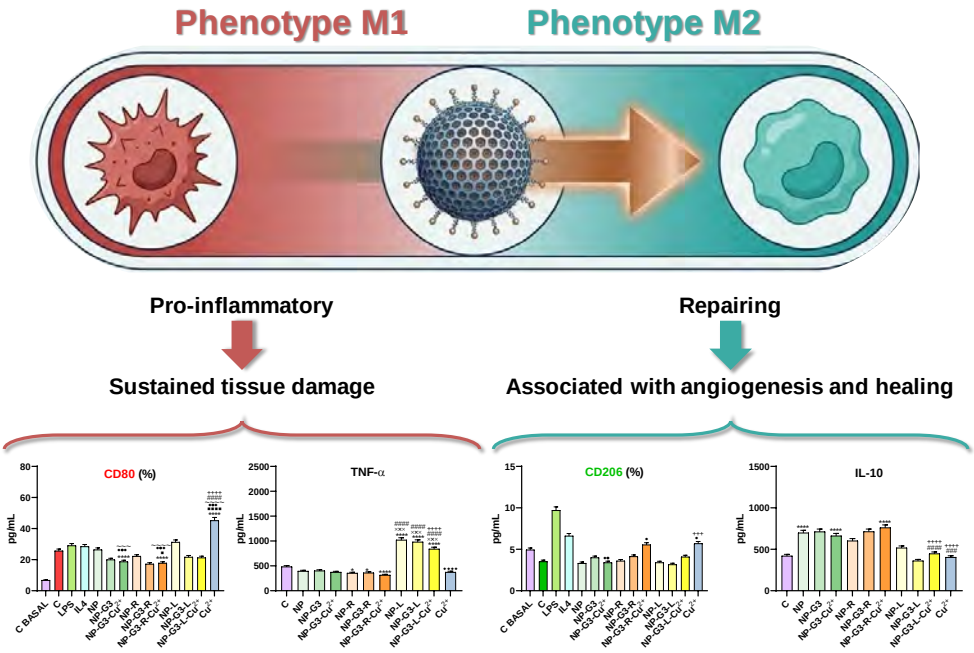

References

[1]Arcos D., Portolés M.T. Mesoporous bioactive nanoparticles for bone tissue applications. Int. J. Mol. Sci. 2023, 24, 3249.
[2]Álvarez E., Estévez M., Jiménez-Jiménez C., Colilla M., Izquierdo-Barba I., González B., Vallet-Regí M. A versatile multicomponent mesoporous silica nanosystem with dual antimicrobial and osteogenic effects. Acta Biomateralia 136, 2021, 570
[3]Polo-Montalvo A., Gómez-Cerezo N., Cicuéndez M., González B., Izquierdo-Barba I., Arcos D. Effective actions of ion release from mesoporous bioactive glass and macrophage mediators on the differentiation of osteoprogenitor and endothelial progenitor cells. Pharmaceutics 2025, 17, 519.
[4]Salvo J., Sandoval C. Role of copper nanoparticles in wound healing for chronic wounds: literature review. Burns Trauma. 2022, 10, tkab047.

S99 – O6

Design and Synthesis of a Mussel-Inspired Bioactive Peptide for the Biofunctionalization of Metallic and Biodegradable Scaffolds

Beck-Sickinger A.G.[1], Khrunyk Y.[1]
[1]Institute of Biochemistry, Faculty of Life Sciences, Leipzig University, Brüderstrs. 34, D-04103 Leipzig, Germany.

Introduction

With the increasing life expectancy of the global population, the incidence of fragility fractures and impaired fracture healing is rising, placing a growing burden on healthcare systems and highlighting the need for improved therapeutic strategies in musculoskeletal repair. Although conventional metallic implants, such as titanium and its alloys, are generally considered biocompatible, their bioinert surfaces limit cell adhesion and may benefit from further functionalization. Similarly, biodegradable scaffolds are attractive due to their resorbable nature, but their capacity to promote cell adhesion can be limited. These limitations highlight the need for biofunctionalization strategies, such as the incorporation of bioactive peptides, to enhance cell adhesion and improve the performance of both metallic implants and biodegradable scaffolds. The aim of this work is the synthesis of a novel bioactive peptide suitable for the biofunctionalization of biomaterials used in bone implant applications.

Materials and Methods

Peptides used in this study were synthesized by solid-phase peptide synthesis, both manually and using an automated synthesizer. Peptide identity and purity were confirmed by MALDI-TOF mass spectrometry (Bruker Daltonics) and analytical RP-HPLC. For *in vitro* assays, cells were cultured under standard conditions (37 °C, 5% CO_2, 95% humidity) in T75 flasks.

Results

A mussel-inspired peptide incorporating two DOPA residues, enabling adhesion to a range of biomaterial surfaces, was synthesized and conjugated to an RGD-containing bioactive sequence via thiol–maleimide click chemistry. The resulting peptide was used for the biofunctionalization of medical-grade titanium scaffolds as well as biodegradable substrates (e.g., silk fibroin). *In vitro* cell culture studies using osteoblast-like cells (Saos-2, MG-63) and macrophage-like THP-1 cells suggested improved viability and adhesion of bone cells on biofunctionalized scaffolds compared to uncoated controls. In contrast, no increase in THP-1 cell adhesion was observed, indicating a potentially limited pro-inflammatory or immunogenic response of the functionalized surfaces.

Conclusion

Together, these results indicate the potential of the developed peptide as a biofunctionalization strategy to enhance the performance of biomaterials for bone-related applications.

Acknowledgements

Dr. Khrunyk gratefully acknowledges the financial support provided by the Alexander von Humboldt Foundation.

S99 – O7

3D-printed PCL/INU-PLA scaffolds enabling bulk and surface in situ MnO_2 functionalization as multifunctional bone biomaterials

Auriemma G.[1], Sardo C.[1], Guidone A.[1], Coppola P.[1], Salsano G.[1], Aquino R.P.[1]
[1]Dept. of Pharmacy, University of Salerno, Fisciano (SA), Italy

Introduction

The development of bioengineered scaffolds able to support tissue integration while mitigating excessive post-implant oxidative and inflammatory responses is highly relevant for improving bone repair. In this context, manganese dioxide (MnO_2) has attracted increasing interest because of its redox-regulating, osteogenesis-supporting and immunomodulatory potential in bone-regenerative microenvironments [1,2]. Here, we developed hybrid 3D-printed PCL/INU-PLA scaffolds enabling two complementary in situ MnO_2 functionalization strategies: (i) bulk-dispersed systems, in which MnO_2 is generated within the polymeric matrix before printing, and (ii) surface-functionalized systems, in which MnO_2 is formed on pre-fabricated scaffolds. The aim was to identify the most promising formulations as templates for MnO_2-functionalization while preserving scaffold integrity and printability.

Materials and Methods

PCL was blended with INU-PLA at 5, 7.5 and 10% w/w, selecting formulations from a previously validated platform for bone scaffold fabrication[3]. For bulk-functionalized systems, solvent-cast disks were used as templates for in situ MnO_2 formation, and the resulting materials were subsequently processed by HME and 3D printing. For surface-functionalized systems, pre-printed scaffolds were directly exposed to $KMnO_4$ solution under optimized conditions to promote in situ MnO_2 deposition onto the scaffold surface. The resulting materials were characterized by FTIR and DSC to assess physicochemical integrity, and by SEM/EDX for morphology and manganese distribution. Additional characterization, including shape fidelity, porosity, surface wettability, swelling, mechanical testing, manganese release, and preliminary in vitro catalytic activity, is ongoing.

Results

MnO_2-functionalized constructs were successfully obtained using both bulk and surface approaches. FTIR and DSC analyses indicated preserved polymer integrity, with no evidence of chemical interactions between PCL and INU-PLA after functionalization. SEM showed a uniform distribution of MnO_2-nanoparticles on the scaffold surface without evident aggregate formation, while EDX confirmed manganese deposition on treated samples. Surface-functionalized scaffolds retained high shape fidelity after treatment, indicating that post-printing MnO_2 generation did not affect scaffold architecture or geometrical features. Preliminary TMB assay results suggested peroxidase-like activity, with stronger signal intensity observed for formulations containing higher INU-PLA fractions, consistent with increased MnO_2 deposition.

Conclusion

These preliminary results provide proof-of-concept evidence supporting the use of MnO_2-functionalized PCL/INU-PLA scaffolds as multifunctional templates for bone regeneration. The constructs combined homogeneous functionalization, preserved material properties and good printability, identifying promising candidates for further physicochemical and biological investigation.

References

[1] Yang Y., Yao Z., Sun Y., et al. 3D-printed manganese dioxide incorporated scaffold promotes osteogenic-angiogenic coupling for refractory bone defect by remodeling osteo-regenerative microenvironment. *Bioactive Materials* 2025;44:354-370.
.[2] Hu H., Yang F., Wang C., et al. Regulation of hypoxic stress and oxidative stress in bone repair: Current trends and future perspectives. *Journal of Materials Science & Technology* 2023; 157:144-153.
[3] Tommasino C., Auriemma G., Sardo C., et al. 3D printed macroporous scaffolds of PCL and inulin-g-P(D,L)LA for bone tissue engineering applications. *International Journal of Pharmaceutics* 2023;641:123093.

S100
Sustainable, green, and circular biomaterials

S100 – K1
Sustainable polyaspartic ester coatings for antifouling and antibacterial applications

Bernaerts K.V.[1], Cao H.[1,2], Ferro[2], A., Dimech, D.[2], Baker M.B.[2]
[1]Sustainable Polymer Synthesis Group, Maastricht University, 6167 RD Geleen, the Netherlands; [2]Department of Complex Tissue Regeneration, MERLN Institute for Technology-Inspired Regenerative Medicine, Maastricht University, 6229 ER Maastricht, the Netherlands

Introduction
The development of environmentally benign coatings remains challenging in marine and biomedical applications due to persistent biofouling and infection risks. Biofouling arises from accumulation of (micro)organisms on surfaces, leading to reduced material performance and severe economic losses. In marine environments, this results in increased drag, fuel consumption, and maintenance costs, while in biomedical settings, protein adsorption and cell or bacterial adhesion can cause implant failure, chronic inflammation, and device-associated infections. The growing incidence of hospital-acquired infections and widespread use of indwelling medical devices further emphasize the need for intrinsically antibacterial coatings that limit microbial colonization at material–tissue interfaces. Conventional antifouling and antibacterial systems often rely on toxic additives, solvent-intensive synthesis routes, or exhibit limited durability under operational conditions. In this work, we present biobased polyaspartic ester networks combining sustainable synthesis, self-healing functionality, and resistance against fouling and bacteria.

Materials and Methods
On one hand, zwitterionic-modified polyaspartic esters were developed through straightforward, solvent-free polycondensation for the development of antifouling coatings. On the other hand, quaternary ammonium functionalities were introduced on polyaspartic esters through post-polymerization alkylation, yielding antibacterial coatings. The thermo-mechanical properties of the networks were evaluated.

Results
Incorporation of zwitterionic moieties promotes strong hydration under aqueous conditions, generating a tightly bound water layer that effectively suppresses the adhesion of cells and microorganisms. Cell adhesion assays showed that the zwitterionic coating markedly reduced L929 fibroblast attachment compared with polyaspartic ester, the commercial control, and tissue culture plastic, confirming its strong antifouling behavior. Indirect contact assays with L929 fibroblasts confirmed good cytocompatibility of both polyaspartic ester and zwitterionic polyaspartic ester coatings, with cell viabilities exceeding 75%, no significant morphological alterations, and no evidence of acidic degradation products.

Quaternary ammonium-functionalized polyaspartic ester coatings exhibited bacteriostatic activity against both Gram-negative *E. coli* and Gram-positive *S. aureus*, significantly inhibiting bacterial growth and surface colonization, with a more pronounced effect against S. aureus.
Both coating types are dynamically crosslinked networks that enable bond exchange and structural rearrangement, addressing growing demands for sustainable and self-healing materials with extended service lifetimes.

Conclusion
These studies demonstrate how the unique chemistry of polyaspartic esters can be leveraged to create multifunctional protective coatings with either antifouling or antibacterial performance, while simultaneously providing self-healing and environmentally responsible manufacturing. This work highlights dynamic polyaspartic ester networks as a promising class of sustainable coating materials for both marine and biomedical environments.

Acknowledgements
Huixing Cao (CSC202106920010) gratefully acknowledges financial support from China Scholarship Council.

S100 – O1

Plant-Derived Glycoprotein Bioink for 3D Bioprinting and Soft Tissue Regeneration

Sonali Garje, Ashok M.Raichur
Department of materials engineering,Indian Institute of Science,Bengalore

Introduction

Extrusion-based 3D bioprinting is a widely used additive manufacturing technique that fabricates three-dimensional tissue-like structures by extruding bioinks containing living cells through a nozzle layer by layer. The bioink plays a crucial role in 3D bioprinting by providing a microenvironment that is conducive to cell attachment, growth, and proliferation, which are essential for tissue regeneration. Materials used for bioink formulation must satisfy specific criteria, including printability, high shape fidelity, viscoelasticity, shear-thinning behavior, bioactivity, biocompatibility, and appropriate mechanical properties tailored to the target tissue regeneration application. Natural polymers such as gelatin, hyaluronic acid, alginate, and collagen are commonly used in bioink formulations due to their biocompatibility and bioactivity. However, these polymers exhibit limitations, including poor printability, low shape fidelity, and insufficient mechanical strength. To overcome these drawbacks, synthetic polymers are frequently blended with natural polymers; nevertheless, this approach often reduces cell attachment and biocompatibility due to the generation of toxic byproducts and the absence of cell adhesion motifs in synthetic materials. Therefore, there is a pressing need to identify natural materials that possess all the requisite properties for bioink applications.

Aim

To develop and characterize a photocrosslinkable plant-derived glycoprotein-based bioink and evaluate its rheological properties, printability, and biocompatibility for extrusion-based 3D bioprinting applications**.**

Materials and Methods

A novel plant-based material was extracted, and its composition was determined. The material was chemically modified with photocrosslinkable groups, which were confirmed by NMR analysis. Rheological properties, including shear-thinning and viscoelastic behavior, were evaluated using a rheometer, and shape fidelity was assessed through extrusion-based 3D bioprinting. Scaffold morphology was analyzed by SEM, while biocompatibility was evaluated using MTT assay, and cell attachment and proliferation were studied via Live–Dead assay.

Results

A novel plant-derived glycoprotein-rich material containing carbohydrates (230 ± 60 µg/mg), proteins (71 ± 20 µg/mg), polyphenols (30 ± 5 µg/mg), and essential minerals (K, Ca, Mg) was investigated as a bioink candidate. It mimics the extracellular matrix and exhibited suitable rheological properties with high viscosity, shear-thinning **(Figure 1b)**, viscoelastic behavior **(Figure 1c)**, and excellent printability with shape fidelity at 40–60 mg/mL **(Figure 1a)**. Hydroxyl groups were modified with photocrosslinkable groups confirmed by NMR **(Figure 1d)**, enabling visible light (405 nm) crosslinking to enhance mechanical strength. SEM revealed a porous scaffold with an average pore size of 83 ± 16 µm **(Figure 1f)**, favorable for cell migration and nutrient/oxygen transport. Biocompatibility studies using NIH-3T3 fibroblast cells showed more than 100% cell viability **(Figure 1g)** with confirmed attachment and proliferation **(Figure 1h)**, while inherent antioxidant properties help neutralize ROS.

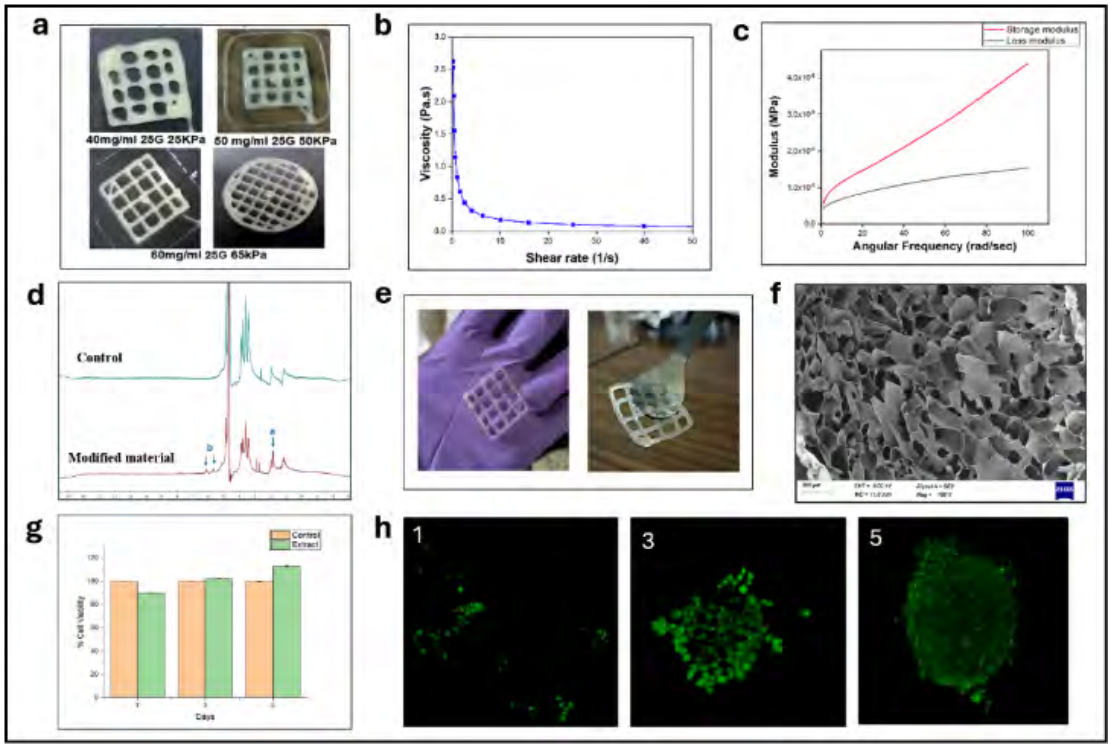

Figure 1. (a) Shape fidelity of the bioink at different concentrations (b) Shear-thinning behavior of material (5mg/ml) (c) Frequency sweep analysis of material (5mg/ml) (d) NMR analysis of chemically modified material (e) Photo-crosslinked scaffolds after exposure to visible light (405 nm) (f) SEM analysis of crosslinked scaffold (g) Cell viability assessment using the MTT assay (h)Live/dead assay using acridine orange and propidium iodide showing cell attachment and proliferation on days 1, 3, and 5

Conclusion

The plant-derived glycoprotein-based bioink exhibited suitable rheological properties, good printability, porous scaffold morphology, and high biocompatibility. These results indicate its strong potential as a sustainable bioink for extrusion-based 3D bioprinting and tissue engineering applications.

S100 – O2

Non-Cytotoxic Binary Mixtures of Cationic Nanoparticles and Polymer Chains Kill Polymicrobial Communities

Buksa H.[1], Trebell M.[1], Suzuki R.[2], Holt N.[3], Tanaka M.[2,4], Durham W. M.[1], Corrigan R. M.[5], Armes S. P.[1]
[1]School of Mathematical and Physical Sciences, University of Sheffield, Sheffield, United Kingdom; [2]Center for Integrative Medicine and Physics, Kyoto University, Kyoto, Japan; [3]GEO Specialty Chemicals, Southampton, United Kingdom; [4]Institute of Physical Chemistry, Heidelberg University, Heidelberg, Germany; [5]School of Medicine, University College Dublin, Dublin, Ireland

Introduction

Antimicrobial resistance (AMR) is an escalating global health concern driven by antibiotic misuse and a limited pipeline of new therapeutics. Amphiphilic antimicrobial peptides (AMPs) disrupt bacterial membranes but suffer from poor stability and high production costs. Synthetic antimicrobial polymers (SNAPs) offer a promising alternative, combining AMP-like activity with enhanced stability, tunable composition and scalable synthesis. Recent studies highlight the importance of multivalency and polymer architecture in enhancing membrane interactions and bactericidal efficiency, yet their influence on killing kinetics, cytocompatibility and broad-spectrum activity remains to be explored.[1,2]

Aim. To compare the antimicrobial activity and cytocompatibility of cationic and cationic amphiphilic polymer multivalent nanoparticles and the corresponding polymer chains to achieve broad-spectrum antibacterial activity.

Materials and Methods

Cationic and cationic amphiphilic polymer multivalent nanoparticles, along with their corresponding polymer chains, were assessed for antibacterial activity against Gram-positive *Staphylococcus aureus* and Gram-negative *Escherichia coli*. Bacterial killing assays were conducted for monocultures and co-cultures, including clinically relevant methicillin-resistant *S. aureus* (MRSA) and uropathogenic *E. coli* (UPEC). Transmission electron microscopy (TEM) and fluorescence microscopy were used to examine nanoparticle-bacteria interactions and membrane disruption. Cytotoxicity was evaluated using human umbilical vein endothelial cells (HUVECs) to identify therapeutic windows. Binary mixtures of polymer chains and nanoparticles were tested to assess synergistic antibacterial effects.

Results

Transmission electron microscopy and fluorescence microscopy confirmed rapid adsorption of nanoparticles onto bacteria and localized disruption of their membranes. Such assays also revealed subtle differences in killing kinetics: purely cationic nanoparticles induce rapid lysis of *S. aureus*, whereas cationic amphiphilic nanoparticles lead to slower, sustained killing of *E. coli*. In contrast, the corresponding cationic amphiphilic chains exhibit only transient lethality for the latter pathogen. Cell survival assays utilizing HUVECs enable identification of a therapeutic window whereby nanoparticles can be deployed at concentrations that are lethal for both bacterial organisms yet are non-toxic for mammalian cells. Importantly, a judicious binary mixture of purely cationic polymer chains and cationic amphiphilic nanoparticles provides broad-spectrum activity against both monocultures and co-cultures of Gram-positive and Gram-negative bacteria, including clinically relevant MRSA and UPEC (see Figures 1 and 2). This synergistic combination leverages rapid (albeit transient) killing by individual cationic polymer chains with sustained killing by nanoparticles over 24 h.

Conclusion

We demonstrate that multicomponent synthetic antimicrobial polymer formulations provide a versatile platform for next-generation antimicrobial therapies targeting both polymicrobial and drug-resistant infections.

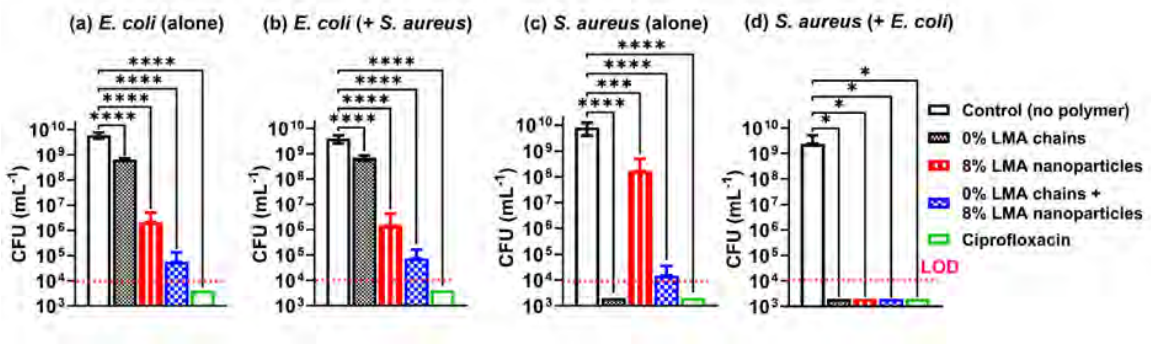

Figure 1. A binary mixture of polymer nanoparticles and chains offers broad-spectrum antibacterial activity towards co-cultures containing Gram-positive and Gram-negative microorganisms. Bacterial killing assays performed for (a) *E. coli* MG1655; (b) *E. coli* MG1655 plus *S. aureus* Newman; (c) *S. aureus* Newman; (d) *S. aureus* Newman plus *E. coli* MG1655. Bacteria were mixed with 0% LMA chains at 200 µg mL⁻¹ (black), 8% LMA nanoparticles at 1000 µg mL⁻¹ (red) and their binary mixtures (blue) prior to incubation for 24 h at 37ºC. *E. coli* strains were plated on McConkey agar, while *S. aureus* strains were selected using Mannitol Salt agar. Ciprofloxacin (at 2 µg mL^{-1}) was used as a positive antibiotic control in both experiments (green). The dashed horizontal line denotes the limit of detection (LOD). Statistical significance was determined by one-way ANOVA with post hoc testing [$p < 0.05$ (*), $p < 0.01$ (**), $p < 0.001$ (***), $p < 0.0001$ (****)]. Each experiment was performed in triplicate.

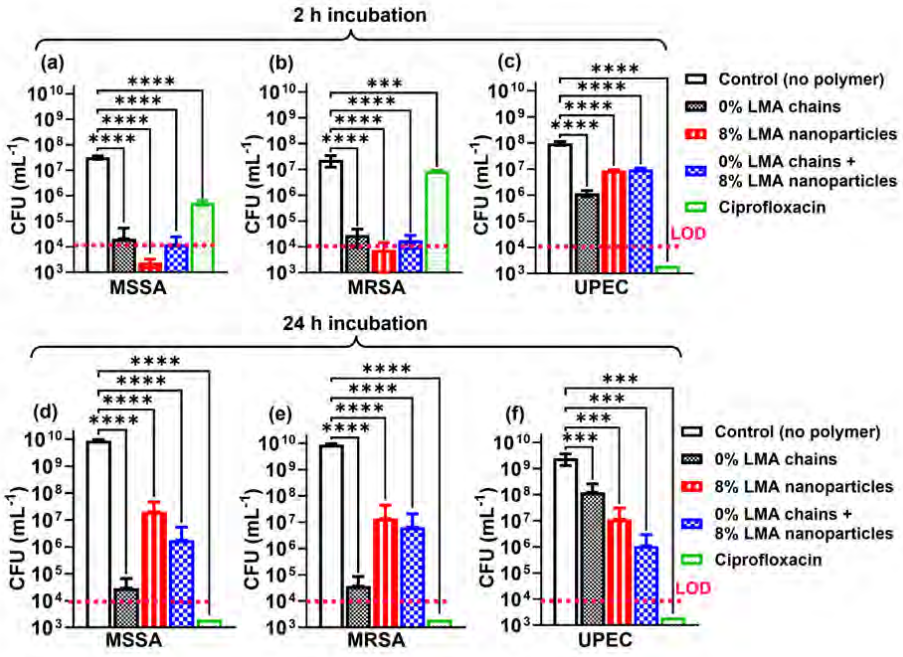

Figure 2. Selected amphiphilic cationic nanoparticles, cationic homopolymer chains and their corresponding binary mixture are effective against clinically relevant strains. Bacterial killing assays performed for (a) Methicillin-susceptible *S. aureus* (MSSA) Newman; (b) Methicillin-Resistant *S. aureus* (MRSA) COL; (c) Uropathogenic *E. coli* (UPEC) following incubation for 2 h at 37ºC with 0% LMA chains at 200 µg mL⁻¹ (black), 8% LMA nanoparticles at 1000 µg mL⁻¹ (red) or their binary mixture (blue). Bacterial killing assays performed for (d) MSSA Newman; (e) MRSA COL; (f) UPEC following incubation for 24 h at 37ºC with 0% LMA chains at 200 µg mL⁻¹ (black), 8% LMA nanoparticles at 1000 µg mL⁻¹ (red) or their binary mixture (blue).

Acknowledgements
We acknowledge EPSRC for a CASE PhD studentship for the first author and thank GEO Specialty Chemicals (Hythe, UK) for additional financial support of this project and for permission to publish these results. RMC thanks the Wellcome Trust and the Royal Society (104110/Z/14/A) for a Sir Henry Dale Fellowship and acknowledges a 2018 Lister Institute Research Prize. MT thanks Japan Society for the Promotion of Science (JSPS, JP24H00796) for support. We thank Christopher Hill and Dr. Svetomir Tzokov of the University of Sheffield Biomedical Science Electron Microscopy Suite for their technical assistance. Finally, the first author thanks Prof. Yoshihiro Sasaki for inspiring discussion.

References
[1]Haktaniyan, M., Bradley, M. Polymers Showing Intrinsic Antimicrobial Activity. *Chem. Soc. Rev*; 2022; 51; 8584–8611.
[2]Concilio, M., Garcia Maset, R., Lemonche, L. P., Kontrimas, V., Song, J. I., Rajendrakumar, S. K., Harrison, F., Becer, C. R., Perrier, S. Mechanism of Action of Oxazoline-Based Antimicrobial Polymers Against Staphylococcus Aureus: In Vivo Antimicrobial Activity Evaluation. *Adv. Healthc. Mater.* 2023; 12; 2301961

S100 – O3

Cerium-crosslinked Porphyridium cruentum EPS/bone ECM composite gels for injectable and moldable bone regeneration

Duarte M.M[1], Suprinovych A.[1], Veiga A.[1], Lopes A.I.[1], Tavaria F.K.[1], Morais R.[1], Oliveira A.L.[1]
[1]Universidade Católica Portuguesa, CBQF - Centro de Biotecnologia e Química Fina – Laboratório Associado, Escola Superior de Biotecnologia, Rua Diogo Botelho 1327, 4169-005 Porto, Portugal

Introduction

Extracellular polysaccharides (EPS) from *Porphyridium cruentum* are sulphated biopolymers with rheological versatility and antioxidant, antibacterial, and immunomodulatory potential, making them attractive candidates for multifunctional biomaterials[1]. Cerium has attracted interest in bone tissue engineering due to its redox-active behavior, ability to modulate oxidative stress and support osteogenic microenvironments, while bone-derived extracellular matrix (ECM) provides tissue-specific biochemical cues and a mineralized framework for bone regeneration[2,3]. In this work, cerium-crosslinked EPS gels were combined with decellularized bone ECM in particulate and digested formats to develop composite systems with cerium-driven bioactivity and dECM improved mechanical integrity.

Materials and Methods

Bone ECM was obtained following decellularization of porcine bone tissue involving sequential washes in 1M NaCl and 10 mM Tris-HCl in an ultrasonic bath for 15 minutes, immersion in 1% TnBP for 1h, and $scCO_2$ cycles for 30 min at 200, 150, and 100 bar. dECM was milled, then characterized for particle size, DNA and collagen content. EPS were dissolved in dH_2O (2.5 wt%) and ionically crosslinked with Ce^{3+} (10.0 wt%) to produce an EPS-cation gel. EPS-cerium-dECM gels were prepared by mixing milled (100, 250, 350 mg/mL) or digested (in 1mg/mL pepsin-HCl) dECM with EPS-cation gels. Rheological characterization before and after ECM incorporation was performed to assess viscoelastic behavior and flow response.

Results

Ce^{3+}-crosslinked EPS hydrogels were bioactive, inhibiting the growth of *S. aureus* and *E. coli* after 24h, showed antioxidant activity (~40 Trolox Equivalents (µM)/mg), and were cytocompatible with both HDF and HaCaT cells. Rheological analysis confirmed gel-like behavior (G' > G''), although values and the frequency-dependent behavior of elastic modulus were characteristic of a weak gel network. Preliminary incorporation studies (Figure 1) appear to show that bone dECM integrated into the EPS-cerium network in both particulate and digested formats. Notably, the addition of dECM increased the elastic modulus of 2.5 wt% EPS gels from ~100-400 Pa to ~15,000 Pa, and exhibited frequency-independent behavior, indicative of a more stable, solid-like network. Additionally, our decellularization protocol managed to reduce DNA content to below 50ng/mg, while preserving collagen content (~250 µg/mg), without demineralization.

Conclusion

Preliminary results support the feasibility of combining *P. cruentum* EPS, cerium, and porcine bone ECM into composite gel systems for bone regeneration. EPS-cerium gels showed strong bioactive potential, while bone ECM incorporation enhanced gel's mechanical integrity. Further studies are needed to evaluate how the incorporation of dECM affect the biological activity previously observed for Ce^{3+}-crosslinked EPS gels.

References

[1] Raposo M.F., de Morais A.M., de Morais R.M. Influence of sulphate on the composition and antibacterial and antiviral properties of the exopolysaccharide from Porphyridium cruentum. *Life Sciences* 2014 Apr 17;101(1-2).
[2]Meng X., *et al.* Harnessing cerium-based biomaterials for the treatment of bone diseases. *Acta Biomaterialia* 2024; 183; 30-49.
[3]Lin X., Patil S., Gao Y.G., Qian A. The Bone Extracellular Matrix in Bone Formation and Regeneration. Frontiers in Pharmacology. 2020; 11; 757.

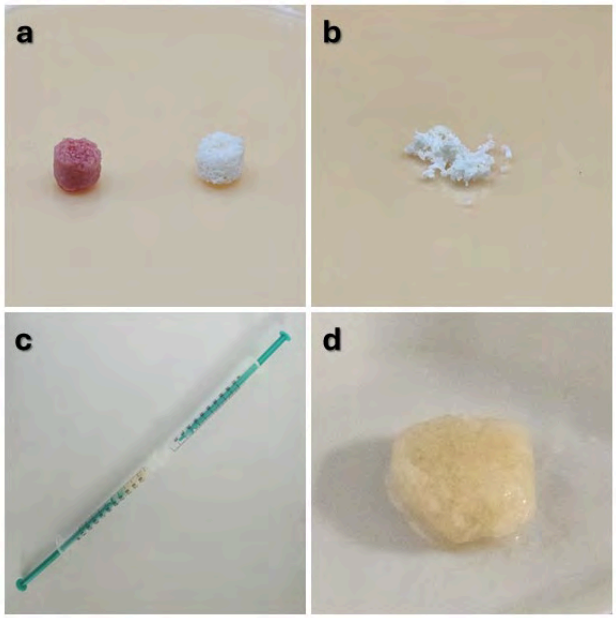

Figure 1. Preliminary incorporation studies of Ce^{3+}-crosslinked EPS hydrogels with bone dECM. a) Porcine native bone (left) and decellularized bone (right). b) Milled dECM particles. c) Mixing of EPS solution and dECM particles using a dual-syringe system with luer-lock connector. d) Ce^{3+}-crosslinked EPS-dECM gel.

S100 – O4

Marine-inspired hydrogels for treatment of diabetic chronic wounds

Correia, C.[1,2], Sousa, R.O.[1,2], Ibrahim, N.A.[3,4], Fadilah, N.I.M.[3,4], Maarof, M.[3,4], Silva, T.H.[1,2], Reis, R.L.[1,2], Fauzi, Mh B.[3,4], Pashkuleva, I.[1,2], Alves, N. M.[1,2]

13B's Research Group, I3Bs – Research Institute on Biomaterials, Biodegradables and Biomimetics, University of Minho, Headquarters of the European Institute of Excellence on Tissue Engineering and Regenerative Medicine, AvePark, Parque de Ciência e Tecnologia, Zona Industrial da Gandra, 4805-017 Barco, Guimarães, Portugal; 2 ICVS/3B's–PT Government Associate Laboratory, Braga/Guimarães, Portugal;3 Department of Tissue Engineering and Regenerative Medicine, Faculty of Medicine, Universiti Kebangsaan Malaysia, Jalan Yaacob Latif, Cheras, Kuala Lumpur 56000, Malaysia;4 Advance Bioactive Materials-Cells UKM Research Group, Universiti Kebangsaan Malaysia, Bangi 43600, Malaysia

Introduction

Diabetes is a chronic metabolic disease characterized by high blood glucose levels due to reduced insulin production. In 2017, about 451 million people were affected, and this number is projected to reach 693 million by 2045. Chronic wounds are a major complication of diabetes and often lead to amputation and increased mortality. Current treatments show limited efficacy, highlighting the need for advanced wound dressings. Adhesive hydrogels effectively treat soft and irregular wounds by creating a moist, protective environment that adapts to the wound shape and promotes healing. Inspired by mussel adhesion, catechol functionalization enhances polymer adhesion due to its strong interactions, biocompatibility, and feasibility.

Aim. This study evaluated the therapeutic potential of bioadhesive hydrogels based on Chitosan (Chit) in a diabetic wound model in mice.

Materials and Methods

Chit was modified with catechol groups (Chit-Cat), achieving a substitution degree of 19%, confirmed by ^{1}H-NMR and UV–vis spectroscopy. Thermoresponsive hydrogels were obtained via electrostatic crosslinking by mixing Chit-Cat with β-glycerophosphate (56%) on ice, followed by incubation at 37°C for 6h[1]. Control hydrogels were produced using unmodified Chit.

Diabetes was induced in C57BL/6 mice by intraperitoneal injection of streptozotocin (40mg/kg) for five consecutive days. Animals were divided into: (1) non-diabetic untreated wounds (NDB-NT), (2) diabetic untreated wounds (DB-NT), (3) diabetic wounds treated with commercial Integra® patch, (4) diabetic wounds treated with Chit hydrogels, and (5) diabetic wounds treated with Chit-Cat hydrogels. Full-thickness skin wounds (1cm diameter) were created and immediately treated with the respective materials, followed by non-adherent dressing and suturing.

Results

Wound area decreased in all groups (Fig.1): untreated wounds closed rapidly through contraction, often resulting in poor tissue organization, whereas Chit-Cat hydrogels showed good tissue integration and promoted faster closure with minimal contraction (Fig.2). Picrosirius Red staining revealed presence of mature collagen in Chit and Chit-Cat groups, while untreated and Integra-treated wounds contained predominantly immature collagen. Immunohistochemistry showed thicker K5-positive layers and increased CD31 and α-SMA expression in Chit-Cat-treated wounds, indicating enhanced epidermal regeneration and angiogenesis. By day 14, Chit-Cat hydrogels degraded 85% without systemic toxicity, confirming their biocompatibility.

Conclusion

Chit-Cat hydrogels enhance diabetic wound healing by promoting re-epithelialization, collagen maturation, and angiogenesis, while safely degrading *in vivo*. They offer a promising strategy for treating chronic diabetic wounds.

Acknowledgements

The authors acknowledge the EC through: SHIFT (grant 101008041) and APTADEGRAD (HORIZON-EIC-2022-PATHFINDEROPEN-01-101099063), and FCT for PD/BD/150519/2019, UID/50026/2025, SeaJellySpine(COMPETE2030-FEDER-00653700), Jelly4Bone(COMPETE2030-FEDER-00710400), and TERM-RES-Hub infrastructure(PINFRA/22190/2016).

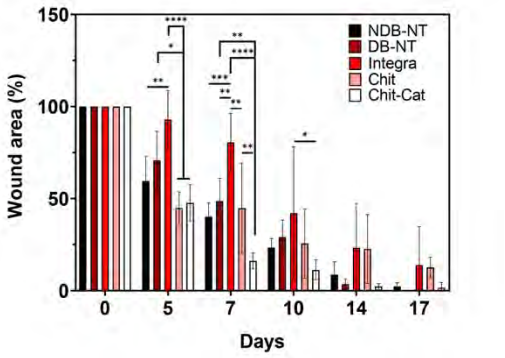

Fig. 1: Quantitative assessment of wound closure up to 17 days after the implantation. Quantitative results are expressed as the mean ± standard deviation, where n= 3, *p < 0.05, **p < 0.01, ***p < 0.001, **** p < 0.0001, two-way ANOVA with Tukey multiple comparison post-test.

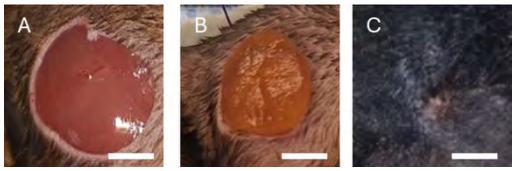

Fig. 2: Representative macroscopic images of wounds treated with Chit-Cat hydrogels showing healing progression (scale bar = 5 mm): (A) immediately after treatment, (B) during hydrogel treatment, and (C) 17 days post-treatment.

References

[1] Correia,C. et al. Biomaterials Advances,2025,167,214090.

S100 – O5

The response of human pulmonary cells cultured on cellulose-based membranes under physiological fluid shear stress – a focus on artificial lung applications

Fruleux T. [1], Chagas R. [2], Ferreira L. M. [2], Wang J. [1], Vallejo-Giraldo C. [1] and Biggs M. [1*]
[1] CURAM, SFI Research Centre for Medical Devices, University of Galway, Galway, Ireland; [2] LAVQ-REQUIMTE, Chemistry Department, NOVA School of Science and Technology, Universidade NOVA de Lisboa, Caparica, Portugal

Introduction

End-stage lung disease represents the third leading cause of death worldwide, accelerated by increasing rates of tobacco smoking and exposure to air pollutants, creating an urgent need for new therapeutic strategies. Extracorporeal membrane oxygenation (ECMO) and mechanical ventilation can be temporarily used as a bridge to lung transplantation for patients too sick to wait until a donor lung becomes available. These devices utilise a porous membrane which allows for gas transfer at the blood-device interface, facilitating blood oxygenation. Although ECMO can prevent patient death, challenges include device-related infection, bleeding, thrombosis, cost, and low patient quality of life. Current ECMO devices are made of polymethylpentene (PMP) or polypropylene (PP), hydrophobic materials which can promote platelet aggregation and thrombosis, giving rise a lifetime of only approx. 7 days. Due to the high surface area, high mechanical strength, high cytocompatibility and hemocompatibility, a cellulose composite is here described as a novel alternative material for the fabrication of cytocompatible, sustainable, renewable and highly porous membranes for ECMO.

Materials and Methods

Cellulose-based bilayer membranes were investigated under static and dynamic (σ= [0.5,1,2] Pa) flow conditions to reproduce the physiological environment of human pulmonary system. The cytocompatibility of human microvascular lung cells (HULEC-5a) was compared to tissue culture plates (TCP) and the industry standard polymethylpentene (PMP) in vitro.

Results

The proliferation of HULEC-5a under static and dynamic flow conditions on four different cellulose composites formulations made of cellulose methacrylate (CellMA), microfibrillated cellulose (MFC) and zwitterionic sulfobetaine methacrylate (SBMA) were investigated over one week in culture (Figure 1) and compared to control conditions. Under static flow conditions, CellMa + MCC (50%) exhibited the highest cell proliferation at day 7, exceeding those of tissue culture control and PMP. Cells were subsequently assessed via immunostaining assay and were pictured after 1 day at different initial cell density. (Figure 2)

Conclusion

Microvascular lung cells HULEC-5a proliferated on cellulose-based materials, forming a complete monolayer after 1 day of culture under static conditions. Under dynamic conditions, the cell proliferation was significantly altered by the applied shear stress.

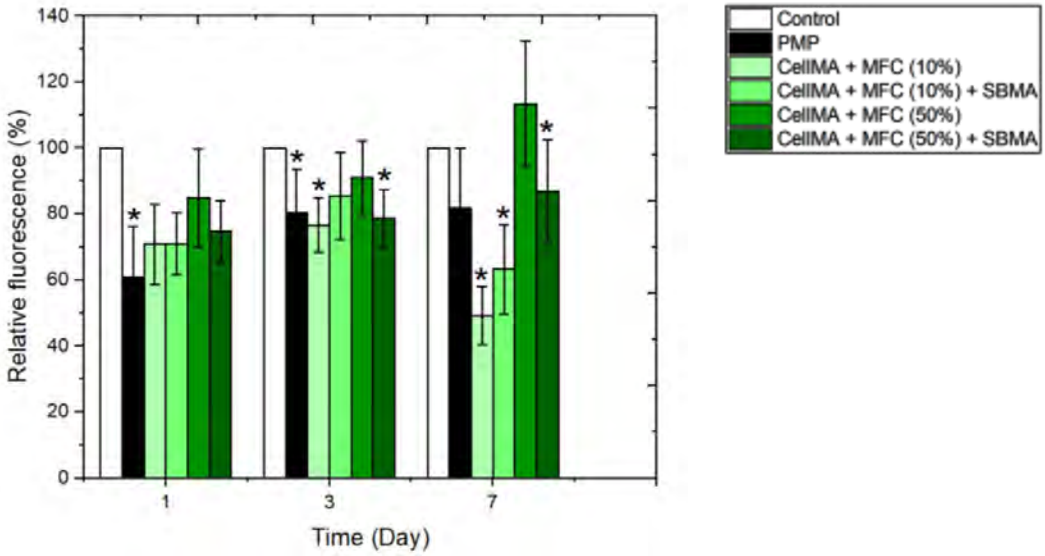

Figure 1: Proliferation of HULEC-5a at the surface of nanocellulose-based membrane after 1, 3 and 7 days of culture.

Figure 2: Immunostaining assay (Rhodamine) of HULEC-5a cells after 24h at the surface of nanocellulose-based membranes with an initial cell density of (a) 0.5 x10^5, (b) 1 x10^5 and (c) 2x10^5 cells.cm^{-2}. Scale bar = 100 µm.

S100 – O6

From waste to high-value biomaterial: gellan gum hydrogels enriched with pomegranate peel extract for cartilage regeneration

Busto F.[1], Scalia A. C.[2], Gentile P.[3,4], Girón-Hernández J.[3,4], Cometa S.[5], Brosio T.[2], Mastrorilli P.[6], Cochis A.[2], De Giglio E.[1]

[1]Dept. of Chemistry, University of Bari, Bari, Italy; [2]Dept. of Health Sciences, Università del Piemonte Orientale, Novara, Italy; [3]Centre for Biomaterials and Tissue Engineering, Universitat Politècnica de València, València, Spain; [4]Biomedical Research Networking Centre on Bioengineering, Biomaterials and Nanomedicine (CIBER-BBN), Carlos III Health Institute, Valencia, Spain; [5]Jaber Innovation s.r.l, Rome, Italy; [6] DICATECh, Politecnico di Bari, Bari, Italy.

Introduction

Cartilage microtrauma can lead to degradation and limited capacity for tissue regeneration. Agri-food waste represents a promising alternative source of bioactive compounds. Pomegranate peel is an agri-food byproduct rich in polyphenols, which possess significant anti-inflammatory properties. These characteristics are especially valuable for materials intended for cartilage tissue regeneration.[1]

The aim of this work is to integrate a pomegranate peel extract (PPE) within a gellan gum network. This strategy provides a multifunctional hydrogel demonstrating antibacterial, antioxidant, anti-inflammatory, and chondrogenic activities in addition to enhanced mechanical properties (Figure 1).[2]

Materials and Methods

PPE was prepared by dissolving pomegranate peel powder in distilled water at room temperature. High- and low-acyl gellan gum (1.2:0.8% w/v) were added to PPE at 70°C under continuous stirring. The hydrogel solution was transferred into multi-well plates and stored at 6°C for 24 hours. Then, a cross-linking was performed by dipping the hydrogels in $MgCl_2$ solution. The chondrogenic potential of GG_{HL}/PPE hydrogels was assessed under both physiological and IL-1β/TNFα-induced inflammatory conditionsin hMSC-seeded prototissues using histology and qRT-PCR. Antibacterial and antibiofilm efficacy were evaluated against multidrug-resistant Gram-positive and Gram-negative bacteria.

Results

FT-IR/ATR, TGA, and SS-NMR indicated that PPE polyphenols interact with carbohydrate via hydrogen bonds. The hydrogel showed excellent mechanical performances (compressive Young's modulus up to ~145 kPa, strain at break up to ~54 %). PPE in the hydrogel created a supportive environment for hMSCs, enhancing SOX9, COL2, and ACAN expression, even under inflammatory conditions. PPE-loaded hydrogel promoted anti-inflammatory effects by modulating key cytokines and reducing PBMC migration *in vitro*. Moreover, GG_{HL}/PPE inhibited Gram-positive and Gram-negative bacterial growth and biofilm formation by over 95%.

Conclusion

The promising mechanical, chondrogenic, antinflammatory, antibacterial, and antibiofilm properties of this hydrogel derive from the high bioactivity of the polyphenol-rich extract, which is retained within the polymer network. GG_{HL}/PPE represents an *in vitro* sustainable material suitable for in situ cartilage regeneration.

References

[1]Bernini, R., Campo, M., Cassiani, C., Fochetti, A., Ieri, F., Lombardi, A., Urciuoli, S., Vignolini, P., Villanova, N., & Vita, C. Polyphenol-rich extracts from agroindustrial waste and byproducts: Results and perspectives according to the green chemistry and circular economy. Journal of Agricultural and Food Chemistry (2024); 72(23), 12871–12895.

[2]Busto, F., Scalia, A. C., Gentile, P., Girón-Hernández, J., Cometa, S., Brosio, T., Mastrorilli, P., Cochis, A., & Giglio, E. D. Analytical and biological characterization of Gellan Gum-Pomegranate Peel Extract hydrogel: Combining mechanical, antibacterial, anti-inflammatory and pro-regenerative properties for cartilage healing. Carbohydrate Polymer Technologies and Applications (2025); 12, 101032.

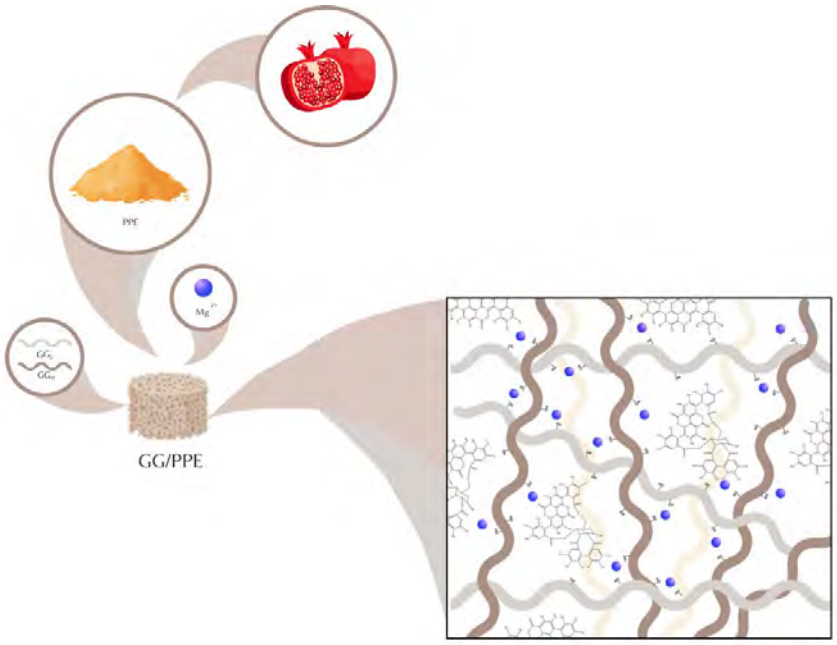

Figure 1. Graphical representation of the GG_{HL}/PPE hydrogel.

S101
Biomaterials for bone and cartilage regeneration (II)

S101 – K1
Multi-Material and Multi-Wavelength Volumetric 3D Printing

Thijssen Q.[1,2], Ortega A.J.[1], Itzel F.[1], Wechsler F.[3], Belfiore A.[1], Carroll J.A.[2], Moser C.[3], Barner-Kowollik C.[2,4], Van Vlierberghe S.[1]
[1] Polymer Chemistry and Biomaterials Group, Centre of Macromolecular Chemistry, Dept. of Organic and Macromolecular Chemistry, Ghent University, Ghent, Belgium; [2] School of Chemistry and Physics, Queensland University of Technology, Brisbane, Australia; [3] Laboratory of Applied Photonics Devices, School of Engineering, Ecole Polytechnique Fédérale de Lausanne, Switzerland; [4] Institute of Functional Interfaces, Karlsruhe Institute of Technology, Eggenstein-Leopoldshafen, Germany

Most objects used in everyday life are inherently multi-material, combining distinct mechanical, thermal, optical, or chemical properties within a single structure. In contrast, volumetric 3D printing has so far largely remained limited to single-material fabrication, restricting the functional complexity that can be achieved.[1–4] Expanding volumetric 3D printing toward multi-material and multi-functional fabrication is therefore an important step toward the production of more realistic and application-relevant three-dimensional objects.

In this talk, I will present two complementary strategies to overcome this limitation. First, we demonstrate that multi-functional structures composed of entirely different base materials can be fabricated through sequential volumetric 3D printing, in which distinct materials are introduced in consecutive printing steps. Second, I will present our progress toward simultaneous multi-material volumetric 3D printing from a single resin. In this context, multi-wavelength photochemistry becomes key, as it enables different photochemical pathways to be controlled independently during fabrication and thereby paves the way for increased contrast in volumetric 3D printing, as well as for the simultaneous generation of spatially defined and heterogeneous functionalities from a single resin.

Together, these results show how volumetric 3D printing can evolve beyond rapid shape formation toward the fabrication of complex three-dimensional materials with integrated, spatially defined, and heterogeneous functionalities.

1. Thijssen, Q., Toombs, J., Li, C. C., Taylor, H. & Van Vlierberghe, S. From pixels to voxels: A mechanistic perspective on volumetric 3D-printing. *Prog. Polym. Sci.* **147**, 101755 (2023).
2. Thijssen, Q., Ortega, A. J., Vieira, R. P. & Van Vlierberghe, S. Radical inhibition in tomographic volumetric 3D printing for thiol-Ene photoresists: From Photorheology to printability. *React. Funct. Polym.* **205**, 106096 (2024).
3. Thijssen, Q. *et al.* Beyond absorption maxima: the impact of wavelength-resolved photochemistry on materials science. *Mater. Horiz.* **11**, 6184–6191 (2024).
4. Thijssen, Q. *et al.* Volumetric Printing of Thiol-Ene Photo-Cross-Linkable Poly(ε-caprolactone): A Tunable Material Platform Serving Biomedical Applications. *Adv. Mater.* **35**, 2210136 (2023).

S101 – O1

A coacervate-based approach to achieve controlled mineralization in bulk collagen constructs

Vergara-Vera N.S.[1,2,4], Sümbelli Y.[3,4], Rodríguez-Abetxuko A.[3,4], Leurs, Y.[3,4], Ito K. [2,4], Van Hest J.[3,4], Castilho M.[1,4]
[1]Biomaterial Engineering & Biofabrication; [2]Orthopaedic Biomechanics; [3]Bio-organic Chemistry, Dept. of Biomedical Engineering; [4]Institute for Complex Molecular Systems, Eindhoven University of Technology, Eindhoven, The Netherlands

Introduction

Achieving uniform mineralization within bulk collagen scaffolds remains a major challenge in bone tissue engineering, as current methods often yield surface-dominated mineral deposition. Although physiological mineralization mechanisms remain debated, matrix vesicles are thought to transport mineral precursors into collagen, while acidic non-collagenous proteins (NCPs) contribute to driving mineral formation. Inspired by these vesicles, we developed a poly(aspartic acid)–based complex coacervate (COV) system to stabilize and deliver calcium phosphate. As no synthetic platform has yet replicated such vesicles, we aim to use COVs to elucidate their role in collagen mineralization. We hypothesize that COVs enable mineral delivery and provide early nucleation sites for hydroxyapatite formation and growth.

Materials and Methods

COVs were prepared using poly-L-lysine, poly-(L-aspartic acid), and nano-hydroxyapatite (HAp) powder. HAp incorporation was confirmed using confocal laser scanning microscopy (CSLM). COVs were incorporated into poly(ethylene glycol)-supplemented collagen and cast into gels by neutralization with PBS followed by incubation at 37°C for 90 minutes. Constructs were mineralized for four weeks at 37°C using a PILP-mineralization treatment[1]. Collagen-only gels and collagen mixed with an HAp suspension were included as control groups. Mineral distribution and morphology were evaluated using SEM, while EDS quantified Calcium:Phosphate (Ca:P) ratios as an indicator of mineral growth and chemical stability. Apparent stiffness was measured using unconfined compression testing.

Results

COVs were successfully synthesized, and hydroxyapatite (HAp) incorporation was confirmed by CSLM (Fig1). SEM showed that COV-treated constructs contained finely dispersed mineral granules integrated throughout the fibrillar network at Weeks 1 and 4, without forming large aggregates (Fig2a). In contrast, HAp-treated samples displayed patchy surface coatings, while controls developed dense aggregates as early as Week 1. EDS analysis (Fig2b) revealed stable Ca:P ratios for COV samples (2.0-2.1) with low variability over time, indicating controlled mineral maturation. HAp and control samples showed lower or fluctuating ratios (1.7-2.2), consistent with heterogeneous deposition. Mechanical testing (Fig2c) showed lower apparent stiffness for COV constructs (4 kPa vs. 21-22 kPa), reflecting uniform but non-aggregated mineral rather than mineral absence.

Conclusion

COV-mediated mineralization enables uniformly distributed, chemically stable mineral formation within bulk collagen constructs, avoiding surface aggregation and producing architectures resembling early bone matrix. We anticipate that this system will support physiologically relevant mineral networks in millimetre-thick constructs and promote integrated collagen-mineral architectures. Ongoing work focuses on implementing COVs in 3D-printing workflows, performing detailed physicochemical analyses, and using TEM to elucidate the nanoscale mechanisms underlying COV-driven mineral formation.

References

[1]De Wildt B., *Adv. Funct. Mater.* 2022; 32; 2206992.

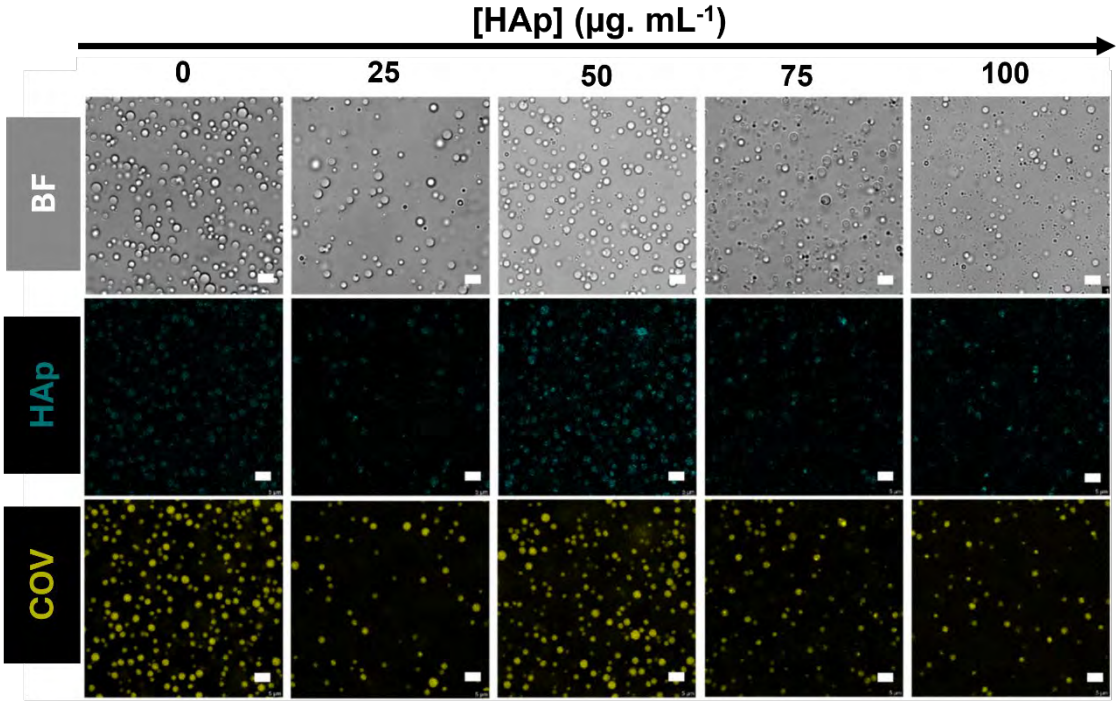

Figure 1. Brightfield and CLSM images showing how increasing HAp concentration (0–100 µg mL⁻¹) affects COV formation. Brightfield images reveal liquid-like droplets with HAp incorporation at intermediate levels. CLSM shows rising HAp fluorescence (cyan) and reduced droplet stability (yellow) at high concentrations, with optimal, homogeneous HAp incorporation at 50–75 µg mL⁻¹. Scale bar = 5 µm.

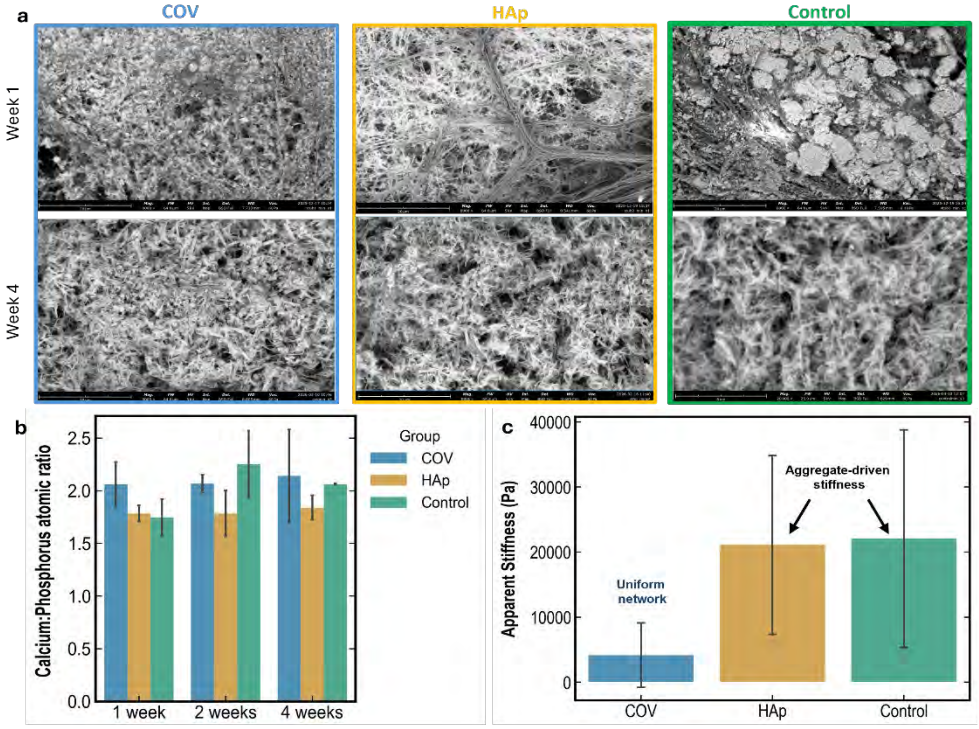

Figure 2. COV-mediated mineralization yields uniform and chemically stable mineral networks. (a) SEM images of COV constructs reveal uniform and integrated mineral growth. (b) EDS show stable Ca:P ratios over time, and mechanical testing (c) after four weeks demonstrated controlled mechanical properties.

S101 – O2

Collagen-catechol hydrogels combined with gallium-bioglass nanoparticles for bone regeneration

Fernandes M.[1,2,3], Correia C.[1,2], Franco R.A.[1,2], Reis L.R.[1,2], Vieira M.[3], Peixoto D.[1,2], Alves M.N.[1,2]
[1]3B's Research Group, I3Bs – Research Institute on Biomaterials, Biodegradables and Biomimetics, University of Minho, Guimarães; [2]ICVS/3B's–PT Government Associate Laboratory, Guimarães; [3]RISE-Health, Center for Translational Health and Medical Biotechnology Research (TBIO), ESS, Polytechnic of Porto, Porto, Portugal

Introduction

Bone presents a self-healing capacity in response to an injury. When fractures are extensive, it may be necessary to use bone grafts. Conventional treatments have limitations, such as a lack of antibacterial activity, non-biodegradability, and limited biocompatibility, which increase the risk of inflammation, infection, and rejection. Due to these limitations, hydrogels appear to be an alternative for bone regeneration, given their ECM-like structure, biocompatibility, and ability to incorporate bioactive molecules into their structure. Collagen (Coll) is the principal component of bone, making it ideal for developing scaffolds for bone applications. Hydrogels based on coll modified with catechol (coll-cat) groups were developed. This biomimetic approach is inspired by the adhesion capacity of marine mussels to wet irregular surfaces.

Aim

To develop coll-cat hydrogels combined with Gallium Bioglass nanoparticles (Ga-BGNPs) to enhance antibacterial properties, osteoblast cell viability, and proliferation.

Materials and Methods

Coll was modified with catechol by reaction with hydrocaffeic acid and characterized by NMR and UV-Vis. The Ga-BGNPs were produced by the sol-gel method and characterized by HR-SEM, EDS, and zeta sizer. Hydrogels were produced via intramolecular interactions and combined with Ga-BGNPs. The physical and chemical properties of hydrogel, as well as their antimicrobial activities and cytocompatibility with human osteoblast cells, were analyzed. The biomineralization was conducted by immersing the hydrogel in SBF solution, and the surface was analyzed by HR-SEM, EDC, and XRD.

Results

The modification of Coll with catechol groups increased the hydrogel's adhesion properties, as proven in adhesion tests using rat femur and porcine skin. The incorporation of 1% Ga-BGNPs promoted the formation of hydroxyapatite and exhibited antibacterial activity against clinically relevant microorganisms. The hydrogel/Ga-BGNPs system showed higher activity against *P. aeruginosa*, a pathogen known for its antibiotic resistance and clinical challenges in bone infections. Also, Coll-cat/Ga-BGNPs hydrogels promoted and supported osteoblasts' adhesion and proliferation (Figure 1).

Conclusion

Overall, bioadhesive hydrogel composites represent a promising system for bone regeneration, combining enhanced adhesive capacity, biomineralization, antibacterial/antibiofilm properties, cytocompatibility, and stimulation of cell proliferation.

Acknowledgements

We acknowledge projects SHIFT (funded by the European Union's Horizon 2020 Research and Innovation Programme under the Maria Sklodowska-Curie grant agreement no. 101008041), SeaJellySpine – Operação nº15520 (COMPETE2030-FEDER-00653700) and Jelly4Bone – Operação nº15969 (COMPETE2030-FEDER-00710400), co-financed by ERDF through the Innovation and Digital Transition Thematic Programme (COMPETE 2030), under Portugal 2030. Also, TERM RES Hub-reference PINFRA/22190/2016 (Norte-01-0145-FEDER-022190), funded by the FCT in cooperation with CCDR-N and UID/50026/2025, financed by FCT I.P (component OE) (https://doi.org/10.54499/UID/50026/2025).

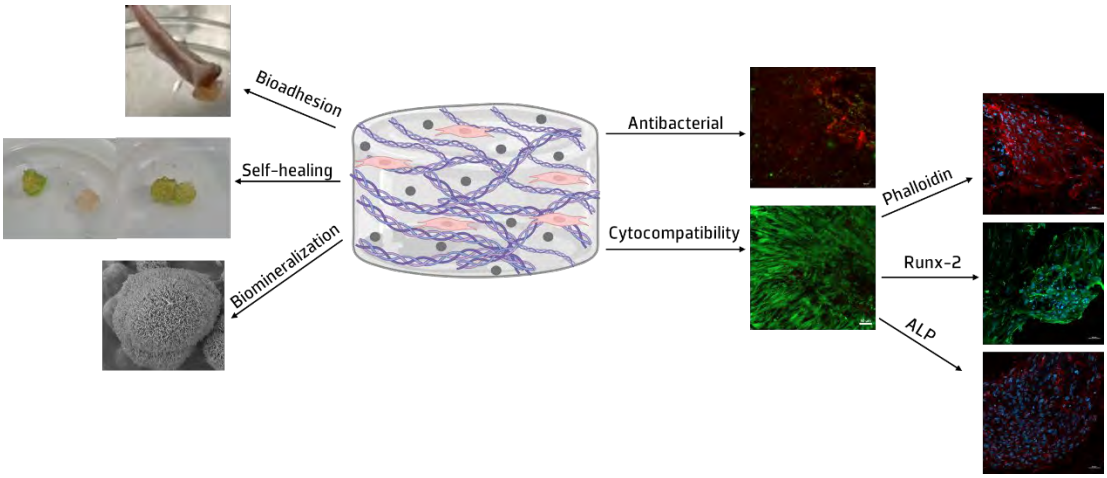

Figure 1- Coll-cat hydrogels combined with Ga-BGNPs properties

S101 – O3

3D bone tissue model by triculture of human primary cells on methacrylated gelatin bioink, supported by biphasic calcium phosphate

Durvin N.[1,2], Hammad M.[1], Custodio Morena A.[1], Lepage M.L.[2], Fournier Noel C.[1], Layrolle P.[1]
[1]INSERM/Toulouse University UMR 1214, Toulouse Neuro Imaging Center (ToNIC), CHU Toulouse Purpan; [2]CNRS /Toulouse University UMR CNRS, Laboratoire Hétérochimie Fondamentale et Appliquée (LHFA), Toulouse, France

Introduction

In 3D bioprinting technologies, bioinks are commonly used to encapsulate cells. Widely reported as a biocompatible material, crosslinked gelatin-methacrylate (GelMA) can promote cell adhesion and proliferation in a 3D environment. However, these matrices are still not optimized for bone tissue remodeling. Biphasic calcium phosphate (BCP) is widely known for its osteoconductive properties and used as a synthetic bone substitute. BCP particles can support cells attachment, proliferation and production of an osteogenic matrix to form a 3D construct. The aim of this study is to develop a 3D bone model with vascularization and remodeling capacity by co-culturing human bone marrow mesenchymal stem cells (hBMSC), human umbilical vein endothelial cells (HUVEC) and peripheral blood-derived monocytes (PBMC) in GelMA-BCP matrices.

Materials and Methods

Functionalized GelMA was prepared by reaction of gelatin with methacrylic anhydride. The modified biopolymer was isolated by dialysis and freeze-dried. The degree of functionalization (DoF) was determined by NMR spectroscopy and ninhydrin assay. Based on results obtained in our lab on the triculture supported by BCP, different ratio of GelMA/BCP were tested. Photopolymerization was performed using LAP (405 nm). Constructs 3D bioprinting were tested by digital light processing and microextrusion (Cellink, LumenX, BioX) and mechanical properties using a texturometer. After cell encapsulation, adhesion, proliferation and osteogenic differentiation as well as formation of microvasculature were observed by fluorescence confocal microscopy after immunololabeling and histology sections. Gene expression was evaluated using RTqPCR.

Results

GelMA with different DoF and BCP content were prepared and crosslinked giving a range of stiffness for the artificial matrices. Preliminary results indicated that hBMSC and HUVEC co-cultured in crosslinked GelMA supported osteogenic differentiation and vasculogenesis. After one-week of culture, cell growth was observed for both cell types, while HUVEC organized into vessel-like structures. However, the degradation of GelMA matrix after three weeks of culture is limiting the maturation of the 3D construct. Monocytes were induced to form multinucleated osteoclasts able to resorb bone matrix. The study currently in progress is exploring the tri-culture of hBMSC, HUVEC and monocytes on GelMA 3D construct, stabilized and promoted by the BCP biomaterial.

Conclusion

This bioink could be used for 3D bioprinting of bone constructs. The study of hBMSC, HUVEC, monocytes triculture in a GelMA-BCP construct is a promising approach to build a 3D bone model with remodeling capacity for studying osteoporosis disease in vitro as an alternative to animal experiments.

Acknowledgements

Funded by the European Commission ORTHO ALLO UNION.

S101 – O4

Enhancement of osteogenic differentiation using gelatin-coated $BaTiO_3$ in PLLA scaffolds

Nakagawa S.[1], Yamamoto K.[2], Morita Y.[2]
[1]Graduate School of Life and Medical Sciences, Doshisha University; [2]Faculty of Life and Medical Sciences, Doshisha University, Kyoto, Japan

Introduction

Poly-L-lactic acid (PLLA) is used as a scaffold for bone regeneration. However, bone formation requires a long period, and scaffolds should promote cell proliferation and differentiation. Previous studies have improved osteogenesis by incorporating $BaTiO_3$ (BTO) microparticles to mimic bone electromechanical properties. Both PLLA and BTO lack integrin-binding ligands such as RGD, resulting in poor cell adhesion. Integrin-mediated adhesion is essential for cellular responses to scaffold-derived stimuli. In this study, coating BTO microparticles with gelatin was proposed to introduce cell-adhesive sites. Incorporation of gelatin-coated BTO microparticles (Ge-BTO) into PLLA scaffolds may enable effective electrical stimulation by modulating cell-adhesive properties. The purpose was to develop Ge-BTO to promote osteogenic differentiation.

Materials and Methods

Ge-BTO was prepared by dispersing BTO in a gelatin solution, followed by collection of the particles, crosslinking, and freeze-drying. Morphology and composition of the particles were analyzed by SEM and EDS. Three types of films were prepared by spin-coating: PLLA, PLLA films containing BTO (PLLA/BTO) and PLLA films containing Ge-BTO (PLLA/Ge-BTO). Surface properties were evaluated by fluorescence microscopy, KFM, and contact angle measurement. MC3T3-E1 cells were seeded at 1.0×10^4 cells/cm² and cultured for 7 days in α-MEM with 10% FBS and 1% antibiotics. Cell adhesion (Day 1) was evaluated by DNA quantification and F-actin staining. Osteogenic differentiation was assessed by RT-qPCR (*Runx2*, *Col1a1*, *Alp*) and ALP activity (Day 7).

Results

SEM and EDS confirmed spherical Ge-BTO microparticles (0.5–1.5 μm). Fluorescence imaging confirmed gelatin coating on Ge-BTO microparticle surfaces. KFM demonstrated that Ge-BTO retained BTO-derived surface potential after gelatin coating. Fig. 1 shows enhanced cell spreading and F-actin organization on Ge-BTO due to gelatin-derived cell-adhesive sites. Cell adhesion on PLLA/Ge-BTO (Day 1) was approximately fivefold higher than that on PLLA and PLLA/BTO. Proliferation from Day 1 to Day 3 was comparable among groups. Fig. 2 shows that Ge-BTO induced the highest osteogenic gene expression, with *Runx2* and *Alp* significantly upregulated, while *Col1a1* expression was highest in PLLA/BTO. ALP activity showed no significant difference between PLLA and PLLA/BTO but was significantly higher on PLLA/Ge-BTO at Day 7. These results suggest that enhanced integrin-mediated adhesion improves cellular responsiveness to BTO-derived electrical stimulation, resulting in enhanced osteogenic differentiation.

Conclusion

Ge-BTO was successfully developed, providing cell-adhesive sites while retaining surface potential. Ge-BTO improved cell adhesion and enhanced osteogenic differentiation in PLLA scaffolds through the combined effects of cell adhesion and electrical stimulation.

Acknowledgements

This work was supported by JST SPRING.

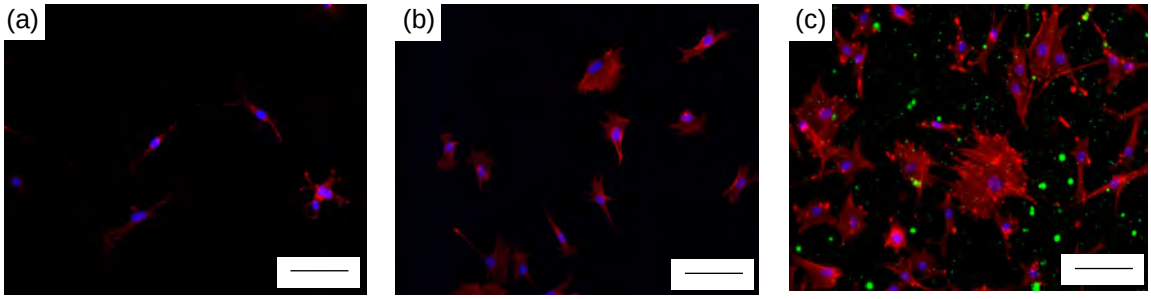

Figure 1 Fluorescence images of MC3T3-E1 cells on Day 1. (a) PLLA, (b) PLLA/BTO, (c) PLLA/Ge-BTO. (×200, Scale bar: 50 µm, blue: nucleus, green: gelatin, red: F-actin.)

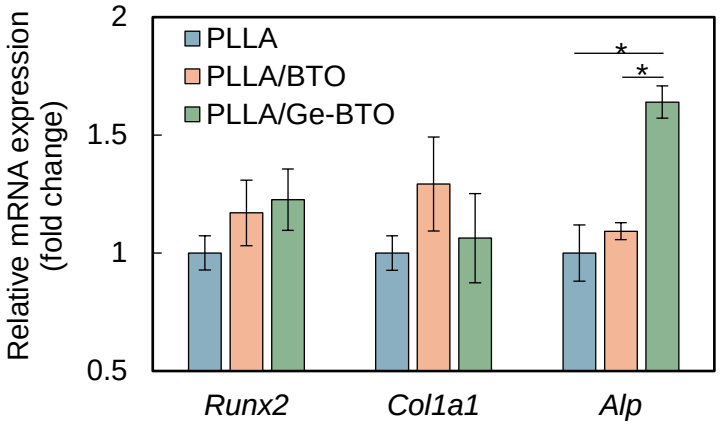

Figure 2 Relative mRNA expression of *Runx2*, *Col1a1*, and *Alp* in MC3T3-E1 cells, normalized to *Gapdh* and expressed as fold change relative to PLLA. (mean ± S.D., *$p < 0.01$, n = 3).

S101 – O5

Osteoinductive effect of an ectopic hydroxyapatite synthetic bone graft – A µCT and histopathology-focused study

Rondahl V.[1], Carlsson E.[2], Torres Rodriguez C.[3], Hedenqvist P.[3], Höglund O.[3], Hulsart Billström G.[2]
[1]Dept of Animal Bioscience, Swedish University of Agricultural Sciences (SLU); [2]Dept. Medical Cell Biology - BMC, Uppsala University; [3]Dept. Clinical Sciences, SLU, Uppsala, Sweden

Introduction

Surgical intervention with bone grafting is used to facilitate fusion of complicated bone lesions and subsequent healing. However, autogenous bone grafts have issues with donor site morbidity. Vast knowledge has been generated about how to tailor artificial, synthetic bone substitutes – ceramic biomaterials, but there is a lack of knowledge regarding the osteoinduction pathways involved, if any, for many of these materials. Studies on osteoinduction are complicated by the fact that frequently used laboratory animals - mice and rats - have different metabolic pathways for bone formation compared to humans, whereas rabbits have many more similarities to human bone metabolism, as do dogs.

Aim

To determine if a hydroxyapatite synthetic bone graft is osteoinductive in an ectopic (subcutaneous) rabbit model.

Materials and Methods

A new commercially available hydroxyapatite synthetic bone graft (Xcyte, CAVIX AB, Uppsala, Sweden) with calcium pyrophosphate, 3-phase calcium phosphate, and α-tricalcium phosphate was placed subcutaneously in the flank of eight 4-month-old, female New Zealand White rabbits: Xcyte granules in a plastic cage; Xcyte free granules (on one side); Xcyte+putty in a cage and an empty cage (on the other side). One day (n=1), three months (n=2) and six (n=5) months after surgery, the rabbits were euthanised and necropsied. Tissue samples of the flank skin including the implanted materials were immediately formalin-fixed, and the fixed material was analysed with µCT, histopathology (both hard-tissue and after decalcification) and immunohistochemistry.

Preliminary results

µCT imaging showed no to minimal extragranular mineralisation or bone formation (Figure). Histopathology of hard-tissue sections, stained with modified Paragon stain, showed that granules were surrounded by few to numerous mononuclear (black arrows) and giant multinuclear cells (asterisk) of either macrophage or osteoclast origin. The mononuclear cell morphology was plasmacytoid to osteoblastic (black arrows), some with intracytoplasmic material suggestive of osteoid production (white arrows). µCT of the empty plastic cages showed no mineralisations or bone material, and histopathologically the cages contained connective tissue with occasional giant multinuclear macrophages (MM) lined along the cage (C) surface, with adjacent macrophages (M).

Conclusion

The preliminary µCT results show no extagranular mineralisations or bone formation, and additional analyses will show if there are effects on e.g. granule size or profile that suggest *in vivo* modifications. Likewise, there are ongoing histopathology and immunohistochemistry analyses to determine the origin of mononuclear and multinuclear cells. The cell morphology strongly suggests that there are cells with ongoing differentiation to osteoblastic or osteoclastic cell types.

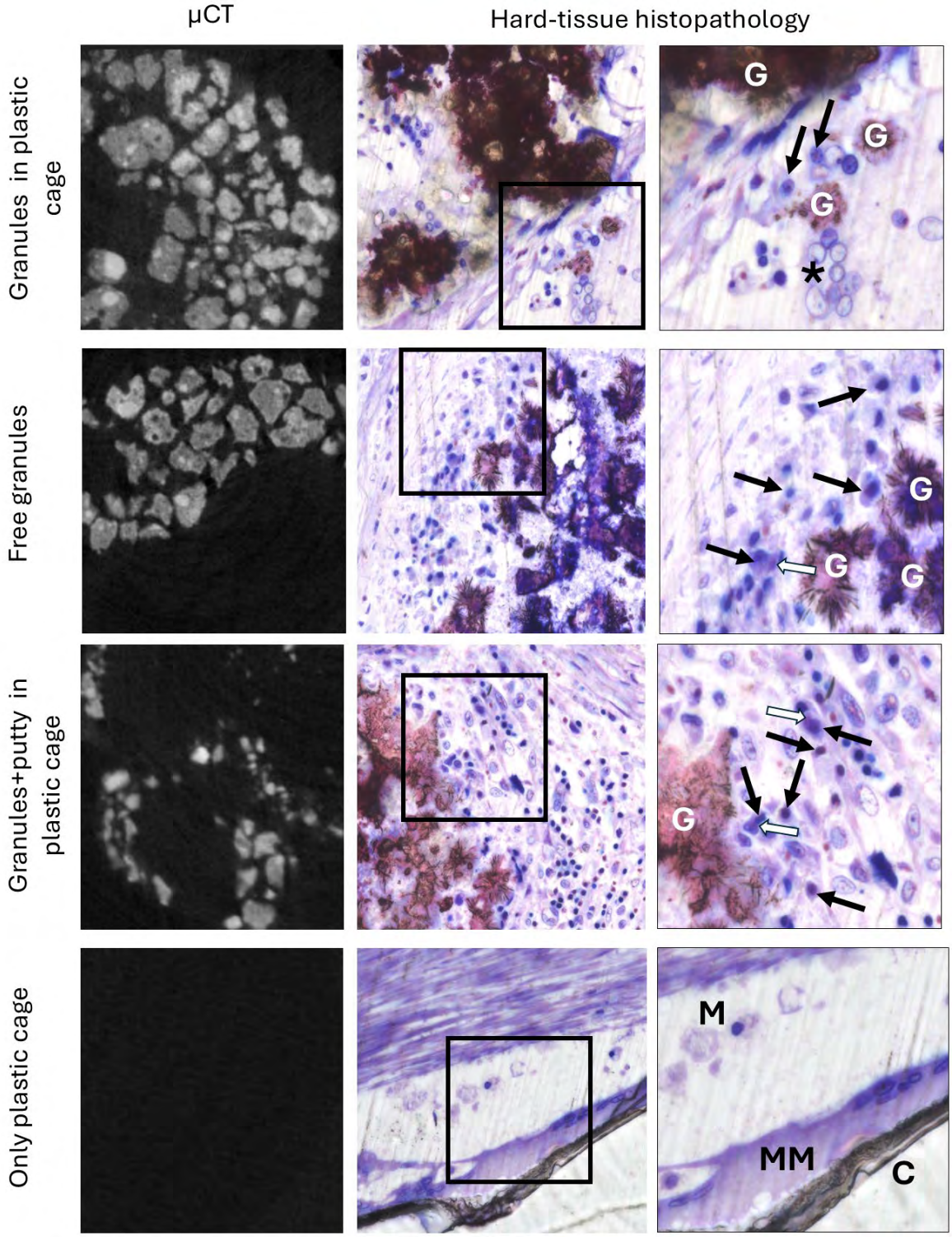

Figure Representative µCT and hard-tissue histopathology images. Black squares indicate area enlarged in right-most column. G = granules, M = macrophage, MM = multinucleated macrophage, C = cage material. * = giant multinucleated cell of unknown origin. Black arrow = mononuclear cells with plasmacytoid/osteoblastic morphology, white arrows = osteoid-like intracellular material in some mononuclear cells.

S101 – O6

Metal oxide modified fluorophosphate nano glass filled polymeric scaffolds for enhanced bone repair

Ganesan S.M.[1], Balasubramanian M.[1], Kandaswamy R.[1], Sankaralingam P.[2], Thangavel V.C.[2]
[1]Dept. of Rubber and Plastics Technology, Madras Institute of Technology Campus, Anna University, Chromepet, Chennai; [2]Bone Substitutes, Madurai, Tamil Nadu, India

Introduction

The design of biomimetic scaffolds capable of supporting bone regeneration remains a central challenge in orthopedic biomaterials research. Conventional metallic implants provide structural support but lack bioactivity and may cause long term complications such as stress shielding and poor osseointegration. Bioactive glass systems have gained significant interest because of their ability to stimulate osteogenesis and bond chemically with bone tissue. Fluorophosphate glasses represent an advanced class of bioactive materials with tunable degradation and ion release properties. Incorporating therapeutic metal oxides into fluorophosphate nano glass structures and integrating them into biodegradable polymeric scaffolds may provide improved mechanical compatibility and enhanced biological performance for bone regeneration.

Aim

This study aims to develop metal oxide modified fluorophosphate nano glass filled polymeric scaffolds with enhanced mechanical strength, bioactivity, and osteogenic potential for bone tissue engineering applications.

Materials and Methods

Fluorophosphate nano glass compositions containing P_2O_5, CaO, Na_2O, and CaF_2 were synthesized via the melt quenching technique. Metal oxides such as Ag_2O and ZnO were incorporated as dopants to enhance structural stability and biological functionality. The resulting nano glass particles were incorporated into polymeric scaffold matrices composed of biodegradable polymers (Figure 1). Structural and physicochemical properties were characterized. Bioactivity was evaluated by immersing scaffolds in simulated body fluid (SBF) for 21 days. Cytocompatibility and osteogenic responses were investigated using MG-63 and SAOS-2 osteoblast like cell lines through alkaline phosphatase activity and osteocalcin secretion assays[1]. In addition, in vivo bone regeneration capability was evaluated using a rabbit defect model, followed by radiographic and histopathological analysis to assess bone formation, scaffold integration, and vascularization.

Results

The developed nano glass filled scaffolds exhibited mechanical properties comparable to natural bone with a Young's modulus of approximately 1.8 GPa[1]. Incorporation of 5 wt.% metal oxide dopants improved the chemical stability and bioactivity of the glass network while maintaining favorable degradation characteristics (Table 1). Following SBF immersion, the scaffold surfaces demonstrated rapid hydroxyapatite formation within 14 days, confirmed by XRD patterns corresponding to crystalline apatite. SEM analysis revealed homogeneous apatite deposition, while EDS confirmed a Ca/P ratio close to 1.67, characteristic of biologically relevant mineral phases. In vitro biological evaluation demonstrated greater than 90% cell viability, along with increased ALP activity and approximately two-fold enhancement in osteocalcin secretion, indicating strong osteogenic stimulation. In vivo studies further demonstrated accelerated bone regeneration, with radiological analysis showing progressive defect healing and histological evaluation confirming new bone formation, vascularization, and integration of the scaffold within the surrounding tissue.

Conclusion

Metal oxide modified fluorophosphate nano glass filled polymeric scaffolds demonstrate excellent mechanical compatibility, bioactivity, and cytocompatibility. The combined in vitro osteogenic responses and in vivo bone regeneration results highlight their strong potential as bioactive scaffolds for bone tissue engineering and orthopedic regenerative applications.

Acknowledgements

The research was fully supported by Bone Substitutes, Madurai 625014, India. The authors are much grateful to the Department of Rubber and Plastics Technology, MIT campus, Anna University, Chennai-600044.

References

[1]Balasubramanian M., Ganesan S.M., Thangavel V.C., Sankaralingam P., Kandaswamy R. Nanofluorophosphate glasses as biocompatible and bioactive materials in porous biopolymeric scaffolds for bone tissue engineering. *Polymeric Scaffolds and Their Role in Biomedical Engineering*. *IntechOpen* 2025; DOI: 10.5772/intechopen.1012729.

Table 1. ***Physicomechanical properties and 21-day bioconversion of fluorophosphate nano glass filled scaffold formulations, highlighting variations in pore size, porosity, compressive strength, and bioactivity.***

Formulation	Glass wt. (%)	Mean pore size (µm)	Open porosity (%)	Compressive strength (MPa)	Bio-conversion [21 days] (%)
Base polymer blend	35	420 ± 60	71 ± 3	9.1	62
Base polymer blend + AgFP	35	405 ± 55	69 ± 4	16.3	67
Base polymer blend + ZnFP	35	398 ± 50	70 ± 2	14.8	57

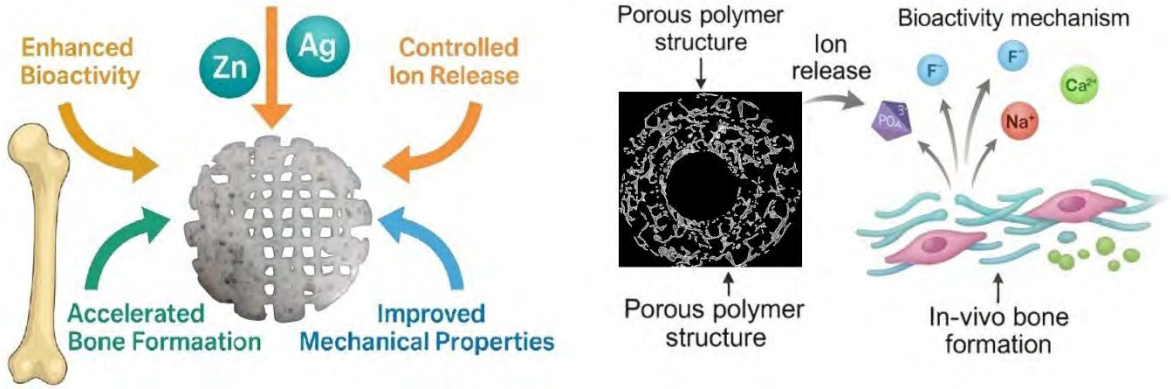

Figure 2. ***Schematic of fluorophosphate nano glass filled porous scaffolds demonstrating ion release, bioactivity, and mechanical reinforcement for bone repair.***

S101 – O7

New injectable composites featuring dual responsiveness for trabecular bone repair

Pillai A.S[1], Maciejewicz-Kamiński N.[1], Sać P.[1], Demirci G.[1], Prowans P.[2], El Fray M.[1]
[1]Dept. of Polymer and Biomaterials Science, West Pomeranian University of Technology in Szczecin, Poland; [2]Dept. of Plastic, Endocrine and General Surgery, Pomeranian Medical University, Szczecin, Poland

Introduction

Repairing and regenerating injured bone after tumour resection, trauma, and injury is challenging especially for trabecular (highly porous) bone at distal end. To address the pressing need for the development of more advanced solutions than Kirschner's wires, PMMA or calcium-phosphate bone cements, new composite polymer networks were developed to meet these needs.

Aim. Aim of the work was to develop novel composite materials based on supramolecular networks containing cyclodextrins and thermo-responsive poly(N-isopropylacrylamide) units. Next, composite formulations containing hydroxyapatite (HAp) and alginate beads were prepared. The amount of additives was optimized to reach good dispersion in polymer networks and to facilitate injectability and provide immediate mechanical stability in seconds under UV light at body temperature.

Materials and Methods

The preparation protocol involved synthesis of photoresponsive macromonomer and complexation with α-cyclodextrin. Photocurable and thermosensitive formulations were prepared by incorporating N-isopropylacrylamide (NIPAM) into the methacrylated macromonomers and further irradiated with UV light at 365 nm. A composite hydrogel containing HAp were finally developed. Characterization of chemical structure was performed with ATR FT-IR and NMR. Material viscosity was evaluated for injectability. Cell viability was assessed for biological response.

Results

A photoresponsive macromonomer has successfully been synthesised and its chemical structure was confirmed with ^{1}H NMR. GPC revealed the M_n of 1200 g/mol with dispersity of 2. Maximum conversion of a system cured under UV light was reached at 20 seconds. Photo-DSC analysis indicated fast photopolymerization kinetics, with maximum conversion of 80%, confirming efficient UV-induced network formation. Among the investigated formulations, the system containing 20% HAp exhibited the most efficient curing behavior. Compression tests of the cured composites containing 20% HAp and 1% alginate microbeads revealed reproducible mechanical behavior reaching a maximum compressive stress of approximately 10-11 MPa at around 19-21% strain, indicating good mechanical stability of the photocured composite structure. Preliminary biological evaluation demonstrated cell viability exceeding 80%, confirming good cytocompatibility of the developed materials.

Conclusion

Dual-responsive injectable composite hydrogels based on cyclodextrin supramolecular networks and thermo-responsive poly(N-isopropylacrylamide) units were successfully developed. The materials demonstrated rapid UV-induced polymerization containing 20% HAp and 1% Alg, good injectability, and sufficient mechanical stability after curing. The structural properties and high cytocompatibility indicate that the developed composites are promising candidates for minimally invasive treatment of trabecular bone defects and may serve as potential alternatives to conventional bone cements.

Acknowledgements

This work has been supported by research „New biomaterials based on supramolecular and thermosensitive polymer networks", UMO-2023/49/B/ST11/04005.

S102
Bioinspired and biometric materials II

S102 – K1

More than 50 years of Fibrin-based biomaterials

Heinz Redl (1,2)
1) Ludwig Boltzmann Institute for Traumatology
2) Austrian Cluster for Tissue Regeneration

Fibrin, a natural hydrogel, is the end product of the physiological blood coagulation cascade and naturally involved in tissue healing. We started more than 50 years ago to support the development process of fibrin as a surgical sealant therapeutic product both from the material side and the application tools. Beyond its role in haemostasis and tissue sealing (i.e. commercial products), it acts as a local reservoir for growth factors and as a provisional matrix for invading cells that drive the regenerative process. Its unique intrinsic features do not only promote wound healing directly via modulation of cell behavior but it can also be fine-tuned to evolve into a delivery system for sustained release of therapeutic biomolecules, cells and gene vectors. Despite its extensive history in the field, this biomaterial continues to demonstrate a high degree of versatility and frequent utilization. This presentation will elucidate the contributions of fibrin to the domain of biomaterials in regenerative medicine.

S102 – O1

EMC derived matrix bound nanovescicole: An innovative biomaterial in TERM

Di Francesco D.[1,2], Di Varsavia C1, Boccafoschi F.[1,2]
[1]Dept. of Health Sciences, University of Piemonte Orientale, 28100 Novara, Italy; [2]Tissuegraft srl, 28100 Novara, Italy

Introduction

Matrix bound nanovesicles (MBV) are a recently discovered subtype of extracellular vesicles (EV) entrapped in collagen of the extracellular matrix (ECM). These nanovesicles differ from other EV in terms of biological, chemical and physical properties, and they have been identified in a number of decellularized ECM (dECM) biomaterials1,2. Importantly, MBV have displayed great bioactivity for regenerative medicine, also demonstrating ability to replicate the biological activity of the source dECM material they are derived from3,4. This discovery has allowed to better understand both ECM physiological involvement in regeneration, the mechanisms underlying the biological potential of dECM, and to explore an innovative type of ECM-derived biomaterial. Given the recent discovery there is still a lot unknown on MBV and their full potential for TERM applications has not yet been uncovered.

Aim

The aim of this research was to characterize MBV derived from pericardium dECM (dBP), to understand their bioactive properties, such as angiogenic and wound healing potential, and their application in regenerative medicine.

Materials and Methods

MBV derived from dBP have been characterized in terms of chemical-physical properties, such as size-concentration (NTA, TEM) and protein cargo (LC-MS/MS, immunoassays). Cytocompatibility has been tested using varied human cell lines (fibroblasts, endothelial cells, corneal epithelial cells), evaluating cell metabolic activity and MBV internalization. The angiogenic potential was assessed in vitro by immunofluorescence staining, eNOS expression, angiogenic cytokine release and tube formation assay, ex vivo with aortic ring assay, and in vivo with a hind limb ischemia (HLI) model. Involvement in wound healing pathways was also tested using human fibroblasts.

Results

MBV derived from dBP showed excellent regenerative potential in different applications. Cytocompatibility was confirmed for all cells lines, with MBV internalization, increase in cell metabolic activity, maintenance of cell morphology and significant enhancement of cell specific phenotype markers. The angiogenic potential has been extensively demonstrated in all the conditions (in vivo, ex vivo and in vivo), indicating ability to induce neovascularization and increase angiogenic markers. Furthermore, MBV also show ability to induce the expression of markers involved in wound healing, such as α-SMA.

Conclusion

MBV from dBP have demonstrated to be incredible multitasking ECM components. The results confirm their involvement in tissue repair, displaying angiogenic, wound healing potential and regenerative ability in different tissue contexts. This confirms their potential use as innovative biomaterials derived from ECM.

Acknowledgements

Authors thanks Tissuegraft s.r.l. for the unconditioned financial support.

References

[1]Huleihel L., et al. *Sci. Adv.* 2016; 2; e1600502.
[2]Di Francesco D., et al. *Matrix Biology* 2025.
[3]Huleihel L., et al. *Tissue Eng.* 2017; Part A 23; 1283–1294. [4]Turner N.J,. et al. *Tissue Eng*. 2022; Part A 28; 879–892.

S102 – O2

Development of the next generation of biomaterials through glycan-functionalized polyethylene glycols

Hariharan A.[1], Mora-Boza A.[1], Uribe-Gomez J[1*], Russo L[1,2,3*], and Pandit A.[1*]

[1]CÚRAM, Research Ireland Centre for Medical Devices, Biomedical Sciences, University of Galway, Galway, H91 W2TY, Ireland
[2]School of Medicine and Surgery, University of Milano-Bicocca, Milan, Italy
[3]Fondazione IRCCS San Gerardo dei Tintori, Monza, Italy

Introduction

The therapeutic efficacy and longevity of implantable biomaterials are frequently constrained by the host's foreign-body response. It is crucial to develop biomaterials that are compatible with the host and can interact with the host's immune system. Immune cells possess surface receptors that recognize and bind to glycans. Glycans are monosaccharides linked in either a linear or branched configuration. In this study, we propose that the surface functionalization of biomaterials with glycans may attenuate the foreign-body response by engaging glycan-binding receptors.

Materials and Methods

A comprehensive library of linear polyethylene glycol (PEG) functionalized with eleven distinct monosaccharides was developed. The modified PEGs were characterized using FT-IR, ^{1}H and ^{13}C NMR. To evaluate the immunomodulatory effects, the secretome of IFN-γ-activated MSCs was analysed in the presence of the modified PEGs using a multiplex assay. Furthermore, glycosylated biomaterial coatings presenting sialyllactoses were developed. Sialic acids were conjugated to lactose using a three-enzyme chemoenzymatic approach[1] and functionalized onto a PEG backbone for biomaterial coatings. The synthesis was confirmed using FT-IR and NMR.

Results

The developed library exhibited no cytotoxic effects on HDFs and MSCs. Among the 13 paracrine factors analysed in activated MSCs, reductions in MCP-1, IP-10, IL-6, and IL-8 levels were observed following treatment with modified PEGs for 48 h. This immunomodulatory effect of monosaccharides serves as the basis for the development of glycosylated coatings. The successful synthesis of sialyllactose coatings was confirmed by the presence of carboxyl and methyl-N-acetyl peaks at 172.45 and 174.70 ppm, respectively, in the ^{13}C NMR spectra. Primary human monocytes, derived from peripheral blood mononuclear cells and cultured on sialyllactose-coated well plates, show a marked reduction in the expression of inflammatory markers and a diminished secretion of inflammatory cytokines, including TNF-α, in contrast to classically activated macrophages.

Conclusion

In this study, we demonstrated that glycan-modified PEGs can modulate the inflammatory responses of MSCs. Additionally, we established the development of glycosylated PEG coatings with immune-instructive properties. This research provides a foundation for the advancement of next-generation biomaterials with enhanced interactions between materials and host tissues.

Acknowledgement

Funding was provided by Research Ireland (grant number 18/EPSRC-CDT/3583).

Reference

[1]Yu, H., Chokhawala, H. A., Huang, S., & Chen, X. One-pot three-enzyme chemoenzymatic approach to the synthesis of sialosides containing natural and non-natural functionalities. Nature Protocols 2006; 1(5); 2485–2492.

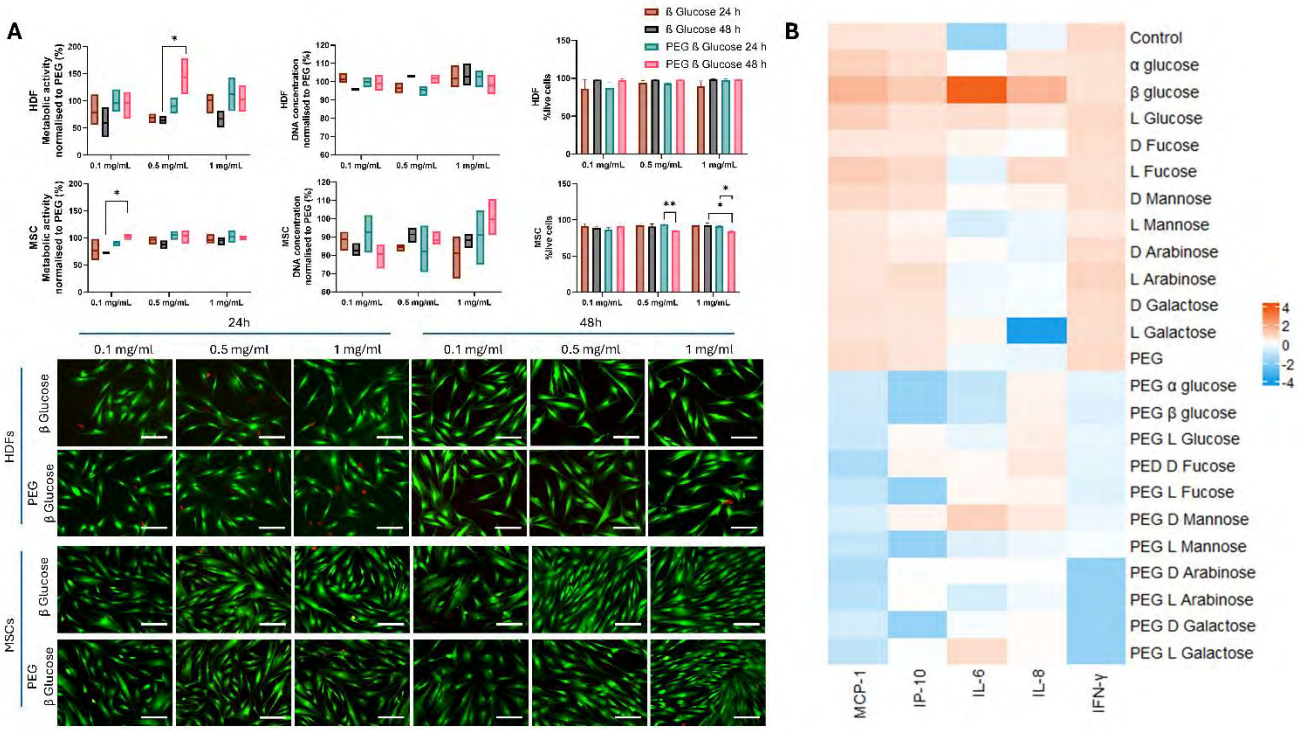

Figure 1: Library of monosaccharide modified-PEGs. (A) Cell viability and cytotoxic analysis of the library. (PEG beta glucose is shown). (B) Multiplex analysis of paracrine factors secreted from IFN-gamma activated MSCs.

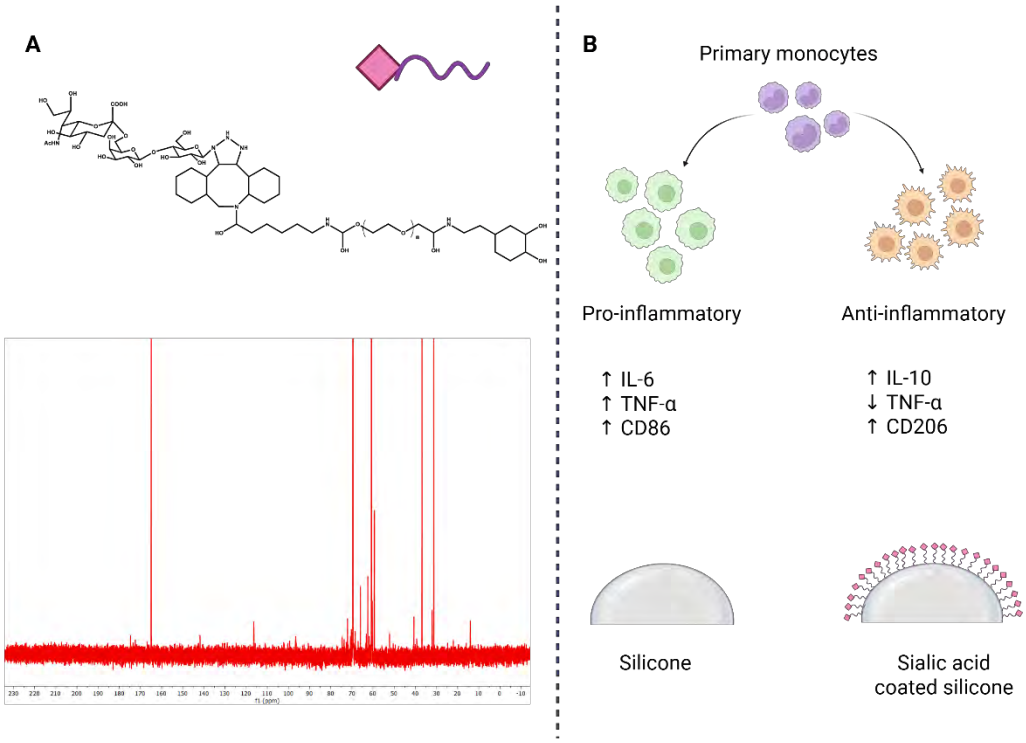

Figure 2: Development of sialic acid-presenting PEG coatings. (A) Structure and ^{13}C NMR of sialic acid functionalised coating. (B) Predicted immunomodulatory effects of the coating.

S102 – O3

Liquefied-Core Microcapsules as a Platform for In Vitro Endochondral Ossification

Bakht S.M[1], Carreira M[1], Mano J.F[3]
[1]CICECO – Aveiro Institute of Materials, Department of Chemistry, University of Aveiro, Campus Universitário de Santiago, 3810-193, Aveiro, Portugal

Introduction

Bone tissue possesses a unique intrinsic capacity for self-repair. However, large bone defects can exceed this regenerative capacity, leading to impaired healing. Bone tissue engineering has traditionally relied on intramembranous ossification strategies, which frequently lack a functional vascular supply and may result in necrotic core formation. In contrast, endochondral ossification (ECO) represents a promising alternative due to its ability to promote both osteogenesis and angiogenesis. In this study, a novel in vitro ECO model was developed using liquefied compartments incorporating 3D cartilaginous microtemplates, umbilical cord-derived mesenchymal stem cells (UCMSCs), and human umbilical vein endothelial cells (HUVECs) to mimic key stages of bone formation.

Aim. This study aimed to develop and evaluate a 3D in vitro ECO model within liquefied microcapsules capable of supporting vascularized bone tissue development.

Materials and Methods

Umbilical cord-derived cells were isolated from human newborns. Three-dimensional UCMSC microtemplates were generated using Aggrewell microplates and cultured in chondrogenic differentiation medium for 21 days. Alginate microbeads containing microtemplates, dispersed UCMSCs, and HUVECs were produced via electrohydrodynamic atomization in a calcium chloride bath. A multilayered membrane was assembled using a layer-by-layer technique with poly(L-lysine), alginate, chitosan, and alginate. The alginate core was subsequently liquefied using EDTA. The resulting liquefied-core microcapsules were cultured dynamically in spinner flasks for an additional 21 days. Chondrogenic and osteogenic differentiation were assessed over time using biochemical assays and imaging techniques.

Results

Chondrogenic differentiation of UCMSCs within microtemplates was confirmed by aggrecan and collagen II expression, along with increased sulfated glycosaminoglycan production. Collagen X expression indicated progression toward hypertrophy. High cell viability was maintained throughout the culture period. Immunofluorescence tracking demonstrated progressive adhesion of UCMSCs and HUVECs to the microtemplates. Osteogenic differentiation was evidenced by osteopontin and osteocalcin expression. Mineralization was confirmed by hydroxyapatite detection and SEM/EDS analysis of calcium and phosphorus, with Ca/P ratios comparable to native bone. Endothelial marker expression further confirmed recruitment of HUVECs into the developing microtissues.

Conclusion

This study presents a novel 3D in vitro ECO model based on liquefied microcapsules that supports cellular organization, differentiation, and matrix mineralization. The system enables integration of multiple cell types while promoting vascularization, highlighting its potential as a versatile platform for bone tissue engineering, disease modeling, and drug screening applications.

Acknowledgements

This work was financed by national funds (OE) through the Portuguese Foundation for Science and Technology (FCT)/MCTES in the scope of “O2Cells” (2022.04237.PTDC) and the European Research Council for project “REBORN” (ERC-2019-AdG-883370). This work was developed within the scope of the project CICECO-Aveiro Institute of Materials, UIDB/50011/2020, UIDP/50011/2020& LA/P/0006/2020, financed by national funds through the FCT/MEC (PIDDAC). M. Carreira acknowledges the financial support given by FCT with the doctoral grant (2021.04542.BD).

S102 – O4

Bone-guided biomaterials to modulate nerve-bone crosstalk during regeneration

Nóbrega A[1,2*], Osório de Valdoleiros B[1,3], Reis J[1,2], Couto M[1], Lamghari M[1], Ribeiro CC[1,2] and Vasconcelos DP[1,2]

[1]i3S – Instituto de Investigação e Inovação em Saúde, Universidade do Porto, Portugal; [2]ISEP – Instituto Superior de Engenharia do Porto, Instituto Politécnico do Porto, R. Dr. António Bernardino de Almeida 431, 4249-015 Porto, Portugal; [3]FCUP – Faculdade de Ciências da Universidade do Porto, Rua do Campo Alegre s/n, 4169-007 Porto, Portugal

Introduction

Bone has an intrinsic regenerative capacity, restricted to small defects. Larger defects remain a global orthopedic challenge, leading to repeated surgeries and disability [1]. Bone tissue engineering (TE) has progressed significantly with the development of biomaterials that support osteogenesis and modulate immune responses. In biomaterials-guided-bone regeneration, a major gap persists, as innervation is overlooked in biomaterial design for TE [2]. Addressing these interactions requires models capable of capturing both biomaterial-induced osteogenesis and neuronal contributions. Microphysiological systems (MPS) offer a versatile platform for controlled and physiologically relevant testing, enabling the investigation of mechanisms inaccessible to traditional *in vivo* models. Among emerging biomaterials, kefiran, an exopolysaccharide, has recently gained attention, due to its safety profile and promising physiochemical and biological characteristics for TE [3]. This study aimed to develop a nerve–bone organ-on-chip (OoC) platform to decipher the nerve-bone crosstalk mediated by a kefiran-based biomaterial, with the goal of enhancing bone regeneration.

Materials and Methods

Kefiran production was performed as previously established [3]. Biocompatibility of kefiran hydrogels at 5 %, 2 % and 1 % (w/v) was evaluated using human osteoblasts (HOB) and sensory neurons (dorsal root ganglia (DRGs)) employing lactate dehydrogenase (LDH) and Live/Dead assays. Neurite outgrowth was quantified using the AxoFluidic software [4]. Alkaline phosphatase (ALP) activity in HOB was measured on days 7, 14 and 21. Engineered 3D bone microtissues (EBM) were generated by encapsulating HOB within kefiran hydrogels and subsequently evaluated for viability, morphology and extracellular matrix (ECM) deposition.

Results

These findings indicate that kefiran not only supports osteogenesis but also facilitates neuro-integration. Together, these results validate kefiran as a promising biomaterial for advancing bone-regeneration strategies with integrated neural components. Current studies are investigating how neuronal integration into EBM influence osteogenesis.

Conclusion

Data demonstrate that kefiran-based biomaterials are well tolerated by sensory neurons, supporting both neuronal viability and neurite extension. HOB cultured on kefiran hydrogels showed enhanced viability and significantly increased ALP activity at day 7. The resulting EBM exhibited well-defined architectures and improved cell morphology compared with control hydrogels (Figure 1). Importantly, when co-cultured with sensory neurons in a MPS, EBM embedded in kefiran hydrogels promoted clear structural interactions between axons and the bone microtissues, in contrast to control EBM.

Acknowledgements

This work was supported by the Funding Neuro-skeletal group (Centro 8089901H22) and the MOBILIsE_Plus project, co-funded by the European Union through the NORTE 2030 Regional Program of the European Regional Development Fund (FEDER), under the operation with the code NORTE2030-FEDER-01801000. DPV received funding from Fundação para a Ciência e Tecnologia - FCT (2021.03374.CEECIND).

References

[1]Nauth, A.; Schemitsch, E.; Norris, B.; Nollin, Zachary; Watson, J. Tracy. Critical-Size Bone Defects: Is There a Consensus for Diagnosis and Treatment?. Journal of Orthopaedic Trauma 32; 2018; S7-S11.

[2]Sun, W., Ye, B., Chen, S. et al. Neuro–bone tissue engineering: emerging mechanisms, potential strategies, and current challenges. Bone Res. 11, 65; 2023.

[3]Gentry B., Cazón P., O'Brien K. A comprehensive review of the production, beneficial properties, and applications of kefiran, the kefir grain exopolysaccharide. International Dairy Journal; 144; 2023.
[4]Neto, E., Alves C.J., Sousa, D.M. et al. Sensory neurons and osteoblasts: close partners in a microfluidic platform. *Integrative Biology* 6, 2014; 586–595.

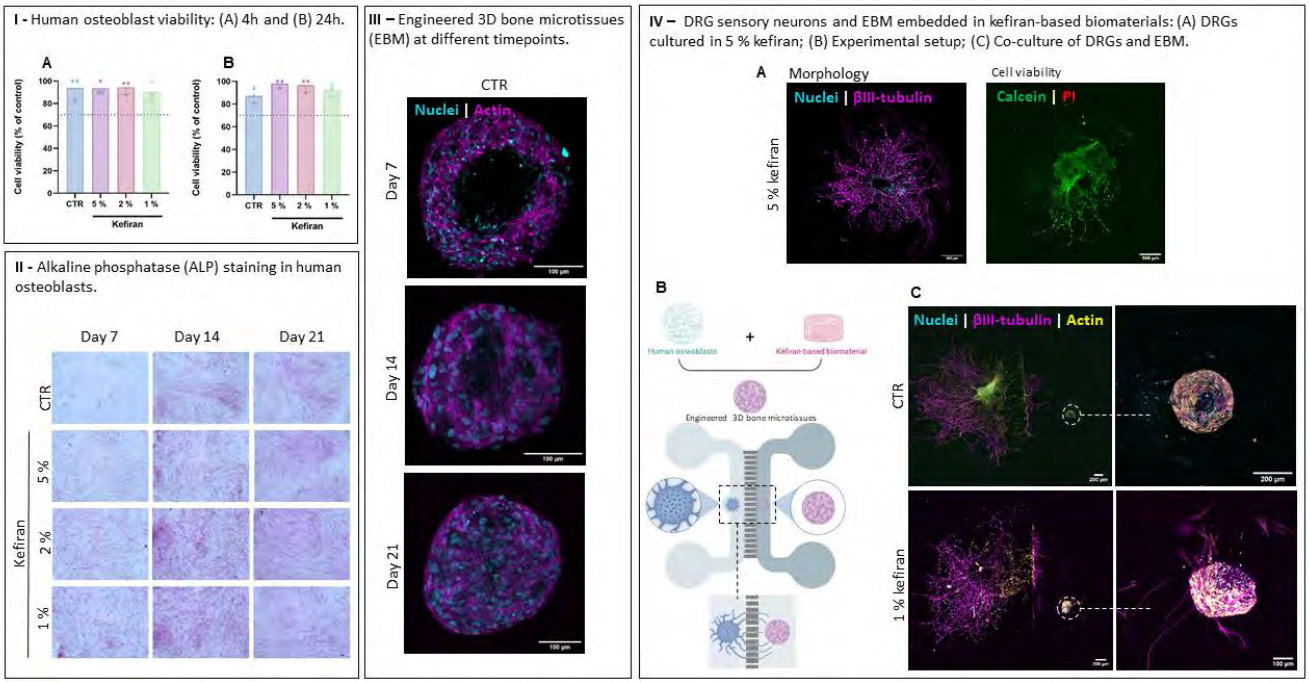

Figure 1: Experimental setup.

S102 – O5

Lignocellulosic material blend for melt electrowriting to alter mechanical and bacterial properties

Kumauchi T[1], Mussoni C[1], Kronberger V[1], Lamberger Z[1], Stahlhut P[1], Ewald A[1], Kumar A[2], Jungst T[1], Groll J[1], Bartolf-Kopp M[1]

[1] Department for Functional Materials in Medicine and Dentistry, University Würzburg, Würzburg, Germany

[2] Natural Resources Institute Finland (Luke), Ministry of Agriculture and Forestry of Finland, Helsinki, Finland

Introduction

Melt Electrowriting (MEW) is a novel manufacturing process that relies on electrohydrodynamic interactions with the processed materials to fabricate micro- to nanometer scale fiber constructs. Polycaprolactone (PCL) is the most ubiquitously processed material and due to its biocompatibility and material properties well suited for biofabrication with MEW. The number of materials for MEW beyond PCL is still limited, especially in the group of renewable additives like wood components, which have become more relevant in processes like fused filament fabrication. Evaluating the processability of lignocellulosic additives for MEW is therefore a promising approach to diversify the material library of the method.

Aim

Expand processable material library of MEW with a new renewable material additive and investigate the effects on the generated constructs.

Materials and Methods

Ligninocellulosic materials were extracted from wood waste and grouped by their origin and constituents into powdered substrates. A defined number of particles have been melt-blended into PCL until homogenous. Using a custom-made MEW printer setup, different ratios of blended materials were tested and optimized for processability with MEW. Mechanical testing, TG, DSC and rheology have been used to record changes in material properties. Micro biotic interaction essays have been conducted to evaluate the effect of the included particles compared to pure PCL constructs.

Results

A ratio of 10% w/w lignocellulosic particles in PCL yielded the best printing results and enabled fabrication of grid structures. Fiber diameter with optimized printing temperatures were between 50 and 100 µm depending on used particles and increases if particle amount increases. Rheology TG and DSC confirm semi-miscibility of the melt and focus ion beam measurements reveal inclusion of particles within the processed melt. Mechanical measurements reveal an increase in recorded stress and higher ultimate tensile stress for GX and BLCC compared to pure PCL. Bacterial attachment essays reveal that inclusion of particles lessens the amount of attached bacteria on scaffolds with comparable geometry. It was found that by processing GX at high temperatures, a significantly elevated bacterial retention could be shown, indicating a tunability of procaryotic interaction with the scaffold.

Conclusion

We present here a new material blend processable with MEW that utilizes natural materials in the form of lignocellulosic particles extracted from wood, a renewable resource. The addition not only strengthens the mechanical properties of PCL but also allows for tunable pro- or anti-microbial properties depending on extrusion temperature. Thereby the material library of MEW is expanded and simultaneously made more recyclable.

S102 – O6
Design of a Targeted Peptide Nanocarrier for Nucleic Acid Delivery

McCarthy HO.[1] & Dunne N.[2]
[1]School of Pharmacy, Queen's University Belfast, Belfast, United Kingdom
[2] School of Mechanical and Manufacturing Engineering, Dublin City University, Dublin, Ireland

Introduction

Nucleic acids (NA) such as DNA, mRNA, miRNA require delivery systems that encapsulate, protect and ensure the payload reaches its destination site, namely the cytoplasm or nucleus of cells. The gold standard for NA delivery is Lipid Nanoparticles (LNPs). Although functional, these remain sub-optimal with accumulation in the liver, which means there is a need to refine the LNPs or even investigate other delivery technologies for NA where targeted delivery is critical. This project explains how we have created the first peptide delivery system termed HAWC for NA that i) bypasses the liver and targets the lung and spleen when injected IV and ii) can be used to load NA into biomaterials for wound healing.

Aim

The aim of this study was to design and develop a new peptide delivery system using Machine Learning and validate the results in biological systems.

Materials and Methods

A Machine Learning platform extracted information from the Human Protein Atlas in relation to proteins that transport across cell membranes. This was then cross-referenced with APCs, and sequences were automatically pulled from the NCBI website. Clustal Omega then extracted consensus motifs. Consensus sequence 1 (8 Amino Acids) was found in the Pleckstrin, and Sec7 Domain-containing protein 4 (PSD4), and consensus sequence 2 (7 Amino Acids), was found in the dynamin-binding protein (DNMBP). Neither individual consensus sequence nor the 15 aa combination functioned as a delivery system. Through a series of mutational events, the HAWC 24 aa peptide was generated (PCT/EP2025/075098).

Results

The HAWC peptide was complexed with GFP mRNA and formed Nanoparticles <100 nm with a PDI <0.1 (industrial level homogeneity). NPs successfully transfected in NCTC-929s and DC 2.4 cells with transfection efficiencies as high as 80% and 62%, respectively (Figure.1). Biochemical analysis showed that the NPs enter cells via two mechanisms. The HAWC-mRNA nanoparticles were lyophilised into a product and have shown stability out to 1 month so far at room temperature. Using mRNA encoding luciferase, NPs were injected intravenously, they bypassed the liver, and expression was detected in the lungs and spleen. Finally, the NPs were loaded into a biomaterial for wound healing and outperformed commercial controls.

Conclusion

Using AI, a new peptide has been designed for nucleic acids that bypasses the liver and has huge applicability for biomaterials. This green technology offers accelerated manufacturing, reduced NA wastage, and solvent-free processing, with the potential to substantially lower the cost of goods.

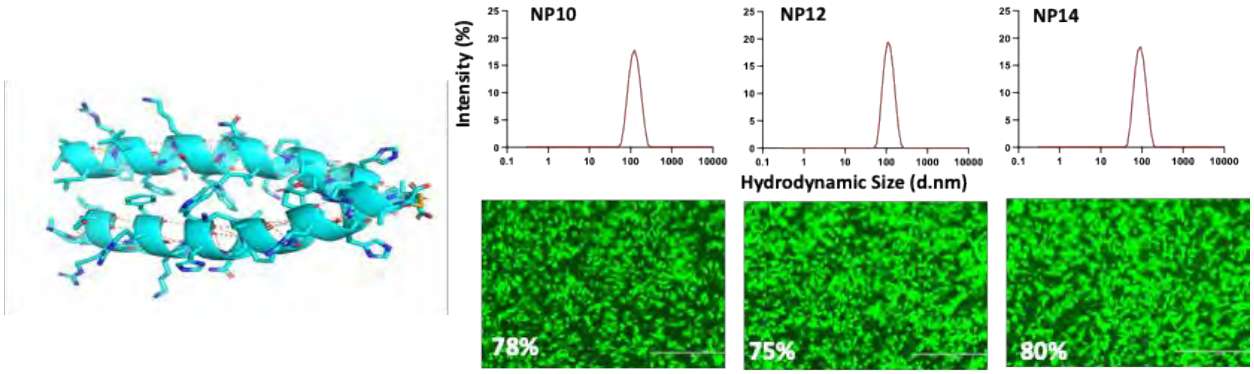

Figure 1: *A pymol representation of the 24aa HAWC peptide. HAWC-mRNA nanoparticle transfections in NCTC-929 fibroblast cells. Nanoparticles were formulated at room temperature using 1 µg of mRNA in a final volume of 50 µL. Particle size was measured using a Malvern Zetasizer Nano ZS. Representative fluorescence microscopy images of cells 24 h after transfection using peptide NPs as indicated using FACs analysis*.

S103
Advanced manufacturing and functionalization strategies for Next-Generation biomaterials

S103 – K1
Reducing Uncertainty in Mechanical Characterization of Soft Biomaterials: Lessons from the C4Bio Community Challenge

Famaey N.[1,2], Yadav D.[1,2], Loeckx M.[1,2], Fehervary H.[1],
[1]FIBEr Core Facility for Biomechanical Experimentation, KU Leuven, Belgium, [2]Soft Tissue Biomechanics Group, Dept. of Mechanical Engineering, KU Leuven, Belgium

Introduction
Characterizing the mechanical properties of biological tissues is essential for understanding function, diagnosing disease, and designing biomedical devices. Because many organs exhibit strong structure-function relationships, changes in tissue mechanics due to aging or pathology can provide clinically relevant indicators. In tissue engineering, matching the mechanical behavior of native tissues is critical for functional integration, while accurate mechanical data are equally important for the design of implants, prosthetics, and surgical tools. Moreover, experimentally derived properties enable development of constitutive models that support computational simulations in *in silico* medicine.

To address this challenge, the international C^4Bio (Community Challenge towards Consensus on Characterization of Biological Tissue) initiative was established to quantify and reduce variability in soft tissue mechanical testing. Initial campaigns focusing on uniaxial testing of porcine aorta demonstrated that interlaboratory variability remains substantial, even when a consensus testing protocol is adopted, indicating the presence of important uncontrolled methodological factors[1].

Keynote overview
This presentation will discuss how the lessons learned from C^4Bio are helping shape a roadmap towards more credible mechanical characterization of biomaterials and biological tissues. First, the development of robust and biofidelic reference materials will be highlighted as an essential step towards benchmarking testing systems and protocols across laboratories. Such materials provide a means to isolate methodological variability from biological variability and establish traceable quality-control procedures.

Second, recent efforts aimed at systematically unraveling methodological variability will be presented, including combined experimental and computational sensitivity analyses investigating the effects of gripping conditions, device configurations, specimen geometry and strain measurement approaches on measured material properties.

Third, the talk will argue that future characterization frameworks should embrace, rather than oversimplify, the inherent inhomogeneity related to mechanical testing of biological tissue. Experimental methodologies including multi-axial loading strategies and full-field deformation measurements enable a richer characterization of material behaviour than conventional testing methods.

Finally, the importance of uncertainty quantification and propagation throughout experimental and computational workflows will be discussed. Rather than reporting single deterministic parameter values, future databases and constitutive models should capture the uncertainty associated with biological variability and measurement processes, thereby supporting more reliable model-informed decision making.

Acknowledgements
Samples were mechanically tested at FIBEr. The equipment used in this study was funded by Research Foundation Flanders (FWO: AKUL/15/25 & I011822N)
This work is supported by KU Leuven (C2M/24/031)

References
[1]Famaey, Nele, et al. "Community challenge towards consensus on characterization of biological tissue: C4Bio's first findings." *Journal of Biomechanics* (2025): 113021.

S103 – O1

Implementation of PCL/AgNPs electrospun coatings onto Ti6Al4V additive manufactured samples with biomedical applications

Ibáñez Losantos S.[1,2], Castaño A.[1], Veiga F.[1,4], Lasa Í.[3], Rodríguez R.J.[1,2], Rivero P.J.[1,2]
[1]Engineering dept. - Public University of Navarre (UPNA), Pamplona, Spain; [2]Institute of Advanced Materials and Mathematics (INAMAT2) - Public University of Navarre (UPNA), Pamplona, Spain; [3]Microbial Pathogenesis Laboratory, Navarrabiomed–Navarre Hospital Complex (CHN)–Public University of Navarre (UPNA), IDISNA, Pamplona, Spain; [4]Institute of Smart Cities (ISC) - Public University of Navarre (UPNA), Pamplona, Spain

Introduction

This study reports the development of functional polymeric coatings based on PCL and later doped with silver nanoparticles, produced via electrospinning. The work focused on optimizing nanofibrous mats with antimicrobial properties to create surfaces capable of responding to pathogenic threats. The coatings were extensively characterized using SEM-EDX, confocal microscopy, XRD, GD-OES, wettability, and roughness analyses. Their antimicrobial performance was evaluated through Kirby–Bauer inhibition halo assays and direct-contact tests, assessing both ion-diffusion activity and pathogen–surface interaction. The incorporation of AgNPs significantly enhanced antimicrobial behavior, highlighting the potential of these electrospun coatings for biomedical and hygienic applications.

Materials and Methods

A polymeric solution of PCL and AgNPs in chloroform was prepared to fabricate electrospun coatings. Initial tests on glass substrates optimized the electrospinning parameters, after which coatings were produced on LPBF manufactured Ti6Al4V samples. The materials underwent detailed physicochemical characterization to assess morphology, composition, and microstructure. Finally, standardized assays against *S. aureus* and *E. coli* including inhibition halo and direct contact tests, evaluated the antimicrobial performance of the PCL/AgNPs coatings.

Results

Electrospun PCL and PCL/AgNPs coatings were successfully obtained and assessed for antimicrobial activity. Incorporating silver nanoparticles significantly reduced microbial growth of *Escherichia coli* and *Staphylococcus aureus*. The nanofibrous structure enhanced microorganism–surface interaction, improving antimicrobial effectiveness. These results highlight the potential of these coatings as effective antimicrobial surfaces for biomedical environments where bacterial contamination is critical.

Conclusion

The results show that electrospun PCL/AgNPs coatings effectively reduce microbial activity on polymeric surfaces. Silver nanoparticles markedly enhanced the antimicrobial response against *Escherichia coli* and *Staphilococcus aureus*, confirming the efficiency of the nanofibrous structures. These findings highlight their potential for biomedical and protective applications, including complex geometries.

Acknowledgements

This project has been made possible thanks to funding from the FactorIA Misiones de Ciencia e Innovación TransMisiones 2024 project (PLEC2024-011165 UFG 30.30.00.558A) and the FABTI project (PID2024-158908OB-C33), to which we express our deepest gratitude.

S103 – O2

Process design for large-scale manufacturing of microneedle arrays

Velayudhan S.[1], Jayahanumaiah P.[2]
[1]Dept. of Biomaterials Science and Technology, Biomedical Technology wing, Sree Chitra Tirunal Institute for Medical Sciences and Technology, Trivandrum, India; [2]Centre for Sensors & Vision Technology, Central Manufacturing Technology Institute, Bangalore, India

Introduction

Microneedle arrays are emerging as a transformative platform for minimally invasive transdermal delivery of drugs, vaccines, and biologics. By penetrating the stratum corneum without stimulating pain receptors, they combine the efficacy of hypodermic injections with the convenience of transdermal patches. However, despite extensive research, the translation of microneedle technology into practical healthcare products remains constrained by the lack of scalable and reproducible manufacturing methods. This work addresses the critical challenge of bridging laboratory-scale microneedle fabrication with industrial production by developing and evaluating a scalable automated-processing fabrication strategy.

Materials and Methods

A batch-processing system was developed for scalable fabrication of polymeric microneedle arrays. The process involved controlled dispensing of polymer formulations into microstructured molds followed by vacuum-assisted degassing (~10^2 mbar) to remove entrapped air and ensure uniform mold filling. Drying and curing were carried out under controlled thermal conditions to stabilize needle geometry. The fabricated arrays were transferred onto surgical-grade backing substrates and sterilized using chemical or ultraviolet treatment prior to packaging. Meloxicam-loaded microneedle patches were used as a model system to evaluate morphology, mechanical integrity, and drug release performance. Micro-molded microneedles fabricated using conventional slow-drying conditions served as the reference system.

Results

Micro-molded microneedles demonstrated well-defined pyramidal geometry with sharp tips, uniform spacing, and needle heights of approximately 620–650 µm within a 529-needle array (Fig. 1), resulting in reliable insertion and efficient drug release. In contrast, rapid-drying conditions in the scalable automated-processing workflow introduced surface skin formation, shrinkage gradients, and microbubble entrapment. These defects caused partial needle deformation, tip rounding, and reduced needle height (Fig. 2). Consequently,automated-processed microneedles initially exhibited reduced drug release (~60%) compared with micro-molded systems (~90%).

Process analysis identified drying dynamics, temperature gradients, and degassing efficiency as critical determinants of microneedle morphology and functional performance. Iterative optimization of these parameters enabled uniform solvent evaporation, minimized internal stresses, and improved mold filling consistency. As a result, the microneedle arrays exhibited sharper tip geometry, improved structural stability, and significantly enhanced drug release efficiency approaching ~90%.

Conclusion

The study establishes a scalable fabrication framework for microneedle arrays and highlights the importance of process-parameter optimization in achieving reproducible morphology and performance. The optimized automated-processing strategy provides a practical pathway for translating microneedle technology from laboratory prototypes to industrial-scale manufacturing.

Acknowledgements

The authors acknowledge funding support from DST/TDT (DST/TDT/AM/2022/166 (C)/2) and the support of SCTIMST, Trivandrum, India, and CMTI, Bengaluru, India.

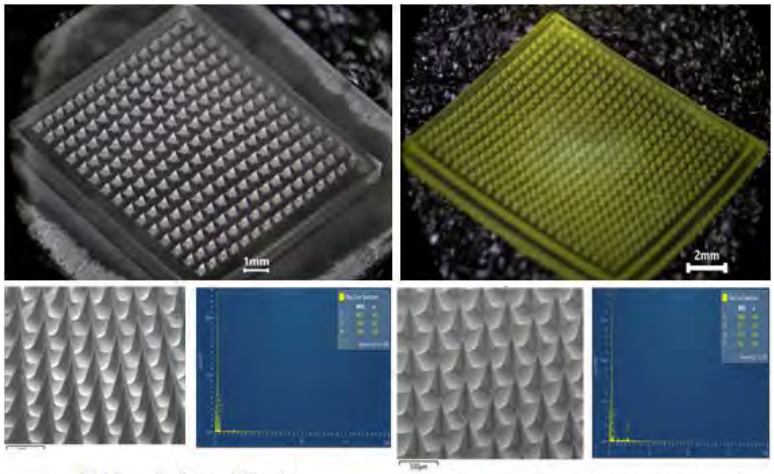

MN patches: Virgin

MN patches: Drug loaded

Figure 1. Microneedles fabricated by conventional micromolding

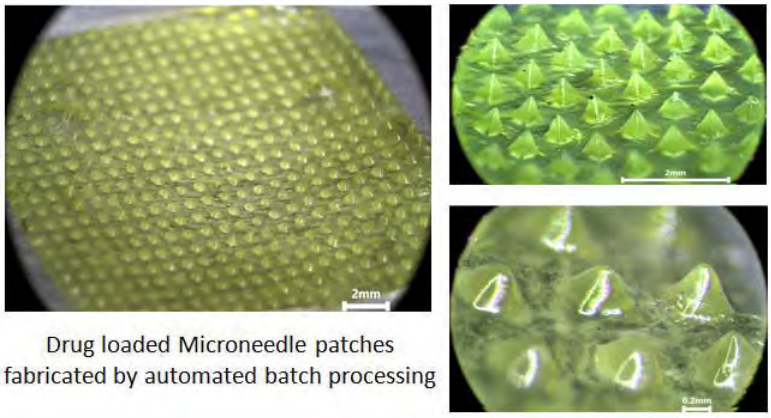

Drug loaded Microneedle patches fabricated by automated batch processing

Figure 2. Microneedles fabricated by scalable automated process

S103 – O2

Biochemical transformations during chitosan extraction from crab anatomical fractions revealed by FTIR spectroscopy

Tapia A.[1], Gutierrez Pua L.[1], Pérez-Cervera C.[2], Andrade-Pizarro R.[3], Paredes Mendez V.[4]
[1]Dept. Mechanical Engineering, Universidad del Norte, Barranquilla; [2]Agro-Industrial Engineering Program, Pontificia Bolivariana University, Montería; [3]Dept. of Food Engineering, Universidad de Córdoba, Montería; [4]Dept. Biomedical Engineering, Universidad Simón Bolívar, Barranquilla, Colombia

Introduction

Marine crustacean waste is an abundant biomass resource with potential for the sustainable production of biopolymers such as chitin and chitosan. Crab residues generated during industrial processing contain structurally diverse exoskeletal components whose biochemical composition may vary depending on the anatomical region. Although chitosan extraction from mixed crab biomass has been previously reported for *Callinectes sapidus* and *Callinectes bocourti,* the specific contribution of individual anatomical fractions to the biochemical transformations occurring during extraction remains poorly understood.
Fourier Transform Infrared Spectroscopy (FTIR) provides an effective method to identify functional groups associated with chitin and chitosan and to detect biochemical differences among biological materials.

Aim

This study investigates the influence of crab species (*Callinectes sapidus* and *Callinectes bocourti*) and anatomical fractions (carapace mixture, claw and chest) on the biochemical transformations occurring during chitin extraction and chitosan production, using FTIR spectroscopy.

Materials and Methods

Crab residues from *Callinectes sapidus* and *Callinectes bocourti* were separated into three anatomical fractions: carapace mixture, claw, and chest (Figure 1). The biomass was washed, dried, and milled prior to chitin extraction. The extraction process included sequential chemical treatments consisting of deproteinization (NaOH) and demineralization (HCl), followed by two alkaline deacetylation stages to convert chitin into chitosan.
FTIR spectroscopy (599–4000 cm^{-1}) was used to evaluate biochemical changes during the extraction process by comparing spectra from raw material, deproteinization, demineralization, and the two deacetylation stages.

Results

FTIR spectra revealed biochemical differences among the crab fractions (carapace mixture, claw, and chest) during the extraction process (Figure 2). All samples showed characteristic chitin bands including amide I (1650–1620 cm^{-1}), amide II (~1590 cm^{-1}), and amide III (~1317 cm^{-1}), along with C–O–C stretching bands in the ~1150–1020 cm^{-1} region.

Spectral evolution reflected the sequential treatments: deproteinization reduced amide band intensity, demineralization enhanced polysaccharide-related signals, and the two deacetylation stages showed changes in amide and amine bands associated with the conversion of chitin into chitosan.
The chest and claw fractions exhibited more pronounced spectral transitions and clearer definition of the polysaccharide region compared to the carapace mixture, indicating differences in biochemical composition among anatomical fractions.

Conclusion

FTIR analysis showed that crab anatomical fractions present distinct biochemical transforming during chitosan extraction. The chest and claw fractions exhibited clearer spectral transitions during the processing stages, suggesting a more effective conversion toward chitosan.
These results highlight the influence of biomass selection and anatomical origin for sustainable chitosan production from crab waste.

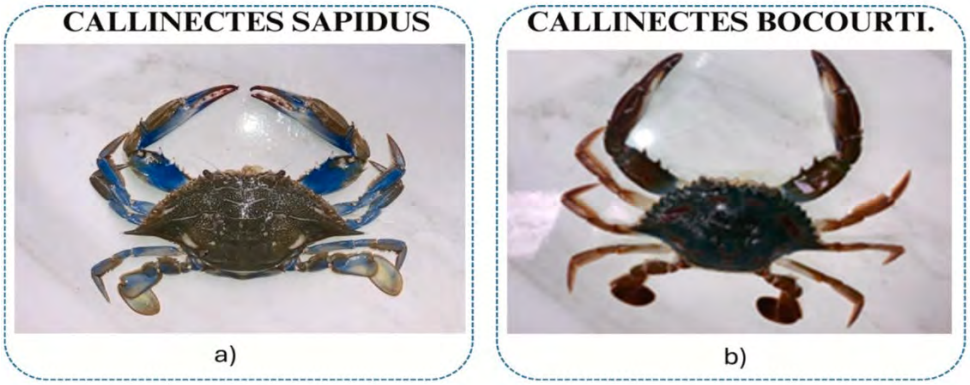

Figure 1. Representative species used as biomass sources for chitosan extraction: (a) Callinectes sapidus and (b) Callinectes bocourti. These crustaceans are commonly processed in the seafood industry, generating exoskeletal residues valorized for chitin and chitosan production.

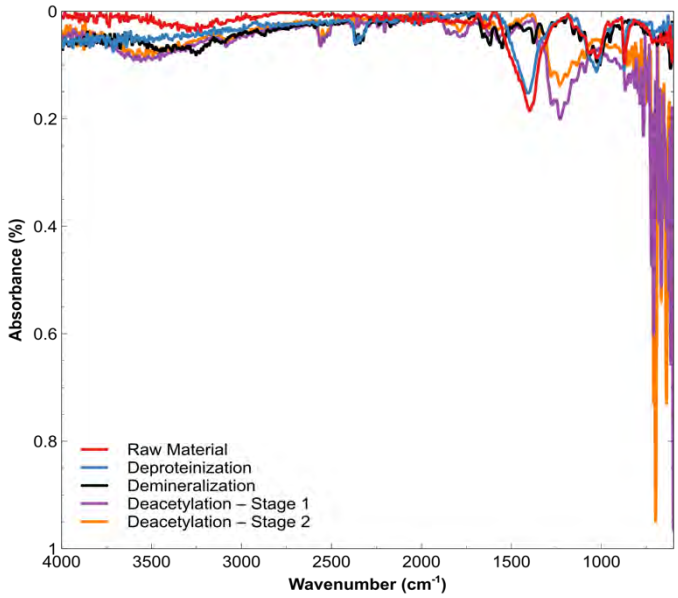

Figure 2. FTIR spectra showing the biochemical evolution during chitosan extraction from crab biomass across the sequential processing stages: raw material, deproteinization, demineralization, and two deacetylation stages

S103 – O4

Impact of degradation and strain on the fatigue of degradable magnesium

Hindenlang B.[1], Tolnai D.[1], Wiese B.[1], Bohlen J.[2], Höche D.[3], Willumeit-Römer R.[1], Wieland D.C.F.[1]
[1]Institute of Metallic Biomaterials, Helmholtz-Zentrum Hereon, Geesthacht; [2]Institute of Material and Process Design, Helmholtz-Zentrum Hereon, Geesthacht; [3]Institute of Surface Science, Helmholtz-Zentrum Hereon, Geesthacht, Germany

Introduction

Magnesium-based biodegradable implants promise advanced treatments, e.g. for cardiovascular applications or bone repair, due to their mechanical properties and potential transient use as they dissolve on their own after successful treatment. One issue is the complex degradation of Mg under biological conditions, where factors such as alloy composition, environment, and mechanical loads need to be considered. To better understand the mechanistic interaction, static tensile and compressive tests have been performed on Mg-10Gd under degradation conditions that closely resemble the physiological environment.

Materials and Methods

Experiments have been performed on C-ring samples, which were compressed and subjected to degradation for up to 4 weeks. The deformation was set to 0%, 30%, 50%, and 70%, respectively. The degradation was either observed by longitudinal µCT measurements of the C-ring or, for a second set of samples, by mass loss after chromic acid treatment. The strain distribution in the samples at specific degradation times and under deformation was monitored using scanning X-ray diffraction experiments. Furthermore, the samples were characterized by electron backscattering.

Results

Monitoring of the degradation showed that under compression, a thick and homogeneous degradation layer was observed, with small cracks within it (see Figure 1, blue arrows). The degradation was even faster, than in the undeformed state. On the tensile side, a different behavior can be observed. An increase in pitting is observed as analyzed by µCT, accompanied by the formation of a thin degradation layer. High-resolution µCT investigation could show that the degradation was penetrating deep into the material, triggering stress corrosion cracking and directly attacking the metal matrix; see Figure 1 (left). Strain profiles acquired for these conditions also show a reduction in strain at the interface with ongoing degradation, indicating weakening of the samples' integrity; see Figure 2.

Conclusion

Our experiments show that strain significantly affects the degradation behavior and, thus, the service life of a potential implant. Compressive and tensile loads have different impacts on the degradation behavior of magnesium alloys. For compressive strain, the degradation behavior remains similar to the undeformed state, with a higher degradation rate as cracks allow the media to access the bulk of the sample. On the tensile strained side, the formation of large cracks can be observed even after 1 week, with only minor degradation in the uncracked region, which might be hindered due to the presence of a high dislocation density.

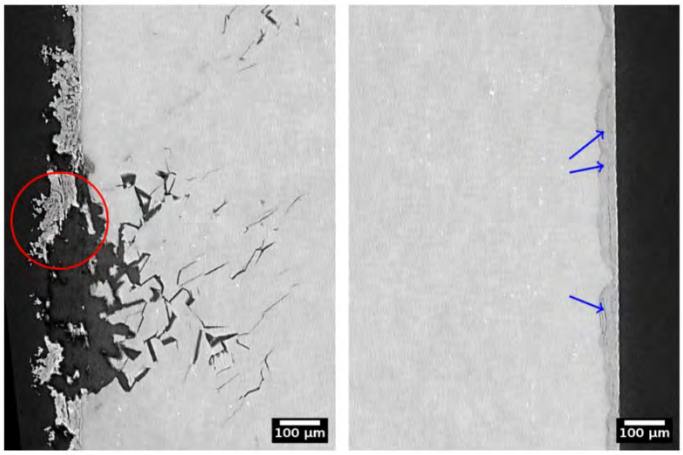

Figure 3: Slice through a tomographic reconstruction of the C-ring with 70% deformation and 4 weeks of degradation. On the left the tensile strain influence is seen, on the right the compressive strain. The blue arrows point on tiny cracks in the degradation layer.

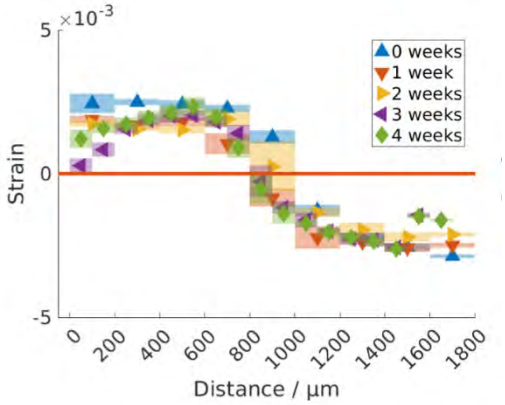

Figure 4 Strain profile across the C-ring at 50% deformation for different degradation times as determined by scanning X-ray diffraction

S103 – O5

Two-photon polymerized 3D microscaffolds for architecturally controlled stem cell culture platforms

Buccioli G.[1], Cortesi C.[1], Gavazzoni B.[2,4], Behrouzitabar M.[3], Martinelli C.[1], Conci C.[1], Nardini A.[4], Martínez Vázquez R.[4], Vanna R.[4], Polli D.[2,4,5], Antonacci G.[5], Raimondi M.T.[1], Jacchetti E.[1]
[1]Dept. of Chemistry, Materials and Chemical Engineering "Giulio Natta", Politecnico di Milano; [2]Dept. of Physics, Politecnico di Milano; [3]Dept. of Physics, University of Milano-Bicocca; [4]Institute for Photonics and Nanotechnologies, IFN-CNR; [5]Specto Photonics, Milan, Italy

Introduction

Mesenchymal stromal/stem cells (MSCs) are widely investigated for regenerative and immunomodulatory applications; however, their in vitro expansion is often associated with loss of stemness and functional potency. Mechanical cues play a central role in regulating stem cell state, yet conventional flat culture systems fail to reproduce the mechanical constraints experienced by cells in vivo. While three-dimensional (3D) culture is increasingly adopted, it remains unclear whether dimensionality alone is sufficient to generate biologically meaningful models, or whether the architectural distribution of mechanical constraints critically determines stem cell behaviour. Advanced fabrication strategies are therefore required to engineer 3D culture platforms with multiscale control over geometry and mechanics.

Materials and Methods

Optically accessible, highly porous 3D microscaffolds were fabricated by two-photon polymerization using the biocompatible hybrid photoresist SZ2080 and patterned onto glass substrates. The technique enables subcellular-scale resolution, allowing precise control of adhesion-regulating features while simultaneously defining cellular-scale confinement through scaffold geometry. The microscaffolds consisted of lattice architectures with overall dimensions on the order of tens of micrometers, designed either with graded pore sizes (10 × 10 × 15, 20 × 20 × 15 and 30 × 30 × 15 μm³) or with isotropic pores (15 × 15 × 15 μm³). MSCs were cultured on flat substrates as two-dimensional controls and within the two 3D microscaffold architectures, and were analyzed using optical microscopy techniques, including confocal microscopy, FLIM and Brillouin microscopy.

Results

Two-photon polymerization enabled the fabrication of 3D microscaffolds with well-defined architectures and optical accessibility. Compared to flat glass substrates, MSCs cultured within 3D microscaffolds exhibited pronounced differences in cell morphology, confirming that two-dimensional culture provides an incomplete description of stem cell mechanical state. Cellular responses within 3D environments were strongly architecture-dependent. Graded-pore microscaffolds promoted distinct cytoskeletal organization, nuclear morphology, metabolic activity and mechanical properties compared to isotropic architectures, demonstrating that scaffold microarchitecture critically modulates stem cell state beyond dimensionality alone.

Conclusions and perspectives

Ongoing and future work will integrate transcriptomic and proteomic analyses to quantitatively assess stemness maintenance and immunomodulatory signatures in cells cultured within architecturally defined microscaffolds. This will enable a mechanistic understanding of how micro- and cellular-scale mechanical constraints regulate cell function. In parallel, the development of biodegradable photopolymerizable materials will be explored to create application-specific platforms, allowing the design of transient or long-lasting 3D scaffolds depending on therapeutic needs, such as acute versus chronic pathologies. Together, this combined materials-driven and biology-oriented strategy aims to guide the development of next-generation photopolymerized devices for stem cell–based immunomodulatory and regenerative applications.

Acknowledgements

ERC (project BEACONSANDEGG, G.A. 101053122), MSC-DN, project flIMAGING3D, G.A. 101073507, MIUR (PRIN2022-VISION, cod. 2022FLXS8T).